



**Proceedings of the 40th
International Symposium on
Automation and Robotics in
Construction**

Chennai, India, July 5-7, 2023

Proceedings of the 40th International Symposium on Automation and Robotics in Construction

ISSN (for the proceedings series): 2413-5844

ISBN (for this issue of the proceeding series): 978-0-6458322-0-4

The proceeding series is Scopus indexed.

Scopus[®]

All papers are available in the IAARC Website and presentations in the IAARC YouTube Channel



Copyrights reserved.

© 2023 International Association on Automation and Robotics in Construction

This work including all its parts is protected by copyright. Any use outside the narrow limits of copyright law without the consent of the individual authors is inadmissible and punishable. This applies in particular to reproductions, translations, microfilming and saving and processing in electronic systems.

The reproduction of common names, trade names, trade names etc. in this work does not justify the assumption that such names are to be regarded as free within the meaning of the trademark and trademark protection legislation and can therefore be used by everyone, even without special identification.

Cover design: Samuel Prieto and Borja García de Soto. Image: Robotic platform developed by the S.M.A.R.T. Construction Research Group at NYUAD with a thermal camera and laser scanner for the autonomous collection of information in construction sites.

Editorial Board

Editors in Chief

García de Soto, Borja (New York University Abu Dhabi)

Gonzalez, Vicente (University of Alberta)

Brilakis, Ioannis (University of Cambridge)

Editors (Area Chairs)

Adán, Antonio (University of Castilla La Mancha)

Arashpour, Mehrdad (Monash University)

Brosque, Cynthia (Stanford University)

Bugalia, Nikhil (Indian Institute of Technology Madras)

Carbonari, Alessandro (Università Politecnica delle Marche)

Du, Jing (University of Florida)

Feng, Zhenan (Massey University)

Gheisari, Masoud (University of Florida)

Hall, Daniel (TU Delft)

Hamzeh, Farook (University of Alberta)

Hu, Rongbo (Technical University of Munich)

Isaac, Shabtai (Ben-Gurion University of the Negev)

Iturralde, Kepa (Technical University of Munich)

Li, Nan (Tsinghua University)

Liang, Ci-Jyun (National Institute for Occupational Safety and Health)

Mahalingam, Ashwin (Indian Institute of Technology Madras)

Ng, Ming Shan (Kyoto Institute of Technology)

Zhang, Jiansong (Purdue University)

Zou, Yang (University of Auckland)

Local Organizing Committee

Raphael, Benny (Chair)
Varghese, Koshy (Co-chair)
Babu, Ramesh
Bugalia, Nikhil
Chaunsali, Piyush
Gettu, Ravindra
Kirupakaran, Keerthana
Mahalingam, Ashwin
Palaniappan, Sivakumar
Pillai, Radhakrishna
Ramamurthy, K.
Santhanam, Manu
Satyanarayana, K. N.

Sponsors

PLATINUM SPONSOR



GOLD SPONSOR



SILVER SPONSOR



BRONZE SPONSOR



WORKSHOP PARTNER



MEDIA PARTNER



Foreword

The International Association for Automation and Robotics in Construction (IAARC) and the local organizing committee are pleased to present the Proceedings of the 40th International Symposium on Automation and Robotics in Construction (ISARC 2023) held on July 5-7, 2023, at IIT Madras, Chennai, India. The 40th ISARC was proudly hosted by the Department of Civil Engineering at IIT Madras. This ISARC marks the 40th anniversary of this emblematic symposium. A total of 133 papers were submitted, and after a rigorous peer-review process, 103 papers (77%) were accepted, and 100 were included in the proceedings. Two hundred eighty-six authors representing 115 universities and 29 private/public research organizations and firms from 28 countries, including the Americas, Europe, Asia, and the Middle East, were selected after a two-step (including rebuttal phase) peer-review process with over 170 reviewers managed by 19 Area Chairs taking care of the 8 technical areas of interest of ISARC/IAARC including “Sustainable construction with automation”, the theme proposed by the local organizers for this edition. Submission of full papers with no prior submission of abstracts was requested, making the revision cycles and iterations more effective. The peer-review of the papers was single-blinded. Most of the papers (66%) had 2 reviews. In some cases, papers went through additional reviews before a decision could be made. Twenty-nine percent had 3 reviews, and 6% had 4. That allowed us to address situations where consensus by the reviewers was not reached, and additional reviews were required. During the review process, a rebuttal phase was incorporated to allow authors to address the comments by the reviewers. In general, authors appreciate the comments and feedback provided by the reviews. The peer-review process enabled the identification of high-quality papers, including short papers, in the proceedings. In terms of presentations, the traditional keynote, plenary and parallel presentations were identified. On top of that, this edition of ISARC includes a “poster category”. The posters were showcased during the symposium.

ISARC is the premier global event in the domain of automation and robotics in construction, and as such, the IAARC Technical Committee, with the support of the Area Chairs, strived to secure the acceptance of high-caliber papers. Along with the consolidation of ISARC/IAARC technical areas of interest, an explicit effort to consolidate the knowledge accumulated this year (and from prior years) was undertaken by the IAARC Technical Committee. In that regard, a supporting framework for Area Chairs and reviewers was put in place, including guidelines and standards, to include papers in the proceedings that were carefully curated. The establishment of this review framework and additional “standards” represent an incremental improvement to the ongoing efforts from IAARC to continue improving the standing of ISARC.

We trust that this year’s proceedings are interesting for readers, and they will find the papers included stimulating and inspiring. Please enjoy.

Borja García de Soto (New York University Abu Dhabi)

Vicente A. Gonzalez (University of Alberta)

Ioannis Brilakis (University of Cambridge)

Table of Contents

K – Keynote talks

Automated Progress Monitoring in Modular Construction Factories Using Computer Vision and Building Information Modeling.....	1
Roshan Panahi, Joseph Louis, Ankur Podder, Shanti Pless, Colby Swanson, and Melika Jafari	
BIM-based construction quality assessment using Graph Neural Networks.....	9
Navid Kayhani, Brenda McCabe, and Bharath Sankaran	
Discrete Event Simulation Based Approach for Tracking Performance of Segmental Production at Precast Yard	17
Ashutosh Kumar Rai, Varun Kumar Reja, and Koshy Varghese	

P – Plenary talks

Reducing Uncertainty in Multi-Robot Construction through Perception Modelling and Adaptive Fabrication.....	25
Daniel Ruan, Wes Mcgee, and Arash Adel	
Identifying key parameters for BIM-based disassembly planning.....	32
Benjamin Sanchez, Pieter Herthogs, and Rudi Stouffs	
Building insulation renovation: a process and a software to assist panel layout design, a part of the ISOBIM project.....	40
Michel Pierre Aldanondo, Julien Lesbegueries, Andrea Christophe, Elise Vareilles, and Xavier Lorca	
Automatic point Cloud Building Envelope Segmentation (Auto-CuBES) using Machine Learning.....	48
Bryan P. Maldonado, Nolan W. Hayes, and Diana Hun	
Contribution of Dual-tree Complex Wavelet to Three-dimensional Analysis of Pavement Surfaces.....	56
Kazuya Tomiyama, Yuki Yamaguchi, and Kazushi Moriishi	
How Can ChatGPT Help in Automated Building Code Compliance Checking?.....	63
Jiansong Zhang	
Making Uncoordinated Autonomous Machines Cooperate: A Game Theory Approach.....	71
Kohta Sakurai, and Masahide Horita	

A – Automated/robotic machines, devices, & end-effectors

Full-Scale Prototype for Bricklaying Activity.....	79
Michele Ambrosino, Fabian Boucher, Pierre Mengeot, and Emanuele Garone	
Bettan – Industrial robot and application for Finja Exakt build system.....	86
Maike Klöckner, Mathias Haage, Ronny Andersson, Klas Nilsson, Anders Robertsson, and Helena Eriksson	
Optical Process Control for extrusion-based Additive Manufacturing methods in construction.....	94
Rafay Mohiuddin, Miranda Cruz Policroniades, Martin Slepicka, and André Borrmann	
RTDE robot control integration for Fabrication Information Modeling.....	102
Martin Slepicka, Jalal Helou, and André Borrmann	
Realtime damage detection in long conveyor belts using deep learning approach.....	110
Uttam Kumar Dwivedi, Ashutosh Kumar, and Yoshihide Sekimoto	
Low-light Image Enhancement for Construction Robot Simultaneous Localization and Mapping.....	116
Xinyu Chen, and Yantao Yu	
Mobile-robot and Cloud-based Integrated Defect Inspection System for Indoor Environments.....	124
Vengatesan Govindaraju, Takrit Tanasnitikul, Zheng Wu, and Pongsak Lasang	
Vehicle Trajectory-Tracking Model for AV using LiDAR in Snowy Weather Under Different Snowing Environments.....	132
Padmapriya J, Ravi Prasath M, and Murugavalli S	
Quantified Productivity Evaluation of Autonomous Excavation Systems using a Simulation Approach.....	140
Xiaoyu Bai, Beiji Li, Yong Zhi Koh, Soungcho Chae, C.S. Meera, and Justin K.W. Yeoh	
Prototypical digital twin of multi-rotor UAV control and trajectory following.....	148
Lanh Van Nguyen, Trung Hoang Le, and Quang Phuc Ha	
Development of a Blade Lifting Control Assist System for a Motor Grader.....	156
Ekin Cansu Özkan Öztürk, Ufuk Akpınarlı, İlhan Varol, Yavuz Samim Ünlüsoy, and Klaus Werner Schmidt	
Development and evaluation of a low-cost passive wearable exoskeleton system for improving safety and health performance of construction workers: A pilot study.....	164
Shahnawaz Anwer, Heng Li, Mohammed Abdul-Rahman, and Maxwell Fordjour Antwi-Afari	
Automated construction process for foundation engineering.....	172
George Meshcheriakov, and Anatolii Andryushchenko	
Bulldozer sensing technique for the purpose of automation for bulldozer's workflow.....	180
Alexey Bulgakov, Thomas Bock, Georgii Tokmakov, and Sergey Emelianov	
Proposal of an Open Platform for Autonomous Construction Machinery Development.....	186
Genki Yamauchi, Endo Daisuke, Hirotaka Suzuki, and Takeshi Hashimoto	
Real-time evaluator to optimize and automate crane installation of prefabricated components.....	192
Nolan W. Hayes, Bryan P. Maldonado, Diana Hun, and Peter Wang	
Mathematical description of concrete laying robots.....	200
Vladimir Travush, Alexey Bulgakov, Thomas Bock, Wen-der Yu, and Ekaterina Pakhomova	
Structural organization of robotic building and mounting complexes.....	208
Alexey Bulgakov, Jens Otto, Wen-der Yu, Vladimir Rimshin, and Alexey Shleenko	

B – Construction management techniques

Proof-of-concept for a reliable common data environment utilizing blockchain and smart contracts for supply-chain of public civil works.....	214
Fumiya Matsushita, and Kazumasa Ozawa	
An Extensible Construction Ontology to Guide Job-Site Sensing and Support Information Management.....	222
Ran Ren, Jiansong Zhang, and Pingbo Tang	
Impact of Reinforcement Design on Rebar Productivity.....	230
Amith G Mallya, Varun Kumar Reja, and Koshy Varghese	
Prospects of Integrating BIM and NLP for Automatic Construction Schedule Management.....	238
Akarsth Kumar Singh, Aritra Pal, Pavan Kumar, Jacob J. Lin, and Shang-Hsien Hsieh	
Design based Constraint Handling for Site Layout Planning.....	246
Abhishek Raj Singh, Venkata Santosh Kumar Delhi, and Sagar Jain	
Digital Twin Framework for Worker Safety using RFID Technology	254
Anikesh Paul, Sagar Pulani, and J. Uma Maheswari	
Evaluation of ground stiffness using multiple accelerometers on the ground during compaction by vibratory rollers.....	262
Yusuke Tamaishi, Kentaro Fukuda, Kazuto Nakashima, Ryuichi Maeda, Kohei Matsumoto, and Ryo Kurazume	
Optimized Production Scheduling for Modular Construction Manufacturing	270
Angat Pal Singh Bhatia, Osama Moselhi, and SangHyeok Han	
AWPIC: Advanced Work Packaging Improvement Canvas	278
Hala Nassereddine, Makram Bou Hatoum, and Fernando Espana	
Assessment of Financial Risk Parameters Associated with Public-Private Partnership Port Projects in India	286
Krushna Shivaji Raut, and Gayatri S. Vyas	

C – Human factors & human-system collaboration

From Lab to Field: A Sociotechnical Systems View of the Organisational Cycle for Intelligent Robotics Technologies Ideation, Planning, Design, Development and Deployment	294
Karyne Ang, Shankar Sankaran, Dikai Liu, and Pratik Shreshta	
Digital Twin Approach for the Ergonomic Evaluation of Vertical Formwork Operations in Construction	302
Vigneshkumar Chellappa, and Jitesh Singh Chauhan	
Impact of Crew Diversity on Worker Information Access and Performance	309
Bassam Ramadan, Hala Nassereddine, Timothy Taylor, and Paul Goodrum	
Understanding BIM through a Simulation Game - Case study of Indian Students subjected to this course	317
Vasanth K. Bhat, Gregor Grunwald, and Tobias Hanke	
Towards interfacing human centered design processes with the AEC industry by leveraging BIM-based planning methodologies	325
Marc Schmailzl, Michael Spitzhörn, Friedrich Eder, Georg Krüll, Thomas Linner, Mathias Obergrießer, Wassim Albalkhy, and Zoubeir Lafhaj	

Research on the Relationship between Awareness and Heart Rate Changes in the Experience of Safety Education Materials Using VR Technology	333
Shunsuke Someya, Kazuya Shide, Hiroaki Kanisawa, Zi Yi Tan, and Kazuki Otsu	

D – Information modeling techniques

An Integrated Approach for Automated Acquisition of Bridge Data and Deficiency Evaluation.....	341
Abdelhady Omar, and Osama Moselhi	
Coupling asphalt construction process quality into product quality using data-driven methods.....	349
Qinshuo Shen, Faridaddin Vahdatikhaki, Seirgei Miller, and Andre Doree	
BIM-GIS integration and crowd simulation for fire emergency management in a large diffused university.....	357
Silvia Meschini, Daniele Accardo, Mirko Locatelli, Laura Pellegrini, Lavinia Chiara Tagliabue, and Giuseppe Martino Di Giuda	
Transformation of Point Clouds to Images for Safety Analysis of Scaffold Joints.....	365
Jeehoon Kim, Sunwoong Paik, Yulin Lian, Juhyeon Kim, and Hyoungkwan Kim	
Occlusion-free Orthophoto Generation for Building Roofs Using UAV Photogrammetric Reconstruction and Digital Twin Data.....	371
Jiajun Li, Frédéric Bosché, Chris Xiaoxuan Lu, and Lyn Wilson	
Geometric control of short-line match casting using Computational BIM	379
Nandeesh Babanagar, Ashwin Mahalingam, Koshy Varghese, and Vijayalaxmi Sahadevan	
A pre-trained language model-based framework for deduplication of construction safety newspaper articles	387
Abhipraay Nevatia, Soukarya Saha, Sundar Balarka Bhagavatula, and Nikhil Bugalia	
Development of a BIM-based spatial conflict simulator for detecting dust hazards	395
Leonardo Messi, Alessandro Carbonari, Alessandra Corneli, Stefano Romagnoli, and Berardo Naticchia	
MN-pair Contrastive Damage Representation and Clustering for Prognostic Explanation	403
Takato Yasuno, Masahiro Okano, and Junichiro Fujii	
Indoor Defect Region Identification Using an Omnidirectional Camera and Building Information Modeling	411
Yonghan Kim, and Ghang Lee	
Subword Tokenization of Noisy Housing Defect Complaints for Named Entity Recognition	418
Kahyun Jeon, and Ghang Lee	
A Framework of Reconstructing Piping Systems on Class-imbalanced 3D Point Cloud Data from Construction Sites	426
Yilong Chen, Seongyong Kim, Yonghan Ahn, and Yong Kwon Cho	
Information Modelling Guidelines for the Mining Sector	434
Jyrki Salmi, and Rauno Heikkilä	
Automated Layout Zoning: A Case of the Campus Design Problem	442
Vijayalaxmi Sahadevan, Kane Borg, Vishal Singh, and Koshy Varghese	
Deep learning for construction emission monitoring with low-cost sensor network.....	450
Huynh Anh Duy Nguyen, Trung Hoang Le, Quang Phuc Ha, and Merched Azzi	

Restructuring Elements in IFC Topology through Semantic Enrichment: A Case of Automated Compliance Checking.....	458
Ankan Karmakar, and Venkata Santosh Kumar Delhi	
Towards Automation in Steel Construction: Development of an OWL Extension for the DSTV-NC Standard.....	466
Victoria Clarita Jung, Lukas Kirner, and Sigrid Brell-Cokcan	
Quality monitoring of Concrete 3D printed elements using computer vision-based texture extraction technique.....	474
Shanmugaraj Senthilnathan, and Benny Raphael	
Digital twins of bridges: notions towards a practical digital twinning framework.....	482
Kamil Korus, Marek Salamak, and Jan Winkler	

E – Sensing systems & data infrastructures

Marker-based Extrinsic Calibration for Thermal-RGB Camera Pair with Different Calibration Board Materials.....	490
Bilal Ali Sher, Xuchu Xu, Guanbo Chen, and Chen Feng	
Online Safety Risk Management for Underground Mining and Construction Based on IoT and Bayesian Networks.....	498
Milad Mousavi, Xuesong Shen, and Binghao Li	
Evaluating Road Segmentation Performance in Participatory Sensing: An Investigation into Alternative Metrics.....	506
Jeongho Hyeon, Minwoo Jeong, Giwon Shin, Wei-Chih Chern, Vijayan K. Asari, and Hongjo Kim	
Microservice-Based Middleware for a Digital Twin of Equipment-Intensive Construction Processes.....	513
Anne Fischer, Yuling Sun, Stephan Kessler, and Johannes Fottner	
BIM-SLAM: Integrating BIM Models in Multi-session SLAM for Lifelong Mapping using 3D LiDAR.....	521
Miguel Arturo Vega Torres, Alex Braun, and André Borrmann	
A review of Computer Vision-Based Techniques for Construction Progress Monitoring	529
Shrouk Gharib, and Osama Moselhi	
A corpus database for cybersecurity topic modeling in the construction industry	537
Dongchi Yao, and Borja García de Soto	
Lessons Learned from ‘Scan to BIM’ for Large Renovation Projects by the U.S. Army Corps of Engineers.....	545
Tony Cady, Anoop Sattineni, and Junshan Liu	
Demonstration of LiDAR on Accurate Surface Damage Measurement: A Case of Transportation Infrastructure	553
Nikunj Dhanani, Vignesh V P, and Senthilkumar Venkatachalam	
DeepGPR: Learning to Identify Moisture Defects in Building Envelope Assemblies from Ground Penetrating Radar.....	561
Bilal Ali Sher, and Chen Feng	
Using AI for Planning Predictions – Development of a Data Enhancement Engine.....	569
Ashwath Kailasan, Vikas Patel, Viranj Patel, and Bhargav Dave	

Lessons Learned from the “Hack My Robot” Competition and Considerations for Construction Applications	577
Muammer Semih Sonkor, and Borja García de Soto	

F – Services & business applications / Industry papers

HLE-SLAM: SLAM for overexposed construction environment	585
Xinyu Chen, and Yantao Yu	
AprilTag detection for building measurement.....	589
Kepa Iturralde, Jungcheng Shen, and Thomas Bock	
UAV for target placement in buildings for retrofitting purposes.....	593
Kepa Iturralde, Wenlan Shen, Tao Ma, Soroush Fazeli, Hükar Suci, Runfeng Lyu, Weihang Li, Jui Wen Yeh, Phillip Hübner, Nikhita Kurupakulu Venkat, and Thomas Bock	
BIM Implementation Strategy- A proposal for KMRL.....	597
Dona James, Berlin Sabu, and Dyna James	
Object Detection in Construction Department.....	601
Pralipa Nayak	
Online Modelling and Prefab Layout definition for building Renovation.....	605
Kepa Iturralde, Sathwik Amburi, Sandhanakrishnan Ravichandran, Samanti Das, Danya Liu, and Thomas Bock	
Overview of robotic shotcrete technologies with basalt reinforcement.....	609
Thomas Bock, Viacheslav Aseev, and Alexey Bulgakov	
Automatic Design of various Reinforced Concrete Structures based on AutoCAD AutoLISP.....	613
Dharani V P, and Parvatham Vijay	
PEXCon: Design and Development of Passive Exoskeleton for Construction.....	617
Sachin Kansal, and Jiansong Zhang	

G – Technology management & innovation

The Analysis of Lean Wastes in Construction 3D Printing: A Case Study.....	621
Wassim AlBalkhy, Scott Bing, Saad El-Babidi, Zoubeir Lafhaj, and Laure Ducoulombier	
Exploring the Digital Thread of Construction Projects.....	628
Makram Bou Hatoum, Hala Nassereddine, Nadine AbdulBaky, and Anwar AbouKansour	
The impact of the combined innovations at the Hungarian National Athletics Stadium steel roof structure construction.....	636
Heidenwolf Orsolya, Juhász Márton István, Kocsis András Balázs, Gáncs Dániel, Kézsmárki Zoltán, Kis Attila, and Szabó Ildikó	
Generative Design for Prefabricated Structures using BIM and IoT applications – Approaches and Requirements.....	644
Veerakumar Rangasamy, and Jyh-Bin Yang	
LeanAI: A method for AEC practitioners to effectively plan AI implementations.....	652
Ashwin Agrawal, Vishal Singh, and Martin Fischer	
Digital Twin as enabler of Business Model Innovation for Infrastructure Construction Projects.....	660
Sascha van der Veen, Elias Meusburger, and Magdalena Meusburger	

H – Sustainable construction with automation

Using BIM to Facilitate Generative Target Value Design for Energy Efficient Buildings.....	667
Saurav Bhilare, Diya Khatri, Salonee Rangnekar, Qian Chen	
Hardware/Software solutions for an efficient thermal scanning mobile robot.....	675
Alejandro López-Rey, Amanda Ramón, and Antonio Adán	
Construction Automation and Robotics for Concrete Construction: Case Studies on Research, Development, and Innovations.....	683
Rongbo Hu, Wen Pan , Kepa Iturralde, Thomas Linner , and Thomas Bock	
3D Printing: An opportunity for the sustainable development of building construction.....	691
Christopher Joseph Núñez Varillas, Marck Steewar Regalado Espinoza, and Angela Cecilia Gago Gamboa	
Crack Detection and Localization in Stone Floor Tiles using Vision Transformer approach.....	699
Luqman Ali, Hamad Aljassmi, Medha Mohan Ambali Parambil, Muhammed Swavaf, Mohammed AlAmeri, and Fady Alnajjar	
Integrating Building Information Modeling, Deep Learning, and Web Map Service for Sustainable Post-Disaster Building Recovery Planning.....	706
Adrianto Oktavianus, Po-Han Chen, and Jacob J. Lin	
Life cycle-oriented decision making based on data-driven building models.....	714
Niels Bartels, Josephine Pleuser, and Timo Schroeder	
Sustainability in Construction Projects: Setting and measuring impacts.....	722
Priyanka Ramprasad, Bhargav Dave, Martin Zilliacus, and Viranj Patel	
State of the art Technologies that Facilitate Transition of Built Environment into Circular Economy.....	730
Aparna Harichandran, Søren Wandahl, and Lars Vabbersgaard Andersen	
A review on the Smartwatches as IoT Edge Devices: Assessing the end-users continuous usage intention using structural equation modelling.....	738
Udit Chawla, Hena Iqbal, Harsh Vikram Singh, Varsha Mishra, Sarabjot Singh, and Vishal Choudhary	

Automated Progress Monitoring in Modular Construction Factories Using Computer Vision and Building Information Modeling

R. Panahi¹, J. Louis², A. Podder³, S. Pless⁴, C. Swanson⁵, and M. Jafari⁶

^{1,2} School of Civil and Construction Engineering, Oregon State University, Oregon, USA

^{3,4} National Renewable Energy Laboratory, Colorado, USA

⁵ Momentum Innovation Group, USA

⁶ College of Built Environments, University of Washington, Washington, USA

E-mail: panahir@oregonstate.edu, joseph.louis@oregonstate.edu,
ankur.podder@nrel.gov, shanti.pless@nrel.gov, colby@miginnovation.com, melikaj@uw.edu

Abstract –

Modular construction methods have recently gained interest due to the advantages offered in terms of safety, quality, and productivity for projects. In this method, a significant portion of the construction is performed off-site in factories where modular components are built in different workstations, assembled on the production line, and shipped to the site for installation. Due to the labor-intensive nature of tasks, cycle times in modular construction factories are highly variable, which commonly leads to major bottlenecks and delays in construction projects. To remedy this effect, recent methods rely on sensors such as RFID to monitor the production process, which is reportedly expensive, and intrusive to the work process. Recently, computer vision-based methods have been proposed to track the production process in modular construction factories. However, these methods overlook monitoring the assembly process on the production line. Therefore, this paper presents a method to monitor the assembly process by integrating computer vision-based methods with Building Information Modeling (BIM). The proposed method detects the modular units using object segmentation; superimposes the installation area with the corresponding 2D region using BIM, and identifies the installation of the components using image processing techniques. The proposed method has been validated using surveillance videos captured from a modular construction factory in the US. Successful implementation of the proposed method can lead to timely identification of delays during the assembly process and reduce delays in modular integrated construction projects.

Keywords –

Modular Construction; Computer Vision; Building Information Modeling

1 Introduction

Off-site and modular construction is increasingly being seen as a promising method of project delivery due to the advantages offered in terms of productivity, schedule, and cost [1]. Here, building components are produced in a controlled environment such as a prefabrication factory, and shipped to the site for installation, leaving relatively minimal work to be performed on-site [2]. It also enables incorporation of energy-efficient building strategies at scale to reduce first cost of installation for affordable housing. Despite these advantages and the recent advancements in the application of robotics inside modular construction factories [3], [4], the current state of these factories in the U.S. still highly relies on manual labor. In addition, variability in design [5] and the stochastic nature of the orders [6], all, lead to the high variability of cycle times and result in major bottlenecks. These bottlenecks reportedly can account for up to 15% of work time, reduce productivity, and cause delays in modular integrated construction projects [7]. Therefore, it is important to identify and mitigate these bottlenecks in order to prevent such delays from negatively affecting construction projects.

Monitoring and control systems inside factories can be used to identify bottlenecks inside the factories and enable optimal tactical and strategic responses to dynamic changes on the factory floor [8]. However, the current state of the monitoring practice inside modular

construction factories commonly relies on manual methods such as five-minute rating, and work sampling [9], which are prohibitively expensive and error-prone when implemented in a large scale [10]. Alternatively, sensors such as radio-frequency identification (RFID) [5], audio [11], and inertial measurement units (IMU) [12] were used to automatically collect the process data from the shopfloor in modular construction factories. However, these systems are expensive to maintain and can cause intrusion into the progress of work, which can impede their practical application [13].

Computer vision-based methods can overcome these challenges by remotely monitoring the progress of work. During the past decade, these methods have attracted much attention from the construction community at large [14]. However, despite these advancements, recent research unveils an array of challenges computer vision-based methods face when applied inside modular construction factories. Examples of such challenges are the fast-paced environment which causes inter-object occlusions [15], high variability of tasks which reduces the performance of activity recognition methods [16], and fundamental differences in processes compared to on-site tasks which hinder the vision-based knowledge transfer across on-site and off-site environment [17].

To address these challenges, computer vision-based methods were used to monitor the ergonomics of workers [18], their activities [15], and tackle technical challenges such as occlusion in tracking the workers [16]. To monitor the processes, Zheng et al. [19] proposed a framework that extracts the cycle time for the installation of modules after being delivered to the construction site. They fine-tuned a Mask R-CNN object segmentation algorithm on a total of 1100 synthetic and real images of finished prefabricated modules. In order to monitor the progress of work in panelized construction factory workstations, Martinez et al. [17] proposed a vision-based monitoring method that detects the crane and the workers in a single station and updates the parameters of a finite state machine to track the progress of work. More recently, Park et al. [20] [21] created a synthetic image dataset of modular units inside the factory and evaluated a CNN-based 3D reconstruction network from the collected 2D synthetic images.

Based on the conducted review of the related literature following gaps are identified and targeted in this study: (1) drawbacks of contact-based sensors: majority of the previously proposed monitoring methods inside modular construction factories rely on contact-based sensors. Despite the accuracy these methods provide, they are expensive to implement at large scale; they are susceptible to noise, and they are intrusive to the progress of work; (2) drawback of vision-based monitoring methods: previous research identifies the movement of equipment and uses this information as

queues to monitor the progress of work. However, in many cases the movement of equipment is not related to the progress of work, such as the assembly process, and (3) limitation of detection vs. segmentation: previously proposed progress monitoring methods inside modular construction factories rely on detection methods, however, detection bounding boxes are not reliable for progress monitoring as they entail a large background area, unrelated to the object of interest, especially in oblique views of CCTV video footage.

This study attempts to propose a computer vision-based progress monitoring method to overcome the drawbacks of contact-based sensors, use object segmentation to detect the modular units at pixel level, and monitor the assembly progress of components on the modular unit on the production line.

The remainder of this paper is structured as follows. First, the proposed method is presented. This is followed by a brief explanation of a case study that demonstrates the applicability of the framework. The paper ends with conclusions and future work.

2 Methodology

The goal of the proposed method is to monitor the assembly progress in modular construction factories. Figure 1 shows the objectives to achieve this goal.

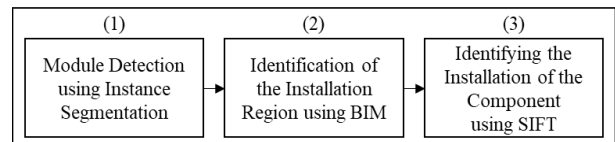


Figure 1. Workflow of the proposed method

As shown in Figure 1, the objectives of this study are: (1) module detection: to detect and segment the modular units on the shop floor; (2) identification of the installation region: to detect the installation region of interest (RoI) on the video, and (3) identifying the installation of the component: to classify the state of the components as installed or not-installed. These objectives are explained in further detail, in following sections.

2.1 Module Detection

Here, the modular units are detected and their boundary is segmented using an object detection and segmentation method. Doing so, Mask R-CNN instance segmentation is used to demarcate the modular units on the shop floor, at a pixel level. Mask R-CNN is a state-of-the-art model for instance segmentation, developed on top of Faster R-CNN. Faster R-CNN is a region-based convolutional neural networks [22], that returns

bounding boxes for each object and its class label with a confidence score. Figure 2 shows the architecture of the Mask R-CNN algorithm used on this study.

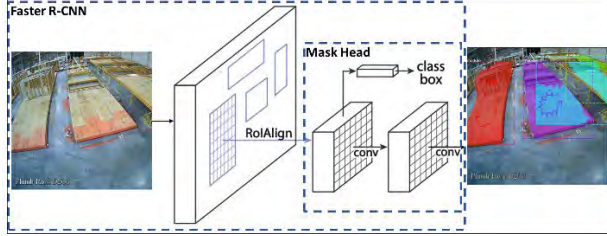


Figure 2. Architecture of the Mask R-CNN algorithm

As shown in figure 2, the algorithm first performs detection by drawing a bounding box around the object of interest. However, this bounding box commonly includes a large portion of the background area, since CCTV cameras are commonly installed in highly oblique orientation to cover a large portion of the factory. As a result, these bounding boxes cannot be efficiently used to extract precise reference points on the modular unit and use them to identify the installation regions. Therefore, the Mask Head in the segmentation algorithm is used to precisely annotate the boundaries of the modular unit. Finally, in order to identify the left corner of the module, the lowest point in each detected instance is identified as the reference point.

2.2 Identification of Installation Region

Here, the installation region of each component on the modular unit is annotated in the video using the BIM model. Figure 3 shows the pipeline that creates this association between the points in the virtual and real space using projective geometry, and equation 1 shows the projective transformation formula using the homography matrix H.

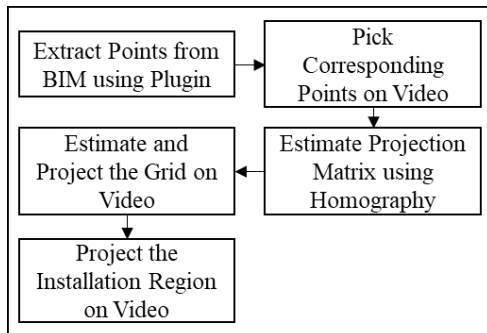


Figure 3. Region of Interest Identification

$$\begin{bmatrix} x'_1 \\ x'_2 \\ x'_3 \end{bmatrix} = \begin{bmatrix} h_1 & h_2 & h_3 \\ h_4 & h_5 & h_6 \\ h_7 & h_8 & h_9 \end{bmatrix} \begin{bmatrix} x_1 \\ x_2 \\ x_3 \end{bmatrix} \quad (1)$$

In equation 1, (x'_1, x'_2, x'_3) denotes the pixel coordinates of a point on the image, (x_1, x_2, x_3) denotes the pixel coordinates of a point on in the virtual space, and h_1 to h_9 denote the translation, rotation, and scale parameters. In this case, x'_3, x_3 are set to zero as both sets of points are constrained to planes.

As shown in Figure 3, a plugin is designed in Revit software to extract four points located on the modular unit. Specifically, the designed plugin uses Revit API to loop through all the coordinates of a the “floor” type, and exports the four corners of the element to an excel sheet. Subsequently, these four corner points are manually identified on the video and the projection matrix is estimated using the homography formula shown in equation 1. It is important to note that this process needs to be done only once for each CCTV camera, since all the future in-coming modules are at the same height and therefore on the same plane. Therefore, the same homography matrix can be used for all stations visible in the same camera. However, the module detection step and identifying a reference point on the module has to be performed each time a module comes into the station since the exact location of the module inside the station is not fixed. Furthermore, the simple template-based matching expands the generalizability and practicality of this method to other factories by allowing the domain experts to easily annotate two templates for each station in the new factory. This approach also made this method robust to the changes in the appearance of the modular unit which occurs across the production line as the modular units are developed.

A grid parallel to the edges of the modular unit is projected on the plane of the modular units in the video, using the corner of the unit as the reference point. Finally, extracted points of the component, which needs to be installed, are projected on the generated grid. Equation 2 shows how the homographic matrix is used to calculate the pixel location of installation regions and what input BIM points are used.

$$\begin{bmatrix} h_1 & h_2 & h_3 \\ h_4 & h_5 & h_6 \\ h_7 & h_8 & h_9 \end{bmatrix}^{-1} \begin{bmatrix} X \\ Y \\ 0 \end{bmatrix} = \begin{bmatrix} x \\ y \\ 0 \end{bmatrix} \quad (2)$$

In Equation 2, the inverse of the H matrix, computed from the previous equation, is used and multiplied by $(X, Y, 0)$, which denotes the coordinates of one corner of the region of interest from the BIM model. In the proposed method, the $(X, Y, 0)$ coordinates are exported from the BIM model, where the designed API performs a search for elements with type “bath pod” and returns the corner

coordinates of the element. Finally, the $(x, y, 0)$ is computed which denotes one corner of the installation point in the pixel space. Using four corners of the region of interest from the BIM model in equation 2 provides the RoI of the installation point in the pixel space.

2.3 Identifying the Installation of Component

Here, the objective is to use computer vision techniques to identify if the component has been installed in the pre-planned location on the modular unit, or not. Figure 4 shows the pipeline that classifies each installation region of interest as installed or not-installed.

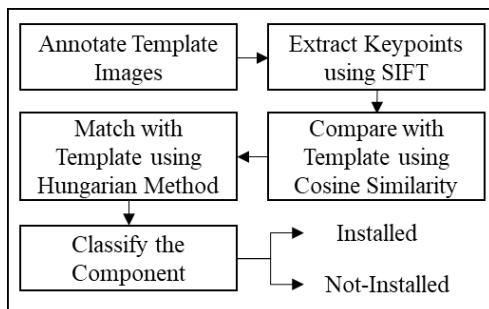


Figure 4. Identifying Installation of Component

As shown in Figure 4, a template-based matching approach is employed to compare the current state of the region of interest with template images of two possible states. Doing so, for each installation region of interest; template images of ‘installed’ and ‘not-installed’ are first annotated. Specifically, two images for each station is annotated as template from the ‘installed’ and ‘not-installed’ states. In the proposed method images are extracted and annotated from the same factory, and the same camera view. Scale Invariant Feature Transform method [23] is used to extract and describe the keypoints in the video and the templates; Cosine similarity function is used to estimate the cost of matching between the regions of the interest in the video and the template; Hungarian method is used to match the region of interest in the video with the most similar template. Finally, the component is classified as installed or not-installed based on the result of matching. Specifically, if the cost of matching between the image and the ‘installed’ template is less than the cost of matching between the image and the ‘not-installed’ state then the component is classified as installed.

The next section evaluates the proposed method on the videos collected from a modular construction factory.

3 Case Study

The proposed method was evaluated using surveillance videos captured from a modular construction

factory in the US. Collected videos include five days of 12-hour shifts in a single workstation. In these videos, modular units move from one station to the next as components such as walls, and bath pods are installed. The goal of this implementation is to evaluate the proposed method by identifying the installation of a bath pod unit on a modular unit in a single workstation, and comparing the results to manual monitoring of videos.

3.1 Module Detection

Here, the modular units were detected and segmented by training the segmentation algorithm on the created dataset. Using the collected videos, an image dataset comprising 200 train and 60 test instances of modular units was annotated. Both sets were from the same factory, however, the test set was created using a camera view similar to the one in Figure 5, while the train set was created using other cameras covering other stations further down the production line. The appearance of these modules differed from the ones in the test set as the components such as walls were being installed. Next, the Mask R-CNN object segmentation algorithm with Resnet-50 backbone was pre-trained on COCO dataset using PyTorch framework. The last layer of the network was fine-tuned on the training dataset for 40 epochs, with an initial learning rate of 0.001, a momentum of 0.9, and a decay of 0.0001, using an RTX1080 GPU for 0.5 hour. Validation of the model on the test set resulted in average precision of 0.75 when Intersection over Union (IoU) parameter was set to 0.75. Figure 5 shows an example image where four modular units are detected with a bounding box and segmented with different colors. In this figure, workstation three is annotated with color purple. Figure 6 shows the annotated ground truth of this image.

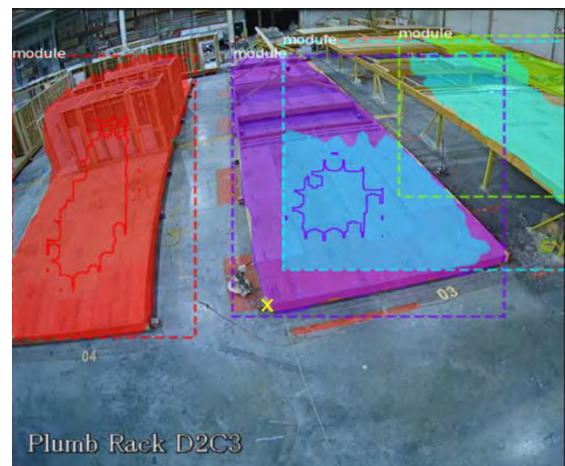


Figure 5. Example instance segmentation result



Figure 6. Ground truth annotated with yellow line

Finally, one point from each detected instance is picked as a reference at the lowest point of the detection instance. This point is annotated with a yellow cross in Figure 5. The radial distortion of the camera is disregarded, since the both source and target datasets are capture from similar cameras, however, rectification of the lens distortion can improve the performance of the detection algorithm which was left for future work.

3.2 Installation Region Identification

Here, the projection matrix was estimated and the installation region of interest was projected on the video. As shown in Figure 7, four corresponding corner points on the video are picked manually.

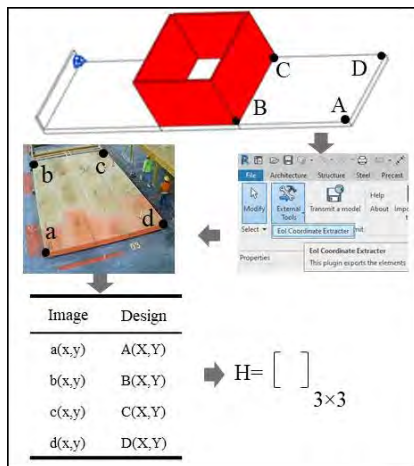


Figure 7. Extracting the corresponding points using the designed plugin

As shown in Figure 7, the corresponding points are extracted automatically using the designed BIM plugin in Revit. Here, the meta-data of the 3D module is augmented with a ‘type’ custom field. The designed plugin performs a search through all elements in the model filter by ‘FilteredElementCollector’ constructor

to identify the element with type ‘floor’, and extracts the corner coordinates of the element and stores the data in an excel sheet. These coordinates are then used to estimate the projection matrix.

Finally, the grid and the location of the installation region is projected from the BIM model onto the video. Figure 8 shows the projected axis grids with smaller red dots and the projected boundary of the location of the installation component with purple color.

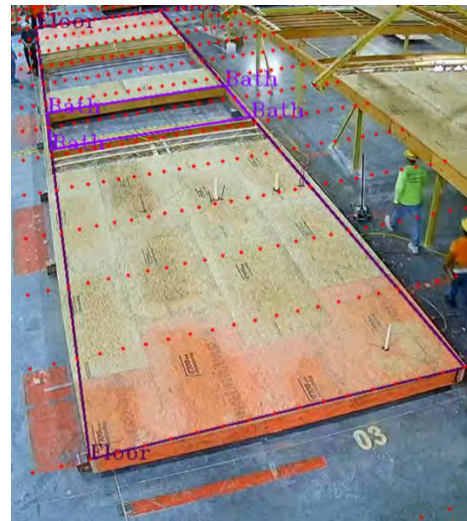


Figure 8. Projected installation location on the detected instance of modular unit

3.3 Identifying the Installation of Component

Here, the installation of a bath pod unit is monitored and identified using the proposed computer vision-based method. Figure 9 shows an example result for matching the identified installation region of interest in the detected modular unit in workstation three, with the template.

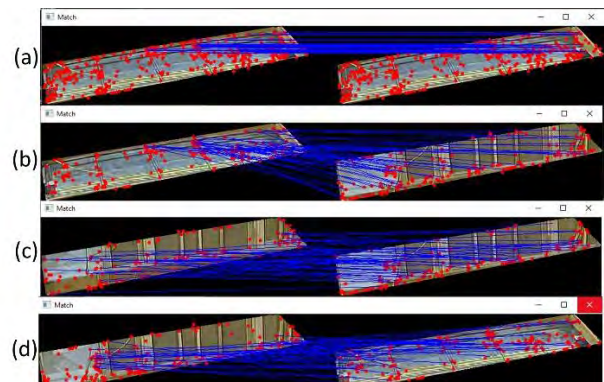


Figure 9. Matching template RoIs of the installation region on the left column with query

RoIs of the installation region on the right column: (a) matching an empty template with an empty query, (b) matching an empty template with an occupied query, (c) matching an occupied template with an occupied query, (d) matching an occupied template with an empty query

As shown in Figure 9, the ‘installed’ and ‘not-installed’ video images on the left column are matched with the templates on the right via parallel blue lines indicating strong matches. Figure 10 shows a qualitative assessment of the proposed method for identifying the installation for the bath pod unit on the video.



Figure 10. Installation of bath pod, as detected in the pre-planned location, on the modular unit

In Figure 10, on the right, the bath pod unit has not yet been installed in the pre-planned region which is annotated with color green. Figure 11 shows a quantitative assessment of the classification for the region of interest. Here, the same test dataset used for the module detection step, comprising 60 instances for the module, was used to evaluate the performance of the proposed installation identification method.

True Label	Installed	0.95	0.05
	Not-Installed	0.03	0.97
		Installed	Not-Installed
		Classified Label	

Figure 11. The evaluation performance of SIFT-based classification for region of interest

As shown in the confusion matrix in figure 11, the proposed method was able to correctly identify the installation of the bath pod on the planned location in the detected modular unit with 96% accuracy.

Analysis of the failed cases reveals that the proposed method is sensitive to occlusions caused by the presence

of workers in the evaluation dataset, which lead to false positives and false negatives. Additionally, movement of the gantry crane and transportation of components such as walls, created partial occlusions and resulted in false positives due to the similarities between the bath pod and the side walls. To mitigate these temporary occlusions, median-smoothing functions can be used to classify the installation based on the median of the neighboring frames.

4 Conclusions and Future Work

This research proposed a method to monitor the progress of assembly inside modular construction factories. The proposed method relies on integration of hand-crafted and deep learning-based computer vision with building information modeling. Specifically, object detection and instance segmentation were used to precisely locate the modular units as they move from one station to the next; building information modeling and principles from projective geometry were used to identify the location of installation, based on the design, and SIFT template-based matching was used to identify the installation of the component in the pre-planned location. The proposed method was successfully evaluated on surveillance videos of a modular construction factory in the U.S. The major limitation of the proposed method is related to cases with high visual occlusion, such as scenes where the wall element was installed earlier and occluded the bath pod region of interest in the back, and manually calculating the homography matrix. To improve the proposed method, and overcome this limitation the future work will focus on improving the performance of segmentation using data augmentation and deep learning-based boundary refinement models; synthesizing the camera view using the BIM environment; projecting the 3D region of interest on the video scene, and classifying the region of interest using deep learning-based Siamese network. Furthermore, future work will consider automatically computing the homography matrix by extracting the points from the masked image without the need for user involvement.

5 Acknowledgement

This article was developed based upon funding from the Alliance for Sustainable Energy, LLC, Managing and Operating Contractor for the National Renewable Energy Laboratory for the U.S. Department of Energy. The authors also gratefully acknowledge Volumetric Building Companies for their help with data collection for this research.

5.1 References

- [1] M. Arashpour and R. Wake, "Autonomous production tracking for augmenting output in off-site construction," *Autom. Constr.*, p. 9, 2015.
- [2] I. Y. Wuni and G. Q. P. Shen, "Holistic Review and Conceptual Framework for the Drivers of Offsite Construction: A Total Interpretive Structural Modeling Approach," *Buildings*, vol. 9, no. 5, p. 117, May 2019, doi: 10.3390/buildings9050117.
- [3] B. M. Tehrani, C. G. Ozmerdiven, and A. Alwisy, "A Decision Support System for the Integration of Robotics in Offsite Construction," in *Construction Research Congress 2022*, Arlington, Virginia, Mar. 2022, pp. 849–858. doi: 10.1061/9780784483961.089.
- [4] B. M. Tehrani, S. BuHamdan, and A. Alwisy, "Robotics in industrialized construction: an activity-based ranking system for assembly manufacturing tasks," *Eng. Constr. Archit. Manag.*, Dec. 2022, doi: 10.1108/ECAM-02-2022-0143.
- [5] M. S. Altaf, A. Bouferguene, H. Liu, M. Al-Hussein, and H. Yu, "Integrated production planning and control system for a panelized home prefabrication facility using simulation and RFID," *Autom. Constr.*, vol. 85, pp. 369–383, Jan. 2018, doi: 10.1016/j.autcon.2017.09.009.
- [6] A. Varyani, A. Jalilvand-Nejad, and P. Fattahi, "Determining the optimum production quantity in three-echelon production system with stochastic demand," *Int. J. Adv. Manuf. Technol.*, vol. 72, no. 1–4, pp. 119–133, Apr. 2014, doi: 10.1007/s00170-014-5621-1.
- [7] I. Y. Wuni and G. Q. Shen, "Risks identification and allocation in the supply chain of modular integrated construction (MiC)," *Modul. Offsite Constr. MOC Summit Proc.*, pp. 189–197, 2019.
- [8] Q. Chang, J. Ni, P. Bandyopadhyay, S. Biller, and G. Xiao, "Supervisory Factory Control Based on Real-Time Production Feedback," *J. Manuf. Sci. Eng.*, vol. 129, no. 3, pp. 653–660, Jun. 2007, doi: 10.1115/1.2673666.
- [9] J. Gong and C. H. Caldas, "Computer vision-based video interpretation model for automated productivity analysis of construction operations," *J. Comput. Civ. Eng.*, vol. 24, no. 3, pp. 252–263, 2009.
- [10] A. Pal Singh Bhatia, S. Han, O. Moselhi, Z. Lei, and C. Raimondi, "Data Analytics of Production Cycle Time for Offsite Construction Projects," *Modul. Offsite Constr. MOC Summit Proc.*, pp. 25–32, May 2019, doi: 10.29173/mocs73.
- [11] K. M. Rashid and J. Louis, "Activity identification in modular construction using audio signals and machine learning," *Autom. Constr.*, vol. 119, p. 103361, Nov. 2020, doi: 10.1016/j.autcon.2020.103361.
- [12] K. M. Rashid and J. Louis, "Automated Active and Idle Time Measurement in Modular Construction Factory Using Inertial Measurement Unit and Deep Learning for Dynamic Simulation Input," in *2021 Winter Simulation Conference (WSC)*, Phoenix, AZ, USA, Dec. 2021, pp. 1–8. doi: 10.1109/WSC52266.2021.9715446.
- [13] M. Ahmed, C. T. Haas, and R. Haas, "Using digital photogrammetry for pipe-works progress tracking¹ This paper is one of a selection of papers in this Special Issue on Construction Engineering and Management.," *Can. J. Civ. Eng.*, vol. 39, no. 9, pp. 1062–1071, Sep. 2012, doi: 10.1139/l2012-055.
- [14] B. F. Spencer, V. Hoskere, and Y. Narazaki, "Advances in Computer Vision-Based Civil Infrastructure Inspection and Monitoring," *Engineering*, vol. 5, no. 2, pp. 199–222, Apr. 2019, doi: 10.1016/j.eng.2018.11.030.
- [15] R. Panahi, J. Louis, N. Aziere, A. Podder, and C. Swanson, *Identifying Modular Construction Worker Tasks Using Computer Vision*. 2021.
- [16] B. Xiao, H. Xiao, J. Wang, and Y. Chen, "Vision-based method for tracking workers by integrating deep learning instance segmentation in off-site construction," *Autom. Constr.*, vol. 136, p. 104148, Apr. 2022, doi: 10.1016/j.autcon.2022.104148.
- [17] P. Martinez, B. Barkokebas, F. Hamzeh, M. Al-Hussein, and R. Ahmad, "A vision-based approach for automatic progress tracking of floor paneling in offsite construction facilities," *Autom. Constr.*, vol. 125, p. 103620, May 2021, doi: 10.1016/j.autcon.2021.103620.
- [18] W. Chu, S. Han, X. Luo, and Z. Zhu, "Monocular Vision-Based Framework for Biomechanical Analysis or Ergonomic Posture Assessment in Modular Construction," *J. Comput. Civ. Eng.*, vol. 34, no. 4, p. 04020018, Jul. 2020, doi: 10.1061/(ASCE)CP.1943-5487.0000897.
- [19] Z. Zheng, Z. Zhang, and W. Pan, "Virtual prototyping- and transfer learning-enabled module detection for modular integrated construction," *Autom. Constr.*, vol. 120, p. 103387, Dec. 2020, doi: 10.1016/j.autcon.2020.103387.
- [20] K. Park, S. Ergan, and C. Feng, "Towards Intelligent Agents to Assist in Modular Construction: Evaluation of Datasets Generated in Virtual Environments for AI training," presented at the 38th International Symposium on Automation and Robotics in Construction, Dubai, UAE, Nov. 2021. doi: 10.22260/ISARC2021/0046.
- [21] K. Park and S. Ergan, "Toward Intelligent Agents to Detect Work Pieces and Processes in Modular Construction: An Approach to Generate Synthetic Training Data," in *Construction Research Congress*

2022, Arlington, Virginia, Mar. 2022, pp. 802–811.
doi: 10.1061/9780784483961.084.

- [22] S. Ren, K. He, R. Girshick, and J. Sun, “Faster R-CNN: Towards Real-Time Object Detection with Region Proposal Networks,” in *Advances in Neural Information Processing Systems 28*, C. Cortes, N. D. Lawrence, D. D. Lee, M. Sugiyama, and R. Garnett, Eds. Curran Associates, Inc., 2015, pp. 91–99. Accessed: Feb. 13, 2020. [Online]. Available: <http://papers.nips.cc/paper/5638-faster-r-cnn-towards-real-time-object-detection-with-region-proposal-networks.pdf>
- [23] D. G. Lowe, “Distinctive Image Features from Scale-Invariant Keypoints,” *Int. J. Comput. Vis.*, vol. 60, no. 2, pp. 91–110, Nov. 2004, doi: 10.1023/B:VISI.0000029664.99615.94.

BIM-based construction quality assessment using Graph Neural Networks

Navid Kayhani^{1,2}, Brenda McCabe¹, and Bharath Sankaran²

¹Department of Civil and Mineral Engineering, University of Toronto, Canada

²Naska.AI (formerly Scaled Robotics), Spain

navid.kayhani@mail.utoronto.ca, brenda.mccabe@utoronto.ca, bharath@naska.ai

Abstract -

Automated construction quality control and as-built verification often involve comparing 3D point clouds captured on-site with as-designed Building Information Models (ad-BIM) at the individual element level. However, signal noise and occlusions, common in data captured from cluttered job sites, can negatively affect the performance of these methods that overlook the semantic relationships between elements. In this paper, we introduce a novel approach to automated quality control that enhances element-wise quality assessments by exploiting semantics in BIM. The proposed method represents ad-BIM as a graph by encoding elements' topological and spatial relationships. Exploiting this representation, we propose a Graph Neural Networks (GNNs)-based algorithm to infer element-wise built quality status. Our method significantly outperforms classical methods and allows for inference on partially observed or unobserved elements.

Keywords -

GNN; Quality Control; BIM; Semantic Enrichment; Point Cloud; Machine Learning.

1 Introduction

With the growing adoption of BIM within the construction industry, quality control processes are being automated to optimize cost and improve efficiency [1]. This is accomplished by comparing reality capture data (laser scanning, photogrammetry) to the as-designed BIM (ad-BIM) to detect errors in construction, thereby preventing costly downstream effects that subsequently affect the project cost and schedule [2].

Current approaches to automated quality control report element-wise quality where the as-built status of the building elements are evaluated in isolation [1, 3, 4] without considering the surrounding context. Irrespective of the reality capture system used, the data captured by these devices are plagued by noise and occlusions, which lead to inaccurate assessments. On cluttered construction sites, the reality capture data are affected by occlusions, sensor noise, weather conditions, and material properties, thereby resulting in the partial observability of the built structure

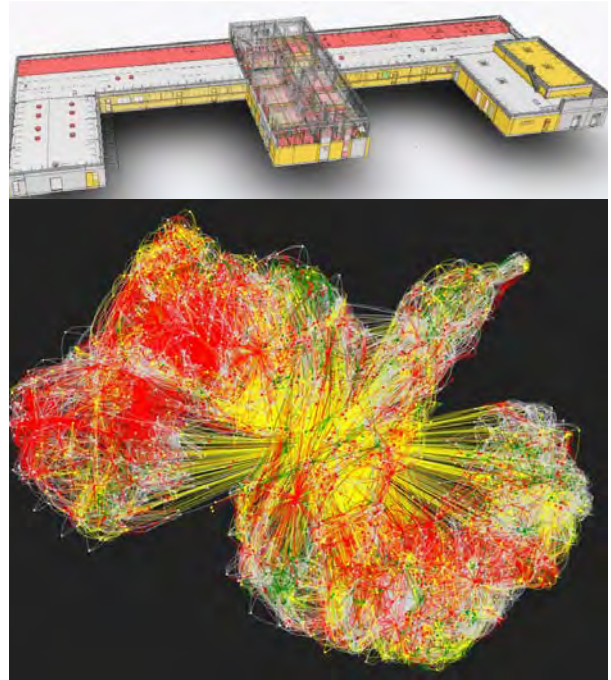


Figure 1. Graph representation of ad-BIM. The top shows the ad-BIM for an institutional building, with element-wise construction quality status labels. The bottom displays the same ad-BIM represented as a graph to leverage semantic relationships between elements to enhance as-built quality assessments.

(Figure 2). To cope with these sources of noise, it is essential to consider the semantic (e.g., spatial, topological, and temporal) relationships between building elements to enhance the quality control assessments.

In this paper, we present BIM-GNN, a novel method for detecting the built quality of building elements on a construction site using Graph Neural Networks (GNNs), incorporating semantic information extracted from ad-BIM. Our contributions are twofold. Firstly, we propose a method for constructing a graph representation of buildings from their ad-BIM (Figure 1), which is amenable to graph-based inference. In this representation, the nodes

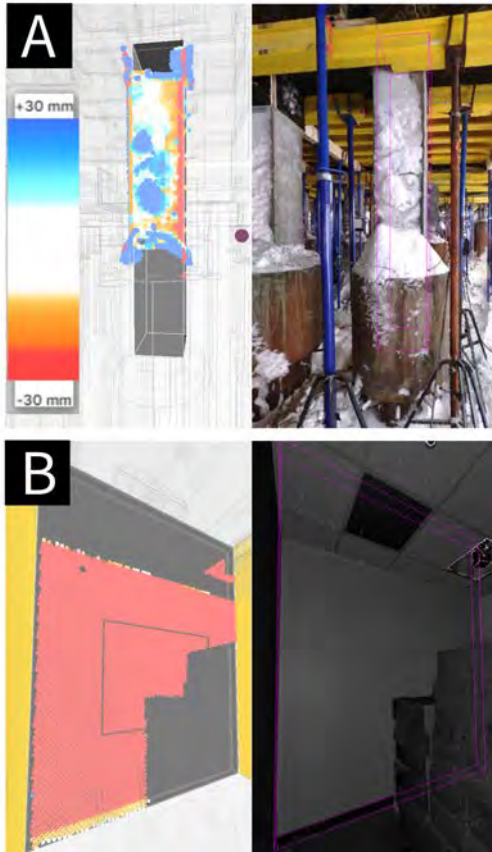


Figure 2. Noise and occlusion in on-site data. (A) Column covered by snow (noise) and occluded by ad-BIM elements (pedestal and steel beam). (B) Wall occluded by ad-BIM elements (ceiling) and clutter (boxes). Registered 3D point cloud data are shown as spheres indicating deviations as heatmaps.

represent BIM objects, and the edges represent their topological and spatial associations. Secondly, we propose a graph inference algorithm that utilizes the graph structure and the features computed on its nodes to classify the building elements using *Graph Attention Networks* [5] into one of four quality classes, namely, *verified* - element built within the desired tolerance, *deviated* - element built outside of desired tolerance, *missing* - element not built and *no data* - not enough information to make an assessment. Our experiments in Section 4 show that leveraging our graph representation allows our inference algorithm approach to significantly outperform existing element-based methods.

2 Background

In this section, we briefly review what most automated quality control techniques have in common and why we need to revisit the problem. Then, we provide a short

overview of graph neural networks, graph representation of buildings, and the applications of GNNs in the architecture, engineering, and construction (AEC) domain.

2.1 Automated construction quality control

Automated quality control of construction projects is a well-studied area of research [6, 7]. Typically, solutions to this problem involve comparing the ad-BIM to 3D point clouds of the construction site captured with cameras [8] or laser scanners [7]. These comparisons can be done manually or using machine learning techniques. The machine learning-based solutions often treat the individual building elements as independent and identically distributed (iid) data which are fully observed. This is seldom the case, as the data are prone to noise and occlusions and the building elements are semantically linked. In this paper, we deal with the problem of partial observability by leveraging the graph structure and semantic relationships between elements of the ad-BIM to make robust quality control assessments of individual building elements.

2.2 Graphs and graph neural networks

As our ad-BIM is represented as a graph, we need learning algorithms that are capable of operating on non-euclidean permutation invariant data [9]. Most graph learning algorithms map the information the graph represents to a vector in a high-dimensional linear embedding space. These learned vectors can then be used for downstream learning tasks such as classification, regression, clustering, and generation. Graph Neural Networks (GNNs) typically use message-passing to update the representation of a node by processing its neighborhood's embedding from a previous layer to update the representation of the node in the current layer, as shown in Figure 3. The set of nodes that are directly connected to a given node via an edge is referred to as its neighborhood, which can include the node itself. In other words, GNNs with l layers allow nodes to capture information within their l -hop neighborhood [10]. These networks take a graph as input and compute node embeddings through a series of non-linear transformations, allowing for prediction at the node, edge, or graph level. Many GNN architectures have been proposed that vary in their definitions of message, transformation, and aggregation operations. These architectures also differ in how they stack layers using different graph manipulation techniques to accomplish supervised or unsupervised tasks at the node or graph level.

2.3 Graph representation of BIM

Graph representation of buildings has been used for accessibility analysis [11], generative design [12], and large BIM file processing [13]. These representations capture

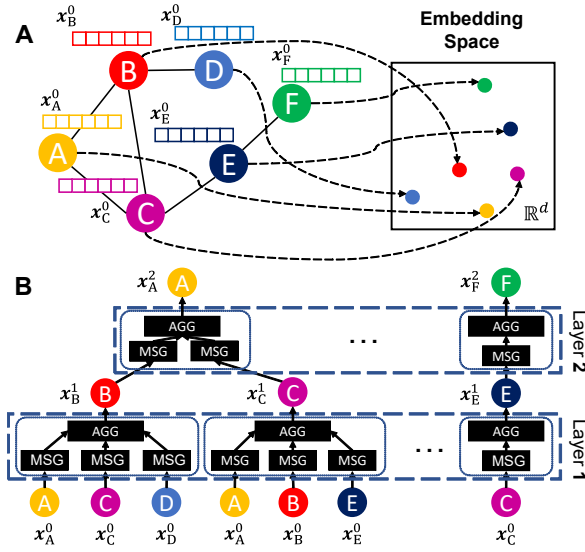


Figure 3. Graph neural networks (GNNs). (A) GNNs map information in the graph domain to a d -dimensional vector representation. (B) A 2-layer GNN example with a message-passing mechanism, where x_N^l indicates representation of node N at layer l . Each node has its own computational graph, through which its representation is updated by transformation and aggregation of its neighborhood’s representation. Here we only show nodes A and F. The transformed representation of the neighbor, self, and the connecting edge in layer $l - 1$ constitute a message (MSG) in layer l . Every node aggregates (AGG) the messages it receives, using a permutation-invariant aggregation function (e.g., sum or average), and updates its representation.

geometries, semantics, and some spatial and topological relationships. They can be used to filter out irrelevant information, group related data, and identify key components. For instance, graphs were used to represent the relationships between IFC instances to enable topological querying, with semantic information being incorporated as the node and edge weights [14]. However, using these representations for learning-based quality control inference models has not been previously explored.

2.4 GNN in AEC domain

GNNs have seen limited use in the AEC domain but are gaining attention due to their potential applications [15]. For example, GNNs were used in conjunction with spatial vector data to classify patterns among groups of buildings for urban planning [16]. In architectural design, GNNs were used for the automated generation of floor plans that follow specific space planning rules [17]. In construction, these techniques were utilized to identify the most time-

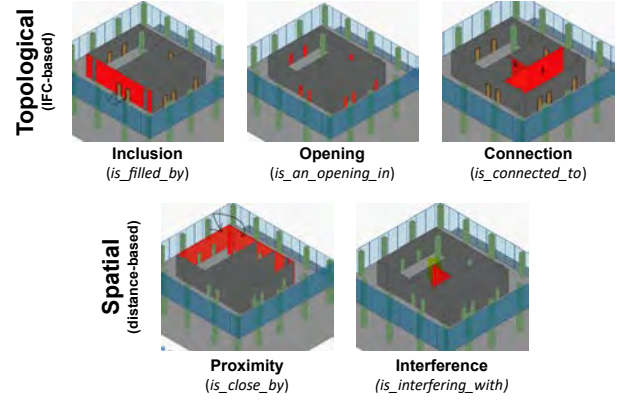


Figure 4. Topological and spatial relationships extracted from ad-BIM IFC.

efficient construction sequence and to improve scheduling productivity and accuracy [18]. Finally, the automatic classification of room types [19] and the automation of the classification of BIM objects into different Industry Foundation Classes (IFC) [20] categories are two of the few examples of the use of BIM and GNNs.

3 Methods

In this section, we explain how we convert the ad-BIM IFC into a graph structure that can be used for automated machine learning-based quality control assessments. In Section 3.2, we describe the GNN model used for semantic-aware quality status classification of building elements.

3.1 Converting BIM to a graph

In this work, we consider the elements in ad-BIM as nodes and their associations with other elements as the edges of the graph. Two nodes are connected through an edge if they are topologically or spatially related. Incorporating temporal relationships is not considered in this paper. The topological and spatial relationships between BIM objects are extracted from ad-BIM in IFC format. The topological relationships are directly extractable from the hierarchical inheritance associations of objects in the IFC schema. Spatial relationships are determined by quantifying the distance between the various BIM objects’ axis-aligned bounding boxes (AABB). We identified three types of topological relationships (Figure 4): (1) inclusion; (2) opening; (3) connection; and two types of spatial relationships: (1) proximity; (2) interference.

An inclusion relationship refers to the relationship between a container element (e.g., wall) and a filler element (e.g., door). For example, a wall instance of the *IfcWall*

class (e.g., *IfcWallStandard*) would be connected to an *IfcOpeningElement* through an *IfcRelVoidsElement*. A door in the same wall would be an instance of the *IfcDoor* class and would be connected to the same *IfcOpeningElement* through an *IfcRelFillsElement*. An opening relationship describes the association between a void and its container, which may or may not be filled by a filler element. A connection relationship is defined using *IfcRelConnectsElements*, which describes the elements' connectivity with a connection geometry (such as a point, curve, or surface). For example, walls A and B in Figure 4 would be connected through a surface and not through any other element.

Our proposed method for identifying spatial relationships between BIM objects calculates a distance matrix based on the minimum distance between the objects' AABBs. The distance between two AABBs can be calculated using the coordinates of their bottom-left and top-right corners in 3D space. We then parametrize the proximity and interference relationships between objects. In the equation below, d is the distance between the two BIM objects, $d_{min, max}$ are the proximity thresholds and d_{int} is the interference threshold. Finally, semantics such as element's type and floor are extracted from the ad-BIM to build the ad-BIM graph $G = (V, E)$, where V and E refer to the set of its nodes and edges, respectively. Nodes in V contain features extracted from ad-BIM, graph structure, and on-site data, while edges in E have no attributes.

$$\text{spatial} = \begin{cases} d_{min} \leq d \leq d_{max} & \text{proximity} \\ d \leq \min(d_{int}, d_{min}) & \text{interference} \end{cases} \quad (1)$$

3.2 BIM-GNN Classifier model

3.2.1 Architecture and training settings

Graph Attention Network (GAT) [5] is a GNN architecture that is built by stacking graph attention layers (GAT convolution). GAT convolutions use attention mechanisms to implicitly specify weights to different nodes in a neighborhood, indicating their importance. They may consist of multiple "heads", each with its own set of parameters. These heads attend to different aspects of the graph, allowing the model to learn multiple representations of the graph simultaneously. Mathematically, the attention coefficient between node i and node j is computed as:

$$\alpha_{i,j} = \frac{\exp(\text{LeakyReLU}(a^T [\mathbf{W}h_i \parallel \mathbf{W}h_j]))}{\sum_{k \in \mathcal{N}_i} \exp(\text{LeakyReLU}(a^T [\mathbf{W}h_i \parallel \mathbf{W}h_k]))} \quad (2)$$

where $\alpha_{i,j}$ is the attention coefficient between node i and j , a is a learnable parameter vector, h_i and h_j are the node representations for nodes i and j , \parallel is the concatenation operator, \mathcal{N}_i is the set of all the neighbors of node i , and W is a learnable weight matrix.

Finally, the new hidden representation of node i (h'_i) in a GAT convolution with K heads is calculated as:

$$h'_i = \parallel_{k=1}^K \sigma \left(\sum_{j \in \mathcal{N}_i} \alpha_{ij}^k \mathbf{W}^k h_j \right) \quad (3)$$

As depicted in Figure 5, our model has a sequential architecture and consists of two multi-headed GAT convolutions and a fully connected layer with ReLU activations. We apply dropout before each layer and to the normalized attention coefficients in GAT convolutions. The output is a four-dimensional array that is normalized using a log-softmax function. The training is performed following a transductive learning approach. In this approach, the model is trained on training labels while accessing the entire graph structure and node features. We used the negative log-likelihood as the loss, Adam optimizer with a learning rate of $5e-3$, and weight decay of $5e-4$. The model was trained for 10K epochs with early stopping.

3.2.2 Baseline model

In this work, we use an ensembled baseline model (*ML-Vanilla*) to predict element-wise quality status. The baseline model is trained on features learned on point cloud data [21] and engineered features that relate to scans-BIM coverage as discussed in Section 4.1.3. This baseline model *ML-Vanilla* was trained on a large number of individual element data from multiple different construction projects yet without considering relationships between elements.

4 Experiments & Discussion

In our experiments, we are interested in answering the following questions:(1) How robust is our method on a dataset with a mixture of graphs with both highly imbalanced and balanced labels? (2) What are the impacts of the size of the training, validation, and test sets on the model performance? (3) How does the BIM-GNN model perform compared to the *ML-Vanilla* model, which does not consider the element relationships and graph structure? (4) How do different feature types contribute to the model's expressiveness? (5) How can BIM-GNN help label unobserved or partially observed elements?

4.1 Dataset

4.1.1 Description

The dataset used in this work contains ad-BIMs and scans captured from three institutional building projects in Europe, including two scans from a university building (UB1 and UB2), one scan from a hospital (LH), and one scan from a special school (SS) project. All scans were

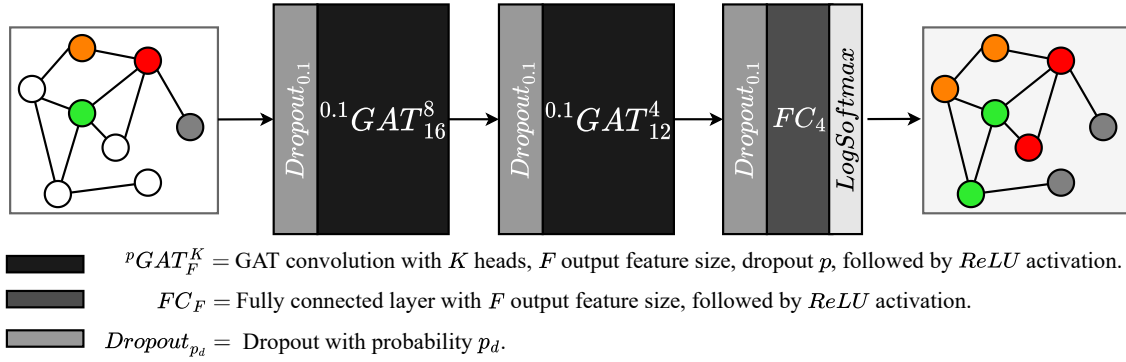


Figure 5. BIM-GNN Classifier architecture.

processed and registered with their ad-BIMs, such that only a subset of the elements of the ad-BIM are associated with the 3D point cloud. Then engineered and learned features for each element are computed solely based on the processed (partial) per-element scan of the on-site observations. An automatic ML-based process assigns each element a label based on the extracted features. A post-processing review is conducted to ensure the reliability of the assigned labels. We call a processed scan an analysis.

4.1.2 Statistics

As summarized in Table 1, each analysis was converted to a graph with an average node count of 3103 and an average degree of 50. The edge counts varied between tens to hundreds of thousands. However, the relationships extracted from the ad-BIM turned out to be dominated by spatial relationships across all analyses.

Figure 6 depicts the distribution of ground truth quality status labels for nodes in each graph. Imbalanced label distribution across all scans was observed where *No Data* accounts for a large proportion of the elements mainly due to data incompleteness in real-world projects.

4.1.3 Features

Nodes in the created ad-BIM graphs contain three features: BIM-based, graph-based, and scan-based. BIM-based features include semantics such as element type and floor. Graph-based features capture information about a

Table 1. Dataset summary

Name	Nodes	Edges	Spatial Edges	Avg. Deg.
SS	6264	242k	99.7%	77
LH	919	21k	100%	46
UB1	3256	55k	100%	26
UB2	2014	25k	100%	34

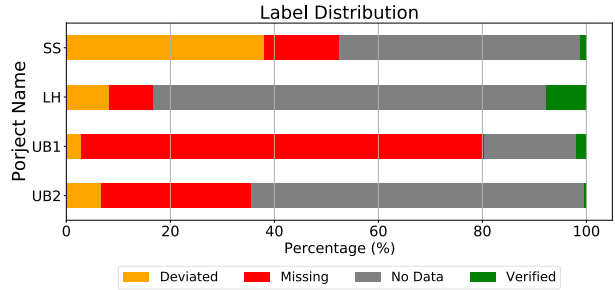


Figure 6. Distribution of the ground truth labels in the dataset.

node's local neighborhood and include node degree, eigenvector centrality, and clustering coefficient. The node degree is the number of edges incident to that node. Eigenvector centrality measures the importance of a node in a graph. The clustering coefficient measures how the node's neighbors are connected to one another. Scan-based features include BaselineML and PointNet features. BaselineML is a set of hand-engineered features that quantify the degree to which the ad-BIM elements match the scans and include features such as scanned fraction, relative alignment error, etc. PointNet features are extracted from the hidden representation of the last two layers of a pre-trained Pointnet [21] model.

4.2 BIM-GNN Classifier performance

In our experiments, we used nine randomized training/validation/test splits. We started our evaluations with a split of 60% training, 20% validation, and 20% test, considering all features defined in Section 4.1.3. We denote this combination of features and data split as the *original* dataset. We chose the F1-Score with weighted average as the metric for evaluation since it is suitable for evaluating both balanced and imbalanced datasets. Table 2 summarizes the performance of our model on the test sets

Table 2. Model performance

Name	F1-Score (weighted) <i>ML-Vanilla</i>	F1-Score (weighted) Ours
SS	61.53 ± 1.20%	70.51 ± 5.05%
LH	62.17 ± 2.06%	74.20 ± 2.38%
UB1	75.41 ± 1.09%	79.99 ± 1.52%
UB2	22.26 ± 1.79%	88.44 ± 1.59%
Total	55.34 ± 20.26%	77.99 ± 7.37%

across 9 runs based on the metric above. The results suggest that our model outperforms the baseline significantly. The average F1-Score of *ML-Vanilla* is 55.34% with a standard deviation of 20.26%, while the average F1-Score of our model is 77.99% with a standard deviation of 7.37%. The average improvement is 22% with a lower variance. The improvement is more significant when the dataset is imbalanced. For example, the average F1-Score of *ML-Vanilla* on the UB2 graph is 22.26%, while the average F1-Score of our model is 88.44%.

Figure 9 depicts a low-dimensional representation of node logits pre- and post-training using t-distributed stochastic neighbor embedding (t-sne). T-sne maps high-dimensional data to a lower-dimensional space while preserving its structure. Figure 9 reveals separate clusters for each label. While our model can differentiate between *missing*, *no data*, and the other two classes, it struggles to differentiate between *deviated* and *verified* in certain cases. Further investigation is needed as mistakenly detecting *deviated* as *verified* may lead to unnoticed quality issues, although this is partly due to labeling subjectivity.

4.3 Influence of training data percentage

The *original* dataset allows the model to access 60% of the labels in the training set directly and 20% in validation indirectly, meaning if we have access to 80% of the labels, node features, and ad-BIM, we could outperform the baseline. However, to address the practicality of such a high percentage of available labels, we decreased the percentage of available labels (training 3: validation 1) and repeated the experiments. Results in Figure 7 show that even with 10% of the node labels (7% training), our proposed method achieved considerably higher F1-Score than the classical approach.

4.4 Ablation study

An ablation study is performed to investigate the importance of different features. We retrained our model by removing one feature or feature set at a time from the *original* dataset, namely, PointNet (*no_pnet*), type (*no_type*), and BaselineML (*no_bsln*) features, plus graph-based (*no_graph*) and scan-based (*no_bsln_pnet*)

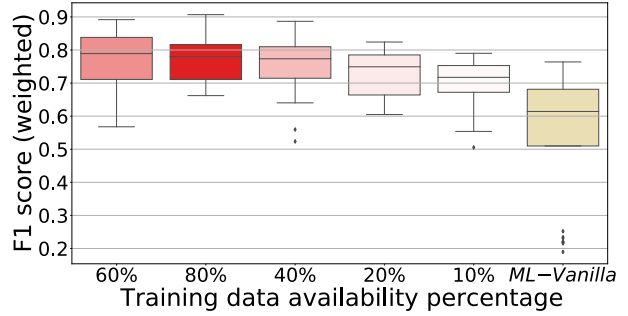


Figure 7. Impact of labeled data availability percentage during training on F1-Score and comparison with *ML-Vanilla*.

feature sets (Table 3). The results, shown in Figure 8, suggest that the PointNet features (learned scan-based features) do not positively contribute to the model’s expressiveness, while hand-engineered BaselineML features seem to be more essential. Removing the type and the graph-based features can worsen the model’s performance while removing the scan-based features has the most negative impact. The results indicate that all features, except for PointNet, contribute to the superior performance of our model. Nonetheless, we retained the PointNet features to ensure smoother performance, as a significant increase in F1-Score variance across various analyses is observed when excluded (*no_pnet*).

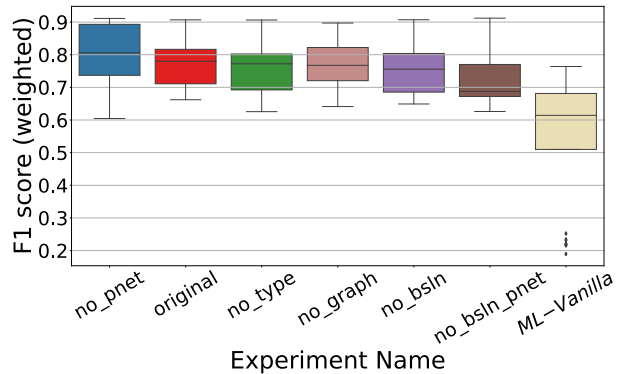


Figure 8. Impact of feature ablation on F1-score and comparison with *ML-Vanilla*.

More interestingly, comparing *ML-Vanilla* and *no_bsln_pnet* results suggests that our model can still outperform the baseline even without the scan-based features. This essentially means that given the graph structure and the labels for some elements (60% training), we can better predict the quality status of elements even if they are unobserved. This is a significant improvement on the baseline, which views the elements in isolation and solely relies

Table 3. Ablation study experiment settings

Name	Scan-based		BIM-based		Graph-based	
	BaselineML	PointNet	Type	Floor	Eigen, Deg.,	Cluster
<i>original</i>	✓	✓	✓	✓	✓	✓
<i>no_pnet</i>	✓		✓	✓	✓	✓
<i>no_bsln</i>		✓	✓	✓	✓	✓
<i>no_type</i>	✓	✓	✓	✓	✓	✓
<i>no_bsln_pnet</i>			✓	✓	✓	✓
<i>no_graph</i>	✓	✓	✓	✓		

on scan-based features. Our results suggest that incorporating semantics can improve element-wise quality status classification performance despite the partial observability of elements as an essential building block in construction quality assessment applications.

5 Conclusion and future work

In this work, we demonstrated the utility of exploiting the semantic (i.e., topological and spatial) relationships encoded within the ad-BIM graph to improve automated construction quality assessment despite partial observability of elements. To enhance our approach, we plan to explore additional graph learning algorithms and incorporate more relationship types to better capture the relationships between mechanical, electrical, and plumbing (MEP) elements. Additionally, we aim to add relationship types as edge features and further evaluate the generalizability of our method by applying it to more projects. We also hope to leverage the temporal relationships in 4D-BIM to predict element labels based on time- and sequence-dependent contexts.

6 Acknowledgements

This study was supported by Mitacs through the Mitacs Accelerate program and by the EU Horizon project, HumanTech, under GA 101058236. The first author is grateful to colleagues at Naska.AI (formerly Scaled Robotics SL) for their invaluable support. Special thanks go to Adarsh Jois and Alba Maria Herrera for their contributions and discussions. The first author thanks Sara Villuendas and CEO Stuart Maggs for their exceptional administrative support. We also thank the Natural Science and Engineering Research Council (NSERC) for their financial support through grant number RGPIN-2017-06792.

References

- [1] Burcu Akinci, Frank Boukamp, Chris Gordon, Daniel Huber, Catherine Lyons, and Kuhn Park. A formalism for utilization of sensor systems and integrated project models for active construction quality control. *Automation in construction*, 15(2):124–138, 2006. doi:10.1016/j.autcon.2005.01.008.
- [2] James L Burati Jr, Jodi J Farrington, and William B Ledbetter. Causes of quality deviations in design and construction. *Journal of construction engineering and management*, 118(1):34–49, 1992. doi:10.1061/(ASCE)0733-9364(1992)118:1(34).
- [3] LiJuan Chen and Hanbin Luo. A bim-based construction quality management model and its applications. *Automation in construction*, 46:64–73, 2014. doi:10.1016/j.autcon.2014.05.009.
- [4] Stan Vincke and Maarten Vergauwen. Vision based metric for quality control by comparing built reality to bim. *Automation in Construction*, 144:104581, 2022. doi:10.1016/j.autcon.2022.104581.
- [5] Petar Veličković, Guillem Cucurull, Arantxa Casanova, Adriana Romero, Pietro Liò, and Yoshua Bengio. Graph Attention Networks. *International Conference on Learning Representations*, 2018. URL <https://openreview.net/forum?id=rJXmpikCZ>.
- [6] Thomas Czerniawski and Fernanda Leite. Automated digital modeling of existing buildings: A review of visual object recognition methods. *Automation in Construction*, 113:103131, 2020. doi:10.1016/j.autcon.2020.103131.
- [7] Erzhuo Che, Jaehoon Jung, and Michael J Olsen. Object recognition, segmentation, and classification of mobile laser scanning point clouds: A state of the art review. *Sensors*, 19(4):810, 2019. doi:10.3390/s19040810.
- [8] Navid Kayhani, Wenda Zhao, Brenda McCabe, and Angela P Schoellig. Tag-based visual-inertial localization of unmanned aerial vehicles in indoor construction environments using an on-manifold extended kalman filter. *Automation in Construction*, 135:104112, 2022. doi:10.1016/j.autcon.2021.104112.
- [9] Michael M Bronstein, Joan Bruna, Yann LeCun, Arthur Szlam, and Pierre Vandergheynst. Geometric deep learning: going beyond euclidean data. *IEEE Signal Processing Magazine*, 34(4):18–42, 2017. doi:10.1109/MSP.2017.2693418.
- [10] William L Hamilton. Graph representation learning. *Synthesis Lectures on Artificial Intelligence and Machine Learning*, 14(3):1–159, 2020. doi:10.2200/S01045ED1V01Y202009AIM046.
- [11] Nimalaprakasan Skandhakumar, Farzad Salim, Jason Reid, Robin Drogemuller, and Ed Dawson. Graph theory based representation of build-

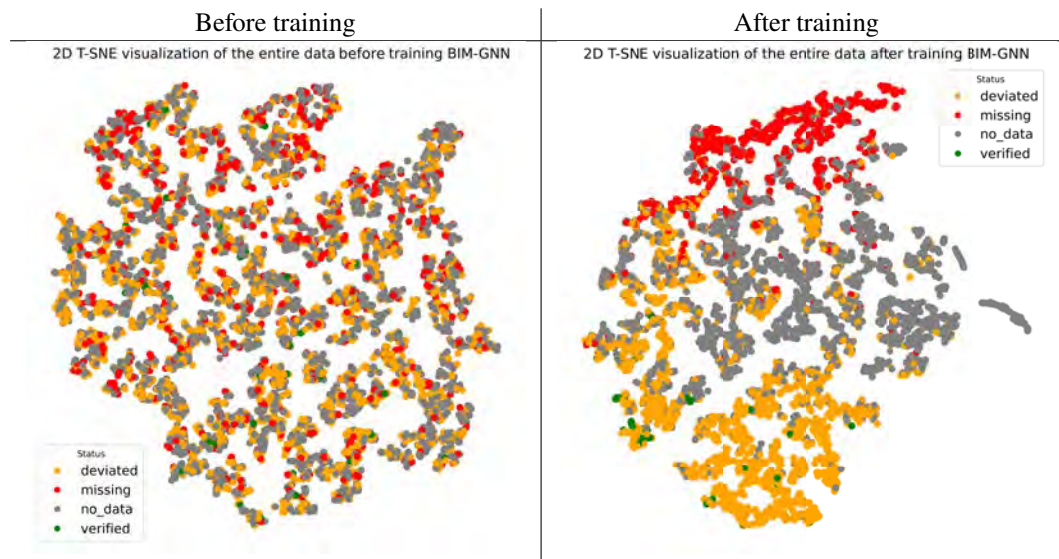


Figure 9. T-SNE embedding of the node-wise logits in SS graph.

- ing information models for access control applications. *Automation in Construction*, 68:44–51, 2016. doi:10.1016/j.autcon.2016.04.001.
- [12] Vincent JL Gan. Bim-based graph data model for automatic generative design of modular buildings. *Automation in Construction*, 134:104062, 2022. doi:10.1016/j.autcon.2021.104062.
- [13] Xiaoping Zhou, Jichao Zhao, Jia Wang, Ming Guo, Jiayin Liu, and Honghong Shi. Towards product-level parallel computing of large-scale building information modeling data using graph theory. *Building and Environment*, 169:106558, 2020. doi:10.1016/j.buildenv.2019.106558.
- [14] A Khalili and DK H Chua. Ifc-based graph data model for topological queries on building elements. *Journal of Computing in Civil Engineering*, 29(3):04014046, 2015. doi:10.1061/(ASCE)CP.1943-5487.0000331.
- [15] Yilong Jia, Jun Wang, M Reza Hosseini, and Wenchi Shou. Graph neural networks in building life cycle: a review. In *EC3 Conference 2022*, volume 3, pages 0–0. University of Turin, 2022. doi:10.35490/EC3.2022.164.
- [16] Xiongfeng Yan, Tinghua Ai, Min Yang, and Hongmei Yin. A graph convolutional neural network for classification of building patterns using spatial vector data. *ISPRS Journal of Photogrammetry and Remote Sensing*, 150 (September 2018):259–273, 2019. ISSN 09242716. doi:10.1016/j.isprsjprs.2019.02.010.
- [17] Ruizhen Hu, Zeyu Huang, Yuhan Tang, Oliver van Kaick, Hao Zhang, and Hui Huang. Graph2Plan: Learning Floorplan Generation from Layout Graphs. *ACM Transactions on Graphics*, 39(4):1–14, apr 2020. ISSN 0730-0301. doi:10.1145/3386569.3392391.
- [18] Ying Hong, Haiyan Xie, Vahan Hovhannisyan, and Ioannis Brilakis. A graph-based approach for un-packing construction sequence analysis to evaluate schedules. *Advanced Engineering Informatics*, 52(May):101625, apr 2022. ISSN 14740346. doi:10.1016/j.aei.2022.101625.
- [19] Zijian Wang, Rafael Sacks, and Timson Yeung. Exploring graph neural networks for semantic enrichment: Room type classification. *Automation in Construction*, 134(October 2021):104039, 2022. ISSN 09265805. doi:10.1016/j.autcon.2021.104039.
- [20] Fiona C. Collins, Alexander Braun, Martin Ringsquandl, Daniel M. Hall, and André Borrmann. Assessing IFC classes with means of geometric deep learning on different graph encodings. In *Proceedings of the 2021 European Conference on Computing in Construction*, volume 2, pages 332–341, 2021. doi:10.35490/EC3.2021.168.
- [21] Charles R Qi, Hao Su, Kaichun Mo, and Leonidas J Guibas. Pointnet: Deep learning on point sets for 3d classification and segmentation. In *Proceedings of the IEEE conference on computer vision and pattern recognition*, pages 652–660, 2017. URL <http://arxiv.org/abs/1612.00593>.

Discrete Event Simulation Based Approach for Tracking Performance of Segmental Production at Precast Yard

Ashutosh Kumar Rai ^a, Varun Kumar Reja ^{a, b}, Koshy Varghese ^a

^aDepartment of Civil Engineering, IIT Madras, India

^bFaculty of Engineering and Information Technology, UTS, Australia

E-mail: theashutoshrai@gmail.com, varunreja7@gmail.com, koshy@iitm.ac.in

Abstract –

Efficient performance tracking and monitoring systems can facilitate timely decision-making by management. However, cycle time, which is commonly employed as a monitoring system in segmental production sites, can be time-consuming and only allows for the identification of inefficiencies, rather than supporting decision-making. In this context, operational management concepts with broad applications in manufacturing industries should be utilized. While several tools are offered by operational management, this paper focuses on the implementation of a process analysis tool as a performance tracking system for superstructure construction at a precast yard. Process analysis tools incorporate several operational performance measures, including cycle time, total idle time, direct labor content, and direct labor utilization. These performance measures serve as indicators for evaluating process productivity and can be estimated using an excel spreadsheet. Simulation tools, which enable visualization of the process and the identification of potential issues before implementation, can be valuable. In this regard, modeling in ExtendSim can be beneficial as the segmental production process can be easily visualized, aiding in the identification of station dependencies and allowing for the acquisition of performance measure results with a single click. This study therefore aims to explore the integration of process analysis tools with ExtendSim simulation as a performance tracking system at the precast yard. The values of these operational performance measures will provide management with multiple dimensions for enhancing the efficiency and effectiveness of the segmental production process.

Keywords –

Productivity, Production, Superstructure, Operational Management, ExtendSim, Simulation, Performance Measurement, Segmental Construction, Process Analysis, Modelling, Precast yard

1 Introduction

The construction industry lacks a practical framework for performance measurement [1][2]. This even applies to segmental bridge construction. The precast team uses cycle time as the only performance measure for monitoring segmental construction progress.

Though the production output can be increased by several means, one is by reducing cycle times i.e., either through product or process innovation. But the identification of problems and implement changes in the process will take time and it is just one measure to look at the performance of the precast yard. Also, several decisions have to be made to manage the production process, this decision will be regarding production planning, capacity, process design, operation strategy, and inventory control. Precast yard lacks this kind of monitoring system. Making the production system efficient, requires effective management. Manufacturing industries use operational management concepts which help in making these decisions and it is concerned with designing and controlling the process of production. All the concepts, tools, and techniques of operational management help make the production system efficient [3]. The major task at precast yard is shown in Figure 1.

1. Cutting and bending of rebars at the rebar yard.
2. Tying at rebar jigs.
3. Segment shutter & concrete work at casting bed.



Figure 1. Segmental Production Process

Hence, the current study explores an option of looking at the operational management tools which can be used in precast yards as performance tracking systems to point out the right areas for improvement. The two

objectives of this study are as follows:

1. To develop a simulation model based on a process flow diagram of a short-line segmental production system and determine monthly performance parameters.
2. To determine operational performance measures of a segmental construction process using simulation.

For this paper, the scope is limited to improving the performance of precast yard superstructure production.

This paper can be broadly divided into seven sections. Section 2 provides a literature review, while Section 3 outlines the methodology used in the study. Section 4 elaborates on the process analysis tool implemented through Simulation. Section 5 presents the simulation results and offers improvement suggestions. Section 6 offers a detailed discussion of the study findings. Section 7 presents limitations and future research directions. Finally, Section 8 concludes the study.

2 Literature Review

In the current system, performance indicators related to processes include planned percent complete (PPC), waste, safety, and quality process improvement for enhancing site performance [1].

Also in that context, lean principles are effective in enhancing the performance of the construction process. These principles will improve the entire process of production, by eliminating waste in the process and ultimately increasing the performance of the business [4]. Many construction companies have also started integrating some of the principles of the Lean Production System (LPS). Companies applying these techniques can decrease their production cost, reduce rework, and increase production capacity.

Even research revealed that lean construction principles led to 41% improvement in process productivity, 14% enhancement in process efficiency, and 17% reduction in cycle time [5]. Lean production can improve operational performance [6]. The four dimensions of operational performance i.e., cost, quality, variety, and responsiveness are positively related to the lean production practice in the manufacturing industry [7]. And even its tools help in maximizing profit through high productivity and are applicable in any industry [3]. Hence, use of these tools in construction should be explored.

There are different ways to track the performance of the process, but it would not help the site management in decision making i.e., decision-related to resource allocation based on the project's scope and duration [8]. In this context, simulation tools which are widespread in various industries such as education, health, information technology, robotics, economics, business, logistics, and

transport services can be helpful. The simulation outputs are the most valuable for production companies during the initial stages of business development. Also, the simulation methods can be utilized when there is a need to improve manufacturing and business processes and during the reengineering of technology and all business process [9][10]. Even many operations in construction projects show high potential for improvement through the application of lean principles and simulation, but it has not been used widely [11]. Simulation tools like ExtendSim are used for creating the real production process model and identifying the bottleneck and also help in redesigning the production process [12]. It has powerful capabilities to model and study complex systems [13].

The literature indicates a lack of performance indicators in the current system, and construction industries have turned to lean principles to enhance the construction process. While operational performance measures are linked to lean production and have been widely used in manufacturing industries, they are not commonly employed in construction processes.

In summary, through the literature study, it was found that simulation if used within lean approach helps in identifying problems in production processes, documenting the process, ranking the various opportunities for process improvement and finally helps in predicting the impact of accepted improvements before implementations. Therefore, it can be inferred that operational performance is positively related to lean production. In that reference, implementing operational management concepts to improve the construction process is one area that needs to be explored. Also, previous studies on simulation programs suggest that they can be useful in decision-making in the beginning stage. Therefore, using simulation for improving the segmental production process and for making decisions relevant to the production system is the other area to explore. Therefore, this study intended to fill the gap by integrating the process analysis tool of operational management with ExtendSim simulation as a performance tracking system for improving segment production rate at the precast yard.

3 Methodology

Figure 2 shows the methodology adopted for this study. The first stage of research consisted of a basic literature review to introduce previous studies and findings, after construction's professional opinion has been taken into consideration, and finally going through current adopted practices at the site level helps in defining the problem statement.

The second stage collecting data from the site. Data was collected and maintained in an excel spreadsheet

during segmental production and were used to determine the average processing time (delay) at each station.

The final stage is the integration of operational performance measures with simulation., the first step is to draw a process flow diagram to understand the flow of materials from one station to another station. In the second step, the model was constructed using ExtendSim simulation according to the process flow diagram and inputting delay as constant. Third, to check the simulation model accuracy, a model was validated through a comparison between model outputs and site outputs i.e., obtained from the monthly production spreadsheet. After model validation, operational performance measures are estimated using a simulation function. And based on the results, a few scenarios are assumed to improve the performance measures and help the management in the decision-making process.

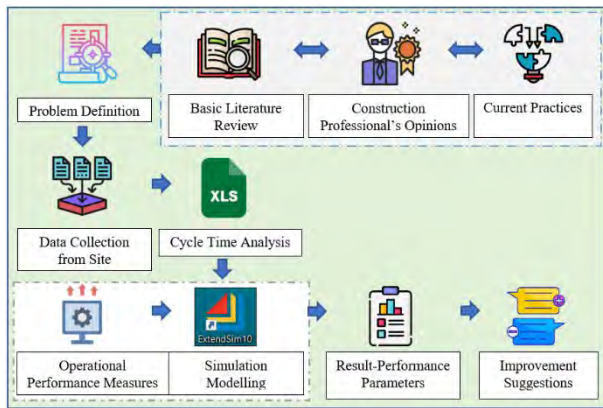


Figure 2. Methodology Adopted

4 Process Analysis Tool Implementation at Precast Yard

4.1 Operational Performance Measures

The performance measures that are determined in this study are the capacity at each station, process capacity, flow rate, utilization at each station, cycle time, total idle time, direct labor content, and direct labor utilization. All the terms used in this study are defined in Table 1.

Table 1. Term Definition

Terms	Definitions
Processing Time (PT)	Time spent by the worker or crew on the task.
Capacity (C)	It is estimated as (m/processing time) with m being the number of resources (e.g., workers or crews) being devoted to the station.
Bottleneck	It is defined as the process step in the

	flow diagram with the lowest capacity.
Process Capacity (PC)	The process capacity is always equivalent to the capacity of the bottleneck.
Flow Rate (FR)	Minimum between demand rate and process capacity.
Utilization (U)	It is calculated as flow rate divided by capacity. The utilization tells us, how well a resource is being used.
Cycle Time (CT)	It is defined as the time between the output of two successive flow units.
Direct labor content (DLC)	It is defined as the time sum of all process steps.
Idle Time (IT)	It is defined as cycle time minus processing time. The time when a resource is not doing anything and waiting for another resource.
Total Idle Time (TIT)	The total idle time is the time sum of all idle time within a process.
Direct Labour Utilization (DLU)	It is defined as the direct labor content divided by the sum of direct labor content and total idle time. The average labor utilization tells us the overall performance or productivity of the process.

4.2 Process flow diagram

It is the visual representation of the process flow. In which, rectangles represent tasks and activities; triangles represent inventory and arrows indicate the flow of the process. Figure 3 is the process flow diagram for the short-line bed model.

Short-line bed (SLB)

In a short-line bed, the casting of the next segment can begin only after shifting a previously casted segment. The casting of pierhead and expansion joints (EJ) segments is done on a short-line bed.

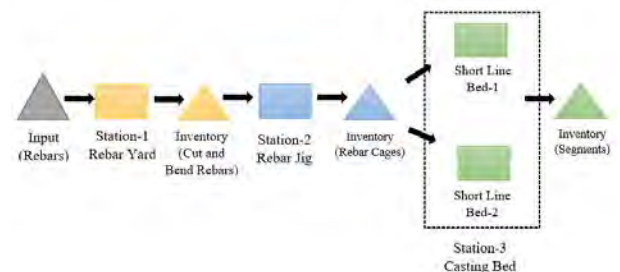


Figure 3. Short-line bed process flow diagram

For short-line segmental construction, work started at station-1 (rebar yard) on one cut-and-bend machine

(C&B), and these cut-and-bend rebars are shifted to station-2 (rebar jig) for tying purposes. Depending upon the front availability on station-2, cage-tying work will start. In general, short-line beds have one front available for cage tying. Once the cage is ready and the front is available at the casting bed, cage lowering is done at the casting bed (station-3). For segment casting work, two short-line beds are operational. Casting work goes parallelly at both beds. After casting and gaining sufficient strength for lifting, segments are shifted at the stacking yard for finishing purposes, and station-3 is made ready for cage lowering of the next segment.

4.3 Data collection

ExtendSim requires average processing time (delays) as input data. This data is manually recorded by the site engineer or supervisor in the daily-progress register and maintained in a cycle-time excel spreadsheet by the site-planning engineer. This spreadsheet gives information on the time taken for the completion of activities required for the casting of segments. Table 2 corresponds to the average processing time data recorded at the segmental construction site for the short-line bed.

Table 2. Average Processing time as input

Stations	Station's Name	Avg. PT (In hours)
1	Rebar Yard	30
2	Rebar Jig	35
3	Short line Bed	82

4.4 Modelling in ExtendSim

In this study, the ExtendSim 10.0.7 license version is used for modelling a short-line bed production system at the precast yard with the following basic assumptions.

1. Processing time (delay) as constant.
2. Sufficient demand per month of segments.
3. Most of the construction works are performed in a group not as an individual hence, the crew will be used in place of labor.

Steps required for modeling in ExtendSim:

- Firstly, using create, activity, queue, exit blocks in ExtendSim to imitate a process flow diagram for a short-line bed.
- Secondly, as construction works operate in day and night shifts, shift block is used to input details of workers' working time in a day.
- Lastly, simulating for 624 hours (assuming total working days in a month =26).

Figure 4 corresponds to the process flow diagram of the short-line bed in ExtendSim with all these settings.

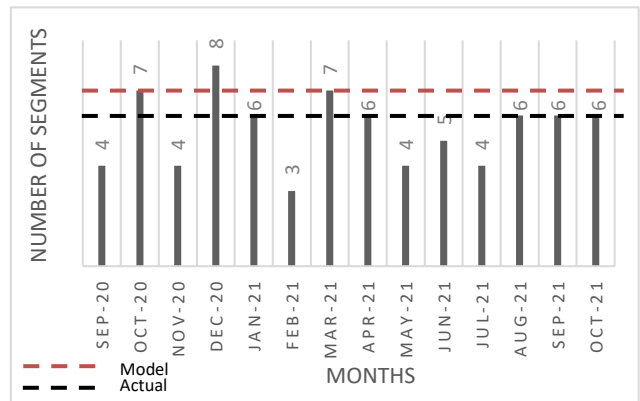


Figure 5. Short-line bed production (Actual)

4.4.1 Model Validation

To make sure that the model made in ExtendSim mimics the real segmental production process, inputs

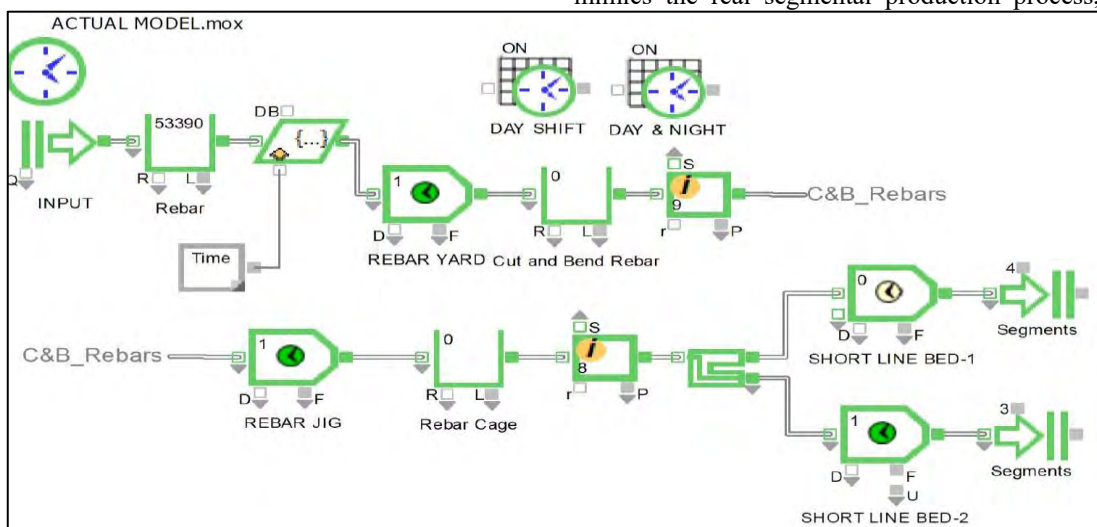


Figure 4. Short-line bed production system (Predicted by Model)

from the segmental production site was used in the modelling. If the model made in ExtendSim simulation gave nearly the same output as the precast team executed at the site, it will confirm model validation and can be used further for determining performance parameters.

Short-line Bed (SLB): Rebar yard works in the day shift; jig station and casting bed station work in both shifts. Figure 5 corresponds to the actual production capacity of the short-line bed.

It is indicated from Figure 4 and Figure 5, that the average monthly production capacity obtained from a site (i.e., 6 segments are produced per month) and from the model (7 segments per month) are closer. Hence, the model is validated and can be used for obtaining performance measures.

4.4.2 Determining performance measures

Operational performance measures are estimated through equation function under the value library. For determining these measures, processing time (delay) and crew deployed are used as input. Figure 6 demonstrates capacity and process capacity calculation.

```

Real a, b, c, d; // Crew deployed at each station
a = 1;
b = 1;
c = 1;
d = 1;
C1 = floor(a*10.5*26/PT1); //Station-1 Capacity
C2 = floor(b*20.5*26/PT2); //Station-2 Capacity
C3 = floor(c*20.5*26/PT3) + floor(d*20.5*26/PT4); //Station-3 Capacity
IF(C1<=C2 && C1<=C3)
PC=C1; //PC is the process capacity
else
IF(C2<=C1 && C2<=C3)
PC=C2;
else
PC=C3;
    
```

Figure 6. Determining Operational performance

Similarly, other performance measures can be determined. Due to space constraints, the link to the repository for estimating operational performance measures for short-line beds is:

<https://github.com/ashurai21/Performance-Measures>

5 Result and Improvement Suggestions

5.1 Results

Operational performance measures are estimated with a single click in ExtendSim for the short-line bed shown in Figure 7. The result of the simulation models is presented in

Table 3.

Table 3. Short-line Bed Results

Operational Performance	Output	Unit
Capacity, C1	9	Segments/month
Capacity, C2	15	Segments/month
Capacity, C3	12	Segments/month
Process Capacity	9	Segments/month
Flow Rate	9	Segments/month
Cycle Time	140.75	Hours/Segment
Utilization, U1	1	-
Utilization, U2	0.6	-
Utilization, U3	0.75	-
Total Idle Time	275.25	Hours/Segment
DLC	229	Hours/Segment
DLU	0.45	-

From Table 3 and Figure 7, rebar jigs (station-2) can produce fifteen cages in a month, but due to less capacity of the rebar yard (station-1), only the tying of eight cages

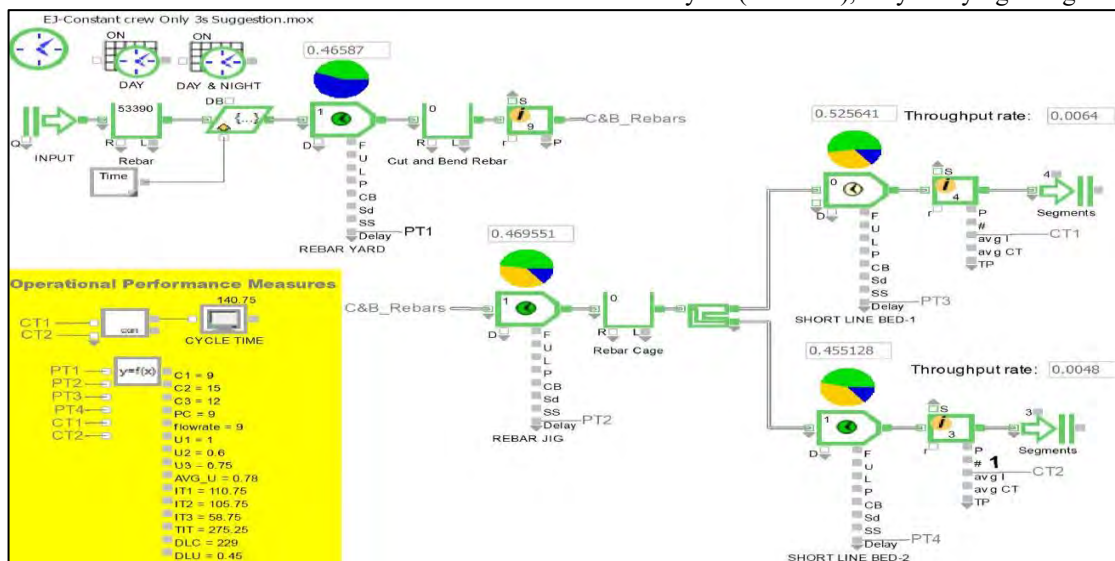


Figure 7. Short-line bed Operational Performance Measures Values

is completed and at one jig tying work is in progress. Further, the only casting (station-3) of seven segments is achieved, one segment casting is work-in-progress, even though it can cast twelve segments. It shows waste in utilization at station-2 and 3, which is the major reason for an increase in cycle time, and idle time in the process. The rebar yard (station-1) has the lowest capacity as compared to other stations. Therefore, it is the bottleneck station, and the capacity of the entire process will depend on it. Direct labor utilization values indicate productivity of the process which is just 0.45 in this case.

5.2 Suggestions

In this section, two scenarios are considered for a short-line bed to achieve the following objectives.

1. The first objective is to reduce cycle time and idle time.
2. The second objective is to increase the capacity, hence process capacity, flow rate, utilization, and direct labor utilization.

Percentage improvement (%I) is calculated for all the operational performance measures to determine whether the measures are improved or not after switching from the actual site scenario to the proposed site scenario.

For cycle time, idle time (objective is to decrease the values of these measures), and percentage improvement is estimated by using the following equation (1).

$$\%I = (\text{Actual}-\text{Proposed})/\text{Actual} \times 100 \% \dots (1)$$

For capacity, process capacity, flow rate, utilization, and direct labor utilization (the objective is to increase the values of these measures), percentage improvement is estimated by using the following equation (2).

$$\%I = (\text{Proposed}- \text{Actual})/\text{Actual} \times 100 \% \dots (2)$$

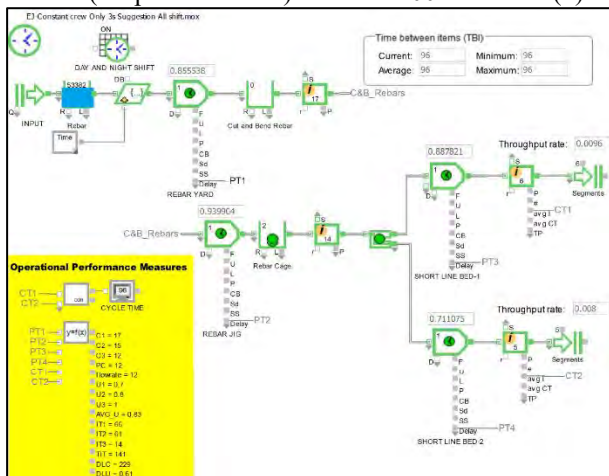


Figure 8. Scenario-1 Short-line bed

Scenario-1 All stations are operational on both day and night shifts without deploying any additional resources.

Figure 8 shows the operational performance values obtained through simulation in this scenario. Percentage improvement values are presented in Table 4.

Table 4. Scenario-1 Short-line Bed

Operational Performance	Actual	Scenario-1	
		Proposed	% I
Capacity, C1	9	17	88.88
Capacity, C2	15	15	0
Capacity, C3	12	12	0
Process Capacity	9	12	33.33
Flow Rate	9	12	33.33
Cycle Time	140.75	96	31.79
Utilization, U1	1	0.7	-30
Utilization, U2	0.6	0.8	33.33
Utilization, U3	0.75	1	33.33
Total Idle Time	275.25	141	48.77
DLC	229	229	0
DLU	0.45	0.61	35.55

In scenario-1 short-line bed, the bottleneck station is changed to station-3 (casting bed) from station-1. Cut and bend rebars are always available in buffer for tying purposes, and extra cages are always ready for casting purposes. Figure 9 illustrates the percentage improvement from the actual to the proposed scenario.

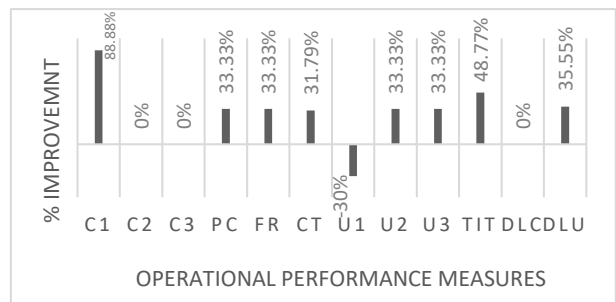


Figure 9. % Improvement Scenario-1 SLB

Percentage Improvement shows that in the proposed scenario almost all of the desired objectives are achieved. However, utilization at station-1 decreased by 30%.

Scenario-2 Balancing capacity by allowing work at each station till the time requires, to meet the demand. Hence, in this scenario assuming:

- Rebar yard is operational till 4 A.M.
- Rebar jig is operational till 1 A.M.
- The casting bed is operational on both day and night shifts.

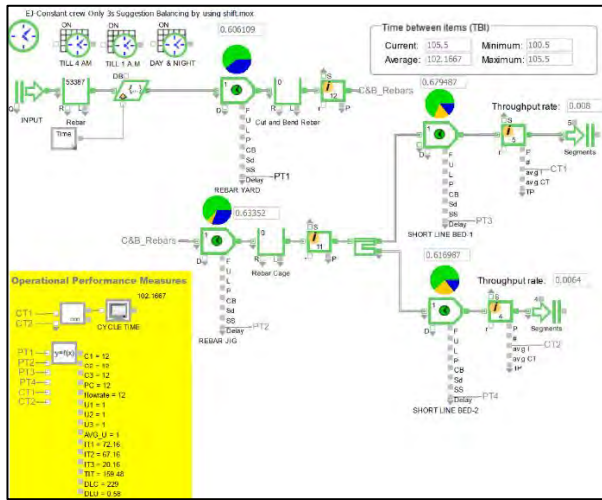


Figure 10. Scenario-2 Short-line bed

Table 5. Scenario- 2 Short-line bed

Operational Performance	Actual	Scenario-2	
		Proposed	%I
Capacity, C1	9	12	33.33
Capacity, C2	15	12	-33.33
Capacity, C3	12	12	0
Process Capacity	9	12	33.33
Flow Rate	9	12	33.33
Cycle Time	140.75	102.2	27.41
Utilization, U1	1	1	0
Utilization, U2	0.6	1	66.67
Utilization, U3	0.75	1	33.33
Total Idle Time	275.25	159.5	42.05
DLC	229	229	0
DLU	0.45	0.58	28.88

Figure 10 shows the operational performance values obtained through simulation in this scenario. Percentage improvement values are presented in Table 5.

Though the overall productivity of the segmental production process is increased to 0.58 in this scenario, still, it is not desirable to have a balanced process. This is because, if there is uncertainty in rebar procurement at the site, cutting and bending get delayed, which ultimately delays tying works. Therefore, it will be more beneficial to add slack capacity (rebar cages) at the jig station, which means it needs to be imbalanced to deal with this uncertainty. Figure 11 illustrates the percentage improvement from the actual to the proposed scenario. A positive value of % improvement indicates that almost all of the desired objectives are achieved in scenario 2. However, capacity at station-2 is decreased by 33.33%.

The other possible scenario in which productivity of the process can be increased is by deploying additional resources which are not covered in this study.

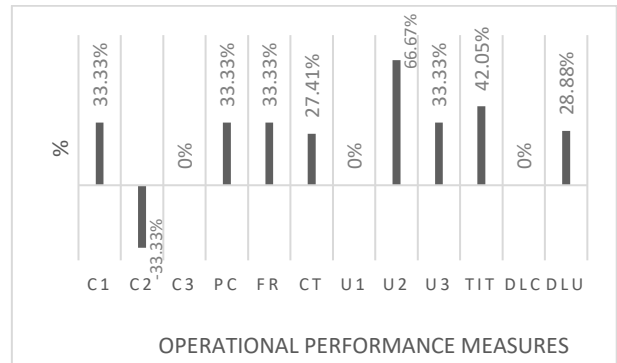


Figure 11. % Improvement Scenario-2 SLB

6 Discussion

This section deals with evaluating the usefulness of operational performance measures at the precast yard. Through performance measures, the actual capacity of each station is determined and by comparing it with on-site production, waste incapacity can be determined. Depending upon the resource availability and front availability, the process flow diagram will vary at sites. The model made in ExtendSim helps in visualizing the process flow of the segmental production process, which further helps in identifying the dependencies of stations on each other and determining monthly performance parameters. The process capacity depends upon the bottleneck station, hence knowing this parameter will help the precast team to look at the bottleneck station first, rather than focusing on other stations. Hence, the precast team should focus on achieving higher process capacity, i.e., achieved either by doing process innovation (which will cut down processing time) or allowing workers to work in more shifts to meet demand. Higher process capacity means achieving a greater number of segments casting in the same timeframe.

In this study, demand assumed was sufficient, but if demand is lower than production capacity, i.e., segments produced are more than segments erected, the flow rate of the process will depend upon segment erection. And in this case, the segment has to be stacked as inventory in the stacking yard. This may trouble site management for segment storage as the inventory at the site will exceed stacking capacity. Hence, the flow rate will help the precast team in tracking the mismatch between demand and capacity. High cycle time and idle time values indicate waste in the process, which ultimately affects profit margins. These two-performance measures will tell the site team that there is still scope for improvement in the process flow. Based on the productivity of the process, the precast team can decide on the requirement of deploying an additional crew and additional resources or allowing the crew to work in more shifts to meet the demand. All these measures will help the precast team in eliminating waste and inefficiencies and in scaling up the

profit margins. Finally, with the help of these measures site-management can track the segmental construction progress which helps in making right strategies, and thus saving the project from schedule and cost overruns.

7 Limitations and Future Directions

The current scope of this study is restricted to the precast yard, but the process flow could be expanded to include segmental erection. This addition would provide a more comprehensive view of the superstructure's performance, allowing for better monitoring and tracking by management. Also, to further enhance the analysis, in future, 3D simulation software (e.g., AnyLogic) could be utilized to visualize the precast yard stations and compare the differences in results obtained.

8 Conclusion

The research presented in this paper tries to find the operational performance measures of the segmental production process with the help of ExtendSim simulation for a short-line bed production system. The key findings of this study are:

- The process flow diagram of segmental production with the help of ExtendSim simulation helps in visualizing the entire process. And thus, the flow of material or products from one station to another, or dependencies of stations on each other are analysed.
- Based on these values, management can focus on increasing the capacity of the bottleneck station.
- These performance measures will help management on focusing on the right areas for improvement and in supporting their decision. These decisions can be regarding deploying additional crew or asking crew to work over shifts.

Through the study done, it is confirmed that process analysis tools can be integrated with ExtendSim simulation and can be used as a performance tracking system at the precast yard.

9 References

- [1] A. Pekuri and H. Haapasalo, "Productivity and Performance Management – Managerial Practices in the Construction Industry," 2014.
- [2] M. Jayesh Jain, V. K. Reja, and K. Varghese, "Exploring the Critical Factors Affecting The Productivity of Microtunneling Pipe Installation," in *38th International No-Dig*, 2022. [Online]. Available: <https://www.researchgate.net/publication/364309638>
- [3] A. Maralcan and I. Ilhan, "Operations management tools to be applied for textile," *IOP Conf Ser Mater Sci Eng*, vol. 254, no. 20, 2017.
- [4] D. Manea, "Lean Production – Concept and Benefits," *Review of General Management*, vol. 17, no. 1, pp. 164–171, 2013.
- [5] M. S. Bajjou and A. Chafi, "Lean construction and simulation for performance improvement: a case study of reinforcement process," *International Journal of Productivity and Performance Management*, vol. 70, no. 2, pp. 459–487, 2021, doi: 10.1108/IJPPM-06-2019-0309.
- [6] A. K. Rai, V. K. Reja, and K. Varghese, "Application of Operational Management Tools at Precast Yard," in *Indian Lean Construction Conference (ILCC)*, 2022.
- [7] A. R. Ibrahim, G. Imtiaz, B. Mujtaba, X. Vinh Vo, and Z. U. Ahmed, "Operational excellence through lean manufacturing: Considerations for productivity management in Malaysia's construction industry," *Journal of Transnational Management*, vol. 25, no. 3, pp. 225–256, Jul. 2020, doi: 10.1080/15475778.2020.1749809.
- [8] R. Larsson, *An integrated simulation-based method for considering weather effects on concrete work tasks' productivity and concrete curing*, no. September. 2020.
- [9] M. Straka, M. Malindzakova, P. Trebuna, A. Rosova, M. Pekarcikova, and M. Fill, "Application of extendsim for improvement of production logistics' efficiency," *International Journal of Simulation Modelling*, vol. 16, no. 3, pp. 422–434, 2017.
- [10] S. Bait, A. Di Pietro, and M. M. Schiraldi, "Waste reduction in production processes through simulation and VSM," *Sustainability (Switzerland)*, vol. 12, no. 8, 2020, doi: 10.3390/SU12083291.
- [11] A. Nikakhtar, A. A. Hosseini, K. Y. Wong, and A. Zavichi, "Application of lean construction principles to reduce construction process waste using computer simulation: A case study," *International Journal of Services and Operations Management*, vol. 20, no. 4, pp. 461–480, 2015.
- [12] M. Ondov, A. Rosova, M. Sofranko, J. Feher, J. Cambal, and E. F. Skrabulakova, "Redesigning the Production Process Using Simulation for Sustainable Development of the Enterprise," *Sustainability (Switzerland)*, vol. 14, no. 3. 2022.
- [13] R. Larsson, "An Integrated Simulation-Based Methodology for Considering Weather Effects on Formwork Removal Times," *Advances in Informatics and Computing in Civil and Construction Engineering*, pp. 415–422, 2019, doi: 10.1007/978-3-030-00220-6_49.

Reducing Uncertainty in Multi-Robot Construction through Perception Modelling and Adaptive Fabrication

D. Ruan¹, W. McGee¹, and A. Adel^{1*}

¹University of Michigan, USA

*Corresponding Author

deltar@umich.edu, wesmccgee@umich.edu, aaadel@umich.edu

Abstract

One of the significant challenges for robotic construction with dimensional lumber and other construction materials is the accumulation of material imperfections and manufacturing inaccuracies, resulting in significant deviations between the as-built structure and its digital twin. This paper presents and evaluates methods for addressing these challenges to enable a multi-robot construction process that adaptively updates future fabrication steps to accommodate for perceived inaccuracies, improving build quality. We demonstrate through a physical stacking case study experiment that our methods can decrease fabrication deviations due to setup and calibration errors by utilizing robot perception and adaptive processes. Overall, this research advances current toolpath and task optimization strategies to help shape a comprehensive system for working with tolerance-aware robotic construction.

Keywords –

Robotic Assembly, Adaptive Fabrication, Perception, Timber Structures, Multi-Robot Construction

1 Introduction

Robotic construction with dimensional lumber and other construction materials imposes significant challenges for robotic systems due to material imperfections and fabrication tolerances [1], [2]. Depending on the quality of the lumber (e.g., grade 2 or 3), the cross-sections of elements could deviate from nominal values. Furthermore, due to the length of the full-height elements (e.g., 3 m), lumber elements are usually not completely straight and include considerable deformations (e.g., twists and bends), contributing to their positioning errors. Compounding these issues, wood can shrink and expand due to temperature and moisture variability. Material imperfections and manufacturing inaccuracies accumulate during the

assembly process, resulting in a significant deviation between the as-built structure and its digital twin. Our previous experiments have shown deviations up to 60 mm while assembling a light timber wall assembly, and due to these inaccuracies, the automated process often must be interrupted and errors addressed manually, decreasing build quality and increasing time taken for fabrication.

The current challenge in autonomous manufacturing and assembly of building-scale structures is the high intrinsic complexity of construction tasks and the lack of human-robot interfaces designed for the specific operational needs of construction [3]. This is in part due to the adoption of robotic systems from other industries such as the automotive industry, which operates in a highly structured and repetitive environment. Through the integration of more intelligent perception, reasoning, and control algorithms, a streamlined digital design-to-fabrication workflow can better address potential unforeseen collisions and part imprecisions, especially when compounded with the challenge of operating multiple robots cooperatively. This paper presents and evaluates methods for addressing the discussed challenges to enable a multi-robot construction process that adaptively updates future fabrication steps to accommodate for perceived inaccuracies due to material imperfections and manufacturing inaccuracies, improving build quality.

2 Related Work

Multi-robot systems have long been established for assembly line applications, with well-synchronized repetitive tasks [4], [5]. Cooperative robotic fabrication for construction, however, is still being explored, with applications including foam wire cutting [6], masonry vault construction [7], spatial metal structure assembly [8], and timber construction [1], [9]–[15]. In addition to distributing workload, robotic cooperation can also be utilized to perform construction tasks that cannot be achieved by a single robot, as is often the case when working with spatial assemblies.

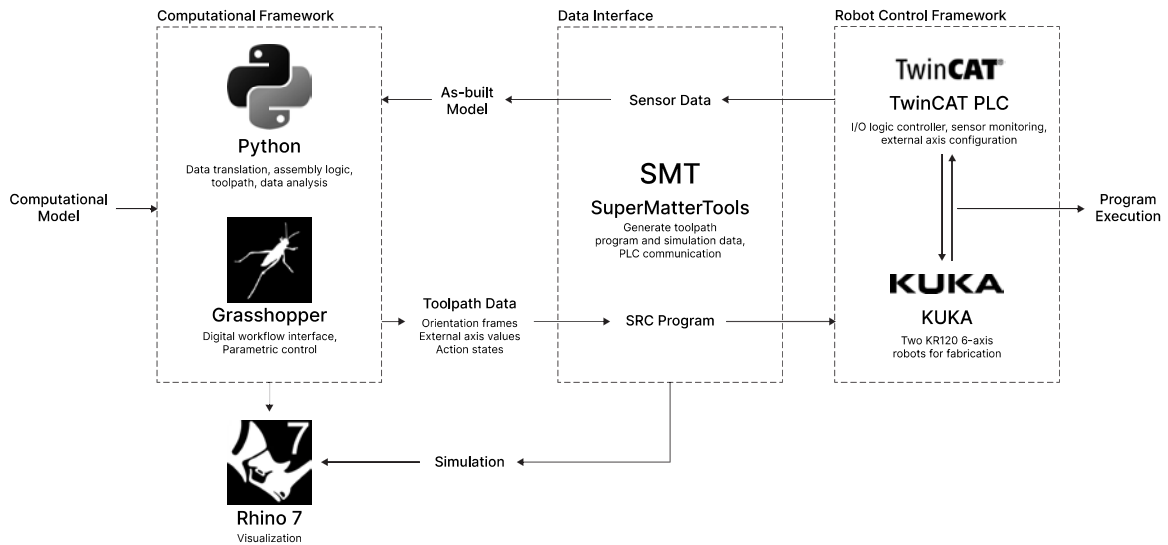


Figure 1. Digital design to fabrication workflow, highlighting the transfer of data between the computational model and the robot, adapted from previous research [9].

Focusing specifically on light timber assembly, the tight tolerances required for structural integrity coupled with the imperfect nature of timber studs make fully automated assembly challenging. The calibration of the robots and their tooling becomes a critical factor in determining as-built tolerances, with the real possibility of failure due to part collision. An end-effector positioning system utilizing static and dynamic correction through external pose tracking can reduce average positioning error down to 0.10 mm [16]; however, this solution has limited application outside of a defined workspace and is not suitable for adapting to material and process deviations.

There has been research to develop methods for dynamically adapting to these deviations. Gandia et al. [2] present a tolerance-aware computational design method for spatial timber structures, demonstrating how an optimal assembly sequence can be generated to minimize propagated tolerances. Eversmann et al. [17] use scanning to calculate the gripping and placement of differently sized shingles, however there was no feedback for updating post-placement tolerances, presumably due to the flexibility of a shingle system. Devadass et al. [18] reference a haptic fiducial to dynamically calibrate the workpiece cutting process for a mobile robotic setup, although assembly was still assisted through human robot collaboration. These approaches focus on minimizing tolerances during material processing and design computation, and as such there exists a gap in current literature on how to address deviations during the fabrication and assembly steps.

Adaptive fabrication techniques have long been embedded into the culture of craft, overcoming materials and environments with uncertain conditions by utilizing

visual and haptic perception to inform decision-making in real-time [19]. When translated to robotic processes, computer vision technologies such as three-dimensional (3D) laser scanning and force/torque sensing form a basis for robotic perception, which then informs how the robot reasons with its surroundings to perform its next action in a feedback loop.

Recent research has demonstrated the application of adaptive robotic subtractive manufacturing processes for stone carving [19] and wood [20], where the visualization and predictive techniques afforded by adaptive processes enable human-like responsiveness towards working with the material. Adaptive processes have also been utilized for the localization and calibration of a mobile robotic fabrication system for building-scale mesh welding [21], increasing accuracy through continuous mapping of the environment and surveying of the fabrication process.

Overall, the main objective of this research is to develop and evaluate adaptive assembly techniques that enable cooperative multi-robot timber assembly by minimizing positional and process deviations, as well as handling material imperfections. These adaptive techniques will be evaluated through a set of physical stacking experiments to determine their effectiveness based on fabrication tolerance metrics.

3 Methods

3.1 Fabrication Setup

The fabrication testbed for this research consists of two KUKA [22] KR 120 R2700 6-axis industrial robot arms, named ‘North’ and ‘South’, mounted on parallel linear tracks, which allows full access to a raised

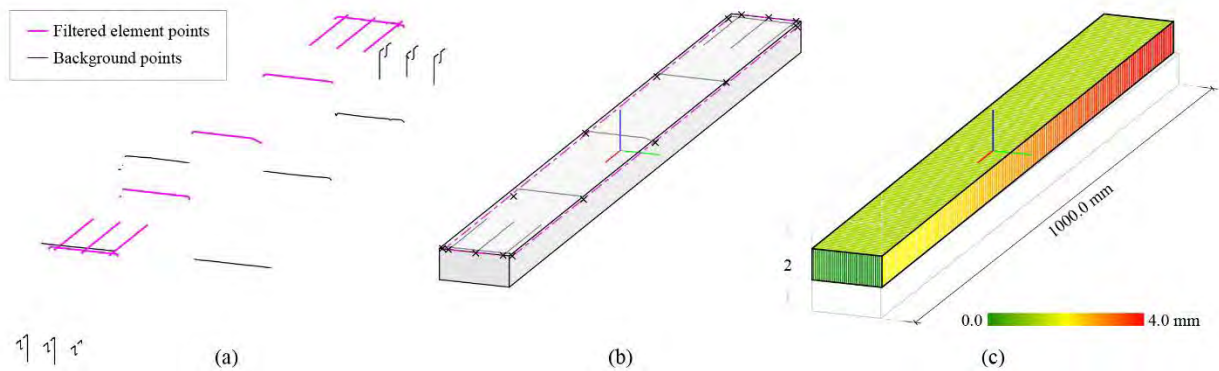


Figure 2. The scan processing begins with filtering the profile pointcloud (a), isolating the points scanned from the top face of the element. The filtered profiles are then used to generate a geometric representation and its central frame (b). The as-built model is updated with the newest element, which can be used to calculate deviations from the digital model (c).

assembly platform and a custom 3-axis computer numerical controlled (CNC) table saw. Each robot is equipped with a pneumatically controlled gripper end effector, which can be swapped out for an LMI Technologies Gocator 2350 [23] two-dimensional (2D) laser profiler for all scanning operations. Control of the workcell and collection of sensor data is processed through a programmable logic controller (PLC, Beckhoff TwinCAT [24]).

3.2 Timber Assembly Process

The basic timber assembly process, as the main case study process for this research, starts with a human operator loading a standard 2x4 piece of lumber down the center of the saw table, with one end roughly aligned with the center of the table, with one end roughly aligned with the edge of the table. The active robot then picks up the raw stock and performs two cuts on the saw for the model-specified length and end-plane angles. The gripping frame is located on the stock such that the first cut safely minimizes offcut volume, while the second cut maximizes the remaining material for future cuts, also making sure to avoid any potential collision between the saw blade and the gripper. Without regripping, the cut 2x4 element is brought over to the assembly platform and inserted into its final position within the sub-assembly. The human operator then fastens the element into place (e.g., with screws to previously placed elements, or with clamps if directly attached to the platform) before the robot releases the element and retracts. This process repeats until the sub-assembly is complete.

3.3 Digital Design-to-Fabrication Workflow

We have adapted a digital design-to-fabrication workflow based on previous research [9], which integrates Rhinoceros 3D [25], its plugin Grasshopper [26] and Python [27] with Super Matter Tools [28], a custom computational design tool for offline

programming and simulation (see Figure 1). This workflow enables a seamless connection between the digital design of the fabrication module and the robotic simulation, control, and manufacturing.

The forward loop of the workflow translates each timber element's modelled geometry into frames (consisting of position and orientation) that can be interpreted by our control algorithm for path planning. The primary frame for each element is chosen to be located at the centroid of the element, aligned with its long axis, ensuring safe and stable gripping while cutting and placing the element during assembly. Cutting attributes (such as cutting distance, saw blade angles) are generated parametrically from the modelled end planes. The pickup and saw locations are taught, while the path traversal and gripping states are configured prior to fabrication. All of these parameters are then automatically post-processed into Kuka Robot Language (KRL) to be executed by the robot.

The backward loop of the workflow enables feedback into the digital design loop, allowing for alterations to the model based on observed as-built conditions. This loop is what enables the adaptive adjustment of model parameters to reduce deviations in the fabricated sub-assembly.

Perception of the workpiece occurs both before and after each pick-cut-place operation to assist in the adaptive processes, as discussed in the following section. At this point in the process, the active robot swaps to the laser profile scanning end effector and performs a series of profile scans of the placed element to generate a digital as-built model. Profile scanning was selected over sweep scanning due to its minimal memory and processing requirements, while still being able to capture the critical boundary points to reconstruct the element digitally within reasonable accuracy. The reconstructed element is then used to update the as-built model, which can be compared with the original model to perceive deviations (see Figure 2).

3.4 Adaptive Processes

In order to reduce deviations between the digital and as-built models, we introduce adaptation into the fabrication workflow. Adaptation is enabled through the robots' usage of the laser profile scanner, which defines a perceptual coordinate space model in relation to the base world coordinate system for each robot. This process utilizes the physically placed elements as an anchor point to align the digital model with the perceptual spaces of each robot.

Two adaptation steps are added to the fabrication process – in the first, the active robot scans the previously placed element to determine the current deviation and estimate the correction (i.e., changes placement position and orientation) required to minimize deviations in the next element. After placing the next element, the active robot scans the new element to evaluate and update its estimation model.

The true as-built frame of a placed element in the world coordinate system is notated as p_n^W , where n is the element index. The relation between this true frame and the scanned frame is as follows:

$$p_n^L = T_{LW} p_n^W + \varepsilon_n^L \quad (1)$$

Where p_n^L is the scanned frame relative to the robot laser's tool center point (TCP, T_{LW} is the transformation between the laser and world spaces, and ε_n^L is the measurement noise due to the scanning process. T_{LW} is, in turn, comprised of transformations from the scanner TCP to the robot flange (T_{LF}), robot flange to the robot root (T_{FR}), and robot root to the world (T_{RW} , see Equation (2)).

$$T_{LW} = T_{LF} T_{FR} T_{RW} \quad (2)$$

Of these transformations, T_{LF} is calibrated by the user, T_{FR} is calculated by the robot controller and assumed to be accurate, leaving T_{RW} as the primary source of deviation between the laser and world spaces. This deviation is trivial in a single robot workcell with a fixed root, as the world space can be defined to be the same as the robot root. However, in a multi-robot workcell, any deviation in installation or calibration may result in a mismatch between each robot's perception of the world space. As an example, the two robots used in this paper have world spaces that are offset by approximately 4 mm, which translates to deviations in fabrication when operating without adaptation processes. To address this, one robot is arbitrarily chosen as the primary robot, setting the world space equal to its root (i.e., $T_{RW}^0 = I$). T_{RW} can then be estimated for the remaining robots $k \geq 1$ by relating their scanned element frame to the primary robot's.

$$\hat{T}_{RWn}^k = \underbrace{(T_{LF}^k T_{FR}^k)^{-1} p_n^{Lk}}_{\text{robot } k} \underbrace{[(T_{LF}^0 T_{FR}^0)^{-1} p_n^{L0}]^{-1}}_{\text{primary robot}} \quad (3)$$

As the number of elements increases, \hat{T}_{RW}^k is refined through linear least squares approximation. With a model for the transformation between the robot's perceptual space the world space, an estimate of the true as-built frame can be derived from Equation (4) and applied to determine the current deviation T_{WDn} between the digital and as-built models.

$$\hat{p}_n^W = T_{WDn} p_n^D \quad (4)$$

This transformation is then applied to the modelled frame of the next element p_{n+1}^D alongside an estimated gripper error \hat{T}_{GE} to obtain the gripper target position in the robot perceptual space \hat{p}_{n+1}^R (see Equation (5)), which is input into the toolpath program generation.

$$\hat{p}_{n+1}^R = \hat{T}_{GEN} \hat{T}_{RWn} T_{WDn} p_{n+1}^D \quad (5)$$

The gripper error is derived from the second adaptation step after placing and scanning the new element. This model is initialized (before the start of a fabrication task, for example) with a test piece assuming $T_{GE} = I$. With the post-placement scanned frame p_{n+1}^L , the gripper error is updated with linear least squares.

$$p_{n+1}^L = T_{LR} (\hat{T}_{GEN+1})^{-1} \hat{p}_{n+1}^R + \varepsilon_{n+1}^P \quad (6)$$

Where ε_{n+1}^P is the process noise error, which can result from material deformation, shifting while fastening, etc., assumed to have a mean of 0. Altogether, there is now a forward adaptation step for adjusting the position and orientation of the next element, as well as a backward adaptation step for evaluating and updating the error estimation model.

Adaptation can be applied in two ways in a multi-robot fabrication workflow – in the first, the arbitrarily designated primary robot does not incorporate any adaptation steps, and instead, the other robot(s) adapt and work around the primary robot. In this case, the primary robot establishes a ground truth throughout the fabrication process by adhering strictly to the digital model but is therefore reliant on its initial calibration to minimize deviations. The second method of adaptation is for all the robots to incorporate adaptation, which increases the primary robot's ability to respond to deviations at the cost of decreased protection against cumulative tolerances. To investigate the effectiveness of these adaptative processes, we conducted an experiment to compare the average deviation of a fabrication task with and without adaptation.

3.5 Experiment

The experiment was tasked with cutting and stacking ten 1000 mm lengths of standard 2x4 lumber from 8 ft (2.4 m) stock, alternating between the two robots of the experimental workcell, North and South, as the active robot. Although the model design is architecturally trivial,

the rotational alignment and positional accuracy of both robots is critical to the success of the task (i.e., forming a flat vertical wall), demonstrating the effectiveness of adaptation in a multi-robot fabrication setup. The effectiveness of the fabrication process was evaluated based on the average and per-element frame deviations.

The first experimental process was the base case, with no adaptation on either robot. In the second experimental process, North was set as the non-adapting primary robot while South adapted to its placements. In the third experimental process, both robots utilized adaptation. One stack of ten timber elements was fabricated for each of the three processes, generating ten sample points each (five per robot). Each sample point is a 6-dimensional vector (x, y, z , roll, pitch, yaw) representing an element's deviation (transformation) relative to its original modeled configuration frame. The results of the second and third processes are benchmarked with the base case.



Figure 3. The South robot placing the final element in a timber stacking task (with no adaptation).

4 Results

Figures 4-6 plot the x and y components of each sample point across the three experimental processes. The perception of each robot (colored red for North, blue for South) is consistently offset for each process, indicating the base difference between the two robots' perceptual spaces. Within each perceptual space, the base case (Figure 4) highlights the calibration error between North-placed elements (circles) and South-placed elements (triangles), as the result of no adaptation, with the offset between the average deviation of each cluster being 2.5 mm. The average deviation of a cluster is calculated by averaging the Euclidean distance of each sample point to their respective reference frame (modeled element frame). The second process (Figure 5) shows a marked improvement with South's adaptation

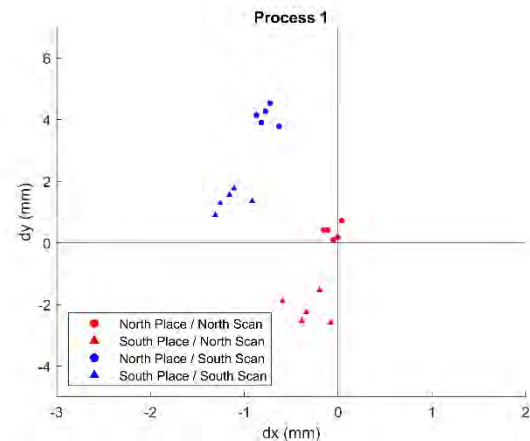


Figure 4. XY frame deviation for Process 1 (base case), with no adaptation.

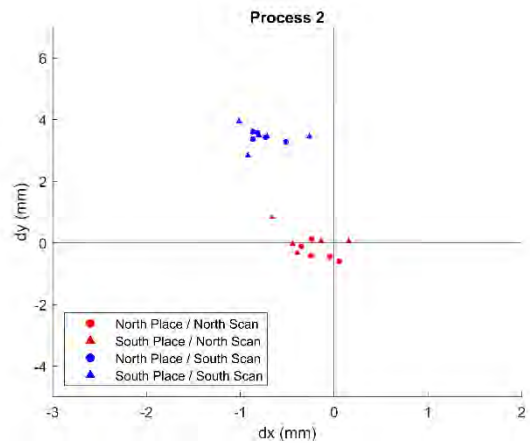


Figure 5. XY frame deviation for Process 2, with South adapting to North.

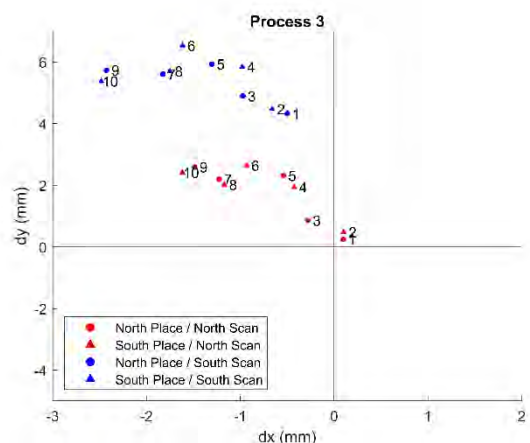


Figure 6. XY frame deviation for Process 3, with both North and South robots utilizing adaptation.

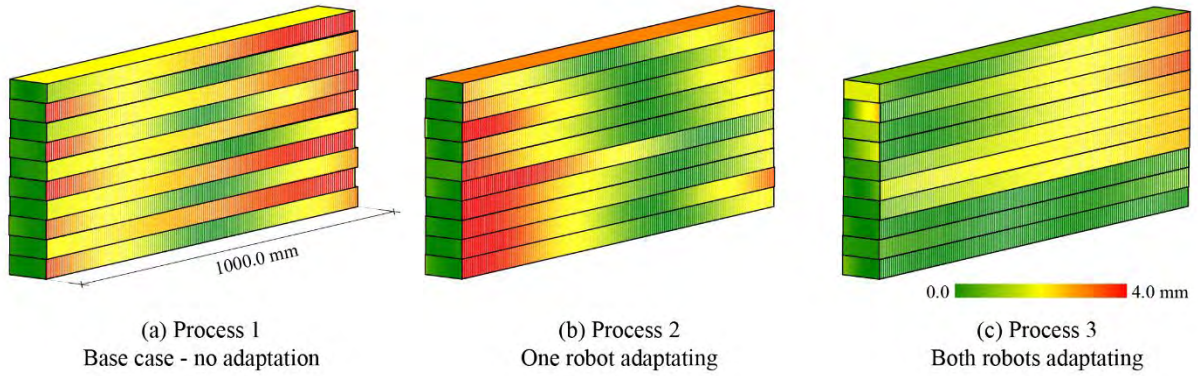


Figure 7. Heat maps indicating the deviations between the scanned and reconstructed as-built model and the digital blueprint model.

aligning its elements with North's, decreasing the offset to 0.4 mm and reducing the overall average deviation from 1.28 mm down to 0.45 mm (as measured by North).

The third experimental process shows the effect of cumulative deviations – each element in Figure 6 is labelled for legibility, with the elements having a clear drift direction, tending to deviate further from the modelled position as the task progresses. This is likely due to the fact that the two estimation models for the robot-world transformation \hat{T}_{RW} and gripper error \hat{T}_{GE} are still rough at the beginning of a new task, especially with the lack of an established ground truth as present in the case of the second process. Utilizing a larger initial dataset (e.g., gathered from previous tasks) could potentially alleviate most of this drift; however, more robust control logics are required to completely eliminate cumulative deviations.

Table 1. Element frame deviation translation (mm)

Process	Scanned by North		Scanned by South	
	Average	Stdev.	Average	Stdev.
1	1.28	1.01	3.00	1.28
2	0.45	0.26	3.53	0.28
3	1.96	1.03	5.66	0.77

Table 2. Element frame deviation rotation (°)

Process	Scanned by North		Scanned by South	
	Average	Stdev.	Average	Stdev.
1	0.107	0.255	0.108	0.263
2	0.377	0.053	0.354	0.055
3	0.484	0.086	0.452	0.090

5 Conclusion and Outlook

In this paper, we have introduced an adaptive process for multiple robots working cooperatively on a construction task. Initial experimental results

demonstrate the potential for this adaptive process to decrease fabrication deviations due to setup and calibration errors by utilizing robot perception. The research also highlights future work to further refine the estimation models and cooperative fabrication workflow.

As next steps, we intend to apply the adaptive processes to light timber framed wall assembly tasks at building-scale as well as implement real-time control to drive the fabrication workflow. Part of this implementation will include a probabilistic model that accounts for the currently unaddressed measurement and process noise error terms. These advances will push the adaptive process in line with other current toolpath and task optimization strategies to create a comprehensive system for working with tolerance-aware robotic construction.

Acknowledgement

This research was partially supported by the National Science Foundation (NSF, Award No. 2128623) and the Taubman College of Architecture and Urban Planning at the University of Michigan (U-M). Any opinions, findings, conclusions, or recommendations expressed in this paper are those of the authors and do not necessarily reflect the views of the NSF or U-M.

References

- [1] Adel Ahmadian A. Computational Design for Cooperative Robotic Assembly of Nonstandard Timber Frame Buildings. ETH Zurich, 2020.
- [2] Gandia A., Gramazio F., and Kohler M. Tolerance-aware Design of Robotically Assembled Spatial Structures. In *Proceedings of the 42nd Annual Conference of the Association for Computer Aided Design in Architecture (ACADIA)*, 2022.
- [3] Davila Delgado J. M., Oyedele L., Ajayi A., Akanbi L., Akinade O., Bilal M., and Owolabi H. Robotics and automated systems in construction:

- Understanding industry-specific challenges for adoption. *Journal of Building Engineering*, 26100868, 2019.
- [4] Dong Sun and Mills J. K. Adaptive synchronized control for coordination of multirobot assembly tasks. *IEEE Transactions on Robotics and Automation*, 18(4):498–510, 2002.
- [5] Pellegrinelli S., Pedrocchi N., Tosatti L. M., Fischer A., and Tolio T. Multi-robot spot-welding cells for car-body assembly: Design and motion planning. *Robotics and Computer-Integrated Manufacturing*, 4497–116, 2017.
- [6] Rust R. Spatial Wire Cutting: Integrated Design, Simulation and Force-adaptive Fabrication of Double Curved Formwork Components. ETH, Zurich, 2017.
- [7] Parascho S., Han I. X., Walker S., Beghini A., Bruun E., and Adriaenssens S. Robotic vault: a cooperative robotic assembly method for brick vault construction. *Construction Robotics*, 4(3–4):117–126, 2020.
- [8] Parascho S., Gandia A., Mirjan A., Gramazio F., and Kohler M. Cooperative Fabrication of Spatial Metal Structures. In *Fabricate 2017*, UCL Press, Apr. 05, 2017, 24–29.
- [9] Adel A. Co-Robotic Assembly of Nonstandard Timber Structures. In *Proceedings of the 42nd Annual Conference of the Association for Computer Aided Design in Architecture (ACADIA)*, 2022.
- [10] Thoma A., Jenny D., Helmreich M., Gandia A., Gramazio F., and Kohler M. Cooperative robotic fabrication of timber dowel assemblies. *Research culture in architecture*, 77–88, 2018.
- [11] Craney R. and Adel A. Engrained Performance: Performance-Driven Computational Design of a Robotically Assembled Shingle Facade System. In *Proceedings of the 40th Annual Conference of the Association for Computer Aided Design in Architecture (ACADIA)*, 2020, 604–613.
- [12] Wagner H. J., Alvarez M., Kyjanek O., Bhiri Z., Buck M., and Menges A. Flexible and transportable robotic timber construction platform – TIM. *Automation and Construction*, 120103400, 2020.
- [13] Adel A., Thoma A., Helmreich M., Gramazio F., and Kohler M. Design of Robotically Fabricated Timber Frame Structures. In *Proceedings of the 38th Annual Conference of the Association for Computer Aided Design in Architecture (ACADIA)* 2018, 394–403.
- [14] Graser K., Adel A., Baur M., Pont D. S., and Thoma A. Parallel Paths of Inquiry: Detailing for DFAB HOUSE. *Technology|Architecture + Design*, 5(1):38–43, 2021.
- [15] Thoma A., Adel A., Helmreich M., Wehrle T., Gramazio F., and Kohler M. Robotic Fabrication of Bespoke Timber Frame Modules. In *Robotic Fabrication in Architecture, Art and Design 2018*, Cham: Springer International Publishing, 2018, 447–458.
- [16] Stadelmann L., Sandy T., Thoma A., and Buchli J. End-Effector Pose Correction for Versatile Large-Scale Multi-Robotic Systems. *IEEE Robotics and Automation Letters*, 4(2):546–553, 2019.
- [17] Eversmann P., Gramazio F., and Kohler M. Robotic prefabrication of timber structures: towards automated large-scale spatial assembly. *Construction Robotics*, 1(1–4):49–60, 2017.
- [18] Devadass P., Stumm S., and Brell-Cokcan S. Adaptive Haptically Informed Assembly with Mobile Robots in Unstructured Environments. 2019.
- [19] Shaked T., Bar-Sinai K. L., and Sprecher A. Adaptive robotic stone carving: Method, tools, and experiments. *Automation and Construction*, 129103809, 2021.
- [20] Brugnaro G. and Hanna S. Adaptive Robotic Carving. In *Robotic Fabrication in Architecture, Art and Design 2018*, Cham: Springer International Publishing, 2019, 336–348.
- [21] Dörfler K., Hack N., Sandy T., Giftthaler M., Lussi M., Walzer A., Buchli J., Gramazio F., and Kohler M. Mobile robotic fabrication beyond factory conditions: case study Mesh Mould wall of the DFAB HOUSE. *Construction Robotics*, 3(1–4):53–67, 2019.
- [22] KUKA. <https://www.kuka.com/en-us> (accessed Mar. 30, 2023).
- [23] LMI Technologies. Gocator 2300 series. <https://lmi3d.com/series/gocator-2300-series/> (accessed Mar. 30, 2023).
- [24] Beckhoff. TwinCAT automation software. <https://www.beckhoff.com/en-us/products/automation/twincat/> (accessed Mar. 30, 2023).
- [25] Robert McNeel & Associates. Rhinoceros 3D, version 7.0. <https://www.rhino3d.com/> (accessed Mar. 30, 2023).
- [26] Rutten D. and Robert McNeel & Associates. Grasshopper 3D. <https://www.grasshopper3d.com/> (accessed Mar. 30, 2023).
- [27] van Rossum G. and Drake F. L. Python 3 Reference Manual. Scotts Valley, CA, 2009.
- [28] Pigram D. and McGee W. Formation embedded design. In *Proceedings of the 31st Annual Conference of the Association for Computer Aided Design in Architecture (ACADIA)*, 2011, 122–131.

Identifying key parameters for BIM-based disassembly planning

Benjamin Sanchez¹, Pieter Herthogs¹ and Rudi Stouffs²

¹Singapore-ETH Centre, Future Cities Lab Global Programme, CREATE campus, 1 CREATE Way, #06-01 CREATE Tower, Singapore 138602

²Department of Architecture, School of Design and Environment, National University of Singapore, Singapore 117566, Singapore

benjamin.sanchez@sec.ethz.ch, pieter.herthogs@sec.ethz.ch, stouffs@nus.edu.sg,

Abstract

Reuse of building systems and components has the potential of taking full advantage of the residual utility of building materials. In this matter, disassembly planning plays a critical role for retrieving reusable components in an optimized way. Unfortunately, the implementation of disassembly planning for buildings, at a component level, is still limited due to the lack of standardized methods and the lack of the definition of necessary characteristics (parameters) for building disassembly models. Therefore, the aim of this paper is to identify the necessary parameters for disassembly models and collate them into a framework. The approach in this study uses BIM as the main platform and graphic interface for managing the disassembly parameters for building components. First, the necessary information for building disassembly models is investigated. Then, the parameters for disassembly models are suggested and they are instrumented using BIM for a case study. The results of the enriched BIM disassembly model are verified according to the analytical solution for disassembly models for buildings.

Keywords –

Building Information Modeling; Disassembly planning; Building components reuse; Building disassembly model

1 Introduction

Reuse of building components has become a very important matter since year by year the construction industry is responsible for about 40% of the global natural resources exploitation, and 40% of waste diverted in landfills [1]. To overcome this challenge, technological advancements, such as Construction Waste Management (CWM), Materials Passports (MP), Product Recovery Management (PRM), and Life Cycle

Assessment (LCA) [2], have been implemented to increase the rates of reuse and recycling of building components. However, the implementation for reuse of building components and systems is still scarce due to the lack of research about reclamation protocols [3]. In this matter, disassembly planning is a strategic approach for the recovery of building components and systems for their future reuse or recycling [4,5]. Disassembly planning is the process of recognizing the required consecutive steps for dismantling a building, defining deconstruction activities, and ordering them logically. Figure 1 shows the disassembly planning methods for buildings according to the nature, type, and mode of disassembly.

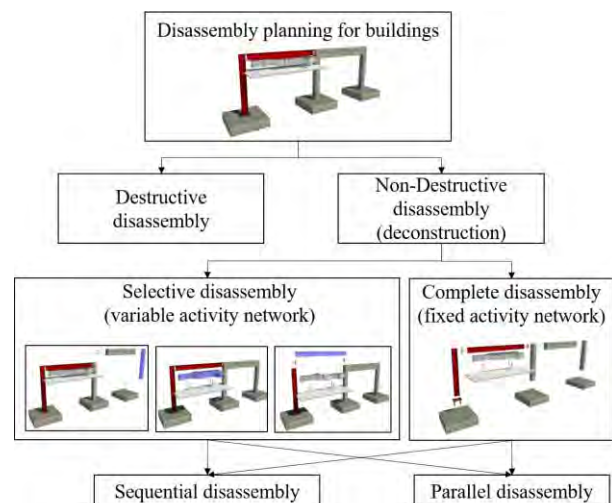


Figure 1. Disassembly planning methods for buildings

Unfortunately, disassembly planning for buildings is still underdeveloped in comparison to other industries such as manufacturing, automobile, and electronic industries [4,6]. The definitions of the characteristics (parameters) that a disassembly model should have are

critical for the implementation of disassembly planning methods. This field is still underdeveloped for buildings. In the following section we identify the parameters needed for disassembly models of buildings, based on a literature review and on previous studies in this domain.

2 Required information for disassembly models of buildings

In this study we identify three consecutive disassembly modelling stages in agreement to the study presented by Zhou et al. [7] for manufacturing products. The three stages are: (1) preprocessing stage, (2) analytical disassembly model stage, and (3) performance stage. According to these stages, we present in Table 1 the parameters for disassembly planning of buildings based on (1) lessons learned from previous studies for the implementation of disassembly planning for building archetypes [6] and (2) a literature review of disassembly planning methods for buildings.

2.1 Preprocessing stage

In this stage the critical information regarding parts and the interdependency relationships among the parts of

a disassembly model must be defined. Each disassembly element that is meant to be part of the disassembly model under study must have associated the relationship parameters that link it with the rest of the assembly. The *global disassembly model identifier* is the unique descriptor for identifying all the parts that conform to the same disassembly model. The identifier is an alphanumeric value (e.g., $c_{\#}$, $beam_{\#}$, $part_{\#}$). The *disassembly part type* is the classification for any disassembly part either as a component or a connection. For products' and buildings' disassembly, this classification has been standardized identifying components as c and connections as fasteners f [7,22]. The *disassembly part identification* assigns a numerical identifier for part types, e.g., c_1 and f_1 . *Hosted components* and *hosted connections* register the parts that structurally depend on a host component.

Connection disassembly is the degree of difficulty for a connection to be disassembled usually expressed as a grade of a rating scale. This is a characteristic that has been explored deeply for manufacturing products [7,22]. In contrast, for buildings' disassembly there are just a few studies that have integrated this metric to measure the affordability for deconstruction. The main reason is the lack of studies directed specifically to the assessment of deconstructability of buildings' connections, and with it

Table 1 Required information for disassembly planning of buildings

Source	Preprocessing stage										Analytical disassembly model stage					Performance stage										
	Global disassembly model	Disassembly part type	Disassembly part	Hosted components	Hosted connections	Connection disassembly	Fastener constraint type	Physical interface	Global coordinate system	Local coordinate system	Assembly elements location	Structural composition	Graph data structure	Extraction directions	Object geometry (2D, 3D)	Physical constraints	Modular subassemblies	Working space	Disassembly tool	Disassembly method	Environmental impacts	Disassembly time	Disassembly cost	Disassembly revenue	Disassembly distance	Operation number
[6]	✓	✓	✓	✓	✓	✓	✓	✓	✓	✓	✓	✓	✓	✓	✓	✓	✓	✓	✓	✓	✓	✓	✓	✓	✓	✓
[4]	✓	✓	✓	✓	✓	✓	✓	✓	✓	✓	✓	✓	✓	✓	✓	✓	✓	✓	✓	✓	✓	✓	✓	✓	✓	✓
[8]	✓	✓	✓	✓	✓	✓	✓	✓	✓	✓	✓	✓	✓	✓	✓	✓	✓	✓	✓	✓	✓	✓	✓	✓	✓	✓
[9]	✓	✓	✓	✓	✓	✓	✓	✓	✓	✓	✓	✓	✓	✓	✓	✓	✓	✓	✓	✓	✓	✓	✓	✓	✓	✓
[10]	✓	✓	✓	✓	✓	✓	✓	✓	✓	✓	✓	✓	✓	✓	✓	✓	✓	✓	✓	✓	✓	✓	✓	✓	✓	✓
[11]	✓	✓	✓	✓	✓	✓	✓	✓	✓	✓	✓	✓	✓	✓	✓	✓	✓	✓	✓	✓	✓	✓	✓	✓	✓	✓
[12]	✓	✓	✓	✓	✓	✓	✓	✓	✓	✓	✓	✓	✓	✓	✓	✓	✓	✓	✓	✓	✓	✓	✓	✓	✓	✓
[13]	✓	✓	✓	✓	✓	✓	✓	✓	✓	✓	✓	✓	✓	✓	✓	✓	✓	✓	✓	✓	✓	✓	✓	✓	✓	✓
[14]	✓	✓	✓	✓	✓	✓	✓	✓	✓	✓	✓	✓	✓	✓	✓	✓	✓	✓	✓	✓	✓	✓	✓	✓	✓	✓
[15]	✓	✓	✓	✓	✓	✓	✓	✓	✓	✓	✓	✓	✓	✓	✓	✓	✓	✓	✓	✓	✓	✓	✓	✓	✓	✓
[16]	✓	✓	✓	✓	✓	✓	✓	✓	✓	✓	✓	✓	✓	✓	✓	✓	✓	✓	✓	✓	✓	✓	✓	✓	✓	✓
[17]	✓	✓	✓	✓	✓	✓	✓	✓	✓	✓	✓	✓	✓	✓	✓	✓	✓	✓	✓	✓	✓	✓	✓	✓	✓	✓
[18]	✓	✓	✓	✓	✓	✓	✓	✓	✓	✓	✓	✓	✓	✓	✓	✓	✓	✓	✓	✓	✓	✓	✓	✓	✓	✓
[19]	✓	✓	✓	✓	✓	✓	✓	✓	✓	✓	✓	✓	✓	✓	✓	✓	✓	✓	✓	✓	✓	✓	✓	✓	✓	✓
[20,21]	✓	✓	✓	✓	✓	✓	✓	✓	✓	✓	✓	✓	✓	✓	✓	✓	✓	✓	✓	✓	✓	✓	✓	✓	✓	✓

the establishment of a standardized metric. In this respect, some recent studies have proposed and implemented a BIM-based disassembly score system such as the Disassembly and Deconstruction Analytics System (D-DAS) [23] and Deconstructability Assessment Scoring (DAS) [24]. Both approaches propose innovative ways to measure deconstructability of buildings based on a qualitative description of the demountability of the building connections. Other studies have developed weighted ranking lists to score the grade of deconstructability based on the description of different types of connections and material characterization [13,25,26].

Fastener constraint type indicates the condition of a fastener being removed in either one direction or two directions. *Physical interface characterization* defines the geometrical and mechanical specifications associated to different types of connections (e.g., bolts, screws, rivets, washers, welding). None of the current approaches for disassembly planning of buildings have included this characteristic. However, the *physical interface characterization* plays a critical role for the accurate study of the disassembly properties of a connection type. We consider this characteristic of high relevance for buildings' disassembly. In comparison to manufacturing products, buildings' connections have a higher level of importance for obvious reasons. First, the structural integrity and reliability of any component (structural and non-structural) depends on the appropriate selection, design, dimensioning, and installation of its connections. Failing to achieve this might produce damages to the building and, more important, injuries to its users. Second, buildings' connections represent a higher percentage on the investment.

The *global coordinate system* defines the origin of a 3D cartesian coordinate system associated to all the parts of the disassembly model. The *local coordinate system* defines the local origin of a 3D cartesian coordinate system associated to each disassembly part. The *assembly elements location* constitutes the 3D coordinates that define the location of each disassembly part in the global coordinate system. This characteristic is exclusive for those methods in which the geometrical representation of the disassembly model is the basis for determining physical constraints among components (e.g., contact, motion, and projection constraints).

2.2 Analytical disassembly model stage

The analytical disassembly model is the mathematical representation of the disassembly model, disassembly constraints, and the disassembly precedence relationships. According to the literature review on disassembly planning for products and buildings the most studied analytical disassembly models are interference graphs, Petri nets, and constraint matrices [7]. These

approaches have the objective of describing the composition of the disassembly model in a consistent data structure for its computational processing. In this respect, a *graph data structure* is necessary for establishing the mathematical configuration of the disassembly model. A graph data structure is the abstract representation of a disassembly model through nodes (vertices) and liaisons (edges). For building disassembly, some studies have implemented Graph Data Models (GDM) [10,12,13] and liaison graphs [4,6] as graph data structures for disassembly models. Other studies have used GDM to represent the connectivity between building components [14,15]. In this paper we propose an approach for determining the appropriate parameters for disassembly models at a component level, including the graph data structure. This can be achieved by registering for each component the liaison relationship(s) (fasteners f_n) with the component(s) (c_n) in the next upper level of the disassembly hierarchy (the components that are physically attached and supported by the component under study), as demonstrated in a previous study [6]. Then, in a next processing stage, the registered information for all of the components can be arranged in a matrix (liaison matrix) for the computation of the disassembly sequence.

The *structural composition relationship* is an important characteristic for disassembly models of buildings. This characteristic indicates the structural composition of components inside a disassembly model. For manufacturing products, any fastener can be removed from the disassembly model as long as the fastener is physically accessible. In comparison, in a building composition some fasteners could be physically accessible and removed but required for the structural stability of the assembly.

Extraction directions are the possible paths for removing any disassembly part. As a generality for disassembly planning methods the number of extraction directions is four in a 2D environment (+x, -x, +y, -y) and six in a 3D environment (+x, -x, +y, -y, +z, -z) [7,27,28]. The *object geometry* is the information related to the geometrical characteristics of the disassembly parts. *Physical constraints* are the physical restrictions of a disassembly part in any extraction direction (contact constraints, motion constraints, and projection constraints) [7,27,28].

Modular subassemblies is the property that form modules conformed by two or more disassembly parts which are to be retrieved together. Finally, the *working space* is an important characteristic for buildings' disassembly related to the necessary physical space for a human worker to develop disassembly works. The working space has also been explored for products' disassembly [7,29]. However, due to the significant difference of scale and the nature of the disassembly

works, the implications for buildings are significantly different. For buildings it is necessary to add more detailing to the process of executing dismantling works in order to make the disassembly planning estimations significant. This includes analyzing the necessary space for manipulating disassembled components inside and outside the building, investigating the disassembly activities that need the participation of more than one human worker or mechanical manipulator (or the combination of both), and resolving resource allocation and scheduling (e.g., the possibility of developing disassembly works on different work fronts simultaneously). These are topics that have been continuously under development in Project Management (PM) for building construction. We argue the need to extend the scope of the investigations to disassembly planning of buildings.

2.3 Performance stage

This stage is related to the objectives to optimize the disassembly planning. The optimization objectives can change according to the particularities of the project and according to the goals of the stakeholders. The most common optimization objectives are low cost, low environmental impact, high revenue, and decreased time execution [7]. For a given optimization, objective specific information per disassembly part must be defined as a numerical value and unit.

Disassembly tool information establishes the instrumentation to be used for disassembly. The use of mechanical tools decreases the time for the disassembly process but increments the cost [7]. The *disassembly method* refers to the depiction of disassembly works per building component, such as perfect disassembly, destructive disassembly, and selective demolition [8]. *Environmental impacts* refer to the associated environmental impacts (e.g., Global Warming Potential [GWP], Primary Energy Demand [PED]) per building component according to the definition and scope of an LCA. *Disassembly time, cost, and revenue* are the designated amount of time, cost, and profit for disassembling a building component depending on the disassembly method and instrumentation used. The *disassembly distance* is the distance moved in disassembling a component.

The *operation number* is the total number of activities developed for the disassembly process. This domain has only been studied for the disassembly planning of manufactured products. Here, the quantified activities depend on the disassembly approach. For example, some studies have quantified the number of change of directions of a disassembly tool (manipulated by a worker) that are needed to remove fasteners [7]. Other studies have quantified the total distance traveled by a worker through different working stations in a

disassembly line. Similarly, the consideration of *operation number* must be included as part of the disassembly planning for buildings in future investigations, to determine the correct approach and appropriate metrics.

Disassembly energy consumption is relevant when robotic disassembly is considered for total or partial execution of the works. It refers to the energy consumption of robots and heavy machinery in the disassembly process. It is important to mention that the last three parameters of *disassembly distance, operation number, and disassembly energy consumption* were gathered from a literature review, developed by Zhou et al. [7], of disassembly planning for manufactured products. Even though none of the approaches for buildings presented in Table 1 includes these parameters, we consider they are relevant to the disassembly of buildings and should be included, adapted, and implemented for buildings assets.

3 BIM disassembly parameters

BIM is arguably the most important technology used in the construction industry for planning and monitoring building processes along the entire life cycle of a building project [30]. BIM is a highly organized 3D model-based graphical interface for the efficient planning, designing, constructing, and management of buildings assets. In the last three decades, plenty of investigations have explored the benefits of implementing BIM in different life cycle stages of building projects, however its implementation for the End-of-Life (EoL) stage is still underdeveloped [4,6]. In this paper we argue that the current information included in BIM is incomplete and undefined for specific tasks in the EoL stage of buildings such as disassembly planning. Some of this information is indirectly embedded in BIM elements according to the Industry Foundation Classes (IFC) schema, which is the universal data format for BIM. Therefore, according to the disassembly model characteristics presented in the last section we define the BIM parameters needed for disassembly models for buildings and map the corresponding IFC entities for their definition (Table 2). These parameters can be gathered from an information model, during the planning and design stage. The parameters can be categorized according to their nature as: type parameter and instance parameter. Type parameters are the same for all the existences of BIM elements that belongs to the same family type, while instance parameters are unique to a kind of BIM object. Overall, 27 parameters (9 type parameters, 18 instance parameters) were identified (see Table 2). Figure 2 shows the mapped parameters for disassembly models into the IFC schema. The definitions of the type and instance parameters displayed in Figure 2 are a suggested first

Table 2 BIM parameters for disassembly models

Stage	Parameter	Unit	Type/instance	Available/new/retrievable	
Preprocessing	Global disassembly model	Numeric	Instance	Available/read	
	Disassembly part type	Binary	Instance	New/write	
	Disassembly part identification	Alphanumeric	Instance	New/generate	
	Hosted components	Alphanumeric	Instance	New/write	
	Hosted connections	Alphanumeric	Instance	New/write	
	Connection disassembly	Numeric	Type	New/write	
	Fastener constraint type	Numeric	Type	New/write	
	Physical interface	Numeric	Instance	Available/read	
	Global coordinate system	Numeric	Type	Available/read	
	Local coordinate system	Numeric	Instance	Available/read	
Analytical disassembly model	Assembly elements location	Numeric	Instance	New/generate	
	Structural composition	Alphanumeric	Instance	New/generate	
	Graph data structure	Alphanumeric	Instance	New/generate	
	Extraction directions	Numeric	Type	Available/read	
	Object geometry (2D, 3D)	NA	NA	Available/read	
	Physical constraints	Numeric	Instance	New/generate	
	Modular subassemblies	Numeric	Type	Available/read	
	Working space	Numeric	Type	New/write	
	Performance	Disassembly tool	Alphanumeric	Type	New/write
		Disassembly method	Alphanumeric	Type	New/write
Environmental impacts (LCA)		Numeric	Instance	Retrievable/read	
Disassembly time		Numeric	Instance	Retrievable/read	
Disassembly cost		Numeric	Instance	Retrievable/read	
Disassembly revenue		Numeric	Instance	Retrievable/read	
Disassembly distance		Numeric	Instance	New/generate	
Operation number		Numeric	Instance	New/generate	
Disassembly energy consumption	Numeric	Instance	Retrievable/read		

approach for simple BIM archetypes. This approach needs future revisions and investigations to demonstrate their functionality at a large scale for disassembly projects. As it happens for building projects, the definition of type or instance parameters for BIM elements can be customized depending on the objectives and characteristics of each project.

The parameters can be categorized according to the nature of the registered information such as *available*, *new*, and *retrievable* [31]. The *available* category is embedded information in the BIM elements that can be accessed (*read*) directly from the IFC schema. The *new* category refers to information missing in the BIM elements that can either be entered (*write*) by the user during the modeling process, or it can be estimated (*generate*) with a customized subroutine. The *retrievable* category is information that is not embedded in the BIM elements. However, the information is available in external databases and it can be accessed (*read*) and registered with an appropriate subroutine.

As it is displayed in Figure 2, we propose the mapping of the disassembly model parameters into the IFC schema. In this study, the process of retrieving, updating, and registering information in the IFC file is done through a Visual Programming Interface (VPL) in the BIM modeler Revit. In this stage of development, the whole process is manual, as a proof of concept, by entering the

information of a disassembly model archetype from a previous study [6]. In future stages of development, the appropriate subroutines will be developed for the automated retrieving, updating, and registering of information in the IFC file.

4 Case study – BIM for disassembly planning

For the functional demonstration of the presented framework of assembly model characteristics and corresponding BIM parameters, we developed an information model with all the required parameters for developing the disassembly planning for retrieving targeted components. The archetype used in this demonstration comes from a previous study [6]. Similarly, the validation of the model is achieved through the comparison of the parameters included in the BIM model with the ones resolved for the analytical disassembly model of the previous study. Figure 3 shows the BIM interface with the parameters of the BIM element c_1 (structural steel column). Some of the parameters of the performance stage do not have an associated value. The reason is the lack of availability of

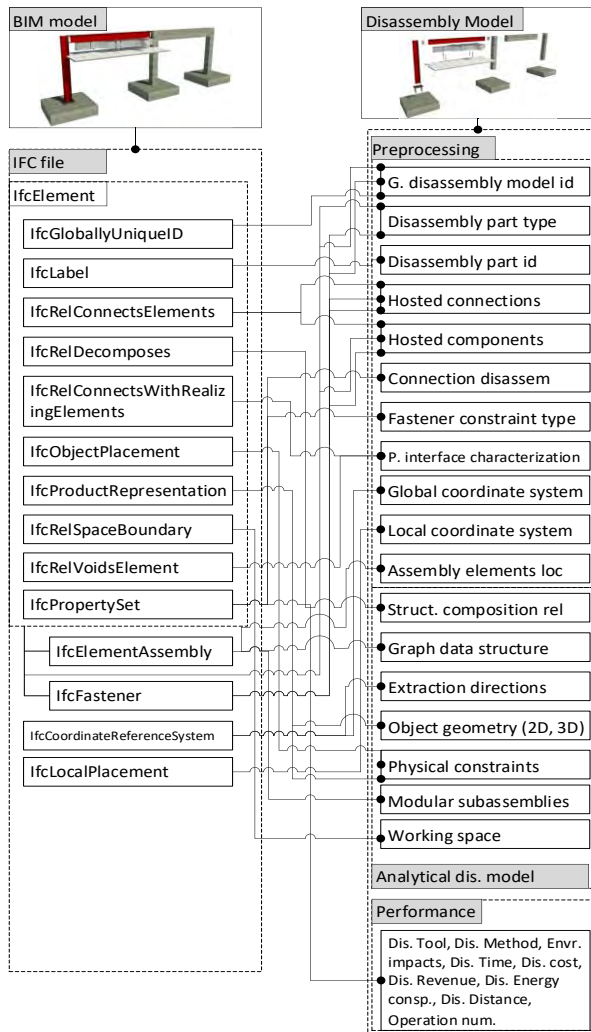


Figure 2. Mapped parameters into IFC for disassembly models

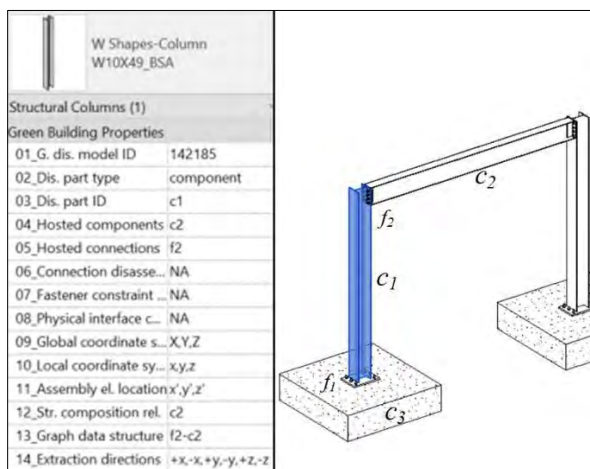


Figure 3. BIM disassembly planning parameters

reliable sources to gather such information. As discussed in subsection 2.3, that information depends on the kind of optimization assessment to perform.

5 Conclusions and future work

The results of this study demonstrate that it is possible to set the appropriate parameters for disassembly models using BIM. In this respect the IFC schema can be used to determine most of the disassembly parameters. The parameters can be retrieved directly from the IFC schema, or they can be calculated using a combination of them. It is demonstrated that it is technically feasible to develop semantically enriched BIM disassembly models using a commercial BIM software. With the disassembly BIM model ready, in the next steps it will be possible to implement any of the disassembly planning theories to develop assessments for the partial or total disassembly of the building structures. This study provides a comprehensive overview of the necessary information for disassembly models of buildings. The framework presented in this study can help to overcome the technical barriers that nowadays limit the implementation of disassembly planning in a systematic and standardized way.

A future step for this research is the development of a BIM-based automated semantic enriching engine for disassembly models. This approach will improve the generation of correct and fully semantically enriched BIM models. As discussed in Section 3, some of the proposed parameters can be retrieved from the BIM model (*available/read*), some can be entered by the users during the modelling process (*new/write*), some others can be estimated (*new/generate*), and others can be retrieved from external databases (*retrievable/read*). For any of these cases it is possible to develop the appropriate technology, e.g. Visual Programming Language (VPL) or Application Programming Interphase (API) subroutines, for the systematization and automation of the process. These techniques have become very popular in the field of open BIM in the last years. They have demonstrated efficiency for the manipulation of information in BIM environments, technical feasibility for interconnecting multiple digital technologies, and the interoperability of the processes. Therefore, the whole process of semantic enrichment of a BIM disassembly model, the verification of the completeness and correctness of the information, and the development of the disassembly assessments can be integrated in a BIM platform.

One of the limitations of the proposed approach is the elevated amount of data to integrate into a BIM model, for each one of the BIM elements (components and fasteners). This high Level of Detail (LoD) of

information could be difficult to compute for large building assemblies. However, it could be possible to implement this approach for representative subassemblies to reduce the computational requirements. Also, with the development of the computational technology, in the future this kind of high LoD assessments could be possible and technically affordable. Another limitation, is the lack of available and reliable information regarding disassembly/deconstruction works. This is related to the performance stage of the proposed approach where it is necessary to have access to disassembly information for building components such as cost, time, environmental impacts, disassembly methods, among others. Nevertheless, the current reliable information in this field is very limited to the most recurrent and traditional techniques in the construction industry. This field has attracted the attention of researchers, companies, and governments in the last two decades due to the global climate emergency. Therefore, more investigations and regulations in the industry have appeared and it is expected that they will keep increasing in the coming years. The evidence shows that there is huge potential for the reuse of materials in the built environment, and the new trends of reusable buildings will lead the future for sustainable urban development.

Acknowledgements

This research was conducted at the Future Cities Lab Global at Singapore-ETH Centre. Future Cities Lab Global is supported and funded by the National Research Foundation, Prime Minister's Office, Singapore under its Campus for Research Excellence and Technological Enterprise (CREATE) programme and ETH Zurich (ETHZ), with additional contributions from the National University of Singapore (NUS), Nanyang Technological University (NTU), Singapore and the Singapore University of Technology and Design (SUTD).

References

- [1] S. Badi, N. Murtagh, Green supply chain management in construction: A systematic literature review and future research agenda, *Journal of Cleaner Production*. 223 (2019) 312-322, <https://doi.org/10.1016/j.jclepro.2019.03.132> ISSN 0959-6526.
- [2] F. Jalaei, Integrate Building Information Modeling (BIM) and Sustainable Design at the Conceptual Stage of Building Projects, Doctoral Dissertation, 2015, University of Ottawa, .
- [3] A. Mahpour, Prioritizing barriers to adopt circular economy in construction and demolition waste management, *Resources, Conservation and Recycling*. 134 (2018) 216-227.
- [4] B. Sanchez, C. Rausch, C. Haas, Deconstruction programming for adaptive reuse of buildings, *Automation in Construction*. 107 (2019) 102921, <https://doi.org/10.1016/j.autcon.2019.102921> ISSN 0926-5805.
- [5] C. Rausch, B. Sanchez, C. Haas, Spatial Parameterization of Non-Semantic CAD Elements for Supporting Automated Disassembly Planning, *Spatial Parameterization of Non-Semantic CAD Elements for Supporting Automated Disassembly Planning*, 2019 Modular and Offsite Construction (MOC), Banff, AB, Canada, 2019, pp. 108-115, <https://doi.org/10.29173/mocs83> .
- [6] B. Sanchez, C. Haas, A novel selective disassembly sequence planning method for adaptive reuse of buildings, *Journal of Cleaner Production*. 183 (2018) 998-1010, <https://doi.org/10.1016/j.jclepro.2018.02.201> ISSN 0959-6526.
- [7] Z. Zhou, J. Liu, D.T. Pham, W. Xu, F.J. Ramirez, C. Ji, Q. Liu, Disassembly sequence planning: Recent developments and future trends, *Proceedings of the Institution of Mechanical Engineers, Part B: Journal of Engineering Manufacture*. (2019), 10.1177/0954405418789975.
- [8] B. Sanchez, C. Rausch, C. Haas, R. Saari, A selective disassembly multi-objective optimization approach for adaptive reuse of building components, *Resources, Conservation and Recycling*. 154 (2020), <https://doi.org/10.1016/j.resconrec.2019.104605> ISSN 0921-3449.
- [9] B. Sanchez, C. Rausch, C. Haas, T. Hartmann, A framework for BIM-based disassembly models to support reuse of building components, *Resources, Conservation and Recycling*. 175 (2021) 105825, <https://doi.org/10.1016/j.resconrec.2021.105825> ISSN 0921-3449.
- [10] F. Denis, C. Vandervaeren, N.D. Temmerman, Using network analysis and BIM to quantify the impact of Design for Disassembly, *Buildings*. 8 (2018) 113, <https://doi.org/10.3390/buildings8080113> ISSN 2075-5309.
- [11] M. Mahmoudi Motahar, S.H. Hosseini Nourzad, A hybrid method for optimizing selective disassembly sequence planning in adaptive reuse of buildings, *Engineering, Construction and Architectural Management*. 29 (2021) 307, 10.1108/ECAM-12-2020-1023 ISSN 0969-9988.
- [12] C. Vandervaeren, W. Galle, A. Stephan, N. De Temmerman, More than the sum of its parts: Considering interdependencies in the life cycle material flow and environmental assessment of demountable buildings, *Resources, Conservation and Recycling*. 177 (2022),

- 10.1016/j.resconrec.2021.106001.
- [13] A. Menasce, N. Kobylinska, Exploratory development of graph-based models for disassembly, 2021, .
- [14] A. Khalili, D.K.H. Chua, IFC-based graph data model for topological queries on building elements, *Journal of Computing in Civil Engineering*. 29 (2015), 10.1061/(ASCE)CP.1943-5487.0000331.
- [15] S. Isaac, T. Bock, Y. Stoliar, A methodology for the optimal modularization of building design, *Automation in Construction*. 65 (2016) 116-124, <https://doi.org/10.1016/j.autcon.2015.12.017> ISSN 0926-5805.
- [16] S. Schaubroeck, R. Dewil, K. Allacker, Circularity of building stocks: Modelling building joints and their disassembly in a 3D city model, *Circularity of building stocks: Modelling building joints and their disassembly in a 3D city model*, *Procedia CIRP*, vol. 105, 2022, pp. 712-720, 10.1016/j.procir.2022.02.119 Available at <https://www.scopus.com/inward/record.uri?eid=2-s2.0-85127526824&doi=10.1016%2fj.procir.2022.02.119&partnerID=40&md5=3a839546b9cc29633b611091e7723072>, .
- [17] E. Durmisevic, Transformable building structures: design for disassembly as a way to introduce sustainable engineering to building design & construction, (2006).
- [18] E. Durmisevic, A. Guerriero, C. Boje, B. Domange, G. Bosch, Development of a conceptual digital deconstruction platform with integrated Reversible BIM to aid decision making and facilitate a circular economy, Development of a conceptual digital deconstruction platform with integrated Reversible BIM to aid decision making and facilitate a circular economy, *Proc. of the Joint Conference CIB W78-LDAC*, vol. 2021, 2021, pp. 11-15, .
- [19] P.R. Beurskens, The development of an evaluation method to support circular building design, (2021).
- [20] D. Schwede, Application of RecyclingGraphs for the Optimisation of the Recyclability in Building Information Modelling, Application of RecyclingGraphs for the Optimisation of the Recyclability in Building Information Modelling, *IOP Conference Series: Earth and Environmental Science*, vol. 323, IOP Publishing, 2019, pp. 012044, .
- [21] D. Schwede, E. Störl, System for the analysis and design for disassembly and recycling in the construction industry, *Central Europe towards Sustainable Building Prague 2016 (CESB16)*. (2016).
- [22] A.J.D. Lambert, Disassembly sequencing: A survey, 41 (2003) 3721-3759, 10.1080/0020754031000120078 ISSN 0020-7543.
- [23] L.A. Akanbi, L.O. Oyedele, K. Omoteso, M. Bilal, O.O. Akinade, A.O. Ajayi, J.M. Davila Delgado, H.A. Owolabi, Disassembly and deconstruction analytics system (D-DAS) for construction in a circular economy, *Journal of Cleaner Production*. 223 (2019) 386-396, 10.1016/j.jclepro.2019.03.172.
- [24] A. Basta, M.H. Serror, M. Marzouk, A BIM-based framework for quantitative assessment of steel structure deconstructability, *Automation in Construction*. 111 (2020) 103064.
- [25] L. Mattaraia, M.M. Fabricio, R. Codinhoto, Structure for the classification of disassembly applied to BIM models. *Architectural Engineering and Design Management*. (2021), 10.1080/17452007.2021.1956420.
- [26] D. Cottafava, M. Ritzen, J. van Oorschot, Report: D6. 1 Report on benchmarking on circularity and its potentials on the demo sites, (2020).
- [27] S.S. Smith, W. Chen, Rule-based recursive selective disassembly sequence planning for green design, *Advanced Engineering Informatics*. 25 (2011) 77-87, <http://dx.doi.org/10.1016/j.aei.2010.03.002> ISSN 1474-0346.
- [28] S. Smith, G. Smith, W.-. Chen, Disassembly sequence structure graphs: An optimal approach for multiple-target selective disassembly sequence planning, *Advanced Engineering Informatics*. 26 (2012) 306-316, <https://doi.org/10.1016/j.aei.2011.11.003> ISSN 1474-0346.
- [29] Z.-. Li, S. Wang, W.-. Yin, Determining optimal granularity level of modular product with hierarchical clustering and modularity assessment, *Journal of the Brazilian Society of Mechanical Sciences and Engineering*. 41 (2019), 10.1007/s40430-019-1848-y.
- [30] H. Mattern, M. König, BIM-based modeling and management of design options at early planning phases, *Advanced Engineering Informatics*. 38 (2018) 316-329, <https://doi.org/10.1016/j.aei.2018.08.007> ISSN 1474-0346.
- [31] F. Karim, F.H. Abanda, V. Christos, W. Graham, Taxonomy for BIM and Asset Management Semantic Interoperability, *Journal of Management in Engineering*. 34 (2018) 04018012, 10.1061/(ASCE)ME.1943-5479.0000610.

Building insulation renovation: a process and a software to assist panel layout design, a part of the ISOBIM project.

Michel Aldanondo¹ Julien Lesbegueries¹ Andréa Christophe^{1,2} Elise Vareilles³ Xavier Lorca¹

¹ Université de Toulouse / IMT Mines Albi / Centre Génie Industriel – Albi, France

² Armines – Paris, France

³ Université de Toulouse / Isae-SUPAERO / DISC – Toulouse, France
firstame.lastname@mines-albi.fr, firstame.lastname@isae-supaeero.fr

Abstract –

In order to lower the huge carbon dioxide emissions due to building heating, the goal of this communication is to show how the design of insulation panel layout can be strongly computer-aided during façade building energy renovation projects.

The work has been achieved during an applied collaborative research project (ISOBIM), whose purpose is to develop open web integrated decision-aided tools to support a whole digital engineering retrofitting processes using modular timber framing panels.

First, the panel layout design problem is analyzed and permit to identify a four steps design process supported by three data models. Then, once the problem is preprocessed to remove some singularities, an automatic layout design algorithm is proposed and discussed. An example illustrates the propositions and support discussions.

Keywords –

Building insulation renovation, Panel layout design, Aiding design system, Constraint-based problem

1 Introduction

According to the European commission [1] “Today, roughly 75% of the European Union (EU) building stock is energy inefficient. This means that a large part of the energy used goes to waste. Such energy loss can be minimized by improving existing buildings”. The same report enhances that such building renovation can reduce the EU’s total energy consumption by 5-6% and lower carbon dioxide emissions by about 5%.

Consequently, many European and national research agencies have launched research programs to encourage the systematic renovation of buildings. In France the national research agency (ANR) supports a collaborative project called ISOBIM. The goal of the project is to develop open web integrated decision-aided tools to

support a digital engineering retrofitting processes using modular timber framing panels. In this project we consider “heavy” retrofitting panels, meaning that they integrate doors and windows in opposition with “light” solutions that by-pass them, the reader can consult [2] or [3] for more details.

It is important to note that “light solutions” require a significant amount of work in sizing, cutting and fitting the panels which must be done on the building site during the renovation. In contrast, “heavy solutions” assume that all panels are prefabricated in the factory and then assembled without rework on site. The “light solutions” are more often related to a craft approach while the “heavy solutions” correspond more to an industrial activity. The solutions proposed in this article are fully within the scope of an industrial approach which allows to reduce the manufacturing and assembly costs and the duration of the renovation on site.

In order to provide ideas about “heavy solution”, some order of magnitude about panels used in “heavy solutions” are provided. In terms of dimensions, maximum panel sizes are around 3.5 meters by 13 meters because of transportation constraint. In terms of weight such a panel (3.5x13) can weigh between 1.5 to 4 tons. For cost, including manufacturing and installation, a panel without any door or window is between 150 to 250 €/m² in Europe. In terms of energetic performance improvement, it is too much case dependent to provide exact result, but such solution can be used only if the heating cost are at least divided by 2 to 4.

Considering the “heavy solution”, some global retrofitting process models can be found in the literature. For our work, we consider the one published in [4] that considers four main steps: (i) building digitalization, (ii) panels layout design, (iii) panel manufacture planning (iv) on site project management (figure 1).

Within the framework of the ISOBIM collaborative research project, these 4 steps have been distributed to

various partners and we are in charge of the second step (panels layout design) and with the transition between the first and second step (preparation of the layout design just after building digitalization). Consequently, this paper is dedicated to panel layout design.

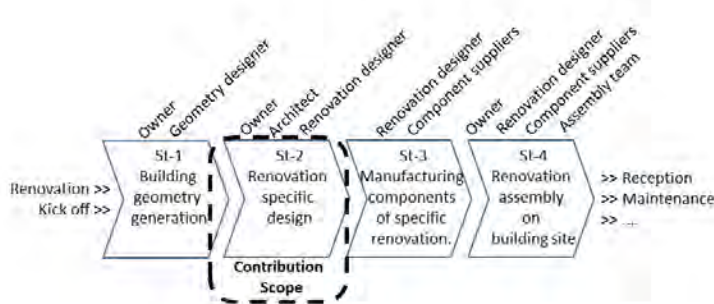


Figure 1. Work situation

The research work and this communication follow a progressive problem-solving approach where three issues are successively addressed. First, the tasks of the complete design process are defined. Then the data feeding and resulting from these tasks are identified and modeled. Finally, the core task of the design is instrumented with a solution finding algorithm.

Consequently, the contribution is organized as follows. In a first section, we will discuss and propose a process model that starts after the building digitalization and finishes after the final design of the panel's layout, shown as the "contribution scope" in figure 1. In a second section, we will discuss and propose three building facade models that support the tasks of the previous process. In a third part we will discuss and propose an algorithm that can automate the panel layout design.

2 The layout design process

The goal of this section is to clarify and to detail the tasks necessary before the panel layout design. We will first detail the need of a manual design step and then the need of a preparation step before automatic design. We will conclude with the global process and add a final correction step.

2.1 About a manual layout design step

According to some authors, as Hillebrand et al. [5] or Barco et al. [6], the algorithms that are able to solve the panel layout design problem requires strong hypothesis relevant to the considered entities.

We follow these ideas and first assume that our automatic layout design algorithm considers only rectangle building facade and only rectangle panels. Consequently, facades with triangular gable ends will require manual layout.

We also assume that the panels must be fixed at the

top (mainly for support) and bottom (mainly for wind). As a consequence, specific parts of the facade as acroterion (facade top) or sub-basement (facade bottom) that don't have resisting area at their top or bottom will also require a manual layout design.

2.2 About preparation before manual design

If building facades have windows and doors that will be replaced and integrated into the panels, they also can have multiples singularities as: air conditioning unit, solar panel, balcony, lights, garage door, pipes... For all these singularities, it must be decided during the preparation task, if they should be associated with a hole in the panel or if they should be by-passed by the panels. Rectangle elements gathering: (i) singularities associated with panel holes, (ii) windows and (iii) doors will be called from now panel "outin". Elements gathering singularities by-passed by panels will be called from now panel "outout".

As we have assumed before, panel are fixed at their top and bottom with mechanical supports. These supports are sealed in the facade at specific places called resisting areas that can handle high effort, note that a large isolating panel (12 meters by 3 meters) can weight up to 4 tons. During the preparation task, these specific areas must be identified on the building geometry by building experts and correspond most of the time with floor-end, partition-wall or their crossing. Furthermore, for automatic layout algorithm, they should be approximated by support lines where panel supports will be sealed. These support lines can be either vertical or horizontal.

2.3 Proposed layout design process

Given previous assumptions, we propose the following panel layout process in four steps (figure 2).

The first one, "Preparation" identifies and transforms resisting areas in support lines and associates any facade element with either outin (that will be integrated in a single panel) or outout (that will be by-passed by the panels).

A second one, "Manual design" that allows the user to manually design the panels that can not be taken into account by the automatic algorithms as: non-rectangular panels, panels for acroterion or sub-basement.

A third one, "Automatic design" that will be detailed in a following section.

A last step, "Manual touch up" allows the architect or building owner to manually correct the proposed panel layout.

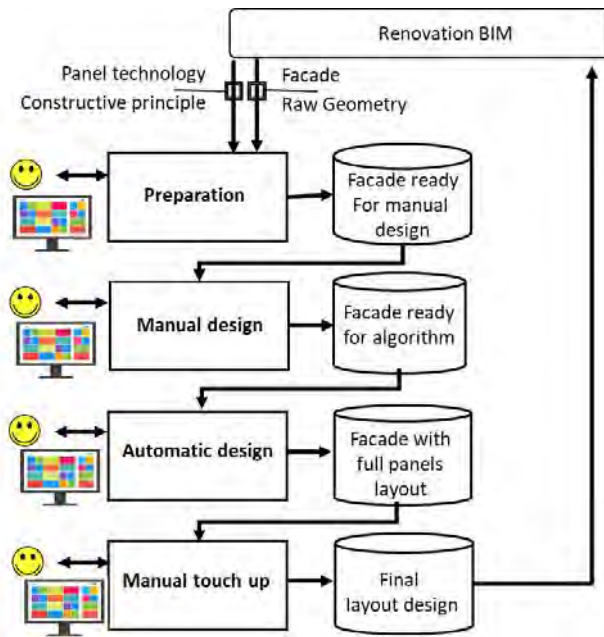


Figure 2. Panel layout design process

3 The facade models

Given previous process, we describe in this section the tree facade models that are used during the layout design.

In order to represent the façade models, we use the standard class diagram of the Unified Modeling Language that can show how systems can be decomposed in sub-systems. We use mainly the two relations : (i) composition aggregation (AND represented with a diamond symbol) that shows the physical composition of the system and (ii) Generalization/Inheritance (OR represented with a triangle symbol) that shows various possibilities for each sub-system.

The first model (figure 3) is the first description or raw geometry of the building’s facades. The building is a set of facades, where each facade gathers four kinds of elements: non-resisting, resisting, singularity and add-on. All of them are rectangle except the add-on non-rectangle element.

The second model (upper part of figure 4) is the facade ready for manual and automatic layout design. This model gathers only three kinds of elements: Resisting Support lines, Outin elements (that should be integrated in a single panel) and Outout elements (that should be by-passed by panels).

The last model shows the layout solution as a set of panels including outin elements and mechanical supports (lower part of figure 4).

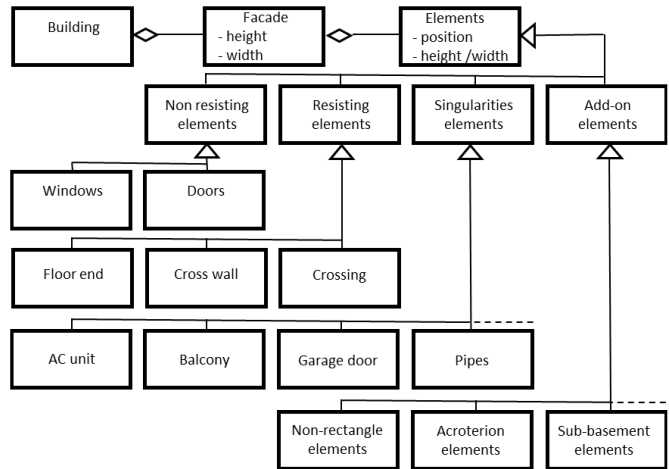


Figure 3. Facade raw geometry model

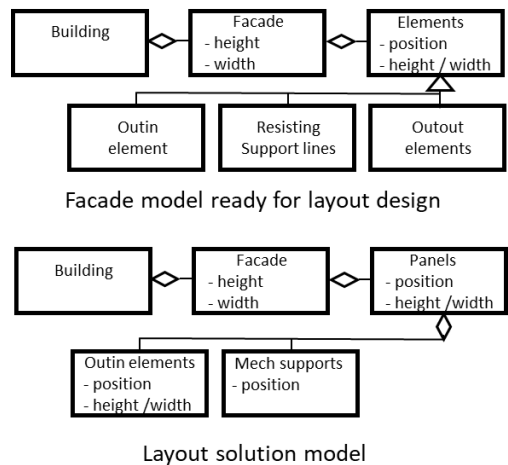


Figure 4. Facade model before and after design

4 The proposed layout design algorithm

In a first part, we summarize the problem inputs, the panel technology constraints and optimization criteria. Then we propose a small problem analysis in order to introduce our heuristic approach. Finally, we will present the main ideas of our layout design algorithm.

4.1 Inputs, panel constraints and criteria

Given previous elements, the layout design automatic algorithm only considers as an input the three elements: support lines, outin and outout, an example is given in figure 5. This case does not need any manual panel design because everything is rectangular and there is no special panel for facade top and bottom. According to most panel manufacturers each couple of balcony and window element must be associated in a single outin rectangle.

In terms of panel technology, a panel has minimum and maximum dimensions (width and height). For transportation constraints, each dimension should be less than the truck length (around 14 meters) and one dimension should be lower than the truck height (around 3.5 meters). The layout solution, is a set of panels that covers the facade except "outout". Panel dimensions should be larger than the integrated elements outin. For panel rigidity, a minimum distance between the outin edge and the panel border can exist. Each panel has a weight more or less proportional to its area. Lower panel border can be supported either by a lower horizontal support line or by its lower corners on a vertical or horizontal support line. Panels can have two orientations, horizontal or vertical. Horizontal panels have a width larger than height while it is the opposite for vertical ones. Panel providers prefer most of the time horizontal panels if this is possible.

The problem is consequently to find a set of panels that cover the facade. As many solutions can exist, different criteria can be considered. The most frequent are: minimize the number of panels, maximize the panel size or minimize the length of joins between panels. They all globally go towards the same direction that is to minimize heat loss.

4.2 Problem analysis

Given the proposed elements, this problem can be classified with respect to two types of problems: "cutting and packing" [7] and "product configuration" [8].

Cutting and packing problems deal with small and large objects and try to place the small ones into the large ones. Classic examples are: steel bars and plates production, fabrics cutting, vehicle loading, memory allocation... For problem with two dimensions, as our panel layout problem, four characteristics impact the solution complexity [9] :(i) the quantity of large objects, 1 or more than 1 (ii) the quantity of small objects, given as an input or to be identified, (iii) the size of small objects, identical or not, and (iv) the sizes of small objects, given as an input or to be identified.

Product configuration considers that a product is a set of predefined components (standard or configurable) that respect various constraints (coming from marketing, design, manufacturing...). The characteristics impacting the problem complexity are: (i) the quantity of components in a product: given as an input or to be identified, (ii) the fact that the components are: standard (frozen dimensions) or configurable (dimensions to be identified but limited) and (iii) the constraints complexity acting on all of these objects.

For these two approaches, when the quantity of small objects and relevant dimensions are given as an input, it is quite easy to define the space of solutions as a tree and to define systematic search algorithms. When the problem size and/or complexity are moderate, it is possible to scan the total solution space and to identify optimal solutions by combining solving and filtering algorithms. When we quit these kinds of situations, it is much more difficult to define systematic algorithm and the definition of heuristics becomes most of the time necessary.

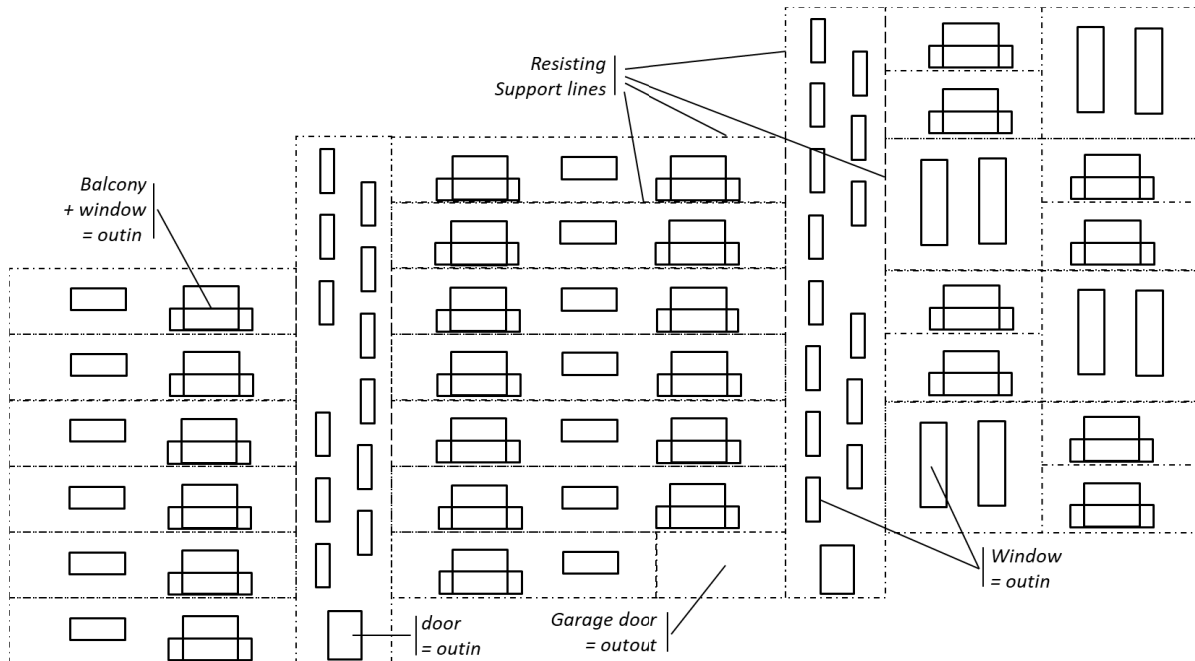


Figure 5. Example of facade model ready for automatic layout design

It sounds rather obvious that our panel layout design problem is at the top of the complexity scale due to: (i) the quantities, dimensions and positions of all the small objects (panels) than must be identified and (ii) the diversity and quantity of geometric constraints that should be respected. The most delicate characteristic to handle is that the number of small objects is to be identified. This effectively implies that the variable quantity of the problem (or problem size) is not known when the algorithm is launched. Authors, as Barco et al. [10], have modeled this whole problem as a constraint satisfaction problem and shown that there is no generic constraint-based algorithm able to handle it.

As this work belongs to a collaborative operational project, it is necessary to provide a robust solution that works with all previous characteristics, we therefore designed a heuristic-based algorithm. But we also try to figure out how constraint-based solvers could deal with our problem. The next section presents the main ideas of our automatic panel layout design algorithm.

4.3 Layout design algorithm

After a small introduction, we describe the general structure algorithm then we detail the algorithm for horizontal panels and finish with some experimental results and discussion.

4.3.1 Algorithm key parameters

The heuristic we propose is parameterized according to two key parameters:

- Orientation strategy: HORIZONTAL or VERTICAL. This parameter defines the preferred orientation of the panels defined by the user. A panel can be horizontal: in this case it is attached at the bottom and top of support lines, or vertical: in this case, the panel is fixed on its 4 corners.
- Direction strategy: RIGHT or LEFT. This parameter defines if the heuristic path starts by going to the right or to the left.

However, regardless of the chosen parameters, the heuristic as a whole traverses the facade from bottom to top, i.e., the first panels will be positioned at the bottom and the last ones at the top. This is compliant with the assembly process that always start at the bottom and goes up floor by floor.

In order to start the design algorithm, we need to set some initial starting points. These points will be stored in a list, that will be filled while traveling through the facade, and removed once taken into account. The termination predicate of the algorithm is then the emptiness of this list. Initially, the starting points list is filled with each lower right and left corner of the perimeter of the facade.

4.3.2 Algorithm general structure

The general algorithm behavior is a loop running while starting points remain in a stack ordered from the bottom to the top (Algorithm 1). While running, it tries to find a panel in the desired orientation and direction. If the first attempt fails, another try is made with the other available orientation. For instance, if the algorithm is launched with RIGHT and HORIZONTAL parameters, the algorithm will first look for a right-directed horizontal panel, and if it's not possible a right-directed vertical panel. If a panel is found, it is added to the solution list that will be returned at the end of the loop. Consequently, possible new starting points are added based on the new panel : for right direction the two added points are panel top left and bottom right, while for the other they are top right and bottom left.

Algorithm 1 General layout design structure.

```

1: Let Panel := x, y, width, height, out-ins
2: Let p a Point variable x, y
3: Let panel a panel variable
4: direction ← RIGHT
5: orientation ← HORIZONTAL
6: startingPoints ← findStartingPoints(F, direction) // ordered stack
7: Let solution := [Panel]
8: solution = []
9: while startingPoints is not empty do
10:  p ← selectNextPoint(startingPoints) // bottom to top, then direction
11:  panel = addPanel(p, F, cp, direction, orientation)
12:  if panel is null then
13:    panel = addPanel(p, F, cp, direction, other(orientation))
14:  end if
15:  if panel is null then throw Error (No solution found.)
16:  else
17:    solution.add(panel)
18:    addStartingPoints(startingPoints, panel)
19:  end if
20: end while
21: return solution

```

Lines 1 to 8 are variable definitions and input parameters:

1. A Panel data structure is defined (basically a rectangle with some out-ins)
2. A p variable of type Point
3. A panel variable of type Panel
4. Direction parameter set
5. Orientation parameter set
6. A set of points is calculated to start the algorithm, using one of the preparation algorithms
7. The type of the return value is set (an array of panels)
8. Return value set

The addPanel() function used in Algorithm 1 is a simplification for addHorizontalPanel() and addVerticalPanel() combination. They are very similar and differs only on their supporting technique. Both functions are given a starting point and have for main goal to find the best second point defining the largest valid panel. For clarity, the first function is detailed in the next paragraph.

4.3.3 Horizontal panels detailed algorithm

The horizontal panel design algorithm is divided into 2 main actions (see Algorithm 2). First it builds a hash map of possible coordinates - for each possible y, possible x are stored (line 2). Then the biggest valid panel is found by browsing ordered possible coordinates (line 25 to 35).

Given a starting point p of coordinates {xp, yp}, the algorithm is looking for a support-line that touches p. Then a geometry collection of all contiguous support-lines found from the first one is gathered (findSupportLines() line 3). As a result, we can obtain a horizontal line that has got minimum and maximum X coordinates.

We store then the maximum x (or minimum x if direction is LEFT) in the bottomMaxX variable (bottomMinX). This gives us the range [xp, bottomMaxX] ([bottomMinX, xp]) of all the possible X coordinates regarding the bottom side of the panel (line 5 and 16). But we have to test also the possible Xs regarding the top side of the panel.

Then the possible Y coordinates are calculated, given the initial p point. For each possible y, we can deduce the maximum x (minimum x) for both bottom and top support lines (by using findSupportLines() again - line 9 and 19). Once ordered, possible coordinates are stored.

The second step of the algorithm is a double loop trying to build and return the biggest valid panel candidate. By ordering the coordinates we ensure that the first valid panel found will be the biggest one. The valid function evaluates the validity of the following constraints of each panel candidate:

Algorithm 2 Horizontal panel design algorithm.

```

1: function addHorizontalPanel(point, facade, cp, direction) → Panel
2:   coordCandidates := Map{Y, [X]} = {} // possible x list for each y
3:   bottomSupportLines ← findSupportLines(point)
4:   if direction == RIGHT then
5:     bottomMaxX ← maxX(bottomSupportLines)
6:     possibleYs ← findPossibleYs(point)
7:     possibleYs ← possibleYs.reverse()
8:     for y in possibleYs do
9:       maxX ← min(bottomMaxX, maxX(findSupportLines(point.x, y)))
10:      possibleXs ← findPossibleXs(point, maxX, y)
11:      possibleXs ← possibleXs.reverse()
12:      coordCandidates.put(y, possibleXs)
13:    end for
14:  else /* direction == LEFT */
15:    bottomMinX ← minX(bottomSupportLines)
16:    possibleYs ← findPossibleYs(point)
17:    possibleYs ← possibleYs.reverse()
18:    for y in possibleYs do
19:      minX ← max(bottomMinX, minX(findSupportLines(point.x, y)))
20:      possibleXs ← findPossibleXs(point, minX, y)
21:      coordCandidates.put(y, possibleXs)
22:    end for
23:  end if
24:  /* Browses possible coordinates for the 2nd point of panel */
25:  for x in coordCandidates.keys() do
26:    for y in coordCandidates[x] do
27:      panel ← createCandidate(point, x, y)
28:      if isValid(panel, facade, cp) then
29:        addResistingElements(panel)
30:        addFixingElements(panel)
31:        return panel
32:      end if
33:    end for
34:  end for
35:  return null
36: end function

```

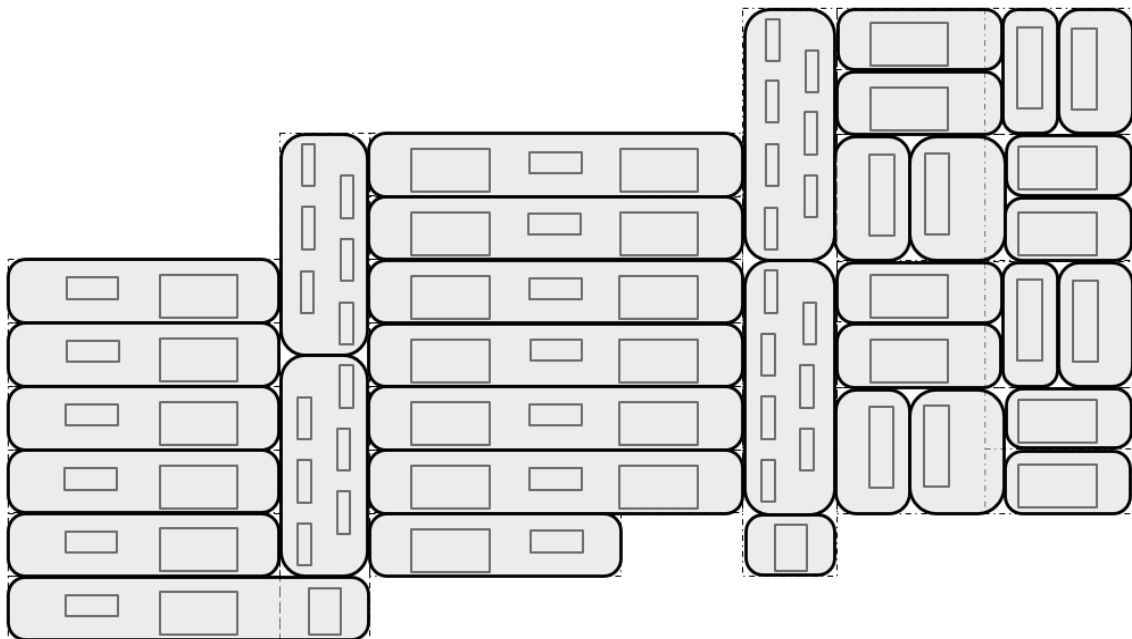


Figure 6. Horizontal solution for the example of figure 5

- Dimensions validation: panel dimensions must respect the minimum and maximum values of width and height coming from the constructive principle,
- Borders validation: if the distance between a panel border and a facade edge or outout edge is greater than 0 but lesser than the minimal width / height of a panel, the panel is not valid,
- Outin containment validation: outin must be fully contained in one panel,
- Other panels overlapping validation: panels must not overlap the other panels (the ones of the solution or the ones manually placed initially),
- Resistance validation: the minimal resistance of the resisting support lines must be compliant with the weight of the panel (computed from its area).

4.3.4 First results and discussion

When this algorithm is used with the example of figure 5, a solution gathering 34 panels is found and shown in figure 6 (panels have rounded corner to see them easily). It can be seen that even if horizontal panels are preferred, at least 12 vertical panels are necessary for staircase and duplex with two floors windows.

In terms of optimality, it must be pointed out that the panel orientation has a major influence on the solution and can sometimes decrease the optimality level of a solution. In the example of figure 6, it is possible to see that when the panel at the bottom of the right staircase is designed, the horizontal orientation forces a small horizontal panel (with a door in the center). Architects would most of the time prefer a single large vertical one that would replace two panels as shown in figure 7.

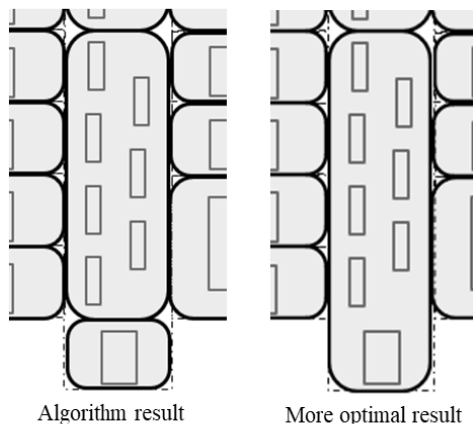


Figure 7. A more optimal result

A more optimal algorithm could be to compute for each panel design the two alternatives (horizontal and vertical) and to keep the best one. This could have been easily done, but this would lead to layout solutions mixing the two orientations. These solutions can be confusing because panels don't seem to be logically arranged and are very delicate to manage during on-site assembly due to a lack of a logical assembly.

This is why we have kept the strength of the orientation parameter in the algorithm, but add a last manual correction, with the manual touch up step, at the end of the design process after automatic design (figure 2). During this last step, manual modification can be inputted in order to change some panel size, to regroup panels or to line up panel edges. This can improve the optimality of the solution and also take into account specific requirements of the building architect and/or owner.

In order to avoid the previous hazardous mix of panel orientations, some authors, as Aldanondo et al. [11], propose to decompose the whole facade in sub-facades either fully horizontal or vertical (meaning accepting only horizontal or vertical panels) before launching the layout algorithm. The main interest is that the problem size can be decreased significantly. But the drawback is that some cases cannot be considered. For example, the right part of our example cannot be processed with fully vertical or horizontal panels. But a mix of the two approaches would merit to be investigated.

The presented solution was obtained with a direction from left to right. When the opposite direction is used (left to right), the modification of the layout concerns only the right part of the facade and are shown in figure 8. This is the result of the outin (windows and balconies) that forbid to use horizontal panels with a larger width.

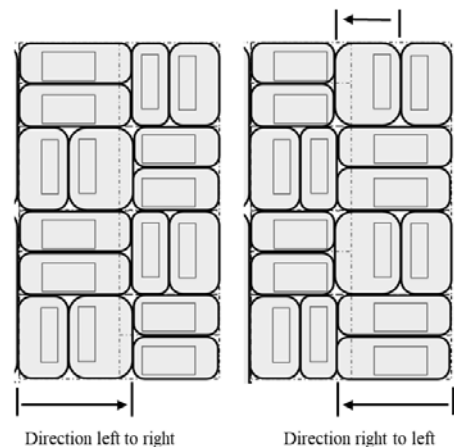


Figure 8. Comparing different directions

5 Conclusion

Our goal was to present a global supported approach to assist the panel layout design for Building insulation renovation. We have proposed a four steps process, three data models and a layout design algorithm that allows to find solutions with a preferred orientation.

As far as we know, we couldn't find in the communities close to the subject, "cutting and packing" and "product configuration", any exact approach able to model and to optimally solve the problem as defined. The proposed algorithm is a greedy heuristic which purpose

is to design panels as larger as possible. As panels get larger, the panel quantity and joint length get smaller. Consequently, the building energetic performances are much better which fulfill the ultimate goal. However, our automatic algorithm only considers rectangular shapes limited by resisting zones. In order to have an operational solution that works, a manual design task where more or less “every design is possible” can be achieved before automatic layout design.

At an operational level, the result is quite robust, it has been used on various facades with no problem. The feedback from the project partners is quite good, they can generate in less than one hour panel layout solutions that require manually at least a day of work. Consequently and this is a key interest, our approach allows us to quickly test and compare different solutions, which is usually never done when layout design is achieved manually.

Some comments about the sustainability aspects of the proposition can address two aspects : the technical “heavy” panel-based solution, the proposed process and software. About the panel solution, we cannot provide any detail figures about energy efficiency, we just know that such project is launched when the cost reduction is at least 50%. But we can say that this industrial process is the only solution in order to reduce building carbon dioxide emissions. For example, in France : (i) much more than 12 million of building apartments are considered as energy strainer (ii) each year no more than 300 thousand of new building apartments are built, (iii) consequently it will take more than 40 years to upgrade the French building stock without industrial retrofit. About the process and software, it is not possible to quantify the benefit of the computerized assistance on sustainability. But as we said in the previous section, the ease and rapidity in the elaboration and comparison of insulation solutions offered by our proposal undoubtedly allows the development of more effective solutions.

At the present time we are trying to use the constraint-based solver Choco Solver library [12] to reprogram the algorithm in order to have a more declarative program. This will allow to update or modify much more easily the constraints relevant to the panel technology and/or constructive principle of the panels. Another research direction is to develop an approach to analyze the “manual touch up” steps in order to systematize the search for improvements concerning the proposed process and algorithm.

Acknowledgments

The authors want to thank the French Research National Agency (ANR) for funding the ISOBIM project that has supported the presented works.

References

- [1] European Commission. In focus: Energy efficiency in buildings. In https://ec.europa.eu/info/news/focus-energy-efficiency-buildings-2020-lut-17_en
- [2] Urbikain MK. Energy efficient solutions for retrofitting a residential multi-storey building with vacuum insulation panels and low-E windows in two European climates. *J. of Cleaner Production*, Vol 269, Elsevier, 2020.
- [3] International Energy Agency. Prefabricated Systems for Low Energy Renovation of Residential Buildings. *IEA ECBCS Annex 50* or https://nachhaltigwirtschaften.at/resources/iea_pdf/iea_ecbcs_annex_50_anhang10b-moduledesign.pdf 2011.
- [4] Aldanondo M., Barco-Santa A., Vareilles E. and Falcon M. Towards a BIM Approach for a High Performance Renovation of Apartment Buildings. In *Proceedings of the PLM 2014 conference*, Springer, pages 21–30, Yokohama, Japan, 2014.
- [5] Hillebrand G., Arends G., Streblow R., Madlener R. and Müller D. Development and design of a retrofit matrix for office buildings. *Energy and buildings*, Vol 70, pages 516-522, Elsevier, 2014.
- [6] Barco A., Vareilles E., Aldanondo M. and Gaborit P. A Recursive Algorithm for Building Renovation in Smart Cities. *Lecture Notes in Computer Science*, LNAI Vol 8502 Springer, pages 144–153, 2014.
- [7] Kendall, K., Daniels, K. and Burke, E.. Cutting, packing, layout, and space allocation. *Special issue Annals Operation Research*. n°179, p. 1-3, 2010.
- [8] Felfernig, A., Hotz, L., Bagley, C., and Tiihonen, J. *Knowledge-Based Configuration: From Research to Business Cases*. Morgan Kaufmann, 2014.
- [9] Huang, E., and Korf, R.E. Optimal rectangle packing: An absolute placement approach. *J. of Artificial Intelligence Research*. Vol. 46, p. 47-87, 2012.
- [10] Barco-Santa, A., Fages, J.G., Vareilles, E., Aldanondo, M., and Gaborit, P. Open packing for facade-layout synthesis under a general purpose solver. In *CP conference - Lecture Notes in Computer Science*, vol. 9255, pages 508-523. 2015.
- [11] Aldanondo M., Vareilles E., Lesbegueries J., Christophe A. and Lorca X. Buildings energetic improvement: first elements about isolating panels layout design. In *Proceedings of the conference 14th IFAC Workshop on Intelligent Manufacturing Systems*, pages 487–492, Tel Aviv, Israel, 2022.
- [12] Prud’homme C. and Fages J. An introduction to choco 3.0 an open-source java constraint programming library. In *CP solvers: modeling, applications, integration, and standardization*. Int. workshop, Uppsala Sweden, 2013.

Automatic point Cloud Building Envelope Segmentation (Auto-CuBES) using Machine Learning

Bryan P. Maldonado, Nolan W. Hayes, Diana Hun

Buildings and Transportation Science Division, Oak Ridge National Laboratory*, United States of America

maldonadopbp@ornl.gov, hayesnw@ornl.gov, hunde@ornl.gov

Abstract -

Modern retrofit construction practices use 3D point cloud data of the building envelope to obtain the as-built dimensions. However, manual segmentation by a trained professional is required to identify and measure window openings, door openings, and other architectural features, making the use of 3D point clouds labor-intensive. In this study, the Automatic point Cloud Building Envelope Segmentation (Auto-CuBES) algorithm is described, which can significantly reduce the time spent during point cloud segmentation. The Auto-CuBES algorithm inputs a 3D point cloud generated by commonly available surveying equipment and outputs a wireframe model of the building envelope. Unsupervised machine learning methods were used to identify facades, windows, and doors while minimizing the number of calibration parameters. Additionally, Auto-CuBES generates a heat map of each facade indicating non-planar characteristics that are crucial for the optimization of connections used in overlaid envelope retrofits. With a scan resolution of 3 mm, the resulting window dimensions showed a mean absolute error of 4.2 mm compared to manual laser measurements.

Keywords -

point cloud, segmentation, unsupervised learning

1 Introduction

Buildings are responsible for 30% of the total carbon dioxide emissions in the US [1]. To mitigate the impact of building operations on climate change, the application of energy codes in construction practices has reduced the energy use in buildings by more than 40% since their insertion in the 1980s. However, about 52% of residential and 46% of commercial buildings were built before energy codes [2]. Hence, large energy savings can be achieved by retrofitting older buildings and bringing them up to code.

Overclad envelope retrofits are an attractive solution since they minimize occupant disruption and shorten construction time at the job site. However, they require pre-

cise measurements of the existing envelope to adequately design and manufacture the retrofit panels. Current state-of-the-art retrofit panel design and sizing consists of three steps: 1) 3D point cloud data generation of the building envelope using commonly available surveying equipment, 2) manual segmentation of 3D point cloud data by a trained professional to identify and dimension window openings, door openings, wall protrusions, and other non-planar architectural features, and 3) modular panel layout optimization and sizing by an architect or engineer [3, 4]. The process of manually segmenting the point cloud data can be difficult and costly, often requiring third-party software and a trained professional to spend several man-hour-weeks depending on the size of the existing building. Additionally, after segmentation of the point cloud into different components of the envelope, the position and size of each component (window, door, etc.) must be extracted from the point cloud which often includes human-introduced errors due to the difficulty and tediousness of the process. Although commercially available software has been optimized to handle point clouds for manual segmentation, automated feature identification and measurement extraction are still challenging. Thus, the automation of these processes could save a significant amount of time and money while also minimizing errors.

Recent advances in machine learning have enabled the development of automatic segmentation algorithms for extracting building envelope features. Common practices include the use of photogrammetry (RGB cameras) data [5] or a combination of photogrammetry and light detection and ranging (LiDAR) data [6]. Although such algorithms can identify the locations and dimensions of windows and doors, they are limited to the resolution of the camera (~10s of mm) and might not achieve the millimetric accuracy needed for retrofit panel design. Deep learning techniques that analyze LiDAR data for point cloud segmentation are capable of automatically identifying the constituent components of common objects [7]. However, this requires a large amount of correctly labeled points for training neural networks. For the segmentation of large structures, the scarcity of training samples and inaccurate boundary segmentation have limited the scope of their usage [8]. For building envelope segmentation specifi-

*This manuscript has been authored by UT-Battelle, LLC, under contract DE-AC05-00OR22725 with the US Department of Energy (DOE). The publisher acknowledges the US government license to provide public access under the DOE Public Access Plan (<https://energy.gov/downloads/doe-public-access-plan>).

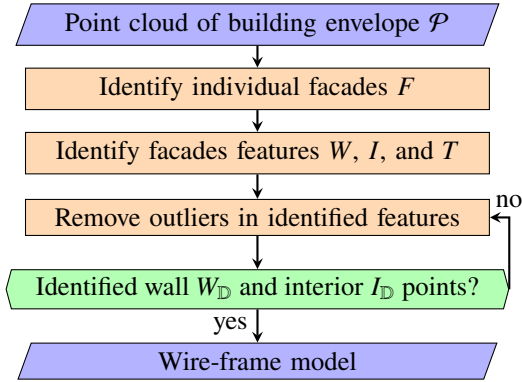


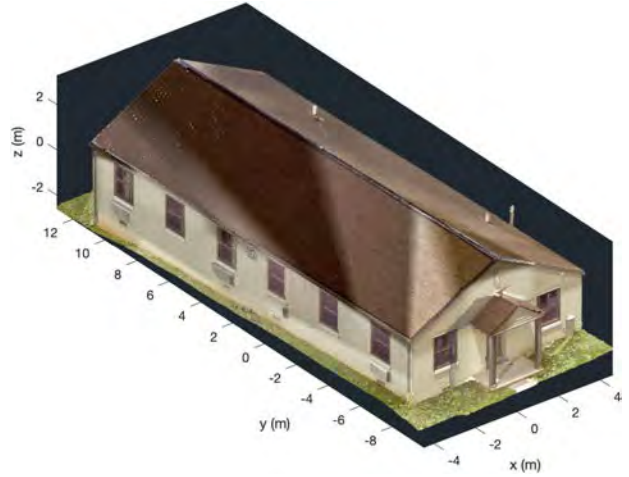
Figure 1. Flowchart of Auto-CuBES algorithm.

cally, such a training set could require additional labor time and cost. Moreover, the variety and uniqueness of facade topologies exacerbate the real-world training sample scarcity problem. Unsupervised machine learning methods that do not need training data present a solution for the building envelope segmentation task. Even though unsupervised methods require the explicit definition of sequential tasks and task-dependent calibration parameters, they have been successful at generating architectural floor plans from point clouds of building interiors [9].

In this study, we introduce the Automatic point Cloud Building Envelope Segmentation (Auto-CuBES) algorithm based on unsupervised machine learning that can automatically label 3D point cloud data and reduce the time spent in manual segmentation. The algorithm can process high-resolution point clouds and generate a wire-frame building envelope model with a small set of calibration parameters. The remaining sections are as follows. Section 2 describes in detail each component of the Auto-CuBES algorithm. Section 3 shows the algorithm results. Finally, Section 4 presents conclusions and future research.

2 Auto-CuBES algorithm

Figure 1 shows the flowchart of the Auto-CuBES algorithm starting from the input point cloud file to the output wire-frame model. In contrast to deep learning methods where layers of neurons are placed between inputs and outputs, unsupervised methods are typically divided into sequential tasks. Each task of the Auto-CuBES algorithm plays an important role in segmentation and outlier removal. Although each task has its own set of calibration parameters, empirical observations suggest that most of them do not need to be recalibrated for different input files. However, the decision step in Fig. 1 might require some recalibration based on the level of accuracy defined by the user. The following subsections describe the unsupervised machine learning methods, calibration parameters, and preliminary results of each task.

Figure 2. Point cloud \mathcal{P} of a residential building.

2.1 Input point cloud file structure

The Leica Nova MS60 MultiStation was used to collect point cloud data with 7-dimensional elements of the form:

$$\mathcal{P} = [P \ L \ C] = [x \ y \ z \ L \ r \ g \ b] \quad (1)$$

where $P = [x \ y \ z]$ are the rectangular coordinates, L is the LiDAR intensity recorded as the return strength of a laser beam, and $C = [r \ g \ b]$ are the corresponding pixel colors obtained from the camera. A duplex residential house was scanned by placing the LiDAR scanner in front of each facade and stitching the scans together using four control points located near the corners of the building. Figure 2 shows the resulting point cloud used in this study. The point cloud encompasses a total of 32.2 million points with an average distance of 3 mm between points.

2.2 Identify and extract individual facades

The algorithm starts by identifying the four facades of the building and removing the roof points. To achieve this, and assuming that the LiDAR scanner was leveled, the point cloud was rotated about the z -axis to align the walls with the x, y canonical basis. To determine the angle of rotation, a plan view of the envelope was generated by selecting a subset of points corresponding to a section passing through the center of the building's height. In other words, the plan view of the envelope is the set:

$$E = \{[x \ y \ z] \in \mathcal{P} \mid |z - \mathbb{E}[z]| < \delta\}. \quad (2)$$

Here, $\mathbb{E}[\cdot]$ is the expected value function and $\delta = 0.4$ m is a calibration parameter. The rotation angle was calculated by solving the minimum-volume oriented bounding box problem using the method described in Chang *et al.* [10].

The top-left plot of Fig. 3 shows the resulting plan view of the building envelope. By aligning the envelope E with

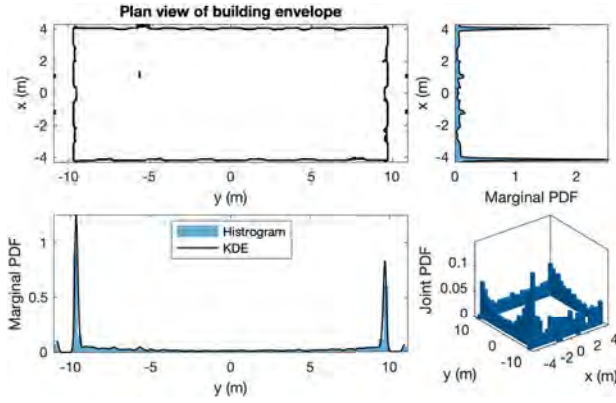


Figure 3. Plan view of building envelope E with joint and marginal PDFs of the x and y components.

the x - and y -axis, the individual facades can be identified by looking at the distribution of points over each axis. The histograms in Fig. 3 correspond to the joint and marginal distributions of $[x \ y] \subset E$. The marginal probability density functions (PDFs) $\text{pdf}(x)$, and $\text{pdf}(y)$ where approximated using kernel density estimators (KDEs). The Gaussian kernel was used in the KDE and the bandwidth was selected following Silverman's rule of thumb [11].

Note that the marginal PDFs have two main modes, each of which corresponds to one of the four facades of the building envelope. Let $\bar{x}_{>0} = \arg \max_{x>0} \text{pdf}(x)$ be the largest mode for the positive values in the x -axis. Similarly, define $\bar{x}_{<0}$ for the negative x -axis, and $\bar{y}_{>0}, \bar{y}_{<0}$ for the y -axis. Although each mode defines the average location of a facade, the facade thickness was obtained by selecting the interval between the inflection points around each mode. Let $\bar{x}_{>0}^L = \arg \max_{x>0} \frac{d}{dx} \text{pdf}(x)$ and $\bar{x}_{>0}^R = \arg \min_{x>0} \frac{d}{dx} \text{pdf}(x)$ be the inflection points around $\bar{x}_{>0}$. Note that the inflections points bound the corresponding mode on the left and right as follows: $\bar{x}_{>0}^L < \bar{x}_{>0} < \bar{x}_{>0}^R$. Using similar definitions for the remaining modes, the four facades of the building envelope can be extracted as:

$$F_x^{y<0} = \{p \in \mathcal{P} \mid \bar{x}_{<0}^R \leq x \leq \bar{x}_{>0}^L, \bar{y}_{<0}^L \leq y \leq \bar{y}_{<0}^R\} \quad (3a)$$

$$F_x^{y>0} = \{p \in \mathcal{P} \mid \bar{x}_{<0}^R \leq x \leq \bar{x}_{>0}^L, \bar{y}_{>0}^L \leq y \leq \bar{y}_{>0}^R\} \quad (3b)$$

$$F_y^{x<0} = \{p \in \mathcal{P} \mid \bar{x}_{<0}^L \leq x \leq \bar{x}_{>0}^R, \bar{y}_{<0}^L \leq y \leq \bar{y}_{>0}^L\} \quad (3c)$$

$$F_y^{x>0} = \{p \in \mathcal{P} \mid \bar{x}_{>0}^L \leq x \leq \bar{x}_{>0}^R, \bar{y}_{<0}^R \leq y \leq \bar{y}_{>0}^L\} \quad (3d)$$

Figure 4 shows the automatically identified facades. Note that the procedure described here is intended for a traditional envelope with four perpendicular facades. A more complex geometry will require a modified approach.

2.3 Identify and extract facade features

Each facade was individually analyzed to extract its main features (doors and windows). Based on traditional

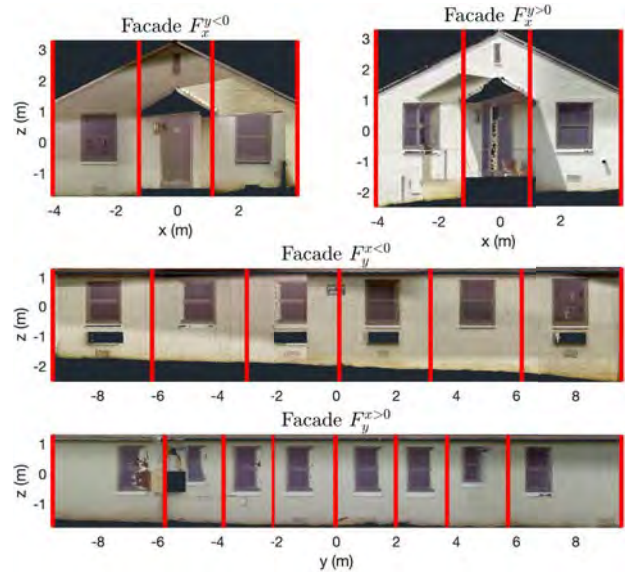


Figure 4. Four perpendicular facades from building envelope sectioned according to identified features.

residential construction practices, it was assumed that the window and door frames are recessed with respect to the exterior wall surface. Therefore, and thanks to the high resolution of the point cloud data, the facade thickness can be sliced into three main subsets: 1) interior points corresponding to windows and doors, 2) wall points, and 3) exterior points corresponding to features such as roof overhangs and window sills. In order to slice the facade, the point cloud distribution with respect to the thickness axis was considered. However, this method assumes that the facade is flat, which is not always the case. To remove flatness assumptions, the facade was decomposed into different sections depending on the number of features in the facade. The unsupervised k-means clustering algorithm was used to segment each facade into k sections [12]. Here, k is a parameter given by the user. Figure 4 shows how each facade can be automatically divided into sections corresponding to the number of features.

The algorithm assumes that each section is locally flat, even though the combined facade is not. Therefore, for each section within a facade, interior, wall, and exterior features were identified using the point cloud distribution of the thickness axis. As an example, consider dividing the first facade in Fig. 4 into the sections $\{F_{x,k}^{y<0}\}_{k \in \{1,2,3\}}$. Under the locally-flatness assumption, the facade section will be align with a plane of the form $y = a_k x + b_k z + c_k$. Moreover, consider the following coordinate transformation to align each section with the xz -plane:

$$y_{<0}^k = y - (a_k x + b_k z + c_k) + \mathbb{E}[y]. \quad (4)$$

The parameters of the linear function were found using

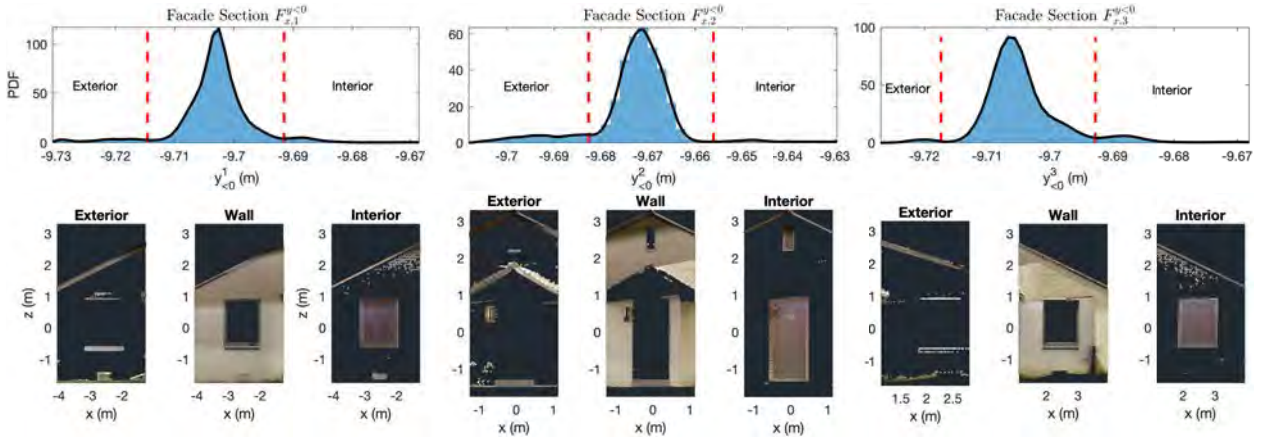


Figure 5. Segmentation of the facade $F_x^{y<0}$ into exterior, wall, and interior points by analysing individual sections.

robust least squares with bisquare weights due to the existence of outliers [11]. The top row of Fig. 5 shows the pdf($y_{<0}^k$) for each section. Although the resulting PDF is not unimodal, there is a clear dominant mode where the wall points are located. Let $\hat{y}_{<0}^k = \arg \max \text{pdf}(y_{<0}^k)$ be the dominant mode, then the thickness interval corresponding to wall points was defined as $\hat{y}_{<0}^{k,L} \leq y_{<0}^k \leq \hat{y}_{<0}^{k,R}$, where:

$$\hat{y}_{<0}^{k,L} = \max \left\{ y_{<0}^k < \hat{y}_{<0}^k \mid \frac{d}{dy} \text{pdf}(y_{<0}^k) = 0 \right\} \quad (5a)$$

$$\hat{y}_{<0}^{k,R} = \min \left\{ y_{<0}^k > \hat{y}_{<0}^k \mid \frac{d}{dy} \text{pdf}(y_{<0}^k) = 0 \right\}. \quad (5b)$$

Note that the bounds in Eqn. (5) correspond to the first critical points of the PDF to the left and to the right of the dominant mode, respectively. This interval for each section is pictured in Fig. 5 by the red dashed lines. Consequently, the exterior points satisfy $y_{<0}^k < \hat{y}_{<0}^{k,L}$ while the interior points correspond to $y_{<0}^k > \hat{y}_{<0}^{k,R}$. This is also true for facade $F_y^{x<0}$, with the appropriate reformulation of the PDFs over the x -axis. However, keep in mind that the reverse is true for facades $F_x^{y>0}$ and $F_y^{x>0}$ because of the positive sign of the thickness component. Finally, let $W_{x,k}^{y<0}$, $I_{x,k}^{y<0}$, and $T_{x,k}^{y<0}$ be the point clouds corresponding to wall points, interior points, and exterior points, respectively. The second row of Fig. 5 shows the resulting point clouds. Note that the original assumption of recessed window/door placement holds and the interior points correspond mostly to the windows and door points. However, one can observe that roof and ground features are also present in the set of interior points. This highlights the need for outlier removal, where the roof, ground, and other facade characteristics are purposely removed in order to extract the dimensions of windows and doors.

2.4 Outlier removal

A distanced-based outlier removal was used to clean up the individual point cloud sections in order to extract accurate dimensions and locations of building features. A previous study by the authors used the Mahalanobis distance to determine outliers [13]. Although the properties of the Mahalanobis distance allowed for statistical hypothesis testing to determine outliers, the underlying Euclidean metric is not well suited for handling rectangular features such as windows and doors. Therefore, we present a new custom metric developed for rectangular point clouds.

Let $p \in \Pi$, where Π is a point cloud corresponding to wall or interior points. Consider the normalization:

$$\tilde{p} = \frac{p - \mathbb{E}[p]}{\mathbb{M}[|p - \mathbb{M}[p]|]} \in \tilde{\Pi}. \quad (6)$$

Here, $\mathbb{M}[\cdot]$ is the median function. The zero-mean and unit median absolute deviation transformation is a robust normalization approach to deal with outliers in each point cloud. Note that Eqn. (6) transforms the Cartesian coordinates of rectangular prisms, such as windows, doors, and rectangular walls, into cubes centered at the origin. In order to draw a boundary around the cube and remove outliers, consider using the Chebyshev metric applied to the rectangular coordinates of the normalized point cloud:

$$D_C(\tilde{p}) = \max \{ |\tilde{x}|, |\tilde{y}|, |\tilde{z}| \mid [\tilde{x} \ \tilde{y} \ \tilde{z}] \in \tilde{p} \}. \quad (7)$$

Moreover, outliers are generally miss-classified points that are not only physically distant from the cluster centroid but also correspond to a different material. For example, note that point clouds of interior points $I_{x,k}^{y<0}$ in Fig. 5 have outliers corresponding to brick cladding and roof tiles. Such outliers are made of materials different from those of window frames. Therefore, the normalized light intensity

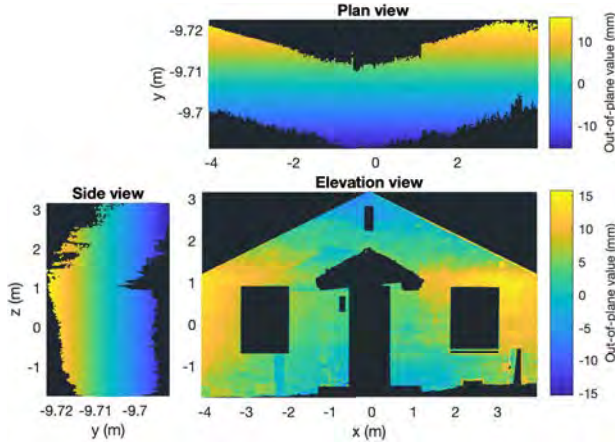


Figure 6. Plan, side, and elevation views of $W_{x,\mathbb{D}}^{y<0}$ with heat map describing flatness of outside surface.

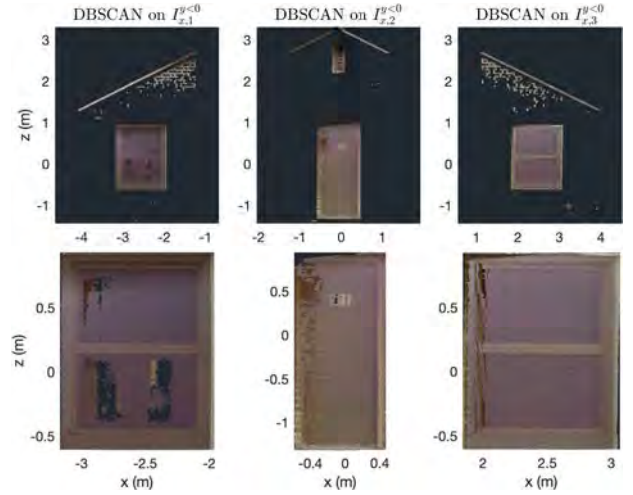


Figure 7. Outlier removal for $I_{x,k}^{y<0}$ using DBSCAN.

\tilde{L} can also be used to identify outliers since it correlates well with the reflectivity of the material. Finally, consider the following metric for identifying outlier points:

$$\mathbb{D}: \mathbb{R}^7 \mapsto \mathbb{R}^+, \quad \mathbb{D}(\tilde{p}) = D_C(\tilde{p}) + \alpha|\tilde{L}|. \quad (8)$$

Here, $\alpha > 0$ is a calibration parameter that captures the relative importance of the light intensity component with respect to the rectangular coordinates within the point cloud.

The outlier removal task consists on discarding the elements of a point cloud with a distance $\mathbb{D}(\cdot)$ larger than a preset threshold D_{thres} . In other words, the reduced point cloud after the outlier removal task was defined as:

$$\Pi_{\mathbb{D}} = \{p \in \Pi \mid \mathbb{D}(\tilde{p}) < D_{\text{thres}}, \tilde{p} \in \tilde{\Pi}\}. \quad (9)$$

2.4.1 Outlier removal for wall points

For this study, the calibration parameter $\alpha = 1$ worked well for all facades. On the other hand, the threshold D_{thres} was not uniform along all sections. As described by the flowchart in Fig. 1, the outlier removal task of the AutoCuBES may require some iteration by the user. In this case, after a visual inspection of the resulting point cloud, the user can decide to pick a larger or smaller threshold D_{thres}^{i+1} at iteration i . It was empirically found that a value of $D_{\text{thres}}^0 = 4$ provides a good starting point for the iteration.

Following the same example as before, consider the wall points $W_{x,k}^{y<0}$. After outliers were removed from each section, the wall points of the entire facade correspond to the union of all different sections, i.e., $W_{x,\mathbb{D}}^{y<0} = \bigcup_k W_{x,k,\mathbb{D}}^{y<0}$. Figure 6 shows the plan, side, and elevation views of the remaining elements after outlier removal. From the plan view, note that the cladding is not flat, but it rather bows in. The side view indicates that the wall is slightly leaning

forward and is not perfectly plumb. The bowing, leaning, or bulging of external walls can be summarized in the elevation view by coloring the points according to the out-of-plane value, define as the position of each point with respect to the facade's average plane. The average plane was calculated with respect to the axis at the thickness of the wall, similar to Eqn. (4) but keeping a zero mean. The coloring not only helps to determine sections where wall stability could be a problem, but it also assists in the design of optimized connections for overlaid panel retrofits.

2.4.2 Outlier removal for interior points

The top row of Fig. 7 shows the interior points $I_{x,k}^{y<0}$ for all three sections of the facade. Note that, in contrast to the wall points $W_{x,k}^{y<0}$, distinct clusters can be identified corresponding to window/door points, roof points, and other clusters such as vents. Hence, unsupervised clustering was performed. The algorithm chosen for this task was DBSCAN [14], which is a density-based clustering algorithm well suited to identify the cluster of each section corresponding to windows and doors. The DBSCAN algorithm determines if a point p belongs or not to a dense cluster by considering a neighborhood of radius $\epsilon = 12$ cm around p , if there are less than $m = 100$ points in the neighborhood, then the point is an outlier. Finally, the dense cluster corresponding to a window/door was decided based on its proximity to the centroid of $I_{x,k}^{y<0}$. The bottom row of Fig. 7 shows the resulting clusters after the DBSCAN algorithm was performed. Although the algorithm can correctly identify the dense clusters corresponding to the facade features, it cannot distinguish outliers within points at the edge of the clusters. It was observed that, in most cases, the subsequent use of the outlier removal method in Eqn. (9) was needed to obtain accurate dimensions.

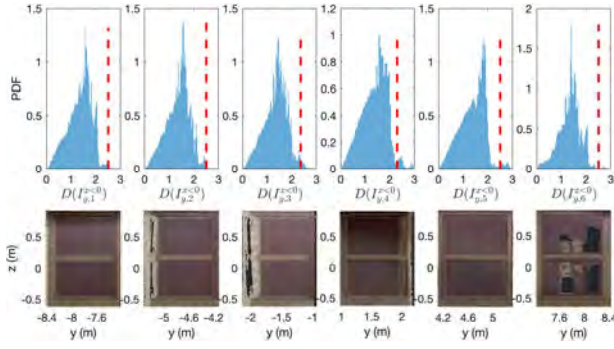


Figure 8. Clusters $I_{y,k,D}^{x<0}$ corresponding to windows.

Figure 8 shows the resulting windows extracted from facade $F_y^{x<0}$ after the sequential application of DBSCAN and the outlier removal metric $\mathbb{D}(\cdot)$. The top row of Fig. 8 shows the histograms of the distance $\mathbb{D}(I_{y,k,D}^{x<0})$ calculated for each window after running the DBSCAN algorithm. For all the interior points, a value of $\alpha = 0.1$ was used to remove outliers mainly based on the cuboid shape of windows and doors. Even though the windows are physically similar, the histograms show some variability. This is due to the sensitivity of the point cloud scan with respect to scanner position, laser's angle of incidence, and window recessed distance from the wall. Nonetheless, we observed a general triangular distribution with a sharp drop after the main mode. Similar to the wall points, the distance threshold for removing outliers was not uniform for all windows and doors, and some iteration was needed. However, it was empirically found that a value of $D_{\text{thres}}^0 = 2.5$ provided a good starting point. The individual values $D_{\text{thres},k}$ for each window are pictured by the red dashed lines over the histograms. Finally, the bottom row of Fig. 8 shows the resulting point clouds to be used for extracting the dimensions and relative positions of each window.

2.5 Wire-frame model generation

Once the original point cloud \mathcal{P} has been segmented into wall points ($W_{x,D}^{y<0}$, $W_{x,D}^{y>0}$, $W_{y,D}^{x<0}$, $W_{y,D}^{x>0}$) and interior window/door points ($I_{x,k,D}^{y<0}$, $I_{x,k,D}^{y>0}$, $I_{y,k,D}^{x<0}$, $I_{y,k,D}^{x>0}$), the position and dimensions of the building envelope and its features can be extracted to create a simple wire-frame model. First, the exact dimension of each feature can be obtained by solving the minimum-volume oriented bounding box problem. This approach considers the possibility that windows and doors might not be aligned with the building facade. Moreover, as seen in Fig. 6, the facades are not perfectly flat, hence it should not be assumed that the windows are aligned. Thus, the bounding box not only provides the dimensions of each feature but also generates

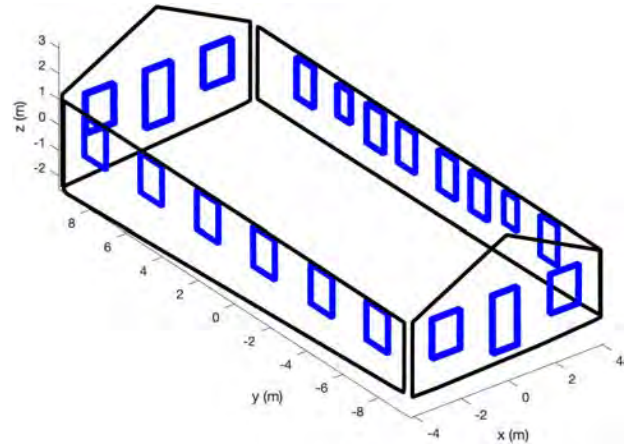


Figure 9. Wire-frame model of building envelope.

the rectangular prism needed for the wire-frame model. Given that the wall points do not have a rectangular shape, the facade dimensions and wire-frame model were obtained using the convex hull. Note that, in either case, the wire-frame generated is limited to convex point clouds. Non-convex facades, such as those with towers, will need a different approach to generate a wire-frame model.

Figure 9 shows the resulting wire-frame model when combining the convex hulls of wall points and the bounding boxes of windows and doors. Ultimately, the Auto-CuBES algorithm was able to reduce the highly detailed point cloud of the building envelope from 32.2 million points to a simplified wire-frame model with 309 points that summarized the essential information needed for retrofit panel design. Moreover, the wire-frame model combined with the out-of-plane coefficient in Fig. 6 can be a powerful tool to obtain necessary as-built dimensions for accurate overlaid panel retrofits and for optimizing the position and dimensions of connections on existing facades previous to the retrofit process.

3 Results

Even though the Auto-CuBES algorithm has few calibration parameters for a single point cloud, the total number of parameters scales linearly with the number of facades and the number of features per facade in the building envelope. Ignoring the time needed to iterate over D_{thres}^i for windows and doors in each facade, the Auto-CuBES algorithm took a total of 12 m 22 s to run when implemented in MATLAB on a computer running on a quad-core Intel Core i7. Table 1 shows the breakdown of the time taken to run each task in the Auto-CuBES algorithm. Note that the DBSCAN algorithm takes the longest to run, taking 71% of the total running time. Although all other tasks in the Auto-CuBES algorithm have been optimized to some level using in-house developed code, the density-based

Table 1. Time taken to run Auto-CuBES algorithm

Identify and extract individual facades:	0 m 14 s
Identify wall and interior points:	2 m 03 s
DBSCAN only:	8 m 47 s
Outlier removal using metric $\mathbb{D}(\cdot)$:	1 m 05 s
Wire-frame model generation:	0 m 13 s
TOTAL TIME:	12 m 22 s

clustering for interior points was done using the single MATLAB command `dbscan`. Future work will explore alternatives to accelerate DBSCAN in order to reduce the overall Auto-CuBES execution time.

The accuracy of the Auto-CuBES was quantified by comparing the resulting dimensions for windows and doors versus manual laser measurements. Before discussing the results, it is important to mention two main caveats:

1. Manual measurements contain human errors: The person measuring needs to aim the laser at the exact interface between the window frame and the brick.
2. Only corner points were used to generate manual measurements: This assumes that the rough openings of windows and doors are square and straight.

Figure 10 shows the difference between the window dimensions obtained using the Auto-CuBES and the manual measurements for all facades. The calculated error is shown as a bar plot for each window's width (top row) and height (bottom row), and the scanner resolution (3 mm) is depicted with the dashed line. Facades $F_x^{y<0}$ and $F_x^{y>0}$ show errors comparable to the scanner resolution. They also correspond to the narrow section of the envelope, in which the scanner could maintain a high resolution throughout. Although not shown in the plot, the door dimensions for the facades showed comparable levels of accuracy. Facade $F_y^{x<0}$ shows a low error on window height, but some larger errors on window width. This is probably due to variable resolution across the facade. Although, on average, the scan has a 3 mm resolution, the actual controllable variable in the scanner is the angle increments for the robotic laser head. This means that surfaces that are scanned at an angle (e.g., edge of a wide facade) can have lower resolution than points directly in front of the scanner head. Finally, facade $F_y^{x>0}$ shows the largest errors among all. This was probably due to the scanner location with respect to the facade. In contrast to the other scans, the scanner position was not perpendicular to the facade due to the topographical constraints of the terrain around the building. Thus, the scan was taken at an angle and at a different altitude compared with the rest of the scans. This caused resolution and line-of-sight issues for the scanner.

To summarize the results, the mean absolute error (MAE) was calculated for all features in the building en-

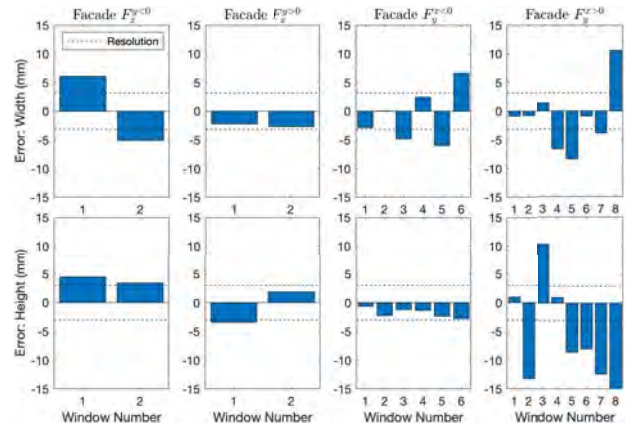


Figure 10. Error between bounding box dimensions and manual laser measurements for windows.

velope. The width MAE was 4 mm while the height MAE was 4.4 mm when the four facades were included. This resulted in an overall MAE of 4.2 mm with an average scan resolution of 3 mm. If, however, facade $F_y^{x>0}$ is excluded due to the non-ideal scanning conditions, the overall MAE is closer to 3.2 mm. This indicates that, during ideal scanning conditions, the point cloud resolution is maintained and the error is minimized when the dimensions were automatically extracted from the point cloud. To cope with resolution and line-of-sight issues, future studies will look at a larger number of scans with overlapping areas.

4 Conclusions

This study introduces the Auto-CuBES algorithm for extracting as-built dimensions of facades, windows, and doors from a 3D point cloud of a building envelope. In its current version, the algorithm is intended for simple one-floor structures comprising four main perpendicular convex facades, and rectangular windows and doors. The Auto-CuBES can process 32.2 million elements of a 3D point cloud and extract the minimum required points (309 in this study) to generate a wire-frame model of the building envelope. Additionally, the flatness of the external cladding is evaluated to optimize the design of connections for overlaid panel retrofits. The individual tasks of the Auto-CuBES algorithm were based on unsupervised machine learning methods which do not require a training set with labeled data. This methodology was chosen due to the scarcity of labeled training samples for building envelopes and the inaccurate boundary segmentation of current supervised machine learning algorithms. The performance of the Auto-CuBES algorithm was evaluated in terms of computation time and accuracy compared to manual measurements. Without including the calibration time taken to find the optimal thresholds for distance-based

outlier removal, the Auto-CuBES processed 32.2 million points in 12 m 22 s. However, 71% of the computation time was taken by the DBSCAN task, which will be optimized in future versions. Manual laser measurements were compared against the automatically generated dimensions, resulting in an overall MAE of 4.2 mm for the point cloud in this study with 3 mm resolution. However, if only the facades that were scanned under ideal conditions are considered, then the MAE is comparable to the point cloud resolution. Therefore, the Auto-CuBES present a solution to expedite and reduce the cost of accurate overlaid retrofits to bring old buildings up to energy codes.

Future research will focus on expanding the capabilities of the algorithm to include protruding and/or non-rectangular architectural features, as well as dealing with non-convex facades and non-rectangular envelopes. Current efforts on non-convex hull optimization and on random sample consensus (RANSAC) for arbitrary shape detection are being considered to expand the applicability of the Auto-CuBES. Additional development will include the integration with advanced construction methods such as the real-time evaluator (RTE) that is currently being developed by the authors.

5 Acknowledgements

This research was supported by the DOE Office of Energy Efficiency and Renewable Energy (EERE), Building Technologies Office, under contract DE-AC05-00OR22725, and used resources at the Building Technologies Research and Integration Center, a DOE-EERE User Facility at Oak Ridge National Laboratory.

References

- [1] U.S. Energy Information Administration. Annual Energy Outlook 2022. Technical report, U.S. Department of Energy, 2022.
- [2] The Alliance to Save Energy. Energy Efficiency Impact Report. Technical report, The American Council for an Energy-Efficient Economy, 2022.
- [3] G. Iannaccone, G. Salvalai, M.M. Sesana, and R. Paolini. Integrated Approaches for Large Scale Energy Retrofitting of Existing Residential Building through Innovative External Insulation Prefabricated Panels. In *Sustainable Built Environment (SBE) Regional Conference*, pages 636–643, Zurich, 2016.
- [4] G. Salvalai, M. M. Sesana, and G. Iannaccone. Deep renovation of multi-storey multi-owner existing residential buildings: A pilot case study in Italy. *Energy and Buildings*, 148:23–36, 2017.
- [5] Norhan Bayomi, Mohammed El Kholly, John E. Fernandez, Senem Velipasalar, and Tarek Rakha. Building envelope object detection using yolo models. In *2022 Annual Modeling and Simulation Conference (ANNSIM)*, pages 617–630, 2022.
- [6] E. Özdemir and F. Remondino. Segmentation of 3d Photogrammetric Point Cloud for 3d Building Modeling. *ISPRS - International Archives of the Photogrammetry, Remote Sensing and Spatial Information Sciences*, 6210:135–142, September 2018.
- [7] R. Charles, H. Su, M. Kaichun, and L. J. Guibas. Pointnet: Deep learning on point sets for 3d classification and segmentation. In *2017 IEEE Conference on Computer Vision and Pattern Recognition (CVPR)*, pages 77–85, Los Alamitos, CA, USA, jul 2017. IEEE Computer Society.
- [8] Xiaofei Yang, Enrique del Rey Castillo, Yang Zou, and Liam Wotherspoon. Semantic segmentation of bridge point clouds with a synthetic data augmentation strategy and graph-structured deep metric learning. *Automation in Construction*, 150:104838, 2023.
- [9] Minju Kim, Dongmin Lee, Taehoon Kim, Sangmin Oh, and Hunhee Cho. Automated extraction of geometric primitives with solid lines from unstructured point clouds for creating digital buildings models. *Automation in Construction*, 145:104642, 2023.
- [10] Chia-Tche Chang, Bastien Gorissen, and Samuel Melchior. Fast Oriented Bounding Box Optimization on the Rotation Group SO(3,R). *ACM Trans. Graph.*, 30(5), oct 2011.
- [11] Kevin P. Murphy. *Machine Learning: A Probabilistic Perspective*. The MIT Press, 2012. ISBN 0262018020.
- [12] D. Arthur and S. Vassilvitskii. K-means++: The advantages of careful seeding. In *Proceedings of the Eighteenth Annual ACM-SIAM Symposium on Discrete Algorithms*, SODA '07, page 1027–1035. Society for Industrial and Applied Mathematics, 2007.
- [13] Bryan P. Maldonado, Nolan W. Hayes, Daniel Howard, and Diana Hun. Automatic Segmentation of Building Envelope Point Cloud Data Using Machine Learning. In *ASHRAE Topical Conference Proceedings*, 12 2022.
- [14] Martin Ester, Hans-Peter Kriegel, Jörg Sander, and Xiaowei Xu. A Density-Based Algorithm for Discovering Clusters in Large Spatial Databases with Noise. In *Proceedings of the Second International Conference on Knowledge Discovery and Data Mining*, KDD'96, page 226–231. AAAI Press, 1996.

Contribution of Dual-tree Complex Wavelet to Three-dimensional Analysis of Pavement Surfaces

Kazuya Tomiyama¹, Yuki Yamaguchi² and Kazushi Moriishi²

¹Division of Civil and Environmental Engineering, Kitami Institute of Technology, Japan

²Obayashi Road Corporation, Japan

tomiyama@mail.kitami-it.ac.jp, yuki-yamaguchi@obayashi-road.co.jp, kazushi-moriishi@obayashi-road.co.jp

Abstract –

Pavement industries in Japan enhance the application of three-dimensional (3D) modeling as a part of the policy called "i-Construction" which applies 3D point cloud data to pavement works. However, distinctive approaches in terms of signal processing are required in practical applications of 3D point clouds to pavement surfaces. An effective and efficient filtering algorithm is then necessary for the analysis. The purpose of this study is to verify the ability of the dual-tree complex wavelet transform (DTCWT) applied to the 3D point clouds measured for pavement surfaces. Unlike conventional continuous and discrete wavelet transforms, the DTCWT allows nearly shift invariant and directional decomposition in two and higher dimensions with less redundant manners. This study conducts a field experiment at a test site paved with precast concrete blocks for the verification. The result shows that the DTCWT provides superior decomposition algorithm to the discrete wavelet transform by enabling effective filtering based on the directional multiresolution analysis. Finally, the performance of DTCWT is proved for the identification of pavement distress and deformation effectively and reasonably in terms of wavelengths and locations in this study.

Keywords –

Dual-tree complex wavelet; Point cloud; Pavement surface; ICT; i-Construction

1 Introduction

Pavement industries in Japan enhance the application of three-dimensional (3D) modeling as a part of the policy called "i-Construction" which applies 3D point cloud data in design, construction, maintenance, and rehabilitation stages of pavements [1]. An advantage of the i-Construction is capable of improving productivity and quality of pavement works by use of Information and Communication Technologies (ICTs). The use of terrestrial laser scanner (TLS) which is one of the unique applications of i-Construction has been studied in terms of establishing

technical standards [1], measurement accuracy [2], and measurement efficiency [3,4]. The demand for 3D measurement has also been increasing in the implementation of area-based pavement management rather than line-based one by detecting localized distress and deformation of pavement surfaces [5-8].

On the other hand, distinctive approaches in terms of signal processing are required in practical applications of 3D point clouds. For example, the approaches include removing unwanted noises [9], generating a reference plane [10], and detecting information of interest [11]. In other words, an effective and efficient filtering algorithm is necessary for the analysis of 3D point clouds measured for pavement surfaces in practice. Various filtering techniques to identify features of a signal have so far been developed with convolution digital filters (CDF) [12], short-time Fourier transform (STFT) [7], continuous wavelet transform (CWT) [13], and discrete wavelet transform (DWT) [14]. However, the CDF needs to design different specifications corresponding to different wavebands of interest. It results in the increase of the number of calculations. The STFT allows the simultaneous identification of wavelengths and locations whereas it requires the stationarity assumption of a signal for the analysis. Unlike the CDF and STFT, the CWT and DWT realize efficient filtering and feature identification in the wavelength and location information simultaneously without the assumption of stationarity [15]. Nevertheless, the calculation redundancies of CWT and the shift variant properties of DWT are still remaining as issues in the decomposition of a signal [15,16]. Against the properties of these methods, the dual-tree complex wavelet transform (DTCWT) has been developed to achieve nearly shift invariant and directional decomposition in two and higher dimensions with less redundant manners [16, 17]. This advantage was applied to a pavement distress analysis based on photographic images [18].

In the light of this background, the purpose of this study is to verify the ability of DTCWT applied to the 3D point cloud rather than photographic images acquired for pavement surfaces. For this purpose, this study conducted a field experiment at a test site paved with precast

concrete blocks as an example to verify the diagnostic performance of DTCWT applied to the pavement surfaces.

2 Theory of DTCWT

The basic theory of DTCWT obeys the manner of DWT [15] whereas the DTCWT introduces the concept of complex numbers for the scaling and wavelet functions as same as the Fourier transform [17]. This chapter reviews the theory of DTCWT with describing the difference from DWT. The details can be seen elsewhere [15-17]. Note that when point cloud data of pavement surfaces are defined as function of length, the frequency of cycle per length is called wave number. However, the term frequency is used in this chapter unless otherwise specifically noted.

2.1 DWT

Any finite-energy analog signal $x(t)$ as a function of time or distance t can be decomposed in terms of wavelets $\psi(t)$ and scaling functions $\varphi(t)$ via

$$x(t) = \sum_{n=-\infty}^{\infty} c(n)\varphi(t-n) + \sum_{j=0}^{\infty} \sum_{n=-\infty}^{\infty} d(j,n)2^{\frac{j}{2}}\psi(2^j t - n) \quad (1)$$

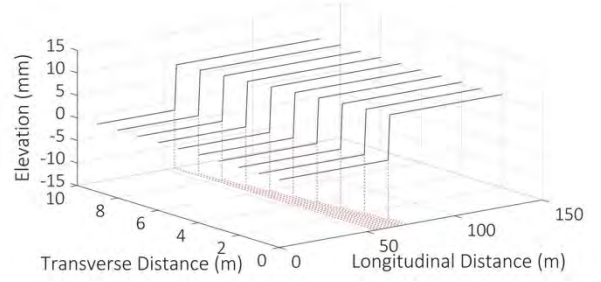
The scaling coefficients $c(n)$ and wavelet coefficients $d(j,n)$ are computed by the following equations

$$c(n) = \int_{-\infty}^{\infty} x(t)\varphi(t-n)dt \quad (2)$$

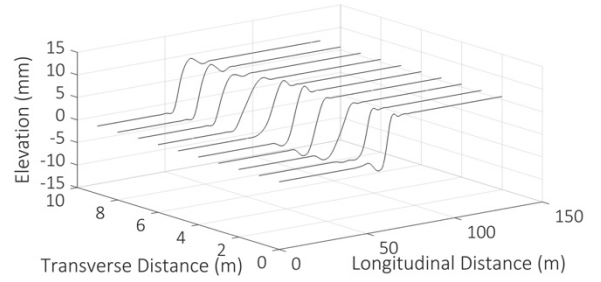
$$d(j,n) = 2^{j/2} \int_{-\infty}^{\infty} x(t)\psi(2^j t - n)dt \quad (3)$$

Where j and n denote the scale factor and the shift parameter corresponding to the frequency content and time/distance, respectively. That is, the DWT transforms an original signal into low-pass ‘‘approximation’’ components via the scaling functions and high-pass ‘‘detail’’ components via the wavelets, which can be seen in the first and second term, respectively, on the right-hand side of Equation (1). With this representation, the DWT allows multiresolution analysis using a fast pyramid algorithm.

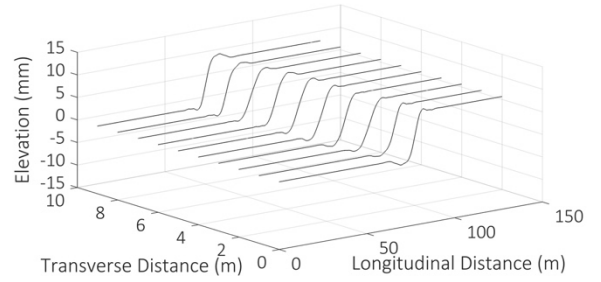
However, the DWT lacks the property of shift invariance. As a result, the energy of the wavelet coefficient changes significantly against a small time/distance shift in the phase of an input signal [16]. For instance, Figure 1(a) shows step functions which had offsets longitudinally at an interval of 2 m. The steps can be decomposed into level 2 as shown in Figure 1(b) on the basis of 7th order Symlet wavelet [19]. As can be seen in the figure,



(a) Original Signals



(b) DWT Result



(c) DTCWT Result

Figure 1. Wavelet Analysis Results for Step Functions with Longitudinal Offset

the oscillations of steps clearly depend on the location.

2.2 DTCWT

The signal processing with DTCWT follows that with the DWT shown in Equation (1)-(3). However, the DTCWT involves the concept of complex numbers for the scaling and wavelet functions as same as the Fourier transform [17]. That is, the DTCWT employs complex valued wavelets $\psi_c(t)$ and scaling functions $\varphi_c(t)$ shown in Equation (4) and (5), respectively.

$$\psi_c(t) = \psi_r(t) + \mathbf{i}\psi_i(t) \quad (4)$$

$$\varphi_c(t) = \varphi_r(t) + \mathbf{i}\varphi_i(t) \quad (5)$$

Where \mathbf{i} denotes the imaginary unit. In Equation (4), $\psi_r(t)$ and $\psi_i(t)$ are the real part and the imaginary part

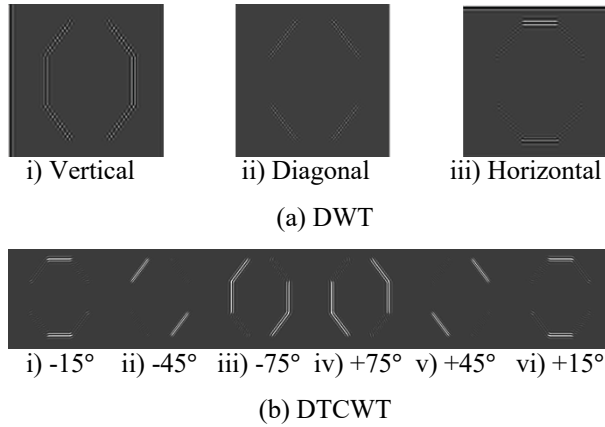


Figure 2. Directional Wavelet Analysis of an Octagon Image

of the complex wavelet functions, respectively. Here, $\psi_r(t)$ and $\psi_i(t)$ are Hilbert transform pair to each other which is supported on only a Nyquist frequency range. Same is true for the complex scaling functions shown in Equation (5). The complex wavelet coefficient and the magnitude can be computed by Equation (6) and (7), respectively.

$$d_c(j, n) = d_r(j, n) + \mathbf{i}d_i(j, n) \quad (6)$$

$$|d_c(j, n)| = \sqrt{[d_r(j, n)]^2 + [d_i(j, n)]^2} \quad (7)$$

In practice, the DTCWT can be simply implemented with two real DWTs: the first DWT gives the real part of the transform while the second DWT gives the imaginary part [17]. Figure 1(c) indicates the result of level 2 DTCWT with a filter bank based on 9/7 biorthogonal wavelet [20] applied to Figure 1(a). As shown in the figure, the effect of shift variance obviously decreased in comparison with the result of DWT shown in Figure 1(b).

2.3 Directional Analysis

When the transform is expanded in multi-dimensions, the DTCWT performs directional decomposition toward the angles of $\pm 15^\circ$, $\pm 45^\circ$, and $\pm 75^\circ$. This ability allows analyzing and processing oriented singularities such as edges, joints and unevenness in 3D pavement surfaces [17]. Although the DWT is possible to directional decomposition toward the horizontal ($\pm 0^\circ$), diagonal ($\pm 45^\circ$), and vertical ($\pm 90^\circ$) directions, it brings the aliasing for the diagonal orientations.

Figure 2 illustrates the level 3 decomposition of an octagon image by the DWT and DTCWT. As shown in the figures, the DWT produces a checkerboard artifact on the diagonal orientation whereas the result obtained with DTCWT is free of it. The directional decomposition result of DTCWT can be reconstructed for any combinations of orientations. The applicability of this performance to a 3D measured pavement surface is described

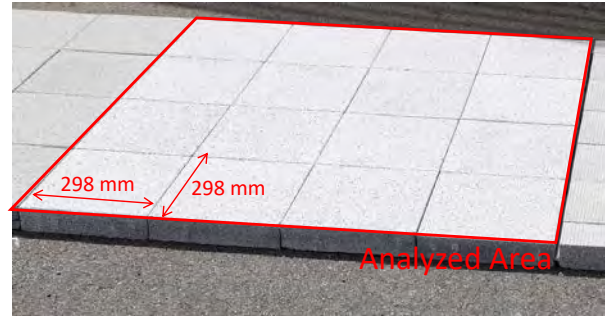


Figure 3. Overview of Target Pavement



Figure 4. TLS (RIEGL VZ-400i)

in the rest of this paper.

3 Verification Field Experiment

A field experiment was conducted to verify the diagnostic performance of DTCWT applied to the pavement surfaces. The target surface was paved with precast concrete blocks as shown in Figure 3. The point clouds were acquired with a TLS (RIEGL VZ-400i) shown in Figure 4.

3.1 Pre-processing of Point Clouds

As a pre-processing, measured data are rotated to obey the mathematical coordinate system for exploiting the directional performance of DTCWT. Then, since the density of point clouds depends on the distance from the TLS to the target object, intervals between each point are resampled to be a constant value according to the purpose of analysis. In this study, a constant interval of 1 mm is set in respect to the interaction between surface properties and micromobilities [21]. Figure 5(a) shows the contour map of measured point clouds after the pre-processing. At a glance, only a slope from the top left to bottom right can be observed in the figure whereas no diagnostic findings in terms of pavement surface characteristics are recognized.

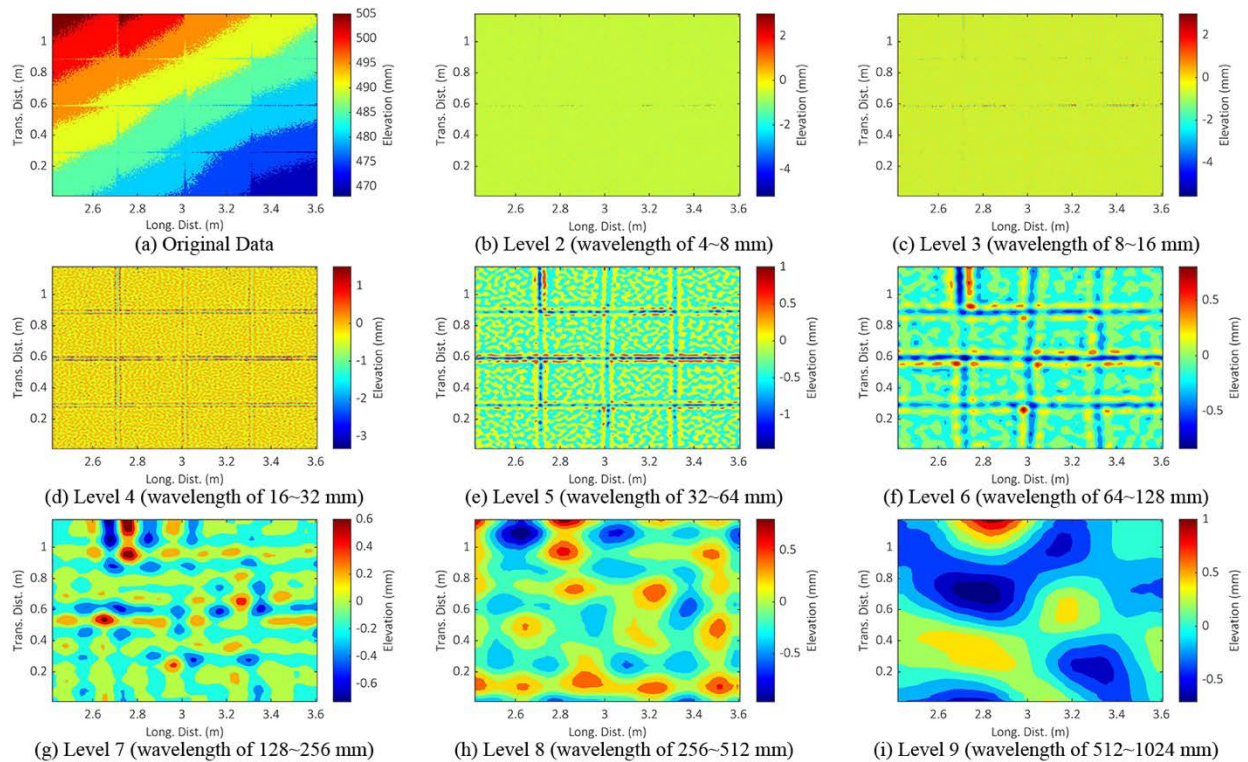


Figure 5. Multiresolution Analysis of Block Pavement

3.2 Result of Multiresolution Analysis

The DTCWT performs a multiresolution analysis by decomposing an original signal into low-pass approximation and high-pass detail components. The approximation component is further decomposed repeatedly with the same manner. This technique contributes to the diagnosis of pavement surface characteristics in terms of the simultaneous identification of wavelengths and locations.

Figure 5 indicates the result of omnidirectional multiresolution analysis from level 2 to 9 without the direct current component for the measured pavement surface. Here, the result of level 1 is excluded because no meaningful information is detected. As shown in the figure, the result provides diagnostic viewpoints based on the decomposition levels as follows:

- Level 4 component depicts the edge deterioration of precast concrete blocks,
- Level 5 to 6 components emphasize the localized joint faults, and
- Level 7 to 9 components illustrate the unevenness of the surface due mainly to the irregularity of base course.

When a practical application that identifies blocks deviated vertically is considered, level 4 highlighting edge locations and level 7 to 9 associated with unevenness can

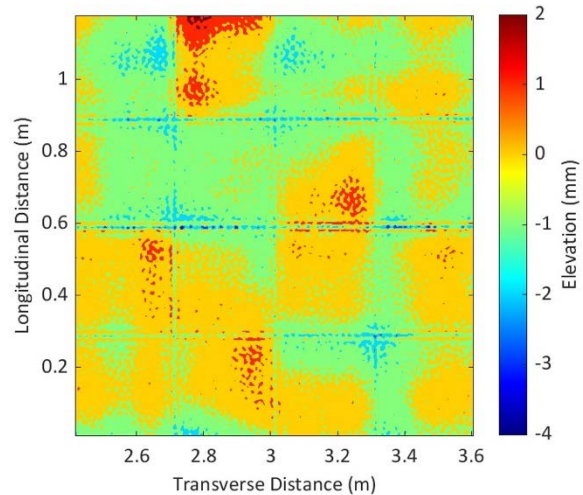


Figure 6. Reconstruction of Specific Levels Associated with Edge and Unevenness Components

be integrated by the reconstruction of wavelets as shown in Figure 6. As shown in the figure, the severe vertical displacement of a block located at the first row of the second column from the top left can be identified. This result demonstrates that the DTCWT achieves the effective vis-

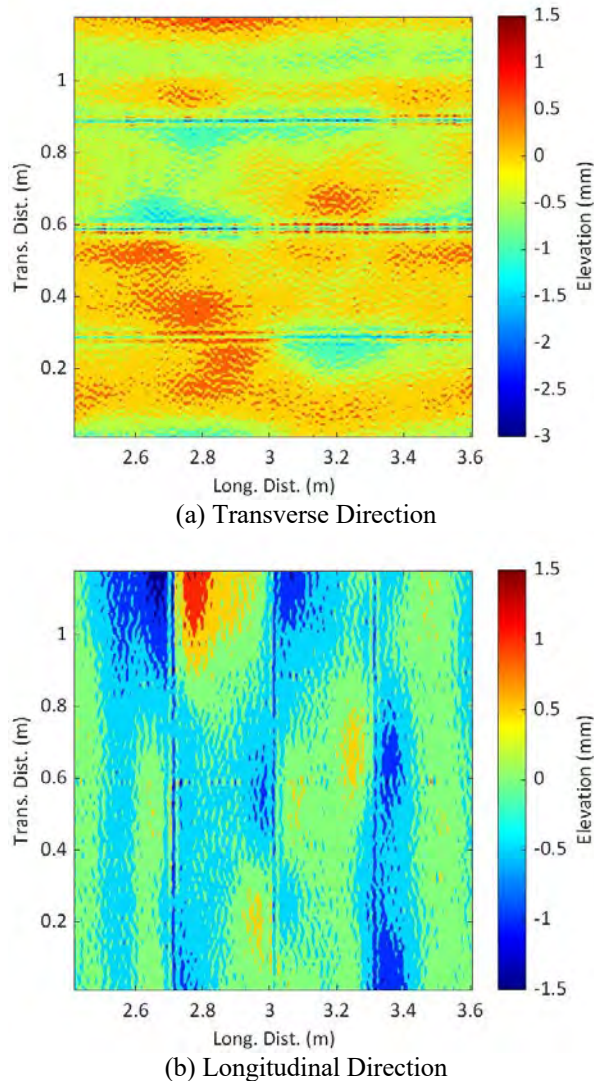


Figure 7. Result of Directional Multiresolution Analysis

ualization and evaluation of pavement distress and deformation considering wavelengths and locations.

3.3 Directional Multiresolution Analysis

A distinctive ability of DTCWT realizes a directional multiresolution analysis of 3D point clouds. It allows the recognition of orientation and spread of pavement distress and deformation. Figure 7 shows the result of directional multiresolution analysis for the target pavement. Here the longitudinal direction is defined with a combination of the orientations at $\pm 75^\circ$ whereas the transverse direction consists of a combination between the orientation at $\pm 15^\circ$ and $\pm 45^\circ$.

According to Figure 7, the deviation of the block identified in the previous section mostly occurs at the

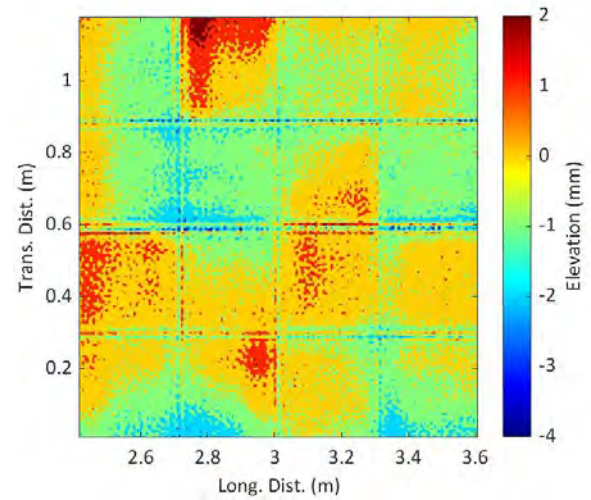


Figure 8. Reconstruction of Specific Levels Associated with Edge and Unevenness Components

longitudinal direction. This fact corresponds visually to the actual situation of the site. Thus, the longitudinal correction of the base course needs to be planned as a possible rehabilitation activity of the pavement.

3.4 Comparison with Conventional DWT

As theoretically described above, the DTCWT overcomes the shortcomings of conventional DWT in terms of the shift variant properties. This section performs the DWT for the same measured pavement surface. Figure 8 shows the reconstruction result based on the DWT in the same manner of Figure 6. As shown in Figure 8, trivial differences with Figure 6 are observed at first glance. Here, note that the result of DWT is shift variant and suffers from aliasing effects in diagonal orientation components. Figure 9 and Figure 10 show the oriented DWT and DTCWT, respectively. As shown in the figures, checkerboard artifacts due to aliasing effects can be apparently seen in the diagonal components of DWT unlike the result of DTCWT. The artifact leads to misinterpretation on the inspection result of pavement surfaces. Consequently, the capability of the directional multiresolution analysis with the DTCWT contributes to providing the evidence for the reasonable decision on pavement maintenance and rehabilitation activities.

4 Discussion and Conclusions

The pavement engineering fields nowadays widely attempts to apply 3D measurement technologies against the demand for improving construction quality as well as the productivity. However, the effective use of 3D data is still challenging due to the requirement of distinctive

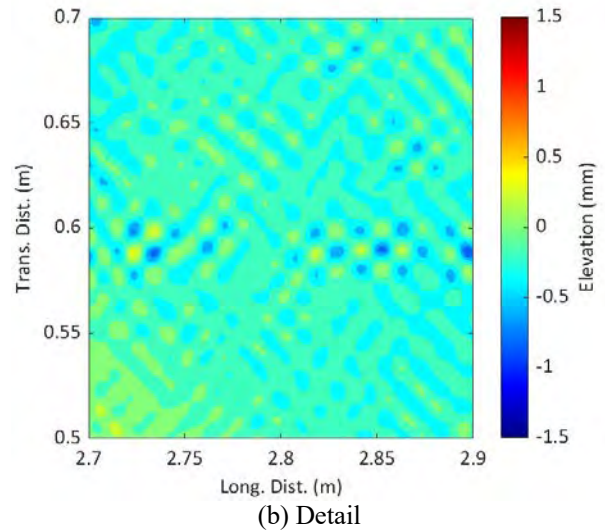
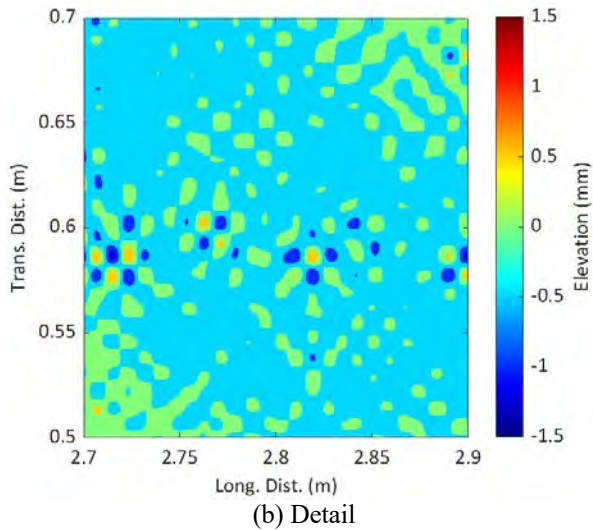
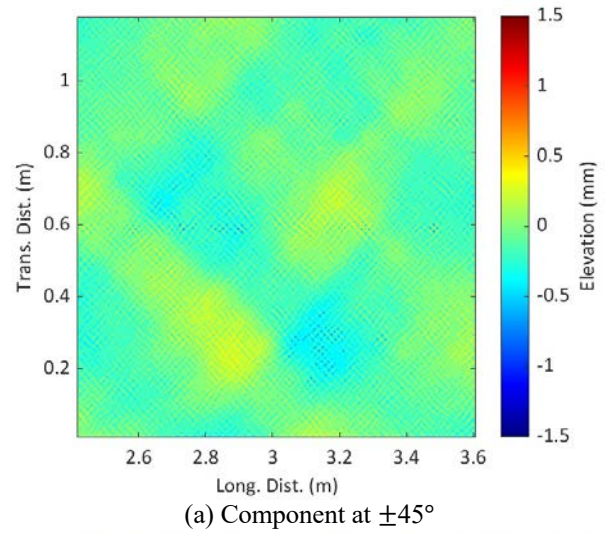
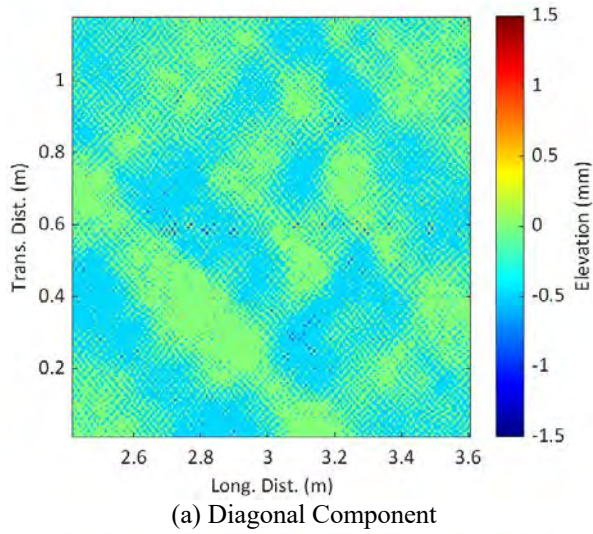


Figure 9. An Example of Oriented DWT

Figure 10. An Example of Oriented DTCWT

analysis techniques apart from conventional 2D-based methods. In the light of this background, this study has introduced a novel approach applying the DTCWT to 3D measured pavement surfaces. The DTCWT overcomes the shortcomings of conventional DWT by introducing the imaginary part in wavelet and scaling functions. The performance of DTCWT allows the effective filtering to identify pavement distress and deformation based on the directional multiresolution analysis. This study has validated the capability of the DTCWT in pavement surface analysis.

In this study, a field experiment which was subject to the pavement with precast concrete blocks was conducted to prove the capability of DTCWT. Although the measured original data provided no diagnostic findings

in terms of the pavement surface characteristics, the multiresolution analysis based on the DTCWT emphasized the specific wavelengths and locations related to the edge, joint, and unevenness. Consequently, the performance of DTCWT has been demonstrated for the effective visualization and evaluation of pavement distress and deformation.

This study also described the directional multiresolution analysis of 3D point clouds as a unique ability of DTCWT. As a result, the DTCWT was able to identify the orientation and spread of distress and deformation in the measured pavement. The advantage of DTCWT over DWT in terms of the oriented transform was validated as well. Finally, this study concluded that the directional multiresolution analysis with the DTCWT provides the evidence for the reasonable decision on pavement

maintenance and rehabilitation activities.

According to the findings acquired with this study, the performance of DTCWT has been proved for the analysis of 3D point clouds effectively and reasonably in terms of the data filtering.

References

- [1] Kondo, K., Morikawa, H., Masuta, Y., Yamaguchi, A., Takemoto, N., and Kumamoto, Y. New Standard for Dimensional Control with Lidar in Public Pavement Work, *Journal of Japan Society of Civil Engineers, Ser. F3 (Civil Engineering Informatics)*, 73 (2), pages I_83-I_91, 2017.
- [2] Higuchi, T., Sada, T., Emori, H., Murayama, S., and Fukumori, H. Study on the Measurement Finished Shapes by TLS in Pavement Work, *Journal of Japan Society of Civil Engineers, Ser. F3 (Civil Engineering Informatics)*, 75 (2), Pages II_71-II_78, 2019.
- [3] Moriishi, K. and Tomiyama, K. Efficient Improvement of Point Cloud Data Acquisition and Expansion of Application Fields into ICT Pavement Construction, *Journal of Japan Society of Civil Engineers, Ser. E1 (Pavement Engineering)*, 75 (2), Pages I_77-I_85, 2019.
- [4] Moriishi, K., Tomiyama, K., Nishikawa, K., and Yamaguchi, Y. Improvement of Operational Efficiency on Road Surface Control using 3-D Measurement Devices, *Journal of Japan Society of Civil Engineers, Ser. E1 (Pavement Engineering)*, 76 (2), Pages I_169-I_177, 2020.
- [5] Moriishi, K., Nakamura, H., and Watanabe, K. A Study of the New Road Surface Evaluation Method using Three-Dimensional Coordinate Data, *Journal of Japan Society of Civil Engineers, Ser. E1 (Pavement Engineering)*, 69 (3), Pages I_9-I_16, 2013.
- [6] Eguchi, M., Kawamura, A., Tomiyama, S., Takahashi, S., and Endo, K. A Basic Study on Evaluation of Spotted Surface Defects by a 3-dimension Formulating System using Transverse Profile Data, *Journal of Japan Society of Civil Engineers, Ser. E1 (Pavement Engineering)*, 73 (3), Pages I_71-I_78, 2017.
- [7] Hirano, H., Mizutani, T., Ishida, T., Annaka, S., and Suzuki, K. Evaluation of Local Deterioration of Pavement Surface by Spatial Frequency Analysis based on Short-Time Fourier Transform, *Journal of Japan Society of Civil Engineers, Ser. E1 (Pavement Engineering)*, 74 (3), Pages I_113-I_120, 2018.
- [8] Eguchi, M., Kawamura, A., Tomiyama, K., and Omachi, S. A Simplified Method of Detecting Spot Surface Defects by using Quasi-3D Data from a Conventional Road Profiler, *Transportation Research Record*, 2673 (11), pages. 1-11, 2019.
- [9] Han, X.F., Jin, S.J., Wang, M., Jiang, W., Gao, L., and Xiao, L. A Review of Algorithms for Filtering the 3D Point Cloud, *Signal Processing: Image Communication*, 57, pages103-112, 2017.
- [10] Liang, J., Gu, X., Chen, Y., Ni, F., and Zhang, T. A Novel Pavement Mean Texture Depth Evaluation Strategy based on Three-dimensional Pavement Data Filtered by a New Filtering Approach, *Measurement*, 166 (108265), 2020.
- [11] PIARC. Optimization of Surface Characteristics, Technical Committee Report on Surface Characteristics, *Technical Committee Report on Surface Characteristics*, pages 13-19, PIARC Xviii World Road Congress, 1987.
- [12] Deng, Q., Zhan, Y., Liu, C., Qiu, Y., and Zhang, A. Multiscale Power Spectrum Analysis of 3D Surface Texture for Prediction of Asphalt Pavement Friction, *Construction and Building Materials*, 293 (123506), 2021.
- [13] Puri, N., Valero, E., Turkan, Y., and Bosché, F. Assessment of Compliance of Dimensional Tolerances in Concrete Slabs using TLS Data and the 2D Continuous Wavelet Transform, *Automation in Construction*, 94, pages 62-72, 2018.
- [14] Parrish, C. Exploiting Full-Waveform Lidar Data and Multiresolution Wavelet Analysis for Vertical Object Detection and Recognition, *IEEE International Geoscience and Remote Sensing Symposium (IGARSS)*, 420, 2007.
- [15] Mallat, S. *Wavelet Tour of Signal Processing*, Academic Press, New York, 1999.
- [16] Kingsbury, N. Complex Wavelets for Shift Invariant Analysis and Filtering of Signals, *Applied and Computational Harmonic Analysis*, 10 (3), pages 234-253, 2001.
- [17] Selesnick, I.W., Baraniuk, R.G., and Kingsbury, N.C. The Dual-tree Complex Wavelet Transform, *IEEE Signal Processing Magazine*, 22 (6), pages 123-151, 2005.
- [18] Wang, J. and Gao, R., Pavement Distress Analysis based on Dual-Tree Complex Wavelet Transform, *International Journal of Pavement Research and Technology*, 5 (5), pages 283-288, 2012.
- [19] Daubechies, I. *Ten Lectures on Wavelets*, Society for Industrial and Applied Mathematics, 1992.
- [20] Antonini, M., Barlaud, M., Mathieu, P., and Daubechies, I., Image Coding Using Wavelet Transform, *IEEE Transactions on Image Processing*, 1 (2), pages 205-220, 1992.
- [21] Tomiyama, K. and Moriishi, K. Pavement Surface Evaluation Interacting Vibration Characteristics of an Electric Mobility Scooter, *Lecture Notes in Civil Engineering*, 76, pages 893-900, 2020.

How Can ChatGPT Help in Automated Building Code Compliance Checking?

Jiansong Zhang, Ph.D.¹

¹School of Construction Management Technology, Purdue University, United States of America

zhan3062@purdue.edu

Abstract

One main challenge in the full automation of building code compliance checking is in the extraction and transformation of building code requirements into computable representations. Semantic rule-based approach has been taken mainly due to its expected better performance than machine learning-based approach on this particular task. With the recent advancement in deep learning AI, particularly the launch of ChatGPT by OpenAI, there is a potential for this landscape to be shifted given the highly regarded capabilities of ChatGPT in processing (i.e., understanding and generating) natural language texts and computer codes. In this paper, the author preliminarily explored the use of ChatGPT in converting (i.e., extracting and transforming) building code requirements into computer codes, and compared it with the results from cutting-edge semantic rule-based approach. It was found that comparing to the semantic rule-based approach, the conversion results from ChatGPT still has limitations, but there is a great potential for it to help speed up the implementation and scale-up of automated building code compliance checking systems.

Keywords –

Automated building code compliance checking; AI; ChatGPT; SNACC; Natural language processing

1 Introduction

Automated building code compliance checking has been one promising application of artificial intelligence (AI) since its inception. Earlier efforts, however, mainly hard-coded building code requirements into computable representations. While effective in addressing various types of building code requirements, the large amount of efforts required in such hard-coding tasks coupled with the large number and different types/versions of building codes adopted at different authorities having jurisdictions (AHJs), in fact prohibited automated building code compliance checking systems from easy scaling up or even implementation in the field in the first place. In the

last two decades or so, efforts have been made to automatically or semi-automatically convert building code requirements from natural language texts into computable representations. Such efforts are considered critical in overcoming this major barrier to full automation of code compliance checking systems. Semi-automated approach requires manual labeling (or marking up) of the building code requirements using predefined tag set such as Requirement, Applicability, Selection, and Exceptions (RASE) [1] which was used in the *SMARTCodes builder* software of International Code Council [2]. While the improvement was salient comparing to the hard-coding approach, such semi-automated approach still failed to lead to wide implementation or scaling up of automated building code compliance checking systems. When it comes to investigating full automation of information extraction from building codes and their transformation into computable representations, two main approaches have been taken: machine learning-based and rule-based. In spite of the high initial rule development efforts required in the rule-based approach, it has been shown to achieve better performance than machine learning-based approach (e.g., 96.9% precision vs. 93.1% precision; 94.4% recall vs. 92.9% recall) [3,4]. Now, with the highly promising launch of GPTChat of OpenAI which inundated the AI community and our society at large recently, can the landscape of automated conversion of building codes into computable representations be shifted? To answer this question, the author conducted an initial but systematic investigation of the capabilities of GPTChat on this task, and compared it with the cutting-edge rule-based approach.

2 Background

In the automated processing (i.e., extraction and transformation) of building code requirements, for both rule-based approach and machine learning approach, natural language processing (NLP) techniques are employed. This section provides some relevant backgrounds in NLP, information extraction, building code compliance checking, and GPTChat.

2.1 Natural language processing

Natural language processing (NLP) aims to enable computers to understand and process natural human languages in a human-like manner [5]. It is an important field of AI, with multiple NLP-based systems benchmarking milestones of AI development such as the ELIZA ChatterBot program developed by Joseph Weizenbaum at MIT in the 1960s [6] and the IBM Watson that outperformed human champions in the “Jeopardy!” game in 2011 [7].

In construction research, NLP has been used to analyze and process various types of construction documents to: automate the classification of project documents [8]; extract key elements of change orders [9]; identify poisonous clauses or extract concepts and relations from construction contracts [10,11]; review and analyze construction specifications [12-15]; extract precursors and outcomes from construction injury reports [16]; and retrieve similar construction risk cases for project risk management [17]. Nora El-Gohary’s group pioneered the use of NLP in analyzing and processing building codes [3,18-20].

2.1.1 Information Extraction

Information extraction is a classic task/application in NLP, together with others such as part-of-speech tagging, named entity recognition, word sense disambiguation, information retrieval, etc. While information retrieval has achieved huge success in the commercial sector as represented by popular search engines such as Google Search and Microsoft Bing Search, information extraction is a similar but slightly different task in terms of: (1) results being monotonous; and (2) task provided with predefined information template. Information extraction is typically the first step of converting building code requirements to computable representations, with machine learning and rule-based as the two main approaches used [3,4]. In addition, semantic modeling has played important roles in this task, by enabling/augmenting extraction algorithms with semantic relations and associations, and simplifying disambiguation at the word level and phrase level.

2.1.2 Machine Translation

Machine translation aims to translate one language into another using computers. It is an even more important task to help with automated conversion of building codes to computable representations, comparing to information extraction. Modern machine translation algorithms predominately took a machine learning approach. Because features are the main ingredient of machine learning models, and feature engineering can be a labor-intensive task, information extraction is sometimes used to help generate features for training machine learning models.

In spite of the maturity of machine translation tools and techniques, the direct application of machine learning models to conquering the building code conversion problem has been under-investigated.

2.2 Building code compliance checking

Building code compliance checking is traditionally an intelligent manual task that requires deep expertise in the architecture, engineering, and construction (AEC) domain. The manual compliance checking operation is time-consuming, costly, and subjective/error-prone [3,4]. Efforts in automating the code compliance checking task date back to the 1960s when Fenves et al. [21] encoded American Institute of Steel Construction (AISC) specifications into decision tables. Since then there have been many efforts in automating the compliance checking for various building regulations such as those summarized in [22,23]. However, these efforts/systems still hard-code building code requirements or at most provided pre-defined templates to allow some flexibility in defining rules to reflect code requirements. A more efficient and flexible conversion of building codes into computable representations would significantly increase the usability of such systems. In view of that, the author jumped on a journey to harness the power of NLP and other modeling and AI techniques to pursue full automation of building code compliance checking 12 years ago and created semantic NLP-based information extraction and transformation algorithms that can automatically convert building code requirements into logic programs.

2.3 GPTChat

“GPT-Chat is a GPT-3 based conversational AI that allows users to interact with the language model to generate human-like text. GPT-Chat uses OpenAI’s GPT-3 model, which is a state-of-the-art language model that has been trained on a massive dataset of text data. It can generate text that is highly coherent and contextually appropriate, making it well-suited for a wide range of natural language processing tasks such as text generation, language translation, and question-answering.” [24]. This is the definition provided by GPTChat when asked “What is GPTChat?”

Trained using Reinforcement Learning from Human Feedback (RLHF) and fine-tuned using Proximal Policy Optimization (PPO), GPTChat has been demonstrated strong capabilities (close to completely correct and only required minor manual adjustments) in generating and translating computer codes (especially Python and Java, at the time of test) based on natural language human instructions [25,26,27]. In the context of building code conversion, the following questions naturally emerge: How well can GPTChat convert building code requirements to computer codes? How will the

performance compare to the state-of-the-art rule-based conversion?

3 Approach

This study is explorative in nature. A simple comparative evaluation approach is taken by comparing the conversion results on representative regulatory requirements.

4 Experiment

Regulatory requirements from International Building Codes in different types and in an increasing level of complexity were selected, consistent with the test cases developed in the author's previous studies for automated code compliance checking [3,18].

The tool used to generate logic programs is the most recent version of the semantic NLP-based automated compliance checking (SNACC) system which was initially described in [28,29] and has been constantly refined with more training data [30]. Although SNACC could batch process regulatory requirements, for better clarity in the comparative evaluation, the selected regulatory requirements were processed/tested one at a time. Then the same regulatory requirement was formed as a question/command in form of "Please convert "... into Python code." where the "..." will be replaced by the regulatory requirement (RQ) text with the double quotes surrounding it reserved (see an example in Fig. 1).

Time measurement was performed for both conversion processes on each RQ. When using the SNACC, time benchmarking function in Java was used to tell/record the start and finish times of the conversion process, whereas the processing time in GPTChat was measured using an online timer. Note that the GPTChat also automatically generated code explanations the time consumption of which was not included.

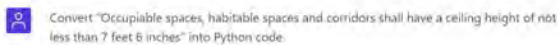


Figure 1. Example question/command in GPTChat.

5 Experimental Results and Analysis

The experimental results are listed below.

RQ1: "Spacing of transverse reinforcement shall not exceed 8 inches." [31]

Logic rules generated by SNACC:
*compliance_Spacing_of_transverse_reinforcement1(Transverse_reinforcement):-
 spacing(Spacing),transverse_reinforcement(Transverse_reinforcement),has(Transverse_reinforcement,Spacing),not_greater_than(Spacing,quantity(8,inches)).*

*check_Spacing_of_transverse_reinforcement1(X):-
 (compliance_Spacing_of_transverse_reinforcement1(X)
 ->writeln((X,is,compliant,with,section,1904-
 3,rule1));writeln((X,is,noncompliant,with,section,1904-*

3,spacing,should,be,not,greater_than,8,inches,rule2))).

Python code generated by GPTChat: Figure 2.

Time consumption by SNACC: 21.32 s.

Time consumption by GPTChat: 12.75 s.

```
max_transverse_reinforcement_spacing = 8 # in inches

def check_transverse_reinforcement_spacing(reinforcement):
    if reinforcement.spacing > max_transverse_reinforcement_spacing:
        print("Spacing of transverse reinforcement exceeds the maximum limit of 8 inches.")
    else:
        print("Spacing of transverse reinforcement meets the maximum limit of 8 inches.")
```

Figure 2. Python code for RQ1 by ChatGPT

Code explanation generated by GPTChat: "This code defines a variable 'max_transverse_reinforcement_spacing' that holds the maximum allowed spacing of transverse reinforcement in inches, and a function 'check_transverse_reinforcement_spacing' that takes an object as an input (could be a class or instance) that represent the transverse reinforcement and compares its spacing property to the maximum allowed spacing. If the spacing is greater than the maximum allowed spacing, the function will output a message indicating that the spacing exceeds the limit, otherwise it will output a message indicating that the spacing meets the limit."

RQ2: "Courts shall not be less than 3 feet in width." [32]

Logic rules generated by SNACC:
*compliance_width_of_courts1(Courts):-
 courts(Courts),width(Width),has(Courts,Width),not_less_than(Width,quantity(3,feet)).*
*check_width_of_courts1(X):-
 (compliance_width_of_courts1(X)->writeln((X,is,compliant,with,section,1904-3,rule1));writeln((X,is,noncompliant,with,section,1904-3,width,should,be,not,less_than,3,feet,rule2))).*

Python code generated by GPTChat: Figure 3.

Time consumption by SNACC: 20.58 s.

Time consumption by GPTChat: 11.16 s.

```
min_court_width = 3 # in feet

def check_court_width(court):
    if court.width < min_court_width:
        print("Court width does not meet the minimum requirement of 3 feet.")
    else:
        print("Court width meets the minimum requirement of 3 feet.")
```

Figure 3. Python code for RQ2 by ChatGPT

Code explanation generated by GPTChat: "This code defines a variable 'min_court_width' that holds the minimum required court width in feet, and a function

‘check_court_width’ that takes a court as an input and compares its width to the minimum required width. If the width of the court is less than the minimum required width, the function will output a message indicating that the court width does not meet the requirement, otherwise it will output a message indicating that the court width meets the requirement.”

RQ3: “The unit shall have a living room of not less than 220 square feet of floor area.” [32]

Logic rules generated by SNACC:

```
compliance_unit1(Unit):-
unit(Unit),living_room(Living_room),has(Unit,Living_r
oom),floor_area(Floor_area),has(Living_room,Floor_a
rea),not
less_than(Floor_area,quantity(220,square_feet)).
check_unit1(X):-
(compliance_unit1(X)->writeln((X,is,compliant,with,sec
tion,1904-
3,rule1));writeln((X,is,noncompliant,with,section,1904-
3,rule2))).
```

Python code generated by GPTChat: Figure 4.

Time consumption by SNACC: 20.45 s.

Time consumption by GPTChat: 12.41 s.

```
min_living_room_area = 220 # square feet

def check_living_room_area(unit):
    if unit.living_room_area < min_living_room_area:
        print("Living room area does not meet the minimum requirement
of 220 square feet.")
    else:
        print("Living room area meets the minimum requirement of 220
square feet.")
```

Figure 4. Python code for RQ3 by ChatGPT

Code explanation generated by GPTChat: “This code defines a variable **‘min_living_room_area’** that holds the minimum required living room area in square feet, and a function **‘check_living_room_area’** that takes a unit as an input and compares its living room area to the minimum required area. If the living room area of the unit is less than the minimum required area, the function will output a message indicating that the living room area does not meet the requirement, otherwise it will output a message indicating that the living room area meets the requirement.”

RQ4: “The thickness of concrete floor slabs supported directly on the ground shall not be less than 31/2 inches.” [31]

Logic rules generated by SNACC:

```
compliance_thickness_of_concrete_floor_slabs_sup
ported1(Concrete_floor_slabs_supported):-
thickness(Thickness),concrete_floor_slabs_supported(C
```

```
oncrete_floor_slabs_supported),has(Concrete_floor_slab
s_supported,Thickness),ground_prep(Ground),on(Con
crete_floor_slabs_supported,Ground),not
less_than(Thickness,quantity(31/2,inches)).
```

```
check_thickness_of_concrete_floor_slabs_supported
1(X):-
```

```
(compliance_thickness_of_concrete_floor_slabs_suppor
ted1(X)->writeln((X,is,compliant,with,section,1904-
3,rule1));writeln((X,is,noncompliant,with,section,1904-
3,thickness,should,be,not,less_than,31/2,inches,rule2))).
```

Python code generated by GPTChat: Figure 5.

Time consumption by SNACC: 19.03 s.

Time consumption by GPTChat: 17.22 s.

```
min_concrete_thickness = 3.5 # in inches

def check_concrete_thickness(slab):
    if slab.is_supported_directly_on_ground and slab.thickness <
min_concrete_thickness:
        print("Thickness of concrete slab does not meet the minimum requirement
of 3.5 inches for slabs supported directly on the ground.")
    else:
        print("Thickness of concrete slab meets the minimum requirement of 3.5
inches for slabs supported directly on the ground.")
```

Figure 5. Python code for RQ4 by ChatGPT

Code explanation generated by GPTChat: “This code defines a variable **‘min_concrete_thickness’** that holds the minimum required thickness of concrete floor slab supported directly on the ground in inches, and a function **‘check_concrete_thickness’** that takes an object as an input (could be a class or instance) that represent the slab, checks if it is supported directly on the ground and compares its thickness property to the minimum required thickness. If the thickness is less than the minimum required thickness, the function will output a message indicating that the slab does not meet the requirement, otherwise it will output a message indicating that the slab meets the requirement.”

RQ5: “Occupiable spaces, habitable spaces and corridors shall have a ceiling height of not less than 7 feet 6 inches.” [32]

Logic rule generated by SNACC:

```
compliance_Occupiable_spaces1(Occupiable_space
s):-
(occupiable_spaces(Occupiable_spaces);habitable_spa
ces(Occupiable_spaces);corridors(Occupiable_spaces))
,ceiling_height(Ceiling_height),has(Occupiable_spaces
_habitable_spaces_corridors,Ceiling_height),not
less_than(Ceiling_height,quantity(7,feet)),associated(O
ccupiable_spaces,Habitable_spaces),associated(Occupi
able_spaces,Ceiling_height).
```

```
check_Occupiable_spaces1(X):-
```

```
(compliance_Occupiable_spaces1(X)->writeln((X,is,co
mpliant,with,section,1904-
3,rule1));writeln((X,is,noncompliant,with,section,1904-
```

3,rule2))).

Python code generated by GPTChat: Figure 6.

Time consumption by SNACC: 18.04 s.

Time consumption by GPTChat: 17.99 s.

```
min_ceiling_height = 7 * 12 + 6 # convert 7 feet 6 inches to inches

def check_ceiling_height(space):
    if space.type in ["occupiable", "habitable", "corridor"] and
    space.ceiling_height < min_ceiling_height:
        print("ceiling height of space does not meet the minimum requirement of
        7 feet 6 inches")
    else:
        print("ceiling height of space meets the minimum requirement of 7 feet 6
        inches")
```

Figure 6. Python code for RQ5 by ChatGPT

Code explanation generated by GPTChat: “This code defines a variable ‘**min_ceiling_height**’ that holds the minimum required ceiling height in inches (7 feet 6 inches converted to inches), and a function ‘**check_ceiling_height**’ that takes a space as an input, checks if it is of type "occupiable", "habitable", or "corridor", and compares its ceiling height to the minimum required height. If the ceiling height of the space is less than the minimum required height, the function will output a message indicating that the space does not meet the requirement, otherwise it will output a message indicating that the space meets the requirement.”

RQ6: “Bars shall not be smaller than No. 4 and shall have a total area of not less than 0.002 times the gross cross-sectional area of the footing.” [31]

Logic rule generated by SNACC:

```
compliance_Bars1(Bars):-
bars(Bars),times_gross_cross_sectional_area(Times_gross_cross_sectional_area),footing(Footing),has(Footing,Times_gross_cross_sectional_area),not_less_than_or_equal(Bars,quantity(1,no_4)).
compliance_Total_area3(Total_area):-
total_area(Total_area),times_gross_cross_sectional_area(Times_gross_cross_sectional_area),footing(Footing),has(Footing,Times_gross_cross_sectional_area),not_less_than(Total_area,quantity(0.002,Times_gross_cross_sectional_area)),associated(Total_area,Times_gross_cross_sectional_area).
check_Bars1(X):-
(compliance_Bars1(X)->writeln((X,is,compliant,with,section,1904-3,rule1));writeln((X,is,noncompliant,with,section,1904-3,bars,should,be,not,less_than_or_equal,1,no_4,rule2))).
check_Total_area3(X):-
(compliance_Total_area3(X)->writeln((X,is,compliant,with,section,1904-3,rule3));writeln((X,is,noncompliant,with,section,1904-3,total_area,should,be,not,less_than,0.002,times_gross_cross_sectional_area,rule4))).
```

Python code generated by GPTChat: Figure 7.

Time consumption by SNACC: 19.45 s.

Time consumption by GPTChat: 21.03 s.

```
min_bar_size = 4
min_bar_area_ratio = 0.002

def check_footing_reinforcement(footing):
    for bar in footing.bars:
        if bar.size < min_bar_size:
            print("Bar size does not meet the minimum requirement of
            No. 4.")
            return
        if bar.area < footing.gross_cross_sectional_area *
        min_bar_area_ratio:
            print("Total area of bars does not meet the minimum
            requirement of 0.002 times the gross cross-sectional area of
            the footing.")
            return
    print("Footing reinforcement meets the requirements.")
```

Figure 7. Python code for RQ6 by ChatGPT

Code explanation generated by GPTChat: “This code defines a variable ‘**min_bar_size**’ that holds the minimum required size for bars in the footing, a variable ‘**min_bar_area_ratio**’ that holds the minimum required ratio of total area of bars to the gross cross-sectional area of the footing, and a function ‘**check_footing_reinforcement**’ that takes an object as an input (could be a class or instance) that represent the footing and check each bar in the footing against the minimum required size, and the minimum required ratio of total area of bars to the gross cross-sectional area of the footing. If any bar does not meet these requirements, the function will output a message indicating that the footing reinforcement does not meet the requirement, otherwise it will output a message indicating that the footing reinforcement meets the requirements.”

RQ7: “Any room with a furred ceiling shall be required to have the minimum ceiling height in two thirds of the area thereof, but in no case shall the height of the furred ceiling be less than 7 feet.” [32]

Logic rules generated by SNACC:

```
compliance_a_furred_ceiling1(A_furred_ceiling):-
room(Room),a_furred_ceiling(A_furred_ceiling),has(Room,A_furred_ceiling),minimum_ceiling_height(Minimum_ceiling_height),area(Area),height(Height),furred_ceiling(Furred_ceiling),has(Furred_ceiling,Height),has(Furred_ceiling,A_furred_ceiling),have_in(Room,quantity(2/3,Area)),not_less_than(Height,quantity(7,feet)).
check_a_furred_ceiling1(X):-
(compliance_a_furred_ceiling1(X)->writeln((X,is,compliant,with,section,1904-3,rule1));writeln((X,is,noncompliant,with,section,1904-3,rule2))).
```

Python code generated by GPTChat: Figure 8.

Time consumption by SNACC: 20.54 s.

Time consumption by GPTChat: 24.45 s.

```
min_ceiling_height = 7 * 12 # convert 7 feet to inches
min_ceiling_height_ratio = 2/3

def check_furred_ceiling_height(room):
    if room.has_furred_ceiling:
        if room.ceiling_height < min_ceiling_height:
            print("ceiling height of room does not meet the minimum
requirement of 7 feet")
        elif room.furred_ceiling_area < min_ceiling_height_ratio *
room.area:
            print("Furred ceiling area does not meet the minimum
requirement of two thirds of the room area")
        else:
            print("Ceiling height and furred ceiling area of room
meet the minimum requirements")
    else:
        print("Room does not have a furred ceiling")
```

Figure 8. Python code for RQ7 by ChatGPT

Code explanation generated by GPTChat: “This code defines a variable ‘**min_ceiling_height**’ that holds the minimum required ceiling height in inches (7 feet converted to inches), a variable ‘**min_ceiling_height_ratio**’ that holds the minimum required ratio of the area of furred ceiling to the room area, and a function ‘**check_furred_ceiling_height**’ that takes a room as an input, checks if it has a furred ceiling, if yes it compares its ceiling height and furred ceiling area to the minimum required”

RQ8: “In dwellings assigned to Seismic Design Category D or E, the height of the wall shall not exceed 8 feet, the thickness shall not be less than 71/2 inches, and the wall shall retain no more than 4 feet of unbalanced fill.” [31]

Logic rules generated by SNACC:

*compliance_Height_of_wall1(Height):-
dwellings(Dwellings),in_prep(Wall,Dwellings),assigned_to(Dwellings,Seismic_Design_Category_D_or_E),seismic_design_category_d_or_e(Seismic_Design_Category_D_or_E),height(Height),wall(Wall),has(Wall,Height),thickness(Thickness),unbalanced_fill(Unbalanced_fill),not_greater_than(Height,quantity(8,feet)).*

*compliance_Thickness_of_wall3(Thickness):-
dwellings(Dwellings),in_prep(Wall,Dwellings),assigned_to(Dwellings,Seismic_Design_Category_D_or_E),seismic_design_category_d_or_e(Seismic_Design_Category_D_or_E),height(Height),wall(Wall),thickness(Thickness),has(Wall,Thickness),unbalanced_fill(Unbalanced_fill),not_less_than(Thickness,quantity(71/2,inches)).*

*compliance_Unbalanced_fill_of_wall5(Unbalanced_fill):-
dwellings(Dwellings),in_prep(Wall,Dwellings),assigned_to(Dwellings,Seismic_Design_Category_D_or_E),seismic_design_category_d_or_e(Seismic_Design_Category_D_or_E),height(Height),wall(Wall),thickness(Thickness),unbalanced_fill(Unbalanced_fill),has(Wall,Unbalanced_fill),not_greater_than(Unbalanced_fill,quantity(4,feet)).*

*ss),unbalanced_fill(Unbalanced_fill),has(Wall,Unbalanced_fill),not_greater_than(Unbalanced_fill,quantity(4,feet)).
check_Height_of_wall1(X):-
(compliance_Height_of_wall1(X)->writeln((X,of,wall,is,compliant,with,section,1904-3,rule1));writeln((X,of,wall,is,noncompliant,with,section,1904-3,height,should,be,not,greater_than,8,feet,rule2))).
check_Thickness_of_wall3(X):-
(compliance_Thickness_of_wall3(X)->writeln((X,of,wall,is,compliant,with,section,1904-3,rule3));writeln((X,of,wall,is,noncompliant,with,section,1904-3,thickness,should,be,not,less_than,71/2,inches,rule4))).
check_Unbalanced_fill_of_wall5(X):-
(compliance_Unbalanced_fill_of_wall5(X)->writeln((X,of,wall,is,compliant,with,section,1904-3,rule5));writeln((X,of,wall,is,noncompliant,with,section,1904-3,unbalanced_fill,should,be,not,greater_than,4,feet,rule6))).*

Python code generated by GPTChat: Figure 9.

Time consumption by SNACC: 20.50 s.

Time consumption by GPTChat: 27.52 s.

```
max_wall_height = 8 # in feet
min_wall_thickness = 7.5 # in inches
max_unbalanced_fill = 4 # in feet

def check_wall_requirement(dwelling):
    if dwelling.seismic_design_category in ["D", "E"]:
        if dwelling.wall_height > max_wall_height:
            print("wall height exceeds the maximum limit of 8 feet for Seismic
Design Category D or E.")
        elif dwelling.wall_thickness < min_wall_thickness:
            print("wall thickness is less than the minimum limit of 7.5 inches
for Seismic Design Category D or E.")
        elif dwelling.unbalanced_fill > max_unbalanced_fill:
            print("wall retains more than 4 feet of unbalanced fill for Seismic
Design Category D or E.")
        else:
            print("wall meets the requirements for Seismic Design Category D or
E.")
    else:
        print("This check is only applicable for Seismic Design Category D or
E.")
```

Figure 9. Python code for RQ8 by ChatGPT

Code explanation generated by GPTChat: “This code defines a variable ‘**max_wall_height**’ that holds the maximum allowed height of the wall in feet, a variable ‘**min_wall_thickness**’ that holds the minimum required thickness of the wall in inches, a variable ‘**max_unbalanced_fill**’ that holds the maximum allowed unbalanced fill that the wall should retain, and a function ‘**check_wall_requirement**’ that takes an object as an input (could be a class or instance) that represent the dwelling and checks if the dwelling is assigned to seismic design category”

5.1 Analysis

It was found that with the increase of complexity in the regulatory requirement, the processing time of SNACC stayed relatively flat whereas the processing time of GPTChat stably increased (Figure 10). This can be caused by the inherent complexity of GPTChat's deep learning models which is much more complex than the rule-based core of SNACC.

In terms of the quality of the conversion results, both SNACC and GPTChat captured the logic in each regulatory requirement reasonably well. One interesting observation is that the Python codes generated by GPTChat did not directly handle units of measures in most cases. For example, "8 inches" will be implemented as the numeric value 8 with the unit of measure "inches" left to the comment section. In one case, it did convert "7" feet to "7*12" inches but still only kept the numeric value in the code and left the units to the comment section. Yet, based on the code explanations automatically generated, it appeared GPTChat did clearly understand the meaning and the use of units of measures. In addition, the code explanations appear to be smooth natural language without any error (some has period in the end some has not). Another finding was that the GPTChat struggled a little bit in dealing with domain-specific concepts such as the "No. 4" size bars. The Python code generated directly treated "No. 4" size of bars as the numeric value "4". Without domain knowledge in construction, it will be difficult to use this Python code in compliance checking applications.

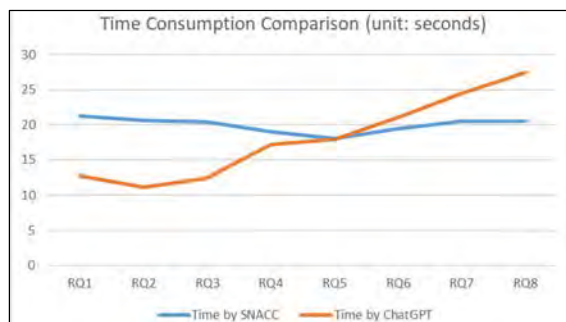


Figure 10. Time Consumption of SNACC and ChatGPT

6 Conclusion

Automated conversion of building code requirements into computable representations is one main barrier to the full automation of building code compliance checking, and thus in turn one main barrier to the wide implementation and scale-up of automated building code compliance checking systems. The state of the art in building code conversion still favored rule-based approach which had better performance than machine

learning-based approach. The recent development in deep learning especially the release of GPTChat has a potential to shift that landscape. To investigate if that is the case, the author did a preliminary but systematic set of tests on eight building code requirements with different types and increasing levels of complexity. The most recent semantic NLP-based automated compliance checking (SNACC) system was comparatively evaluated with GPTChat in converting each of the regulatory requirement. SNACC converted requirements into logic rules, whereas GPTChat converted requirements into Python codes. It was found that the processing time curve by SNACC was relatively flat with regard to the complexity of regulatory requirements whereas the processing time by GPTChat stably increased. This could be due to the nature of deep learning behind GPTChat which is inherently more complex than the rule-based algorithm behind SNACC. Furthermore, the Python codes generated did not explicitly treated units of measures, and it will require construction domain knowledge to modify the Python codes to use them in practical building code compliance checking tasks. In conclusion, the GPTChat did not immediately change the landscape in building codes conversion research but it has great potential to facilitate a faster implementation and even scaling up of existing automated code compliance checking systems by reducing the amount of efforts needed in coding. Furthermore, providing specific domain knowledge as part of the prompt could further improve the results, which the author is planning to test in his future work. More holistic testing in the future is also planned to use precision, recall, F1-measure, ROC curve, etc.

References

- [1] Hjelseth E. and Nisbet N. Capturing normative constraints by use of the semantic mark-up RASE methodology. Proc., 30th CIB W102, pages 1–10, Queensland University of Technology, Brisbane, Australia, 2011.
- [2] Wix J. and Nisbet N. Using constraints to validate and check building information models. Proc., eWork and eBusiness in Architecture, Engineering and Construction, pages 467–476, Sophia Antipolis, France, 2008.
- [3] Zhang J. and El-Gohary N. Semantic NLP-based information extraction from construction regulatory documents for automated compliance checking. *J. Comput. Civ. Eng.*, 30(2): 04015014, 2013.
- [4] Zhang R. and El-Gohary N. A deep neural network-based method for deep information extraction using transfer learning strategies to support automated compliance checking. *Autom. Constr.* 132(December 2021): 103834, 2021.
- [5] Cherpas, C. Natural language processing,

- pragmatics, and verbal behavior. *Analysis of Verbal Behavior*, 10: 135–147, 1992.
- [6] Ireland C. Alan Turing at 100. On-line: <https://news.harvard.edu/gazette/story/2012/09/alan-turing-at-100/>, Accessed: 12/01/2023.
- [7] Markoff J. Computer Wins on ‘Jeopardy!’: Trivial, It’s Not. Online: <https://www.nytimes.com/2011/02/17/science/17jeopardy-watson.html>, Accessed: 12/01/2023.
- [8] Caldas C.H., Soibelman L. and Han, J. Automated classification of construction project documents. *J. Comput. Civ. Eng.*, 16(4): 234–243, 2002.
- [9] Ko T. and Jeong H.D. Syntactic approach to extracting key elements of work modification cause in change-order documents. Proc., Construction Research Congress (CRC) 2020, pages 134–142, Tempe, Arizona, USA, 2020.
- [10] Lee J., Yi J.-S. and Son J. Development of automatic-extraction model of poisonous clauses in international construction contracts using rule-based NLP.” *J. Comput. Civ. Eng.*, 33(3): 04019003, 2019.
- [11] Al-Qady M. and Kandil A. Concept relation extraction from construction documents using natural language processing. *J. Constr. Eng. Manag.*, 136(3): 294–302, 2010.
- [12] Moon S., Lee G., Chi S. and Oh H. Automated construction specification review with named entity recognition using natural language processing. *J. Constr. Eng. Manag.*, 147(1): 04020147, 2021.
- [13] Akanbi T. and Zhang J. Automated design information extraction from construction specifications to support wood construction cost estimation. Proc., CRC 2020, pages 658–666, Tempe, Arizona, USA, 2020.
- [14] Akanbi T. and Zhang J. Design information extraction from construction specifications to support cost estimation. *Autom. Constr.*, 131(November 2021): 103835, 2021.
- [15] Ren R. and Zhang J. Semantic rule-based construction procedural information extraction to guide jobsite sensing and monitoring. *J. Comput. Civ. Eng.*, 35(6): 04021026, 2021.
- [16] Tixier A.J.P., Hallowell M.R., Rajagopalan B. and Bowman D. Automated content analysis for construction safety: A natural language processing system to extract precursors and outcomes from unstructured injury reports. *Autom. Constr.* 62: 45–56, 2016.
- [17] Zou Y., Kiviniemi A. and Jones, S.W. Retrieving similar cases for construction project risk management using natural language processing techniques. *Autom. Constr.*, 80: 66–76, 2017.
- [18] Zhang J. and El-Gohary N. Automated information extraction from construction-related regulatory documents for automated compliance checking. Proc., CIB W078 / W102, Sophia Antipolis, France, 2011.
- [19] Salama D. and El-Gohary N. Automated compliance checking of construction operation plans using a deontology for the construction domain. *J. Comput. Civ. Eng.*, 27(6): 681-698, 2013.
- [20] Salama D. and El-Gohary N. Natural language processing for automated regulatory and contractual document analysis. Proc., 2011 CSCE Annual Conference, Ottawa, ON, Canada, 2011.
- [21] Fenves S.J., Gaylord E.H. and Goel S.K. Decision table formulation of the 1969 AISC specification. *Civ. Eng. Studies: Struct. Res. Series*, 347, 1969.
- [22] Eastman, C., Lee, J., Jeong, Y., and Lee, J. Automatic rule-based checking of building designs. *Autom. Constr.*, 18(8): 1011-1033, 2009.
- [23] Dimyadi, J. and Amor, R. Automated building code compliance checking - where is it at? Proc., CIB World Build. Congress, Brisbane, Australia, 2013.
- [24] GPTChat. What is GPTChat? Online: <https://chat.openai.com/chat>, accessed: 10/01/2023.
- [25] Kim S. Writing code snippet using AI – OpenAI ChatGPT. Online: <https://medium.com/geekculture/>, accessed 11/01/2023.
- [26] Doglio F. I asked ChatGPT to build a To-Do app – Have we finally met our replacement? Online: <https://blog.bitsrc.io/>, accessed 11/01/2023.
- [27] OpenAI. CHATGPT: Optimizing language models for dialogue. Online: <https://openai.com/blog/chatgpt/>, accessed 13/02/2023.
- [28] Zhang, J. Automated code compliance checking in the construction domain using semantic natural language processing and logic-based reasoning. Ph.D. Dissertation, University of Illinois at Urbana-Champaign, Urbana, Illinois, USA, 2015.
- [29] Zhang J. and El-Gohary N. Integrating semantic NLP and logic reasoning into a unified system for fully-automated code checking. *Autom. Constr.*, 73, 45-57, 2017.
- [30] Wu J., Xue X. and Zhang, J. invariant signature, logic reasoning, and semantic natural language processing (NLP)-based automated building code compliance checking (I-SNACC) framework." *ITcon*, 28, Special Issue of The Eastman Symposium, 1-18.
- [31] International Code Council (ICC). 2009 International Building Code. Online: <https://codes.iccsafe.org/content/IBC2009>, accessed 01/01/2023.
- [32] ICC. 2006 International Building Code. Online: <https://codes.iccsafe.org/content/IBC2006>, accessed 01/01/2023.

Making Uncoordinated Autonomous Machines Cooperate: A Game Theory Approach

Kohta Sakurai and Masahide Horita

School of Engineering, University of Tokyo, Japan
sakurai-kohta655@g.ecc.u-tokyo.ac.jp

Abstract –

The construction industry in Japan is facing an increasing shortage of labor that has resulted viable demands for automation and robotics. This research study applies an approach based on game theory to model cooperation in an uncoordinated autonomous environment. A set of construction machines have been designed to complete a joint task that needs cooperation without a priori knowledge of how willing or likely other agents are to cooperate. Our simulation results show that the crisped strategy model best-promoted cooperation and successfully executed the model construction task by using the robot operating system 2.

Keywords –

Dynamic collaboration; game theory; deep reinforcement learning; multiagent determination model

1 Introduction

Automatic construction is being promoted strongly in the construction field in Japan. This field is suffering from the aging population problem that mainly comprises the construction industry and the shortage of skilled labor who can operate construction machines. To deal with these problems, efforts are currently expended to take advantage of the rapidly improving digital technology to automate constructions in ways in which operations can be conducted remotely and autonomously [1].

In the construction field, it is crucial for machines to cooperate with each other. This is because many types of machines are involved and they must achieve one common goal by associating various operations and tasks. For example, a machine should conduct its task in a rush if it is the bottleneck in the entire construction, or it should yield its resources and its flow line to others if it has some freedom to do so. To achieve the autonomous construction goal, it is important to adopt task-management approaches and cooperation mechanisms in the construction field.

Therefore, this study aims to design a dynamic

collaboration mechanism that enables construction machines to engage in their assigned tasks and cooperate with each other by applying the mathematical cooperation game theory models to the construction field. This study is based the concept that cooperative construction can be realized through individual efforts by deriving the optimal decision that considers interactions among multiple agents (i.e., without the coordination through central control) and established models that enable machines to make individual judgments. We focused on borrowing tasks conducted by more than two machines as an example of construction tasks and solves the borrowing flow-line designing problem in an actual working environment.

2 Related and Previous Research

2.1 Mathematical Approach of Cooperation Using a Game Theory Approach

Rational choice theory is a field in mathematics that is based on model cooperation. Based on this theory, the components of society are modeled as the agents or mathematical expressions of the environment, and the interaction of each component is described using a specific equation. For example, Bonabeau [2] describes complex social systems to enable the expression of emergent phenomena based on the interactions of all individual agents with others. Dynamic collaboration is considered an emergent phenomenon that appears as the result of the interactions of agents involved in task execution (e.g., making a concession effort not to prevent the flow line of other machines reduces the completion time of the overall task); accordingly, machine cooperations can be reproduced by describing interactions in agent-based models and with the use of mathematics.

Gambetta [3] studied the relationship between cooperation and risk of choice. In addition, they defined the trust of agents in other components from a prediction viewpoint; they suggested that the observation of other components would transit in accordance with their subjective intention, as a means of expression in the

subjective provability, and discussed the relationship between the freedom of choice and subjective trust probability. Additionally, Vives and Feldman [4] analyzed prosocial behavior, i.e., cooperation, from the viewpoint of absolute risk and ambiguity, and observed the relationship between one's patience to ambiguity and the emergence of prosocial behavior. The term ambiguity used in the study by Vives and Feldman [4] can be reworded to the term "subjective volatility to future events." Therefore, it is mentioned [4] that the degree of preference toward the volatility to future events may have a strong affection on the emergence of prosocial behavior.

This study considers the emergence of cooperation in the context of optimization in agent-based simulation. Generally, in agent-based simulation that uses game theory approach, a certain pay-off game and the space of actions for it in the environment are proposed (such as those proposed by Chen et al. [5]) and the relationship between cooperation and action determination way are discussed. However, this study focuses on task optimization in the dynamic programming designed by Bellman equation and evaluates the degree of system optimization. In other words, this study contributes to the total system optimization by enabling the agents to cooperate in their action space by game theory approach without coordinating with each other. This approach helps the agents to determine their actions more flexibly from the environment with cooperation in the optimization context, and this enables the efficient globally-optimized autonomous construction.

2.2 Deep Reinforcement Learning

One of the major deep reinforcement learning approaches is achieved by the Deep Q-Network (DQN) [6]. This approach adopts an optimum solution that assimilates the method of deep machine learning into value-based reinforcement learning.

In the value-based reinforcement learning method represented by DQN, Q-value, the totality of the present value of future rewards, and the assembly of the action strategy of the agent itself $\{a_s\}$ (or the probability of action choice of the agent itself, $\pi(a, s)$) are being explored. This method enables the exploration of maximized rewards from a prospective viewpoint (by solving this equation, system optimization will be completed).

At some time point t_0 , the totality of the net present value of rewards can be written as (1) using the action a and the state s :

$$\begin{aligned} E(s_{t_0} | a) & \quad (1) \\ & = r(s_{t_0}, a) + \gamma \left[\max_{\{a_{t_i}\}_{i=1}^{\infty}} \sum_{i=1}^{\infty} \gamma^{i-1} r(s_{t_i}, a_{t_i}) \right] \end{aligned}$$

where $r(s, a)$ is a rewarding function that decides the

amount of reward from states s and the agent's actions a , and γ is the time-discount rate (hereinafter, the subscripts of time are abbreviated.) Furthermore, $\{s_t\}$, the assembly of transition s is dependent on action a . The indentation of t on the action a and the state s indicates that the value is for time t .

The agent makes its choice that maximizes its total net present value of rewards; in other words, the action that maximizes equation (1) at each time t . From this perspective, the total net value of rewards in this circumstance is called the value (or value function) of the state s_t , $Q(s_t)$, at time t (however, $Q(s_t)$ can be determined only by the state s_t and not from $\{a_s\}$ or $\pi(a, s)$). This is because the agent can select its choice only by observing the state at each time point.

Thus, the value function $Q(s_t)$ can be expressed by equation (2),

$$Q(s_t) = \max_a \left\{ r(s_t, a) + \gamma \left[\max_{\{a_{t'}\}_{t'=1}^{\infty}} \sum_{t'=1}^{\infty} \gamma^{t'-1} r(s_{t'}, a_{t'}) \right] \right\} \quad (2)$$

Focusing on the recursive part on the right side, equation (2) can be rewritten as follows:

$$Q(s_t) = \max_a \{ r(s_t, a) + \gamma Q(s_{t+1}) \} \quad (3)$$

Equation (3) is called the Bellman equation and is extensively used to solve the optimization problem in dynamic programming, such as reinforcement learning. The estimation of $Q(s_t)$ in this equation is equivalent to the explosion of optimized action a_t at an optional time t (this is because the optimized action a_t can be expressed according to equation (4):

$$a_t = \operatorname{argmax}(r(s_t, a) + \gamma Q(s_{t+1})) \quad (4)$$

2.3 Deterministic Policy Gradient Algorithms (DDPG)

DDPG is a deep-learning algorithm that was presented by Silver et al. [7]. This algorithm consists of two models, namely, the actor-critic. Because the application of the concept of dividing estimation into these two models was very convenient for estimating the value function in multiagent tasks, this study established a multiagent, deep-learning model which was based on the DDPG network.

DDPG is the model used for estimating the value function $Q(s_t)$ in equation (3), as well as the DQN model. However, this model can be divided into two networks. The first one is the actor network which determines the action of the agent depending on the state s_t , and the second one is the critic network which estimates the structure of the task. The combination of these two networks enables the estimation of $Q(s_t)$ (the value where the action and the state are given). Figure 1 illustrates the concept of DDPG.

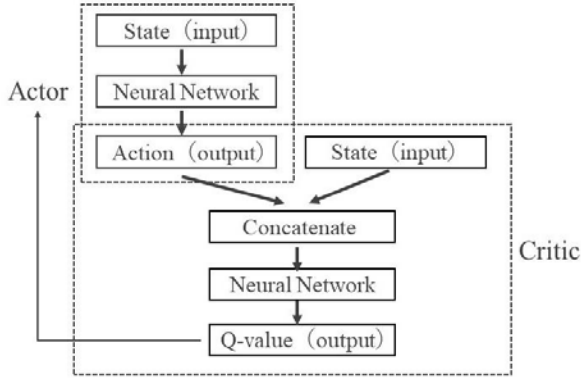


Figure 1. Actor–Critic Networks in Deterministic Policy Gradient Algorithms (DDPG)

When the function value is estimated in the DDPG model, the assembly of the action in response to the state $\{a(s_t)\}$ and the Q-value function $Q(s_t)$ are respectively replaced by the action policy [depending on the state $\mu(s_t)$] and the estimated conditional total net present value of rewards $E(s, \mu(s))$. This enables the division of the Q-value function into the actor and critic networks. The same as the DDPG model, this study adopts the actor and critic network system which estimates the agent's action policy (actor) and the relationship between the agent's action and rewards (critic) in the effort to estimate of the Q-value function.

2.4 Robot Operating System 2 (ROS2)

ROS2 is an integrative software platform that includes the tools and libraries that are necessary to develop robots. This study established the task execution environment of the real borrowing tasks of machines that was conducted by multiple agents who were already trained in the simulation by using the commands and instructions in ROS2.

3 Models and Simulation

3.1 Derivation of Multiagent Q-value Function

First, the Bellman equation, which was presented in Subsection 2-1, is extended to the model which can be applied to the multiagent system.

In a multiagent system, the competitiveness and altruism of tasks should be considered. This is because it is assumed that one's choice will have some effect (reduce or increase total net present rewards) on other agents in the case in which multiple agents engage in their tasks collaboratively at the same time. For example, if two agents engage in a major task together, they can

complete it within a short time. Alternatively, if one's flow line disturbs other machines, this reduces the entire total net present value of rewards the agent can receive). Specifically, the reward r that the agent can get in the state s is determined by both the action of the agent itself a_s and the action of another agent a_p if the number of engaging agents is equal to two (the same is true for the multi-agent systems that consist of more than three agents.) Hereafter, the action of the agent conducting the task itself is represented as a_s , and the action of another agent, who can be recognized as a partner from the perspective of the agent conducting the task itself, is represented as a_p . This difference is very important to understand which action can be controlled or not by the focused agent.

Considering the following points, the total net present value of the agent itself depending on the state s_t , the assemble of the action of the agent itself a_s , and that of a_p (equation (1) in the single-agent system case) is represented as follows (5),

$$\begin{aligned}
 E(s_t | a_s = a_s, a_p = a_p) &= r(s_t, a_s, a_p) \\
 &+ \gamma \int_{a_{p,t} \in \{a_{p,t}\}} da_{p,t} w(a_{p,t}) \left[\max_{\{a_{s,t}\}_{t=1}^{\infty}} \sum_{t=1}^{\infty} \gamma^{t-1} r(s_t, a_{s,t}, a_{p,t}) \right]
 \end{aligned} \quad (5)$$

Regarding the rewarding function, the reward that the agent can receive at time t depends on s_t , a_s , and a_p ; therefore, the argument of the reward function is extended to these three elements.

However, attention should be paid so that the argument of the left side is only s_t because all $\{a_{s,t}\}$ and $\{a_{p,t}\}$ values that emerge after the time point t are determined uniquely at time point t , including the probabilistic representation. This determination is because the partner agent is assumed that makes repeatedly the best judgment for itself (or the one which seemed to be the best at some specific time point); this helps the pruning of the transition tree. In addition, as the agent repeatedly makes the best choice for itself, this enables the pruning of the transition tree. Therefore, the total net present reward value can be determined by s_t at any time point; this is the departure from the estimated multiagent Q-value function in this study.

Meanwhile, the first term on the right side of equation (5) $r(s_t, a_s, a_p)$ is a function that depends only on s_t because a_s and a_p are constant in this situation as the left side is set to the conditional total net present value where the actions a_s and a_p are selected at time point t . However, regarding the second term $\max_{\{a_{s,t}\}_{t=1}^{\infty}} \sum_{t=1}^{\infty} \gamma^{t-1} r(s_t, a_{s,t}, a_{p,t})$ is the function that depends on state s and the assembly of its partner's choices $\{a_{p,t}\}$ because $a_{p,t}$ remains in the equation (the

argument $a_{s,t}$ is deleted by the maximization function). Thus, the arguments are not unified if the right and left sides are integrated directly into the equation.

Consequently, the integral of a function in a definite interval should be calculated to unify the arguments by multiplying it with the voluntary weighting function $w(a_{p,t})$ (when the maximization function is considered as the integration of a function multiplied by the delta function $\delta(x)$, this can be regarded as the same variation as the single-agent Q-value derivation). In this situation, the range of integration is the entire range of $\{a_{p,t}\}$.

The weighting function is an appropriate function based on the partner's action a_p . This weighting function corresponds to the idea of "belief" in game theory. Agents have some rational beliefs about the actions of others that exist outside their own optimization space (this means that they perform their own optimization by multiplying some of their appropriate weights by elements), and they determine their own choices. From this perspective, the belief is usually represented by the expression of the estimated choice probability of the partner's action $p(a_p)$, so the weighting function $w(a_{p,t})$ in equation (5) can be replaced into $w(p(a_p))$. In this case, $w(p(a_p))$ is determined voluntarily such that $\int_{a_p \in \{a_p\}} da_{p,t} w(p(a_p)) = 1$ is required following the definition of probability.

Finally, like the situation of the single-agent version, the Q-value function in the multiagent system is represented by equation (6) by replacing the conditional total net present value of rewards with the Q-value function.

$$Q(s_t) = \int da_p \max_{a_s} w(p(a_p)) \{r(s, a_s, a_p) + \gamma Q(s_{t+1})\} \quad (6)$$

The next key point is to identify a way to determine the weights $w(p(a_p))$, i.e., the way to determine one's belief according to assumptions for optimized actions of others.

One way that seems to be rational from the perspective of game theory is to determine the weights simply based on the probability density function $w(p(a_p)) = p(a_p)$. In this case, the right side of equation (6) is regarded as the expected value of the total net present value at time point t depending on the partner's choice a_p . This study refers to the determination weighting approach as the *expected action choice pattern* (this determination way is the expression that allows the volatility to future events caused by other choices).

Conversely, if the action choice probability of other

agents' $p(a_p)$ is fixed at some time point t , it can be rationally assumed that the partner agent must just select the unique choice that maximizes the choice probability (and the Q-value for the partner) because a) the partner is exploring the best actions for itself during the training and b) the partner can select just one action in the transition from s_t to s_{t+1} . (The probabilistic expression can represent one's choice; however, its action is not probabilistic but definitive). Thus, by using the delta function,

$$w(p(a_p)) = \delta(a_p - \operatorname{argmax}(p(a_p))) \quad (7)$$

where,

$$\int_{x \in \{a_p\}} dx \cdot \delta(x - \operatorname{argmax}(p(a_p))) f(x) = f(\operatorname{argmax}(p(a_p))) \quad (8)$$

This study refers to this determination weighting approach as the *maximum action choice pattern*. Herein, two ways of choice determination were set, namely, the expectative and the maximum action choice patterns; in other words, the determination ways of agents' beliefs. Additionally, this study discusses the relationship between the determination belief and the behavior of task execution represented by the swarms which were generated by the models.

3.2 Multiagent Actor-Critic Estimation Network (MA-DDPG Model)

As was presented by Silver et al. [7], the Q-value function was first replaced by the expression that depended on the self-action determination policy $\mu_s(s_t)$ and the partner's action determination policy $\mu_p(s_t)$, as follows (10):

$$(s_t) \cong Q(s_t, \mu_s(s_t), \mu_p(s_t)) \quad (9)$$

According to equation (7),

$$\begin{aligned} \mu_s(s_t) &= a_s|_{s=s_t} = \operatorname{argmax}(Q(s_t)) \\ \mu_p(s_t) &= f(a_p)|_{s=s_t} \end{aligned} \quad (10)$$

As mentioned before, this is because the self-action (which depends on s_t) can be determined definitively as it maximizes the Q-value of the agent itself. However, the partner's action will be estimated by determining rationally the weighting parameters in the model in some way (this paper used the estimations performed according to the observations of the others during training based on past experiences and periodically substituted the outcomes to the model). In the situation presented in this study, agents could only predict some types of laws for the action choice depended on s_t based

on deep-learning networks.

The multiagent actor–critic model that enabled the dynamic collaborated task execution in this study is shown in Figure 2. In the function estimation used in this study, the weighting function $w(p(a_p))$ was set out of the actor’s network (partner-action policy estimation network) because setting the output of this network as the estimated value of the partner’s action choice probability was more convenient for making the training labels based on past experiences, and the weighting function was multiplied during the transition from the actor’s network to the critic network.

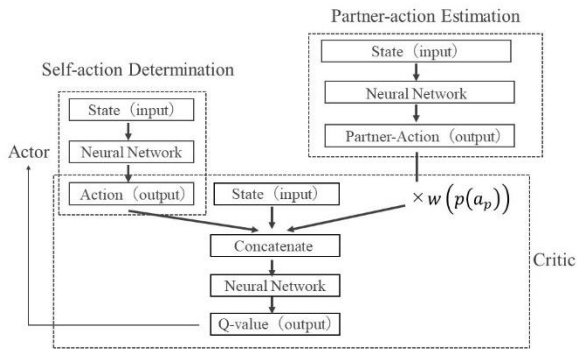


Figure 2. Multiagent Actor–Critic Estimation Network

The appropriate training of these networks enables the estimation of the Q-values of given tasks and the entire output of the model. The training targets of the three networks (self-action determination network, partner-action estimation network, and critic network) were respectively the action which maximized the Q-value at the time point t , the states-actions corresponding vectors which were stocked in the replay buffer (this enabled the estimation of the action choice probability, that is, the action policy), and the Q-value which was calculated based on the target networks. The adopted loss function of the critic model was the mean squared error (MSE) and the previous research findings, and the adopted loss functions of two actor networks were categorical cross-entropy functions because the actions were discretized in the conducted simulations.

Adopting the model shown in Section 3.2, the multiagent actor–critic estimation networks enabled the construction task execution based on dynamic collaborated cooperation between the agents.

3.3 Cooperation Fee

Changing the determination mechanism and the cooperation fee are ways to encourage the agents to cooperate.

The cooperation fee is a way of distributing its rewards to other agents as compensation for the

commitment of others. For example, the study by Miyakzaki [7] focused on the application of reward allocation methods to other agents as in indirect compensation for the commitment of others. This study also focused on the way of indirect rewards as a way of encouraging the agents to cooperate, and considered the effects associated with the use of the cooperation fee by distributing a certain proportion of rewards to the other agents at the time one agent received rewards (in cases in which an agent received a chunk of the soil or discharged it, or in the case of the borrowing task on which this study was focused on). The cooperation fee was considered as the distribution of the rewards in the task, and is defined based on equation (11),

$$r_{\text{cooperation fee}} = r_{\text{direct}} \times \delta \quad (11)$$

where r_{direct} represents the rewards that will be received directly by the task, and δ is a dummy binary variable which takes the value of one in the case in which the cooperation fee becomes available and the value of zero in the case the cooperation fee is not available. This study considered the effect of changing the availability of cooperation fee on the emergence of cooperative behaviors (the result is described in Section 4.1.2).

3.4 Construction Task Simulation

This study set a borrowing task of machine dump cars as an example of simulated and simplified construction cooperation tasks. A dump car received a clump of beads from an excavator and the dump carried it to a particular filling area in the borrowing task. This effort was completed by two dump machines, and the clump of beads was alternatively substituted with clumps of sand. The task was finished when a specific quantity of beads was carried. The training task (for machine learning) was pursued and completed based on computer simulations, and the actual execution environment was designed by using ROS2 commands. The overhead view of the site is shown in Figure 3. Solid lines in Figure 3 represent flow lines through which the machines can pass.

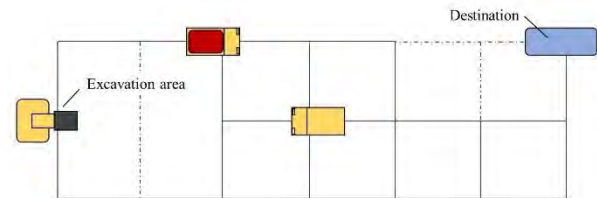


Figure 3. Overhead view of task execution area

3.5 Simulation and Learning Flow

Figure 4 depicts the learning flow diagram of agents.

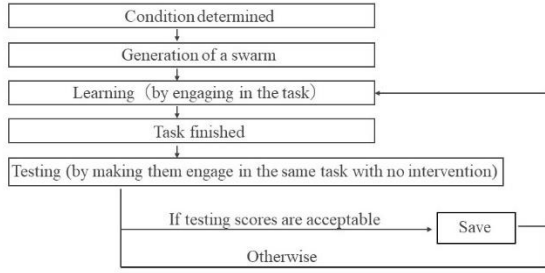


Figure 4. Flow Diagram of Training Agents and Simulations

Based on this flow diagram, the swarms of trained agents were generated, and their behaviors were observed at each point. The scores of the swarms that could finish the test task in 200 time steps were saved and the transition of their scores was observed. The score of the task execution was defined according to equation (12) by considering that the earlier agents could finish the task and that they had high scores; negative scores were not recorded.

$$\begin{cases} \text{Learning score} = 10000 - TL \\ \text{Test score} = 200 - TS \end{cases} \quad (12)$$

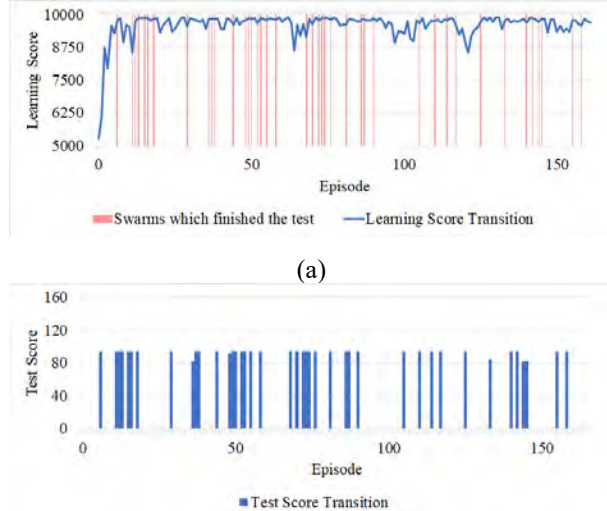
where TL is the time of the learning task execution and TS is the testing task execution.

4 Results and Discussion

4.1 Simulation Results

4.1.1 Choice theory differences

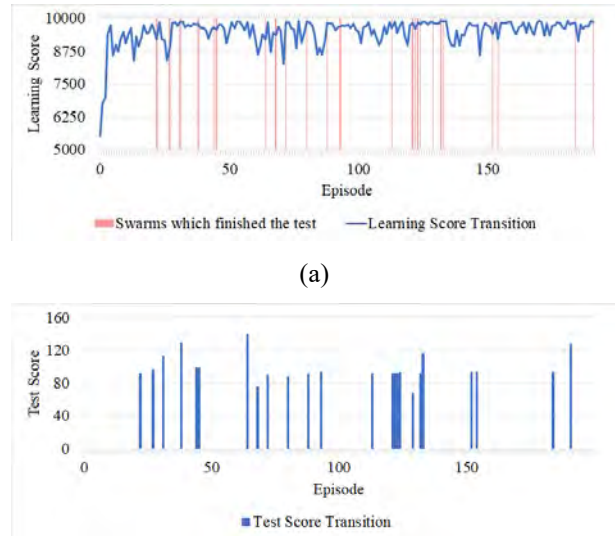
Figure 5 describes the learning and testing results of the performances which were observed by the swarms generated by the *expectative action choice* model (presented in Section 3.2).



(b)

Figure 5. a) Learning Score Transition and b) Test Score Transition in the Expectative Action Choice Model

Figure 6 describes the learning and test results of the performances which were observed by the swarms generated by the *maximum action choice* model which was presented in Section 3.2 (the cooperation fees of models used in Figures 5 and 6 were both 60% of their maximum values to eliminate the effects of cooperation fee changing; $\delta = 0.6$ was thus used in equation (11)).



(a)

(b)

Figure 6. a) Learning Score Transition and b) Test Score Transition in the Maximum Action Choice Model

Table 1. Comparison of the simulation results of the expectative action choice and maximum models

Model	Expectative model	Maximum model
Number of episodes	161	191
Number of swarms which finished the test	41 (25.5% of all swarms)	24 (12.6% of all swarms)
Number of swarms with high score (>100)	0 (0.0% of tested swarms)	5 (20.8% of tested swarms)

By comparing Figures 5 and 6, the behavioral differences of agents that were attributed to the weighting function $w(p(a_p))$ differences were considered. First, regarding the score that was observed in learning, the fluctuation of the scores was less in the expectative action choice model (Figure 5a) than that in the maximum

action choice model (Figure 6a); thus, the learning scores were more stable in the executive action choice model. These differences were considered to be attributed to the facts that a) the executive action choice was more redundant to the exploration randomness compared with the maximum action choice and b) the probability that the swarms could execute the borrowing task without being affected by the external elements was higher.

Conversely, a comparison of Figures 5b and 6b shows the probability that the generated swarms had higher test scores in the case of the maximum action choice model than those in the case of the expectative action choice model. The borrowing task could be finished in a shorter period if two agents were cooperative (if they could concede their flow lines to each other) because they could execute the task in parallel without disturbing each other. Therefore, it was considered that in the case of the maximum action choice model, the probability of generating more cooperative swarms was higher compared with that associated with the expectative action choice model. This was because the weighting function of the maximum action choice model enabled the agents to expect the choices of others to make the high-risk and high-return choices. Additionally, this point was considered to contribute to the generation of agents that could finish the task within a shorter period.

4.1.2 Cooperation Fee Differences

The effect of the cooperation fee which was discussed in Section 3.3 was also analyzed. Figure 7 shows the agents' outcomes in the case in which the cooperation fee was not available ($\delta = 0$ in equation (11)). The corresponding agents' outcomes in the case in which the cooperation fee was available ($\delta = 1$) is shown in Figure 8.

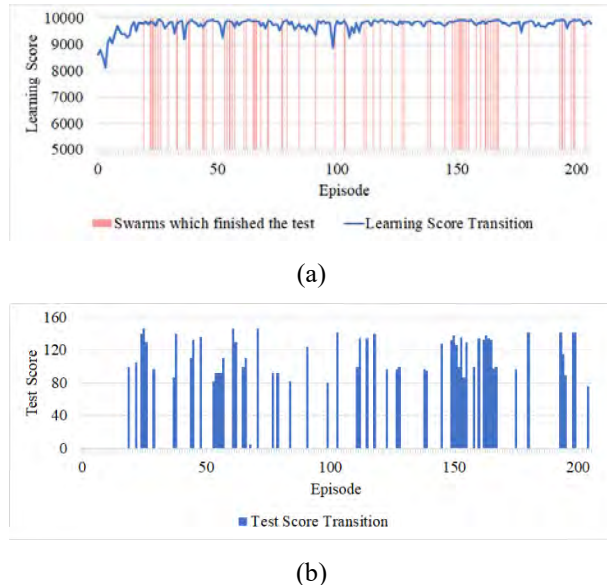
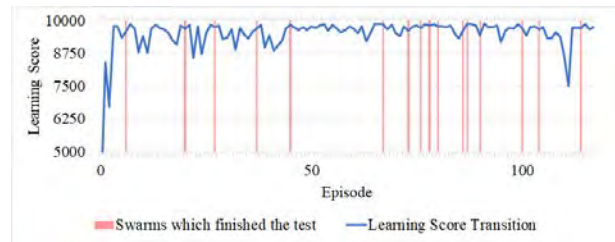
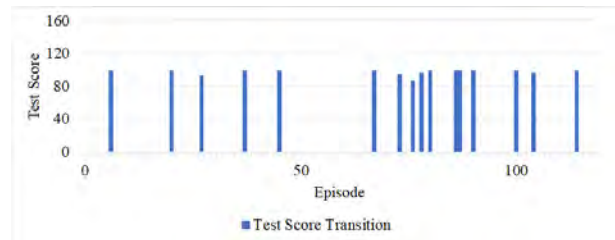


Figure 7. a) Learning Score Transition and b) Test Score Transition in the Case Wherein the

Cooperation Fee was Unavailable ($\delta = 0$)



(a)



(b)

Figure 8. a) Transition of Learning Score Transition and b) Test Score Transition in the Case Wherein the Cooperation Fee was Available ($\delta = 1$)

Table 2. Comparison of the simulation results of the expectative action choice and maximum models

Cooperation fee availability	Not available ($\delta = 0$)	Available ($\delta = 1$)
Number of episodes	206	117
Number of swarms which finished the test	64 (31.1% of all swarms)	16 (13.7% of all swarms)
Number of high-score swarms (>100)	34 (53.1% of tested swarms)	0 (0.0% of tested swarms)

In the case in which the cooperation fee was available, the task was not executed cooperatively compared with the case in which the cooperative fee was unavailable. This seemed to be because the cooperation fee may affect positively the degree of sabotage. When the cooperation fee was available, the agents could obtain the rewards without engaging in the task; accordingly, this may lead to the sabotage of the agents. Conversely, in the task design of this study, the situation in which all the agents engaged enthusiastically in their tasks made the total borrowing task time shorter. Therefore, the dedication to its task seemed to assign a cooperative effect to the task.

Based on the experiments in Subsections 4.1.1 and 4.1.2, the maximum action choice model and the unavailability of the cooperation fee were the primary contributory factors in the achievement of increased machine cooperation in borrowing tasks.

4.2 Experiments in an Actual Environment

Using the conclusion that was reached in Section 4.1 and simulation results, a swarm was generated based on the learning flow diagram and it was adequately trained. The borrowing outcomes using radio-controlled machinery in an actual environment are shown in Figure 9.



Figure 9. Task Execution in an Actual Environment

5 Conclusion

This study structured a determination algorithm that enabled the autonomous operation of machines in the construction field, focused on a method of reinforcement learning that encouraged agents to obtain an autonomous determination model by repeating training to achieve dynamic collaboration in the construction field, and used game theory to represent cooperation mathematically. In the borrowing task set as a virtual step of the construction task in this study, agents could determine cooperative choices following the model of the maximum action choice in the case in which the cooperation fee was unavailable. We verified that agents could complete set tasks within a shorter time by structuring their determination models cooperatively.

In this study, we developed a globally optimizing method of realizing an optimized multiagent system that enabled agents to determine each action efficiently in an environment that changes depending on the actions of others without coordination and performed a virtual step of an autonomous construction task. The findings of this study indicate that an agent can be encouraged to acquire optimized decisions by applying game theory to a deep-learning model in an event that the interaction of multiple agents is considered. This approach will enable cooperative agents to easily achieve a single construction project.

However, regarding the volatility of a future event, the uncertain transition of an environment caused by the uncertainty of the observation can also be considered in addition to the uncertainty caused by the actions of others. Such uncertainty can be addressed by creating an

elaborate building information modeling (BIM) model and setting appropriate weightings to the uncertainty of the environment. In the latter method, the Bellman equation, which describes a game with complete information, must be extended to an equation that can represent a game with incomplete and uncertain information. Further, improvement is required, as the game theory can contribute to achieving a sufficiently autonomous construction.

Acknowledgement

This work was supported by JSPS KAKENHI Grant Number JP22H01561 and Japan Science and Technology Agency (JST) - Moonshot Research and Development Program, Grant Number: JPMJMS2032.

References

- [1] Ministry of Land, Infrastructure, Transport and Tourism, Japan. Automated and autonomous technology for construction equipment installation. Online: https://www.mlit.go.jp/sogoseisaku/constplan/sosei_constplan_tk_000049.html, Accessed: 01/12/2022.
- [2] Bonabeau, E. Agent-based modeling: Methods and techniques for simulating human systems. *Proceedings of the National Academy of Sciences*, 99(Suppl 3):7280–7287, 2002.
- [3] Gambetta, D. Can we trust. *Trust: Making and breaking cooperative relations*, 13:213–237, 2000.
- [4] Vives, M. L., & Feldman Hall, O. Tolerance to ambiguous uncertainty predicts prosocial behavior. *Nature Communications*, 9(1):1–9, 2018.
- [5] Chen, Y. S., Yang, H. X., Guo, W. Z., & Liu, G. G.. Promotion of cooperation based on swarm intelligence in spatial public goods games. *Applied mathematics and computation*, 320:614–620, 2018.
- [6] Mnih, V., Kavukcuoglu, K., Silver, D., Graves, A., Antonoglou, I., Wierstra, D., & Riedmiller, M. Playing atari with deep reinforcement learning. *arXiv preprint arXiv:1312.5602*, 2013.
- [7] Silver, D., Lever, G., Heess, N., Degris, T., Wierstra, D., & Riedmiller, M. Deterministic policy gradient algorithms. In *International Conference on Machine Learning*, pages 387–395, Beijing, China, 2014.
- [8] Miyakzaki, K., Arai, S., & Kobayashi, S. A theory of profit sharing in multi-agent reinforcement learning. *Jinkouchinou (in Japanese)*, 14(6):1156–1164, 1999.

Full-Scale Prototype for Bricklaying Activity

Michele Ambrosino¹, Fabian Boucher², Pierre Mengeot², and Emanuele Garone¹

¹Service d'Automatique et d'Analyse des Systèmes, Université Libre de Bruxelles, Brussels, Belgium.

²NV BESIX SA, Brussels, Belgium.

Michele.Ambrosino@ulb.ac.be, fabian.boucher@besix.com, pierre.mengeot@besix.com,
egarone@ulb.ac.be

Abstract -

A major challenge for construction robotization concerns the use of robots for building activities on site. Several innovative ideas have been tried out in recent years. One of these is the idea of a mechanical mason to make the construction of walls as automated as possible. However, most of the solutions proposed so far have not gone beyond the prototype stage. In this work, we propose a new idea of a multi-robot system able to build walls with large and heavy blocks. After a detailed analysis of the current manual masonry process, the proposed mechanical design is analyzed. To test the feasibility of this innovative approach, a full-scale demonstrator and the entire control algorithm are presented and explained in detail. Experimental results show the efficiency of the proposed multi-robotic system.

Keywords -

Construction robotics; Control Architecture; Bricklaying activity; Multi-robotic System

1 Introduction

Among the different construction operations, masonry has always been an excellent candidate for robotization. It is a quite repetitive and almost deterministic activity that requires setting, in the same way, thousands of identical blocks. Moreover, especially with heavy and large blocks, masonry is one of the most dangerous construction activities. For more than 150 years, research groups around the world have been trying to develop innovative solutions to perform this type of construction activity. As a matter of fact, patents for bricklaying machines have already been announced in 1875 [1] and in 1904 [2]. These first attempts were purely mechanical bricklayers that could not sense anything about their environment. They applied a layer of mortar and mechanically placed a brick at regular intervals. However, all of these attempts never made it far beyond the demonstration stage, and never found any sort of commercial success. Beginning in the late 1980s and early 90s, we start to see attempts based on robotic arms. Unlike the previous machines, which were purely mechanical, these machines had an information processing component. These solutions were based on a high degree-

of-freedom robotic arm with sensors and control systems to “feel” the construction environment and to interact with blocks. Despite all the efforts, these attempts saw the same level of success as the previous ones. Most did not get past the level of technical descriptions, and a few reached the level of prototypes, but essentially no progress was made beyond that. Over the years, masonry has declined in importance as a construction technology in the developed world, and with it the interest in automating it. Nowadays, there is one commercial machine, SAM100, offering automation of bricklaying for large straight building facades [3]. SAM is a masonry robot built by Construction Robotics, and has been in use on commercial projects since 2015. This machine is based on a standard industrial manipulator with a gripper mounted on a large mobile base. The bricks are stored in the mobile base. A conveyor belt and a mortar dispenser serve the robotic arm with new bricks covered with mortar. A drawback of this product is that the mobile base moves on rails. Therefore the environment for this system must be structured. Moreover, the robot is a typical industrial rigid arm that is able to work only with bricks of small size. Another commercial machine is Hadrian X by Fastbrick Robotics [4]. This system consists of a big truck equipped with a telescopic robotic arm and a conveyor belt that brings the blocks to the tip of the arm. So far, this robot has been tested only to build low-rise detached houses. The adaptability of this solution in high-rise buildings and in dense urban environments is at the current stage doubtful. Other advanced prototypes on the same subject are DimRob [5], In Situ Fabricator [6], ABLR [7], and a parallel-kinematic manipulator [8]. However, to the best of our knowledge, none of them has gone beyond the advanced prototypical state. The reasons why most attempts so far have failed are different [9]. Several of the proposed solutions are designed to work in very well-structured environments and this is hardly compatible with the reality of most construction sites. Moreover, all of the previous robotic attempts require custom or small blocks which leads to increased cost and poor re-usability of the system. In the project, which this paper is part of, we propose a robotic solution that aims at overcoming some of the main limitations of the designs proposed so far (see also [10, 11]). We propose a robotic solution capable of

laying large and heavy construction blocks while remaining lightweight and maneuverable. This innovative design is based on a 'non-rigid' robot, such as a crane, in charge of the macro-movement and of holding most of the weight of the block, and a small rigid robot mounted on an aerial work platform to achieve the desired precision during the fine placement of the block.

The aim of this paper is to show the implementation and preliminary experimental validation of the proposed multi-robot bricklayer system. The experimental validation is performed on a full-scale prototype based on an industrial robotic arm and a custom-made overhead crane. The proposed control scheme will be implemented following a modular development approach, breaking down the entire architecture into several sub-modules, each of which implements a feature of the control system.

The remainder of this paper is organized as follows. In Section 2, an analysis of the process of laying sand lime blocks is proposed. In Section 3, the mechanical design of the proposed robotic solution is described. The current full-scale prototype is explained in detail in Section 4. In Section 5, the whole control architecture that allows us to properly control the system is explained and realistic experiments are shown in Section 6. Section 7 concludes the paper.

2 Bricklaying activity

To deeply understand the building process for the foreseen robotization, in this section we analyse the manual masonry process, focusing on the actions required to build walls and the type of blocks used in this operation. As a case study, we focus on sand-lime block masonry. As this type of block is widely used in the European context, and due to their size and weight, none of the robotic solutions proposed so far could handle them.

2.1 Manual masonry process

The manual masonry process to build walls with sand-lime blocks is characterized by repetitive action steps and the use of a lifting mechanism (i.e. a small crane). Typically, this activity is carried out by a team of two masons (see Fig. 1): one mason controls the crane to move the block from the pallet to its final position, and the second mason guides manually the block toward its final location. Therefore, the entire laying activity can be divided into two crucial phases. The first phase is the macro-movement performed by the crane. In this phase, the crane lifts the block and brings it close to its final position. The main difficulty of this first phase concerns the oscillations of the payload which must be counteracted with proper handling of the crane by the operator. As demonstrated by the authors in [12, 13, 14], these problems can be solved by properly



Figure 1. Pose of Silka Sand-Lime blocks

controlling the crane by making use of nonlinear control in combination with constrained control techniques. The second phase is the precision placement, which is mainly performed by the second mason. When the block is close to the final position, the mason guides the block to the final position while the other mason only operates the winch of the crane to gradually lower the load. This second operation is the subject of this work.

3 Mechanical Design

Based on the analysis carried out in the previous sections, we propose a new robotic concept for the bricklaying with large and heavy blocks based on a 'non-rigid' robot, such as a crane, in charge of the macro-movement and of holding most of the weight of the block, and a small rigid robot mounted on an aerial work platform to achieve the desired precision during the fine placement of the block. A schematic of the envisioned solution is reported in Fig. 2 where (1) is the crane, (2) the aerial work platform, (3) is the robotic arm, (4) is the block to be placed, and (5) is the existing wall.

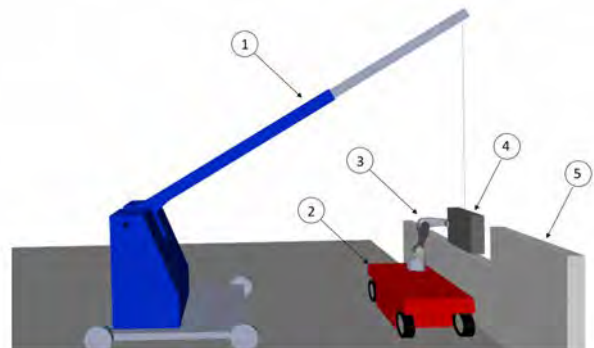


Figure 2. Layout of the robotic solution

There are a number of factors that advocate the effec-

tiveness and feasibility of this solution:

- **R&D Cost Effectiveness:** singularly taken boom cranes, aerial platforms, and industrial manipulators are well-engineered and mature devices that do not require any major research or redesign. Accordingly, the R&D needed to bring to the real world the solution proposed in this paper concerns mainly the integration and the cooperative control of the components.
- **Flexibility:** the proposed solution makes use of standard units that can be possibly used independently also for other building operations.
- **Simplicity:** once connected to the block, the rigidity of the robotic manipulator allows to sense and control the exact position and orientation of the block w.r.t. the basis of the robot. This allows for avoiding an overly complex sensory suite for the fine placement of the block.
- **Extensibility :** the concept based on the cooperation between the crane and the robotic arm can be used not only for masonry work with heavy blocks but also to perform other construction tasks where heavy materials need to be positioned precisely (e.g. steel structures, prefabricated buildings/elements assembly).

4 Experimental Setup



Figure 3. Robotic Prototype.

To test the proposed multi-robotic architecture, we built a full-scale demonstrator (see Fig. 3). The prototype consists of a robotic arm and an overhead crane to mimic the behavior of the lifting mechanism used in manual operations. In this work, the robot is fixed in one position. The idea of using a mobile base (see the mechanical design explained in Section 3), will be the subject of future implementations. The robotic arm used is a KUKA LBR IIWA14 R820. The lifting mechanism is composed of two

motors electric motors. The electric motor for the horizontal motion of the cart, subsequently called the “x-motor”, is an LK4ESZ by Holzmann Maschinen. The electric motor for the motion of the cable, from now on called the “z-motor” is an LHM1011 by FERM. The sensor for measuring the position of the x-motor is an ESA02 AH006820 (from now on referred to as the “x-sensor”), and the one keeping track of the position of the wire (from now on the “z-sensor”) is a Hengstler Incremental Encoder 1024 by RS. To be able to send commands to the motors and to read measures from the sensors, the communication is ensured by a NIDAQmx (NI USB-6008), one of National Instruments’ current-generation acquisition drivers. Moreover, a vision system based on an Intel Camera D455 is used to measure the oscillations of the suspended block thanks to the presence of markers on the surface of the block.

5 Control Architecture

This section describes the multi-robot control architecture and its sub-components (see Fig. 4). In this work, we focus on a specific task of the laying activity, namely the positioning of the block in the desired position once the robotic arm has grasped the block. From a control viewpoint, this phase is the most challenging and nonstandard one. In fact, to perform this operation an adequate control scheme should be designed so that the two units collaborate in the correct and safe way in order to guarantee that the block is placed in the final position and during the operation, the robot is never overloaded by the weight of the block since the block to be placed weighs more than the maximum admissible payload that the robot alone can handle. The other steps of the construction activity under investigation will be the subject of future exploitation of the proposed control architecture.

The control architecture in this study was developed on two devices: a Windows-based machine and an Ubuntu-based machine. A Controller Area Network (CAN bus) standard protocol is used to implement the communication between the two devices to allow the exchange of information. Moreover, in the Ubuntu-based machine, we used the Robot Operating System (ROS) framework since it provides an environment where a developer can combine numerous sub-processes called ROS nodes into an application package. In this study, five ROS nodes were developed and linked to each other in the system architecture (see Fig. 4). These nodes and their interactions are described below.

The goal of the proposed control architecture is to send commands to the crane and to the robotic arm in order to move the common payload to a desired final position. As mentioned in Section 4, the communication between the computer and the crane is ensured by a NI USB-6008.

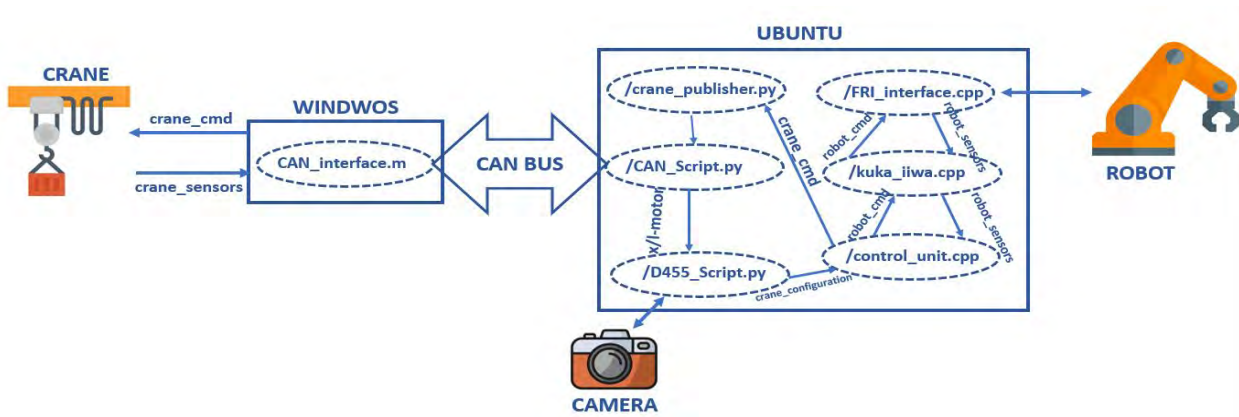


Figure 4. Robot Control Architecture

This device is only compatible with Windows and the Data Acquisition Toolbox of Matlab[®] allows a quick interface with its driver. However, the robotic arm used in this paper (i.e. a KUKA LBR IIWA14 R820), can be controlled only via an Ubuntu machine. Therefore, CAN-based communication was established between the two computers. The CAN-communication used in this work is a PCAN-USB adapter that enables simple connection to CAN networks. The **CAN_interface.m** is a Matlab[®] script that sends commands to the x-motor and the l-motor of the crane in order to move the block to the desired position. The script is also used to read measures from the x-sensor and the l-sensor. The desired commands are sent via CAN from the **/control_unit.cpp**, a ROS node. The measures from the sensors are sent instead to the Ubuntu computer. In this communication, each message is characterized by a custom and unique ID: **#ID200** x-motor command, **#ID201** l-motor command, **#ID100** x-sensor measure, and **#ID101** l-sensor measure. These messages are exchanged between **CAN_interface.m** and **/CAN_Script.py**. This ROS node runs on the Ubuntu computer and makes the interface with the CAN Bus. It receives the desired motor commands from the node **/crane_publisher.py** and it sends the measures from the sensor to the node **/D455_Script.py**. The latter node uses camera data and crane sensor data to compute all degrees of freedom of the suspended brick that cannot be measured directly (i.e. the oscillations of the cable and the three angles of the orientation of the block, see Fig. 10). The entire configuration of the crane (i.e. the position of the cart, the length of the cable, and the un-actuated degree of freedom of the block) are then sent to the node **/control_unit.cpp**. This script computes the desired commands (based on a pre-planned trajectory) to be sent to the robot and crane in order to move the common load to its final desired position. The current configuration of the crane is sent by the node **/D455_Script.py**. The current configuration of the robot is sent by the node

/kuka_iiwa.cpp. Instead, the desired commands are sent from the control node to the node **/crane_publisher.py** to actuate the crane and to the node **/kuka_iiwa.cpp** to move the robot. The last node in the proposed control architecture is the **/FRI_interface.cpp**. This node sends the desired commands to the robotic arm to make it move and receives the measurements from the sensors of the robot that are then sent to the node **/kuka_iiwa.cpp**. The pipeline between the computer and the robotic arm is illustrated in detail in Fig. 5.

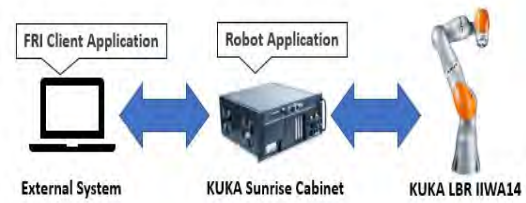


Figure 5. Robotic arm control scheme pipeline

The robot used in the proposed prototype (i.e. a KUKA LBR IIWA14), is especially suited for research in robotics, as it is accessible through a real-time interface named *Fast Robot Interface* (FRI) [15]. FRI is an interface via which data can be exchanged continuously and in real time between a robot application running on the robot controller and an FRI client application running on an external system. The FRI can be switched between position or torque control modes, accepting commands for motor position or joint torque respectively. As shown in Fig. 5, this architecture is comprised of several elements:

- **Robot application.** The Robot application is programmed in Java and executed on the robot controller. In this paper, we used KUKA Sunrise.OS 1.17, KUKA Sunrise.Workbench 1.17 and KUKA Sunrise.FRI 1.17 to program the robot.

- **FRI client application.** FRI client application can be created in C++ and is executed on an external system, in our case, on a Laptop with Intel(R) Core(TM) i7-6500U CPU 2.50GHz 2.60 GHz. In the proposed control architecture, the client application is implemented in the node `/FRI_interface.cpp`.

The code explained in this section is made available by the authors. Please send an e-mail to one of the authors to receive all information on how to download it.

6 Experimental Results

In this section, we will demonstrate via experiments the feasibility of the proposed approach. In particular, we will show that the full-scale demonstrator presented in Section 3 and the control scheme in Section 5 allows a lightweight robotic arm to manipulate a large and heavy block. The dimensions of the block used in the experiments are reported in Tab.1.

Table 1. Block Dimension

Length [m]	Height [m]	Thickness [m]
0.8	0.6	0.12

The experiment we performed is the following: the robotic arm has to move the suspended object with a weight of **30kg**, along the x-axis of *18cm* and along the z-axis of *13cm*, in order to place the object in its final position, Fig. 6. The robotic arm used in the simulations, a KUKA IIWA14 R820, can handle a payload of up to **14kg**, [16]. However, due to the fact that the mass of the block is sustained almost entirely by the cable, we can still use a lightweight robotic arm to perform the foreseen operations. A video of the experiments can be found at <https://youtu.be/XTEwk9j-W7A>.

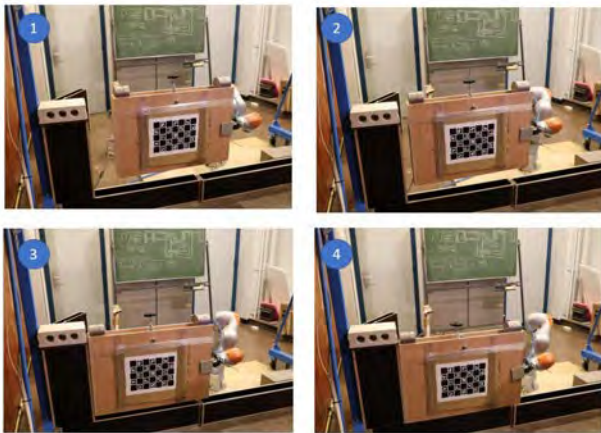


Figure 6. Experiments, pose of block

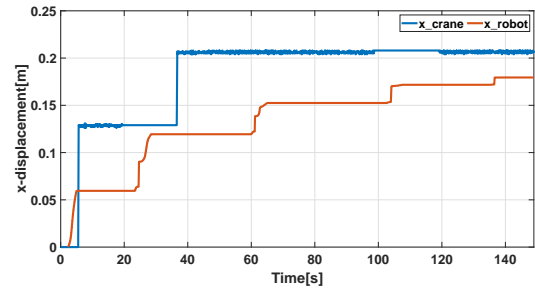


Figure 7. Time evolution of along the x direction. Red Line. Robot end-effector. Blue Line. Crane x-motor.

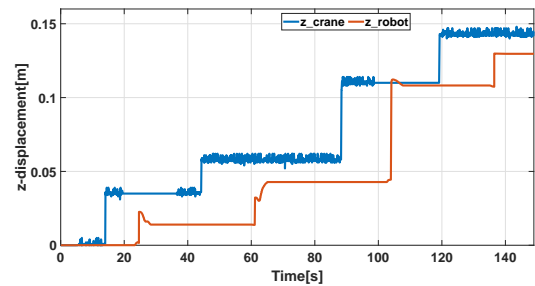


Figure 8. Time evolution of along the z direction. Red Line. Robot end-effector. Blue Line. Crane z-motor.

The desired operation is performed by combining two movements. The first movement is along the horizontal-axis. This part of the trajectory is planned so that: *i*) the robot end-effector reaches the final desired pose in the horizontal plane (see Fig. 7); *ii*) the crane follows the movement of the payload in the horizontal plane (i.e. it keeps as low as possible the angle of the cable w.r.t. to gravity) while keeping the altitude of the block constant. From Fig. 7, one can clearly see that while the cart reaches its limit after only two steps, the robot continues to move (and push) the load for the last few centimeters in order to reach the desired position and alignment with the pre-existing wall. During this operation, the parameters of the internal controller of the robotic arm are tuned so as to ensure sufficient compliance when the block enters in contact with the existing wall.

The second part of the trajectory consists of movements along the vertical-axis. Once the block is sufficiently well aligned above its horizontal desired position, the block is lowered toward the vertical destination as shown in Fig. 8. During this operation, the robot is controlled aiming to keep the horizontal position and the alignment of the block, while along the vertical axis, it follows the block in a compliant way. Moreover, as one can see in Fig. 9, during

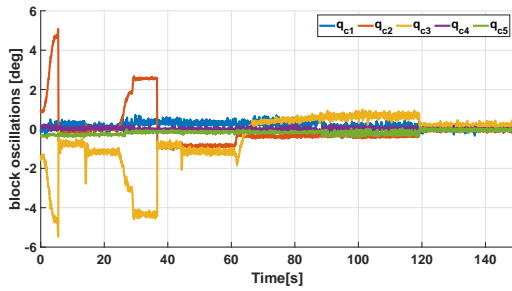


Figure 9. Time evolution of block oscillations.



Figure 10. Block configuration

the operations, the robotic arm is able to damp almost all the oscillations of the block in order to place it in the correct position with a high level of precision. In fact, there are no residual oscillations once the block has been positioned, and all the oscillation angles of the block are almost zero degrees. This allows us to conclude that the block has been positioned correctly. The two first oscillations that can be seen in the behavior of q_{c2} and q_{c3} in Fig. 9 are due to the first two movements of the block with respect to the horizontal axis. Please, refer to Fig. 10 to understand the meaning of each oscillation of the block.

It is important to notice that, despite the limitations of the payload that can be managed by the robot, the cooperation between the two robotic units ensures that the robot is never overloaded. In fact, as one can see in Fig. 11, the torques required to the robotic actuators are well within the joint torques limits.

7 Conclusion

This paper proposes a novel concept for the bricklaying of large sand-lime blocks and provides a possible embodiment to perform the construction activity. The main idea is to use the crane currently used in manual bricklaying operations in conjunction with a lightweight robotic arm. The role of the crane is to move the payload and sustain

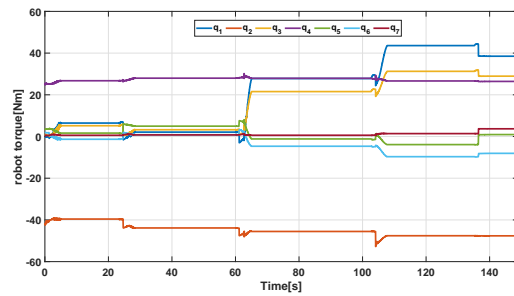


Figure 11. Time evolution of robot torques.

most of the weight of the block. The role of the robot is to place the block within the expected precision levels. The control architecture that allows the multi-robot system to perform brick-laying operations is explained in detail, highlighting its modularity that can be easily modified and extended for other technologies. We demonstrated via experimental analysis performed with a KUKA LBR IIWA14 R820 and with two industrial electric motors the feasibility of this novel approach. The preliminary results shown in this work will be exploited in the future for two activities. Firstly, the control law will be modified to be able to perform the block-grabbing activity by the robot. Secondly, the mobile platform will be implemented and tested, so that the robot can be moved around and increase its working space.

8 Acknowledgments

This research has been funded by The Brussels Institute for Research and Innovation (INNOVIRIS) of the Brussels Region through the Applied PHD grant: Brickiebots - Robotic Bricklayer: a multi-robot system for sand-lime blocks masonry (réf : 19-PHD-12).

References

- [1] C. Franke. Improvement in brick-laying machines. 1875.
- [2] J. Thomson. Brick-laying machine. 1904.
- [3] Sam100. <https://www.construction-robotics.com/sam100/>.
- [4] Hadrian x. <https://www.fbr.com.au/view/hadrian-x>.
- [5] V. Helm, S. Ercan, F. Gramazio, and M. Kohler. Mobile robotic fabrication on construction sites: Dimrob. pages 4335–4341, 2012. doi:10.1109/IROS.2012.6385617.

- [6] Markus Gifftthaler, Timothy Sandy, Kathrin Dörfler, Ian Brooks, Mark Buckingham, Gonzalo Rey, Matthias Kohler, Fabio Gramazio, and Jonas Buchli. Mobile robotic fabrication at 1: 1 scale: the in situ fabricator. *Construction Robotics*, 1(1-4):3–14, 2017.
- [7] Ablr. <https://constructionautomation.co.uk/ablr/>.
- [8] Maike Klöckner, Mathias Haage, Helena Eriksson, Henrik Malm, Klas Nilsson, Anders Robertsson, and Ronny Andersson. Insights into automation of construction process using parallel-kinematic manipulators. In *Proceedings of the 39th International Symposium on Automation and Robotics in Construction*, July 2022. doi:[10.22260/ISARC2022/0006](https://doi.org/10.22260/ISARC2022/0006).
- [9] Balaguer Carlos, Abderrahim Mohamed, Balaguer Carlos, and Abderrahim Mohamed. Trends in robotics and automation in construction. 2008.
- [10] Michele Ambrosino, Philippe Delens, and Emanuele Garone. Control of a multirobot bricklaying system. *Advanced Control for Applications*, 3(4):e90, 2021. doi:<https://doi.org/10.1002/adc2.90>.
- [11] Michele Ambrosino, Fabian Boucher, Pierre Mengot, and Emanuele Garone. Constrained control scheme for the manipulation of heavy pre-fabricated elements with lightweight robotic arm. In *Proceedings of the 39th International Symposium on Automation and Robotics in Construction*, July 2022. doi:[10.22260/ISARC2022/0053](https://doi.org/10.22260/ISARC2022/0053).
- [12] Michele Ambrosino, Arnaud Dawans, and Emanuele Garone. Constraint control of a boom crane system. In *Proceedings of the 37th International Symposium on Automation and Robotics in Construction (ISARC)*, October 2020. doi:[10.22260/ISARC2020/0069](https://doi.org/10.22260/ISARC2020/0069).
- [13] Michele Ambrosino, Marc Berneman, Gianluca Carbone, Rémi Crépin, Arnaud Dawans, and Emanuele Garone. Modeling and control of 5-dof boom crane. In *Proceedings of the 37th International Symposium on Automation and Robotics in Construction (ISARC)*, October 2020. doi:[10.22260/ISARC2020/0071](https://doi.org/10.22260/ISARC2020/0071).
- [14] Michele Ambrosino, Arnaud Dawans, Brent Thierens, and Emanuele Garone. Oscillation reduction for knuckle cranes. In *Proceedings of the 37th International Symposium on Automation and Robotics in Construction (ISARC)*, October 2020. doi:[10.22260/ISARC2020/0221](https://doi.org/10.22260/ISARC2020/0221).
- [15] Günter Schreiber, Andreas Stemmer, and Rainer Bischoff. The fast research interface for the kuka lightweight robot. In *IEEE workshop on innovative robot control architectures for demanding (Research) applications how to modify and enhance commercial controllers (ICRA 2010)*, pages 15–21. Citeseer, 2010.
- [16] Kuka. <https://www.kuka.com/>.

Bettan – Industrial robot and application for Finja Exakt build system

M. Klöckner¹, M. Haage¹, R. Andersson², K. Nilsson³, A. Robertsson⁴, H. Eriksson⁵

¹Department of Computer Science, Lund University, Sweden

²AChoice AB, Malmö, Sweden

³Cognibotics AB, Lund, Sweden

⁴Department of Automatic Control, Lund University, Sweden

⁵Winsome Consulting AB, Lomma, Sweden

E-mail: maike.klockner@cs.lth.se, mathias.haage@cs.lth.se, ronny.andersson@achoice.se, klas@cognibotics.com, anders.robertsson@control.lth.se, helena@winsomeconsulting.se

Abstract – This paper reports on efforts to create a robotized construction build system, based on the Finja Exakt manual build system. The equipment used is a generic off-the-shelf industrial arm robot integrated with a spindle crane carrier for mobility. The approach offers technical, safety and usability challenges as well as integration and business challenges for placing a generic industrial robot onsite as part of an automation solution. The question we address is if a robotized build system is a viable niche for industrial robotics in construction. In this paper the question is partially answered by reporting on an industrial robot partially adopted for work on a construction site with evaluation of individual processes in a build system.

Keywords – construction robotics, build system automation, Finja Exakt build system

1 Introduction

The electric industrial robot arm is the main work horse of the robotized part of manufacturing industry. It is typically used as automation solution in several niche applications such as palletizing, welding, assembly, conveyor picking and cutting as well as bin picking and 3D print. The robot is optimized for high performance in repeatable accuracy and cycle time. It is considered part of a “machine” and is therefore according to regulations certifiable only in its application [1]. Typically, safety aspects demand protection from human access during operation. Therefore, automation solutions utilizing robots are usually organized in work cells with protection barriers and structured input/output material handling. Recent years have seen the development of cobots (collaborative robots) to somewhat loosen safety restrictions, but such robots are typically severely limited



Figure 1. The mobile robot system Bettan (top) and the house type targeted by the robotized Finja Exakt build system (bottom) [11].

in capacity.

Placing an off-the-shelf robot arm onsite at the construction site poses challenges. Literature lists hampering factors such as high initial investment, risk for subcontractors, lack of interoperability, lack of tolerance management, immature technology, unproven effectiveness, lack of experts [2,3,4]. But there are also concerns for low productivity of regular construction equipment [10]. There are basic challenges, i.e., withstanding conditions of a new environment,



Figure 2. Steps in the manual masonry process in the Finja Exakt block system. From left to right: a) First layer. b) Customization of blocks. c) Door openings. d) Mortar application. e) Reinforcement application. f) Customization for cabling. [12]

withstanding splashes and dirt from new materials used in the process, as well as transport logistics and usability onsite. Current industrial robots are built for environments in manufacturing which could be harsh, such as foundry, but it is still not possible to purchase a robot branded for construction environment. Available tools for setup and installation of robots are optimized to support batch production. Flexibility to quickly change task and/or re-localize a robot setup with minimal and non-expert human intervention is less supported. Regarding basic robot properties, an industrial robot is optimized for cycle time and requires a stable mounting surface for full performance utilization. At the same time the payload to weight ratio is low, to guarantee repeatable accuracy at high speeds and accelerations. That said, the industrial robot is a robust automation solution within its niche tasks.

The transfer and adaptation of an industrial robot automation solution from the manufacturing sector to the construction sector is examined in this paper. Early indications has shown that the typical tasks within a build system, as the one examined in this paper, maps well to existing robot niche tasks. Solutions for handling variation through workspace sensing is also becoming more common with the technology possibly being transferable to the construction site. Being able to build on available automation experience and re-use established roads to automation solutions with current off-the-shelf technology would benefit automation solutions for construction. It is an avenue worth visiting to gain experimental data on the feasibility of the approach. Related efforts are seen in [5,6].

There are basically two views for onsite material manipulation using industrial robot automation solutions. One is to build a specialized machine where the robot is integrated in the machine as part of the solution. The SAM100¹ bricklaying machine and the Hadrian² block laying machine are examples of this approach. The other approach is to view the construction task as an

application for the industrial robot and provide application-specific packaged software, tooling and setup means for the robot on the construction site. It offers a bit more flexibility in the sense that the application is more tightly knit to a generic industrial robot and therefore might scale better with the possibility of switching applications. On the other hand, it does require to solve safety and certification of robots in applications on site. The robot presented here together with tooling and software explores creation of a construction robot and an application for a robotized Finja Exakt build system.

2 Finja Exakt build system

The Finja Exakt build system³ consists of a family of insulated blocks. The family consists of three separate siblings with different width: 290, 350 and 400 mm, respectively. Typically, one width is selected and used. Within each sibling a few block variants exist, mainly varying in placement of insulation in order to handle different build situations such as corners. Blocks exist with two heights, slightly less than 200 and 100 mm, with a praxis of adjusting wall heights using one layer of half height blocks and the rest with full height. The length is slightly less than 600 mm to allow for a 600 mm placement zone in the wall. From the standard length there is a need to cut and customize blocks into specific variants. This typically happens at windows, doors and corners. The weight of a block is between 15 to 20 kg depending on variant. The system is named Exakt (Swedish for high accuracy) because the blocks are manufactured with high tolerance in measurements. This allows blocks to be assembled into walls with small accumulation of errors. There is therefore little to no need to compensate for errors so the mortar layer between blocks can be very thin. In the Exakt system blocks are used with a mortar interlayer spacing of 3 mm. This is also the motivation for the selection of this build system

¹ <https://www.construction-robotics.com/>

² <https://www.fbr.com.au/>

³ Finja Exakt system, <https://youtu.be/S6NdghrdLkI>

for robotization as low variation in the main work object makes the system better suited for robot handling. The weight of the block and the size of the wall also fits medium-sized industrial robots well. The selection of robot for this build system, the ABB IRB 4600, handles double the payload of one block leaving around 20 kg for tooling and dressing. The robot reach of 2.5 meters matches well to the height requirement of a wall of 2.9 meters. The weight around 550 kg fits the selection of spindle crane as carrier well with the combined weight of carrier and the robot doable for a concrete slab.

2.1 Robot tasks

A mapping of robot tasks to Finja Exakt build tasks reveals standard robot operations to be performed; pick and place, depalletization, machine tending and 3D print of mortar. However, calibration procedures, normally part of an initial setup, here need to be part of the ongoing process. Because of non-rigidity in the robot structure the robot base system is non-Euclidean (curved) and not easily globally aligned with a house system. Also, the work object (house) is much larger than the robot workspace requiring a smaller robot to move around to reach the entire house with a need for recalibration to not lose position accuracy. These error sources together with other possible uncertainties (one example is placement of the robot on loose ground outside the slab) require the robot to maintain the robot base system or even local work frame relation to the house system as part of the process.

Manual operations in the Finja Exakt build system follow predefined steps, as illustrated in Figure 2 and specified in the Finja Exakt build instruction⁴, used with blueprints. In short, the first layer of blocks is laid down with care for accurate placement of openings and care taken to achieve an even layer height. The application of mortar is performed by using a special tool (white box, Figure 2). Reinforcement is applied every few layers. Custom block sizes which are needed for corners and openings (windows and doors), are generated by on-site sawing of blocks. The first layer requires robot operations to be performed in a global coordinate system requiring millimeter-accurate external references and/or metrology systems. The second layer and up can be solved with local alignment techniques using surrounding blocks as references even though care must be taken to avoid error build-up. The current state of the robotized build system focuses on solving local alignment for utilization in the second layer and up. Besides calibration needs in-process, placement of blocks is a standard robot operation.

The Exakt blocks come factory packaged on pallets,

⁴ <https://www.finja.se/produkter/block/isolerblock-exakt?id=16292060>

requiring depalletization. A complication is that the blocks are oriented on the pallet with the block top surface vertical instead of horizontal. Also, the packaging is tight making it difficult to utilize mechanical gripping techniques. The isolation layer on the block makes vacuum a possible gripping technique but the need to grip from the side and coping with dirt makes long term robustness an open question. The current state of the build system is that it will depalletize using vacuum but assemble using mechanical gripper. In the longer run a change to Exakt block geometry to allow for mechanical gripping is to be proposed.

Manual distribution of mortar between layers is done using a distribution tool in the Finja Exakt build system, as seen in Figure 2. The mortar is pumpable, so the robot utilizes a 3D print technique to distribute mortar. A complication is the need to add reinforcement every few layers. The build system utilizes a nylon sheet being pressed into the mortar after mortar distribution before adding a layer of blocks on top. In the current state of the robotized build system automatic placement of reinforcement is not addressed.

Customization of blocks is the last task in the Finja Exakt build system. There are two basic cuts used. The straight cut is used to adjust the length of the block and is mostly used to adjust blocks to suit openings, doors and windows. The other cut is a rectangular cut-out for corners to optimize use of insulation. The needed block size is measured and cut to fit in-place for each individual placement, but a common cut is the half block to allow for an interleaved layering of blocks. For the robotized build system tending of an automatic saw is utilized. The robot is responsible for accurate placing of a block in the saw, and removal of block pieces after a cut. The cut is performed by the saw.

3 Further challenges

This section develops the discussion of challenges further. Besides basics of deploying an industrial off-the-shelf robot onsite as mentioned in the introduction and challenges in development of robot tasks for a new environment as discussed in section 2, we have also encountered and/or foreseen several other challenges:

- Safety, ergonomics and certification for onsite
- Usability, collaboration and sensing onsite
- Preparation onsite
- Impacts of mobility and reachability on execution of a build plan
- Material flow and tending in execution of a build

- plan
- Tooling
 - Outdoor environment
 - Level of autonomy
 - Integration into digital tooling
 - Business case

The list is by no means complete but a reflection of work-in-progress. There are ergonomic reasons for considering a robot solution. On a general level construction sites belong to the most dangerous workplaces, including injuries through unergonomic work, injuries through accidents and fatal accidents [7,8,9]. A study performed early on at a construction site using the Finja Exakt build system revealed several risks associated with heavy lifting, working on heights and sawing. The risks were not necessarily specific for the build system but nevertheless exists with the build system. To provide a safe work environment for human and robot on the construction site, safety concepts are required meeting the requirements of the machinery regulation [1] in combination with construction directives. In Bettan safety is currently managed by requiring an operator with a deadman switch, within enclosure or with requirement on (non-)presence of personnel. However, design of a non-monitored and CE-brandable safety solution is still an open question.

The same construction site revealed the challenge associated with moving equipment around the slab with obstructions such as placement of material and hoses sticking up from the slab. In Bettan physical repositioning is a manual operation using built-in tracks. There is currently no data on possible repositioning issues caused by obstructions. Repositioning without concern for obstruction is a quick operation.

3.1 Robotized build process

The traditional work scheme for a robot is to stay stationary, protected in a cell, and manipulate material flowing in and out of the cell. For part of a build system this might work well, such as customization of blocks through sawing in the Finja Exakt build system. For other tasks, needing manipulation of a work object much larger than the work volume of the industrial robot, there is need to extend the reach. In the Finja Exakt build system this occurs during placement of blocks and distribution of mortar for blocks.

Our selected approach is a semi-automatic system where an operator utilizes the robot equipment as a tool to perform tasks in the build process. To make the robot usable for construction site workers, the robot system need to be simple to use with little robot knowledge required.

Using industrial robot equipment require planning in where to place material and planning of a build route. The

current concept is to plan the robot build process in digital tooling together with the house design and provide robot build process information with the blueprint that can be used in a preparation of a slab, for instance using bluelineing.

Experimentally, we have selected as first step the adaptation of the manual building process for straight wall segments in one-story housing as illustrated in Figure 1. This includes adaptation of processes like placing strategies of blocks, strategies for mortar application and onsite sawing as well as transport logistics, tooling, cleaning and setup.

4 Preparations

4.1 Mobile robot for Finja Exakt build system

To adapt the Finja Exakt build processes for automation we configured an industrial arm robot on a mobile platform. The equipment was chosen to put a generic industrial robot onsite to evaluate challenges in doing that and challenges in application development for the selected build system. The equipment is not necessarily the optimum selection but rather the selection we opted for to perform experiments. The equipment is called Bettan (Figure 1). It consists of an ABB IRB 4600 foundry robot mounted on a Maeda spider crane (MC174CRM) where we dismounted the crane and attached the robot with a custom-made connection plate mounted on the rotational part of the crane. This offers the possibility to enlarge the robot's workspace, by rotating the adapter plate. The spindle legs suffice to keep the robot stable during operation if acceleration is constrained. There is no rollover risk with legs extended. The legs somewhat constraint reach since there is a limit on how close to a work object the robot can be placed. With a collapsed robot and retracted legs, the form factor is sufficiently small to pass through a door.

The tooling is developed specifically for the Exakt system and is multi-functional. It consists of a gripper for pick and place operations, currently a pneumatic Schunk gripper (SCHUNK PHL-W 40-100), equipped with fingers for Exakt blocks and vacuum cups for depalletization. This is combined with an extruder for mortar distribution as well as mounting positions for sensing, currently several RGBD cameras but also touch probe and force sensor for evaluation.

Since the form factor with robot and spindle crane is rather small there is little to no room for additional necessary equipment. This is currently solved by a trailing "umbilical cord" connecting the robot to external equipment being considered as extra "payloads" in the Bettan system. Each payload is usually mounted on an EU pallet or a movable trolley with the size of an EU

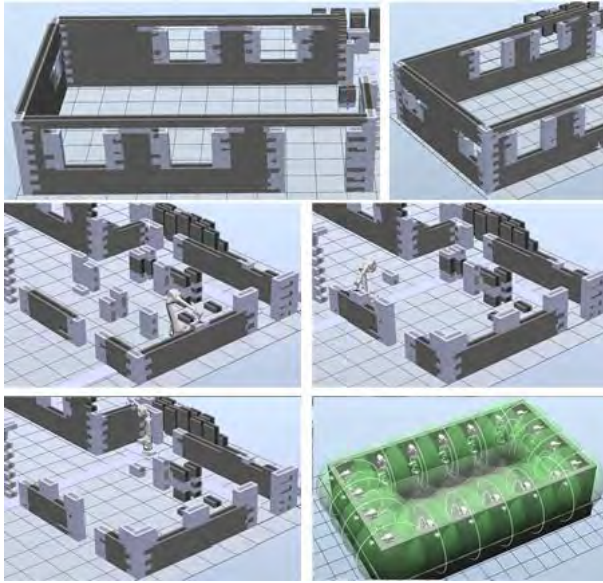


Figure 3. Digital preparation. From top to bottom: a) Parts of test house to build including straight walls, corners, openings for windows and doors (top). b) Disassembly producing stacks of blocks as material supply to a given assembly task of part of a test house (middle and bottom left). c) Calculating the amount of needed robot positions to disassemble/assemble the test house (bottom right).

pallet. The ABB compact robot controller (IRC5), the mortar pump equipment and air compressor are considered payloads. The idea is to form an “equipment island” that is moved seldom connected to a movable robot through the umbilical cord. In Bettan the equipment that is not weatherproofed is currently placed in the transport container. Construction tents are considered as well. The length of the cord is selected to allow for reach in the small houses that the system currently targets.

4.2 Digital preparation for process planning

It is common to develop offline simulations for robotized processes into CAD-like software tools to develop and validate the robot process. For a Finja Exakt robotized build process we also require a simulation. Apart from validation a simulation is also required as an end point to receive digital blueprints from external sources. The idea is to receive digital blueprints at block granularity level in nominal house coordinates, then add tolerances and letting the physical equipment solve tolerances through in-process sensing, also offering possibilities for logging sensor data for an as-built trace. This digital chain has been partly tested towards two external actors with different blueprint generation software, AChoice AB and Fojab. See Figure 3 for a generated one-story house blueprint imported into the ABB RobotStudio simulation software.

Another need is to prototype necessary planning methodology/algorithms regarding material and robot logistics to generate an execution plan and enrich a blueprint so this information can be utilized in prepping a slab for the actual physical execution.

The process planning addresses several aspects: Robot positioning, pallet (material) positioning, order of blocks to pick and order of blocks to place. For the robot re-positioning we calculated the amount of needed robot positions to build the whole house with the requirement to move the robot as little as possible to avoid wasting time for robot movement. The positioning of pallets is based on the calculated robot positions and the reachability of the robot. The generated sequence order of blocks to pick and blocks to place is based on time as well as on reachability demands. Figure 3 illustrates robot positions that might need consideration when build a house with four walls based on the robot’s workspace. A suggested starting methodology for planning is to “go backwards” and disassemble blocks of a test house and then rebuild. This to indicate a sequence of needed robot positions and required material supply at each position. Producing a timeline of build events with material supply in this manner is tested in a simulation, see Figure 1. A set of rules determine which blocks will be disassembled in which order and from which robot position. A sample rule is “If the block is a full block and lies completely in the area of the picked block from the layer above, pick the block”. The method awaits practical evaluation onsite using the robot equipment to execute a planned build sequence. It is likely that bluelining or a metrology system will be needed to support the build.

5 Experiments

The robotized build system has in addition to extensive module tests in lab also been exposed to out-of-lab tests at two occasions so far. One occurring during summer and one during winter/spring weather conditions. The main focus of the first test was to test logistics and deployment onto a site with the second test focusing more on the application and gaining experience in repeating deployment.

5.1 Outdoor tests

Pre-outdoor testing at lab facilities included building small wall segments and trying out calibration techniques such as touch probing for fine localization. The build system requires between 2-5 mm accuracy per block for a wall to be approvable at inspection with individual block positioning errors not adding up to create overhangs. For a visually pleasing result it is also important that orientation errors are kept low to keep blocks in the wall aligned. Touch sensing has the advantage of being impervious to variations in lighting



Figure 4. Robotized Finja Exakt processes. a) Wall segment assembly (top left). b) Mortar application (right). c) Sawing (bottom left).

conditions. On the other hand, touch require multiple contacts to determine a coordinate system but is feasible if the number of necessary contacts is kept low. Unfortunately, the outcome of lab experiments showed that introduced errors because of non-rigidity in the robot and carrier platform made the robot absolute coordinate system sufficiently non-Euclidean for correspondence with a house coordinate system to be outside allowed tolerance limits. Consequently, frequent local measurements were necessary for local alignment.

Integration with external measurement equipment, i.e., trackers, could be used to uphold correspondence with a house system. Trackers are sensitive equipment and operate on a line-of-sight basis. There is a need to consider occlusion in a potentially cluttered work site. The lab facilities have access to trackers with limited work volume. Exploration of this option has until now been limited to lab experiments.

The first outdoor test was performed early September 2021 with fine weather. The experiment place was located some 20 km from the lab facilities with logistics solved using two trucks, as the lift capacity was not enough for a standard smaller truck with a 400 kg lift to solve transportation of the combined weight of carrier and robot. Payloads necessary to run the system was transported on the second truck while the robot with

carrier was transported on the first truck. The system was powered from a portable construction diesel generator. The experiment consisted of packing (day before experiment), unpacking and deployment, performing part of the build system processes, packing and transportation back to lab facilities, performed during a six-hour experiment run. At the experiment site, the robot was positioned to work directly on the ground (the site did not have a slab yet). Despite one of the spindle legs being positioned on loose ground the robot behaved well during initial repeated pick and place tests performed at payload limit (40 kg tool + work object) with max speed but reduced acceleration profile (20 % of max). Lab experiments had determined the reduced acceleration profile threshold to be safe to avoid inducing potentially equipment-moving impulses. The process of constructing a wall segment was tested by picking blocks from stacks and placing to assemble the segment. A semi-manual calibration technique was employed in preparation of development of sensor-assisted local calibration techniques. The technique consisted of executing a nominal program as generated by our digital preparation tool chain, but with tolerance offsets to keep outside collision danger zones. At suitable positions in the program execution user interaction was asked for in terms of correcting the positioning of a held block

towards the wall segment. Corrections were performed in a coordinate system suitable for human interaction with manual visual inspection of correctness. The manual correction process turned out to be rather effective with less than 30 secs needed for a correction. It does require entering the robot work area though. Still, the idea is to replace the manual correction process with an automated sensor-assisted process, with the manual process as a fallback option. As for the number of corrections needed for a program run of 4-5 layers of blocks two corrections were initially tried at the beginning of the program, at the start and end of the first layer. However, it turned out, that this was not enough and several more corrections were needed, either each layer or every second layer. Also, runs for gluing were performed.

The second outdoor test was executed during spring 2022 over longer period of time. The experiment site was located around 100 km from the lab facilities. Weather conditions varied from snowing to sunny with experiments being performed below roof or open sky. As lesson learned from the first test a container was rented for the equipment and was used for transport. This test featured several one-day deployment experiments to exercise setup and packaging of the equipment. It also saw a more full-ranged execution of build system processes, including wall segment assembly (Figure 4 top left), mortar application (Figure 4 right), and sawing (Figure 4 bottom left). Appropriate equipment was used with the robot for these tests, i.e., saw, pump, air, control cabinet and logistics for use of additional equipment was tested. Data was gathered to evaluate RGBD cameras as assistive sensing technology for local calibration in-process. Partial gathering of performance data was done.

5.2 Results

Table 1 summarizes the experiment results in terms of a scenario of building a small house similar to the one shown in Figure 1. The house consists of 1200 Exakt blocks (based on simulation in Figure 3) and around 20 % of those need adjustment through sawing. Measured values from experiments are marked with M. Estimated values are marked with P. Operations O1-2 involve repositioning of the robot. The number of repositioning's is estimated using the work volume of the robot and Exakt system regulations allowing stacking of only three layers of blocks in a short time. Operation O3 considers the robot at a fixed position, and not performed together with O1-2 in this scenario.

Table 2 shows estimated total time spent by operator (tending robot) and robot (automatic operation) for the operations shown in Table 1. Table 2 reflects our current target for Bettan, which is semi-autonomous operation using automatic calibration (current work-in-progress) and manual repositioning performed by operator (in the scenario every 9th minute). Automatic repositioning, we

consider future work.

Table 1. Bettan time study for a small house scenario consisting of 1200 Exakt blocks. Headline Man = manual operation, Auto = automatic operation, Reps = repetitions. Operation O1 = place 1200 blocks at 100 robot positions, O2 = mortar application on 1200 blocks at 100 robot positions, O3 = sawing of 20 % of 1200 blocks. Time is measured in minutes and annotated with M = measured value from experiments, P = estimated value based on experience from experiments and/or simulation.

Operation	Man [min]	Auto [min]	Reps
O1a: Reposition robot	M 2	P 2	P 100
O1b: Recalibrate	P 5	P 0.5	P 100
O1c: Pick n place x 12		M 4	P 100
O2a: Recalibrate	P 5	P 0.5	P 100
O2b: Mortar startup		M 0.17	P 300
O2c: Mortar application		M 0.13	P 1200
O3a: Recalibrate	P 5	P 0.5	P 24
O3b: Replace material	P 5		P 24
O3c: Pick n place x 3		M 1	P 240
O3d: Sawing	M 0.17	M 0.17	P 240

Table 2. Interpretation of experiment data as total operator (manual tending of robot) and robot (automatic execution) time spent in a 1200 block house scenario based on data from Table 1. Assuming automatic calibration and manual repositioning. Note that time spent is based partially on estimated data. Time not directly related to robot operation, such as digital and onsite preparation for robot operation, is left out.

Use case	Tending [h]	Auto [h]
O1+O2	4	12
O3	2	5

6 Conclusion & Future work

The paper reports on efforts to automate a build system using an industrial robot made mobile as automation solution. The prototype is called Bettan. The build system selected is the Finja Exakt build system. Development of a Finja Exakt build system application for the robot has progressed so far that individual build system processes are fully or partially implemented and in the phase of being tested. The next step is further evaluation to approach the question of viability for industrial off-the-shelf robots as automation tools in build systems. The focus is not to build a fully optimised robot solution but to build a low cost robot that already in the short run is cost effective in a high cost country. The authors consider that such an application would have

the largest impact on the use of robots in construction.

There is a need to allow spending of effort to develop higher level TRL complex prototype systems in risk sectors. In this case to try out a hypothesis of technology transfer from mature industry to immature (from an automation perspective). Higher TRL is necessary to reach and expose problems and issues only visible at higher TRLs, such as regulation, certification, business case, cost effectiveness, role among actors and in market, quantifiable societal and climate impact, besides technical issues. The Bettan demonstrator is currently developed throughout four research projects.

7 Acknowledgement

The authors gratefully acknowledge the support received from project "Innovative Agile Construction for globally improved sustainability (ACon4.0)", Vinnova UDI 1 2018-03362, for initially exposing the question. Project "Innovativt bostadsbyggande genom flexibla robotar i samverkan med människor" (Boverket 181006) for initial equipment acquisition and application development. Project Vinnova UDI 2 (ACon4.0) 2019-04750 for further application development, first outdoor testing and business evaluation with proposal (the ACon4.0 model). Project "Systemdemonstration av affärsmodell för flexibel produktion av enfamiljshus baserad på digitaliserad integrerad informationshantering, robotiserad bygglats produktion och kundmedverkan" (Formas 2021-00334) for second outdoor testing and development of sensing for calibration in-process as well as planning in simulation. Finally, we are grateful towards the Center for Construction Robotics at Lund University for hosting the work and associated partners for participating in the projects and aiding system development. In particular, we acknowledge AChoice AB for allowing use of their digital construction document preparation pipeline and their interest in adapting it for robot solutions, Petra Jenning and Henrik Malm at Fojab for early consideration of robot solutions in building design and in architecture design tools, Cognibotics AB for aiding equipment developments, Robert Larsson at Cements AB for aid with 3D print, Miklos Molnar at Dept. of Structural Engineering, Lund University for work on alternative reinforcement methods for the Finja Exakt build system to better suit automation solutions. Finally, to our regrets, Anders Robertsson, one of the authors of this paper, passed away during the processing of the paper. We will miss him dearly.

References

[1] Proposal for a REGULATION OF THE EUROPEAN PARLIAMENT AND OF THE

- COUNCIL on machinery products COM/2021/202 final. Online: <https://eur-lex.europa.eu/legal-content/EN/TXT/?uri=CELEX:52021PC0202>, Accessed: 30/03/2023.
- [2] Saidi, K. S., Bock, T., & Georgoulas, C. (2016). Robotics in construction. In *Springer handbook of robotics* (pp. 1493-1520). Springer, Cham.
- [3] Buchli, J., Giftthaler, M., Kumar, N., Lussi, M., Sandy, T., Dörfler, K., & Hack, N. (2018). Digital in situ fabrication-Challenges and opportunities for robotic in situ fabrication in architecture, construction, and beyond. *Cement and Concrete Research*, 112, 66-75.
- [4] Delgado, J. M. D., Oyedele, L., Ajayi, A., Akanbi, L., Akinade, O., Bilal, M., & Owolabi, H. (2019). Robotics and automated systems in construction: Understanding industry-specific challenges for adoption. *Journal of Building Engineering*, 26, 100868.
- [5] Hunhevicz J. et al. Construction Processes for the Future - Using the NEST dfab Unit as a Case Study. 2017.
- [6] Van Hoogstraten J. CyBe: Robot Crawler. Online: <https://cybe.eu/3d-concrete-printing/printers/cybe-robot-crawler/>, Accessed: 10/01/2023.
- [7] Bavafa A. et al. Identifying and assessing the critical factors for effective implementation of safety programs in construction projects. *Safety Science*, 106 (2018), pp. 47-56.
- [8] Dillon A. et al. Precursors of construction fatalities. II: Predictive modeling and empirical validation. *Journal of Construction Engineering and Management*, 143 (7),(2017), pp. 04017024-1 – 04017024-12.
- [9] Jin R. et al. A science mapping approach based review of construction safety research. *Safety Science*, 113 (2019), pp. 285-297.
- [10] Manikandan, M. et al. A study and analysis of construction equipment management used in construction projects for improving productivity. *Journal of Engineering and Technology*, 3, (2018), pp. 1297 – 1303.
- [11] Klöckner M. et al. Insights into automation of construction process using parallel-kinematic manipulators. *Proceedings of the 39th International Symposium on Automation and Robotics in Construction (ISARC)*, pp. 25 - 32, Bogotá, Colombia, 2022.
- [12] Klöckner M. et al. Parallel kinematic construction robot for AEC industry. In *Proceedings of the 37th International Symposium on Automation and Robotics in Construction (ISARC)*, p. 1488 - 1495, Kitakyushu, Japan, 2020.

Optical Process Control for extrusion-based Additive Manufacturing methods in construction

Rafay Mohiuddin^{1*}, Miranda Cruz Policroniades^{1*}, Martin Slepicka^{1*}, and André Borrmann^{1*}

¹Chair of Computational Modeling and Simulation, Technical University of Munich, Germany

* all authors have contributed equally.

martin.slepicka@tum.de

Abstract -

Additive Manufacturing (AM) provides many advantages when applied to the field of construction. However, due to the large scale of construction projects, time requirements for the printing process are also large, making AM processes susceptible to the influence of external variables. Accordingly, it is advisable to employ methods that can ensure the stability of the extrusion process. This study demonstrates a method to increase the reliability of extrusion-based concrete 3D printing processes through automated monitoring and controlled material extrusion process. In order to maintain a consistent width of the extruded material, a closed-loop optical process control system capable of tracking extruded layers has been developed. It utilizes a mounting system for the monitoring system (RGB camera) that can automatically rotate and moves relative to the printing nozzle and tracks the extruded filament. A computer-vision-based algorithm monitors the filament's width in real-time and continuously transmits the information to a PID controller regulating the material extrusion rate. Overall, the system can effectively track the extruded filament and adjust the extrusion rate based on the vision system, demonstrating significant potential in real-time process control applied in robotic construction.

Keywords -

Digital Fabrication; Automation in Construction; Additive Manufacturing; Process Monitoring; Real time Control, Computer Vision;

1 Introduction

Additive Manufacturing (AM) has been an established technology in many industries for a long time; in particular, it is often used to produce sample components (rapid prototyping). This technology has already revolutionized various industries and shows great potential for the construction industry as it improves construction projects' speed, efficiency, and sustainability [1]. Due to various scaling problems, this technology was not adopted in the construction industry for a long time but is now gaining more acceptance [2]. Many research projects focus on developing new and improved methods and exploring suitable material mixtures.

Another emerging field of research related to AM in construction is the development of appropriate process monitoring systems. Monitoring and progress reporting

are essential management functions in delivering construction projects while minimizing delays and cost overruns [3]. The typical workflow for AM with concrete is that the machine control code is created in advance and transmitted to the AM system. Human operators then continuously monitor the corresponding process to intervene in critical deviations.

This type of process control takes a passive approach in which process conditions are initially assumed to be ideal, and recalibration is performed only in response to observed deviations. In addition, deviations can occur at any time that negatively affect, if not completely ruin, the printing process affecting the aesthetics and stability of the component; Even minor deviations can have a critical effect in the further course of the printing process due to superposition effects. Large-scale 3D printing projects, as is common in construction, are also expected to have long production times [2], making the corresponding process monitoring time-consuming and susceptible to human error. In other words, the quality of the printed component hinges on the long-term vigilance, responsiveness, and judgment of the operator.

Thus, an automated monitoring system for AM processes is of high importance. Reliable systems could not only support human supervision but replace it entirely. In this context, and in order to achieve optimal printing results, systems must be developed that can monitor various aspects of the manufacturing process and translate the collected data into suitable feedback signals in near real-time [4].

Computer vision techniques make it possible to monitor the geometry of a component in real-time during the manufacturing process. This work proposes an adaptive control system that can use RGB camera data to regulate the filament width during an extrusion-based concrete 3D print. Contrary to comparable systems, the proposed control methodology is also equipped with a tracking mechanism that can be adapted to different printer configurations and a more precise segmentation method (which also works on a small scale) that can be calibrated for different materials and lighting conditions.

2 Background

AM, also known as 3D printing, generally describes a manufacturing principle in which an object is created based on a digital model by applying or binding material layer by layer using a robotic actuator. According to this principle, methods capable of processing concrete, steel, and wood have been developed for the construction industry. In fact, for these materials, various methods have been developed that can be categorized according to the type of material application, i.e., deposition or particle bed methods [2]. For the present study, concrete printing processes by material deposition are particularly important.

2.1 Concrete 3D printing by material deposition

In concrete printing methods by means of deposition, often also referred to as extrusion-based methods, the cementitious material is deposited layer by layer in a continuous filament through a nozzle [5]. Different variants of this technique vary in nozzle shape and guidance [6, 2, 7] but also in the strategy with which the material is deposited. P. Carneau et al. [8] distinguish between “infinite brick”, free flow, and layer pressing strategy (cf. Fig. 1). In addition, the material composition is of great importance [9, 10, 11].

To achieve an optimum print result, it is important that all the previously mentioned parameters are attuned to each other. Among these parameters, properties of material used for printing are most susceptible to variation

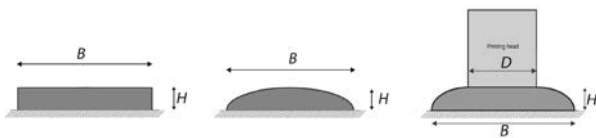


Figure 1. Different concrete extrusion strategies. From left to right: “infinite brick”, free flow, and layer pressing strategy [8]

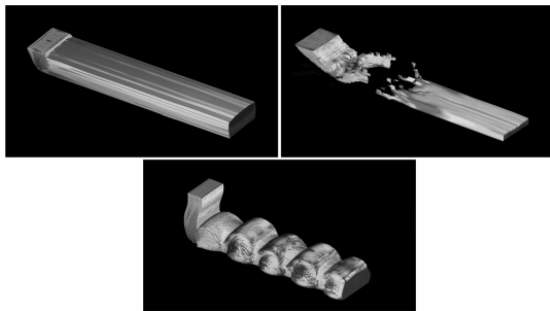


Figure 2. Filament integrity: ideal (left), tearing (right), and buckling (bottom) [7]

of the external conditions, introduced by longer printing time. It is to be noted that AM processes for large-scale projects take a considerable time to complete. Any deviation in material properties over time can either result in under-extrusion (tearing) or over-extrusion (buckling) of the material (cf. Fig. 2) [7]. This not only reduce the quality of the print but also makes the structure unstable when consecutive layers are added.

2.2 Process control

One solution to stabilize the process is to use an extrusion force-velocity controller [12]. The thickness of the extruded filament depends on how much material is deposited at a particular instant. This can be controlled by adjusting the robot speed (speed of print nozzle) or the extruder speed (material extrusion rate). Advanced methods like synchronization between extrusion and robot speed [13] and model-aware control [14] can make the extrusion process even more reliable.

Another approach is to actively measure the extruded filament’s dimension and correct the extrusion process’s speed to get the desired dimension. This approach thus consists of two tasks, dimension monitoring on the one hand and extrusion control on the other. For the first task, current advances in computer vision technology make it possible to measure dimensions with ordinary cameras effectively. For the second task, a control loop feedback mechanism can be employed. A commonly used controller is the so-called proportional-integral-derivative (PID) controller, which constantly calculates an error term (difference between measured and nominal value of the control variable) and determines a control value by utilizing proportional, integral and derivative terms [15].

Kazemian et al. [16] proposed a solution to measure the dimension of an extruded filament using a 720p web camera in their study. One of the features of their dimension measurement system is that it averages the measurement over a specified time, which allows them to reduce noise in the measured value. Based on the obtained camera data, a proportional controller then corrects the material extrusion rate (volume flow) by adjusting the speed of the extruder.

Similarly, Shojaei Barjuei et al. [17] proposed a methodology for dimension measurement based on edge detection in their study. Instead of averaging camera-based measurements, their approach used the real-time data feed of an industrial camera with a high frame rate directly for their control system. Via a PI controller, this data was used to control the speed of the AM robot (printing head), to adjust the rate of material deposition. Both of these systems were tested on industrial robots for a large-scale system, which was demonstrated by controlled material extrusion in a straight line.

In another study, Wolfs et al. [18] proposed to use a precise laser line profiler for the dimension measurement. They developed a clash control system that compares point cloud data with the “as-planned” geometry to control the printing process.

In the present study, a near real-time optical process control system was developed and tested on a scaled-down 3D printing setup consisting of a 6-DOF robotic manipulator with a fixed (non-rotating) round nozzle configuration.

A separate rotating head was developed that automatically orientates an RGB camera along the extruded filament using “as-planned” fabrication information. A Computer-vision-based algorithm is then employed to dynamically track and determine the extruded filament’s width. A closed-loop feedback control utilizes the measured dimension, determined at every frame from the camera, and evaluates a correction value using a PID controller. Based on the correction value from the controller, the material extrusion rate is adjusted. In contrast to the relevant studies [16, 17, 18], key differences of the proposed method are the printing configuration, synchronization of robot and printer, as well as the employed computer vision algorithm. The small scale of the print, combined with the unclear edges due to the layer-pressing strategy of the print and the fixed nozzle configuration, required some adaptations compared to the other systems.

3 Equipment setup

A small-scale experimental setup was used for testing, as illustrated schematically in Fig. 3. The individual components are described in detail in the following sections.

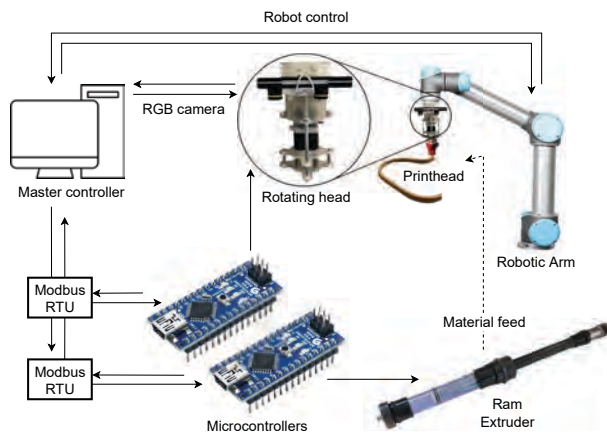


Figure 3. Experimental setup architecture

3.1 Robot/Hardware communication

The main component of the setup is a Universal Robot UR10e robotic arm with 6 degrees of freedom (DoF),

which operates independently of a 1.5L ram extruder. The ram extruder conveys the material through a build-up pressure generated by a stepper motor. Once the motor is activated, the material is pumped via a tube toward the printhead. At the printhead, a second stepper motor operates an auger screw, which finally extrudes the material through the nozzle. The stepper motors are controlled by the master controller via a microcontroller using the serial transmission protocol, Modbus RTU.

The robot movement is currently programmed offline and manually transmitted to the robot as an URscript file. During execution, the velocity can vary or remain stable depending on the geometry. The print information is transmitted per TCP/IP connection to the master controller using the so-called RTDE interface (Real Time Data Exchange) provided by UR.

3.2 Printhead

The printhead is outfitted with a round nozzle with which the material can be deposited utilizing the layer-pressing strategy. Due to the material intake, i.e., the tube between the printhead and the ram extruder, the freedom of movement of the robot is limited to 5 DoF, the sixth axis must not be rotated. However, since the relative orientation of the filament to the printhead can change during the process depending on the geometry, the field of view of a camera mounted directly on the printhead would be very limited. To increase the field of view, a camera mount was developed that can rotate around the printhead independently of the robot’s motion (cf. Fig. 3). A second microcontroller was installed for controlling the rotating camera mount, which is also connected via a serial link using Modbus RTU.

3.3 Camera

For the optical monitoring task of the proposed process control system, an RGBD camera (ZED mini) was installed on the rotating camera mount. Although the camera can be used for depth measurements, only one of the camera’s lenses was used, effectively downgrading the monitoring system to a simple RGB camera. During the printing process the camera is set up to transmit a continuous 720p video feed.

4 Methodology

4.1 Optical process monitoring

The objective of the monitoring system is to measure the width of the extruded filament. To realize this, the image frames of the camera’s video feed are processed utilizing computer vision algorithms to extract the filament width.

The approach used for image processing is similar to the method proposed by Kazemian et al. [16]. The key difference is the segmentation method (separating target object from surrounding) and utilization of all frames (60 frames per second) instead of sampling for more accuracy, in order to decrease the reaction time of the control system, making the system more reliable in highly dynamic processes [17]. For segmentation, a mask is created based on HSV (hue saturation value), and the value range for HSV value is adjusted manually using track bars (cf. Fig. 4). The value of the range predominantly depends on the background and luminous intensity.

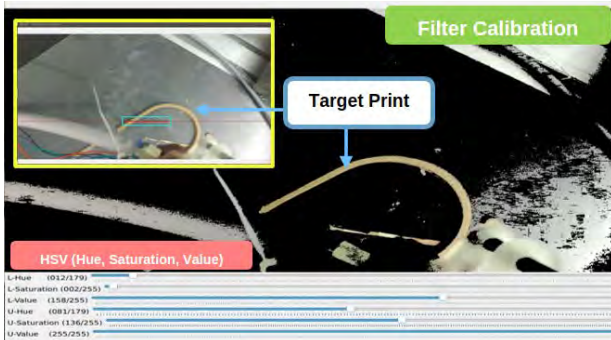


Figure 4. GUI for calibrating HSV range values

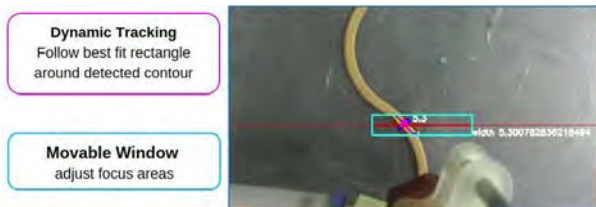


Figure 5. Contour tracking by estimating rectangle with smallest area over detected contour in focus area.

As illustrated in Fig. 5, only a small cropped segment of every image frame focusing the region around the target object (printed filament) is used for the width detection. The position of this cropping rectangle is set manually. It should be chosen as small as possible to minimize noise but large enough so that the filament can be detected even if the camera mount is rotated imprecisely. Cropping the image speeds up the computation time by reducing the number of pixels and the probability of noise.

HSV-based segmentation mask is then applied to the cropped frame to separate the target object from its surrounding. The HSV-based method mainly relies on the difference in color gradient between the background and printed material and thus can be made flexible for intensity value making it less prone to erroneous measurement because of lighting conditions. On each frame with the

segmented object, the full family of contours is retrieved in a hierarchical list, including all boundary points of the contour [19]. All contours of each individual frame are filtered based on the minimum pixel area to prevent any unnecessary noise. The minimum pixel area of a contour is another hyperparameter along with the HSV value range. It addresses the sensitivity of the monitoring system as it limits the minimum size that can be detected. In the last step, the dimension is measured by converting the pixel width of the rectangle to centimeters.

For all the presented steps, a calibration must first be performed once when the system is set up or exterior influences change (e.g., lighting). In order to make this more convenient, a user interface (UI) has been implemented that can be called when necessary, providing:

- **Scaling (pixels per cm):** User input prompt requiring a calibration measurement of an object with known dimensions. It takes the correct measurement as input and calculates the scaling factor.
- **Movable Window:** Sliders allow the user to adjust the position and size of the focus area (cf. fig. 5) by moving two corner points in relation to the center of the image.
- **HSV Calibration:** The user can adjust maximum and minimum HSV-values and thus the upper (U) and lower (L) segmentation thresholds. The values must be adjusted until only the specimen is visible (cf. fig. 4).

4.2 Process control

Once a printing process is started on the UR10e robot controller, the process control algorithm (Main controller, cf. Fig. 6) obtains input from the robot via its RTDE interface. In parallel, the camera provides a continuous video feed to the main controller. As soon as the printed filament is detected on any video frame and its width is measured (skipping the first 20 valid frames for good measure), the PID controller (part of the main controller) is enabled. The PID controller returns a cumulative term that is to be added to the extrusion speed as a correction value. The calculated extrusion speed (adapted to the current robot speed) and the PID value are continuously transmitted to Microcontroller 1, which controls the ram extruder and the print head (cf. Fig. 6).

In parallel to the optical process control, a second microcontroller is employed to control the camera position via the rotating mounting system. This system ensures that the focus area of the camera (cropping rectangle, cf. Section 4.1) is centered on the filament. The necessary rotation angle is calculated using the current and two previous waypoint positions of the robot and sent to

Microcontroller 2 (cf. Fig. 6, see also section 4.4). Microcontroller 2 controls the motor of the camera mount and adapts the position accordingly. In contrast to the extrusion speed, this process only occurs at each waypoint change and terminates once the position is reached.

The process control is terminated once the final waypoint is detected.

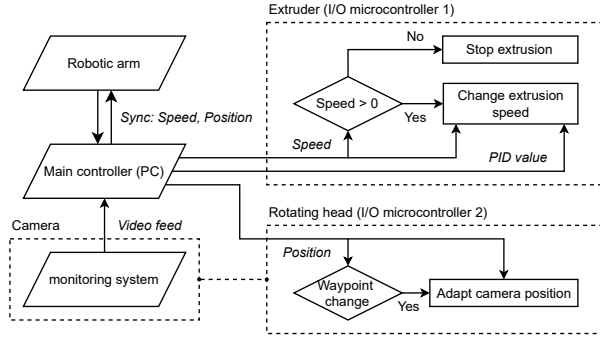


Figure 6. Optical process control monitoring system execution flowchart

4.3 Robot data exchange

As discussed above, a pivotal point for online monitoring is the robot data exchange (current speed and position). Via the UR robots Real-Time Data Exchange (RTDE) interface, it is possible to continuously exchange data between the robot and a computer using a TCP/IP connection. The update rate of this data exchange can be set to up to 500 Hz. Also, the interface is able to skip packages in case of any process holdups so that always the most recent data is exchanged. During the printing process, a constant RTDE feed between the robot and the main controller (PC, cf. Fig. 6) is maintained.

4.4 Rotating head

As mentioned in section 3.2, the system proposed in this study was developed for a 5-DoF system (limitation due to the used print head). Due to the fixed sixth robot axis, a camera mounted directly on the printhead would be limited in its field of view to only one direction. However, since arbitrary geometries can be printed with the AM system, it is necessary to integrate a dynamic camera mount into the monitoring system. For this purpose, a rotating camera mount was implemented that is controlled using the mentioned RTDE position updates from the robot. As the robot path is known in advance (defined by the component's geometry), waypoints for camera position updates can also be defined in advance. Every time the robot gets close enough to such a waypoint a signal is sent to the respective microcontroller which then initiates a position

change. From the current position the last three waypoints (A, B, C) are considered for the calculation of the rotation angle. Between these three points, it is possible to calculate an angle by calculating the slopes (m_1 and m_2) of the lines \overline{AB} and \overline{BC} and solving equation 1 to θ .

$$\tan \theta = \frac{m_1 - m_2}{1 + (m_1 \cdot m_2)} \quad (1)$$

The result is translated into motor steps and direction and sent via Modbus RTU to Microcontroller 2 controlling the camera mount (cf. Fig. 3 and 6). This function runs independently of the extrusion speed and is only executed when needed. The Modbus protocol allows each microcontroller to work simultaneously or independently from the other.

4.5 Extrusion speed

The extrusion speed is calculated using the sync speed as the main parameter. By formulating a relation between the extruder motor speed and the robot's actual speed, the extrusion rate ($Q_{extruder}$) can be synchronized with the filament deposition rate ($Q_{filament}$):

$$Q_{extruder} \left[\frac{mm^3}{s} \right] = Q_{filament} \left[\frac{mm^3}{s} \right] \quad (2)$$

On the right side of equation 2, the filament deposition rate is calculated with equation 3 using the user input parameters, filament width (d_f) and the layer height (h_l) which are unique to the setup and the geometry, and actual robot speed (v_{TCP}), i.e. the Tool Center Point (TCP) movement speed obtained via the RTDE interface (cf. section 4.3). It should be noted that the equation 3 is based on the assumption that the filament has a rectangular shape, which is not exactly the case with the layer pressing strategy [8]. The inaccuracy acts as a constant factor, which is, however, compensated for by the proposed PID controller (cf. section 4.6) and is therefore negligible.

$$Q_{filament} = v_{TCP} \left[\frac{mm}{s} \right] \cdot d_f [mm] \cdot h_l [mm] \quad (3)$$

On the left side of equation 2, the extrusion rate is based on the extruder setup. When a mechanical conveying system powered by a stepper motor is employed, as is the case in this study, the extrusion rate can be expressed as the product of the turn frequency f_{motor} of the motor and a specific volume flow q_{ram} defined by the extruder geometry (cf. equation 4).

$$Q_{extruder} = f_{motor} \left[\frac{step}{s} \right] \cdot q_{ram} \left[\frac{mm^3}{step} \right] \quad (4)$$

By using equations 4, 3 and 4 and by solving to f_{motor} it can be derived that the motor speed of the ram extruder is

linear proportional to the filament width (d_f). Due to that fact, a PID controller can be used to control the extrusion rate when monitoring the filament width.

4.6 PID controller

As mentioned before, a PID controller was chosen as the control architecture for the optical process control system proposed in this paper. The controller calculates the error term e as the difference between the measured “as-manufactured” filament width and the “as-designed” width. With this error value e , the PID output $u(t)$ is calculated via equation 5.

$$u(t) = K_P e(t) + K_I \int e(t) dt + K_D \frac{de}{dt} \quad (5)$$

In equation 5, the frame rate of the camera is used as the time domain to avoid conversions. Using the equations 2, 3 and 4, the calculated PID value $u(t)$ can finally be converted into a motor frequency f_{PID} , which is transferred to the extruder controller (microcontroller 1, see Fig. 6) as a correction value. Since every frame is processed during monitoring (see section 4.1), additionally a failsafe was implemented in case incorrect values were determined, e.g. due to noise. With a simple threshold value procedure, measured values that are too small or too large are simply discarded and the unregulated motor frequency is used as the control variable (cf. Fig. 7).

The PID tuning – setting of the PID constants K_P , K_I and K_D – was performed utilizing several test prints of a very simple geometry, a single straight line (cf. [15]). The measured data for each individual test print were plotted

and examined for their convergence behavior. Depending on the behavior, the PID factors were then adjusted accordingly, first the K_P value, then K_D and finally K_I . The tuning outcome setting for our system is ($K_P = 20$), ($K_D = 1$) and ($K_I = 0.01$).

5 Experimental validation

To evaluate the performance of the proposed optical process control, a small scale clay 3D printing setup was used printing along a curved print path. For the first run, the camera and the rotating head algorithm were activated to be able to observe the width of the extruded material, but the PID extruder control was disabled (cf. Fig. 8, left). In the second run, the complete optical process control, including PID, was activated (cf. Fig. 8, right). The initial configuration was set to be the same as in the first run. The expected filament width for both experiments was $6mm$.

As a result of an uneven print bed, the uncontrolled 3D print produced a filament with variable filament width. Additionally, with the used setup, an exact initial configuration of the nozzle height is not possible. As illustrated in Fig. 8, both of these issues accumulate to a clearly visible error in the filament width – the width is not constant and with a value of around $12mm$, depending on the position, too large.

As illustrated in Fig. 8, right, the developed process control applied in the same setup is not only able to detect the changes of the filament throughout the print, but it is also able to update the control value correctly, maintaining a filament width of close to $6mm$. The results of this experiment demonstrate the potential of our process control as it provides automatic supervision and in-time corrections during the printing process. Further improvements to the system are discussed in the following section.

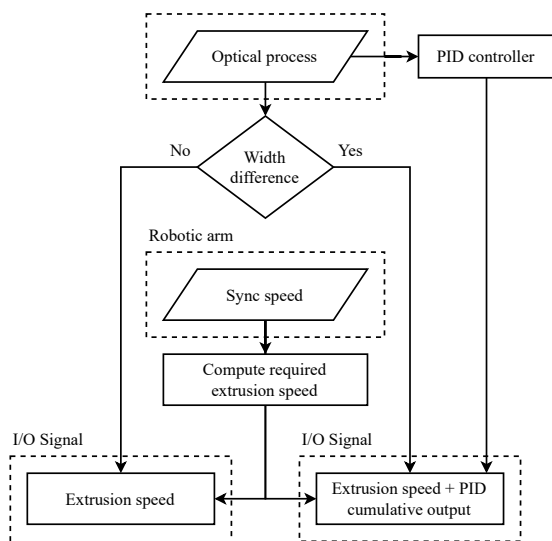


Figure 7. Data exchange for extrusion speed control.

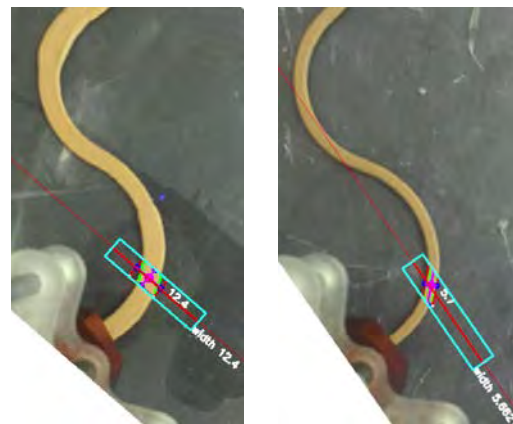


Figure 8. Test print using a curved print path: uncontrolled (left) and controlled (right).

6 Limitations and future work

One of the limitations of the proposed system is tracking sharp curves with small angles of rotation. By reducing this distance between printhead and camera, it will be possible to track and test such complex geometries. Reducing distance to the printhead will also reduce the distance between the nozzle and the camera objective. As visible in Fig. 8, there is a lag of information between what is being printed and what is being measured. The implemented PID helps regulate this disturbance but reducing this distance with a different camera mount could improve the efficiency of the system.

If multiple layers are being printed and in the case of under extrusion with very little difference between the current and previous layer, HSV based filters might ignore the current layer and return the measurement of previous layer. This can be avoided by using depth based filters. However, a RGBD camera cannot sufficiently resolve depth at such small scales. Alternatively, for a small scale experimental setup, laser profilers that provide a much larger resolution can be used, as proposed by Wolfs et al. [18].

The implemented HSV-based segmentation performs more reliable compared to the noisy measurements of the segmentation method proposed in [16], but in the current state of the implementation it relies on manual calibration. To limit the need for manual calibration, automatic thresholding techniques and methods like mask RNN can be explored in detail for automated segmentation, making the vision system completely independent of external environmental variables. An automated calibration process can help get rid of the user-induced error but a reference still needs to be set when using HSV. For instance, the material color might not always be the same and this will still have to be adjusted manually.

For the experimental validation, a small-scale clay 3D printing setup was used. While the developed process control system is in principle applicable to any scale of additive manufacturing, an experimental proof for larger scales and other materials (concrete) has not yet been performed. This is subject to future work.

7 Conclusion

In this paper, a methodology to increase the reliability of additive manufacturing process in the field of construction, through automated monitoring and controlled material extrusion process has been introduced. In order to maintain a consistent width of the extruded material, a closed loop optical process control system capable of tracking the extruded filament has been developed. It utilizes an independent rotating head for a camera that moves relative to the nozzle and tracks the extruded filament. A computer-vision based algorithm, monitors the width of

the filament in real time, which is then used to regulate the material extrusion rate using a PID controller. Overall, the system is able to effectively track the path and adjust the extrusion rate based on a simple RGB vision system and demonstrates great potential in the area of real-time process control applied in robotic construction. In particular, it provides the basis for implementing the comprehensive concept of cyber-physical production systems in construction.

In contrast to the previous studies mentioned in section 2.2 the proposed control system was able to perform reliable even on a small-scale – the segmentation methods proposed in the previous studies resulted in a noisy measurement of the print path. It was shown that with a 1920x1080 *px* resolution camera with 60 *fps* satisfactory control was obtained without averaging frames, mainly because of the difference in segmentation method. Additionally, the control system represents a novel approach for use with extruder systems that have a fixed printing nozzle (layer pressing strategy), where an additional filament tracking system is required.

Acknowledgments

The research presented is part of the Transregio 277 ‘Additive Manufacturing in Construction – The Challenge of Large Scale’, funded by the Deutsche Forschungsgemeinschaft (DFG, German Research Foundation) – project number 414265976 – TRR 277.

References

- [1] Seyed Hamidreza Ghaffar, Jorge Corker, and Mizi Fan. Additive manufacturing technology and its implementation in construction as an eco-innovative solution. *Automation in Construction*, 93:1–11, September 2018. doi:10.1016/j.autcon.2018.05.005. URL <https://doi.org/10.1016/j.autcon.2018.05.005>.
- [2] Alexander Paolini, Stefan Kollmannsberger, and Ernst Rank. Additive manufacturing in construction: A review on processes, applications, and digital planning methods. *Additive Manufacturing*, 30, 12 2019. ISSN 22148604. doi:10.1016/j.addma.2019.100894.
- [3] D Shamsollahia, O Moselhib, and K Khorasanic. Construction progress monitoring and reporting using computer vision techniques—a review. *39th International Symposium on Automation and Robotics in Construction (ISARC 2022)*, pages 467–472, 2022.
- [4] Rob JM Wolfs, Freek P Bos, Emiel CF van Strien, and Theo AM Salet. A real-time height measurement and feedback system for 3d concrete printing. In *High*

Tech Concrete: Where Technology and Engineering Meet, pages 2474–2483. Springer, 2018.

- [5] Manu K. Mohan, A.V. Rahul, Geert De Schutter, and Kim Van Tittelboom. Extrusion-based concrete 3d printing from a material perspective: A state-of-the-art review. *Cement and Concrete Composites*, 115:103855, 2021. ISSN 0958-9465. doi:<https://doi.org/10.1016/j.cemconcomp.2020.103855>. URL <https://www.sciencedirect.com/science/article/pii/S0958946520303607>.
- [6] Xiangpeng Cao, Shiheng Yu, Hongzhi Cui, and Zongjin Li. 3d printing devices and reinforcing techniques for extruded cement-based materials: A review. *Buildings*, 12(4):453, April 2022. doi:10.3390/buildings12040453. URL <https://doi.org/10.3390/buildings12040453>.
- [7] R.J.M. Wolfs, T.A.M. Salet, and N. Roussel. Filament geometry control in extrusion-based additive manufacturing of concrete: The good, the bad and the ugly. *Cement and Concrete Research*, 150:106615, December 2021. doi:10.1016/j.cemconres.2021.106615. URL <https://doi.org/10.1016/j.cemconres.2021.106615>.
- [8] Paul Carneau, Romain Mesnil, Nicolas Ducoulombier, Nicolas Roussel, and Olivier Baverel. Characterisation of the Layer Pressing Strategy for Concrete 3D Printing. In Freek P. Bos, Sandra S. Lucas, Rob J.M. Wolfs, and Theo A.M. Salet, editors, *Second RILEM International Conference on Concrete and Digital Fabrication*, pages 185–195, Cham, 2020. Springer International Publishing. ISBN 978-3-030-49916-7.
- [9] Rjm Rob Wolfs, Freek P. Bos, and Tam Theo Salet. Early age mechanical behaviour of 3d printed concrete: Numerical modelling and experimental testing. *Cement and Concrete Research*, 106:103–116, 2018.
- [10] A. Perrot, D. Rangeard, and A. Pierre. Structural built-up of cement-based materials used for 3d-printing extrusion techniques. *Materials and Structures*, 49(4):1213–1220, February 2015. doi:10.1617/s11527-015-0571-0. URL <https://doi.org/10.1617/s11527-015-0571-0>.
- [11] A.S.J. Suiker. Mechanical performance of wall structures in 3d printing processes: Theory, design tools and experiments. *International Journal of Mechanical Sciences*, 137:145–170, March 2018. doi:10.1016/j.ijmecsci.2018.01.010. URL <https://doi.org/10.1016/j.ijmecsci.2018.01.010>.
- [12] Bradley K. Deuser, Lie Tang, Robert G. Landers, Ming C. Leu, and Greg E. Hilmas. Hybrid extrusion force-velocity control using freeze-form extrusion fabrication for functionally graded material parts. *Journal of Manufacturing Science and Engineering*, 135(4), July 2013. doi:10.1115/1.4024534. URL <https://doi.org/10.1115/1.4024534>.
- [13] Pinyi Wu, Keval S. Ramani, and Chinedum E. Okwudire. Accurate linear and nonlinear model-based feedforward deposition control for material extrusion additive manufacturing. *Additive Manufacturing*, 48:102389, December 2021. doi:10.1016/j.addma.2021.102389. URL <https://doi.org/10.1016/j.addma.2021.102389>.
- [14] Hesam Zomorodi and Robert G. Landers. Extrusion based additive manufacturing using explicit model predictive control. In *2016 American Control Conference (ACC)*. IEEE, July 2016. doi:10.1109/acc.2016.7525169. URL <https://doi.org/10.1109/acc.2016.7525169>.
- [15] Pid controller explained, n.D. URL <https://pidexplained.com/pid-controller-explained/>.
- [16] Ali Kazemian, Xiao Yuan, Omid Davtalab, and Behrokh Khoshnevis. Computer vision for real-time extrusion quality monitoring and control in robotic construction. *Automation in Construction*, 101:92–98, 5 2019. ISSN 09265805. doi:10.1016/j.autcon.2019.01.022.
- [17] E. Shojaei Barjuei, E. Courteille, D. Rangeard, F. Marie, and A. Perrot. Real-time vision-based control of industrial manipulators for layer-width setting in concrete 3d printing applications. *Advances in Industrial and Manufacturing Engineering*, 5, 11 2022. ISSN 26669129. doi:10.1016/j.aime.2022.100094.
- [18] Rob J.M. Wolfs, Freek P. Bos, Emiel C.F. Van Strien, and Theo A.M. Salet. A real-time height measurement and feedback system for 3d concrete printing. In *High Tech Concrete: Where Technology and Engineering Meet*, pages 2474–2483. fib. The International Federation for Structural Concrete, 2018. ISBN 9783319594705. doi:10.1007/978-3-319-59471-2_282.
- [19] Opencv contours documentation, 2022. URL https://docs.opencv.org/3.4/d3/d05/tutorial_py_table_of_contents_contours.html.

Real-time data exchange (RTDE) robot control integration for Fabrication Information Modeling

Martin Slepicka¹, Jalal Helou¹ and André Borrmann¹

¹Chair of Computational Modeling and Simulation, Technical University of Munich, Germany

martin.slepicka@tum.de, jalal.helou@tum.de, andre.borrmann@tum.de,

Abstract -

In response to its stagnating productivity and growing demand for sustainability, the architecture, engineering, and construction (AEC) industry is increasingly pushing ahead regarding digitization and automation. Building Information Modeling (BIM) and Additive Manufacturing (AM) are two technologies that contribute significantly to this development. Although these technologies have similar basic principles — both are based on computer-aided methodologies and used for automation purposes — they have long been developed independently in the construction industry. However, recently, studies on integrating AM into BIM methodology have gained momentum. One approach is the Fabrication Information Modeling (FIM) methodology which aims at interfacing digital design with automated manufacturing by providing a fabrication-aware intermediate layer, a digital model that contains all the information necessary for automated fabrication. This study focuses on extending FIM by providing a new robot control methodology that can directly utilize FIM data to control an AM system and is better suited to extrusion-based concrete 3D printing needs. The proposed robot control method aims to be more flexible regarding the recalibration of printing parameters and prepares the basis for developing systems for automated quality control.

Keywords -

Fabrication Information Modeling; AM; Robotics

1 Introduction

The architecture, engineering, and construction (AEC) industry has been stagnant for a long time regarding the industry's productivity. In response to this, and to satisfy the growing demand for sustainability, the industry is increasingly pushing ahead in digitization. Critical components of this development include Building Information Modeling (BIM) and Additive Manufacturing (AM). On the one hand, there is BIM, a methodology developed to enable seamless use of digital data throughout the lifecycle of a building [1]. On the other hand, there is AM, a term that refers to various additive manufacturing processes that can resource-efficiently generate complex geometries from building materials based on digital data. However,

although both technologies are based on computer-aided methodologies, they have long been developed separately in the industry. Among other things, this has also prevented the development of uniform data modeling guidelines, which has made it challenging to synergize the two technologies. This fact has led to various efforts to combine the two technologies [2]. Among other things, a methodology was developed to derive manufacturing information from BIM data for use with extrusion-based AM methods, i.e., Fabrication Information Modeling (FIM) [3].

With the help of FIM, tool paths for 3D printing of building components can be generated based on parametric patterns. In addition, with interfaces to various robot control frameworks, printing can be included in the digital workflow, regardless of which robot system is used. However, it should be noted that the FIM data are mostly not read directly or conversion-free by the robot control system but are interpreted via the interface.

Another problem is that concrete printing is a highly delicate matter. For fresh concrete to be processed using extrusion-based 3D printing, it must be pumpable, extrudable, and buildable [4]. These three properties contradict each other to some extent. On the one hand, the concrete must be flowable to be pumped. However, on the other hand, it must remain dimensionally stable as it is extruded through the nozzle and must be load-bearing fast enough to withstand further printing layers. In addition, external influences can change these rheological properties; among other things, pumping too fast can negatively affect the material's composition, while printing too slow can lead to poor inter-layer bonding [4]. Further negative influences are time-dependent due to the long curing time of the concrete. Others originate from, e.g., inertia effects during rapid changes of direction [4] or simply from environmental influences, such as temperature or humidity [5].

For these reasons, AM processes in construction are heavily dependent on human supervision. Concrete printing often fails without quality control and recalibrations, resulting in inferior component quality. In order to increase the degree of automation, this study proposes a robot control methodology that is significantly more adapt-

able than other comparable systems. On the one hand, the system can process the FIM data directly without intermediate steps. On the other hand, it is suitable to plan a velocity profile taking inertia effects at direction changes into account. Furthermore, the system enables adaptation of the fabrication information during the printing process and thus provides new possibilities to integrate sensor systems into the AM system for automated quality control. It can quickly be recalibrated, and parameters relevant to 3D printing can be changed by user input.

In the following, we will first show how conventional methods are carried out. Then the proposed methodology is described in detail, and improvements compared to conventional methods are discussed.

2 Background

In this study, the focus is on extrusion-based concrete printing methods. One of the first, and still representative, processes developed is Contour Crafting (CC), in which concrete is forced through a nozzle to form a strand (or filament) and then deposited layer by layer according to a digital model. CC was developed in analogy to the Fused Deposition Modeling (FDM) 3D printing method, processing a thermoplastic in the same functional principle.

As with FDM, the corresponding digital model is created as a volume model using computer-aided design (CAD) and stored in a data format suitable for the subsequent slicing operation, usually as Stereolithography (STL) file. The subsequent slicing process cuts the volume model into several equidistant 2D slices. These slices are then converted into tool paths that describe the movement of the nozzle and, thus, the location where the material is applied. Usually, these paths first follow the contour of the slice and then fill the rest of the surface following a specific pattern (hatching). After that, the planned path is transformed into a robot trajectory, i.e., a series of robot poses that the machine must traverse, and communicated to the 3D printer along with the extrusion rates via G-Code or other specific interfaces [6]. Executing this robot control code will then start the printing process.

This trajectory translation depends on the selected robot system, e.g., for an industrial robot arm with six degrees of freedom (6-DoF), six coordinates describe each pose. In the Cartesian representation, three coordinates (X , Y , Z) describe the position of the robot's end-effector, and another three coordinates (R_X , R_Y , R_Z) describe its orientation. However, the robot requires these coordinates as a list of joint positions (θ_1 , θ_2 , θ_3 , θ_4 , θ_5 , θ_6), which must be calculated by inverse kinematics (usually done by the robot control unit) [7].

Inverse kinematics transforms a robot's end-effector coordinate frame from Cartesian space into Joint space using Denavit-Hartenberg-Transformations. For a 6-DoF robot

arm, six chained transformations must be solved for the respective Joint angles, which is a very time-consuming calculation and usually provides multiple results (more than one possible pose). The transformation from Joint space to Cartesian space is called forward kinematics, a more straightforward problem that provides only one solution.

2.1 Digital model

The representation of the geometry (digital model) is the output of the design process that usually describes the product's final form. As previously stated, the digital model is usually created using the user's preferred CAD tool. However, with CAD, it is only possible to generate the geometry of the component to be manufactured. Additional information, e.g., the material to be used or varying feed rates, cannot be considered in this process [8]. Additionally, the representation requires several preparation steps for fabrication, such as meshing into the STL format and layer-wise slicing, introducing multiple areas of deviations, and hindering automation.

Furthermore, an STL mesh exhibits numerous redundancies and cannot model curved segments accurately except with significantly large file sizes [9]. Thus, the aspects needed for fabrication are handled after the design process rather than incorporated into it. Nevertheless, with the extensive knowledge and support for CAD files regarding meshing, optimization, and simulation, concrete 3D printing (C3DP) processes based on regular CAD are the current standard [6, 10].

On the other hand, BIM has been proven to offer multiple advantages to the construction industry and C3DP, such as the support for additional parameters for fabrication and standard support for Industry Foundation Classes (IFC), which is advantageous for AM applications [8, 9]. Several studies have taken advantage of the flexibility of BIM and developed automated BIM-based AM fabrication processes [8, 11].

The proposed methodology in this study uses the FIM methodology developed by Slepicka et al. [3] for generating the required digital model instead of using a simple CAD tool. FIM offers a pattern-based approach where voids, inserts, supports, and other functional inserts can be integrated directly into the design. Another advantage of using FIM is that the path-planning tasks are already incorporated in this step. Therefore most of the tasks are semi-automatically applied already in the design phase.

2.2 Planning and Execution

As mentioned before, for path planning, it is standard practice to use slicing software, which converts an STL file into tool paths that can be exported as robot control code. The slicer program will use a specific in-fill pattern,

density, and material based on user input, specifying how the end-effector's tool path is generated. Typical slicing software solutions provide different output formats, but the old industry standard DIN 66025, commonly known as G-Code, is often used for 3D printing [8, 11]. A different approach gaining much interest is using the Robot Operating System (ROS) framework, which provides MoveIt!, a motion planning framework, for path planning [12]. MoveIt! can plan the path, calculate inverse kinematics, and detect collisions, among other features.

When the path planning is complete, the manufacturing information is transmitted to the robot, which performs the 3D printing. There are two different methods for this task, offline and online programming. In this context, offline programming refers to transmitting manufacturing information as a whole, which is then executed sequentially. Online programming, on the other hand, describes the continuous transmission of manufacturing information in small packages, which enables more control and room for feedback [13].

Using MoveIt!, offline programming is the standard, where the complete path and the joint coordinates are pre-calculated. Although this approach allows collision checking, it does not allow real-time checks and adaptations to the printing path.

With FIM, the planning process for the fabrication is, as mentioned in the previous section, shifted to the design phase, when the digital model is created and, in part, automated. Using FIM, BIM data is extracted and processed by applying design patterns, generating semi-automatically (the user must choose design parameters) fabrication information for a selected component. While the outer shape of the component is retained from the BIM design, the pattern is applied to generate the interior structure of the component. In contrast to conventional slicing methods, with FIM, the voids are designed by path planning, not the other way around [3]. The fabrication information (path and parameters for material, process, and machinery) is stored in the BIM exchange format IFC (cf. fig. 5).

When combining FIM with the methodology proposed in this study (cf. section 3), the manufacturing information can be directly transmitted with the online programming strategy to an AM system. As discussed in section 3.1.2, an object-oriented planning algorithm is proposed that complements the FIM-IFC representation [3], enabling direct data access and the generation of an adapted velocity profile. The proposed high-frequency online communication uses the Real-Time Data Exchange (RTDE) offered by Universal Robots™ (UR), which synchronizes the UR controller with an external client over TCP/IP. While this communication protocol is specific to UR CB-Series and e-Series robots, other industrial robots offer similar protocols for data exchange, e.g., KUKAs Robot Sensor Inter-

face (RSI) [14].

3 Methodology

The proposed methodology consists of several modules described in detail in this section, including their execution. In general, the RTDE methodology is supposed to directly process digital models generated by FIM [3] and execute the contained fabrication information. Thus, it extends the FIM framework, providing means to generate system-specific velocity profiles and to directly control AM systems. At the same time, the system also opens up possibilities to feed data back to the FIM model during the printing process. Figure 1 summarizes the different modules and their connections to each other.

3.1 Modules

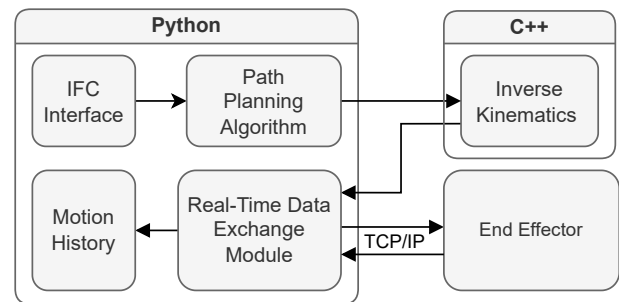


Figure 1. A Flowchart of the Different Modules used within the Methodology

3.1.1 IFC Interface

As discussed in [3], FIM uses the IFC format to store the fabrication information (printing path and other variables relevant to the printing process). Using the available ifcOpenShell library for Python, the IFC file's contents can be read and queried easily. The code queries for layers that are geometrically represented as `IfcCompositeCurve` entities, which in turn contain `IfcCompositeCurveSegment` describing the geometry of each layer segment. While the specific geometry can be of any IFC representation, the current code is equipped to handle `IfcTrimmedCurve`, `IfcPolyLine`, and `IfcSpline` entities. All the `IfcCompositeCurve` entities are stored as layer objects, whereas `IfcCompositeCurveSegment` entities are translated into segment objects within the program. Segments are parametrized and can be evaluated using $t \in [0, 1]$ and discretized into N equal segments or based on an array of step sizes utilized within the path planning module.

This object-oriented approach allows for a more straightforward adaptation of other IFC entities and allows control over the required discretization in later workflow stages. The layer and segment objects can be offset, scaled, and trimmed using their respective method functions.

3.1.2 Velocity profile

Initially, the velocity profile algorithm assumes a constant velocity for the entire layer. It then adds a gradual acceleration and deceleration at the start and end, respectively, represented by a hyperbolic tangent profile. An exemplary velocity profile is shown in Fig. 2 for one layer.

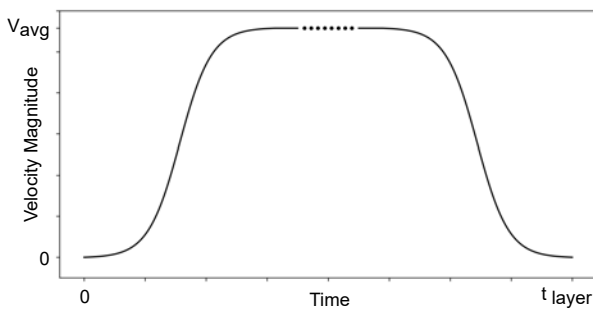


Figure 2. Schematic of the Assumed Velocity Profile of one Layer within the Path Planning Algorithm

The profile is entirely defined by the user input values of the layer printing time and maximum acceleration/deceleration values. Based on the frequency of the established connection with the end-effector, an array of step sizes is calculated, defining the distance between the discretized points. These step sizes are fed sequentially to each segment's `discretize` method to obtain a list of waypoints for the end-effector to follow. The velocity and acceleration in each direction are also calculated to ensure that the machine limits are not exceeded.

3.1.3 Inverse Kinematics

With the printing layer segments discretized into an array of cartesian points, inverse kinematics is performed to obtain an array of joint coordinates that the specific end-effector can execute. These calculations are the most time-consuming among the modules and thus are implemented using C++, utilizing the mathematical library *Eigen* for matrix operations and *pybind11* for Python bindings. The compiled program offers a `kinematicCalculator` object that can be initialized for a specific end-effector currently limited to UR5, UR5e, UR10, and UR10e but can be extended to any end-effector with known Denavit–Hartenberg parameters. The C++ object also has the methods `forward` and `backward` for executing the respective kinematic transformations.

Using C++ ensures the real-time capability of the program, where a look-ahead time of a few seconds can be safely maintained. For instance, at a 125 Hz frequency of communication, the program's ratio of execution time to planning time varies between 1.8 and 2.5 on the reference machine.

3.1.4 Real-Time Data Exchange

As mentioned, the RTDE controller communicates with the robot and performs the printing process. While using the RTDE communication protocol, the user can perform several tasks. The user can manipulate the robot's joints, read its TCP and joint position, and use its general-purpose digital and analog I/O registers. These parameters are continuously transmitted using a high-frequency connection reaching update rates of 125 Hz on CB-series robots and 500 Hz on e-Series robots [15]. Within the control loop of the end-effector, the UR controller has priority over the RTDE communication while allowing the robot to skip packages that interrupt its computations, which minimizes the jerk of the robot.

Additionally, to this end, the inverse kinematics step is done prior, as described in section 3.1.3, allowing greater control over the computational speed. RTDE for UR-robots is provided in C++ and Python APIs and is used in Python for this work. The API works with a URScript running on the robot, which receives the path information and governs the movement of the end-effector.

With the proposed RTDE methodology, the robot motion is controlled by transmitting the individual poses that the robot traverses as joint coordinates at a fixed transmission rate (z.B. 125 Hz). The robot is moved to the pose just transmitted in time until the subsequent transmission (0.008 s at 125 Hz). Accordingly, the speed at which the distance of each successive pose describes the robot moves. Thus it is possible to influence the position and speed of the robot in each of the time intervals, either to insert an unscheduled stop or to react to deviations based on sensor data. In addition, the corresponding data can be processed graphically and made usable for process monitoring (cf. fig. 7).

The packages transmitted are defined using a configuration XML file, with outputs from the robot defined in the `state` recipe, while inputs are defined in the `setp` recipe. The outputs `runtime_state`, `actual_TCP_pose`, `actual_q`, and `output_int_register.0` are used to monitor the robot's state, positions in Cartesian and joint coordinates, and an integer to communicate with the URScript running on the robot, respectively. Meanwhile, inputs are defined as six double registers, `input_double_register.*`, which transmit the joint positions to the URScript.

A URScript program, illustrated in Fig. 3, must be exe-

```

▼ BeforeStart
write_output_integer_register(0, 0)
tmp:=[0,0,0,0,0,0]
setp = get_actual_joint_positions()
Popup
write_output_integer_register(0, 1)
rtde_set_watchdog("input int register 0", 1, "STOP")
▼ Robot Program
servoj(setp, 0, 0, 0.008, 0.1, 300)
▼ Thread 1
setp :=get_actual_joint_positions()
❏ Loop
tmp:=[0,0,0,0,0,0]
tmp[0] = read_input_float_register(0)
tmp[1] = read_input_float_register(1)
tmp[2] = read_input_float_register(2)
tmp[3] = read_input_float_register(3)
tmp[4] = read_input_float_register(4)
tmp[5] = read_input_float_register(5)
x = norm(tmp)
If x
setp:= tmp
write_output_integer_register(0, 0)

```

Figure 3. URScript running on the End-Effector

cuted on the robot's end for the system to receive and apply the transmitted waypoints. The program starts with initializing variables and waits for a pop-up message box to be closed by the user. Then the execution process starts as soon as the RTDE communication from the Python code starts. After that, the script continuously executes `servoj` along with a thread in which it sets the joint position `setp` to the `input_double_register_*`, read by the function `read_input_float_register`. `servoj` is a real-time control function of joint positions, which blocks the computation for a specified parameter t , determined by the frequency of the communication. It uses look-ahead time and gain to predict the future trajectory [16]. If changed, these parameters can further fine-tune the reaction time of the robot and the smoothness of the robot's trajectory. For this study, the standard settings recommended in the documentation were used and proved sufficient. The parameter t can be set to a value as low as 0.002 s (500 Hz) for e-Series robots but was set to 0.008 s in this study to ensure that the inverse kinematics calculations can be performed in parallel to execution (cf. section 3.1.3).

3.2 Program Execution

With each of the modules described, the overall flow and execution of the methodology are illustrated in Fig. 4. After initializing and reading the IFC file using the IFC Reader module and after initializing the RTDE communication via the configuration XML file, three threads are activated. The planning thread is responsible for discretizing the segments and layers provided by the reader into three-

dimensional Cartesian coordinates. The inverse kinematics thread receives the Cartesian coordinates and calculates the joint coordinates. Finally, the communication thread relays the joint coordinates to the URScript with the specified frequency of 125 Hz to maintain real-time control. The communication thread also communicates with the extrusion module, controlled by a serial connection.

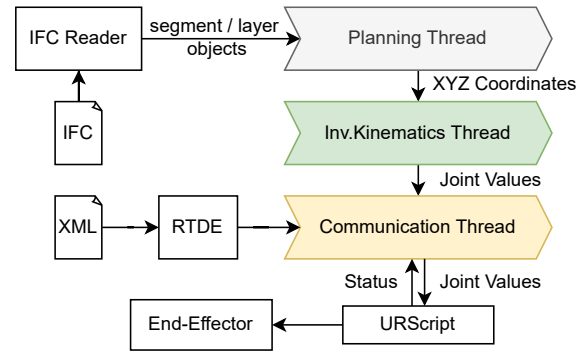


Figure 4. Execution Flowchart of the Proposed Methodology

The Planning and the inverse kinematics thread are put on hold to avoid unnecessary computation when they have calculated enough joint coordinates, defined by look-ahead time limits, and resume when the robot has caught up. Using this sequence, the segment, layer, and coordinate information can be changed and fed into the thread within or after the look-ahead time has passed. Accordingly, this also enables the user to change the layer time, extrusion rate, and other parameters depending on the results at the start of the printing process. If changes are made, these will only take effect after a few seconds (depending on the hardware) so as not to interrupt printing.

4 Experimental Validation

The presented robot control methodology has been developed for a small-scale test setup, including a Universal Robot UR10e industrial robot arm and an extrusion-based clay printing tool. The following validation shows that the developed planning and control modules can directly process FIM models into robot motion in a robust and smooth process. From the preparation of the design to the finished printed component, only a few steps are required. For controlling the robot, a regular laptop with the following specifications was connected via TCP/IP to the robot:

- i7-6700HQ 2.6 GHz Processor (8 Cores)
- 12 GB of Random Access Memory (RAM)
- Ubuntu 22.04 LTS

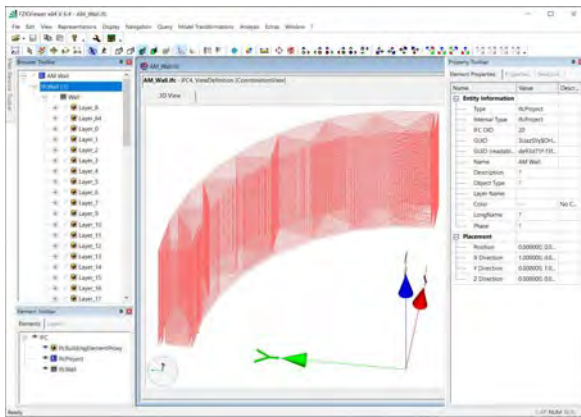


Figure 5. Fabrication Information Model used for testing the robot control method [3].

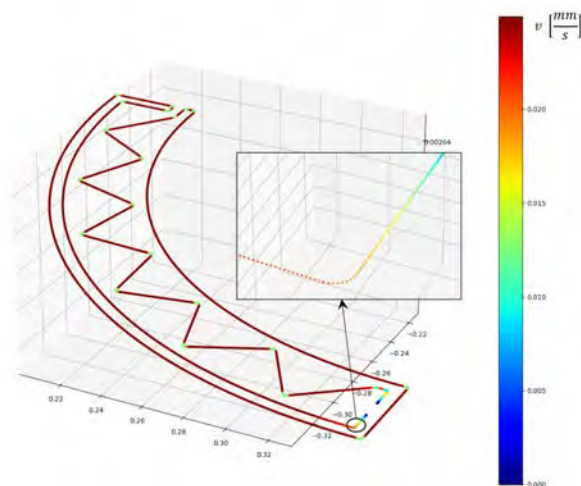


Figure 6. Velocity profile for the imported FIM model.

Using the FIM framework [3], a BIM-based design – a quarter-circular wall with a zigzag in-fill – was created to be fabricated with the clay printer (cf. Fig. 5). As a first step, a suitable velocity profile was generated for this printing path, which was limited by a maximum acceleration of $250 \frac{mm}{s^2}$ and by a layer time of $70s$. As shown in Fig. 6, using a single layer as an example, the speed is reduced in regions where a rapid change of direction occurs. In addition, the slow acceleration and deceleration at the beginning and end of the printing path can be seen. The magnification shows that the path is discretized into individual waypoints, and each waypoint gets a velocity value assigned.

Before executing the clay print, the control system was tested on a simulated robot, illustrated in Fig. 7, also depicting the GUI developed for this system. All the relevant

information can be seen on the GUI, and some values can be adapted during print time. Finally, the system was tested with the clay extruder, as shown in Fig. 8. The simulated robot and the actual clay print were executed using an update rate of $125 Hz$, thus sending a new waypoint every $0.008s$. The resulting robot movement seemed much smoother than with an offline programmed test print using URscript, even at higher printing speeds. With the proposed system, it is thus possible to produce components faster compared to other control methods.

The RTDE control system was also successfully coupled with the extruder control system, allowing the extrusion rate to adapt automatically to the robot's speed. The general print quality of the system still needs to be assessed but will be done in a coordinated test setup. Most importantly, the system processed the manufacturing information piece by piece while controlling the robot at a $125 Hz$ update rate without any jerking.

5 Conclusion

At its core, the proposed RTDE control method is similar to other robot control frameworks, e.g., ROS, but it follows a more streamlined approach, which fits the overall concept of FIM. It can directly process FIM models and convert the data into robot movement without data conversion. Additionally, since the FIM data is not processed all at once before printing begins but piece by piece, the system remains adaptable if the printing path or any print parameters need to be changed. Although the path planning and robot control modules are separate in the current implementation of FIM, both systems could be run simultaneously. Any changes to the print path could be done automatically based on sensor input. Only a few steps are required to process a digital model into a finished component.

However, the main advantage of the proposed RTDE robot control method is its simplicity. Although open-source robot control frameworks are being developed to provide a common platform for controlling different robots, these systems are mainly developed for scientific purposes, i.e., mainly for lightweight robots. For example, in ROS, various Kuka robot systems are integrated up to the size KR210/150, but none of the larger robot models are supported. The control method presented in this study can always be used, provided that parameters can be transmitted to the robot via a suitable communication interface and the Denavit-Hartenberg parameters corresponding to the robot are available. For UR robots, the RTDE functionality has been demonstrated in this study. However, in the same way, it can be done for Kuka robots, via the RSI interface or the KukaVarProxy tool [14], or for ABB robots, via the OPC UA or MQTT interface.

The system is easily expandable and opens up many pos-

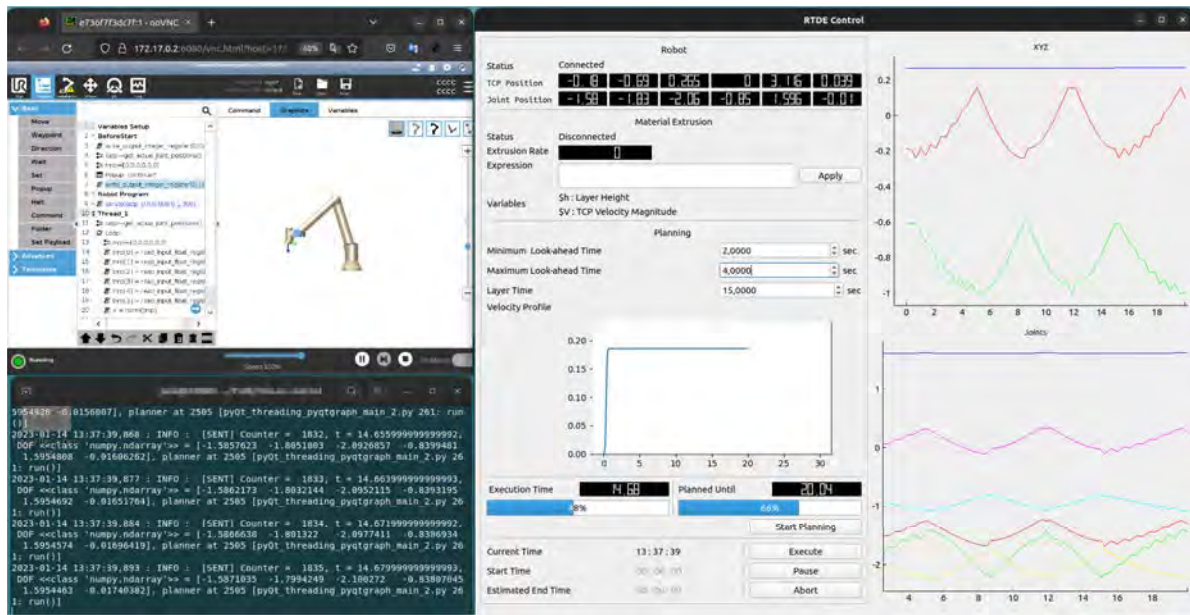


Figure 7. Using the robot control system with a simulated UR10e robot (left), showing the GUI of the system (right).



Figure 8. Clay print using the implemented robot control system. The shown clay extruder nozzle is mounted on a UR10e robot.

sibilities, such as integrating different (closed loop) control loops. For this reason, the proposed RTDE method is invaluable for setting up automatic quality control systems and thus increasing AM systems' automation level. The implementation shown in this study also provides a lightweight GUI and enables the user to interact with the printing process while it is running.

Compared to the offline control of the robot (using the URScript functionality), the printing process seems much smoother with the RTDE control, which is easily explained by the velocity smoothing at sharp corners in the print path impossible otherwise. A fact that is taken as an indication that velocity smoothing positively affects the overall print quality. However, as this study is mainly focused on robot

control, the performance of the printed specimens was not evaluated quantitatively. Nevertheless, the RTDE control can be used to study the effects of speed smoothing when printing with viscous materials such as concrete or clay.

Acknowledgments

The research presented is part of the Transregio 277 'Additive Manufacturing in Construction – The Challenge of Large Scale', funded by the Deutsche Forschungsgemeinschaft (DFG, German Research Foundation) – project number 414265976 – TRR 277.

References

- [1] André Borrmann, Markus König, Christian Koch, and Jakob Beetz. Building information modeling: Why? what? how? In *Building information modeling – Technology Foundations and Industry Practice*, pages 1–24. Springer, 2018.
- [2] Klodian Gradeci and Nathalie Labonnote. On the potential of integrating building information modelling (BIM) for the additive manufacturing (AM) of concrete structures. *Construction Innovation*, 2019.
- [3] Martin Slepicka, Simon Vilgertshofer, and André Borrmann. Fabrication Information Modeling: interfacing building information modeling with digital fabrication. *Construction Robotics*, 6(2):87–99, 2022. ISSN 2509-8780. doi:10.1007/s41693-

- 022-00075-2. URL <https://doi.org/10.1007/s41693-022-00075-2>.
- [4] R.A. Buswell, W.R. Leal de Silva, S.Z. Jones, and J. Dirrenberger. 3D printing using concrete extrusion: A roadmap for research. *Cement and Concrete Research*, 112:37–49, 2018. ISSN 0008-8846. doi:<https://doi.org/10.1016/j.cemconres.2018.05.006>. URL <https://www.sciencedirect.com/science/article/pii/S0008884617311924>. SI : Digital concrete 2018.
- [5] Nicolas Roussel. Rheological requirements for printable concretes. *Cement and Concrete Research*, 112:76–85, 2018. ISSN 0008-8846. doi:<https://doi.org/10.1016/j.cemconres.2018.04.005>. URL <https://www.sciencedirect.com/science/article/pii/S000888461830070X>. SI : Digital concrete 2018.
- [6] Pinar Urhal, Andrew Weightman, Carl Diver, and Paulo Bartolo. Robot assisted additive manufacturing: A review. *Robotics and Computer-Integrated Manufacturing*, 59:335–345, 2019. doi:10.1016/j.rcim.2019.05.005.
- [7] Serdar Kucuk and Zafer Bingul. *Robot kinematics: Forward and inverse kinematics*. INTECH Open Access Publisher London, UK, 2006.
- [8] Lieyun Ding, Ran Wei, and Haichao Che. Development of a BIM-based automated construction system. *Procedia Engineering*, 85:123–131, 2014. ISSN 1877-7058. doi:<https://doi.org/10.1016/j.proeng.2014.10.536>. URL <https://www.sciencedirect.com/science/article/pii/S187770581401902X>.
- [9] Alexander Paolini, Stefan Kollmannsberger, and Ernst Rank. Additive manufacturing in construction: A review on processes, applications, and digital planning methods. *Additive Manufacturing*, 30:100894, 2019. ISSN 2214-8604. doi:<https://doi.org/10.1016/j.addma.2019.100894>. URL <https://www.sciencedirect.com/science/article/pii/S2214860419309029>.
- [10] Filipe Monteiro Ribeiro, J. Norberto Pires, and Amin S. Azar. Implementation of a robot control architecture for additive manufacturing applications. *Industrial Robot: the international journal of robotics research and application*, 46(1):73–82, 2019. doi:10.1108/ir-11-2018-0226.
- [11] Omid Davtalab, Ali Kazemian, and Behrokh Khoshnevis. Perspectives on a BIM-integrated software platform for robotic construction through Contour Crafting. *Automation in Construction*, 89:13–23, 2018. ISSN 0926-5805. doi:<https://doi.org/10.1016/j.autcon.2018.01.006>. URL <https://www.sciencedirect.com/science/article/pii/S0926580517307975>.
- [12] Xuchu Xu, Ruoyu Wang, Qiming Cao, and Chen Feng. Towards 3D Perception and Closed-Loop Control for 3D Construction Printing. In *Proceedings of the 37th International Symposium on Automation and Robotics in Construction (ISARC)*, pages 1576–1583, Kitakyushu, Japan, October 2020. International Association for Automation and Robotics in Construction (IAARC). ISBN 978-952-94-3634-7. doi:10.22260/ISARC2020/0219.
- [13] Arturo Laurenzi, Enrico Mingo Hoffman, Luca Muratore, and Nikos G. Tsagarakis. Cartesi/o: A ros based real-time capable cartesian control framework. In *2019 International Conference on Robotics and Automation (ICRA)*, pages 591–596, 2019. doi:10.1109/ICRA.2019.8794464.
- [14] M.H. Arbo, I. Eriksen, F. Sanfilippo, and J.T. Gravdahl. Comparison of kvp and rsi for controlling kuka robots over ros. *IFAC-PapersOnLine*, 53(2):9841–9846, 2020. ISSN 2405-8963. doi:<https://doi.org/10.1016/j.ifacol.2020.12.2688>. URL <https://www.sciencedirect.com/science/article/pii/S2405896320334509>. 21st IFAC World Congress.
- [15] Real-time data exchange (RTDE) guide - 22229, 2022. URL <https://www.universal-robots.com/articles/ur/interface-communication/real-time-data-exchange-rtde-guide/>.
- [16] Universal robots - script manual - e-series - sw 5.11, 2022. URL <https://www.universal-robots.com/download/manuals-e-series/script/script-manual-e-series-sw-511/>.

Realtime damage detection in long conveyor belts using deep learning approach

Uttam Kumar Dwivedi ^{ab}, Ashutosh Kumar ^b and Yoshihide Sekimoto ^b

^aHazama Ando Corporation, Japan

^bDepartment of Civil Engineering, University of Tokyo, Japan

E-mail: uttam.kumar.dwivedi@ad-hzm.co.jp, uttamdwwivedi04@gmail.com, sekimoto@iis.u-tokyo.ac.jp

Abstract —

Japan's Road networks rely heavily on the mountain tunnels due to its topology. During the construction of these tunnels, mucking process is conducted to remove crushed rocks and rubbles in the tunnel with the use of long conveyor belts with the size of 3 to 10km. Regular visual inspections of these belts are carried out tediously by the workers to ensure belt integrity. To reduce the burden on workers, the paper proposes a vision based deep learning solution deployed on an edge device. Proposed framework detects the size of damage ranging from 1 cm to 100cm. Edge device deployment helps the workers to receive the result in real-time regardless of internet availability or working conditions. The effectiveness of the proposed framework is confirmed on 3 tunnel construction sites, with the estimated mean average precision of 85% for crack detection. The study can be applied in other domains of construction industry such as road damage or concrete damage categorization.

Keywords —

Internet of things (IoT); Edge computing; Deep learning; Smart construction; Damage detection; Real-time

1. Introduction

Japan has a long-standing reputation for excellence in construction engineering, particularly in the area of tunnels. This is due to the country's complex geology and densely populated urban areas. Japan has a vast network of road and railway tunnels, with recent data showing that there are over 5000 kilometers of road tunnels and

3800 kilometers of railway tunnels [1][2]. With the advancement of new tunneling technologies [3][4], there is renewed focus on sustainable development through shorter construction periods, cost savings, environmental preservation, and improved quality. One of the frequently used methods is the New Austrian Tunneling Method (NATM) [5][6], which is the basis of modern tunneling techniques. This method involves breaking rocks using explosives, followed by removal of the crushed rocks using conveyor belts. However, sharp rocks of various sizes can damage the conveyor belts, leading to accidents or belt failures [7]. It is therefore essential to regularly inspect the belt surfaces for damage to prevent such occurrences.

The inspection of conveyor belts in mountain tunnel construction continues to rely on manual visualization, which is a strain on inspectors and reduces the frequency of inspections due to fatigue. Additionally, stopping the conveyor belt during inspections decreases the work efficiency of the mucking process and causes delays. To address these problems, a new edge AI based deep learning framework is proposed to automatically detect damage in real-time and provide real-time alerts to safety engineers. The proposed system consists of three parts: damage detection, frame tracking, and real-time alerting. The effectiveness of the proposed method has been tested on three different mountain tunnel construction sites and has shown potential to enhance productivity and safety with an average mean average precision of 0.85 for damage detection. This solution uses deep learning and image processing on an offline edge device [8] to provide a real-time alerting platform for damages on long conveyor belts.

2. Literature Review

Automated inspection of tunnel constructions is a challenging but fascinating area for researchers in the construction field [9][10][11]. Over time, various devices have been developed to address these issues. Infrared thermal imaging technology and X-ray based nondestructive techniques [12] have been devised to detect damage in coal mines. These methods can detect cracks, but they require specific image processing and high-end, expensive equipment. Recently, AI-based methods, especially deep learning algorithms [13][14], have been widely used in image classification, detection, and segmentation. These methods use high-speed CMOS cameras and high-performance computing devices to extract features from images. Researchers have proposed MATLAB's deep learning solution[15] with two-layer neural networks to detect and locate conveyor belt damage in real-time. These methods provide a good balance of network architecture depth, image resolution, detection speed, and mean average precision (mAP). They can locate damages of different sizes and identify the numbers marked on the side of conveyor belts, which indicate the distance and make repair easier.

3. Research methodology

The methodology for this study has been framed around three main areas: data collection to include a range of scenarios, experimental setup and applied computer vision techniques-

A. Data collection

The conveyor belt crack detection (CBCD) dataset was developed by collecting 9,362 images from various mountain tunnel construction sites. The images were passed through data annotation tool [16] to create bounding box around different cracks. Figure 1(A) shows a sample of data, where the damage area is annotated with class id. The annotations are saved for each image as the equation [1].

$$\langle class\ id \rangle \langle \frac{x_o}{x} \rangle \langle \frac{y_o}{y} \rangle \langle \frac{w}{x} \rangle \langle \frac{h}{y} \rangle \quad (Eq. 1)$$

[Where, class id = label index of the class to be annotated; x_o = X coordinate of the bounding box's center.

y_o = Y coordinate of the bounding box's center.

w = Width of the bounding box.

H = Height of the bounding box.

X = Width of the image

Y = Height of the image]

The CBCD dataset is split into training, validation and testing set with 70%, 20% and 10% respectively.

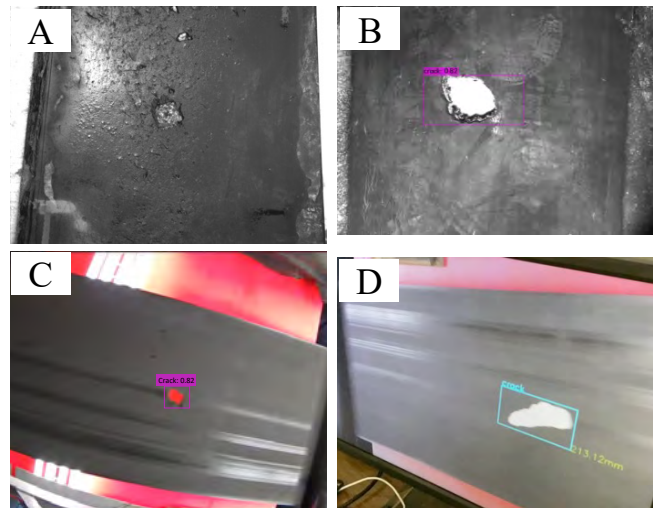


Figure 1. Training dataset for Conveyor belt crack detection (CBCD). (A) shows reflecting surface with non-through cracks, (B) shows through cracks while (C) shows through cracks with orange lights reflecting through it. (D) show scratched surface detected by AI. B and C also shows the bounding box around the crack area.

B. Experimental setup

Figure 2 shows a setup diagram is shown. The camera was positioned at the ground facing upwards with 1.5 meters between it and the conveyor belt. This configuration was intended to be used in construction scenarios. In order to maintain the belt's cleanliness, water from a stream was poured onto the belt to wash away any sled debris. A dark room was prepared with a camera mounted inside and lighting set up next to it. This provided optimal lighting conditions for filming.

Cameras require a specific lighting condition to properly record footage. A second LED light with an orange hue was added to the camera setup to indicate the severity of damage. Camera equipment used at construction sites in mountain tunnels has a rubber, polyester, and rubber layer construction. Each layer is 10mm thick and the total width of the belts is 0.6 meters. The conveyor belts operate at average speed of 200m/min.

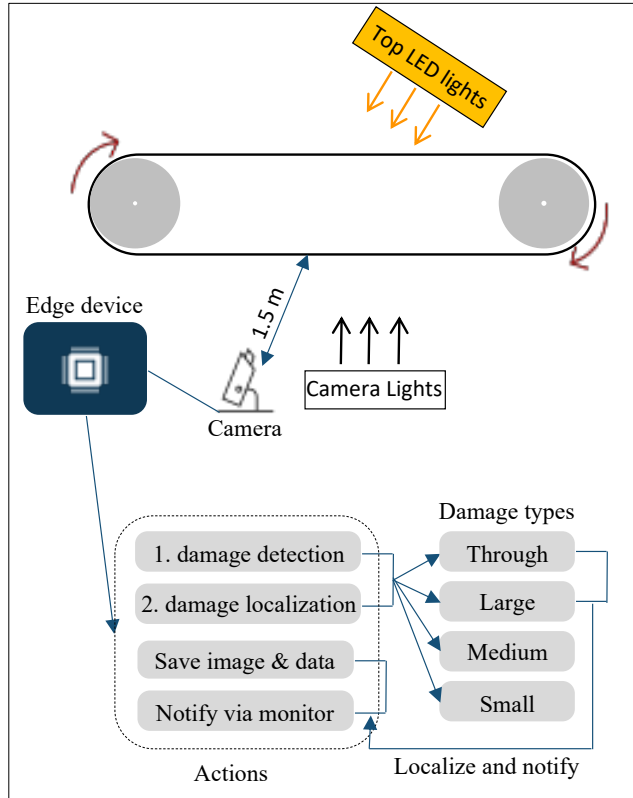


Figure 2. Simplified diagram of experiment setup and expected output. Edge device’s deep learning and image processing program provides output. Top LED orange lights provide contrast with respect to bottom white lights.

Table 1. Hyperparameters of the YOLOv5 network for training on the CBCD dataset.

Hyperparameter	Value
Input size	608
Learning rate	0.001
Batch size	64
Sub-division	16
Optimizer	SGD with momentum

C. Applied computer vision techniques

The section provides the details of deep learning models and image processing techniques used in proposed paper.

a) Deep learning-based detector model –

Object detection is used for identifying the location of cracks. Proposed paper uses a single instance target detection algorithm YOLOv5 [17] as a deep learning model to detect cracks in real-time. Since the original model is trained on the COCO dataset [18] with 80 general classes like person, cars, trucks etc. However, the original model doesn’t include specific object type such as cracks in conveyor belts.

In general, the training dataset contains around 200,000 images to train the model from scratch. With the help of transfer learning technique [19], where the original pretrained trained model is reused as a starting point for a model on second task. We train YOLO model using around 6,550 images from the CBCD dataset for 30,000 iterations with a batch size of 64 using the initial pre-trained weights from ImageNet dataset [20] for the first 137 convolutional layers. For training, NVIDIA RTX 3090 with 24GB memory was used for continuous 10 hours. The hyperparameters for the training is shown in Table 1.

b) Optimization of the neural network –

To run the detection framework effectively in real-time on the edge devices, proposed paper optimizes the YOLOv5 model. Neural networks generally use FP32 (32-bits floating point precision) [21] to store parameters such as weights and biases. Using a higher precision increases computational complexity and increases the size of the model. Through experiments, it has been found that the neural network model using half-precision FP16 (16-bit floating point) as parameters has similar performance to the neural network model using single-precision FP32. Therefore, the precision can be reduced to FP16 without severe loss of performance. This may be because neural networks are very resilient to noise. Decreasing the precision value from FP32 to FP16 is considered to introduce noise. Furthermore, half-precision models are very lightweight and show a significant increase in inference speed compared to single-precision models [21]. Proposed paper performs optimizations in the TensorRT framework [22] by reducing floating-point precision to FP16 and incorporating layers that perform conventional operations.

c) Crack size estimation –

Proposed paper deploys the optimized TensorRT model on the edge device NVIDIA Jetson NX, which localizes the cracks. To estimate the crack size in metric units, a distance estimation technique proposed by

Karney et al. [23] is used. Their approach is essentially limited to estimating the distance of an object when its true size is known and the focal length, camera sensor size and image resolution are fixed. In our approach, the distance from the camera to the conveyor belt is fixed (1.5 meter) as shown in Figure 2. The only parameter that remains to be determined is the crack size, which can be evaluated using Equation 2.

$$\mathcal{H}_{crack} = \frac{d \times h_{crack,px} \times \mu_h \times 1000}{f \times I_h} \quad (Eq.2)$$

[Where, \mathcal{H}_{crack} = Crack size in metric units (mm); d = Fixed distance of the conveyor belt surface from the camera; $h_{crack,px}$ = Height of the crack in pixels obtained from the bounding box; μ_h = Height of the camera sensor; f = Focal length of the camera; I_h = Height of the image resolution]

Size of the cracks are divided into 3 range as large damage size ($H_{crack} > 10\text{cm}$), medium damage ($10\text{cm} < H_{crack} < 5\text{cm}$) and small damage ($H_{crack} < 5\text{cm}$) shown in the table 2.

4. Result

Three different mountain tunnel construction sites were selected to run the crack detection and size estimation framework on long conveyor belts. The trained YOLOv5 model on CBCD dataset achieved a combined mean average precision (mAP) of 87% with FP32 and 85% with optimized FP16-TRT [21] on small edge device. The test was run on 500 images completely different from original CBCD dataset. However, the optimized model with TensorRT framework (FP16-TRT) provides significance speed on the edge device NVIDIA Jetson NX [8] from 5 FPS (frames per second) to 15 FPS as shown in the Figure 3. The frames per second (FPS) is calculated by averaging the inference FPS for 5,000 iterations. Figure 1 (D) shows a sample of the detection result with colored bounding box around the crack area with estimated size of 213mm (21.3 cm).

In Table 2, proposed paper shows the accuracy of crack detection by its size. The results presented in Table 2 are based on crack detection results carried out at the mountain tunnel site using NVIDIA Jetson Xavier NX device. We collect the samples from the image frames of the moving conveyor belt. Thus, the light reflections, water and dust on the conveyor belts require us to capture the testing data using multiple cameras at different locations and angles. We notice that a very

small false positive for no damages, while the accuracy of crack detection reduces as the size of the crack reduces. We achieve the highest accuracy of 89.23% for large damages and the lowest accuracy of 64.13 for smaller damages as smaller damages can get difficult to detect due to light reflections or dust appearing on top of conveyor belt.

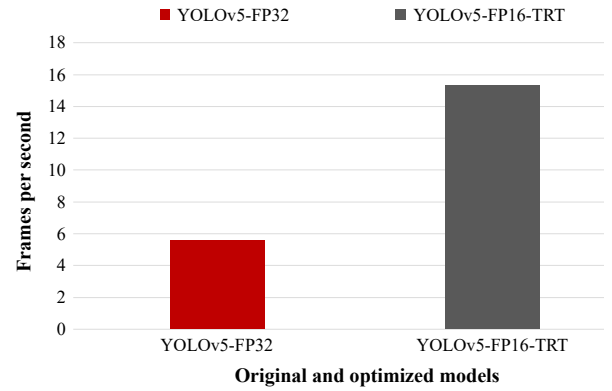


Figure 3. The comparison of inference speed of the original YOLOv5 model and its optimized version. Comparison of YOLOv5(YOLOv5-FP32) with 608x608 input resolution and its optimized version in TensorRT (YOLOv5-FP16-TRT). The frames per second (fps) is calculated by averaging inference fps for 5,000 iterations.

Table 2: Table shows the accuracy of the detection for various crack sizes

Damage size	# Of sample	Detected	Not detected	Accuracy (%)
Large damage (size >10cm)	103	92	11	89.3
Medium damage (10<size <5cm)	120	91	29	75.8
Small damage (size <5cm)	92	59	33	64.1
Through damage	34	28	6	82.4
No damage	500	4	496	99.2

5. Discussions and Conclusions

Long conveyor belts are widely used in various industries for transporting rocks, sand, and other heterogeneous materials over long distances. However, the manual inspection of these belts to detect damage is time-consuming and expensive, and current methods that use infrared laser light, x-rays, sound, magnetic, and ultrasound energy are also costly and have limited ability to detect large damage. In this study, we propose a simple and cost-effective method to detect and locate conveyor belt cracks in real-time. Our proposed system runs on edge devices and uses a server that operates offline. The system uses a CBCD dataset of 9,362 images to train a YOLOv5 model, optimized to execute inference on lightweight devices. The optimized model can detect cracks and track on the conveyor belt with a mean average precision of 85% and can process 15 frames per second on resource-constrained devices. The severity of the damage is estimated by fixing the camera's distance from the conveyor belt and using a monocular camera to categorize the size of the damage. Further improvement can be made by combining multiple video frames to identify crack regions in the conveyor belt.

At this stage, our proposed model for detecting and locating conveyor belt cracks in real-time is novel and compares favorably to existing methods in the field. To check the novelty of our proposed model, we reviewed the literature for belt tear detection, a vision-based method developed by Guo et al. [13] detects large size damages using YOLOv5-m [17] with a mean average precision (mAP) of 82.5%. However, this method fails to identify small or medium size damages. Similarly, Agata et al. [15] proposed an artificial intelligence-based approach for the classification of conveyor belt damage using a two-layer neural network and achieved an accuracy of 80%. Another method based on Haar-Ada Boost and Cascade algorithm was proposed by Wang et al. [14], where longitudinal tears of a conveyor belt under uneven light were detected with an accuracy of 97%. These methods can only detect large types of damage, whereas our proposed method can detect various types of damage and improve the overall detection accuracy, as shown in Table 2.

In conclusion, our proposed method provides a simple, inexpensive, and sustainable solution for detecting and locating conveyor belt cracks in real-time. The optimized model has a high accuracy and can detect

both cracks and digits on the conveyor belt, while categorizing the severity of the damage using a monocular camera. Our proposed method has the potential to revolutionize the field and make manual inspection of conveyor belts a thing of the past. A more detailed study will be presented in an upcoming journal.

6. Acknowledgement

This study is supported by Tokyo Kizai Kogyo co. ltd. and University of Tokyo, Japan. The authors declare no conflict of interest. We acknowledge Mr. Takeshi Hosokawa of Tokyo Kizai Kogyo Co., Ltd., and Mr. Tsuneo Koike of Ando Hazama Corporation for their cooperation in filming the continuous belt conveyor of this research.

7. Conflict of Interest

There are no conflicts to declare.

8. Reference

- [Internet]. Japan-tunnel.org. 2022 [cited 12 July 2022]. Available from: https://www.japan-tunnel.org/en/sites/www.japan-tunnel.org/en/files/tunnel_book_aspects/Tunnel%20Activity%202020%20Overview_0.pdf
- [Internet]. Ejrcf.or.jp. 2022 [cited 12 July 2022]. Available from: <https://www.ejrcf.or.jp/jrtr/jrtr66/pdf/38-51.pdf>
- Miura K. Design and construction of mountain tunnels in Japan. *Tunnelling and Underground Space Technology*. 2003 Apr 1;18(2-3):115-26.
- Karakuş M, Fowell RJ. An insight into the new Austrian tunnelling method (NATM). *Proc. ROCKMEC*. 2004 Oct 21.
- Tran TH. A Study on Tunnel Lining Concrete with Crushed Aggregate from NATM Muck. *In Proceedings of the 3rd International Conference on Sustainability in Civil Engineering 2021* (pp. 145-151). Springer, Singapore.
- Phadke V, Titirmare N. Construction of tunnels, by new austrian tunneling method (NATM) and by tunnel boring machine (TBM). *International Journal of Civil Engineering (IJCE)*. 2017 Oct 21;6(6):25-36.
- Bortnowski P, Kawalec W, Król R, Ozdoba M. Types and causes of damage to the conveyor belt-review, classification and mutual relations. *Engineering Failure Analysis*. 2022 Jun 16:106520.
- Feng H, Mu G, Zhong S, Zhang P, Yuan T. Benchmark analysis of Yolo performance on edge

- intelligence devices. *Cryptography*. 2022 Apr 1;6(2):16.
9. Montero R, Victores JG, Martinez S, Jardón A, Balaguer C. Past, present and future of robotic tunnel inspection. *Automation in Construction*. 2015 Nov 1;59:99-112.
 10. Gambao E, Balaguer C. Robotics and automation in construction [Guest Editors]. *IEEE Robotics & Automation Magazine*. 2002 Mar;9(1):4-6.
 11. Trybała P, Blachowski J, Błażej R, Zimroz R. Damage detection based on 3d point cloud data processing from laser scanning of conveyor belt surface. *Remote Sensing*. 2020 Dec 25;13(1):55.
 12. Ming-sheng W, Zheng-shi C. Researching on the linear X-ray detector application of in the field of steel-core belt conveyor inspection system. In 2011 International Conference on Electric Information and Control Engineering 2011 Apr 15 (pp. 701-704). IEEE.
 13. Guo X, Liu X, Zhou H, Stanislawski R, Królczyk G, Li Z. Belt Tear Detection for Coal Mining Conveyors. *Micromachines*. 2022 Mar 17;13(3):449.
 14. Wang G, Zhang L, Sun H, Zhu C. Longitudinal tear detection of conveyor belt under uneven light based on Haar-AdaBoost and Cascade algorithm. *Measurement*. 2021 Jan 15;168:108341.
 15. Kirjanów-Błażej A, Rzeszowska A. Conveyor Belt Damage Detection with the Use of a Two-Layer Neural Network. *Applied Sciences*. 2021 Jun 13;11(12):5480.
 16. [Internet]. Tzutalin (2015), 'LabelImg', Free software: MIT License. Available from: <https://github.com/heartexlabs/labelImg>
 17. Nelson J. Yolov5 is here [Internet]. Roboflow Blog. Roboflow Blog; 2021 [cited 2022Nov24]. Available from: <https://blog.roboflow.com/yolov5-is-here/>
 18. Lin TY, Maire M, Belongie S, Hays J, Perona P, Ramanan D, Dollár P, Zitnick CL. Microsoft coco: Common objects in context. In European conference on computer vision 2014 Sep 6 (pp. 740-755). Springer, Cham.
 19. Torrey L, Shavlik J. Transfer learning. In *Handbook of research on machine learning applications and trends: algorithms, methods, and techniques 2010* (pp. 242-264). IGI global.
 20. Deng J, Dong W, Socher R, Li LJ, Li K, Fei-Fei L. Imagenet: A large-scale hierarchical image database. In 2009 IEEE conference on computer vision and pattern recognition 2009 Jun 20 (pp. 248-255). Ieee.
 21. FP32 (Floating point format for Deep Learning) [Internet]. OpenGenus IQ: Computing Expertise & Legacy. 2022 [cited 12 July 2022]. Available from: <https://iq.opengenus.org/fp32-in-ml/>
 22. Jeong E, Kim J, Ha S. TensorRT-based Framework and Optimization Methodology for Deep Learning Inference on Jetson Boards. *ACM Transactions on Embedded Computing Systems (TECS)*. 2022.
 23. Karney CF. Transverse Mercator with an accuracy of a few nanometers. *Journal of Geodesy*. 2011 Aug;85(8):475-85.

Low-light Image Enhancement for Construction Robot Simultaneous Localization and Mapping

Xinyu Chen¹ and Yantao Yu¹

¹Department of Civil and Environmental Engineering, Hong Kong University of Science and Technology

xchengl@connect.ust.hk, ceyantao@ust.hk

Abstract -

Visual Simultaneous Localization and Mapping (V-SLAM) is widely used in construction robots because it is an efficient and inexpensive information acquisition method. However, low-light construction scenes pose significant challenges for V-SLAM detection and positioning. In low-light scenes such as underground garages or dim indoor scenes, V-SLAM is difficult to detect enough valid feature points, which causes navigation to fail. To address this issue, we propose an Unsupervised V-SLAM Light Enhancement Network (UVLE-Net) to enhance low-light images. After image enhancement, we add a robust Shi-Tomasi method in ORB-SLAM2 to detect feature points and use the sparse optical flow algorithm to track the feature points. By using UVLE-Net, the brightness and contrast of the images can be significantly increased, and feature points can be detected easily. The optical flow and Shi-Tomasi method improve the ability of feature point extraction and tracking in low light. To validate the robustness and superiority of our method in low-light conditions, we conduct comparison experiments with other enhancement techniques on published and real-world construction datasets.

Keywords -

Low-light enhancement; Retinex; Simultaneous Localization and Mapping; Construction robots

1 Introduction

The productivity, quality, and other aspects of construction have significantly increased as a result of the rapid development of construction robotics[1]. Autonomous mobile robots can perform specific tasks by navigating the construction site[2]. For example, a waste recycling robot can inspect construction sites and find nails and screws[3]. Construction monitoring robots with scanning sensors and cameras can move automatically and monitor progress [4]. The autonomous task of construction robots depends on the navigation system. Mobile robots typically use Simultaneous Localization and Mapping (SLAM) technology to generate maps of unknown environments while locating robots in the map. Construction robots can move and work automatically using the SLAM system.

Construction robots need to collect enough on-site data in order to operate autonomously. At present, laser point clouds and RGB cameras are mainly used in positioning and working system. Visual data contains rich data information, and provides a data basis for construction site work. In comparison to other SLAM sensors like LiDAR, the RGB camera is typically lightweight, inexpensive, and contains rich visual information. State-of-the-art visual-based algorithms such as ORB-SLAM2 perform well in both datasets and real-world experiments[5]. However, the SLAM algorithm is set in a well-lit environment[6][7]. The low-light construction sites pose significant challenges for V-SLAM. For example, in an interior building environment, a robot moving from an area with good lighting to an area far away from artificial lighting facilities, such as a backlit area or an underground garage with many occlusions, can experience location errors or even failure. Insufficient light in image shooting can significantly reduce the visibility of the image. V-SLAM methods rely on feature point extraction, but low-light frames provide few high-quality points. Therefore, V-SLAM systems would lose their localization and detection abilities in low light conditions due to low light and low contrast. Moreover, due to dynamic lighting and halos in a dark scene, it is difficult to track the same feature points as the lighting changes. In order to improve the visibility of the low-light construction environment and the usability of the current robot navigation and positioning system, low-light images need to be enhanced.

Although there have been some studies on enhancing low-light images in the field of computer vision, most low-light image enhancement techniques, such as LIME[8], Low-light GAN[9], MSRCR[10], are optimized to enhance the image perception by human eyes rather than the V-SLAM performance. The existing low-light image enhancement approaches have limited ability to address low-light difficulties in construction robots V-SLAM, given the following existing problems: (a) Due to the limitation of manual parameter setting, the manual enhancement method based on image features can only solve one of the problems in challenging low-light construction scenarios. (b) Data-driven enhancement methods require training on pairs of data sets. In dynamic construction environments,

it is challenging to collect paired data sets with exactly the same content. (c) The existing low-light enhancement methods lack research on feature point extraction of construction robots V-SLAM. Therefore, it is necessary to build a low-light enhanced method for construction robot localization and mapping in low light.

In this paper, we propose an Unsupervised V-SLAM Light Enhancement Network (UVLE-Net) to enhance low-light images, which helps construction robots to locate under low light. To address the issue of construction robots in low light, we preprocess the image using the deep neural network of the Retinex theory. Following image preprocessing, we detect feature points with the Shi-Tomasi method and uniformly assign feature points to track. Finally, we test UVLE-Net on the EuRoc dataset[11] and construction environment. Experiments show that our proposed method has better detection performance in both open datasets and real low-light construction environments. The contributions of our work are summarized as follows: (a) We propose an UVLE-Net for low-light construction robots to enhance frames' lightness and contrast. It can help construction robots to get more gradient information and feature points in low light. (b) We design novel loss functions to train the image enhancement network in an unsupervised way, thereby drastically reducing the requirement of coupled image collection. (c) We combine the Shi-Tomasi and sparse optical flow algorithm into ORB-SLAM2 to detect and track the feature points in low-light construction. It can usefully reduce the requirement of ORB-SLAM2 feature points and improve positioning accuracy in low-texture and low-light construction environments.

Our approach is innovative in three aspects: (a) Based on Retinex theory, we use a deep neural network to iteratively solve the reflectance map of the image, which has better generalization performance in construction scenes. (b) The enhancement network can be trained on any lightness dataset by designing unsupervised learning mode loss functions. (c) The Shi-Tomasi and sparse optical flow method is introduced in ORB-SLAM2 to increase its low-light positioning ability.

2 Literature review

2.1 SLAM in construction robotics

In construction, SLAM has gained more and more attention from researchers as an effective autonomous movement and location method[12]. SLAM algorithms can be divided into LiDAR-based and visual-based methods. Regarding LiDAR SLAM, Cebollada et al.[13] used a monocular camera with a 2-D laser sensor to locate and map the underground space. It used the bilinear filter function to estimate grid occupancy and the Gauss-Newton method to optimize scan matching. However, these methods lack

closed-loop detection and optimization. Therefore, it is not capable of eliminating accumulated localization errors. Kim et al.[14] used 3-D laser SLAM to locate and match point cloud objects. It is limited by laser detection range and cannot be modelled in large construction scenes. It costs lots of computing resources in point cloud location and matching. Meanwhile, laser SLAM lacks the semantic information of the maps, which cannot help robots to do some work.

Regarding visual SLAM, it only needs inexpensive cameras and a few computing resources. It is economical and suitable for construction environments. Peel et al.[15] combined adaptive monte carlo localization with SLAM, using a small robot to detect bridge supports. Zhang et al.[16] used mobile robots for large-scale 3D printing construction. These robots mapped the environment using Gmapping and adaptive monte carlo localization to locate themselves. Asadi et al.[17] proposed a mobile robot platform equipped with an RGB camera. It used visual SLAM and semantic segmentation techniques to navigate daytime construction scenes. Although there has been a lot of work to demonstrate the effectiveness of SLAM in construction, most of them have been done under sufficient lighting conditions. These methods will not work in low-light conditions. In the low-light and low-texture construction environment, visual SLAM hardly extracts and tracks feature points due to the loss of gradient information. So there are some robustness and reliability issues with V-SLAM in a low-light environment.

2.2 Low-light image enhancement

The low-light image enhancement methods can be divided into conventional and data-driven methods. Regarding conventional methods, local statistics and intensity mapping are the primary earlier conventional methods. Histogram-based solutions expand the enhanced dynamic range by modifying the light distribution of global or local images[18]. Then, researchers used the Retinex theory to enhance images. Reflection mapping was used as the result of enhancement in Multiscale Retinex with Color Restoration (MSRCR) [10]. To enhance image lighting conditions, Fu et al.[19] used a weighted variational model to estimate the reflectivity and illuminance of images. By determining the RGB channel's maximum pixel intensity for each pixel, LIME[8] calculated the rough illumination map. Most conventional methods depend on carefully designed parameters and fail to generalize to various low-light construction conditions.

With the development of deep neural networks, many enhanced methods use deep learning techniques. For instance, the first low-light enhanced network in the GAN model was low-lightgan[9]. To simulate lighting images, it created a discriminator and generator using paired

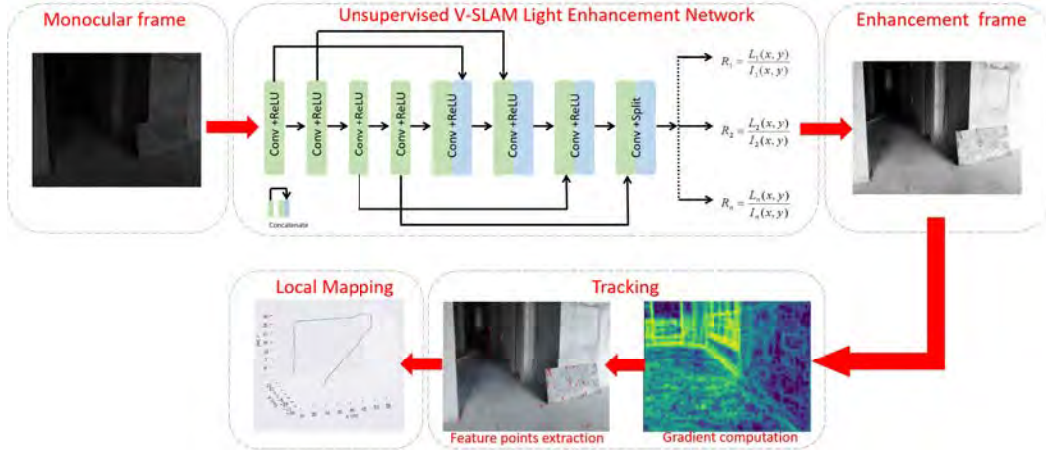


Figure 1. Architecture of the low-light construction robot navigation system.

Table 1. Detailed architecture of UVLE-Net.

Input	Dimensions	Operator	Output
Image	$256 \times 256 \times 1$	Conv+ReLU	Conv1
Conv1	$256 \times 256 \times 32$	Conv+ReLU	Conv2
Conv2	$256 \times 256 \times 32$	Conv+ReLU	Conv3
Conv3	$256 \times 256 \times 32$	Conv+ReLU	Conv4
Conv1+Conv4	$256 \times 256 \times 64$	Conv+ReLU	Conv5
Conv2+Conv5	$256 \times 256 \times 64$	Conv+ReLU	Conv6
Conv3+Conv6	$256 \times 256 \times 64$	Conv+ReLU	Conv7
Conv4+Conv7	$256 \times 256 \times 64$	Conv+ReLU	Conv8
Conv7+Conv8	$256 \times 256 \times 8$	Split	$R_1 \cdots R_n$
Image $\times R_n$	-	-	Enhanced image

datasets. Zero-DCE [20] extended the solution by establishing numerous particular image curves based on zero-inference. However, the model based on light recovery curves exhibits unstable performance under different levels of darkness. Therefore, in order to enhance the robustness of the image, it is necessary to estimate the image features.

3 Methodology

In this section, we first introduce the Retinex theory. On this basis, we present an Unsupervised V-SLAM Light Enhancement Network (UVLE-Net). Then, we introduce our robot positioning mapping method based on ORB-SLAM2. Figure 1 shows the overall structure of our method. First, the low-light images are fed into the enhancement network. We incorporate the Retinex theory into a deep neural network model to solve the reflectance iteratively. Our data-driven reflectance model can enhance images accurately under various illumination conditions. Then, ORB-SLAM2 computes gradients and feature points for robot localization and mapping.

3.1 UVLE-Net for low-light image enhancement

The traditional Retinex theory simulates human color perception. It is assumed that the image can be broken down into two parts: reflectance and illumination. The image $I(x, y) \in R^{W \times H \times 1}$ represents the source image, then it can be decomposed by

$$I(x, y) = R(x, y) \cdot L(x, y), \quad (1)$$

where $L(x, y)$ is the spatial distribution of source illumination, $R(x, y)$ denotes the distribution of scene reflectance. Reflectance denotes the intrinsic property of captured objects, which is consistent under all illumination conditions. The illumination depicts the varying degrees of brightness of objects.

We attempt to estimate the reflectance as guidance for automatic low-light image enhancement, with the merits of a simple and differentiable expression relying on the input images and preserving the differences of neighbouring pixels. Assuming that the illumination map under normal light condition L is an identity matrix, according to the effective formulation of Retinex, the reflectance for enhancement can be obtained. Arguably, the formulation of $R(x, y)$ is an ill-posed problem, and direct decomposition

results in unnatural artifacts. So we design the enhanced model and use iterative algorithms to gradually eliminate the impact, which is

$$\log R_i(x, y) = \log I_i(x, y) - \log L_i(x, y), \quad \forall i = 1 \dots n. \quad (2)$$

where n is the number of iterations. Here we set $n = 5$ empirically, which we will detailedly discuss in the ablation study.

The detailed architecture of the enhanced model is demonstrated in TABLE 1. Input frames in SLAM are grey images, so the UVLE-Net is designed to enhance brightness in grey images. The proposed enhanced images model consists of 8 convolutional layers with skip connections. Specifically, the first 7 layers have 32 convolutional kernels of size 3×3 and stride 1 followed by the ReLU activation function, and the last one has 8 convolutional kernels of size 3×3 and stride 1 followed by the Tanh activation function. Essentially, the last convolutional layer splits the estimated lighting reflectance R_i , and the given image I_i is enhanced iteratively in terms of the parameter maps R_1 to R_n .

It is challenging to capture different lighting-paired images of a uniform dynamic construction scene. So we adopt unsupervised learning to overcome this problem. We devise several differentiable loss functions to facilitate the unsupervised reflectance illumination model training.

Loss functions:

(1) Information Difference Loss. In robot location tasks, the quality of feature point extraction is important. Thereby, an information difference loss is devised to quantify the differences between the improved image and the original image, which is expressed as:

$$L_{idl} = \|V(I_n) - V(I_0)\|_2^2, \quad (3)$$

where $V(I)$ is the feature extraction operator based on VGG-16. I_0 is the original raw image and I_n is the corresponding enhanced image after n time iterations. The VGG network is leveraged here for its concise architecture to compute information differences effectively.

(2) Exposure Control Loss. The stable exposure intensity in SLAM is the key to the position. Therefore, the exposure control loss is required to equalize exposure. To obtain an average intensity Y , the image is split into $16 * 16$ non-overlapping local regions. According to exposure fusion theory, a well-exposedness level E is defined as the grey level in grey space. As a result, the exposure control loss, which measures the distance between average intensity Y and well-exposedness level E , is calculated as follows:

$$L_{ecl} = \frac{1}{M} \sum_{m=1}^M |Y_m - E|, \quad (4)$$

where M represents the number of non-overlapping local regions, E is set as 0.6 empirically.

(3) Illumination Smoothness Loss. An illumination smoothness loss is applied to the estimated reflectance parameter map R_i to ensure the smoothness of the illumination component in grey space for maintaining the monotonicity of pixel-level surrounding context during iteration, which is expressed as:

$$L_{isl} = \frac{1}{N} \sum_{i=1}^N (|\nabla_x R_i| + |\nabla_y R_i|)^2, \quad (5)$$

where N represents the number of iterations, ∇ is the first-order differential operator, accordingly ∇_x and ∇_y denote the horizontal and vertical gradient operations respectively. We will explain them in the experimental section.

To sum up, the total loss is expressed as:

$$L = \omega_a L_{idl} + \omega_b L_{ecl} + \omega_c L_{isl}, \quad (6)$$

where ω_a , ω_b , and ω_c are the weights controlling the significance of losses.

3.2 ORB-SLAM2 for localization and mapping

In this paper, ORB-SLAM2 is selected as the navigation algorithm for construction robots. The workflow of ORB-SLAM2 consists of four steps: detection of feature points, stereo matching, feature tracking, and motion estimation. When ORB-SLAM2 receives a frame, it first extracts the feature points. A stereo-matching process follows feature detection. Then the field points created in the previous frame are projected to the current frame and matched with the current frame to obtain several corresponding features. The ORB-SLAM2 system relies on extracting and matching many feature points, and all the foundations are built on the accurate extraction of rich feature points. Therefore, system position and pose tracking will fail when operating in a construction scene with low texture and low light.

We adopt the Shi-Tomasi[21] and Kanade-Lucas-Tomasi (KLT)[22] sparse optical flow algorithm to solve these problems. The average distribution of feature points in the low illumination environment reduces the matching requirement of feature points. New feature points will be added if not enough features are left after the uniform procedure to reach the necessary 200. The next frame will be considered a new keyframe if the difference between the two frames' parallaxes is significant.

4 Experiments and results

The main focus of our work is the visual navigation of construction robots to work reliably in low-light environments. Therefore, we experiment on low-light open datasets and real construction scenes. First, we train the UVLE-Net model. Then we compare our method with

other low-light enhancement methods and evaluate their accuracy on public datasets. Finally, we test them in real low-light construction scenes.

4.1 UVLE-Net training and ablation experiment

The UVLE-Net is trained in an unsupervised way on SICE[23]. SICE is a dataset consisting of 589 image sequences and 4,413 high-resolution samples with significant exposure levels. We use multi-exposure datasets to train the enhanced image model. It can reduce the impact of varying lighting conditions. These datasets are guaranteed to improve the generalization performance of UVLE-Net under various lighting conditions in construction scenes. UVLE-Net training experiments are conducted on a desktop Dell 7000 workstation. It has an Intel I7-12700 CPU running at 3 GHz, 16 GB of RAM, and an NVIDIA 3060 GPU. The network is optimized using the ADAM optimizer with default parameters and a fixed learning rate of 0.001. The weights of loss functions: w_a, w_b , and w_c are set as 0.01, 50, and 100 empirically.

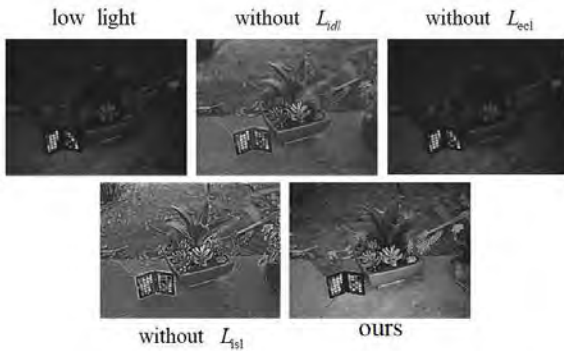


Figure 2. Ablation study on the contribution of loss functions.



Figure 3. Qualitative comparison of the different iterations.

We use the same dataset and parameter to train the UVLE-Net model with different loss functions to verify the effects

of each loss function, as shown in Figure 2. The loss of information difference L_{idl} enhanced the features produced from the input image, improving the model's ability to interpret semantics. Without the loss of exposure control L_{ecl} , the brightness decreases, and the low-light area fails to recover. The illumination smoothness loss L_{isl} acts as a link between surrounding pixel-level changes, Ensuring the unity of the overall brightness. We respectively test $n = 0, 1, 3, 5, 7$ and 9 iterations. It reveals that the peak performance appears when n equals five. Figure 3 depicts a visual example adapted to the different number of iterations. Increasing the number of iterations improves the lightness intuitively. However, when $n > 5$, performance barely improves. To verify the availability of our method in low light, we compare it with other advanced enhancement methods in SLAM feature point extraction and gradient calculation, as shown in Figure 4. It can be seen that the global overexposure of MSRCR reduces the information gradient and makes it difficult to extract feature points. The LIME approach has local confusion and ambiguity. Our method can improve brightness and contrast steadily. It has clearer gradient information and more feature points.

4.2 Low-light SLAM experiment

All experiments are conducted on a Ubuntu 22.04 laptop with an Intel I7-7700 CPU at 2.1Hz and ROS kinetic energy 2GB of memory. Camera FPS in the EuRoc data and real construction data are 20Hz, and UVLE-Net can run at 22Hz on CPU and 67Hz on GPU. So it can run in real time.

A.Public dataset experiment

We use MH sequences in EuRoc MAV as the test datasets. The EuRoc MAV datasets consist of 5 sequence micro aircraft vehicles (MAVs) flying rooms around two different directions (V1 and V2 sequences) and one large industrial (MH sequences). Depending on MAVs' speed, lighting, and texture, the sequences are classified as easy, medium, and difficult. In MH datasets, there are many low-light and complex light scenes. These indoor lighting problems are very similar to low-light problems in construction scenes, so they are used to test algorithms in low-light environments. As shown in Figure 5, we use MSRCR, LIME and UVLE-Net to enhance low-light images in MH datasets.

Table 2 compares the performance of UVLE-Net in monocular sensors with original, MSRCR and LIME; all tests are in KLT ORB-SLAM2. As shown in the table, our method achieves lower error results in all sequences than other enhanced methods, in most cases by a large margin. In most sequences, using enhancement methods can reduce the error. Nevertheless, MSRCR produces a larger error because overexposure destroys gradient and

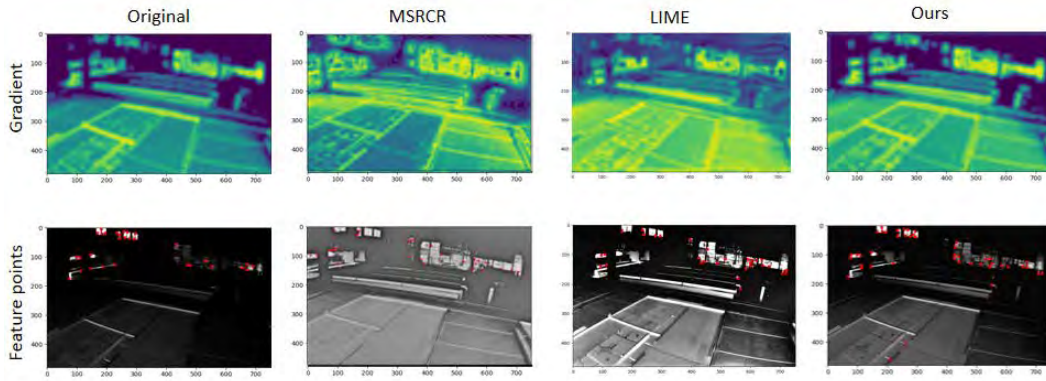


Figure 4. The gradient and feature point results of original, MSRCR, LIME and our method.

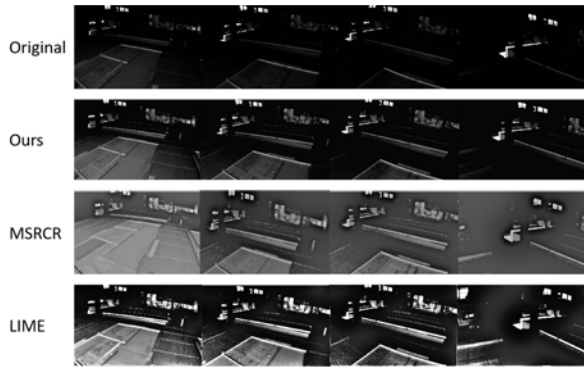


Figure 5. The results of image preprocessing in MH datasets. MSRCR shows global overexposure, LIME has local overexposure and blurring, and our method steadily increases brightness, showing more detail and no overexposure.

Table 2. Performance comparison in the EuRoC MH datasets (Root mean square error in m).

Sequence	Original	MSRCR	LIME	Ours
MH01 easy	0.039	0.031	0.034	0.024
MH02 easy	0.036	0.028	0.033	0.025
MH03 medium	0.055	0.059	0.055	0.053
MH04 difficult	0.089	0.084	0.079	0.073
MH05 difficult	0.077	0.062	0.064	0.055

feature points in some normally lit scenes in MH-03. In addition to the table, we demonstrate the result of the MH-01 sequence on both 2D and 3D pose graphs in Figure 6 and Figure 7. In the pose graphs map, X-Z represents the ground, and Y represents the height. From the enlarged part in the figures, we can see that under the original low-light environment, the SLAM algorithm has a significant error in this section. MSRCR and LIME can reduce these errors. The estimated trajectory of our method is almost

consistent with the real value.

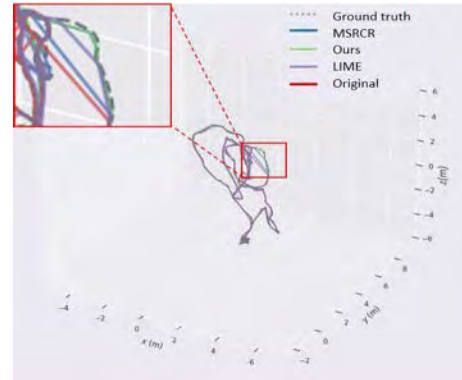


Figure 6. 3D pose graph. The broken line is SLAM ground truth. The blue line is MSRCR. The green line is our method. The purple line is LIME. The red line is the original frames (X-Z represents the ground, and Y represents the height).

B. Real construction dataset experiment

We use the Intel Realsense 435 camera to conduct real experiments in low-light indoor construction scenes. We lack the pose motion capture system in construction scenes to collect the actual moving position. So we only compare our low-light enhanced method with the original method in the real-world experiment. In Figure 8, we compare the original image with our enhanced image. The processed image has higher brightness and contrast. It shows more gradient information and feature points. In order to further verify the performance of our algorithm, we conduct location estimation and mapping experiments. The results are shown in Figure 9. As can be seen, in the latter part of the navigation (left part), the original frames cannot provide enough feature points for tracking and matching, so the mapping is lost. In addition, there is a large deviation in the corner part.

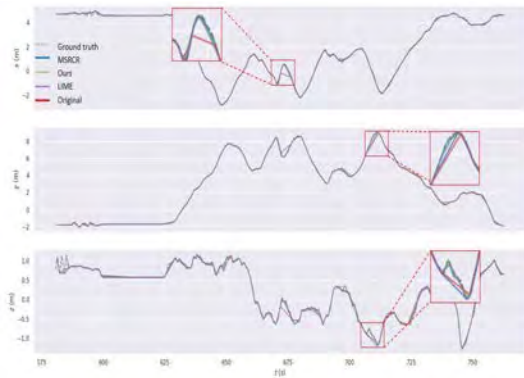


Figure 7. 2D pose graph. The broken line is SLAM ground truth. The blue line is MSRCR. The green line is our method. The purple line is LIME. The red line is the original frames.

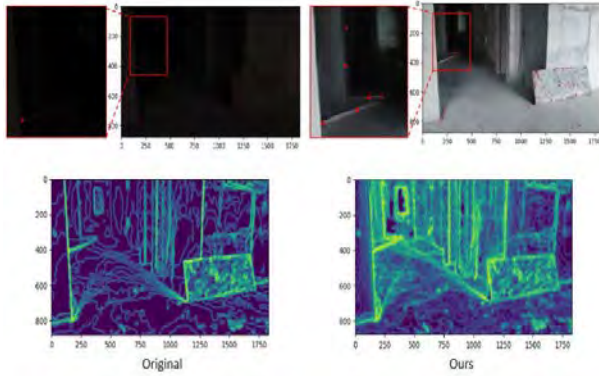


Figure 8. Original image captured by the Intel Realsense 435 camera and processed image in UVLE-Net.

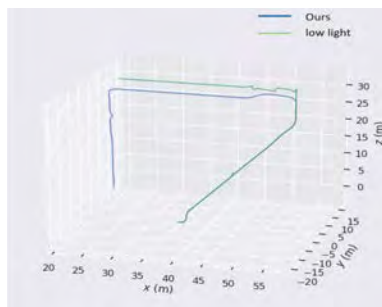


Figure 9. 3D pose graph. The green line is the original method in low light. The blue line is our method(X-Z represents the ground, and Y represents the height).

5 Conclusions

This paper proposes a visual-based monocular construction robot SLAM system for low-light challenges. We design a low-light enhancement network for robot construction scenes. The deep network based on Retinex theory trains the enhancement model using self-supervised learning. This method improves the brightness and contrast of the frame and helps the construction robot to track feature points in low light environments. We add the Shi-Tomasi and optical flow method to the ORB-SLAM2 system to reduce the difficulty of feature point tracking in the SLAM system. We validate our method in the public and real-world datasets. The results show that our method has better performance than MSRCR and LIME. Our method solves the positioning failure problem in low-light construction scenes. Our method can be run in real-time on mobile computers and it is suitable for deploying robots or portable devices in low-light environments.

6 Acknowledgement

This work was financially supported by the HKUST-BDR Joint Research Institute Fund, No. OKT23EG01.

References

- [1] Xinge Zhao and Chien Chern Cheah. Bim-based indoor mobile robot initialization for construction automation using object detection. *Automation in Construction*, 146:104647, 2023. ISSN 0926-5805.
- [2] Hongling Guo, Jia-Rui Lin, and Yantao Yu. Intelligent and computer technologies' application in construction, 2023.
- [3] Zeli Wang, Heng Li, and Xiaoling Zhang. Construction waste recycling robot for nails and screws: Computer vision technology and neural network approach. *Automation in Construction*, 97:220–228, 2019.
- [4] Muhammad Ilyas, Hui Ying Khaw, Nithish Muthuchamy Selvaraj, Yuxin Jin, Xinge Zhao, and Chien Chern Cheah. Robot-assisted object detection for construction automation: data and information-driven approach. *IEEE/Asme Transactions on Mechatronics*, 26(6):2845–2856, 2021.
- [5] Raul Mur-Artal and Juan D Tardós. Orb-slam2: An open-source slam system for monocular, stereo, and rgb-d cameras. *IEEE transactions on robotics*, 33(5):1255–1262, 2017.

- [6] Myriam Servières, Valérie Renaudin, Alexis Dupuis, and Nicolas Antigny. Visual and visual-inertial slam: State of the art, classification, and experimental benchmarking. *Journal of Sensors*, 2021, 2021.
- [7] Xinyu Chen and Yantao Yu. Image illumination enhancement for construction worker pose estimation in low-light conditions. In *Computer Vision–ECCV 2022 Workshops: Tel Aviv, Israel, October 23–27, 2022, Proceedings, Part VII*, pages 147–162. Springer, 2023.
- [8] Xiaojie Guo, Yu Li, and Haibin Ling. Lime: Low-light image enhancement via illumination map estimation. *IEEE Transactions on image processing*, 26(2):982–993, 2016.
- [9] Guisik Kim, Dokyeong Kwon, and Junseok Kwon. Low-lightgan: Low-light enhancement via advanced generative adversarial network with task-driven training. In *2019 IEEE International Conference on Image Processing (ICIP)*, pages 2811–2815. IEEE, 2019.
- [10] Daniel J Jobson, Zia-ur Rahman, and Glenn A Woodell. A multiscale retinex for bridging the gap between color images and the human observation of scenes. *IEEE Transactions on Image processing*, 6(7):965–976, 1997.
- [11] Michael Burri, Janosch Nikolic, Pascal Gohl, Thomas Schneider, Joern Rehder, Sammy Omari, Markus W Achtelik, and Roland Siegwart. The euroc micro aerial vehicle datasets. *The International Journal of Robotics Research*, 35(10):1157–1163, 2016.
- [12] Lichao Xu, Chen Feng, Vineet R Kamat, and Carol C Menassa. An occupancy grid mapping enhanced visual slam for real-time locating applications in indoor gps-denied environments. *Automation in Construction*, 104:230–245, 2019.
- [13] Sergio Cebollada, Luis Paya, Miguel Julia, Mathew Holloway, and Oscar Reinoso. Mapping and localization module in a mobile robot for insulating building crawl spaces. *Automation in Construction*, 87:248–262, 2018.
- [14] Pileun Kim, Jingdao Chen, and Yong K Cho. Slam-driven robotic mapping and registration of 3d point clouds. *Automation in Construction*, 89:38–48, 2018.
- [15] H Peel, S Luo, AG Cohn, and R Fuentes. Localisation of a mobile robot for bridge bearing inspection. *Automation in Construction*, 94:244–256, 2018.
- [16] Xu Zhang, Mingyang Li, Jian Hui Lim, Yiwei Weng, Yi Wei Daniel Tay, Hung Pham, and Quang-Cuong Pham. Large-scale 3d printing by a team of mobile robots. *Automation in Construction*, 95:98–106, 2018.
- [17] Khashayar Asadi, Hariharan Ramshankar, Harish Pullagurla, Aishwarya Bhandare, Suraj Shanbhag, Pooja Mehta, Spondon Kundu, Kevin Han, Edgar Lobaton, and Tianfu Wu. Vision-based integrated mobile robotic system for real-time applications in construction. *Automation in Construction*, 96:470–482, 2018.
- [18] Chulwoo Lee, Chul Lee, and Chang-Su Kim. Contrast enhancement based on layered difference representation of 2d histograms. *IEEE transactions on image processing*, 22(12):5372–5384, 2013.
- [19] Ying Fu, Antony Lam, Imari Sato, Takahiro Okabe, and Yoichi Sato. Separating reflective and fluorescent components using high frequency illumination in the spectral domain. In *Proceedings of the IEEE International Conference on Computer Vision*, pages 457–464, 2013.
- [20] Chunle Guo, Chongyi Li, Jichang Guo, Chen Change Loy, Junhui Hou, Sam Kwong, and Runmin Cong. Zero-reference deep curve estimation for low-light image enhancement. In *Proceedings of the IEEE/CVF Conference on Computer Vision and Pattern Recognition*, pages 1780–1789, 2020.
- [21] Jianbo Shi et al. Tomasi. good features to track. In *1994 Proceedings of IEEE Conference on Computer Vision and Pattern Recognition*, pages 593–600. sn, 1994.
- [22] Myung Hwangbo, Jun-Sik Kim, and Takeo Kanade. Inertial-aided klt feature tracking for a moving camera. In *2009 IEEE/RSJ International Conference on Intelligent Robots and Systems*, pages 1909–1916. IEEE, 2009.
- [23] Jianrui Cai, Shuhang Gu, and Lei Zhang. Learning a deep single image contrast enhancer from multi-exposure images. *IEEE Transactions on Image Processing*, 27(4):2049–2062, 2018.

Mobile-robot and Cloud based Integrated Defect Inspection System for Indoor Environments

Vengatesan Govindaraju, Takrit Tanasnitikul, Zheng Wu, Pongsak Lasang

Panasonic R&D Center Singapore, Singapore
vengatesan.govindaraju@sg.panasonic.com

Abstract –

Conventional defect inspections in newly constructed indoor environments still rely heavily on manual checking and judgement, which can be costly, time-consuming, superficial, and prone to human errors. In this paper, we have proposed a novel complete integrated system where a mobile-robot platform capable of autonomous navigation, performs data collection in indoor environments and transmits this data to a remote server on the cloud. Here, our AI and 3D fusion analysis software detect defects such as alignment, evenness, cracks, damages, and finishing defects as per the Construction Quality Assessment System (CONQUAS) standards. The results are then published to a well-designed web-based User-Interface system where stakeholders can view/track the defects. By integrating these core technologies and addressing most of the practical concerns, our proposed approach is able to conduct inspections with higher accuracy and efficiency compared to traditional manual assessments.

Keywords –

Mobile-robot; Defect Inspection; Cloud; Construction Quality, Alignment, Evenness, Crack, Damages, Stains, User Interface

1 Introduction

Conventional inspection tasks in many of the building construction processes, such as soil investigation, excavation, structural, architectural and mechanical and electrical inspection are conducted manually by skilled inspectors. Manual inspections have several associated problems such as inaccuracies (prone to subjectivity of inspection professionals), difficulty to find skilled inspectors or high cost to upskill existing inspectors to prevent incorrect use of tools and failure to spot defects, incompleteness (areas like external walls, facade, ceilings, etc. are difficult to be assessed and evaluated), physical fatigue and safety hazards due to long working hours and unsafe working environment. The data collected during an inspection is owned by the individual



Figure 1. Overview of the System: It consists of (i) Mobile-robot platform, (ii) 3D and AI Analysis software on the cloud, (iii) Web-based user interface for robot control and defect

entities responsible for the inspection task and this data cannot be distributed across multiple stakeholders for further tracking or management of defects. For these reasons, it is imperative to consider automated solutions for inspection tasks using robots.

One of the common inspection tasks is the assessment of the quality of finishing in newly completed units such as unevenness, wall corner right-angleness, wall verticality, etc. In Singapore, this assessment is based on workmanship standards set in the Construction Quality Assessment System (CONQUAS), which is maintained by Building and Construction Authority (BCA), a statutory board under the Ministry of National Development of the Government of Singapore. The latest revision to the standards was released in 2022 [1]. There is generally a higher demand for Quality Mark (QM[®]) tested residential units which are 100% thoroughly inspected (compared to sample tested units). Therefore, there is a real need to automate these tedious inspection tasks using mobile robots that overcome the

disadvantages of conventional manual methods. The Government of Singapore is actively working towards the integration of digital technologies in various construction processes through its Integrated Digital Delivery (IDD) program. [2].

Based on our interviews with the building inspectors, ‘architectural’ inspections (which consider internal and external finishes, material & functional tests) constitute the major workload (more than two-thirds) compared to ‘structural’ and ‘M&E (Mechanical and Electrical)’ inspections. Therefore, we are considering primarily architectural inspection for this project. From our preliminary investigation, automating this inspection process called for a complete integrated solution that addressed several key concerns: (i) a portable and automated robot system with safe navigation, (ii) ease of control for a person with limited robotics skills, (iii) fast, thorough and accurate inspection, (iv) real-time analysis to detect defects such as cracks, stains and unevenness, and (v) render visualizations and generate reports of defects. Overall, the target is to achieve high accuracy and higher productivity compared to manual inspection.

In this paper, we introduce an autonomous mobile-robot-based inspection system to facilitate ‘Accurate Construction Quality inspections’ with an ‘Intuitive User Interface’. The contributions of our work include:

- 1) Integrated mobile-robot inspection platform with safe autonomous navigation and data collection capabilities. The robot uses Building Information Model (BIM) or 2D floorplan drawing as a prior map for robot navigation and scanning position determination for data collection.

- 2) AI and 3D-based analytic engines for room structure understanding and defect inspection from 3D point-cloud and image data. AI semantic segmentation and 3D geometry analysis technologies are combined to facilitate analysis.

- 3) Intuitive user interface for robot control, inspection results visualization/editing, report generation and information sharing with multiple stakeholders.

In this paper, we have discussed the related works in Section 2, described the overview of our inspection system in Section 3, and the operations and methods in Section 4. We have provided the results from on-site testing in Section 5 and concluded in Section 6.

2 Related Works

Recently, many robotics related open-source software (such as ROS) have simplified the adoption of robot systems and it can be easily observed in the rise in the number of construction related research papers [3, 4, 5, 6, 7]. Paper [5] develop a scaffold scanning dog robot with all computation such as SLAM, scaffold detection algorithm running in an onboard PC. Paper [6] developed

a mobile for point cloud scanning with SLAM and context awareness for navigation all on the on-board PC. For such an architecture, scaling the robot to larger area or more complex algorithms requires upgrading the computational capacity of the computer. This eventually increases the power-requirement, and thereby the battery weight. To avoid this problem, our method off-loads some of the computationally heavy tasks (that are not so time-sensitive) to the remote server on the cloud. This introduces new challenges such as network connectivity and data transmission efficiency, which we have also addressed in this paper.

In paper [7], the authors describe the development of an autonomous robot that performs data collection through autonomous navigation. The paper focuses on the data collection process and only for construction progress monitoring purpose. Data collection for an inspection operation needs to consider many other factors such as sensor characteristics, floor plan geometry, total inspection time, etc. In papers [8] and [9], the authors describe methods to find optimal scan positions that improve coverage and minimize data collection time. In paper [8], it simplifies the problem by considering only a discrete grid of candidate scan points on the floorplan for optimization. Our approach improves this method by considering an iterative approach to optimize over a continuous space. Although, many of these research techniques focus on the autonomous capability, construction workers mostly look forward to using a product that is easy-to-use and intuitive. We address this by providing multiple modes of operation of the robot through a simple user interface.

In recent years, we have seen an uptick in the number of technology companies that have started working in this domain. A Singapore start-up company, Transforma Robotics developed Quicabot, an autonomous wheeled robot used for 3D and visual data collection and defect detection [10, 11]. The robot has at least four types of sensors (a 2-D laser scanner, a colour camera, a thermal camera with heater, and an inclinometer) for detecting hollowness, alignment and evenness, crack and inclinations. While the system claims to cover many of the defect types to be inspected faster than manual, there is not much information on how the defect information is stored and reported to the user. Based on interviews, during defect rectification, the main pain points for most construction companies are miscommunication and non-traceability of defects. In this paper, we present solutions to address these pain-points through our defect visualization and report generation techniques.

A startup based in Barcelona, Naska.ai (previously Scaled Robotics), works on construction site data capture, analysis and reporting services for quality control and coordination [12]. Its software is not attached to any specific sensor or robot hardware. Doxel, a startup based

in Silicon Valley, provides software services for automated progress tracking, cost scheduling and estimation. Another Silicon Valley startup company Holobuilder (developed the ‘Spotwalk’ robot), primarily uses a 360-degree camera for Construction Progress Monitoring. Naska, Doxel and Holobuilder do not work on defect detection and the robot hardware is not their primary focus. For defect inspection application, the accuracy and reliability of defect analysis depends a lot on the data acquisition process. Early defect detection can save significant time and money by avoiding rework. In this paper, we focus on problems and solutions with respect to defect inspection process and present methods to improve the data acquisition process.

Differing from existing players, our solution aims to provide a complete integrated solution with an autonomous mobile robot platform equipped with high-resolution 3D scanning and surround-view image capture, capable of traversing safely in a newly constructed unit, real-time defect detection (both structural and visual defects) with 3D and AI analytical engines. Our solution addresses practical concerns and aims to deliver superior accuracy and faster inspections compared to traditional manual methods.

3 Overview and Physical setup

The overall inspection system consists of 3 main components corresponding to (i) data collection (mobile robot platform with sensors), (ii) data analysis (remote server with AI/3D analysis engines), and (iii) data visualization (web-based UI). The connections between these components are shown in Figure 1.

The data collection platform mainly consists of a wheeled mobile robot platform fitted with a variety of sensors, computing platform and internet connectivity. The robot is built from scratch using mostly off-the-shelf components. The chassis is modified from Ubiquity Robotics Magni robot by replacing the non-driving caster wheels with two larger omni-wheels of 20 cm diameter. This makes the mobile platform capable of climbing small steps less than 5cm. This is to take care of the movement of the robot in and out of the toilet or balcony whose floor levels are usually lower than other rooms. The robot is not designed to climb stairs. However, we have designed the robot to be under 25kgs, allowing for manual lifting to different floor levels, if elevators are not available. Within the same floor level, the robot can be either remote-controlled or be pushed like a trolley to the testing site. The suspension design was modified to allow for the driving wheels to be always in contact with the floor to avoid slippage.

The robot uses a multitude of sensors such as Hokuyo UST-10LX 2D laser range scanner, Intel Real-sense D435 RGB Depth cameras, and Leica BLK360 3D



Figure 2. Data captured by scanner on the robot.

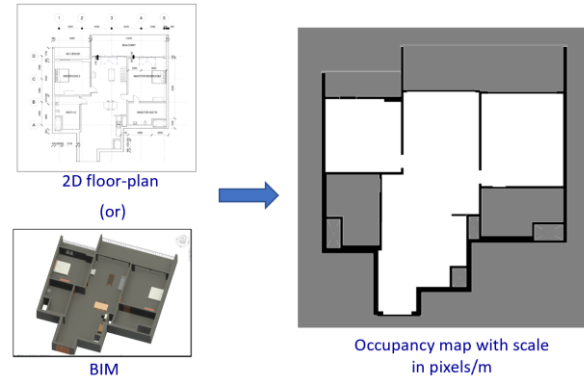


Figure 3. Occupancy map is created from 2D floor plan. The pixel colors represent free space (white), obstacles (black), keep-out region (grey).

terrestrial laser scanner. The 2D laser range scanner and the depth cameras are for navigation purposes (localization, safety and teleoperation). The terrestrial laser scanner is for collecting high resolution and high accuracy point cloud and image data. The robot is required to stop and then perform scanning (stop-scan-go) as BLK360 is a static laser scanner. The specification of this sensor is shown in Table 1.

Each scan takes less than two minutes to complete the scan and each scan captures high-resolution point cloud and 28 pictures covering 360° space, as well as generates a panoramic image, as shown in Figure 2. The laser scanner is mounted at a certain height on a pole and the robot connects to this sensor via Wi-Fi. The robot footprint dimensions are 63cm x 42cm and height is 50cm (with sensor pole folded) and 1.20m (with sensor pole upright). The battery life is above 6 hours for nominal usage (70% travel time) and further it supports hot-swapping to prolong the operation time. The entire robot is designed to be modular for easy development and troubleshooting.

As the computation power of the robot is limited, all

Table 1 BLK360 Specifications

Field-of-view	360° (horiz) / 300° (vert)
Scanning range	min. 0.6 - up to 60 m
Accuracy	6mm @ 10m
Camera system	15 MPixel 3-camera system, 150Mpx full dome capture, HDR

the scan data collected gets uploaded to the remote server on the cloud through the internet for 3D and AI analysis and defect report generation. At the remote server, the high computational power hardware is able to process the data very fast. Speed is very critical for inspections as the longer it takes to detect a defect, the more the rework that must be done. Apart from the scan data, other necessary information such as robot position in the map, calibration details and analysis results are also stored on the remote server. The data management software and intuitive user interface are also developed to share the information among multiple stakeholders to visualize the inspection data and check the reported defects.

4 Operation and Methods

In this section, we will first introduce three operation modes of the robot, the 3D and AI analysis flow and integrated robot control and data management UI.

4.1 Robot Operation

In a typical CONQUAS inspection, two inspectors are involved. However, our inspection routine is designed to streamline the process by combining the efforts of one robot and one human inspector. In this setup, a single inspector brings the robot to the test site. Using a hand-held tablet's user interface, the inspector selects the map corresponding to the residential unit number. They then set an approximate initial pose for the robot on the map by utilizing a click and drag action. The robot utilizes this information for localization, estimating its current position within the map.

Our localization algorithm (based on AMCL - Adaptive Monte-Carlo Localization) relies on odometry data from laser scan matching instead of the wheel encoders, and therefore, does not lose localization even if the map information is not very precise. We only use an approximate occupancy map image obtained from either BIM (IFC) model or 2D floor-plan map drawing (with some manual cleanup to ensure that the occupancy map is safely navigable by the robot) as shown in the Figure 3. This alleviates the necessity to conduct any prior mapping for autonomous navigation. This saves any time required for setting up the robot (at least 30% of the total time needed) and improves productivity compared to existing automated systems. Our navigation algorithms (based on open-source ROS Navigation stack) ensure that the robot does not enter the unknown areas or collide with obstacles. Once the inspector verifies that the robot has localized properly from the UI, then he/she can choose one of three modes of operation for the robot.

The robot has three modes of operation (Mode 1, Mode 2, and Mode 3). Mode 1 is the manual mode where the robot is controlled manually using a joystick button on the UI. It also allows the inspector to teach scan-routes

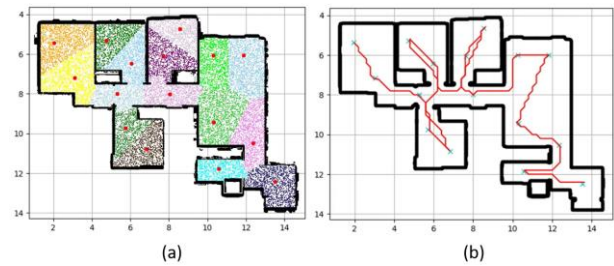


Figure 4. Mode 3 of the robot operation (a) Optimal computation of scan-points, (b) Shortest path through the scan points.

to the robot. Scan-route are made up of waypoints (where the robot passes through) and scan-points (where the robot stops to scan). Although we have the option to handcraft the scan-routes directly on the UI (without moving the robot), it is recommended to use the robot to ensure that the scan-route is navigable with high confidence. In the Mode 2, the user simply selects along one of the previously created scan-routes in the same or similar floorplan unit. This is very useful for high-rise buildings, where the same scan-route can be used for units with similar floorplans across different levels of the building. The robot then autonomously and safely navigates along this selected scan route and collects the scan data.

When the robot moves to the scan location, it triggers the scan command wirelessly to BLK360 sensor. The robot waits until the scan is complete and then navigates to the subsequent scan position. While the robot is working, the inspector is free to do other inspection tasks such as functionality tests and hollowness checking. As the robot is not capable of opening doors by itself, the inspector ensures that the doors are already open before starting autonomous navigation. This implies that surfaces behind the open doors will not be scanned by the robot.

Manually creating an optimal scan-route to maximize coverage and minimize inspection time, is very difficult without much experience and knowledge about the sensor and the robot. Therefore, we have developed Mode 3, where the robot does automatic selection of good scanning positions that guarantee full coverage with

Table 2 CONQUAS Inspection Requirements

Items	Description
Wall / floor evenness	No more than 3mm per 1.2m
Wall meet at right angles	No more than 4mm per 0.3m
Wall verticality	No more than 3mm per m
Wall / floor / ceiling / door finishing/damage defect	No stain marks. No rough / patchy surface No visible damage / defects
Floor level height	Minimum 2.8 m
Ramp slope	A gentle gradient of 1:20 to 1:15 is preferred

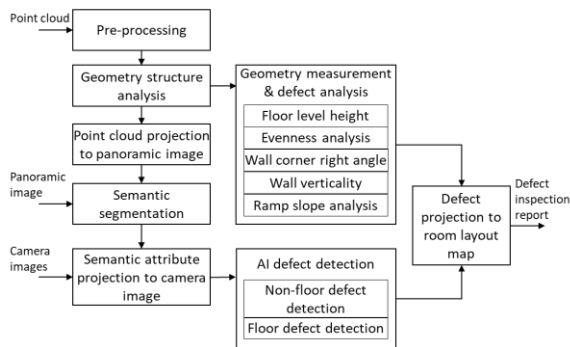


Figure 5. 3D/AI analysis flowchart

minimum number of scans, given a floorplan image. We observed that the noise of the measurement increases with the distance from the scanner and decreases with the incidence angle at the surface to be inspected. It also increases with the reflectivity of the material surface. Based on our experiments with BLK360, the nominal range could be set at 3 meters for achieving the required high inspection accuracy up to 3mm per 1.2m length as per CONQUAS standards. For a dense grid of points uniformly distributed on the navigable free space of the floor plan, we compute a score for each point that quantifies the scanning efficiency at that point based on the visibility, incidence angle and distance requirement from the walls. Given the floorplan area and scanner range we compute the required number of scan-points. The scan points are seeded at random positions in the floorplan and then we use these points as Voronoi centers for the Lloyd's algorithm to construct a weighted Centroidal Voronoi Tessellation. The weighting density function is obtained from the dense grid scores. Over several iterations, the scan-points (also Voronoi centers) converge to an optimal position that maximizes the scan scores. Figure 4 shows the resulting optimal scan positions for covering a sample unit. We then use an open-source Travelling Salesman Problem (TSP) solver to get the optimal path to these scan-points.

The robot can travel along the same path, stop at same locations and collect data whenever it sent for inspection. That provide the advantages of being able to compare images or point cloud from several inspections over a long period of time. It requires multiple scans to cover the entire apartment to handle occlusions and meet the accuracy requirement at all surface points. As the data size is humongous, we use MPEG point-cloud compression technique to compress the data by more than 80% before uploading. The raw images are compressed to lossy JPEG compression (85% quality). The final data size (including the point-cloud and the images per scan) is only about 12~15 Mb. All the scan data is further compressed to a zip file and then it becomes easier to transmit the data to the remote server via 4G/LTE modem on the robot.

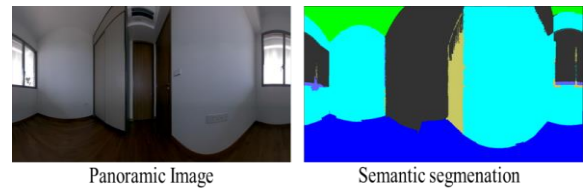


Figure 7. Room structure analysis

4.2 3D and AI analysis flow

Once all the scan data is uploaded, the remote server conducts the 3D and AI analysis on both the point cloud and image data. It is essential to link defects or non-compliances with the relevant structural components of the rooms, such as walls, floors, ceilings, doors, and windows (see Table 2). Therefore, the key step is to understand the room's structure.

A framework is devised to combine both point cloud and image data. In Figure 5, the process begins with point cloud cleanup, including de-noising and removal of low reflectance points. Geometric analysis is then employed to extract planes, eliminating objects unrelated to the room structure, such as the robot operator. Position and direction information for the floor, ceiling, and walls can be derived from the point cloud. Utilizing AI technique PointNet++ [13], we extract more semantic information like doors and windows in the point cloud. Semantic segmentation results of point cloud are then further refined by projecting onto the panoramic image. This information is later used by visual defect detection system on camera images to remove false detections. A sample result of panoramic image is shown in Figure 7.

Defect inspection is conducted by 3D and AI analysis parallelly. 3D point cloud measurement is used for ceiling height measurement, evenness of walls, floor and ceiling, wall verticality, wall corner angle, and ramp slope. To reduce computation complexity, sampling method is used. For example, for unevenness analysis, the points on each plane are sampled and the up-down variance in the local area around the sampled point is

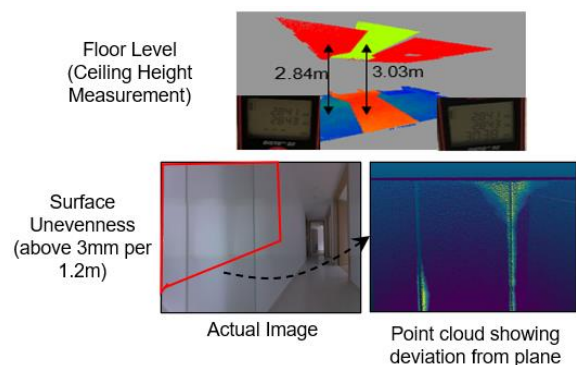


Figure 6. 3D analysis for structural defects

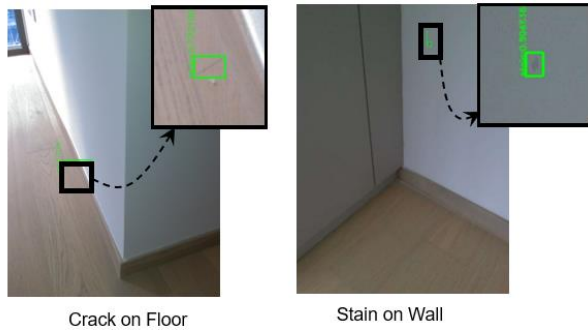


Figure 8. Visual defects at actual site

computed for evenness. The sampled measurements are interpolated to obtain the dense output for each point on the plane.

Figure 6 demonstrates the measurement of floor level height for individual points on the floor. Additionally, it illustrates the measurement of evenness for each point relative to its own plane surface. In the image, purple color indicates an even surface, green indicates unevenness of 3mm and yellow indicates unevenness of 4mm or higher. This example highlights the robot system's ability to easily detect door warpage that could be overlooked by inexperienced inspectors. In Figure 8, the sample visual defect detection results are shown for floor and non-floor part separately.

To detect finishing and damage defects, we project the semantic segmentation information onto camera images to distinguish between floor and non-floor components. The defect object detection is conducted separately because floor and non-floor parts are different in their characteristics. Non-floor components, like walls and ceiling, are usually white painted which lacks textures. On the contrary, floor contains more textures due to different materials such as wood, marble, and ceramic tiles. Therefore, detection methods and models are trained for floor and non-floor parts separately by using YOLOv5's architecture [14]. Our approach involves utilizing multiple public datasets for pre-training, followed by fine-tuning the model using a combination of both public datasets and our collected datasets. By employing this technique, we achieve a recall rate of up to 80%.

Defect analysis is performed on each scan independently. To facilitate accurate record-keeping and effective communication with stakeholders for necessary repairs, it is crucial to determine the precise defect positions relative to the entire unit. By leveraging the recorded robot position at the time of the scanning, we can register point-cloud of each scan to the map. Thus, the defect position identified in each scan can be transformed and mapped onto the floorplan layout and are linked to corresponding room segment (living room, kitchen, bedroom, etc.).

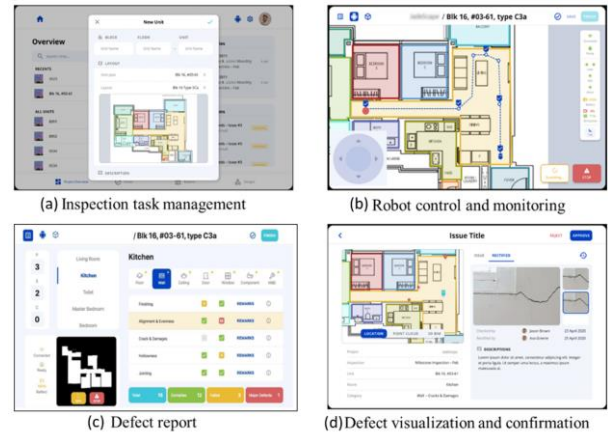


Figure 9. User interface

4.3 User interface

A web-based user interface (UI) is developed for robot control and visualization. The data is organized hierarchically, categorizing it based on the construction project, unit number, and inspection time. Each unit is associated with floorplan information and room segment details, represented by polygons on the floorplan image (refer to Figure 9(a)). To accommodate inspectors without robotics expertise, the UI only exposes essential controls, ensuring a user-friendly and intuitive experience. The UI also provides real-time updates on the robot's position and logging information, enabling inspectors to monitor the autonomous inspection process effectively. Following the analysis, the detected defects are displayed on the issue page, organized under the relevant room segment (refer to Figure 9(c)). The defect position is also visualized on the floorplan and the panorama viewer. The inspector has the option to add/modify the issues listed before generating the final report as a PDF file in the CONQUAS report format. The



Figure 10. A panoramic visualization showing accurate defect-positions with close-up image.

report also contains the exact pin-point location of the defects marked on a panoramic image as illustrated in Figure 10.

5 Results

Tests were conducted in a newly constructed residential units, before the actual CONQUAS inspection by the inspection personnel. The floorplan was obtained from the brochure of the construction project and occupancy map image is prepared as seen in Figure 11. After the robot is brought to the construction unit, the initial position was set, the robot was observed to localize and navigate well just based on the approximate floorplan map and did not require prior mapping.

We have provided a comparison of timing and detection performance of the robot with a manual counterpart in Table 3 from one of our site tests. The inspection was carried out in a newly constructed three-bedroom apartment. With the assistance of a trained inspector, we identified a total of about 61 finishing defects in the whole unit. Subsequently, we evaluated and compared the performance of a robot against that of an actual inspector. For a total of 11 scans, robot takes roughly 22 minutes for the data collection for the entire

Table 3 Comparison of the Timing and Defect detection

Items	Mobile-Robot (+ 1 Inspector)	Manual (2 Inspectors)
Defects (numbers)	40	61
Set-up time	< 2 min	NA
Total Inspection Time	46 min 51 sec	~35 min
- Data Collection	22min 37 sec	
- Scanning Time (11 scans)	~18 min	NA
- Movement (Mode2)	~4 min	NA
- Data downloading from Scanner	15 min 15 sec	NA
- Data Upload to Server	3 min 24 sec	NA
- AI and 3D Analysis	5 min 35 sec	NA
Report generation	15 sec	Several Hours
Accurate location referencing	Yes	No
Digital photographic record for evidence and traceability	Yes	No

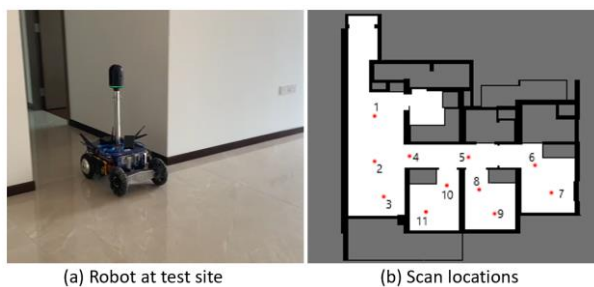


Figure 11. Testing at Actual Site

unit. The raw data generated from these 11 scans amounts to approximately 1.6GB, but after compression, it reduces to around 150MB. For data downloading from the scanner and uploading to server (which highly depends on network connectivity), it takes another 18 minutes. Analysis takes around 5 minutes at the remote server. Altogether, the data collection, transmission and processing take a total of about 45 minutes. Initially, the inspection process carried out by our system may seem slightly slower compared to a human inspector team, which typically takes around 35 minutes to complete visual and structural defect detection in the same area. However, significant time savings are achieved during the photographic evidence capturing and report generation phase. This particular process can take several hours for a human inspector, whereas the robot is capable of producing location-referenced images within a few seconds.

In terms of inspection performance, the robot is able to detect at least two thirds of the total visual defects reported by human inspector team. The human inspector excels in identifying certain minute defects that are observed up close and may not be captured by the robot's camera due to factors such as poor lighting or significant distance (as shown in Figure 12). Lighting plays a critical role in determining the accuracy of visual defect detection results. The analysis indicates comparable performance between the robot and human inspectors in detecting larger defects measuring over 2 cm. However, further improvement is necessary for identifying smaller defects. As an improvement measure, we conducted tests by equipping additional lights on the robot, which led to enhanced inspection results, especially on cloudy days. In terms of structural defect inspection, our system surpasses manual inspection effortlessly. Human inspectors are limited to conducting sampling tests on reachable surfaces, whereas our system can examine every single point on the surface. Furthermore, we have observed instances where the robot successfully identifies new visual and structural defects that were previously unnoticed by human inspectors.



Figure 12. Some defects not observed from far distance with bad light conditions

6 Conclusion

In this paper, we introduce the integrated mobile-robot and cloud-based defect inspection system for indoor built environments and discuss the practical challenges that the system addresses. We present a complete system with a mobile-robot platform powered by advanced navigation technology, defect inspection using novel 3D and AI analytic engines, intuitive user interface for robot-system control and data management. Our system has been tested in actual construction sites for robot navigation and indoor building quality analysis. The results demonstrate that our system outperforms manual inspection methods in terms of accuracy and speed. Moving forward, we plan to enhance the defect detection rates by incorporating more training data and leveraging manual defect entries as feedback for the learning process. Additionally, we aim to reduce inspection time significantly by conducting tests with multiple robots. The global construction robotics industry is experiencing steady growth, and we are actively exploring opportunities for commercialization in this rapidly expanding market.

Acknowledgements

This work is partly funded by A*STAR (Agency for Science, Technology and Research of Singapore) under its National Robotics Programme (NRP) – Robotics Domain Specific (RDS) (Grant No. W2122d0155). Any opinions, findings and conclusions or recommendations expressed in this material are those of the authors and do not reflect the views of the A*STAR.

We are grateful to Building and Construction Authority (BCA) Singapore for the valuable advice for construction quality assessment, as well as the strong support for site trial.

References

- [1] B. Singapore, “BCA Construction Quality Assessment System (CONQUAS),” 2022. [Online]. www1.bca.gov.sg/buildsg/quality/conquas
- [2] Building Construction Authority (BCA), Singapore., “Integrated Digital Delivery (IDD),” [Online]. <https://www1.bca.gov.sg/buildsg/digitalisation/integrated-digital-delivery-idd>.
- [3] S. Haldera, K. Afsaria, J. Serdakowskib and S. DeVitob, “A Methodology for BIM-enabled Automated Reality Capture in Construction Inspection with Quadruped Robots,” in *38th International Symposium on Automation and Robotics in Construction (ISARC)*, 2021.
- [4] E. M. Wetzel, L. E. T. Leathem and A. Sattineni, “The Use of Boston Dynamics SPOT in Support of LiDAR Scanning on Active Construction Sites,” in *39th International Symposium on Automation and Robotics in Construction (ISARC)*, 2022.
- [5] D. Chunga, S. Paik, J. Kim and H. Kim, “Autonomous operation of a robot dog for point cloud data acquisition of scaffolds,” in *39th International Symposium on Automation and Robotics in Construction (ISARC)*, 2022.
- [6] K. Asadia, “Building an Integrated Mobile Robotic System for Real-Time Applications in Construction,” in *35th International Symposium on Automation and Robotics in Construction (ISARC)*, 2018.
- [7] S. Prieto, B. García de Soto and A. Adan, “A Methodology to Monitor Construction Progress Using Autonomous Robots.,” in *37th International Symposium on Automation and Robotics in Construction (ISARC)*, 2020.
- [8] E. Frías, L. Díaz-Vilariño, J. Balado and H. Lorenzo, “From BIM to Scan Planning and Optimization for Construction Control,” *Remote Sensing*, vol. 11, no. 17, p. 1963, 2019.
- [9] J. Knechtel, L. Klingbeil, J.-H. Haurert and Y. Dehbi, “Optimal Position and Path Planning for Stop-And-Go Laserscanning for the acquisition of 3D Building Models.,” *ISPRS Annals of the Photogrammetry, Remote Sensing and Spatial*, vol. 4, pp. 129-136, 2022.
- [10] R.-J. Yan, E. Kayacan, I.-M. Chen, R. Tiong and J. Wu, “QuicaBot: Quality Inspection and Assessment Robot.,” *IEEE Transactions on Automation Science and Engineering.*, vol. 16, no. 2, pp. 506 - 517, 2019.
- [11] “QuicaBot - QBB30,” Transforma Robotics, [Online]. transformarobotics.com/quicabot.
- [12] “Naska.ai Website,” [Online]. <https://naska.ai/>.
- [13] C. R. Qi, “Pointnet++: Deep Hierarchical Feature Learning on Point Sets in a Metric Space.,” *arXiv: 1706.02413*, 2017.
- [14] G. Jocher, “ultralytics/yolov5: v6.1 - TensorRT, TensorFlow Edge TPU and OpenVINO Export and Inference,” Zenodo, Feb 2022. [Online]. <https://doi.org/10.5281/zenodo.6222936>.

Vehicle Trajectory-Tracking Model for AV using LiDAR in Snowy Weather Under Different Snowing Environments

Padmapriya J¹, Ravi Prasath M² and Murugavalli S³

¹Panimalar Engineering College Chennai City Campus, Tamilnadu, India

²National Institute of Technology Tiruchirappalli, Tamilnadu, India

³Panimalar Engineering College Chennai City Campus, Tamilnadu, India

padmapriyaj.panimalar@gmail.com, 110121051@nitt.edu, principal@panimalarengineeringcollegechennai.ac.in

Abstract -

Autonomous cars are frequently fitted with radars, cameras, and LiDAR due to their complimentary capacities of environment awareness. However, when the host vehicle's LiDAR is negatively impacted by challenging weather circumstances like snow in varied snowfall conditions, precisely following the trajectory of the previous vehicle becomes imperative. Due to the sparse nature of LiDAR data, which can be influenced by a variety of variables such as the wind or snow conditions, it is also increasingly difficult to precisely remove the snow while maintaining the point clouds' details. The complete, learning-based strategy put out in this study attempts to address this urgent issue. Intensity and spatial-temporal feature-based de-snowing, QLGM, weighted technique, and switch RNN with a dual-level long short-term memory (LSTM) are used to track the trajectory path in snowy weather for various snowing levels.

Keywords -

De-noising; Trajectory Tracking; GMM; LiDAR; Autonomous Vehicle

1 Introduction and Background

A major challenge for fully autonomous military vehicles is navigating in bad weather since they lack the sensors to estimate depth, locate obstacles, and maintain traction. By getting troops out of high-risk environments such as snowstorms, autonomous vehicles can reduce casualties in the coldest places, such as Kargil in India, where the lowest temperature in winter can be as low as -35 degrees and the likelihood of contracting hypothermia is high. Because of the high level of precision in the ranging results, point clouds created by LiDAR could be a useful complement [1]. Environmental elements like snowflakes, fog, and raindrops cause noise in the point clouds [2],[3]. These airborne particles deflect laser beams, causing noise to appear in the corresponding locations in point clouds. However, studies on de-noising for snow have not been conducted [4],[5].

De-snowing for LiDAR, or fusing the de-noised point

clouds with the radar data stream, could help predict trajectory tracking under different snow conditions. Intensity is part of the LiDAR measurement outcomes [6], and this paper focuses on how to measure intensity in different types of snowfall. The intensity of snow points, which reflects the details of the environment, can be used to work out how much snow should be de-snowed [7]. One problem to be solved is how to use the intensity without harming the environment.

In accordance with the angles of incidence as well as Time of Flight (TOF), LiDAR points' locations could be calculated [8]. Snowflakes move in various directions and at various speeds, unlike raindrops. The motion of snow points is readily influenced by outside variables like wind and snowy conditions [9], [10].

The method for excluding snow-points from LiDAR data is presented in the paper. The central concept of our strategy is derived from two observations made in [11]. In temporal space, snow points are discrete, whereas the placement of non-snow points is typically constant. Our method first removes snow using an intensity-based filter that was based on the work in [12]. A restoring method is suggested to recover the lost points in the following stage of the process in order to enhance the accuracy of the point clouds. This paper proposes a de-snowing technique that combines the snow's intensity with the spatial-temporal characteristics of point clouds'. Additionally, it also proposes that the points in width and time (W-T) space, that can differentiate between snow points and point clouds, be restored.

Millimeter-wave (MMW) radars, LiDARs, and cameras are frequently found in fully autonomous vehicles (FAVs) in order to provide them with a driving experience that is as human-like as possible [13]. The motion capture of on-road users is the preliminary step in carrying out complex self-driving tasks. Precise tracking employing sensor fusion is a topic that both educators and corporate are very interested in. Spatial reasoning on complex data and the integration of multiple-projected paths, however, present two significant implementation challenges.

K-means [14] and the Gaussian mixture model (GMM)

[15] are two techniques that have been developed to group dense data in the existing literature on spatial reasoning. Thereinto, A complex object can be presented as a combination of a finite number of Gaussian density functions with unknown parameters, and GMM offers cutting-edge model-free technology for fitting it. To determine the maximum likelihood to estimate submodel parameters iteratively, the expectation-maximization (EM) algorithm is introduced [16].

It is possible to fit complex components with the Gaussian Mixture Model using cutting-edge model-free technology (GMM). A small amount of Gaussian density functions with uncertain attributes are combined to form the GMM. The expectation-maximization (EM) algorithm is used [5] to ascertain which submodel parameters have the highest probability of being estimated accurately. The two following significant drawbacks of the GMM-EM method are: 1) The quantity of clusters and 2) The probability that the submodel mean coincides with the values of real-world objects. If the centroids are not correctly reconfigured, the target vehicle's estimated trajectory will be off.

Motion traceability for the vehicle ahead becomes an important step in challenging snowy conditions, particularly when LiDAR information is disrupted by snow particles. It is important to move the GMM centroids which correlate with the velocity data. The integration of multi radar information is a critical issue that must be resolved in radar fusion.

Vision-based fusion frameworks have made it possible to detect and track multiple objects [17] [18]. However, because these algorithms rely on LiDAR information or camera streams, their motion predictions are unreliable. Recurrent neural networks (RNNs) exhibit a considerable advantage in designing dynamic systems and trajectories [19]. Furthermore, experiments have demonstrated the effectiveness of vehicle motion prediction using an RNN with LSTM cells. [20].

In previous works [21] - [22], methods for obtaining effective performance by sensor fusion were investigated. Saleh et al. proposed a three-layer LSTM network to track the trajectory of the pedestrian [23] and Yang et al. proposed a JTSM for customized trajectory prediction. [22]. Accurate trajectory tracking has been hindered by RADAR valid-range changes and LiDAR difficulties. The expansion of automated driving's operating environment and application space faces a significant challenge during snowfall. When it snows, the surrounding roads are in a different state than they are during fair weather. This is likely to be employed for tasks like operating snowplows that call for previous driving experience. One problem is that, due to snowfall and other factors, it is difficult to match the map data with the road surface. This makes it difficult to engage in safe automated driving because the lane a vehicle

is in can be hard to tell.

A number of studies have been conducted to address the issue by simulating the uncertainties associated with error propagation and afterwards comparing radar images [24]. In [25] LiDAR and millimetre wave radar were proposed as a localization system. Radar image alignment was incorrect because the confidence estimation was only done for LiDAR data, which resulted in inaccurate confidence level estimation. Additionally, it only takes into account the two environmental conditions of snow and no snow.

Therefore, a learning-based method has been proposed to track trajectories in the snow - covered climate under various snowing conditions. The three significant contributions are listed below: 1) the input LiDAR data stream is de-snowed using intensity and spatial-temporal features to separate snow points from point cloud data using spatial geometric data. 2) To acquire the precise positions of the clusters of compact short-range radar data, the amount of clusters is then investigated using a Q-learning method which is given to GMM-EM. The centroids are realigned in order to further mitigate the position deviation based on velocity inputs. (3) In addition, a switch dual-level LSTM (SDL) network approach is used that relies on the recommended radar-vision binary fusion technique to work with three snowing conditions. The vehicles that are ahead of them are tracked using SDL networks in challenging snowy conditions.

2 Approach

Fig. 1 depicts the proposed approach's framework. There are three steps in the framework. Prior to restoring non-noise, snow is first removed using an intensity filter and spatial-temporal features. The second step involves fusing the short-range radars (SRR) and electronically scanning radar (ESR) to assist in the prediction of trajectory tracking, which is done with the help of the de-snowed LiDAR points. And the final step is to use a Switch Dual-Level LSTM Network with combined filtered point clouds and fused radar data in order to predict the trajectory for three different modes.

2.1 De-snowing

2.1.1 Intensity-Based Filter

The ranging distance R , the incident angle, and the reflectance all play a significant role in intensity, according to the LiDAR principle in Eq. 1 [26].

$$I = H\left(\frac{P_t D_r^2 \rho \cos(\alpha)}{4R^2} \eta_{sys} \eta_{atm}\right) \quad (1)$$

Applying the settings in [27], the snowflake structure [28] and the LiDAR [11], α and the reflectance of snowflakes

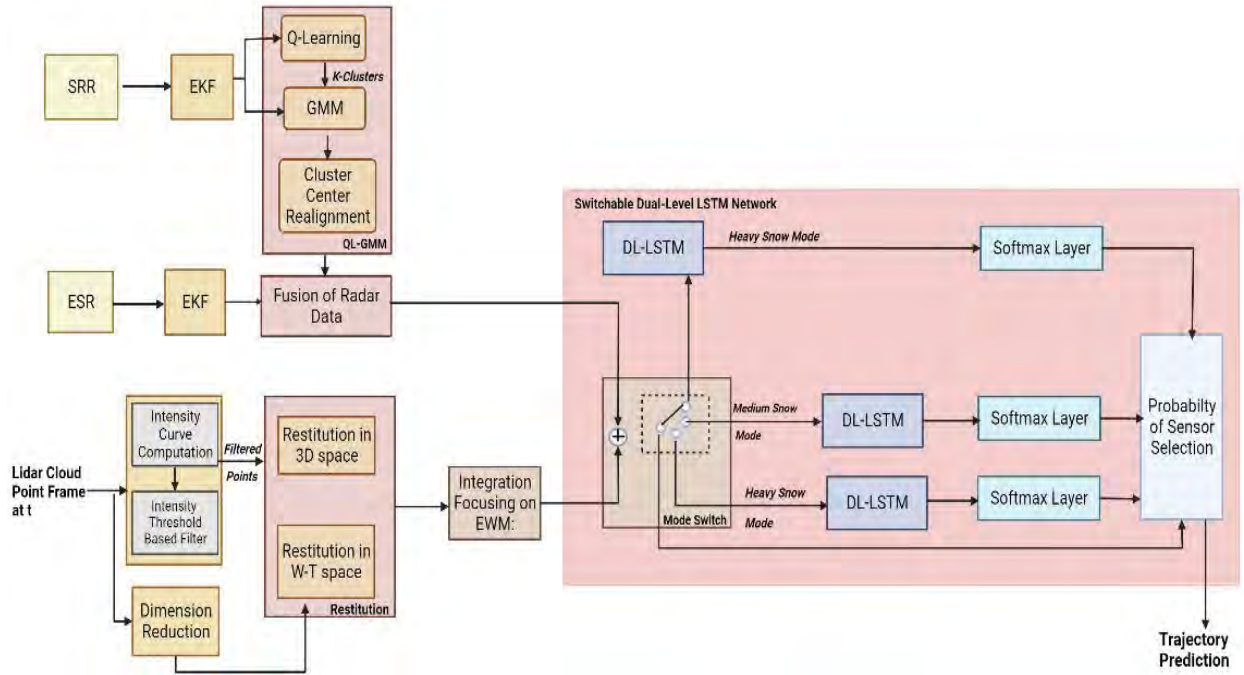


Figure 1. An Illustration of the proposed trajectory tracking framework.

are set . Using the measured intensity I_{ref} and the range R_{ref} , another intensity I_m with the range R_m could be calculated as in Eq. 2. In this manner , an intensity gradient of the snowflakes is obtained from several I_m at different R_m .

$$I_m = I_{ref} \frac{R_{ref}^2}{R_m^2} \quad (2)$$

2.1.2 Restitution

To recover the removed points with the same characteristics as snow points, spatial-temporal geometry features in typical 3D and width and time (W-T) space have been used. [11]. The amount of neighbour of a LiDAR point p_i in normal 3D space and W-T space, respectively, is denoted as symbols $|3d|_{p_i}$ and $|wt|_{p_i}$.

1) 3D space Restitution: Based on prior hypotheses, it is concluded in this paper that non-snow points are not isolated. A point is almost certain that it is a non-snow point if it has a lot of neighbours. The number of LiDAR points expressed as $p_i(x, y, z)$ for which Euclidean Distance to p_i is lower than r is known as $|3d|_{p_i}$ of p_i .

Because LiDAR is a sparse sensor, when r is set too low, there are not many neighbours in the distance. Distanced points will be taken into consideration as noise. The neighbour numbers resemble one another when r is set too high. Snow and point clouds are difficult to separate. r is set based on the experimental findings in [27].

2) W-T Space restitution: W-T space refers to the point of view whose centerline is parallel to the width and time axes . Images are viewed in W-T space using the height direction. As a result, from the frames, it was possible to view the movement of the pixels migrated at a particular height. Dimension reduction is used to reduce a collection of point cloud frames with a 4D tensor P to a 3D tensor P' is regarded as a collection of 2D frames for the W-T space. When snow points are produced around the LiDAR, it is not feasible to have $|3d|_{p_i}$ alone to differentiate the snow. Since the trajectory of some weak-intensity points, like those from moving objects or the surface, is continuous, these points are grouped together in W-T space. As a result, it was possible to distinguish between non-snow points and weak- intensity points.

The amount of the nearest neighbour is used to specify the temporal feature given the constant trajectory and position of point clouds in W-T space. $p_i(w, h, t)$, in which $w, h,$ and t denote the positions and stamp in the point clouds, respectively, can be used to represent a LiDAR point in W-T space. From time $t - n/2$ to time $t + n/2$, the number n indicates how many point clouds are in the area. The amount of points in a $(n + 1) \times (n + 1)$ searching mask in W-T space is indicated by the symbol $|wt|_{p_i}$ of p_i at height h .

Prior to computing $|wt|_{p_i}$, point clouds are preprocessed. In the W-T space, $|wt|_{p_i}$ is computed. Each point's 3D coordinates ($x, y,$ and z) cannot be used directly. The Principal Component Analysis (PCA) is used to transform 3D

point clouds into 2D [29].

3) Integration Focusing on EWM: Entropy is an indicator of system disorder, based on information theory. It is used to determine the degree of discreteness. The degree of discreteness increases with decreasing entropy value, and this has a greater impact primarily on extensive assessment. As a result, entropy may be used to compute weights for various indicator models. The entropy weight method (EWM) is a weight computation method that produces results according to the data dispersion.

In this case, $|3D|_{pi}$ and $|wt|_{pi}$ will be combined to calculate a weighted average confidence score to decide if the point must be recovered [11]. As a result, EWM is used to compute the weights. P_i 's calculated $|3D|_{pi}$ as well as $|wt|_{pi}$ is saved in $F_{m \times 2}$. Weights w_j , distribution of $|3D|_{pi}$ and $|wt|_{pi}$ expressed as pro_{ij} , and entropy values e_j are calculated using EWM as in [11]. After calculating w_1 and w_2 , Eq. 3 computes a weighted Score I of pi using the normalised $|3D|_{pi}$ and $|wt|_{pi}$. Score i is the confidence score used to decide if pi is the snow point when compared to a threshold. The threshold is set as mentioned in [11].

$$Score_i = w_1 \cdot \frac{|3D|_{pi}}{|3D|_{pi} + 1} + w_2 \cdot \frac{|wt|_{pi}}{|wt|_{pi} + 1} \quad (3)$$

2.2 Fusion of Radar Data

The Extended Kalman Filter (EKF)-filtered data from SRRs is given to the Q-learning GMM clustering component. To produce the fused radar stream Φ_R^R , EKF-processed SSR data is paired with the EKF-processed ESR data. Φ_R^R and de-snowed Lidar Cloud Points Φ_D^D are then combined to form Φ_{RD}^{RD} . It is sent to the snowing condition switch, a finite state machine (FSM). A dual-level LSTM network layer and a softmax layer are coordinated by each snowing mode. Following that, the sensor fusion block and network blocks can be used to achieve the predicted trajectory.

2.2.1 GMM for Clustering Based on Q-Learning

The standard GMM-EM algorithm is explained and illustrated in [16], [23], and [22], and it can be written as

$$p(\xi_{ip}|\theta) = \sum_{k=1}^K \rho_k \mathcal{N}_k(\xi_{ip}|\Sigma_k) \quad (4)$$

where $\xi_{ip} = (X_{SRR_{ip}}, Y_{SRR_{ip}})$ as well as $\Theta = \{\rho_k, \mu_k, \Sigma_k\}_{k=1}^K$ are model parameters and the position data sequence. The coordinates' index is i_p , and the length of the sequence is indicated by n_p . Gaussian submodels are represented by the number K . Multivariate Gaussian distribution is denoted by $N_K(\xi_{ip}|\mu_k, \Sigma_k)$, where Σ_k

and μ_k are the covariance matrix and mean vector. The k^{th} Gaussian sub model that satisfies has a component weight of $0 < \rho_k \leq 1$, and this value is represented by. However, there is one significant flaw with plain K-means or traditional GMM. That is to say, it is unknown how many clusters K there will be.

K was specified in advance as a constant for the duration of the implementation in the literature [15] and [22]. However, given the ambiguity and time-varying nature of driving conditions, it is irrational to assume that the surroundings can be divided. Noise and initialization can have a significant impact on clustering performance, even though K can be automatically determined by Bayesian non parametric [16].

To this end, it is possible to develop a Q-learning-based strategy to figure out K in this section [30]. In addition to offering an offline Q-value table for implementation at a lower cost in terms of computation, Q-learning can also maintain good performance even when clustered targets are close together. QLGM is also unaffected by initial conditions, noise in the data, and outliers.

2.2.2 GMM Algorithm Based on Q-Learning

A commonly applied model selection criterion, BIC [16], [21],[31], can be employed to determine the amount of Gaussian components K . The BIC function, denoted as $g(\hat{L})$, is given by

$$g(\hat{L}) = BIC = -2 \ln(\hat{L}) + M_p \ln(M) \quad (5)$$

For Q-learning-based selection of K , a Markov decision process (MDP) is presented [32]. Given that action space A , the amount of clusters K with K being the finite number of model components, the BIC results necessitates the log-likelihood estimation \hat{L} feedback. The prior likelihood of the chosen course of action is represented by P_a . A one-to-one correspondence can be established as a result to increase the effectiveness of training [33].

The state-action integration Q is used by Q-learning to derive a Q-value table [34]. Every Q-value table item is initially set to $Q_0 = \frac{K_0}{BIC_0}$ rather than 0, reducing the iterative computation. K_0 is a positive weight, and BIC_0 stands for the previously calculated BIC value at various K .

Using the Q-value component the result of carrying out action at in state s_t while governed by π at time interval τ_s is denoted by the symbol $Q_\pi(s_t, a_t)$, which is used to serve the Q-value table. This value is calculated by starting in state s_{τ_s} , carrying out action a_{τ_s} , and then carrying out policy π . The Q-value table can be constantly monitored from the ω^{th} iteration to the $(\omega + 1)^{\text{th}}$ iteration by adopting a learning rate of $(0 < \alpha \leq 1)$ and the temporal

difference in [34].

The quantity of radar-data clusters in the T-frame scenario can be determined after the optimal policy π^* is achieved. The position data for each cluster is then determined by feeding π^* into the standard GMM-EM algorithm. In contrast to using a constant [15] or the BIC traversal calculation [16], Therefore, it is necessary to determine how many clusters are present in each frame [15]. This method can also offer a novelty to choose the best course of action for time-series LiDAR data during a driving scenario without losing generality [30].

2.2.3 Cluster Center Realignment

The Gaussian sub-models don't take into account the velocity information v_k^{SRR} ($v_{x|k}$, $v_{y|k}$) as a potential centering mismatch cause [31]. Furthermore, it is unclear how much each vehicle weighs. So the cluster centres realigned using a kinetic-energy-element method. Each point's kinetic energy per unit mass (KEUM) is represented by the notation $\tilde{E}_{kin|k_i k}$ and its relocated centre by the notation $\tilde{\zeta}_k^{SRR}$. Because of the introduction of KEUM, the re-alignment results now correspond to the actual vehicle positions. By using this method, the suggested SRR cluster centres could be more effectively linked to the ESR data.

2.2.4 Radar Data Association

The suggested QLGM method was used to cluster the SRR results in the previous section. But another problem that needs to be solved is how to combine the data from multiple radars.

In addition to these other data, the acquired radar data streams textPhi_T^{SRR} and Φ_T^{ESR} contain position coordinates ξ , velocity signals v , relative distance D , and the direction Ψ of the vehicle ahead. The integrated T-frame radar stream RT is created by combining the reconfigured QLGM SRR data $\text{textPhi}_{QLGM}^{SRR}$ as well as the EKF ESR data Φ_{EKF}^{ESR} . which is given as

$$\Phi_T^R = \lambda_1 \Phi_T^{SRR} + \lambda_2 \Phi_T^{ESR} \quad (6)$$

The proximity of a target to the radar system and the amount of radar points on a vehicle both affect how well a vehicle detects objects with radar [35]. Due to the unknown designed fusion weights of SRR (λ_1), detection-area-based method is addressed focused on the radar specifications as well as fitting boundaries [30]. The detection area is divided into five sections as in [30].

In a data-driven manner, λ_1 can be developed as a hybrid linear function in accordance with the fitting boundaries. As a result, the filtered LiDAR data stream and fused radar data are combined as Φ_T^{RD} and given to the SDL networks for trajectory prediction.

2.3 LiDAR-Fault-Tolerant Trajectory Prediction

2.3.1 FSM for Snowing Mode Switch

In this paper, the signals of the de-snowed LiDAR point clouds can be used to determine three snowing modes: heavy snow mode, medium snow mode, and light snow mode. FSM [36] [37] is created to change between various snowing modes. The swapping logic and the Snowing modes are represented by three states and six transitional conditions in this FSM, similar to [30]. The $I_{th1} > I_{th2}$ and $0 < I_{th1} < I_{th2}$ conditions are met by the thresholds of snowing intensity for state transition. Depending on how much snow is falling, the FSM holds each state or switches to another. As long as the snowfall intensity stays within a certain range, the current snowing mode would be retained. Otherwise, upon meeting or exceeding the thresholds, the state transition is enabled. As defined below, the FSM's switching actions include:

- 1 Maintain the Light Snow mode: $I \geq I_{th1}$.
- 2 Swap between Light Snow and the Medium Snow mode: $|I| \leq I_{th1}$.
- 3 Maintain the Medium Snow mode: $I_{th2} < I < I_{th1}$.
- 4 Swap between Medium Snow and the Heavy Snow mode: $I_{th1} < |I| < I_{th2}$.
- 5 Maintain the Heavy Snow mode: $I \leq I_{th2}$.
- 6 Swap between Heavy Snow and the Light Snow mode: $|I| \geq I_{th2}$.

2.3.2 Dual-Level LSTM Network for Trajectory Prediction

The RNN with LSTM cells enable a workable alternative to estimate the future trajectory because of their improved ability of capturing long temporal correlations [37]. The performance of a single LSTM layer, however, is sub-par in the actual implementation [38]. Additionally, an excessive number of LSTM layers will cause the computational load to rise exponentially [39]. The hidden state h between LSTM cells and then a softmax probability vector y are created by each snowing mode coordinating a dual-level-LSTM layer and a softmax layer [30]. The LSTM (.) operator is used as the LSTM to prevent gradient vanishing.

The prediction accuracy is further improved by a cooperative dynamic binary fusion approach by including the SDL layers [30]. The binary sensor choice following the softmax operation should be represented by a block matrix $P_\tau = [I_\tau, O_\tau], [O_\tau, I_\tau], I_\tau, O_\tau \in \mathbb{R}$, where O_τ and I_τ are the zero matrix and the identity matrix at a time step, respectively. $y_\tau = P_\tau (1) = [I_\tau, O_\tau]$ indicates using radar data, and $y_\tau = P_\tau (2) = [O_\tau, I_\tau]$ indicates choosing de-snowed LiDAR data. The foremost sources to the suggested SDL network are orientation, relative distance

and longitudinal velocity signals from LiDAR and radar streams. The results of selection probability indicate "1" for radars only whereas "0" for only de-snowed LiDAR.

2.4 Light Snow Mode

Due to the sparse snow or clear weather in the Light Snow mode, the result of the proposed method would be from LiDAR data. In this mode the LiDAR point clouds will not have noise from the snow as the amount of snow will be less or none, therefore the point clouds from the de-snowed LiDAR can be used to predict the trajectory tracking.

2.5 Medium Snow Mode

The outcome of the suggested approach might alter between fused radar data and the de-snowed LiDAR method in medium snowing condition as the intensity may vary from low to high and the LiDAR data might have more noise. Therefore, the proposed QL-GMM+SDL method is the optimal solution for the given mode.

2.6 Heavy Snow Mode

In this condition with de-snowed LiDAR data, there is the possibility of two types of detection failures: miss detection and mishap. Detecting objects is more challenging when using de-snowed LiDAR data in this mode. In this initialization region, the radar stream is a necessary component of the proposed data fusion.

3 Conclusion

Navigating inclement weather presents a significant challenge for fully autonomous vehicles. Snow particularly confounds pivotal sensor data that a vehicle needs to gauge depth, find obstacles, and maintain traction. For autonomous vehicles operating in a variety of snowy circumstances, a de-snowing method for LiDAR point clouds and an integrated learning-based vehicle tracking solution is suggested in this paper. The spatial-temporal features retrieved from 3D and W-T space are used to filter out snow points and restore non-snow points. This solution includes a weight scheduling approach for multi-radar integration, an SDL network for trajectory tracking in three snowfall conditions, and a Q-learning-based GMM-EM algorithm for compact data aggregation. One of the two promising enhancements of the QLGM algorithm is the statistical determination of the number of clusters by Q-learning. Suggested re-alignment concepts, in contrast, can eliminate the positional incompatibilities between the GMM cluster centres and actual automobiles. Additionally, to create a fused radar data stream, QLGM SRR cluster centres can be linked to ESR data

based on the EKF. To improve the accuracy of vehicle tracking, an FSM-based SDL network model with a binary fusion method that matches the different snowfall conditions is designed. The proposed method ingeniously enhances the radar-vision tracking efficiency when faced with different environmental conditions, such as snowy weather in difficult snowy circumstances, making it a promising replacement for humans in dangerous military operations.

The results of the simulation model and evaluation of the proposed method will be compared and analyzed in the future. The emphasis of upcoming work will be on implementing suggested algorithms in real-time. In conditions with snowfall, it may not be possible to match the pattern of the road surface, so a robust system must reject matching results or use additional sensors to make up for them. There this idea will be further extended to have an integrated multi-sensor fusion Vehicle Localization and Trajectory Tracking Framework under different snow conditions.

References

- [1] Y. Zhou and O. Tuzel. "voxelnet: End-to-end learning for point cloud based 3d object detection". In *IEEE/CVF Conf. Comput. Vis. Pattern Recognit. (CVPR)*, page 4490–4499, 2018.
- [2] M. Colomb Y. Li P. Duthon and J. Ibanez-Guzman. "what happens for a tof lidar in fog?". *IEEE Trans. Intell. Transp. Syst.*, page 1–12, 2020.
- [3] M. Byeon and S. W. Yoon. "analysis of automotive lidar sensor model considering scattering effects in regional rain environments". In *IEEE Access*, page 102669–102679, 2020.
- [4] J. Shi W. Xu Y. Wang F. Fu and J. Wang. "efficient moving objects detection by lidar for rain removal". In *Int. Conf. Intell. Comput. (ICIC)*, page 697–706, 2016.
- [5] A. U. Shamsudin K. Ohno T. Westfechtel S. Takahiro Y. Okada and S. Tadokoro. Fog removal using laser beam penetration, laser intensity, and geometrical features for 3d measurements in fog-filled room". *Advanced Robotics*, 30(11-12):729–743, 2016.
- [6] P. Vacek O. Jaek K. Zimmermann and T. Svoboda. "learning to predict lidar intensities". *IEEE Trans. on Intell. Transp. Syst.*, page 1–9, 2021.
- [7] S. Ronnback and A. Wernersson. "on filtering of laser range data in snowfall". In *Proc. Int. Conf. Intell. Syst.*, volume 2, page 17–33, 2008.

- [8] J. Liu Q. Sun Z. Fan and Y. Jia. “tof lidar development in autonomous vehicle”. In *Proc. IEEE Optoelectron. Global Conf. (OGC)*, page 185–190, 2018.
- [9] B. Yang Z. Jia J. Yang and N. K. Kasabov. “video snow removal based on self-adaptation snow detection and patch-based gaussian mixture model”. *IEEE Access*, 8:160188–160201, 2020.
- [10] C. H. Bahnsen and T. B. Moeslund. “rain removal in traffic surveillance: Does it matter?”. *IEEE Trans. Intell. Transp. Syst.*, 20(8):2802–2819, 2019.
- [11] B. Li J. Li G. Chen H. Wu and K. Huang. “de-snowing lidar point clouds with intensity and spatial-temporal features”. In *2022 International Conference on Robotics and Automation (ICRA)*, pages 2359–2365, 2022. doi:10.1109/ICRA46639.2022.9812241.
- [12] J. I. Park J. Park and K. S. Kim. “fast and accurate desnowing algorithm for lidar point clouds”. In *IEEE Access*, volume 8, page 160202–160212, 2020.
- [13] M. Cao and J. Wang. “obstacle detection for autonomous driving vehicle with multi-lidar sensor fusion,”. *J. Dyn. Syst., Meas., Control*, 142(2), 2020.
- [14] J. Melo A. Naftel A. Bernardino and J. Victor. “detection and classification of highway lanes using vehicle motion trajectories. *IEEE Trans. Intell. Transp. Syst.*, 7(2):188–200, May. 2006.
- [15] W. Wang J. Xi and D. Zhao. “learning and inferring a driver’s braking action in car-following scenarios”. *IEEE Trans. Veh. Technol.*, 67(5):3887–3899, May 2018.
- [16] W. Wang D. Zhao W. Han and J. Xi. “a learning-based approach for lane departure warning systems with a personalized driver model”. *IEEE Trans. Veh. Technol.*, 67(10):9145–9157, Oct. 2018.
- [17] H. Gao B. Cheng J. Wang K. Li J. Zhao and D. Li. “object classification using cnn-based fusion of vision and lidar in autonomous vehicle environment,”. *IEEE Trans. Ind. Informat.*, 14(9):4224–4231, Sep. 2018.
- [18] D. Kim B. Kim T. Chuang and K. Yi. “lane-level localization using an avm camera for an automated driving vehicle in urban environments,”. *IEEE/ASME Trans. Mechatronics*, 22:280–290, Feb. 2017.
- [19] S. Xie and J. Ren. “recurrent-neural-network-based predictive control of piezo actuators for trajectory tracking,”. *IEEE/ASME Trans. Mechatronics*, 6: 2885–2896, Dec. 2019.
- [20] A. Zyner S. Worrall and E. Nebot. “naturalistic driver intention and path prediction using recurrent neural networks,”. *IEEE Trans. Intell. Transp. Syst.*, 21(4): 1584–1594, Apr. 2020.
- [21] K. Saleh M. Hossny and S. Nahavandi. “intent prediction of pedestrians via motion trajectories using stacked recurrent neural networks”. *IEEE Trans. Intell. Veh.*, 3(4):414–424, Dec. 2018.
- [22] X. Li W. Wang and M. Roetting. “estimating driver’s lane-change intent considering driving style and contextual traffic”. *IEEE Trans. Intell. Transp. Syst.*, 20(9):3258–3271, Sep. 2019.
- [23] W. Wang J. Xi and J. K. Hedrick. “a learning-based personalized driver model using bounded generalized gaussian mixture models”. *IEEE Trans. Veh. Technol.*, 68(12):11679–11690, Dec. 2019.
- [24] K. Yoneda N. Hashimoto R. Yanase M. Aldibaja and N. Sukanuma. “vehicle localization using 76 ghz omnidirectional millimeter-wave radar for winter automated driving,”. In *Proc. IEEE Intell. Vehicles Symp. (IV)*, page 971–977, Jun. 2018.
- [25] N. Yanase R. Hirano D. Aldibaja M. Yoneda, K. Sukanuma. “lidar- and radar-based robust vehicle localization with confidence estimation of matching results”. *Sensors*, 22:3545, 2022.
- [26] S. Kaasalainen A. Jaakkola M. Kaasalainen A. Krooks and A. Kukko. “analysis of incidence angle and distance effects on terrestrial laser scanner intensity: Search for correction methods”. *Remote Sens.*, 3(10):2207–2221, 2011.
- [27] J. I. Park J. Park and K. S. Kim. “fast and accurate desnowing algorithm for lidar point clouds”. *IEEE Access*, 8:160202–160212, 2019.
- [28] Su-Hyun Kim Dae-Hong Ko Dae-Kyung Seong Seung-Hee Eun Byung-Gon Kim Baek-Jo Kim Chang-Geun Park and Ju-Wan Cha. “quantitative analysis of snow particles using a multi-angle snowflake camera in the yeongdong region”. *Atmosphere*, 29(3):311–324, 2019.
- [29] Y. Duan C. Yang H. Chen W. Yan and H. Li. “low-complexity point cloud denoising for lidar by pca-based dimension reduction”. *Opt. Commun.*, 482: 26567, 2021.
- [30] N. Chen M. Cao R. Wang and J. Wang. “a learning-based vehicle trajectory-tracking approach for autonomous vehicles with lidar failure under various lighting conditions”. *IEEE/ASME Transactions*

on *Mechatronics*, 27(2):1011–1022, April 2022.
doi:10.1109/TMECH.2021.3077388.

- [31] P. J. Huber. “robust statistics,”. *International Encyclopedia of Statistical Science*. Berlin, Germany: Springer, page 1248–1251, 2011.
- [32] H. Ko S. Pack and V. C. Leung. “mobility-aware vehicle-to-grid control algorithm in microgrids”. *IEEE Trans. Intell. Transp. Syst.*, 19(7):2165–2174, Jul. 2018.
- [33] T. Back. *Evolutionary Algorithms in Theory and Practice: Evolution Strategies, Evolutionary Programming, Genetic Algorithms*. Oxford Univ. Press, London, U.K., 1998.
- [34] R. S. Sutton and A. G. Barto. *Reinforcement Learning: An Introduction*. MIT Press, Cambridge, MA, USA, 2018.
- [35] H. Sun J. Xin X. Wang L. Xu and N. Zheng. “on-road vehicle detection and tracking using mmw radar and monovision fusion”. *IEEE Trans. Intell. Transp. Syst.*, 17(7):2075–2084, Jul. 2016.
- [36] Y. Chen J. Zha and J. Wang. “an autonomous t-intersection driving strategy considering oncoming vehicles based on connected vehicle technology,”. *IEEE/ASME Trans. Mechatronics*, 24(6): 2779–2790, Dec. 2019.
- [37] Y. Chen C. Hu and J. Wang. Human-centered trajectory tracking control for autonomous vehicles with driver cut-in behavior prediction,”. *IEEE Trans. Veh. Technol.*, 68(9):8461–8471, Sep. 2019.
- [38] L. Zhang R. Gao J. Wang P. Fu and R. Zhao. “multilevel information fusion for induction motor fault diagnosis”. *IEEE/ASME Trans. Mechatronics*, 24(5): 2139–2150, Oct. 2019.
- [39] X. Yang C. Lv and D. Cao. “personalized vehicle trajectory prediction based on joint time series modeling for connected vehicles”. *IEEE Trans. Veh. Technol.*, 69(2):1341–1352, Feb. 2020.

Quantified Productivity Evaluation of Autonomous Excavation Systems using a Simulation Approach

Xiaoyu Bai¹, Beiji Li¹, Yong Zhi Koh^{1,2}, SoungHo Chae³, Meera C.S.⁴ and Justin K.W. Yeoh¹

¹Department of Civil and Environmental Engineering, National University of Singapore, Singapore

²Koh Kock Leong Enterprise Pte Ltd, Singapore

³Kajima Technical Research Institute Singapore (KaTRIS), Singapore

⁴Advanced Remanufacturing & Technology Centre (ARTC), Agency for Science, Technology and Research (A*STAR), Singapore

xiaoyu.b@nus.edu.sg, lbj@nus.edu.sg, yzkoh@kkle.com.sg, s.chae@kajima.com.sg, chitra_sunil_meera@artc.a-star.edu.sg, justinyeoh@nus.edu.sg

Abstract -

Autonomous excavation systems are currently being developed to help address issues of poor productivity, by automating the excavation process and reducing manpower onsite. However, the impact of automation on the productivity of the excavation process remains to be determined. This paper uses a simulation approach to study this question. A typical excavation operation scenario is modeled and subsequently modified to account for the impact of automation. A comparative study between the typical and modified scenarios demonstrates the impact of automation on productivity. Three modes of automation are modeled in the excavation process: autonomous excavation, autonomous navigation of excavators, and autonomous lorry fleets. The models are validated using actual site data, and results suggest the impact of automation on the excavation process is severely limited.

Keywords -

Autonomous Excavation Systems; Simulation; Productivity Impact

1 Introduction

With the rapid advancement of technology, automation in civil engineering has brought about great benefits with regard to safety, cost, and productivity, as noted in several studies [1]. Excavators, one of the most commonly found heavy equipment on construction sites, are a prime example of where automation can improve operations [2]. Unmanned autonomous excavators are a trending research direction and have significant commercial interest [3].

Presently, construction companies all over the world that use traditional excavators are facing engineering problems, such as high labor intensity, low efficiency, and high safety risks [4, 5, 6]. Critical shortage of skilled operators for large machinery, and the dangerous working environment of some excavators may result in safety and health issues for on-site operators [6].

In response to some of the abovementioned issues, autonomous excavation systems hold some promise in mitigating productivity problems. Autonomous excavation systems encompass both autonomous (robotic) excavators and autonomous dump trucks (lorries). Development of these systems involves various areas of robotics research, including autonomous navigation, robotic path-planning, localization, and integration of digital terrain with survey data [7]. Robotic excavation also involves trenching, leveling, and slope cutting via remote teleoperation to

achieve maximum work efficiency, precision, profitability, and safety.

The industry has several examples of commercially available or near commercialization autonomous excavators. Komatsu developed the PC210LCi-10 in 2013, which is based on the iMC (Intelligent Machine Control) technology, equipped with GNSS antenna, inertial measurement unit, stroke sensing cylinder, and controller. In 2021, an intelligent excavator developed by the Aviation Industry Control Institute and Sany Heavy Industry Co., Ltd., realized automatic planning and remote control, automatic moving, automatic trenching, and 5G remote control. FJ DYNAMICS has also developed a complete set of unmanned and digital solutions that include 3D spatial sensing integrated with guidance and control systems. These excavators are equipped with an excavation guidance system with 3D images that display the movement of the machine in real-time, and high-precision construction can be carried out at any time, even in low visibility and restricted access conditions.

However, despite the potential benefits of autonomous excavators, further development in several areas is required. A recent study found that remote operation of excavators may not be as effective as initially thought [8]. Current teleoperated systems may suffer from control delays compared to manual controls and may encounter difficulties in acquiring and understanding surrounding information such as soil, machines, nearby human workers, and other obstacles [4]. Full automation of every process on the job site remains challenging, given the uncertainties of the dynamic and complex excavation tasks onsite [5]. Thus, analyzing the impact of autonomous excavators on productivity is necessary to help justify whether there is a return on investment for autonomous excavators.

In this paper, a simulation model is used to study the excavation process. The model is validated using real-world data, and different modes of automation are modeled and studied. Finally, conclusions are drawn regarding the efficacies of automation on productivity and its practical implications discussed.

2 Literature Review

2.1 Autonomous excavator system

Automatic excavator systems are an emerging field of research that combines civil engineering and robotics. In

recent years, there has been significant progress in the development of autonomous excavator systems that can operate continuously for extended periods without human intervention, such as the system developed by researchers from Baidu Robotics, Research Robotics and Auto-Driving Lab (RAL), and the University of Maryland, College Park, in 2021 [9]. The system is equipped with sensors that can perceive the 3D environment and identify materials, which significantly enhances productivity. An overview is provided in Figure 1.

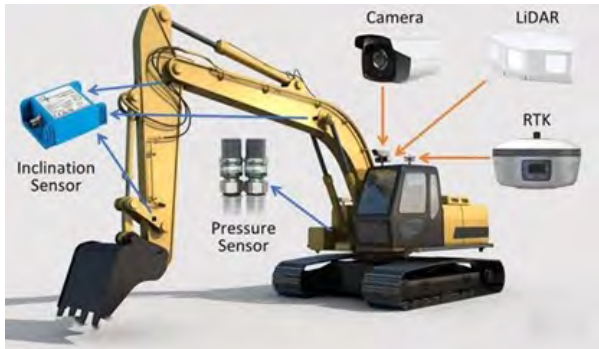


Figure 1. Autonomous excavator system from Baidu Robotics and Research Robotics and Auto-Driving Lab (RAL) and the University of Maryland, College Park (Zhang et al., 2021)

Navigation planning is a crucial aspect of autonomous excavator systems. The combination of point-to-point (PTP) and complete coverage path planning (CCPP) methods is one solution that has been proposed to achieve this. PTP is a technique that uses an algorithm such as the A^* algorithm, which relies on a heuristic function $h(n)$ to estimate the lowest-cost path from the start node to the goal node $g(n)$ [10]. CCPP algorithms are designed to split the workspace into square cells and use a cost function to optimize the path planning, taking into account various parameters such as water flow, travel distance, elevation, accessibility, and environmental constraints [6]. An algorithm proposed by Kim et al. in [11] provides an example of a CCPP algorithm that considers earthwork and environmental constraints as an optimization problem. The algorithm's cost function additionally takes into account the accessibility of the lorries and the external conditions of the work environment, such as the distance between cells, distance from the entrance, and isolation. These parameters are critical in determining the cost of excavation and the overall efficiency of the system [6].

2.2 Earthwork Simulations

Simulation systems play a crucial role in civil engineering and construction management by helping professionals understand and predict complex engineering problems, with the objective of potentially increasing work productivity. AbouRizk [12] showed that simulation plays an integral role in construction engineering and management by summarizing the key factors of deploying simulation models and key attributes of construction problems that make them more amenable for simulation modeling than

other methods. In addition, simulation models are capable of capturing complex variables, analyzing the impact on the productivity of tunneling construction projects, and carrying out further sensitivity analysis [13].

One benefit of simulation systems is its ability to provide integrated simulation and optimization approaches to reduce CO₂ emissions from the on-site construction process. For example, Li et al. [14] used a discrete-event simulation (DES) approach to model the construction process in cold regions, quantifying the amount of CO₂ emissions, and optimizing on-site labor allocation using a genetic algorithm. This reduced the carbon footprint of construction activities in cold regions.

Another benefit is its ability to create simulation models for earthwork operations to enhance productivity. Symphony.Net, a simulation environment developed by AbouRizk et al. [15], provides construction simulation solutions that can handle both discrete event and continuous simulations. One important feature of this simulation environment is its extensibility and flexibility, which allows it to create special-purpose simulations for specific construction systems such as earth-moving, paving, etc.

In conclusion, simulation systems have become an essential tool for civil engineers and construction professionals. They provide a way to better understand complex engineering problems, optimize construction activities, and enhance productivity.

2.3 Gap in Current Studies

In recent years, there has been a rapid development of autonomous excavator technology. The potential for this technology in the civil engineering industry is immense. Autonomous excavation systems combine various technologies such as 3D vision, machine learning, and other artificial intelligence techniques to achieve fully autonomous operations. Earthwork operations analysis using simulation is also gaining popularity as it is proven to enhance the productivity of infrastructure projects.

However, the current application of autonomous excavators in the civil engineering industry is still in its experimental phase. Due to the uncertainties of dynamic and complex excavation tasks in the workplace [5], it is necessary to investigate and verify whether autonomous excavation systems can improve overall productivity. Therefore, it is essential to develop a baseline productivity measure to test the usability of autonomous excavators.

This paper identifies different strategies of autonomy for automated excavation systems, but there have been few studies on the impact of automation on the productivity of autonomous excavation systems, considering these different strategies. Therefore, it is important to measure productivity and compare it accordingly [16]. Therefore, the objective of this study is to define these strategies of automation for autonomous excavation systems and quantify their impact accordingly. Both of the objectives are realized by simulating the excavation process in Symphony.Net. By doing so, the study aims to provide a better understanding of the potential for autonomous excavation systems in the civil engineering industry.

3 Proposed Research Method

3.1 Overall simulation methodology

The overall methodology of this research is presented in Figure 2. It consists of four main sections, namely Data preparation, Simulation model building, Output analysis, and Discussion. Each of these sections can be further broken down into several sub-steps. The following paragraphs will introduce the activities in each sub-step in more detail.

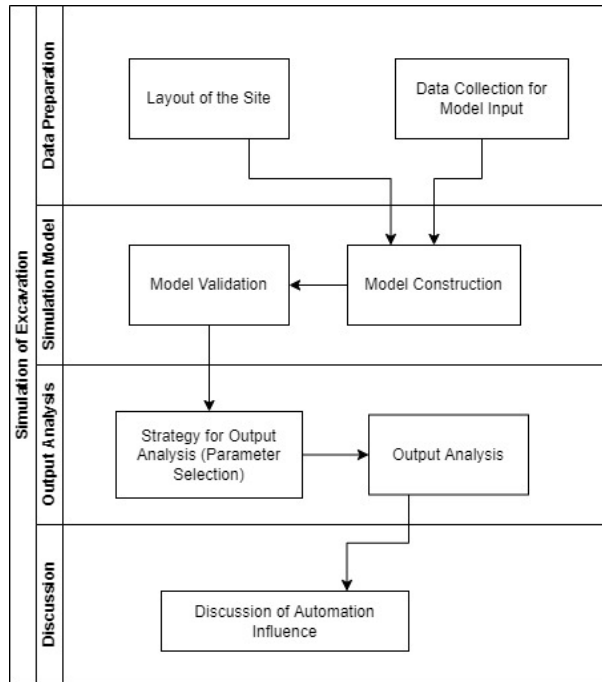


Figure 2. Research Method of the Research

To realistically simulate the excavation activity, data from an actual construction site is used. In the first step of data preparation, the layout of the site is analyzed, and project information is collected. The information gathered is then used to design the simulation model.

In the next step, the simulation model is built. The model is made up of several sub-cycles, including Excavators, Lorries, and Personnel. The earthwork is transferred as units flowing through different nodes. Once the simulation model has been constructed, input data is used to fit the simulation model.

To ensure the accuracy of the input data, a statistical t-test is conducted to establish a baseline model. This helps to validate the data input, as well as to identify any inconsistencies or errors that may have occurred during data preparation.

Finally, various automation strategies are formulated and tested on the simulation model. Metrics for assessment are selected, and a sensitivity analysis is carried out to investigate the results further. The results obtained from the simulation model are analyzed and discussed, with a focus on the impact of automation on the productivity of autonomous excavation systems. In conclusion, the overall methodology of this research is designed to provide a systematic and rigorous approach to investigating the

impact of automation on the productivity of autonomous excavation systems.

3.2 Site Information: Layout of Site and Data Collection

To simulate the excavation process at a construction site, an open-cut bulk excavation project is selected here as a reference project to build the simulation model. The layout of the site is presented in Figure 3, which shows that the site has been divided into two zones, with each zone serviced by an individual gate. Lorries enter and exit the site from either Gates 1 or 2. There are no intermediate storage areas for excavated earth. The average travel distances of the excavators and lorries are estimated to be similar for both zones, and the size of each zone is about $350m^2$.

The overall objective of the excavation operation is to excavate 1000 cubic meters of soil from the construction site and move it to the dump site situated externally from the site. The excavators carry out two different activities: Some excavators carry out excavation and slope grading when not excavating, while others are tasked to load the excavated soil material onto the lorries. Other project machinery such as lorries and personnel including banksman, operators, supervisors, etc., are also incorporated into the simulation. These elements make up the fundamental components of the project, with further details listed below in Table 1.

Element	Description	Units
Excavator	Bucket Capacity: $1.5m^3$	1
Lorry	Capacity: $8m^3$	15
Banksman	-	3
Safety Personnel	-	3
Operator	-	9
Supervisor	-	3
Traffic	-	3

Manpower is divided into three groups: those in charge of excavation, loading, and dumping, respectively. Lorries enter and exit the site via the two major gates at an average interval of 7 minutes due to the dumping activity. Excavators, lorries, and manpower are assumed to operate continuously over the working period. This assumption allows the simulation to operate at a steady state, thus allowing for more consistent results to be obtained.

Overall, the comprehensive simulation model created closely mirrors the excavation process at a real construction site. By incorporating all the key elements of the excavation project, including personnel, machinery, and different operational activities, the simulation model provides a realistic and accurate representation of the excavation process. This model will enable the impact of different automation strategies on excavation productivity and efficiency to be evaluated.

4 Simulation Model

4.1 Model Construction in Symphony.NET

The model is constructed within Symphony.NET, a modeling environment composed of simulation services and a

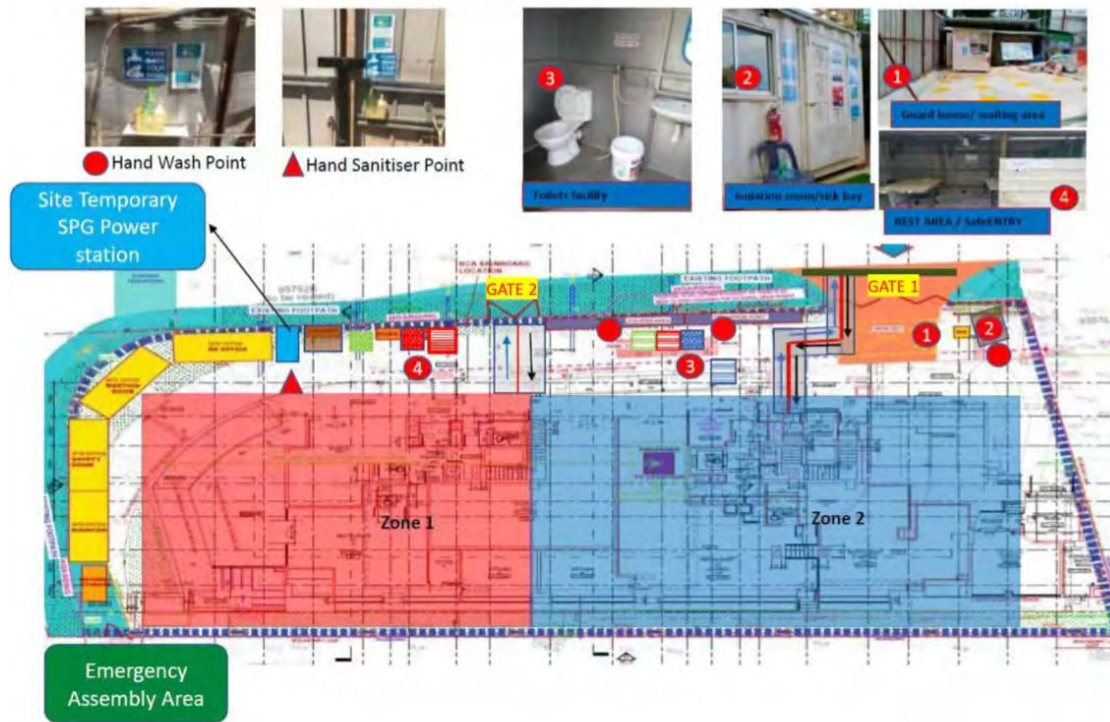


Figure 3. Layout of Test Site

modeling user interface that provides a visual representation of the excavation process. The overall excavation process is simulated in Symphony.NET as shown in Figure 4. The model is designed to simulate the sub-cycles within the excavation process, which mainly include the excavation sub-cycle, the loading sub-cycle, and the lorry cycle. These sub-cycles are connected to the soil sub-cycle, which depicts the transfer of earth from its original state to its excavated state, and finally to its dumping site.

By adjusting and tuning the parameters of the model and running simulations, output analysis can be conducted to determine how these parameters impact the total operation time and production rate. This output analysis refers to the evaluation of strategies and is used to evaluate the effect of different classes of autonomous excavation systems.

In Figure 4, green nodes depict major resource units utilized by the simulation. Deep yellow nodes represent processes whose duration follows an estimated statistical distribution from historical data. Light yellow nodes indicate activities where the time durations are estimated from video data collected onsite, and used to tune the model.

To integrate the simulation model, data is required, including the duration of processes and unit quantities. Table 2 lists the data required for the simulation.

Cycle times for normal excavation, excavator maneuver, and loading are estimated based on video recordings of the site excavation works. The time spent on internal travel and external travel of lorries is estimated using a statistical distribution, with lognormal distribution assumed for the two durations. Examples of such data are often recorded in site lorry logs. Table 3 provides the complete data input

set for the simulation.

4.2 Model Validation

Validation of simulation models is a crucial step in the modeling process to ensure the model accurately reflects the actual situation of the construction site. In this case, the simulation model is validated using data records of lorries coming in and out of the site, and durations of internal and external travel are used as a metric. Internal travel refers to the time lapse between the entry and exit of a specific lorry from the site, and the mean and standard deviation of these durations are computed. T-tests are then conducted to determine if there is a statistical difference between the simulation results and the observed data. The computed p-values of the two durations indicate a high probability that the observed data is not significantly different from the simulated results. Therefore, the model structure is deemed acceptable, and the simulated model is representative of the actual situation on-site.

With the validated simulation model, two modes were further developed, each with the same structure and node layout. The first mode, “Real Situation” depicts the scenario where the validated model was used as-is. The second mode, “Optimized Situation” shows the scenario where further resource balancing was carried out on the validated model to optimize the resources. In this “Optimized Situation”, the resources of manpower, excavators, and lorries were analyzed and balanced to match the interaction of the different cycles. By doing so, the resources are adjusted to match the needs of the excavation, loading, and lorry cycles. The optimization process ensures the re-

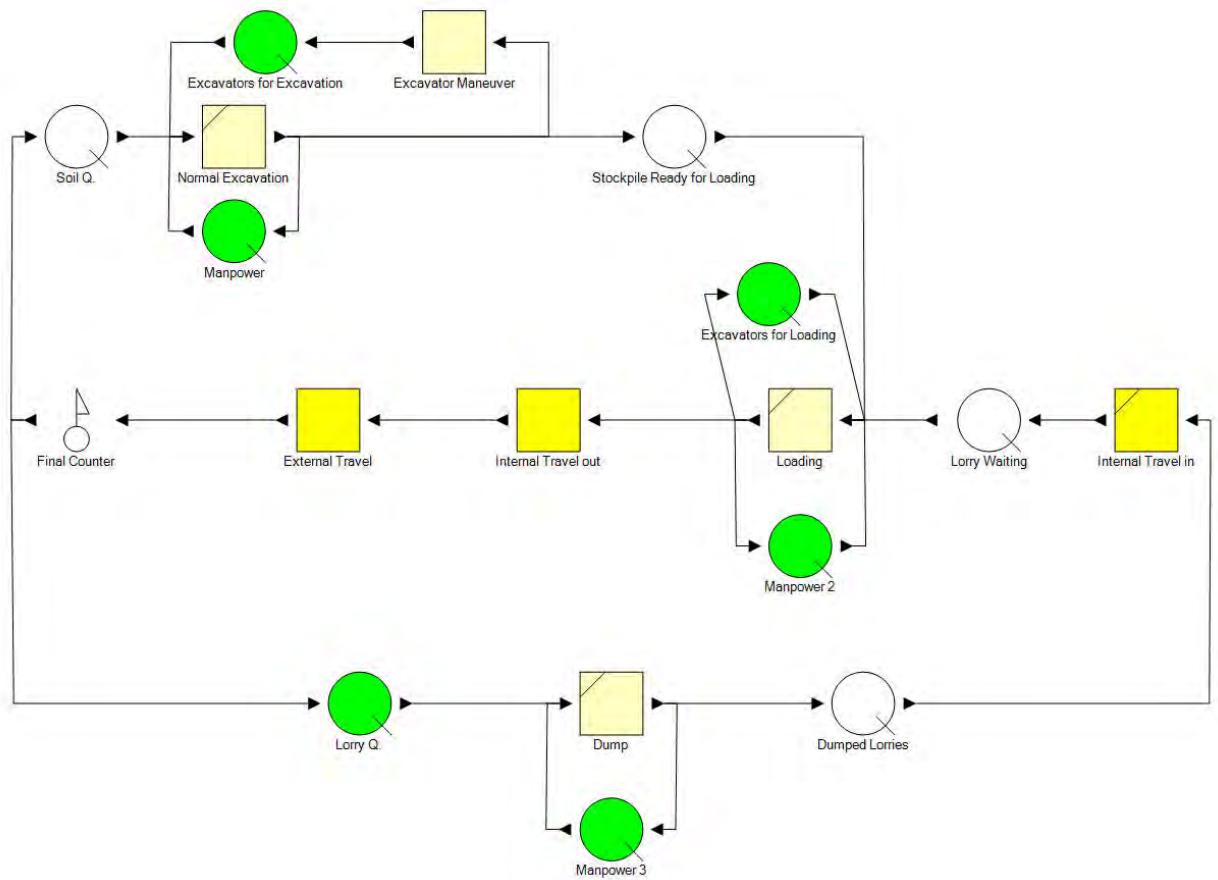


Figure 4. Overall Symphony.NET Model

Table 2. Data Requirements for Simulation Model

Data Requirements	Description
Capacity of Excavator Bucket and Lorries	Capacity is used for unit balancing
Number of Excavators, Lorries, and Manpower	The major resources used for maintaining the cycles
Soil Amount	The target amount of soil that needs to be transported outside the site
Internal Travel	Duration of lorries traveling in the site
Loading	Duration for excavator loading the lorries
External Travel	Duration when lorries are traveling outside the site
Normal Excavation	Duration of one excavator finishing a single excavation cycle
Excavator Maneuver	Duration of excavator maneuvering to excavation point

Table 3. Data Input Values used in Model

Parameter	Value
Internal Travelling Time	$\sim LN(1.996, 0.272)$
External Travelling Time	$\sim LN(4.705, 0.160)$
Normal Excavation Duration	0.25 minutes
Number of Excavators	3
Number of Lorries	30
Loading Duration	1.5 minutes
Excavator Bucket Capacity	$1.5m^3$
Lorry Capacity	$9m^3$
Number of Manpower	6
Excavator Maneuver Duration	0.5 minutes
Soil Amount	$1000m^3$

sources are utilized to their full potential, thus reducing the overall operation time and increasing the production rate. The rationale of comparing the results from the two modes is to isolate the effect of automation from the impact of resource optimization. This allows a more accurate evaluation of the effect of automation on the excavation process.

5 Output Analysis

5.1 Strategies for Autonomous Excavation systems

This paper identifies three modes or strategies of automation that will improve excavation: autonomous excavation, autonomous navigation and automated lorry fleet. Autonomous excavation is achieved through the use of

bucket sensors and posture detection techniques. Bucket sensors enable the excavator to detect the location and depth of the earth being excavated, while posture detection ensures the excavator maintains the correct posture while performing the excavation. These techniques work together during the excavation process to ensure greater accuracy and speed than a human operator.

Autonomous navigation is another key area where robotics can help improve excavation processes. By using real-time data to identify the boundaries of excavation activity, autonomous navigation can help to allocate dynamic zones of excavator operation and reduce conflicts inside the site. This can significantly reduce the duration for maneuvering and control of the excavator, resulting in increased efficiency and productivity.

Automating the fleet of lorries is also a potential strategy that can help to reduce the amount of travel within the site. By using autonomous navigation techniques to optimize the routes taken by lorries, it is possible to reduce the time and fuel consumption required for transportation.

To simulate these three strategies in the Symphony.NET model, the effects of these strategies are modeled by decreasing the expected durations of their associated activities, as shown in Table 4. In the simulation, each strategy is modeled as a simulation scenario, wherein a different level of automation is depicted. Additional simulation scenarios are also defined where the different strategies are combined. The effects of the strategies are obtained from expert judgment found in Li et al. [16].

Table 4. Strategies for Automation of Excavation Process

Strategies	Associated Nodes	Change
Autonomous Excavation (Strategy 1)	Normal Excavation	-30 %
Autonomous Navigation (Strategy 2)	Excavator Maneuver	-30 %
Automated Lorry Fleet (Strategy 3)	Internal Travel Time	-30 %

As each of the above strategies may be used in conjunction, this research further identifies the following scenarios. This creates a total of seven possible strategies, arising from the possible combinations of the above three strategies.

- Strategy 1&2: Autonomous Excavation with Autonomous Navigation
- Strategy 1&3: Autonomous Excavation with Autonomous Lorry Fleet
- Strategy 2&3: Autonomous Navigation with Autonomous Lorry Fleet
- Strategy 1&2&3: Autonomous Excavation with Autonomous Navigation and Autonomous Lorry Fleet

Several metrics are defined that are used as indicators of the overall productivity of the excavation process:

- Metric 1: The “Last Arrival Time” is the total time taken within the simulation to excavate $1000m^3$ of earth.

- Metric 2: The “Average waiting times” of excavators for loading activities.
- Metric 3: The “Average waiting times” of excavators for excavation activities.

This paper uses three metrics to evaluate the impact of automation on the excavation process. The first metric, Metric 1, is used to measure the overall productivity of the entire excavation process. This metric is commonly used by earthwork contractors to assess their productivity, making it a valuable tool to assess the effectiveness of the different automation strategies. Metrics 2 and 3 are used to track the utilization of the equipment. This information can be used to identify any inefficiencies or idling of the equipment, which may occur as a result of automation.

The study focuses on measuring the change in the numerical values of these metrics, as different automation strategies are implemented. The objective is to identify any negative effects, such as excessive idling of the equipment, and develop strategies to mitigate them. By monitoring these metrics, insights can be gained into the effectiveness of the different automation strategies and their impact on the excavation process.

5.2 Results and Discussion

The aforementioned 7 simulation scenarios refer to the possible combinations of the automation strategies; these scenarios were then applied to both the “Real Situation” and “Optimized Situation” modes respectively. The purpose was to determine if there was a significant difference in the mean values of the simulation results obtained from applying the strategies compared to the base cases from either the “Real Situation” or the “Optimized Situation.” To determine this, a t-test was performed. The results of these hypothesis tests are presented in Table 5 for the “Real Situation” and Table 7 for the “Optimized Situation”. In both tables, $m1$ represents the mean value of the metric used obtained from applying the strategy, and $m2$ represents the mean value of the same metric obtained from the base scenario. The results in bold indicate significant differences between the two mean values.

Table 5 presents the quantitative results of the three metrics tracked in the study. The table shows that only ‘Strategy 3’, ‘Strategy 1&3’, ‘Strategy 2&3’, and ‘Strategy 1&2&3’ have a significant difference in productivity (Metric 1). The corresponding improvements in the “Real Situation” were measured and compared against the base results from the same situation, as well as the “Optimized Situation” results. Table 6 shows these results, with the actual mean values obtained for each set of simulations presented in parentheses. Negative percentage values indicate a percentage decrease in the metric measured, and values in parenthesis indicate the absolute mean values obtained for each set of simulations. Values in parentheses within the header of the table indicate the mean value of the base ‘Real Situation’ scenario.

Table 7 and Table 8 refer to the hypothesis tests and their corresponding quantitative results in the “Optimized Situation”. The table shows that only ‘Strategy 1&3’ and ‘Strategy 1&2&3’ have statistically significant results in the optimized scenario.

In the “Real Situation”, the unbalanced number of resources means that there are not enough lorries to support the excavation and loading operations. As a result, the

Table 5. Results of Hypothesis Testing of Strategies in Real Situation

	Metric 1	Metric 2	Metric 3
Strategy 1	$m_1 = m_2$	$m_1 = m_2$	$m_1 < m_2$
Strategy 2	$m_1 = m_2$	$m_1 = m_2$	$m_1 < m_2$
Strategy 3	$m_1 > m_2$	$m_1 > m_2$	$m_1 > m_2$
Strategy 1&2	$m_1 = m_2$	$m_1 = m_2$	$m_1 < m_2$
Strategy 1&3	$m_1 > m_2$	$m_1 > m_2$	$m_1 < m_2$
Strategy 2&3	$m_1 > m_2$	$m_1 > m_2$	$m_1 < m_2$
Strategy 1&2&3	$m_1 > m_2$	$m_1 > m_2$	$m_1 < m_2$

Table 6. Quantitative Metrics for “Real Situation”

	Metric 1 (1097.13)	Metric 2 (7.35)	Metric 3 (2.93)
Optimized Situation	-18.08% (878.78)	-24.56% (5.54)	106.85% (6.05)
Strategy 1	0.17% (1099.05)	0.27% (7.37)	15.85% (3.39)
Strategy 2	0.11% (1098.32)	0.21% (7.36)	5.45% (3.09)
Strategy 3	-1.84% (1076.98)	-2.19% (7.19)	-2.66% (2.85)
Strategies 1&2	-0.00% (1097.18)	-0.03% (7.35)	20.49% (3.53)
Strategies 1&3	-1.85% (1076.84)	-2.13% (7.19)	12.41% (3.29)
Strategies 2&3	-1.68% (1078.69)	-1.9% (7.21)	2.46% (3.00)
Strategies 1&2&3	-2.00% (1075.24)	-2.19% (7.18)	17.48% (3.44)

Table 7. Results of Hypothesis Testing of Strategies in Optimized Situation

	Metric 1	Metric 2	Metric 3
Strategy 1	$m_1 = m_2$	$m_1 = m_2$	$m_1 < m_2$
Strategy 2	$m_1 = m_2$	$m_1 = m_2$	$m_1 < m_2$
Strategy 3	$m_1 = m_2$	$m_1 = m_2$	$m_1 = m_2$
Strategy 1&2	$m_1 = m_2$	$m_1 = m_2$	$m_1 < m_2$
Strategy 1&3	$m_1 > m_2$	$m_1 = m_2$	$m_1 < m_2$
Strategy 2&3	$m_1 = m_2$	$m_1 = m_2$	$m_1 < m_2$
Strategy 1&2&3	$m_1 > m_2$	$m_1 > m_2$	$m_1 < m_2$

Table 8. Quantitative Metrics for “Optimized Situation”

	Metric 1 (898.78)	Metric 2 (5.54)	Metric 3 (6.05)
Strategy 1	0.19% (900.51)	0.11% (5.55)	7.54% (6.51)
Strategy 2	-0.08% (898.02)	-0.13% (5.54)	2.27% (6.19)
Strategy 3	-0.26% (896.48)	-0.09% (5.54)	-0.37% (6.03)
Strategies 1&2	-0.03% (898.50)	-0.02% (5.54)	9.75% (6.65)
Strategy 1&3	-0.28% (896.27)	0.02% (5.54)	7.08% (6.49)
Strategy 2&3	-0.12% (897.71)	0.15% (5.55)	2.34% (6.20)
Strategy 1&2&3	-0.18% (897.14)	-0.03% (5.54)	9.47% (6.63)

excavators used for excavating have to wait for longer periods of time, which reduces the efficiency of the operation. The waiting time for loading excavators, on the other hand, does not show much variation in different scenarios, indicating that automation does not have a significant impact on the utilization of loading excavators.

The quantitative results presented in Table 6 show that the Last Arrival Time (Metric 1) decreases from 1.68% to 2% in the statistically significant scenarios from Table 5. The average waiting time for loading (Metric 2) shows little variation in different scenarios. This indicates that automation does not affect the utilization of loading excavators significantly. However, the waiting time for excavators used for excavating increases significantly by up to 17.5%. This increase in waiting time is due to the lack of enough lorries to support the operation. When the excavating machinery finishes the work faster, but the subsequent loading is not fast enough, significant delays may occur during excavation, hence reducing the overall efficiency of the operation.

For “Optimized Situation”, where resources are balanced, the overall production time drops by about 20% when compared to the “Real Situation”. This reduction in production time is due to the smoother and more efficient operation arising from balanced resources. However, the effect of automation on total productivity is not as significant as one might expect. The decrease in last arrival time (Metric 1) and loading excavator waiting time (Metric 2) in the “Optimized Situation” is almost trivial, ranging from -0.18% to -0.28%. The waiting time for excavators used for excavating (Metric 3) is also longer than that of the “Real Situation” although the increase in waiting time is not as significant, ranging from 7% to 9%.

In conclusion, resource constraints (the lack of lorries to balance production) is inferred to dominate productivity, despite the availability of automation. From both Real and Optimized Situations, the impact of automation on productivity is observed to be minimal.

6 Conclusion

Simulations are valuable tools for modeling complex processes and predicting their potential outcomes. In this study, an excavation simulation model was created using real-world site data. The model aimed to represent the standard workflow of an open-cut excavation project, which includes excavating, maneuvering, and loading. The simulation model was built using Symphony.NET, a powerful software tool for creating dynamic simulations of industrial processes. The required data for the simulation model was gathered from actual site data or estimated from secondary sources. The model was then validated using various techniques to ensure that it accurately represented the real processes.

Once the simulation model was set up successfully, an output analysis was conducted to determine the potential impact of automation on the overall excavation productivity and equipment utilization. The analysis revealed that the changes to the metrics were not significant within the simulation model. This may be due to the shortage of lorries which limits the effect of automatic excavators.

Although automatic excavators help reduce the time for excavation, maneuvering, and loading, the changes made to the overall productivity (Last Arrival Time) and uti-

lization (average waiting time for excavators) are minimal. The study showed that the lack of lorries constrains the effect of automatic excavators on productivity. This suggests that the effect of automation may not be as significant as expected, especially if there is a shortage of resources.

As future work, the simulation study can be significantly improved by comparing the results to the reported performance of autonomous excavator systems. This verification may be obtained in the future through collaboration with developers of autonomous excavator systems. Such collaboration can help to further validate the simulation model and enhance its accuracy, which can in turn provide valuable insights for optimizing excavation processes.

7 Acknowledgements

This project is supported by Building Construction Authority (BCA) Singapore and National Robotics Programme (NRP) under its Built Environment Robotics R&D programme W2122d0153. Any opinions, findings and conclusions or recommendations expressed in this material are those of the author(s) and do not reflect the views of BCA or NRP.

References

- [1] Behrokh Khoshnevis. Automated construction by contour crafting—related robotics and information technologies. *Automation in Construction*, 13(1):5–19, 2004. ISSN 0926-5805. doi:10.1016/j.autcon.2003.08.012.
- [2] Masakazu Haga, Watanabe Hiroshi, and Kazuo Fujishima. Digging control system for hydraulic excavator. *Mechatronics*, 11(6):665–676, 2001. ISSN 0957-4158. doi:10.1016/S0957-4158(00)00043-X.
- [3] Kwangmin Kim, Minji Kim, Dongmok Kim, and Dongjun Lee. Modeling and velocity-field control of autonomous excavator with main control valve. *Automatica*, 104:67–81, 2019. ISSN 0005-1098. doi:10.1016/j.automatica.2019.02.041.
- [4] Masaru Ito, Chiaki Raima, Seiji Saiki, Yoichiro Yamazaki, and Yuichi Kurita. Effects of Machine Instability Feedback on Safety During Digging Operation in Teleoperated Excavators. *IEEE Access*, 9:28987–28998, 2021. ISSN 2169-3536. doi:10.1109/ACCESS.2021.3059710.
- [5] Dominic Jud, Simon Kerscher, Martin Wermelinger, Edo Jelavic, Pascal Egli, Philipp Leemann, Gabriel Hottiger, and Marco Hutter. HEAP - The autonomous walking excavator. *Automation in Construction*, 129:103783, 2021. ISSN 0926-5805. doi:10.1016/j.autcon.2021.103783.
- [6] Jeonghwan Kim, Dong-eun Lee, and Jongwon Seo. Task planning strategy and path similarity analysis for an autonomous excavator. *Automation in Construction*, 112:103108, 2020. ISSN 0926-5805. doi:10.1016/j.autcon.2020.103108.
- [7] Jin Sol Lee, Youngjib Ham, Hangu Park, and Jeonghee Kim. Challenges, tasks, and opportunities in teleoperation of excavator toward human-in-the-loop construction automation. *Automation in Construction*, 135:104119. ISSN 0926-5805. doi:10.1016/j.autcon.2021.104119.
- [8] Hikaru Nagano, Hideto Takenouchi, Nan Cao, Masashi Konyo, and Satoshi Tadokoro. Tactile feedback system of high-frequency vibration signals for supporting delicate teleoperation of construction robots. *Advanced Robotics*, 34(11):730–743, 2020. ISSN 0169-1864. doi:10.1080/01691864.2020.1769725.
- [9] Liangjun Zhang, Jinxin Zhao, Pinxin Long, Liyang Wang, Lingfeng Qian, Feixiang Lu, Xibin Song, and Dinesh Manocha. An autonomous excavator system for material loading tasks. *Science Robotics*, 6(55), 2021. doi:10.1126/scirobotics.abc3164.
- [10] A. R. Soltani, H. Tawfik, J. Y. Goulermas, and T. Fernando. Path planning in construction sites: Performance evaluation of the Dijkstra, A*, and GA search algorithms. *Advanced Engineering Informatics*, 16(4):291–303, 2002. ISSN 1474-0346. doi:10.1016/S1474-0346(03)00018-1.
- [11] Sung-Keun Kim, Jeffrey S. Russell, and Kyo-Jin Koo. Construction Robot Path-Planning for Earthwork Operations. *Journal of Computing in Civil Engineering*, 17(2):97–104, 2003. ISSN 0887-3801. doi:10.1061/(ASCE)0887-3801(2003)17:2(97).
- [12] Simaan AbouRizk. Role of Simulation in Construction Engineering and Management. *Journal of Construction Engineering and Management*, 136(10):1140–1153, 2010. ISSN 0733-9364, 1943-7862. doi:10.1061/(ASCE)CO.1943-7862.0000220.
- [13] Yasser Ebrahimi, Simaan M. AbouRizk, Siri Fernando, and Yasser Mohamed. Simulation modeling and sensitivity analysis of a tunneling construction project's supply chain. *Engineering, Construction and Architectural Management*, 18(5):462–480, 2011. ISSN 0969-9988. doi:10.1108/09699981011074600.
- [14] Hong Xian Li, Limao Zhang, Don Mah, and Haitao Yu. An integrated simulation and optimization approach for reducing CO2 emissions from on-site construction process in cold regions. *Energy and Buildings*, 138:666–675, 2017. ISSN 0378-7788. doi:10.1016/j.enbuild.2016.12.030.
- [15] S AbouRizk, S Hague, R Ekyalimpa, and S Newstead. Symphony: A next generation simulation modelling environment for the construction domain. *Journal of Simulation*, 10(3):207–215, 2016. ISSN 1747-7778. doi:10.1057/jos.2014.33.
- [16] Beiji Li, Xiaoyu Bai, and Justin K.W. Yeoh. Review and Classification of Autonomous Excavation Systems. In *Proceedings of the 22nd International Conference on Construction Applications of Virtual Reality (CONVR 2022)*, Seoul, South Korea, 2022.

Prototypical digital twin of multi-rotor UAV control and trajectory following

L.V. Nguyen¹, T.H. Le¹, and Q.P. Ha¹

¹School of Electrical and Data Engineering, University of Technology Sydney (UTS), Australia

{vanlanh.nguyen; hoang.t.le; quang.ha}@uts.edu.au

Abstract -

This paper presents the development of a prototypical digital twin package for multi-rotor aerial vehicle (MAV) systems, with potential application for monitoring a construction site. The focus is how to create a virtual representation of an actual surveillance system that can be updated from real-time data to effectively help with its control, conditional monitoring, and decision-making via a versatile platform. Here, a simulation framework is developed to include the system dynamics, operation environment, and other control and tracking requirements for a wide range of MAV mission circumstances. Real-world examples from a construction site are used to illustrate the concept. A prominent advantage is that we can thoroughly test, validate, verify and evaluate the MAV control and monitoring in abnormal conditions without the need for physical implementation and field experiments for the whole system in reality. This will substantially reduce extensive testing efforts throughout the development cycle to achieve optimal performance in terms of cooperation, safety, smoothness, fault tolerance, and energy efficiency.

Keywords -

Digital twin, multi-rotor aerial vehicle, 3D modelling, control and tracking.

1 Introduction

With the technological advancements of the Industrial Revolution 4.0, multi-rotor aerial vehicle (MAV) systems are gradually becoming popular in civilian life and industrial activities. In the construction sector, they are well-established in multiple project stages such as site monitoring and 3D mapping [1], building and damage assessment [2], as well as package delivery logistics [3], indicating the potential for widespread use of MAVs.

The MAV technology recognizes simulation as an effective approach for testing and validating drone functionality. The flying environment includes a wide range of factors such as cooperative missions, traveling distances, vehicle dynamics, and obstacles. The number of possibilities increases exponentially with the number of factors and has the potential to explode. To obtain dependability certification via real drone testing, the vehicle often has to fly hundreds of miles, even in complicated circumstances, which is highly time-consuming and risky. Furthermore, these circumstances cannot be simply manufactured and replicated in real life. It is worth noting that real flight testing is only valid for a certain mechanical, electrical, and

software setup. If a new configuration or software update is required, the test must be repeated. As a result, simulations will be used to test the majority of MAV features, and a framework that can mix multiple technological components and validate the design development in the early stages of functional development is critical.

Digital twin, an emerging technology, could be used for that purpose. The digital twin concept was first introduced in [4] by creating virtual digital representations of physical systems. To imitate dynamic behaviours of actual objects, their virtual versions are developed in digital form. The computerized model can describe the object's state using perceptual data, anticipating, evaluating, and interpreting dynamic changes. So far, the use of digital twins has been proven successful in industrial robots and self-driving cars [5, 6]. This technology enables an autonomous system to comprehend complex commands, determine the best action, and carry out tasks independently.

In the field of MAVs, a digital twin framework has been recently introduced in [7], made up of three parts: the virtual simulation environment, the actual MAV, and the service centre. Physical and virtual MAVs can communicate bidirectionally, allowing for the continuous assembly and updating of physical models. For multiple MAVs, a digital twin-based intelligent cooperative architecture for MAV swarms was presented in [8]. In this framework, a digital twin model is built to accurately replicate the physical entity, i.e., the MAV swarm, with high fidelity and monitor its entire process. Integrated with this model, a machine learning algorithm is built to explore the global optimal solution and control the behaviors of the swarm.

In civil engineering areas, the idea of a digital twin can find applications in architecture, infrastructure, machinery, and construction processes [9]. From the virtual viewpoint, it makes extensive use of modelling, simulation, calculation, analysis tools, and cutting-edge algorithms. Accordingly, the development of smart construction is promoted. For instance, a digital twin-enabled intelligent modular integrated construction system was introduced with a testbed robotic demonstration for cooperative decision-making and daily operation during on-site assembly [10]. The focus of existing works, however, is mostly on replicating the digital structures and tracking the

building's state. Including MAV systems, a digital twin of a building inspection scenario for reanimation and data validation has been conducted in [11]. In this study, realistic system workflow creation, comprehensive research for regulating the digital twin in the settings, and the cross-application of geographic information systems (GIS) are used to manage the geographic information production process. It includes a variety of virtual environment creation procedures, such as analyzing available GIS data, installation in the simulator, applying GIS-based real-world environment transformation tools, and gathering data with MAVs.

Although certain digital twin platforms for MAV are available in the literature, the above-mentioned works are mainly developed for system verification or communication. To the best of our knowledge, no digital twin of MAV control and trajectory following has been designed. Therefore, this paper proposes a prototype digital twin for incorporating the dynamic behaviors of typical MAVs, as well as the implementation of a MAV swarm and a cooperative path-planning algorithm. The co-simulation framework will be illustrated through construction applications in normal and faulty operations. The contribution of this paper is twofold: (i) a 3D model of the MAV and its environment for better visualization; (ii) a testing framework based on the co-simulation to demonstrate the response of MAV control and trajectory following algorithms when performing an on-site surveillance task.

2 Preliminaries

This section presents an overview of MAV operation, modelling, cooperative path planning, and control algorithms. These concepts are crucial to the design of a prototypical digital twin of MAV.

2.1 Description of MAV

Consider MAVs powered by $2N_p$ motors, where N_p denotes the number of rotor pairs, as shown in Figure 1. For symmetry, each pair of rotors are arranged on two opposite sides of the airframe. For $i = 1, 2, \dots, 2N_p$, the i -th rotor rotates clockwise if i is odd or anticlockwise if i is even. Each rotor is supported by its arm of length l_i . The angles formed by two successive arms are equal. By varying the speed of the rotors, the MAV can generate roll, pitch, yaw, and altitude movements with six degrees of freedom. The pitch angle, varied in accordance with the longitudinal motion of the MAV, is produced by unbalancing the sum of the front and rear propellers' velocities, which generate the total front force, $(F_1 + F_2 + F_8)$, and the total rear force, $(F_4 + F_5 + F_6)$. Meanwhile, its lateral displacement is governed by the roll angle, which is regulated by unbalancing the sum of the speeds of the right and left rotors, resulting in total right forces, $(F_2 + F_3 + F_4)$, and total left forces,

$(F_6 + F_7 + F_8)$. Yaw torque is obtained by adjusting the average speed of the clockwise and anticlockwise rotating rotors. Finally, all of the rotors contribute to the overall thrust input. In general, the MAVs operate on a similar operating principle. Differentiating features include rotor layout, size, and quantity. In practice, numerous alternative variations of MAVs are conceivable by changing the main configuration.

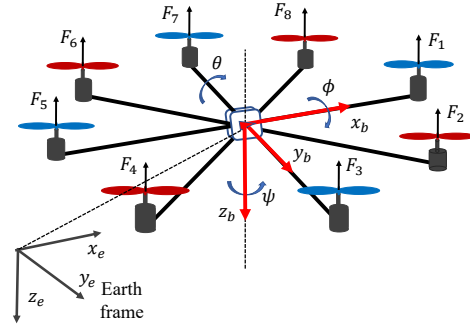


Figure 1. Configuration of the MAV system.

2.2 MAV Modelling

The goal of modelling is to express in mathematical terms the physical principles that govern the behaviours of a system in an environment or the motion of a control system. From this interpretation, calculations and simulations can be performed to analyze the system performance numerically and graphically. For MAVs, a parametric model of the vehicle is also required in order to execute the proper control. In this study, a multi-rotor system with $N_p \geq 2$ pairs of rotors is taken into consideration, assuming that the framework is rigid and symmetrical with regard to the roll and pitch axes. Besides, it is considered that the MAV's centre of gravity (CoG) is located at the origin of the body-fixed frame, and each propeller spins in the opposite direction of its two neighbors.

As illustrated in Figure 1, an earth frame, $\{x_e, y_e, z_e\}$, is attached to the ground, and a body frame, $\{x_b, y_b, z_b\}$, is mounted to the MAV's CoG, both with the z axis pointing downward. A vector $P = (x, y, z)^T$ defines the location of the CoG in the earth frame. Angles $(\phi, \theta, \psi)^T$, which correspond to roll, pitch, and yaw motion, respectively, are used to indicate the MAV orientation. These angles are limited for attitude control as $\phi \in [-\pi/2, \pi/2]$, $\theta \in [-\pi/2, \pi/2]$ and $\psi \in [-\pi, \pi]$. According to the MAV description, the total thrust force F , represented in the body coordinate, is computed as

$$F = \sum_{i=1}^{2N_p} f_i = b \sum_{i=1}^{2N_p} \omega_i^2, \quad (1)$$

where $f_i = b\omega_i^2$ is the thrust force exerted by i th rotor, ω_i is its corresponding rotational speed, and $b > 0$ is

the thrust coefficient. The components of torque vector $\tau = [\tau_\phi \ \tau_\theta \ \tau_\psi]^T$, which represent rotation in the roll, pitch, and yaw directions, can be obtained as:

$$\tau_\phi = bl \sum_{i=1}^{2N_p} -\sin\left((i-\epsilon)\frac{\pi}{N_p}\right) \omega_i^2, \quad (2a)$$

$$\tau_\theta = bl \sum_{i=1}^{2N_p} \cos\left((i-\epsilon)\frac{\pi}{N_p}\right) \omega_i^2, \quad (2b)$$

$$\tau_\psi = \beta \left(\sum_{i=1}^{N_p} \omega_{2i}^2 - \sum_{i=1}^{N_p} \omega_{2i-1}^2 \right) = \beta \left(\sum_{i=1}^{2N_p} (-1)^i \omega_i^2 \right), \quad (2c)$$

where l is the length of rotor's arm, β is the apparent radius for converting the force into the yaw torque, and $\epsilon = 1$ if the MAV has a "+" configuration, or $\epsilon = 1/2$ if the MAV has an "X" configuration. In the MAV dynamic, we consider the propeller gyroscopic, τ_p , and aerodynamic torques, τ_a , as external disturbances, i.e., $d = [d_\phi \ d_\theta \ d_\psi]^T = \tau_p - \tau_a$, where d_ϕ , d_θ , and d_ψ are disturbance components.

It is important to note that the thrust force F is the only control input of the 3D translational dynamics, whereas the active torques govern completely the MAV orientation. Hereafter, the vector of virtual control inputs will be denoted as $u = (u_1, u_2, u_3, u_4)^T$, with $u_1 = F, u_2 = \tau_\phi, u_3 = \tau_\theta$, and $u_4 = \tau_\psi$. A unified dynamical model for MAV is then given as below [12]:

$$\ddot{x} = \frac{1}{m}(c_\phi s_\theta c_\psi + s_\phi s_\psi)u_1, \quad (3a)$$

$$\ddot{y} = \frac{1}{m}(c_\phi s_\theta s_\psi + s_\phi c_\psi)u_1, \quad (3b)$$

$$\ddot{z} = \frac{c_\phi c_\theta}{m}u_1 - g, \quad (3c)$$

$$\ddot{\phi} = I_{xx}^{-1} [(I_{yy} - I_{zz})\dot{\theta}\dot{\psi} + u_2 + d_\phi], \quad (3d)$$

$$\ddot{\theta} = I_{yy}^{-1} [(I_{zz} - I_{xx})\dot{\phi}\dot{\psi} + u_3 + d_\theta], \quad (3e)$$

$$\ddot{\psi} = I_{zz}^{-1} [(I_{xx} - I_{yy})\dot{\phi}\dot{\theta} + u_4 + d_\psi], \quad (3f)$$

where s_x and c_x respectively represent $\sin x$ and $\cos x$, m is the total mass of the MAV, and $I = \text{diag}(I_{xx}, I_{yy}, I_{zz})$ is the inertia matrix of the MAV.

2.3 MAV cooperative path planning

Consider a group of M vehicles that operate in a particular flight region with multiple obstacles. The MAV group's location in an earth frame is defined as $\mathcal{P} = [P_1, P_2, \dots, P_M]$, where $P_m = [x_m, y_m, z_m]^T$ is the position of the m -th vehicle. The goal of cooperative path planning is to find the best routes for all MAVs to take from their starting point to target positions while meeting all formation shape, path length, threat avoidance, and turning angle limit requirements. The problem can be expressed as [13]

$$P_m(0) \xrightarrow[\text{s.t. } J(\mathcal{P}_m(k), \mathcal{P}_m^-(k))]{\mathcal{P}_m(k)} P_m(\text{end}), m = 1, 2, \dots, M, \quad (4)$$

where $P_m(0)$ and $P_m(\text{end})$ represent the initial and final postures of m -th MAV, respectively, k signifies the way-point instant, $\mathcal{P}_m(k)$ and $\mathcal{P}_m^-(k)$ represent MAV $_m$'s path and a set of its neighbors' paths, which includes a total of K nodes subject to the multi-vehicle cost $J(\mathcal{P}_m(k), \mathcal{P}_m^-(k))$. We formulate it into an optimization problem, and we solve this problem with a cost function for each MAV in the team. The cost function for one MAV is defined as [14]:

$$J(\mathcal{P}(k)) = \omega_1 \sum_{k=1}^K E(k) + \omega_2 \sum_{k=1}^{K-1} L(k) + \omega_3 \sum_{k=1}^{K-1} \sum_{\tau=1}^{\mathcal{T}} D_\tau(k) + \omega_4 \sum_{k=1}^K H(k) + \omega_5 \sum_{k=1}^{K-2} \theta(k) + \omega_6 \sum_{k=1}^{K-1} |\varphi(k) - \varphi(k+1)|, \quad (5)$$

where formation error $E(k)$, path length $L(k)$, and safety cost $D_\tau(k)$ associated with threats \mathcal{T} are concerned. The altitude payoff is denoted by $H(k)$, the turning angle and climbing angle are denoted by $\theta(k)$ and $\varphi(k)$, respectively, and the weight coefficients are denoted by ω_i for $i = 1, 2, \dots, 6$.

Given the cost function $J(\mathcal{P}_m(k))$ defined for each MAV, the cooperative path planning problem becomes finding paths $\mathcal{P}_m, m = 1, 2, \dots, M$ to simultaneously minimize $J(\mathcal{P}_m, \mathcal{P}_m^-)$. Since this cost depends on not only path \mathcal{P}_m generated for MAV $_m$ but also its rivals' paths \mathcal{P}_m^- , finding optimal solutions is a challenging problem. Meanwhile, game theory has been well-recognized for resolving conflicts and handling interactions. The players of a game can decide to pursue their individual objectives by simultaneously considering the possible goals, behaviors, and countermeasures of other decision-makers to achieve a win-win situation. Therefore, this paper employs a recently developed game theory-based particle swarm optimization (GPSO) [14] to effectively generate MAV cooperative paths. The GPSO solves the collaborative path planning problem by finding the equilibrium of a Stackelberg-Nash game using a PSO hierarchical optimization framework.

2.4 MAV trajectory tracking control

The aim of trajectory tracking control is to derive the control laws that apply to each MAV's actuator to reach the desired position and attitude. Figure 2 depicts a general cascaded control structure for MAVs. The controller is designed in a hierarchical scheme, in which the inner loop is the control of the angles, and the outer loop is the position control. There are four control signals. For the fully-actuated subsystem, the control action u_1 is to control the altitude and u_4 is to control yaw motion. For the under-actuated subsystem, u_2 and u_3 are control roll angle and the pitch angle, respectively, and hence control x, y positions. The reference or desired position is typically

given by the ground operation remotely, or by a trajectory planner. To fine-tune the output of the MAV, i.e., the position and orientation, the classical PID (proportional-integrator-derivative) controller is widely employed due to its simple structure and implementation, overall good control performance, and robust design.

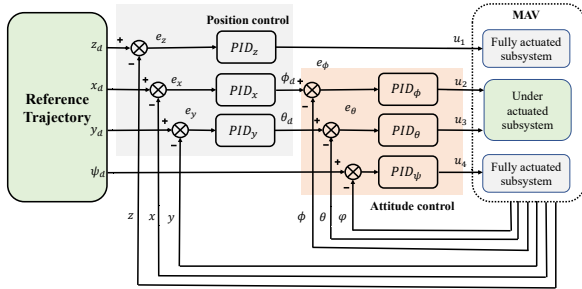


Figure 2. Control architecture of MAVs.

3 Tool development and Simulation

Given flying environments, vehicle dynamics, cooperative path planning, and control algorithms, this section provides a co-simulation framework for testing, verifying, and validating MAV technologies. Firstly, the 3D CAD model of a MAV is assembled in Solidworks to visually depict its physical twin along with its dynamic parameters obtained from the geometry and material inputs to the software. The virtual aerial vehicle is then exported to Matlab/Simulink through the supported plug-in between the two environments. Similarly, the virtual world of a case study, reflecting a construction site, is realized in the Simulink Simscape Multibody environment. The tower cranes, earthmoving vehicles, and incomplete buildings, which pose obstacles to drone navigation, are imported from their respective CAD files.

3.1 Computer-aided design MAV model

The use of computer-aided design (CAD) has proved useful and profitable for a wide range of professions. This practice assures effortless perception for users and promises growing productivity and straightforward modification in engineering endeavours. Specifically, a CAD model possesses the capability to accurately represent its physical counterpart. Hence, using this strategy encourages the visualization of the multi-rotor system, which is an essential part of the proposed digital twin platform.

In the first step, the CAD model of an actual MAV, such as the 3DR Solo drone in this work, is reconstructed and assembled using component-based and parametric modeling for visualization of the model. Therefore, modular design is possible with consideration for compatibility with the digital twin platform. The quadcopter's structural frame

consists of an attached battery, replicated legs forming the landing gear, and a propulsion system comprising two pairs of contra-rotating brushless DC motors and corresponding propellers. Lastly, the materials and surface textures of each component are specified. This is a crucial step to ensure the modelling software numerically produces acceptable mass, the moment of inertia, and other intrinsic values and visually depicts its physical twin, as illustrated in Figure 3.



Figure 3. Rendered model of the 3DR Solo Drone.

The software allows for obtaining all dynamic parameters of the drone from the manufacturer's specifications and measurements. The numerical values can be stored in a compatible file format for later use. Securing inertial figures, whether by rigorously performing measurements on specialized instruments or analytically conducting calculations, is an arduous task. Hence, by embracing CAD modeling, the developed digital twin can quickly accommodate a variety of drones on the platform.

3.2 Virtual flight environment

In general, a digital twin for MAV systems requires a virtual flight environment that accurately simulates the motion of aerial vehicles. While existing simulators such as AirSim, Gazebo, jMAVSim, and Flight-gear are useful, these simulators do not reflect in full dynamics of the UAVs in a visualized environment without a significant computational cost. To address this limitation, Solidworks is used to create 3D models of complex objects while being compatible with numerical simulation tools, such as Matlab and Simulink, reducing additional software dependencies.

To demonstrate the digital twin platform, simplified versions of construction objects were created to simulate a hypothetical construction site. These objects include crawler excavators, cement mixer trucks, luffing jib tower cranes, and unfinished buildings, all of which are utilized to simulate realistic construction activities in the virtual scenario. For example, earthwork operations and concrete-pouring processes in real construction require the use of excavators and mixer trucks, which are selected from open-source designs [15], as shown in Figures 4(a) and 4(b). Similarly, the tower crane for heavy lifting and moving materials, such as steel beams or other construction materials, is represented using component-based and parametric design

processes, as illustrated in Figure 4(c). The construction site is also simulated with unfinished buildings featuring exposed concrete floors and columns, and a general floor plan is sketched and duplicated for the upper levels, with supportive pillars patterned accordingly, as depicted in Figure 4(d). In addition, the tower blocks of the building complex appear here as an obstacle for aerial missions. By incorporating these elements into the simulated environment, the digital twin platform provides a more comprehensive and realistic representation of a construction site, enabling users to test and optimize different construction scenarios before real-world execution. Finally, the desired waypoints resulting from the cooperative path planning algorithm are represented as spherical markers, and the interpolated polynomial trajectory is featured to visually examine the MAVs' responses. A virtual environment is then created, as shown in Figure 5.

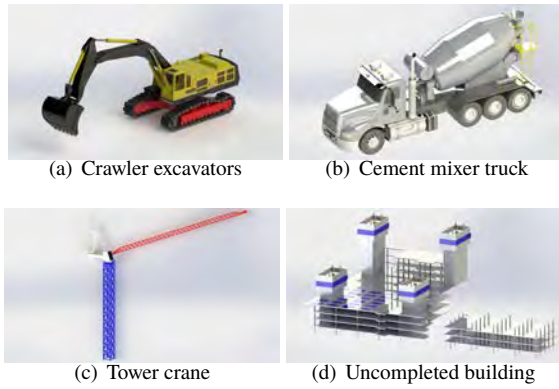


Figure 4. CAD models of equipment and structure

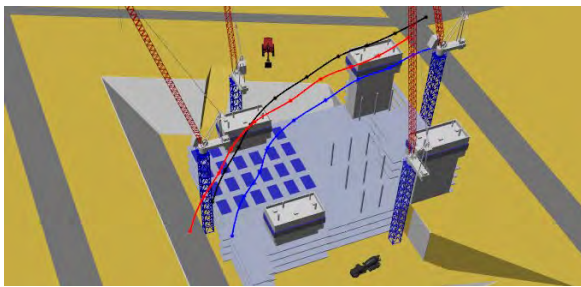


Figure 5. Virtual flight environment.

3.3 Numerical simulation

Given the MAV dynamic model, cooperative path planning and trajectory control algorithms, presented in Section 2, Matlab/Simulink are used to encode the algorithms. The digital twin of the 3DR Solo drone is also rigorously tested through tailored scenarios to verify the validity of the hierarchical control scheme. Figure 6 depicts the simulation model, including three main subsystems: trajectory

generation and control, the MAV swarm, and the environment. Details of these subsystems are presented as follows.

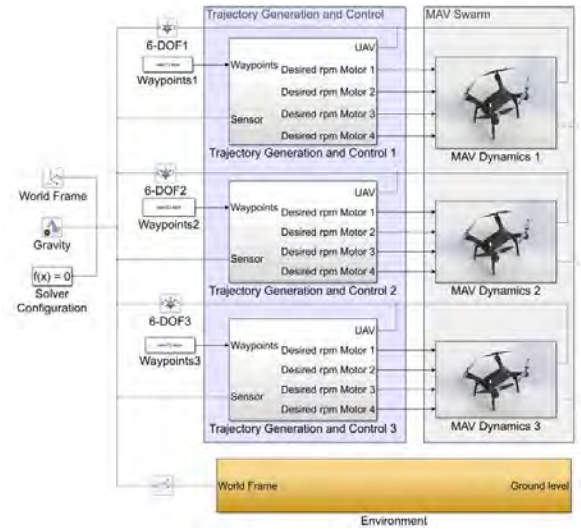


Figure 6. Simulation model

Figure 7 shows a subsystem of a MAV quadcopter. The highest level of this subsystem comprises its structural frame and the propulsion system as designed in Section 3.1. The virtual aerial vehicle is exported from Solidworks through the supported Simscape Multibody Link plug-in between the two environments. As a result, an extensible markup language (.xml) file is generated that describes all of the intrinsic, geometric relationships between each part in a CAD assembly model. After loading this file, a Simscape Multibody model of the multi-rotor is automatically constructed. Minor modifications are conducted to align the CAD model built with common practices in 3D modeling software with the simulation purposes of the digital twin platform. A graphically intuitive way of arranging the propulsion system is intentional for user-friendly purposes. Immobile parts of the drone, such as the four legs and battery, are grouped with the "Quadcopter Chassis" block. This step should vary with different multi-rotor vehicles and depend on how intricate the models need to be in the simulations.



Figure 7. MAV subsystem

Figure 8 displays the environment subsystem, consist-

ing of the blocks for the visualization of the terrain and surroundings of the construction site along with the trajectories of the MAV swarm. For the Simscape Multibody simulation, the world origin connects to every block that is visually represented in the animation. Thus, the "World Frame" is the input to all internal blocks. Exploring the options from the TouchTerrain website, the topography of the construction site is secured in the standard triangulation language (.stl) file format. The terrain is included in the digital twin platform via a script that reads and converts a .stl file into a compatible data type for the "Rigid Terrain Grid Surface" block. Besides, the "Construction Site" block allows the direct integration of stationary CAD models of background objects into the interested test cases. Meanwhile, the "Trajectory" block enables the incorporation of markers for waypoints and the visualization of planned paths. Utilizing these blocks, the surroundings for different MAV missions can be realized within the Mechanics Explorer.

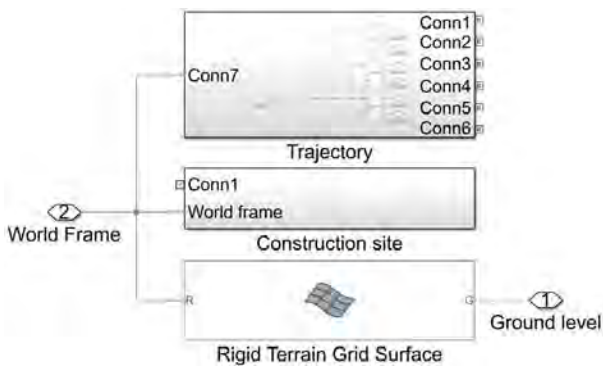
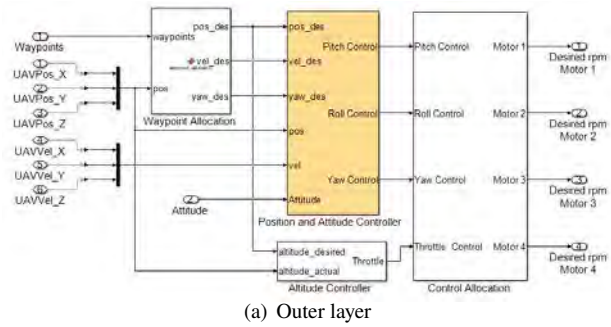
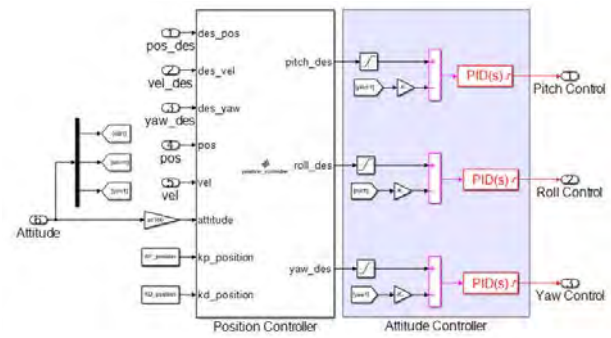


Figure 8. Environment subsystem

Figure 9(a) depicts the outer layer of the "Trajectory Generation and Control" block for one MAV. In the figure, the "Waypoint Allocation" block receives the waypoints produced by the cooperative path planning algorithm. The logic of the block sequentially assigns a new destination to the vehicle when an acceptable range to a waypoint is reached. The block will attempt to steer the vehicle to the final waypoint. The positional references are then sent to the controllers. In the "Position and Attitude Controller" block, as expanded in Figure 9(b), the position control initially receives the desired longitudinal and latitudinal values. Three major steps are executed in this block. Firstly, corrections are applied to the position errors in the form of PD gains. Then, an intermediate conversion from x and y positions to the required orientation, in this case, roll-pitch-yaw angles, is completed. Finally, the attitude PID controller attempts to improve the current rotational values accordingly. Simultaneously, the desired altitude is fed to the "Altitude Controller", at the outer layer, for appropriate adjustments to the resultant thrust. The outputs



(a) Outer layer



(b) Position and attitude controller block

Figure 9. Trajectory generation and control block

of the attitude and altitude controllers are converted into more intuitive motor revolutions for the following operations, performed in the "Control Allocation" block. The required RPM for each specific motor is then available for employment from the "MAV Dynamics" subsystem.

4 Results

4.1 Case study

To demonstrate the capabilities of our digital twin model, we conducted a virtual surveillance scenario at the Western Sydney International Nancy-Bird Walton Airport, located at coordinates $33^{\circ}53'17''S$ $150^{\circ}42'53''E$, which is currently under construction in Badgerys Creek, New South Wales, Australia [16]. The digitalized airport comprises integrated 3D models organized into a singular scenario. The terrain within the terminal building has been tailored to mimic specific steep and smooth areas, while the surrounding landscape remains flat due to the initial earthwork phase of construction. To supplement a realistic layer, asphalt roads for material transportation and future runways were introduced. The number of earthmoving equipment in the simulation was carefully selected to balance computational demands and visualization characteristics, resulting in a necessary number of construction vehicles being imported into the simulation. The rising tower blocks of the main building and the height of the luffing jib cranes pose the primary challenges for the aerial inspection task, with all objects being positioned on the

map to reflect the actual construction site.

The aim is to deploy a team of MAVs, configured with desired geometrical shapes from the initial to final locations, to carry out an on-site surveillance task. Our model utilized the GPSO algorithm to generate optimized, collision-free, and formation-preserving routes for the team, taking into account the environment's obstacles, as depicted in Figure 10. To ensure safe navigation of MAVs around obstacles while maintaining the desired formation, yellow cylinders were created around the tower mast to represent threat zones. The MAVs' altitudes were also constrained by the tops of the unfinished buildings and the minimum height of the crane's boom. Additionally, a cascade trajectory tracking controller was employed to ensure that the MAVs followed their planned routes accurately. This controller continuously monitored each MAV's position and velocity, comparing them to the planned trajectories, and made necessary adjustments to keep the MAVs on track.

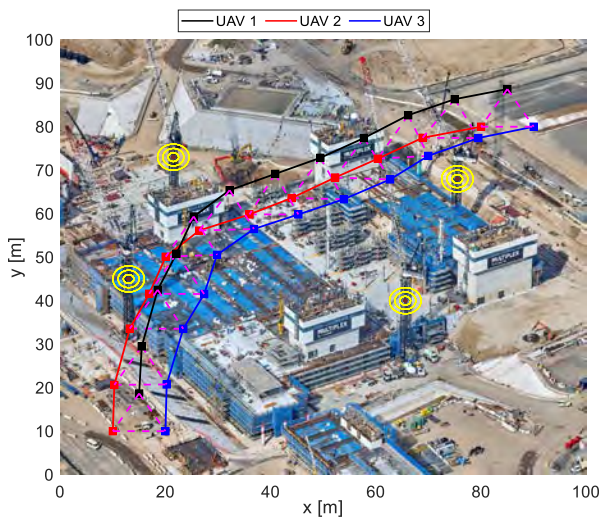


Figure 10. MAV paths on a construction site.

4.2 Normal operation

In the first test, a team of three MAVs using cascade controllers performed their mission, i.e., tracked their desired trajectory as in a normal operation. To evaluate the controller's robustness under any external excitation sources, e.g. winds, a random disturbance was introduced into the simulation model. Using the proposed digital twin platform, one can evaluate the response of MAVs as well as the performance of control and trajectory tracking algorithms, and hence improve them. A simulation scenario is depicted in Figure 11. As can be seen in the figure, the team of MAV can follow their reference without colliding with obstacles. However, the tracking error employing the current cascade controller is apparent. Accordingly, other advanced control techniques are suggested, such as iter-

ative learning sliding mode control [17]. This is a huge benefit of the proposed digital twin.

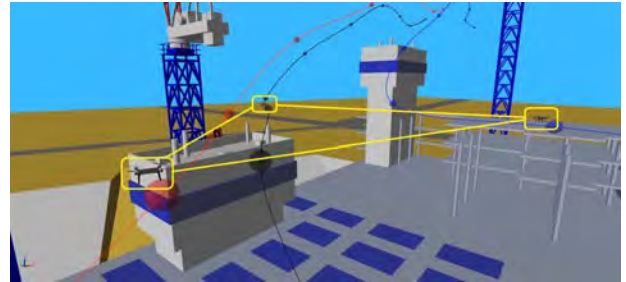


Figure 11. A visualization scenario.

4.3 Faulty operation

To further demonstrate the merit of the digital twin, another simulation is conducted with a faulty motor in one MAV. In this test, the electrical signal sent to one motor of the leader drone is disconnected during the mission. The result is shown in Figure 12. As can be expected, the 3DR Solo drone using cascade PID control is unable to continue flying and drops to the ground. For tolerance control, it is suggested to develop other types of MAV with more rotors, e.g., hexacopters or octocopters, and design a fault controller such as the one presented in [18].

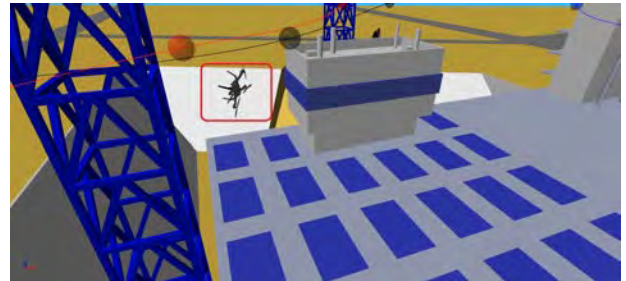


Figure 12. MAV in a faulty operation.

4.4 Discussion

Simulation results demonstrate that the digital twin model was able to generate optimal routes and trajectories for the MAV team, resulting in a safe and efficient completion of the inspection mission. The real-world scenario highlights the potential of the digital twin model to visually test the operation of a MAV team in complex and dynamic environments, such as construction sites, for safety purposes. By providing a virtual replica of the environment, the digital twin model can help optimize the flight paths of MAV teams before they are deployed to the actual site, reducing the risk of accidents and improving the quality and efficiency of the operation.

5 Conclusion

This paper has presented a digital twin platform for MAV path planning and trajectory tracking control. The physical quadcopter, one of the most typical MAVs, was digitalized into a 3D CAD model in the Solidworks software. The virtual construction site was formed by integrating CAD models of structures, vehicles, and MAVs in the common Simscape Multibody environment. Matlab/Simulink was employed to encode the working principles, path planning, and tracking algorithms of the MAV swarm. The simulation platform was validated with a team of MAVs employed in an inspection task on a construction site, demonstrating the efficacy of the proposed digital twin approach. While the system is computationally efficient and accurate in simulating the motion of aerial vehicles, validation in complex real-world scenarios will be necessary to fully assess its effectiveness. Our future work will also focus on extending the framework to dynamic environments.

References

- [1] A. Bulgakov, D. Sayfeddine, T. Bock, and A. Fares. Generation of orthomosaic model for construction site using unmanned aerial vehicle. In *ISARC. Proceedings of the International Symposium on Automation and Robotics in Construction*, volume 37, pages 900–904. IAARC Publications, 2020.
- [2] N. Bolourian, M. M. Soltani, A. H. Albahria, and A. Hammad. High level framework for bridge inspection using lidar-equipped uav. In *ISARC. Proceedings of the International Symposium on Automation and Robotics in Construction*, volume 34. IAARC Publications, 2017.
- [3] J. Grzybowski, K. Latos, and R. Czyba. Low-cost autonomous uav-based solutions to package delivery logistics. In *Advanced, Contemporary Control*, pages 500–507. Springer, 2020.
- [4] Michael W Grieves. Product lifecycle management: the new paradigm for enterprises. *International Journal of Product Development*, 2(1-2):71–84, 2005.
- [5] E. G. Kaigom and J. Roßmann. Value-driven robotic digital twins in cyber-physical applications. *IEEE Trans. Industr. Inform.*, 17(5):3609–3619, 2020.
- [6] Z. Hu, S. Lou, Y. Xing, X. Wang, D. Cao, and C. Lv. Review and perspectives on driver digital twin and its enabling technologies for intelligent vehicles. *IEEE trans. intell. veh.*, 2022.
- [7] Y. Yang, W. Meng, H. Li, R. Lu, and M. Fu. A digital twin platform for multi-rotor uav. In *2021 40th Chinese Control Conference (CCC)*, pages 7909–7913. IEEE, 2021.
- [8] L. Lei, G. Shen, L. Zhang, and Z. Li. Toward intelligent cooperation of uav swarms: When machine learning meets digital twin. *IEEE Network*, 35(1): 386–392, 2020.
- [9] F. Jiang, L. Ma, T. Broyd, and K. Chen. Digital twin and its implementations in the civil engineering sector. *Autom. Constr.*, 130:103838, 2021.
- [10] Y. Jiang, M. Li, D. Guo, W. Wu, R. Y. Zhong, and G. Q. Huang. Digital twin-enabled smart modular integrated construction system for on-site assembly. *Computers in Industry*, 136:103594, 2022.
- [11] J. Zhang, R. Wang, G. Yang, K. Liu, C. Gao, Y. Zhai, X. Chen, and B. M. Chen. Sim-in-real: Digital twin based uav inspection process. In *2022 International Conference on Unmanned Aircraft Systems (ICUAS)*, pages 784–801. IEEE, 2022.
- [12] K. Benzaid, N. Mansouri, and O. Labbani-Igbida. A generalized dynamical model and control approach applied to multirotor aerial systems. In *2016 8th International Conference on Modelling, Identification and Control (ICMIC)*, pages 225–230. IEEE, 2016.
- [13] L. V. Nguyen, I. T. Herrera, T. H. Le, M.D. Phung, R. P. Aguilera, and Q. P. Ha. Stag hunt game-based approach for cooperative uavs. In *ISARC. Proceedings of the International Symposium on Automation and Robotics in Construction*, volume 39, pages 367–374. IAARC Publications, 2022.
- [14] L. V. Nguyen, M. D. Phung, and Q. P. Ha. Game theory-based optimal cooperative path planning for multiple uavs. *IEEE Access*, 10:108034–108045, 2022.
- [15] URL <https://grabcad.com/library>.
- [16] URL https://en.wikipedia.org/wiki/Western_Sydney_Airport.
- [17] L. V. Nguyen, M. D. Phung, and Q. P. Ha. Iterative learning sliding mode control for uav trajectory tracking. *Electronics*, 10(20):2474, 2021.
- [18] G. Michieletto, M. Ryll, and A. Franchi. Control of statically hoverable multi-rotor aerial vehicles and application to rotor-failure robustness for hexarotors. In *2017 IEEE International Conference on Robotics and Automation (ICRA)*, pages 2747–2752. IEEE, 2017.

Development of a Blade Lifting Control Assist System for a Motor Grader

Ekin Cansu Özkan Öztürk¹, Ufuk Akpınarlı¹ İlhan Varol¹ Yavuz Samim Ünlüsoy² and Klaus Werner Schmidt³

¹Hidromek-Hidrolik ve Mekanik Makina İmalat Sanayi ve Ticaret A.Ş., Turkey

²Middle East Technical University, Mechanical Engineering Department, Turkey

³Middle East Technical University, Electrical and Electronics Engineering Department, Turkey
ekin.ozkan@hidromek.com.tr, ufuk.akpinarli@hidromek.com.tr, ilhan.varol@hidromek.com.tr,
unlusoy@metu.edu.tr, schmidt@metu.edu.tr

Abstract –

Precise blade control is a central task when automating the operation of motor graders. This paper focuses on the parallel lifting movement using a combination of feedforward and feedback control for controlling the respective lifting cylinders. To this end, the paper first examines the blade mechanism of a motor grader and defines its blade movements. Specifically, the mathematical relationship between the edge points of the blade and the lifting cylinders were obtained using 3D CAD data. Then, the hydraulic behavior of the system was analysed in a test environment with wire encoders that are embedded in the lifting cylinders of the real mechanism. Using the input/output relationship between the ‘Desired Stroke’ and the ‘Actual Stroke’ values in different experiments, system identification was applied and the system transfer functions were obtained. Then, a combination of feedforward and feedback control enables moving to desired positions fast while applying precise blade control.

Keywords – motor grader; automatic blade function control; system control algorithm

1 Introduction

Motor graders are construction machines used in specific works such as road construction and leveling/grading. Motor graders can reach high driving speeds. Since they perform machine functions while traveling, their operation can be challenging. Issues such as accidents that may occur at work sites, the accuracy of the levelling, fuel consumption and time have paved the way for studies on assistive systems to help operators [1-4].

Automatic function control from these systems is not only in demand in motor graders but also in other construction machines such as excavators and wheel loaders. GPS, laser, ultrasonic, and distance sensors are

used in such assist systems. The aforementioned system items can be mounted outside of the vehicles. In this study, a control system was developed to assist the parallel lifting movement of the blade during fine grading by using the data obtain from the sensors mounted in the lifting cylinders.

2 Background

Hashimoto and Fujino [5], pointed out that the number of experienced operators will decrease in the near future and the results of this will negatively affect the construction industry. They compared experienced and inexperienced motor grader operators with reference to working time, working efficiency and work quality. Then, both operators tested the automatic control system for the blade control. The study showed that inexperienced operators had better results in terms of work when they have used machine control systems. The shortage of experienced operators foreseen in the near future can be substituted by using automatic control systems.

Sobczyk et al. [6] stated in their studies that the leveling errors created by the motor graders were also caused by the positioning of the front wheels. They aimed to prevent the errors with the stabilization system presented in their study. The model they created serves to determine the position of the blade during movement of the front frame. The position of the blade is constantly compared with the selected reference point in the working area. Accordingly, the cylinder stroke values are recalculated and the blade is positioned correctly.

Felas et al. [7], developed a detailed nonlinear dynamic model using hydraulic system equations and the wheel loader mechanism analysis. The machine they have used in their study is equipped with a load-sensing hydraulic pump, various cylinders and electro-hydraulic valves. While obtaining the hydraulic equations in the study, it is necessary to know the parameters of the elements from which the system is formed.

Shevchenko and Bezsennaya [8] mentioned in their study that the loads on the motor grader lifting cylinders have a significant effect on the mechanism design. To express the changes in the loads on the axes occurring at the connection points of the lifting cylinders, the reference coordinate frame is positioned at the connection point of the blade with the front chassis. As a result of the movement of the cylinders, it has been observed that the loads vary according to the axes.

3 Methodology and Development

In this section, first, all mechanism movements are defined. Then, analysis was made within the necessary mechanism constraints for parallel lifting and the equations required for mechanism analysis are obtained using least squares regression using Matlab [11]. In the last chapter of Section 3, the obtained equations are verified on the real mechanism.

3.1 Blade Mechanism

The motor grader blade mechanism consists of six hydraulic cylinders and one hydraulic motor. Figure 1 and Figure 2 show the mechanism components. The Right and Left Lifting Cylinders move the blade upwards and downwards. The Right and Left Tilting Cylinders create a different soil cutting angle on the blade edge concerning the working terrain. The side shift cylinder moves the blade in sidewise right and left directions. Finally, the hydraulic motor mounted in the circle rotates the mechanism clockwise or counter-clockwise [10]. See Figure 1 and Figure 2.

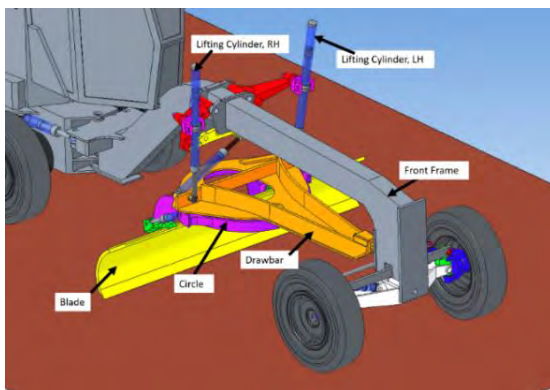


Figure 1. Blade Mechanism-Front View

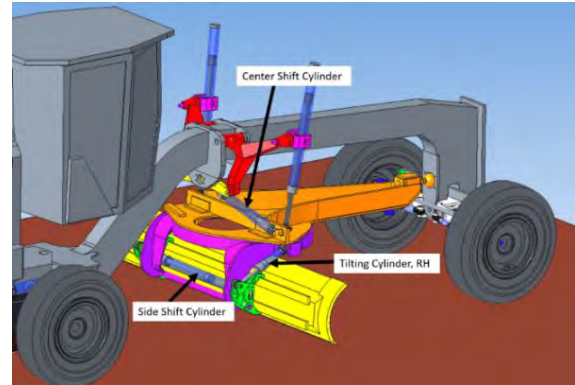


Figure 2. Blade Mechanism-Rear View

3.2 Mechanism Analysis

The motor grader blade mechanism analysis is very challenging since the mechanism has many different combinations of positions [9]. In this study, the main coordinate frame is placed on the grader's front frame and is taken as a reference while the blade edge position values are recorded. The points at the right and left sides of the blade edge are named B1 and B2, respectively.

3.2.1 Collecting Data Using CAD Model

The drawbar and front chassis connection is provided by a spherical joint as pointed out in Figure 1. The position of this connection point is not affected by blade mechanism movements. Only the tire size can change the ground clearance of this anchor point. This connection point on the vehicle is suitable for positioning the XYZ reference coordinate system. In the neutral position defined in Figure 3, XYZ coordinate systems are placed on the right and left edges of the blade. The X-axis represents the vehicle's driving direction, and the Z-axis represents the vertical axis of the machine itself as indicated in Figure 4.

The mechanism tool of PTC Creo 7.0.1.0 [12] was used to find the positions of the cutting edge of the blade in 3-axes concerning a fixed point on the machine at various stroke values of the lifting cylinders. Values were recorded at 1 mm intervals.

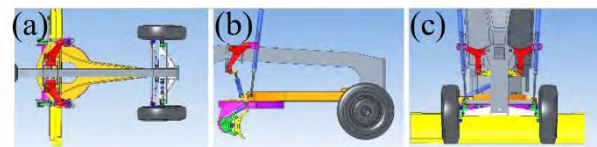


Figure 3. Restriction of Blade Mechanism:
(a) 0° Circle Rotation, (b) 0° Blade Cutting Edge Angle, (c) Side Shift Cylinder is Centered

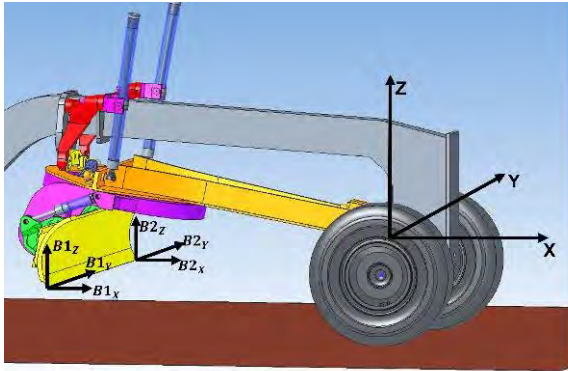


Figure 4. Edge Points B1 and B2 and Coordinate Frames XYZ

3.2.2 Mechanism Equations Using Basic Fitting Method

Considering the limitations in Figure 3, parallel lifting is used to determine the height of the blade from the ground. In other words, the z-axis values from the data collected for the cutting edges of the blade will be sufficient to describe the parallel lifting. The least squares regression method was used to express the relations between the stroke values of the lifting cylinders and the edge points of the blade. For parallel lifting, the right lifting cylinder affects the right edge, and the left lifting cylinder affects the left edge of the blade. Figure 5 and Figure 6 show the basic fitting results for both edges.

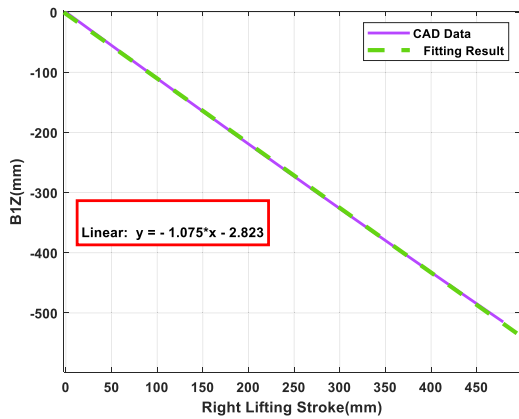


Figure 5. Right Lifting Stroke vs B1Z

The resulting equations (1) and (2) characterize the mathematical relation between the respective lifting stroke and z-coordinate of B1 and B2.

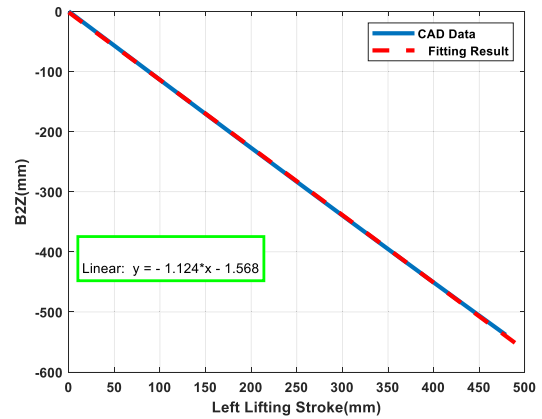


Figure 6. Left Lifting Stroke vs B2Z

$$B1_z = -1.075(RightLiftingStroke) \quad (1)$$

$$B2_z = -1.124(LeftLiftingStroke) \quad (2)$$

3.3 Implementation and Verification

A test environment was set up to test the accuracy of the equations obtained in Section 3.2.2 on the machine. Wire encoders are mounted inside the right and left cylinders to measure their stroke value (See Figure 7 and Figure 8). The wire is attached to the cylinder's rod, and it lengthens or shortens during the movement of the cylinder. The sensor calculates the length of the wire from each turn of its mechanism with the movement of the cylinder rod. Thus, the stroke values can be read.

During the test, the system is given a value for the movement of the blade on the z-axis. The system converts this height value to stroke value and the cylinders start to move. Wire encoders [13] measure stroke values. Then, the initial and final positions of the edge points of the blade are compared.



Figure 7. Draw-wire Encoder



Figure 8. Sensor-Cylinder Integration

The machine is positioned on a flat ground to examine the initial and final positions of the blade cutting edge. The mechanism is placed on the neutral position. The distance of the blade's cutting edge from the ground is measured. Then, the 'Desired Height' value is entered into the system and the lifting cylinders start to move. When the movement is complete, the distance from the ground for the new position of the blade is re-measured and the 'Desired Height' value is compared with the 'Actual Height'. As a result of the comparisons, it has been revealed that (1) and (2) are applicable equations for the real mechanism.

4 Controller Design

The flow generated by the hydraulic pump drives the cylinders through electro-hydraulic valves. The joystick movements provide the amount of flow that will pass through the valve. When the joystick moves forward or backward on the x and y axes, it generates a current for each movement on the axis (See Figure 9). These movements in the joystick axes are expressed as percentages. The rest position of the joystick is called the zero position, and it takes 0% of joystick value (JV). This generated joystick value is converted into a PWM signal with a PID controller, and the valve spool is energized by the generated PWM (See Figure 10). The higher the joystick value, the more flow passes through the electro-hydraulic valve.

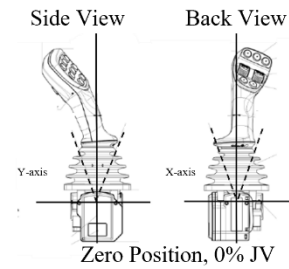


Figure 9. Joystick Representation

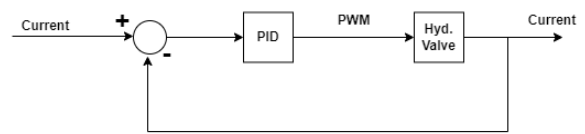


Figure 10. Electro-hydraulic Valve Working Principle

Draw-wire sensor data obtained from the machine can be used to describe the behavior of the hydraulic system. Using equations (1) and (2), the stroke values of the right and left cylinders are calculated from the 'Desired Height' value entered in the system. These values are hereafter referred to as 'Calculated Stroke'. By using the input/output relationship of the 'Actual Stroke' values coming from the sensor denoted as $y(t)$ in (4) and 'Calculated Stroke' values denoted as $u(t)$ in (5), the transfer function $G(s)$ can be calculated with reference to certain joystick values of the hydraulic system by system identification. Joystick values can range from 0% to 100%. To define the system behavior, three different joystick values have been selected for the first tests. These values represent slow, medium, and fast cylinder speeds. (See Figure 11). When tests were performed, the machine was in parking mode and had an engine speed of 800 RPM. Data were taken at 100 ms (10 Hz) intervals (see sampling time T_s in (5)).

$$u(t) = [u(Ts), u(2Ts), \dots, u(NTs)] \quad (3)$$

$$y(t) = [y(Ts), y(2Ts), \dots, y(NTs)] \quad (4)$$

$$T_s = 0.1 \text{ sec} \quad (5)$$

$$G(s) = \frac{y(s)}{u(s)} \quad (6)$$

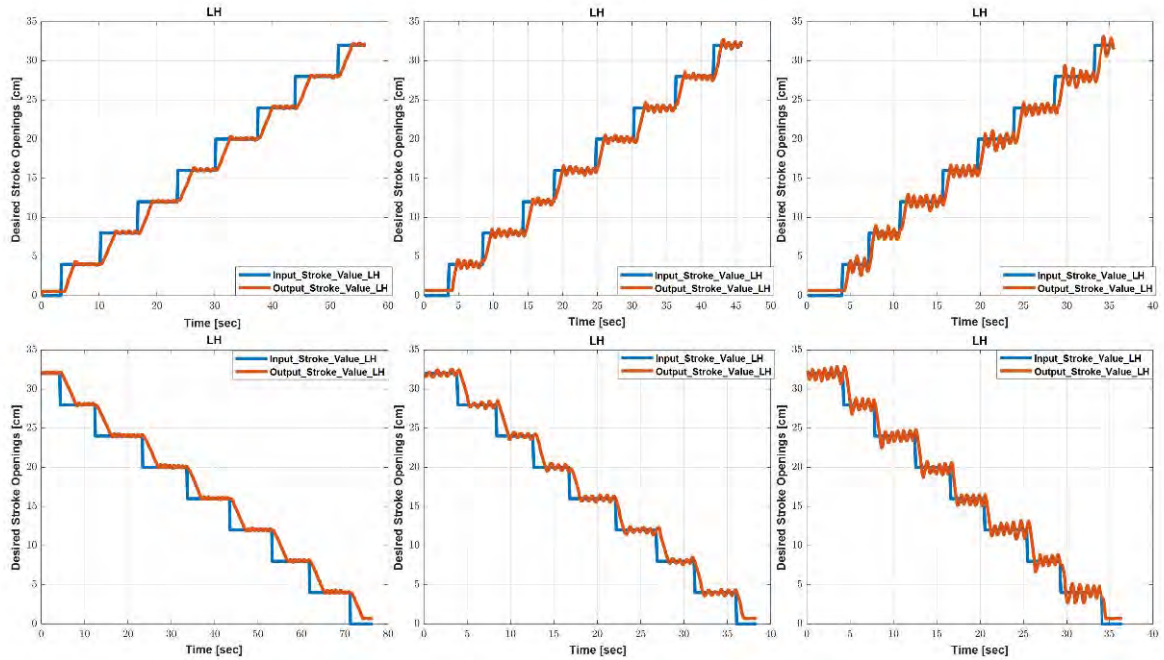


Figure 11. JV Effects with Desired and Actual Stroke Openings

The following relation is shown to exemplify the transfer functions obtained.

$$TFLH = e^{-0.214s} \frac{0.1453s + 1.5471}{s^2 + 1.7544s + 1.5467} \quad (7)$$

$$TFRH = e^{-0.428s} \frac{0.3036s + 1.2182}{s^2 + 1.6008s + 1.2182} \quad (8)$$

Here, TFLH, and TFRH define the transfer function of Left Side and Right Side, respectively.

Also, it has been observed that there is a delay between the input/output stroke values while obtaining transfer functions. These delays may occur for different reasons originating from hydraulics or electronics. To have a better understanding of this delay, Current/PWM graphs were plotted and the parameters were compared at different joystick values. When the graphs are examined, it can be seen that there is no any delay between PWM and Current. An example measurement is shown in Figure 12.

A certain amount of time is required when hydraulic oil fills or drains from the cylinders. The reason for the delay between input/output is that the response speed of the hydraulic system cannot reach the response speed of the electronics.

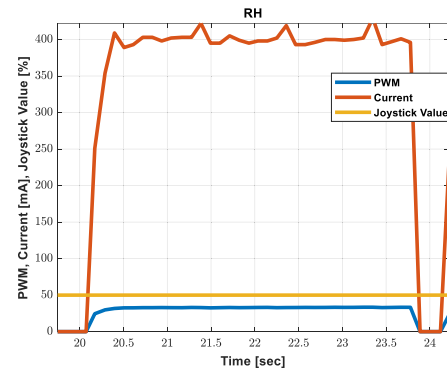


Figure 12. PWM/Current Graph for %50 JV

When the input/output relations in Figure 13 are examined, it is seen that the behavior of the hydraulic system is similar at different JVs. In response to the 'Desired Stroke' value given to the system as step input, the system always reacts as an integrator. Depending on the joystick values, the extraction and retraction speeds of the cylinders vary. The higher joystick values are given, the higher the hydraulic oil flowing through the valves, since the current equivalent of the joystick values is converted to PWM and activates the valves (See Figure 13).

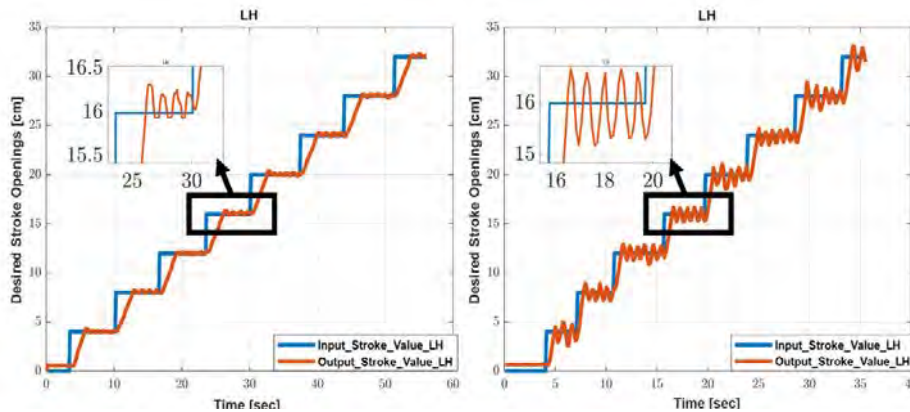


Figure 13. JV Effects with Desired and Actual Stroke Openings in 20% and 80% JVs

The slopes of the graphs give the cylinder velocities in cm/sec. Table 1 represents the cylinder velocities for the test results in Figure 13. The reason for obtaining the values in Table 1 was to see if there was a linear proportionality between the cylinder speeds and joystick values. However, such a relationship could not be seen for these three joystick values. For this reason, cylinder velocities from 10% to 80% of joystick values were calculated. As seen in Figure 14, cylinder speeds from 10% to 30% show linear behavior. This means that in the control algorithm to be created, the hydraulic cylinders can be activated up to a certain level with a constant joystick value of 30%.

Table 1. Calculated Cylinder Speeds

cm/sec	RH	LH
JV20_Down	1.07	1.07
JV20_Up	1.68	1.72
JV50_Down	2.90	3.50
JV50_Up	4.80	3.95
JV80_Down	6.48	6.98
JV80_Up	5.88	6.17

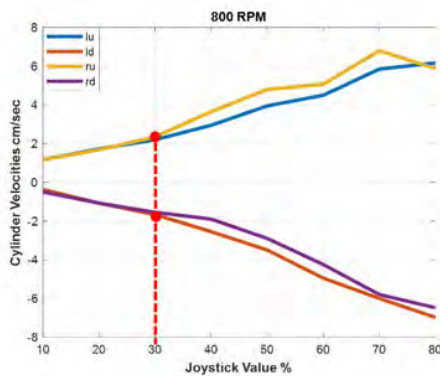


Figure 14. Cylinder Velocities Calculation

Equations (7), (8), (9) ve (10), indicate the relationship of cylinder velocities with joystick values x in % for upward and downward directions.

$$lu = 0.076 \cdot x \quad (7)$$

$$ld = -0.097 \cdot x \quad (8)$$

$$ru = 0.081 \cdot x \quad (9)$$

$$rd = -0.089 \cdot x \quad (10)$$

Here, lu , ld , ru and rd are cylinder velocities in upward and downward directions.

Figure 15 shows the control algorithm flow diagram. According to the figure, the value of ‘Desired Height’ is entered into the system. Then, the system calculates the ‘Desired Stroke’ value and compares it with the ‘Actual Stroke’ value read from the sensor. If the two values are very close to each other (a 5 mm difference was taken in this study), the PI controller is switched on to ensure precise control. Here, the system continuously calculates the joystick value according to the distance to provide precise position control, PWM is produced accordingly and the valves are activated. If the difference between the ‘Desired Stroke’ and ‘Actual Stroke’ values is large, a feedforward controller is used. The cylinders start to move with a 30% joystick value until the distance where the PI controller run is reached. The decision of which controller to operate is made in the switch block. The block called plant represents the characteristics of an electro-hydraulic valve (See Figure 16).

To determine the coefficients of the PI controller, the algorithm was first tested on the machine for different KP coefficients. Figure 17 and Figure 18 show the test results with a KP value of 2.5. In the tests taken for both the right and left cylinders, precise cylinder position control up to 3 mm was achieved.

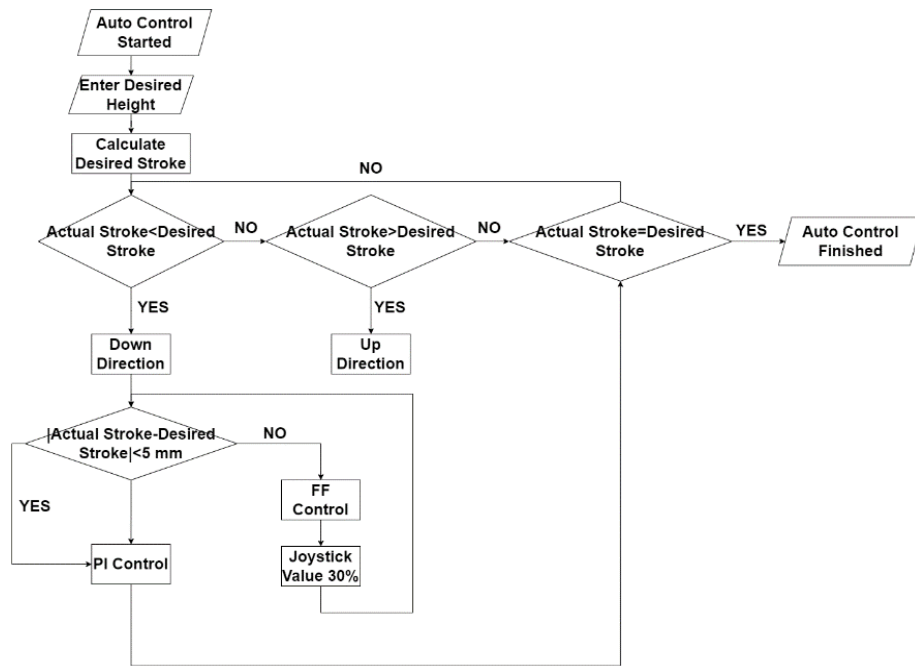


Figure 15. Control Algorithm

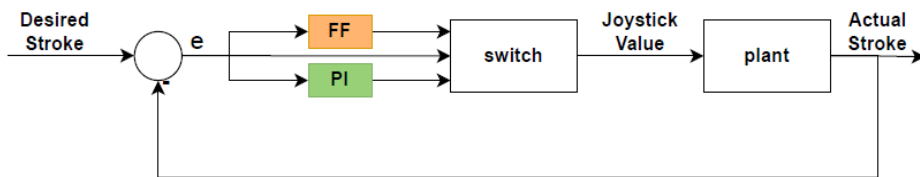


Figure 16. Overall Control Structure

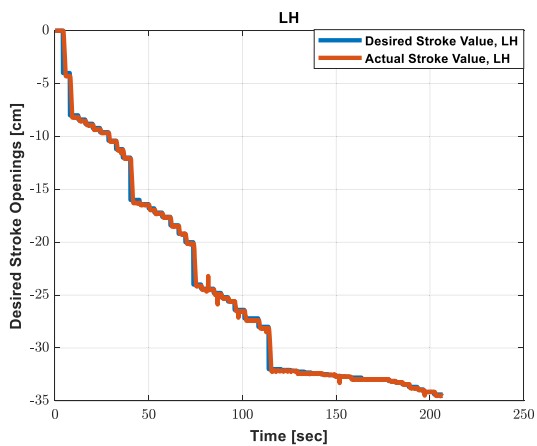


Figure 17. Left Lifting Cylinder, Down Direction, KP Value is 2.5

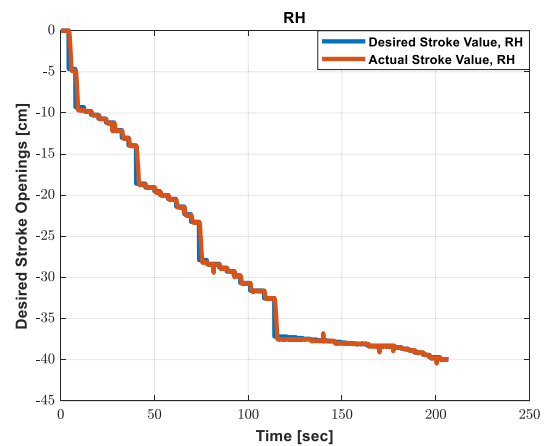


Figure 18. Right Lifting Cylinder, Down Direction, KP Value is 2.5

5 Conclusion and Future Work

This study provides parallel lifting control, which is the first stage of automatic function control for the motor grader blade mechanism. Since the expression of the motor grader blade mechanism using kinematic equations is challenging, the analysis technique used in this study can be applied for similar mechanisms which have 3D CAD data. However, the important point is that the obtained equations should be continuous, that is a single equation should be applicable for many models.

The created control algorithm provides precise stroke control, and the algorithm has been verified by various tests taken on the machine. The control algorithm parameters were obtained using data taken at 800 RPM engine speed but can be used at other RPM values, because the controller was created by considering the distance, not fluid displacement. The external loads on the blade will be a subject of further research.

Certain mechanism constraints were accepted for the analysis. Specifically, this study has aimed at developing an assist system where operators can easily adjust the height of the blade from the terrain. In future studies, improvements can be made by adding sensors to the system for circle rotation, blade tilt angle, and blade slope. In this way, automatic function control will be provided for different terrain conditions by considering both blade and machine positions. In this way, automatic function control will be provided for different terrain conditions by considering both blade and machine positions. Accordingly, the assist system will be extended by improved control algorithms based on the additional sensor measurements.

Acknowledgment

This study is supported by Hidromek-Hidrolik ve Mekanik Makina İmalat Sanayi ve Ticaret A.Ş. and is within the scope of a project supported by TUBITAK-TEYDEB.

References

- [1] Galitskov K. S., Nazarov M. A. and Lukyanov A. S. Studying the dynamics of the automatic control system for the elevation position of a motor grader blade with an alternative position sensor. *IOP Conference Series: Materials Science and Engineering*, 103: 012021, 2021.
- [2] Shevchenko V., Chaplyhina O., Pimonov I., Reznikov O. and Ponikarovska S. Mathematical model of a motor-grader movement in the process of performing working operations. *IOP Conference Series: Materials Science and Engineering*, 985:012009, 2020.
- [3] Zhulai V., Tyunin V., Shchienko A., Volkov N. and Degtev D. Analytical determination of fuel economy characteristics of earth-moving machines. *Energy Management of Municipal Transportation Facilities and Transport*, 282-289, 2019.
- [4] Kumar V., Malleth G. and Radhakrishna K. R. Finite Element Analysis of a Two-Post Rollover Protective Structure of an off-Highway Motor Grader. *Trends in Mechanical and Biomedical Design*, 355-366, 2021.
- [5] Hashimoto T. and Fujino K. Comparative Study of Experienced and Inexperienced Operators with Auto-controlled Construction Machine, *36th International Symposium on Automation and Robotics in Construction*, 658-664, Banff, Canada, 2019.
- [6] Sobczyk A. and Grezegorz T. Grader blade stabilization system, *Automation in Construction*, 7: 385-389, 1998.
- [7] Fales R. and Kelkar A. Robust control design for a wheel loader using H_∞ and feedback linearization-based methods. *ISA Transactions*, 48: 312-320, 2009.
- [8] Shevchenko V. and Beztseynaya Zh. A Method to Estimate Loading of a Motor-Grader Blade Control Hydraulic Cylinders. *International Scientific Journal "Machines, Technologies, Materials"*, 12: 75-77, 2015.
- [9] Pan Y. and Callojo A. Identification, design and kinematic analysis of an earthmoving mechanism, *Journal of Terramechanics*, 66: 27-39, 2016.
- [10] Ozkan E.C. and Ergezer H. Kinematics Analysis and Position Control of Motor Grader Blade Mechanism for Automatic Levelling. In *8th International Conference on Control, Decision and Information Technologies (CoDIT)*, 237-242, İstanbul, Turkey, 2022.
- [11] <https://www.mathworks.com/products/matlab.html>
- [12] <https://www.ptc.com/en/products/creo>
- [13] <https://www.siko-global.com/en-de/products/linearline-draw-wire-encoders/position-sensors-for-hydraulic-cylinders>

Development and evaluation of a low-cost passive wearable exoskeleton system for improving safety and health performance of construction workers: A pilot study

Shahnawaz Anwer¹; Heng Li¹; Mohammed Abdul-Rahman¹; and Maxwell Fordjour Antwi-Afari²

¹Department of Building and Real Estate, The Hong Kong Polytechnic University, Hong Kong SAR

²Department of Civil Engineering, College of Engineering and Physical Sciences, Aston University, United Kingdom

shah-nawaz.anwer@polyu.edu.hk, heng.li@polyu.edu.hk, dr-mo.abdulrahman@polyu.edu.hk,
m.antwifari@aston.ac.uk

Abstract –

Construction workers have an increased risk of having muscle fatigue and musculoskeletal injuries, among other non-fatal workplace injuries. As a result, this project aimed to develop and evaluate a low-cost passive wearable exoskeleton system for improving construction workers' safety and health performance, mainly by mitigating the risk of developing musculoskeletal pain and fatigue. Surface electromyography (sEMG) was used to evaluate muscle activity in the Thoracic Erector Spinae (TES) and Lumbar Erector Spinae (LES) at the L3 and T12 vertebrae level, respectively, during repetitive handling tasks. In addition, both subjective (e.g., rating of the fatigue scale) and objective fatigue indicators (e.g., heart rate, skin temperature) were employed to assess fatigue. Exoskeleton use was associated with a 30% decrease in LES muscle activation compared to baseline. The application of an exoskeleton had a similar effect on the TES, decreasing muscle activity by 12%. When using an exoskeleton, a participant's neck kinematics were reduced by 23%, their low back kinematics by 11%, their hip kinematics by 5%, and their knee kinematics by 36%. Exoskeleton use was associated with a 13% decrease in heart rate and a 67% decrease in perceived fatigue. Nonetheless, skin temperature was raised by around 2% while using an exoskeleton compared to when not using one. Our preliminary findings suggest that the passive exoskeleton system could be an effective ergonomic intervention tool for assisting construction workers engaged in manual repetitive handling activities.

Keywords –

Construction safety; Exoskeleton device; Fatigue; Musculoskeletal injury

1 Introduction

Both developed and emerging economies rely heavily on the construction industry [1]. In many countries around the world, the construction industry contributes between 9

and 15% of GDP [2]. Despite its immense economic contribution, the construction industry is widely seen as a high-risk sector with poor safety, health, and productivity performance around the world. More than 700 people are killed and over 200,000 are injured while working every year in the United States, according to the Bureau of Labor Statistics (BLS) [3]. The annual cost of construction injuries exceeds \$48 billion, having a significant impact on the success of projects, profit margins, and the financial sustainability of construction companies [4]. Exposure to frequent motions, vibration, force, and awkward working positions are all recognized to contribute to or worsen the increased risk of fatigue and injury among construction workers [5].

Several engineering, ergonomic, and management interventions have been used in previous studies to reduce the risk of musculoskeletal injuries, such as: (1) reducing the weight of lifting loads (e.g., concrete blocks); (2) increasing the initial lifting height [6,7]; (3) team working, but not alone [8]; (4) estimating the normative duration of lifting before subjective fatigue [9]; and (5) education and awareness [10]. In theory, these interventions should have a positive impact on worker productivity and safety, but in practice, the dynamic and unpredictable nature of construction sites makes implementation difficult. In addition, many construction activities are still carried out by personnel in laborious, repetitive tasks. Other potential ergonomic measures may be necessary to reduce the high incidence of these risk factors among construction workers.

Researchers are increasingly interested in developing human-robot collaboration to alleviate the burden of monotonous and repetitive tasks on human employees. [11]. As a human-robot collaboration idea, wearable exoskeletons are one of the most promising for construction-related jobs such as repetitive lifts and lowering. When worn, an exoskeleton is a mechanical support device that helps sustain the user's weight by applying torque. Worker fatigue, productivity, and risk management can all be improved using exoskeletons. This technology can be used for both return-to-work and prevention activities. In addition to allowing a worker to execute a task with less effort and thus less danger of

damage, certain exoskeleton technologies provide workers with feedback to ensure safe actions [12]. Return-to-work programs and productivity could both benefit from the use of these tools. For example, a shoulder support exoskeleton that holds the weight of the arm could allow a worker to remain in an awkward position for a longer period with substantially less effort [13]. An exoskeleton, on the other hand, has the potential to improve the quality and productivity of workers as well as reduce the risk of injury [14].

Exoskeletons can be described based on 1) whether they are powered or not (passive or active), 2) which body parts they cover (e.g., entire body, upper limb, lower limb, and body extension), and 3) the materials used to make them (e.g., rigid, or soft). Exoskeleton suits have become increasingly popular in the construction industry because of technological advancements in both wearable and robotic technology. A previous study has investigated the feasibility of exoskeleton for construction workers and highlighted the necessity to evaluate their short- and long-term effects on safety and health, user acceptability, and productivity [15]. Therefore, it is important to understand the interplay between exoskeleton systems, workers, and tasks to make the most use of these technologies, and past research suggests that the benefits of exoskeleton suits may differ based on the kinds of construction works [16]. When it comes to exoskeletons, as with any new technology, we need to be aware of both the positive and negative aspects of this technology and address them before implementing it in the construction industry. Exoskeleton research has just begun to surface, shedding light on their effects. Some studies have shown that wearing an exoskeleton when stooping reduces spinal muscle use significantly [17,18]. The exoskeleton reduced the load on the back by minimizing muscular usage, which may assist in reducing fatigue and maybe preventing an accident [19]. However, this new technique has only a small amount of research.

To analyze the advantages of exoskeletons in the construction sector, it is best to use wearable sensor technology, which is accurate, unobtrusive, and provides a plethora of data for the study. Construction workers will benefit greatly from the comparative data that these studies may supply. For example, wearable sensing technology can collect data on the effects of a device on a user's posture in addition to metabolic expenses [20]. Furthermore, wearable sensing technology can capture dynamic data and then use that data to quantify the differences in the way the worker is moving with or without the devices [21]. Worker safety and health can benefit greatly from the development of exoskeleton technology, which incorporates wearable sensors. As a result, sensors like these are critical to the advancement and use of exoskeleton technology in the construction industry. In the construction industry, wearable sensors will enable the expansion of exoskeleton devices, which could lead to safer and more productive work. When it comes to exoskeleton technology, there is still plenty to learn, both pros and cons. Workplace health and safety relies on wearable sensors because they may give professionals access to data on a wide range of topics, from exoskeletons and their return-to-work and injury

prevention applications to a wide range of other worker health solutions.

Research gap: Despite the obvious promise of exoskeleton devices, additional research is required to determine the positive and negative effects of exoskeletons and to address them prior to implementing and using this technology in the construction industry. There are no clear criteria available to evaluate the effects of exoskeletons on construction workers. Many standard ergonomic assessment approaches are mostly based on static models of work and do not take the potential implications of an exoskeleton into account. Although wearable sensing technology is the greatest method for evaluating the benefits of exoskeletons in the construction sector, no research studies have examined the application of this technology to quantify the effects of exoskeletons on construction workers.

2 Research Methodology

2.1. Design considerations

Low back injuries are widely recognized as the most common WMSDs. Construction workers mostly develop low back injuries mainly due to risk factors such as awkward postures and repetitive motions that are associated with workplace activities (e.g., repetitive lifting, carrying, lowering). To mitigate these injuries, there is a necessity to develop an ergonomic intervention (e.g., a robotic wearable passive exoskeleton system) that can assist the trunk and waist movements (i.e., lumbar flexion/extension, lateral bending, axial rotation) in the direction of anti-gravity. Unlike a robotic human-powered amplifier based on end-effector inputs [22] and an electric motor-assisted device to aid with trunk flexion and extension [23], the passive wearable exoskeleton system is a non-motorized device that helps individuals with lifting activities. This wearable technology borrows ideas from human muscles by using elastic components that can be interpreted as external muscular force generators. Generally, the proposed robotic passive wearable exoskeleton system was configured to transmit assistive torque or forces to a user's lower extremities (i.e., thigh and leg) through actuators and springs allocated at both hip joints.

2.2. Structure of the robotic passive wearable exoskeleton system

As shown in **Figure 1**, a robotic exoskeleton system that is both passive and wearable has been designed. At the shoulders, trunk, and thighs, this novel passive wearable exoskeleton system was articulated to synchronize with hip rotation. System components include a shoulder, trunk, and two leg pieces for each leg joined by Velcro straps in four parts. In order to release elastic energy during repetitive movements, two springs were linked from the shoulder to the hip region [24]. Additional benefits include load transfers from the spine to the legs, which enhances the user's capacity to do tasks that are both ergonomic and physical. This exoskeleton may be attached to the user's body using straps without any assistance from a professional. In choosing the harnesses and cuffs, we

looked for ones that are lightweight, flexible, and less likely to cause internal joint damage from incorrect alignment. The proposed design and structural development of the robotic passive wearable exoskeleton system aims to make the mechanical structure as basic as feasible, specifically to mitigate risk factors for WMSDs during manual repetitive handling duties, which is why it is crucial to remark (i.e., lifting, lowering, and carrying activities).

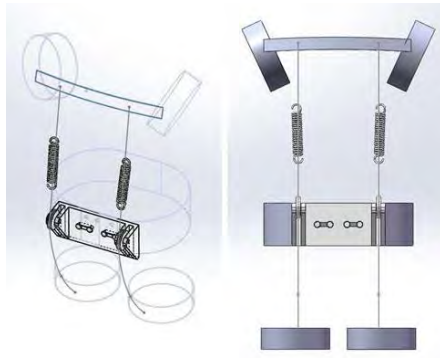


Figure 1. A prototype design of the proposed robotic passive wearable exoskeleton system.

2.3. Experimental design and procedures

The current project implements a design for a randomized crossover research that required only one testing session. Ten healthy university male student participants were selected to take part in the experimental endeavor. If the participants did not have a history of mechanical pain or injury to their upper extremities, lower extremities, or back, then they were allowed permission to take part in the activity. Each participant received an explanation of the in-depth procedures of the experiment, which covered the research objectives, the protocol, and any potential dangers. Participants provided demographic information and written consent after being informed about the study, following a process approved by the Human Subject Ethics Panel of Hong Kong Polytechnic University (reference number: HSEARS20220819005).

The lifting postures (stooping versus squatting) and systems (with vs. without passive exoskeleton) were the independent variables in this study. The muscle activity (i.e., right, and left sEMG: Lumbar Erector Spinae (LES) at L3 vertebrae level, Thoracic Erector Spinae (TES) at T12 vertebrae level), joint kinematics (neck, low back, hip, and knee kinematics), and physical fatigue (e.g., heart rate, HR; skin temperature, ST; and the perceived fatigue score) were the dependent variables in this study. During the performance of the lifting task, EMG data were gathered from these muscles on both sides utilizing Biometrics Ltd Data LITE, a wireless surface EMG sensor system. On the other hand, twin-Axis Electrogoniometer, which can measure angles in up to two planes of movement, was utilized to evaluate the kinematics of the neck, low back, hip, and knee regions. These movements include flexion/extension, and lateral bending. Physical fatigue indicators such as HR and ST were captured using a

wearable sensor (i.e., Empatica E4). Perceived fatigue level was assessed using the rating-of-fatigue scale. **Figure 2** indicates a range of wearable sensors used for the data collection in this study.



Figure 2. Wearable sensors used for data collection.

The principal experimental task in this study was manual, repetitive handling. In this exercise, participants are instructed to stoop or squat to pick up a heavy box (i.e., 15 kg), carry it along a predetermined route, and then drop the box at a given destination using their stooping or squatting position. The experimental procedures are depicted in Figure 3, which depicts the laboratory setting. Following the training, every participant conducted ten iterations of the experiment, one for each of the conditions that were randomly assigned. To lessen the amount of fatigue experienced by the participants, there was a five-minute break in between each of the consecutive experimental trials.

After the trial, participants were told to do two sets of Maximum Voluntary Contractions (MVCs) against physical resistance for each muscle. The participants were instructed to lay prone with their torsos hanging over the side of a table during the MVC trials for the TES and LES muscles. This was carried out in preparation for the trials currently under way. The participants were then instructed to manually resist the researcher by stretching their trunk upward and twisting to the left and right. After each trial, there were a rest period of two minutes, and during that time, each muscle was contracted to its fullest extent for five seconds [25]. The MVCs trials are performed to attain the maximal amplitude of surface electromyographic (sEMG) activity for the aim of normalizing the sEMG signals and, as a result, permitting comparisons of muscle activity between various muscles, lifting positions, and systems.

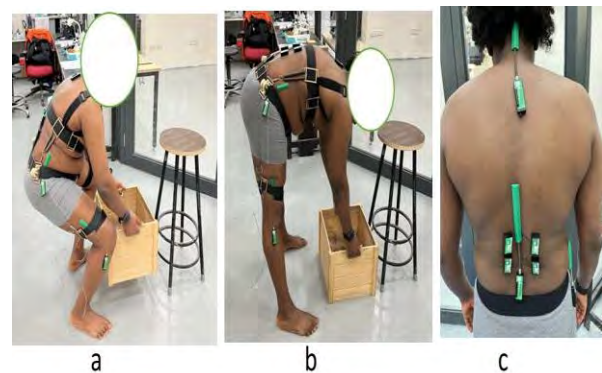


Figure 3. Laboratory experimental setup: (a) Squat Lifting; (b) Stoop Lifting; (c) Placement of EMG and Electrogoniometer sensors

2.4. Data processing and analyses: surface electromyography (sEMG), Electrogoniometer, and HR sensors

The positioning of the sEMG electrodes and Electrogoniometer sensors is shown in Figure 3. It is planned to conduct research on both the right and left sides of the two muscles (TES, LES.). This was executed with a biomechanical perspective. DataLITE Wireless sEMG sensors (LE230) (UK Biometrics Ltd) were attached bilaterally to each muscle to record electrical activity. The distance between the electrodes is 20 millimeters, while the diameter of the electrode is 15 millimeters. All surface electromyography (sEMG) data are going to have their raw electrocardiography signals sampled at a frequency of 2000 Hz with a common-mode rejection ratio of 100 decibels. Using a moving window of 1000 milliseconds that passes across the sEMG signals recorded during the two MVCs, we determined the sEMG signal that has the highest root mean square (RMS) value for each muscle. The sEMG signal with the highest RMS value for each muscle was the one used for normalization.

Each trial of the experiment underwent a visual examination for artifact effects. In the following step, a band-pass filter operating between 20 and 500 Hz was applied to each single sEMG signal. To get rid of power-line interference, we utilized a notch filter with its center frequency set to 50 Hz. To provide an accurate estimation of the RMS sEMG signals, the rectified and processed sEMG signals, in conjunction with an average constant window of 1,000 milliseconds, were utilized. The collected sEMG signals were utilized to derive the mean root-mean-square value of the EMG activity. The highest percent MVC sEMG is shown as a percentage of the maximum percent RMS during MVC, which was used to normalize the obtained data. Because of its sensitivity to transient changes in body loading, the highest amplitude, also known as the maximum percent of the maximum velocity component, was chosen for this study as a useful indicator of human exoskeleton interaction across brief time periods. Its amplitude is also useful as a long-term indicator of human exoskeleton interaction [25]. The Biometrics DataLITE Explore Wireless dongle served as the bridge between the sensors and the PC software, allowing for the transfer of raw data.

Four Electrogoniometer sensors, manufactured by Biometrics Ltd, were affixed to the spinous processes at the T1, S1, lateral to hip, and lateral to knee for measuring cervical, low back, hip, and knee motion, respectively (Figure 3). The rate of sampling was set at 1000 samples per second. To convert Goniometer readings into engineering units usable by the Biometrics Ltd. program, we employed unfiltered ASCII encoding. Sub-sampling was established, and 100 data points were sampled for each activity. The final step was to determine the average of the subsamples. Using the Biometrics Ltd. data acquisition software, all the data were recorded, and subsamples were taken.

2.5. Assessment of fatigue

Participants were given the Rating-of-Fatigue Scale

with 11 possible responses, from 0 (no fatigue) to 10 (total exhaustion), to rate their level of perceived exertion [26]. Each subject's level of exertion during the experimental sessions with and without an exoskeleton was measured using this scale. Additionally, a wearable sensor (i.e., Empatica E4) was used to monitor HR and ST continuously during each task.

2.6. Statistical analyses

To ensure that the data were normally distributed, we ran the Shapiro-Wilk test. Then, a two-factor (2 x 2) mixed-model repeated-measures analysis of variance (ANOVA) was used to assess the differences in muscle activity between subjects who lifted in a stoop versus a squat position (within-subject factors) and who lifted with or without an exoskeleton system (between-subject factors). A two-way (2 x 2) repeated-measures ANOVA was also used to examine the correlation between the number of repetitions performed and the amount of fatigue experienced by the participants. Post hoc comparisons between pairs were calculated using the Bonferroni adjustment. The analyses were performed in SPSS 27.0 (Statistical Program for the Social Sciences) (IBM, USA). Statistical significance was determined at the p 0.05 level.

3. Results

3.1. Descriptive statistics

Table 1 details descriptive statistics. The LES muscle activity with the use of exoskeleton showed a reduction of about 30% as compared to without exoskeleton. Similarly, TES muscle activity was reduced by 12% with the use of exoskeleton as compared to without exoskeleton. The reduction of the neck, low back, hip, and knee kinematics were 23%, 11%, 5%, and 36%, respectively, with the use of exoskeleton as compared to without exoskeleton. HR and fatigue scores were reduced by nearly 13% and 67%, respectively, with the use of exoskeleton as compared to without exoskeleton. However, ST was slightly increased by about 2% with the use of exoskeleton as compared to without exoskeleton.

Table 1. Descriptive statistics

Variables	Without Exoskeleton		With Exoskeleton	
	Mean	SD	Mean	SD
Age, Y	29.50	2.17		
Height, m	1.71	0.07		
Weight, kg	70.30	3.47		
Body mass index, kg/m ²	24.20	0.81		
TES, amplitude	6.56	1.66	5.83	0.72
LES, amplitude	4.61	1.75	3.41	0.17
Neck motion, degrees	8.26	1.76	6.56	0.92
Low back motion, degrees	7.35	1.18	6.56	0.76
Hip motion, degrees	4.43	1.23	4.20	0.25
Knee motion, degrees	5.18	1.02	3.59	0.15
Heart rate, beats/m	83.09	13.05	73.16	6.08
Temperature, °C	31.49	1.59	32.21	1.52
Fatigue score, 0 – 10	7.80	0.89	3.90	0.72

3.2. Effects of exoskeleton system lifting posture on muscle activity

Muscle activity in ANOVA data is shown in Table 2. All muscles examined showed significant changes in sEMG activity when comparing the primary effects of lifting posture ($p < 0.05$) and system ($p < 0.05$). Furthermore, sEMG activity for the LES muscle significantly interacted with lifting posture and systems. However, there was no interaction effect of lifting posture and system was observed for TES muscle.

Table 2. Summary of ANOVA results for muscle activity

Independent Variables	LES		TES	
	F	p	F	p
Main effect				
System	13.43	0.001	4.46	0.042
Posture	10.71	0.002	14.98	0.001
Interaction				
System * Posture	8.28	0.007	0.77	0.385

3.3. Effects of exoskeleton system and lifting posture on joint kinematics

Findings of ANOVA on joint kinematics are reported in **Table 3**. When examining the primary effects of lifting posture and system, there were statistically significant changes in the kinematics of the neck and low back. Knee kinematics for the exoskeleton showed substantial alterations due to the lifting posture, while hip kinematics did not. For low back kinematics, a notable interaction impact between lifting posture and exoskeleton use was observed. However, no system-lifting posture interaction effect was found for any of the other kinematics we looked at.

Table 3. Summary of ANOVA results for joint kinematics

Independent Variables	Neck motion		Low back motion		Hip motion		Knee motion	
	F	p	F	p	F	p	F	p
Main effect								
System	20.38	0.001	7.85	0.008	0.712	0.404	50.43	0.001
Posture	16.97	0.001	11.40	0.002	5.36	0.026	1.88	0.179
Interaction								
System * Posture	.038	0.846	4.16	0.049	0.871	0.357	2.38	0.131

3.2. Fatigue assessment

The HR, ST, and subjective fatigue scores are shown in Table 4 along with the analysis of variance (F ratios and p-values). The major effects of lifting posture and exoskeleton used were statistically significant for HR and subjective fatigue scores. However, changes in ST were unrelated to both lifting posture and exoskeleton used. There was an interaction effect between lifting posture and exoskeleton used for changes in HR and ST, not for subjective fatigue scores.

Table 4. Summary of ANOVA results for fatigue assessment

Independent Variables	HR		ST		Fatigue	
	F	p	F	p	F	p
Main effect						
System	14.38	0.001	2.45	0.126	536.82	0.001
Posture	7.43	0.010	2.86	0.103	50.80	0.001
Interaction						
System * Posture	13.95	0.001	4.16	0.049	1.42	0.243

4. Discussion

The purpose of this research is to evaluate the effects of a passive exoskeleton system on muscle activation, joint kinematics, and fatigue ratings while performing laboratory simulations of manual repetitive handling tasks. The findings were as follows: (1) there was a statistically significant difference between the effects of lifting posture and the exoskeleton system on sEMG activity of the muscles studied; (2) there was a statistically significant difference between the effects of lifting posture and the kinematics of all regions studied except for the knee region; (3) there was a statistically significant difference between the effects of the exoskeleton and the kinematics of all regions studied except for the hip region; and (4) there was a statistically significant difference between the effects of lifting posture and using an exoskeleton on HR and subjective fatigue scores, except for ST.

4.1. Effects of exoskeleton system and lifting posture on muscle activity

Both TES and LES muscles tested showed a statistically significant ($p < 0.05$) increase in muscle activity (sEMG activity) while lifting using stoop posture, regardless of whether an exoskeleton system was used. Most notably, the results showed that sEMG activity in TES and LES was considerably ($p < 0.05$) lower while utilizing the exoskeleton system as opposed to not using it for manual repetitive handling tasks. In general, these results showed that people who utilized the passive exoskeleton system had less sEMG activity and, hence, a lower risk of developing WMSDs. Exoskeleton systems have been shown to lower LES muscle activation during manual repetitive handling tasks [27-30]. Like current findings, Bosch et al. [29] found that participants using an exoskeleton system saw a 35%-38% decrease in maximal voluntary contractions (MVC) during a simulated assembly work simulation involving a protracted forward bending task. The LES muscle's activity was found to be significantly reduced by 12-15% MVC in an evaluation conducted by Huysamen et al. [27]. Cardoso et al. [31] found that while performing trunk bending duties in the furniture production industry, the wearer's back muscles were less active by between 0.8% and 3.8% while wearing a passive exoskeleton system. These results provide support for the hypothesis that the passive exoskeleton system may help reduce the risk of WMSDs among construction workers by mitigating the effects of internal muscle activity and spinal strains.

4.2. Effect of exoskeleton system on joint kinematics

In the current study, evaluation of spinal and peripheral joint kinematics shows that using a passive back exoskeleton changes joint kinematics. In a similar vein, prior research suggests that donning a passive back support exoskeleton modifies joint kinematics [32]. Similarly, Sadler et al. [33] compared the kinematic changes between lifting with and without a back-support passive exoskeleton. According to their research, employing the back-support passive exoskeleton significantly reduces trunk flexion during the whole lift cycle. Another study using a passive exoskeleton also demonstrated an increase in peak lumbar flexion, however this time it was limited to lifts from the ankle level and not the knee level [34]. Moreover, the range of motion was not affected by either exoskeleton in a second study that examined two passive exoskeletons [35]. Furthermore, the kinematics of lifting while wearing a passive exoskeleton was investigated in a separate study [36]. Joint angles in the knee, hip, low back, and upper back did not change noticeably when wearing the exoskeleton. Increases in ankle flexion, decreases in lumbar and thoracic (mid back) flexion, and equal hip flexion were seen in people wearing a passive exoskeleton compared to those not wearing the exoskeleton [37].

4.3. Effect of exoskeleton system on fatigue

Both objective fatigue indicators such as HR and subjective fatigue scores were significantly reduced during lifting tasks while using a passive exoskeleton system.

This study confirms the findings of previous studies showing that using an exoskeleton system considerably reduces the perception of effort during physical activity [28, 38]. Yet, another study found that RPE significantly increased by 0.75 points following exoskeleton-assisted physical task performance [39]. Nevertheless, no research has been done to determine what the minimally clinically important difference (MCID) in exertion level is when utilizing the Borg CR 10 for a lifting task. Consequently, the 0.75 RPE change in their study is debatable in terms of its clinical importance. The results of this study show that compared to when no exoskeleton was used, HR decreased by about 13% when using an exoskeleton. While one study observed a 10% reduction in HR when utilizing a back-supported passive exoskeleton for a lifting task [38], another found an increase of 7% [40]. Yet, contrary research has found little evidence that utilizing an exoskeleton significantly alters HR while carrying out a task [41]. These conflicting findings suggest that it is not possible to draw any firm conclusions about the effect of exoskeleton use on HR, across a variety of tasks and exoskeletons.

4.4. Limitations

Like with any research, the current study was subject to some limitations. First, measurements were conducted in a laboratory setting. The subjects selected for this study were university students who lacked experience with manual materials handling; as a result, the group employed was not exactly representative of construction industry workers. In addition, individuals were not trained on the tested

exoskeleton for an extended period, and task performance was not assessed in this study. It is unknown if participants would become significantly more/less comfortable with the exoskeleton or would perform significantly more/less consistently with longer use. Even though all subjects were instructed on how to do the task prior to data collection, two distinct postures were used. In a real-world construction setting, however, other postures are anticipated.

5. Conclusions and recommendations

Preliminary results suggest that using the passive exoskeleton system decreased sEMG activity. In addition, when using the exoskeleton system, participants showed increased spinal and peripheral joint kinematics. Finally, participants reported less fatigue during the tasks while using the exoskeleton system, as measured by HR and subjective fatigue scores. The key findings of this study are that (1) the passive exoskeleton system has promising applications as an ergonomic intervention tool to aid construction workers while conducting manual repetitive handling activities; (2) findings have provided evidence that the system is not only practical but also portable, convenient, and user-friendly; and (3) this research may help safety managers select the best passive exoskeleton for use in the construction industry by shedding light on the effects of exoskeleton use on muscle activation, kinematics, and physical exertion. Despite these advantages, more studies are required to determine how this passive exoskeleton system affects other peripheral and spinal muscles (e.g., abdominals, glutei etc.), physiological metrics (e.g., respiratory rate, oxygen consumption, etc.), and labor task performance across a variety of construction trades. Additionally, it would be interesting for future research to investigate the feasibility of using passive exoskeleton devices to improve the health and efficiency of construction workers.

Declaration of Competing Interest. No authors have reported any financial or other conflicts of interest that could be considered as influencing the work provided in this paper.

Acknowledgements. The authors acknowledged the funding support received for this project under the Hong Kong PolyU start-up fund (Project number: BD34).

References

- [1]. Australian Bureau of Statistics. Australian National Accounts: National Income, Expenditure and Product, 2022. On-line: [Australian National Accounts: National Income, Expenditure and Product, December 2022 | Australian Bureau of Statistics \(abs.gov.au\)](https://www.abs.gov.au/AustralianNationalAccounts/NationalIncomeExpenditureandProduct/December2022), Accessed: 28/03/2023.
- [2]. Oesterreich, T.D. and Teuteberg, F. Understanding the implications of digitisation and automation in the context of Industry 4.0: A triangulation approach and elements of a research

- agenda for the construction industry. *Computers in industry*, 83: 121-139, 2016.
- [3]. Bureau of Labor Statistics (BLS). *Injuries, Illnesses, and Fatalities, 2017*. (Accessed: July 2021).
- [4]. Sunindijo, R. Y., and Zou, P. X. *Strategic safety management in construction and engineering*. John Wiley & Sons, 2015.
- [5]. Wang D, Dai F, and Ning X. Risk assessment of work-related musculoskeletal disorders in construction: State-of-the-art review. *Journal of Construction Engineering and management*, 141(6):04015008, 2015.
- [6]. Antwi-Afari MF, Li H, Chan AH, Seo J, Anwer S, Mi HY, Wu Z, Wong AY. A science mapping-based review of work-related musculoskeletal disorders among construction workers. *Journal of Safety Research*, Vol. ahead-of-print, No. ahead-of-print. DOI: <https://doi.org/10.1016/j.jsr.2023.01.011>. 2023.
- [7]. Anwer S, Li H, Antwi-Afari MF, Wong AY. Associations between physical or psychosocial risk factors and work-related musculoskeletal disorders in construction workers based on literature in the last 20 years: A systematic review. *International Journal of Industrial Ergonomics*, 83:103113, 2021.
- [8]. Visser, S., van der Molen, H. F., Kuijter, P.P.F.M., Hoozemans, M.J.M., Frings-Dresen, M.W.H. Evaluation of team lifting on work demands, workload and workers' evaluation: an observational field study. *Applied Ergonomics*, 45(6): 1597–1602, 2014.
- [9]. Antwi-Afari, M. F., Li, H., Edwards, D. J., Pärn, E. A., Seo, J., and Wong, A. Y. L. Biomechanical analysis of risk factors for work-related musculoskeletal disorders during repetitive lifting task in construction workers. *Automation in Construction*, 83: 41-47, 2017.
- [10]. Karsh, B., Moro, F.B.P., and Smith, M. J. The efficacy of workplace ergonomic interventions to control musculoskeletal disorders: a critical examination of the peer-reviewed literature. *Theoretical Issues Ergonomics Science*, 2: 23–96, 2001.
- [11]. Hentout, A., Aouache, M., Maoudj, A., and Akli, I. Human–robot interaction in industrial collaborative robotics: a literature review of the decade 2008–2017. *Advanced Robotics*, 33(15-16): 764-799, 2019.
- [12]. Schwerha, D. J., McNamara, N., Nussbaum, M. A., and Kim, S. Adoption potential of occupational exoskeletons in diverse enterprises engaged in manufacturing tasks. *International Journal of Industrial Ergonomics*, 82: 103103, 2021.
- [13]. Maurice, P., Čamernik, J., Gorjan, D., Schirrmeister, B., Bornmann, J., Tagliapietra, L., ... and Babič, J. Objective and subjective effects of a passive exoskeleton on overhead work. *IEEE Transactions on Neural Systems and Rehabilitation Engineering*, 28(1): 152-164, 2019.
- [14]. Zhu, Z., Dutta, A., and Dai, F. Exoskeletons for manual material handling—a review and implication for construction applications.” *Automation in Construction*, 122: 103493, 2021.
- [15]. Cho, Yong K., Kinam Kim, Shaojun Ma, and Jun Ueda. "A robotic wearable exoskeleton for construction worker's safety and health." In *Construction Research Congress 2018*, pp. 19-28. 2018.
- [16]. Alabdulkarim, S., and Nussbaum, M. A. Influences of different exoskeleton designs and tool mass on physical demands and performance in a simulated overhead drilling task. *Applied Ergonomics*, 74: 55-66, 2019.
- [17]. Koopman, A. S., Kingma, I., Faber, G. S., de Looze, M. P., and van Dieën, J. H. Effects of a passive exoskeleton on the mechanical loading of the low back in static holding tasks. *Journal of Biomechanics*, 83: 97-103, 2019.
- [18]. Koopman, A. S., Näf, M., Baltrusch, S. J., Kingma, I., Rodriguez-Guerrero, C., Babič, J., ... & van Dieën, J. H. Biomechanical evaluation of a new passive back support exoskeleton. *Journal of Biomechanics*, 105: 109795, 2020.
- [19]. Howard, J., Murashov, V. V., Lowe, B. D., and Lu, M. L. Industrial exoskeletons: Need for intervention effectiveness research. *American journal of industrial medicine*, 63(3): 201-208, 2020.
- [20]. Leone, A., Rescio, G., Diraco, G., Manni, A., Siciliano, P., and Caroppo, A. Ambient and Wearable Sensor Technologies for Energy Expenditure Quantification of Ageing Adults. *Sensors*, 22(13): 4893, 2022.
- [21]. Vijayan, V., Connolly, J. P., Condell, J., McKelvey, N., and Gardiner, P. Review of wearable devices and data collection considerations for connected health. *Sensors*, 21(16): 5589, 2021.
- [22]. Kazerooni, H. Human power amplifier for lifting load including apparatus for preventing slack in lifting cable. U.S. Patent 6,386,513, 2002.
- [23]. Luo Z, Yu Y. Wearable stooping-assist device in reducing risk of low back disorders during stooped work. In 2013 IEEE international conference on mechatronics and automation 2013 Aug 4 (pp. 230-236). IEEE.
- [24]. Antwi-Afari, M. F., Li, H., Edwards, D. J., Pärn, E. A., Owusu-Manu, D., Seo, J., and Wong, A. Y. L. Identification of potential biomechanical risk factors for low back disorders during repetitive rebar lifting. *Construction Innovation: Information, Process, Management*, 18(2), 2018.
- [25]. Hermens, H. L., Freriks, B. F., Merletti, R., Stegeman, D., Blok, J., Rau, G., Disselhorst-Klug, C., and Haugg, G. Seniam-European

- recommendations for surface electromyography. *Roessingh Research and Development*, 8(2): 13–54, 1999.
- [26]. Micklewright D, St Clair Gibson A, Gladwell V, Al Salman A. Development and validity of the rating-of-fatigue scale. *Sports Medicine*, 47:2375-93, 2017..
- [27]. Huysamen, K., de Looze, M., Bosch, T., Ortiz, J., Toxiri, S., and O'Sullivan, L. W. Assessment of an active industrial exoskeleton to aid dynamic lifting and lowering manual handling tasks. *Applied Ergonomics*, 68: 125-131, 2018.
- [28]. Graham, R. B., Agnew, M. J., and Stevenson, J. M. Effectiveness of an on-body lifting aid at reducing low back physical demands during an automotive assembly task: assessment of EMG response and user acceptability. *Applied Ergonomics*, 40(5): 936-942, 2009.
- [29]. Bosch, T., van Eck, J., Knitel, K., and de Looze, M. The effects of a passive exoskeleton on muscle activity, discomfort and endurance time in forward bending work. *Applied Ergonomics*, 54: 212-217, 2016.
- [30]. Antwi-Afari MF, Li H, Anwer S, Li D, Yu Y, Mi HY, Wuni IY. Assessment of a passive exoskeleton system on spinal biomechanics and subjective responses during manual repetitive handling tasks among construction workers. *Safety science*, 142:105382, 2021.
- [31]. Cardoso, A., Colim, A. and Sousa, N., 2020. The effects of a passive exoskeleton on muscle activity and discomfort in industrial tasks. *Occupational and Environmental Safety and Health II*: 237-245, 2020.
- [32]. Almosnino S, Huangfu R, Cappelletto J. Effects of a Back-Support Exoskeleton on Pelvis-Thorax Kinematics and Coordination During Lifting. In Proceedings of the 21st Congress of the International Ergonomics Association (IEA 2021) Volume V: Methods & Approaches 21 2022 (pp. 131-138). Springer International Publishing.
- [33]. Sadler EM, Graham RB, Stevenson JM. The personal lift-assist device and lifting technique: a principal component analysis. *Ergonomics*, 54(4):392-402, 2011.
- [34]. Simon, A. A., Alemi, M. M., & Asbeck, A. T. Kinematic effects of a passive lift assistive exoskeleton. *Journal of Biomechanics*, 120: 110317, 2021.
- [35]. Madinei S, Alemi MM, Kim S, Srinivasan D, Nussbaum MA. Biomechanical evaluation of passive back-support exoskeletons in a precision manual assembly task: "Expected" effects on trunk muscle activity, perceived exertion, and task performance. *Human factors*, 62(3):441-57, 2020.
- [36]. Baltrusch SJ, Van Dieën JH, Koopman AS, Näf MB, Rodriguez-Guerrero C, Babič J, Houdijk H. SPEXOR passive spinal exoskeleton decreases metabolic cost during symmetric repetitive lifting. *European Journal of Applied Physiology*, 120(2):401-412, 2020.
- [37]. Abdoli-E M, Agnew MJ, Stevenson JM. An on-body personal lift augmentation device (PLAD) reduces EMG amplitude of erector spinae during lifting tasks. *Clinical Biomechanics*, 21(5):456-65, 2006.
- [38]. Lotz CA, Agnew MJ, Godwin AA, Stevenson JM. The effect of an on-body personal lift assist device (PLAD) on fatigue during a repetitive lifting task. *Journal of Electromyography and Kinesiology*, 19(2):331-40, 2009.
- [39]. So BC, Cheung HH, Liu SL, Tang CI, Tsoi TY, Wu CH. The effects of a passive exoskeleton on trunk muscle activity and perceived exertion for experienced auxiliary medical service providers in cardiopulmonary resuscitation chest compression. *International Journal of Industrial Ergonomics*, 76:102906, 2020.
- [40]. Marino M. Impacts of using passive back assist and shoulder assist exoskeletons in a wholesale and retail trade sector environment. *IIEE Transactions on Occupational Ergonomics and Human Factors*, 7(3-4):281-290, 2019.
- [41]. Luger T, Bär M, Seibt R, Rieger MA, Steinhilber B. Using a back exoskeleton during industrial and functional tasks—Effects on muscle activity, posture, performance, usability, and wearer discomfort in a laboratory trial. *Human Factors*, 65(1):5-21, 2023.

Automated construction process for foundation engineering

G.N. Meshcheriakov^a and A.M. Andryushchenko^b

^aDepartment of civil construction, “Engineering Center Transzvuk”, Odesa, Ukraine

^bOdesa Polytechnic National University, Ukraine

E-mail: ectranszvuk@gmail.com, amandr@op.edu.ua

Abstract –

The purpose of this manuscript is to outline a scientific task aimed at improving the technological and organizational methods for pressing piles into the ground. The study proposes the development of conceptual piling equipment and construction methods for various structural and technological solutions for pile fields, especially under complicated conditions. The efficiency indicators are confirmed experimentally on real sites. The ratio of the specific weight of the load moved by a service crane to the total number of project piles and the number of modules used, as well as the organizational and technological schemes for their use, are determined. Additionally, mathematical models are used to estimate the efficiency of various methods and options of pile work. A three-stage algorithm is proposed for the variant design of complex technological processes. Overall, this manuscript presents a comprehensive approach to solving the task of automating the construction of pile foundations, providing valuable insights for engineers and researchers in the field.

Keywords –

Construction automation; Technological process modeling; Foundation engineering; Piling machine

1 Introduction

Construction automation strategy, through the integration of cyber-physical systems into construction processes, aims to improve industry efficiency by overcoming the nonconformity between the pace of urbanization and the limitations of conventional technologies. For this purpose, equipment that combines conceptual design with automated processes, such as large-scale Printing Systems [1], is being developed worldwide. However, the problem of the disparity between the pace of erecting the overground parts of the building and the installation of the underground parts remains unsolved. The underground parts require significant labor costs and can account for up to 50% of total construction, and remains slow, one of the most hazardous and expensive [2].

Analysis of information sources [9] shows that pile foundations can be made reliable by using prefabricated building elements that are pressed into the ground, resulting in minimal environmental impact. Research has demonstrated that conventional piling techniques do not provide sufficient labor productivity in constrained working environments. Inefficient auxiliary processes used by machinery in such conditions can consume more than 75% of the machining time, resulting in decreased productivity and increased, labor and operating costs.

The relevance of the topic is determined by the lack of research on aggregate-modular type piling systems when they are used in foundation engineering.

2 Automated Construction Equipment

The development of automated construction process for pressing precast pile elements into the ground begins with the creation of the Modular Aggregate Piling System (MAPS). Developed by EC “Transzvuk” in Ukraine, this system is used for the construction of pile foundations and sheet pile structures for civil and industrial buildings [7]. The MAPS, shown in Figure 1, consists of the original piling machine of pressing type and a modular skidding system.

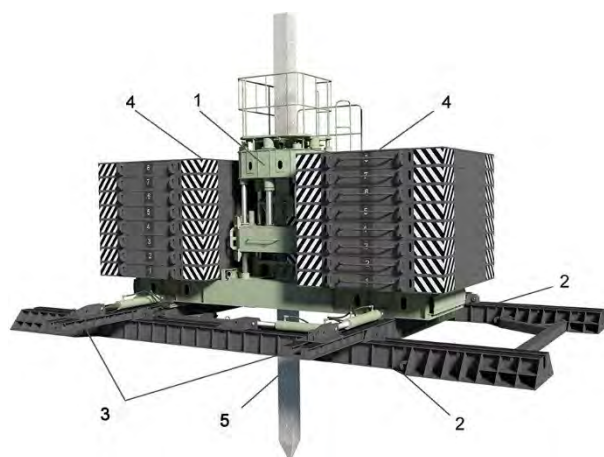


Figure 1. Modular Aggregate Piling System: 1 – piling machine, 2 – basic module, 3 – cross carriage, 4 – anchor loads, 5 – concrete pile

The concept of using MAPS provides precise, two-axis (X-Y) controlled repositioning of the Piling Machine, without remounting and re-anchoring operations and without the interruption of the main technological processes: pile installation – machine displacement.

Specifications of the MAPS are given in Table 1.

Table 1. Technical Specifications

Indicator	Value
Nom. pressing force	2000 kN
Pile pressing speed	1.5 ÷ 3 m/min
Displacement speed	2.1 m/min
Positional precision	± 10 mm

2.1 Hydraulic Piling Machine

The Piling Machine (PM) CO-450 is intended for pressing into the ground precast elements: concrete piles with cross-sections up to 450×450 mm, sheet piles not more than 500 mm width, and metal pipes. The pressing force of PM is up to 2300 kN. It works on the principle of self-centering the pile utilizing a side wedge-operated clamping system and cyclically pressing a pile into the ground in manual or automatic mode.



Figure 2. Piling Machine CO-450

The pile pressing force (soil resistance) is controlled by the hydraulic system of the PM. The PM is a gravity type and is anchored with metal loads by a service crane.

Total weight is up to 200 tonnes and is defined by ground resisting forces. Self-weight of the PM is 14.3 tons. It is the best performance for existing equipment in relation: to the pressing force of the machine to its weight. This property is important for limited space conditions.

The pile to be installed is fed into the PM by a crane. When installing piles below the ground level (up to 12 m), a metal inventory tool is used. The team consists of an operator, a crane operator, and two slingers.

2.2 Modular Skidding System

Modular Coordinating Skidding System (MCSS) is a hydraulic push-pull system of the ground type consisting of the main (aggregative), auxiliary longitudinal module (fixed), and a cross carriage (movable). It was designed according to the general principles of the international standard for building engineering [6]. This ISO specifies the aims of modular coordination and defines the dimensions of buildings, foundations, and the positioning of their components, piles, equipment, and assemblies.

The modules used are identical and interchangeable, allowing them to be connected in various combinations.

The system utilizes four hydraulic drive cylinders of 500 kN to achieve synchronized skid motion controlled along two axes. MCSS could also be used to move heavy equipment or structures (up to 350 t) on it in both longitudinal and transverse directions [8]. Specific pressure on the ground when using 1 (2) module: 15,7 (8,3) tons per square meter. That allows working on slopes and sites with weak or water-saturated soils.

3 Construction Methods

To unify and typify the technological solutions, the authors proposed to classify the existing methods of pile work, by the technological sequence of pile installation and positional displacements of the equipment. It refers to the ability of the equipment used in piling work to complete the installation process without requiring any readjustments or interruptions to the main technological process. The classification distinguishes:

1) Point; 2) Lineal (X); 3) Coordinate (X, Y) methods. Based on this classification, three piling methods have been developed, with each method utilizing an automated Piling Machine CO-450. When developing the piling methods, the geometric parameters of pile foundations for civil buildings [6] were taken into account in order to ensure maximum architectural flexibility.

3.1 Point Method

The point (P) method is based on PM repositioning by a service crane. It is used for the installation of single piles, including the piles of increased liability in a case when the safety of nearby buildings is the determining factor. This method remains indispensable in conducting pile works under conditions of maximum proximity to existing buildings (1m for piles and 0.5m for sheet piles). Unfortunately, the productivity of the P-method is low [10]. It is one pile per hour, with 25% of the time spent pressing a 16m pile into the ground and the remaining 75% of the time spent on inefficient auxiliary processes such as mounting, anchoring, disassembly, and repositioning of the Piling Machine CO-450 by service crane.

3.2 Lineal Method

The lineal (L) method is based on the PM one-coordinated positional movement along the longitudinal X coordinate, along the axis of the pile row, using fixed longitudinal skid guides 2, as exemplified in Figure 3.

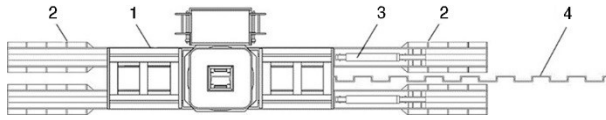


Figure 3. Sheet piling by the lineal method: 1 – piling machine, 2 – longitudinal guides, 3 – drive cylinders, 4 – sheet pile wall

This method is used for the single-row arrangement of building elements: concrete piles, tubes, sheet piles, etc. The advantages of the L-method are obvious for all types of linear works, be it cutoff or retaining walls of a sheet pile type or anti-landslide structures.

The labor productivity is significantly increased in comparison with the P-method, but it is still insufficient for multi-row pile structures, because of the frequent need for equipment readjustments.

3.3 Coordinate Method

The coordinate (C) method is based on PM two-coordinated positional movement along the longitudinal axis, using the cross carriage 3, as shown in Figure 4, option C. It is used for a cluster and multi-row disposition of piles. The technological process for C-method using two modules with sequential reconnection was presented in the paper [8]. It was displayed, that the implementation of the C-method together with the accuracy of the pile installation (position and inclination control) cuts down the production time providing higher productivity.

However, in a restricted workspace, the sequential reconnection of modules is difficult due to the limitations of the service crane operation area [4]. There is a need for additional operations that rising the machining time, such as the equipment being repositioned by crane into a new working space, MCSS re-mount, and PM re-anchor.

When the pile row on the X axis is over, again there is a need to readjust the main process: pile installation – machine displacement, together with the positioning control interruption. The parallel mounting of modules when PM moves in the transverse direction Y does not ensure the continuity of the modular grid system, and as a consequence, the impossibility of complex automation.

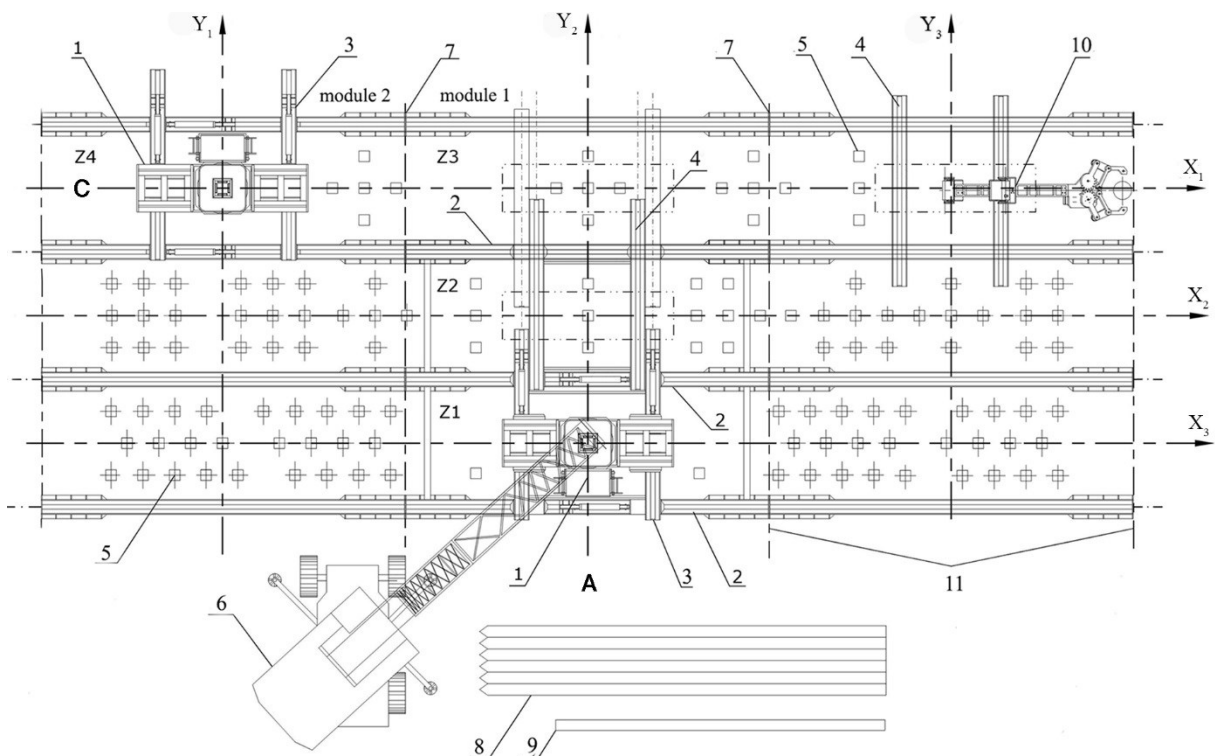


Figure 4. The layout of the coordinate method: 1 – piling machine, 2 – longitudinal guides, 3 – cross carriage (transverse), 4 – auxiliary carriage, 5 – pile point, 6 – service crane, 7 – modules connection unit, 8 – concrete piles, 9 – metal inventory tool, 10 – additional equipment, 11 – a coordinating grid system

3.3.1 Flow-production method

The use of MAPS has been proposed as a new flow-production method for pressing piles into the ground [7].

The system consists of three longitudinal guides and two cross carriages that enable the PM to move along two axes, X and Y, as shown in Figure 4, option A.

When assembling the MAPS, the main axes (X, Y) of the modules are controlled concerning the modular coordinating grid system of the building. This approach ensures proper alignment and integration of the MAPS with the building structure. The preparatory process involves mounting the longitudinal guides 2. The main carriage 3 is then mounted on the longitudinal guides, followed by mounting machine 1 on carriage 3. The hydraulic system of the modules is then connected to the PM and the anchor weights are installed using a crane.

Once the anchors have been secured, the horizontal position of the PM is checked to complete the process.

The main technological process, pile installation - machine displacement, is carried out inside working space Z1. Additional longitudinal guide 2 and auxiliary carriage 4 are mounted by the crane, without interrupting the main process. Coordinating axis distance (X–Y) to the modular grid system is permanently under control.

After all the piles are installed in Z1, PM moves to the next workspace Z2. The main process is performed.

At the same time, the modular system is reassembled. The PM moves from the auxiliary carriage 4 to the main cross carriage 3 by driving cylinders. The main process is carried out inside workspace Z3. After installing all piles inside Z3, the PM shifts to the next workspace, depending on the desired direction. Parallel to this, module 2 can be attached by crane to the extension of module 1, as shown in Figure 4, option C.

When piling is completed within the working space of module 1 (Z3), the PM moves to module 2 (Z4). The movement along the X-axis is carried out by a method of sequentially re-connecting the modules. At the same time, the auxiliary carriage 4 can be used to mount additional equipment 10 on it: a boring machine, crane manipulator, mechanisms for stone columns, vertical energy wells, etc.

This method offers modularity and flexibility for configuring different pile foundations and is suitable for use in large-scale and mass construction for multi-row and continuous pile fields. It is also most suitable for complex automation.

4 Construction Process Parameters

The study of developed piling methods using MAPS was carried out from 2014 to 2022 in Ukraine during the construction of pile foundations for civil buildings [10].

Full-scale experiments under production conditions were conducted to gather reliable data on piling processes using specified technological schemes at real sites.

The initial construction parameters can be illustrated in the example of a multistory residential complex with its underground space 'Park Fontanov', Odesa, 2018.

- Land plot size: 12.8 hectares
- Number of buildings: 10
- Height of buildings: 9 floors
- Car parking: Underground

Foundation: more than 1800 piles, 180 per building.

Pile type: reinforced C140.35 and C120.35 with a cross-section of 350×350 mm and length of 14 m and 12 m, multi-row arrangement, with a step of 1.05 m (3d).

Site conditions: clay loam with limestone layers, soil subsidence properties category – II. The category of soils is II, according to seismic properties.

Groundwater depth: 3.5 m and 10.5 m.

Equipment: Piling Machine CO-450 and MCSS.

The standard architectural and planning solutions of these buildings allowed for the implementation of a combination of options considered earlier. For example, the C-method uses two modules, as shown in Figure 5.



Figure 5. Coordinate piling method by using two modules with their sequential reconnection

Piling data: the pressing force was from 1600 kN to 2000 kN, respectively, for the pile length 12 m and 14 m. The pressing speed was from 1.5 m/min (automate) to 2.5 m/min (manual). The speed of PM displacement (manual) was 2.1 m/min. Productivity: from 20 to 30 piles per shift.

According to the project, full-scale physical modeling [3], and pile testing were made without any additional equipment, essentially requiring no temporary work.

The research methodology involved determining the duration, labor input, and the total weight of the movable load during the implementation of the complex technological process on allocated sections of 126 and 396 piles. During the study, the focus was on the main and auxiliary processes and their readjustment. The study of auxiliary processes allowed for the determination of efficiency indicators for single piles and multi-row pile fields. The comparison of these indicators, as a result of the preliminary processing of the construction datasets, is presented in the following section.

4.1 Efficiency Indicators comparison

Full-scale experiments made it possible to obtain actual data on main and auxiliary technological processes for different foundation designs, organizational and technological schemes for pile work, as well as the various site conditions and scale of construction.

The study of the main process – pile pressing into the ground, performed in automatic mode, determined that the speed of pile pressing remains unchanged (1.5 m/min) for different soil conditions if the force of soil resistance does not exceed 1600 kN at a nominal pressing force of the machine is up to 2000 kN.

To compare the efficiency indicators of the specified methods, a technological model of an anti-slide structure of 126 piles (C100.35) in a three-row arrangement on a site with a total length of 50 meters, was chosen.

The selected technological scheme is easily scalable, and its decomposition makes it possible to analyze single-row and double-row structures, as well as various pile arrangements. The following efficiency indicators have been determined for the three methods: duration, productivity, labor input, and machining time to the entire scope of piling work and per unit of output. Unit of output: 1 concrete pile with section 350×350 mm, length 10 m, pressed into a depth of 12 m.

4.1.1 Process Duration and Labor Input

The duration of separate technological processes and operations was determined in hours by timing at construction sites. Process duration is given in Table 2.

Table 2. Processes Duration

Indicator (hour)	P	L	C
Preparatory work	0.3	0.7	1.1
Assembly, anchoring	116	3.7	1.4
Piles pressing (automated)	31.5	31.5	31.5
Modules reconnection	–	2.0	0.6
Unloading, disassembling	52.5	1.8	1.2
Summary	200.3	39.7	35.8

The duration of the main automated process remains unchanged for the three piling methods.

Labor input for the entire scope of work was determined by multiplying the duration of processes by the team composition. Labor inputs are given in Table 3

Table 3. Labor Input

Indicator (man–hour)	P	L	C
Preparatory work	1.2	2.8	4.9
Assembly, anchoring	537	16.5	6.7
Piles pressing (automated)	54.5	58.7	58.7
Modules reconnection	–	6	2
Unloading, disassembling	263	7.8	4.4
Summary	856	92	77

There was a significant decrease in labor input for the identified most labor-intensive process – PM re-anchor by service crane. It is more than twice for C-method, in comparison with the L-method, and more than thirty times compared to the P-method. The process of modules sequential reconnection was decreased three times from 6 man–hours (L) to 2 man–hours (C), with constant characteristics for the basic automated process.

4.1.2 Labor Productivity

Based on the data on labor input and the total duration of the processes for the entire scope of work of 126 piles, presented in Tables 2 and 3, the following specific (unit) productivity indicators have been calculated.

Overall productivity (pile/hour) is the ratio of the entire scope of work to the total duration of its implementation. Hourly output is the number of installed piles per hour. Work output per man (man–hours, number of piles) is the ratio of the amount of work to the total labor input. Output per pile (man–hour) is the ratio of total labor input to the entire scope of work. Data given in Table 4 display the labor productivity indicators for three methods on a section of 126 piles.

Table 4. Labor Productivity

Unit Indicator	P	L	C
Overall productivity	0.63	3.17	3.52
Hourly output	1	3	4
Work output per man	0.15	1.37	1.64
Output per 1 pile	6.8	0.7	0.6

The labor productivity for C-method is increased, up to 4 piles in 1 hour, due to the non-interrupted process: pile installation – machine displacement. This is the main distinguishing feature of the automated process.

4.1.3 Machining Time

Machining time is the time taken by machines and mechanisms to install one pile. Data given in Table 5 display the machining time for tree piling methods.

Table 5. Machining Time

Unit Indicator (mach.–hour)	P	L	C
Service Crane KS-5363	1.39	0.19	0.16
Piling Machine CO-450	0.17	0.17	0.17
Modular Skidding System	–	0.03	0.03

The data in Table 5 shows that the machine time for PM and MCSS remain unchanged for the three methods.

At the same time, the most time-consuming and labor-intensive processes are provided by a service crane.

To determine a crane operating input in large-scale production (Section 396 piles), the weight of a movable load: piles, inventory tools, and piling equipment was investigated, according to identified processes.

Data given in Table 6 display the total weight of the load by elements. There are PM, anchor loads, MCSS elements, and inventory tools we have to move by a crane to install 396 piles for identified piling methods.

Table 6. Load Weight

Indicator (ton)	P	L	C	A
Concrete piles	1228	1228	1228	1228
Inventory pile	594	594	594	594
Anchor loads, PM	164000	3857	1286	429
Longitudinal guides	–	435	160	72
Transverse guides	–	–	34	51
Summary	165822	6114	3302	2374

Specific (unit) weight was decreased from 419 tons per pile for P-method to 8.5 tons for C-method and almost two times, in comparison with the L-method (16 tons). If a flow method (A) is used, this indicator is 6 tons per pile, while the weight of the concrete pile (C100.35) fed by the crane, is more than 3 tons.

The ratio in Figure 6 shows the balance between the summary weight of the piles, inventory tool, and elements of the equipment, moved by the service crane, with a fixed output volume of 396 piles.

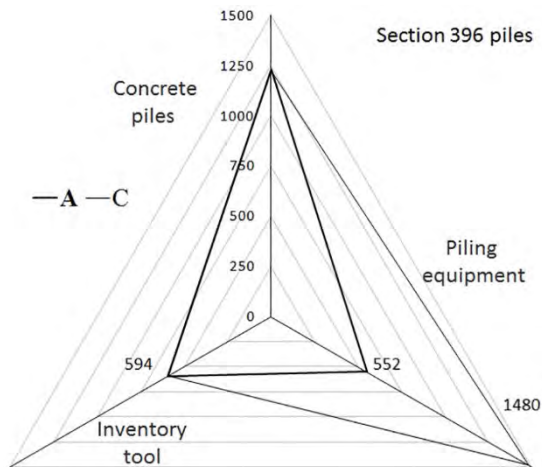


Figure 6. Summary weight by elements: A – flow-production method, C – coordinate method

The diagram illustrates the conditions under which the developed technology reaches its maximum performance at the lowest labor inputs, as well as the lowest operational cost of the equipment.

The use of an additional longitudinal guide and auxiliary cross carriage with a weight of up to 17 tons, makes mounting and anchoring processes achievable once. At the same time, the summary weight of movable equipment and inventory tool is less than the summary weight of the piles which have to be fed by a crane.

5 Technological Process Modeling

The different configuration and heterogeneity of construction objects, as well as the different number of piles and their mutual arrangement in foundation designs, necessitate the use of various methods and options for piling works. Technological modeling of construction processes was performed for three classified methods: Point (P), Lineal (L), and Coordinate (C).

Options are models of complex processes, developed according to standardized technological schemes:

1. Option C1 – one aggregate module with dimensions: 4.2×12 m, up to 24 piles in one grip;
2. Option C2 – two modules connected in series with dimensions: 4.2×24 m, up to 60 piles in one grip;
3. Option C3 – sequential reconnection of modules, which involves the flow method, more than 60 piles;
4. Option L1 – two longitudinal guides with a grip dimensions: 1.2×12 m, up to 8 piles in one grip;
5. Option L2 – four longitudinal guides connected in series, dimensions: 1.2 (4.2)×24 m, up to 20 piles;
6. Option L3 – sequential reconnection of four longitudinal guides, more than 20 piles;
7. Option P1 – single piles while conducting soils control tests with a piling machine: 1.6×6 m, 1 pile;
8. Option P2 – involves work in the construction flow, when the quantity of piles is more than one.

The most significant factors affecting all efficiency indicators are the total number of project piles (scale of production) and the weight of the load (piles, machines, modules, inventory tools, and anchor loads) moved by the service crane during the piling process.

The scale of production is the main design factor that affects all elements of the organizational and technological structure. With an increase in the number of piles, the number of processes for moving the specified loads by service crane increases.

The selected efficiency indicator (specific weight of the load) does not depend on the duration of processes and operations, soil conditions, and configuration of the foundation, as well as random factors, which can be used for a comparative assessment of various work options.

The main and auxiliary technological processes, in which the crane is used, are determined by three methods:

- MCSS assembly, mounting, and anchoring
- Pressing a pile (basic automated process)
- Positional displacement of the machine
- Modules sequential reconnection
- Machine unloading, MCSS disassembling

The unit of output is one precast concrete pile (C100.35), with section 350×350 mm, length 10 m, pressed to a depth of 12 m in automatic mode. The speed of positional displacement is 2.1m/min, in manual mode.

5.1 Generalizing Mathematical Models

It has been found [10] that the dependence of the efficiency indicators, calculated per one pile, on the scale of production for three piling methods and different options of work is described by a single formula (1).

$$E = A + B/N \quad (1)$$

E – efficiency indicator, A and B – constant coefficients, N – number of project piles.

The relation of the specific (unit) weight of the load, moved by the crane, on the total number of project piles for various options, is described by formula (2).

$$w = \Sigma W/N \quad (2)$$

w – specific weight, ΣW – summary weight
A graphical illustration is shown in Figure 7.

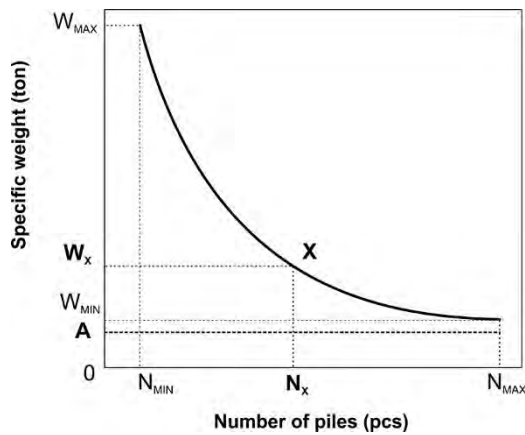


Figure 7. Relation between the specific weight of the load and the number of project piles

Graphically, function (2) represents a hyperbolic curve that approaches "A" asymptotically as "N" approaches infinity. The minimum number of piles required for any work option is one pile, which corresponds to the maximum value of the specific weight of the load. The minimum value of the specific weight is achieved when the maximum number of piles is used in the module space. For the current number of piles, a perpendicular line is drawn from the abscissa axis to the point of intersection with the hyperbola, and the corresponding value of the specific index on the ordinate axis is determined. If the number of piles exceeds N_{max} , then the equipment is moved to a new workspace, which is represented by the corresponding step (not shown), after which the hyperbolic nature of the relationship is preserved. Mathematical models have been developed to quantify efficiency indicators, such as the specific weight of the load moved by a service crane, as a function of the total number of project piles, the number of modules used,

and the different options for their use. These models are accompanied by graphic illustrations [10] and have practical value, making them suitable for use in the design and preparation stages of piling work. Similar approaches can be used to evaluate other specific efficiency indicators, such as productivity or direct cost, using appropriate algorithms and recommendations.

5.2 Technological Solutions Optimization

The algorithm for the variant design of the complex technological process is based on obtained mathematical models. It consists of three main stages:

1. Analysis of the foundation design
2. Evaluation of options for technological structure
3. Development of the final organizational solution

At each stage, the following main tasks are expected to be performed.

Stage 1: Selection of the main direction of MAPS movement along the longest (longitudinal) axes of the building; possible options for the production of works using a modular structural-planning (technological) grid are considered; a qualitative critical analysis of the planned options is carried out, taking into account the limitations of a particular construction site.

Stage 2: Using graphic illustrations, the planned options are evaluated according to the criterion of the specific (unit) weight of the load; the required production resources are determined, a set of equipment is selected and its layout is carried out at the installation site; the most effective option or a combination of options is determined, taking into account the restrictions of the site.

Stage 3: A decision is made on the choice of the final version, taking into account the possibility of its implementation under specified conditions; a typified technological scheme and appropriate set of machines and documents are selected; the calculation of efficiency indicators (productivity, labor input, machining time and cost of work) of the final version is performed.

Variant design of complex technological processes, using the indicated mathematical models, is based on the choice of optimum solution, according to the value of the specific efficiency indicator. The proposed methodology makes it possible to evaluate all methods of pile work, at the stage of foundation designing, and choose the most effective combination of options, especially, under complicated conditions, such as confined spaces and weak soils. It should be noted that complex automation should also include the system for positional movement and control, together with the list of parts and phases which have been described [5]. The trained network can then be used to make informed decisions that optimize the construction process based on the specific objectives and constraints of the pile fields.

6 Conclusions

This manuscript appears to be a technical report or research paper on the development of technology for the automated construction of pile foundations, based on the use of a Modular Aggregative Piling System (MAPS).

The system incorporates a modular approach to pile construction, which provides architectural flexibility and adaptability for different construction projects, especially in challenging conditions.

Currently, the main process of pressing piles into the ground is automated. However, the concept implemented in MAPS involves the automation of the positional movements of the equipment concerning the building's coordinating grid system. This can serve as a common platform for the interaction of construction machinery, compatibility of the CAD/CAM interface, and existing Building Information Models.

Full-scale experimental tests have been carried out, to establish a database, on real construction sites during the industrial operation of MAPS from 2014 to 2022.

The technological process modeling for 126 concrete piles in a multi-row arrangement on a site with a length of 50 m provided the basis for determining the efficiency indicators of the developed flow-production method and comparing it with the basic point method.

The total duration was reduced from 200 h to 36 h;

Labor inputs for the entire scope of pile work were from 856 man–hours to 77 man–hours;

Hourly productivity increased from one pile per hour up to four piles per hour;

Labor input for pressing one pile was reduced from 6.9 man–hours to 0.61 man–hours;

Machining time for one pile was reduced from 1.56 machine–hours to 0.36 machine–hours;

The volume of auxiliary processes was reduced from 84% to 8% of the total time spent on the production of the entire volume of work.

Mathematical models have been determined to establish the relationship between the specific weight of the load on the total number of project piles and the number of modules used, for various options of work.

The asymptotic minimum, for the equipment used and pile type C100.35, is 420 tons per pile for the point method and 6 tons for the flow coordinate method.

The further direction of research is focused on solving the problem of complex automation.

Since objects are heterogeneous and many factors have to be taken into account, a new approach to solving optimization tasks is needed, both in the design phase and in the construction process. One potential approach is to use machine learning to optimize the piling processes in a way that maximizes the desired outcomes while minimizing negative impacts or costs.

The following practical results of this study can be used to optimize data using artificial neural networks.

A database of construction processes and operations collected during industrial equipment operation is utilized. A single standardized mathematical function is used to describe these processes for various work options.

An optimization algorithm based on mathematical models is utilized to improve construction solutions.

The approach utilizes a framework that combines a modular grid of equipment with a building-coordinating grid system to capture data from building processes.

Overall, the use of a database, mathematical models, algorithms, and frameworks can improve the efficiency of aggregate-modular type piling systems in foundation engineering, particularly under challenging conditions.

References

- [1] Khoshnevis B., Hwang D., Yao, Yeh Z. Mega-scale fabrication by contour crafting. *Industrial and Systems Engineering*, 1 (3): 301, 2006.
- [2] Abou-Zeid, M., & El-Rayes, K. Underground construction: A risky business. *Journal of Construction Engineering and Management*, 131(9), 1001-1009, 2005.
- [3] Doubrovsky M. and Meshcheriakov G. Physical modeling of sheet piles behaviour to improve their numerical modeling and design. *Soils and Foundations*, vol. 56, Issue 4. *Official Journal of the Japanese Geotechnical Society*. Elsevier, 2015.
- [4] Wahler E., Meshcheriakov G., Doubrovsky M., Research and development of piling technology in a restrained urban environment *Proceedings of Geotechnical Challenges in Megacities*, Vol.2, pages 479–486, Moscow, 2010.
- [5] Rauno Heikkilä, Teemu Kivimäki, Katja Puolitaival. Development of Automation for Foundation Engineering–Case Piling Machine and the Working Process of Driven Piling. *Proceedings of the conference*, ISARC 27th International Symposium on Automation and Robotics in Construction, pages 73–80, Bratislava, Slovakia, 2010.
- [6] ISO 2848:1984 Building construction – *Modular coordination – Principles and rules*.
- [7] Meshcheriakov G. Method for construction of pile foundations and piling system, *Patent of Ukraine # 114055 Bulletin # 7/2017*.
- [8] Meshcheriakov G. and Vakulin N. Mechanism for moving heavy machinery or other structures, *Patent of Ukraine # 62369 Bulletin # 16/2011*.
- [9] Shinnosuke M. Construction Revolution. On-line: <https://www.giken.com>, Accessed: 23/03/2023.
- [10] Meshcheriakov G. Technology for pressing piles by using a modular aggregative system. On-line: http://odaba.edu.ua/upload/files/Meshcheriakov_pdf. Ph.D. Thesis, page 15, Accessed: 02/01/2023.

Bulldozer sensing technique for the purpose of automation for bulldozer's workflow

Alexey Bulgakov¹, Thomas Bock², Georgiy Tokmakov³ and Sergey Emelianov⁴

¹Central Research and Development Institute of the Ministry of Construction of Russia, Russia

²Department of Architecture, Technical University of Munich, Germany

³Department of Mechatronics, South-Russian State Polytechnic University (NPI), Russia

⁴Southwest State University, Russia

agi.bulgakov@mail.ru, thomas.bock@br2.ar.tum.de, tokmakov_ge@npi-tu.ru, esg@mail.ru

Abstract –

Recently, global positioning systems - GLONASS and GPS are increasingly used for road construction machines. Often, mobile stations installed on the construction site are used, which increase positioning accuracy, but have a limited range. Providing a signal source to every running machine is very costly. Taking into account the often large length of construction sites, it is laborious to move the mobile station. It is also worth considering the insufficient positioning accuracy of these systems in some areas of the world.

Therefore, in order to implement an effective workflow, it is necessary to develop and apply systems for monitoring and controlling the workflow of a bulldozer based on an alternative approach.

The purpose of the research is to collect data on the parameters of working processes in dynamics to identify the working process of the bulldozer, assess the statistical characteristics of disturbing influences and confirm the mathematical models of the working processes of the bulldozer.

In the article, the authors propose a method for digitizing experimental data based on the provisions of the theory of random processes and digital signal processing. A technique for changing the sampling rate of measured signals while maintaining working signal, used to characterize measured process indicators, analyze dynamics and identify a bulldozer's workflow.

Keywords –

Mechatronic system; Bulldozer blade; Leveling control; Sensing system

1 Introduction

There is a very common laser control system is a high-tech earthmoving installation that allows you to perform work without the usual use of building poles and

leveling rods. The use of laser technology, components of the used machinery, and a remote laser transmitter allows the machine control system to obtain accurate information about the terrain, displaying it on the display located in the cab, and, ultimately, setting the blade in the desired position.

A laser transmitter located outside the cab on a tripod emits a thin beam of light that rotates 360 ° to create a slope calculation above the construction site. The cutting edge, located above the surface to be graded, is controlled by a signal sent from an electrically driven tripod that automatically locates the laser receiver within 1.5 mm of the center of the laser beam [1].

The display located in the cab of the bulldozer shows information about the position of the knife blade relative to the ground, at the same time showing where the construction site should be excavated, and where - dumping. The automatic control of the position of the blade allows precise adjustment of the cutting edge. Depending on the content of the correcting signals, the hydraulic double control valve automatically raises or lowers the blade edge, constantly holding it in the desired position, which ensures precise work execution and guarantees an optimal level of labor productivity [2].

The advancement of GLONASS / GPS technology and its use in construction helps to reduce labor requirements and helps heavy equipment operators to complete the work order under the design solution, through careful excavation and filling of soil, it can achieve material cost savings [3].

The system operates as follows: on-board equipment is installed on vehicles, which includes a satellite GLONASS / GPS receiver, a microcontroller, and information collection and transmission facilities. The on-board equipment is used to determine the current coordinates, speed, course, collect information about the status of sensors, control actuators, and signals. All this information is processed specially and transmitted/received to the dispatch center. The accumulated information from the database is used to

analyze and generate the necessary reports and logs.

Such a control system is a high-tech machine control system and a dialogue control system that allows you to reach the proper level of earthwork without elevation marks and leveling rails. Digital design inputs, manuals, and instructions in the dozer's automatic blade position control system help you achieve the desired result faster, more efficiently, and economically, with lower costs.

Bulldozers equipped with modern navigation and information systems are mobile mechatronic objects, and they can be integrated into general process of intellectual construction. The integration will provide optimal efficiency of the construction cycle and will ensure lean production process.

On the basis of bulldozer's workflow dynamics modeling and analyses described in a variety of works, we have concluded that the models to describe kinematics and dynamics of its working equipment, hydraulic and transmission features tend to be analytical formulas derived from well-known laws of physics and from information on bulldozer's structure and mechanisms. If some parameters of the workflow are unknown or constantly changing, the models are either statistical tables or empiric dependences summarizing experimental data. The models depict interaction of end-effectors, engines and environment as well as statistic features of bulldozer's complex units.

Application of regulators based on classical control theory is difficult due to the frequent changes in workflow conditions. Thus, it is necessary to develop adapted control systems to eliminate the difficulties described. The system includes both the bulldozer's dynamics modeling and bulldozer's workflow control method to take into consideration the complex non-linear dependencies between workflow parameters and incomplete information on its working conditions changes.

Having reviewed adaptive and intellectual control methods [4, 5], we propose to create an adaptive control system for technological processes to increase efficiency of bulldozer's control in comparison with traditional control methods.

2 Mathematical model to estimating the position of blade cutting edge

Observations [6-8] show that quite often while designing a face its roughness is progressing, reaching a size at which the control over the workflow is lost. In this case, the operator has to align the face deliberately, trying to ensure its "tranquil" profile that allows doing excavation works smoothly, without frequent control system switching and reducing the dozer's operating speed that causes a slowdown and shows inferiorities of the blade control system. Obviously, if the control system

operates in the antiphase towards deviations of the tractor frame with sufficient accuracy, the initial face roughness will not evolve and will be gradually cut. One of the most likely causes of the opposite phenomenon observed in practice, is the disparity between the velocity of the dozer V_p and actual conveying speed of the working body V_{ot} required in certain areas S_i of the digging operating cycle, where i – is the number of the speed change V_{ot} . Speed ratio depends on the dozer's geometrical dimensions (Fig. 1) and its control system.

Mathematical model of the dozer's movement on a straight line tracking (frame alignment) is built using the Lagrange equations of the 2nd kind, under the assumption that the contribution to the dynamics of the drive gears and a track is small, compared with the contribution of the remaining parts of the dozer.

$$\begin{cases} \frac{d}{dt} \left(\frac{\partial T}{\partial \dot{x}} \right) - \frac{\partial T}{\partial x} = Q_x, \\ \frac{d}{dt} \left(\frac{\partial T}{\partial \dot{\varphi}} \right) - \frac{\partial T}{\partial \varphi} = Q_\varphi. \end{cases} \quad (1)$$

where kinetic energy:

$$T = \frac{1}{2} m_1 \dot{x}^2 + \frac{1}{2} m_2 (\dot{x}^2 + (l_2 l_{c2} \dot{\varphi})^2 + 2 \dot{x} l_2 l_{c2} \dot{\varphi} \sin(\varphi)) + \frac{1}{2} J_{c2} \dot{\varphi}^2 + \frac{1}{2} \sigma h x (\dot{x}^2 + (l_2 \dot{\varphi})^2 + 2 \dot{x} l_2 \dot{\varphi} \sin(\varphi)) + \frac{1}{2} \sigma h x i_{rz}^2 \dot{\varphi}^2; \quad (2)$$

generalized forces acting on a dozer:

$$\begin{aligned} Q_x &= -\sigma h g l_2 \sin \varphi + F_T - F_S, \\ Q_\varphi &= -(m_2 l_{c2} + \sigma x h) g l_2 \cos \varphi + M; \end{aligned} \quad (3)$$

m_1 – tractor mass; m_2 – blade frame mass; σ – soil surface density; F_T machine pulling power; F_S ground cutting resistance; h – depth of the soil cutting; l_{c2} – center of the blade mass; i_{rz} – gyration radius of the dumping soil.

$$m_1 \ddot{x} + m_2 \ddot{x} + m_2 l_2 l_{c2} \ddot{\varphi} \sin \varphi + m_2 l_2 l_{c2} \dot{\varphi}^2 \cos \varphi + \sigma h \ddot{x}^2 + \sigma h x \ddot{x} + \sigma h \dot{x} l_2 \ddot{\varphi} \sin \varphi + \sigma h x l_2 \dot{\varphi} \ddot{\varphi} \sin \varphi + \sigma h x l_2 \dot{\varphi}^2 \cos \varphi - \frac{1}{2} \sigma h \dot{x}^2 - \frac{1}{2} \sigma h i_{rz}^2 \dot{\varphi}^2 - \frac{1}{2} \sigma h (\dot{x}^2 + l_2^2 \dot{\varphi}^2 + 2 \dot{x} l_2 \dot{\varphi} \sin \varphi) = -\sigma h g l_2 \sin \varphi + F_T - F_{comp}. \quad (4)$$

$$m_2 l_2^2 l_{c2}^2 \ddot{\varphi} + m_2 \dot{x} l_2 l_{c2} \sin \varphi + m_2 \dot{x} l_2 l_{c2} \cos \varphi \dot{\varphi} + J_{c2} \ddot{\varphi} + \sigma h \dot{x} l_2^2 \dot{\varphi} + \sigma h x l_2^2 \dot{\varphi} + \sigma h \dot{x} l_2 \sin \varphi + \sigma h x l_2 \cos \varphi \dot{\varphi} + \sigma h \dot{x} i_{rz}^2 \dot{\varphi} + \sigma h x i_{rz}^2 \dot{\varphi} - m_2 \dot{x} l_2 l_{c2} \dot{\varphi} \cos \varphi - \sigma h \dot{x} l_2 \dot{\varphi} \cos \varphi = -(m_2 l_{c2} + \sigma x h) g l_2 \cos \varphi + M. \quad (5)$$

The system (1) solution allows getting the differential equations (4) and (5) that describe the dozer's movement on a straight line track, and determining control actions through the parameters of the machine in areas S_i of the digging operating cycle as the coefficients a_i in the dependence $V_{ot} = a_i V_p$. Such a dependence is typical for dozers with a single-motor drive with a hard pump hydraulic drive connection to the motor shaft.

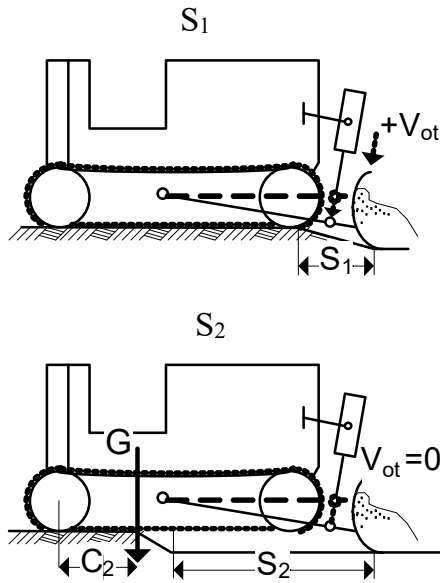


Figure 1. The movement of the tractor frame the beginning of digging

At the beginning of digging (Fig. 1), the frame of the tractor makes a strictly forward movement over a distance of S_1+S_2 without hesitation relatively its mass center. The blade cutting edge in the area S_1 dives into the soil to a depth equal to a predetermined cutting thickness h . Thus, the control action a_1 may be determined by the formula:

$$a_1 = \frac{30i_{tr}m l_2}{\pi r_k F_z i_{pr} C_5 n}, \quad (6)$$

where i_{tr} , i_{pr} - tractor transmission and hydraulic pump ratios; n - number of hydraulic cylinders; m - fluid mass in the hydraulic cylinders;

In the area S_2 the movement is made with $a_2=0$ until the mass center of the tractor won't move to the buttonhole edge.

On further movement the dozer "dives" in the drawn buttonhole (Fig. 2), so in the area S_3 it is necessary to lift the blade at a rate of V_{ot} , determined by the coefficient a_3 :

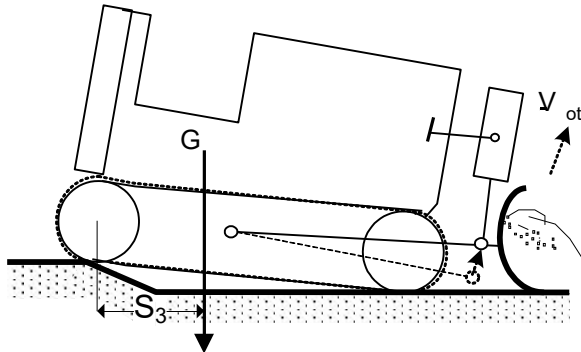


Figure 2 The movement the dozer "dives" in the drawn buttonhole

$$a_3 = \text{tg } \beta \left[e^{\frac{aV_{nt}}{C_1+V_{nt}}} \left(1 + \frac{aC_1}{C_1+V_{nt}} \right) - 1 \right]. \quad (7)$$

The area S_3 ends after the dozer's back gear hits the edge of the face and reverse alignment of tractor frame starts. Length of the alignment area is $S_4 \approx S_1$. Obviously, during this period it is necessary to start dropping the blade. The a_4 determines the rate of dropping the blade in the given area:

$$a_4 = \frac{C_3 S_1}{(C_4 + S_3 + V_{nt})^2}. \quad (8)$$

To implement control actions $a_i = f(S_i, t, h)$ the dozer must be equipped with a vertical blade control system.

The developed models for bulldozer workflow elements are to be used for separate bulldozer units study with the help of analytical dependences between workflow parameters as well as for bulldozer general workflow simulation [8].

Elements models of bulldozer workflows being developed are intended both for the research of individual bulldozer units using analytical relationships between the parameters of the workflows and simulation of bulldozer workflows in general [9-10].

When constructing a discrete simulation model, the following assumptions are taken:

- the linear motion of the machine is investigated;
- the design is considered to be rigid;
- backlash and friction between the elements of the working equipment are not considered;
- the elastic- damping properties of movers are not considered;
- the dynamic characteristics of a diesel engine with fuel regulator and hydro mechanical transmission torque converter are replaced with static;
- coordinates of the treated soil surface are completely determined by the coordinates of the cutting edge of working organ;
- engine power selection to the drive of the working organ and auxiliaries are neglected;
- rate of motion of hydraulic cylinders rods for lifting and burial of the working organ is identical and does not depend on the applied load;
- mover rolling resistance is constant.

A simulation model is implemented in MATLAB / Simulink [7, 10, 13].

3 System configuration for the purpose of automation for bulldozer's workflow

The purpose of the experimental studies was to compare the performance of a bulldozer equipped with modernized and serial working equipment. The main goal of the experiment is to collect the data needed to identify the bulldozer's workflow [8-12].

The sensors connection scheme is shown in Figure 3. As a result of measurements, signals $P(t)$, $v(t)$ and

digging depth $l(t)$ were obtained, used to identify the working process of the bulldozer.

To collect experimental information on the parameters of the working process of the bulldozer in dynamics, laboratory studies of the process of cutting the soil with a flat knife during movement were carried out. The automated collection of the values, of the speed V and the resistance force movement P was carried out. Experimental signals are used to identify the workflow using neural network mathematical models.

Experimental data loaded simulation model. Simulation tasks:

- To single out the main sub-systems in bulldozer's structure and interrelations between the sub-systems;
- To develop analytic and simulation models for workflow elements and to include them into the general structure of the model.

The structure meets the goals of workflow control. When moving soil by the bulldozer, it is necessary to utilize bulldozer's traction capacity in full keeping the nominal traction value; when surfacing, the altitudes of the right and left side of the blade are to correspond the design marks. The key element at the scheme (Figure 4) shows the choice for the first or the second operational mode.

At developing the models, we use mathematical apparatus of the random processes theory, transfer

functions, table interpolation, numerical solution of algebraic equations and ordinary differential equations in the Cauchy form. Random changes in the coordinates of untreated soil surface, as well as normalized fluctuations in the resistance forces on the working organ, caused by the heterogeneity of the soil are highlighted among the disturbing effects on the working organ of the bulldozer from soil conditions. Loading conditions on the working organ are due to random variation in the dig depth and heterogeneity of soil properties.

Soil digging process with bulldozer working organ is studied on the base of the finite element model of the soil mass, a mathematical model of random forces of resistance on the working organ being developed. The actual bulldozer velocity depends on the strength and the properties of the mover, transmission and the power unit. In its turn, disturbance parameters, movement of the working organ and the formation of stress depend on the velocity. Bulldozer drive model and mover interaction with the soil include engine model, mechanical and hydro mechanical transmission, as well as slipping. Control system regulator depending on the objectives, control algorithm and the incoming data from the bulldozer as a control object produces electrical signals to the electrohydraulic distributors being part of the working organ hydro drive. Lifting or burying the blade is done to control either the pulling power, or the blade coordinates.

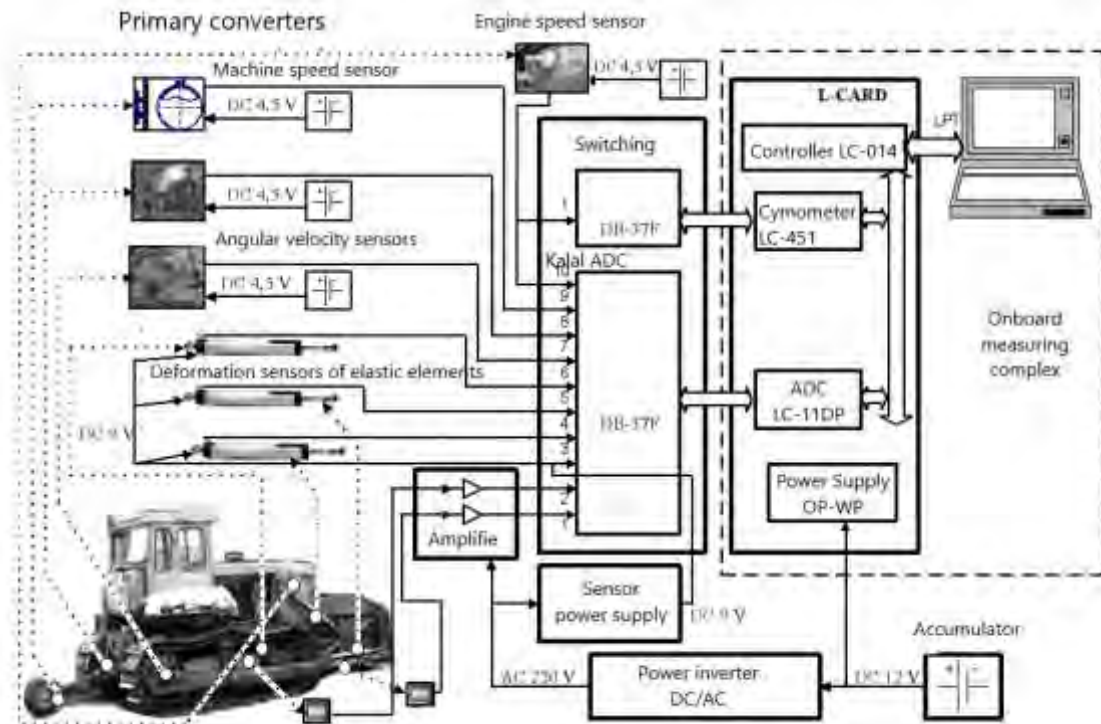


Figure 3. Connection scheme of sensors

After training the model, load the data into the on-board complex of the bulldozer to check the adequacy of the model. To evaluate the proposed system, two experiments were carried out:

- Operator controlled without using an automatic system (Fig. 4a);

- When controlling the operator using the developed system (Fig. 4b);

After that, the results were compared.

Thus, it can be noted that the system allows you to simulate a bulldozer digging surface with a deviation not exceeding 2 cm.

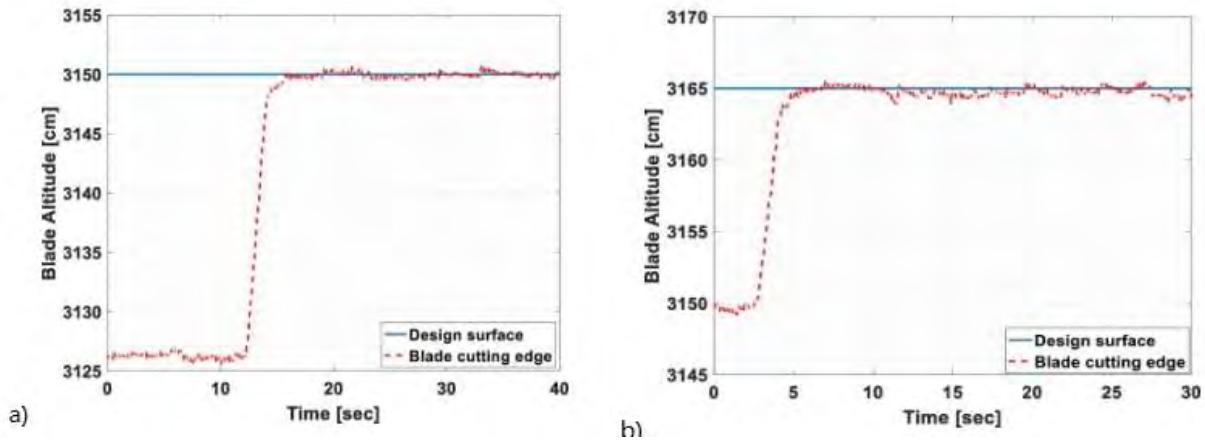


Figure 4. Verification system modeling surface

4 Conclusions and Results

Input model signal, used for training, simulation and verification is presented in Fig. 5a. Adaptive learning for the model is stopped at time $t=9,5$ sec. Receiving at this moment a neural network model parameter values,

modeled digging resistance force and speed of the machine (Fig. 5b, 5d) are accomplished, as well as the forecast for another 0.5 seconds is developed [10].

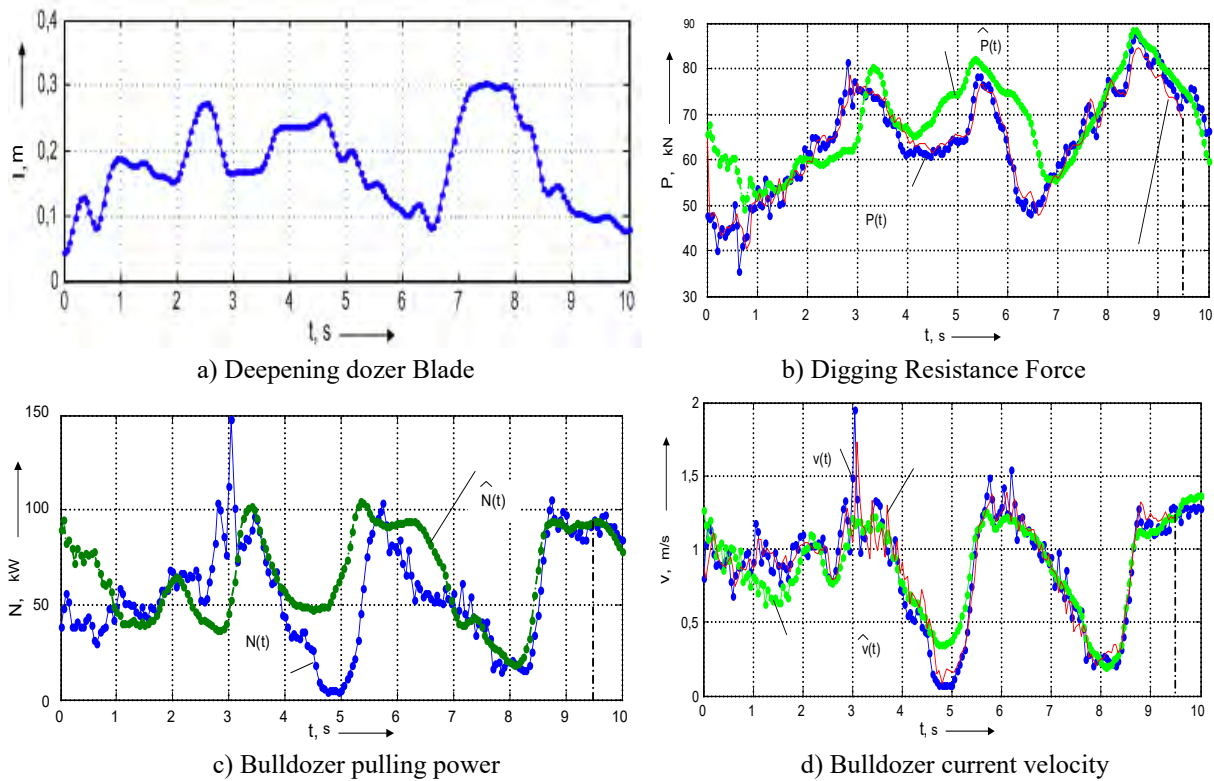


Figure 5. Comparison of Bulldozer operational parameters obtained with the Model and actual operational parameters

Figure 5c shows the output of neural network models-pulling power of the bulldozer. In modeling and prediction of the neural network output is close to the experimental data only in the time interval of 7-10 sec. This is due to a change in unmeasurable chip thickness, as well as the rapidly changing conditions of the mover clutch with the ground. Therefore, the parameters of the adaptive neural network model must be adjusted in real time. The accuracy of prediction of pulling power $N(t)$ has been estimated; the average relative error being 14.7 % on an interval from 7 to 10 s [7]. Identification Technique of bulldozer workflows and models obtained on its basis, are designed for use in the development of adaptive systems of automatic workflow management of bulldozer [11-14].

Identification technique of the dozer's working processes and models obtained on its base, are intended to be used in the development of adaptive systems of automatic control of the dozer's working process.

For the formation of the control actions influencing the bulldozer, particularly electrical signals actuating control valves of hydraulic cylinders lifting and lowering the working organ, the structure and algorithms of adaptive neural network controller have been designed.

References

- [1] Roberts G., Dodson A. and Ashkenazi V. Global Positioning System aided autonomous construction plant control and guidance *Atom. Constr.*, 8 (5) (1999), pp. 589-595, 10.1016/S0926-5805(99)00008-4.
- [2] Trimble Corporation. Civil Engineering and Construction, Grade Control for Dozers. On-line <https://construction.trimble.com/products-and-solutions/grade-control-dozers>, Accessed 4th Jul 2019.
- [3] Komatsu Corporation. Intelligent Machine Control. On-line <https://www.komatsu.eu/en/Komatsu-Intelligent-Machine-Control>, Accessed 4th Jul 2019.
- [4] Roberts G., Ogundipe O. and Dodson A. Construction plant control using RTK GPS *Proceedings of the XXII International Congress of the FIG*, 6 (2002), pp. 1-13 https://www.fig.net/resources/proceedings/fig_proceedings/fig_2002/TS6-2/TS6_2_roberts_ogundipe_dodson.pdf
- [5] Jehle P., Bulgakov A. and Tokmakov G. Mechatronics Systems and Logistic Service for Ensuring the Smooth Construction Process. // *Creative Construction Conference 2014 June 21–24, 2014 Prague, Czech Republic. – Budapest, Szent István University, Proceedings CC2014*, pp. 242-247.
- [6] Bulgakov, A. and Tokmakov, G. ERP-systems, logistics and mechatronics systems for ensuring the smooth construction process // *Journal of Applied Engineering Science Volume 16, Issue 1, 2018, Pages 1-4. ISSN: 14514117 DOI: 10.5937/jaes16-14653*
- [7] Bulgakov, A., Tokmakov, G., Otto, J. and Langosch, K. Evaluation of the construction project success with use of neural networks // *Proceedings of the Creative Construction Conference (2018), 30 June - 3 July 2018, Ljubljana, Slovenia, pp. 46-50. ISBN 978-615-5270-45-1 DOI: 10.3311/CCC2018-007 http://2018.creative-construction-conference.com/wp-content/uploads/CCC2018_Proceedings.pdf*
- [8] Krapivin D., Nefedov V. and Tokmakov G. Mathematical model for the movement of mechatronischen devices for the intelligent building site, *Mechatronik, Lik, Nowotscherkassk, 2010.- S. 50-54.*
- [9] Shestopalov K. Hoisting-and-transport, building and road machines and equipment. Moscow: Academy, 2009. P. 67-72.
- [10] Bulgakov A., Bock, T. and Tokmakov G. Adaptive control of bulldozer's workflows // *5th International Construction Specialty Conference, Vancouver, June 7 - 10, 2015, pp. 434-442.*
- [11] ROBO Industries Autonomous Machine Control System On-line <http://www.aee.us.com/page-video.html>, Accessed 4th Jul 2019
- [12] Guangqiu Yin, He Fuyin, Zhanfu Li, Jingxiu Ling Workspace description and simulation of a backhoe device for hydraulic excavators, *103325 Automation in Construction Volume 119, November 2020.*
- [13] Yong-Seok Lee, Sang-Ho-Kim, Jongwon Seo, Jeakweon Han and Chang-Soo Han. Blade control in Cartesian space for leveling work by bulldozer, *Automation in Construction Volume 118, October 2020/*
- [14] Rutkovskij L. and Pilinskij M. Neural networks, genetic algorithms and fuzzy systems., *Gorzachaza Liniza TELEKOM, 2004.*

Proposal of an Open Platform for Autonomous Construction Machinery Development

Genki Yamauchi¹, Endo Daisuke¹, Hiroataka Suzuki¹, and Takeshi Hashimoto¹

¹Public Works Research Institute, Japan

yamauchi-g573bs@pwri.go.jp, endou-d177cl@pwri.go.jp, suzuki-h574cl@pwri.go.jp, t-hashimoto@pwri.go.jp

Abstract -

We are currently experiencing a shortage of skilled labor in the construction industry, thus it is imperative to improve productivity at construction sites. One of the most effective ways to address this issue is through the implementation of autonomy. Machine control systems have been utilized for heavy equipment for over a decade, providing a measure of autonomy through control in 3D environments. However, fully autonomous systems that are able to recognize and navigate their environment, plan their motions, and control their actions, have yet to be developed. Autonomy in the realm of construction is particularly challenging due to the vast array of construction equipment, different types of construction work, diverse environments, and complex interactions between machines and the earth. To promote research and development of autonomous construction technology, we have developed an open-source based platform. This paper presents the open platform for autonomous construction machinery, including its fundamental rules and systems, to accelerate research and development.

Keywords -

Autonomous Construction; Open Platform; OPERA;

1 Introduction

Construction industry is facing a severe labor shortage, which is expected to further accelerate in the future. The Ministry of Land, Infrastructure, Transport, and Tourism (MLIT) of Japan has been promoting "i-Construction," a strategy that leverages information and communications technology to enhance efficiency across all stages of the construction process, from surveying and design to construction and maintenance. i-Construction has enabled more efficient information acquisition and communication methods, as well as improved support for the operation of construction equipment[1].

To further improve productivity, it is expected to realize autonomous construction, which would allow a single operator to simultaneously manage multiple construction machines while performing construction work. Autonomous construction necessitates the development of construction machines that are able to automatically and appropriately

plan their movements based on design drawings and the surrounding environment as recognized by the construction machines.

Incorporating new players in the construction industry with advanced technologies such as robotics, and AI is crucial for the realization of autonomous construction. However, it can be difficult for those who are not familiar with the construction industry to set-up construction equipment, modify it to enable automated operation, and prepare a field to verify the results of development. Research and development for autonomous construction have traditionally been carried out by individual companies, leading to duplication of effort across the industry and making it difficult to achieve cost-effectiveness. To address this problem, standardization and cooperation are considered to be important[2]. In response to these social needs, the Public Works Research Institute (PWRI) has been developing an open-source-based autonomous construction technology platform, named OPERA (Open Platform for Earthwork with Robotics and Autonomy), with the aim of facilitating the efficient development and easy dissemination of autonomous construction technology. OPERA aims to improve the reusability of development products, avoid duplication of research and investment, and enable the participation of universities and start-up companies with advanced technologies. This paper presents the open platform for autonomous construction machinery, including its fundamental rules and systems.

2 Related Works

Rauno et al. [3] developed a platform for the development of automation systems for hydraulic excavators. They modified the hydraulic system and created a research and development platform comprising hydraulic excavators and simulators that are compatible with autonomous operation. The platform is specific to one hydraulic excavator model and there is no indication of its expansion to include other types of construction equipment. Ashish[4] conducted survey research on a heavy equipment platform ecosystem utilizing the Robot Operating System (ROS). They interviewed software providers, consultants, and manufacturing organizations and found that

these companies have an interest in utilizing ROS. However, both of these studies do not target the development and publication of an open-source-based platform that includes actual machines and simulators.

Autoware[5] is an open-source software platform for autonomous driving technology. It is built on the basis of ROS (Robot Operating System), an open-source middleware for robots, and provides various functions for autonomous driving based on information obtained from sensors such as LiDAR, cameras, and GPS. Autoware is a system for autonomous driving of automobiles, and the control of work machines that come with construction equipment is beyond the scope of the system.

3 Open Platform for Autonomous Construction Machinery Development

Our aim is to establish standards for autonomous construction technology through OPERA for more efficient technology development and on-site operation among stakeholders as shown in Figure 1. OPERA comprises a set of common control messages, middleware, simulators, a demonstration environment including construction equipment and an experimental field. Common control messages standardize the data format of construction machinery control signals, various sensors, switches, etc., making it easy to utilize and share the data. This eliminates the need to consider control signals for each manufacturer or model. Simulators allow for testing and verification of operation under various conditions and control algorithms in a virtual environment. This is expected to shorten the development cycle and reduce costs. Actual machines and fields that correspond to common control signals are provided, and the results verified by simulators can be demonstrated through actual machine testing and experimentation.

Figure 2 shows the system configuration of OPERA schematically. The following subsections provide a detailed description of each component. OPERA also includes some application software required to control construction machinery.

3.1 Common Control Message

Ensuring the reusability of the system to be developed is important to improve the cost-effectiveness of the development and it is desirable to have the ability to control different models from various manufacturers. As shown in Figure 3, We propose a common control message for construction machinery that abstracts hardware, enabling the control of different hardware in a consistent manner and thereby improving interoperability among machines.

The proposed common control message is based on ISO 15143 Part 3[6]), an international data exchange standard

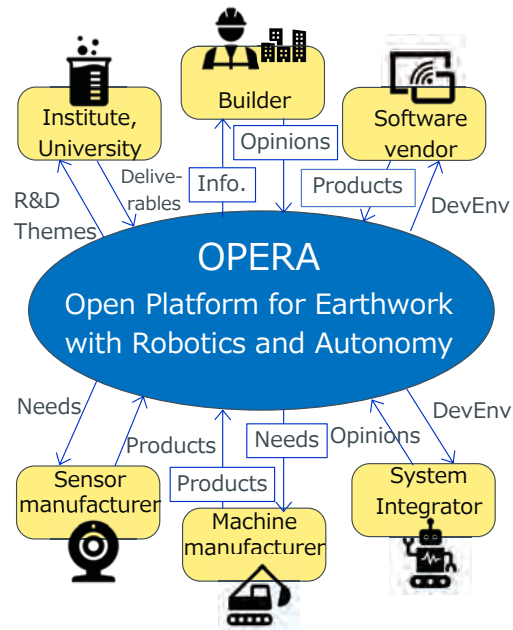


Figure 1. Overview of OPERA Utilization

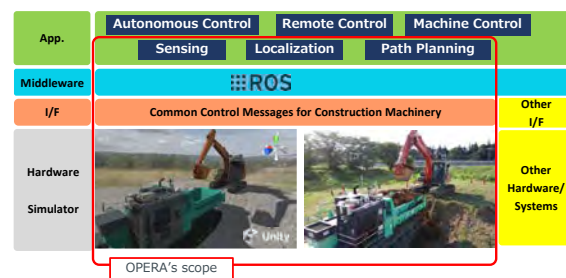


Figure 2. Overview of OPERA System

for construction work-site. From the perspective of dependence on the control characteristics of the machine, functional blocks (blue box) were configured as shown in Figure 4.

Taking a hydraulic excavator as an example, we examined the control message requirements. One of the functional modules, the vehicle controller manages the sequential output of each actuator of the construction machinery and the ON/OFF of the vehicle console switches while monitoring the information from the sensors attached to the vehicle and the emergency stop signal. A motion controller is installed as a higher-level controller for the vehicle controller, which is used for controlling the overall vehicle, such as position control of the bucket tip and trajectory tracking control, and driving control. The vehicle and motion controllers depend on control characteristics such as vehicle mass and hydraulic system. These controllers are considered to be equivalent to "construction machinery" in the system architecture specified in ISO 15143 Part 1. The

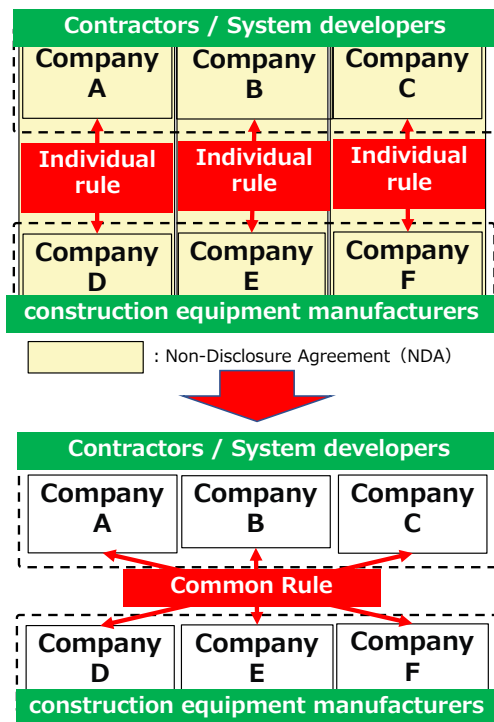


Figure 3. Conventional and Proposed Communication

motion controller communicates with the task controller, which corresponds to the "operation system," a higher-level system specified in ISO 15143 Part 1. It controls the construction machine according to the motion commands output by the task controller, while transmitting a task state. The task controller communicates with the construction planner and management system (i.e., software that plans the excavation area and depth of the target area from a design drawing), which is a higher-level system in the same operation system. The task controller is a functional block that is less dependent on the control characteristics of the machine.

Table 1 provides an overview of the study results of the common control message (C1, C2, D1, D2) among the task controller, motion controller, and vehicle controller. They are part of the data dictionary specified in ISO 15143 Part 2. Further details of the common control signals are available on the PWRI homepage[7].

3.2 Middleware

ROS (Robot Operating System) was adopted as the middleware that facilitates communication between software, which are the functional units of software, to realize autonomous construction. This middleware supports hardware abstraction and system integration of the autonomous

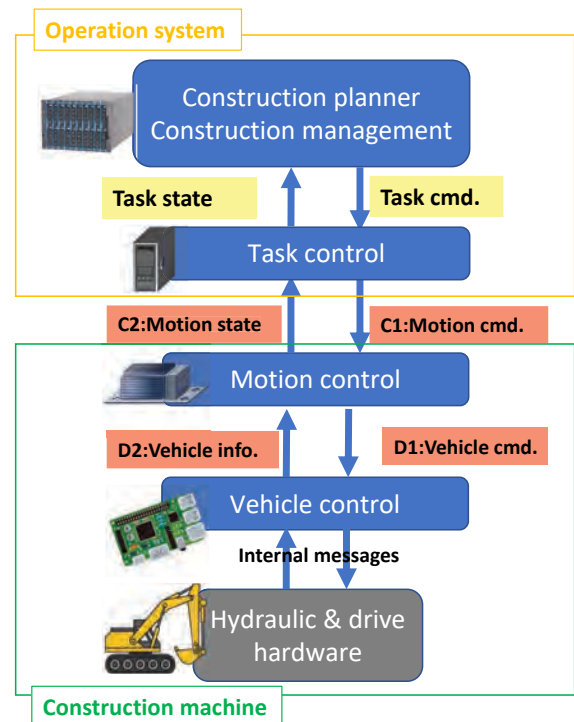


Figure 4. System Architecture

distributed system, making it easy to ensure the reusability of deliverables. Additionally, it is expected that the use of ROS will enable the efficient diversion of existing libraries, many of which have been used for autonomous robots, for use in autonomous construction.

3.3 Simulator

OPERA provides two simulators that support common control message as well as actual machine controllers. Software developed on the simulator can be operated and verified on the actual machine without modification of the source code.

Both simulators are built on Unity, a widely-used game development platform, and they employ different physics engines, Nvidia PhysX[8] (hereinafter referred to as the "PhysX version") and AGX Dynamics[9] (hereinafter referred to as the "AGX version") to realize the following functions.

- (1) To read various physical parameters of construction equipment from a configuration file and calculate the physical behavior of construction equipment in the simulator.
- (2) To compute the physical behavior of earth and sand in the simulator.
- (3) To perform real-time calculations on a general-purpose PC.

Table 1. Part of Common Control Message

Division	Message Name	Parameter Name	Content
C1	Bucket position control	Target position	X,y,z position on machine coordinate
		Target posture	Posture quaternion on machine coordinate
	Direct control	Target speed	Velocity of bucket tip
		Target angle	Swing, boom, arm, bucket angle
Locomotion	Target Velocity	Translational velocity of machine	
	Target Angular Velocity	Angular velocity of machine	
C2	Machine state	Remaining fuel	-
		Engine speed	-
		Oil temperature	-
D1	Working lever input	Each actuator	Swing, boom, arm, bucket input
	Locomotion lever input	Each actuator	Left and right track input
D2	Sensor information	Angle information	Swing, roll, pitch, yaw angle

- (4) Software developed for actual equipment works on the simulator without modification of the source code.
- (5) Visual presentation of the results of the aforementioned items.

The AGX version has a default soil model that calculates soil and machine interaction. Conversely, the PhysX version lacks such a model, thus we implemented our own simplified soil model based on [10]. While the use of the PhysX version does not incur any additional costs as long as you have a Unity license, AGX Dynamics is a paid software.

Users of the simulator can select between the PhysX and AGX versions based on their performance and cost requirements, such as the accuracy of dynamics, the soil model, and the speed of calculations.

3.4 Experimental Environment

OPERA provides actual equipment and field to conduct demonstration tests of functional modules and applications created based on the common control message and middleware. This section describes the current status of these as of the end of August 2022.

PWRI owns one 12-ton hydraulic excavator and one 11-ton crawler carrier as actual construction equipment provided by OPERA. Figure 5 shows an overview of the machines and the schematic diagrams of the system configuration.

Each construction machine is equipped with a RTK-GNSS compass, which can measure latitude, longitude, altitude, and azimuth information. The excavator is fitted with absolute encoders on each joint of the swing, boom, arm, and bucket to acquire angles. In addition, a 6-dof IMU is mounted on the cabin to measure the attitude of the upper body. The crawler carrier has a rotary encoder mounted on each of the left and right sprockets of a track, which measure the rotation velocity of tracks. In addition, a 6-dof IMU is mounted on the cabin and vessel to measure the attitude of the vehicle and the inclination of the vessel.

Each construction machine has a motion controller which receives motion commands from a task controller. The motion controller communicates a vehicle controller which controls hydraulic actuators. A mesh WiFi station and private 5G station are installed for communication with other system, and a specified low power radio station is mounted for emergent safety system.

OPERA also provide the experimental field (Figure 6) established in PWRI and the National Institute for Land and Infrastructure Management in Tsukuba City, Ibaraki Prefecture, as a test site. The field has an area of approximately 26,000 m^2 , and approximately 1,500 m^3 of soil materials are available for testing in the field. The field has a control building for remote control and autonomous construction, as well as infrastructure facilities such as power supplies, PCs, internet lines, security cameras, and RTK-GNSS base station for experiments. Three mesh WiFi and two private 5G base stations are permanently installed to cover the entire field.

4 Future prospects

4.1 Common Control Message

Based on the draft that has been released, the draft and its scope will be revised as necessary through joint research with construction equipment manufacturers and other relevant companies.

4.2 Middleware

As described in section 3.2, OPERA utilizes the ROS as its middleware. However, Open Robotics, the developer of ROS, has announced the cessation of development for the latest version of Noetic Ninjery and the termination of maintenance and support in May 2025. They has announced that the development of ROS will be terminated with the latest version of Noetic Ninjery and that the maintenance and support will be terminated in May 2025. As a successor to ROS, ROS2 has been released

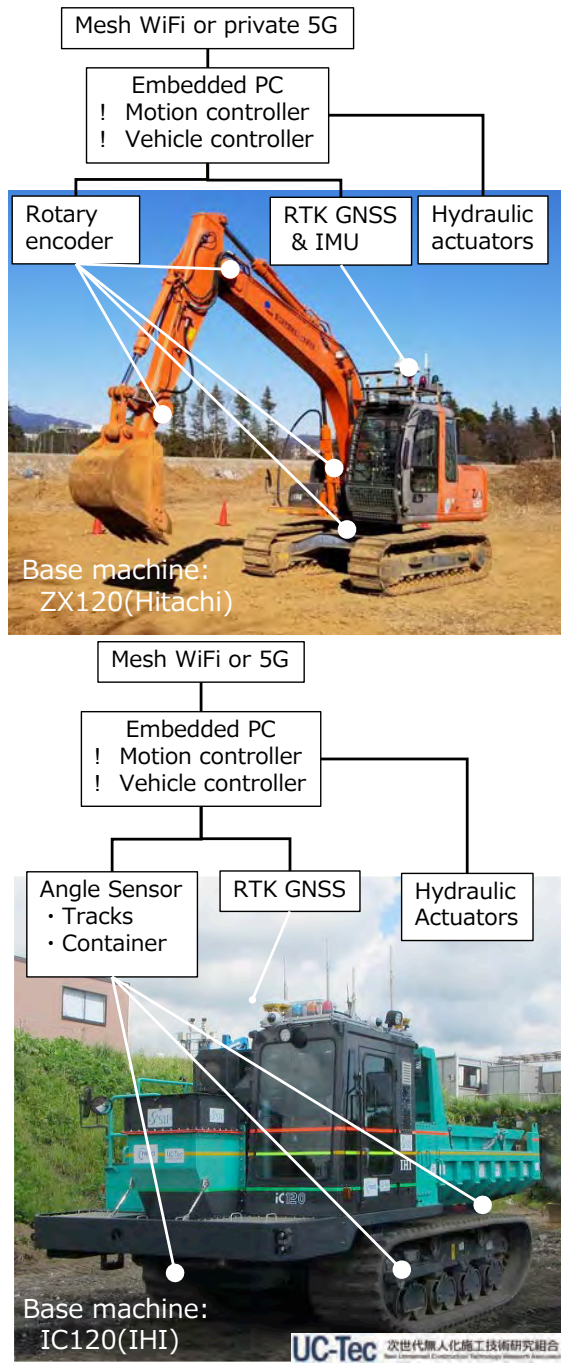


Figure 5. Construction machines and their devices

and is expected to continue to be developed and maintained with major updates. In light of this, OPERA has developed a system compatible with ROS2 and plans to release it in the current year. Currently, MoveIt[11] and Navigation Stack[12] are being used for motion planning and control. These software packages assume the use of responsive electric motors, and it has been found that their



Figure 6. Experimental Field

performance is poor when directly applied to hydraulic machinery. In the future, there is a need to develop planning and control systems that take into account the dead time and nonlinearity specific to hydraulic machinery.

4.3 Simulator

As described in section 4.2, the adoption of ROS2 as middleware is planned in this year, and given that the mechanism of inter-process communication will be fundamentally altered in ROS2, the simulator will also be adapted accordingly. Furthermore, as detailed in section 4.4, the construction equipment provided by OPERA is slated to be expanded, and the variety of construction equipment models represented by the simulator will also be expanded. Additionally, while the current simulator is designed to run on a single PC, it is limited in its ability to simulate real-time operation of more than one or two construction machines. On the other hand, considering that the majority of actual construction sites have a larger number of machines, it is desirable to be able to handle such use cases. Therefore, we plan to redesign the architecture level and verify its effectiveness from both hardware and software perspectives, aiming to improve the scalability of the simulator so that it can simulate large-scale construction sites. Given the typical larger scale of actual construction sites, it is desirable to enhance the scalability of the simulator to accommodate such use cases.

4.4 Experimental Environment

In addition to the two machines described in Section 3.4, We plans to add a 20-ton class hydraulic excavator, a 9-ton class bulldozer, and a compaction roller for OPERA. This will facilitate the development of autonomous technology for primary earthworks such as soil spreading and compaction, excavation, loading, and transportation.

As for the experimental field, a variety of infrastructure updates are planned. Specifically, the following items are intended to be added:

- (1) Additional mesh WiFi equipment
- (2) Fueling facilities for construction equipment
- (3) Additional network surveillance cameras
- (4) Installation of loudspeakers for on-site announcements

4.5 Joint Research

In September of 2022, a joint research project was initiated in collaboration with 14 private companies and universities with the goal of developing technology to enhance productivity in earthwork using OPERA. The project is set to span a period of two and a half years, and will be presented for trial at construction sites. Additionally, a joint research project on the development of a common control message for construction equipment is currently calling for proposals, with the draft proposal expected to be prepared within two years.

5 Conclusion

This paper has presented an overview of the current status and future prospects of OPERA, developed by PWRI, with the aim of increasing the reusability of development results, avoiding duplication of research and investment, and encouraging new entrants such as universities and start-up companies with advanced technologies.

The software and simulators of OPERA are available on GitHub[13], and anyone can use all or parts of the components to suit their own purposes. Any feedback by GitHub issues or email with questions or requests for improvements to OPERA from those who have actually used OPERA is very valuable for us. In response to these requests, a continuous cycle for improving the usability of OPERA will be the core of our future efforts.

References

- [1] Status of i-construction initiatives(in japanese). On-line: https://www.mlit.go.jp/tec/i-construction/pdf/06.7_kikaku_siryoku6.pdf, Accessed: 10/01/2023.
- [2] Japan Federation of Construction Contractors. Survey on robots for the construction industry (in japanese). *Public Works Management Journal*, 11: 47–51, 2020. doi:10.22260/ISARC2017/0001.
- [3] Rauno Heikkilä, Tomi Makkonen, Ilpo Nishanen, Matti Immonen, Mikko Hiltunen, Tanja Kolli, and Pekka Tyni. Development of an earthmoving machinery autonomous excavator development platform. In *Proceedings of the 36th International Symposium on Automation and Robotics in Construction (ISARC)*, pages 1005–1010, May 2019.
- [4] Ashish Sonawane. Software-platform based ecosystem in heavy duty mobile machine industry : “a case study on ros ecosystem”. Master’s Program in Industrial Engineering and Management, Business and Technology, October 2022.
- [5] Shinpei Kato, Shota Tokunaga, Yuya Maruyama, Seiya Maeda, Manato Hirabayashi, Yuki Kitsukawa, Abraham Monrroy, Tomohito Ando, Yusuke Fujii, and Takuya Azumi. Autoware on board: Enabling autonomous vehicles with embedded systems. In *2018 ACM/IEEE 9th International Conference on Cyber-Physical Systems (ICCP)*, pages 287–296. IEEE, 2018.
- [6] ISO 15143-1:2010, Earth-moving machinery and mobile road construction machinery – Worksite data exchange – Part 1: System architecture.
- [7] Draft of common control messages for construction machinery(in japanese). On-line: <https://www.pwri.go.jp/team/advanced/papers.html>, Accessed: 10/01/2023.
- [8] NVIDIA.DEVELOPER:PhysX. On-line: <https://developer.nvidia.com/physx-sdk>, Accessed: 10/01/2023.
- [9] Algorix: AGX Dynamics. On-line: <https://www.algorix.se/agx-dynamics/>, Accessed: 10/01/2023.
- [10] Daniel Holz and Adam Galarneau. Real-time mud simulation for virtual environments. In *ACM Siggraph Symposium on Interactive 3D Graphics and Games*, 05 2018. doi:10.13140/RG.2.2.29015.62885.
- [11] MoveIt Motion Planning Framework. On-line: <https://moveit.ros.org>, Accessed: 10/01/2023.
- [12] ROS Navigation Stack. On-line: <https://github.com/ros-planning/navigation>, Accessed: 10/01/2023.
- [13] Github: pwri-opera. On-line: <https://github.com/pwri-opera>, Accessed: 10/01/2023.

Automated tracking of prefabricated components for a real-time evaluator to optimize and automate installation

Nolan W. Hayes¹, Bryan P. Maldonado¹, Diana Hun¹, and Peter Wang¹

¹Oak Ridge National Laboratory, United States of America

hayesnw@ornl.gov, maldonadopbp@ornl.gov, hunde@ornl.gov, wangpl@ornl.gov

Abstract -

Trade associations for prefabricated construction estimate that about 50% of prefabricated wall projects have alignment problems that lead to defects and rework. Additionally, component installation times average between 30 and 60 minutes per component. To address these issues, a real-time evaluator (RTE) system was introduced to decrease cost and automate prefabricated component installation by reducing the installation time, decreasing rework, and enhancing energy performance through higher installation quality. The RTE uses commonly available hardware and software to perform autonomous tracking to measure the real-time location and orientation of components as they are crane-lifted and installed. The hardware, software, and algorithms that allow the autonomous tracking of components are detailed. An algorithm to automate the initial search for a component with three attached retroreflectors is proposed. Algorithms to automate the measurement of component position and orientation are also proposed. Simple lab-scale proof-of-concept experiments were conducted to assess the algorithms for automation of component searching, measurement of real-time movement, and measurement of component orientation. With additional development, the system can be used as a tool to generate the commands for autonomous crane operation or single-task construction robots.

Keywords -

prefabrication, installation, real-time, automation, accuracy, time

1 Introduction

Trade associations for prefabricated construction, such as the Precast/Prestressed Concrete Institute (PCI), estimate that about 50% of prefabricated wall projects for new construction have alignment problems that lead to defects and rework [1]. Additionally, for the precast concrete industry, typical component installation times average between 30 and 60 minutes per component with a significant amount of time spent performing small adjustments, plumbing, and leveling near the final installation point [1]. Misalignment issues are common when the final connections are made from the prefabricated components to the

substructure, resulting in delays of hours or more to rectify the issue onsite. Additionally, for multi-story buildings, wall panel installers are working from the interior of the building and are often unable to see the exterior surface of the panel to easily manipulate components to align architectural features, when present. In some cases, the as-built substructure dimensional variations are beyond the construction tolerances of the design documents leading to fitment issues of wall panels as they are attached to the substructure. Other industries in prefabricated construction have similar issues which lead to cost overrun and delays. Despite these issues, installation techniques for prefabricated components at the job site have experienced minimal innovation.

Recent advances in surveying technology include laser-based technologies such as robotic total stations that expedite and improve the accuracy of building and land surveying, as well as 3D scanners that produce point cloud data for the development of 3D models. Unfortunately, as shown in Figure 1, these tools are primarily used in prefab construction for as-built surveys after prefabricated component installation. That is, they merely point out errors after installation that can require expensive corrections to maintain the continuity of the air and water barriers in the building envelope and to meet the expected aesthetics of the facade. A better alternative is to actively check the quality of construction during the installation of prefabricated components so that errors can be compensated in real-time.

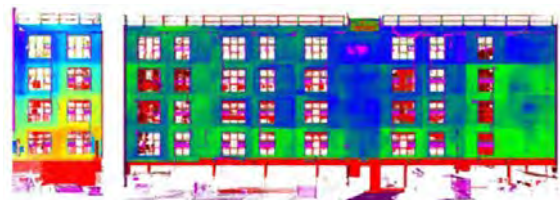


Figure 1. Measured normal point-plane distance of installed volumetric modules [2]. Maximum variation is approximately 3 cm.

The industrial construction industry needs a tool that

uses as-built measurements from these laser-based devices to provide corrective guidance in real time to improve installation speed and quality, increase productivity, and decrease rework. Additionally, for automated crane applications or single-task construction robots to be applicable to a wide variety of construction sites, a feedback-in-the-loop position monitoring system is necessary to correctly position the crane payload or robot [3, 4, 5, 6, 7]. To address these issues, a real-time evaluator (RTE) system was developed to decrease cost and automate prefabricated component installation by reducing the installation time, decreasing rework and enhancing energy performance through higher installation quality. To assess the plausibility of the real-time evaluator system, initial research efforts focused on the development of an automated tracking system which could identify, monitor, and measure the position and orientation of components in real-time during installation. The selection of hardware and development of algorithms to automate the tracking system of the real-time evaluator is described in this work.

2 Methods and materials

For a real-time evaluator to be feasible, an autonomous tracking system needed to be designed and validated. An autonomous tracking system that measures the real-time locations of prefabricated components as they are being installed was designed using off-the-shelf hardware. An automated laser tracker and custom software monitor the location and orientation of each component during installation. The primary work of this paper will describe in further detail the algorithms, processes, and hardware of the autonomous tracking system.

The real-time evaluator is intended to be applicable to a wide variety of types of construction. The initial design focus was on prefabricated overlaid panel retrofits which involve attaching insulated panels over the existing facade of residential or commercial buildings to improve the thermal performance. However, the system is agnostic to construction type and can be extended to monitor, optimize, and automate the installation of a variety of prefabricated components including prefabricated wall panels, prefabricated roof structures, prefabricated floor assemblies, volumetric modular units, and more. Additionally, the RTE workflows could allow the monitoring, optimization, and automation of installing individual structural members to create frames and load-resisting systems such as structural steel frames and prefabricated concrete frames.

2.1 Specifications and current installation methods

By engaging with stakeholders in the prefabricated construction industry, the research team was able to develop a list of minimum requirements or specifications that would

enable the autonomous tracking system of the real-time evaluator to achieve impact in the industry. Partners in precast concrete construction and residential prefabrication were consulted to gauge the potential impact of the real-time evaluator and gather input that could improve the system. A list of basic specifications was drafted as minimum requirements of the RTE (Table 1).

Table 1. Specifications for the real-time evaluator

Requirement	Measure	Value
Position Measurement	Frequency	1 Hz
Position Measurement	Accuracy	3.175 mm
Orientation Measurement	Frequency	0.03 Hz
Orientation Measurement	Accuracy	30 "

The basic requirements requested from industry partners were specified measurement accuracy and speed. Because of the weight and size of most prefabricated components, the crane lifting and movement of these components are slow, especially when in close proximity to other components or the existing structure to which it will be attached. For these reasons, the required frequencies of positional and orientation measurements are not the primary concern, although any time savings in this process results in overall time savings during installation. In most cases, stakeholders were more concerned with measurement accuracy as compounding errors lead to issues that can create the most significant loss of time such as required on-site reworks or re-manufacturing of components.

For position measurements, industry partners recommended a measurement frequency of 1 Hz with positional accuracy of approximately 3 mm or less. Positional accuracy is important because joints between components are commonly 13 mm or smaller; therefore, a high degree of accuracy is necessary for positioning these components next to existing components or to meet installation tolerances of connections. If positional errors of more than 3 mm commonly exist for each installed component, this error can compound to create significant issues for adjoining components.

Stakeholders in the industry also recommended that the measurement of component orientation should be accurate to 30" (seconds of angle) of rotation and take at most 30 seconds in order to significantly impact the speed at which components could be installed. Stakeholders expressed that it is common for a component to remain in place very near to the final design location for 15 minutes or longer while it is precisely plumbed and leveled [1]. Erectors often measure plumbness and levelness by hand using plumb lines and levels which can take longer than a few minutes for each iteration. Components that are not plumb or level must be shimmed at joints or connections to correct orientation; then, the measurement process must be repeated until the installation tolerances are achieved.

Therefore, a high degree of orientation measurement accuracy is required, and an orientation measurement time of less than 30 seconds was deemed to most significantly reduce installation time.

2.2 Hardware and software

The real-time evaluator was designed to operate with a robotic total station. For the initial design and prototyping, a Leica Multi-Station 60 (MS60, shown in Figure 2) was selected to use as the base system on which to build the RTE. However, algorithms and software were designed in such a way that the RTE is hardware agnostic, only requiring communication between the software and robotic total station to be established. The survey-grade multi-station acts as a laser tracker to locate, measure, and track targets attached to components.

Modern multi-stations are capable of performing automated searching algorithms for a single retroreflector [8]; however, it is not possible for the multi-station to identify which retroreflector has been located when multiple prisms are present, especially when prisms are attached to movable objects. The novelty of this research includes the development of algorithms which can automate the process of searching, locating, and measuring three retroreflectors attached to a prefabricated component. By using predetermined information about the component and setup of retroreflectors, algorithms were developed to automate the workflow so that a modern multi-station could measure position and orientation of a prefabricated component with little to no human input required.

Multiple types of retroreflector systems and fixtures are used to enable the identification and laser tracking of connections and components. Three target reflectors must be placed on the prefabricated components during installation to track position and orientation. Leica 360° prisms (full size and miniature shown in Figure 2) were used in the design and prototyping of the RTE. These 360° retroreflectors, at any orientation, can be searched for and tracked by the multi-station.

These retroreflectors are intended to be reused and attached to components using a fixture capable of quick-release, rigid attachment. Fixtures, shown in Figure 2, were designed and prototyped for insulated panels. The first prototype is a simple mechanical clamp with an adjustable clamping distance. The second prototype is a clamp that is affixed to a smooth surface using the force of a generated vacuum. The accuracy of retroreflector distance measurements depends on the angle of the reflector in relation to multi-station location; optimal accuracy is achieved when laser-line is as close to perpendicular to the longitudinal axis of 360° prisms. The modular designs allow the 360° retroreflectors to be rigidly attached to wall panels at different orientations to accommodate a variety

of station setup distances, locations, and building heights. When installing components near the top floors of a multi-story building, a prism with longitudinal axis angle near to horizontal can be used to accommodate a total station setup close to the building on ground (e.g. total station is looking nearly straight up). Additionally, 360° retroreflectors have been shown to generate small measurement error (in most cases less than 2 mm) when the prism is rotated around the longitudinal axis [9]; however, we expect that prisms will not be rotated more than 15° after attachment to components, and therefore, measured errors will be constant and within specifications of 3 mm.

Disposable tape reflectors (Figure 2) are another reflector option. Unfortunately, tape reflectors differ in function from retroreflectors and cannot be easily searched for or tracked by modern total stations; hence, traditional retroreflectors (prisms) are necessary for the operation of the RTE. However, tape reflectors can be used as control points placed on the existing building structure to orient the station setup in relative space (e.g. to tell where the multi-station is set up relative to the building) which will be required to compare the actual location of a component to the goal location. Future development of cheap, disposable retroreflectors, similar in applicability to tape reflectors, would increase the affordability of RTE.

For this research, the RTE software was written in Python and interfaces with the robotic total station using a Bluetooth connection and Leica GeoCOM commands. Alternatively with some additional development, the software can be installed and operated directly on the total station. However, since different types of laser scanners and trackers use varying communication styles, the responsibility falls to the user to make the connection between the RTE and hardware. For the initial design of the system, the software utilizes a graphical user interface on a personal computer to perform the RTE procedures and monitor component position.

2.3 Autonomous tracking system

The basic function of RTE is the active tracking of components during installation. Using a series of retroreflective prisms, the RTE can autonomously identify and locate each to calculate the component positions and orientations in six degrees of freedom: translation and rotation about each axis. Modern multi-stations can search for, lock on to, and measure prisms. Novel algorithms were created to integrate basic knowledge about the component to automate the location process of the first (isolated) prism. The algorithm then commands the multi-station to turn angles to find and measure the next prism on the component.

The RTE, knowing the dimensions of the prefabricated components, can cycle through prisms and determine coordinates of the component's location and orientation about



Figure 2. Hardware required by the real-time evaluator

primary axes. The frequency of autonomous tracking will depend on the communication settings and hardware capabilities. For the Leica MS60 used in this research, measurement frequency of single prism position was possible to 10 Hz. To calculate orientation, the hardware must turn to and measure the location of a minimum of three prisms. The speed of orientation measurement also depends on the hardware used and is most limited by the speed of motorized turning and searching of the total-station. For the Leica MS60 used in this research, a cycle time of approximately 15 seconds was achievable.

Several assumptions are made to enable simple calculation of component position and orientation:

1. The prefabricated component is a simple rectangular prism with a known width, height, and depth.
2. Reflector targets are rigidly fixed at a known distance from external corners of the component.
3. During initial prism search, the primary measurement face of the component is assumed to be oriented near to perpendicular to the view of the total-station.
4. During measurement of the component position, any motion is assumed to be rigid body translation.
5. During measurement of the component orientation, the component is assumed to be stationary.

Using these assumptions, an automated workflow was developed to calculate and monitor the position and orientation of a component. First, the component must be instrumented with retroreflectors (hereafter referred to as prisms). Three prisms must be rigidly attached to the component so that position and orientation can be calculated. The location of each prism in reference to component corners must be known to calculate the position of the perimeter of the exterior face of the component as shown in Figure 3. Each *prism_offset* is recorded assuming that the component is level and plumb. The layout type of prisms must also be pre-programmed so that the RTE can automate the process of identifying and locating the prisms attached to the component. Four distinct layout types are possible for a set of three reflectors attached to corners of a rectangular prism (i.e. top two corners and

bottom left corner, bottom two corners and top right corner, etc.). Each layout produces an isolated reflector that is either on the right or left side of the component. This isolated reflector is what allows the RTE algorithms to be fully automated since it can be uniquely identified by a directional search. Using this layout, RTE can determine from which direction (left or right) the isolated prism can be identified.

The general algorithm to initially find and measure prisms on a component is shown in Algorithm 1. The first, isolated reflector is identified on the stationary component using an automated search procedure. The RTE commands the multi-station to scan either left-to-right or right-to-left depending on the isolated prism location using existing search functions. Horizontal and vertical turn angles are calculated from the positions of measured prisms and known component geometry. RTE commands the multi-station to turn each angle based on the layout of reflectors. After each robotic turn of the multi-station, a spiral search pattern is conducted to locate the prism and acquire a lock before measuring. The entire process takes approximately 30 seconds using the Leica MS60. With the known location of three reflectors attached to the component, the RTE calculates the position and orientation of the component.

After measurement of the three prisms, the RTE automatically enters tracking mode to monitor the real-time position of the component (Algorithm 2). The last prism measured in *find_prisms* will be locked-on and continuous measurements will be collected to determine the rigid body translation of the component. At each measurement cycle, a displacement vector is calculated between two subsequently measured points. This displacement vector is added to the positions of all prisms to determine the new estimated positions of prisms. The frequency of measurement will depend on the multi-station; with the Leica MS60, consistent measurement frequency of up to 10 Hz was possible. During movement, rotations about the X and Y axes of the component (shown in Figure 3) should be small due to the rotational limitations of most rigging configurations for cranes. However, larger rotations about the

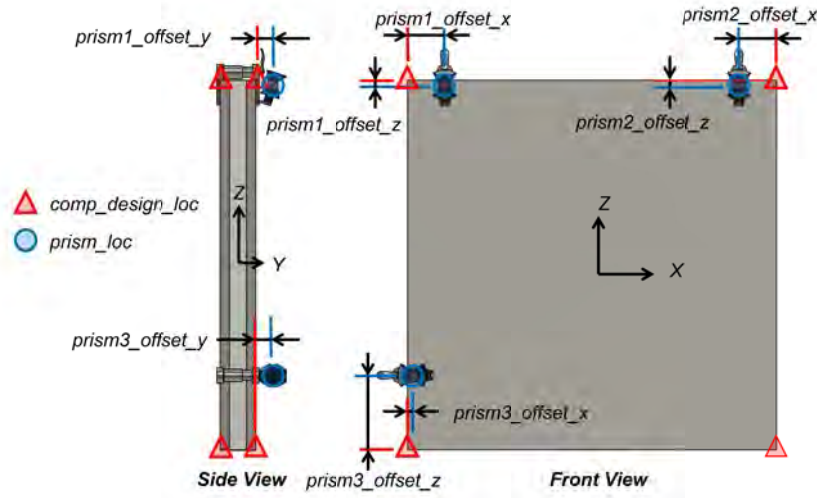


Figure 3. Parameters used to determine the location of components from measured prism locations

Z axis can occur; despite this, the RTE assumes that any movement during active tracking is rigid body translation. As such, the recorded prism locations are simply approximations until another measurement cycle of all prisms is conducted.

After movement, a *cycle_prisms* command (Algorithm 3) can be given to the RTE to measure the real locations of all prisms and determine component positions and orientation. This algorithm is intended to be used when the component is near its design location and only minor adjustments are needed to position, orient, and finalize the placement. Because the *track_position* function assumes rigid body translation of the component, it is possible that prisms are not at exactly their expected locations. Therefore, after each turn, a search is commenced to locate the prism before measurement. This search process allows the RTE to account for minor degrees of rotation of the component about the Z-axis (less than 45°). After returning the three prism locations, the orientation of the component (defined by the Euler angles) can be calculated. The goal of placement is commonly for orientation to be plumb and level; however, RTE can also allow for other solution states defined by the user.

3 Lab-scale demonstration and experiments

Because the autonomous tracking system enables the remainder of the RTE, initial research efforts focused on developing and demonstrating this system. After creation of the algorithms/software and acquisition of hardware, the system configuration was tested using a setup that included a mock-up prefabricated wall panel instrumented with prisms. Both real-time tracking and orientation measurements were achieved in the mock-up, lab-scale test

shown in Figure 4.

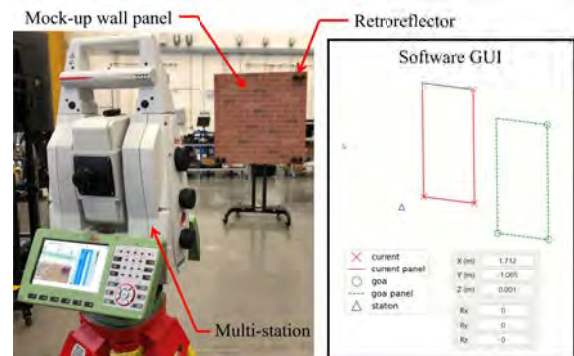


Figure 4. Mock-up lab-scale test of the RTE

A multi-station was set up in a laboratory environment along with a mock-up prefabricated panel on a frame with wheels. Prisms were attached to the mock-up panel at three corners. The RTE software was installed on a personal computer and connected to the multi-station using Bluetooth. The graphical user interface (GUI) was used to control the RTE and track the movement of the panel in real time. The GUI was also set up to simulate the installation of the panel by specifying a design, goal panel location in space, and required movement was given to the installer to move the panel to this goal location.

3.1 Experiments

A series of experiments was performed to determine the performance, repeatability, and limitations of the automated tracking algorithms of the RTE. It is important to note that observed values are dependent on the hardware used and software configurations. The use of different

Algorithm 1: *find_prisms*: automated initial search and measurement of all prisms attached to component

Data:
 Layout of prisms: *prism_layout*
 Offsets of prisms: *prism_offset*
 Dimensions: *comp_width*, *comp_height*
Result:
 Position of prisms: *prism1*, *prism2*, *prism3*
 $hz \leftarrow$ angle from Y-axis (bearing)
 $v \leftarrow$ angle from Z-axis (vertical)
 // Find first prism
 from *prism_layout* determine
 approach_direction
 search(*approach_direction*)
prism1 = measure()
 set_orientation()
 // Find second prism, using a horizontal turn
 $prism2.x = prism1.x - prism1.offset.x +$
 $comp_width + prism2.offset.x$
 $hz = atan2(prism2.x/prism1.y)$
if $hz < 0$ **then**
 | $hz = 2\pi + hz$
end
 turn_to_angle(hz)
 search()
prism2 = measure()
 // Find third prism, using vertical turn
 $prism3.z = prism2.z - prism2.offset.z +$
 $comp_height + prism3.offset.z$
 $v = atan2(prism2.y/prism3.z)$
if $v < 0$ **then**
 | $v = 2\pi + v$
end
 turn_to_angle(v)
 search()
prism3 = measure()
 lock(*on*)
 return *prism1*, *prism2*, *prism3*

models of multi-stations or total-stations will result in different results.

3.1.1 Performance and repeatability

The performance and repeatability of Algorithms 1, 3, and 2 were investigated under standard laboratory conditions. The RTE was commanded to perform each algorithm for a number of iterations. For each iteration, the total time elapsed between start and end of the algorithm was recorded. The same *prism_layout* and *prism_offset* were used for all iterations. The parameters, *comp_width*: 0.7 m and *comp_height*: 0.6 m, were accurately measured manually using the multi-station and used as input for the algorithm. The mock panel was positioned at a distance of 4 m away from the multi-station and was kept stationary for all iterations. First, the RTE was commanded to per-

Algorithm 2: *track_position*: automated tracking of position of moving component

Data:
 Position of prisms: *prism1*, *prism2*, *prism3*
 $V \leftarrow$ displacement vector of moving prism
 // Initialization:
TargetPrism = *prism3*
TargetPrism0 = measure()
while *toggle = moving* **do**
 | *TargetPrism1* = measure()
 | $V = TargetPrism1 - TargetPrism0$
 | $prism1 = prism1 + V$
 | $prism2 = prism2 + V$
 | $prism3 = prism3 + V$
 | *TargetPrism0* = *TargetPrism1*
 | wait *X* milliseconds
end
 return *prism1*, *prism2*, *prism3*

form Algorithm 1 a total of 10 times. The time trial results are shown in Table 2. On average, the algorithm was able to meet the required specification of 30 seconds identification time. There were no failed iterations of performance of Algorithm 1 for this setup within the 10 iterations.

Second, the achievable frequency of Algorithm 2 was experimentally investigated for the software and hardware reported in this study. A similar setup to the previous time trial was used. The mock panel was positioned at a distance of 4 m away from the multi-station and was kept stationary. Algorithm 2 was set to a wait time of 0 milliseconds and allowed to repeat in-loop at maximum speed for 100 repetitions. The amount of time spent within each loop was recorded. Results are shown in Table 3. On average, the algorithm running on specified hardware and software was able to achieve an average tracking measurement frequency of approximately 18 Hz, with maximum frequency of 32 Hz and minimum frequency of 10 Hz for the experiment. However, tracking of crane-installed prefabricated components that are moving slowly will not require high measurement frequency; therefore, it will likely be beneficial to reduce measurement frequency to reduce software and hardware resource requirement.

Next, the RTE was commanded to perform Algorithm 3 a total of 20 times. A similar setup to the previous time trials was used. The mock panel was positioned at a distance of 4 m away from the multi-station and was kept stationary. The time trial results are shown in Table 4. On average, the algorithm completed in nearly half the specified time requirement of 30 seconds cycle time. There were no failed iterations of performance of Algorithm 3 for this setup within the 20 iterations.

To investigate the sensitivity of input data on the repeata-

Algorithm 3: *cycle_prisms*: automated cycling through prisms to measure component position and orientation

```

Data:
Position of prisms: prism1, prism2, prism3

hz ← angle from Y-axis (bearing)
v ← angle from Z-axis (vertical)

// At end of tracking, locked-on to prism3:
prism3 = measure()
lock(off)

// Turn to estimated position of next prism
hz = atan2(prism2.x/prism2.y)
if hz < 0 then
  | hz = 2π + hz
end
v = atan2(prism2.y/prism2.z)
if v < 0 then
  | v = 2π + v
end
turn_to_angle(hz, v)
search()
prism2 = measure()

// Turn to estimated position of last prism
hz = atan2(prism3.x/prism3.y)
if hz < 0 then
  | hz = 2π + hz
end
v = atan2(prism3.y/prism3.z)
if v < 0 then
  | v = 2π + v
end
turn_to_angle(hz, v)
search()
prism1 = measure()
lock(on)

// Reverse prism order for next cycle
order = flip(order)

return prism1, prism2, prism3

```

Table 2. Performance of Algorithm 1: 10 iterations

Parameter	Completion Time (seconds)
Average	26.95
Minimum	26.48
Maximum	27.57
Standard Deviation	0.43

Table 3. Performance of Algorithm 2: 100 iterations

Parameter	Completion Time (milliseconds)
Average	54.4
Minimum	30.7
Maximum	98.9
Standard Deviation	13.6

bility of Algorithm 3, another experiment was performed. A setup similar to the previous time trials was used; the

Table 4. Performance of Algorithm 3: 20 iterations

Parameter	Completion Time (seconds)
Average	13.68
Minimum	13.40
Maximum	14.11
Standard Deviation	0.24

mock panel with prisms was positioned at a distance of 4 m away from the multi-station and was kept stationary. In this experiment, Algorithm 1 was first performed to accurately measure the positions of the three prisms attached to the component. A percent error was applied to the measured width and height of the component, and Algorithm 3 was performed with the error-included *comp_width* and *comp_height*. The completion time of each cycle was recorded. Table 5 shows the setup of the experiment and reported completion times for each iteration. With increasing error up to 30%, the algorithm took longer to complete because more time was spent searching for the prisms. Error beyond 30% caused the algorithm to fail because the prism fell outside of the search radius for the given settings. However, error beyond 5% for the specified component dimensions is unlikely because prefabricated components are often manufactured to dimensional tolerances of millimeters.

Table 5. Sensitivity analysis of Algorithm 3 with errors in component dimensions

Iteration No.	Input Error (%)	Input Width (m)	Input Height (m)	Completion Time (seconds)
1	-30	49.1	39.1	19.19
2	-20	56.1	44.7	18.62
3	-10	63.1	50.2	16.48
4	-5	66.6	53.0	13.58
5	-1	69.4	55.3	13.50
6	0	70.1	55.8	13.08
7	1	70.8	56.4	13.40
8	5	73.6	58.6	14.51
9	10	77.2	61.4	17.35
10	20	84.2	67.0	18.73
11	30	91.2	72.6	19.92

3.1.2 Limitations

The limitations of the hardware and algorithms were investigated using simple tests. First, the maximum usable range of the hardware and algorithms were determined. The total-station with RTE software was setup at a great distance away from a full-scale mock-up of a building retrofit. Two prisms were placed at approximately 10 meters apart, and the hardware was instructed to perform a portion of Algorithm 1, which only included the successful identification of the isolated prism on the left from searching. Upon successful completion of the algorithm, the

total-station was moved further away from the prisms in increments of approximately 10 meters until the algorithm could not successfully identify the correct prism. Distance between prisms was kept constant during the process. Algorithm 1 failed to complete at a maximum distance of approximately 300 meters. The search function was not able to find the prism at this distance, which aligns with the manufacturers specified maximum prism search distance of 300 meters.

To further expand on the limitations of the algorithm, an experiment was designed to determine the minimum component width that could be tracked at maximum distance. Two prisms were spaced apart at increments of set distance approximately 300 meters away from the total-station. The prisms were progressively moved closer together in increments of approximately 0.5 meters until Algorithm 1 failed to complete. The minimum track-able component width was approximately 2.5 meters at a distance of 300 meters. When two adjacent prisms were spaced at this distance, the algorithm would routinely identify the incorrect prism (i.e. when searching from left-to-right, the search would lock onto the right prism instead of the left prism). This limitation is hypothesized to occur because of the search angle of the hardware. Based on equivalent angles, this minimum component width would translate to 0.84 meter minimum component width at a distance of 100 m which would accommodate most prefabricated elements.

4 Conclusions and next steps

A real-time evaluator (RTE) tool was developed to optimize and automate the process of installing prefabricated components. By actively monitoring the real-time position and orientations of components as they are crane-lifted into position, the real-time evaluator can improve installation speed and quality, increase productivity, and decrease rework. The hardware, software, and algorithms that allow the autonomous tracking of components were detailed. The autonomous tracking algorithms and software can be used as an installation tool to expedite prefabricated construction, reduce errors of installation, and enable complete automation of crane installation.

Future research expanding the RTE is planned in the following areas: 1) development and testing of a connection positioning system, 2) development and testing of an installation assistant system, 3) lab-scale testing of multiple prefabricated elements on a mock-up wall, 4) full-scale testing of a retrofit project utilizing prefabricated overlaid wall panels.

4.1 Acknowledgements

This manuscript has been authored by UT-Battelle, LLC, under contract DE-AC05-00OR22725 with the

US Department of Energy (DOE). The publisher acknowledges the US government license to provide public access under the DOE Public Access Plan (<https://energy.gov/downloads/doe-public-access-plan>).

The authors would like to thank Jared Brewe, Steve Brock, Gary Lentz, and Mike Milkovitz from the Precast/Prestressed Concrete Institute and various manufacturers for participating on the advisory board which provided specifications for the research.

References

- [1] Jared Brewe, Steve Brock, Gary Lentz, and Mike Milkovitz. Private Communication, 2020.
- [2] TOCCI. <https://www.tocci.com>, 2022. Accessed: 2022-09-11.
- [3] Hiroshi Miyakawa, Jyunichi Ochiai, Katsuyuki Oohata, and Takashi Shiokawa. Application of automated building construction system for high-rise office building. In Ming-Teh Wang, editor, *Proceedings of the 17th IAARC/CIB/IEEE/IFAC/IFR International Symposium on Automation and Robotics in Construction*, pages 1–6, Taipei, Taiwan, September 2000. International Association for Automation and Robotics in Construction (IAARC). ISBN 9789570266986. doi:10.22260/ISARC2000/0083.
- [4] Kepa Iturralde, Thomas Linner, and Thomas Bock. Comparison of automated and robotic support bodies for building facade upgrading. In Mikko Malaska and Rauno Heikkilä, editors, *Proceedings of the 32nd International Symposium on Automation and Robotics in Construction and Mining (ISARC 2015)*, pages 1–8, Oulu, Finland, June 2015. International Association for Automation and Robotics in Construction (IAARC). ISBN 978-951-758-597-2. doi:10.22260/ISARC2015/0078.
- [5] K. Iturralde, M. Feucht, D. Illner, R. Hu, W. Pan, T. Linner, T. Bock, I. Eskudero, M. Rodriguez, J. Gorrotxategi, Jean Baptizste Izard, J. Astudillo, J. Cavalcanti Santos, M. Gouttefarde, M. Fabritius, C. Martin, T. Henninge, S. M. Normes, Y. Jacobsen, A. Pracucci, J. Cañada, J. D. Jimenez-Vicaria, R. Alonso, and L. Elia. Cable-driven parallel robot for curtain wall module installation. *Automation in Construction*, 138(May 2021), 2022. ISSN 09265805. doi:10.1016/j.autcon.2022.104235.
- [6] Cynthia Brosque and Martin Fischer. A robot evaluation framework comparing on-site robots with traditional construction methods. *Construction Robotics*, 6(2):187–206, 2022.
- [7] Rongbo Hu, Kepa Iturralde, Thomas Linner, Charlie Zhao, Wen Pan, Alessandro Pracucci, and Thomas Bock. A simple framework for the cost-benefit analysis of single-task construction robots based on a case study of a cable-driven facade installation robot. *Buildings*, 11(1), 2021. ISSN 2075-5309. doi:10.3390/buildings11010008. URL <https://www.mdpi.com/2075-5309/11/1/8>.
- [8] Matthias Ehrhart and Werner Lienhart. Object tracking with robotic total stations: Current technologies and improvements based on image data. *Journal of Applied Geodesy*, 11(3):131–142, 2017. doi:doi:10.1515/jag-2016-0043. URL <https://doi.org/10.1515/jag-2016-0043>.
- [9] Stefan Lackner and Werner Lienhart. Impact of prism type and prism orientation on the accuracy of automated total station measurements. In *Proc. 3rd Joint International Symposium on Deformation Monitoring*, 2016.

Mathematical description of concrete laying robots

Vladimir Travush¹, Alexey Bulgakov², Thomas Bock³, Wen-der Yu⁴ and Ekaterina Pakhomova⁵

¹Urban Design Institute for Residential and Public Buildings (GORPROJECT), Russia

²Central Research and Development Institute of the Ministry of Construction of Russia, Russia

³Technical University of Munich, Germany

⁴Chaoyang University of Technology, Taiwan

⁵Southwest State University, Russia

travush@mail.ru, agi.bulgakov@mail.ru, thomas.bock@br2.ar.tum.de, wenderyu@cyut.edu.tw, egpakhomova@yandex.ru

Abstract –

The object of the research is robots with a manipulation system for concrete-laying operations. The kinematic scheme of a robot with an articulated distributive arm, providing delivery of concrete to any point of the erected object and allowing to bypass various kinds of encountered obstacles, is presented. The closed loops in the form of three- and four-links, which make up the manipulation system, are considered and mathematically described, which is conditioned by the use of a hydraulic drive. On the basis of geometrical approach connections between them are defined, as well as dependences of their velocities and accelerations are established. The description of the dynamics of the manipulating system is made on the basis of the Lagrange method, formulated through the D'Alamber principle, which allowed to obtain the resulting equations in a convenient vector-matrix form. The problem of planning the trajectories of a robotized concrete-laying arm nozzle on the examples of monolithic buildings and structures erection by means of sliding, repositionable and volumetric formwork has been solved. Approximation methods are used to form the time laws of changes in the generalized coordinates of the manipulation system.

Keywords –

Robot; Manipulator; Concrete; Path Planning; Mathematical Modell; Approximation

1 Introduction

Modern construction is characterized by large volumes of concrete work. Monolithic concrete and reinforced concrete are widely used for the construction of chimneys, cooling towers, silos, heavy columns, various tanks, energy facilities, retaining walls, complex arched and vaulted coverings. Monolithic structures are used for construction of high-rise public buildings and residential buildings. Monolithic reinforced concrete is

used for the construction of high-rise buildings with complex, expressive plans and combinations of volumes. The development trends of concrete work technology provide a priority solution to the problems of comprehensive mechanization of supply, distribution and placement of concrete mix. At construction sites, machines and equipment are required that would perform continuous feeding and placement of concrete mixture in the structure and ensure a specified rate of concreting. Concrete pumps, concrete placing equipment, concrete placing booms and robots are capable of reducing the laboriousness of concrete placing and transporting the concrete mix, eliminating drastic manual labor and increasing the level of productivity. They are especially effective when concreting large areas and construction of monolithic reinforced concrete buildings.

Analysis of features of the technology of concrete work shows that for distribution and laying of concrete mixture it's advisable to use articulated distribution arms (Fig. 1) having 4-5 degrees-of-freedom. Such structure ensures delivery of concrete to any point of the object being erected and allows you to bypass various kinds of

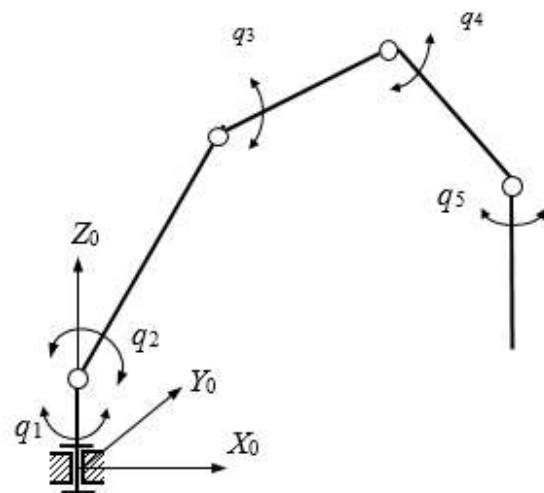


Figure 1. Kinematic diagram of a concrete-laying manipulator

obstacles.

It is known that manipulation systems near special positions (singularities) have sharply reduced load capacity associated with loss of controllability [1,2]. A number of studies are devoted to the consideration of trajectories that do not contain special positions, as well as the definition of the singularity criterion [3,4]. It is worth mentioning that one of the most applicable approaches to solving this issue is based on Jacobi matrices, which express the correlation between the force and kinematic parameters corresponding to a finite link and the input influences - generalized coordinates and forces. In this article, we will not focus on this question, treating it as solved.

For concrete-laying operations performed in monolithic construction, it is reasonable to use a manipulator system located on a rotary tower (Fig. 2). The arm manipulator links are equipped with an electro-

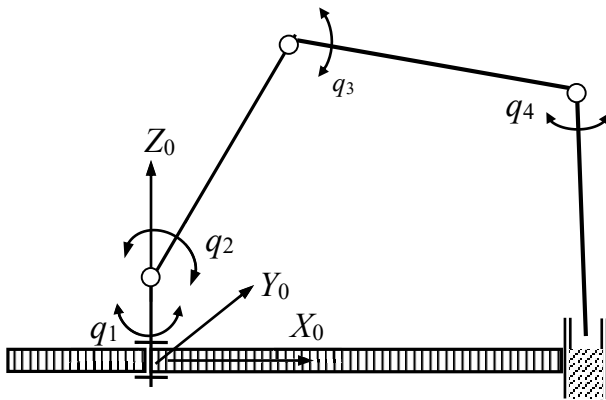


Figure 2. Structure of the articulated arm for concrete laying in the formwork

hydraulic drive. The last link is equipped with a flexible nozzle that produces a horizontal linear movement in any direction. The handling system can cover a wide area and ensures delivery of concrete to any point on the work site.

When laying and distributing concrete over large horizontal areas, it is advisable to use manipulators whose structure is a horizontal multi-link (4-5 links) structure equipped with concrete feeders with a hydraulic drive and remote control (Fig. 3).

The control of concrete-laying manipulators is based

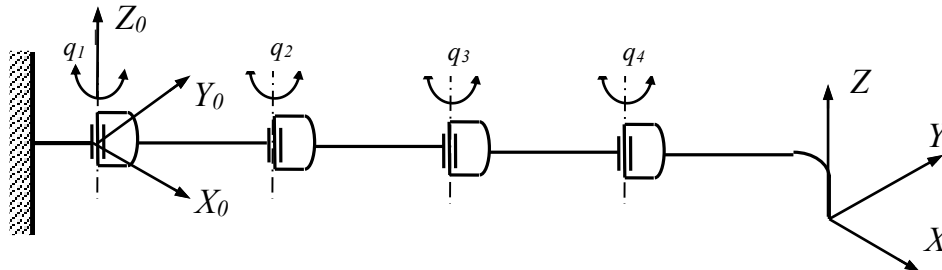


Figure 3. Kinematic diagram of a manipulator for horizontal concrete laying

on the peculiarities of the objects being erected and the volume of concrete work. For concrete-laying manipulators designed to work in line-of-sight conditions, interactive control from a console located on the manipulator's stand is used. The transition to remote control from the site of work makes it possible to significantly simplify the control of concrete mixer trucks with articulated arms and to increase the quality of concrete mix distribution in the formwork. In this case, radio and infrared control devices are used. The proportional radio remote control system makes it possible to regulate all the functions of the concrete pump and the concrete placing arm very accurately from a distance. This allows the operator to move freely around the construction site and constantly monitor the concrete delivery point. When using radio control equipment at the same time provides the ability to remotely control the equipment via cable. When using radio remote control and radio control, it is necessary to strive for minimizing the control operations of the concrete placing arm, contributing to facilitate the work of the operator. This can be achieved by implementing remote control on a strategic level and by using special controls. For example, joysticks with velocity vector control are used to control the horizontal movement of the robot arm. However, in most cases, preference should be given to software control systems for controlling the movement of the arm-manipulator links. Installation of the link position sensors and ultrasonic sensors for obstacle control in a manipulator makes it possible to ensure program control of the concreting process with the help of microprocessor technology. In this case, it must be provided for remote termination of the manipulator in the program mode and the transition to the command control from the remote control. Taking into account the conditions of movement of manipulator links when laying concrete into the formwork, the presence of reinforcement, jacking rods and equipment in the laying area, concrete-laying robots with adaptive control should be used. To implement adaptive control, it is necessary to solve a number of problems: monitoring the state of the service area, building models of the working environment, adjusting the state of the model in real time, building adaptive control algorithms.

The automation of concrete laying requires the automation of the process of compaction of the concrete mixture in the formwork. When using manipulators for concrete laying, the mixture can be compacted by remotely controlled vibrators installed at the output end of the concrete conveyor. High economic performance gives the use of arm manipulators, equipped with compaction devices in the construction of high-rise monolithic buildings and structures in the repositionable and sliding formwork. In this case, the structural arrangement of concrete laying complexes additionally includes concrete compaction and control facilities. Concrete compacting vibrators are installed on the manipulator. It can also be outfitted with tools for finishing work. The installation of link position sensors and ultrasonic sensors for obstacle control in a manipulator makes it possible to control the concreting process by means of microprocessor technology [5,6].

The robotization of concrete-laying operations, based on the use of arm manipulators, should be solved by building robotized concrete-laying complexes (RCLC). Such RCLCs, apart from a concrete-laying manipulator, include concrete conveyors, concrete pumps, receiving hoppers, mechanisms for concrete compaction, robots for laying and welding of reinforcement grids and frameworks.

Many scientific researches and practical developments are devoted to robotization of concrete-laying works using manipulators. At the same time, it should be noted that there is still no systematic approach in solving these problems. It consists primarily in the necessity of mathematical identification of concrete-laying robots and unambiguous representation of them as objects of automatic control. On this basis, it is possible to synthesize various control systems and plan optimal trajectories for the movement of actuators. This article is devoted to the consideration of these issues.

2 Mathematical models of concrete-laying robots

When a hydraulic drive is used in concrete-laying robots, closed loops in the form of three- and four-links are formed (Fig. 4). These mechanisms are described by nonlinear functions and it is necessary to build kinematic and dynamic models to control them. The task of the kinematic analysis of these structures is to establish relations between movements of the drives and the angle of turn of the link, as well as dependences of velocities and accelerations of these parameters. In accordance with the kinematic scheme of the manipulator, local coordinate systems are constructed, on the basis of which the transition matrices from one coordinate system to another $T_{i-1,1}$ are written. These matrices allow to obtain the

equations of interrelation of the basic coordinates with the generalized:

$$\bar{x} = f_1(\bar{q}), \bar{r}_p = T_{01}T_{12}T_{23} \cdots T_{n-1,n}\bar{r}_p = T_{0n}\bar{r}_p^*$$

where \bar{r}_p^* - position vector of point P in the grip coordinate system; $T_{i-1,1}$ - transformation matrix of coordinate systems. To solve the inverse kinematics problem ($q = f^{-1}(x)$) it is convenient to use recurrence relations of the form:

$$q_{k-1} = q_k + J_n^{-1}(q_k) \cdot (x - f(q_k)), \quad (1)$$

where $J_n = \partial f / \partial q$ is Jacobi matrix.

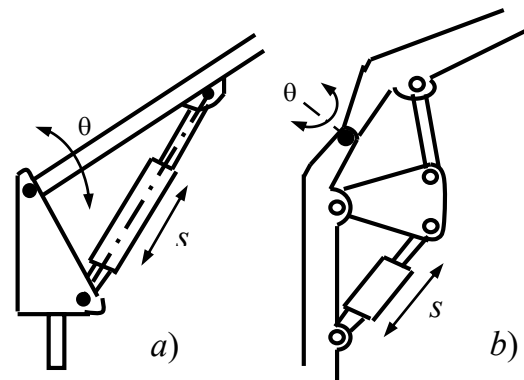


Figure 4. Schematics degrees of mobility of hydraulic arm manipulators

Kinematic models of the considered structures besides the given equations must contain equations of connection of generalized coordinates q_i with displacements of hydraulic actuators s_i : $q_i = f_1(s_i)$, which allow to set dependences between vectors \bar{x} and \bar{s} : $\bar{x} = f_2(\bar{s})$. For the considered structures the required functions $q_i = f_1(s_i)$ are easily obtained on the basis of the geometric approach. For kinematic structure of the second link with a hydraulic jack, providing lifting and lowering of a jib (fig. 4) this interrelation is described by the equation like:

$$\theta(s) = \arctg(a/b) + \arccos\left(\frac{l_1^2 + l_2^2 - s^2}{2l_1l_2}\right) + \arctg(e/d) - \pi, \quad (2)$$

where a, b, c, d, e - structural parameters; $l_1 = \sqrt{a^2 + b^2}$ and $l_2 = \sqrt{d^2 + e^2}$ - interaxial distances. This type of structure, in the first place, refers to the second degree of mobility, where, for the convenience of reporting the generalized coordinate q_2 , it is convenient to use an angle γ , equal to $\gamma = \theta + \pi/2 - \arctg(a/d)$. In this case the generalized coordinate is related to the drive displacement by the relation:

$$\theta(s) = \arctg(a/b) + \arccos\left(\frac{l_1^2 + l_2^2 - s^2}{2l_1l_2}\right) - \pi/2. \quad (3)$$

To solve inverse problems about the position of the considered structure, its kinematic model includes coupling equations $s_i = f_2(q_i)$, which are also defined on the basis of the geometric approach:

$$s(\theta) = (l_1^2 + l_2^2 + 2l_1l_2 \cos(\theta - \alpha - \varphi)). \quad (4)$$

Similarly, the relationship equations between the generalized coordinates q_i and the hydraulic actuator movements s_i are found: $q_i = f_2(s_i)$ for the kinematic structures representing a Witt chain with the three- and four-links connected in series (Fig. 5b). These relations are obtained by pre-recording the expressions:

$$\varphi_{1i}(s) = \angle O_{1i}O_{2i}O_{3i} = \arccos((a_{0i}^2 + a_{1i}^2 - s_i^2) / 2a_{0i}a_{1i}) \bar{e}_i = \bar{e}_{i-1} + (1 - \xi_i) \cdot \bar{\omega}_i \times \bar{e}_i \cdot q_i' + (1 - \xi_i) \cdot \bar{e}_i \cdot \bar{q},$$

$$\varphi_{2i}(s) = \angle O_iO_{2i}O_{4i} = \pi + \alpha_0 + \alpha_1 - \varphi_{1i}(s),$$

$$\varphi_{2i}(s) = \angle O_{2i}O_iO_{3i} = \arccos\left(\frac{d_i^2 + b_{0i}^2 - b_{1i}^2}{2b_{0i}d_i}\right) + \arccos\left(\frac{d_i^2 + b_{3i}^2 - b_{2i}^2}{2b_{3i}d_i}\right),$$

where $d_i(s) = \sqrt{b_0^2 + b_1^2 - 2b_0b_1 \cos(\varphi_{1i}(s))}$.

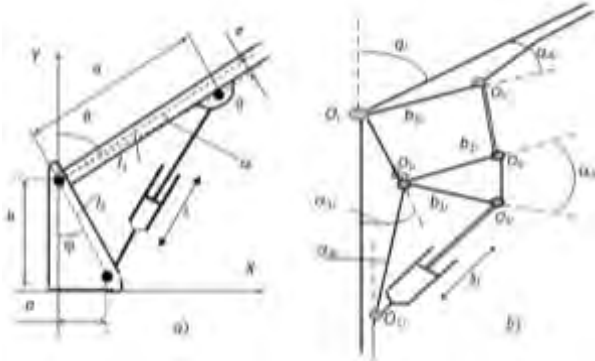


Figure 5. Calculation diagrams of degrees of mobility of a hydraulically driven concrete laying manipulator

Using these expressions, the coupling equations for generalized coordinates are written:

$$q_i(s) = \alpha_{1i} + \alpha_{4i} - \pi + \varphi_{3i}(s). \quad (5)$$

In accordance with the above relations, the dependence has a non-linear nature. However, modeling of the above equations has shown that at certain ratios of design parameters it is possible to obtain dependences close to linear in the operating range of the hydraulic cylinder. In this connection at designing of manipulating mechanisms with the hydraulic drive it is necessary to carry out optimization of a parity of parameters of kinematic structures providing reception of quasi-linear characteristics: $q_i = f_1(s_i)$; $s_i = f_2(q_i)$. It gives an opportunity to carry out linearization of the given equations and to receive convenient relations for construction of control algorithms.

The equations for velocities and accelerations are required to obtain complete kinematic models of the considered structures [6]. The structures under consideration use a linear motion drive, which is converted into angular displacements of manipulator links through

multilink elements. The angular and linear displacement velocities of the i -th link are expressed through the velocities of the $i-1$ st link in the form:

$$\begin{aligned} \bar{\omega}_i &= \bar{\omega}_{i-1} + (1 - \xi_i) \bar{e}_i q_i' \\ \bar{v}_i &= \bar{v}_{i-1} + \bar{\omega}_{i-1} \times \bar{r}_{i-1,i} + \bar{e}_i \cdot q_i' \end{aligned} \quad (6)$$

Where $\bar{r}_{i-1,i}$ is the vector connecting the axes of degrees of mobility $i-1$ and i -th; ξ_i is the logical coefficient describing

the type of kinematic pair: rotational $\xi=0$; translational $\xi=1$. Linear and angular accelerations of two coordinate systems on the basis of the Coriolis theorem are written in the form

$$\bar{e}_i = \bar{e}_{i-1} + (1 - \xi_i) \cdot \bar{\omega}_i \times \bar{e}_i \cdot q_i' + (1 - \xi_i) \cdot \bar{e}_i \cdot \bar{q},$$

$$\bar{a}_i = \bar{a}_{i-1} + \bar{e}_{i-1} \times \bar{r}_{i-1,i} + \bar{\omega}_{i-1} \times (\bar{\omega}_{i-1} \times \bar{r}_{i-1,i}) +$$

$$+ \xi_i \cdot \bar{e}_i \cdot q_i'' + 2\xi_i \cdot \bar{\omega}_i \times \bar{e}_i \cdot q_i',$$

where \bar{e}_{i-1} , \bar{e}_i are vectors of angular accelerations of $i-1$ and i -th manipulator link; \bar{a}_{i-1} , \bar{a}_i are vectors of linear accelerations of $i-1$ and i -th manipulator link. Final dependences of linear and angular velocities as functions of generalized velocities and generalized coordinates are obtained as sums of:

$$\begin{aligned} \bar{\omega}_i &= \sum_{j=1}^n \bar{\omega}_i^j q_j', \quad \bar{v}_i = \sum_{j=1}^n \bar{v}_i^j q_j', \quad \bar{\omega}_i^j = \sum_{j=1}^n (1 - \xi_j) \bar{e}_j \cdot \\ \bar{v}_i^j &= \bar{\omega}_i^j \times \bar{r}_{j,i} + \xi_j \bar{e}_j \cdot q_j'. \end{aligned} \quad (7)$$

Similarly, we can write down the final expressions for accelerations:

$$\bar{e}_i = \sum_{j=1}^n (\bar{\omega}_i^j q_j'' + (\sum_{k=1}^n (\bar{\omega}_i^k \times \bar{\omega}_i^j) q_k') q_j'). \quad (8)$$

The description of drive mechanisms in kinematic models is represented by a system of equations linking drive state parameters with generalized coordinates, velocities and accelerations. The generalized coordinates are calculated from the drive coordinates based on the following equations:

$$\partial q_i = k_{ji}^s \partial s_i, \quad k_{ji}^s = \frac{\partial f_s(s_i)}{\partial s_i}. \quad (9)$$

The description of the generalized velocities and accelerations of the robot is conveniently represented in the form of a vector-matrix equation:

$$\bar{q}' = k_q^s \cdot \bar{s}' = \text{diag} \left\{ \frac{\partial f_s(s)}{\partial s} \right\}. \quad (10)$$

By differentiating the last equations, we obtain the coupling equation for accelerations:

$$\bar{q}'' = k_q^s \bar{s}'' + (k_q^s)' \bar{s}' = k_q^s \bar{s}'' + \text{diag} \left\{ \frac{\partial^2 f_s(s)}{\partial s^2} \right\} \cdot (\bar{s}')^2 \quad (11)$$

For the structural scheme of type 1 (Fig. 4a), the equations of generalized and drive velocity relations are represented in the form:

$$\theta'(s') = k_{\theta}^{(1)}(s) \cdot s' = \frac{s \cdot s'}{(4l_1^2 l_2^2 - (l_1^2 + l_2^2 - s^2)^2)^{1/2}}, \quad (12)$$

$$s'(\theta') = k_s^{(1)}(\theta) \cdot \theta' = \frac{l_1 l_2 \sin(\alpha + \varphi - \theta) \cdot \theta'}{(l_1^2 + l_2^2 + 2l_1 l_2 \cos(\theta - \alpha - \varphi))^{1/2}}.$$

Similarly, the equations of generalized and drive-velocity relations for the structural scheme of type 2 can be written down (Fig. 4b):

$$\theta'(s') = k_{\theta}^{(1)}(s) s', \quad s'(\theta') = k_s^{(1)}(\theta) \theta'.$$

The structural features of concrete-laying robots complicate the construction of their dynamic models. The analysis of methods for describing the dynamics of manipulating mechanisms has shown that, for concrete-laying robots based on articulated arms, it is expedient to build dynamic models using a method based on the Lagrange method formulated through the D'Alembert principle [7]. This makes it possible to obtain the resulting equations in a convenient vector-matrix form. For the manipulation system of concrete-laying robots with closed kinematic chains of hydraulic actuators, the balance of virtual forces is as follows:

$$\sum_{i=1}^n \sum_{v=0}^{N_i} \{m_{iv}(\ddot{\mathbf{r}}_{iv} - \bar{\mathbf{g}})\delta \mathbf{r}_{iv} + (\mathbf{I}_{iv} \varepsilon_{iv} + \omega_{iv} \times \mathbf{I}_{iv} \omega_{iv})\delta \gamma_{iv}\} = \sum_{i=1}^n \tau_i \delta q_i, \quad (13)$$

where \mathbf{r}_i is vector-vector of link i with mass m and moment of inertia j in the point of gravity; $\bar{\mathbf{g}}$ is vector of gravitational interaction; τ is drive moment of drive forces in the i -th link; N is a number of links of the i -th kinematic pair.

For a virtual representation of the movement of manipulator links, the equations of dynamics should be applied in the form of:

$$\sum_{k=1}^n \sum_{v=0}^{N_k} \{m_{kv} v_{kv}(\ddot{\mathbf{r}}_{kv} - \bar{\mathbf{g}}) + (\mathbf{I}_{kv} \varepsilon_{kv} + \omega_{kv} \times \mathbf{I}_{kv} \omega_{kv})\delta \gamma_{kv}\} = \sum_{i=1}^n \tau_k \delta q_k. \quad (14)$$

Equations in drive coordinates are needed to control the drive coordinates. To obtain them, use the virtual work balance equations in articulated coordinates and the relationship equations between the generalized coordinates and the drive coordinates. This results in dynamic equations in drive coordinates:

$$\mathbf{M}(\mathbf{s})\ddot{\mathbf{s}} + \mathbf{h}(\mathbf{s}, \dot{\mathbf{s}}) + \mathbf{g}(\mathbf{s}) = \mathbf{F}_A, \quad (15)$$

where $\mathbf{M}(\mathbf{s}) = k_q^i \mathbf{M}(\mathbf{q}) k_q^i + \mathbf{h}(\mathbf{s}, \dot{\mathbf{s}}) + \mathbf{g}(\mathbf{s}) = \mathbf{F}_A$;

$$\mathbf{h}(\mathbf{s}, \dot{\mathbf{s}}) = \mathbf{k}_q^i \mathbf{M}(\mathbf{q}) \mathbf{k}_q^i \dot{\mathbf{s}}^2 + \mathbf{k}_q^i \mathbf{h}(\mathbf{q}, \dot{\mathbf{q}}) = \mathbf{k}_q^i \mathbf{M}(\mathbf{q}) \mathbf{k}_q^i \dot{\mathbf{s}} + \mathbf{k}_q^i \mathbf{h}(\mathbf{q}, \dot{\mathbf{q}});$$

$$\mathbf{g}(\mathbf{s}) = \mathbf{k}_q^i \mathbf{g}(\mathbf{q})$$

An analysis of the dynamic properties of a concrete-laying manipulator requires the construction of a dynamic model of the complex system, taking into account the

dynamics of the hydraulic drives. In addition to modeling of individual components, it is important to describe the relationship between the mechanical and hydraulic parts of the manipulator, because on the one hand the dynamic characteristics of the mechanical subsystem is determined by the resulting forces of the hydraulic drives, and on the other hand the impact of the mechanical part on the hydraulic drives has a significant impact on their own dynamics.

In the process of modeling such a drive, its static and dynamic models are considered, as well as the simulation of the hydraulic cylinder friction is performed. The main functional blocks of the hydraulic part of the actuator are a double-acting power hydraulic cylinder, an electromechanical converter and a two-stage electro-hydraulic amplifier that includes a three-position hydraulic distributor and a jet amplifier of "nozzle-slide" type. Feedback is provided by the hydraulic motor load. The hydraulic directional control valve, which is hydraulically controlled and determines direction of flow and flow rate of the fluid supplied to the hydraulic cylinder, has a significant influence on static and dynamic characteristics of the electro-hydraulic drive.

3 Path planning of concrete-laying robots

Let's consider the planning of concrete-laying robots trajectory on the examples of monolithic buildings and structures erection by means of sliding, repositionable and volumetric formwork. Analysis of the construction of monolithic pipes, silos, building cores and residential buildings showed that laying the next layer of concrete is done in the horizontal plane. Therefore, the problem of constructing a trajectory of the nozzle of the robotic concrete-laying arm is reduced to the description of the sequence of motions in the plane $X_p Y_p$ parallel to the plane $X_0 Y_0$ of the coordinate system of the robot. The coordinate Z_p does not change within one laying cycle and then increases by the value Δh corresponding to the step of the formwork raising. Fig. 6 shows examples of the most frequently erected monolithic objects. As can be seen from the figures the movement trajectories are either a set of rectangles or circles. When erecting the frame of a residential building (Fig. 6a), it is necessary to formulate an array of coordinates of points P_1, P_2, \dots, P_{10} on the basis of the building plan and determine the sequence of rectilinear sections $P_i \rightarrow P_j$: for sections parallel to the axis $X_0 \rightarrow P_{js}(x_{js}, y_{js}), P_{je}(x_{je}, y_{je})$

$$y = y_{js} \vee y_{jk} \rightarrow x_{js} \leq x \leq x_{je}; \quad (16)$$

and for sections parallel to the axis $Y_0 \rightarrow P_{is}(x_{is}, y_{is}), P_{ie}(x_{ie}, y_{ie})$

$$x = x_{is} \vee x_{ie} \rightarrow y_{is} \leq y \leq y_{ie}. \quad (17)$$

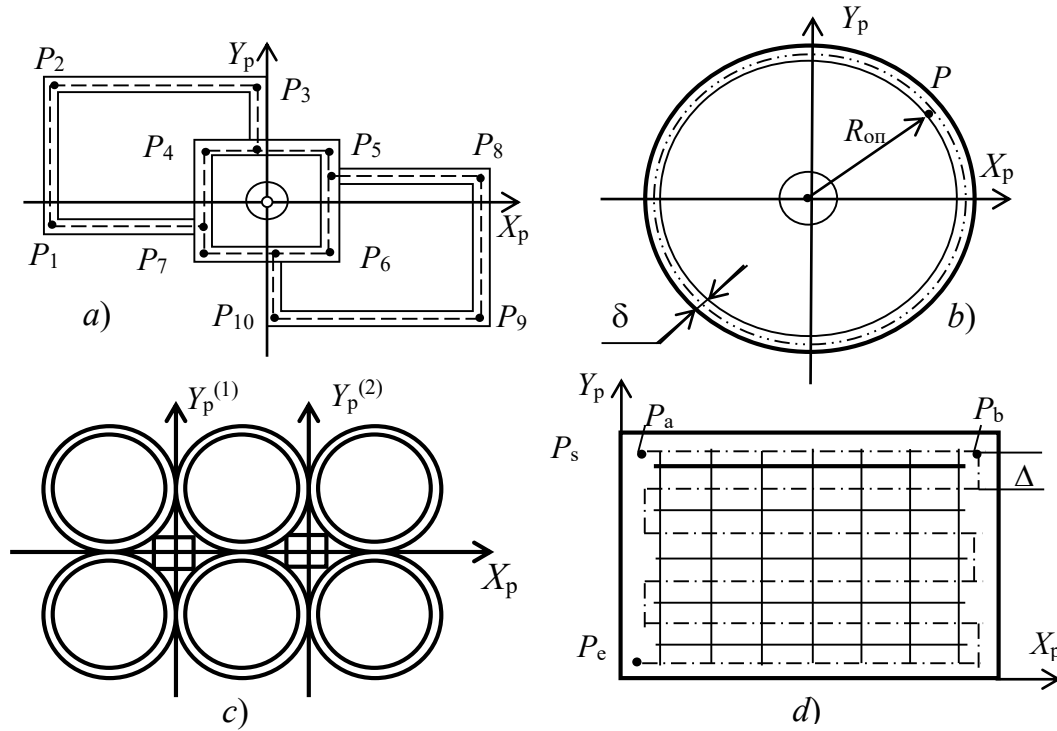


Figure 6. Plans of monolithic objects and concrete laying paths

When erecting chimneys, the concrete-laying robot is positioned on a load shaft in the center of the structure. Therefore, its trajectory is a circle of radius R_{cp} lying in the horizontal plane $X_M Y_M$ of concrete-laying works is performed on the basis:

$$(x - \Delta x_{cm})^2 + (y - \Delta y_{cm})^2 = R_{cp}^2,$$

where $\Delta x_{cm}, \Delta y_{cm}$ is the deviation of the formwork from the design axis.

When planning the trajectories of concrete-laying robots, there are a number of cases that require the use of approximation methods to form the time laws of variation of the generalized coordinates:

$$q(t) = [q_1(t), q_2(t), \dots, q_n(t)].$$

The first of them is associated with displacement of a working body from the initial stationary state, where

$$\dot{q}_s = \ddot{q}_s = 0, \text{ to a given final state } \dot{q}_e = \ddot{q}_e = 0.$$

The problem is to form a law $q(t)$ using the given vectors of generalized coordinates at the end points of the trajectory and the zero values of velocities and accelerations of generalized coordinates at these points. When solving this problem, the limit conditions imposed on the derivatives of the generalized coordinates must be taken into account:

$$q_i^{(k)}(t) \leq (q_i^{(k)})_{add} \quad (k = 1, 2, \dots, m).$$

The limits $(q_i^{(k)})_{add}$ are determined by the maximum forces and moments developed by the robot drives. Given that there are six boundary conditions in this case, we can obtain a function $q_j(t)$ for each generalized coordinate in the form of a polynomial of order 5:

$$q_j(t) = \sum_{k=0}^5 a_{jk} t^k \rightarrow j = 1, 2, \dots, n.$$

The coefficients of the interpolation polynomial a_{jk} are determined according to the boundary conditions from the expressions:

$$a_{j0} = q_{js}; a_{j1} = a_{j2} = 0; a_{j3} = \frac{10(q_{je} - q_{js})}{T^3}$$

$$a_{j4} = \frac{15(q_{je} - q_{js})}{T^4}; a_{j5} = \frac{6(q_{je} - q_{js})}{T^5}.$$

Taking into account the above coefficients, the law of change of the j -th generalized coordinate that ensures the movement of a grab to a given point in the workspace is written in the form:

$$q_j(t) = g_{js} + \Delta g_j \tau^3 (10 + 15\tau + 6\tau^2),$$

where $\tau = t/T$ is the relative time of motion, is the displacement $\Delta q_j = q_{je} - q_{js}$ of the j -th generalized coordinate.

The duration of the time interval T is chosen from the condition that for each generalized coordinate the maximum values of velocities and accelerations do not exceed the maximum allowable values:

$$\left| \dot{q}_j \right|_{\max, j=1, n} \leq \left| \dot{q}_j \right|_{\text{add}}; \left| \ddot{q}_j \right|_{\max, j=1, n} = \left| \ddot{q}_j \right|_{\text{add}}.$$

To ensure this condition, the interval of travel time T must satisfy the condition:

$$T = \max_j \left[\max_{j=1, n} (1,878 \frac{|q_{jk} - q_{js}|}{|\dot{q}_j|_{\text{add}}}), \max_{j=1, n} (5,7735 \frac{\sqrt{|q_{jk} - q_{js}|}}{|\ddot{q}_j|_{\text{add}}}) \right]$$

This algorithm can be used to implement rectilinear motions of construction robots. The analysis of processing such movements by concrete layers showed the effectiveness of using approximating polynomials of order 5 to implement the command movements associated with the movement of the working body to a given point.

Variation laws of generalized coordinates $q(t)$ based on polynomials of degree 3 are used for construction robots when the vectors of generalized coordinates at the initial q_s , final q_e and intermediate node points $q_k (k=1, 2, \dots, m-1)$ are known.

This case is encountered when executing commands related to the movement of a working organ along a given trajectory, which is defined by a set of points. The number of intermediate points is determined by the nature of the trajectory and the required accuracy of its execution. The formation of laws of motion of generalized coordinates is based on the following requirements. The approximating polynomials must be able to pass through a sequence of vectors of generalized coordinates corresponding to each node point of the planned trajectory. In addition, for each generalized coordinate, continuity of the function itself and its first and second derivatives must be ensured. Fulfillment of these conditions ensures the continuity of velocities and accelerations and the smoothness of the trajectory to be realized [7].

Based on the initial information and requirements, a set of spline functions is constructed for each generalized coordinate:

$$P_j(t) = a_{j0} + a_{j1}t + a_{j2}t^2 + a_{j3}t^3.$$

The solution of this problem is performed on the basis of global interpolation. Two variants are possible: at zero velocities at the initial and final points of the motion trajectory; at given (nonzero) values of initial and final velocities of motion. The most interesting for construction robot control is the 1st method of spline construction. The input data in this case are: the trajectory of motion, defined by a set of node points; the values of velocity at the beginning and at the end of the trajectory; the value of the operating velocity along the trajectory. In addition, for each node point of the trajectory we set the orientation vector of the working body, as well as the constraints on the

trajectory, on kinematics and dynamics of the manipulator. The limiting positions and admissible values of velocities and accelerations by degrees of mobility are considered as constraints. The purpose of the planning is to formulate laws of change $q_i(t); \dot{q}_i(t); \ddot{q}_i(t)$. The advantages of this planning method are its real-time execution and the direct generation of the controlled variables in the form of:

$$q_{ji}(t) = a_{ji0} + a_{ji1}(t - t_{i-1}) + a_{ji2}(t - t_{i-1})^2 + a_{ji3}(t - t_{i-1})^3, t_{i-1} \leq t \leq t_i,$$

where $i = 1, 2, \dots, m$ is the number of the spline; $j = 1, 2, \dots, n$ is the number of the degree of mobility of the generalized coordinate.

Determination of spline parameters is based on using the conditions of approximation of functions, continuity of splines and continuity of velocities and accelerations. For one degree of mobility, the system of equations that allows to determine the coefficients of splines has the form:

$$\begin{cases} P_i(t_i) = P_{i+1}(t_i) \rightarrow i = 1, 2, \dots, m-1 \\ \dot{P}_i(t_i) = \dot{P}_{i+1}(t_i) \rightarrow i = 1, 2, \dots, m-1 \\ \ddot{P}_i(t_i) = \ddot{P}_{i+1}(t_i) \rightarrow i = 1, 2, \dots, m-1 \\ P_i(t_i) = q_i, P_1(t_0) = q_0 \end{cases}$$

This system of equations is supplemented by initial conditions:

$$P_i(t) = \frac{M_{i-1}}{6\tau}(t-t)^3 + \frac{M_i}{6\tau}(t-t_{i-1})^3 + (q_{i-1} - M_{i-1} \frac{\tau^2}{6}) \frac{t-t}{\tau} + (q_i - M_i \frac{\tau^2}{6}) \frac{t-t_{i-1}}{\tau} \rightarrow t_{i-1} < t < t_i; i = 1, 2, \dots, m.$$

where M_{i-1}, M_i are the accelerations at the $i-1$ and i -th node points; the interpolation time at the i -th site.

The accelerations at the node points are determined on the basis of vector-matrix equations based on the condition of continuity of velocities at the node points and their equality to zero at the boundary points:

$$\begin{bmatrix} M_0 \\ M_1 \\ M_2 \\ \dots \\ M_m \end{bmatrix} = \begin{bmatrix} 4 & \lambda_0 & 0 & 0 & \dots & 0 \\ \mu_1 & 4 & \lambda_1 & 0 & \dots & 0 \\ 0 & \mu_2 & 4 & \lambda_2 & \dots & 0 \\ \dots & \dots & \dots & \dots & \dots & \dots \\ 0 & \dots & \dots & \dots & \dots & \mu_m & 4 \end{bmatrix}^{-1} \begin{bmatrix} d_0 \\ d_1 \\ d_2 \\ \dots \\ d_m \end{bmatrix}$$

$$\text{or } M = \Delta^{-1} \cdot D.$$

The parameters of the right part of the equation are calculated using the formulas:

$$\begin{aligned} \lambda_0 &= \mu_m = 2; \mu_i = \tau_i / (\tau_i + \tau_{i+1}); \lambda_i = 1 - \mu_i \\ d_0 &= 3(q_1 - q_0) / \tau_1^2; d_m = 3(q_{m-1} - q_m) / \tau_m^2; \\ d_i &= 3[(q_{i-1} - q_i) / \tau_{i+1} - (q_i - q_{i-1}) / \tau_i] / (\tau_{i+1} + \tau_i). \end{aligned}$$

When performing concrete laying as well as such technological operations as painting, priming, welding, cutting material, it is required not only to ensure the continuity and smoothness of movement, but also to plan the speed and acceleration of movement. In this case, when planning movements of the manipulator it is required to determine the speed of links

$$\dot{q}(t) = [\dot{q}_1(t), \dot{q}_2(t), \dots, \dot{q}_n(t)]^T,$$

which provides the estimated technological speed of the tool during the development of the trajectory. It is necessary to formulate the laws of change of the generalized coordinates $q(t) = [q_1(t), q_2(t), \dots, q_n(t)]$, if their values in the nodal points of the trajectory and the speeds of each degree of mobility in these points, corresponding to the technological speed of the tool movement are determined:

$$q_{j_i}(t_i) = q_{j_i}; \dot{q}_{j_i}(t_i) = \dot{q}_{j_i} \rightarrow i = 1, 2, \dots, n-1.$$

The law $q(t)$ is formed as a sequence of contiguous sections described by an interpolation polynomial. In this case, the cubic Hermite interpolation polynomial may be preferred. If at the node points t_i , except for function values $q_j(t_i) = q_{j_i}$, we also know the values of derivatives $\dot{q}_j(t_i) = \dot{q}_{j_i}$, then on each segment $[t_{i-1}, t_i]$ we can construct a spline according to the equation:

$$q_j(t) = q_{j_{i-1}} \cdot \frac{(t_i - t)^2 \cdot (2(t - t_{i-1}) + \tau)}{\tau^3} + \dot{q}_{j_{i-1}} \cdot \frac{(t_i - t)^2 \cdot (t - t_{i-1})}{\tau^2} + q_{j_i} \cdot \frac{(t - t_{i-1})^2 \cdot (2(t_i - t) + \tau)}{\tau^3} + \dot{q}_{j_i} \cdot \frac{(t - t_{i-1})^2 \cdot (t - t_i)}{\tau^2},$$

where $\tau = t_i - t_{i-1}$ is the interpolation step.

The feature of motion planning of manipulation systems in this case is that the time moments corresponding to the node points are initially defined, and the interpolation step is usually chosen uniformly. If the monotonicity of the functions is broken, the interpolation step should be changed and the calculation should be repeated.

4 Conclusion and results

The article presents for the first time a systematic approach to solving the problem of mathematical identification of robots for laying concrete mixture as objects of automatic control. For mathematical description there are multilink manipulators with a hydraulic drive, which most fully reflect the features and requirements of the performed operations, working environment conditions, transportation requirements and installation into a working condition. The feature of such manipulators is the presence of branched structures that provide the best kinematic and dynamic characteristics. The description of drive mechanisms in kinematic models is represented by a system of equations linking the parameters of the drive

state with the generalized coordinates, velocities and accelerations. Analysis of methods for describing the dynamics of manipulating mechanisms has shown that for concrete-laying robots based on articulated manipulators, it is reasonable to build dynamic models by the method based on the Lagrange method formulated through the D'Alembert principle. This makes it possible to obtain the resulting equations in a convenient vector-matrix form and to realize an original approach to planning the trajectory of concrete-laying robots by the example of monolithic buildings and structures erection using sliding, repositionable and volumetric formwork. Since layers of concrete in this case are placed in a horizontal plane, the trajectory of a robotic concrete-laying head is reduced to the description of a sequence of movements in a plane parallel to the plane of the robot's coordinate system. In this case, all the requirements for preventing the appearance of singularity points in the system under consideration are observed, although this issue is not considered separately.

References

- [1] Briot S., Arakelian V., Guégan S. Design and prototyping of a partially decoupled 4-DOF 3T1R parallel manipulator with high-load carrying capacity // *Transaction of the ASME. Journal of Mechanical Design*. 2008. V. 130. No. 12. P. 612–619.
- [2] Arakelian V., Briot S., Glazunov V. Increase of singularity-free zones in the workspace of parallel manipulators using mechanisms of variable structure // *Mechanism and Machine Theory*. 2008. V. 43. P. 1129–1140.
- [3] Hubert J., Merlet J.-P. Static of parallel manipulators and closeness to singularity // *Transactions of the ASME. Journal of Mechanisms and Robotics*. 2009. V. 1. P. 1–6.
- [4] Bonev I., Zlatanov D., Gosselin C. Singularity analysis of 3-DOF planar parallel mechanisms via screw theory // *Transactions of the ASME. Journal of Mechanical Design*. 2003. V. 125. P. 573–581.
- [5] Travush V., Erofeev V., Bulgakov A. and Buzalo, N. Mechatronic complex based on sliding formwork for the construction of monolithic high-rise buildings and tower-type structures made of reinforced concrete. *IOP Conf. Series: Materials Science and Engineering* 913 (2020) 022009 DOI:10.1088/1757-899X/913/2/022009
- [6] Bulgakov A., Bock T., Otto J., Buzalo N. and Linner T. Requirements for Safe Operation and Facility Maintenance of Construction Robots. 2020 *Proceedings of the 37th ISARC, Kitakyushu, Japan*, pp. 369-376. DOI: doi.org/10.22260/ISARC2020/0053
- [7] Lin Lee-Kuo. The research of automatic concrete placing. *In Proceedings of the 17th ISARC 2000*, pp. 1-5, Taipei, Taiwan.

Structural organization of robotic building and mounting complexes

Alexey Bulgakov^{1,5}, Jens Otto², Wen-der Yu³, Vladimir Rimshin⁴ and Alexey Shleenko⁵

¹Central Research and Development Institute of the Ministry of Construction of Russia, Russia

²Technical University of Dresden, Germany

³Chaoyang University of Technology, Taiwan

⁴Research Institute of Building Physics of the Russian Federation Academy of Architecture and Construction Sciences (NIISF RAACS), Russia

⁵Southwest State University, Russia

agi.bulgakov@mail.ru, jens.otto@tu-dresden.de, wenderyu@cyut.edu.tw, rimshin@niisf.ru, shleenko77@mail.ru

Abstract –

The object of the research is construction robot manipulators for mounting works. The results of mathematical identification of mounting manipulators on the basis of a tower crane model are presented. The design of movement trajectories of a manipulator or technological equipment is performed taking into account the limitations both on the trajectory itself and on the movements of the manipulator links. The trajectory of movement is represented as a sequence of typical elementary sections. Recommendations on creation of databases for manipulators operating according to a cyclic program for their use at the stage of trajectories design are given.

Keywords –

Robot; Building and Mounting Works; Mathematical Modell; Path Planning

1 Introduction

Construction and installation work belongs to the main and labor-intensive activities on the construction site. They account for about 23 % of the total labor costs for the construction of the above-ground part of the building. They are divided into two groups: installation cycle operations and auxiliary operations. The most labor-intensive are the assembly cycle operations, the share of which exceeds 65% of the total installation labor costs. Important and often repetitive are the basic operations of the installation cycle, including picking up the panel, lifting it and transporting it to the installation site, positioning and seating it in place, aligning the planned position of the panel and securing it. These

operations completely determine the cycle time and account for 50 % of all installation labor. In addition, they are characterized by difficult and hazardous working conditions. At present, these tasks can be solved on the basis of using crane manipulators, positioning robots and special mounting equipment.

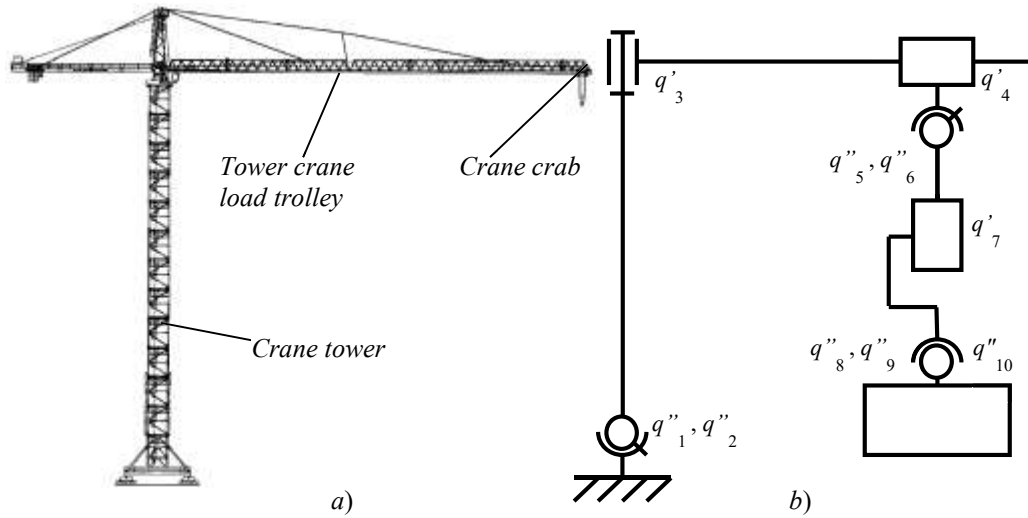
Recent years have seen an increasing use of robotic manipulators in the construction industry. Their kinematic diagrams differ in a great variety, which is associated with different areas of their application and functional tasks [1,2]. The number, type, and mutual arrangement of the degrees of mobility of construction robots are determined by the features of the technological operation performed, the required service area, and the needed orientation ability.

Kinematic schemes of construction manipulators are developed on the basis of formulated functional, design and operational requirements. The functional requirements are primarily those determining the shape, size and location of the working area, the possible technological forces on the working elements, the necessary speed and acceleration ranges of the working elements. In addition, in the case of the mounting robot, the specific shape, size and weight of the structure to be assembled must also be taken into account. When developing the kinematic schemes, the design requirements must include the shape and dimensions of the workspace in which the robot is to operate, the permissible compression ratio and the permissible static and dynamic errors. The operational requirements should include the reliability and compactness of the handling system in the working and transport position. The choice of the structure of the kinematic scheme of the robot, the determination of the number of degrees of mobility, the optimum length of the links and their limiting

displacements is one of the most important tasks in the design of specialized construction robots. The solution of this problem must be based on optimization methods that ensure the minimization of the robot's work envelope for a given operating envelope [3].

2 Mathematical identification of construction robot manipulators for mounting work

To present an approach for mathematical



identification of a robotic assembly complex as an object

Fig. 1. Tower crane (a) and its kinematic diagram (b) used to build the mathematical model.

neglected. During the construction of the crane model, its mechanical part with the load is considered as a manipulation structure [4,5]. At this stage, the elastic displacements and vibrations of the rope are replaced by holonomous couplings. Further, to the Lagrange equations describing the dynamics of the holonomy system, the terms taking into account the action of elastic and dissipative forces are added.

It is better to build the crane dynamic model based on Lagrange equations. In this case, the dynamics of the crane without taking into account the forces generated in the elastic elements is described by the following equation:

$$\mathbf{M} = D(\mathbf{q})\ddot{\mathbf{q}} + \mathbf{b}(\mathbf{q}, \dot{\mathbf{q}}) - \sum_{k=1}^l G^T(\mathbf{q}, \Delta \mathbf{x}^{(k)}) \mathbf{F}_s^{(k)} - \mathbf{M}_w,$$

from which

$$\ddot{\mathbf{q}} = D^{-1}(\mathbf{q}) \left(\mathbf{M} - \mathbf{b}(\mathbf{q}, \dot{\mathbf{q}}) + \sum_{k=1}^l G^T(\Delta \mathbf{x}^{(k)}, \mathbf{q}) \mathbf{F}_s^{(k)} + \mathbf{M}_w \right), \quad (1)$$

where \mathbf{M} is the vector of generalized forces arising in the joints of the manipulator; $\mathbf{D}(\mathbf{q})$ – dynamics matrix; $\mathbf{b}(\mathbf{q}, \dot{\mathbf{q}}) = \mathbf{h}(\mathbf{q}, \dot{\mathbf{q}}) + \mathbf{c}(\mathbf{q})$, $\mathbf{h}(\mathbf{q}, \dot{\mathbf{q}})$ – vector of Coriolis and

of research, consider a crane (Fig. 1a) consisting of a stationary tower 1 on which a horizontal rotary boom 2 with a trolley 3 moving along it is located. The crane is equipped with a rope, which holds the load on an hinged suspension.

A special feature of the crane mathematical model is the need to consider the elastic deformations in its structure arising from the action of wind and dynamic loads. Since the installation process is carried out at low speeds, the amplitude of the cable oscillations is negligible and the wave processes in the cable can be

centrifugal forces; $\mathbf{c}(\mathbf{q})$ – vector of gravitational forces; $\mathbf{F}_s^{(k)}$ – vector of forces arising in the k -th grip, measured in the absolute coordinate system; $\Delta \mathbf{x}^{(k)}$ – a vector of displacement of the point of application of the k -th external force, measured in the crane's crosshead coordinate system; l – number of attachment points of the positioning robot's gripping devices; \mathbf{M}_w – a vector of generalized forces, caused by external influences on the crane mechanism apart from the influence of the positioning robot [6,7].

The elements of the dynamics matrix D and the vectors h and c are calculated from the expressions:

$$D_{ik} = \sum_{j=\max(i,k)}^n \text{Tr}(U_{jk} J_j U_{ji}^T), \quad i, k = \overline{1, n},$$

$$h_i = \sum_{k=1}^n \sum_{m=1}^n h_{ikm} \dot{q}_k \dot{q}_m, \quad h_{ikm} = \sum_{j=\max(i,k,m)}^n \text{Tr}(U_{jkm} J_j U_{ji}^T), \quad (2)$$

$$c_i = \sum_{j=1}^n (-m_j \mathbf{g} U_{ij} \mathbf{r}^{(j)}), \quad i = \overline{1, n},$$

where J_j – is the matrix of moments of inertia of the j -th link; \mathbf{g} is the vector of free fall acceleration; m_j is the mass of the j -th link; $\mathbf{r}^{(j)}$ is the position vector of the centre of mass of the j -th link in its coordinate system.

During mounting work, the crane is heavily influenced by wind loads. In order to mathematically describe the distributed force caused, it is necessary to break down the crane structure into elements that have a sail and then replace the distributed forces acting on the elements with equivalent concentrated forces:

$$\mathbf{F}_w^{(k)} = (\mathcal{G}_x^{(k)}(\mathbf{q})w_x \quad \mathcal{G}_y^{(k)}(\mathbf{q})w_y \quad \mathcal{G}_z^{(k)}(\mathbf{q})w_z)^T, \quad k = \overline{1, n_w}, \quad (3)$$

where $\mathcal{G}_x^{(k)}(\mathbf{q})$, $\mathcal{G}_y^{(k)}(\mathbf{q})$, $\mathcal{G}_z^{(k)}(\mathbf{q})$ is the wind load factor of the k -th element in the direction of the axes of the absolute coordinate system; w_x, w_y, w_z are the projections of wind speed [m/c].

If the force $\mathbf{F}_w^{(k,i)}$ has an application point with coordinates $\mathbf{r}_w^{(k,i)}$, measured in the coordinate system of the i -th link to which the k -th mass is rigidly connected, then the transition to generalized crane forces is of the follows form:

$$\mathbf{M}_w = \sum_i \sum_{k=1}^{l_{wi}} G_i^T(\mathbf{r}^{(k,i)}, \mathbf{q}) \mathbf{F}_w^{(k,i)} = \widehat{G}^T(\widehat{\mathbf{r}}, \mathbf{q}) \widehat{\mathbf{F}}_w, \quad i = 2, 3, 4, 7, 10,$$

where l_{wi} is the number of bodies with sail associated with the i -th link.

By separating the generalized crane coordinates into controllable coordinates \mathbf{q}' and those introduced to simulate elastic deformation \mathbf{q}'' , this equation is transformed to the form:

$$\mathbf{M}' = D'(\mathbf{q})\ddot{\mathbf{q}}' + \bar{D}(\mathbf{q})\ddot{\mathbf{q}}'' + \mathbf{b}'(\mathbf{q}, \dot{\mathbf{q}}) - \sum_{k=1}^3 G'^T(\mathbf{dx}^{(k)}, \mathbf{q}) \mathbf{F}_s^{(k)} - \mathbf{M}'_w,$$

$$\mathbf{M}'' = \bar{D}^T(\mathbf{q})\ddot{\mathbf{q}}' + D''(\mathbf{q})\ddot{\mathbf{q}}'' + \mathbf{b}''(\mathbf{q}, \dot{\mathbf{q}}) - \sum_{k=1}^3 G''^T(\mathbf{dx}^{(k)}, \mathbf{q}) \mathbf{F}_s^{(k)} - \mathbf{M}''_w$$

The generalized forces \mathbf{M}' are generated by the crane drives and the generalized forces which simulate the elastic displacements of the crane are determined by the stiffness and dissipation of the crane components:

$$\mathbf{M}'' = -\alpha \mathbf{q}'' - \beta \dot{\mathbf{q}}'', \quad (4)$$

where α, β – diagonal stiffness and dissipation matrices.

On the basis of the obtained equations it is possible to construct a structural diagram of the model of the crane with the plate to be mounted (Fig. 2). The resulting model of the elastic deforming mechanism of the crane in matrix form is convenient for constructing a model of the mounting complex and control algorithms [8].

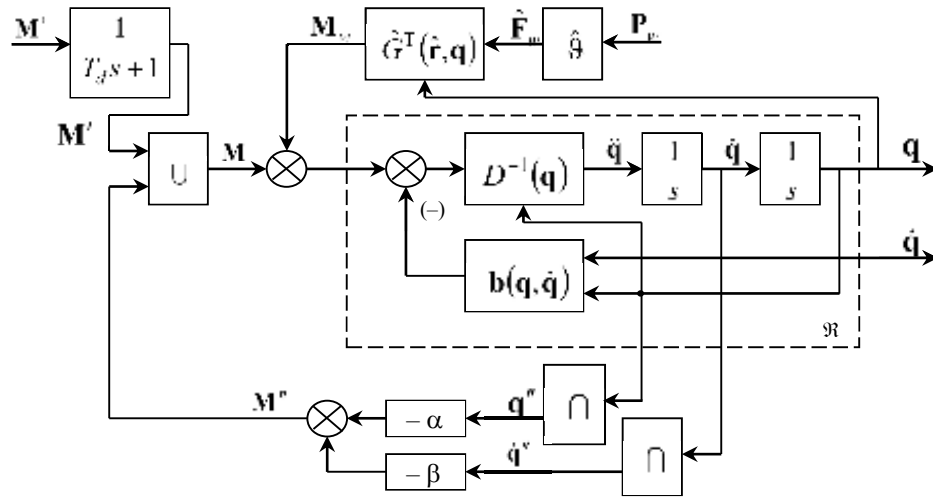


Fig. 2. Crane model structure diagram.

3 Path planning for construction mounting robots

The robot's construction and mounting operations require motion planning of the robot arm in space and time. Movement planning is performed based on constructed movement trajectories, node point tables and movement speeds. The planning task is to develop a mathematical description of the desired movements of

the complex mechanisms. In most cases the motion trajectories of mounting robots are complicated spatial trajectories consisting of rectilinear sections, contiguous arcs of circles or smoothed curvilinear sections. When designing the motions of a robot handling system, the requirements for the character of the motion are also taken into account, ensuring the desired smoothness and continuity of the trajectory, the continuity of the velocities and accelerations. Thus, any complicated movement trajectory is represented as a sequence of typical elementary sections, for which typical motion

planning algorithms are included as part of the robot software. In this connection, motion planning of any construction robot is reduced to the planning of typical elementary movements of the executive mechanism. The design of movement trajectories of a manipulator or technological equipment is performed taking into account the limitations both on the trajectory itself and on the movements of the manipulator links. When planning a trajectory in a non-dimensional environment, the possible nature of its change is taken into account [9].

The robotization of mounting operations by means of specialized cranes with software and adaptive control involves the transportation of components to the mounting area, its orientation and installation into the designed position. When constructing the trajectory of the part moving into the installation zone, changes in the position of mechanisms during the work, changes in the environment in the installation zone are taken into account. In order to avoid emergency situations, when designing the trajectory of the parts, it is necessary to take into account the shape, overall dimensions and inertial properties of the structure, the dimensions of the installation area, and wind loads. Analysis of mounting technology shows that it is more appropriate to use transport trajectories that consist of two or three rectangular sections (Fig. 3), including vertical lifting of

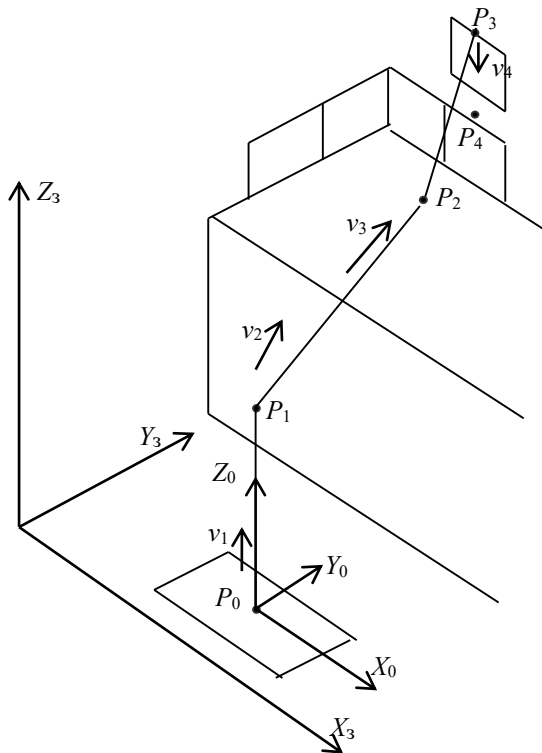


Fig. 3. Trajectories for transporting the building structure into the mounting area.

the part to a given height, its horizontal movement in a straight line to the positioning point and vertical lowering of the part during mounting. For high and long objects, the transport of parts can be done with an inclined trajectory formed after the vertical lift of the part from the cassette. In this way, the motion trajectory of an mounting robot can be divided into 4 segments, each of which corresponds to a certain type of operation: vertical lifting of the building item to be mounted ($P_0 \rightarrow P_1$); linear movement to the designated area ($P_1 \rightarrow P_2$); horizontal movement to the installation site ($P_2 \rightarrow P_3$); orientation and positioning of the item to the designed position ($P_3 \rightarrow P_4$).

The constituent sections of a trajectory are normally straight. When constructing a trajectory, between the 1st and 2nd section and the 2nd and 3rd sections there are contiguous sections to ensure a smooth transition from one section of the trajectory to the other and non-stop movement until the point P_4 , where, in accordance with installation technology requirements, the movement speed should be set to zero. The trajectory points P_0, P_1, P_2, P_3, P_4 are defined in the building coordinate system. To describe them, it is convenient to use the matrix S_T , each column of which contains the coordinates of points P_i and Euler angles describing the orientation of the grip in each point:

$$S_T = \begin{bmatrix} x_i \\ y_i \\ z_i \\ \theta_i \\ \varphi_i \\ \psi_i \end{bmatrix} = \begin{bmatrix} x_0 & x_1 & x_2 & x_3 & x_4 \\ y_0 & y_1 & y_2 & y_3 & y_4 \\ z_0 & z_1 & z_2 & z_3 & z_4 \\ \theta_0 & \theta_1 & \theta_2 & \theta_3 & \theta_4 \\ \varphi_0 & \varphi_1 & \varphi_2 & \varphi_3 & \varphi_4 \\ \psi_0 & \psi_1 & \psi_2 & \psi_3 & \psi_4 \end{bmatrix}. \quad (5)$$

The values of the elements of this matrix are determined analytically. The accuracy of the position values is $\pm (0.5-1)$ mm and the accuracy of the orienting angles is no more than 2 arcmin.

For each section of the trajectory, process speeds are specified. The lifting operation is performed at medium speeds v_1 , the transportation on the 2nd and 3rd sections can be performed at maximum speeds v_2, v_3 , which are limited by the weight of the load and its dimensions. On the last section, where mounting operations, which require increased positioning accuracy, are performed, the speed v_4 of the construction element to be mounted is selected to be reduced. A velocity matrix is produced when constructing the trajectory V_T :

$$V_T = \begin{bmatrix} \dot{x}_i \\ \dot{y}_i \\ \dot{z}_i \\ \dot{\theta}_i \\ \dot{\phi}_i \\ \dot{\psi}_i \end{bmatrix} = \begin{bmatrix} 0 & \dot{x}_1 & \cdot & \cdot & \cdot & 0 \\ 0 & \dot{y}_1 & \cdot & \cdot & \cdot & 0 \\ \dot{z}_0 & \dot{z}_1 & \cdot & \cdot & \cdot & \dot{z}_m \\ 0 & \dot{\theta}_1 & \cdot & \cdot & \cdot & 0 \\ 0 & \dot{\phi}_1 & \cdot & \cdot & \cdot & 0 \\ 0 & \dot{\psi}_1 & \cdot & \cdot & \cdot & 0 \end{bmatrix}. \quad (6)$$

The first and last columns of the matrix are made based on the technological requirements of lifting and lowering the structure to be mounted. Before the structure is moved to the installation area, it must be lifted off the fixture or platform in an upright, torsion-free manner. The structure is also placed in its intended position without changing its orientation angles, by means of a vertical landing.

The analytical description of the trajectory sections is as follows:

– 1st section:

$$x = x_0 = \text{const}, \quad y = y_0 = \text{const}, \quad z_0 \leq z \leq z_1 \rightarrow P_0 \leq P(x, y, z) \leq P_1;$$

– 2nd and 3rd section:

$$\frac{x - x_1}{x_2 - x_1} = \frac{y - y_1}{y_2 - y_1} = \frac{z - z_1}{z_2 - z_1} \rightarrow P_1 \leq P(x, y, z) \leq P_3;$$

– 4th section: $x = x_3 = \text{const}, y = y_3 = \text{const} \rightarrow$

$$P_3 \leq P(x, y, z) \leq P_4.$$

For the convenience of the planning algorithms, the transformation matrices T_i for each of the node points of the trajectory are written on the basis of the matrix S_T , describing the node points of the trajectory. In doing so, the coordinate system of the building is converted to the crane coordinate system. These transformations can be performed based on the following transformations. The position vector $T_0^{(i)}$ of the matrix can be derived from the first three elements of the i -th column of the matrix S_T as:

$$P_0^{(i)} = \begin{bmatrix} x_0^{(i)} \\ y_0^{(i)} \\ z_0^{(i)} \end{bmatrix} = \begin{bmatrix} x_i^{(3)} + x_0^{(3)} \rightarrow \text{var} \\ y_i^{(3)} + y_0^{(3)} \rightarrow \text{const} \\ z_i^{(3)} + z_0^{(3)} \rightarrow \text{const} \end{bmatrix}, \quad (7)$$

where $x_0^{(3)}, y_0^{(3)}, z_0^{(3)}$ - the position of the system $X_0Y_0Z_0$ starting in the building coordinate system $X_3Y_3Z_3$.

The matrix of directional cosines $A_0^{(i)}$ characterizing the orientation of the working body in the manipulator coordinate system $X_0Y_0Z_0$ is compiled on the basis of the Euler angles $\theta_0^{(i)}, \phi_0^{(i)}, \psi_0^{(i)}$, which correspond to the

angles $\theta_3^{(i)}, \phi_3^{(i)}, \psi_3^{(i)}$ since the building $X_3Y_3Z_3$ and manipulator coordinate systems $X_0Y_0Z_0$ are orthogonal and coaxial. The parameters $\theta_3^{(i)}, \phi_3^{(i)}, \psi_3^{(i)}$ are the elements of matrix S_T for the i -th point of trajectory (last three elements of i -th column). Using position vectors $P_0^{(i)}$ and matrices of directional cosines $A_0^{(i)}$ the transformation matrices are compiled:

$$T_0^{(i)} = \begin{vmatrix} A_0^{(i)} & P_0^{(i)} \\ 0 & 0 & 0 & 1 \end{vmatrix}. \quad (8)$$

After these transformations, each node point of the trajectory is obtained represented in the robot coordinate system $X_0Y_0Z_0$ by the obtained matrices $T_0^{(i)}$. The transition of the gripper with the building element $T_0^{(i-1)}$ to $T_0^{(i)}$ be mounted from to is planned as a rectilinear movement between the points P_{i-1} and P_i , if this is not hindered by objects in the environment.

This is where the process of constructing mounting robot trajectories ends in principle. Transition smoothing sections are described during the planning phase of the manipulator movement. The return of the gripper for the next part follows the same trajectory. However, travel speeds can be set differently, using a matrix V_T .

Robotic mounting is only effective if the installation of the next prefabricated component is cyclically repeated. To organize an mounting robot in a cyclic program, a database including a matrix S_T for each cycle or a law of variations in its parameters must be created at the design stage of the motion paths. In large-panel housing erection, parts are usually taken from one or more reference platforms that are rigidly connected to the building coordinate system (Fig. 4). The position of

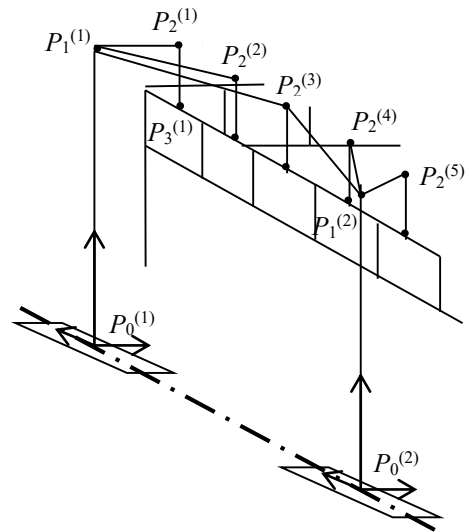


Fig. 4. Technological scheme for the erection of large panel buildings.

the points P_2 and P_3 the orientation of the gripper at these points is determined by the process flowchart of the building element installation sequence. The position of the first two points can be multiple, depending on the number of platforms (fixtures) from which the elements are taken. The movement between the points $P_0^{(k)}$ and $P_1^{(k)}$ is described by the matrix $S_{01}^{(k)}$, where k is the number of the element to be taken.

Before executing the next i -th cycle, the matrix $S_{01}^{(k)}$ corresponding to the location of the next element is selected and the element installation matrix is generated according to the mounting plan:

$$S_{24}^{(j)} = \begin{bmatrix} 0 & 0 & x_2^{(j)} & x_3^{(j)} & x_4^{(j)} \\ 0 & 0 & y_2^{(j)} & y_3^{(j)} & y_4^{(j)} \\ 0 & 0 & z_2^{(j)} & z_3^{(j)} & z_4^{(j)} \\ 0 & 0 & \theta_2^{(j)} & \theta_3^{(j)} & \theta_4^{(j)} \\ 0 & 0 & \varphi_2^{(j)} & \varphi_3^{(j)} & \varphi_4^{(j)} \\ 0 & 0 & \psi_2^{(j)} & \psi_3^{(j)} & \psi_4^{(j)} \end{bmatrix}. \quad (9)$$

By adding the generated matrices $S_{01}^{(k)}$ and $S_{24}^{(j)}$, the matrix $S_T^{(j)} = S_{01}^{(k)} + S_{24}^{(j)}$ describing the coordinates $P_i^{(k)}$ of the trajectory of the next cycle is obtained. Finally, the trajectory lengths and their running times are evaluated. If there are no obstacles in the way of movement, the length of each trajectory segment is chosen to be equal to:

$$l_i = \sqrt{(x_i - x_{i-1})^2 + (y_i - y_{i-1})^2 + (z_i - z_{i-1})^2},$$

and the total length is determined by adding up the individual sections:

$$L_{mp} = \sum_{i=1}^n l_i, \quad (10)$$

where n is the number of sections, i – the section number. As for planning of technological process it is necessary to estimate time of performance of operations at each stage, at this stage a preliminary estimation of time of trajectory passage and installation of an element mounted in the given position is carried out:

$$t_c = \left(\sum_{i=1}^n \frac{l_i}{V_i} \right) + t_{or}, \quad (11)$$

where t_{or} is the element orientation time.

Conclusion

The system approach to the structural organization of robotic construction-assembly complexes was proposed and implemented during the research for the first time. For mathematical identification of construction robot

arms and construction of their dynamic model, Lagrange equations were used. In order to take into account and mathematically describe the influence of wind loads on the performance of installation works, for the first time a model of an elastically deforming crane mechanism in matrix form has been proposed, which makes it possible to develop control algorithms and motion trajectories ensuring the required smoothness and continuity of the trajectory, constancy of speeds and accelerations. When planning a trajectory in a dimensionless environment, the possible nature of its change is taken into account. A further direction of research is the planning of movements of construction robots with speed optimization based on the use of two-level interpolation, which allows to reduce the velocity search area taking into account the constraints and significantly increase the speed of calculations. This will make it possible to create an effective system of robotic installation and assembly of building blocks and elements on the basis of a tower crane and a positioning robot.

References

- [1] Bock T., Bulgakow A., Parshin D. Automation and robotization of mounting operations in building. In *Proceedings of the of the ISARC-2001*, pages 13–17, Krakow, Poland, 2001.
- [2] Bock T. and Bulgakov A. Planning of Movements of Building Robots with Speed Optimization. *Journal of Robotics and Mechatronics*, 2016, Vol.28 No.2, pp. 158-161
- [3] Bock T., Parschin D. and Bulgakov A. Robotization of mounting and finishing operations in building. *Robotica*, Vol. 20, Iss. 02, March 2002, pp. 203-207.
- [4] Manuel H. Robotics and automated systems in construction: Understanding industry specific challenges for adoption, 2019.
- [5] Jayaraj A., Divakar H. Robotics in construction industry. 2018. <https://doi.org/10.1088/1757-899X/376/1/012114>.
- [6] Patle B.K., Babu G., Pande A., Parhi D.R.K., Jagadeesh A. A review: on path planning strategies for navigation of mobile robot, *Defence Technology*, 15 (2019), pp. 582-606.
- [7] Dangaard M.R., Pedersen R., Hansen K.D., Bak T. Control of Wall Mounting Robot: Practical Implementation and Experiments. *IFAC-PapersOnLine*, Vol. 53, Issue 2, 2020, Pages 10025-10030.
- [8] Sloth C. and Pedersen R. Control of wall mounting robot. In *Proceedings of the 2017 IFAC World Congress*.
- [9] Saidi K.S., Bock T., Georgoulas C. Robotics in construction, in: *Springer Handbook of Robotics* Springer Inter. Publ., Cham (2016), pp. 1493-1520.

Proof-of-concept for a reliable common data environment utilizing blockchain and smart contracts for supply-chain of public civil works

Fumiya Matsushita¹ and Kazumasa Ozawa²

¹Institute of Engineering Innovation, School of Engineering, The University of Tokyo, Japan

²Institute of Engineering Innovation, School of Engineering, The University of Tokyo, Japan
matsushita@i-con.t.u-tokyo.ac.jp, ozawa@i-con.t.u-tokyo.ac.jp

Abstract –

To rationalize and automate public civil engineering works, it is crucial to directly utilize the information produced by the contractor for quality/ as-built inspection, and progress measurement. In this study, a highly reliable common data environment that utilizes blockchain and smart contracts to ensure tamper resistance and traceability of construction management information on quality and progress was developed and proved through verification tests in two project sites.

Keywords –

Blockchain; Smart contract; As-built inspection; Progress measurement; Common data environment

1 Introduction

With the introduction of information and communications technology (ICT) in construction, it has become possible to measure and verify construction progress using various devices and collecting the information necessary for construction management (hereinafter referred to as “construction management information”) at the construction site. Among civil engineering works, in earthwork, many efforts that utilize building information modeling (BIM) and ICT for excavation, leveling, compaction, and as-built surveying are being promoted [1] and its productivity has been improved in recent years. However, on-site inspections which are confirmed by using various measurement methods, are still required by the client similar to the case in the past. Thus, to justify construction costs and efforts, including the number of inspections, it is required to develop a common data environment (CDE) that can detect falsification of measured data and ensure its credibility. Here, CDE means a mechanism for sharing information between involved players in a project defined by ISO19650.

To rationalize and automate public civil engineering

works, it is crucial to directly utilize the information produced by the contractor for quality/ as-built inspection, and progress measurement. Productivity can be improved by directly using the data collected from the site by the contractor for inspection. On the other hand, if the data would be falsified to hide a defect in quality and as-built, safety and reliability of infrastructure as well as involved stakeholders might be damaged when revealed, and its social loss and impact would be enormous. For this purpose, the risk of falsification must be reduced. For payments, in addition to inspection results, a mechanism to appropriately manage and trace construction progress measurement according to conditions of contract must be developed.

In this paper, a reliable CDE that can realize these mechanisms utilizing with blockchain and smart contracts is proposed and its concept is proved.

2 Literature review

A blockchain is technically a chain of blocks of information. What makes it special is that the chain is copied across several devices and exists in many copies. Once “chained,” the contents of the blocks cannot be modified, and despite data being copied on several devices, the blockchain algorithm ensures that there are no conflicts and that all copies are identical [2]. In contrast to a conventional centralized data management system, blockchain technology integrates data in a unique ledger while maintaining consistency where management is decentralized. Therefore, it is a trailblazing technology for implementing low-cost information management systems with tamper resistance and high availability that is expected to form the basis for next-generation ICT [3]. In addition, the blockchain has traceability of information [4].

In contrast, smart contracts refer to an ambiguous concept proposed by legal scholar and cryptographer Nick Szabo in the late 1990s [5]. Nick Szabo described smart contracts as “reducing transaction costs by signing

and fulfilling contracts over a network.” In recent years, smart contracts have also been used to refer to computer programs implemented on a blockchain. In this sense, smart contracts are defined as computer codes that execute a contract partially or fully automatically and are stored on a blockchain platform [6]. In recent years, various smart contracts has been proposed and developed, and some of them can implement computer programs on blockchain. Ethereum [7] is an example of a blockchain with this function.

Blockchain technology is still relatively new but is widely regarded as having the potential to solve many business problems. Many organizations and governments are attempting to incorporate blockchain technology into their processes [8]. In particular, blockchain and smart contracts are expected to offer benefits to construction projects on key issues, such as timely payments [6]. For example, one study [9] introduced a semi-autonomous payment based on Hyperledger by the confirmation of qualified work quantities, though the confirmation process itself is manual. Another paper focuses on construction quality information management using blockchains [10]. By applying blockchain, it is possible to realize accurate recording of quality information in the construction process. This information can assist coordination among project participants and reduction of disputes caused by inaccurate documentation of nonconformances. However, because the original data of quality inspection results are not stored on the blockchain, the rationalization of the inspection process itself has not been achieved. For payments, the blockchain-based crypto assets to integrate the physical and financial supply-chains have been proposed [11]. This paper validated through a series of experiments in which crypto assets were used for processing payments. However, it does not include the inspection by the client, which is the target of this research. The CDE using blockchain at the design stage has been proposed [12].

This research focuses on the rationalization of the production process itself at the construction stage, such as quality/ as-built inspection, progress measurement and payment by clients. To achieve this rationalization, blockchain is used to ensure the credibility of information collected from the site by the contractor, and the contract information and contract performance information are managed using smart contracts. Furthermore, it is necessary to develop a smart contract that can connect the results of quality inspections to payment. In contrast to previous research, the proposed CDE with blockchain has advantage of rationalizing the production process itself by directly utilizing data collected from the site for quality/as-built inspection by eliminating the risk of falsification.

3 Requirements and scope of construction management information as input

A reliable CDE using blockchain and smart contracts has to meet the following requirements to ensure the credibility of collected information, rationalize inspections, and automate payments:

1. Information on quality and progress measurement can be stored on the premise of high availability in the blockchain.
2. Because the information collected from the site is directly used for quality/as-built inspection and progress measurement of the construction process, the tamper resistance of construction management information is guaranteed, and the presence or absence of tampering can be detected.
3. Contract information and contract performance information can be managed to make inspections and autonomous payments based on contracts possible.

In the supply-chain of construction projects, a multi-layered subcontracting structure is often formed by various companies, such as a subcontractor, and a material supply company, which makes a sales contract, starting from the main contractor (Figure 1). The construction object comprises a combination of specialized work types and materials carried out by many subcontractors. Hence, in addition to the main contractor, the information on civil engineering works, which is the input value to the as-built inspection system handled in the construction management system, includes the quality and as-built information of construction by a subcontractor and the quality certificate of the material supplied by the manufacturer. In the inspection by the client, the main contractor manages the suppliers, such as specialized construction companies and manufacturers, and the generated information is summarized in the inspection form included in the specifications by the main contractor. Therefore, in the system, the primary data generated by each supplier before the main contractor aggregates the information for inspection, and it is also used as the input value.

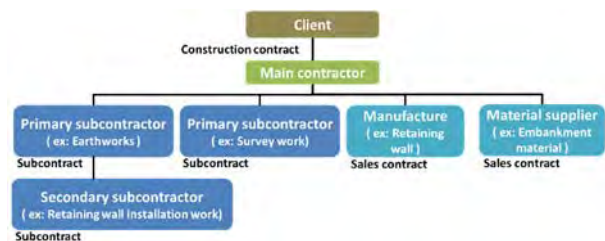


Figure 1. Example of a construction supply chain

4 System design

In order to realize a reliable CDE, it is necessary to consider the mechanism of tamper resistance in order to rationalize inspection. All inspections and payments are then carried out according to the contract. For this reason, smart contract functions are defined to realize inspection and payment workflows. Finally, the necessary system configuration is designed.

4.1 System design for tamper resistance of quality and progress information

Ensuring the tamper resistance of quality/ as-built and progress information is necessary to improve the credibility of the information saved by the contractor. The term “tampering” here refers to a situation wherein the main contractor or the subcontractor makes an intended revision during the inspection or assessment after the information is obtained. As shown in Figure 2, intended corrections have two types: falsification of input values and falsification of stored data. However, the act of redoing the construction and saving again the correction of information does not correspond to falsification.

Here, we assume situations of falsification that may occur and consider how to handle these situations. Specifically, falsification of stored data refers to the act of accessing the information stored in the data storage of the CDE and falsifying the information. For example, if the main contractor finds that some of the results from the surveying company do not meet the required level, some of the survey results stored in the data storage may be falsified by the main contractor. Falsification of input value refers to the act of falsifying and saving the false value by the contractor. Falsification of input values can be detected because true input values are obtained through devices and instruments directly connected to the data storage of the CDE through WebAPI. Therefore, here how to detect falsification of stored data is discussed.

The CDE uses a one-way hash function [13] to obtain the hash of the data when storing the data and stores this value in the blockchain. This makes it possible to be checked by reacquiring and collating the hash value of the file saved on the blockchain with the hash value of the file saved in the data storage at the time of inspection. If the stored data is tampered, it can be detected because the hash values will not match, as shown in Figure 3. In addition, the hash value stored on the blockchain cannot be tampered because of the characteristics of the data structure of the blockchain.

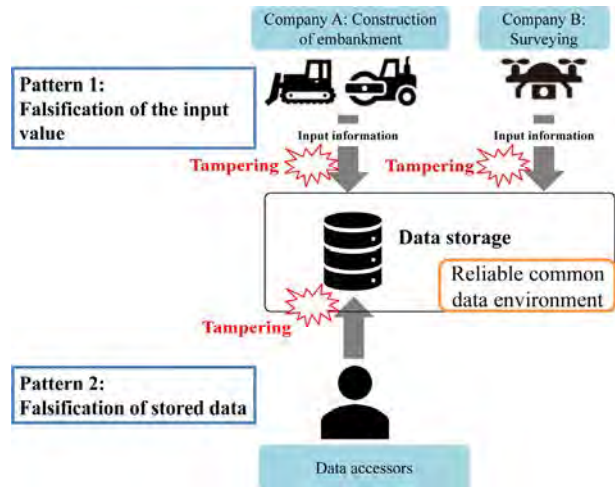


Figure 2. Tampering pattern

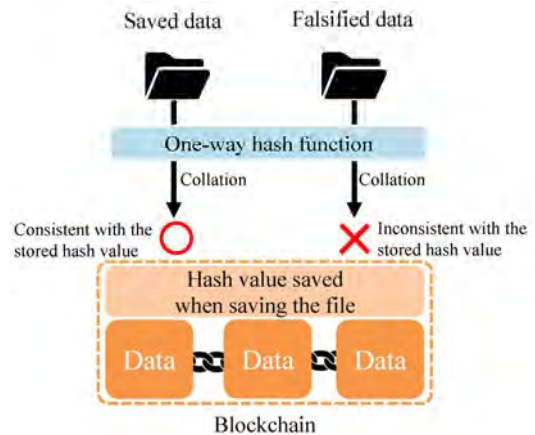


Figure 3. Falsification resistance of stored data

In addition, a company or a person suspected of falsifying data should be traced after the falsification is detected. To realize this, the system design requires an externally owned account [14] at the time of storage of the data to ensure the traceability of the company or the person. This design makes it possible to associate saver information with saved data and to describe it on the blockchain.

4.2 Definition of function for smart contract

When conducting inspections and payments based on smart contracts, the conditions of the contract and the performance of the contract based on those conditions should be managed. For that purpose, “non-tampering information” and “information to be traced at each stage” are needed to be defined appropriately as the functions of the smart contract using a program that implements the

smart contract.

The items of information that should not be tampered include conditions of contract and its performance. Here, conditions of contract cover the following:

- information on contractors (owners and contractors)
- contract amount (unit price and contract amount).

And contract performance includes the following:

- pass/fail of quality and as-built inspection
- construction progress rate by progress measurement
- determination of the payment amount
- management of paid amount on contractors (owners and contractors)

Regarding the conditions of contract, the contents agreed by both parties cannot be changed and tampered by a third party on the network unless both parties allow it. Regarding its performance, the information must not be tampered and updating of the information according to the construction progress should be performed through the joint measurement process. Furthermore, the person who can update the state transition needs to be limited to the client (i.e., project owner).

The information to be input and that to be traced at each stage are determined as shown in Figure 4. Stages 2–5 aim to trace the necessary information (i.e., site ID, contract number, and owner and contractor information) entered when making the contract. The site ID is an ID number assigned to the construction contract and is used to identify the project. The contract number is assigned to the unit price item and is used to identify the contract item. In addition, because inspections and payments are performed between the parties who have signed the contract, the information of the owner and the contractor is traced at stages 2–5. For stages 2 and 3, the obtained results are input from the as-built inspection system and construction progress measurement system. At stage 4, progress payment is made according to the construction progress measurement determined by stages 2 and 3. It is necessary to make the final inspection at completion for the final payment of stage 5, and the performance of construction period, required submissions, and results of the technical proposal, needs to be entered. The final payment is determined by inspection results based on the comparison between the conditions of contract and its performance. The contractor sometimes needs to pay penalty or to receive bonus according to the results based on the conditions of contract.

To handle the performance and its transition on the smart contract, the necessary information is described in the contract ID in strut. Strut is a data type in Solidity and is called a structure type [15], which is prepared by the user to categorize variables described in the contract ID. The categorized variables are shown in Figure 5.

	Contents to be decided at each stage	The content to trace
1. Determination of contract details	Site ID, Contract number Contract amount, Client Contractor	—
2. Quality / as-built confirmation	Result of Quality / as-built inspection	• Site ID, contract number (1) • Client, Contractor (1)
3. Construction progress assessment	Construction progress assessment results	• Site ID, contract number (1) • Client, Contractor (1)
4. Partial payment	Payment	• Site ID, contract number (1) • Client, Contractor (1) • Contract amount (1) • Result of Quality / as-built inspection (2) • Assessment result of volume rate (3) • Payment amount up to the last time (4)
5. Completion payment	Confirmation result of contract performance status payment	• Site ID, contract number (1) • Client, Contractor (1) • Contract amount (1) • Result of Quality / as-built inspection (2) • Assessment result of volume rate (3) • Payment amount by partial payment (4)

The numbers in parentheses indicate the stage at which the information to be traced was entered.

Figure 4. Input and traced information at each stage

In addition, the developed smart contract needs to be placed on the blockchain to execute its function. Several methods are available to place smart contracts on the blockchain; here, Ethereum was used as the blockchain using Truffle. Truffle [16] is a framework for arranging programs that implement smart contracts developed in Ethereum.

Contract performance status	
Item	Variable name
Contract ID	contractId
Client account	sender
Subcontractor account	receiver
Contract price	unitPrice
Contract quantity	unitVolume
Construction progress assessment rate that passed quality and as-built inspection	isPassedVolume
Construction progress rate determined by assessment	progress

Figure 5. Schematic diagram of variables categorized by contract ID

4.3 System configuration

To execute quality/as-built inspection, construction progress measurement, and payment, it is necessary to trace the data held by the CDE and to execute the processing according to the purpose. Figure 6 shows the overall picture of the system, including the system that executes these processes. As shown in this figure, the CDE consists of several sub-system.

System for tampering confirmation is the falsification confirmation system to ensure the reliability of the data. This system is used before carrying out the necessary inspections using the as-built inspection system and construction progress measurement system to utilize the information directly for inspection.

System for as-built inspection uses information that detects the presence or absence of falsification by the system of the CDE. It has a function to check whether the acquired information matches within the allowable range described in the standard required by the client, and input the inspection result to the smart contract of the CDE. The as-built inspection system must have this function to check whether the criteria are satisfied and to visualize its results.

The system for construction progress measurement includes functions to save the construction progress rate that the contractor applies for progress payment, to check the construction progress rate by the client, and to determine the construction progress rate. To confirm the applied construction progress rate, it has a function to calculate the construction amount for assessment using the value confirmed by the falsification detection system as an input value.

System for payment amount confirmation has the function to appropriately trace the information for each progress payment and completed payment via a program on the smart contract, and to determine the payment amount.

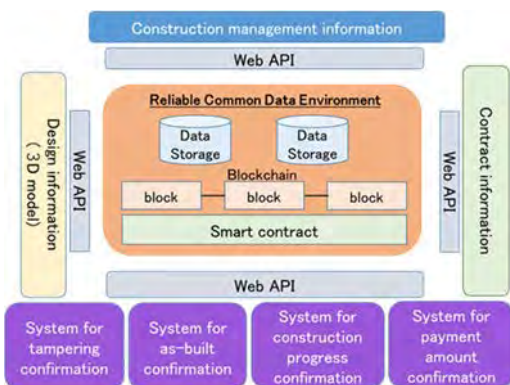


Figure 6. Input information and trace information at each stage

5 Proof-of-concept (PoC) using prototype

In the proof-of-concept, a prototype of a reliable CDE was developed to verify the following two items:

- It is possible to make quality and as-built inspection after confirming that the information produced by the supplier has not been tampered.
- The information of the contract performance status can be updated based on the result of the construction progress measurement conducted by the client or the owner. Furthermore, it is possible to calculate automatically the payment amount by tracing conditions of contract and its performance.

It was applied to the cut and embankment work, and a proof test was conducted. Verification item 1 is the content to be verified for the rationalization of the on-site inspection, and verification item 2 is the item to be verified for the rationalization of payment.

5.1 Outline of PoC

PoC is consisted of two verification tests in total for each verification item1 and item2. In conducting the verification test, the client and contractor participated in the verification test, and each of them played the necessary role. In the verification test, it was verified whether the falsified data and the companies involved in the falsification can be identified. If the falsified data cannot be detected, the product that should be rejected may pass its inspection, which will result in loss of safety and reliability of infrastructure. Therefore, verification is needed whether the falsified data can be detected. For this reason, we rewrote part of the information collected by the contractor from the site and created falsified data intentionally.

5.1.1 PoC for as-built inspection (verification item1)

The verification test related item1 was carried out at Higashi-Saitama Road in Okawado district improvement and other works (embankment work) project under the jurisdiction of the Northern Capital National Highway Office, Kanto Regional Development Bureau, Ministry of Land, Infrastructure, Transport and Tourism. Figure 7 shows a standard cross-sectional view of the target construction. The inspection items that require on-site inspection include the rolling compaction frequency inspection and as-built inspection, and a verification test was conducted for these two inspections. Table 1 shows the design model and information for this inspection item as a list of input values. Regarding this PoC, a total of seven inspection patterns were prepared for vilification test (Table 3).

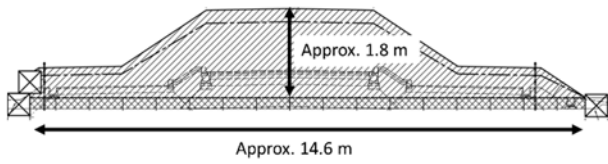


Figure 7. Cross section

Table 1. List of input values

Item	Input value
Design model data	3D design model (LandXML)
Position data for machinery	Coordinate values (x,y,z) and reception time (GNSS data)
Point cloud data	Coordinate values (x,y,z)

5.1.2 PoC for construction progress measurement and payment (verification item2)

The verification test related item2 was carried out using data from the 2018 Kamanashi River channel correction and other works project under the jurisdiction of the Kofu River National Highway Office, Kanto

Regional Development Bureau, Ministry of Land, Infrastructure, Transport and Tourism. This project aims to straighten the river channel and excavate the coloured parts in Figure 8. The input values used in the verification tests are listed in Table 2. In this PoC, payment term was set as twice. Regarding this PoC, a total of 9 inspection patterns were prepared for vilification test (Table 4).

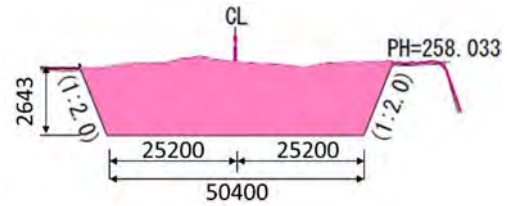


Figure 8. Cross section

Table 2. List of input values

Item	Input value
Design model data	3D design model (LandXML)
Position data for machinery	Coordinate values (x,y,z) and reception time (GNSS data)
Point cloud data	Coordinate values (x,y,z)

Table 3 Inspection pattern for PoC for as-built inspection

No.	Item	Confirmation of quality and as-built	Confirmation of falsification of input value	Judgment
1	Check the number of rolling compactions	Satisfied	Tampered	Failure
2	Check the number of rolling compactions	Satisfied	No tampering	Pass
3	Check the number of rolling compactions	Satisfied	—	Failure
4	Check the number of rolling compactions	Not satisfied	—	Failure
5	Confirmation of as-built	Satisfied	—	Failure
6	Confirmation of as-built	Satisfied	No tampering	Pass
7	Confirmation of as-built	Satisfied	There is tampering	Failure

Table 4 Inspection pattern for PoC for construction progress measurement and payment

No.	Contractor	Partial payment	Confirmation of falsification of saved data	Confirmation of construction progress measurement	Judgment
1	A company	First	Tampered	—	Fail
2	B company	First	—	—	Fail
3	C company	First	No tampering	OK	Pass
4	D company	Second	Tampered	—	Fail
5	E company	Second	No tampering	OK	Pass

5.2 Implementation of PoC

5.2.1 System flow

As shown in the inspection pattern of each verification test, checking the falsification of information is performed on the stored data in the as-built inspection, construction progress measurement, and payment. In addition, for each, the as-built is confirmed, the construction progress is confirmed, and the payment amount is confirmed. Figure 9 shows the overall flow of this system.

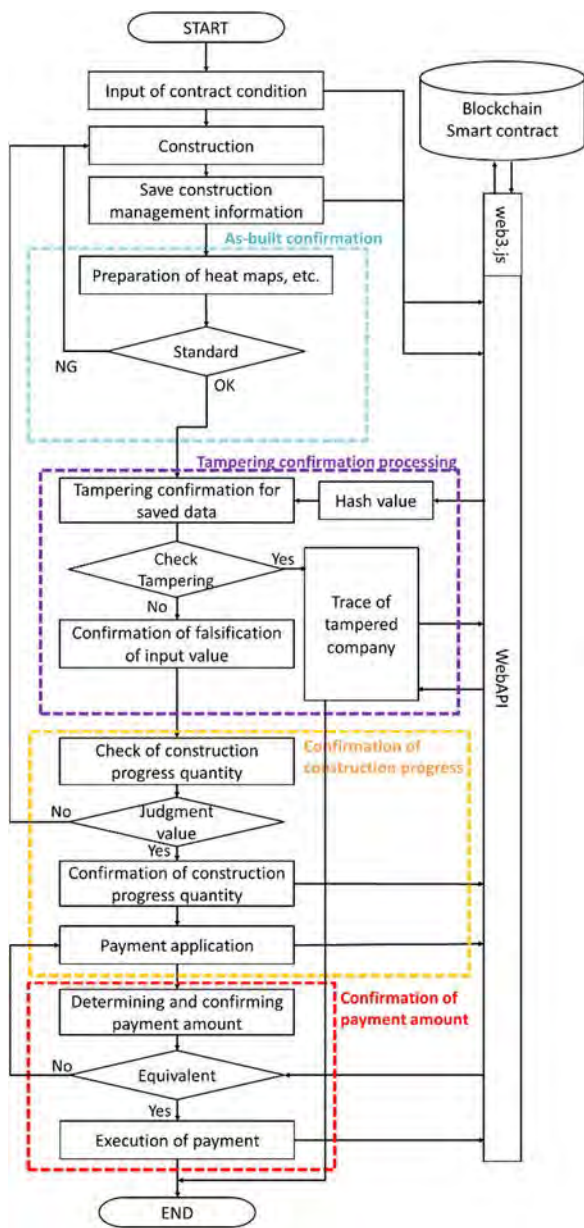


Figure 9. Overall system flow

5.2.2 As-built confirmation

The number of compactations can be checked using a heat map. The required level set by the test construction is six times, and if it is coloured, it indicates that the required level is satisfied. The as-built was also confirmed using a heat map from the design information and point cloud survey results.

5.2.3 Tampering detection process

To check the falsification of the saved data, the URL of the saved data was added to the body and the HTTP request was executed as shown in Figure 10. As a result, a true or false response is returned to check whether the data have been tampered. If true is returned, tampering does not occur; however, if false is returned, the data are tampered. For example, No. 1 (Table 3) returns true, whereas No. 3 returns false.

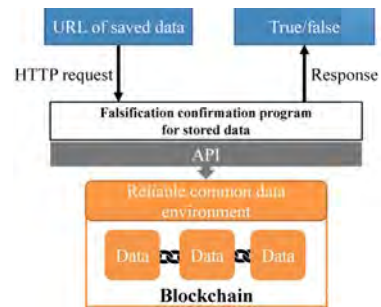


Figure 10. Detection of falsification of saved data

5.2.4 Progress calculation program

The construction amount (excavated soil volume) was calculated from the point cloud data, design model data, and bulldozer blade position information. For the test, an excavated soil model was generated using the extracted blade position information and point cloud data of the site.

5.2.5 Payment

The contractor makes a progress payment by inputting the construction amount using the contract information storage function of the construction progress measurement system. When making a payment, it is first checked whether the applied construction progress rate matches the value confirmed by the measurement stored on the blockchain using the payment confirmation system's functions. If they match, the value obtained by multiplying the contract amount and the construction progress rate is remitted between the owner and contractors. In addition, the amount paid at the time of the second and subsequent payments should be traced.

5.3 Result of PoC

In the verification test related to the as-built inspection, Nos. 1, 3, 4, 5, and 7 (Table 3) were identified as failures. In addition, in the verification test related to the construction progress measurement, Nos. 1, 2, and 4 (Table 4) were failed, and the expected amount of payment was also calculated. Thus, the proposed system was able to identify all instances of tampering, and it is valid to execute as-built inspection, construction progress measurement and payment.

6 Conclusion and future work

In this study, a reliable CDE was designed that utilizes blockchain and smart contracts to ensure the credibility of information, rationalize inspections, and automate payments. It was also confirmed by PoC to the reliable CDE works appropriately to identify falsification of data in quality and as-built, which will secure safety and reliability of infrastructure as well as improve efficiency for quality inspection and measurement. The conclusions are summarized as follows:

1. To detect the falsification of information, the stored data and the input value were assumed to be falsified and the hash value stored on the blockchain was compared with the inspection data.
2. To manage contract information and its performance and to realize inspection and payment based on the contract, “non-tampering information” and “information traced at each stage” were stored in the smart contract. In addition, a system was proposed in which each site ID and contract ID was assigned in a tree structure to handle this information on a smart contract and to update and trace the information appropriately.
3. After checking the falsification of the information, it was confirmed that the quality and as-built form inspection can be successfully carried out.
4. Based on the results of the construction progress measurement conducted by the client, it was confirmed that the smart contract information can be updated as the contract performance status.
5. It was confirmed that the payment amount can be calculated automatically by tracing the contract conditions and contract performance status.

Based on the above, a proof-of-concept for a reliable CDE utilizing blockchain and smart contracts was successful.

In this study, a prototype for an ICT earthwork was developed. Regarding falsification detection of input values, it was possible to directly save the data acquired by the device through WebAPI and to confirm the input values. As a result, the risk of tampering can be reduced.

References

- [1] Tateyama K. A new stage of construction in Japan – i-Construction, *IPA News Letter*, Volume 2, 2017.
- [2] Turk Ž. and Klinc R. Potentials of blockchain technology for construction management, *Creative Construction Conference 2017*, pp. 638–645 2017.
- [3] Kogure J., Kamakura K., Shima T. and Kudo T. Blockchain technology for next generation ICT, *FUJITUS Sci. Tech. J.*, Vol. 53, 2017.
- [4] Oinghua L. and Xiwei X. Adaptable blockchain based systems, *IEEE Software*, Voume34, 2017.
- [5] Szabo N. Formalizing and securing relationships on public networks, *First Monday* 9, 1997.
- [6] Atlay H. and Motawa I. An investigation on the applicability of smart contracts in the construction industry, *ARCOM Doctoral Workshop*, March 2020
- [7] Ethereum. On-line: <https://ethereum.org>, Accessed: 8/January/2023.
- [8] Yang R., Wakefield R., Lyu S., Jayasuriya S., Han F., Yi X., Yang X., Amarasinghe G. and Chen S. Public and private blockchain in construction business process and information integration, *Automation in Construction*, Volume 118, 2020.
- [9] Luo H., Das M., Wang J. and Cheng J., Construction payment automation through smart contract-based blockchain framework, *ISARC*, 2019.
- [10] Sheng D., Ding L., Zhong B., Love P.E., Luo H., and Chen J. Construction quality information management with blockchains, *Automation in Construction*, Volume 120, 2020.
- [11] Hesam H. and Martin F. The application of blockchain-based crypto assets for integrating the physical and financial supply chains in the construction & engineering industry, *Automation in Construction*, Volume 127, 2021.
- [12] Xingyu T., Moumita D., Yuhan L. and Jack C. Distributed common data environment using blockchain and Interplanetary File System for secure BIM-based collaborative design, *Automation in Construction*, Volume 130, 2021.
- [13] Naik R.P. Optimising the SHA256 hashing algorithm for faster and more efficient Bitcoin mining, *MSc Information Security, Department of Computer Science, UCL*, 2013.
- [14] Bahg A. and Madiseti V.K. Blockchain platform for industrial internet of things, *J. Soft. Eng. Appl.*, 533-546, 2016.
- [15] Andreas M. and Antonopoulos G.W., *Mastering Ethereum*, O'Reilly, 2018.
- [16] Truffle. On-line <https://www.trufflesuite.com/>, Accessed: 8/January/2023.

An Extensible Construction Ontology to Guide Job-Site Sensing and Support Information Management

Ran Ren¹, Jiansong Zhang^{2*}, and Pingbo Tang³

^{1,2}School of Construction Management Technology, Purdue University, P.O. Box 47906, City, West Lafayette, IN; e-mail: {ren153@purdue.edu; zhan3062@purdue.edu [* Corresponding Author]}

³Department of Civil and Environmental Engineering, Carnegie Mellon University, P.O. Box 15213, City, PA; e-mail: ptang@andrew.cmu.edu

Abstract

Real-time sensing data and continuously updated project documents pose challenges to project managers who need to analyze these data and documents to derive meaningful information necessary for decision-making. To collect and incorporate heterogeneous data both from offsite and onsite sources, the authors: (1) developed a construction tasks, resources, and techniques integrated (ConTaRTI) ontology to classify construction site information that is extensible; and (2) encoded recommendations regarding sensing technique selection into the proposed ConTaRTI ontology, which aims to help collect data for meeting real-time construction information needs. The proposed ConTaRTI ontology offers a novel way to classify construction information that needs to be collected, measured, and detected on the site, given its real-time decision contexts. The ConTaRTI ontology also helps provide sensing technique recommendations to guide the selection of methods and tools for the data collection on specific construction tasks and resources. Therefore, the ontology enables a new method for construction information management by linking construction site information with suitable data collection methods. In addition, the extensibility and flexibility of the proposed ontological model opens a new door to organizing and integrating specific information needs with its collection/process methods to support information management. The quantitative and qualitative evaluation results indicate that the developed ontology can recommend sensing techniques that effectively support field data collection and information management.

Keywords –

Construction Ontology; Sensing Techniques; Job Site Data; Automation; Information Management

1 Introduction

Construction site contains various types of data represented in different ways, including labor-related, equipment-related, and material-related information coded in textual [1] and graphic [2] formats, among others. Successful collection and use of such data plays an essential role in supporting construction information management, such as information transfer between different stakeholders. The heterogeneous data for construction management can be from offsite (e.g., construction plans and documents) and onsite (e.g., execution of tasks) sources, covering labor, materials, equipment, etc. [3] They provide helpful information to support other construction applications, such as construction monitoring [4]. Therefore, leveraging different types of data efficiently and accurately is an essential research topic of great interest to support various construction applications.

The research presented in this paper examines a new construction tasks, resources, and techniques integrated (ConTaRTI) ontology that is extensible. This ontology classifies construction site information based on their nature and the data collection requirements, then provides encoded sensing technique recommendations regarding data collection methods for specific construction site information. The proposed ConTaRTI ontology was developed in Web Ontology Language (OWL) and further implemented with an app that allows users to explore: (1) construction tasks (i.e., construction activities) and resources (i.e., labor, material, and equipment) on the construction site; (2) sensing technique recommendations regarding data collection methods suitable for specific tasks and resources; and (3) relationships between (1) and (2) with corresponding literature references. This work forms the basis for an ontology-based information management framework that can integrate textual procedural information extraction (IE), sensing technique recommendation and selection, and information analysis application into one framework

to support construction information management.

2 Background

Sensing techniques are essential in transferring traditional manual data collection to automated ones to support business operations, such as site conditions monitoring, equipment, and material management, worker safety, and facility management, among others [5]. With the advancement of sensing techniques, various construction management applications (e.g., construction monitoring and risk analysis) and duties (e.g., construction resources tracking and allocation) can be supported by the increasingly available sensing data. With their various applications and performances in precision, cost, bandwidth, and measurement range, different sensing techniques have distinguished purposes, advantages, and limitations [6]. Accordingly, it is necessary to leverage different sensing techniques to collect the construction site data. For example, photogrammetry can be used to obtain distance information [7], global positioning systems (GPS) can be used to collect information of moving objects and changes in large facilities [8], and three-dimensional (3D) imaging systems (e.g., laser scanners) can be used to capture detailed spatial information about construction workspaces [9].

In the construction domain, the state-of-the-art computer vision applications support object detection, image classification, object segmentation, and pose estimation [10], among others. In addition to imaging sensors, many other sensors have found applications in the construction domain. For example, wearable sensors [e.g., inertial measurement unit (IMU), electromyography (EMG), accelerometer, and gyroscope sensors] can detect movements. Versatile and portable wearable sensors have shown great potential for construction activity recognition [11]. Radio-frequency identification (RFID) and radio-frequency tags can track and locate materials and components on the construction site actively and accurately to better assist construction tasks on the job site (e.g., material tracking) [12]. Augmented reality (AR) and virtual reality (VR) can support various construction management applications, such as construction project planning and scheduling, progress monitoring, workers' training, and site management and visualizations [13-15].

With the technological development and innovation in the construction domain, operations at construction job sites have become increasingly complex and dynamic, posing challenges in managing resources (e.g., labor, materials, and equipment). Sensors can monitor a variety of physical objects and parameters in the field. Therefore, using sensors on the construction job site has become popular, which can help stakeholders in supporting their

decision-making with needed data and information.

Despite the wide variety of sensors and corresponding data analytic methods, no "ideal" sensing technique can serve as a comprehensive solution to universally support all construction applications and management issues. For instance, the widely used computer vision technique still has limitations due to limited annotated datasets and objects with special appearances (e.g., shiny surfaces), causing detection errors [16]. Consequently, effectively selecting and leveraging a target sensing technique to support a specific construction task or application is an important need in the AEC domain. To address this, the authors proposed an extensible construction ontology by considering both construction site information and sensing techniques to guide job-site sensor planning and construction information management.

The main challenge in construction information management is the presence of various data types, including structured data files, semi-structured data files, unstructured text data files, to name a few [17]. Therefore, the effective selection and use of different information for various construction field applications (e.g., process control and manufacturing, detecting and preventing risks) are imperative. The augmentation of sensor networks with sensor information management methods can help collect and process data for efficient and effective data-driven decision-making on construction sites [18].

To summarize, by adopting, improving, and adjusting new sensing technologies on construction sites, construction information management can be supported and facilitated by leveraging and processing heterogeneous data collected by these emerging sensing techniques. In this paper, the authors proposed an extensible construction ontology to help efficiently and accurately provide sensing technique recommendations for guiding construction site data collection, given the characteristics of field applications.

3 Ontological Model Development

Ontology aims to simplify the point of view to represent something for a specific purpose, which is a straightforward specification of an abstract [19]. An ontology defines a list of terms (i.e., concepts), the relationships among them, and the axioms (i.e., definitions of concepts and relationships, and their constraints) coded in hierarchical structures [20]. Concepts define the "things" (e.g., entities and categories) either abstractly or concretely in the domain of interest. An entity represents an action, actor, product, resource, project, or mechanism [20]. An entity has an attribute, and a modality. Concepts in the ontology are associated with three relationships: is-a, part-of, and cross-concept relationships. Is-a relationship is also known as subsumption relationship, representing the specialization

of a super-concept into a specialized sub-concept. The part-of relationship captures the decomposition of a concept into corresponding comprised parts. The cross-concept relationship represents non-hierarchical semantic links between concepts, demonstrating the reason for assigning each link. One important nature of an ontology is in its reusability, so that “reinventing the wheel” can be avoided [20]. Because parts and pieces of any existing related ontology can be reused, it is therefore feasible and necessary to target the development of one ontology for a specific domain and purpose. There was no lack of ontology development for the construction domain, examples include ontology for construction safety knowledge management [21], ontology for sustainable construction [22], among others. However, as far as the authors are concerned, there is a need of an ontology for linking construction site data to their suitable sensing techniques.

Five main steps form the general procedure of ontology development following the top-down approach to ensure a clear structure from the beginning, including (1) defining the purpose and scope of the ontology; (2) building classes and class hierarchy in the ontology; (3) defining relationships between classes; (4) implementing ontology; and (5) evaluating ontology [23]. In this research, the authors developed an extensible ConTaRTI ontology to demonstrate the connections between construction site information and their corresponding sensing techniques, for targeted job-site data collection with appropriate sensing techniques. One main hypothesis is that all construction data and sensing techniques of interest can be found in literature. A computational reasoning framework powered by ConTaRTI is also proposed to provide sensing technique recommendations and further support construction information management. This purpose dictates the represented information in the ontology, including construction site information and sensing techniques classified hierarchically. In addition, the sensing technique recommendations for different construction site information are provided with their literature references. Figure 1 illustrates the ConTaRTI ontology development procedure.

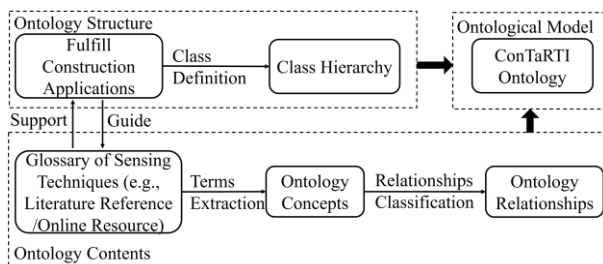


Figure 1. ConTaRTI Ontology Development Process

The purpose of the ConTaRTI ontology is to identify sensing techniques that fulfill given construction applications and site conditions (Figure 1). This purpose dictates the structure of the proposed ontology and helps define the classes and class hierarchy. The authors conducted a literature review regarding construction site information and sensing techniques for data collection, which helped define the concepts and their relationships. The proposed ConTaRTI ontology is encoded in the Protégé (version 5.5.0) using OWL. Protégé is an open-source ontology development editor for developing knowledge-based intelligent systems [24]. The ontology development process involves iterative evaluations and improvements of the ConTaRTI ontology from quantitative and qualitative perspectives.

Associating construction tasks and resources with their corresponding sensing techniques for data collection is the core theme for the ConTaRTI ontology development. Therefore, the ConTaRTI ontology could guide engineers, managers and other site personnel in collecting job-site data and further support construction information management. It is not expected/intended to be the “only” information management model for guiding the job site sensing data collection because “there is no “perfect” ontology and no “optimum” classifications or concept hierarchies” [20]. The authors design this extensible ontology with flexibility and extensibility in mind while keeping the fundamental requirements of connecting information needs and attributes of sensing techniques. Thus, developing this extensible ontology supports the intelligent provision of sensing technique recommendations for collecting construction site information.

4 Ontology Implementation, Experimental Results and Analysis

The ConTaRTI ontology covers construction site information that affects the sensing techniques to select from (for site data collection), including (1) resources class: labor, materials, and equipment; and (2) tasks class: labor-based activities, equipment-based activities, labor and equipment-based activities, labor and equipment and material-based activities, and equipment and material-based activities. The corresponding sensing techniques for each construction resource and task were incorporated into the extensible ontology and assigned to the specific resource and/or task. The information mentioned above was encoded in the proposed ConTaRTI ontology using Web Ontology Language (OWL) in Protégé (version 5.5.0). Then the encoded ontology was implemented with a user-friendly interface. Python programming language (Python 3.5.3) was used for implementing the developed ontology interface.

The method for implementing the ConTaRTI ontology includes five steps. Step 1: Construction Tasks and Resources Information Development – This step classifies construction site information into different categories to support ontology development. Step 2: Construction Sensing Techniques Information Development – This step lists the sensing techniques used to collect different categories of construction site information as identified in Step 1. The selected sensing techniques were identified based on academic literature such as those from Scopus, Google Scholar, and ASCE library, which provides evidence to support further sensing technique recommendation provisions in Step 3. Step 3: Technical Recommendation Regarding Sensing Technique Selection – This step connects the selected information in the ontology in Step 1 and their corresponding sensing technique information in Step 2 to guide sensing technique selection and uses. Step 4: Ontology Integration – This step incorporates the defined construction site information in Step 1, sensing techniques in Step 2, and their relationships in Step 3, and implements them into an ontology-based user-friendly app for guiding job-site data collection. The developed app makes job-site sensing guidance one step closer to full automation, to support construction information management and decision-making. In the app, the corresponding sensing technique(s) for the specific type of construction site information will be provided based on the user selection of specific tasks (i.e., construction activity) or resources (i.e., labor, material, and equipment) in the ConTaRTI ontology. Step 5: Ontology Evaluation – This step evaluates the developed ontology from quantitative and qualitative perspectives. The evaluation results will inform the improvements of the ontology.

4.1 Step 1: Construction Tasks and Resources Information Development

The developed ConTaRTI ontology covers three main areas: (1) construction site information, (2) sensing techniques, and (3) their relationships. Construction site information includes construction tasks and resources. Furthermore, construction resources include labor (e.g., construction worker), equipment (e.g., hydraulic excavator), and materials (e.g., concrete). In addition, construction tasks contain all the resource-related activities, including labor-based activities (e.g., walking), equipment-based activities (e.g., tower crane boom's movement), labor and equipment-based activities (e.g., welding), labor and material-based activities (e.g., inspection of windows/doors), labor and equipment and material-based activities (e.g., pouring concrete from concrete truck), and equipment and material-based activities (e.g., tower crane loading concrete). Our hypothesis was construction tasks that need such explicit resources are the ones that need sensing for data

collection. The ConTaRTI ontology covers various information on the construction job sites that need sensing techniques to capture.

4.2 Step 2: Construction Sensing Techniques Information Development

To facilitate data collection on construction sites, the sensing techniques are incorporated into the ConTaRTI ontology to fill the need. In the ConTaRTI ontology, the construction tasks and resources with corresponding sensing techniques (for data collection) follow one-to-one or one-to-many relationships. All the sensing techniques in the ConTaRTI ontology were selected based on and backed up by literature. Literature provides both the data source and reference information, demonstrating the relationships between sensing techniques and corresponding construction site information they can be used to collect data for.

4.3 Step 3: Technical Recommendation Regarding Sensing Technique Selection

In this step, the relationships between the construction tasks and resource information identified in Step 1 and the corresponding types of sensing techniques identified in Step 2 are defined and encoded into the ontology. For example, the recommendation of the Crossbow MICA2s with sensor board MTS310CA and tri-axial accelerometer will be provided based on the ConTaRTI ontology to collect data for the walking activity which is a labor-based activity [25]. Linking the construction tasks and resources with their data collection sensing techniques integrates the two parts of the ConTaRTI ontology.

4.4 Step 4: Ontology Integration

In this step, the ConTaRTI ontology is encoded in OWL using Protégé. An ontology-based app is developed to support the use of the ontology in a user-friendly manner (Figure 2). There are nine main categories regarding sensing technique recommendations (Figure 2(b)), with 55 classes and 63 properties (relations). Users could select specific terms of construction tasks or resources in different categories when running the app by activating the corresponding functions. The app will then demonstrate the sensing technique recommendations with their literature references in the text display box in color coding. Figure 2(a) illustrates the ontology-based app with zoomed-in looks, Figure 2(b) demonstrates the steps of using the developed interface. In Figure 2(a), the sensing technique Crossbow MICA2s with sensor board MTS310CA and tri-axial accelerometer with literature references are provided for walking in the labor-based activity category (pink color coding).

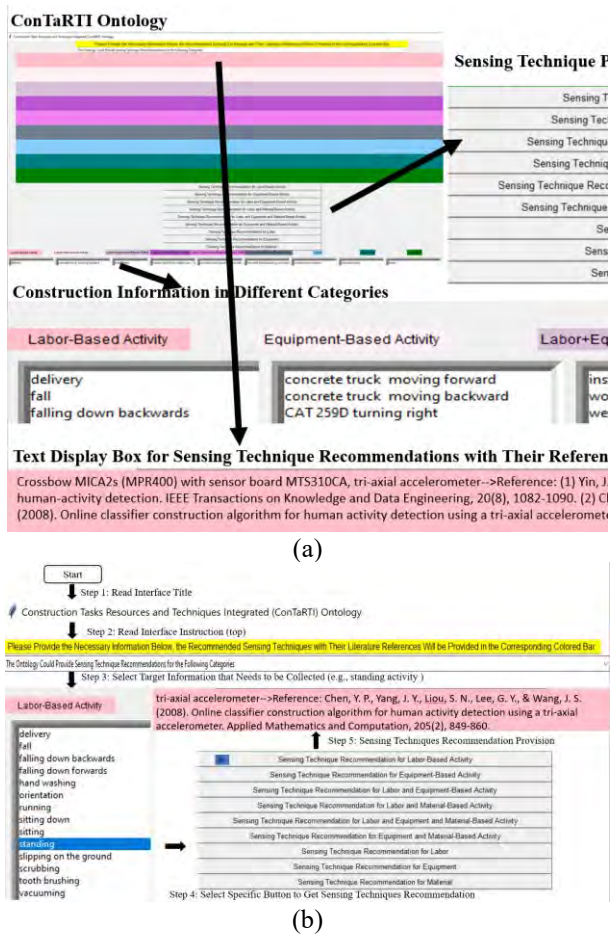


Figure 2. (a) ConTaRTI Ontology-Based App; (b) Ontology-based Interface Explanation with an Example

4.5 Step 5: Ontology Evaluation

Ontology evaluation is critical for ensuring reliable information management in multiple domains. Hlomani and Stacey pointed out that quality and correctness are two critical metrics for evaluating ontologies. Several specific criteria of the above-mentioned metrics include conciseness, accuracy, adaptability, completeness, computational efficiency, clarity, and consistency [26].

Raad and Cruz [27] identified four categories for methods to evaluate an ontology, including “gold standard-based, corpus-based, task-based and criteria-based” methods, respectively. Gold standard-based methods are the most straightforward and widely used type. When using the gold standard-based methods, a newly developed ontology is compared against a reference ontology. Corpus-based methods are used to mainly evaluate the coverage of a newly developed ontology for a specific domain in a data-driven manner. When using the corpus-based methods, the newly developed ontology is compared against a domain-

specific text corpus. Task-based methods are used to mainly assess the improvement to a certain task when using an ontology, which therefore only evaluates the ontology’s performance for a specific task without considering its structural characteristics or broader use. Task-based methods can also be used to evaluate the adaptability of an ontology to a specific task. Based on Raad and Cruz [27], “adaptability measures how far the ontology anticipates its uses.” Criteria-based methods are used to assess the adherence of a newly developed ontology to a specific criterion. Table 1 summarizes different criteria for each ontology evaluation method, in which three levels (i.e., high, medium, and low) are assigned to the corresponding criterion in different methods [27].

Table 1 Overview of ontology evaluation methods [27]

	Gold standard-based methods	Corpus-based methods
Accuracy	High	High
Completeness	High	High
Conciseness	High	High
Adaptability	Medium	Low
Clarity	Medium	Medium
Computational efficiency	Low	Low
Consistency	Medium	Medium

Table 1 (continued)

	Task-based methods	Criteria-based methods
Accuracy	Low	Medium
Completeness	Medium	Low
Conciseness	Medium	Medium
Adaptability	High	Medium
Clarity	Medium	High
Computational efficiency	High	High
Consistency	High	High

4.6 Experimental Test

An experiment was conducted to evaluate the developed ConTaRTI ontology using the task-based method because the nature of our developed ontology is serving construction tasks. The proposed ontology was implemented with an interface to perform the assigned task. Accordingly, a given task was assigned to use the ontology to recommend sensing techniques for specific construction site information (i.e., construction resources and tasks) in terms of data collection in the given scenario. Figure 3 demonstrates an example procedure of using the ConTaRTI ontology. Firstly, a user could select specific construction resources and tasks in different categories (e.g., labor-based activity). Then, the user activates the

corresponding function (e.g., Sensing Technique Recommendation for Labor-Based Activity). The sensing technique selection recommendation with its literature reference will then be provided in a text display box with the same color coding as the name of the selected category (e.g., pink for Labor-Based Activity).

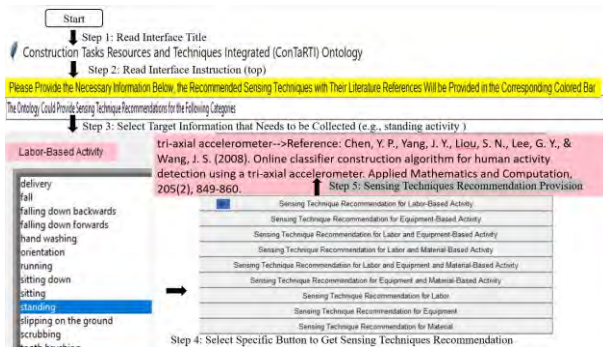


Figure 3. Ontology-based App Explanation with an Example

4.7 Evaluation

The proposed ontology was evaluated in providing recommendations regarding appropriate sensing technique selection for supporting the collection of specific construction site information in a given scenario. In this research, three criteria are considered for ontology evaluation [23]: adaptability, computational efficiency, and consistency, which represent the criteria well covered by task-based ontology evaluation methods (Table 1).

Computational efficiency and consistency were used for quantitative analysis, and adaptability was used for qualitative analysis. Based on Raad and Cruz [27], “Computational efficiency measures the ability of the used tools to work with the ontology.” Accordingly, in this research, the computational efficiency demonstrates the time consumption with and without the use of the ConTaRTI ontology, which is reflected/implemented with a user-friendly app, to obtain sensing technique selection recommendations. With the implemented ConTaRTI ontology, users only needed to activate the corresponding function to get sensing technique recommendations backed by literature references. On the contrary, without using the implemented ConTaRTI ontology, the users needed to either browse online or check publications/websites or other resources to get the sensing technique recommendations, which is time-consuming and labor-intensive. Three independent researchers conducted the evaluation of computational efficiency. They randomly tested twenty-five construction tasks and resources in the ConTaRTI ontology, then calculated the time spent on each of the twenty-five selections to get the average time

consumption.

The average time consumption when using the ConTaRTI ontology to get sensing technique recommendations was 4.664 seconds (standard deviation = 1.36 seconds). Meanwhile, the average time consumption without using the ConTaRTI ontology was 5.489 minutes (standard deviation = 73.45 seconds). Figure 4 shows the line chart of the computational efficiency testing results. In Figure 4, the x-axis represents the number of trials. The y-axis demonstrates the time consumption (unit: second). Accordingly, the time consumption using ConTaRTI ontology (i.e., blue line) is much less than without using the ontology (i.e., red line). In addition, the time consumption with the use of the ontology is much more stable than without using it, as reflected in the computational efficiency testing results (Table 2). It shows that the time consumption efficiency improved 98.58% when using the ConTaRTI Ontology. It demonstrates that the proposed ConTaRTI ontology is promising to provide efficiency in sensing technique recommendation/selection for construction site data collection.

Table 2 An overview of ontology evaluation methods

Method	Without the use of the ConTaRTI ontology	With the use of the ConTaRTI ontology	Evaluation result
Computational efficiency	On average 5.489 minutes	On average 4.664 seconds	98.58% improvement

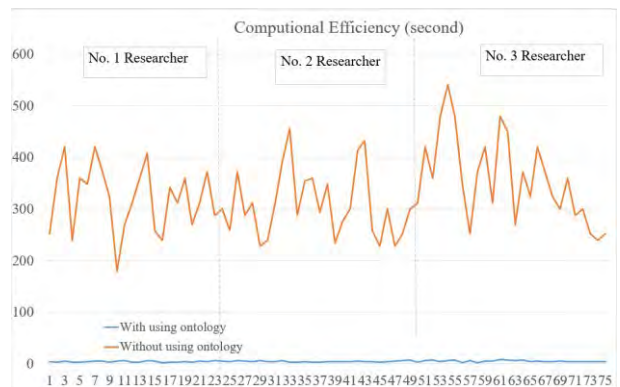


Figure 4. Line Chart of Computational Efficiency Testing Results

Adaptability illustrates how far the ConTaRTI ontology is anticipated for different tasks/applications/scenarios [27]. The authors considered other potential applications of the ConTaRTI ontology in several broad areas (e.g., educational, commercial, and research areas), such as (1) illustrating sensing technique

recommendations for specific construction site information, which can be used as an educational tool to motivate students' learning in advanced construction technology; (2) supporting commodity purchase decision for construction contractors in selecting the most suitable sensor for specific data collection needs and budget available; and (3) providing research tool guidance for target construction site-related research in an efficient way, in areas such as safety management, construction worker monitoring, and smart construction, among others. In addition, the developed ontology provides the conceptual foundation for anticipated construction site management tasks. The extensible ontology was implemented in a user-friendly app, in which the two types of information (i.e., construction site information and sensing techniques) and their relationships were encoded into the ontology. This can be put to use directly, or the contents can be easily adjusted and extended to other applications, such as in providing recommendations regarding project delivery methods based on different types of projects and organizational structures, in which the only adjustment needed is in the relevant concepts and relationships to fulfill the intended usage. For example, within the same structure of the ConTaRTI ontology, the two main parts (i.e., construction information and sensing techniques) could be replaced with different types of project and organizational structures, and project delivery methods, respectively. Then the relationships between them could be assigned based on literature references accordingly. Therefore, the ConTaRTI ontology provides a structural foundation for documenting mapping relationships to support many tasks/applications.

Consistency is an evaluation metric to check if "the ontology does not include or allow for any contradictions" [27]. In this paper, an open-source reasoner named HermiT [28] was used to evaluate the consistency of the proposed ontology. HermiT is an OWL ontology reasoner, which determines if "the ontology is consistent, and identifies subsumption relationships between classes" [29]. In this research, the ontology was imported into Protégé, then HermiT reasoner was executed to evaluate the ontology, in which the majority of the ontology contents were found to be consistent (95%). After minor revisions (e.g., adjustment of *DisjointWith* relationships between different categories), the ontology was found to be completely consistent (100%).

In summary, based on the evaluation results in adaptability, computational efficiency, and consistency, the ConTaRTI ontology: (1) could provide the conceptual and structural foundations for anticipated construction tasks, (2) achieved a 98.58% time efficiency improvement compared with the manual approach, and (3) achieved high/complete consistency. These results show that the developed ConTaRTI ontology is

promising in providing sensing technique selection recommendations to different construction resources and tasks and other construction applications. It is expected to support construction information management.

5 Conclusion and Future Work

This paper presented an extensible construction tasks, resources, and techniques integrated (ConTaRTI) ontology by encoding construction site information, its corresponding sensing technique for data collection, and the relationships between them. It covers the major types of information on the construction site that may need support by sensing techniques in data collection. In the ConTaRTI ontology, both the recommended sensing techniques and their corresponding literature references are provided to demonstrate the sensing technique selection recommendations, which can support decision-making in the construction domain efficiently and accurately. The developed ConTaRTI ontology was quantitatively and qualitatively evaluated using a task-based approach to assess its adaptability, computational efficiency, and consistency. It demonstrates that the developed ConTaRTI ontology is extensible and flexible, and could be implemented in the construction domain to: (1) help provide sensing technique selection recommendations regarding data collection methods for specific construction resources and tasks, and (2) support other tasks in construction information management. In their future work, the authors plan to extend the categories of construction information and sensing technologies in the proposed ontology to cover a broader scope for use in different types of construction projects.

References

- [1] Ren, R., and Zhang, J. (2021). Semantic Rule-based Construction Procedural Information Extraction to Guide Jobsite Sensing and Monitoring." *Journal of Computing in Civil Engineering*, 35(6), 04021026.
- [2] Ren, R., and Zhang, J. (2021). An Integrated Framework to Support Construction Monitoring Innovation. International Conference on Computing in Civil Engineering 2021.
- [3] Ren, R. (2021). Heterogeneous Data Processing to Support BIM Interoperability and Project Management in the Architecture, Engineering, and Construction (AEC) Domain. (Doctoral dissertation, Purdue University).
- [4] Bhokare, S., Goyal, L., Ren, R., and Zhang, J. (2022). Smart Construction Scheduling Monitoring Using YOLOv3-based Activity Detection and Classification. *Journal of Information Technology in Construction*, 27, 240-252.
- [5] Ellis, G. (2020). Sensing the Future of Building:

- The Role of Sensors in Construction. Autodesk Construction Cloud. Retrieved from: <https://constructionblog.autodesk.com/sensors-in-construction/>
- [6] Ziegler, S., Woodward, R. C., Iu, H. H. C., and Borle, L. J. (2009). Current sensing techniques: A review. *IEEE Sensors Journal*, 9(4), 354-376.
- [7] Piñeres-Espitia, G., Cama-Pinto, A., DE LA ROSA, D., Estevez, F., and Cama-Pinto, D. (2017). Design of a low cost weather station for detecting environmental changes. *Revista Espacios*, 38(59). Retrieved from: <https://www.revistaespacios.com/a17v38n59/17385913.html>
- [8] Poku, S. E., and Arditi, D. (2006). Construction scheduling and progress control using geographical information systems. *Journal of Computing In Civil Engineering*, 20(5), 351-360.
- [9] Ajayi, O. G., Palmer, M., and Salubi, A. A. (2018). Modelling farmland topography for suitable site selection of dam construction using unmanned aerial vehicle (UAV) photogrammetry. *Remote Sensing Applications: Society and Environment*, 11, 220-230.
- [10] Wiley, V., and Lucas, T. (2018). Computer vision and image processing: a paper review. *International Journal of Artificial Intelligence Research*, 2(1), 29-36.
- [11] Yan, X., Li, H., Li, A. R., and Zhang, H. (2017). Wearable IMU-based real-time motion warning system for construction workers' musculoskeletal disorders prevention. *Automation in Construction*, 74, 2-11.
- [12] Ren, Z., Anumba, C. J., and Tah, J. H. M. T. (2011). RFID-facilitated construction materials management (RFID-CMM)—A case study of water-supply project. *Advanced Engineering Informatics*, 25(2), 198-207.
- [13] Ahmed, S. (2018). A review on using opportunities of augmented reality and virtual reality in construction project management. *Organization, Technology & Management in Construction: an International Journal*, 10(1), 1839-1852.
- [14] Yu, Y., Zhang, J., and Guo, H. (2017). Investigation of the relationship between construction workers' psychological states and their unsafe behaviors using virtual environment-based testing. Proc., 2017 ASCE Intl. Workshop on Comput. in Civ. Eng. (IWCCE 2017), ASCE, Reston, VA, USA, 417-424.
- [15] Mastali, M., and Zhang, J. (2017). Interactive highway construction simulation using game engine and virtual reality for education and training purpose. IWCCE 2017, ASCE, 399-406.
- [16] Yu, X., Han, Z., Gong, Y., Jan, N., Zhao, J., Ye, Q., Chen, J., Feng, Y., Zhang, B., Wang, X., and Xin, Y. (2020). The 1st Tiny Object Detection Challenge: Methods and Results. arXiv preprint arXiv:2009.07506. 2020 Sep 16.
- [17] Su, C. (2007). Analyzing Management Processes Within a Distributed Team Context: The Case of a Canada-China Construction Project (Doctoral dissertation, École polytechnique).
- [18] Thuraisingham, B. (2004). Secure sensor information management and mining. *IEEE Signal Processing Magazine*, 21(3), 14-19.
- [19] Guarino, N., Oberle, D., and Staab, S. (2009). What is an ontology?. In *Handbook on ontologies* (pp. 1-17). Springer, Berlin, Heidelberg.
- [20] El-Gohary, N. M., and El-Diraby, T. E. (2010). Domain ontology for processes in infrastructure and construction. *Journal of Construction Engineering and Management*, 136(7), 730-744.
- [21] Park, H., Liu, R., and Zhang, J. (2018). Ontology modeling for construction safety knowledge management. Proc., 17th International Conference on Computing in Civil and Building Engineering, The International Society for Computing in Civil and Building Engineering (ISCCBE), Tampere, Finland.
- [22] Howsawi, A., and Zhang, J. (2017). An ontology to support the move towards sustainable construction in Saudi Arabia. IWCCE 2017, ASCE, 296-303.
- [23] Noy, N. F., and McGuinness, D. L. (2001). Ontology development 101: A guide to creating your first ontology.
- [24] Gennari, J. H., Musen, M. A., Fergerson, R. W., Grosso, W. E., Crubézy, M., Eriksson, H., ... and Tu, S. W. (2003). The evolution of Protégé: an environment for knowledge-based systems development. *International Journal of Human-Computer Studies*, 58(1), 89-123.
- [25] Yin, J., Yang, Q., and Pan, J. J. (2008). Sensor-based abnormal human-activity detection. *IEEE Transactions on Knowledge and Data Engineering*, 20(8), 1082-1090.
- [26] Elhassouni, J., El-Qadi, A., Bazzi, M., and El Haziti, M. (2020). Modeling with ontologies design patterns: credit scorecard as a case study. *Indonesian Journal of Electrical Engineering and Computer Science*, 17(1), 429-439.
- [27] Raad, J., and Cruz, C. (2015). A survey on ontology evaluation methods. Proc., 7th International Joint Conference on Knowledge Discovery, Knowledge Engineering and Knowledge Management.
- [28] Motik B., Glimm. B., Stoilos. G., Horrocks. I., and Shearer. R. (2021). HermiT. Protégé.
- [29] Bakhsh, B. (2017). Research on Social Context Acquisition and Reasoning Techniques for Online Social Networks (Doctoral dissertation, Auckland University of Technology).

Impact of Reinforcement Design on Rebar Productivity

Amith G Mallya ^a, Varun Kumar Reja ^{a,b}, and Koshy Varghese ^a

^a Department of Civil Engineering, IIT Madras, India

^b Faculty of Engineering and Information Technology, UTS, Australia

E-mail: amithmallya96@gmail.com, varunreja7@gmail.com, koshy@iitm.ac.in

Abstract –

Scheduling is an essential part of project management, and many processes like procurement, fabrication, and resource mobilization are based on these schedules. If the actual targets lag from the pre-planned schedules, waste is generated in the form of idle inventory. It also results in an increased workload on man and machinery, leading to errors and rework. Schedules are impacted by unreliable productivity estimates assumed during planning stages. In construction, project productivity can vary based on several factors. Reinforcement productivity is affected by factors like site layout, labour skill, design, learning effect, etc. The impact of reinforcement design on productivity is poorly studied, especially in heavily reinforced structures. Thus, the main objective of this study is to validate the hypothesis that reinforcement design affects productivity, which can be used to predict productivity for future structures. The methodology for this study is divided into 3 phases; 1st phase involves data collection and literature review, 2nd phase involves modelling rebar productivity by data fitting models to understand the factors of reinforcement design that affect productivity. MATLAB and Microsoft Excel are tools used in the data fitting process. In the final phase, based on this model, appropriate actions are suggested to improve productivity. Discussion on the aspects of reinforcement design that are found to have an impact on productivity is also detailed.

Keywords –

Reinforcement productivity, Data fitting, Regression analysis, MATLAB, Excel, heavily reinforced structures, rebar density, complexity in design, Delay, work productivity, Buildability, Rebar placement, lean construction management.

1 Introduction

The lean methodology's core concept involves identifying waste and reducing or eliminating it. This study deals with waste due to improper planning and

scheduling. Scheduling is the process of planning and arranging various activities to optimize resource utilization.

The main challenge in preparing a schedule is estimating the time required for completion, which involves predicting productivity. Productivity is affected by several factors like weather, site layout, labour skill, etc. [1]. The literature study found that the effect of reinforcement design on productivity, especially in heavily reinforced structures like industrial structures, bridges, and power plants, is not well understood.

Figure 1 shows the productivity variation for reinforcement placed at a construction site with heavy reinforcements. The graph found that for three months, between September – November 2021, the productivity varied between 0.025 MT/man-day to 0.076MT/man-day with an average of 0.055 MT/man-day and a standard deviation of 0.0108MT/man-day. This variation in productivity was seen even when external factors like site layout/weather/labour skills were constant. So, it would be reasonable to deduce that some inherent factors about certain structures affect productivity.

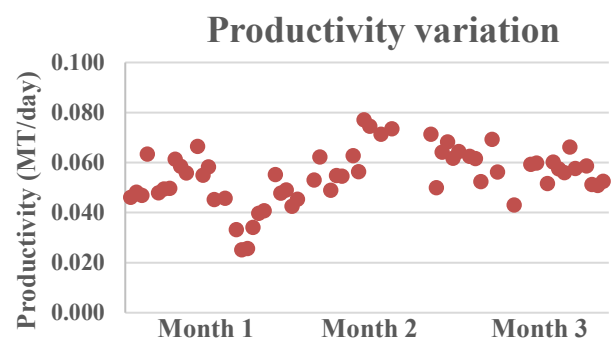


Figure 1. Productivity variation was observed for reinforcement placed at the site.

This paper hypothesizes that heavy reinforcement influences productivity, and using data modelling, this relationship is demonstrated, and an attempt is made to predict productivity based on specific design parameters.

The site chosen for the study is a structure subjected to heavy loads and characterized by large and closely

spaced heavily reinforced columns with deep beams. Some critical parts of the structure have reinforced concrete walls with heavy reinforcements. Numerous embedded parts in the concrete structures enable the installation of ducts, pipes, and cables. The shape of the structure is complex and varies from floor to floor. Figure 2 shows an example of a heavily reinforced slab for a structure with an opening to understand better the challenges faced at the site.



Figure 2. Representative picture of heavy reinforcement taken by the author at a similar construction site.

From the literature review, several studies have been found that list the various factors that affect productivity. However, most of these studies deal with residential/commercial projects and focus on factors like equipment, labour efficiency, and construction methods to improve productivity [2]. Very few papers explore challenges in heavily reinforced structures.

Although past studies list design as a factor affecting productivity, they do not explain and model what aspects of design affect productivity. Thus, the objectives of this study are as follows:

- To develop a method to help predict the productivity of structures based on reinforcement design to validate the hypothesis that reinforcement design affects productivity in heavily reinforced structures.
- Identify possible reasons for low productivity for heavily reinforced structures and suggest appropriate measures to deal with the same.

In terms of structure, this paper is broadly divided into seven sections. After the introduction, Section 2 discusses the literature review. Section 3 highlights the methodology used. Section 4 details the data fitting principles and complexity parameters. Section 5 deals with the data fitting models considered. Section 6 presents the result and analysis of the developed models. Section 7 presents the limitations and future directions. Finally, the study is concluded in Section 8.

2 Literature Review

In the construction industry, lean construction first appeared in 1992 [3] and has been applied to several construction sites [4]. According to B. Jørgensen et al. [5], in general, all methods encompassing lean construction focus on some common elements like reducing waste concerning the end customer expectation, managing the supply chain from a demand-pull approach, approaching production through a focus on processes and flow.

Literature shows that schedules are one of the most critical success factors contributing to the success of a project [6]. Unrealistic schedules cause waste in excess inventory and idle time and pressure men and machinery to achieve unrealistic targets, leading to safety and quality issues.

Accurate productivity rates are needed to have accurate schedules, but in construction, productivity is affected by several external and internal factors [7]. Based on a questionnaire study, Parthasarathy et al. [8] have found several factors that might affect productivity in tall residential building constructions. They have ranked them based on their relative importance. They reported improper planning and scheduling as the leading cause of productivity issues [9].

Rebar fixing is one of the essential activities generally seen in construction, accounting for the most significant percentage of the cost and time of total construction, especially in heavily reinforced structures [10]. There are studies for productivity improvement for activities like formwork, concreting, and blockwork [11,12], but a comparatively lesser number of studies focused on reinforcement [13]. One such study documents the challenges faced in nuclear construction due to the high reinforcement density in reactor building constructions and subsequent issues due to loss in productivity and quality [14].

Though the literature suggests reinforcement design as a factor that can affect productivity [15], it doesn't detail or quantifies what characteristics of reinforcement design causes productivity issues, especially in heavily reinforced structures. This study tries to fill this gap by modelling and predicting productivity using data-fitting software.

To model productivity, machine learning, neural networks, simulation software, and regression analysis have been suggested by various studies [14,16–18]. Based on different factors, this study tries to model productivity using regression analysis of complex factors defined based on inputs from the site.

MATLAB is a software developed by MathWorks primarily for numerical computing. It has features that can automate data fitting, like the fit command [19]. The curve fitting toolbox is an add-on to MATLAB software which makes the curve fitting process more interactive and brings in more functionality [20]. This study will use

these features to model productivity data based on factors in section 4.

3 Methodology

As shown in Figure 3, the study is divided into 3 phases. The 1st phase involves a basic literature review and site consultations to understand the current situation on the topic. The second phase involves data collection, defining complexity parameters for various concrete elements, and then using fitting data software to fit a surface using the complexity parameters as independent variables and productivity as the dependent variable. The model is also validated with independent data.

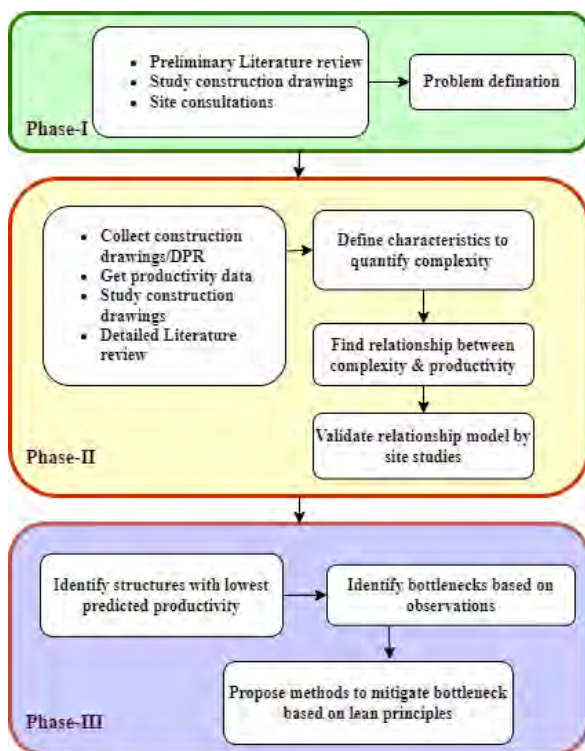


Figure 3. Methodology flowchart

In the final phase, the validated models were then used to predict productivity for concrete elements scheduled in the future. Based on the analysis of the model and predicted productivity, appropriate measures to improve schedules are discussed. The data is also analyzed to understand the factors of reinforcement design that affect productivity, and some conclusions are drawn.

4 Curve Fitting

We can see significant variations between different structures from the productivity data, but it is difficult to

understand why one structure might have better productivity over the other. The reinforcement design affecting productivity can be quantified and better explained using data fitting models and predicting productivity values.

The first part of data fitting is identifying the dependent and independent variables to isolate them.

4.1 Data collection procedure

As productivity is affected by multiple factors other than design, to have a good prediction model, it is required to isolate the data which are only affected by the factors that are of interest to this study. To achieve this, the following steps were taken during data collection.

1. The test data was collected within a short span of 2 weeks, and it was ensured that the weather-related factors did not vary for the data points.
2. All the data were collected from a similar elevation, thus eliminating variation due to equipment bottlenecks like cranes.
3. Distance between the stockpile and work area was similar for most of the data points, thus eliminating variation due to site layouts.
4. The lack of materials and operational delays did not affect the data points.

4.2 Converting subjective metrics into numerical factors

Complexity is subjective; when comparing two structures, one can be estimated to be more complex, but quantifying that difference is a difficult task. Discussions were conducted with multiple foremen at the site, and the following points were noted to be factors affecting productivity.

1. Large diameter bars and long bars are heavier and more difficult to handle at the site where space is limited.
2. Rings and stirrups for columns and beams are more difficult to place when compared to main bars.
3. Heavy reinforcement and congestion make inserting stirrups/shear/column ring difficult.
4. Openings in walls increase the number of bars, and rework will be needed when reinforcement fouls with openings. Thus, increasing complexity.
5. Different reinforcement spacing in a structure requires additional marking and placing reinforcement.
6. Joggling of reinforcement is needed in beams to prevent fouling with reinforcement of intersecting beams and columns.
7. The nonlinear shape of the structure, short-length walls, and non-standardized column dimensions add to confusion and complexity.

To convert these factors into a quantifiable number, some approaches in literature were studied, like a point system to determine a score to define various properties for rebar bending, which was then subsequently used in a classification algorithm [17]. In another study, a metric like the weight of reinforcement per unit of concrete to define congestion was used to compare congestion between nuclear construction and typical construction [15]. Based on literature analysis and site experience, several different parameters were analyzed. The following two factors were the best representation of the subjective factors as they were directly related to the complexity of heavily reinforced structures.

1. **Parameter 1 - Density of reinforcement:** This parameter is the ratio of the weight of reinforcement to the volume of concrete for the structure in question (in MT/cum). The weight of reinforcement is calculated based on the bar bending schedule provided by the designer or BBS procured from the steel yard. The weight of concrete is obtained by considering the dimensions and openings of the structure. This parameter accounts for the close spacing of reinforcements, the diameter of reinforcements, congestion, and the length of bars. This parameter shall be denoted as 'P1' in this paper.
2. **Parameter 2 - Non-linearity of reinforcement:** This parameter is the ratio of the number of bends of all bars to the total length of reinforcement for a given structure multiplied by 10 (in bends/10m). The total length and number of bends are extracted from the BBS. This parameter accounts for complexity due to stirrups/column rings, openings, short wall sections, complex wall shapes, and reinforcement joggling. This parameter shall be denoted as 'P2' in this paper.

The two parameters defined above consider most of the subjective metrics described above and, according to this study, are assumed to represent the complexity of reinforcement holistically.

4.3 Calculating the parameters

To calculate the two parameters for a particular structure, the following four values must be first estimated: concrete volume, reinforcement weight, reinforcement length, and the number of bends in reinforcement. These values can be obtained manually from the bar bending schedule (BBS) provided by the designer. Alternatively, with the help of a Revit model, the BBS can be exported into a .csv file, which can then be read using MATLAB. Data fitting can be done automatically to have a continuously updated model.

5 Data Fitting Models

Depending on the process, data modelling could be parametric modelling (E.g., Regression modelling) or non-parametric modelling (E.g., Interpolation). In this study following two models were developed.

- **Polynomial model:** Regression analysis is a set of statistical processes for estimating the relationships between one or more independent variables. Polynomial regression analysis is a multiple linear regression analysis case where the relationship between dependent and independent variables is modelled as an n^{th} -degree polynomial function.
- **Interpolant model:** Interpolation is a method to connect discrete data points to get reasonable estimates of data points between the given points. Depending on the surface required, one or more functions can be used to estimate values between data points. It is also possible to extrapolate data outside the original dataset using splines.

5.1 Determining the best fit

During the data collection, several precautionary steps were taken to remove the influence of factors other than the design parameters. But due to the nature of data collection, there will always be errors in the data even after taking these precautions. Generally, a metric called the coefficient of determination (R^2) determines how well the predicted values match the actual values assuming the data is accurate with only slight variations. But as explained by Prakash R [21], it was found that the measured productivity deviates from actual productivity due to measurement errors.

For a given set of data points, creating multiple surfaces with varying R^2 values is possible. To determine the best fit, two approaches can be taken.

1. The easiest method is to find the surface with the highest R^2 value; this method assumes the test data is accurate and no other factors influence it. However, we know from the literature that productivity is affected by multiple factors, and even though some of the factors are accounted for, some data points might distort the data.
2. Comparing possible models with data independent from the data set used to make it is also a viable method to determine the best fit. This method is used in this study to determine the best fit.

5.2 Curve fitting using MATLAB

MATLAB offers various methods to fit data by parametric and non-parametric models. The curve fitting toolbox available in MATLAB is one such tool that lets you perform exploratory data analysis and compare

candidate models. The toolbox also supports non-parametric modelling techniques, such as splines, interpolation, and smoothing [19,20].

After creating a fit, one can apply various post-processing methods for plotting, interpolation, and extrapolation, estimating confidence intervals, and calculating integrals and derivatives.

6 Result of Data Fitting, Validation, and Discussion

The test data was added to the MATLAB workspace, and using the curve fitting toolbox, the following models were developed:

6.1 Polynomial modelling (parametric)

The polynomial function with the best R² rating for the data is:

$$f(x, y) = 0.06299 + (0.01943 * x) - (0.01943 * y - 0.006567 * x^2) + (0.00145 * x * y) + (0.00145 * y^2) + (0.002058 * x^3) - (0.00113 * x^2 * y) - (10^{-5} * x * y^2) - (7.5 * 10^{-5} * y^3) \quad (1)$$

Where 'x' refers to the P1 (rebar density) and 'y' refers to the P2 (non-linearity), and 'f' gives the predicted productivity, Figure 4 and Figure 5 shows the 3D and contour plots of the polynomial model.

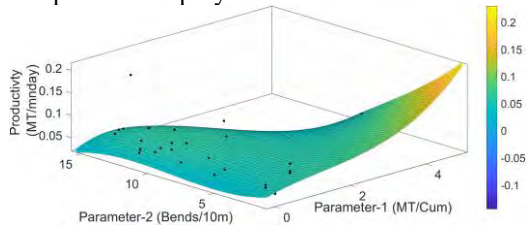


Figure 4. Polynomial model 3D plot

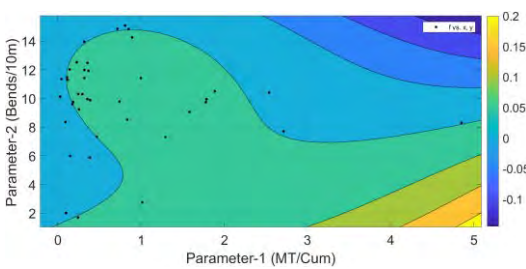


Figure 5. Polynomial model contour plot

Table 1 shows the productivity for eleven independent data points from January to validate the model, compared with the corresponding predicted productivity.

From this data, the predicted productivity varies from actual productivity. This variation is up to 25% of the productivity. Still, for five of the eleven data points, the variation was within ±10% of the productivity, considerably less than the variation seen in the non-

parametric model. Thus, it is better at predicting productivity than the non-parametric model.

Table 1. Validation of the polynomial model

Structure	P1	P2	Productivity (MT/man-day)		Var.
			Act.	Pred.	
Column1	0.05	11.3	0.05	0.0482	7.31%
Wall 1	0.19	13.8	0.04	0.047	-11.90%
Column2	1.81	9.68	0.06	0.0571	1.55%
Column3	1.48	13.7	0.05	0.0521	-6.33%
Column4	2.74	8.97	0.05	0.0451	-0.22%
Column5	2.03	8.14	0.05	0.0546	-21.33%
Column6	4.10	8.65	0.04	0.0351	14.39%
Column7	4.29	8.59	0.05	0.0363	21.09%
slab1	0.52	8.64	0.07	0.0545	25.34%
column8	0.30	10.3	0.04	0.054	-22.73%
column9	0.39	9.88	0.06	0.0552	1.43%

6.2 Interpolant modelling (non-parametric)

For the interpolant modelling, the thin plate spline method was chosen so that the extrapolation of data was possible. Figure 6 and Figure 7 show the 3D plot and the contour plot of the interpolant model.

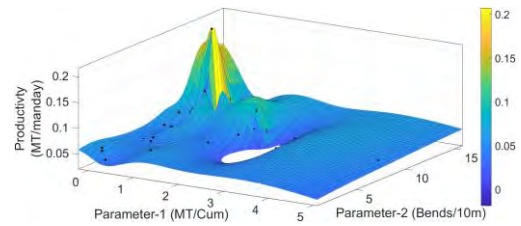


Figure 6. Interpolant model 3D plot

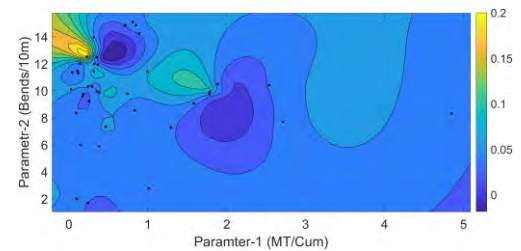


Figure 7. Interpolant model contour plot

Table 2 shows the productivity for eleven data points from January compared with the corresponding predicted productivity.

From this data, the predicted productivity varies from actual productivity. This variation is up to 217% of the productivity. For only two of the eleven data points, the variation was within ±10%, considerably more than the variation seen in the parametric model. Thus, even though this model is a better fit for the data, it is poorer at predicting productivity than the parametric model.

This can be because the test data contains certain data points that are too erratic and influenced by factors irrelevant to this study, thus skewing the model in the vicinity.

Table 2. Validation of interpolant model

Structure	P1	P2	Productivity (MT/man-day)		Var.
			Act.	Pred.	
Column1	0.05	11.3	0.05	0.0490	5.77%
Wall 1	0.19	13.8	0.04	0.1332	-217.14%
Column2	1.81	9.68	0.06	0.0481	17.07%
Column3	1.48	13.7	0.05	0.0745	-52.04%
Column4	2.74	8.97	0.05	0.0496	-10.22%
Column5	2.03	8.14	0.05	0.0047	89.56%
Column6	4.10	8.65	0.04	0.0603	-47.07%
Column7	4.29	8.59	0.05	0.0576	-25.22%
slab1	0.52	8.64	0.07	0.0635	13.01%
column8	0.30	10.3	0.04	0.042	4.55%
column9	0.39	9.88	0.06	0.0685	-22.32%

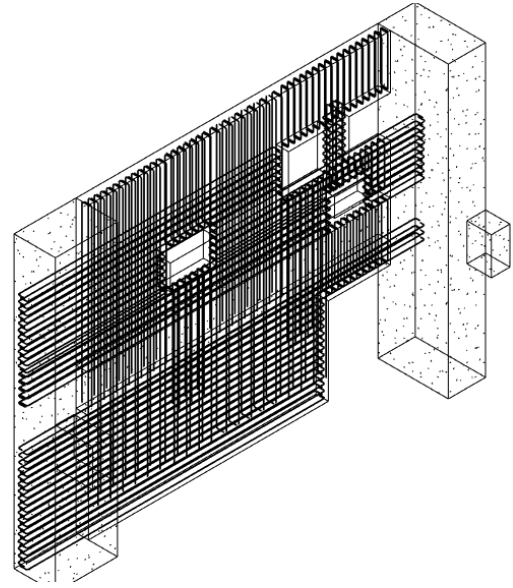


Figure 8: Revit model

6.3 Limitation of models

Even though data fitting models can predict productivity with some accuracy, the absolute productivity values are only valid if no new factors get involved. In addition to this, some other limitations were noted for both these models, like,

- Parametric model: Parametric models help understand the general relationship between the variables, but they may not give a perfect fit, especially for data with a high amount of variability. As the initial data set used for creating the model will be limited to a certain range based on the structure, predicting productivity for structures with parameters outside this range is difficult.
- Non-parametric model: As non-parametric models do not provide a function as an output, it is difficult to interpret compared to parametric models. Also, to predict/visualize the model, MATLAB application/other software is needed. It was also observed from the model that the non-parametric model was less reliable than the parametric model in this scenario.

6.4 Automating data fitting procedure

Calculating the design parameters and data fitting in MATLAB can be automated using Revit and excel. The bar bending schedule can be exported from Revit as a .csv file which can then be read using MATLAB. MATLAB can be coded to predict productivity or to automate data fitting to keep the model up to date.

Table 3: Sample BBS obtained from Revit.

Bar Mark	Type and size	Quantity	Length of each	Shape code	A* mm	B* mm	C* mm
1	H12	12	4375	11	4205	205	0
2	H12	11	6500	11	6345	180	0
3	H12	14	4350	11	4205	180	0
4	H12	5	6525	11	185	6350	0
5	H12	14	2175	21	180	1860	180
6	H12	34	1525	21	180	1210	180
7	H12	4	2050	21	165	1740	180
10	H12	6	3250	11	3095	180	0
11	H12	8	4300	11	4130	180	0
12	H12	6	2700	11	2540	180	0
13	H12	8	3800	11	3650	180	0

6.5 Characteristics of reinforcement affecting productivity

The two models shown above can predict values for a better understanding of the factors affecting productivity. A classification system was used to understand better the variation of productivity based on the variation of independent parameters.

In this method, the dependent variable, independent variable, and productivity are classified into three categories, i.e., below average, average, and above average (Table 4 shows the limits for each variable). The result was then analyzed to find any trends in the data. Classification helps minimize variations in the data by clubbing a similar range of data together.

Table 4. Classification limits

	Below average	Average	Above average
Productivity (MT/man-day)	≤ 0.04	0.04 to 0.06	≥ 0.06
Rebar density (MT/Cum)	≤ 0.25	0.25 to 1	≥ 1
Non-linearity (Bends/10m)	≤ 4	4 to 10	≥ 10

Table 5 shows the result of classifying 64 data points into the abovementioned categories. From this table following are the observations.

1. For a given reinforcement density (except for light reinforcement), productivity tends to decrease with an increase in non-linearity. The aberration in light reinforcement could imply that non-linearity is relevant only for heavier reinforcement.
2. For a given non-linearity, productivity tends to increase with reinforcement density.
3. By analyzing various structures, this can be explained by the following observations. Data points considered in this model refer to structural elements like columns, beams, walls, and slabs. With column and beam forming, most of the data points were collected.
4. In a column/beam, there are generally two reinforcement bars, a reinforcement element parallel to the length of the structure (main bars) and reinforcement perpendicular to the length (stirrups, rings, etc.). Main bars are generally larger in diameter and are easier to fix in place as they are usually long and straight. Stirrups/rings, on the other hand, are of smaller diameter and take longer to fix in position, thus reducing productivity.
5. A structure with high density will have a greater number of main bars (as the contribution of rings to density is less than the main bars), resulting in better productivity. A structure with high non-linearity will have multiple sets of rings (as main bars are primarily straight, contributing less to the non-

linearity parameter), thus reducing productivity.

6. The classifier model helps understand the relationship between the various factors but cannot predict productivity values like the other models. It can only comment on the range of possible productivity.

7 Limitations and Future work

- A more extensive study with a greater data sample would be necessary to enhance the model's accuracy.
- Considering that various factors influence productivity, the model would require regular updates to accommodate environmental changes, production technology, methods, specifications, logistics, labour skills, etc. The frequency of these updates could be determined based on data collected from a more comprehensive study [22].
- Machine learning-based models will be utilized to model and forecast productivity.

8 Conclusion

From the models developed, it can be concluded that reinforcement design does affect productivity and can be predicted. Other conclusions that can be drawn from this study are:

- Contrary to popular belief, large-diameter heavy reinforcement (high P1 value) does not lead to a loss in productivity; instead, it increases productivity.
- Loss in productivity is seen when the number of bends in the reinforcement increases. So short walls, nonlinear walls, the presence of openings discontinuation in reinforcement, presence of stirrups/column rings affect productivity, especially for structures with a density of more than 0.25MT/cum.
- This study showed that this productivity could be predicted using data fitting models, provided all other factors remain the same.

Table 5 Result of classification.

Density	Non-linearity								
	Below average			Average			Above average		
Below average	2	3	-	3	3	-	1	6	3
	40%	60%	-	50%	50%	-	10%	60%	30%
Average	-	-	-	2	5	5	1	7	4
	-	-	-	17%	42%	42%	8%	58%	33%
Above average	0	3	2	-	10	1	-	3	-
	0%	60%	40%	-	91%	9%	-	100%	-

- This model was also validated using independent data.
- Using the predicted productivity values, schedules can be better optimized to balance low and high-productivity structures.

9 References

- [1] Factors affecting the productivity of reinforcement work labours in low-cost residential buildings, *Malaysian Construction Research Journal*. 29 (2019) 49–64.
- [2] A.M. Jarkas, The Effects of Buildability Factors on Rebar Fixing Labour Productivity of Beamless Slabs, *Australasian Journal of Construction Economics and Building*. 10 (2010) 16. <https://doi.org/10.5130/AJCEB.V10I1/2.1583>.
- [3] L. Koskela, Center For Integrated Facility Engineering Application Of The New Production Philosophy To Construction, (1992).
- [4] U.H. Issa, Implementation of lean construction techniques for minimizing the risks effect on project construction time, *Alexandria Engineering Journal*. 52 (2013) 697–704. <https://doi.org/10.1016/J.AEJ.2013.07.003>.
- [5] B. Jørgensen, S. Emmitt, Lost in transition: the transfer of lean manufacturing to construction, (2008). <https://doi.org/10.1108/09699980810886874>.
- [6] A. Lamprou, D.G. Vagiona, Identification and Evaluation of Success Criteria and Critical Success Factors in Project Success, *Global Journal of Flexible Systems Management*. 23 (2022) 237–253. <https://doi.org/10.1007/S40171-022-00302-3>.
- [7] M. Jayesh Jain, V. Kumar Reja, K. Varghese, Exploring The Critical Factors Affecting The Productivity of Microtunneling Pipe Installation, in: 38th International No-Dig, 2022. <https://www.researchgate.net/publication/364309638>.
- [8] M.K. Parthasarathy, R. Murugasan, K. Murugesan, A critical review of factors affecting manpower and equipment productivity in tall building construction projects, *Journal of Construction in Developing Countries*. 22 (2017) 1–18. <https://doi.org/10.21315/jcdc2017.22.suppl.1>.
- [9] A.K. Rai, V.K. Reja, K. Varghese, Application of Operational Management Tools at Precast Yard, in: Indian Lean Construction Conference (ILCC), Hyderabad, 2022.
- [10] A.G. Mallya, V.K. Reja, K. Varghese, Application of Lean Principles to Improve Rebar Productivity In Heavily Reinforced Structures, in: Indian Lean Construction Conference (ILCC), Hyderabad, 2022.
- [11] A. Pandey, P.K. Chaudhary, B.B. Das, Productivity Analysis of Shuttering Works for Sewage Treatment Plant, *Lecture Notes in Civil Engineering*. 105 (2021) 461–471. https://doi.org/10.1007/978-981-15-8293-6_38.
- [12] M. Sona, The impact of buildability factors on formwork in residential building construction, 99 (2021) 85–96. https://doi.org/10.1007/978-981-15-6828-2_8/FIGURES/5.
- [13] S. Dabirian, M. Moussazadeh, M. Khanzadi, S. Abbaspour, Predicting the effects of congestion on labour productivity in construction projects using agent-based modelling, *International Journal of Construction Management*. (2021). <https://doi.org/10.1080/15623599.2021.1901330>.
- [14] M. Badawy, A. Hussein, S.M. Elseufy, K. Alnaas, How to predict the rebar labours' production rate by using ANN model?, *International Journal of Construction Management*. 21 (2021) 427–438. <https://doi.org/10.1080/15623599.2018.1553573>.
- [15] J. Munshi, J. Saini, Reinforcemnt in construction - how much is too much!, 2019. <https://repository.lib.ncsu.edu/handle/1840.20/37968> (accessed April 24, 2022).
- [16] M. Juszczak, Analysis of labour efficiency supported by the ensembles of neural networks on the example of steel reinforcement works, *Archives of Civil Engineering*. 66 (2020) 97–111. <https://doi.org/10.24425/ace.2020.131777>.
- [17] A. Krawczyńska-Piechna, Modelling labour productivity rates for reinforcemnt works, *Archives of Civil Engineering*. LXV (2019) 87–99. <https://doi.org/10.2478/ace-2019-0036>.
- [18] B. Matejević, M. Zlatanović, D. Cvetković, The Simulation Model for Predicting the Productivity of the Reinforced Concrete Slabs Concreting Process, *Tehnički Vjesnik*. 25 (2018) 1672–1679. <https://doi.org/10.17559/TV-20170627195003>.
- [19] Fit curve or surface to data - MATLAB fit - MathWorks India, <https://in.mathworks.com/help/curvefit/fit.html> (accessed April 20, 2022).
- [20] Curve Fitting Toolbox - MATLAB. <https://in.mathworks.com/products/curvefitting.html> (accessed April 20, 2022).
- [21] R.B. Prakash, Micro and Macro Level Analysis of Labor Productivity, *International Journal of Civil Engineering and Technology*. 8 (2017) 500–507. <http://http://iaeme.com/Home/issue/IJCIET?Volume=8&Issue=8http://iaeme.com>.
- [22] M. Jain, V.K. Reja, K. Varghese, Assessment of Factors Affecting Productivity of Pilot Tube Microtunneling Operation Through Case Study, in: Indian Lean Construction Conference (ILCC), Hyderabad, 2022.

Prospects of Integrating BIM and NLP for Automatic Construction Schedule Management

Akarsth Kumar Singh¹, Aritra Pal¹, Pavan Kumar¹, Jacob J. Lin¹, Shang-Hsien Hsieh¹

¹Department of Civil Engineering, National Taiwan University, Taiwan

akarsth@caece.net, apal@caece.net, pavansk@caece.net, jacoblin@ntu.edu.tw, shhsieh@ntu.edu.tw

Abstract –

In construction, project schedules are still created and updated manually, which takes time, causes errors, and leads to poor planning and scheduling, one of the main reasons for project delays today. Consequently, overcoming these challenges requires an automated schedule management method that extracts information and knowledge from existing and previous databases to improve construction planning and scheduling. Natural Language Processing (NLP) and Building Information Modeling (BIM) are two technologies that can revolutionize construction planning and scheduling by providing the ability to extract and interpret data from project documents, models, and past project knowledge bases. This paper reviews the state-of-the-art to understand the current research and methods that use NLP and BIM to automate construction schedule management (CSM). This in-depth study examines the knowledge potential of both technologies and integration possibilities in the construction planning and scheduling context. It also highlights the popular methods in recent times, a generalized workflow of NLP-based data processing, and limitations of existing approaches in practical applications. Finally, this study introduces three future research directions for integrating BIM and NLP for automated CSM.

Keywords –

Natural Language Processing; Building Information Modeling; Construction Planning and Scheduling; Data Extraction; Data Integration; Information Retrieval; Optimization; ChatGPT.

1 Introduction

Construction Schedule Management (CSM), a vital process in the Architecture, Engineering, and Construction (AEC) industry, includes planning, coordinating, and controlling tasks to complete a project within the prescribed time, cost, and quality. However, the inability to manage construction schedules

significantly contributes to delays and cost overruns. Research has shown that deficiencies in planning and scheduling are the primary causes of cost performance issues among contractors, consultants, and clients [1]. Furthermore, poor planning and scheduling conflicts are among the top reasons for project delays [2][3]. Current approaches toward CSM typically rely on manual procedures (creating and updating schedules), which can be time-consuming and susceptible to human errors [4]. Although software solutions are available, they often require labor-intensive manual input [5]. Delays and cost overruns resulted from poor planning and scheduling, and reliance on manual procedures necessitate automation in CSM. Automation provides benefits such as efficient and precise scheduling, reduced human errors, enhanced update speed and accuracy, and real-time data visualization. Additionally, automating the CSM process can eliminate the labor-intensive manual input required by current software solutions, thereby elevating the overall efficiency and performance of the process.

Researchers have employed several methods in the past three decades to automate the scheduling process in construction projects, such as case-based reasoning, knowledge-based systems, model-based approaches, meta-heuristic algorithms, expert systems, and learning-based methods [6]. However, their widespread adoption is hindered by several reasons. A few of those reasons are: each method follows manually formed and maintained work templates, reducing the chance of generalizability across different projects; lack of flexibility in how construction knowledge is stored in existing construction method model templates; a limited ability to automate the learning of construction knowledge from existing records; lack of validation of the applicability of existing automated planning systems on real-life construction projects; and the decoupled nature of research on automated planning and schedule optimization [7].

In recent years, BIM and NLP have been two emerging information technologies in the Architecture, Engineering, and Construction (AEC) industry [8]. These technologies have significantly impacted project management by improving communication, collaboration, and efficiency of information flow. BIM,

which revolutionized the AEC industry, provides a digital representation of a building's physical and functional characteristics. Building Information Modeling (BIM) can automatically generate and optimize schedules using data embedded in the model, reducing reliance on project planners' knowledge and experience and resulting in more efficient and accurate schedules. BIM data, including spatial, geometric, quantity, relationship, and materials, can be leveraged to automate the generation of construction schedules [5].

Natural Language Processing (NLP) is a sub-field of artificial intelligence (AI) that analyses how computers interact with human language. NLP is divided into three parts: syntactic, semantic, and ontological. Syntactic deals with language structure, semantic deals with the meaning of language, and ontology deals with the representation of knowledge in the language [9]. NLP techniques can speed up information extraction from construction documents and enable automatic interpretation of construction processes and interdependence logic across building activities. Applications of NLP can be seen in many areas of the AEC industry. For example, Shen et al. [8] used NLP to extract, process, and analyze data from BIM models to deliver real-time information for safety compliance. Jafari et al. [10] developed an automated NLP and machine learning (ML) tool to analyze contract documents. Other NLP applications include design and code compliance checking [11] and facility maintenance [12].

The power of NLP can also be leveraged to automate the CSM process. It can automatically learn company-specific construction knowledge from past project schedules, generate new schedules, validate the logic of existing schedules [13], and check the completeness and accuracy of the schedules [9].

Recognizing the potential of BIM and NLP individually for automated CSM, this study explores the integration prospects of BIM and NLP in Automated CSM. For this purpose, it reviews relevant academic papers on automated construction management and highlights the state-of-the-art techniques, their methodologies and generalized data processing workflows, and challenges. Finally, it underlines three possible future research directions to improve the BIM and NLP integration for automated CSM. The paper contributes to identifying data sources and types from which information and knowledge for automated construction schedule management (CSM) can be extracted through NLP.

Section 2 of this paper provides an overview of the automated CSM, Section 3 proposes future research directions, and Section 4 summarizes and concludes the study.

2 Overview of Construction Schedule Management

According to the project management institute (PMI), CSM includes schedule preparation, analysis and optimization, schedule update, and schedule control. The current industry practice for schedule management is as follows. First, the work breakdown structures (WBS) and activities are defined from the project scope documents. Next, expert construction professionals use their experience and expertise to identify activity sequences and resource requirements. Considering the common resource efficiency factors, schedulers calculate activity durations using a three-point estimation method: program evaluation and review technique (PERT) [1] or parametric estimation. Commercial project management software tools (e.g., MS Project and Primavera P6) are used to conduct critical path analysis [14], resource leveling, and time-cost trade-offs to analyze and optimize the baseline schedules. During project execution, schedulers manually update construction programs with progress and resource information from the daily progress reports. Projects with the last planner system [15] necessitate alignment of master schedules and weekly lookahead schedules for an accurate schedule update. Empirical delay analysis: time impact analysis (TIA), window analysis (WA), risk analysis, and recovery schedule preparation are conventional ways of schedule controls in the construction industry. The traditional CSM demands a considerable amount of manual effort and expert judgment. Young schedulers with less experience in the construction industry often face difficulties in producing a good quality schedule. Consequently, the project faces contractual challenges, stakeholder dissatisfaction, and disputes.

Researchers have constantly looked for opportunities to automate the CSM process to overcome these challenges. In recent times, advanced deep learning-based data analytic techniques [16] have created a new opportunity to use NLP techniques to extract the tacit knowledge from past schedules for new schedule development. Simultaneous integration of BIM, computer vision, and NLP has eased the process of schedule updates [17]. ML-based delay and risk prediction models have improved the effectiveness of schedule control methods.

Table 1 highlights the conventional and state-of-the-art techniques in each stage of schedule management. The following sub-sections discuss the state-of-the-art methods, their methodologies, and their limitations.

Table 1: Conventional practices and state-of-the-art techniques for CSM

Schedule management	Conventional practices	State-of-the-art
---------------------	------------------------	------------------

<u>Schedule preparation</u>		
Defining WBS and activities	I	A, B
Defining logic	I	A, B, C, D
Defining resources: Type and work	I	-
Defining durations	II, III, IV	J
Schedule Quality control	VIII	B
<u>Schedule analysis and optimization</u>		
Critical path analysis	V	-
Risk path analysis	V	I
Resource leveling	V	-
Time-cost tradeoff	I	E
<u>Schedule update</u>		
Progress update	VI	F
Resource update	VI	-
Logic update	I	-
Linking long-term and short-term schedules	I	H
<u>Schedule control</u>		
Delay analysis and prediction/ EVM	V, VII	I, G
Schedule recovery	I	-

(A) References of state-of-the-art techniques

Ref. Code	State-of-the-art	Reference Paper
A	Graph-Based Automated Construction Scheduling	[18]
B	NLP-based learnings from past project schedules	[9], [19], [20], [13], [21], [22]
C	Activity and sequencing from the BIM database and schedule ontology	[23]
D	IFC-based 4D	[24]
E	Schedule optimization/ Time-Cost tradeoff through GA	[18], [25]
F	Automatic progress updates from reality models	[17]
G	Digital Twin information system	[26]
H	Aligning master schedule and weekly plans	[27]
I	ML-based schedule risk analysis	[28]
J	NLP-based cost and time prediction	[10]

(B) References of conventional practices

Ref. Code	Standard procedures followed in the construction industry
I	Expert judgment
II	Resource Efficiency Factor
III	PERT
IV	Parametric estimation
V	PM Software
VI	Manually from DPR
VII	TIA/ WA
VIII	DCMA Schedule assessment

2.1 State-of-the-art techniques in automatic schedule management

2.1.1 Model-based automated scheduling

As schedule preparation is highly manual and time-consuming, researchers have tried several methods to automate it in the past few years. Early studies in this direction tried to generate schedules automatically leveraging IFC schemas of BIM [24]. Sigalov & König [29] tried BIM-based construction schedule generation using graph-based and feature-based indexing techniques. Faghihi et al. [30] utilized BIM data and genetic algorithms to generate and optimize construction schedules based on time, cost, and job-site movements. Using BIM attributes of structural elements to develop a list of work packages, estimate their duration, and generate schedules utilizing a combination of rule-based and case-based reasoning was tried by Wang & Rezazadeh Azar [31]. Later, Wu et al. [23] tried querying the BIM database through NLP for BIM object retrieval. One could use BIM object hierarchy to formulate construction sequencing knowledge [14]. Schedule generation from BIM using VBA, Excel, and trade-off analysis through Genetic Algorithm (GA) was investigated by ElMenshawy & Marzouk [25]. Singh et al. [32] introduced an AI framework for automatic scheduling and optimization of pipe system installation using BIM, ML, and heuristic techniques, integrating data and site knowledge. Combined with various optimization algorithms, an automated and optimized 4D BIM approach was proposed by Fazeli [33] for estimating construction time by leveraging resource specifications and geometric information from BIM. Although BIM-based techniques are helpful for automatic schedule preparation, BIM models with low Levels of Development (LOD) are often unsuitable for construction planning and monitoring [34]. Also, design approval, permit application, and procurement-related activities cannot be directly retrieved from BIM information.

2.1.2 Learning-based automated scheduling

Recently, for automated schedule preparation and schedule quality control, researchers have focused on NLP-based construction knowledge extraction from past project schedules [9][13]. Amer and Golparvar-Fard [20] proposed a dynamic process template for modeling construction works' planning and sequencing by learning from past project schedules. Later, Amer et al. [19] leveraged deep-learning-based NLP to predict and critique construction sequences of activity pairs. A recent study by Hong et al. [18] used a Graph Convolutional Network (GCN) to learn and identify activity types and sequences from input features, such as relative activity duration and position, text descriptions of activities and

WBS, logic links, and lags between activities. So far, significant research efforts have gone into learning activity definitions and construction sequences from past projects. Future research on automated schedule preparation may look into the prospects of the resource type and quantity identification and activity duration predictions from the knowledge of past projects.

Optimization of automatically generated schedules is essential to ensure better schedule quality. Hong et al. [28] used Genetic Algorithm (GA) to optimize the resource allocation and duration to generate a time- and cost-efficient schedule. Other meta-heuristic approaches, such as Ant Colony Optimization (ACO) and Particle Swarm Optimization (PSO), could be tried.

Schedule update is another step of CSM where the latest technologies bring significant automation. For updating a project master schedule with the information retrieved from weekly lookahead plans, an automatic schedule alignment method proposed by Amer et al. [27] reduced significant manual efforts. Automatic progress information extraction from reality models (as-built point clouds) and alignment with project schedules through NLP-based information extraction and matching can significantly automate the schedule update process [17]. The digital twin information system integrates 3D models and other digital information for project control. It applies AI tools to compare construction projects' as-planned and as-built status in real-time and predict the future state of the project [26].

ML-based schedule risk analysis and delay prediction methods [28] are a significant development in effective construction schedule control. Project managers can proactively mitigate such risks or delays to maintain the project timeline and budget.

2.2 Details of learning-based methods

Model-based methods generally rely on structured data (e.g., IFC and UML), and construction schedules prepared by human engineers are usually less structured. Learning-based methods can handle unstructured data to extract required knowledge from human language texts. As learning-based methods outperformed model-based methods in the generalizability of applications, this section only discusses the methods related to learning-based techniques.

Currently, three popular deep-learning models that support the learning-based CSM methods are Long Short Term Memory Recurrent Neural Network (LSTM-RNN) [19], the Transformer machine learning model [27], and Graph Convolutional Neural Network (GCN) [18].

Amer et al. [13] attempted to automate construction planning and scheduling by proposing a novel method to learn construction planning. This study introduced a generative model called Dynamic Process Templates (DPT), built upon LSTM-RNN. Testing 78,704 activities

from a historical data set confirmed the learning capability of the model with 76% to 98% accuracy. Amer et al. [13][19] also used LSTM architecture-based model to validate logic and ensure schedule quality. Amer et al. [27] used a transformer machine learning model to learn the dependencies between long-term and short-term plans based on schedule activity and lookahead planning task descriptions. The knowledge learned by the model was used to generate a list of lookahead planning tasks based on an input master schedule activity. A Graph Convolutional Network (GCN) was used by Hong et al. [18] to learn and identify activity types and sequences from input numerical, textural, and graphical features, such as relative activity duration and position, text descriptions of activities and WBS, logic links, and lags between activities.

2.3 Generalized workflow of learning-based methods for CSM

Figure 1 shows a generalized workflow for automated CSM through NLP-based data processing. Creating a construction schedule with NLP involves several steps, starting with the significant part of data acquisition, where all relevant information is collected from BIM and construction documents.

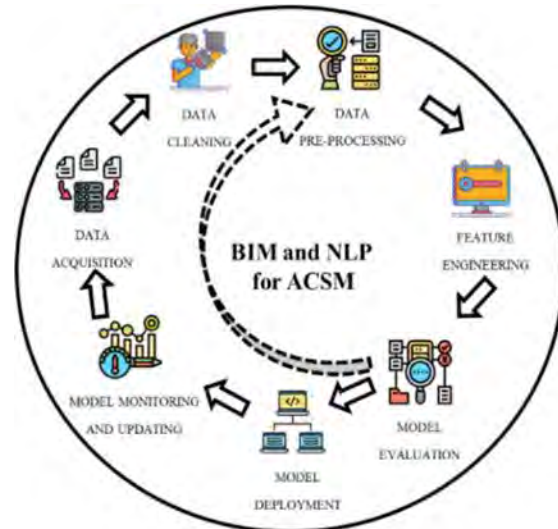


Figure 1. A generalized workflow for NLP-based data processing

The first step is data cleaning, which includes removing duplicated or irrelevant data and correcting errors to ensure data consistency. After cleaning, data pre-processing is performed. This step uses NLP techniques, such as tokenization, lowercasing, stop word removal, POS tagging, stemming, lemmatization, and named entity recognition, for extracting relevant information from the raw data. However, the data

cleaning and pre-processing depend on the input data source and the output data requirement. The output data may need certain information to be extracted, structured, and presented in a specific way, depending on the quality, consistency, format, and level of detail of the input data. The pre-processed data are then transformed into features that are used to train a learning-based schedule-generation model. Also, it is critical to select and alter the data precisely to ensure the features are relevant, high-quality, and representative and reduce the amount of linked and duplicated characteristics. The model is evaluated and refined using co-reference resolution, information modeling, knowledge matching, and text classification techniques. Furthermore, the data evaluation results can help improve the data pre-processing step by identifying issues with the data and providing insight into how to address them. The model can be enhanced by using the evaluation results to improve the data pre-processing step, which ensures high quality of data and captures the relevant features.

Once the model is finalized, it is deployed to manage the construction schedule, which is automated to reduce the time and effort required by management personnel. By ensuring that the data are accurate and up-to-date, data monitoring and updating can assist in improving the data acquisition process and further training the construction schedule generation model for obtaining a more realistic timetable. This procedure can change the model to reflect changes in the real world, and its performance can be enhanced over time.

2.4 Challenges and limitations of learning-based methods

Researchers have identified a few challenges and limitations of using learning-based schedule preparation and management methods. For example, the proposed models learn with an assumption of the same type of precedence dependencies [20]. Considering information regarding productivity and risk factors in the model is still a challenge [20]. Due to different project sizes, activity duration and resource usage cannot be adapted straight away from previous projects [18]. Although the model presented by Amer et al. [19] attempts to validate the logical dependencies, it does not provide an overall assessment of the quality of the schedule; Minimizing biases and irregularities and unpredictability of the impact of the mistakes remains a limitation for the data-driven models [27]. The learning-based models are company-specific [13] and work well mainly for data collected from the same companies.

Overall, achieving high accuracy and moving towards complete automation remained a significant challenge in an attempt to automate CSM. Alternatively, a human-assisted approach could be adopted to support the current automated schedule generation [27].

3 Future research directions

In practice, CSM utilizes information from various construction documents and building models. However, the automated CSM methods have either used information retrieved from BIM or past schedules. There is also limited integration of BIM and NLP observed in past automated CSM literature. This section proposes three research areas where future researchers can focus on improving the state-of-the-art.

3.1 Integration of BIM and NLP in Automated CSM

Integrating BIM and NLP within CSM can prove beneficial in addressing barriers to the widespread adoption of automated planning and scheduling methods. BIM can provide a centralized repository for storing construction knowledge, allowing for greater flexibility in scheduling algorithms. NLP can automate the learning of construction knowledge from existing records, reducing the dependency on manual work templates. Additionally, the integration of BIM and NLP can aid in the automatic generation of dynamic work templates and facilitate their inclusion in integrated planning, scheduling, and optimization systems, allowing for more efficient and accurate management of projects. Furthermore, with the adoption of the BIM methodology, which is centered on producing and exchanging digital models and artifacts [35], the AECO sector is moving towards a model-based approach. Despite this shift, the industry continues to rely heavily on document creation and exchange. NLP can be used to overcome this. By automating extracting and exchanging information from digital models and artifacts, NLP can revolutionize how information is handled in the AEC industry, improving efficiency and accuracy in Automated CSM.

3.2 Data-to-information flow for BIM and NLP-based automated CSM

This section highlights different data sources and types that can contribute to the information requirements for CSM. BIM provides spatial data (location and position of the elements), geometric data (shape and size of the elements), and identification data (element IDs, e.g., GUIDs) [11]. Standards, specifications, and company-specific resource productivity rates are collected for resource (manpower, materials, machinery) requirement calculation, cost estimation, and budget preparation for the project. Besides, the contract documents provide the details of the scope of work, milestones, and other specifications needed to create a realistic construction schedule agreed upon by all stakeholders [10]. Previous project schedules and reports from past projects are used for learning activity

descriptions, logical sequences, and dependencies required for automatic schedule development [8, 29]. Figure 2 shows a mapping between the data collected from construction documents and models and the information requirements for CSM. Based on the construction scheduling experience and literature review, the authors created a data-to-information flow map that connects data types and sources with information requirements for CSM. The mapping is shown in Figure 2. Future research may develop specific methods for multi-source data integration and information and knowledge retrieval for automated CSM.

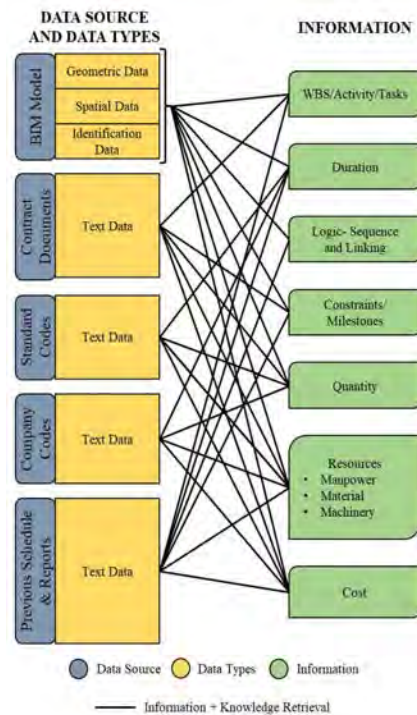


Figure 2. From data to information and knowledge retrieval for automated CSM

3.3 Schedule generation by Large Language Models (LLM): ChatGPT

ChatGPT is a large language model developed by OpenAI based on the GPT-3.5 architecture. It can generate human-like text and has been trained on a massive dataset of internet text, allowing it to create high-quality responses to a wide range of prompts [36]. Using ChatGPT for construction schedule generation can provide a quick and easy way to generate general schedule information for a construction project [37]. It can be beneficial for planning and budgeting, as it can create a schedule quickly and provide a starting point for further refinement and adjustment. This method is not

limited to specific project types, as it includes general information that can be adjusted according to particular project needs. An example schedule generated from ChatGPT can be seen in Figure 3. However, it is important to note that the schedule generated by ChatGPT may not take into account all the specific constraints, risks, and requirements of the project. Prieto et al. [37] study found that ChatGPT performance was promising for project scheduling. Still, significant flaws limit its application in real projects, indicating the potential for specialized tools to benefit the automation of repetitive and time-consuming tasks. Additionally, it may not be as accurate as a schedule created by a construction expert with experience working on similar projects. Therefore, consulting with construction experts and using specialized software to create a detailed schedule is always best. Furthermore, it is essential to validate the information generated by ChatGPT and adjust it to the specific project needs. It is also worth mentioning that ChatGPT can also be used to support construction experts by providing answers to some specific questions they may have during the construction process. Future research can look into including this powerful tool for the BIM and NLP-integrated automated CSM.

Activity Name	Start Date	End Date	Manager	Productivity Rate	Sequence	Linking	Lag Time	Lead Time	Successor	Predecessor
Site clearing and marking	15/01/2022	15/01/2022	10	10	1	FS	0	0	Installation of temporary facilities and hoarding	
Installation of temporary facilities and hoarding	15/01/2022	15/01/2022	8	15	2	FS	0	0	Excavation and backfilling	Site clearing and marking
Excavation and backfilling	15/01/2022	15/01/2022	6	25	3	SS	0	0	Foundation and concrete frame	Installation of temporary facilities and hoarding
Foundation and concrete frame	15/01/2022	15/01/2022	14	35	4	FS	0	0	Installation of scaffolding and concrete frame	Excavation and backfilling
Installation of scaffolding and concrete frame	15/01/2022	15/01/2022	10	35	5	FS	0	0	Roofing of foundation	Foundation and concrete frame

Figure 3. A sample schedule generated from ChatGPT

4 Conclusion

This study reviews the academic literature on BIM and NLP-based automated construction schedule management. It identifies state-of-the-art techniques and their limitations and challenges in widespread adoption in the construction industry. In conclusion, BIM and NLP in CSM have demonstrated significant promise for automating the scheduling process and enhancing project efficiency. However, the integration of these two technologies for CSM is less studied. Previous studies have developed and used model- and learning-based

automated scheduling techniques. However, the flexibility of storing construction information, the reliance on manually created work templates, and the lack of extensive validation on actual construction projects continue to be problems for better solutions. Integrating BIM and NLP is expected to improve the efficiency and accuracy of construction schedule management through the automatic generation of dynamic work templates and the automation of knowledge learning from existing records. This integration aims to minimize the time and effort involved in schedule preparation and update and increase the precision and realism of the construction schedule. Future work will focus on multi-source data extraction and integration to fulfill automated CSM knowledge and information requirements. Research in this direction may also look into integrating large language models such as ChatGPT for automated CSM.

Acknowledgment

The authors thank the National Science and Technology Council, Taiwan, for supporting this research through research grant Nos. MOST 109-2622-E-002-027, MOST 110-2622-E-002-039 and NSTC 111-2622-E-002-041.

References

- [1] H. Doloi, "Cost Overruns and Failure in Project Management: Understanding the Roles of Key Stakeholders in Construction Projects," *J. Constr. Eng. Manag.*, 139(3), 267–279, March 2013, doi: 10.1061/(ASCE)CO.1943-7862.0000621.
- [2] Y. J. T. Zidane and B. Andersen, "The Top 10 Universal Delay Factors in Construction Projects," *Int. J. Manag. Proj. Bus.*, 11(3), 650–672, April 2018, doi: 10.1108/IJMPB-05-2017-0052.
- [3] S. M. E. Sepasgozar, R. Karimi, S. Shirowzhan, M. Mojtahedi, S. Ebrahimzadeh, and D. McCarthy, "Delay Causes and Emerging Digital Tools: A Novel Model of Delay Analysis, Including Integrated Project Delivery and PMBOK," *Buildings*, 9(9), September 2019, doi: 10.3390/BUILDINGS9090191.
- [4] E. Mikulakova, M. König, E. Tauscher, and K. Beucke, "Knowledge-Based Schedule Generation and Evaluation," *Adv. Eng. Informatics*, 24(4), 389–403, November 2010, doi: 10.1016/j.aei.2010.06.010.
- [5] H. Kim, K. Anderson, S. Lee, and J. Hildreth, "Generating Construction Schedules Through Automatic Data Extraction Using Open BIM (BIM) Technology," *Autom. Constr.*, 35, 285–295, November 2013, doi: 10.1016/j.autcon.2013.05.020.
- [6] V. Faghihi, A. Nejat, K. F. Reinschmidt, and J. H. Kang, "Automation in Construction Scheduling: a Review of the Literature," *Int. J. Adv. Manuf. Technol.*, 81(9–12), 1845–1856, May 2015, doi: 10.1007/s00170-015-7339-0.
- [7] F. Amer, H. Y. Koh, and M. Golparvar-Fard, "Automated Methods and Systems for Construction Planning and Scheduling: Critical Review of Three Decades of Research," *J. Constr. Eng. Manag.*, vol. 147(7), July 2021, doi: 10.1061/(asce)co.1943-7862.0002093.
- [8] Q. Shen, S. Wu, Y. Deng, H. Deng, and J. C. P. Cheng, "BIM-Based Dynamic Construction Safety Rule Checking Using Ontology and NLP," *Buildings*, 12(5), April 2022, doi: 10.3390/buildings12050564.
- [9] X. Zhao, K. W. Yeoh, and D. K. H. Chua, "Extracting Construction Knowledge from Project Schedules Using NLP," *10th International Conference on Engineering, Project, and Production Management*, 197–211, Berlin, Germany, September, 2–4, 2019, doi: 10.1007/978-981-15-1910-9_17.
- [10] P. Jafari, M. Al Hattab, E. Mohamed, and S. Abourizk, "Automated Extraction and Time-Cost Prediction of Contractual Reporting Requirements in Construction Using NLP and Simulation," *Appl. Sci.*, 11(13), July 2021, doi: 10.3390/app11136188.
- [11] A. Zahedi, J. Abualdenien, F. Petzold, and A. Borrmann, "BIM-Based Design Decisions Documentation Using Design Episodes, Explanation Tags, and Constraints," *ITcon*, 27, 756–780, March 2022, doi: 10.36680/j.itcon.2022.037.
- [12] Q. Xie, X. Zhou, J. Wang, X. Gao, X. Chen, and L. Chun, "Matching Real-World Facilities to BIM Data Using NLP," *IEEE Access*, 7, 119465–119475, August 2019, doi: 10.1109/ACCESS.2019.2937219.
- [13] F. Amer and M. Golparvar-Fard, "Formalizing Construction Sequencing Knowledge and Mining Company-Specific Best Practices from Past Project Schedules," in *ASCE International Conference on Computing in Civil Engineering*, 215–223, Atlanta, Georgia, June, 17–19, 2019, doi: 10.1061/9780784482421.028.
- [14] K. K. Han, D. Cline, and M. Golparvar-Fard, "Formalized Knowledge of Construction Sequencing for Visual Monitoring of Work-in-Progress via Incomplete Point Clouds and Low-LoD 4D BIMs," *Adv. Eng. Informatics*, 29(4), 889–901, October 2015, doi: 10.1016/j.aei.2015.10.006.
- [15] H. G. Ballard, *The Last Planner System of Production Control*, The University of Birmingham, January 2000.

- [16] A. Pal and S. H. Hsieh, "Deep-learning-based Visual Data Analytics for Smart Construction Management," *Autom. Constr.*, 131, 103892, August 2021, doi: 10.1016/j.autcon.2021.103892.
- [17] A. Pal, J. J. Lin, and S. H. Hsieh, "Schedule-driven Analytics of 3D Point Clouds for Automated Construction Progress Monitoring," in *International Conference on Computing in Civil Engineering 2023*, 1–8, Corvallis, OR, USA, June 25–28, 2023.
- [18] Y. Hong, H. Xie, E. Agapaki, and I. Brilakis, "Graph-based Automated Construction Scheduling (GAS) Without the Use of BIM," *J. Constr. Eng. Manag.*, 149(2), February 2023, doi: 10.1061/JCEMD4.COENG-12687.
- [19] F. Amer, J. Hockenmaier, and M. Golparvar-Fard, "Learning and Critiquing Pairwise Activity Relationships for Schedule Quality Control via Deep Learning-Based NLP," *Autom. Constr.*, 134, February 2022, 104036, 2022, doi: 10.1016/j.autcon.2021.104036.
- [20] F. Amer and M. Golparvar-Fard, "Modeling Dynamic Construction Work Template from Existing Scheduling Records via Sequential Machine Learning," *Adv. Eng. Informatics*, 47, January 2021, doi: 10.1016/j.aei.2020.101198.
- [21] Y. Hong, H. Xie, G. Bhumbra, and I. Brilakis, "Comparing NLP Methods to Cluster Construction Schedules," *J. Constr. Eng. Manag.*, 147(10), 1–11, October 2021, doi: 10.1061/(asce)co.1943-7862.0002165.
- [22] R. Ren and J. Zhang, "Construction Procedural Information Extraction from Textual Sources to Support Scheduling," in *Proc. of Construction Research Congress 2022*, 330–339, Arlington, VA, USA, March 9–12, 2022, doi: 10.1061/9780784483978.035.
- [23] S. Wu, Q. Shen, Y. Deng, and J. Cheng, "Natural-Language-Based Intelligent Retrieval Engine for BIM Object Database," *Comput. Ind.*, 108, 73–88, June 2019, doi: 10.1016/j.compind.2019.02.016.
- [24] H. Hamledari, B. McCabe, S. Davari, and A. Shahi, "Automated Schedule and Progress Updating of IFC-Based 4D BIMs," *J. Comput. Civ. Eng.*, 31(4), 1–16, July 2017, doi: 10.1061/(asce)cp.1943-5487.0000660.
- [25] M. ElMenshawy and M. Marzouk, "Automated BIM Schedule Generation Approach for Solving Time–Cost Trade-Off Problems," *Eng. Constr. Archit. Manag.*, 28(10), 3346–3367, January 2021, doi: 10.1108/ECAM-08-2020-0652.
- [26] R. Sacks, I. Brilakis, E. Pikas, H. S. Xie, and M. Girolami, "Construction with Digital Twin Information Systems," *Data-Centric Eng.*, 1(6), November 2020, doi: 10.1017/dce.2020.16.
- [27] F. Amer, Y. Jung, and M. Golparvar-Fard, "Transformer Machine Learning Language Model for Auto-Alignment of Long-Term and Short-Term Plans in Construction," *Autom. Constr.*, 132, December 2021, doi: 10.1016/j.autcon.2021.103929.
- [28] J. P. Fitzsimmons, R. Lu, Y. Hong, and I. Brilakis, "Construction Schedule Risk Analysis - a Hybrid Machine Learning Approach," *J. Inf. Technol. Constr.*, 27, February 2021, 70–93, 2022, doi: 10.36680/j.itcon.2022.004.
- [29] K. Sigalov and M. König, "Recognition of Process Patterns for BIM-Based Construction Schedules," *Adv. Eng. Informatics*, 33, 456–472, August 2017, doi: 10.1016/J.AEI.2016.12.003.
- [30] V. Faghihi, K. F. Reinschmidt, and J. H. Kang, "Extended Genetic Algorithm for Optimized BIM - Based Construction Scheduling," *Wiley StatsRef: Statistics Reference Online*, December. 2018.
- [31] Z. Wang and E. Rezazadeh Azar, "BIM-Based Draft Schedule Generation in Reinforced Concrete-Framed Buildings," *Constr. Innov.*, 19(2), 280–294, April 2019, doi: 10.1108/CI-11-2018-0094.
- [32] J. Singh and C. J. Anumba, "Real-Time Pipe System Installation Schedule Generation and Optimization Using Artificial Intelligence and Heuristic Techniques," *J. Inf. Technol. Constr.*, 27, 173–190, February 2022, doi: 10.36680/j.itcon.2022.009.
- [33] A. Fazeli, "Automated 4D BIM development : The Resource Specification and Optimization Approach," *Eng. Constr. Archit. Manag.*, December 2022, doi: 10.1108/ECAM-07-2022-0665.
- [34] A. Pal, J. J. Lin, and S. H. Hsieh, "Automated Construction Progress Monitoring of Partially Completed Building Elements Leveraging Geometry Modeling and Appearance Detection with Deep Learning," in *Proc. of Construction Research Congress 2022*, 708–717 Arlington, VA, USA, March 9–12, 2022. doi: 10.1061/9780784483961.074.
- [35] M. Locatelli, E. Seghezzi, L. Pellegrini, L. C. Tagliabue, and G. M. Di Giuda, "Exploring NLP in Construction and Integration with BIM: A Scientometric Analysis," *Buildings*, 11(12), November 2021, doi: 10.3390/buildings11120583.
- [36] Open AI, "ChatGPT: Optimizing Language Models for Dialogue," 2022. <https://openai.com/blog/chatgpt/> (accessed Jan. 15, 2023).
- [37] S. A. Prieto, E. T. Mengiste, and B. G. de Soto, "Investigating the Use of ChatGPT for the Scheduling of Construction Projects," *Buildings*, 13(857), 2023, [Online]. Available: <https://arxiv.org/abs/2302.02805>.

Design based Constraint Handling for Site Layout Planning

Abhishek Raj Singh¹, Venkata Santosh Kumar Delhi² and Sagar Jain³

^{1,2}Department of Civil Engineering, Indian Institute of Technology Bombay, India

³PM group companies, Bangalore, India

arsingh@iitb.ac.in, venkatad@iitb.ac.in

Abstract

Site layout planning (SLP) constraints are handled heuristically or through a mathematical approach, as presented in the SLP literature. The real-life constraints of SLP are modelled as mathematical equations and are attempted to be handled through optimisation models. It is observed that the existing mathematical SLP models handle a limited number of constraints in comparison to what is handled by practitioners in practice. This study outlines a design-based workflow that enables SLP practitioners to handle SLP constraints and reduces the number of infeasible solutions to SLP problem. Firstly, the constraints of SLP are categorised to form constraints typology, and it is understood that the spatial constraints of SLP have facets that can be modelled and handled through design. A test case is developed to demonstrate the design-based handling of SLP constraints. The spatial constraint handling for SLP is presented through single regular-shaped temporary facility (TF) layout variations. The TF's variations enabled ascertaining the possibility of including TFs of different shapes and sizes. The results indicated a reduction in mathematical solution search space; consequently, the search for the optimal solutions for the SLP problem is expected in a timely manner. The implementation of the developed design-based constraint handling approach for SLP needs to be studied in conjunction with the mathematical models and remains an area for further study.

Keywords –

Site Layout Planning, Project Design, Building Information Modelling, Optimisation

1 Introduction

Construction site layout planning (SLP) encompasses organisation of construction project's physical elements in a safe and efficient manner. This includes positioning of temporary facilities (TFs), planning for roads and walkways for internal movement of site personnel, material shifting and equipment [1]. The SLP studies have tried but are not limited to minimise the material handling by finding optimal positions for the TFs [2]. These studies have focused on modelling the SLP

problem as a mathematical problem and solving for an optimal solution to definitive objectives bounded by some constraints [3], whereas in practice there are many constraints handled by the SLP practitioners utilising heuristics while planning layouts [4].

Such incomprehensive problem representation results in sub-optimal layouts and limits the implementation of the SLP optimisation models. These optimisation models present a solution finding approach to the SLP, although the process involves decision-making based on objective and subjective goals. While the objective goals are presented as fitness function in the mathematical form of representation, the subjective goals of SLP are left for the planners to manage [5]. The mathematical representation of a real-life problem of SLP includes objective function(s) subjected to constraints to limit the space for solution search. The parameters like productivity, cost of project, safety on construction site, noise levels, security are mathematically modelled as objective functions to be optimised subjected to some real-life constraints depicted as mathematical bounds. These mathematical bounds restrict the infeasible solutions to become part of the feasible set [5].

Such restrictions mimic the actual solution search strategy adopted by the site layout planners while planning SLP using their experience. In practice the SLP practitioners handle the site constraints utilising the experience gained but considering the intertwined nature of construction projects the handling of multiple objectives subjected to various constraints surpasses the mental computability of humans [6]. Thus the mathematical representation of SLP problem is presented as a method to solve for SLP in the existing literature. These mathematical formulations present limited constraints handling in the optimisation model and thus the unattended practical constraints remain challenges for practitioners to address, resulting in limited adoption of mathematical approaches for SLP [4].

This study reviews the mathematical approaches to SLP, identifies the constraints handled in the SLP literature, develops a constraint typology, and presents a design-based approach to handle the constraints of SLP. The developed design-based strategy is targeted to handle the hard constraints of the SLP problem, consequently lowering the constraints to be handled either mathematically or heuristically.

2 Construction SLP problem and its Constraints

The SLP problem in the literature is represented as either continuous or discrete site space organisation problem targeted to mathematically find optimal positions for TFs. The mathematical models attempt to depict the SLP problem closer to reality, the formulation differs depending upon the geometrical representation considered in the research. Therefore based on geometrical representations presented in SLP studies the problem of SLP can be divided into two namely continuous, and discrete.

The site space is considered as continuous when the TFs can be positioned anywhere on the site. as shown in Figure 1. The centroid of the TFs is considered as decision variable to identify the position of the TFs on the available site area [7] in continuous SLP problem.

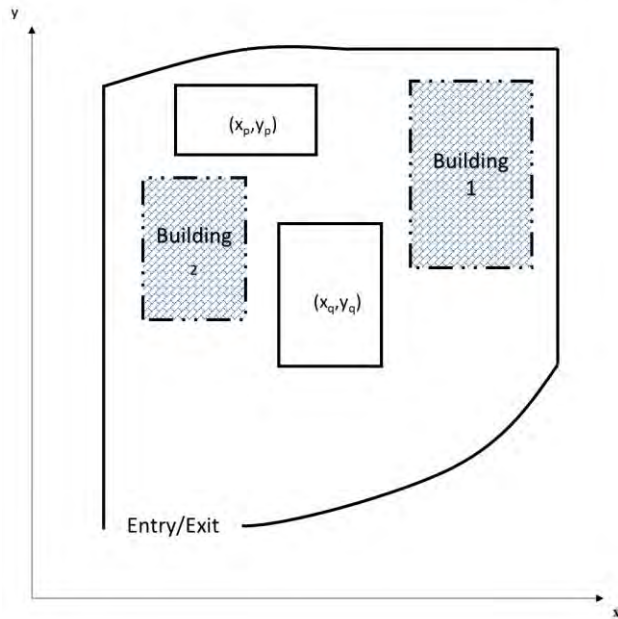


Figure 1. Continuous SLP problem representation.

On the contrary to continuous SLP, the locations to accommodate TFs are identified in prior and then the positioning of TFs is handled as part of the discrete SLP problem [8] as depicted in Figure 2. This formulation poses another challenge for the SLP practitioners of identifying the available locations on the site area for accommodating TFs. Since each TF is distinctive, the area requirement varies and therefore the locations identified by the planners sometimes allow to accommodate more than one TF during any project phase and thus the discrete location becomes a continuous area available for the TFs to be collocated.

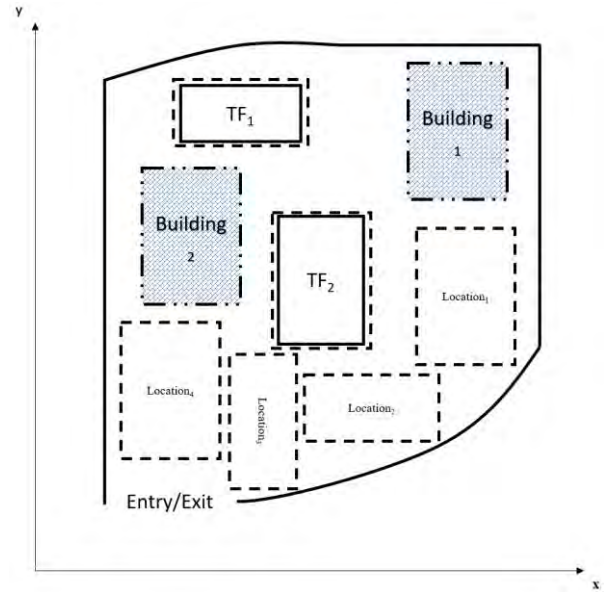


Figure 2. Discrete SLP problem representation.

The studies have indicated some methods to decompose the continuous site space problem to discrete using grid technique whereas this representation still mimics the nature of continuous SLP problem [9]. Although here the approach of using the greatest common divisor (GCD) of the TFs required can help in decomposing the site space into grids [8] as depicted in Figure 3. The TFs are positioned with respect to the cell reference. Such representation restricts irregular shapes of TFs and these TFs are to be divided and modelled into a regular shapes [10].

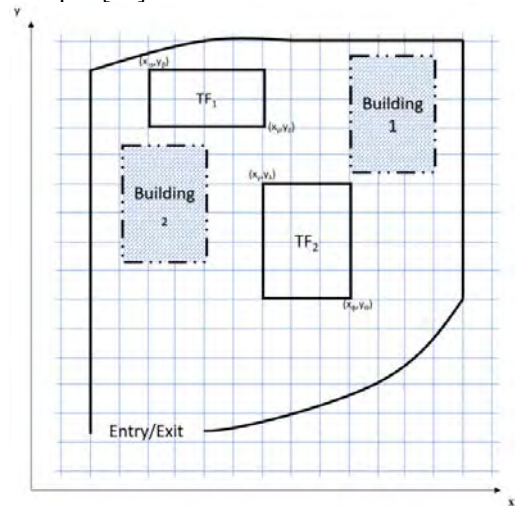


Figure 3. Grid-based SLP problem representation.

Selection of smaller grid size can be a potential solution to the limitation of searching solution between the grid space; but at the same time, it will increase the computation requirements [10], [11]. Considering such

computational needs, researchers have targeted optimisation-based approaches for SLP. The mathematical formulation for SLP problem is depicted in equation 1 and Table 1. The formulation presents the weighted sum method of handling multiple objectives of SLP.

$\sum_{i=1}^n w_i \cdot f_i(x)$	Equation 1
---------------------------------	-------------------

Subjected to multiple constraints for example:

Table 1. Constraints of SLP from literature.

Constraint	Constraint type [modified from]
$\sum_{p=1}^n x_{pl}$	Positioning constraint [12]
$ x_p - x_q \geq 0.5 (\overline{W}_p - \overline{W}_q) \mu_{pq}^x$ $\forall p, q \in F: p < q$	Inclusion constraint [13]
$ y_p - y_q \geq 0.5 (\overline{L}_p - \overline{L}_q) \mu_{pq}^y$ $\forall p, q \in F: p < q$	Inclusion constraint [13]
$\frac{ CXF_p - CXF_q - (LXF_p - LXF_q)}{2} \geq D_{min}$ <p style="text-align: center;">Or</p> $\frac{ CYF_p - CYF_q - (LYF_p - LYF_q)}{2} \geq D_{min}$	Minimum Proximity constraint [9], [14]

Where, the used notations mean as follows:

Symbols	Description
w	Priority weight
$f(x)$	Objective function
x_{pl}	Decision variable indicating positioning of facility p at location l
x_p	Centroid coordinate of facility p in x direction
x_q	Centroid coordinate of facility q in x direction
y_p	Centroid coordinate of facility p in y direction
y_q	Centroid coordinate of facility q in y direction
\overline{W}_p	Width of facility p
\overline{W}_q	Width of facility q

\overline{L}_p	Length of facility p
\overline{L}_q	Length of facility q
μ_{pq}^x	Binary variable, equals one when no overlap takes place between the facilities within the same location in x direction
μ_{pq}^y	Binary variable, equals one when no overlap takes place between the facilities within the same location in y direction
CXF_p	X coordinate of Reference Point of Facility p
CXF_q	X coordinate of Reference Point of Facility q
LXF_p	Length of Facility p on X Axis Direction
LXF_q	Length of Facility q on X Axis Direction
D_{min}	Minimum distance between edges of Facilities
CYF_p	Y coordinate of Reference Point of Facility p
CYF_q	Y coordinate of Reference Point of Facility q
LYF_p	Length of Facility p on Y Axis Direction
LYF_q	Length of Facility q on Y Axis Direction

Since the SLP problem involves multiple constraints to manage, the computer implemented method of solution search through mathematical modelling are explored in SLP research as they promise solution search faster than human generated layouts.

The literature indicates that the constraints of SLP in the developed mathematical formulations are much lesser than the actual constraints the planners handle in practice [4]. This could be due to the more computational requirements the optimisation model will need with an increase in more constraints to handle. Although the technological advancements at present are capable of handling high computational requirements, the problem of SLP is more about achieving feasible solutions as quickly as possible [15]. Site space decomposition is one way to reach optimal solutions faster than searching in large pool of potential solutions. Thus the literature has suggested methods of transforming continuous SLP problem to a grid based SLP. This transformation minimises the search points to be explored for optimal solution in the formulated SLP problem.

Such geometrical transformation(s) are investigated in this study to identify the possible way for handling the SLP constraints that can reduce the computational requirements for solving the SLP problem in a timely manner.

3 Constraints Typology of Construction SLP

The SLP problem is defined as a spatiotemporal

problem, and the spatial and temporal constraints of SLP are handled mathematically in the optimisation-based approach for planning layouts. The developed typology presented in Figure 4 indicates SLP's spatial and temporal constraints. The sub-categories of these two categories highlight the specifics of each constraint modelled in a mathematical SLP optimisation model. These sub-category constraints can further be classified as soft or hard constraints for SLP problem based on the mathematical formulation of SLP. By definition, the hard constraints are mandatory bounds meant to be satisfied with no modification possible to the conditions, whereas the soft constraints provide flexibility in terms of modifications possible to the bound.

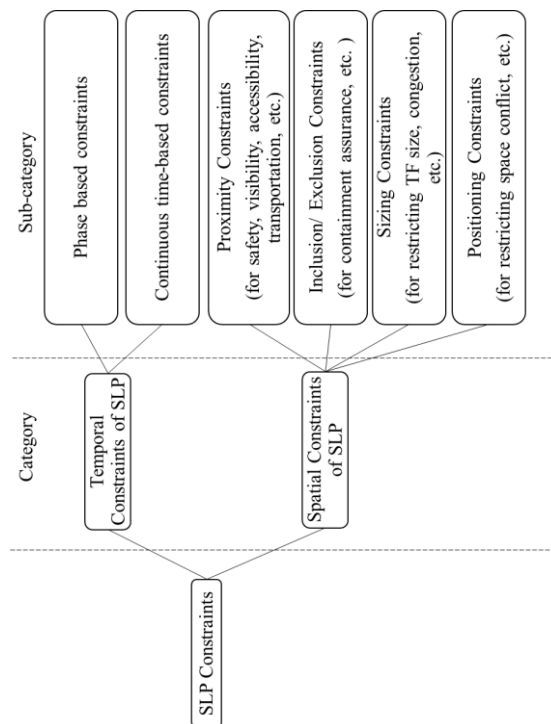


Figure 4. Developed SLP constraints typology.

As like site space, the project duration is sub-divided by researchers in SLP studies into manageable project instances called phases. These phases capture some timeframe of the project duration and are planned for that specific timeframe only. The phased based constraints indicate the need of a TF in a particular project phase and thus the impact of the positioning of TF in preceding phase is not captured on the TF positions in the following phases. Thus to overcome the limitation of phase based SLP the project duration is considered continuous and the impact of positioning TFs on construction site is captured holistically. The category of spatial constraints includes but is not limited to proximity, inclusion or exclusion, sizing, positioning constraints. These sub-categorical

constraints encompass multiple bounds necessary for making SLP decisions like the positioning constraints highlight the zoning requirements for facilities and the orientation in which the TFs are to be located. The sizing constraint on TFs helps in restricting site congestion due to large size TFs located on a congested site. It enables planners to limit the required size of TF to accommodate all machinery associated with the TF along with working place available for performing work. Inclusion or exclusion constraints ensure the TFs must lie within the boundaries of the project site and the exclusion bounds can ensure there are no entry or exit blockages for transporting materials on the site [16]. Another constraint to ensure no blockage of quick egress in situations of accident on site is the proximity constraint. This constraint imposes limits to position certain TFs as far or as close as possible to the execution site. All these constraints of spatial nature [17] are modelled as mathematical bounds in the existing optimisation-based SLP studies [16].

The present research targets the spatial constraints of the SLP, and a design driven framework for handling SLP constraints is conceptualised and demonstrated.

4 Conceptualisation of 'Design for SLP'(DfP)

The intangible benefits of SLP are among the reasons due to which the SLP remains unconsidered by the SLP practitioners. As a result the site conditions adverse over time as construction progresses and therefore the existing SLP literature highlights necessity of planning layout as early as possible in a construction project. The planning of layouts requires inputs for making decisions and these inputs are sought either from past projects or assumed based on experiential learnings of the planners. But such approach results in lapses as the past projects do not reflect the challenges associated with current project. Thus this study proposes utilisation of project design for SLP (DfP) by handling spatial constraints through design.

Designing for construction projects requires ideation and enables planners to plan for execution. Therefore, if all required information that aid in planning can be embedded into project designs, more meaningful planning outcomes are expected. In recent years, the SLP researchers have focused on utilising the building information modelling (BIM) for the SLP purposes. The developed BIM models are used for information inputs to the optimisation models for SLP. Primarily the data-based inputs are retrieved from the BIM model and then fed to the mathematical model to generate optimal layouts [18]. This approach presented the advantage of design for site layout planning (DfP), where BIM provided the necessary quantitative information for layout generation.

This study demonstrates the feasibility of handling constraints through design and the advantage of DfP. An example BIM model is prepared where two industrial buildings as shown in Figure 5 are to be constructed. The proposed pathways for vehicular movement are identified and marked, leaving out seven potential areas for TF allocation depicted as shaded regions. These shaded regions are the result of continuous site space divided into regions due to the road network. Though the representation appears discrete, but the regions represent continuous site space where single region can accommodate more than one TFs.

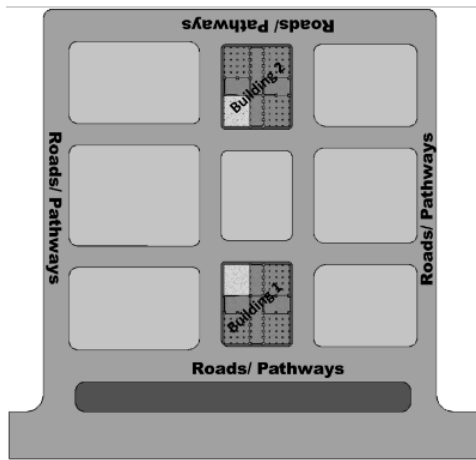


Figure 5. Test case model representation.

The necessary TFs required for the project are identified and required area for accommodating individual TF is mapped in the project design along with the project information. Identifying the area requirement for TFs might appear as an additional task for planners but this is part of the existing SLP practice [19]. Apart from the traditional regular shapes for TFs, the area for consumables can also be mapped in irregular shapes as shown in Figure 6. The shaded area around the location area demarcates the safety zone created as part of the location area for TF to consider the *proximity constraint* of the TFs.



Figure 6. Area requirements for TFs with safety zone modelled as part of the location area.

Along with mapping of area requirements of TFs the whole site area is distributed between 100x100 grids of equal spacing using the GCD method demonstrated in existing SLP studies [20]. Each grid point within the site area as shown in Figure 7 represents a solution for locating a TF.

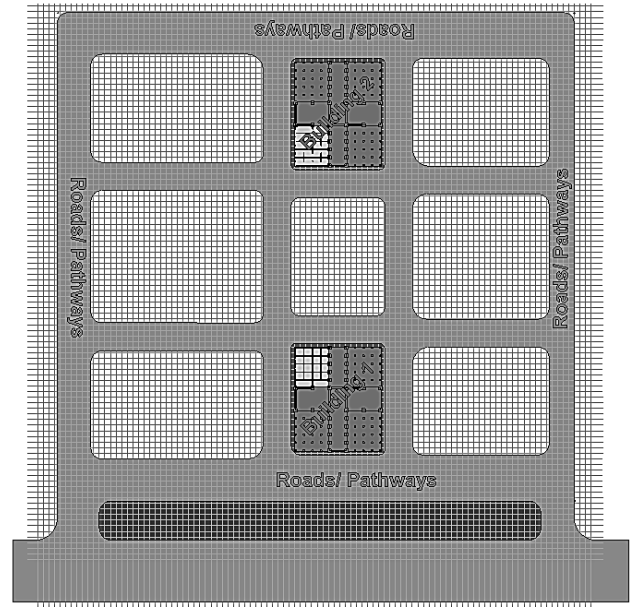


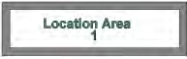





Figure 7. Transformed the test case model to grid-based representation.

Although these 100x100 grid points are possible positions but does not qualify as feasible solutions, and by definition the solutions satisfying the constraints of the problem are feasible solutions [21]. In the considered case the imposition of inclusion constraint will limit the positioning of TFs outside the boundary of the project site resulting in reduction in the number of solutions for exploration in the solution space by eliminating the grid points closer to the site boundary. This research presents a test example to understand this reduction in the solution space through a design based spatial constraint handling approach for SLP.

4.1 Search space decomposition through spatial constraints of SLP

As demonstrated above that how the inclusion constraint of SLP can decrease the number of possible solutions a test case is developed where a TF area requirement of 450 square units is considered. Since the shape of the TFs can vary during the due course of project progress the 450 square units of area is modelled proportionately into eight combinations listed in Table 2 but as a regular shape area shown in Figure 6 as location area 1.

Table 2. Considered TF area dimensions and respective feasible position count.

Sr. no.	Site area dimensions (Length x Breadth)	Orientation	Feasible positions (Count)
1	45x10		27
2	40x11.25		194
3	35x12.857		519
4	30x15		870
5	25x18		1143
6	20x22.5		1296
7	15x30	Serial no. 4 (rotated 90°)	1244
8	10x45	Serial no. 1 (rotated 90°)	559
Total			5852

The choice of regular shape is driven by motivation to demonstrate the functionality through different dimensional variations. Whereas in case of irregular shape the flexibility to iterate through different design variations will result in higher complexity. The Table 2 also reports the results of feasible outcomes from the possible 8x100x100 outcomes when the location area 1 for a TF is taken through all the grid points and the spatial constraints mentioned in Figure 4 are imposed. The location area 1 is dimensionally transformed into different variations to indicate the influence of the *sizing constraints*. Firstly the *inclusion constraints* are imposed to ascertain the TFs are being positioned inside the boundaries of the site. Following the inclusion constraints, the *exclusion constraints* are considered. It helped in ascertaining the non-overlapping of the TF area with the road networks and the upcoming buildings as shown in Figure 8. The grid positions resulting in such violations are removed from the solution pool of the optimisation model to reach optimal solutions faster.

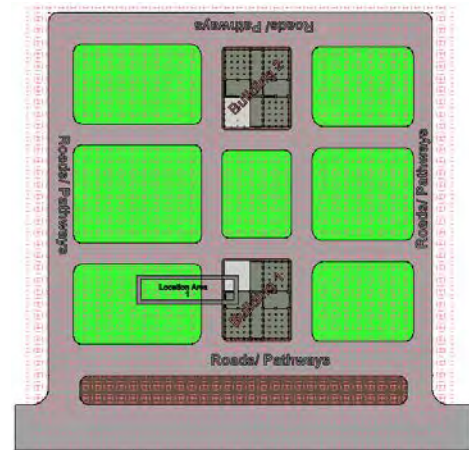


Figure 8. Inclusion constraint satisfied with violation of exclusion constraint.

The imposition of the spatial constraints resulted in 92.6 percent reduction of feasible solution count by eliminating the unfeasible positions through design for the considered case. The studies targeting algorithm based location decomposition for SLP has highlighted that the approach of reducing the solution search area through eliminating infeasible solutions from the solution pool for SLP problem results in generating layouts in timely manner [21]. Similar thrust has been observed in construction safety studies, where the planners were not able to identify the tangible benefits associated with maintaining safety on construction site and consequently numerous incidents had been reported resulting in prevention through design a key research area of construction safety management [22]. This study proposes a concept 'Design for SLP' (DfP) that is similar to 'design for occupational safety and health' (DfOSH) [23], [24]. As like DfOSH, Prevention through Design (PtD) and other design for safety related concepts DfP also advocates for a shared responsibility among project stakeholders for layout planning [23]. These design-based approaches for mitigating safety risks underpin the advantages of proactiveness during project design phase resulting in project success. Although the influence of design is captured in the safety-related domain [25], the design influence on SLP is under explored in the SLP research.

5 Entailments from the proposed DfP

The modelling of TFs for construction projects is not a common practice but doing so will help in managing the project and site workflows. These modelled TFs will be useful in calculating the area requirement of TFs for a project. Such consideration of area requirement of TFs though appears as an additional work but after preparing for a number of projects will result in a database of TFs

required for projects and their area requirements will be a data asset for the organisation. The utilisation of BIM will enable the construction organisations to use the modelled TFs and area requirements for further projects and overtime the database will be enriched significantly that the need for modelling TFs and the area requirements will diminish. The approach of handling the SLP spatial constraints through design as presented in this study offers the search area reduction for the mathematical approach for SLP. Notably, the capture of constraints through design has transformed the solution search space for the mathematical model into a discrete solution search space as depicted in Figure 9.

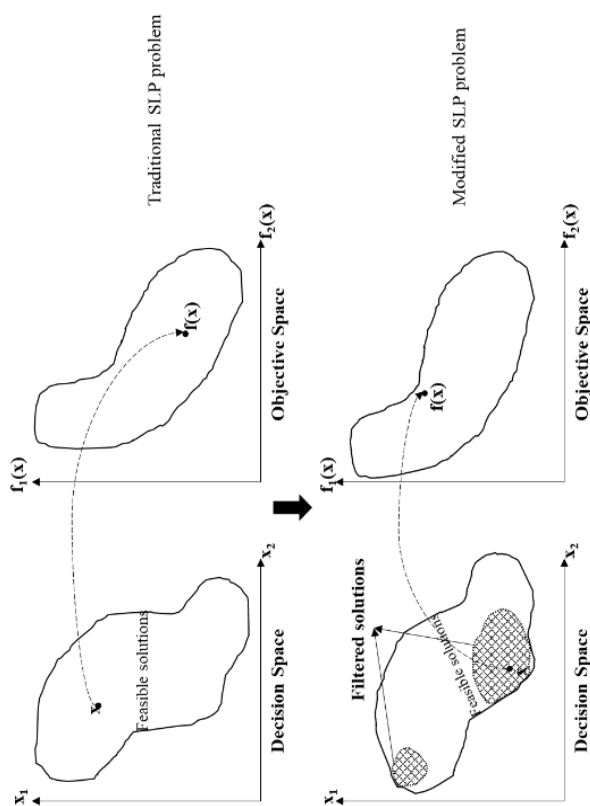


Figure 9. Transformation of traditional SLP to design-based SLP.

The handling of spatial constraints through design though reduces the solution search space but poses another challenge in form of identifying the mathematical algorithms that can help in solving the discontinuous SLP optimisation problem and provides an interesting area of further research. Also a single TF layout is attempted in this test case whereas multiple TF layout is possible using the methodology presented in the study.

6 Conclusion

Traditionally the problem of SLP is considered as decision making problem and is attempted to be benefitted through optimisation models. Although the optimisation models provide mathematical approach to handle the constraints of real-life scenarios, there exist challenges in modelling them. Therefore this study attempted to handle the constraints of SLP through design. In attempt to do so the SLP constraint typology is developed, and the spatial constraints are identified to have features that can be modelled as part of the project design and then the BIM design is put to use for handling the spatial constraints. The presented approach is limited to regular-shaped single TF with variation in dimensions, but the demonstrated case provides evidence of applicability for TFs of different shapes and sizes. The study highlighted the opportunity of utilising design-based constraint handling in SLP problem where visually verifiable results are expected to be generated. The presented workflow for handling SLP constraints filters out the infeasible solutions from the pool of possible solutions to the SLP problem. The optimisation models for SLP are expected to benefit from this study due to reduction in solution search space and to provide optimal solutions to the problem of SLP in a timely manner. The study provides an opportunity for further research focusing on algorithms for SLP optimisation to search in discrete solution search space.

References

- [1] P. P. Zouein and I. D. Tommelein, "Dynamic Layout Planning Using a Hybrid Incremental Solution Method," *J. Constr. Eng. Manag.*, vol. 125, pp. 400–408, 1999.
- [2] R. Gholizadeh, G. G. Amiri, and B. Mohebi, "An Alternative Approach to A Harmony Search Algorithm for A Construction Site Layout Problem," *Can. J. Civ. Eng.*, vol. 37, pp. 1560–1571, 2010.
- [3] D. Prayogo, J. C. Sutanto, H. E. Suryo, and S. Eric, "A Comparative Study on Bio-Inspired Algorithms in Layout Optimisation of Construction Site Facilities," *Civ. Eng. Dimens.*, vol. 20, p. 102, 2018.
- [4] M. Kim, H. G. Ryu, and T. W. Kim, "A Typology Model of Temporary Facility Constraints for Automated Construction Site Layout Planning," *Appl. Sci.*, vol. 11, pp. 1–21, 2021.
- [5] J. Xu and Z. Li, "Multi-Objective Dynamic Construction Site Layout Planning in Fuzzy

- Random Environment,” *Autom. Constr.*, vol. 27, pp. 155–169, 2012.
- [6] K. W. Chau and M. Anson, “A Knowledge-based System for Construction Site Level Facilities Layout,” in *Lecture Notes in Computer Science*, T. Hendtlass and M. Ali, Eds. 2002, pp. 393–402.
- [7] A. W. A. Hammad, “A Multi-Objective Construction Site Layout Planning Problem Solved through Integration of Location and Traffic Assignment Models,” *Constr. Manag. Econ.*, vol. 38, pp. 756–772, 2020.
- [8] A. Al Hawarneh, S. Bendak, and F. Ghanim, “Construction Site Layout Planning Problem: Past, Present and Future,” *Expert Syst. Appl.*, vol. 168, p. 114247, 2021.
- [9] S. Razavialavi and S. M. Abourizk, “Site Layout and Construction Plan Optimization Using an Integrated Genetic Algorithm Simulation Framework,” *J. Comput. Civ. Eng.*, vol. 31, pp. 04017011 (1–10), 2017.
- [10] V. Benjaoran and V. Peansupap, “Grid-Based Construction Site Layout Planning with Particle Swarm Optimisation and Travel Path Distance,” *Constr. Manag. Econ.*, vol. 37, pp. 1–16, 2019.
- [11] N. Č. Babič, P. Podbreznik, and D. Rebolj, “Integrating Resource Production and Construction using BIM,” *Autom. Constr.*, vol. 19, pp. 539–543, 2010.
- [12] A. R. Singh, A. Karmakar, and V. S. K. Delhi, “Decision Support System for Site Layout Planning,” in *37th International Symposium on Automation and Robotics in Construction (ISARC)*, 2020, pp. 1008–1013.
- [13] A. W. A. Hammad, A. Akbarnezhad, and D. Rey, “A Multi-Objective Mixed Integer Nonlinear Programming Model for Construction Site Layout Planning to Minimise Noise Pollution and Transport Costs,” *Autom. Constr.*, vol. 61, pp. 73–85, 2016.
- [14] S. Razavialavi, S. Abourizk, and P. Eng, “Genetic Algorithm – Simulation Framework for Decision Making in Construction Site Layout Planning,” *J. Constr. Eng. Manag.*, vol. 143, pp. 04016084 (1–13), 2017.
- [15] A. AlSaggaf and A. Jrade, “ArcSPAT: An integrated Building Information Modeling (BIM) and Geographic Information System (GIS) Model for Site Layout Planning,” *Int. J. Constr. Manag.*, vol. 1, pp. 1–25, 2021.
- [16] K. El-Rayes and H. Said, “Dynamic Site Layout Planning Using Approximate Dynamic Programming,” *J. Comput. Civ. Eng.*, vol. 23, pp. 119–127, 2009.
- [17] X. Wang and H. Jen, “Designing Virtual Construction Worksite Layout in Real Environment Via Augmented Reality,” in *International Symposium on Automation and Robotics in Construction*, 2006, pp. 757–761.
- [18] A. R. Singh and V. S. K. Delhi, “Automated BIM based SLP for Construction Sites,” in *Construction Research Congress (CRC)*, 2020, pp. 782–791.
- [19] F. Sadeghpour, O. Moselhi, and S. T. Alkass, “Computer-Aided Site Layout Planning,” *J. Constr. Eng. Manag.*, vol. 132, pp. 143–151, 2006.
- [20] X. Ning, J. Qi, C. Wu, and W. Wang, “A Tri-Objective Ant Colony Optimization Based Model for Planning Safe Construction Site Layout,” *Autom. Constr.*, vol. 89, no. December 2017, pp. 1–12, 2018.
- [21] A. W. A. Hammad, D. Rey, and A. Akbarnezhad, “A Cutting Plane Algorithm for the Site Layout Planning Problem with Travel Barriers,” *Comput. Oper. Res.*, vol. 82, pp. 36–51, 2017.
- [22] K. Bhagwat and V. S. K. Delhi, “A Systematic Review of Construction Safety Research: Quantitative and Qualitative Content Analysis Approach,” *Built Environ. Proj. Asset Manag.*, vol. 12, pp. 243–261, 2022.
- [23] E. Adaku, N. A. Ankrah, and I. E. Ndekugri, “Design for Occupational Safety and Health: A Theoretical Framework for Organisational Capability,” *Saf. Sci.*, vol. 133, p. 105005, 2021.
- [24] C. K. I. Che Ibrahim, P. Manu, S. Belayutham, A. M. Mahamadu, and M. F. Antwi-Afari, “Design for Safety (DfS) Practice in Construction Engineering and Management Research: A Review of Current Trends and Future Directions,” *J. Build. Eng.*, vol. 52, no. November 2021, 2022.
- [25] N. Tymvios, D. Hardison, M. Behm, M. Hallowell, and J. Gambatese, “Revisiting Lorent and Szymberski: Evaluating how research in prevention through design is interpreted and cited,” *Saf. Sci.*, vol. 131, no. November 2019, p. 104927, 2020.

Digital Twin Framework for Worker Safety using RFID Technology

Anikesh Paul¹, Sagar Pulani² and Dr. J. Uma Maheswari³

^{1,2,3}Department of Civil Engineering, Indian Institute of Technology Delhi, India
E-mail: cez208406@civil.iitd.ac.in, sagar.pulani@gmail.com, uma.iit@gmail.com

Abstract –

Construction 4.0 and Digital Twin are the emerging concepts of the digital era in the Construction Sector. The crux of these digital technologies lies in capturing the rich “real physical” data to model the “virtual” structure to enable the experiments for specific decision-making. Although protocols for the hazardous operations had been chalked out meticulously across the globe through several organizations using stern safety regulations and codal provisions, still the goal of zero-accidents at the construction site has not been achieved. One of the several reasons for accidents occurrence can be that safety is not always in the minds of the workers and require a third-party intervention. Hence, the objective of this study is to safeguard the workers working in the construction sites using digital platforms (third-party) where the safety is monitored round the clock. The scope of this study is limited to falling of materials, equipments and workers. To achieve this objective, RFID (Radio Frequency Identification System) is used to capture the site data and is modelled in BIM (Building Information Modeling) using Dynamo. Job safety analysis is performed in the BIM software and this experiment is conducted on some hypothetical construction sites-in progress and the initial results have received positive feedback.

Keywords –

Digital Twin; Construction Safety; RFID; BIM

1 Introduction

Construction 4.0 is an emerging digital era concept following the lineage of techniques captured from Industry/Manufacturing Sector to the Construction Sector. The Construction 4.0 framework [1] uses CPS (Cyber-Physical System) as a core driver. Construction 4.0 rules the digital world encompassing several information technologies such as blockchain, big data, AR/VR (Augmented Reality/Virtual Reality), drones, IoT (Internet of Things), cloud-based project

collaboration, BIM (Building Information Modeling), autonomous robots, DfMA (Design for Manufacture and Assembly), PEB (Pre-Engineered Buildings), 3D printing, and the list goes on [1][2]. The crux of many of these technologies lies in capturing the “real physical” world data to generate the “virtual” model to enable the experiments for specific decision-making. Hereafter, the words “virtual” and “digital” are used interchangeably throughout the paper.

The other recent buzz word from the digital era that is popular in the construction industry is the Digital Twin. While many of the above IT techniques focus on physical to virtual models and henceforth the decision-making, the Digital Twin concept follows an iterative loop of physical to virtual and then again to physical for communicating the findings from the “virtual” model into the “real physical-construction site” [3][4] and is portrayed in Figure 1.

Researchers in the past have applied several hardware/software technologies such as IoT/Sensor, GPS (Global Positioning Systems), Tag identification systems, Drones etc. to capture/track real-time data of the mobile resources such as workers, materials, or equipment at the construction site [5][6][7][8][9]. This data can be used to perform several analyses such as scheduling, project performance monitoring, productivity analysis, etc. using a digital platform. In this study, RFID has been used to collect the data for conducting safety performance, which is a very common tag identification system in practice for several decades [10].

Any safety policy whether CDM (Construction Design and Management Regulations, 2015) [11], OSH Act (Occupational health and Safety Act, 1970) [12] or BoCW (Building and other Construction Workers Act, 1996) [13] enforce safety of all the workers working in a construction site. Researchers till date follow the OSHA’s fatal four classifications such as falls, struck-by objects, caught-in/between, electrocutions, and others [14]. In this group of classification, fatality due to falls is ranked as the most hazardous. Despite several fall precautions and preventive measures that are in industry practice today, still the accidents/fatality due to falls cannot be eliminated completely. The other fall hazard

included in this study is the materials/objects/debris/hand tools, etc. falling on the workers which is generally termed as overhead work.

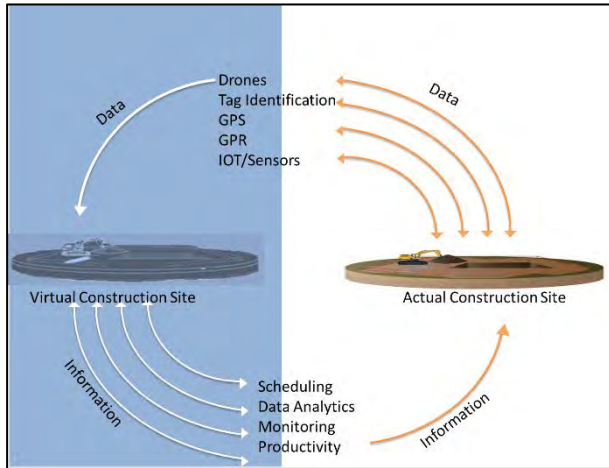


Figure 1. Concept of Digital Twin

Therefore, the objective of this study is to develop a Digital Twin framework that provides worker safety from fall hazards and overhead works during the project progress. To achieve this objective, RFID technology is used to capture the source data from the construction sites and is modeled in BIM (Revit) with the help of Dynamo. The contribution claimed in this study is the use of Dynamo Scripting to capture the data from RFID reader to the BIM software. Job safety analysis is performed in the BIM software and suitable precautions and warnings are conveyed to the site personnel on mobile application, to help sustain a zero-accident site. This experiment is carried out for various scenarios of hypothetical construction sites and the initial results are discussed in Section 4 of the paper. The scope of this study is limited to falling of materials, equipments and workers.

2 Safety Background

Construction Industry is one of the biggest industries that creates a huge employment opportunity to a large spectrum of skilled and unskilled workers [15]. As per ILO (International Labour Organization), the construction industry ranks among the top three industries having the highest accident/fatality rates with a disproportionately high number of recorded accidents globally. Patel & Jha [16] had reported that approximately 48000 workers die each year because of the occupational accidents and one in four workers die in the Indian construction sites. It is a well-known fact that accidents on sites are unavoidable and keeps recurring although the severity and marginally, the number of accidents has been reduced. Despite stern regulations and codal provisions for the hazardous operations being

chalked out meticulously across the globe such as CDM, OSHA, BoCW, etc., still the vision of zero-accidents at the construction site has not been achieved. The term “zero-accident” is more of a philosophy rather than a numeric goal. The zero-accident vision is based on a belief that all accidents are preventable and therefore, must be avoided at all costs at a workplace through strategic policy implementation.

Safety measures due to worker falling from heights are classified into two categories such as fall arrest system or active protection system and fall restraint system or passive protection system. Here, fall arrest system prevents the workers from falling and examples include guard rails, barricades, etc., in addition to safety lanyard, lifeline, anchor point and a harness. On the other hand, fall restraint system protects the workers after the fall incident has occurred and examples include safety nets. Safety measures in case of overhead works include adequate toe boards in the guard rails and scaffolds, debris nets, safety nets, catch platforms, chutes, etc. Despite all these safety precautions, workers are injured in the construction sites due to falls. One of the reasons can be that safety is not always in the minds of the workers and require a third-party intervention.

There are several techniques to capture the real-time data in construction sites i.e., using RFID, vision-based, wireless networks, ultrasound, GPS (Global Positioning System), etc. [17][18][19][20]. It is a well-known fact that RFID is a very common tag identification system that is popular in construction industry practice [10]. The choice of IFC (Industry Foundation Classes) to capture the data from RFID reader into the BIM model has also been reported in some articles [21][22]. In this study, an attempt is made to investigate the Dynamo scripting for capturing the RFID data into the BIM model as it was not attempted earlier.

3 Digital Twin Framework Development using Pilot Example

As mentioned in the earlier section, the objective of the study is to implement safe worker practices in the construction site. The scope of this study is limited to falls and overhead works only. Although there are adequate passive preventive mechanisms before the construction progress happens, still accidents and/or near miss do happen in the construction site and they are unavoidable. Therefore, in this study, a Digital Twin model that has two-way interactions with the virtual model and the real physical model is setup treating it as a third-party monitoring mechanism for establishing safety. This Digital Twin framework is arranged in six simple steps as seen in Figure 2 and is elaborated below.

Step I: Select a construction site for applying the digital twin concept to monitor the safety performance.

To demonstrate this concept, a hypothetical pilot example that mimics a typical construction site-in progress is chosen. This construction site example that is modeled in the Revit software is seen in Figure 3.

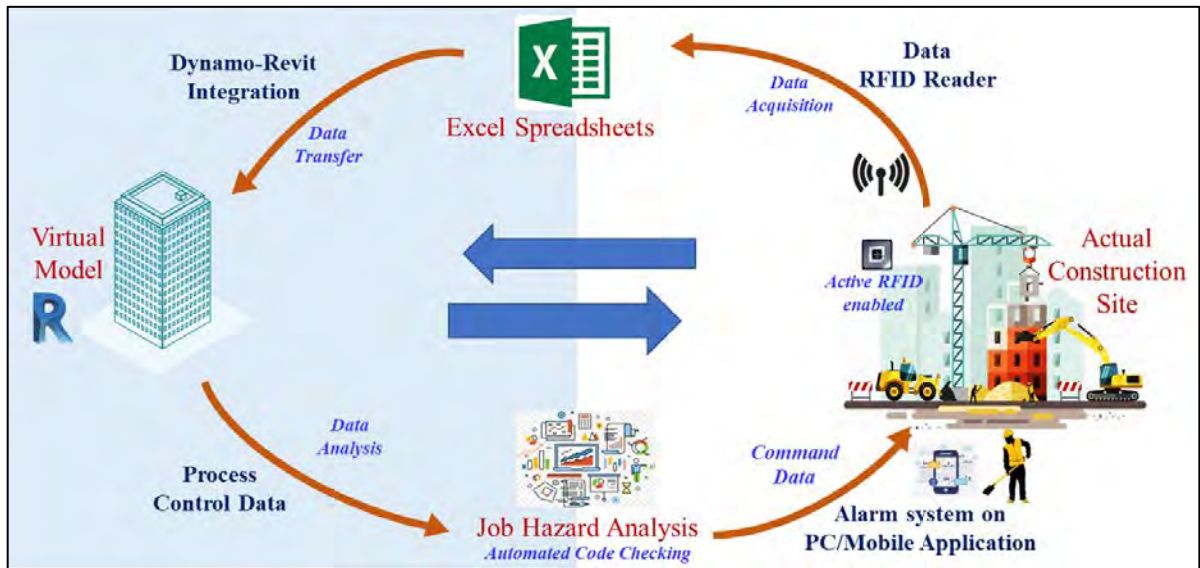


Figure 2. Framework for the Proposed Digital Twin Model

Step II: In this study, the Digital Twin concept is enabled using the RFID technology. A typical RFID system requires the tags to be attached with the resources to be tracked and the reader along with an antenna for reading the information from the tags. Accordingly, the RFID readers are placed at the earmarked locations so that they can detect the presence of the RFID tags and communicate the location to the server as seen in the Figure 2.

stored/updated in the server in the Excel spreadsheets. From this table, it is evident that although the worker is safe about Material-1, the worker can expect a fall hazard regarding Material-2.

Step III: To represent the location of resources in the actual site, this data must be imported in the virtual model. For this purpose, the coordinates from the excel sheet are transferred to the Revit model using the Dynamo scripting.

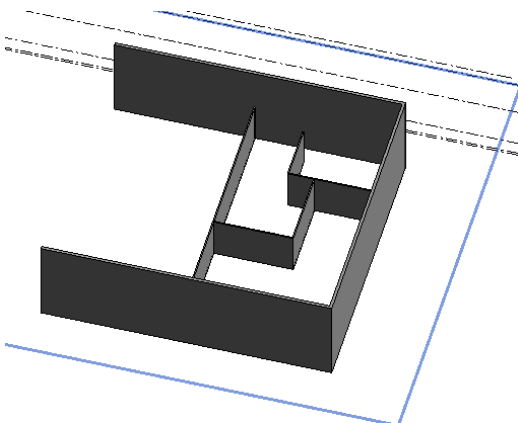


Figure 3. Hypothetical Construction Site (Pilot example)

For instance, if 2 materials and 1 worker location is to be tracked, then the RFID tags are attached to those chosen workers, materials and equipments in the site premises and the location are detected using the RFID reader along X, Y and Z coordinates. Table 1 illustrates the coordinates of the three resources and this is

Table 1 Location Co-ordinates in Spreadsheet

Tag Description	X-co ordinate	Y-co ordinate	Z-co ordinate
Material-1	5	20	30
Material-2	5	5	30
Worker	5	5	5

The first part of the scripting is to trace the location coordinates from the Excel spreadsheet using Dynamo as seen in Figure 4.

Step IV: The next step is to differentiate the two types of resources, i.e., the workers and the materials individually without any confusion as in the screenshot in Figure 5, Figure 6, and Figure 7. Hence, in this example, sphere and polygon are chosen as the two different means of representing the materials and the workers respectively.

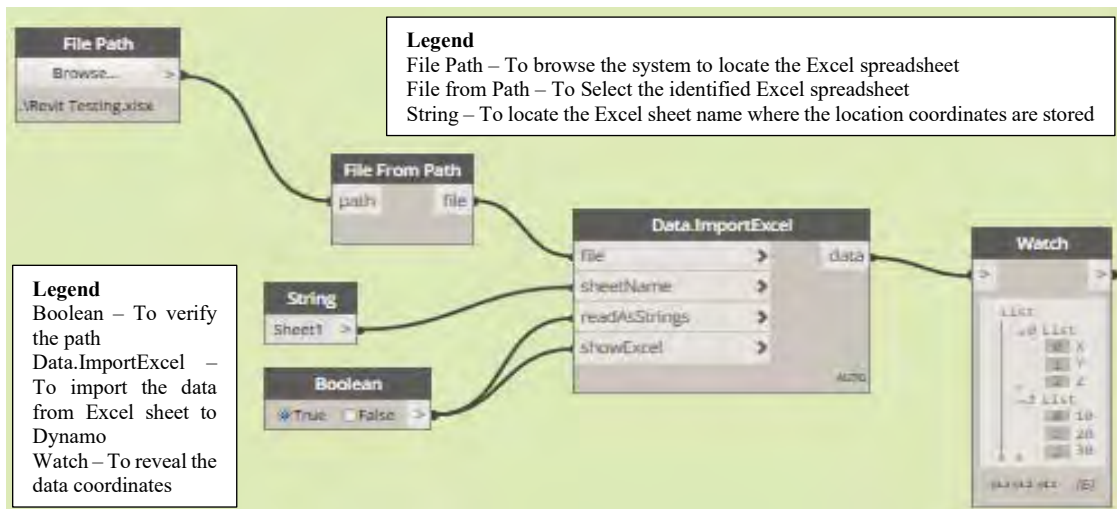


Figure 4. Dynamo Script Part 1 – Import Location Coordinates from Excel

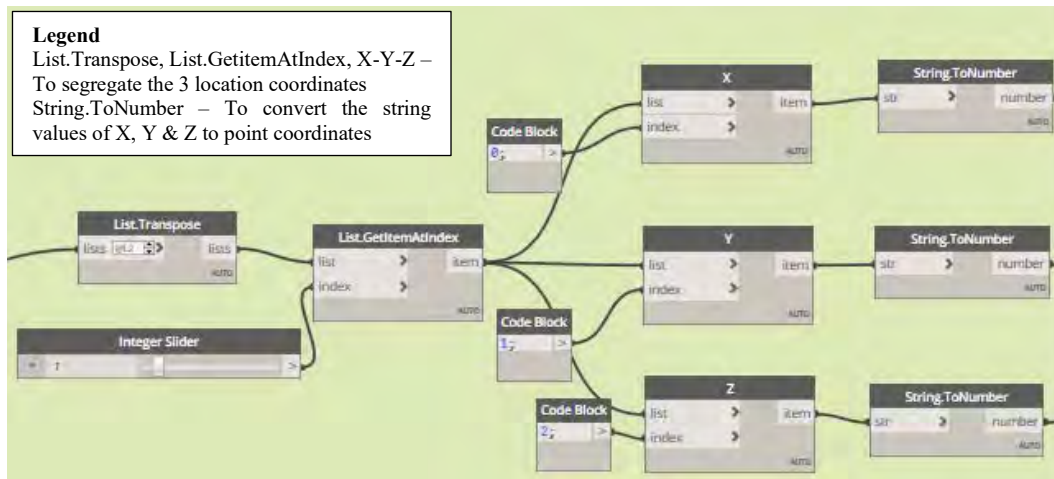


Figure 5. Dynamo Script Part 2 – Coordinates conversion in the desired format

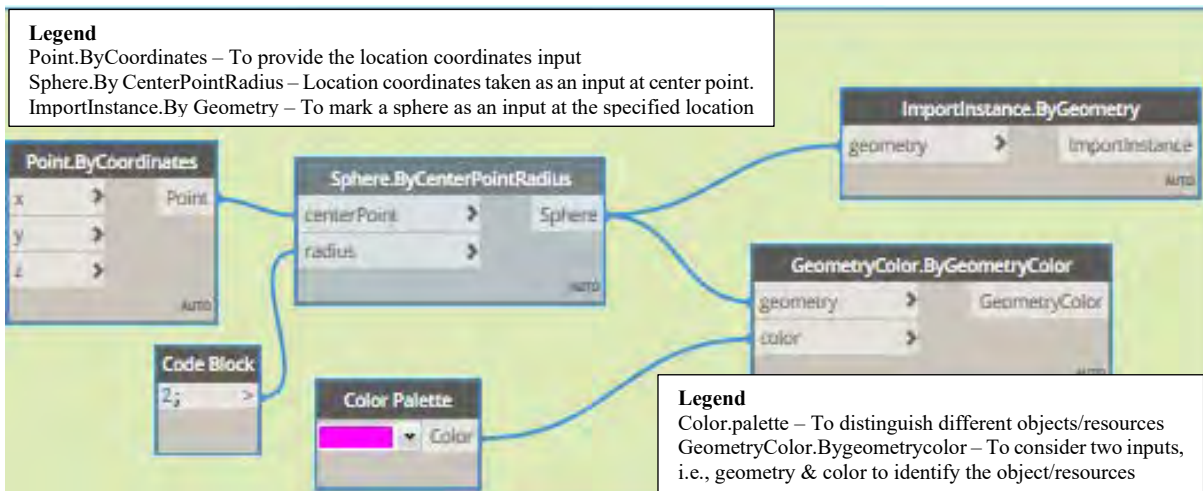


Figure 6. Dynamo Script Part 3 – Locating Materials

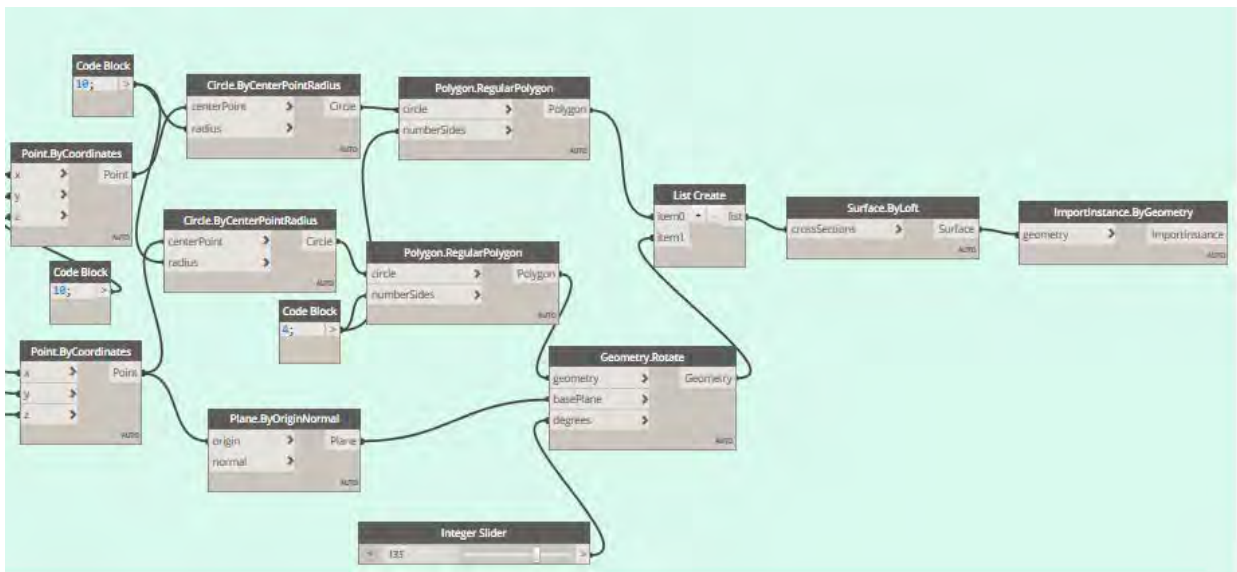


Figure 7. Dynamo Script Part 4 – Locating Worker

Step V: Reload and refresh the Revit Model so that the exact location of material and workers as captured in the construction site will be reflected in the virtual model as seen in the Figure 8 and Figure 9. This new location of workers and materials in the virtual model shall be used to analyse the hazards, if any through backend coding utilizing safety codal provisions.

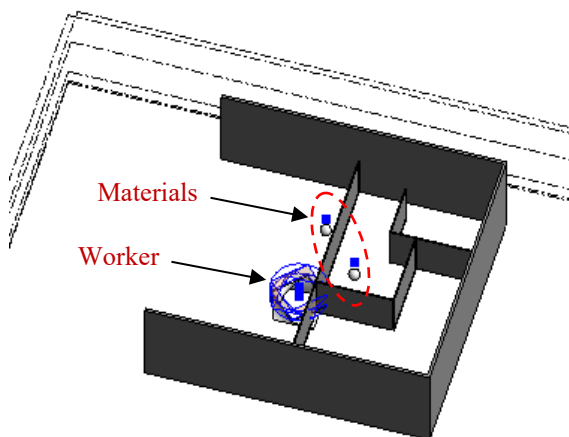


Figure 8. Regenerated Revit Model-I (Pilot example)

Step VI: After the updation of the location data, hazard proximity analysis has been carried out through backend coding (automated code checking) using python and java script (refer Figure 10). Safety guidelines regarding various site scenarios have been obtained from the codal provisions (OSH, BIS, etc.). Upon non-compliance, a warning is first generated in the virtual Revit model. Accordingly, an alarm/notification containing the appropriate safety solution will be communicated to the concerned workers/supervisors

(refer Figure 10) at the construction site on their mobile application, to be safe from the falling objects/fall zone.

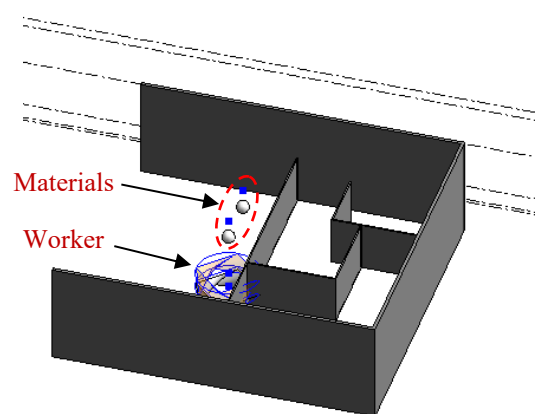


Figure 9. Regenerated Revit Model-II (Pilot example)

Pilot Example Results: Figure 8 presents the location of one worker and two materials of the construction site in the Revit model. This is a safe situation wherein the worker and the materials are far apart from one another and there is rare chance of worker incidents to occur. But there is a possibility of nil progress or idle situation which can be investigated from the site office and thereafter investigated from the crew.

Similarly, Figure 9 presents the location of one worker and two materials of the construction site in the Revit model at another instance. This isometric projection shows that one material is above the worker location and he must be warned for safety measures. The situation assumed is that the material is placed above the forklift and with the movement of the forklift, the material location and worker location are merged in the

planar coordinates except in the space. Accordingly, an alarm is notified to the worker as shown in Figure 10.

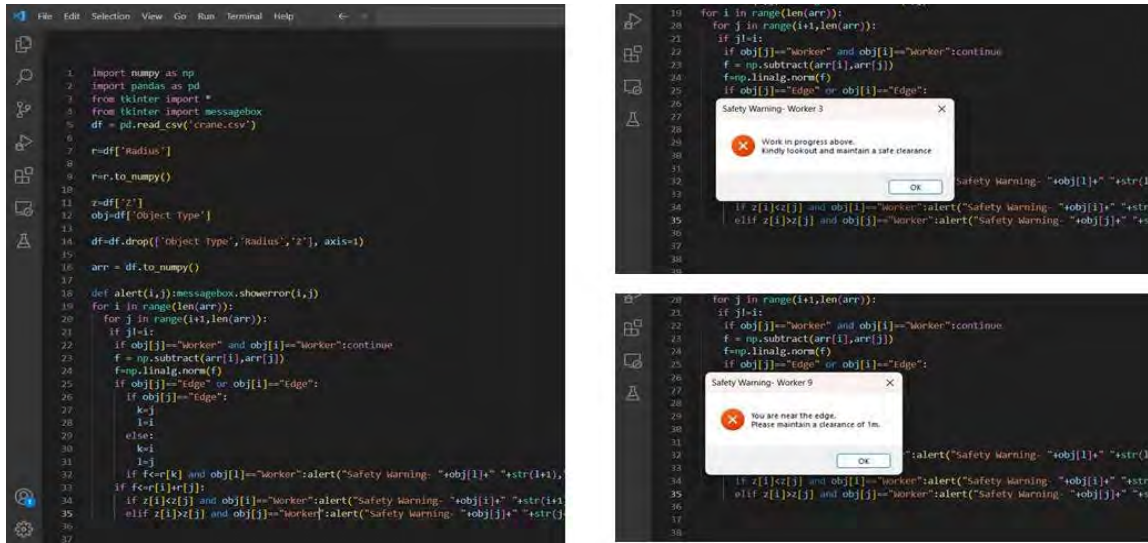


Figure 10. Coding snippet (left) and Safety warning notifications for Pilot example (right)

4 Analysis and Results - Caselets

In this section, two different scenarios about the movement of materials, equipments and worker is captured from the different types of construction sites at a specific time interval and analyzed for safety compliance. The pilot example in the previous section has been used for the development of the framework, which has been further verified by means of the two hypothetical caselets undertaken in this section.

Caselet - 1: Figure 11 illustrates the situation where a tower crane is operating at a construction site. Four different workers are working in the vicinity of the crane, thus raising a safety concern. The workers along with the crane have been provided with the RFID tags. As can be seen in the figure, there are three workers who are working under the swing radius of the crane (here 15 m). They are under the fall zone of the materials that the crane is lifting and thus need to be informed to move outside the swing radius of the crane to safety. But, the fourth worker being in the safe zone need not be notified, thus avoiding a false concern.



Figure 11. Construction Site Scenario (Caselet - 1)

The scenario is modeled in Revit and the location information of the resources are obtained through the RFID sensors, which are further transferred in Revit through the dynamo plugin. Upon hazard analysis, the respective workers in the unsafe zone are notified using the mobile application as shown in Figure 12.

Caselet – 2: The next case showcases a three storey under construction building site as shown in Figure 13.

Five workers along with three equipments namely drilling machine, chipping machine and a crowbar (all with RFID tags) working on different storey have been taken to illustrate the unsafe scenarios at site. As evident in the figure, the worker with crowbar is close to an opening on the third storey. Also, drilling work is happening on the edge of the second storey and another worker is working just beneath on the ground floor. Similarly, chipping works is in progress on the first floor and brickwork is happening just below it on the ground floor.

Similar steps of action, as already explained in the previous section are taken to model the physical site and their allied information through Dynamo-Revit integration. And then, hazard proximity analysis is

performed through coding to check for safety compliance against various codal provisions. Thus, a warning is generated in the Revit model at the main site office to notify the same to the concerned person/s. Further notifications regarding any safety actions are then communicated to the concerned workers on their mobile application (refer Figure 13).

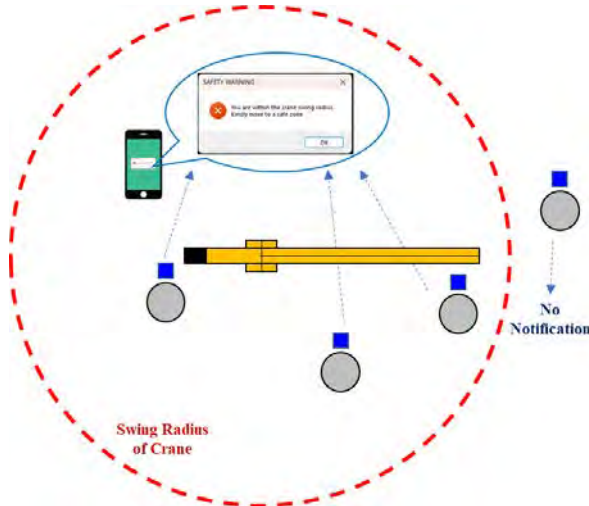


Figure 12. Safety notifications to concerned workers

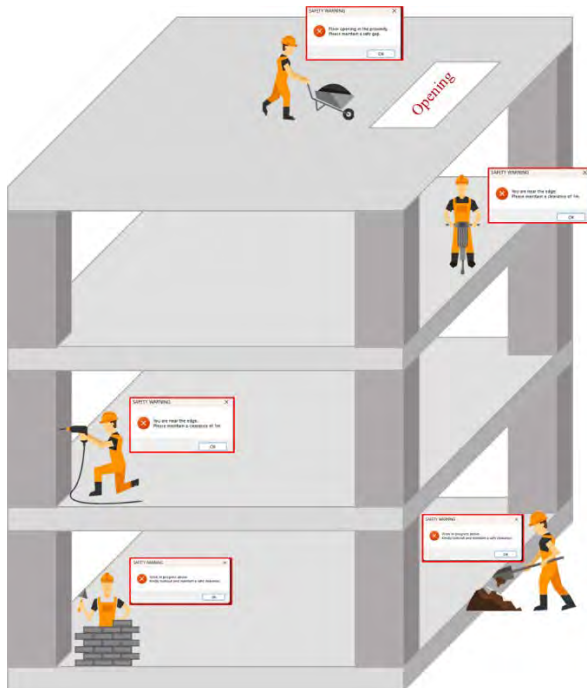


Figure 13. Building site scenario and corresponding safety notifications to workers (Caselet - 2)

5 Discussions

Live data collection from an ongoing construction project and real physical experiments was a great

challenge during the pandemic. Hence, hypothetical case examples have been used to mimic typical construction sites. It is assumed that the physical experiments will generate the data that was assumed in this study and the dynamo scripting was carried out. Verification of this exercise through various hypothetical cases have been carried out in the previous section of the study. Although, the framework has proved effective for these hypothetical case studies, the validation of the framework on an actual live construction site is essential and is therefore, a plan for the future.

Also, this dynamo scripting is highly efficient for locating and monitoring few resources. Hence, in the pilot example, 2 materials and 1 worker were chosen to portray the resources. When this concept is applied in a medium or large construction site, enormous effort is required for scripting as it must be written specifically for each and every resource. Since, this is not a feasible solution, heuristic way of developing the dynamo scripting for any resource independently with minimal effort is required.

6 Summary

The framework for the Digital Twin model based on the integration of RFID-Dynamo-Revit shall provide the seamless data transfer from the actual construction site to virtual model. This combination framework is expected to read and trace the workers, equipments and materials location from the actual construction site into the virtual model for monitoring the site in terms of safety round the clock.

In this study, dynamo scripting was used for reading the resources data from RFID to model the same into the Revit software which was not attempted earlier. With the inputs given from the hypothetical construction site, the Revit model was regenerated at suitable intervals for evaluating safety performance. Hence, dynamo scripting can be applied to small construction sites for digital safety performance, keeping in mind its limitations.

References

- [1] Sawhney, A., Riley, M. & Irizarry, J. Construction 4.0 – An Innovation Platform for the Built Environment. Routledge Taylor & Francis Group, 2020.
- [2] Jazzar, M.E., Urban, H., Schranz, C. and Nassereddine, H. Construction 4.0: A Roadmap to Shaping the Future of Construction. In *Proceedings of 37th International Symposium on Automation and Robotics in Construction (ISARC)*, pages 1314-1321, 2020.
- [3] Boje, C., Guerriero, A., Kubicki, S. and Rezgui, Y. Towards a Semantic Construction Digital Twin:

- Directions for Future Research. *Automation in Construction*, 114:103179, 2020.
- [4] Caramia, G., Corallo, A., and Mangialardi, G. The Digital Twin in the AEC/FM Industry: A Literature Review. In *Proceedings of the Conference CIB W78*, pages 11-15, 2021.
- [5] Xie, M.C. and Pan, W. Opportunities and Challenges of Digital Twin Applications in Modular Integrated Construction. In *Proceedings of 37th International Symposium on Automation and Robotics in Construction (ISARC)*, pages 278-284, 2020.
- [6] Sacks, R., Brilakis, I., Pikas, E., Xie, H.S. and Girolami, M. *Construction with Digital Twin Information Systems, Data-centric Engineering, Vol. 1*. Cambridge University Press, 2020.
- [7] Zhao, J., Seppanen, O., Peltokorpi, A., Badihi, B. and Olivieri, H. Real-time Resource Tracking for Analyzing Value-adding Time in Construction. *Automation in Construction*, 104:52-65, 2019.
- [8] Deng, M., Menassa, C.C. and Kamat, V.R. From BIM to Digital Twins: A Systematic Review of the Evolution of Intelligent Building Representations in the AEC-FM Industry. *Journal of Information Technology in Construction*, 26: 58-83, 2021.
- [9] Hou, L., Wu, S., Zhang, G., Tan, Y. and Wang, X. Literature Review of Digital twins Applications in Construction Workforce Safety. *Applied Sciences*, 11: 339, 2021.
- [10] Kasim, N., Latiffi, A.A. and Fathi, M.S. RFID Technology for Materials Management in Construction Projects – A Review. *International Journal of Construction Engineering and Management*, 2(4A):7-12, 2013.
- [11] CDM (Construction Design and Management Regulations) (2015). On-line: <https://www.legislation.gov.uk/ukxi/2015/51/regulation/17/made>, Accessed: 13/12/2022.
- [12] OSH Act (Occupational Safety and Health Act) (1970). On-line: <https://www.osha.gov/laws-regs/regulations/standardnumber/1926>, Accessed: 10/12/2022.
- [13] BoCW (Building and other Construction Workers Act) (1996). On-line: <https://clc.gov.in/clc/acts-rules/building-and-other-construction-workers>, Accessed: 05/01/2023.
- [14] Albert, A., Pandit, B. and Patil, Y. Focus on the fatal-four: Implications for Construction Hazard Recognition. *Safety Science*, 128:104774, 2020.
- [15] ILO (International Labour Organization) website. On-line: <https://www.ilo.org/>, Accessed: 21/03/2023.
- [16] Patel, D.A. and Jha, K.N. An Estimate of Fatal Accidents in Indian Construction. In *Proceedings of 32nd Annual ARCOM Conference*, pages 577-586, 2016.
- [17] Soltanmohammadlou, N., Sadeghi, S., Hon, C.K.H. & Mokhtarpour-Khanghah, F. Real-time Locating Systems and Safety in Construction Sites: A Literature Review. *Safety Science*, 117:229-242, 2019.
- [18] Calvetti, D., Mêda, P., Chichorro Gonçalves, M., and Sousa, H. Worker 4.0: The future of sensed construction sites. *Buildings*, 10(10):169, 2020.
- [19] Rao, A.S., Radanovic, M., Liu, Y., Hu, S. Fang, Y., Khoshelham, K., Palaniswami, M. and Ngo, T. Real-time Monitoring of Construction Sites: Sensors, Methods, and Applications. *Automation in Construction*, 136:104099, 2022.
- [20] Zhao, J., Zheng, Y., Seppanen, O., Tetik, M. and Peltokorpi, A. Using Real-time Tracking of Materials and Labor for Kit-based Logistics Management in Construction. *Frontiers in Built Environment*, 122, 2021.
- [21] Costin, A.M., Teizer, J. and Schoner, B. RFID and BIM-enabled Worker Location Tracking to Support Real-time Building Protocol Control and Data Visualization. *Journal of Information Technology in Construction*, 20(29):495-517, 2015.
- [22] Sattineni, A. and Azhar, S. Techniques for Tracking RFID Tags in a BIM Model. In *Proceedings of 27th International Symposium on Automation and Robotics in Construction (ISARC)*, pages 346-354, 2010.

Evaluation of ground stiffness using multiple accelerometers on the ground during compaction by vibratory rollers

Y.Tamaishi^{1,2}, K.Fukuda², K.Nakashima³, R.Maeda², K.Matsumoto³, R.Kurazume³

¹Tamaishi Juki Co., Ltd., Japan

²Graduate School of Information Science and Electrical Engineering, Kyushu University, Japan

³Faculty of Information Science and Electrical Engineering, Kyushu University, Japan
tamaishi@irvs.ait.kyushu-u.ac.jp, k_fukuda@irvs.ait.kyushu-u.ac.jp, k_nakashima@irvs.ait.kyushu-u.ac.jp,
maeda@irvs.ait.kyushu-u.ac.jp, matsumoto@irvs.ait.kyushu-u.ac.jp, kurazume@ait.kyushu-u.ac.jp

Abstract –

Soil compaction is one of the most important basic elements in construction work because it directly affects the quality of structures. Compaction work using vibratory rollers is generally applied to strengthen ground stiffness, and the method that focuses on the number of compaction cycles is widely used to manage the ground stiffness by vibratory rollers. In contrast to this method, the continuous compaction control (CCC) using accelerometers installed on the vibratory rollers has been proposed as a quantitative evaluation method more suited to actual ground conditions. This method quantifies the distortion rate of the acceleration waveform of the vibratory roller. However, this method based on acceleration response has problems in measurement discrimination accuracy and sensor durability because the accelerometer is installed on the vibration roller, which is the source of vibration. In this paper, we propose a new ground stiffness evaluation method using multiple accelerometers installed on the ground surface. The proposed method measures the acceleration response during compaction work by vibratory rollers using multiple accelerometers on the ground surface. Experiments show the proposed method has a higher discrimination than the conventional methods.

Keywords –

Vibratory rollers, Ground stiffness evaluation

1 Introduction

Vibratory rollers are used for compaction to strengthen the ground stiffness. To manage the ground stiffness using vibratory rollers, the number of compaction cycles is widely used as a compaction work management method.

In contrast, the continuous compaction control (CCC) method utilizing acceleration response during

compaction has been proposed as a quantitative evaluation method that reflects actual ground conditions [1] [2] [3] [4] [5]. This method uses accelerometers installed on a vibratory roller to quantitatively evaluate changes in ground stiffness owing to compaction. Performance was compared between CCC measurements and location-specific in-situ test results. By including the effect of moisture content using multivariate regression, the consistency between the CCC and in situ test data sets was higher than without inclusion [6].

This method uses the phenomenon in which the acceleration waveform of a vibratory roller is disturbed as the stiffness of the compacted soil increases and quantifies the distortion rate of the waveform. This phenomenon is caused by the vibratory rollers bouncing up and impacting against the stiffened ground.

However, this method based on acceleration response has problems in terms of measurement discrimination accuracy and sensor durability because accelerometers are attached to the vibratory rollers that are the source of vibration.

This paper proposes a ground stiffness evaluation method with a higher discrimination than that in the conventional method using multiple accelerometers installed on the ground surface to measure the acceleration response during compaction by a vibratory roller.

In the experiment, the embankment was compacted using a vibratory roller, and the acceleration signals of the ground surface vibration were measured during compaction using accelerometers installed on the ground (proposed) and on the vibratory roller (conventional). The compaction control value (CCV) [7] was used as an index to evaluate the ground stiffness. The CCV obtained by the proposed method which utilizes the multiple accelerometers on the ground was compared with the conventional CCV obtained by the accelerometer on the vibratory roller. In addition, the coefficient of the ground reaction force was measured using a light falling weight deflectometer (LFW) test and its relationship with the

CCV obtained using the proposed method was also verified.

2 Background

CCC (or the acceleration response method) uses an acceleration sensor fixed to the main body of a vibratory roller to estimate the degree of ground compaction from the acceleration waveform during the compaction process. The phenomenon used in this method is that when compaction by the vibratory roller progresses, a spectrum appears in the amplitude spectrum of the acceleration waveform at a frequency other than the fundamental frequency of the compaction by the vibratory roller.

This phenomenon is considered to be caused by a vibratory roller bouncing up against a rigid ground and impacting it [8]. CCC evaluates the ground stiffness by calculating the spectral turbulence using the compaction meter value (CMV) [1], the resonance meter value (RMV), CCV [5], etc., which calculates turbulence ratio based on the ratio of the spectra at multiple vibration frequencies. CCC can manage the compaction condition in 2-dimensions by combining the obtained spectral disturbance with the positional information obtained by the GNSS installed on the vibratory roller.

However, this conventional method has a problem with measurement discrimination accuracy, particularly in soils with a high water content. In such cases, the spectral turbulence becomes unclear, and evaluating the degree of compaction is often difficult. In addition, because the accelerometer is installed at the vibration source, the measured values contain a significant amount of noise. Furthermore, the proximity of the sensor to the vibration source can cause the sensor to malfunction.

The ground stiffness evaluation method proposed in this study is similar, in that it is based on the amplitude spectrum ratio of the acceleration waveforms. The difference is that the multiple accelerometers are installed on the ground. The installation of the accelerometers on the ground reduces sensor failures and the signal-to-noise ratio; this is expected to improve the measurement discrimination accuracy.

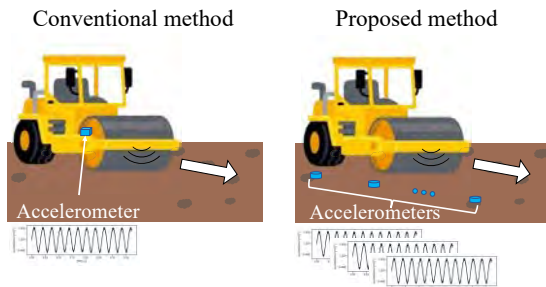


Figure 1. Comparison image of the conventional method and the proposed method

Figure 1 shows the comparison image of the conventional method and the proposed method.

3 Evaluation method

In this study, the ground stiffness during compaction by a vibratory roller is evaluated by integrating the vibration data obtained from several distributed accelerometers on the ground. The vibration data from each sensor are obtained as triaxial acceleration signals corresponding to the operation of the vibratory roller.

The Z-axis is vertical to the ground, and the X-Y axis is horizontal to the ground. This study uses only the X-Y-axis component that is stably obtained because the Z-axis signal is suppressed when the wheel of the vibratory roller passes over the ground.

First, the short-time Fourier transform (STFT) is applied to acceleration signals $a_{i,x}$, $a_{i,y}$ in the X-Y axis at the i -th sensor ($i = 1 \dots N$) (N is the total number of sensors) to obtain spectrogram $S_{i,x}$, $S_{i,y}$. Next, composite spectrogram \tilde{S}_i is calculated as follows:

$$\tilde{S}_i = \sqrt{S_{i,x}^2 + S_{i,y}^2} \quad (1)$$

As explained above, ground stiffness is estimated using the obtained composite spectrogram, \tilde{S}_i . In the evaluation of ground stiffness based on the roller acceleration response, the acceleration waveform is known to be disturbed as the ground stiffness increases.

Unlike conventional methods that directly measure acceleration signals of the vibratory roller, which is a vibration source, this study measures the acceleration signals of vibrations propagating on the ground surface. This method is expected to reduce the signal-to-noise ratio. In this study, CCV [7], defined by the following equation, is used as the ground stiffness index.

$$\text{CCV}(S) = \frac{s'_0 + s'_1 + s_1 + s'_2 + s_2}{s'_0 + s_0} \times 100 \quad (2)$$

s_0 denotes the fundamental component corresponding to oscillation frequency of spectrogram S (the vibratory roller frequency), s_n denotes the high-frequency component corresponding to $n + 1$ times the frequency, and s'_n is the 1/2 fractional harmonic component corresponding to $n + 0.5$ times the frequency. As the ground stiffness increases, high-frequency and fractional harmonic components dominate, and the CCV increases owing to turbulence in the acceleration waveform. Finally, the CCVs obtained from N sensors are averaged.

$$\text{CCV} = \frac{1}{N} \sum_{i=1}^N \text{CCV}(\tilde{S}_i) \quad (3)$$

4 Experiment

4.1 Experimental setup

In this study, an embankment was used as the experimental environment. The ground rolling experiment was conducted at an outdoor test site located on the Ito campus at Kyushu University. The experiment was conducted using a vibration roller (SAKAI, SV512D V) and high-sensitivity 3-axis accelerometers (Onosokki, NP-7310).

In the experiment, compaction and measurement lanes were prepared on the embankment. Accelerometers were placed at 5 m intervals at the top of the embankment, and a vibratory roller ran along the compaction lane. The compaction experiments were conducted on two layers (1st and 2nd layers). In the 1st layer, there were two compaction lanes: the F-lane far from the accelerometers and the N-lane close to them. Figure 2 shows the arrangement of the accelerometers and dimensions of the embankment on each layer, and Figure 3 shows the experimental conditions. The experiments were conducted as follows.

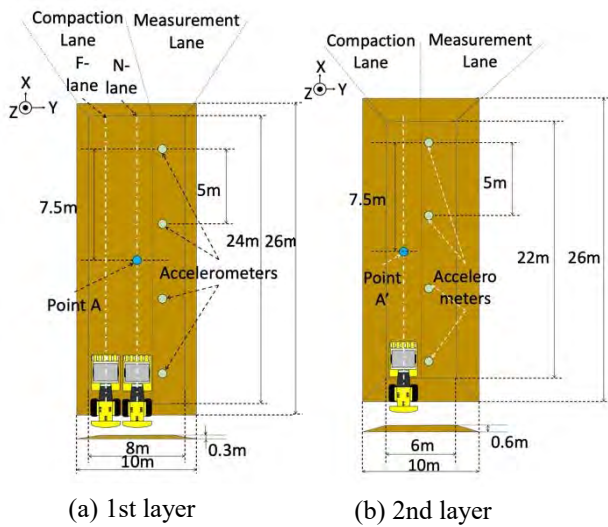


Figure 2. Arrangement of accelerometers



Figure 3. Experimental setup in the outdoor field

(1) A 0.3 m thick layer of soil was spread onto a well-compacted base. (1st layer)

(2) The soil was rolled 12 times back and forth (24 times in total) using a vibratory roller on the measurement lane. After rolling the measurement lane, four accelerometers were fixed to the ground surface of the measurement lane with stakes at intervals of 5 m along compaction lanes.

(3) Twelve round trips (24 times in total) of rolling by the vibratory rollers were repeated on the compaction lane, and the measured values of each accelerometer were recorded.

(4) After removing accelerometers, a 0.3 m thick 2nd layer of soil was spread on the former layer.

(5) The 2nd layer test was subjected to the same procedure (2) to (3) as the 1st layer to measure acceleration.

LFWD tests were conducted during compaction (2, 4, 6, 8, and 10 round trips) on each layer. In the LFWD test, an impact load was applied by free-falling a weight on the loading plate. The displacement caused by the impact was measured at the center of the load and at the radial position from the center of the load to obtain the coefficient of the subgrade reaction [9].

$$K_{P.FWD} = \left(\frac{P_X}{\delta_X} \right) \cdot \left(\frac{D_{Y1}}{D_{Y2}} \right) \quad (4)$$

$K_{P.FWD}$: Coefficient of subgrade reaction by LFWD (MN/m³)

P_X : Load stress at displacement X mm (MN/m³)

δ_X : Displacement X (mm)

D_{Y1}, D_{Y2} : Diameter of LFWD loading plate Y1 (cm), Diameter of FWD loading plate Y2 (cm)

4.2 Soil condition

Figure 4 shows the particle size distribution curve of the fill material used in this experiment. The gravel content was low, but the fine-grained (clay and silt) content was high (> 50%), making the soil difficult to compact. All uniformity coefficients were higher than 10, and the grain size distribution was good. Table 1 shows the result of particle component ratio.

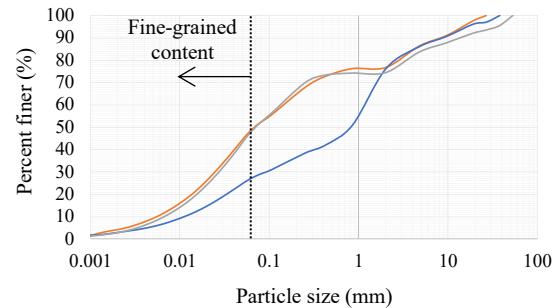


Figure 4. Particle size distribution curve

Table 1 Particle component ratio

Parameters used for classification	Sample		
	No.1	No.2	No.3
Coarse gravel %	2.4	3.9	8.0
Medium gravel %	11.3	10.1	8.4
Fine gravel %	9.6	9.9	9.2
Coarse sand %	0.5	25.2	0.2
Medium sand %	8.4	12.6	4.3
Fine sand %	16.4	9.8	18.7
Silt %	42.1	23.1	43.5
Clay %	9.3	5.6	7.7
Maximum grain size mm	26.5	37.5	53.0
Coefficient of uniformity	30.0	104.2	21.5
Coefficient of curvature	0.8	0.5	0.8

The dry density versus moisture content curve for the same fill material is shown in Figure 5. The samples used for the measurements were prepared using the dry method and were used in the repeat method. Table 2 presents the number of times the samples were rammed and the other test parameters.

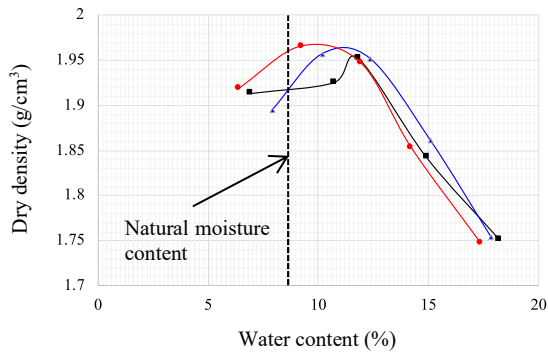


Figure 5. Moisture–density curve for fill materials

Table 2 Dry density versus moisture content test conditions

Type of soil	Decomposed granite
Mass of rammer (kg)	2.5
Falling height (m)	0.3
Number of times tampered per layer	25
Number of layers tampered	3
Inner diameter of mold (m)	0.1
Height of mold (m)	0.1273
Volume of mold (m³)	0.001
Maximum grain size (m)	0.019

The results of the experiment on the samples from the three sites showed that the average optimum moisture content was approximately 10.9%, average maximum dry density was approximately 1.96 g/cm³, and natural moisture content at the time of the experiment was approximately 8.7%.

4.3 Experimental results

Figure 6 shows the CCV. In each figure, the CCV for each position on the forward journey (left), CCV for each position on the backward journey (center), and CCV rate of change averaged over the travel section (right) are also shown. Results of N-lane on the 1st layer are shown in Figure 6 (a), and 2nd layer are shown in Figure 6(b). In these figures, #1 ~ #4 indicate the positions of accelerometers.

The CCV rate of change is defined as relative rate of change r_n with respect to the CCV_n at the n th time of compaction. The r_n is calculated separately for each case of forward and backward journey, thus n is $3 \leq n \leq 24$ when determining the r_n .

$$r_n = \frac{CCV_n - CCV_{n-2}}{CCV_{n-2}} \quad (5)$$

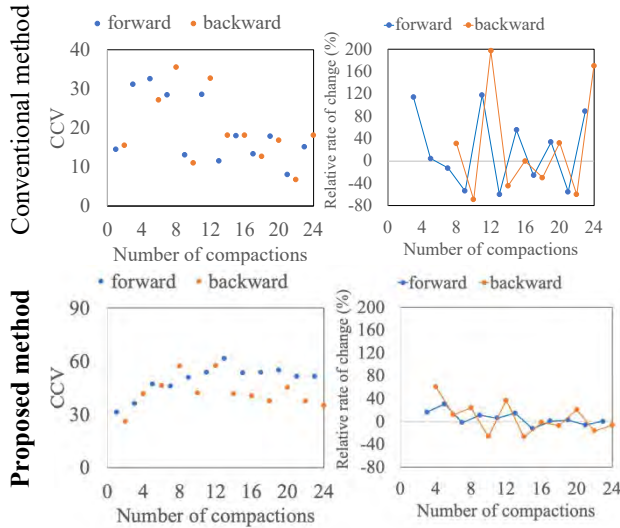
As shown in Figure 6, the CCV of the proposed method increased with the number of compaction cycles, showing a convergence trend on each layer. However, the CCV of the conventional method increased and decreased irregularly and did not converge. This is considered to be owing to the reduction in the signal-to-noise ratio by the separation of the vibration source and the measurement device that improves the convergence and discrimination of the proposed method.

In addition, Figure 7 shows the relationship between CCV and the number of compaction cycles when the vibratory roller passed at the position A on the N-lane and A' (midway position, 7.5m) in Figure 2. The relationship between the rate of change of CCV and the number of compaction cycles with same condition is also shown in Figure 7.

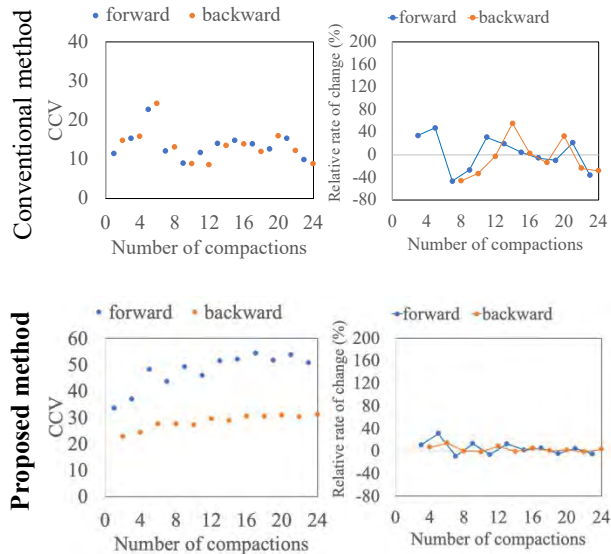
The conventional method has a large variation in CCV. The CCV increased when the number of compaction cycles was small, but decreased when the compaction had progressed on each layer.

On the other hand, the CCV measured by the proposed method tended to increase and converge as the number of compaction cycles increased. The CCV values measured in the forward directions were larger than those measured in the backward direction. It is possible that the rear wheels block the vibrations propagating through the ground when the rear wheels are ahead of the vibratory wheels, but this should be verified in the future.

The CCV rate of change varied widely with the conventional method and the trend was difficult to read, but with the proposed method, it decreased and showed a convergence trend on each layer.



(a) CCVs and r_n evaluated on N-lane of the 1st layer



(b) CCVs and r_n evaluated on the 2nd layer

Figure 7. CCVs and r_n when the vibratory roller passed at the positions A and A' in Figure 2

Figure 8 shows the comparison of CCVs at three points (5m, 7.5m and 10m) on the N-lane of the 1st layer for the conventional and proposed methods. Compared to the conventional method, CCVs of the proposed method are stable and the convergence trend is clearly observed.

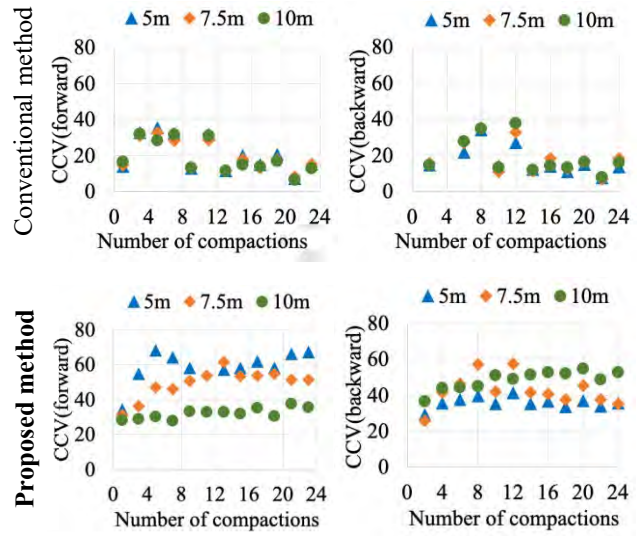
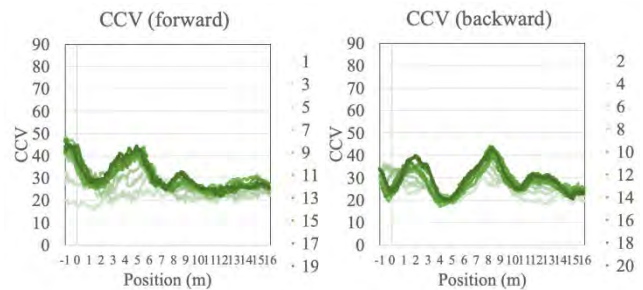


Figure 8. CCVs evaluated on N-lane of the 1st layer on each point

The results of this experiment were obtained under limited soil conditions. It is well known that the change of CCV tends to become unclear with increasing moisture content [10]. A similar trend may be obtained with the proposed method, and this will be discussed in the future.

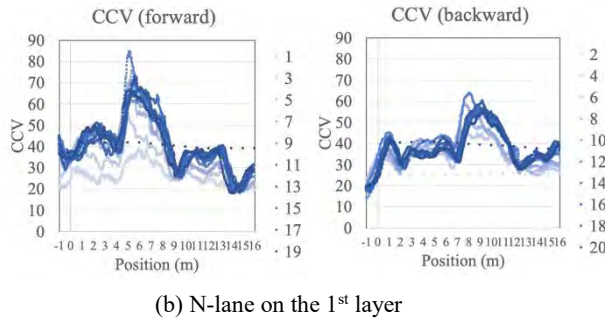
To investigate the effect of the distance from the accelerometers to the vibratory roller, an additional experiment was conducted in which the vibratory roller compacted the compaction lane on the far side (F-lane) and more than 4 m away from the accelerometer.

Figure 9 shows the CCVs of the F-lane and N-lane. Although the CCV is larger on N-lane than on F-lane, the CCVs of both lanes clearly converge. This indicates that the proposed method is effective even when the vibration roller is more than 4 m away from the accelerometer.



(a) F-lane on the 1st layer

Figure 9. CCVs for varying distance from vibration source to accelerometers



(b) N-lane on the 1st layer

Figure 9. CCVs on F-lane and N-lane.

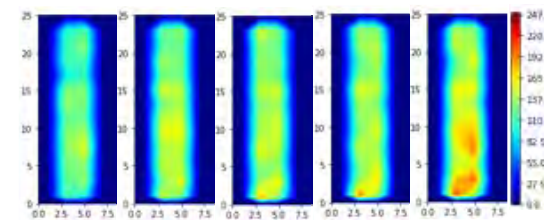
The resulting coefficients of the subgrade reaction (MN/m³) are listed in Table 3 and Table 4. The LFWD test was conducted at the fourth, eighth, 12th, 16th, and 20th of compaction on each layer. The heat map for the case where the embankment traveled in the longitudinal direction is shown in Figure 10.

Table 3 Coefficients of subgrade reaction on 1st layer with LFWD. (MN/m³) (n = 24)

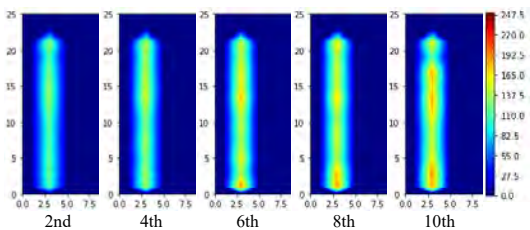
	4th	8th	12th	16th	20th
Ave.	118	137	139	139	155
Max.	155	160	180	189	210
Min.	88	112	118	110	112
SD	15.4	14.4	14.7	17.4	23.5

Table 4 Coefficients of subgrade reaction on 2nd layer with LFWD. (MN/m³) (n = 11)

	4th	8th	12th	16th	20th
Ave.	119	137	155	157	163
Max.	133	152	189	185	187
Min.	109	125	139	139	113
SD	8.7	8.9	15.9	15.5	21.5



(a) Coefficients of subgrade reaction on 1st layer



(b) Coefficients of subgrade reaction on 2nd layer

Figure 10. Coefficients of subgrade reaction with LFWD

The results confirmed that the coefficients of the subgrade reaction tended to increase as the number of compaction cycles increased.

The rate of change of the coefficients of the subgrade reaction obtained by the LFWD was also calculated. Because LFWD measurements were obtained at 4th, 8th, 12th, 16th, and 20th compaction, the unmeasured coefficients of the subgrade reaction were linearly complemented, and the average rate of change was obtained. Figure 11 shows the results and same convergence trend as the CCV rate of change shown in Figure 6.

Because the LFWD is measured over a long period of time at the surface of the compacted ground, it is difficult to measure at construction sites. The acceleration response method proposed in this study can be measured at a location off the compaction ground and is considered to be useful at construction sites.

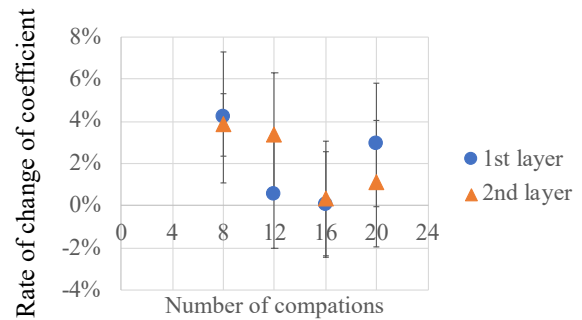


Figure 11. Rate of change of coefficient of subgrade reaction with LFWD

4.4 Simulation results

Simulations were conducted to find out the characteristics of the conventional and proposed methods.

The acceleration of the roller was varied so that the impact amplitude between the roller and the ground increased as the compaction cycles increased. In addition, a low-pass filter was applied to smooth the vibration as it passed through the ground in the proposed method. Since damping decreases as the stiffness of the ground increased, it was assumed that the cutoff frequency increased as the number of compaction cycles increased.

Figure 12 shows the CCVs when the impact amplitude and the cutoff frequency of the low-pass filter were increased in the conventional and proposed methods, respectively. In both cases, the CCVs increase when the impact amplitude or the cutoff frequency increases. In particular, the proposed method showed a nonlinear relationship between the cutoff frequency and the CCVs. From this non-linearity, it is expected that the

CCVs change gradually during initial compaction cycles. On the other hand, the CCVs increase uniformly for any compaction cycles for conventional method. This may cause the different characteristics and may be one of the reasons why the proposed method has higher discriminability than conventional method.

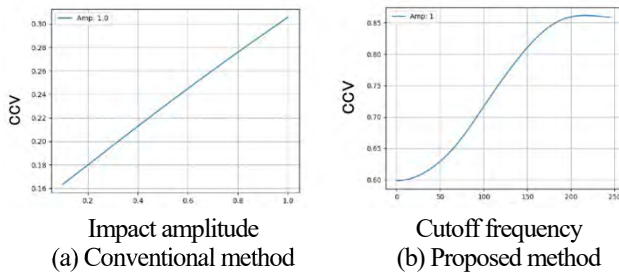


Figure 12. CCVs of conventional and proposed method obtained by the simulation

4.5 Advantages and limitations

The experimental results suggest that the proposed method is more discriminative than the conventional method. The proposed method also shows superiority in failure resistance and signal-to-noise ratio compared to the conventional method.

On the other hand, the proposed method has disadvantages compared to the conventional method in terms of labor and cost required to install sensors. It is also necessary to consider the effects of vibrations generated by surrounding machinery. Furthermore, since absolute values vary depending on the distance from the roller to the acceleration sensor, evaluation by absolute values are currently difficult and can only be compared relatively. Further discussion on this issue is needed in the future.

5 Conclusions

This paper proposes a method for evaluating ground stiffness using multiple synchronous acceleration sensors placed on the ground. The proposed method is superior to the conventional method in terms of discrimination and convergence with respect to the number of compaction cycles, as confirmed by ground rolling tests on embankments. The convergence tendency of the proposed method was similar to that of the coefficient of the subgrade reaction calculated using LFWF.

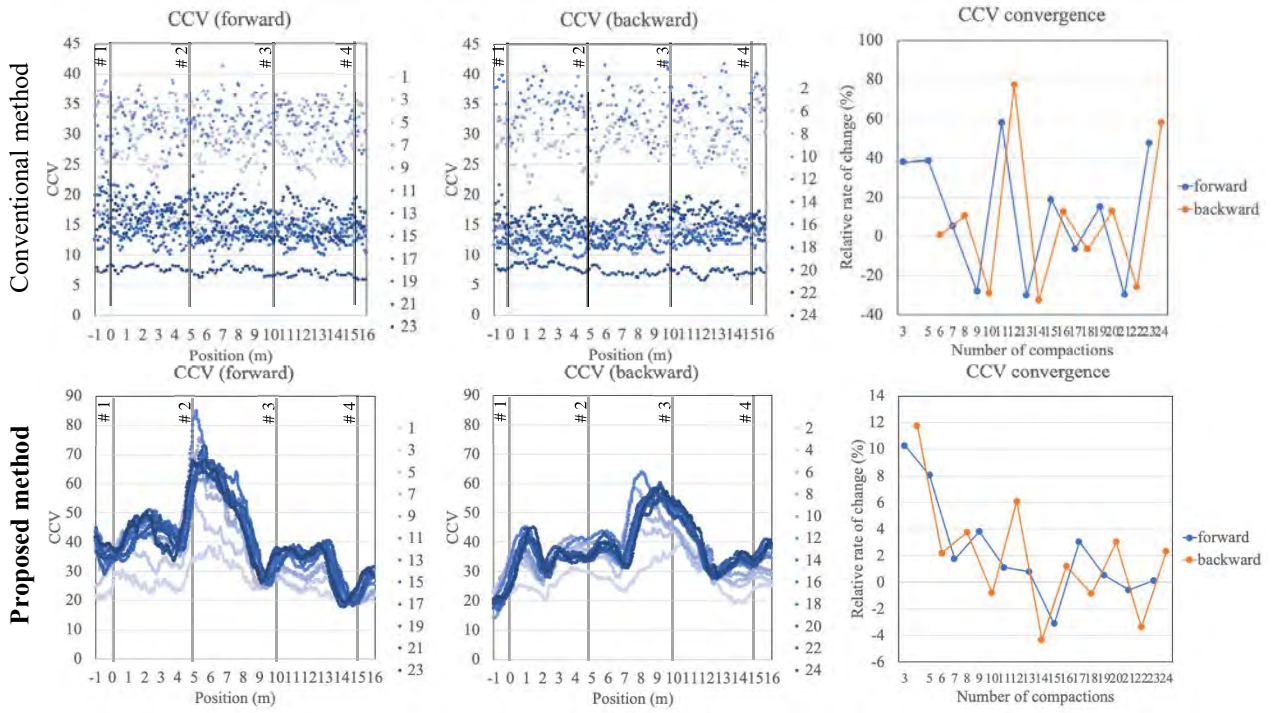
In a future study, experiments will be conducted on soils with various moisture contents to clarify the characteristics of the proposed method.

Acknowledgement

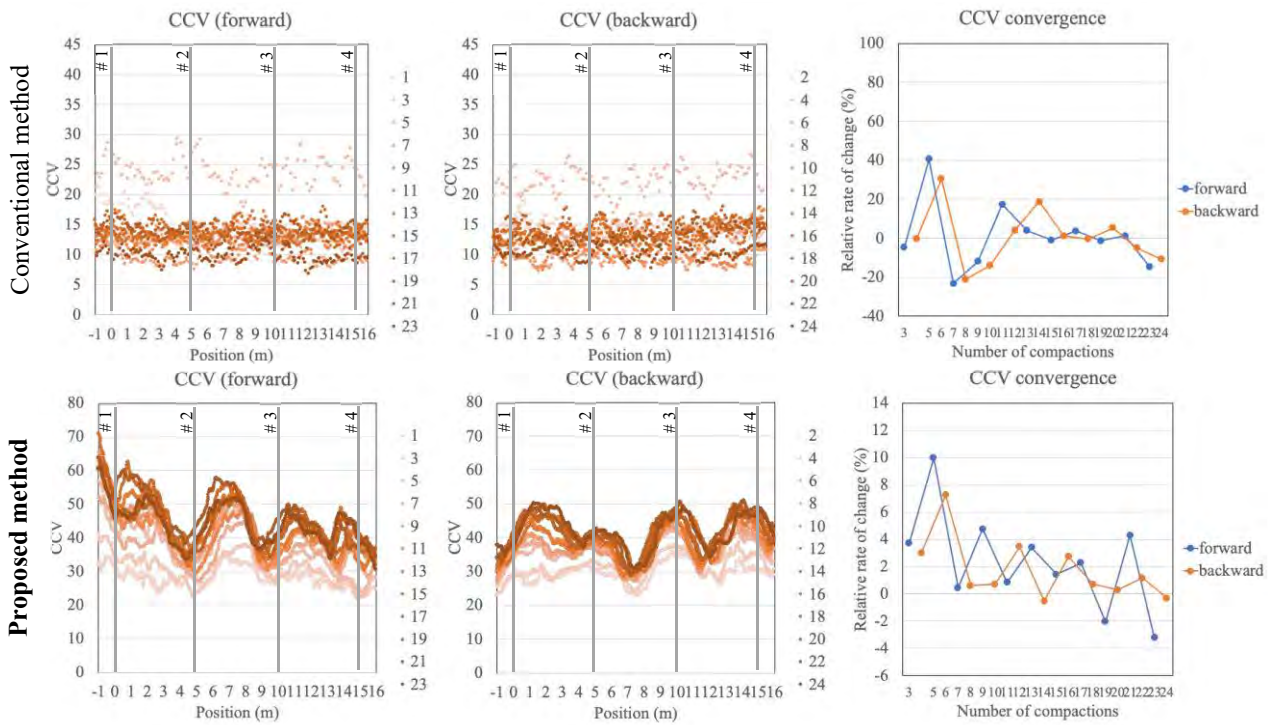
The authors are grateful to Prof. Yasuhiro Mitani and Prof. Hisatoshi Taniguchi for technical assistance with the experiments. This work was supported by the JST [Moonshot R&D] [Grant Number JPMJMS2032].

References

- [1] Thurner H. and Sandstrom A. A New Device for Instant Compaction Control. In *International Conference on Compaction*, Vol. II pages 611-614, France, 1980.
- [2] Forssblad L. Compaction Meter on Vibrating Rollers for Improved Compaction Control. In *International Conference on Compaction*, pages 541– 546, Paris, France, 1980.
- [3] Adam D. Continuous Compaction Control with vibratory rollers. In *Geo Environment 97*, pages 245-250, Rotterdam, Netherlands, 1997.
- [4] Adam D. and Brandl H. Sophisticated roller integrated continuous compaction control. In *12th Asian Regional Conference on Soil Mechanics and Geotechnical Engineering*, Vol. 1 pages 427-430, Singapore, 2003.
- [5] R. Anderegg and K. Kaufmann. Intelligent Compaction with Vibratory Rollers: Feedback Control Systems in Automatic Compaction and Compaction Control. *Journal of the Transportation Research Board*, 1868(1):124-134, 2004.
- [6] Christopher M, Daniel C, Faraz T and William B. Assessing soil compaction using continuous compaction control and location-specific in situ tests. *Automation in Construction*, 73:31-44, 2017.
- [7] Sakai Heavy Industries, Ltd. Vibrating roller type soil compaction quality controller CCV (compaction control value), Operating & Maintenance Instructions, pages 1-5, 2007.
- [8] Hashimoto T. Fujino K. and Tateyama K. Suggestion of the ground stiffness estimative method with the running speed of a plate compactor. In *International Symposium on Automation and Robotics in Construction*, pages 1-6, Alabama, USA, 2016.
- [9] University of Maryland College Park. Standardizing lightweight deflectometer modulus measurements for compaction quality assurance, pages 5-8, Final report for Maryland Department of Transportation State Highway Administration Research Report, 2017.
- [10] Wei H, Pawel P, Xiaoyang J, Hongren G and Baoshan Huange. Visualization and quantification of lab vibratory compacting process for T aggregate base materials using accelerometer. *Transportation Geotechnics*, 25:1-8, 2020.



(a) CCVs and r_n evaluated on N-lane of the 1st layer



(b) CCVs and r_n evaluated on the 2nd layer

Figure 6. CCVs and r_n evaluated results ("#n" denotes the position of the n-th accelerometer)

Optimized Production Scheduling for Modular Construction Manufacturing

A. Bhatia^a, O. Moselhi^{a,b} and S.H. Han^{a,b}

^a Department of Building, Civil and Environmental Engineering, Concordia University, Montreal, QC, Canada

^b Centre for Innovation in Construction and Infrastructure Engineering and Management (CICIEM), Concordia University, Montreal, QC, Canada

angatpalsingh.bhatia@concordia.ca, moselhi@encs.concordia.ca, sanghyeok.han@concordia.ca

Abstract –

Modular construction is becoming a viable construction method in North America due to its support of the concept of circular construction and its inherent ability to provide a faster return on investment. The process of modular construction manufacturing (MCM) operates as a production line, where the number of module components (e.g., wall, roof, and floor panels) with different design specifications and their sequence (i.e., order of prefabricating these module components) dictates the productivity of the production line. This variation in design specifications and impractical sequences of module components leads to imbalanced production lines and prolonged makespan (i.e., total completion time) of prefabricating module components at workstations. To address these challenges, this paper proposes a method that utilizes deep neural network and genetic algorithm (GA) techniques to solve the modular construction manufacturing scheduling problem (MCMSP). The method consists of two processes: (i) developing a deep neural network model based on the historical time data and later hyperparameter tuning using a GA in order to select the optimal neural network configurations; and (ii) subsequently using the predicted process times as input in the optimization model in order to schedule the sequences of module components (e.g., wall panels). The proposed method is implemented in a wood-based wall panel production line of a modular fabricator in Edmonton, Canada. This developed method can assist production managers in efficiently forecasting process times and developing production line schedules.

Keywords –

Modular Construction Manufacturing (MCM); Production Line; Deep Neural Network; Scheduling; Optimization

1. Introduction and Background

Modular construction is a process where module components (e.g., wall, roof, and floor panels) are prefabricated in a controlled factory environment and later transported on-site to be installed as building blocks. Modular construction is increasingly growing in popularity over conventional construction, given its potential to achieve shortened construction schedules and less material waste, facilitate the process of circular construction and lead to a quicker return on investment for project owners [1] and [2]. However, prefabricating modules has been a very complex manufacturing process due to the highly customized nature of module components (i.e., variation in design specifications), leading to varying production rates and imbalanced production lines. Therefore, this process makes it challenging for production line managers to develop a robust production planning and scheduling model without accurately forecasting the process times of module components at workstations along the production line.

In modular construction manufacturing (MCM), the processing time is defined as the time taken (i.e., start and finish time) to complete one module component (e.g., wall panel) at the workstation [3]. Accurately predicting the process times can be seen as a way of: (i) gaining an in-depth understanding of the nature of module components; and (ii) making data-driven decisions with respect to the planning and scheduling of module components in the production line. However, the modular construction industry has not achieved its full potential benefits due to the lack of a systematic, data-driven decision-making approach in order to solve the modular construction manufacturing scheduling problem (MCMSP). In practice, production managers make guesswork based on their experience and rely on the average process times. However, such methods do not provide optimal results due to the stochastic nature (i.e., randomness) of prefabricating module components at

workstations. In this respect, this paper proposes a method combining deep neural networks and GA to develop a model to solve MCMSP efficiently. The proposed method encompasses; *(i)* data preprocessing (e.g., outlier's removal) in order to clean RFID-based production line data for prediction purposes; *(ii)* development of predictive models using the deep neural network; *(iii)* identification of optimal model configuration for the deep neural network using GA optimization; and *(iv)* development of a scheduling model using GA based optimization technique facilitating the data-driven production line schedules.

2. Literature Review

This section provides a literature review from three perspectives: *(i)* Data analytics; *(ii)* Scheduling in MCM; and *(iii)* optimization for production scheduling.

2.1 Data Analytics

Various machine learning and statistical techniques were employed to substantially enhance the accuracy of predictive models in construction and infrastructure engineering [4]. Artificial neural networks (ANN) are a more suitable tool for developing predictive models as they provide superior performance for highly uncertain, nonlinear, and complicated problems [5]. According to Moselhi et al. [6], ANN encompasses a collection of processing elements, usually organized into layers (i.e., input, hidden, and output layers). The input layer accepts the data (i.e., independent variables), which is used by the hidden layers to represent the relationship and the output layer produces the network response (i.e., dependent variable). To make reliable predictions, ANN has been extensively applied in the construction, infrastructure, and manufacturing industry. For example, Zangenehmadar and Moselhi [7] used ANN models to predict the remaining useful life of water pipes in Montreal. Critical factors such as pipe length, diameter, material, and breakage rate were considered to develop robust predictive models. Likewise, Golnaraghi et al. [8] applied the ANN technique, and on that basis, the labor productivity for performing formwork installation operations was predicted. Moon et al. [9] successfully implemented a multilayer perceptron artificial neural network to predict production and latency days for manufacturing production facilities. Although, some studies have advanced the development of forecasting process times at workstations along the production line in modular construction [10]. However, manual and GridSearchCV were used to find the optimal parameters for the machine learning algorithms. This approach is time-consuming and does not ensure optimal parameters. Therefore, various researchers have used GA for

hyperparameter tuning for machine learning models in construction and infrastructure engineering. For instance, Assad and Bouferguene [11] used the GA algorithm in order to optimize the hyperparameter of various data mining techniques to accurately predict the water mains condition. Considering these characteristics of GA, the research presented in this paper seeks to implement GA to select the optimal neural network model configurations for predicting the process times of module components in the production line.

2.2 Planning and Scheduling in Modular Construction Manufacturing

Scheduling in the manufacturing industry is a decision-making process where the sequencing of jobs (i.e., module components) and allocation of resources is performed to achieve specific objectives (e.g., minimization of makespan). According to Piendo [12], the scheduling process can be stochastic or deterministic. Since the process times and release dates of the jobs in the production lines are not known with certainty in advance. The scheduling problem in MCM resembles the stochastic scheduling problem. Therefore, various researchers have implemented methods on lean manufacturing principles and simulation to enhance planning and scheduling in MCM. For example, Yu et al. [13] applied a lean-based approach in the modular construction company's production line, improving labor efficiency by 10 % and reducing labor costs by 18%. On the other hand, Moghadam et al. [14] generated multiple scenarios of production line schedules using discrete event simulation. Later, these developed simulation scenarios were integrated with a visualization model to determine the best scenario for balancing the production line. In general, lean and simulation have been applied individually or integrated to develop plans and schedules; thereby improving the performance of MCM. However, there are the following issues: *(i)* a limited number of scenarios were tested; therefore, not giving optimal sequences of modules to be prefabricated in the production line; *(ii)* does not account for decision variables such as module design specifications in their module sequencing arrangement.

2.3 Optimization for Production Scheduling

Various researchers in industrial engineering have applied optimization techniques to solve scheduling problems (e.g., flow and job shop scheduling). For example, Chen et al. [15] proposed a GA-based method that developed schedules for a hybrid flow shop considering order arrivals in a dynamic manner. GA demonstrated its effectiveness by reducing job waiting time and meeting order deadlines. Meanwhile, An et al. [16] illustrated the application of GA in minimizing the

production time and cost for a metal-cutting production process. Similarly, optimized schedules were developed for modular and offsite construction. For instance, Hyun et al. [17] developed a multi-objective optimization model based on GA to reduce the duration and cost of modular construction production lines. Rashid and Louis [18] integrated GA and discrete event simulation in order to minimize the total makespan (i.e., completion time) for the modular construction production line by allocating an optimal number of workers at each workstation. However, these developed methods assumed the durations of workstations on a production line as only triangular distribution or determined duration based on number of workers allocated to the activities. There is a lack of scheduling methods that utilize the historical production data while developing predictive models to be used as input for scheduling the sequences of module components in the production line. Although the effectiveness of optimization algorithms depends on the type of scheduling problem and objective, the positive reviews of the GA algorithm (i.e., provides an effective solution and good computing capabilities) lead to its selection to solve MCMSP in this research.

3. Developed Method

Figure 1 presents the proposed method that combines a deep neural network and genetic algorithm in order to solve the modular construction manufacturing scheduling problem (MCMSP). A modular fabricator company collected the historical time data using RFID-based technology [19], consisting of an RFID printer, reader, antenna, and paper-based tags. A detailed discussion of the RFID system design and its application for data was reported in the paper of Sadiq et al. [3]. This research starts with extracting the process times and relevant attributes of module components (e.g., number of studs and doors) at each workstation from the RFID raw data file provided by the company. From the timestamps collected using the RFID system, the process times (i.e., the time required to complete one module component at each workstation) is extracted based on Equation (1):

$$\text{Processing Time } i, w = \text{First Read Time } i, w+1 - \text{First Read Time } i, w \quad (1)$$

where i = panel; w = workstation; $w+1$ = next workstation; last read and first read are from antenna description.

In this respect, the next critical step was to perform data preprocessing to clean the data and ensure that the dataset was in the required format for prediction purposes. The first step of data preprocessing is to identify and remove any missing values. In addition, (i) data visualization techniques (i.e., pie charts) are applied in order to gain insights into the data, and (ii) data points that are above and below 'Mean \pm 1.5 SD' are marked as

possible statistical outliers. Another crucial preparation step is combining attributes with the same meaning (e.g., the number of single and large doors). Furthermore, normalization techniques are implemented using Equation (2) in order to reduce the sizes of independent variables and model computation time.

$$V' = (V - \min_A) / (\max_A - \min_A) \quad (2)$$

where \min_A is the minimum value and \max_A is the maximum value of the independent variable, A , and V represents the original value of A .

The dataset, having been preprocessed, was divided into training (80%) and testing (20%) subsets. Based on the training subset, a deep neural network model, is developed. It should be noted that this study used a deep neural network due to its feature of having multiple processing layers, which can efficiently perform complex nonlinear transformations. Each layer entails several nodes representing the input, transfer, and output variables. In this paper, the rectifier activation function is selected, and the range searched for upper bound/lower bound is 3-10 for hidden layers and 6-100 for the number of nodes. The next critical step is to apply the cross-validation technique in order to prevent overfitting and obtain a better evaluation of the predictive model. The present study adopts K-fold cross-validation for testing the performance of a model. The dataset is divided into K groups, where, in turn, the predictive model is trained using $(K-1)$ groups, and the remaining fold is used to test the accuracy of the model. It should be noted that the parameters of the model (i.e., the number of hidden layers and nodes) have a significant impact on the model's performance. For instance, if there are a small number of nodes, the model cannot be trained well, and with a large number of nodes, performance can be enhanced, but a large number of connections will increase the computational time. Therefore, it is critical to establish parameters for neural networks which can be trained in reasonable computation time and provide errors within the tolerance limit. Therefore, hyperparameter tuning is performed, which is a process of identifying an optimum model configuration. This paper uses the GA optimization technique for hyperparameter tuning to minimize the model's prediction error (i.e., mean absolute error (MAE)). The procedure begins with initializing the population, representing a set of random solutions. The fitness of each solution is calculated, and the best solutions are then selected in the population using a tournament selection strategy. The selected solution is used to reproduce by undergoing the process of crossover and mutations. The process is repeated until optimization criteria are met. It should be noted that only MAE is selected as a measure of goodness of fit, which according to various studies is a better alternative to R square while evaluating the performance of model in respect to nonlinear data [20] and [21]. According to

Lsesh [20], utilization of R square for evaluating model performance in nonlinear data, leads to misinterpretations and produces misleading conclusions. Moreover, in the mathematical literature, it has been concluded that the R-square generally do not increase even for better nonlinear predictive models [21]. Later, the unseen data fit into the developed predictive model, and process times were predicted using the deployment function in the python library.

The predictive process times of module components and the type and number of module components were used as input in the optimization model. As mentioned earlier, in a modular construction production line, the duration of each module component at each workstation changes according to its: (i) type and design specification (i.e., exterior/interior and number studs, door, and window) and (ii) procedure required to prefabricate (i.e., framing, nailing and cutting). At a given production line, the allocated module components are conducted in a cyclic manner (i.e., pre-defined sequence), and the process times of each workstation are a major variable. Therefore, the optimization problem can be defined as a combinatorial problem of the number of module components and process times. To solve the MCMSP, the following assumptions are considered: (i) Only module components affect the cycle time of the production line; and (ii) module components will be available in the inventory. The problem is modeled as an operation sequencing optimization problem, where $J = \{J_1, J_2, \dots, J_m\}$ is a set of 'm' number of module components to be scheduled and; $P = \{P_1, P_2, \dots, P_w\}$ is a set of 'w' number of workstations. Every module component in a modular construction production line needs to be prefabricated on several workstations in the pre-defined order (i.e., sequences), which is considered a non-deterministic polynomial-time hard (NP-hard) problem. That means there are multiple sequences to schedule the module components at workstations, and with an increase in the number of combinations, the complexity of the problem (search space) increases, which makes it harder for the techniques to efficiently find the optimal sequences in a reasonable model runtime. The objective of the optimization problem is to find a near-optimal schedule (i.e., sequences of module components) in order to minimize the makespan (i.e., minimum time to complete all module components in the production line from start to end) [25] represented by equation 3:

$$\text{Min} [\text{Max} (C_{1,w}, C_{2,w}, \dots, C_{m,w})] \quad (3)$$

Constraints:

$$S_m + D_i \leq S_{i+1} \quad (4)$$

$$\text{Max } X_{m,w} = 1 \quad (5)$$

The decision variables are the different sequences of module components in the production line. This optimization problem is subject to a set of constraints: (i) constraint 1 (equation 4) defines the production flow of module components, which ensures the module component 'm+1' at station w cannot start before the end of its predecessor module component 'm' at station 'w'; and (ii) constraint 2 (equation 5) represents the workstation capacity, which enforces each workstation 'w' can process max of one module 'm' at a time.

The primary component to develop the optimization model is GA, which optimizes the sequences of module components (i.e., order of module components) to be prefabricated at the workstations, which minimizes the makespan of the modular units. The critical elements of the GA algorithm are initialization, evaluation, selection, crossover, and mutation, which works as follows: (i) an initial population (i.e., comprised of chromosomes representing a list of module components) is generated randomly. In this research, we have used permutation encoding of modules (i.e., arranging the number of module components in different orders) as a chromosome where a primary module component will be assigned first, then the succeeding module component. For instance, a permutation [4,1,8,5,2,7,3,6] is a chromosome that represents a sequence where module component number 4 gets prefabricated first on all the workstations followed by module component 1, 8, and so on; (ii) performing the process of evaluation, where fitness values of each chromosome are evaluated based on the optimization criteria (i.e., minimum makespan); (iii) The best chromosomes from the population is selected as the best solution (i.e., optimal sequences of module components) based on their fitness value. In this research, the selection process is performed using roulette wheel selection. It should be noted that the goal of the selection process is to save better and remove bad chromosomes; (iv) crossover and mutation are implemented in order to generate new chromosomes for the next generation. For each pair of parents to be mated, a crossover point is chosen using a two-point crossover, and the offspring exchanges the parents' genes among themselves until the crossover point. In the mutation process, to introduce variability and diversity, some of the genes in the offspring are flipped. This selection, crossover, and mutation process continues until the optimization criteria are met.

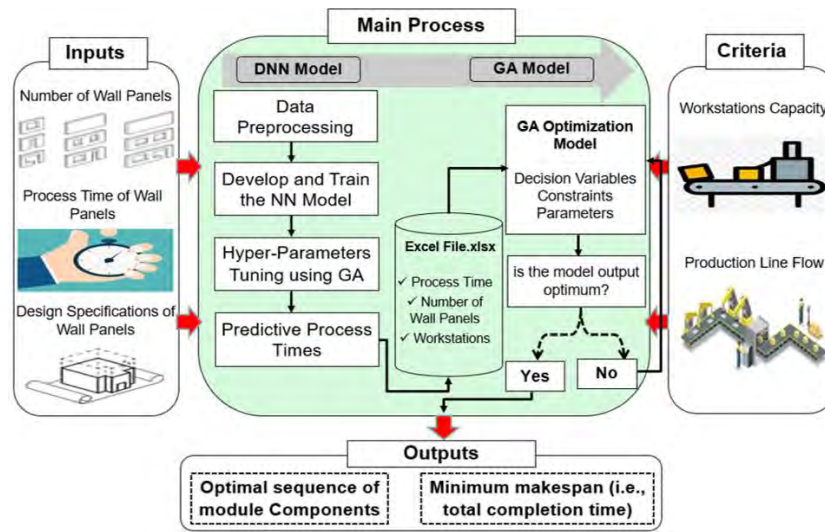
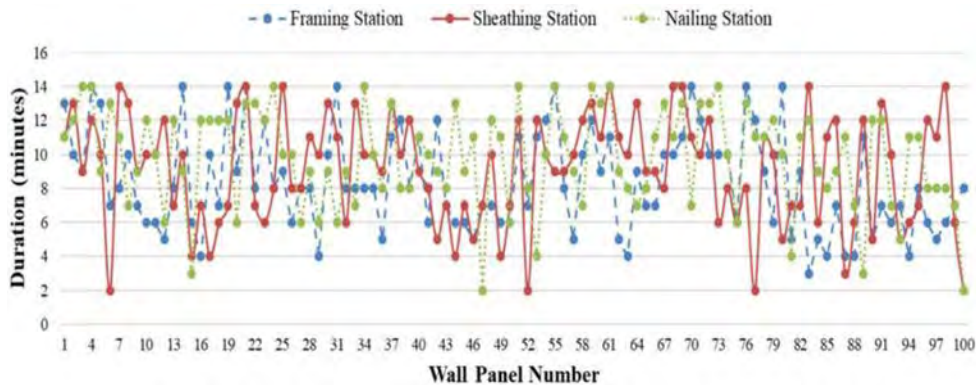


Figure1. Research methodology

4. Case Study and Results

The proposed method was implemented on a wood-frame wall panel production line operated by a modular fabricator in Edmonton, Canada. The wall panel production line consists of the following workstations: (i) framing station where the wall components such as studs, tracks, and headers are fastened together to form a wall panel frame; (ii) sheathing station where drywall/sheets are installed on wall panels; (iii) multifunction bridge where drywalls/sheets are nailed (fixed) and moved to next workstation using transfer cart. It should be noted that interior multiwall panels are moved from the multifunction bridge and are cut at the transfer cart into single-wall panels, which are sent to the window bypass line to store them at the wall magazine line, whereas exterior wall panels are cut into single-wall panels and transferred to the window/door line or window bypass line; (iv) Window/Door installation lines, where windows/doors are installed on the wall panels and transferred to the storage area (i.e., wall magazine line). The wall panels are stored at the storage area as they await delivery to sites. Process times at workstations

were collected by the modular fabricator company using an RFID system. The data in the 'RFID raw data' file for the workstations include the time between July 2015 and May 2017. As such, it contains (i) timestamps for each wall panel along with the workstations; and (ii) design factors of each wall panel (e.g., number of studs, number of windows, and length of wall panel). Considering this, the next critical step in the case study was to extract the process times of wall panels at the workstation using Equation (1). In addition, initial data analysis was performed in order to gain insights into the production line. Figure 2a shows a high level of variance in the process times at workstations due to the influence of the design factors (i.e., number of windows, panel length, and number of studs). For example, at the sheathing station, the processing time of wall panel 3 was 9 minutes, wall panel 4 was 12 minutes, and wall panel 6 was 2 minutes. This variation in process times affects the daily productivity of the workstations. Moreover, Figure 2b illustrates that the daily production on March 30 was 12 panels at the sheathing station, 22 panels at the framing station, and 6 panels at the nailing station, respectively, causing an imbalanced production line.



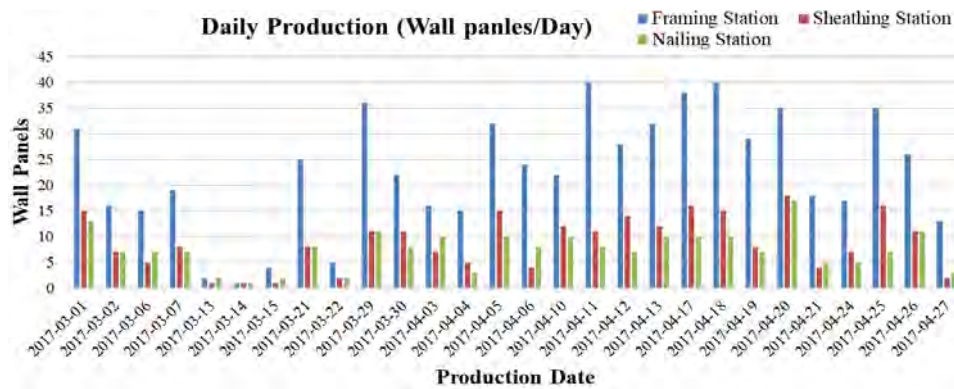


Figure 2 (a): Process times of wall panels at workstations; and (b): Daily production of wall panels

Prior to the development of a predictive model, data preprocessing was implemented. Timestamps of wall panels prefabrication that started on one day and finished on the following day were removed, and wall panels with missing timestamps were also discarded from the dataset. Additionally, similar properties of a panel were combined into a single attribute in order to reduce data dimensions. For example, DStud, LStud, and MStud were combined into a 'stud'; similarly, window and large widow were combined as a 'window.'

Later the outliers were removed based on data visualization (i.e., pie chart), which helps to visualize the distribution of data points that are inconsistent from the data set. For example, at butterfly (i.e., cutting workstation), the process times above 60 minutes were removed (Figure 3). The reason for removing these points is that around 4% of the wall panel's processing times have excessive times (i.e., 61-41000 minutes). Such data points indicated a work disruption due to errors in the shop drawings and resulted from their waiting between the workstations. In addition, data points above and below 'Mean ± 1.5 SD' are data points marked as possible statistical outliers. As a result of the preprocessing tasks, the datasets numbered 7256, 2885, 3035, 19998, 1868, 4101, and 1592 for the framing, sheathing, nailing, cutting, window door, window bypass, transfer table, and storage area workstations, respectively.

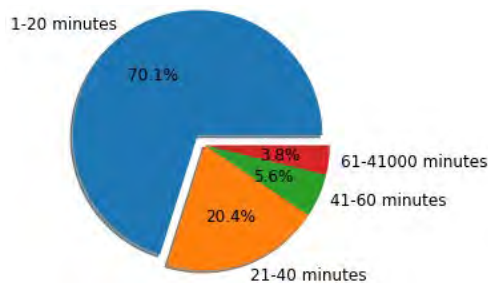


Figure 3. Pie chart

Next, the min-max normalization technique was applied in order to transform values ranging between 0

and 1. As described above, the variation in the process times at workstations due to differences in design factors of wall panels leads to an imbalanced production line. In this respect, the next critical step in the case study was to develop a predictive model by considering the wall panel design factors.

The developed deep neural network consists of input, hidden, and output layers. The independent variables, such as panel length, number of regular studs, number of doors, and number of windows, were used as model inputs, while the process times of wall panels in minutes were the output variable. Each node element was connected and layered with nodes of the next layer. The nodes, which carry weights, were used to process the error rate. In this paper, the rectifier activation function was selected, and the range searched for upper bound/lower bound was 3-10 for hidden layers and 6-100 for the number of nodes.

In order to identify the optimal number of hidden layers and nodes, a GA optimization algorithm was selected to minimize the MAE. In this paper, the optimization parameters were assigned as follows: (i) population size of 20; (ii) the maximum number of generations was 50; (iii) mutation probability of 0.1; (iv) crossover probability of 1 and: (v) number of tournaments were 3. As observed in table 1, most of the workstations (i.e., framing, sheathing, and nailing station) had MAE of less than 2.50 minutes, respectively.

Table 1. Selected values of the predictive model

Workstations	Selected Value		MAE
	Hidden	Nodes	
Framing	3	74	2.17 min
Sheathing	3	72	2.11 min
Nailing	3	14	2.41 min
Butterfly (cutting)	7	70	5.37 min
Window/Door	8	42	30.36 min
Window Bypass	3	86	20.16 min
Transfer Table	9	24	1.11 min

Later the predictive process times were used as input in the optimization model. A genetic algorithm was developed with an objective of minimizing the makespan (i.e., production duration) of prefabricating the wall panels in the production line. The number of wall panels considered for this optimization model are 46 (i.e., 27 exteriors and 19 interiors) to be processed at 7 workstations, respectively. The optimization parameters used in this case study are as follows: 100 generations, each generation containing 30 populations with mutation and crossover rates of 0.2 and 0.8. Figure 4 shows that the Makespan value (i.e., duration) plateaued after 85 generations. The algorithm starts with an initial solution of a makespan equal to 4359 minutes, and the algorithm converges to the best solution in 90 generations with a makespan equal to 4352 minutes.

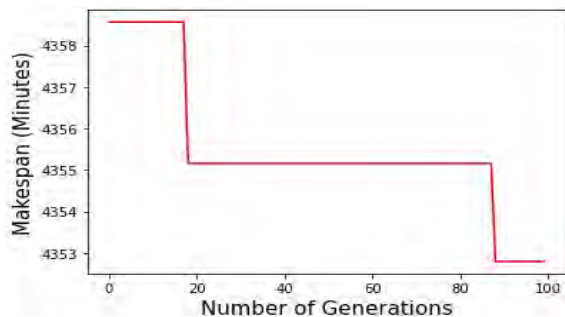


Figure 4. Makespan value

The median makespan to prefabricate 46 wall panels is 4352 min (i.e., 72.32 hours ~ 7 days (10 hours/day working time for the factory)). The optimal sequence is: 9,16,25,14,23,10,44,42,27,5,45,36,26,28,11,13,31,22,29,18,39,38,43,6,22,40,30,2,4,17,12,33,8,34,15,32,41,7,1,4,2,21,3,19,35,37, where the wall panel number 9 is the first panel to be prefabricated at the first station (i.e., framing) followed by 16 and so on. The approach presented in this paper unleashes the potential of a data driven scheduling method, which overcomes the drawbacks of previous studies with respect to: (i) testing limited number of scenarios for sequencing module components, thus not providing near optimal solution and; (ii) assuming the durations on a production line as only triangular distribution or based on number of workers allocated to the activities.

5. Conclusions and Future Work

In modular construction, the module components (e.g., wall, roof, and floor panels) are of various sizes and design specifications, necessitating dynamic changes to the production line. This poses a challenge for production line managers to accurately forecast the process times of module components at each workstation, leading to inefficient production line schedules and reduced

productivity. In this respect, this research proposes a newly developed method that utilizes deep neural network and GA in order to solve the MCMSP. The developed method utilizes the historical time data collected from the manufacturing plant at each workstation as an input in the deep neural network model to predict the process times at these workstations. Next, the GA optimization technique is implemented for hyperparameter tuning and, as such, finds the optimal number of hidden layers and a number of nodes in each layer. Subsequently, the predicted process times are used as an input in the scheduling optimization model in order to provide optimal sequence of module components to minimize the makespan. The case study implementation of the developed method in a wall panel production line demonstrates that the developed method predicted the process times with a MAE of less than 2.50 minutes for most of the workstations. In particular, the optimal sequences of 46 wall panels are prefabricated in 72.32 hours. As illustrated by the case study, this method can be helpful in assisting production managers to understand the insights of the production line by: (i) predicting process times for various types of module components; and (ii) analysing variance in the process times at workstations due to the influence of the module components design factors. In this way, production line managers can reduce duration of prefabricating module components at workstations and don't need to rely on experienced based approach with respect to estimating the process times and developing schedules.

However, the developed method does have limitations in the following respect: (i) other factors important to develop schedules for production line besides duration, (e.g., minimization of the idle time at workstations and allocation of optimal number of workers at workstations), are not taken into consideration in the current method; and (ii) the number of module components considered for this optimization model are not based on multiple projects. Therefore, in order to improve the current method, the future work will seek to expand in the following directions: (i) optimization model will consider module components (e.g., wall panels) based on multi-projects to achieve JIT lean strategy; (ii) the optimization model can be further improved by applying hybrid optimization techniques; and (iii) multi-objective optimization of production line schedules with respect to cost and workers will be explored. It should be noted that this paper focused primarily on developing production line schedule with an objective of minimizing duration, which is an essential factor while solving sequencing problems for production line. However, consideration of quality of work can also be incorporated into future works by measuring the percentage of rework for prefabricating module components at workstations.

Acknowledgments

The authors wish to acknowledge the support of Dr. Mohammed Sadiq Altaf in providing the production line data. Special thanks to Hassan Bardareh for helping in automating RFID-based data extraction of the production line.

References

- [1] Nik-Bakht M., An C., Ouf M., Hafeez G., Dziejdz R., Han S.H., Nasiri F., Eicker U., Hammad A. and Moselhi O. Value Stream Mapping of Project Lifecycle Data for Circular Construction. In *Proceedings of the International Symposium on Automation and Robotics in Construction*, 38, 1033-1042, Dubai, United Arab Emirates, 2021.
- [2] Salama T., Moselhi O. and Al-Hussein M. Overview of the Characteristics of the Modular Industry and Barriers to its Increased Market Share. *International Journal of Industrialized Construction*, 2(1), 30-53, 2021.
- [3] Altaf M.S., Bouferguene A., Liu H., Al-Hussein M. and Yu H. Integrated production planning and control system for a panelized home prefabrication facility using simulation and RFID. *Automation in construction*, 85, 369-383, 2018.
- [4] Chu W., Han S.H., Zhen L., Hermann U. and Hu D. A Predictive Model for Scaffolding Man-hours in Heavy Industrial Construction Projects. In *Proceedings of the International Symposium on Automation and Robotics in Construction*, 37, 976-983, Kitakyushu, Japan 2020.
- [5] Hegazy T., Fazio P. and Moselhi O. Developing practical neural network applications using backpropagation. *Computer Aided Civil and Infrastructure Engineering*, 9(2), 145-159, 1994.
- [6] Moselhi O., Hegazy T. and Fazio P. Neural networks as tools in construction. *Journal of construction engineering and management*, 117(4), 606-625, 1991.
- [7] Zangenehmadar Z. and Moselhi O. Assessment of remaining useful life of pipelines using different artificial neural networks models. *Journal of performance of constructed facilities*, 30(5), 04016032, 2016.
- [8] Golnaraghi S., Zangenehmadar Z., Moselhi O. and Alkass S. Application of artificial neural network (s) in predicting formwork labour productivity. *Advances in Civil Engineering*, 2019.
- [9] Moon S., Hou L. and Han S. Empirical study of an artificial neural network for a manufacturing production operation. *Operations Management Research*, 1-13, 2022.
- [10] Mohsen O., Mohamed Y. and Al-Hussein M. A machine learning approach to predict production time using real-time RFID data in industrialized building construction. *Advanced Engineering Informatics*, 52, 101631, 2022.
- [11] Assad A. and Bouferguene A. Data Mining Algorithms for Water Main Condition Prediction Comparative Analysis. *Journal of Water Resources*, 148(2), 04021101, 2022
- [12] Pinedo M.L., 2012. *Scheduling*, (Vol. 29). New York: Springer.
- [13] Yu H., Al-Hussein M., Al-Jibouri S. and Telyas A. Lean transformation in a modular building company: A case for implementation. *Journal of management in engineering*, 29(1), 103-111, 2013.
- [14] Moghadam M., Barkokebas B. and Al-Hussein M. Post-simulation visualization application for production improvement of modular construction manufacturing. In *Proceedings of the International Symposium on Automation and Robotics in Construction*, 31,1, Sydney, Australia, 2014
- [15] Chen J., Wang M., Kong X.T., Huang G.Q., Dai Q. and Shi G. Manufacturing synchronization in a hybrid flowshop with dynamic order arrivals. *Journal of Intelligent Manufacturing*, 30(7), 2659-2668, 2019.
- [16] An L., Yang P., Zhang H. and Chen M. Multi-objective optimization for milling operations using genetic algorithms under various constraints. *International Journal of Networked and Distributed Computing*, 2(2), 108-114, 2014.
- [17] Hyun H., Yoon I., Lee H.S., Park M. and Lee J. Multi-objective optimization for modular unit production lines focusing on crew allocation and production performance. *Automation in Construction*, 125, 103581, 2021.
- [18] Rashid K., Louis J. and Swanson C. Optimizing labor allocation in modular construction factory using discrete event simulation and genetic algorithm. In *Proceedings of Winter Simulation Conference*, 2569-2576, 2020.
- [19] Bardareh, H. and Moselhi, O. An integrated RFID-UWB method for indoor localization of materials in construction. *Journal of Information Technology in Construction*, 27(32), 642-661, 2022
- [20] Kva Lseth, T.O. Note on the R² measure of goodness of fit for nonlinear models. *Bulletin of the Psychonomic Society*, 21, 79-80, 1983.
- [21] Spiess, A.N. and Neumeier, N. An evaluation of R² as an inadequate measure for nonlinear models in pharmacological and biochemical research. *BMC pharmacology*, 10(1), 1-11, 2010.

AWPIC: Advanced Work Packaging Improvement Canvas

Hala Nassereddine¹, Makram Bou Hatoum¹, Fernando Espana²

¹Department of Civil Engineering, University of Kentucky, USA

²Construct-X, USA

hala.nassereddine@uky.edu, mnbo229@uky.edu, fernando@construct-x.com

Abstract –

Advanced Work Packaging (AWP) is an innovative planning and control method for industrial projects with known parameters that allow organizations to transform the way they plan and control industrial construction projects. As the implementation of AWP is gradual, organizations are constantly looking to improve their practices. However, several organizations struggle with change, making decisions, and taking action. Every change effort impacts a wide array of internal and external stakeholders, and the lack of standard procedures to help organizations effectively navigate a change by making informed decisions and acting on those decisions impedes the progress and growth of the organization. This paper contributes to the notion of decision-making in the construction industry by presenting an “Advanced Work Packaging Improvement Canvas” (AWPIC). AWPIC allows organizations to improve their current AWP practices and transform their businesses by mapping the essential elements that organizations must consider to facilitate the change dialog internally and move toward the desired future state. The paper describes the theoretical underpinnings that embody AWPIC, then introduces AWPIC, and explains its six building blocks: Current State, Problem, Future State, Solution, Investment and Value Creation Analysis, and Action Plan and Follow-Up. AWPIC is developed with the intent to present a holistic framework for improvement and change processes and increase standardization in the industry.

Keywords –

AWP; Improvement; Business Process Reengineering; Canvas

1 Introduction

In a volatile, uncertain, and ambiguous environment, construction stakeholders are pressured to successfully complete complex construction projects with strict budgets and tight timelines. The success of the construction project depends on the effectiveness of planning and control systems [1,2]. However, in the

construction management body of knowledge, the topic of planning and control is considered among the areas in need of improvement in the construction industry [3]. This has yielded various research efforts that have been conducted to develop robust planning and control systems such as work packaging, Last Planner System®, Takt-Time Planning, activity-based methodology, and location-based methodology [4–6].

In industrial construction, and with the increasing project complexity and lack of predictability, Advanced Work Packaging (AWP) was developed as a planning and control method for industrial projects [7]. AWP is an innovative construction-driven process that is based on existing work packaging practices and industry practices [1]. The concept of AWP can be traced back to the 1990s, but it was scientifically formalized in 2009 through research conducted by the Construction Industry Institute (CII) [8,9]. Research on AWP was first launched in Northern America, and soon later, the implementation of AWP expanded and various countries including Peru, Brazil, Argentina, Spain, Norway, South Africa, Nigeria, Saudi Arabia, India, Thailand, China, South Korea, Australia, and Indonesia began integrating AWP into their industrial projects [9].

AWP is formally defined as “a project framework to divide project scope into manageable portions of work for planning and execution to achieve improved productivity and increased predictability. AWP incorporates agile and lean construction methodologies – empowered through automation technology – to optimize capital projects across the entire asset lifecycle” [9]. AWP is also a planning and control system for all stakeholders including the owner, engineer, contractor, subcontractors, vendors, and operators [1,10].

Two key concepts behind AWP include optimizing workflow by integrating discrete packages of work across disciplines into a synchronized plan that will be executed by forepersons and aggressively and collaboratively aligning teams to make that work ready by removing all constraints that would prevent that work from being executed without interruption according to that plan [11]. This requires an effective team that will drive alignment across all key functional groups (design, engineering, procurement, construction, commissioning & start-up) and an integrated supply chain [12].

Readiness gates are set up to ensure work can be released to downstream team members through collective go/no-go decision-making supported by enabling technologies that better inform teams of current conditions to support better decision-making [13].

AWP studies have shown that the implementation of AWP on construction projects results in numerous benefits including improved safety awareness and performance, reduced cost, improved labor productivity, reduced rework, improved overall project cost and schedule predictability, better alignment among stakeholders from planning through construction, and improved overall project quality [7,8,14]. Moreover, with the increased use of AWP on industrial projects, it was found that the level of implementation of AWP practices varies among stakeholders and across projects [1]. [1] developed an AEP maturity assessment form to assist construction stakeholders in evaluating the extent to which an AWP practice of a given project phase is implemented. Additionally, [15] developed an AWP capability assessment tool that enables a project or organization to assess its current state capabilities and desired future state capabilities.

While understanding the shortcomings of current practices and determining the desired future state is instrumental for an organization to begin its journey toward improvement, organizations struggle to structure and institutionalize the change effort [16]. Some organizations wrestle with decidophobia where the fear of making decisions takes over and prevents the organization from moving forward [17]. Other organizations do not provide a collaborative environment that supports change [18]. Organizations, however, are acknowledging that the cost of inaction is far greater than the cost of action. Thus, there is a need to equip organizations with the right decision-making tools to develop a roadmap or execution strategy to attain their desired future state [19].

While the existing research work on AWP discusses AWP practices and benefits, research does not present a standardized methodology to assist AWP organizations to improve their current state and reach a desired future state. This paper builds on the work conducted by [15] and aims to advance strategic thinking and assist construction stakeholders in making incremental improvements in their AWP practices and implementation. The objective of this paper is to develop a simple, yet holistic “AWP improvement Canvas (AWPIC)” that maps the essential elements that organizations must consider to facilitate the change dialog internally and move toward the desired future state. While not discussed in this paper in detail, those essential elements can be described as a blend of *people* who are at the center of any change in construction organizations, *processes* that must be analyzed and re-engineered to

remove waste and enhance their flow, *technology* that can transform tasks and add value to the desired outcome, and *culture* that would require collaboration, communications, and willingness to continuously improve among all related stakeholders [20,21].

2 Theoretical Underpinnings

Projects are executed based on a constant flow of decisions, the timing of those decisions, who makes those decisions, how they are made (collaboratively, committee, individually, etc.), and the implications of those decisions based on the quality and richness of the information used to make that decision [20]. Thus, the decision to improve from a current state to a future state must be driven by scientific thinking [22]. A search on Google Scholar of articles that discuss change and process improvement models and frameworks led to the identification of three research streams that this paper will build on, specifically: business process reengineering, business model canvas, and A3 process.

2.1 Process Reengineering

Studies have indicated that companies aim for process reengineering in three situations: (1) companies are facing difficulties and are desperate to find solutions; (2) companies are in a stable situation with satisfactory performance but their management anticipates difficulties, and (3) companies are in peak positions yet their management are ambitious and innovative and seek continuous process improvements [23]. Major process reengineering methodologies have been published in the literature since the early 1990s – most notably the ones presented in Figure 1 [24–31]. As shown in Figure 1, the methodologies can be distributed on four main processing reengineering phases:

- Defining current state
- Analyzing and re-designing the current state
- Developing future state
- Implementing and monitoring the future state

Moreover, research in the AEC industry has also presented AEC-oriented reengineering methodologies. Examples include studies on reengineering construction processes [32], construction management process reengineering [33–35], cross-organization process integration in the design-build team [36], process reengineering and improvement for building precast production [37], a redesign process model for design companies [38], and a lean-based framework to re-engineer processes in the era of Construction 4.0 [39].

Existing Methodologies		<i>Defining Current State</i>	<i>Analyzing and Re-designing Current State</i>	<i>Developing the Future State</i>	<i>Implementing and Monitoring Future State</i>
	<i>Harrison and Pratt (1993)</i>	1. Set direction for reengineering 2. Baseline and benchmark current process	3. Create the vision to proceed forward 4. Launch problem solving projects	5. Design improvements across processes	6. Implement change 7. Embed continuous improvement
	<i>Furey (1993)</i>	1. Determine customer requirements and goals 2. Map and measure existing process	3. Analyze and modify existing process	4. Design a reengineered process	5. Implement the reengineered process
	<i>Manganelli and Klein (1994)</i>	1. Preparation 2. Identification	3. Vision	4. Technical and social design	5. Transformation
	<i>Underdown (1997)</i>	1. Develop vision and strategy for reengineering	2. Create desired culture to implement reengineering	3. Integrate and improve the enterprise	4. Develop technology solutions
	<i>Mayer and DeWitte (1999)</i>	1. Motivating reengineering and starting correctly 2. Justifying reengineering	3. Planning reengineering projects 4. Setting up for reengineering	5. "To-be" design and validation	6. Implementation
	<i>Adesola and Baines (2005)</i>	1. Understand business needs 2. Understand the process	3. Model and analyze process 4. Redesign process	5. Implement new process	6. Assess new process and methodology 7. Review new process
	<i>Muthu et al. (2006)</i>	1. Prepare for BPR 2. Map and analyze "as-is" process	2. Map and analyze "as-is" process	3. Design "to-be" process	4. Implement reengineering process 5. Improve continuously
	<i>Tiamaz et al. (2018)</i>	1. Define goals 2. Prepare the environment	3. Understand the process	4. Manage wastes	5. Implement 6. Revise 7. Sustain results

Figure 1 Summary of the existing methodologies

2.2 Business Model Canvas

One of the major challenges that organizations face is communication. In fact, businesses can find themselves struggling to "make the unfamiliar familiar" when sharing ideas and plans with different internal and external stakeholders, making it a challenge to "frame ideas in terms, metaphors, or analogies that make them understandable" to all those involved [40]. One way of solving communication problems is business models, which can be used as "analogies for innovating businesses" and framing communication within companies and between them and their investors [40,41].

A business model describes the rationale of how an organization creates, delivers, and captures value [42]. It is an efficient guide that allows businesses to discover value creation, identify customer needs, exploit external opportunities, identify required resources, generate and increase profits, and perform short, medium, and long-term projections [43]. Moreover, clearly-understood business models can support strategic competitiveness by providing organizations with insights into the alignment of high-level strategies and underlying actions in an

organization [44,45].

To develop and communicate business models, Osterwalder and Pigneur [42] proposed the "Business Model Canvas" (BMC). BMC serves as "a blueprint for a strategy to be implemented through organizational structures, processes, and systems", and the canvas includes nine basic building blocks covering the four main areas of a business – customers, offer, infrastructure, and financial viability [42]. Its holistic approach, visual representation, and simplicity The holistic visual and simple approach gained BMC momentum with new business ventures in its early stages, then made its way into incumbent firms with well-defined business models that use BMC to innovate and maintain competitive advantage [46].

BMC also gained momentum in research, as researchers mutate the canvas' building blocks and make them more oriented toward specific industries and transformations [47]. Mutations can include adding, removing, and/or dividing blocks, modifying the blocks' content, linking elements between the blocks, and adding views that reflect the mutated canvas' specific objectives [48]. In the AEC industry, examples of mutated BMC

include the “Business Model Transformation Canvas” (BMTC) which illustrates the construction business model in Industry 4.0 [49], and the “Construction 4.0 Implementation Canvas” (CONiC4.0) that aims to provide implementation practices that can guide AEC organizations towards a successful Construction 4.0 vision [39].

2.3 A3

The A3 tool originally evolved from Toyota Production System where it was traditionally used as a collaborative problem-solving method [50]. It is named after the international paper size of A3 – a single sheet of ISO A3-size paper with SI dimensions of 297 millimeters x 420 millimeters or about 11 inches x 17 inches in the US [51]. At Toyota, A3 became the “standard for telling stories with facts” and “convey information in a single page using bullet points, charts, and graphs” and very few words [22]. The use of A3 evolved from “Problem-solving A3” to using the tool for reporting project statuses work-related proposals, and strategic planning [51].

A3 typically has sections that describe the theme and background, the problem statement or the current condition, the target statement or desired future state, systematic scientific analysis (such as root cause analysis (5 Whys), cost-benefit analysis (CBA), and cause-effect diagrams), possible solutions often involving cross-functional coordination, implementation timeline with actions and responsibilities, the impact of achieved results, follow-up actions with responsibilities and learning points to share [50,51].

With the rise in Lean construction, A3 became a central focus and it was used for different applications such as decision-making [18], simulations and gaming [52], continuous improvement [53], and sharing knowledge and lessons learned among project stakeholders [54].

3 Methodology

The methodology employed to develop the AWP improvement canvas encompasses four tasks. The first task consisted of reviewing existing methods for problem-solving and designing solutions. Existing business process reengineering models were summarized, the business model canvas - the most popular innovative business model - was reviewed, and the A3 process, which emerged at Toyota as part of the Toyota Production System, was examined. The outcome of the first task informed the authors about 1) elements that are crucial for organizations to consider when improving a process and 2) visual methods in which the improvement plan or process can be communicated. The authors then, for the second task, conducted six focus group

discussions with seven AWP subject matter experts. The focus group participants were asked to share their experience developing and implementing workflows and processes within their organization to improve their AWP practices. Content analysis was employed to analyze the interview data and proceeded in three steps: initial reading, coding, and creation of themes. A code is a phrase that represents a single idea and a theme is a word or phrase that describes a group of codes. For example, “prioritize solutions and receive buy-in” was coded from the interviews and assigned to the “Solution” theme.

The rich data collected from the interviews and the content analysis led to the identification of six key themes, or building blocks, that the AWP Improvement Canvas (AWPIC) must include when guiding organizations to successfully improve their AWP implementation (third task). These six Once developed, the canvas was discussed and validated with the AWP subject matter experts (fourth task). The canvas is developed to assist with making process and organizational reengineering decisions but most importantly to help organizations align these decisions to the overall transformation objectives.

4 The Proposed AWPIC

The proposed Advanced Work Packaging Improvement Canvas (AWPIC) is illustrated in Figure 1. AWPIC encompasses six building blocks that illustrate the flow and logic of how an organization can move from a current state that needs improvement to a future desired state.

4.1 Building One: Current State

The first building block is the Current State located on the bottom left of the canvas. This building block documents the current state conditions by clearly articulating shortcomings and the areas in need of improvement.

4.2 Building Two: Problem

The second building block is the Problem located above the Current State. This element aims to contextualize the problem by tackling the what, where, who, and when. In formalizing what the problem is, the team is encouraged to consider the following why questions: (1) Why do we believe to have a problem?; (2) Why do we have this problem? (It is recommended to employ the five why analysis to identify the root causes of the problem); and (3) Why do we need to improve?

Answering these three questions creates agreement on the problem, thus ensuring buy-in from all team members. Following the discussion of the problem, the

team must clearly show where in the project lifecycle of the project the identified problem this.

Next, all internal and external stakeholders (individuals, teams, and organizations) that are impacted by the problem, that will be impacted by the solution,

and those critical to the improvement process must all be identified. The team then discusses the urgency of the problem and devices a timeline to act (immediate action, intermediate action, and long-term action).

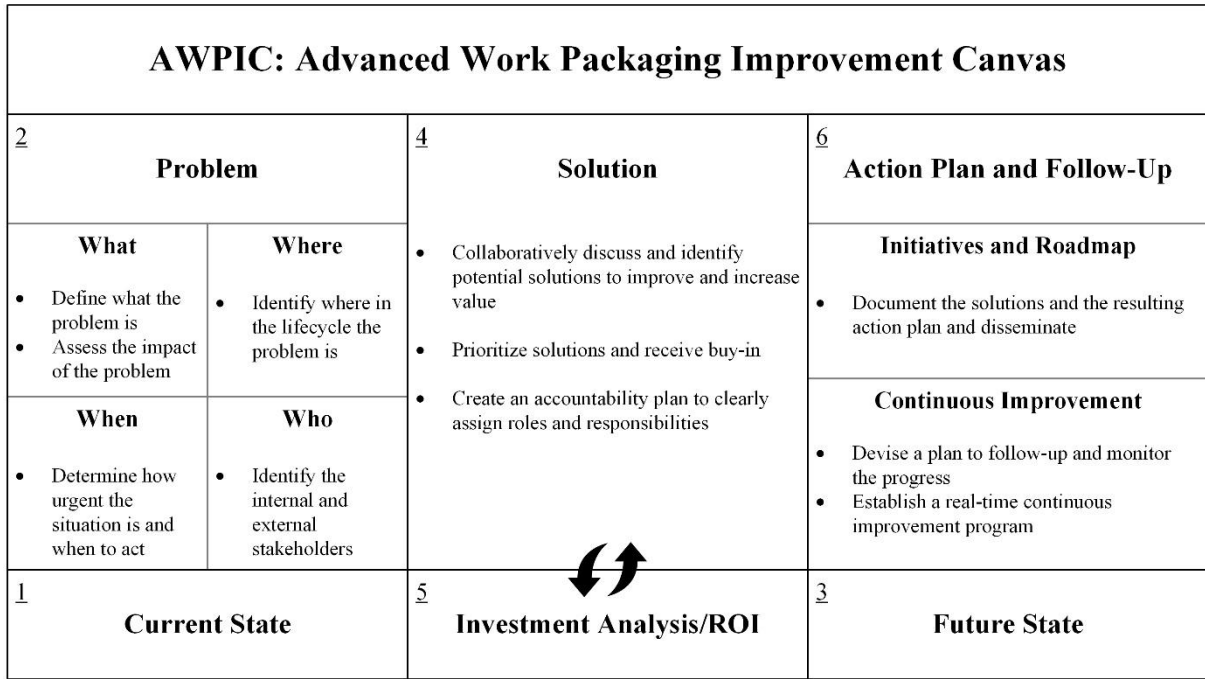


Figure 2 Proposed AWPIC

4.3 Building Three: Future State

Following a thorough understanding of the problem and its implications on the organization, the team then sets the goal for the Future State, i.e., the third building block located on the bottom right corner of the canvas. It is important to note that the Future State block must be continuously referenced and evaluated throughout the improvement process to ensure that the discussions align with the desired objectives.

4.4 Building Four: Solution

The fourth building block is the Solution located in the middle of the Canvas. The team works collaboratively to brainstorm and develop potential, realistic solutions that could be implemented to address the problem and help the organization move from its current state to its desired future state. After expanding the range of possible solutions, the team should define criteria for reducing the number of ideas to a manageable few. The criteria should be specific to the context of the business of the organization but could include factors such as estimation implementation timeline, possible resistance, and impact on competitive advantage.

Moreover, the team must discuss an accountability plan that clearly assigns roles and responsibilities to selected stakeholders to ensure.

4.5 Building Five: Investment and Value Creation Analysis

Simultaneously with Solution, Investment and Value Creation Analysis (the fifth building block) must be also considered because available resources and revenue potential are critical criteria that impact the feasibility of potential solutions. There is a loop connecting the Solution and Investment and Value Creation Analysis building blocks because these two are connected and one influences the other.

4.6 Building Six: Action Plan and Follow-Up

The sixth and last building block is the Action Plan and Follow-Up located to the far right of the canvas and above the Future State. This building block aims to document the solution resulting from the back-and-forth considerations of the fourth and fifth building blocks. An action plan with the proposed solutions, responsible parties, the expected timeline, expected outcomes, and

anticipated challenges must be developed to clearly communicate the initiative and the change roadmap to all involved parties. Zone management can be implemented to structure the action plan [55]. Zone management is a discipline that provides organizations with a strategic plan to allocate resources across three investment horizons: horizon 1 (in the coming fiscal year), horizon 2 (in two to three years), and horizon 3 (in three to five years). In addition to the timeline, zone management differentiates between disruptive and sustaining innovation and revenue performance versus enabling investment. Moreover, to ensure the effectiveness of the plan and create a mechanism for continuous improvement, a follow-up plan must be integrated into the last building block. The team can for instance specify when the team must revisit the plan to evaluate if the set desired future state has been achieved or not.

5 Conclusions, Limitations, and Future Work

Decisions in today's environment will have more consequences on project outcomes. The demand for making the best decisions will be crucial. They need to be earlier, more informed, have visual evidence, leverage enabling tools, and be deeply aligned across stakeholders. They will need to be based on leading indicators to affect work before execution versus lagging indicators that react to events in the past (proactive versus reactive).

This paper presented a proposed Advanced Work Packaging Improvement Canvas (AWPIC) to assist organizations in improving their current AWP practices through a structured decision-making roadmap. AWPIC is the culmination of data collected from seven AWP subject matter experts regarding their experience with AWP improvement and change efforts. AWPIC consists of six building blocks: *Current State*, *Problem*, *Future State*, *Solution*, *Investment and Value Creation Analysis*, and *Action Plan and Follow-Up*. While this paper proposed a new canvas to improve AWP implementation, it has its limitations. The proposed framework is a concept, and its practicability has not been tested yet. Additionally, the authors are expanding on the interconnectivity between people, processes, technology, and culture for each block. The canvas will further progress by conducting a series of case studies with small, medium, and large organizations to understand AWPIC in action and study the effectiveness of the proposed building blocks. Through a longitudinal study, the authors will work with various construction organizations and will use the canvas to guide change efforts.

6 Acknowledgments

The authors would like to thank the members of The Advanced Work Packaging Community for Business Advancement (AWPCBA) for their contribution to the canvas.

References

- [1] Halala YS, Fayek AR. A framework to assess the costs and benefits of advanced work packaging in industrial construction. *Canadian Journal of Civil Engineering* 46(3):216–29, 2019. Doi: 10.1139/cjce-2018-0072
- [2] Nassereddine H, Veeramani D, Hanna AS. Design, Development, and Validation of an Augmented Reality-Enabled Production Strategy Process. *Frontiers in Built Environment* 8:730098, 2022. Doi: 10.3389/fbuil.2022.730098
- [3] Sriprasert E, Danwood N. Next Generation of Construction Planning and Control System - the Lewis Approach. In: Formoso CT, and Ballard G, editors. *10th Annual Conference of the International Group for Lean Construction*, Gramado, Brazil, 2002
- [4] Gao S, Low SP. The Last Planner System in China's construction industry — A SWOT analysis on implementation. *International Journal of Project Management* 32(7):1260–72, 2014. Doi: 10.1016/j.ijproman.2014.01.002
- [5] Lehtovaara J, Coelho RV, Singh VV, Tommelein ID. Takt production in construction planning and control: integrative review. *Journal of Construction Engineering and Management*, 2023
- [6] Kenley R, Seppänen O. *Location-Based Management for Construction: Planning, scheduling and control*. 1st ed. London: Routledge
- [7] Ponticelli S, O'Brien WJ, Leite F. Advanced work packaging as emerging planning approach to improve project performance: case studies from the industrial construction sector. *The Canadian Society for Civil Engineering 5th International/11th Construction Specialty Conference*, Vancouver, Canada, 23001–10, 2015
- [8] CII RT-365. *Promoting the Use of Advanced Work Packaging (Phase 2)*. Construction Industry Institute
- [9] Mikaelsson R. Fundamentals of AWP, 2021
- [10] Calabrese A, Camaioni M, Piervincenzi G. Advanced Work Packaging in capital projects: a standardized model for EPC Contractors. *Journal of Modern Project Management*:1–19, 2019. Doi: 10.19255/JMPM02102
- [11] Wu C, Wang X, Wu P, Wang J, Jiang R, Chen M, Swapan M. Hybrid deep learning model for

- automating constraint modelling in advanced working packaging. *Automation in Construction* 127:103733, 2021. Doi: 10.1016/j.autcon.2021.103733
- [12] Rebai S, Hamdi O, BuHamdan S, Lafhaj Z, Yim P. AWP for residential buildings to modular construction: A proposed framework. *Proceedings of the 2022 Modular and Offsite Construction (MOC) Summit*, Alberta, Canada, 50–7, 2022
- [13] Al Rashdan A, Oxstrand J, Agarwal V. Automated Work Package: Conceptual Design and Data Architecture. *US Department of Energy Office of Scientific and Technical Information*, 2016. Doi: 10.2172/1364774
- [14] O'Connor JT, Leite F, Ma JW. Expanding advanced work packaging to include commissioning and startup for industrial projects. *Construction Innovation ahead-of-print(ahead-of-print)*, 2022. Doi: 10.1108/CI-09-2021-0173
- [15] CII AWP Business Accelerator Committee, 2022. Available at: [https://www.construction-institute.org/resources/advanced-work-packaging-\(awp\)-overview/network-with-the-awp-experts/awp-business-accelerator](https://www.construction-institute.org/resources/advanced-work-packaging-(awp)-overview/network-with-the-awp-experts/awp-business-accelerator)
- [16] Nassereddine H, Hatoum MB, Musick S, El Jazzer M. Implications of Digitization on a Construction Organization: A Case Study. *Proceedings of the Creative Construction e-Conference*, Budapest, Hungary: Budapest University of Technology and Economics, 71–9, 2022
- [17] Šostar M. Decidophobia as a Limiting Factor of Management. *Interdisciplinary Management Research* 7:272–82, 2011
- [18] Arroyo P, Long D. Collaborative Design Decisions. *26th Annual Conference of the International Group for Lean Construction*, Chennai, India, 463–72, 2018
- [19] Noueihed K, Hamzeh F. The Need for a Human Centric Approach in C4.0 Technologies. *Proceedings of the 30th Annual Conference of the International Group for Lean Construction (IGLC)*, Edmonton, Canada, 820–31, 2022
- [20] Bou Hatoum M, Nassereddine H, Badurdeen F. Towards a Canvas for Construction 4.0 Implementation in AECO Organizations. *Proceedings of the Creative Construction e-Conference*, Budapest, Hungary: Budapest University of Technology and Economics, 214–20, 2022
- [21] Ramadan BA, Taylor TRB, Real KJ, Goodrum P. The Construction Industry from the Perspective of the Worker's Social Experience. *Construction Research Congress 2022*, 611–21, 2022
- [22] Liker JK. *The Toyota Way: 14 management principles from the world's greatest manufacturer*. 2nd ed. McGraw-Hill
- [23] Hammer M, Champy J. *Reengineering the Corporation: A Manifesto for Business Revolution*. Zondervan
- [24] Adesola S, Baines T. Developing and evaluating a methodology for business process improvement. *Business Process Management Journal* 11(1):37–46, 2005. Doi: <https://doi.org/10.1108/14637150510578719>
- [25] Furey TR. A six-step guide to process reengineering. *Planning Review*, 1993
- [26] Harrison DB, Pratt MD. A methodology for reengineering businesses. *Planning Review*, 1993
- [27] Manganelli RL, Klein MN. *The reengineering handbook: a step-by-step guide to business transformation*, 1994
- [28] Mayer RJ, DeWitte PS. Delivering Results: Evolving BPR from art to engineering. *Business process engineering*, Springer, 83–129, 1999
- [29] Muthu S, Whitman L, Cheraghi SH. Business process reengineering: a consolidated methodology. *Proceedings of the 4th Annual International Conference on Industrial Engineering Theory, Applications, and Practice, 1999 US Department of the Interior-Enterprise Architecture*, Citeseer, 2006
- [30] Tiamaz Y, Lahboube F, Souissi N. A Business Process Improvement Method. *Industrial Engineering and Operations Management Conference*, vol. 14, 2018
- [31] Underdown DR. *Transform Enterprise Methodology*. The University of Texas at Arlington
- [32] Serpell A, Alarcón LF, Ghio V. A general framework for improvement of construction process. *Annual Conference of the International Group for Lean Construction*, vol. 4, 1996
- [33] Cheng M-Y, Tsai M-H, Xiao Z-W. Construction management process reengineering: Organizational human resource planning for multiple projects. *Automation in Construction* 15(6):785–99, 2006. Doi: 10.1016/j.autcon.2005.10.014
- [34] Cheng M-Y, Tsai H-C, Lai Y-Y. Construction management process reengineering performance measurements. *Automation in Construction* 18(2):183–93, 2009. Doi: 10.1016/j.autcon.2008.07.005
- [35] Cheng M-Y, Tsai M-H. Reengineering of construction management process. *Journal of Construction Engineering and Management* 129(1):105–14, 2003. Doi:

- [https://doi.org/10.1061/\(ASCE\)0733-9364\(2003\)129:1\(105\)](https://doi.org/10.1061/(ASCE)0733-9364(2003)129:1(105))
- [36] Cheng M-Y, Tsai M-H. Cross-Organization Process Integration in Design-Build Team. *Proceedings of the 22nd International Symposium on Automation and Robotics in Construction*, Ferrara, Italy: International Association for Automation and Robotics in Construction (IAARC), 2005
- [37] Chen J-H, Yang L-R, Tai H-W. Process reengineering and improvement for building precast production. *Automation in Construction* 68:249–58, 2016. Doi: 10.1016/j.autcon.2016.05.015
- [38] Mendonça LV, McDermott P. Lean Design Management Applied to Concrete Structures for Retaining Aqueous Liquids: A Redesign Process Model to Portuguese Design Companies, Brighton, UK, 2000
- [39] Hatoum MB, Nassereddine H, Badurdeen F. Reengineering Construction Processes in the Era of Construction 4.0: A Lean-Based Framework. *Proc. 29th Annual Conference of the International Group for Lean Construction (IGLC)*, Lima, Peru, 403–12, 2021
- [40] Sort JC, Nielsen C. Using the business model canvas to improve investment processes. *Journal of Research in Marketing and Entrepreneurship* 20(1):10–33, 2018. Doi: 10.1108/JRME-11-2016-0048
- [41] Lund M, Nielsen C. The Evolution of Network-based Business Models Illustrated Through the Case Study of an Entrepreneurship Project 2(1):105–21, 2014. Doi: <https://doi.org/10.5278/ojs.jbm.v2i1.720>
- [42] Osterwalder A, Pigneur Y. *Business Model Generation: A Handbook for Visionaries, Game Changers, and Challengers*. United States of America: John Wiley & Sons, Inc.
- [43] Murray A, Scuotto V. The Business Model Canvas. *Symphony Emerging Issues in Management* (3):94–109, 2016. Doi: 10.4468/2015.3.13murray.scuotto
- [44] Casadesus-Masanell R, Ricart JE. From Strategy to Business Models and onto Tactics. *Long Range Planning* 43(2):195–215, 2010. Doi: 10.1016/j.lrp.2010.01.004
- [45] Joyce A, Paquin RL. The triple layered business model canvas: A tool to design more sustainable business models. *Journal of Cleaner Production* 135:1474–86, 2016. Doi: 10.1016/j.jclepro.2016.06.067
- [46] Cosenz F, Noto G. A dynamic business modelling approach to design and experiment new business venture strategies. *Long Range Planning* 51(1):127–40, 2018. Doi: 10.1016/j.lrp.2017.07.001
- [47] Fritscher B, Pigneur Y. Visualizing Business Model Evolution with the Business Model Canvas: Concept and Tool. *2014 IEEE 16th Conference on Business Informatics*, vol. 1, 151–8, 2014
- [48] Schoormann T, Behrens D, Kolek E, Knackstedt R. Sustainability in Business Models - a literature-Review-based Design-Science-Oriented Research Agenda. *24th European Conference on Information Systems, ECIS 2016, Istanbul, Turkey, June 12-15, 2016*, 2016
- [49] Das P, Perera S, Senaratne S, Osei-Kyei R. Developing a construction business model transformation canvas. *Engineering, Construction and Architectural Management* 28(5):1423–39, 2021. Doi: 10.1108/ECAM-09-2020-0712
- [50] Sobek II DK, Jimmerson C. A3 reports: tool for process improvement. *IIE Annual Conference Proceedings*, Institute of Industrial and Systems Engineers (IISE), 1–6, 2004
- [51] Koskela L, Broft RD, Pikas E, Tezel A. Comparing the Methods of A3 and Canvas. *Proc. 28th Annual Conference of the International Group for Lean Construction (IGLC)*, Berkeley, California, USA, 13–24, 2020
- [52] Rybkowski ZK, Munankami MB, Shepley MM, Fernández-Solis JL. Development and Testing of a Lean Simulation to Illustrate Key Principles of Target Value Design: A First Run Study. *24th Annual Conference of the International Group for Lean Construction*, Boston, Massachusetts, USA, 2016
- [53] Bordin MF, Dall’Agnol A, Dall’Agnol A, Lantelme EMV, Costella MF. Kaizen - Analysis of the Implementation of the A3 Reporting Tool in a Steel Structure Company. *26th Annual Conference of the International Group for Lean Construction*, Chennai, India, 294–304, 2018
- [54] Gupta AP, Tommelein ID, Blume K. Framework for Using A3s to Develop Shared Understanding on Projects. In: Cuperus Y, and Hirota EH, editors. *17th Annual Conference of the International Group for Lean Construction*, Taipei, Taiwan, 545–56, 2009
- [55] Moore GA. *Zone to win: Organizing to compete in an age of disruption*. Diversion Books

Assessment of Financial Risk Parameters Associated with Public-Private Partnership Port Projects in India

¹Krushna S. Raut and ²Dr. Gayatri S. Vyas

¹MTech student, COEP Technological University, Pune

²Assistant Professor, Civil Engineering department, COEP Technological University, Pune
rautks21.civil@coep.ac.in, gsv.civil@coep.ac.in

Abstract –

In developing countries infrastructure investment is increased in last few decades. Public private partnership plays important role in low- and middle-income countries for providing finance. 95% of India international trade is transport through port sector. Hence it is big infrastructural project for India to connect with other countries. Public private partnership is new way for private investment in port infrastructure project. Central Ministries would oversee implementing the projects listed under the Sagarmala programme mostly in a private or PPP approach. In public private partnership model some issues may arise during whole life cycle of port project. Some of the problems include financial, legal, social, land acquisition as well as construction time delay. The aim of this paper is to investigate risk parameter associated with public private partnership project and further modelling the risk. Monte Carlo simulation is used in the Net Present Value (NPV) @RISK model to mitigate risk. Various risk parameter associated with port project are found out by previous literature survey. The two risks that have the most effects on public-private partnership projects are discount rate and capital cost. The application of this paper helps to identify which sources of risk affect more. The proposed model can be used as decision making for investment by private investors and gives profitability of the project. This will be more helpful for public authorities to identify parameter which have largest impact on investment. It helps to apply corresponding strategy to minimize the financial risk during preconstruction stage.

Keywords –

Financial risk, Monte Carlo simulation, Net Present Value (NPV), port infrastructure, public-private partnership.

1 Introduction

In both developed and developing countries, the financial crisis that began in 2008, brought new interest in Public-Private Partnerships (PPP). By 2047, the government wants to see India become a developed country. To achieve this, the economy will need to grow quickly, driven by strong exports, investments, and domestic demand. A strong increase in exports will be made possible through maritime trade and port facilities. Therefore, to make Indian ports and exports competitive on a global scale, the government must promote the construction of world-class port infrastructure in India. By realizing the full potential of India's coastline and waterways, the ambitious national effort Sagarmala hopes to significantly improve the performance of the logistics sector in that country.

The government faces many constraints on public resources and is therefore looking towards the private sector as a funding source [1]. The Government of India (GOI) took a step forward in the fiscal year 2019–20 by allocating 0.149 million USD in capital expenditure over five years (2020–25) under the National Infrastructure Pipeline (NIP) program. PPP in the infrastructure sector is a key tool for accelerating the development of India's infrastructure and closing the infrastructure development gap envisioned by NIP. In India, the shift toward PPP as a means of enhancing infrastructure and customer service levels started early and has advanced tremendously. The challenges need to be resolved and chance must be provided of learning for various nations hoping to use PPP in the port sector. India is one of the world's largest PPP markets, with over 1500 big national construction industry projects as of March 31, 2014, [7]. Examining PPP as a way of combining private sector innovation and technologies to improve operational effectiveness and provide better public services.

To reap the rewards of speed in project delivery and greater service standards, the performance of the public sector must be competent. Due to the nature of long-term PPP projects and the unpredictability surrounding

predicted future revenue flows, traffic projections, construction delays, and cost overruns, these projects often carry considerable financial risks [12].

This paper aims to investigate and assess the financial risk parameters associated with public-private partnership port projects in India using NPV @RISK decision tool. The objectives of this research are (i) to investigate risk factors associated with the PPP port project, (ii) to identify financial risk parameters associated with the PPP port project that affect the Net Present Value (NPV) of cash flow, (iii) to develop a risk assessment model using the NPV @RISK decision tool of the current case study in India, (iv) to analyse the results.

Using a real-world PPP port project as an example, this study examines the investment risk connected to a PPP port infrastructure project. It employs the Net Present Value (NPV) @RISK model, which generates a cumulative probability distribution curve for NPV by considering a few related parameters and appropriate distributions. The proposed model can be utilized as a decision-making tool by private investors during the planning stage to assess the feasibility of the project and make investment decisions.

2 Literature Review

Using the Scopus search engine, a thorough desktop search on financial risk assessment in the PPP was conducted. Scopus was chosen because it is often used by other studies in this field and because of other factors including its usability, breadth of coverage, potency, and accuracy of the search results. The study objectives and prior literature were carefully considered while choosing and finalising the Scopus search terms. Relevant keywords included phrases like crucial risk elements, risk identification, risk assessment, and risk allocation. The initial search using the above string yielded 22 papers. Some irrelevant papers still appeared in the search from other subject areas. Search results were further scrutinized by manually defining the source type of relevant papers in the search options to 'journal'. This reduced the number of papers to 3.

NPV @RISK is a tool used for analysing the financial feasibility of projects by considering the uncertainty associated with the project's cash flows. In the literature, several studies have used the different approach to assess the financial risk parameters associated with PPP projects in India. Kagne and Vyas (2020) created a financial risk model using NPV @RISK to investigate the major investment risk factors linked with the Build operate and Transfer (BOT) road project in India. Kumar et al., (2018) examined the investment risk related to road projects by defining variables like traffic volume and project costs

and then analyzed the risk by examining actual PPP based projects in India. The authors used the NPV @RISK tool to develop model and performed Monte Carlo simulation.

Gad et al. (2022) classified economical risks like Financial Market Risk (FMR), Financial Operational Risk (FOR) and Financial Credit Risk (FCR). For example, the elements were discovered and found through interviews and surveys with professionals involved in construction industry projects. Modelling of financial risk is done using the Financial Risk Analysis Model (FRAM) model. Kara E. et al. (2021) used the Fuzzy Analytic Hierarchy Process (FAHP) method to assess and rank the risks associated with five construction machines utilized in port loading and unloading activities. Then, recommendations are made for each risk on preventative measures to lessen the listed risks and consequences. Ebrahim Jokar et al. (2021) used case studies of PPP-based freeway projects in Iran to identify the most significant hazards in these projects. The findings of a quantitative risk evaluation using the FAHP method revealed first-level risks in seven distinct groups, including risks to the economy and investment, risks to construction, risks to operations, risks to the law and politics, risks to other entities, and risks to the government.

Several researchers focus on risks in port projects. Xu et al. (2020) analyzed the possible issues associated with investing in port development projects in China and offered recommendations for risk assessment of such investments along with the features of investment risks associated with port construction projects. Joubert & Pretorius, (2020) described a method for identifying risks during the preconstruction phases of a port of shipment and associated container terminal, as well as a questionnaire of 215 potential issues and related risk breakdown structures (RBS).

Numerous studies have been conducted to help PPP projects succeed and get better, including those that take an individualistic approach and include future market conditions, inflation rates, and cost concerns. Only a limited number of research studies could be identified when looking specifically for risk in port projects. There is still a need for further investigation of the use of such models for actual public and private-based port construction work in the world.

3 Research methodology

The parameters related to the PPP port project and the many risk categories influencing it are initially identified in this article. Then, for each factor, a respective probability distribution is allotted to predict the parameter's real worth. The model was created using

NPV @RISK tool. The entire process utilized in this paper is summed up in Figure 1

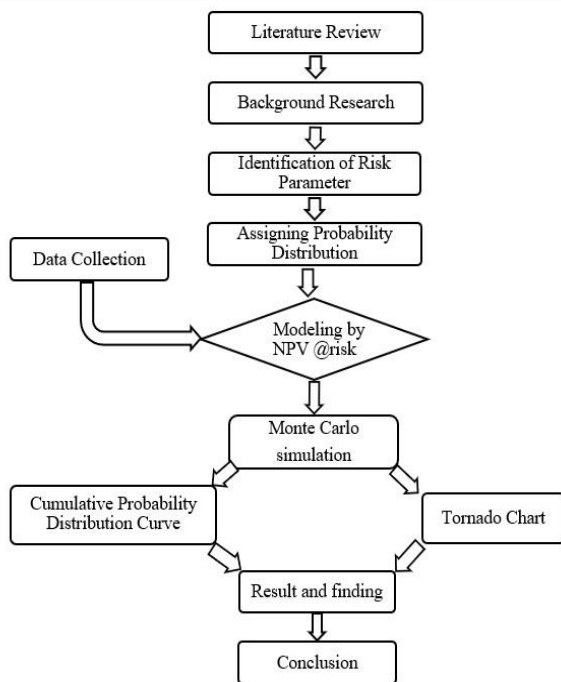


Figure 1. Flowchart of Research Methodology

3.1 Identification of financial risk parameters and probability distribution allocation

Given the complexity of the port construction project, several risk variables could affect it. These elements are interconnected in a complicated way, and the intensity of the effects they could have on the project is also varied. Making decisions about investments while totally ignoring these risk variables or only considering a small portion of them will result in poor choices. These include capital cost, concession period, construction period, discount rate, operating costs, and inflation rate.

3.1.1 Capital cost:

It is among the most significant expenses that the contractor must bear, thus it needs to be expected as accurately as possible while taking all potential unexpected circumstances into account. Since the concessionaire seeks to incur the least amount of expense possible, the largest likelihood happens at cheaper cost levels.

3.1.2 Concession period:

This is the time when the franchisee owns the port infrastructure and has the power to receive payments. It is the most important component of a PPP project because, if revenue is low, the concession period can be extended to allow the franchisee to cover all expenses,

and a decision regarding the length of the concession period is made based on profitability.

3.1.3 Construction Period:

The construction stage is the time when the actual construction of the port is done. Throughout the construction phase, the concessionaire does not make any money. As a result, the franchisee strives to complete the project within the time frame specified to avoid funding issues.

3.1.4 Discount rate:

To calculate the present value of future cash flows, discounted cash flow analysis, uses an interest rate known as a discount rate. This aids in determining if the cash flows from a project or investment will be more valuable than the capital expenditure required to support it in the present. The discount rate must equal or be higher than the cost of capital, which is the lowest rate required to justify the expense of a new endeavor.

3.1.5 Operating cost:

90% of the running expenses incurred during construction are often administrative[9]. Utility and maintenance expenses, however, are predicted to be 20% or less after commissioning. Additionally, it is a very uncertain expense [9].

3.1.6 Inflation Rate:

A state of inflation is one in which there is a steady rise in the price of products over time. Because of this inflation, people's purchasing power may decline, which will have a negative impact on port. Every nation consistently tries with a variety of strategies to keep inflation within the established normal ranges. Variable inflation makes people's welfare unclear and lowers their purchasing power for goods and services.

3.2 Allocation of probability distribution

3.2.1 Normal probability distribution

It is possible to simulate a variety of events using the normal distribution, which is a flexible distribution. Financial risk characteristics, such as concession period, interest rates, and inflation rates, behave similarly to natural phenomena.

3.2.2 Lognormal probability distribution

A few issues with normal distributions may be resolved by log-normal distributions. Log-normal distributions contain all positive variables, whereas normal distributions can also include negative random variables. The analysis of asset prices is one of the most typical uses of log-normal distributions in finance. A representation of a market's projected returns using a

normal distribution is possible. Even though, a log-normal distribution may be graphed for the market's price data. The compound return that the investment is likely to experience over time may thus be better determined using the log-normal distribution curve.

Table 1 shows the identified parameters with allocation of probability distributions.

Table 1. Allocation of the probability distribution

Sr. No.	Parameters	Probability distribution [Authors]
1	Capital cost	For capital cost the probability distribution consider as Lognormal [7], [12]
2	Concession period	Normal [8]
3	Construction period	Lognormal[10]
4	Discount rate	Normal [7], [12]
5	Operating costs	Lognormal [9]
6	Inflation rate	Normal [7], [12]

3.3 Data Collection

The Nhava Sheva International Container Terminal (NSICT) was India's first PPP port container terminal under Jawaharlal Nehru Port Trust (JNPT) and is still one of the country's most extensive ports. Based on the highest NPV of royalty given, a 30-year license for the port was granted in 1997. A total of 90 million USD was spent over two years to develop the terminal project. The financial data of NSICT is taken from GOI website [3], which is shown in Table 2.

Table 2. NSICT Financial Data

Parameter	Values
Concession period (in years)	30
Construction period (in years)	2
Capital cost (in million USD)	90

Operation and Maintenance cost	20% of revenue
Discount rate	7%
Inflation rate	5%

4 Development of model

Since the project involves working capital over a long period, the value of money over time is an important consideration in any investment. By creating a present value cumulative probability graph, the idea of NPV @RISK calculates the NPV generated from a single project within a certain confidence level. The uncertain parameters are then given the corresponding probability distribution along with their mean and standard deviation. The relationship between various parameters and how they affect net present worth is explored with net present worth selected as the appropriate risk output [7]

4.1 Cash flow for simulation

The costs include both the initial capital investment and the operating costs for the successive periods until the concession agreement expires. Revenue is calculated based on container traffic in Twenty feet Equivalent Unit (TEU) per year, tariff charge, and inflation rate and does not initiate until the construction period is complete [10]. The revenue is calculated as follows (see Equation (1)).

$$\text{Revenue} = (\text{Traffic in TEUs/year} \times \text{Tariff}) \quad (1)$$

Considering operation and maintenance cost 20% of the revenue for corresponding year [9]. All values are in Indian rupees. Then cash flow value for each year is calculated and then represented them in cash flow diagram which is shown in Figure 2. NPV of the cash flow diagram is calculated using following Equation (2) and its value is 22.98 million USD.

$$\text{NPV} = \sum_{t=1}^n \frac{\text{CF}_t}{(1+i)^t} \quad (2)$$

Table 3. Cash flow for simulation

Year	Cost	Revenue	Cash Flow	Present Value
1	45	0	-45	-42.056
2	45	0	-45	-39.304
3	0	12.906	10.325	8.428
4	0	30.314	24.251	18.501
5	0	41.178	32.942	23.487
6	0	52.398	41.918	27.932

7	0	53.682	42.945	26.744
8	0	53.765	43.012	25.033
9	0	49.784	39.827	21.663
10	0	44.979	35.983	18.292
11	0	55.050	44.040	20.923
12	0	52.096	41.676	18.505
13	0	59.826	47.860	19.860
14	0	61.993	49.594	19.233
15	0	58.712	46.969	17.024
16	0	43.729	34.983	11.850
17	0	40.602	32.482	10.283
18	0	48.592	38.873	11.501
19	0	57.169	45.735	12.646
20	0	60.027	48.022	12.409
21	0	63.028	50.423	12.177
22	0	66.180	52.944	11.950
23	0	69.489	55.591	11.726
24	0	72.963	58.371	11.507
25	0	76.612	61.289	11.292
26	0	80.442	64.354	11.081
27	0	84.464	67.571	10.874
28	0	88.688	70.950	10.671
29	0	93.122	74.4972	10.471
30	0	97.778	78.222	10.275
NPV= 22.98 million USD				

Table 3 shows the capital cost, revenues, and present value for each financial year for 30-year concession period.

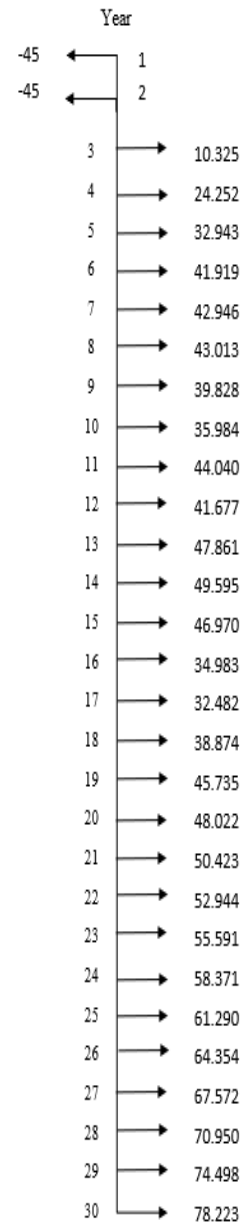


Figure 2. Cash flow diagram shows the net cash flow values of the project

4.2 NPV @RISK decision tool

NPV is a financial statistic used to evaluate the present value of future cash flows, discounted at a specific rate. NPV @RISK decision tool which is excel add-in tool is used for risk analysis and making decisions in uncertain situations. The project inputs, such as the capital cost, concession period, construction period, operation and maintenance cost, discount rate, and inflation rate factors, must first be defined before using

@RISK for NPV analysis. After that, using @RISK to generate a probability distribution based on input data.

4.3 Monte Carlo simulation

The simulation of Monte Carlo is a computer-aided numerical approach for calculating risk in statistical analysis and decision-making, [4]. Monte Carlo

simulation computes the outcomes using repeated random sampling and statistical analysis. The random experiments in which the precise outcome is not known beforehand, are very closely related to this simulation technique. Monte Carlo simulation can be seen as a methodical approach to performing a what-if analysis in this situation. Monte Carlo simulation of 5000 iterations is performed for NPV @RISK.

	A	B	C	D	E	F	G	H	I	J	K
1	NSICT										
2	Concession period	30									
3	Construction period (in years)	2									
4	Capital cost (in million USD)	90									
5	O & M cost	0.2									
6	Discount rate	0.07									
7	Inflation	0.05									
8											
9											
10		1197-98	1198-99	1999-2000	2000-01	2001-02	2002-03	2003-04	2004-05	2005-06	2006-07
11	Year	1	2	3	4	5	6	7	8	9	10
12	Construction cost	45	45	0	0	0	0	0	0	0	0
13	Traffic	0	0	343187	694899	943928	1201119	1230555	1232470	1323801	1359125
14	Tariff charge (in INR)	0	0	3000	3480	3480	3480	3480	3480	3000	2640
15	Conversion of INR to USD	0.01229	0.01229	0.01229	0.01229	0.01229	0.01229	0.01229	0.01229	0.01229	0.01229
16	Tariff charge (in USD)	0	0	36.87	42.7692	42.7692	42.7692	42.7692	42.7692	36.87	32.4456
17	Revenue (in million USD)	0	0	12.9064	30.3147	41.1785	52.3983	53.6824	53.766	49.7847	44.9796
18	O & M cost	0	0	2.58127	6.06294	8.23569	10.4797	10.7365	10.7532	9.95694	8.99592
19	Cash Flow	-45	-45	10.3251	24.2517	32.9428	41.9187	42.946	43.0128	39.8278	35.9837
20	Present Value	-42.056	-39.3047	8.42835	18.5015	23.4877	27.9322	26.7446	25.0338	21.6637	18.2923
21	Net Present Value	22.9764									

Figure 3. Developed financial model

Figure 3 Shows the developed financial model in which firstly, input financial data is inserted (from Table 2) and then detailed cash flow is prepared for concession period i. e., for 30 year and shown here up to 10 years. Then NPV is calculated and then using NPV @RISK Monte Carlo simulation is performed.

5 Results and discussions

In the NPV @RISK tool, a financial risk model is created for the real port project NSICT at JNPT in India. The

NPV for the project is 22.98 million USD, according to the model's calculations. Figure 4 shows the probability of having a positive net present worth is 55.4 %, which implies that this project could occasionally have a negative net present worth under extreme circumstances. As a result, for this project, the likelihood of success is 55.4 % and the likelihood of failure is 42.1 %. When compared to the other 6 elements affecting this project's NPV, the discount rate is the most significant risk parameter which is shown in Figure 5.

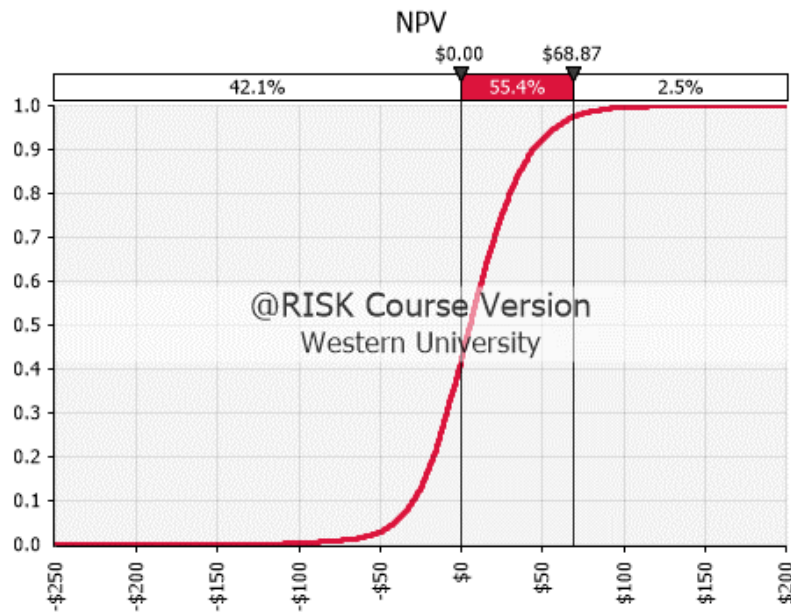


Figure 3 Cumulative probability of positive NPV

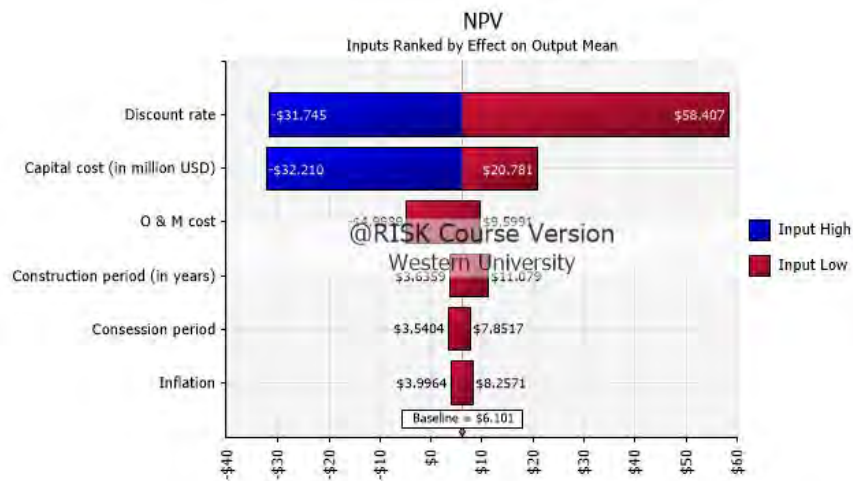


Figure 4 Tornado chart showing critical parameter

6 Conclusion

According to previous literature, several studies have already been done in PPP projects, regardless of the port sector project. The main contribution of this paper is the application of risk-analysis model for analyzing the investment risk associated with PPP-based port infrastructure projects. This will help to prevent the concessionaire from suffering significant losses and from having their money wasted. The PPP-based port projects can be effectively risk analyzed by using NPV @RISK,

as detailed in this work, to identify the related uncertainty. Additional PPP port project financial data can be conducted to modify the financial evaluation. By carefully weighing the profits to the concessionaire, the port sector in the world can use NPV @RISK decision tool. NPV @RISK model is more accurate and take less time for simulation other than FRAM and FAHP. Therefore, by following the example set by this study, more case studies and parameters can modify the results obtained which will reduce financial risk .

References

- [1] Chourasia A. S., Dalei N. N., and Jha K. Critical success factors for development of public-private-partnership airports in India. *Journal of Infrastructure, Policy and Development*, vol. 5, no. 1, 2021.
- [2] Gad N. A., Monem A., and Hamid A. Modeling financial risk contributes to construction projects; case study of expansion food industries. *HBRC Journal*, vol. 18, no. 1, pp. 85–106, 2022.
- [3] Government of India, Public Private Partnership in India. On-line: <https://www.pppinindia.gov.in/>, Accessed: 08/01/2023.
- [4] Hacura A., Jadamus-Hacura M., and Kocot A. Risk analysis in investment appraisal based on the Monte Carlo simulation technique. *The European Physical Journal B*, 2001.
- [5] Joubert F. J., and Pretorius L. Design and construction risks for a shipping port and container terminal: case study. *Journal of Waterway, Port, Coast, Ocean Eng*, vol. 146, no. 1, 2020.
- [6] Juliza H. and Anggiat H. O. S. Identify the operational risk of the port by the risk breakdown structure (RBS) method. *IOP Conference Series: Materials Science and Engineering*, Institute of Physics Publishing, 2019.
- [7] Kagne R. K. and Vyas G. S., Investigation and modelling of financial risks associated with PPP road projects in India. *International conference on transportation and development*, 2020.
- [8] Kakimoto R. and Seneviratne P. N. Financial risk of port infrastructure development. *Journal of Waterway, Port, Coastal, Ocean Eng*. Vol. 126:281-287, 2000.
- [9] Kakimoto R. and Seneviratne P. N. Investment risk analysis in port infrastructure appraisal. *Journal of infrastructure system*, 6:123-129, 2000.
- [10] Kakimoto R. and Seneviratne P. N. Simplified investment risk appraisal in port infrastructure project. *Traffic and Transportation Studies*, 2000.
- [11] Kara E., Menten A., and Akyildiz H. Operational risk management in loading and unloading operations in ports. *GiDB DERGi*, 2021.
- [12] Kumar L., Jindal A., and Velaga N. R. Financial risk assessment and modelling of PPP based Indian highway infrastructure projects. *Transportation Policy (Oxf)*, vol. 62, pp. 2–11, 2018.
- [13] Rybnicek R., Plakolm J., and Baumgartner L. Risks in public-private partnerships: a systematic literature review of risk factors, their impact and risk mitigation strategies. *Public Performance and Management Review*, vol. 43, no. 5, pp. 1174–1208, 2020.
- [14] Sugrue D., Martin A., and Adriaens P. Applied financial metrics to measure interdependencies in a waterway infrastructure system. *Journal of infrastructure system*, 27(1): 05020010, 2020.
- [15] Xu X., Yang Z., Jin L., and Hao L. Research on risk assessment of port project investment and construction. *Journal of Coastal Research*, vol. 2020, no. 115, pp. 187–189, 2020.

From Lab to Field: A Sociotechnical Systems View of the Organizational Cycle for Intelligent Robotics Technologies Ideation, Planning, Design, Development and Deployment

Karyne C.S. Ang¹, Shankar Sankaran¹, Dikai Liu² and Pratik Shrestha³

¹School of Built Environment, University of Technology Sydney, Australia

²School of Mechanical and Mechatronics Engineering, University of Technology Sydney, Australia

³Building Structures, Aurecon Group, Australia

karyne.ang@uts.edu.au, shankar.sankaran@uts.edu.au, dikai.liu@uts.edu.au, Pratik.shrestha@aurecongroup.com

Abstract

Advanced intelligent robotics technologies like autonomous and collaborative robots in construction sites have been explored in the literature for more than a decade. However, there are only a few prototypes that successfully make it to the field due to various reasons. There is burgeoning interest in the design, development and deployment of intelligent robot technologies due to the spread of Industry 4.0.

Ideas for a robot project often stem from a visionary's intention to solve industry challenges such as workplace safety and well-being, productivity, market competitiveness. The translation of the visionary's idea into reality goes through an iterative design and development process before a tangible robot prototype is produced. Within the organisational cycle, the abilities to lead, organise, mediate, plan, communicate and engage are important. At each stage of the cycle, different interactions and considerations are required involving different stakeholders. However, for ultimate success, the proof of concept, acceptance and deployment into field (reality) are equally important aspects of the development for new technologies.

This study examines the sociotechnical systems processes involved in an innovation project about intelligent robot technologies in construction. We examine stakeholder interactions across the system from ideation, planning and design, rapid iterations and prototyping that resulted in a successful development of a proof-of-concept intelligent robot onsite.

Keywords:

socio-technical systems; stakeholders; design-thinking; intelligent robots; construction

1 Introduction

A Socio Technical Systems (STS) perspective is applied to explore how different stakeholders contribute

to organise, plan, design and develop to ultimately deploy and work with robots onsite in construction work. This perspective is important because the study demonstrates useful insights into how co-operative work involving humans and intelligent robots could be designed and structured. Within the larger sociotechnical system, stakeholders are both internal and external and could include project owners, mediators, designers, planners and workers, labour unions and media.

1.1 Industry 4.0 and Construction 4.0

Industry 4.0 promoted 'horizontal, vertical and digital integration' of processes used to design produce and deliver products. [1] (p.22). Based on the strategies and impact of Industry 4.0 the construction sector also realised that it could transform itself. To facilitate this transformation Construction 4.0 was conceived 'to overcome the existing horizontal, vertical, and longitudinal fragmentation and to take a holistic approach to the improvements needed in the industry [2] (p. 301). One of the nine pillars of Industry 4.0 is deployment robots which applies to Construction 4.0. Robots in construction

Robots have been used in construction since the 1970's. Their application in construction has increased evidenced by the number of articles appearing in ISARC proceedings on the application of robotics in construction [3]. De Soto & Skibiniewski [3] predict that Construction 4.0 concept 'makes the construction automation and robotics promising' (p. 292) and will lead to an increase in the use robotics in construction. However, the introduction of robots will require 'human-machine relationship to evolve' [3] (p. 302) requiring more attention towards human-robot interaction that incorporates the 'social aspects of human robot collaboration' [4] (p.669).

1.2 Robot and Human Collaborative workspaces

To facilitate collaboration with humans at work, robots used in collaborative work would be designed differently [5]. Factors considered in designing collaborative robots should ensure that they work at lower speeds than industrial robots used in assembly lines; they are designed to cooperate with humans and not replace them; they are safe to work in shared workspaces; and they are easy to program enabling them to be flexible to carry out different tasks [5].

The popular belief that automation will reduce 'human interaction' is untrue as humans will need to develop new skills when new technologies are introduced [6] (p. 10124). Sony and Naik call for adopting a sociotechnical perspective for a successful and sustainable implementation of new technologies [6]. Adopting such a perspective could help in designing robots for use in the construction sector. We now briefly review the sociotechnical aspects of introducing automation in a workplace.

1.3 Sociotechnical systems and design

STS have their origins in the work of the Tavistock Institute Human Relations in the in the UK [7]. Sociotechnical theory has at its core 'the idea that the design and performance of any organisational system can only be understood and improved if both 'social' and 'technical' aspects are brought together and treated as interdependent parts of a complex system' [8] (p 464).

One of the earliest scholars to develop some rules to guide sociotechnical systems designs was Cherns [9]. Cherns' principles have been updated for the digital age by Clegg [8] by developing a sociotechnical framework that conceptualises modern work as a complex system comprising of social (people, culture and goals and technical (technology, infrastructure and processes) elements. Recently, Eason [10] has suggested further that four principles are important in designing sociotechnical systems:

1. Implementing using minimum critical specifications with flexibility for adaptation during application to fit local circumstances.
2. Aligning the social and technical aspects of a system to the processes they are to undertake using contextual knowledge.
3. Enabling user participation to understand implicit aspects of the social system from people who will use the system.
4. Preparing for evolution of the solution to be effective.

The last point is reinforced by Pasmore et al. [11] who argue that 'In traditional STS [sociotechnical systems], the goal was to design the social system around a fixed

technical system in a way that maximised throughput and quality while satisfying human needs. In the next generation STS, the goal of balanced optimisation is predicated on the notion that everything is in motion' (p. 79). It is further predicted that future organisations introducing changes in their work processes would use design thinking approaches to designing sociotechnical systems [11]. Design thinking 'is a discipline that uses the designer's sensibility and methods to match people's needs with what is technologically feasible and what a viable business strategy can convert into customer value and market opportunity' [12] (p. 85). The design thinking process can be consolidated into five stages – empathise, define, ideate, prototype and test [13] (p. 230). These elements of design thinking are mentioned in numerous STS literature but have not been extensively explored in the construction context.

In sum, STS theory explores how the introduction of new technology in organisations impacts on people, specifically how multi-skilled people work together as self-organised units to optimise social and technical systems [14]. Accordingly, optimal performance requires attendance to both the social and technical aspects of work organisation. Our review of the literature showed that very few cases about intelligent robot technologies in construction are reported.

We draw from the STS worldview to explain how different stakeholders across multiple systems organise, plan, design and develop to ultimately deploy and work with robots in a construction project.

The research questions addressed in this paper are:

1. *How does an innovative idea about intelligent robot technologies translate into practice in the construction industry?*
2. *What roles do various stakeholders play from ideation to deployment in innovation projects in the construction sector?*

The research context is a construction site where an intelligent robot was tested as proof-of-concept in field. Based on a real-life case study of an intelligent robot for automating a construction task we propose further considerations for teams designing collaborative or co-operative working roles, tasks and structures and networks for the construction workplace.

2 Research Methodology

2.1 Data Collection

A single case study was used to explore how ideas about intelligent robot technologies might be translated into practice. Through qualitative semi-structured interviews, the case study drew upon the perspectives of various stakeholders involved in the innovation project. Case studies provide an opportunity to investigate a real-

life, contemporary bounded system (a case) over a set time. Detailed, in-depth data involving multiple sources of information were collected and analysed to offer different in-depth perspectives, thick description and triangulation [14]. In this study we gathered stakeholder insights that traces the ideation, design, development and proof-of-concept test in field of an intelligent robot at a building construction worksite.

Publicly available documents from various media sources (news articles, videos, TV reports), confidential organisational reports and robot technology specifications were used to establish the background and context of the case. Specific references to these sources are not cited to maintain the anonymity of identities of the organisation where the robot was delivered. Profiles of the four interview participants can be found in Appendix 1, Table 1.

2.2 Data Analysis

The analysis used a systematic cycle with iterative coding and recoding that included categorising, sorting, prioritising, integrating, synthesising, abstracting, conceptualising, and finally, theory building [15]. Throughout this process, we applied an STS lens to address the research questions on how innovative ideas about intelligent robot technologies translate into practice in the construction industry. We considered the various roles that stakeholders played from ideation to deployment in this innovation project. The STS lens applied fits well with the interpretive nature of this study as indicated by Lofland et al [16] whereby social life happens at the intersection of one or more stakeholders (e.g. the interviewees) who engage in one or more activities (e.g., the behaviours in strategy, planning, design, development and deployment) and at a particular time in a specific place e.g., the case study of an intelligent robot project that was ultimately deployed at a construction site. We used Nvivo qualitative analysis software to map, organise and conceptualise the themes into conceptual clusters.

The Intelligent Robot Development team composition at the various stages in the cycle of the prototype development from (1) strategy planning and organisation consists of the Mediator as the project lead in engineering Design, Lead Robotics Director, Construction client, Designers and Construction Building experts and crew; while (2) is the design, development and testing team comprising Robotic engineers, Mechanical (hardware) and software engineers who are led by the Robotics Director and (3) Robot operations and proof-of-concept deployment on site that comprises the Operator of the robot, the Robot itself, Supervisor and Laborer. These clusters as illustrated in Figure 1 (developed for this paper) are marked by number and colored boundaries.

External to the team are the secondary stakeholders labelled as (4) comprising the media and labour union. Findings relating to the views of the primary stakeholder groups involved in the innovation project in the stages from (1) to (4) are presented and discussed from an STS perspective in the following section.

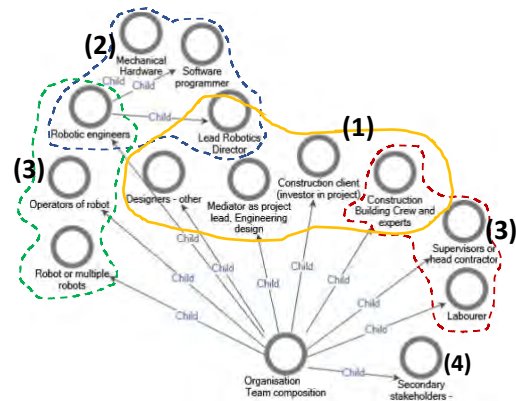


Figure 1. Organisational stakeholders in intelligent robot development from planning and design to deployment (developed for this paper)

2.3 Synopsis of the case study for context

Timber delivers sustainability and environmental benefits, resulting in the increasing popularity for Mass Engineered Timber construction. Building with timber is also faster, quieter and safer, and produces less waste. However, given the repetitiveness of labour-intensive tasks of installing screw fixings in a timber construction site, fatigue and back injury due to prolonged and awkward poses can occur.

In collaboration with MODA (client) and AURORA (construction engineering) and MAXPRO (Building construction firm), researchers at the University of Technology Sydney developed an autonomous robot for a timber building construction. The intelligent robot developed provides an innovative solution to address significant work health and safety issues, while improving efficiency and accuracy of the process.

The intelligent robot comprises of a mobile platform and a robotic arm with six degrees of freedom mounted with a mechanism to perform screw fixings. The robot autonomously navigates and localises itself on a floor at the construction site and makes its way to a section where long screws need to be fixed. Once it reaches the section, the robot calculates the locations of the screws, and moves its robot arm to the desired location while avoiding collisions with the surrounding environment. With advanced control methods the robot installs the screws into the timber floor. Once a section is completed, the robot automatically progresses to the next section to

install more screws.

Workers could monitor the operation and view live data through a simple user interface. At the point of prototype deployment onsite, a human operator was needed to feed the screws to the robot as the self-feeding mechanism was not ready due to time constraints. The prototype and human worker feeding the robot is shown in Figure 2.



Figure 2. Intelligent robot prototype with human operator feeding screws

3 Findings and Discussion

3.1 Findings from stakeholders in each stage of the organisational cycle

In this paper, we trace how the initial idea of having robots in construction moved into intention, strategy, organisation, planning, design, development and eventual deployment in the field. The organisational process provides an insight into how an innovation system works to eventuate intelligent robot technologies deployed at the construction site.

When we consider how innovation projects are organised from an STS perspective, there are different networks at play in the project with different levels of stakeholder interactions at different points in time across the lifecycle of the project.

The research data enabled us to examine the STS processes and stakeholder interactions in the system from the start, including ideation to the boardroom, what happened during the design thinking meetings and how the robots were developed, tested and a proof-of-concept deployed on site.

3.1.1 Ideation, consultation and strategic planning

At the beginning, an idea was proposed with the intention of innovatively addressing some of the issues faced while harnessing the opportunities provided in the construction industry. The project leader from AURORA, an engineering construction firm initiated the idea of using robots for timber construction and proposed it to the client (MODA).

The idea and reasoning: "What's *something cool that we can do and embed in research? It was a joke, really. We just said, 'Wouldn't it be funny if we got robots to build part of the building?'* And MODA said, 'Yeah, let's make it happen!'" (PRAKA). PRAKA also indicated that the client (MODA) was forward-thinking, and research driven. They were willing to invest in advanced technologies that would enhance the systems in construction while addressing the issues of cost and safety for their workers. The ideation was coupled with strong intentions and rationale for the organisation and industry at large, "Why not make a wonderful [timber] material readily available, and couple that with automation, and innovation to make it even faster, even cheaper, even better to build. At the moment, timber construction attracts cost premium. The material has more cost premium than concrete and steel does. If we use automation and innovation and robotics to make timber construction even faster to build, we bring the cost price down, which means it becomes more competitive, so that it becomes a material of choice. We disrupt the construction industry. So that was all of the reasoning and rationalisation behind why we needed the robot to do what we needed to do."

AURORA acknowledged very early on that they were not robot designers and required the consultation and support of other expert stakeholders. Once the idea was embraced and funds were approved by the client, they immediately sourced and form a multi-disciplinary team of consultants and experts.

Harnessing experts: "we're *not robotic designers, we're not robotics experts. We don't even do robotics.... Soon as day one, the contractor is then on board, we need the robotics team to be on board at the same time.... So we started forming working groups with UTS-IRD Director and the robotics team and as well as MODA. In fact, RMIT was also involved at that time. And we looked at various options.*" (PRAKA)

Design thinking and collaboration: "We use design thinking tools, and all that sort of stuff to hone down into a specific aspect of the timber building" (PRAKA).

"We had the German supplier, with their product, connections and their manufacturing processes. For the timber design. the lead was asking questions from about 12 other people. The whole team was made up of design managers, or drafting people, project managers, project engineers, all that sort of very technical process." (PEKA)

Integrating social and technical aspects in the system: Integrating the social and technical aspects of the organisational system as done in this case study contributed to the optimal design and performance of the overall project. This approach aligns well with STS concepts whereby these social and technical aspects are brought together upfront and treated as interdependent parts of a complex system [8]. In the early stages of

consultation and planning, the project lead introduced, led and mediated the various stakeholders including the client, engineers, contractors and robot designers to collaboratively identify processes, workflows and elements that would differ from a traditional construction system. This was critical as the deployment of intelligent robots onsite would disrupt the existing system of works. This was recognised and the consultation process took note of both the planning for the design of the robots and the design of the systems to facilitate anticipated disruptions to traditional construction work, manage workspaces and schedules, and minimise clashes when incorporating human-robot teams onsite. An STS-based mediation scenario was described by PRAKA, *"We needed the robotics and construction teams, and the engineers at AURORA to sit at the round table and say, This is your traditional form of construction. A contractor will say, here's how I'm going to build everything. Then the robotics team will say, well hang on, where am I going to fit in all this? That discussion to say, Hang on a second, you really need to allow for the robotics seem to come into this, come into that, come into here, and really sort of plan their work from there."*

The contractor echoes the facilitation and mediation efforts of AURORA, *"PRAKA from AURORA was the most fantastic organiser of a team. The way that he structured the minutes kept people everybody in line. We were paid as consultants [timber experts] to talk about the constructability of the project, the connections and how to get it built to a certain extent. (PEKA)"*

We refer to the literature on STS on the need to consider the ecosystem while delivering technological solutions. Pasmore et al. [11] set up a two-day lab called the socio-technical action research lab (STARlab) with a team of diverse experts at Silicon Valley, USA to explore how organisations will evolve taking into considerations social and technical aspects of managing change. The research team predicted that socio-technical design will evolve in the future to optimise technical system design; social systems design; organisation design and ecosystems design. STARlab team also predicted that to manage organisational change will be more inclusive of stakeholders in the ecosystem 'who play important roles in which work systems operates' (p.81). Design labs would bring together diverse stakeholders involved in a change initiative and 'design thinking principles and rapid prototyping' would be applied to move towards viable solutions (p. 81-82). This experience was reflected by one of the interviewees involved in the design thinking workshops.

"I had the pleasure of sitting in three or four design meetings a week with Germany, Italy, and east coast, and the MAXPRO design team. My involvement [in the design thinking sessions] was probably a good six months of

knowing that this was gonna happen." (PEKA)

3.1.2 Robot design, development and testing

The second level consists of the technology design, development and testing. Key stakeholders in this system are the Lead Project Engineer as a mediator working very closely with the Robotics team made up of The Director of the Robotics Institution, and the Hardware and Software Robot Engineers.

These stakeholders interacted directly to develop multiple virtual prototypes. Once they were satisfied with the test results, a physical prototype of the intelligent robot was developed, further tested and finally deployed onsite. The approach to experimentation, rapid and iterative prototyping found in new technologies for innovation like Pasmore's STARlab combined with design thinking [11] is described by PRAKA:

Virtual prototype: *"We were able to do a lot of virtual studies for prototyping and failing fast. Rather than building the robot and building 10 of those, we built many in the virtual environment."*

Iterative tests: *"Tested that, it didn't work, tested, it didn't work."*

Physical prototype: *"When we were comfortable with what we wanted, we built a real prototype. And we got some lab testing done."*

Deployment onsite as proof-of-concept: *"Thanks to the whole the testing, we were able to deploy it live on site, which meant that we were able to do it without any issues. Everything was very successful, and we were able to deploy it on site."*

The process of design, development and testing was very iterative. To develop the software programs for the intelligent robot to perform optimally as intended, the software engineer was required to understand the trade nuances of the task of timber drilling and screwing. The robot engineers did not have the initial technical construction expertise and needed to understand this aspect thoroughly before they were able to translate the tasks into hardware and software that made up the robot. To achieve this, the robotics team researched and consulted with expert contractors for industry-specific knowledge and immersed themselves in a hands-on approach to the timber craft of drilling and screwing. This helped them understand the force, torque, angles and alignment of the drills and screws with the boards, appropriate speeds, knowing when to start, stop or adjust the force and ensuring accuracy. This is described by the robotic engineers.

Knowledge transfers and Hands-on immersion: *"They provided us with very specific details about screw sizes, boards that they were using, because we don't know any of that going into the project, we have to get those details slowly."* (GIKA)

"We would buy the tools ourselves, do it ourselves."

He [construction expert] sent us a video, and like a worker I tried to copy it. If we had any issues, we would go to him, 'what are we doing wrong?'" (GIKA)

The robotic engineers also needed to understand the dynamics of construction sites through discussing different scenarios. They were also provided with construction area blueprints and maps by the contractor and construction project engineers.

Scenarios: "Every single scenario that's possible for a robot drilling machine, you have to think about it, you have to think of it and programming into it" (PEKA).

Mapping: "During the design phase, we mapped out different areas for the robot to go to. We worked with the robotics team at UTS" (PRAKA), and reinforced by GIKA, "They gave me the floorplan, blueprints, and metadata of the whole structure about the dimensions of everything that they're building. I designed the whole planning and motion algorithms, where the robot has to go, to sense where it needs to drill, and the robot can actually understand its environment before even going there." (GIKA)

3.1.3 Prototype development and Field trials

Beyond the lab, there was a pragmatic element of 'readiness' coupled by time schedules, client expectations and funding constraints. To ensure that technical tests were not entirely limited to the research lab, once the physical intelligent robot prototype was deemed safe and ready for use, it was deployed as a proof-of-concept in field. An introduction of the intelligent robot onsite changes the overall system. Further social and technical adjustments and improvisations were needed to the construction site, supervision, roles and work allocations needed to be made. For instance,

1. Shared workspaces but separate work sections
2. Human-Robot Teaming requiring collaboration
3. Variation of roles and processes – Robot supervision, quality management and robot operations

1) Shared workspaces but separate sections: Work for the timber workers working on similar tasks as the robot were limited to certain sectioned areas within the shared space with the robot, but not alongside the robot, as evidenced by PEKA, "Physically seeing it doing its job, I did see it. I was part of choosing the location where it was going to be done, and what was the practical thing to be done.... we got very limited access to the robot process when it was on site. The interaction was very limited, because it's a very prototype type process. We were told the size of the screw, the location to put it in, and our guys turned up and did it." (PEKA).

According to the robotic engineer ALKA, one consideration in intelligent robot technologies with collaborative elements is to ensure human safety when

allocating tasks," We can assign this area for human and this area to be done by the robot, or the robot can do it overnight for some tasks." The separation of work sections in a shared working space can be viewed as complementary in human-robot teaming, and a base level for human-robot collaborative work [17].

2) Human-Robot Teaming depicting collaboration onsite: During deployment in this case study, humans worked with the intelligent robot to operate and control the functions of the robot. In this instance the robotics engineers took the role of the human operator due to time constraints in the project.

"I think they need me and GIKA to show them first of all, how to do that step by step, how we can document it, and maybe [later] they can do it." (ALKA)

The screw-feeding mechanism is still human-operated, as the self-feeding mechanism for the robot was not ready at the point of deployment. "So now the worker has to load the screws. But later, the robot can ultimately do that" (ALKA)

"A human has to feed the robot with the screws, and then the screws can be inserted. The human can immediately move the robot or stop the robot, if it thinks it's in any danger, or it's doing the wrong thing. So that's the human collaboration there right now." (GIKA)

These elements of human-robot teaming, in fact, can be considered human-robot collaboration or HRC.

3) Variation of roles and processes: Robot supervision, quality assessment and certifications, robot operations

Workers would need to supervise and operate the robot for monitoring and control, "We have to check that the robot movements are right. Whether the points that the robot is screwing are okay or not. We [humans] have a good perception, with good eyes, rather than the robot where it just scans the floor. That's the collaboration with robots and the human." (ALKA)

Installations by the robot, as with a human labourer would need to be quality-certified, "Part of my quality processes, all our manual installation is checked by an engineer, all of that. So in the robotic component of it would need to be checked by our engineer who's going to sign it off, certified." (PEKA).

Robot operations: "So you have something like a computer, just click the button, and the robot will do that for you. They [workers] can learn and adapt, like using other machines in the construction site. Now it looks like another machine, but it's more intelligent." (ALKA).

Designing for the end-users in mind also meant considering how to make it easy for general labourers to operate and work with an intelligent robot, as commented by ALKA: "From our development and focus, it's whether the interface is good enough for the workers. We try to develop something like look like your phones. And everyone can use that easily."

3.1.4 External stakeholders (Media, Labour Union)

External stakeholders like the media and construction industry labour union had no direct involvement in the design, planning and deployment. However, they have an interest in the construction innovation and power to influence. They were kept in close communication by the key stakeholders, particularly the client, construction companies and lead project engineer in the process. For instance, the external media interactions for public relations and publicity (e.g., news, videos, social media releases) was managed by AURORA to ensure that publicity was accurately featured as intended to communicate the advances in engineering innovation for the construction sector. The publicised messages addressed worker safety, quality, sustainability and enhancement of worker well-being. The project was also careful to address concerns that such innovations would be threat to job-security. *"That's a huge part of the project is communicating to the team that, in fact, we're not taking away jobs, we're letting the robot do unsafe tasks. There's a big difference between taking away jobs versus eliminating unsafe tasks."* (PRAKA). These external stakeholders were managed as part of the critical larger socio-technical system that interacted with the internal human-robot systems.

3.2 Pulling it all together – Integration, collaboration, mediation and flexibility

Integration and mediation in the project team from an STS perspective is important [18]. The extent of involvement for contractors was communicated and managed upfront by the main lead engineering organisation AURORA, so that contractors are aware that they are tendering for a project that is innovative and therefore should not be viewed as a traditional construction project as revealed by these quotes:

"We put a specific requirement in there for the tenders to respond to say, 'we envisage that we will be doing something innovative, and we'll be using automation and construction, you as the tender need to respond to that and give your commitment'. So all the tenders, the construction companies who responded said, 'We don't know what it is, but we'd love to be engaging in that dialogue'." (PRAKA)

"The first question he asked was, 'We want to engage with you guys, but this project requires innovation, sustainability, and all those sorts of things. Can you help us with ticking those boxes?'" (PEKA)

Apart from formal contracts, attributes that contributed to a positive innovation team environment in the construction sector included contractors being forthcoming and collaborative, ability to compromise, willingness to be flexible with the aspiration.

"They were very forthcoming. And very collaborative in the sense that they said, We think we can help you with this. Compromises are important. Whilst we might have had an aspiration to do all of the screw fixings, that was never going to be a reality on this project. So the contractor wouldn't have wanted that because it would have held them up because it's never been done before.... So how do you make it happen? Part of it is collaboration, and part of it is compromise." (PRAKA).

3.3 Research limitations and future research

This study is limited to a single case study in the construction industry. The key stakeholders involved in the design and deployment of an intelligent robot built with the intention of installing timber screws in a large construction site were interviewed, but could be extended to more stakeholders (e.g., workers, external stakeholders). Additionally, researchers were unable to observe workers and the robot on site to examine human-robot teams in action as the building had been completed while this paper was written. This was overcome by videos with information and context for the research. For future research, the following socio-technical systems themes could be studied: human-robot teaming onsite, planning for human-robot teams in construction and multiple systems and levels within the organisational.

4 Implications and Conclusions

Organisations embarking on innovation projects such as intelligent robots in construction and how this is deployed on site as human-robot teams require a clear integration of organisational intention with the views and experiences of different stakeholders in the project from design to deployment. For innovative ideas about intelligent robot technologies to translate into practice in the construction industry, planning and design for workflow processes, roles and task allocations, mapping and zoning, and dynamic workspaces characterised by the construction site are critical in translating a vision into reality.

In practice, this implies that integrating and facilitating sociotechnical aspects of the stakeholders in the system are important considerations when conducting rapid and iterative prototyping and deploying the proof-of-concept onsite. Intelligent robot design, development and deployment onsite require the project lead to harness experts from multiple disciplines in a collaborative design thinking process.

From ideation to deployment, stakeholders hold different roles including leader, mediator, specialist consultant, designer, planner, supervisor, robot operator, expert and learner. Fundamental to the social and cognitive attributes of the various systems stakeholders are a willingness to embrace change (including

uncertainty and ambiguity), improvisation, and flexibility. The willingness of various stakeholders in the system to learn, share knowledge, engage in hands-on immersive learning and experimentation can fill the gaps in a socio-technical systems approach in innovations projects. Furthermore, onsite human-robot teaming requires planning from the start including work zones, and task allocations, robot supervision, accountabilities, safety and quality assessment and certifications and robot operations.

In conclusion, through a single case study about mass engineered timber construction, sociotechnical systems processes in an innovation project about intelligent robot technologies in construction were explored. We examined various stakeholder interactions across the system from ideation, planning and design, rapid iterations and prototyping that resulted in a successful deployment of a proof-of-concept intelligent robot onsite. This paper contributes to the application of sociotechnical systems concepts and design thinking in the planning, design, development and deployment of intelligent robots in construction.

5 References

- [1] Crnjac, M., I. et al., From concept to the introduction of industry 4.0. *International Journal of Industrial Engineering and Management*, 8(1): 21-30, 2017.
- [2] Sawhney, A., et al., A proposed framework for Construction 4.0 based on a review of literature. *EPiC Series in Built Environment*, 1: 301-309, 2020.
- [3] de Soto, B.G. and Skibniewski, M.J. Future of robotics and automation in construction, in *Construction 4.0*. Routledge., London, pages 289-306, 2020.
- [4] Tijani, B. and Feng, Y. *Social impacts of adopting robotics in the construction industry: A systematic literature review*. in *Proceedings of the 23rd international symposium on advancement of construction management and real estate*, pages 668-680, Springer, Singapore. 2021
- [5] Simões, A.C., et al., Designing human-robot collaboration (HRC) workspaces in industrial settings: A systematic literature review. *Journal of Manufacturing Systems*, 62: 28-43, 2022.
- [6] Sony, M. and Naik, S. Industry 4.0 integration with socio-technical systems theory: A systematic review and proposed theoretical model. *Technology in Society*, 61:101248, 2020
- [7] Guest, D.E., *The sociotechnical approach to work organization*, in *Oxford research encyclopedia of psychology*, OUP, Oxford. 2022.
- [8] Clegg, C.W., Sociotechnical principles for system design. *Applied Ergonomics*, 31(5): 463-477, 2000.
- [9] Cherns, A., Principles of sociotechnical design revisited. *Human Relations*, 40(3): 153-161, 1987.
- [10] Eason, K., Afterword: the past, present and future of sociotechnical systems theory. *Applied Ergonomics*, 45(2): 213-220, 2013.
- [11] Pasmore, W., et al., Reflections: Sociotechnical systems design and organisation change. *Journal of Change Management*, 19(2): 67-85, 2019
- [12] Brown, T., Design thinking. *Harvard Business Review*, 86(6): 84-92, 2008.
- [13] Emery, F.E. and E.L. Trist, *Towards a social ecology: contextual appreciation of the future in the present*. Plenum Press, London. 1972
- [14] Carter, N., et al. The use of triangulation in qualitative research. *Oncol Nurse Forum*, 41(5): 545-547, 2014.
- [15] Saldaña, J., *The coding manual for qualitative researchers*. Sage, London. 2021
- [16] Lofland, J., et al., *Analysing social settings: A guide to qualitative observation and analysis*. Wadsworth, Belmont, CA. 2006.
- [17] Michaelis, J.E., et al. Collaborative or simply uncaged? understanding human-cobot interactions in automation. in *Proceedings of the 2020 CHI conference on human factors in computing systems*, pages 1-12, Honolulu, HI, 2020.
- [18] Wihlborg, E. and Söderholm, K. Mediators in action: Organising sociotechnical system change. *Technology in Society*, 35(4): 267-275, 2013.

Appendix 1

Table 1 is based on Figure 1.

Table 1 Profiles of case study participants interviewed.

Participant	Role and responsibilities	Stage in the cycle
ALKA	Mechatronics robot engineer (hardware development)	2, 3
GIKA	Senior software robot engineer (programming)	1, 2, 3
PRAKA	Project lead engineer and mediator (overall project)	1, 2, 3, 4
PEKA	Construction consultant (installation of timber components)	1, 3

AURORA (Engineering Construction Firm, MODA (Construction Client), MAXPRO (Building Construction Organisation)

Digital Twin Approach for the Ergonomic Evaluation of Vertical Formwork Operations in Construction

Vigneshkumar Chellappa¹ and Jitesh Singh Chauhan²

¹Amity School of Design, Amity University, Noida – 201303, India

²Centre for Ergonomics: User-Centred Design and Occupational Wellbeing,
Indian Institute of Technology Guwahati, Guwahati – 781039, India

cvkumar@amity.edu, jiteshsingh@iitg.ac.in

Abstract –

Construction formwork activities are physically demanding and repetitive, increasing the risk of work-related musculoskeletal disorders. This study proposed a digital twin approach to evaluate the ergonomic risks associated with vertical formwork operations using steel formwork systems in Indian construction projects. The on-site observation captured the workers' postures, allowing for more reproducible and thorough evaluations. The researchers selected the significant postures, and the real scenario was replicated in a virtual environment and performed a simulation to evaluate the ergonomic risks involved in the tasks. The findings indicated that the workers were at high risk of developing musculoskeletal disorders in the trunk, neck, wrist, and arm during formwork operations which could result in long-lasting harm to the workers. The recommendations were provided based on the study findings, including changes in methods to avoid and reduce the signs of musculoskeletal disorder risk caused by the original operations. The study findings show how digital twins could be used to evaluate ergonomic risks associated with construction activities.

Keywords –

Digital twin; Vertical formwork; Construction workers; Health and safety

1 Introduction

Work-related musculoskeletal disorders (WMSDs) contribute to non-fatal occupational injuries in the construction industry [1]. Construction workers frequently suffer from WMSDs such as back pain, carpal tunnel syndrome, tendonitis, and sprains [2] due to physically demanding construction tasks involving prolonged awkward static/repetitive postures, long working hours, forceful exertions, and whole-body vibration [3]. Statistics reported that 41.2 out of every

10,000 employees experience WMSDs, which causes them to miss 12 job site work days in the U.S. [4]. Similar cases were recorded in Canada, indicating that 41.9% of all approved lost-time claims were attributed to WMSDs in the construction industry in 2008 [5]. In addition to causing work absenteeism, these WMSDs could also result in permanent impairment [6] and place a significant financial strain on the construction industry owing to lost production and higher workers' compensation costs [7]. Workers at construction workplaces perform specialized tasks, including formwork and roofing, that require physical demands, thus overexerting various body parts. Prolonged overexertion's most common side effects include pain, sprains, strains, and discomfort [8].

Determining the workers' postures and workloads is the first step in reducing their negative influence. Generally, manual observations are used for this, and the data are analyzed quantitatively using ergonomic scales. However, this approach is time-consuming [9] and subjective to deliver accurate evaluations [10]. To overcome these challenges, developing measuring tools has become a priority in the era of Construction 4.0, seeking effective processes. For instance, Yan et al. [11] detect rebar workers' postures using Inertial Measurement Unit (IMU)-based wearable personal protection equipment (PPE) and alerts them about the risk involved with their actions. Similarly, several researchers (e.g., [12]) examined workload using biomechanical assessment tools). Although these methods illustrate the concept, they need the worker to have several sensors attached to their bodies, which may be physically uncomfortable and irritating and have a negative impact on productivity [9].

This study proposed a Digital Twin (DT) approach to evaluate ergonomic risks associated with construction activities, given the limitations of these methods. Kaur et al. [13] define DT as creating a digital replica of a physical object. It offers real-time monitoring, analyzing, simulating, optimizing, and forecasting throughout the lifecycle [14]. Data duplication and information silos can be avoided due to DT application [15]. From

occupational health and safety perspective, DT is a virtual representation of the workplace, activities, and other elements used to forecast hazardous areas by simulating [16]. Wanasinghe et al. [17] reported that risks related to health and safety were reduced by optimizing offshore operations through DT in the oil and gas industry. Similarly, Ogunseiju et al. [8] proposed a DT framework to create awareness among carpenters regarding the ergonomic risks involved in their working postures.

Construction involves a wide variety of activities that require physical demands; hence, evaluating the ergonomic risks involved is necessary to prevent or reduce WMSDs. Compared to other construction activities, vertical formwork operations require a lot of physical demand [6] and have a chance of developing a high risk of WMSDs [19]. Labors and carpenters must carry large weights and squats to perform formwork operations, putting them at significant risk of WMSDs [20]. Formwork workers most frequently sustain low back, shoulder, hand, and wrist injuries and have a high prevalence of "sprains and strains" [21]. Numerous types of research have been undertaken on the causes and preventive measures of WMSDs in construction activities. However, only limited studies (e.g., [19]) reported the risk of WMSDs in formwork operations, especially traditional formwork.

The current study evaluated the ergonomic risks involved in vertical formwork operations while using steel formwork systems in Indian construction through the DT approach. First, a site observation was performed to understand the worker's nature of the job to understand how workers are associated with formwork activities. Second, video cameras were used to capture the working postures of workers involved in formwork operations. The researchers selected significant postures and created digital models for each working posture. Next, a simulation was performed to evaluate the ergonomic risks involved in the tasks. The proposed approach is significant from both a practical and theoretical perspective. Specifically, due to visualized results, construction workers and managers will benefit from an intuitive awareness of ergonomic risks.

2 Background

In 2002, Michael Grieves' presentation on "Product Lifecycle Management" later became "DT" [22]. According to Grieves and Vickers [23], DT is a collection of virtual information models intended to completely represent an existing physical product. The basic framework of DT is illustrated in Figure 1, which involves mapping the virtual worker to the actual worker through the interchange of data and information. DT generally consists of the physical element, its virtual

model, and the information that flows between these physical elements and the virtual model [8]. The National Aeronautics and Space Administration (NASA) applied the concept of DT for the first time in 2010 on the Apollo program to enable mirroring or twinning of the state of the real spacecraft during the mission [14]. Since then, many researchers have defined DT. For example, Tao et al. [24] stated that DT consists of a physical product, a virtual product, and connected data that connects the virtual and physical products.

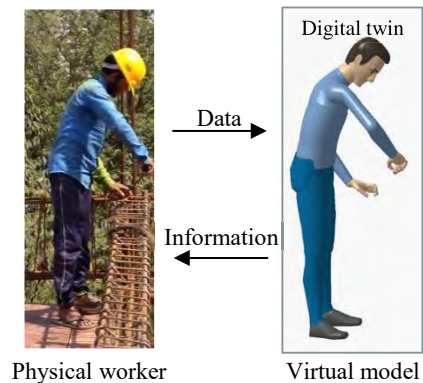


Figure 1. DT model – adaptation of Grieves model [23]

In the past decade, industry interest in DT has grown due to the rapid advancements in emerging technologies. This technology has been mostly adopted in healthcare, manufacturing, and aviation. Particularly in industries like manufacturing, DT technology has advanced significantly. For instance, Zhuang et al. [25] introduced a supervision system based on DT for product assembly shop floors. The findings indicated that by connecting the actual physical assembly with the digital representation, the real-time data capture of the assembly shop floors was able to provide smart manufacturing. The DT could identify the causes of product defects and analyze manufacturing bottlenecks [26]. In healthcare, the individuals' digital representation, including personal information like emotional status, activity data, and health data, may help understand one's well-being and factory working conditions. This can result in upskilling and the greatest production performance through ultrarealistic training programs, improving employees' physical and psychological wellness [27]. In the aviation sector, to secure and monitor data while producing aircraft components, Mandolla et al. [28] merged digital twin and 3D printing.

With the increased interest in DT, researchers in the construction domain explored the potential of DT and discussed how the technology might be used to enhance productivity [29]. Researchers further stated that DT optimizes asset performance by monitoring and diagnosing the asset's condition using simulations and

historical data [30]. Although the definitions of Building Information Modeling (BIM) and DT appear similar, construction researchers have drawn attention to the differences between the two concepts. BIM and DT differ in the technology, purpose, and stages of the project life cycle [31]. Volk et al. [32] stated that BIM can be used for constructability analysis, site safety management, and clash detection and does not function as real-time data. However, Khajavi et al. [31] claimed that to create a real-time view, extracted data from BIM could be an essential component to creating the DT of a building. Recently, Opoku et al. [33] argued that the DT primarily focuses on the operation phase, where BIM is mainly applied in the design and planning stages. With the potential of real-time monitoring, a DT-driven framework was proposed by Kan and Anumba [34] to improve workforce health and safety.

In summary, DT technology is used in various industries, including construction. Few studies have focused on the applications of DT for construction site safety; however, there is limited research on the application of DT for ergonomic evaluation for construction activities [8,20]. This study aimed to propose a DT-based approach for the ergonomic assessment of vertical formwork operations focusing on improving the health and well-being of construction workers.

3 Methodology

Several observational methods enable researchers to record and assess WMSD risk based on worker postures, and observation causes less interruption to worker task performance [19]. Therefore, an on-site observation was conducted to achieve research objectives. Manual observation or video recordings can be a basis for observational methods [35]. The present study used manual and video recordings to collect field data to allow for more reproducible and thorough evaluations. The study was performed on commercial construction projects in northeast India. At the time of the study, the workers at construction sites were associated with vertical formwork operations (panel assembly and panel erection) using steel formwork systems. The worker's task was to assemble formwork panels and lift the assembled panels manually (see Figure 2) to the place for erection.



Figure 2. Workers lifting assembled panels to

erect

The workers then erect the panels around the rebar and lock them with bolts and nuts. Figure 3 shows the workers erecting formwork panels around the rebar. The weight of the panel (108 kilograms) and panel dimensions were gathered from site supervisors. Researchers observed that workers mostly use their upper body and were involved in the repetitive nature of the work and awkward postures. Once the manual observation was performed, a video camera was used to capture the working cycle postures while performing the worker's routine tasks.



Figure 3. Workers erecting formwork panels around the rebar

The recorded videos were transferred to the computer over USB following the observational methods. Selected videos were divided into segments to select the significant postures for the analysis, as shown in Figures 4 and 5. The reason behind choosing these postures was that workers were repeatedly using the same postures while lifting the formwork panels throughout their task cycle. The literature (e.g., [20]) pointed out that the workers involved in formwork operations mostly use their upper body and only minimally involve their legs.



Figure 4. Panel lifting

The selected postures were transferred to CATIA V5 software to perform simulations and risk assessment.

CATIA V5 is a digital human modelling (DHM) software with a module for simulating individuals, enabling precise manual work modeling [9]. CATIA V5 replicates the real working environment of the worker's task (see Figure 6). The simulation was performed based on four following essential steps: (1) setting up a virtual environment that replicates the same workplace; (2) creating a DHM for actual workers; (3) data implementation and operations refining when necessary (e.g., grasping an object, lifting, handling, etc.); and (4) run the simulation. The ergonomics evaluation was carried out after the simulation had been completed.



Figure 5. Panel erection

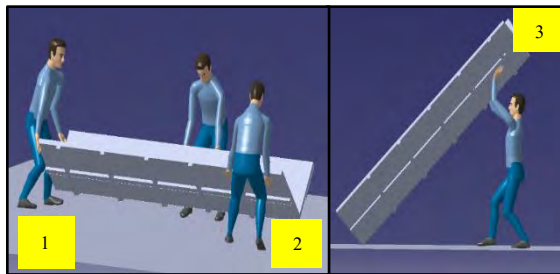


Figure 6. The virtual working environment of worker's tasks for postures 1-3

As previously mentioned, during formwork operations, workers mostly use their upper body parts, and hence, RULA (Rapid Upper Limb Assessment) is a suitable method for ergonomics study under the scenario depicted [5]. RULA, based on the work of McAtamne and Corlett [36], is integrated with the DHM module of the CATIA V5 software. The postural and biomechanical load requirements of workers' tasks/demands on the upper extremities, trunk, and neck are considered by the RULA ergonomic assessment tool. The final RULA score represents the WMSD risks for the evaluated job task. The RULA score ranges between 1 and 7, and the cut points and descriptions of the RULA level of WMSDs are as follows [37]: score 1-2 – acceptable

posture; score 3-4 – further investigation and change may be needed; score 5-6 – further investigation and change soon; and score 7 – investigate and implement change. It should be noted that the Human Model in CATIA V5 does not display which body parts are less comfortable. Figure 7 illustrates the methodological framework of the present study.

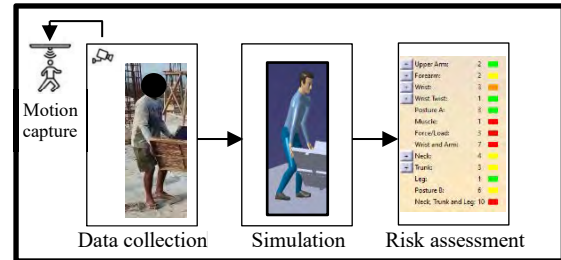


Figure 7. Overview of research methodology

4 Results and discussion

The overall RULA score for three postures is summarized in Table 1. The studies revealed that the postures were awkward, and the workers were at high risk of developing WMSDs. It can be seen in Figure 4 that the workers lifting panels stretch their upper body, causing muscle fatigue. The RULA analysis for both postures 1 and 2 are shown in Figures 8 and 9. It was observed from both these figures that the upper body parts, such as the wrist, arm, neck, and trunk, show red color, indicating that these postures experience muscle fatigue while lifting panels.

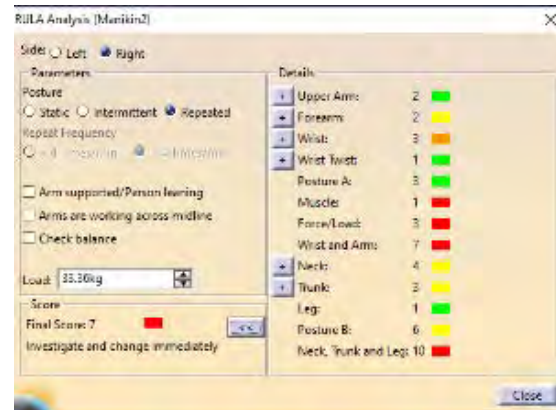


Figure 8. RULA score for posture 1

Similarly, the worker erecting panels had to stretch the upper parts of the body (see Figure 5). Figure 10 depicts the RULA analysis of posture 3, and the upper body parts, including the upper arm and wrist, exhibit a red color, which denotes that these body parts become fatigued from erecting panels.

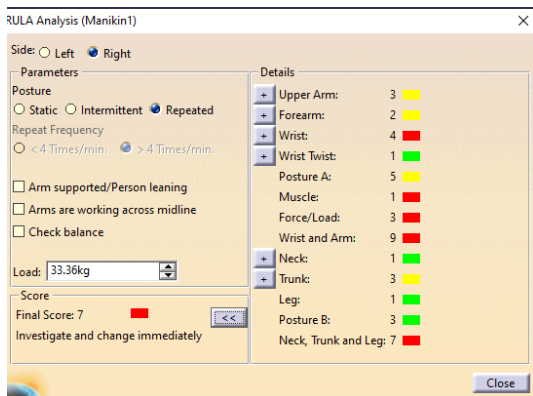


Figure 9. RULA score for posture 2

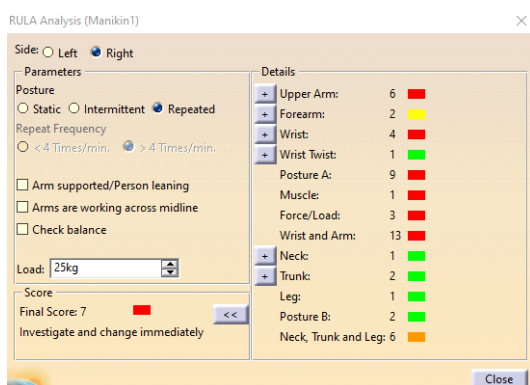


Figure 10. RULA score for posture 3

The overall RULA score is 7 for all the postures indicating that the postures could cause musculoskeletal disorders if it lasts for long time and hence, investigation and changes must be undertaken immediately for the outcomes obtained [30].

The neck, trunk, wrist, and arm are revealed to be the areas with the most risk in all the postures. The analysis made it clear that the workers were at a high risk of developing WMSDs when they repeatedly performed panel erection and lifting tasks.

Table 1 RULA score for vertical formwork operations

Posture	Score	Risk level	Action to be taken
1, 2 and 3	7	High	Investigate and change immediately

Formwork system manufacturers should introduce ergonomic interventions to prevent WMSDs. Based on the study findings and resources provided by National Institute for Occupational Safety and Health (NIOSH; 38) and Gambatese and Jin [19], the recommendations below may aid in preventing WMSDs that occur during formwork operations.

- Construction organizations should try to minimize lifting and overreaching requirements for their formwork workers by providing lifting devices, including hoists and hand tools.
- To reduce wrist-related disorders, formwork system manufacturers should provide handles or grips into formwork components without unnecessarily increasing the weight.
- Manufacturers should design ergonomic tools to eliminate the need for form workers to outreach and bend. For instance, extension clamps could be included in tools to allow users to do these activities while standing up, without elevating their shoulders, and with minimal bending.
- To avoid repetitive activities for an extended period, rotate workers among various tasks during a shift. The research team observed on the job site that employers frequently allocate form workers one or more specific form components at the beginning of the workday; rotating workers between tasks is extremely uncommon.

5 Conclusion

This paper proposed a DT approach to evaluate the ergonomic risks associated with vertical formwork operations. The virtual replica of actual workers allows for performing an ergonomic risk assessment. The study findings indicated a high risk of WMSDs in the trunk, neck, wrist, and arm during formwork operations. Based on the findings, the recommendations, including changes in methods, were provided to formwork system manufacturers to prevent WMSDs among form workers. It is expected that the recommended practices could minimize WMSDs if they are executed. The study findings demonstrate the potential of DT for evaluating ergonomic risks associated with vertical formwork operations. This study adds knowledge to the existing literature on enhancing workers' health through DT techniques. Future research could adopt DT technologies to evaluate the WMSD risks in other formwork systems, such as plywood and aluminum. The DT's potential for reducing further workplace hazards in other construction activities should also be examined.

References

- [1] Wang D. Dai F. and Ning X. Risk Assessment of Work-Related Musculoskeletal Disorders in Construction: State-of-the-Art Review. *Journal of Construction Engineering and Management*, 141(6):04015008, 2015.
- [2] Valero E. Sivanathan A. Bosché F. and Abdel-Wahab M. Musculoskeletal disorders in construction: A review and a novel system for

- activity tracking with body area network. *Applied Ergonomics*, 54:120–130, 2016.
- [3] Sobeih T. Salem O. Genaidy A. Abdelhamid T. and Shell R. Psychosocial factors and musculoskeletal disorders in the construction industry. *Journal of Construction Engineering and Management*, 135(4):267-277, 2009.
- [4] BLS. Fact Sheet: Occupational injuries and illnesses resulting in musculoskeletal disorders (MSDS). Online: <https://www.bls.gov/iif/oshwc/case/msds.htm>, Accessed: 18/01/2022.
- [5] Inyang N. Al-Hussein M. El-Rich M. and Al-Jibouri S. Ergonomic Analysis and the Need for Its Integration for Planning and Assessing Construction Tasks. *Journal of Construction Engineering and Management*, 138(12):1370–1376, 2012.
- [6] Schneider S. and Susi P. Ergonomics and construction: A review of potential hazards in new construction. *American Industrial Hygiene Association Journal*, 55(7):635-649, 1994.
- [7] Hajaghazadeh M. Marvi-milan H. Khalkhali H. and Mohebbi I. Assessing the ergonomic exposure for construction workers during construction of residential buildings. *Work*, 62(3):411-419, 2019.
- [8] Ogunseiju O.R. Olayiwola J. Akanmu A.A. and Nnaji C. Digital twin-driven framework for improving self-management of ergonomic risks. *Smart and Sustainable Built Environment*, 10(3): 403-419, 2021.
- [9] Greco A. Caterino M. Fera M. and Gerbino S. Digital Twin for Monitoring Ergonomics during Manufacturing Production. *Applied Sciences*, 10:7758, 2020.
- [10] Yu Y. Yang X. Li H. Luo X. Guo H. and Fang Q. Joint-Level Vision-Based Ergonomic Assessment Tool for Construction Workers. *Journal of Construction Engineering and Management*, 145(5):04019025, 2019.
- [11] Yan X. Li H. Zhang H. and Rose T.M. Personalized method for self-management of trunk postural ergonomic hazards in construction rebar ironwork. *Advanced Engineering Informatics*, 37:31-41, 2018.
- [12] Kim S, Moore A. Srinivasan D. Akanmu A. Barr A. Harris-Adamson C. Rempel D.M. and Nussbaum M.A. Potential of exoskeleton technologies to enhance safety, health, and performance in construction: industry perspectives and future research directions. *IIEE Transactions on Occupational Ergonomics and Human Factors*, 7(3-4):185-191, 2019.
- [13] Kaur M.J. Mishra V.P. and Maheshwari P. The convergence of digital twin, IoT, and machine learning: Transforming data into action. In *Digital twin technologies and smart cities*, 3–17. New York: Springer, 2020.
- [14] Schleich B. Anwer N. Mathieu L. and Wartzack S. Shaping the digital twin for design and production engineering. *CIRP Annals* 66(1):141–144, 2017.
- [15] Zhang J. Cheng J.C.P. Chen W. and Chen K. Digital Twins for Construction Sites: Concepts, LoD Definition, and Applications. *Journal of Management in Engineering*, 38(2):04021094, 2022.
- [16] Teizer J. Johansen K.W. and Schultz C. The Concept of Digital Twin for Construction Safety. In *Construction Research Congress 2022*, 1156-1165, Virginia, USA, 2022.
- [17] Wanasinghe T.R. Wroblewski L. Petersen B.K. Gosine R.G. James L.A. and De Silva O. Digital Twin for the Oil and Gas Industry: Overview, Research Trends, Opportunities, and Challenges. *IEEE Access*, 8:104175–104197, 2020.
- [18] Schneider S. and Susi P. Ergonomics and construction: A review of potential hazards in new construction. *American Industrial Hygiene Association Journal*, 55(7):635-649, 1994.
- [19] Gambatese A. and Jin Z. Identification and Assessment of Musculoskeletal Disorders (MSDs) Risk for Concrete Formwork Systems. In *CPWR Technical Report*, USA, 2021.
- [20] Chellappa V. Chauhan J.S. and Strukova Z. Ergonomic Risk Assessment for Concrete Formwork activities in Construction Using Digital Human Modeling. In *International Ergonomics Conference*, Zagreb, Croatia, 2022.
- [21] Welch L.S. Hunting K.L. and Anderson J. Concrete form work, injury and musculoskeletal disorders. In *Proceedings of the Human Factors and Ergonomics Society Annual Meeting*, 5-647-5-650, SAGE Publications, Los Angeles, 2000.
- [22] Jazzar M.E. Piskernik M. and Nassereddine H. Digital Twin in construction: An Empirical Analysis. In *EG-ICE 2020 Workshop on Intelligent Computing in Engineering*, 1-10, Berlin, Germany, 2020.
- [23] Grieves M. and Vickers J. Digital twin: mitigating unpredictable, undesirable emergent behavior in complex systems. In *Transdisciplinary Perspectives on Complex Systems*, 85-113, Springer, Cham, 2017.
- [24] Tao F. and Zhang M. Digital twin shop-floor: a new shop-floor paradigm towards smart manufacturing. *IEEE Access*, 5:20418-20427, 2017.
- [25] Zhuang C. Liu J. and Xiong H. Digital twin-based smart production management and control framework for the complex product assembly shop-floor. *International Journal of Advanced Manufacturing Technology*, 96(1-4):1149-1163,

- 2018.
- [26] Lu Q. Xie X. Parlikad A.K. and Schooling J.M. Digital Twin-Enabled Anomaly Detection for Built Asset Monitoring in Operation and Maintenance. *Automation in Construction*, 118:103277, 2020.
- [27] Kendzierskyj S. Jahankhani H. Jamal A. and Jimenez J.I. The transparency of big data, data harvesting and digital twins. In *Blockchain and clinical trial*, 139–148, Springer, New York, 2019.
- [28] Mandolla C. Petruzzelli A.M. Percoco G. and Urbinati A. Building a digital twin for additive manufacturing through the exploitation of blockchain: a case analysis of the aircraft industry. *Computers in Industry*, 109:134-152, 2019.
- [29] Ammar A. Nassereddine H. AbdulBaky N. AbouKansour A. Tannoury J. Urban H. and Schranz C. Digital Twins in the Construction Industry: A Perspective of Practitioners and Building Authority. *Frontiers in Built Environment*, 8:834671, 2022.
- [30] Yitmen I. Alizadehsalehi S. Akıner İ. and Akıner M.E. An Adapted Model of Cognitive Digital Twins for Building Lifecycle Management. *Applied Sciences*, 11(9): 4276, 2022.
- [31] Khajavi S.H. Motlagh N.H. Jaribion A. Werner L.C. and Holmstrom J. Digital Twin: Vision, Benefits, Boundaries, and Creation for Buildings. *IEEE Access*, 7:147406–147419, 2019.
- [32] Volk R. Stengel J. and Schultmann F. Building Information Modeling (BIM) for existing buildings - Literature review and future needs. *Automation in Construction*, 38, 109–127, 2014.
- [33] Opoku D.-G. Perera S. Osei-Kyei R. and Rashidi M. Digital Twin Application in the Construction Industry: A Literature Review. *Journal of Building Engineering*, 40:102726, 2021.
- [34] Kan C. and Anumba C.J. Digital Twins as the Next Phase of Cyber Physical Systems in Construction, In *Computing in Civil Engineering 2019: Data, Sensing, and Analytics*, 256–264, Georgia, USA, 2019.
- [35] Spielholz P. Silverstein B. Morgan M. Checkoway H. and Kaufman J. Comparison of self-report, video observation and direct measurement methods for upper extremity musculoskeletal disorder physical risk factors. *Ergonomics*, 44(6):588-613, 2001.
- [36] Mcatamney L. and Corlett E.N. RULA: a survey method for the investigation of work-related upper limb disorders. *Applied Ergonomics*, 24(2):91–99, 1993.
- [37] Middlesworth M. A Step-by-Step Guide to the RULA Assessment Tool. Online: <https://ergo-plus.com/rula-assessment-tool-guide/>, Accessed: 07.11.2022.
- [38] NIOSH. Ergonomics and Musculoskeletal Disorders, Online: <https://www.cdc.gov/niosh/topics/ergonomics/default.html>, Accessed: 03/08/2022.

Impact of Crew Diversity on Worker Information Access and Performance

Bassam Ramadan¹, Hala Nassereddine¹, Timothy Taylor², Paul Goodrum³

¹Department of Civil Engineering, University of Kentucky, USA

²National Center for Construction Education and Research, USA

³Department of Construction Management, Colorado State University, USA

bara235@uky.edu, hala.nassereddine@uky.edu, ttaylor@nccer.org, paul.goodrum@colostate.edu

Abstract –

Labor shortage has consistently been a challenge in the construction industry for decades. As a data-heavy industry, information access and technological innovations are critical for pique performance. Currently, the industry is witnessing a global trend of workforce diversity, as industry leaders are emphasizing its importance. Research shows that gender and ethnic diversity and inclusion strategies can mitigate the impact of the construction labor shortage. Despite the importance and potential benefits of crew diversity, no research has yet studied how crew diversity impacts the worker's perceived difficulty of the process to access needed information, and their performance. The objective of this paper is to analyze and understand the impact of crew diversity on 1) the difficulty of the process to access information 2) the self-evaluated performance record and, of construction craft workers and construction frontline supervisors in the construction industry. To achieve the research objective, 2394 construction craft workers and frontline supervisors were surveyed using an online questionnaire. The survey participants were asked to self-evaluate 1) the difficulty of the process to receive or get access to information, and 2) their work personal performance record. The participants were asked to report the ethnic and gender composition of their work crew. The collected data was then analyzed. Key findings indicate that the gender and ethnic crew diversity showed a statistically significant positive impact on worker's information access and performance.

Keywords –

Information Access; Performance; Crew Diversity; Technology;

1 Introduction & Background

The aging infrastructure of the United States is in serious need for renovations as we face a major shortage of labor and craft workers [1]. Current trends show that

the construction workforce is aging rapidly causing an industry-wide labor shortage [2]. Most industry leaders and experts believe the construction industry will look drastically different over the next 20 years [3]. At the same time, construction technologies are not being implemented as fast as they are being developed, and the industry is yet to benefit from their full potential [1]. A McKinsey & Company analysis of Venture Capitalist (VC) investments data concluded that VC investment growth in construction technologies has outpaced VC investment growth in other industries by approximately 15-fold, with no clear indication of this momentum slowing down [4].

On a construction project, information is considered the lifeblood of the modern construction industry [5]. Considering the massive amount of knowledge created throughout the different phases of a construction project, the proper management of this information is indispensable due to the compartmentalized nature of the industry [6,7]. The transition from paper-based information to digital information and e-construction has been gaining momentum through the industry [8]. Adequate information access has been found to add massive benefits to the industry. Information can improve construction safety and performance [9,10]. Information access and information technologies improve external and internal collaboration, enhance communication, and employee satisfaction [11]. Information access and management improve work quality, simplify difficult tasks, and increase worker productivity [12]. Information management within an organization eases the process of disseminating critical information to related projects, which potentially facilitates on-time project completion. Among members of construction teams, it facilitates the communication between workers and supervisors, and promotes collaboration, coordination and effective decision-making [13]. Researchers have studied and examined construction 4.0 and information technologies at length [14,15], including the most recent developments in blockchain technologies [16–18], and construction

digital twins [19–22]. The existing literature has highlighted the numerous benefits of such construction technologies, particularly information technologies. One study examined the impact of several technologies on construction performance and information access found that the use of several information technologies improves information access and performance for construction craft workers, particularly for frontline supervisors [23].

In the construction industry, construction craft workers and frontline supervisors play unique and different roles. Still, there is a persistent perception that low productivity is the result of inadequate performance from craft workers. In reality, any problems are more likely to be caused by the lack of adequate supervision and failure of frontline supervisors to provide the necessary planning, information, support, and motivation [24]. Frontline supervisors have the responsibility of ensuring a safe and healthy workplace, and bridging the missing communication link between management and the craft workforce [25–27]. There is a wealth of studies that have thoroughly highlighted the importance of and influence frontline supervisors have on construction efficiency [28–30]

Along the rapidly changing technology landscape, the construction industry, is witnessing a global workforce diversity trend [31]. Still, as the importance of workforce diversity is being emphasized by industry leaders, demographic diversity is a serious concern to the industry, as unconscious biases and structural prejudices have negatively impacted the construction workforce [32]. The impact of ethnic diversity on project productivity is unclear as there are competing theories. A study by [33] claims ethnic diversity can negatively impact project performance and the communication of information and data due to cultural and linguistic barriers. On the other hand, [34] argues that ethnic diversity can benefit a company's performance because diverse groups can outperform uniform groups in problem-solving ability. As for gender diversity, it has been theorized that mixed-gender groups are better equipped to complete tasks, and therefore, potentially benefiting project performance [35,36]. Still, the construction industry faces major headwinds for women in construction. A recent study found that women in construction are on average more likely to feel disrespected at work, treated unprofessionally, and be subjected to derogatory remarks [37].

While the importance and benefits of technology use and crew diversity have been evaluated and highlighted in existing work, no research has yet studied how crew diversity impacts the worker's ability to access needed information and performance. This study attempts to bridge this gap of knowledge using a survey of construction workers and frontline supervisors that investigates, the demographics of crew composition, the

respondent's performance record, and the difficulty of the information access process. The aim of this paper is to analyze and understand the impact of gender and ethnic crew diversity on 1) the difficulty of the process to access information, and 2) the self-evaluated personal performance record of construction craft workers and frontline supervisors in the construction industry.

2 Methodology

The objective of this paper is to analyze and understand the impact of crew diversity on the self-reported difficulty of the process to receive or get access to information, and the personal performance record of construction workers and frontline supervisors in the construction industry. To achieve the research objective, an online questionnaire was developed in "Qualtrics" and distributed to US construction workers. Among other questions, the survey asks construction workers about gender and ethnic diversity of their crew, the types of information technologies used on their construction sites, how hard it is to gain access to information, and their performance. The survey received 2394 responses from all 50 states. Figure 1 details the geographic distribution of the responses. States contributing most to the survey were large population states including New York, California, Texas, Pennsylvania, and Illinois.

Overall, the responses have a gender breakdown of 94.8% male and 4.9% female. This sample breakdown is representative of the US construction craft workforce, where females constituted 3.9% of the construction craft workforce in 2021 according to the bureau of labor statistics [38].

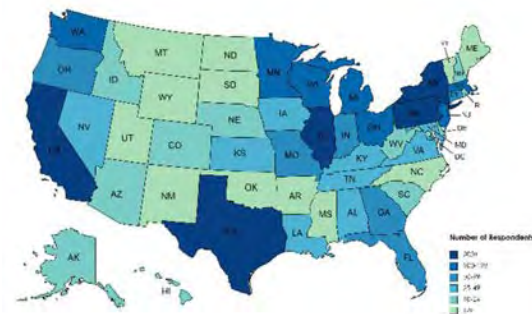


Figure 1. Geographic distribution of the number of respondents across the states – generated by mapchart.net

The breakdown of the survey participants by age showed that 30% are over the age of 55, 25% are in the 45-54 age group, 25% are in the 35-44 age group, 17% are in the 25-34 age group, and 3% are under the age of

25. Additionally, by job title, 41% are craftspersons/journeymen, 14% are foremen, 13% are superintendents, 13% are apprentices/helpers, 7% are general foremen, 3% are project managers, and 9% stated that they have another title. By education, 42% of the respondents indicated that they have received some college education, 29% have a high school equivalent education or less, 16% have completed a technical program, 11% hold a bachelor's degree or a graduate/post-graduate degree, and 2% indicated that they have another type of education.

In this study, the survey asked the construction workforce to select all the information technologies that they are using on their construction sites to measure the current level of technology implementation on US construction sites. The following is a list of information technologies that can be selected: RFID Chip Tracking, Virtual or Augmented Reality (VR or AR), Artificial Intelligence, Barcode Scanning, Building Information Modeling (BIM), Drones, and Robotics. The respondents were allowed to list any "Other" information technologies that they use on their construction site.

Another section of the survey asked the construction workforce to list the number of men and women on their crew, as well as the number of workers of different ethnic backgrounds (White, Black or African American, Hispanic, Asian or Asian American).

Finally, the survey asked participants the two following questions relating to the level of difficulty to gain access to information and their performance record:

- On a scale of 0 to 10, 0 being "instantaneous access", and 10 being "very hard", how hard is the process to receive or get access to required information?
- For the last year, please rate your personal performance record (including safety, attendance, quality, productivity, and initiative) on a scale from 0 to 10, 0 being "weak", and 10 being "superior".

A higher value on the response to the personal performance record indicates a more positive outcome, while a lower value on the response to how hard the process to receive or get access to required information indicates a more positive outcome.

To compare 1) the difficulty of the process to receive or get access to information and 2) the personal performance record based on whether the respondent indicated that their crew includes gender diversity and ethnic diversity, the data was grouped based on whether the crew includes such diversity or not. The corresponding average of the difficulty level of accessing information and the performance record and of these groups is calculated and compared.

In order to examine if the difference between the two groups is statistically significant, the non-parametric Mann-Whitney U- test was completed to obtain the p-

value. This test was used to err on the conservative side of the statistical analysis due to large discrepancies in sample sizes of two groups being compared [39]. The students' t-test was not used due to the large discrepancies in sample sizes between groups. If sample sizes in both conditions are equal, the t-test is very robust against unequal variances. However, if sample sizes are unequal, unequal variances can influence the Type 1 error rate of the students' t-test by either increasing or decreasing the Type 1 error rate from the nominal alpha significance level. In such cases, the Mann-Whitney U-test performs better and is better behaved than the t-test [39]. Thus, the Mann-Whitney U-test was selected for this statistical analysis. A significance level, α , of 0.1 is considered for statistical significance (i.e., 90% confidence level).

This analysis was performed for 1) the survey population as a whole representing the overall construction workforce, 2) among frontline supervisors as one group, and 3) among craft workers as another group.

3 Results and Analysis

3.1 Information Technology Use

Survey respondents were asked what kind of information technologies are used on their sites. Figure 2 shows the current levels of different "Information" technology use on construction sites in the United States. Among information technologies, as can be seen in Figure 2, *Barcode Scanning* and *BIM* have the highest level of implementation at 23% and 21% respectively. *Drones* are used on 9% of construction sites, while *Virtual or Augmented Reality* is used on 7% of construction sites. *Robotics* are used on 6% of sites, and *RFID Chip Tracking* is used on only 5% of construction sites. *Artificial Intelligence* had the lowest implantation percentage at 2%. Finally, 12% of the survey participants indicated that they use other types of information technologies that were not among the listed technologies including laser alignments, tablets, GPS, and telematics, etc. A study of the impact of several technologies on construction performance and information access found that the use of several information technologies improves information access and performance for the construction workforce, particularly for frontline supervisors [23].

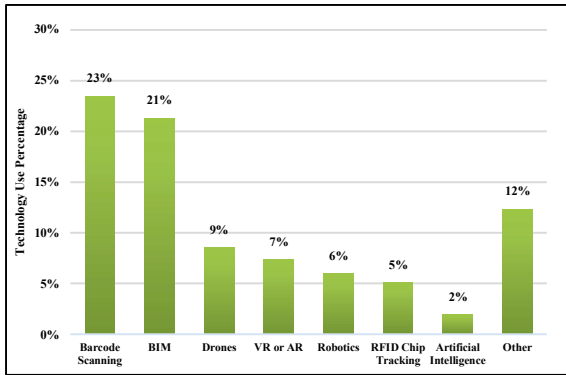


Figure 2. Current implementation level of different information technologies on construction sites in the United States

3.2 Crew Diversity in the Construction Industry

Survey participants were asked about the gender and ethnic composition of their crews. Figure 3 shows the percent of crews in the construction industry in the United States that include and don't include each of gender diversity and ethnic diversity.

The results in Figure 3 show that only 34.8% of construction crews include gender diversity (i.e., the membership of the crew includes women), while 65.2% of construction crews are all men crews that don't include gender diversity. However, a significant majority of construction crews, 70.6%, are ethnically diverse, while 29.4% of construction crews are all white crews that don't include any type of ethnic diversity.

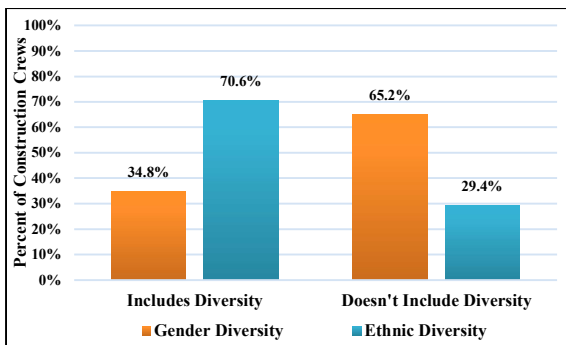


Figure 3. Percent of crews that includes gender and ethnic diversity in the construction industry

3.3 Impact of Crew Diversity

The impact of gender and ethnic crew diversity on the 1) the difficulty to receive or get access to required information, and 2) the personal performance record for the construction workforce, based on whether the respondents indicated their crew includes such diversity

is presented in Tables 1-4. The tables show the average responses for the difficulty of information access and the average personal performance record for respondents who specified whether their crew includes each type of diversity or doesn't. The tables present the p-value of the Mann-Whitney U-test to examine whether any difference in the averages is statistically significant. This analysis was performed for 1) the overall construction workforce, 2) frontline supervisors, and 3) craft workers.

Table 1 shows the average difficulty of information access for the construction workforce based on gender diversity on a scale of 0-10. The results of Table 1 show that gender diversity of the crew, on average, eases the process of information access. This positive impact is statistically significant for the construction workforce as a whole. However, when the analysis is broken down by categories, the positive impact is only statistically significant among frontline supervisors, but not among craft workers. While frontline supervisors benefit greatly from gender diversity with regards to information access, the benefit seen among craft workers is not as significant.

Table 1. Average difficulty of information access of the construction workforce based on gender diversity on a scale of 0-10

Gender Diversity	Includes	Doesn't Include	P-value
Overall Workforce	3.221	3.423	0.02*
Frontline Supervisors	2.930	3.212	0.01*
Craft Workers	3.542	3.597	0.39

*Difference in averages is statistically significant at the 90% level

Table 2 shows the average personal performance record for the construction workforce based on gender diversity on a scale of 0-10. The results of Table 2 show that gender diversity of the crew, on average, improves the personal performance record for the workforce. This positive impact is statistically significant for the construction workforce as a whole. However, when the analysis is broken down by categories, the positive impact is only statistically significant among frontline supervisors, but not among craft workers. While frontline supervisors benefit greatly from gender diversity with regards to performance, the benefit seen among craft workers is not as significant.

Table 3 shows the average difficulty of information access for the construction workforce based on ethnic diversity on a scale of 0-10. The results of Table 3 show that ethnic diversity of the crew, on average, eases the process of information access. However, this positive impact is not statistically significant for the construction workforce as a whole, for frontline supervisors, or for craft workers.

Table 2. Average personal performance record of the construction workforce based on gender diversity on a scale of 0-10

Gender Diversity	Includes	Doesn't Include	P-value
Overall Workforce	8.687	8.537	0.03*
Frontline Supervisors	8.821	8.676	0.10*
Craft Workers	8.477	8.402	0.39

**Difference in averages is statistically significant at the 90% level*

Table 3. Average difficulty of information access of the construction workforce based on ethnic diversity on a scale of 0-10

Ethnic Diversity	Includes	Doesn't Include	P-value
Overall Workforce	3.359	3.428	0.229
Frontline Supervisors	3.123	3.144	0.464
Craft Workers	3.615	3.681	0.393

**Difference in averages is statistically significant at the 90% level*

Table 4 shows the average personal performance record for the construction workforce based on ethnic diversity on a scale of 0-10. The results of Table 4 show that ethnic diversity of the crew, on average, improves the personal performance record for the workforce. This positive impact is statistically significant for the construction workforce as a whole. However, when the analysis is broken down by categories, the positive impact is only statistically significant among frontline supervisors, but not among craft workers. While frontline supervisors benefit greatly from ethnic diversity with regards to performance, the benefit seen among craft workers is slightly smaller.

Table 4. Average personal performance record of the construction workforce workers based on ethnic diversity on a scale of 0-10

Ethnic Diversity	Includes	Doesn't Include	P-value
Overall Workforce	8.652	8.486	0.01*
Frontline Supervisors	8.820	8.613	0.02*
Craft Workers	8.472	8.372	0.14

**Difference in averages is statistically significant at the 90% level*

4 Discussion

Having a better understanding of crew diversity on worker performance, and ability to access information, is critical to helping construction industry leaders identify strategies that improve construction productivity as we face the next chapter of labor challenges in an

increasingly diverse industry. This study presents a statistical analysis of the impact crew diversity has on the construction workforce of the United States. Using the data collected from craft professionals and frontline, survey participants described the gender and ethnic composition of their crews, and then self-evaluated the difficulty of the process to receive or get access to needed information and their personal performance record.

The results show that gender diversity on average, both improves performance and eases the process of information access. These results are statistically significant for the overall construction workforce and frontline supervisors, but not among craft workers. As for ethnic diversity, the results show that it statistically improves performance for the overall construction workforce and frontline supervisors. The improvement in performance among craft workers is not statistically significant. While ethnic diversity, on average, eases the process of information access across all three groups, the positive impact is not statistically significant in any of them. Considering the labor shortage in the industry, industry leaders should actively ramp up the recruitment of diverse demographics to acquire desired benefits, particularly women. Women only represent 4% of the workforce when they make up half the population. This presents a significant opportunity to fill the labor gap from an untapped resource, because not only do women not hurt the difficulty of information access, and construction performance, but the results presented in this paper also show a statistical improvement in information access performance when women are working among the crew.

5 Conclusion, Limitations, and Future Studies

Over the past decade, technological innovations have played a key role in the growth and advancement of an increasingly diverse construction industry. While research has extensively studied workforce diversity, little existing work has studied its direct impact on worker information access and performance. The objective of this paper is to analyze and understand the impact of crew diversity on the worker's self-evaluated difficulty of the process to receive or get access to information, and their personal performance record in the construction industry. Using data from a survey of 2394 construction workers, statistical analysis showed that there are substantial benefits for increasing workforce gender and ethnic diversity. This study found that on average, for the overall construction workforce, gender diversity had a statistically significant positive impact on both information access and performance. While ethnic diversity had a positive impact on both information access and performance, only the results of the impact on

performance had results that were statistically significant.

While this study presents a robust statistical analysis of the impact crew diversity on information access and personal performance, the study does have certain limitations. The survey of construction workers does not ask any multiple-choice questions or open-ended questions that discuss specific benefits, challenges, or perceptions gender and ethnic diversity, or factors that resulted in enhanced access to information and performance. Therefore, while this analysis can empirically measure a positive impact on performance and information access, the study cannot answer the questions related to why crew diversity resulted in improvements. Future research can build on this study and attempt to answer these specific questions, to build a roadmap for the leaders of the construction industry to identify paths that will maximize potential benefits based on their specific construction needs. Further work can also study the ideal demographic composition of work crews to enhance information access, work productivity and workforce cohesion.

6 Acknowledgments

The authors gratefully acknowledge the Construction Industry Institute (CII) for their valuable support and partial funding for the data collection of this research project, and the college of engineering at the University of Kentucky for continuous support. The authors would also like to thank all the survey participants, without whom this research would not be possible. Any opinions, findings, conclusions and recommendations expressed by the authors in this paper do not necessarily reflect the views of the University of Kentucky or the Construction Industry Institute.

References

- [1] Construction Industry Institute: *Workforce 2030: What You Need to Know Now About Your Future Workforce*. Austin, TX, US: Construction Industry Institute
- [2] Construction Industry Institute: *Is There a Demographic Labor Cliff that Will Affect Project Performance*. Austin, TX: Construction Industry Institute
- [3] Ribeirinho MJ., Mischke J., Strube G., Sjödin E., Blanco JL., Palter R., Biörek J., Rockhill D., Andersson T: *The Next Normal in Construction: How disruption is reshaping the world's largest ecosystem*. McKinsey & Company
- [4] Bartlett K., Blanco JL., Fitzgerald B., Johnson J., Ribeirinho MJ: Rise of the platform era: The next chapter in construction technology. *McKinsey & Company*, 2020. Available at: <https://www.mckinsey.com/industries/private-equity-and-principal-investors/our-insights/rise-of-the-platform-era-the-next-chapter-in-construction-technology>
- [5] Nassereddine H., Hanna AS., Veeramani D., Lotfallah W: Augmented Reality in the Construction Industry: Use-Cases, Benefits, Obstacles, and Future Trends. *Front Built Environ* 8:730094, 2022. Doi: 10.3389/fbuil.2022.730094
- [6] Dave B., Koskela L: Collaborative knowledge management—A construction case study. *Automation in Construction* 18(7):894–902, 2009. Doi: 10.1016/j.autcon.2009.03.015
- [7] Kazi AS., Koivuniemi A: Sharing Through Social Interaction: The Case of YIT Construction Ltd. *Real-Life Knowledge Management: Lessons from the Field* (952-5004-72-4):63–80, 2006
- [8] Dadi GB., Nassereddine H., Taylor TR., Griffith R., Ramadan B: *Technological Capabilities of Departments of Transportation for Digital Project Management and Delivery*, No. NCHRP Project 20-05, Topic 52-19, 2022.
- [9] Al-Shabbani Z., Ammar A., Dadi G: Preventative Safety Metrics with Highway Maintenance Crews. *Construction Research Congress 2022*, Arlington, Virginia: American Society of Civil Engineers, 510–9, 2022
- [10] Ammar A., Al-Shabbani Z., Dadi G: Assessing the Safety Climate of a State Department of Transportation through Its Highway Maintenance Crews. *Construction Research Congress 2022*, Arlington, Virginia: American Society of Civil Engineers, 345–55, 2022
- [11] Klinc R., Dolenc M., Turk Ž: Possible Benefits of WEB 2.0 to Construction Industry:10, 2008
- [12] Vasista TG., Abone A: Benefits, Barriers and Applications of Information Communication Technology in Construction Industry: a Contemporary Study. *IJET* 7(3.27):492–9, 2018. Doi: 10.14419/ijet.v7i3.27.18004
- [13] Prasanna SVSNDL., Raja Ramanna T: Application of ICT benefits for building project management using ISM Model. *International Journal of Research in Engineering and Technology* 3(6):68–78, 2014
- [14] Ammar A., Nassereddine H: Blueprint for Construction 4.0 Technologies: A Bibliometric Analysis. *IOP Conf Ser: Mater Sci Eng* 1218(1):012011, 2022. Doi: 10.1088/1757-899X/1218/1/012011
- [15] Forcael E., Ferrari I., Opazo-Vega A., Pulido-Arcas JA: Construction 4.0: A Literature Review. *Sustainability* 12(22):9755, 2020. Doi: 10.3390/su12229755

- [16] Li J., Greenwood D., Kassem M: Blockchain in the built environment and construction industry: A systematic review, conceptual models and practical use cases. *Automation in Construction* 102:288–307, 2019. Doi: 10.1016/j.autcon.2019.02.005
- [17] Sadeghi M., Mahmoudi A., Deng X: Adopting distributed ledger technology for the sustainable construction industry: evaluating the barriers using Ordinal Priority Approach. *Environ Sci Pollut Res* 29(7):10495–520, 2022. Doi: 10.1007/s11356-021-16376-y
- [18] Sadeghi M., Mahmoudi A., Deng X., Luo X: Prioritizing requirements for implementing blockchain technology in construction supply chain based on circular economy: Fuzzy Ordinal Priority Approach. *International Journal of Environmental Science and Technology*:1–22, 2022
- [19] Ammar A., Bhatt B., Dadi G., Nasserredine H: A Blueprint for Creating Digital Twins for Transportation Assets: an Application for Highway Engineering. *Proceedings of the Eleventh International Conference on Engineering Computational Technology*, vol. 2, Edinburgh, United Kingdom: Civil-Comp Press, 2022
- [20] Ammar A., Maier F., Rachel C., Nasserredine H., Gabriel D: Departments of Transportation Efforts to Digitize Ancillary Transportation Asset Data: A Step Toward Digital Twins. *Transportation Research Record*, 2023
- [21] Ammar A., Nasserredine H., AbdulBaky N., AbouKansour A., Tannoury J., Urban H., Schranz C: Digital Twins in the Construction Industry: A Perspective of Practitioners and Building Authority. *Front Built Environ* 8:834671, 2022. Doi: 10.3389/fbuil.2022.834671
- [22] Ammar A., Nasserredine H., Dadi G: STATE DEPARTMENTS OF TRANSPORTATION'S VISION TOWARD DIGITAL TWINS: INVESTIGATION OF ROADSIDE ASSET DATA MANAGEMENT CURRENT PRACTICES AND FUTURE REQUIREMENTS. *ISPRS Ann Photogramm Remote Sens Spatial Inf Sci* V-4-2022:319–27, 2022. Doi: 10.5194/isprs-annals-V-4-2022-319-2022
- [23] Ramadan B., Nasserredine H., Taylor TRB., Goodrum P: Impact of Technology Use on Workforce Performance and Information Access in the Construction Industry. *Frontiers in Built Environment*, 2023. DOI: 10.3389/fbuil.2023.1079203
- [24] Howell GA: What is Lean Construction? IGLC7. *University of California, Berkeley, CA, USA*, 1999
- [25] Oswald D., Lingard H: Development of a frontline H&S leadership maturity model in the construction industry. *Safety Science* 118:674–86, 2019. Doi: <https://doi.org/10.1016/j.ssci.2019.06.005>
- [26] Ramadan B., Nasserredine H., Taylor TRB., Real K., Goodrum P: Impact of Skill Proficiencies on Frontline Supervision Practices in the Construction Industry. *Proceedings of the Creative Construction e-Conference (2022)*, 2022. DOI: <https://doi.org/10.3311/CCC2022-024>
- [27] Uwakweh BO: Effect of Foremen on Construction Apprentice. *J Constr Eng Manage* 131(12):1320–7, 2005. Doi: 10.1061/(ASCE)0733-9364(2005)131:12(1320)
- [28] Gerami Seresht N., Fayek AR: Factors influencing multifactor productivity of equipment-intensive activities. *IJPPM* 69(9):2021–45, 2019. Doi: 10.1108/IJPPM-07-2018-0250
- [29] Hewage KN., Gannoruwa A., Ruwanpura JY: Current status of factors leading to team performance of on-site construction professionals in Alberta building construction projects. *Can J Civ Eng* 38(6):679–89, 2011. Doi: 10.1139/111-038
- [30] Liberda M., Ruwanpura J., Jergeas G: Construction Productivity Improvement: A Study of Human, Management and External Issues. *Construction Research Congress*, Honolulu, Hawaii, United States: American Society of Civil Engineers, 1–8, 2003
- [31] Won D., Hwang B., Chng SJ: Assessing the effects of workforce diversity on project productivity performance for sustainable workplace in the construction industry. *Sustainable Development* 29(2):398–418, 2021. Doi: 10.1002/sd.2155
- [32] Karakhan AA., Gambatese JA., Simmons DR., Al-Bayati AJ: Identifying Pertinent Indicators for Assessing and Fostering Diversity, Equity, and Inclusion of the Construction Workforce. *J Manage Eng* 37(2):04020114, 2021. Doi: 10.1061/(ASCE)ME.1943-5479.0000885
- [33] Glaeser EL., Vigdor JL: *Racial segregation in the 2000 Census: Promising news*. Citeseer
- [34] Hong L., Page SE: Groups of diverse problem solvers can outperform groups of high-ability problem solvers. *Proc Natl Acad Sci USA* 101(46):16385–9, 2004. Doi: 10.1073/pnas.0403723101
- [35] Ali M., Kulik CT., Metz I: The gender diversity–performance relationship in services and manufacturing organizations. *The International Journal of Human Resource Management* 22(7):1464–85, 2011. Doi: 10.1080/09585192.2011.561961

- [36] Sabatier M: A women's boom in the boardroom: effects on performance? *Applied Economics* 47(26):2717–27, 2015. Doi: 10.1080/00036846.2015.1008774
- [37] Ramadan BA:, Taylor TRB:, Real KJ:, Goodrum P: The Construction Industry from the Perspective of the Worker's Social Experience. *Construction Research Congress 2022*, Arlington, Virginia: American Society of Civil Engineers, 611–21, 2022. DOI: 10.1061/9780784483985.062
- [38] US Bureau of Labor Statistics: Employed Persons by Detailed Occupation, Sex, Race, and Hispanic or Latino Ethnicity, 2021. Available at: <https://www.bls.gov/cps/cpsaat11.htm>
- [39] Gibbons JD:, Chakraborti S: Comparisons of the Mann-Whitney, Student's t, and Alternate t Tests for Means of Normal Distributions. *The Journal of Experimental Education* 59(3):258–67, 1991. Doi: 10.1080/00220973.1991.10806565

Understanding BIM through a Simulation Game - Case study of Indian Students subjected to this course

Vasanth K. Bhat¹ Gregor Grunwald² Tobias Hanke³

¹ DESIGN HUB-INDIA, Bangalore, India

^{2,3} Jade University of Applied Sciences, Faculty of Architecture, Oldenburg, Germany
vkbhat@designhubindia.com, gregor.grunwald@jade-hs.de, tobias.hanke@jade-hs.de

Design Hub India and Jade University of Applied Sciences conducted a simulation game in Bangalore, India to teach the networked and digital planning methodology Building Information Modelling (BIM). The teaching format was developed in Germany and has already been implemented and field-tested in teaching. At this event, the format was used in an international context for the first time. It was investigated in a one and a two-day course at Indian universities. The main focus was to give a playful and simple introduction to the new planning method BIM in order to minimize initial fears of contact and to guide an understanding of the digital planning standard for construction projects with a focus on collaboration. To convey the necessary expertise in a relatively simple way, so-called BIM Nuggets were developed as a self-learning tool. They are described in more detail in this article. Results of these events were outstanding design projects, with data structured and submitted according to given specifications. The results were motivated students who worked together on their projects far beyond the required workload, as well as satisfied teachers who enabled a large number of people to gain an introduction to a complex topic in a very short time. This event was a good test ground to check the performance of the teaching format on international level. This event motivates to further develop the training in a cross-cultural format where Indian and German students work together on one project.

Keywords – Information modelling techniques, Building Information Modelling; BIM; business game; international case study

1 Introduction

Introduction of new technologies and ideas are often met with opposition, as it is human nature to resist change. This lack of awareness and experience of

Building Information Modelling (BIM) within the industry is hindering the extensive utilization of the technology. Therefore the education and training of people, while representing a substantial challenge, is essential. When faced with the task of introducing BIM people related issues have been largely overlooked. Issues such as culture, experience, support, education and training need to be addressed.

“BIM facilitates a new way of working: creating designs with intelligent objects. Regardless of how many times the design changes - or who changes it - the data remains consistent, coordinated, and more accurate across all stakeholders” [1]. Eastman defines BIM as "a modeling technology and an associated set of processes for creating, communicating, and analyzing building models." [2]. BIM allows for all key design decisions to be made digitally at the working drawing stage before actual construction starts, resulting in a higher degree of certainty in all aspects of the project, like quality, cost, scheduling, sustainability and targets. BIM will become the planning standard for construction projects all over the world. [3,4].

In India due to the high volume of construction activity both in the public and private sector, great emphasis is laid by the government to transform the construction industry to go digital. This has resulted in a high demand for professionals with good knowledge of Building Information Modelling among the various professionals like architects, structural engineers, MEP, HVAC consultants, etc. involved in the construction industry. Realizing the need for relevant training using new teaching and learning formats, not only at universities but also in the field of continuing education for working experts, Design Hub India [5] a pioneer in co-curricular learning in the field of Architecture invited Prof. Grunwald from Jade University of Applied Sciences, Oldenburg- Germany, to conduct workshop on learning BIM through a simulation Game, which he has devised.

Thus, it was decided to conduct two simulation game sessions in Bangalore – first one at BMS School of Architecture – which was purely for undergraduate students and a second one at the Impact School of Architecture in Bangalore for a mixed group of students and professionals to teach the networked and digital planning methodology BIM.

The teaching format as a “simulation Game” was developed at the Jade University of Applied Sciences two and a half years ago and has already been conducted several times with different groups of participants - both interdisciplinary and in mixed groups of students and professionals together. Reports on these first events are given in the references [3,5,6,7]. In Bangalore, the BIM game could now be tested internationally for the first time and was thus a test run for the course in English-speaking countries. Fifty students participated in a two-day workshop, the second event was reduced to one day and had even more participants: with eighty interested people from the university and the professional planning industry. The event was partly sponsored by Capricot Technologies Bangalore, a partner of Autodesk India, with the noble mission of popularizing the application of BIM in the construction industry. They invited industry experts for the concluding session where Prof. Grunwald presented the successful outcome of the Workshop under the topic of "BIM – Game Changer for Construction Professionals", in which, among other things, the results of the events were presented. [9]

2 BIM Simulation Game

The BIM game is primarily an architectural competition with an increased focus on the correct provision of information. In the game, participants are divided into working groups and assigned different roles. The participants are: the architect, the civil engineer, the visualiser and the BIM coordinator. The teachers act as clients and as coaches who supervise the students. The list of roles is expandable and can be adapted to the needs and teaching topics.

The aim of the group is to create a 3D model for a specific construction task and to practice working together on this model. For this purpose, the play time is divided into different work phases, each phase ending with the submission of certain deliverables as defined in the EIRs issued by the client. Figure 1 shows the basic structure of the workshop

Certain tasks are directly assigned to one of the roles, according to the project-specific role description. Each delivery item is checked, evaluated, an overall group score is created and puts the participants in a direct competitive situation with the other groups, who work out and process their own ideas in parallel. In this way,

the game creates a concentrated and intensive working atmosphere, also due to the limited processing time, in which effort initially remains secondary because the common goal of completing all deliverables motivates the groups.

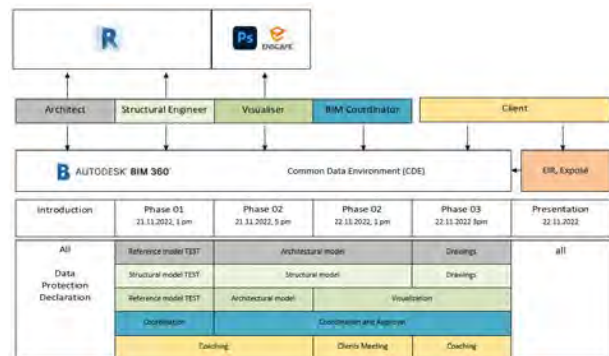


Figure 1: Structure of the workshop – Source: own figure

2.1 Record of progress

Both workshops were organized into similar work steps as described below.

Day 1, 8.30am – 10.30 am: resource persons in the venue, prepare their laptops and study materials and are ready to receive the students. Starting lecture for the students with general instruction in which the programme objective is highlighted time break ups for the next two days are defined and outcomes are defined.

10.30am – 1.00pm: Grouping of five students and role assigning within each group, software is downloaded on to each student’s laptop through cloud computing. Nugget learning phase. – Students start working on their assignments while the resource persons go from group to group giving them advice and clearing their doubts. 2.00pm – 5.00pm: students fully engrossed in their works, the designing part of assignment completed, and they are now working on the 3D aspect of design, improving on their designs, integrating various service aspects, etc.

Day 2, 9.00 am – 2.00 pm: The students have solved their assignments going through all the phases of BIM, like integrating information, extracting the structural model, performing a clash detection, etc. They are ready with their 3D designs of the assignment.

2.30 - 4.00 pm: Each group is called over to the actual site within the campus where they were asked to locate the building. The resource persons feed their designs into the AR glasses which they have brought along with and each student is made to experience their final outcome on augmented Reality using the “Hololens”. The students were mighty excited to see their buildings come alive and

felt a sense of achievement of having got an insight into BIM and its usefulness in the design process.

4.00 – 5.00 pm: The students were back in the studio, each group making its presentation and taking feedback from the resource persons.

The workshop ended with observations from the resource persons and distribution of certificates to the students.

2.2 Working material

The students receive the building task in the form of an exposé. This document contains all the boundary conditions for the design, such as the spatial programme, location, explanations on the use of the building, its urban context and others. The information requirements are summarised in an Employer Information Requirement (EIR). This document contains a project overview, the BIM-goals and use-cases, it highlights the specific BIM-goals of the project, explains the content provided to all participants and briefly describes the organization of the design contest. Most important chapter contains the digital delivery item definition. The document continues with the specification of roles and responsibilities, the strategy of cooperation and ends with handling instructions of the Common Data Environment (CDE), a cloud based data storage with further control and project management functions, described in chapter 2.3.

It is therefore the planners' specification of how information is to be prepared and delivered in the project [10]. The EIR is based on the model template from BIM Germany [11]. The usual response of the planners to the EIR in the form of a BIM execution plan (BEP) will be dispensed with in this event due to time constraints.

2.3 Modelling and information enrichment

When the game starts, the initial focus is on designing and modelling the spatial structure in a modelling software. Revit was used for the events in Bangalore. Considering the given boundary conditions from the exposé, rooms and utilisation units are created by joining individual building elements. They are designed with Revit's own build-in parameters in accordance with the Level of Information (LOI) defined in the EIR. In addition to these standard parameters, however, properties are defined specifically for the BIM Game. In this way the students should learn to define and upload their own parameters independently of the modelling software and to fill them with information. In summary the exercise focuses on enriching the geometry with semantic information.

For all further work steps and for communication with the other group members, the models are exported

as Industry Foundation Class (IFC) files. The teachers subject these IFC files to a model check and can thus automatically examine the file for required information. The models are also reviewed for compliance with the modelling guidelines. The level of detail (LOD) of the model is compared to the specifications from the EIR and evaluated. More information on this automatic model check in chapter 2.4.1

2.4 Collaboration on the model

The collaborative teamwork takes place in a working platform, a Common Data Environment (CDE). At the events in India, Autodesk's BIM360 CDE was used [12,13]. It serves as a storage location for files and is a communication space for the participants. Various planning and coordination processes run on the CDE: The BIM coordinator performs a clash check to compare two 3D models previously created by the architect and civil engineer in Revit. This check trains the merging of different 3D models and the detection of clashes. The conflicts found are to be documented and sent back to the authors for revision as a direct task in the form of the BIM Collaboration Format (BCF). This is to practise generating a coherent coordination model. Communication about the model is also practised in this subtask. The clear protocol structure of the CDE enables the traceability of the performed task and thus simplifies the evaluation of the exercise by the game leaders. The participants are confronted with further planning challenges. Marking and commenting on the model is another function that students should get to know and actively integrate into their planning process. The students can collect points for this activity and positively influence the overall assessment. Furthermore, it is important to initiate an approval process. The architect and the civil engineer can ask the BIM coordinator via the CDE to approve the finished files. The coordinator must review the files and then either approve the file or reject the request and ask for improvements. Only approved files are allowed to be submitted in the competition. Likewise, the use of a standardised naming convention is prescribed. Incorrectly named documents are not considered in the evaluation. Here, too, the CDE with preceding convention helps to comply with the standard.

The data storage structure of the CDE is very simple, as can be seen in table 1. There is a folder with general information for all groups. Each group also has its own working area. Two folders with special properties are built in here. Each group receives a drop-off folder and a coordination folder for performing clash detections. Additional subfolders can be added as required.

Table 1 CDE Structure – source: own figure

Folder	Documents	Access
00_Information	Exposé	all
	EIR	
	Click Tutorial	
01_Work folder	---	group only
01.1_Submission	approved delivery items	
01.2_Coordination	IFC models for clash detection	
01.3 ...	any	

2.5 BIM Nuggets

To convey the necessary expertise for the steps listed above in a relatively simple way, so-called BIM Nuggets are used to introduce participants to digital planning technology. A BIM Nugget is learning material reduced to one topic area and usually consists of a video tutorial, click tutorial, exercise, sample solution and a questionnaire. All material is available to students digitally for self-study and can be accessed at any time. The BIM Nuggets (schedule and structure are presented in Figure 2) are primarily designed for the preparation and qualification of the BIM Game, but they can also be used in the game for reference and as a reminder.

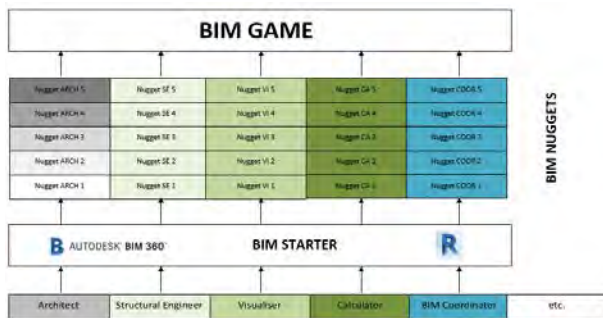


Figure 2. BIM Game Schedule and Structure – source: own figure

In general BIM Nuggets consist out of:

- the video tutorial, which introduces different BIM use cases, explains them and enriches the topic with further information, in order to finally demonstrate the implementation in the corresponding software application step by step. A schematically superimposed mouse records the clicks required for the application, and keyboard shortcuts are also displayed. The workflow is explained via voice recording. The video tutorials serve primarily as preparation for the BIM Game.
- a click tutorial, which provides the learners with a PDF-based reference work. Here, the required work

steps are numbered and summarised. It is a condensed format that is particularly suitable as a reminder during the BIM Game.

- exercises and sample solutions which help learners to apply the knowledge they have learned in self-study and to test it before participating in the BIM Game. In this way, the participants learn how to use the most important applications.
- By means of quizzes, what has been learned is reflected upon and consolidated. In this respect, the quiz is an integral part of the nuggets and serves as a self-check.

2.5.1 Automation and Visualization

The self-learning character of BIM Nuggets is an important feature of the learning offer. Since the university curriculum rarely offers space for the study of digital planning methodology, and when it does, self-learning materials are usually the only way to learn this key technology. Self-study is simplified by automations and thus becomes an interesting feature in this teaching project. Some of the automations used in this simulation are summarised below with corresponding references to relevant publications on these topics.

BIMQ is a web-based database that was developed specifically for the requirements and quality management of BIM projects. With BIMQ, the assignment or understanding of LOD and LOI requirements in relation to planning phases, service profiles and use cases no longer takes place via data sheets, but in a database-oriented manner. With the help of BIMQ, comprehensive and well-structured information requirements for a project can be centrally defined, distributed and processed. [14, 15] With BIMQ, an automation technique is used in the BIM Game that allows to control the input of data and to create a consistent information request. BIMQ is used to generate the checking rules of the final BIM model to verify the students' IFC files with model checking software such as Solibri for rule compliance, content consistency and the properties specified and required in the EIR. This automation technology thus helps in checking the performance in terms of information enrichment of the models in the IFC file. Students can also do this independently as a self-test and thus check their work regarding the quality of the information. A further increase is achieved using process control tools within the BIM Game. Here the authors have experiences in the use and integration of a Bizagi work platform, which can be read in more detail in [6].

In addition to automation, visualisation is also an important and motivating factor in the BIM Game. For

visualising the IFC files of the students Microsoft's Power BI is used to graphically evaluate and display different aspects of information such as number of rooms, size and area of the design. For this purpose, the IFC file is extracted with Bimsheet from Simplebim [16] and exported to an Excel file in order to read it into Power BI and check the students' spatial results. Further information in [6].

The participants of the two-day workshop could also view their designs using Hololens glasses. The 3D model was loaded onto the glasses via the Trimble Connect Cloud and located at the planning site. The students were able to view their design on a scale of 1:1, embedded in the surrounding buildings, and thus had the opportunity to assess their design in terms of proportion, design, orientation and many other aspects. The realistic visualisation of their designs inspired the participants and was another highlight of the event. Figure 3 below shows the use of the AR glasses in the workshop.



Figure 3. AR glasses visualize the 3D model – source: own figure

2.5.2 Project Funding

The creation of the BIM Nuggets and their implementation in a new training structure is funded by the "Stiftung Innovation in der Hochschullehre" (see Figure 4). The aim of the foundation is to enable innovation in teaching and learning at universities. [17].

The funded project is called "AUFLADEN" in English "CHARGING" and is briefly summarised: The journey into the digital future of construction requires ideas, time, courage and energy. The education and training laboratory for digital planning and building is the place to charge energy and knowledge in order to participate in the digital transformation. The aim of the project is to create a suitable training concept for teaching BIM, the didactic preparation of the learning content and the scientific evaluation of the new concept. The

knowledge gained from this should contribute to improving the courses offered at the university, to promoting the standardisation of the education offered and to providing impulses and suggestions across the university. The project is aimed at students of degree programmes along the entire value chain of the construction and real estate industry, especially prospective architects, civil engineers and specialist planners. The project serves to close the gap between beginners and advanced BIM users, to pick up students who are still seeking access to the topic and to involve everyone in the digital transformation.



Figure 4. Logo of the Foundation – source [17]

3 Observations

The aim of conducting this workshop was to test the teaching format in an international environment. Figure 5 and 6 at the end of the article show some final designs that were created in these workshops. Besides the architectural design quality a particular focus lies on the functionality of the BIM Nuggets. In addition the workshops were intended to show whether and to what extent the game-like approach of the business game successfully contributes to increasing the motivation of the participants. The next observation is the cultural aspect: the event should clarify to what extent the learning format can be transferred from Germany to Indian conditions and whether there are cultural differences that need to be taken into account. Final observations examine demographic aspects with regard to the age-structural composition of the two workshops.

3.1 Functionality

The developed format was successfully implemented both in the one-day and in the two-day workshop. The learning content could be conveyed quickly, thus creating a knowledge base for its application. The learning content is summarized in table 2 with a note on the training method used. The topics were either communicated via Nuggets, explained in the starting

lecture or explained in the personal support of the students.

Table 2 Result evaluation in percent

Tool	Criteria	Training Method	Evaluation
R	Access/ Handling	Coaching	90
R	Template Settings	Nugget	85
R	3D-Modelling guidelines	Lecture	45
R	Parameter Settings	Nugget	65
R	Creation of Views	Nugget	70
R	IFC Export	Nugget	60
R	Pset Export	Nugget	55
V	IFC Check	Coaching	75
V	Parameter Check	Coaching	90
B	CDE Access	Nugget	100
B	Handling Documents	Lecture	90
B	Drawing Sets	Nugget	85
B	Naming Convention	none	95
B	Issues (BCF)	none	55
B	Transfers	none	75
B	Marker	Lecture	80
B	Clash Detection	Nugget	70
B	Views	none	95

R=Revit / V=IFC-Viewer / B= BIM360 (CDE)

It should be noted that all topics that could be processed using a BIM Nugget achieved good to very good results. Here, the students knew how to solve the task. The instructions provided helped with the application on their own design. Some tasks were assigned without direct assistance. Their processing can be carried out relatively intuitively in the programs used. This was also confirmed in the evaluation of the results with exceptions in issue management and the use of the BCF data format. Further support is required here. A major challenge in the workshops was adhering to the modeling guidelines. this overwhelmed many students and, in many cases, could not be dealt sufficiently. Additional learning materials are required for this topic.

In addition, the very high number of participants (50/80 people) posed a particular challenge: However, it shows the advantage of the Nuggets as self-learning modules. Only with this help could a large number of students be taught and trained within a very short time with only two teachers as supporting coaches.

3.2 Gamification

The playful approach in the simulation game consists in the competitive situation that the participants are exposed to. Students work together as a team on a design in direct competition with other teams. For their processed Nuggets and completed tasks, they receive points (see table 2) that make their performance status visible at any time. This is motivation for the students to work intensively on the tasks set, with the aim of making progress and achieving good results. A final jury evaluates the works at the end of the workshop and selects the winners.

Another gamification accent is created by the distribution of roles in each of the groups. Participants may take on a task role in the workshop and should play this character Table 3 includes an overview of the role assignment. On the one hand, this limits the workload of each individual, creates identification with a discipline involved in the project and produce an understanding of the problems involved in the division of tasks. Topics such as coordination and communication become relevant, the cooperation between the individual disciplines is trained, the participants get to know the planning process from different perspectives

Table 3 Role Assignment – source: own figure

BIM role	Role assignment	Project-specific role description
Information author	ARCH, STRE	Building modelling and enrichment of the component objects with information, each for its own discipline.
Information user BIM coordinator	ARCH COOR	Use of geometric and alphanumeric building information for visualisations Organisation of the LOIN and coordination of the data flow within the own discipline. Responsible for the composition of the internal coordination model, the collision check and the model-based coordination process.
Consulting	CONS	CONS empowers participants to work in a BIM-compliant manner, if support becomes necessary

ARCH= Architect/ STRE= Structural Engineer/ COOR= BIM Coordinator

3.3 Demographic Structure

In order to investigate the effects of different experience backgrounds and different ages of the participants, it was decided to follow a two-pronged strategy in selecting students for these workshops. Different age and ability groups were formed. Figure 4 shows a group of experienced practitioners.



Figure 4. Group of experienced practitioners – source: own figure

The first group is enrolled by undergraduate students of architecture who have just completed two semesters of study (in their third semester of the ten-semester course), who are yet to even achieve proficiency in computer drafting. The average age of the participants was 20 years. Their knowledge of CAD was very limited – almost nil. Since they have to be taught from scratch, we decided to have a two-day work-shop. This is henceforth described as workshop-1 (WS1).

The next case study for implementation of the Simulation Game was to have professional architects & engineers, who have varied years of experience in the field, but are yet to be introduced to BIM implementation. For these professionals we had a one day workshop as we presumed a certain degree of CAD knowledge and who are exposed to practical experience already handling building projects. For this group a one-day workshop was offered, wherein the entire process of the BIM Game was reduced to eight hours of intensive learning over one day. This is henceforth described as workshop-2 (WS2)

The two events conducted were an experience to examine the influence of age and previous knowledge on the learning curve of the participants. Conclude:

a) The older age group, used to working with CAD software such as AutoCad, showed lethargy when moving from CAD software to BIM – particularly Revit software, and were therefore slow to adapt to BIM processes. The results were similar to those of the novice group. This is surprising, since their lead in knowledge and experience would actually have led to expect a better result.

b) The students who were new to CAD, on the other hand, showed remarkable resilience in dealing with Revit and BIM 360 and were thus able to quickly grasp and apply the principles of the BIM process. No old and practiced application routines and ways of thinking stood in the way here. The fresh and unbiased handling of the matter promoted a quick grasp of the learning content and its implementation in the project.

3.4 Cultural Aspects

Both workshops focused primarily on the communication aspect. As the speakers were both from Germany, the organizers were worried about passing on their instructions to the Indian students. However, within the first hour, we could observe that the students and professionals responded to the resource people's instructions and were able to convey their points easily. This can also be attributed to the fact that the BIM Nuggets were easy to understand for the participants and, in addition to linguistic elements, are very much focused on visual information. The clear numbering of the application steps to be carried out is internationally

understandable and a suitable instrument for explaining the operation of software.

In addition to the language barrier, the number of students was a challenge. Previous experiences from the events in Germany are based on group sizes of around 20 participants. In India, far more people had to be integrated into the teaching format, which in no way harmed the play and the learning process.

4 Conclusion

The two events held were an intercultural experience for understanding BIM. The game format helped to successfully convey the new technology despite cultural differences and the very tight schedule. The evaluation results of the event in India are similar to the results of the workshops held in Germany.

To conclude: The BIM-simulation Game as a teaching aid has high potential irrespective of cultural barriers as proved with the success of implementing the game for the first time outside Germany. The efficacy of BIM Nuggets to effectively instill interest in learning the finer points of BIM operations by using this learning modules over a wide age group has been proved to be successful.

The workshops has been successful in teaching the essence of BIM for beginner students of Architecture and has evoked their interest to further learn BIM process in detail over a period of time.

BIM - Simulation game works as an “Appetizer” and can be effectively used as a tool to increase the awareness of applying BIM process for building projects big or small. This could be an effective tool to communicate the advantages of introducing BIM process by various software companies catering to the building industry.



Figure 5. Student Café Design of a student group: Sumedha, Chethana, Bahuleya, Riya, Saakshi, Syed

References

- [1] Autodesk (2011) Realizing the Benefits of BIM http://images.autodesk.com/adsk/files/2011_realizing_bim_final.pdf last accessed 2023/01/10
- [2] Eastman, Chuck, et al. BIM Handbook : A Guide to Building Information Modeling for Owners, Designers, Engineers, Contractors, and Facility Managers, John Wiley & Sons, Incorporated, 2018. ProQuest Ebook Central, <http://ebookcentral.proquest.com/lib/jade/detail.action?docID=5447327>
- [3] Skye Rayner, Assem Al-Hajj, "Implementing BIM: a change in culture" in Proceedings of International Conference on Civil and Building Engineering Informatics (ICCBEI 2015), 67. Tokyo, Japan, 2015.
- [4] Heins, C., Grunwald, G., Helmus, M.: Gamification and BIM - The didactic guidance of decentralised interactions of a real-life BIM business game for higher education. ISARC 2021 Conference Paper, 38th International Symposium on Automation and Robotics in Construction, November 2021, DOI: 10.22260/ISARC2021/0126
- [5] Design Hub India Homepage, <https://designhubindia.com/events.html>, last accessed 2023/01/10
- [6] Grunwald, G., Heins, C.: BIM Game: a testing ground for specifying, modeling, evaluating and visualising information in IFC formats. ICCEA 2022 Conference Paper, 5th International Conference on Civil Engineering and Architecture, December 2022
- [7] Innovative Hochschule Jade-Oldenburg! Homepage, <https://ihjo.de/bim-game-jade-work/>, last accessed 2023/01/10
- [8] Innovative Hochschule Jade-Oldenburg! Homepage, <https://ihjo.de/55-stunden-spielend-ping-pong-ein-digitales-planspiel/>, last accessed 2023/01/10
- [9] Homepage Capricot <https://capricot.com/contact-us/bim-game-workshop/>, last accessed 2023/01/10
- [10] M. Filardo, J. Krischler, Basiswissen zu Auftraggeber-Informationsanforderungen (AIA), bSD Verlag, 2020, ISBN 978-3-948742-12-6
- [11] Muster AIA (Status: February 2022) <https://www.bimdeutschland.de/leistungen/muster-auftraggeber-informationsanforderungen>, last accessed 2023/01/10
- [12] BIM360 Homepage, <https://www.autodesk.com/bim-360/>, last accessed 2023/01/10
- [13] Wallner, Marcus Michael. "Building project management training using the platform BIM 360." *Управление проектами: идеи, ценности, решения*. 2019.
- [14] BIMQ Homepage, <https://www.bimq.de/en/>, last accessed 2023/01/10
- [15] BIMQ Homepage, <https://bimq.centraldesks.com/de/articles/by2R-einleitung/>, last accessed 2023/01/10
- [16] Simplebim Homepage: <https://simplebim.com/bimsheet/>, last accessed 2023/01/10
- [17] Stiftung Innovation in der Hochschullehre Homepage, <https://stiftung-hochschullehre.de/>, last accessed 2023/01/10
- [18] Besné Yanguas, Alia, et al. "A Systematic Review of Current Strategies and Methods for BIM Implementation in the Academic Field." *Applied Sciences*, 2021, 11 (12) (2021).
- [19] Nikolic, Dragana, Fadi Castronovo, and Robert Leicht. "Teaching BIM as a collaborative information management process through a continuous improvement assessment lens: a case study." *Engineering, Construction and Architectural Management* (2021)

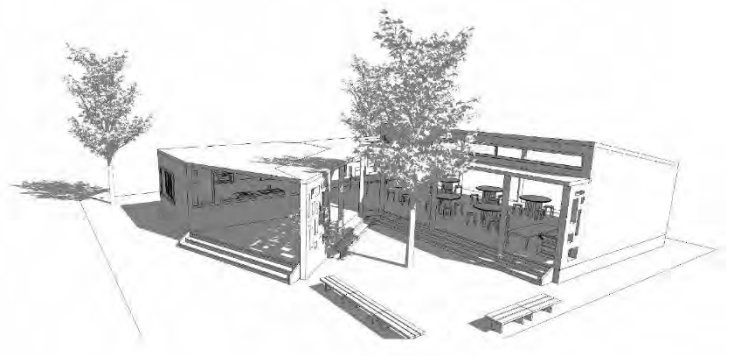


Figure 6. Student Café design of a group 1: Shaik Ahmed Affan, Tanvi Prasad, Y Sai Sushanth, Arpitha Prasad, Ashita S., Murtaza Suterwala

Towards interfacing human centered design processes with the AEC industry by leveraging BIM-based planning methodologies

Marc Schmailzl¹, Michael Spitzhirn², Friedrich Eder¹, Georg Krüll³, Thomas Linner¹, Mathias Obergriesser¹, Wassim Albalkhy⁴ and Zoubeir Lafhaj⁴

¹Faculty of Civil Engineering, Ostbayerische Technische Hochschule Regensburg, Germany

²Imk Industrial Intelligence GmbH, Germany

³Faculty of Mechanical and Systems Engineering, Esslingen University, Germany

⁴Centrale Lille, CNRS, UMR.9013-LaMcube, Lille, France

marc.schmailzl@oth-regensburg.de, michael.spitzhirn@imk-ic.com, friedrich.eder@oth-regensburg.de, georg.kruell@hs-esslingen.de, thomas.linner@oth-regensburg.de, mathias.obergriesser@oth-regensburg.de, wassim.al-balkhy@centralelille.fr and zoubeir.lafhaj@centralelille.fr

Abstract –

Digital workflows in the Architecture, Engineering and Construction (AEC) industry have been working with a wide range of software solutions trying to enable a Design-to-Production (DtP) end-to-end data flow. Thereby, state-of-the-art software solutions attempt to streamline the design and production processes accordingly.

However, most digital workflows lack in terms of adequate sequential data preparation, agglomeration, and interfacing capabilities for consecutive design phases. These issues result in long, tedious correction loops, a wide range of software solutions and extensions to mitigate the issues. In addition, many digital workflows do not consider or integrate construction, production and machine relevant data holistically (respectively geometry and semantics). In this context, the production relevant data in from of human-centered work process data referring to digital human models (DHM), derived human abilities, safety and ergonomic criteria are often neglected. However, this is essential to interface the construction, human and machine relevant data in a holistic manner.

This paper therefore proposes a DtP-workflow which is intended to solve some of the issues by interfacing relevant software solutions incorporating construction, production (including DHM and more) and machine relevant data in a holistic manner using a Building Information Modeling (BIM)-approach (based on the IFC schema). In this regard, the DtP-workflow aims to reverse common top-down digital workflows by considering and integrating the relevant data for consecutive design phases from the

beginning. Subsequently, the DtP-workflow should achieve a reduction in planning effort.

Keywords –

Architecture Engineering and Construction (AEC) industry, Building Information Modeling (BIM), Digital Human Model (DHM), Interoperability

1 Introduction

The AEC industry plays an integral part in the worldwide economy by being not only a major employer, but also responsible for critical infrastructure and is thus systemically relevant. That is why the industry is under enormous economic and social pressure. Socially, it suffers from an omnipresent shortage of skilled labor due to the demographic change and is particularly aggravated by physically intense and dangerous work conditions [1]. Economically, the overall increased productivity rates are lower than in other industries and simultaneously experiences one of the lowest degrees of digitalization [2]. In addition, the growing demand for housing has not been satisfied yet, which has led to increasing real-estate prices [3].

To counteract the aforementioned inhibiting factors, the performance of AEC related tasks has to get more efficient, persistent, quality consistent and human-centered to secure a higher value creation, thereby significant productivity gains and acceptance.

In this context, productivity losses are often caused by interoperability issues between different software solutions. Data is siloed in different software solutions and databases causing data redundancies, as well as inconsistencies. Moreover, different file formats, data

structures and naming conventions lead to data fragmentation.

Current research on improving interoperability and thereby including common data standards (e.g. BIM) are already conducted. However, there is still a need to fully enable a seamless data flow from design to production considering and integrating (not only) construction, but also production and machine relevant data.

The research gap therefore consists of a lack of process relevant data preparation, agglomeration, integration, exchange capabilities and adoption of new technologies (e.g. BIM) to enable an effective, collaborative and seamless workflow. Subsequently, enabling the aforementioned could save millions of working hours and eventually led to more projects being delivered on time and within budget [4] [5].

Therefore, this paper proposes a DtP-workflow, aiming towards a beneficial economic and social impact for the AEC industry by bridging interoperability gaps considering, as well as integrating construction, production, and machine relevant data in early design stages. In this context, it should illustrate a first attempt of interfacing work process simulation software (including DHM and more) with AEC industry related BIM-authoring software and eventually machine control capabilities.

2 State-of-the-art

2.1 Digital workflow tools

Nowadays, a digital workflow in the AEC industry consists of various sequential value adding steps (e.g. planning, detailed planning, production planning, construction or building operation etc.) and therefore incorporates a wide range of different software solutions. In this context, the ISO family of standards (IFC schema and process standards), common data environments and novel management approaches such as lean construction introduced strategies allowing a more integrated workflow. Moreover, digital, parametric planning and modeling using BIM approaches are the basis for integrated planning and communication throughout the value chain. Nevertheless, such approaches usually require complex adaptations cross compartments and value-added steps [6] leading to concepts such as Design for Manufacturing and Assembly (DfMA), Robot Oriented Design (ROD) and considering construction as an integrated production system [7].

In addition, there are further identified challenges regarding the overall data interoperability [8] such as loosely defined object definitions, the coverage of BIM authoring tools and varying levels of parameterization. Furthermore, the introduction of semantic web technologies into the AEC sector are likely to overcome

these problems by introducing a metadata abstraction layer, able to describe heterogeneous data sources [9].

Moreover, possibilities of using simulation software solutions, ever better integration of BIM-to-machine/robot software pipelines and the use of robotic frameworks can further facilitate integration.

In the following sections AEC industry related state-of-the-art software solutions (alias: digital workflow tools) are described further and intended to be used in the proposed DtP-workflow (section 3 and 4). Moreover, correlating challenges are synthesized to identify digital workflow determining bottlenecks which the DtP-workflow is intended to tackle accordingly.

2.1.1 Building Information Modeling (BIM, construction perspective)

In general, an AEC project involves various stakeholders and is therefore increasingly reliant on a BIM-approach incorporating the IFC data model schema to eventually assure a better-information flow throughout the design phases. That is why many sectors started to require BIM in AEC projects and aiming to establish it as a standard practice for the industry since recent years [10].

BIM-based data interoperability is mainly facilitated by the common IFC data model schema which defines AEC industry-specific entities and relations (Industry Foundation Classes) [11]. It allows the creation of BIM models which serve as a repository for all data related to the building itself as well as the construction process. That is why this data model is considered the de-facto standard for exchanging data through an openBIM collaboration process [12].

The data model can utilize existing construction domain-specific entities which can be complemented by custom property sets in order to store all production-specific information (e.g. Materials, Names, Surfaces, Colors, Coating Areas, Gross Areas, Net Areas, Professions, Deliveries, Categories etc.).

Exchange requirements are implemented through a separate schema file (STEP or XML) which makes it possible to check for specific relations and properties among the IFC entities. This so-called 'level information need' as mentioned in [13] is - in terms of the IFC - implemented through either a Model View Definition (MVD), or an Information Delivery Specification (IDS).

In model-based workflows issue management can be accomplished by contextualizing the issue with an entity. In BIM-based workflows this can be implemented through the so-called BIM Collaboration Format (BCF). In practice BCF can be implemented as a file or web-service.

In accordance with the proposed DtP-workflow (section 3) and use-case (section 4), the mechanisms implemented by the Industry Foundation Classes offer a purposeful software solution.

2.1.2 Human-robot-work-process simulation (production perspective)

An AEC project can be also complemented by human-robot-work-process simulations enabling a holistic perspective and thereby human-centered planning process for production.

Planning systems with DHM such as ema Work Designer (emaWD) or process simulate can thereby detect ergonomic risks and are used to analyze and optimize the work process regarding ergonomics and productivity [14].

EmaWD (section 4) includes an integrated task library and a motion generator that allows the DHM to autonomously fulfil user-defined work tasks. Hereby, DHM with different abilities related to age (e.g. anthropometry, mobility, etc.) as well as various robots can be used to ensure an ability- and age-appropriate design of work processes and factories at an early stage [15] [16].

This step is essential to simulate, analyze and optimize task planning or allocations for human- and robot- related work processes in a holistic production related manner (including risk assessment, collision detection etc.).

Subsequently, such software solutions can be beneficial for the DtP-workflow by considering production in a holistic manner considering product, human and machine or robot in accordance to the production periphery.

2.1.3 Machine simulation and control (machine perspective)

An AEC project usually ends with the machine control and thereby subsequent production/realization of the intended product or product.

In general, there are two ways of programming such machines – either offline (e.g. remote via PC and underlying software solutions) or online (at the machine itself e.g. via Teach Pendant).

To establish an end-to-end data flow, an offline programming approach is to be chosen to make sure a sequential software solution usage is established accordingly.

In this context, vendor-agnostic software solutions (e.g. frameworks) for simulating and partly programming/controlling (offline programming, e.g. Gazebo, RoboDK, HAL Robotics Framework, Robot Operating System ROS etc.) play a decisive role for testing new control algorithms, evaluate efficiency, safety, and robustness, as well as optimize the operational behavior [17] [18].

Nevertheless, the general user effort and correlating usage complexity depends heavily on the machine itself and associated Degrees of Freedom (DoF). An NC control for a CNC milling machine with three DoF can already be initiated seamlessly due to a standardized

machine programming language (G-code), whereas the machine control with a robot is more difficult due to more DoF and different manufacturer-specific programming languages. However, this difficulty can be partly conquered by agnostic software solutions (robot frameworks, e.g. ROS, HAL etc.) as mentioned before.

In this regard the proposed DtP-workflow (section 3 and 4) is intended to use aforementioned agnostic software solutions (machine control via offline programming with framework) to prototypically execute a machine control (robot) with the advances of being simulation based and agnostic.

2.2 Resulting challenges of the digital workflow in AEC industry and underlying tools

The preceded research showcased a range of state-of-the-art software solutions for establishing an end-to-end DtP data flow. Nevertheless, there are still several challenges that need to be solved accordingly.

First, the overall low adoption rate of AEC specific human-robot-work simulations for production in connection with BIM-related approaches is an eminently occurring challenge and derived from interoperability issues (e.g. IFC) because certain software solutions missing essential capabilities to process construction industry specific file formats (e.g. IFC, including geometry and semantics).

Moreover, this challenge is additionally exacerbated by a lack of data preparation and agglomeration to enable a better-informed and thereby more efficient or seamless digital workflow. This issue can cause correction loops, redundancies and thereby delays, as well as cost overruns [19].

Despite the BIM-approach with correlating IFC-schema as an attempt to standardize data flow throughout the design phases, there are still different file formats needed/used (e.g. STEP, cpiXML, LandXML etc.) to initiate analyses, simulations, or machine controls due to their proprietary nature, as well as data schema.

Furthermore, the current BIM-approach in combination with consecutive robot control for production is still not sufficient due to the lack of production-relevant data preparation, as well as insufficient consideration of ergonomic standards and human abilities for human-robot-collaboration (HRC) [20]. This can lead to expensive corrections loops and health and safety related risks. A better consideration of human human-robot-work-process could support the development of appropriate work processes. That is why a more detailed production-, as well as human-centered work process data level description is required.

3 DtP-workflow

3.1 General digital workflow and information management

The proposed DtP-workflow is showcased in Figure 1 and focuses on the software layer, which can be divided into three sequential processes. In this regard, the accumulated information derived from each step is transferred through a data exchange following a BIM-based approach (IFC schema). In the CAD-processes (construction perspective) the design intent documentation of the client is getting processed with the aim to provide product level information which describes a product in accordance to the clients requirements for the consecutive Computer Aided Engineering (CAE) processes incorporating a first virtual product model. Product model information thereby consists of geometric (e.g. solids, surfaces etc.) and semantic (e.g. unit-based dimensions, materials, physical properties, mass, product cost etc.) data.

The CAD-processes are followed by the CAE-processes (production perspective) where the product is further detailed in terms of its elements. Furthermore, the related production system is planned, as well as consecutively simulated, analyzed, and optimized in accordance with the elements. The resulting element level information also consists of geometric (e.g. detailing, element aggregations etc.) and semantic (e.g. processes, assembly instructions, production cost, health and safety related information etc.) data.

Afterwards, the prepared and accumulated data (element level information) is processed in the Computer Aided Manufacturing (CAM) processes and used for initiating machine control with correlating simulations, analyses, as well as optimizations. The CAM-processes thereby transfer the implicit assembly instructions of the element level information into explicit ones and eventually generating machine code (production documentation) for production. Furthermore, the CAM-processes utilizes the relevant production level information to generate a better-informed machine control.

This sequential data preparation and agglomeration is consistently processed throughout the CAx processes due to the introduced data exchange layer which allows interoperability accordingly. This data exchange layer is further elaborated in section 3.3.

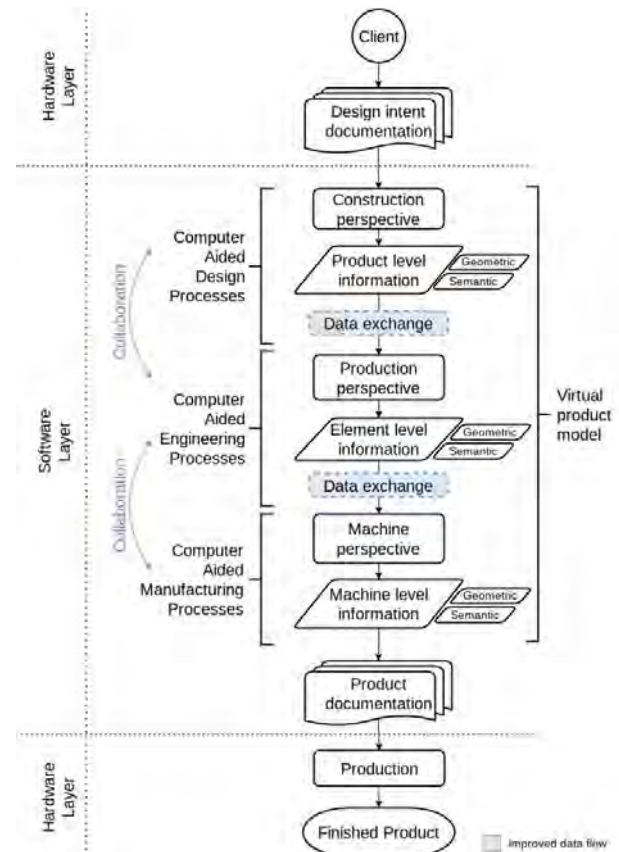


Figure 1: General digital workflow and information management of the DtP-workflow.

3.2 Collaboration loops

Each CAx process has its own collaboration and thereby development loop (Figure 2), where the current process state is reviewed based on the objectives. In case these objectives are not met, the origin of the given issue is determined. If the issue is related to the previous process, proper documentation is created and is handed to the previous process. Otherwise, the loop does not leave the scope of the current process.

In this regard, an integral part of the applied BIM-approach is the utilization of established exchange mechanisms as described in section 2.1.1 - namely MVD for the definition of the actual exchange - BCF for handling model-based issue management between the top-level process steps and the IFC for the persistent storage of model and process data.

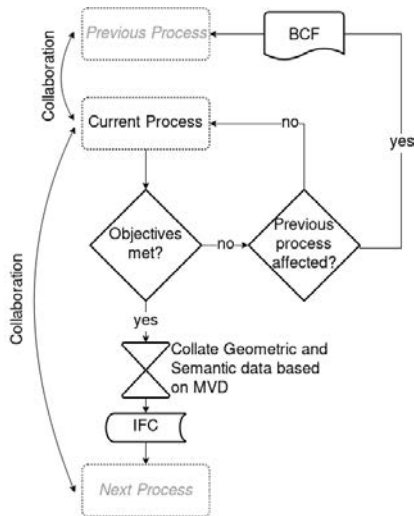


Figure 2: General collaboration loops within the CAx processes.

3.3 Idealistic data exchange

The integrated BIM-based data flow facilitates the proposed DtP-workflow with the underlying digital workflow (section 3.1). This calls for a common data format - namely IFC - which serves as a data storage for all related CAx process related information (geometric and semantic data). In Figure 3 the BIM-based data flow is shown accordingly.

If the user wants to push IFC data to the IFC data storage, the prepared and accumulated IFC data can be integrated via an import data routine.

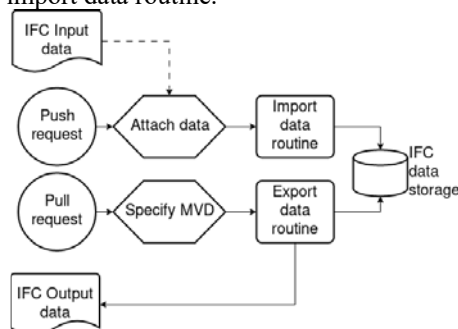


Figure 3: Idealistic data exchange.

If the user wants to pull IFC data from the IFC data storage a pull request can be issued through the specification of a desired MVD and the subsequent export routine delivers the related output IFC file.

4 Use-case

4.1 Production process

The production process describes the manufacturing and assembly of the balcony platform (Figure 4). In this

context, the balcony platform (Figure 4, outlined in red) is assembled from various elements: edge profiles, platform beams and segments, as well as connectors and vary in dimensions from 1x1m to 7x3m.

In the general production process – used for all iterations - the edge profiles (Figure 4, dark grey) are first connected using profiled corner connectors (Figure 4, light grey) and bolts. The platform beams (Figure 4, medium grey) and segments must be glued, sealed, and riveted together after they have been inserted accordingly. Further elements (e.g. railing etc.) are attached in downstream processes.



Figure 4: Balcony and platform for the production process (software: Blender BIM).

4.2 Digital workflow in accordance to the DtP-workflow

The following testing of the DtP-workflow is executed in accordance to the previously introduced general digital workflow and information management (Figure 1).

The desired product is firstly designed by correlating CAD software with BIM-authoring capabilities (e.g. Autodesk Revit, Blender BIM etc.) and afterwards prepared and accumulated with relevant product level information, for example in this case: overall geometry of the balcony and semantics regarding visual and structural boundary conditions (e.g.. location, surface finishes, mounting systems etc.).

Subsequently, the resulting virtual product model can be seamlessly handed over to the CAE processes due to the developed data exchange layer (section 4.3), where the given product level information is further complemented with information at the element level. For the balcony, this includes, but is not limited to designing and considering further geometry of the profiles and semantics (e.g. weights/mass, center of gravity, bearing load etc.).

In order to determine further semantic element level information of the production process (e.g. human-robot-interaction, ergonomics, task allocations etc.) and the corresponding optimization, simulation software with DHM (in this case emaWD) is used accordingly.

This simulation software is used to orchestrate the

previously described elements within the production context (e.g. production line etc.). Therefore, emaWD utilizes the following element level information established by the preceding processes: Element-Identifier, Element-Name, Dimension (e.g. Length, Width, Height) and Weight.

In this use-case three different production process variants were modeled (initial, variant 1, variant 2) in order to assess the capabilities of the DtP-workflow regarding scalability, since each iteration augments the processes and thereby increasing the complexity.

Initially the balcony platform (4x2m) is produced in a manual process (Figure 5) only by humans and characterized by a large number of elements, ergonomically unfavorable work conditions due to long, bulky parts (e.g. up to 4m long), as well as high element weights (e.g. between 3 and 12kg) and very repetitive work processes (e.g. gluing, riveting, pick and place etc.).



Figure 5: Initial production process (software: emaWD).

The first iteration (Figure 6) incorporates the modification of the pick-up height, replacing the euro pallets with elevated racks as well as utilizing a dedicated lifting table and pallet cages. This in turn resulted in an improvement regarding ergonomic and production criteria (e.g. ergonomic assessment EAWS, execution time etc.).



Figure 6: Optimized production process variant 1 (software: emaWD).

In the second variant (Figure 7), the handling of the segments of the outer frame is carried out by a robot (KUKA KR16-2). This leads to further optimization regarding the detailed ergonomic assessment and leading

time. In this regard, a previously developed implementation [18] was used, which enhances robotic simulation functionalities (more realistic robot behaviour model for robot specific tasks derived from ROS-based simulation packages and enabled by data exchange) in emaWD. The use of this developed implementation assures a better simulation result due to more accurate collision-free trajectory planning capabilities taking environmental objects into account.

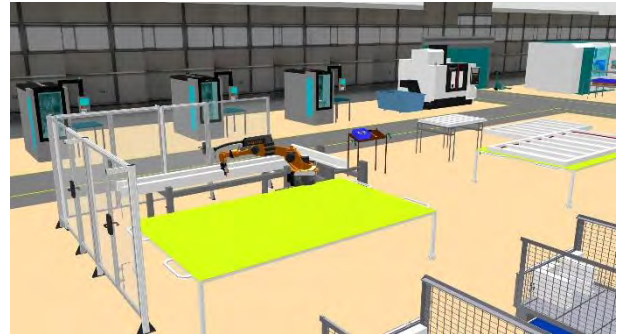


Figure 7: Optimized production process variant 2 (software: emaWD).

Afterwards the optimized robotic movements (assembly instructions) were transferred (data exchange, section 4.3) to the CAM processes in which the element level information is further complemented with machine level information. In this process the further prepared and accumulated data is utilized to introduce a machine/robot control.

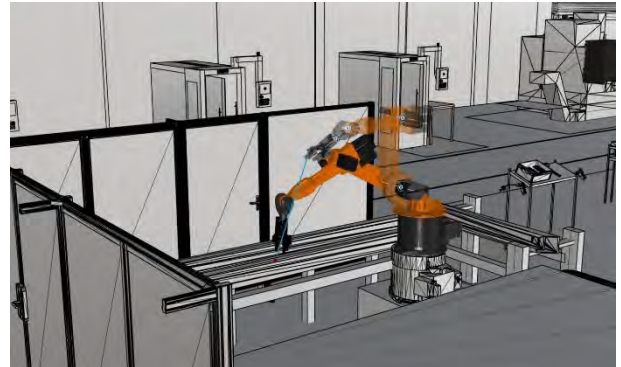


Figure 8: Optimized production process variant 2 and initiated machine/robot control (software: HAL Robotics Framework).

Previous data can be fed into the corresponding data compartments (record) in a machine simulation and control software solution (Figure 8, HAL Robotics Framework). Afterwards the machine code can be uploaded or exported to the robot controller in the joint space (programmable logic controller, PLC) to enable the production accordingly.

4.3 Applied data flow

With the use-case (balcony pre-assembly) we show the prototypically BIM-based DtP-workflow enabled by programmed IFC semantic parsers (leveraging IfcOpenShell) which translate a CSV or XML file to a software readable format assuring previously aggregated data is transmitted seamlessly.

The introduction of this layer is thereby bridging the interoperability gap and being able to extract and integrate various structured (e.g. tabular, hierarchical etc.) data formats expected by the used software solutions. The impact on the proposed data exchange (Figure 3) is shown in Figure 9.

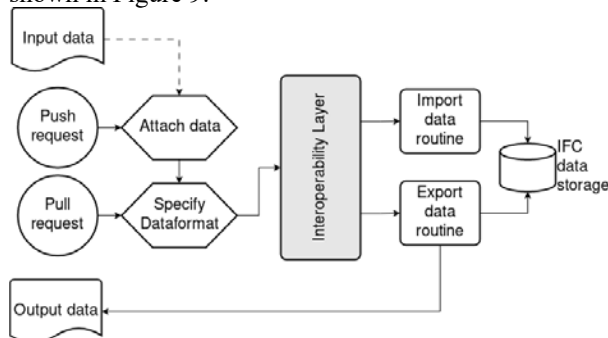


Figure 9: Applied data flow.

5 Results

The described use-case indicates several benefits as well as issues regarding the proposed DtP-workflow.

The application of a collaborative, model-based data exchange led to a reduction in planning effort. Less time was needed to integrate the element-level information from the handed over IFC file into the simulation software (emaWD). Additionally, the model-based approach facilitated communication as well as end-to-end data flow capabilities and thereby further supplementing the overall planning processes. Through reducing the effort in preparation for interfacing between software solutions and corresponding data agglomeration, a reduction in overall susceptibility for failures could be achieved. The usage of human-robot-work-process simulation software (emaWD) in the context of the AEC industry could therefore significantly support in the related tasks by identifying and quantifying risks.

6 Discussion

The proposed DtP-workflow is still at a prototypical stage and more research needs to be conducted in this direction.

In future research the proposed DtP-workflow needs to be tested for several use-cases (especially an on-site AEC-industry related use-case, not only for a

prefabrication use-case), as well as evaluated under real-life production conditions. Additionally, a more detailed DtP-workflow-related stakeholder allocation needs to be conducted. The current state of the developed data exchange layer (section 4.3) relies on a MVD as a means of concurrent data exchange, lacking the description of a schema-based, standardized way of data integrity verification [21]. This could be resolved by utilizing or introducing more specific IFC classes for creating the semantic context in a DtP-workflow (section 3.3).

In addition, there are technical challenges involved when dealing with optimizing data flow utilizing the IFC data schema such as efficiently processing large and complex data, detecting and resolving semantic errors or inconsistencies and ensuring compatibility. These challenges have to be considered accordingly.

In the end the workflow was developed with the intent to perform the data flow automatically. However, a completely automated implementation was considered beyond the scope of the conducted research as it necessitates the extension of proprietary software Application Programming Interfaces (APIs). Therefore, the workflow majorly showcases a solution for solving aforementioned issues without disrupting the underlying software architectures. In addition, the workflow could be used for further developments towards linking different software solutions in the AEC industry.

7 Conclusions

There is still the potential to reduce cost, save time and simultaneously assure quality in modern AEC-related digital workflows. This was demonstrated by enabling human-robot-work process software solutions (emaWD) to utilize and accelerate tasks, based on the DtP-workflow with a derived digital workflow in a BIM-based holistic manner (IFC schema). Thereby data preparation, agglomeration and interfacing software solution capabilities can be alleviated.

With the described combination of BIM, human-robot-work process simulation and consecutive machine control, a virtual product model was prototypically developed from design to production.

8 Acknowledgements

We are especially indebted by the SECIRA-consortium (secira-project.com), which initiated first topic-related approaches in an EU-Horizon proposal. The related discourse laid the first foundations for this paper.

References

- [1] Tender M, Couto JP, Gibb A, Fuller P and Yeomans S. Emerging Technologies for Health, Safety and

- Well-being in Construction Industry. In Bolpagni, M., Gavina, R., Ribeiro, D. (eds) *Industry 4.0 for the Built Environment*. Structural Integrity, 20, pages 369-390. Springer, Cham, 2021.
- [2] Agarwal R, Chandrasekaran S and Sridhar M. Imagining construction's digital future. Online: <https://www.mckinsey.com/capabilities/operations/our-insights/imagining-constructions-digital-future>, Accessed: 28/01/2023.
- [3] OCED. Analytical house prices indicators. Online: https://stats.oecd.org/Index.aspx?DataSetCode=HOUSE_PRICES, Accessed: 28/01/2023.
- [4] Khalfan M. and Raja N. Improving Construction Process through Integration and Concurrent Engineering. *Australasian Journal of Construction Economics and Building*. 5: pages 58-66, 2012.
- [5] Sacks R. Brilakis, I. Pikas E. Xie, H. S. and Girolami M. Construction with digital twin information systems. *Data-Centric Engineering*. 1(e14): 1-26, 2020.
- [6] Ng M. Hall D. Schmailzl M. Linner T. and Bock T. Identifying enablers and relational ontology networks in design for digital fabrication. *Automation in Construction*. 144(1): pages 1-20, 2022.
- [7] Bock T. and Linner T. *Robotic Industrialization. Automation and Robotic Technologies for Customized Component, Module, and Building Prefabrication*. Cambridge University Press. 2015.
- [8] Tchouanguem Djuedja, J.F., Karray, M.H., Foguem, B.K., Magniont, C., Abanda, F.H. (2019). Interoperability Challenges in Building Information Modelling (BIM). In: Popplewell, K., Thoben, KD., Knothe, T., Poler, R. (eds) *Enterprise Interoperability VIII. Proceedings of the I-ESA Conferences*, vol 9. Springer, Cham. https://doi.org/10.1007/978-3-030-13693-2_23.
- [9] Pauwels, P., Zhang, S., & Lee, Y.-C. (2017). Semantic web technologies in AEC industry: A literature overview. *Automation in Construction*, 73, 145–165.
- [10] Moreno C. Olbina S and Issa R. R. BIM Use by Architecture, Engineering, and Construction (AEC) Industry in Educational Facility Projects. *Advances in Civil Engineering*, 2: pages 1-19, 2019.
- [11] buildingSMART. Scope of buildingSMART Standards. Online: <https://technical.buildingsmart.org/>. Accessed: 29/01/2023.
- [12] buildingSMART. openBIM. Online: <https://www.buildingsmart.org/about/openbim/>. Accessed: 29/01/2023.
- [13] ISO 19650-1:2018-1: Organization and digitization of information about buildings and civil engineering works, including building information modelling (BIM) — Information management using building information modelling — Part 1: Concepts and principles.
- [14] Gunther E. P. *Modelling and simulation of human systems*. 5. pages 704-735. John Wiley & Sons, Inc. 2021.
- [15] Spitzhirn M. Ullmann S. and Fritzsche L. Considering individual abilities and age-related changes in digital production planning – human centred design of industrial work tasks with ema software. pages 459-477. *Z. Arb. Wiss.* 76. 2022.
- [16] Spitzhirn M. Ullman S. Bauer S. and Fritzsche L. Digital production planning and human simulation of manual and hybrid work processes using the ema Software Suite. In *Proceedings of the 7th International Digital Human Modeling Symposium*. 7(1). 2022.
- [17] Chong O. W. Zhang J. Voyles R. M. and Min B. C. BIM-based simulation of construction robotics in the assembly process of wood frames. *Automation in Construction*. 137: 104-194, 2022.
- [18] Staranowicz A. and Mariottini G. L. A survey and comparison of commercial and open-source robotic simulator software. In: *Association for Computing Machinery, Proceedings of the 4th International Conference on Pervasive Technologies Related to Assistive Environments*, 56, pages 1-8, New York, USA, 2011.
- [19] Muller M. F. Loures E. R. and Junior O. C. Interoperability Assessment for Building Information Modelling. Grupo BIM PUCPR. In *Conference: 3rd International Conference on Mechatronics, Robotics and Automation*, pages 224-231, Shenzhen, China, 2015.
- [20] Tender M. Couto J. P. Gibb A. Fuller P. and Yeomans S. *Industry 4.0 for the Built Environment . Emerging Technologies for Health, Safety and Well-being in Construction Industry*. 20. pages 369-390. Springer, 2021.
- [21] Lemmerz K. Glogowski P. Hypki A. and Kuhlenkoetter B. Functional Integration of a Robotics Software Framework into a Human Simulation System. In: *ISR 2018. 50th International Symposium on Robotics*, pages 1-8, Munich, Germany, 2018.
- [22] van Berlo, Léon. The curious case of the MVD. Online: <https://blog.buildingsmart.org/blog/the-curious-case-of-the-mvd>, Accessed: 30/01/2023.

Research on the Relationship between Awareness and Heart Rate Changes in the Experience of Safety Education Materials Using VR Technology

Shunsuke Someya ^a, Kazuya Shide ^b, Hiroaki Kanisawa ^b, Zi Yi Tan ^c and Kazuki Otsu ^d

^aDoctoral Course, Graduate School of Eng., Shibaura Institute of Technology, Japan

^bProf., School of Architecture, Shibaura Institute of Technology, Japan

^cLecturer, Department of Construction Management, Faculty of Engineering and Green Technology, Universiti Tunku Abdul Rahman, Malaysia

^dMaster Course, Graduate School of Eng., Shibaura Institute of Technology, Japan
Email: na19501@shibaura-it.ac.jp, shide@shibaura-it.ac.jp, kani@sic.shibaura-it.ac.jp,
tanzy@utar.edu.my, mj21017@shibaura-it.ac.jp

Abstract –

The response of subjects having experienced VR content for safety education was confirmed by their heart rate. Ten male subjects with work experience in construction and ten without such experience used VR content for safety education. The subjects were allowed to walk through scaffolding which was defective in five facilities in that content. Their heart rates were measured, both at rest and during the experience, whereupon they were interviewed about their awareness during said experience. Following this experiment, it was suggested that there were some VR content for safety education to which subjects with work experience reacted only.

Keywords –

VR; Safety Education; Heart rate; Human factor

1 Introduction

Compared to other industries, the construction industry has more occupational accidents and safety education has been implemented in various forms for some time. Materials used vary from those commonly distributed in print, such as books and pamphlets, to videos and presentation materials created independently by each company or workplace. Conversely, declining numbers of skilled and inexperienced workers and foreign workers in recent years have raised expectations of new safety materials that are independent of experience or language. In this study, we focused on experiential teaching materials using VR technology and used physiological sensing technology to quantitatively confirm the response of the experimental subjects and examine the relationship between HR changes and awareness or feeling of fear.

2 Previous Studies and This Purpose

2.1 Previous Studies

Takagi's previous research examined safety materials used in construction companies and their effects, pointing out the mainstream of the so-called 'learning type' such as paper materials, DVD videos and discussions and doubts over their scope to effectively prevent crash disasters [1]. In previous research on the use of VR content, the "experiential" educational material focused on in this study, Ito et al. reported significant individual differences in the standard deviation of heart rate (R-R) intervals during the experience, as well as differing trends between males and females [2][3].

2.2 Purpose of this Study

VR contents have been published or sold by the Ministry of Health, Labour and Welfare [4] and private companies [5] in Japan. It is described that VR contents are characterized by their ability to provide an immersive, near-real experience in those HP. As in previous research [2][3], individual differences emerge in user responses, even for game content, which may mean differences emerging obtained in VR contents. We hypothesized that VR experience for safety education would have different tendencies depending on the presence or absence of work experience, and that difference would appear in the heart rate. In this research, we aim to verify this hypothesis by conducting an experiment in which multiple subjects use VR contents, and discussing differences in trends by interviewing them and measuring their heart rates.

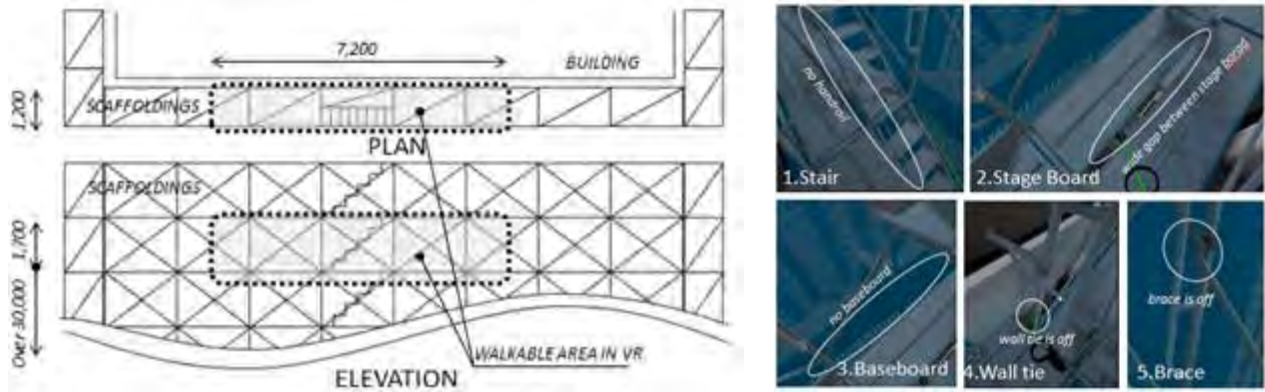


Figure 1. Image example of safety teaching materials using VR

3 Method of hypothesis verification

3.1 VR content used as the subject

In this study, the subject was a walking experience in a VR space of a temporary scaffold installed outdoors and at elevation in order to use the presence or absence of construction management experience as an evaluation index. During the experiment, it is assumed that work to inspect safety equipment is being carried out and the different between subject groups in terms of the sense of danger and reaction to the defective part is examined. Commercially available products are used for the content, which highlights deficiencies in five safety facilities (1. stairs, 2. scaffolding boards, 3. baseboards, 4. wall ties, 5. braces) (Fig. 1).

The movable range within the content is shown in Fig. 1, left. It is one layer of the upper part of the temporary scaffolding, which includes steps in the scaffolding and crossings to the main building. In the experiment, the walkable area was about two rows of scaffolding boards x four spans (W 1, 200 x L 7, 200). Defects in equipment were not mentioned at the start of the experiment and each person was capable of walking freely and performing visual checks.

3.2 Indicators to quantify subject response

In this study, the heart rate is measured to quantitatively capture the unconscious biological response that occurs during a VR experience. Since the heart rate changes immediately compared to the body temperature and other physiological responses, we deemed it suitable to evaluate an experience experiment like this one. In previous research [3] as mentioned above, the purpose was to use the heartbeat to quantify the comfort level or discomfort, etc. Accordingly, if a professional analysis using electrocardiographic data were required, measurements with electrodes placed on the chest would be performed. Conversely however, since this research aimed to detect the presence or absence of biological reactions, with the need for safe measurements that would leave the movement of subjects in the experiment unhindered, heart rate as a

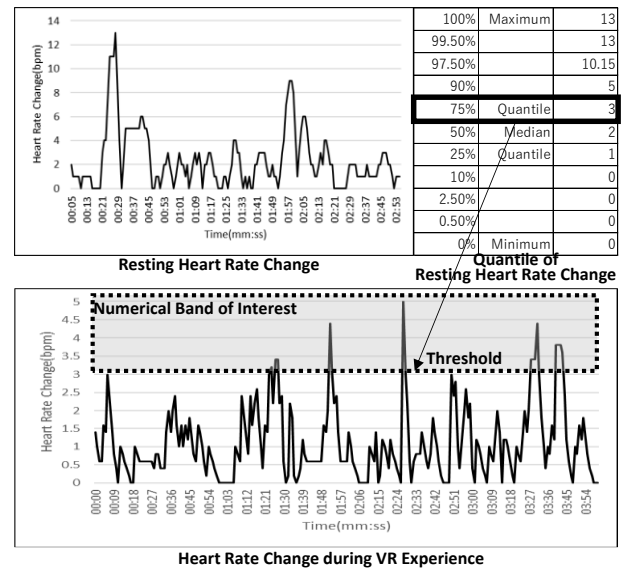


Figure 2. Heart rate analysis method

Table 1. Equipment list

HMD	OculusQuest2(FacebookTechnologies,LLC)
VR contents	Safety VR Experience Training (Tsumiki Seisaku Co., Ltd.)
HR sensor	A370 (Polar Electro)

parameter estimated from the pulse taken at the wrist, etc., was adopted and wristwatch-type devices were selected.

The methods used to determine whether or not a reaction occurred during the experience were as follows: During the experience, heart rate changes over time were recorded, whereupon the absolute value of the change was used as an indicator to determine whether or not a reaction occurred at the threshold. The amount of change in heart rate was taken as the absolute value of a 5-second moving average, referencing the report of Hirota et al. [4]. To detect false responses, Hirota et al. measured heart rate variability during a question and answer session and found some changes having emerged between 5 and 20 seconds had elapsed since the response. In this study, the minimum value of

5 seconds was assumed to be the time required for heart rate variability to occur from the perception of danger. The threshold was based on the resting heart rate of each experimental subject, taking individual differences in heart rate variability into account. In the absolute value of heart rate variability at rest, the third quartile was used as the threshold and any scenario involving an amount of change that exceeded that threshold confirmed during the experience was deemed "significant change."

3.3 Selection of subjects for the experiment

To confirm differences in experiential effects, similar experiments were conducted on two groups: A: subjects with practical construction work experience and B: subjects without any practical experience. There were ten participants in each group, for a total of 20 and considerations were made to ensure the overall analytical results were not impacted by the unique data of some of the experimental subjects. The group A comprised construction managers at a construction company and B comprised students. Only men were surveyed in this study because previous studies exposed differing trends between men and women in terms of heart rate responses when experiencing VR content[3].



Photo 1. Subject wearing devices

Table 2. Background of subjects

experienced subjects	experience of VR game	years of work	inexperienced subjects	experience of VR game	experience of walking on scaffoldings
subject1	×	2	subject11	×	○
subject2	○	15	subject12	○	○
subject3	×	15	subject13	×	×
subject4	×	6	subject14	×	×
subject5	×	6	subject15	×	×
subject6	×	7	subject16	×	×
subject7	○	22	subject17	○	×
subject8	×	16	subject18	○	×
subject9	×	2	subject19	×	○
subject10	×	4	subject20	×	○

3.4 How the results were analyzed

①The relationship between heart rate variability and VR content

The VR content or specific behavior at the time of significant variation in heart rate was identified and any differences emerging between the groups considered.

②Relationship between Heart Rate Variability and Subjective Feedback

Immediately after the VR experience, the subjects were interviewed to determine their subjective awareness and changes in their feelings during the experience. The interview method was based on a study by Sukegawa et al. [6] that revealed the tacit knowledge of experienced carpenters based on protocol analysis and the subjects were shown videos of their own VR experiences, asked to verbalize what they felt thoughts in each scene and their keywords were recorded. The relationship between this subjectivity and heart rate variability was then discussed.

4 Overview of the validation experiment

4.1 Equipment used

Details of the head-mounted displays (Below: HMD),

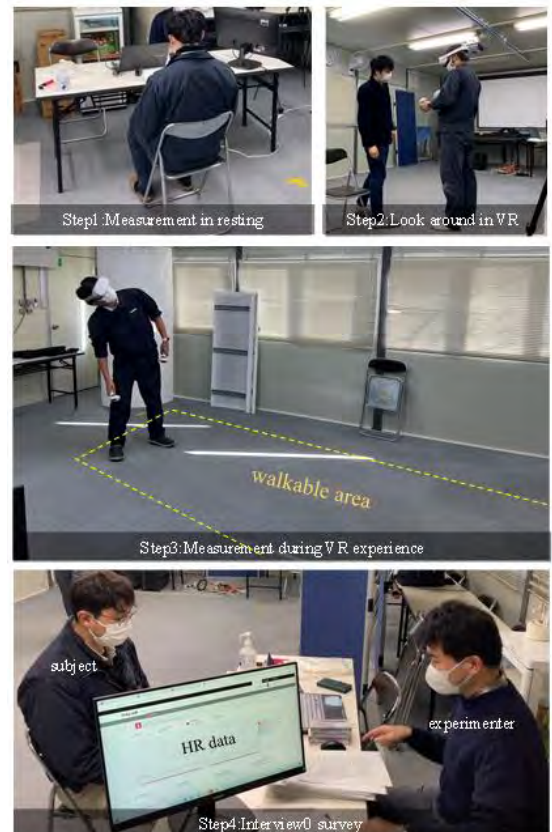


Photo 2. State of VR experiment

VR content and heart rate monitors used are listed in Table 1. The data recording interval was set at 1 Hz, the minimum value specified in the product specifications.

4.2 Experimental summary

The subjects, date, place and procedure of the experiment conducted are described below.

① Subjects, date and place of the experiment

[Group A: No work experience]

- (Subjects)10 male supervisors working for a general contractor
- (Dates)December 17 and 24, 2021
- (Venue)Shibaura Institute of Technology, Toyosu New Campus, Construction Office

[Group B: Work experience]

- (Subjects)10 male students majoring in architecture in a master's degree program
- (Dates)September 22, 2021
- (Venue)Shibaura Institute of Technology, Toyosu

② Experimental procedure

The experiment was performed for each experimental subject according to the following procedure. STEP 2 was set as a break-in time to calm tension, surprise, etc. To show subjects a video of their own experience in STEP 4, VR images reflected in the HMD were captured in STEP 3. In STEP 4, the subjects were asked to verbalize what they had been feeling about in each scene while displaying a video of their VR experience and a heart rate graph on the monitor screen and recorded it in writing. To understand the subjects' knowledge and the context behind their actions, they were asked about their experience walking on temporary scaffolding for those with no experience in practical work, their years of experience for those with practical work experience and their experiences using VR, etc.

- STEP 1: A heart rate monitor was worn and the resting heart rate while seated was measured (5 minutes)
- STEP 2: An HMD was worn and VR content was surveyed while standing (1 minute)
- STEP 3: The subjects were free to walk around and visually inspect the experience area (3 minutes)
- STEP 4: Face-to-face subjective feedback

5 Experimental results

5.1 Experience situation

During the VR content experience, the experimental subjects walked evenly through the walkable area of the content and scanned the VR space. Some of the

experimental subjects also checked areas at elevation or squatted down to look at their feet.

5.2 Heart rate measurement results

The median resting heart rate was 62 ~ 104 and resting heart rate variability was 0 ~ 13, confirming individual differences. The third quartile of heart rate variability for each subject in the experiment was either 2 or 3, with these figures used as thresholds to distinguish between large and small heart rate variability during the experience. Figure 3 shows a graph of the 5-second moving averages in heart rate variability during the experience measured for each subject in the experiment, showing where the thresholds were exceeded. All heart rate variability exceeding the thresholds constituted changes on the rising side.

When the groups with and without work experience were compared, heart rate varied significantly at a median of 3.5 sites in the experienced group and 0.5 sites in the inexperienced group, with a tendency for the experienced group to have greater heart rate variability.

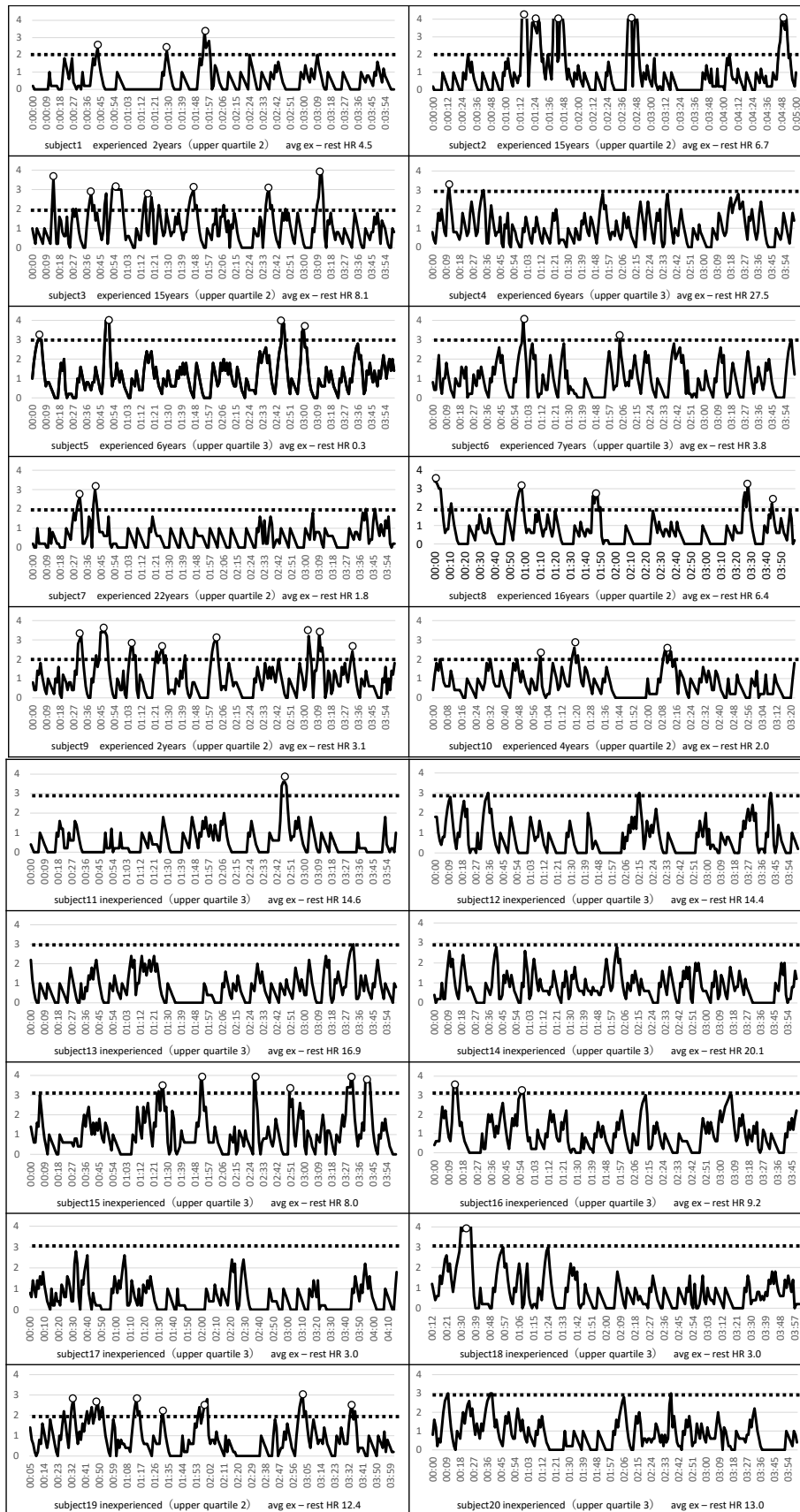
5.3 Feedback Results

First, the results of background interviews related to subjects' knowledge and behavior are shown in Table 2. Among the inexperienced workers, there were both subjects with and without experience walking on scaffolding. The years of work of the experienced subjects ranged from 2 to 22 years. Some subjects had experience using VR games, etc., while others did not.

Feedback on what was noticed and felt during the experience could be broadly divided into ①locations where fear was perceived during this experience and ②deficiencies in safety equipment noted in VR content

①The location where they felt fear the most was around the stairs, in which 7 out of 10 subjects with practical experience and all 10 subjects without practical experience felt fear. Subjects without practical experience were not frightened elsewhere. 5 subjects with practical experience felt fear around the defective scaffolding board, and 3 subjects felt fear while checking the inter-layer net.(Table 2)

②The number of places in which inadequacies in the safety equipment in VR content were noted varied considerably between those with and without practical experience respectively. Several experimental subjects proposed improvements to the installation status of interlayer and shatterproof nets as well as the five facilities that were intentionally flawed in the contents. For the total of seven points pointed out, those with practical experience noticed a median of 5.5 points, while inexperienced people noticed a median of 2.0 points.(Table 3)



(Legend) Vertical axis: HR change (HR at relevant time — average HR for the last 5s [bps]), horizontal axis: elapsed time (mm:ss)
: Threshold for judging the magnitude of change in HR (resting HR 75% quartile), O: Point exceeding the threshold

Figure 3. Changes in HR

Table 3. Location where subjects felt fear or noticed defective equipment

subjects	fear/noticed HR Change	Defective equipments					Other equipments	
		Stairs	Stage board	Baseboard	Wall tie	Brace	Interlayer net	Anti-scattering net
experienced	subject 1 fear	○	○	×	×	×	○	×
	subject 1 noticed	○	○	○	○	×	○	○
	subject 2 fear	○	○	×	×	×	×	×
	subject 2 noticed	○	○	○	○	○	×	○
	subject 3 fear	×	×	×	×	×	×	×
	subject 3 noticed	○	○	○	○	○	○	×
	subject 4 fear	×	×	×	×	×	×	×
	subject 4 noticed	○	×	○	○	×	○	×
	subject 5 fear	○	×	×	×	×	×	×
	subject 5 noticed	○	○	○	○	×	○	○
inexperienced	subject 6 fear	○	×	×	×	×	×	×
	subject 6 noticed	○	○	×	○	×	×	○
	subject 7 fear	○	○	×	×	×	×	×
	subject 7 noticed	○	○	×	○	○	×	○
	subject 8 fear	○	○	×	×	×	○	×
	subject 8 noticed	○	○	○	○	×	○	○
	subject 9 fear	○	○	×	×	×	○	×
	subject 9 noticed	○	○	○	○	○	○	○
	subject 10 fear	×	×	×	×	×	×	×
	subject 10 noticed	○	○	○	○	○	×	×
inexperienced	subject 11 fear	○	×	×	×	×	×	×
	subject 11 noticed	○	○	○	×	×	×	×
	subject 12 fear	○	×	×	×	×	×	×
	subject 12 noticed	○	○	×	×	×	×	×
	subject 13 fear	○	×	×	×	×	×	×
	subject 13 noticed	○	○	×	×	×	×	×
	subject 14 fear	○	×	×	×	×	×	×
	subject 14 noticed	○	○	○	○	○	×	○
	subject 15 fear	○	×	×	×	×	×	×
	subject 15 noticed	○	×	×	×	○	×	×
inexperienced	subject 16 fear	○	×	×	×	×	×	×
	subject 16 noticed	○	×	×	×	×	×	×
	subject 17 fear	○	×	×	×	×	×	×
	subject 17 noticed	○	×	×	×	×	×	×
	subject 18 fear	○	×	×	×	×	×	×
	subject 18 noticed	○	○	×	×	×	×	×
	subject 19 fear	○	×	×	×	×	×	×
	subject 19 noticed	○	○	×	×	○	×	×
	subject 20 fear	○	×	×	×	×	×	×
	subject 20 noticed	○	×	×	×	×	×	○

5.4 Comparison of Heart Rate Variability with VR Content and Subjectivity

Next, we checked the location of the VR content that the experimental subjects were viewing during the time period when heart rate variability could be confirmed. We also compared the results of feedback to confirm any VR content associated with a change in awareness or sentiment, even when the heart rate remained unchanged. A table showing heart rate variability and the presence or absence of awareness by type of safety equipment in the VR content is shown for each experimental subject (Table 4).

When the relationship between heart rate variability and the location of the VR content was examined, heart rate variability around stairs was the most common in the faulty safety equipment, occurring in nine out of ten of the experienced group and five out of ten inexperienced participants. There were five experienced and two inexperienced participants in the scaffolding boards, two experienced participants in the wall connections and no other changes. In other areas, in the safety equipment noted by the experienced participants, there were five experienced participants in the interlayer net, one experienced participant in the vertical net and HR changes. None of the inexperienced group showed any changes here. Accordingly, in terms of HR alone, those with more experience showed changes for all items.

6 Discussion

First, consider the relationship between fear and

Table 4. Location and number of changes in HR data

subjects	Defective equipments					Other equipments		Changes in subject's posture	
	Stairs	Stage board	Baseboard	Wall tie	Brace	Interlayer net	Anti-scattering net		
experienced	subject1	0	0	0	0	0	2	0	1
	subject2	1	1	0	0	0	2	0	0
	subject3	3	0	0	1	0	1	0	2
	subject4	0	0	0	0	0	0	0	1
	subject5	2	0	0	0	0	0	0	2
	subject6	2	0	0	0	0	0	0	0
	subject7	1	1	0	0	0	0	0	0
	subject8	1	1	0	0	0	1	0	1
	subject9	1	1	0	1	0	1	0	2
	subject10	1	1	0	0	0	0	1	0
inexperienced	subject11	1	0	0	0	0	0	0	0
	subject12	0	0	0	0	0	0	0	0
	subject13	0	0	0	0	0	0	0	0
	subject14	0	0	0	0	0	0	0	0
	subject15	3	1	0	0	0	0	0	2
	subject16	1	1	0	0	0	0	0	0
	subject17	0	0	0	0	0	0	0	0
	subject18	1	0	0	0	0	0	0	0
	subject19	5	0	0	0	0	0	0	1
	subject20	0	0	0	0	0	0	0	0

awareness. Distinguishing between (A) locations where at least 1 subject felt fear and (B) places where at least 1 subject pointed out deficiencies but without fear, (A) stairs, scaffolding boards, inter-layer nets (B) Baseboards, wall ties, braces, and anti-scattering nets. Judging from the interviews, this is thought to be because (A) is a location where the person concerned would be endangered and (B) is a location where others would be endangered. In the VR content, it is speculated that the impressions of the experiment subjects differed between the above two. Examining the differences between the experimental groups, a difference in trends was confirmed, particularly in (B). In the group with practical experience, the average number of (B) was 3.9, while in the group without practical experience, the average number was 1.2. (B) is deemed content that is difficult to notice without one. (Table 5)

Next, the relationship between fear/awareness and heart rate changes was considered. We counted the number of locations where heart rate changes occurred in all experimental subjects, and sorted them into three categories: locations where fear was felt, where was only noticed without fear, and those where there was no awareness (Table 6). There were a total of 52 heart rate changes, half of which, 26, were at locations where subjects felt fear. There was no bias among the experimental groups, and all of the locations were (A) in danger for themselves. This implies that the location which generally makes everyone feel afraid of, such as simulation of heights, could feel the same in VR without depending on practical experience.

Conversely, 8 changes in heart rate were confirmed in locations where only awareness and without fear, all of which were experienced workers. Specifically, these were 4 times on the stairs, once at the scaffold board, once at the inter-layer net in (A), and twice at the wall ties in (B). For these, no difference was confirmed according to the number of years of work experience. These can be considered cases in which subjects with practical experience react strongly and unconsciously in contrast to their own senses. Therefore, this case is defined as type (C) in this paper (Table 5).

Based on the above, it can be interpreted that there is

Table 5. Number of subjects noticed defective equipment or felt fear

subjects' consciousness	group	(A)location in danger for themselves			(B)location in danger for others			
		Stairs	Stage board	Interlayer net	Baseboard	Wall tie	Brace	Anti-scattering net
noticed and felt fear	ex	7	5	3	0	0	0	0
	in-ex	10	0	0	0	0	0	0
noticed only	ex	3	4	3	8	10	4	7
	in-ex	0	6	0	2	1	3	3
not noticed	ex	0	1	4	2	0	6	3
	in-ex	0	1	10	8	9	7	7

(C) Unconscious change in HR [8 number of times / 3 subjects]

a difference in the cases where the heart rate changes depending on the presence or absence of practical experience when VR content is used. In other words, it is speculated that practical experience is subconscious, VR evokes memories, and then causes the body to respond unconsciously.

Conversely, when it comes to VR content in which a person clearly perceives a personal danger, such as when gaps emerge under his/her feet at elevation, the results of the experiments suggest that everyone could obtain similar sense regardless of whether or not they have practical experience.

7 Conclusion

In this research, a quantitative verification method using interviews and heart rate as indicators was proposed and verification experiments on experienced and inexperienced users were conducted, aiming to identify differences in experiences obtained by users of VR contents on whether or not they had practical experience. As a result, similar awareness and biological responses, regardless of whether or not they had practical experience with content that made them feel fearful, were confirmed. Conversely, experiences that only those with practical experience could obtain with content that did not make them feel fearful were confirmed. There were cases in which the subject recognized it and cases in which individuals reacted unconsciously. In future, we will use this knowledge to explore how to use VR contents more effectively and propose ways to select materials that are more effective

Table 6. Relationship between HR changed and subject consciousness (number of times)

HR changed or not	group	subjects' consciousness		
		noticed and felt fear	noticed only	not noticed
HR changed	ex	15	9	12
	in-ex	11	0	5
HR not changed	ex	2	31	-
	in-ex	5	14	-

in practice, in conjunction with educational methods other than VR.

This research was conducted with the approval of the Bio-engineering Research Ethics Review Committee of the Shibaura Institute of Technology (No. 21069, August 19, 2021). This experimental subjects were informed of the contents of this experiment in advance and their approval was obtained before this experiment.

Acknowledgments

In this research, Tsumiki Seisaku Co., Ltd. cooperated with the VR content used in this experiments and the employees of Kajima Corporation and the students of Shibaura Institute of Technology as this experimental subjects. Mr. Yohei Koga (a graduate student at the time, now working for Misawa Home Corporation.) also cooperated with this experimental operation. Thank you.

References

- [1] M. Takagi: ANALYSIS OF SAFETY TRAINING IN SMEs — A questionnaire survey among plumbing contractors —, J. JSCE. Ser. F4, 72 (4), I_11-I_22, 2016
- [2] K. Ito, Y. Harada, S. Kishiro, G. Tomiyama, H. Nakatsuji, Y. Tate, H. Seto, M. Ohkura: Evaluation of “Feelings of Excitement” on Presenting Information with “In-vehicle System” by Using Physiological Indices - HRV Analysis of Influence on Giving Prior Information about Landscapes -, Transactions of Japan Society of Kansei Engineering, Volume 16 (2017) Issue 3, pp. 321-331, 2017
- [3] K. Ito, M. Ohkura: Study on Affective Evaluation of VR System using ECG - Evaluation of "Feeling of Excitement" during playing "Summer Lesson" with comparison between genders -, Entertainment Computing Symposium 2017, pp. 301-305, 2017
- [4] Ministry of Health, Labour and Welfare, Learning Materials and Tools, On-line: <https://anzeninfo.mhlw.go.jp/information/kyozaishiryu/eng.html>, Accessed: 03/04/2023
- [5] Tsumikiseisaku, VR TRAINING, On-line: <https://tsumikiseisaku.com/safetyvr/>, Accessed: 03/04/2023
- [6] C.Sukegawa, et al. : SMART HAND FOR DIGITAL TWIN TIMBER WORK THE INTERACTIVE PROCEDURAL SCANNING BY INDUSTRIAL ARM ROBOT, Proceedings of the 27th CAADRIA Conference, pp.131-140, 2022.4
- [7] A. Hirota, K. Yokota, J. Wada, S. Watanabe, N. Takasawa: Heart Rate and Heart Rate Variability in Psychophysiological Detection of Deception, Japanese journal of science and technology for identification, 5(1), pp. 33-53, 2000
- [8] C. Murase, R. Kawamoto, S. Sugimoto: Changing of Emotions by the Stimulation of Visual and Auditory Senses — An Analysis of Heart Rate Variability (HRV) —, Journal of UOEH, 26(4), pp. 461-471, 2004
- [9] H. Hotta, K. Sawamura, T. Inoue: Heart Rate Variability during Music Listening at the Same Tempo as Subject's Heart Rate, Journal of clinical and educational psychology, 33, pp. 1-8, 2007
- [10] R. Horita, A. Komura, S. Chiba: Analysis of Relationship between Intellectual Productivity and Heart Rate, GN Workshop 2019, pp. 107-113, 2019
- [11] M. Uchimura, Y. Eguchi, M. Kawasaki, N. Yoshii, T. Umeda, M. Takata, K. Jo: Spatiotemporal stress indicator using LF/HF, IPSJ SIG technical reports (MPS), 2012 (2), pp. 1-6, 2012
- [12] S. Hayashi, A. Fujiki, M. Sugao, I. Satake, T. Hosoya, I. Kitajima, H. Inoue: New quantitative methods for measurement of QT interval using 24-hour Holter ECG recordings, JPN.J.ELECTROCARDIOLOGY, Vol. 24 No. 4, pp. 199-207, 2004
- [13] Atsushi Sugama, Takahiro Nishimura, Kouki Doi, Shigenobu Shimada, Manabu Chikai, Kiyohiko Nunokawa, Shuichi Ino: Evaluation of musculoskeletal workload of manual operating tasks using a hydraulic jack based on ergonomic postural analysis and electromyography: A case study of non-professional young male users, Work, 72(2), pp. 677-685, 2022
- [14] Mana Nishino, Ryosuke Nakajima, Akiko Takahashi, Atsushi Sugama: A Fundamental Study on Easy-to-Understand Work Procedure Manuals for Safety Work in Construction Sites, 2021 IEEE 8th International Conference on Industrial Engineering and Applications, pp. 79-83, 2021
- [15] Jenni Anttonen, Veikko Surakka: Emotions and heart rate while sitting on a chair, CHI '05: Proceedings of the SIGCHI Conference on Human Factors in Computing Systems, pp. 491-499, 2005
- [16] Andre Pittig, Joanna J. Arch, Chi W. R. Lam, Michelle G. Craske: Heart rate and heart rate variability in panic, social anxiety, obsessive-compulsive, and generalized anxiety disorders at baseline and in response to relaxation and hyperventilation, International Journal of Psychophysiology, 87(1), pp. 19-27, 2013

An Integrated Approach for Automated Acquisition of Bridge Data and Deficiency Evaluation

Abdelhady Omar^{1,2} and Osama Moselhi³

¹Ph.D. Candidate, Department of Building, Civil and Environmental Engineering, Concordia University, Canada.

²Assistant Lecturer, Department of Structural Engineering, Faculty of Engineering, Alexandria University,

Egypt. ³Professor and Director of Center for Innovation in Construction and Infrastructure Engineering and Management (CICIEM), Department of Building, Civil and Environmental Engineering, Concordia University, Canada. Email: abdelhady.omar@mail.concordia.ca, moselhi@encs.concordia.ca

Abstract –

Bridges are essential components of civil infrastructures that enable joining highways and cities, as well as facilitating movement between different geographical locations. Deterioration of bridges can pose a threat to public safety and hinder economic activities. The development of innovative and reliable asset management tools to support the optimization of maintenance and timely intervention plans is of paramount concern to transportation agencies. However, such development is usually impeded by a lack of data and/or difficulties in collecting and organizing data from different sources. This paper introduces an integrated scheme for automated acquisition of bridge-related data. The proposed methodology enables the creation of a unified structured and comprehensive data repository that can be used for further processing and modeling purposes. Data from multiple sources, including web pages and bridge inspection reports, were extracted, collected, prepared, and compiled. As such, web scraping and rule-based information extraction were employed to achieve this objective. Finally, text mining was applied to the inspection comments extracted from bridge inspection reports to get insights into such inspection information and evaluate the severity of bridge deck deficiencies.

Keywords –

Data Acquisition; Data Scraping; Bridge Inspection Report; Document Parsing; Information Extraction; Text Mining; Bridge Deck Deficiencies.

1 Introduction

Bridges are strategic points in the road network because of the severe consequences of their failure or closure to traffic. Measures must therefore be taken to prevent these structures from deteriorating to the point where they compromise the safety of users or require a

diversion. Transportation agencies should offer service levels that meet the users' needs. As such, transportation agencies implement several types of inspection programs to identify defects in the structural elements as soon as possible so that the necessary measures can be taken to ensure the durability of the structures and the safety and comfort of the users. In addition, these programs are carried out at regular intervals or, if necessary, depending on the problem identified to gather all the data needed to plan preventive and corrective actions; hence, ensure the safety of structures and protect the invested capital [1].

A crucial first step in maintaining the integrity of the bridge, preventing deterioration proliferation, and avoiding unnecessary Maintenance, Rehabilitation, and Replacement (MR&R) work is determining the best intervention plan [2]. However, current bridge deterioration models and management systems have limited ability to enable justifiable and well-informed decisions regarding bridge intervention strategies since they have concentrated on using just a small collection of abstract data (e.g., year of construction, material type, and bridge geometry). Due to the absence of thorough descriptions of bridge deficiencies of different bridge components (e.g., deck, superstructure, and substructure), such abstract data are insufficient since they restrict the ability to learn from these data to guide intervention planning decision-making and make deficiency-based forecasts [3]. On the other hand, a lot of information regarding bridge deficiencies and deterioration conditions is buried in textual inspection reports without being used. Federal Highway Administration claims that bridge owners are unable to effectively use the "mountain" of inspection data contained in bridge inspection reports [3, 4]. Even worse, there are instances where the abstract data are either unavailable or difficult to collect, which can impede the development of effective decision-making support tools. This issue is prevalent in Quebec, Canada. In these circumstances, planning and executing preventive or corrective measures becomes challenging, compromising the bridge's and its users' safety.

In this context, this paper serves as a key first step in developing innovative and reliable asset management tools to support the optimization of maintenance and timely intervention plans by introducing an integrated scheme for automated acquisition of bridge-related data and defects' severity evaluation for bridges in Quebec. As such, it enables the creation of a structured comprehensive data repository that can be used for further processing and modeling purposes. The repository of data includes not only information regarding the bridge and crossing road characteristics but also data obtained from bridge inspection reports. This data encompasses a wide range of information, such as inspection frequency, percentages of defective material, structural behavior ratings, and inspection comments made by inspectors, which provide information about the various types of defects observed. Web scraping techniques were used to collect and extract bridge and crossing road characteristics data. This process involved automatically retrieving and parsing relevant information from government agency websites. A rule-based information extraction method was employed to extract the important information buried in bridge inspection reports. These reports were automatically downloaded first by navigating through the website and retrieving the reports without any manual intervention. Moreover, text mining techniques were employed to get insights into inspection comments related to the bridge deck in order to explore the most common types of defects, their association, and their severity.

2 Background

Data acquisition methods are required to automatically identify and extract data/information from different sources and formats, e.g., transportation agencies' websites and unstructured textual bridge inspection reports, and then represent the extracted data in a structured format ready for additional data analytics. In this light, web scraping and rule-based information extraction methods were employed to extract and collect bridge-related data. Web scraping is an automated technique for extracting copious unstructured volumes of scattered data from websites. There are several ways to scrape web pages, including using internet services, Application Programming Interfaces (APIs), or writing particular code [5-7]. The application of web scraping and machine learning algorithms was considered to assess the real estate price in the secondary housing market in Moscow [8]. A data-based price indices research was implemented using web scraping [9]. In addition, web scraping and convolutional neural networks were integrated to verify fraudulent content from social media, news articles, and other web pages [10]. On the other hand, information extraction is the

process of searching through natural language text for information pertinent to an interest, such as entities, relationships, or events. Information extraction methods are either rule-based or machine-learning-based [3, 11]. Among both methods, the most closely related to this work is rule-based information extraction. Rule-based techniques use manually created pattern-matching-based rules to direct the identification and extraction of target information from unstructured textual input [3, 12]. Syntactic and/or semantic text properties are used to construct the pattern-matching-based rules [3]. Zhang and El-Gohary [13] and Zhou and El-Gohary [14] developed pattern-matching-based rules that integrate syntactic and semantic elements to extract building regulation information for compliance assessment.

Once the data have been extracted from bridge inspection reports, performing text mining to analyze and gain valuable insights from the text-based information becomes essential. Text mining is a data analytics technique that involves searching for patterns in text data through various approaches such as data, analysis, visualization, and application of statistical and machine learning algorithms. Williams and Betak [15] used Latent Dirichlet Analysis, a text mining algorithm, to highlight significant issues in railroad equipment accidents from equipment accident reports published by Federal Railroad Administration. Lv and El-Gohary [16] developed a method using text analytics to extract words and phrases describing stakeholders' concerns from comments on early-stage large-scale highway projects. In order to establish a set of decision-making chains to boost workplace safety, Zhao et al. [17] analyzed occupational safety reports and investigations relevant to electrocution accidents. They identified activities and decision-making errors that raise the worker's safety risk. Mostafa et al. [18] used rule-based text mining to extract the type and extent of damage from textual information from school inspection reports. They used Principal Component Analysis and clustering to categorize events and identify assets with a high priority for renewal.

3 Motivation

Quebec bridges experience significant deterioration levels as well as have the highest average age among all provinces in Canada, followed by Nova Scotia [19]. Several agents, such as exposure to de-icing salts, cycles of freeze and thaw, deferred maintenance, aging, and increasing traffic volumes, contribute to the rapid degradation of these critical civil infrastructures posing diverse burdens and challenges to transportation agencies, specifically under budget constraints and limited resources [20]. The failure, or even service interruption, of these infrastructures can be ruinous in terms of human life, social, environmental, and economic impacts.

In September 2006, the Concorde Boulevard overpass in Laval, Quebec, collapsed, resulting in five deaths and six injuries. It was the first time a young structure had collapsed in the province without apparent cause [21]. Less than a year later, the Interstate 35W bridge over the Mississippi River in Minneapolis, Minnesota, USA, collapsed, causing 13 deaths and 145 injuries [22]. These tragedies raised concerns about deficient bridges in North America and prompted transportation agencies and academia to develop innovative asset management tools and techniques to ensure safety and preserve the value of these assets [20]. However, the development of such smart technology-based methods is greatly hindered due to the lack of effective processing/transforming of raw data into valuable information; and hence, into informed decisions regarding the MR&R of bridge structures. A large amount of raw data is available but not used efficiently for various reasons, summarized as follows.

Data are located in different sources and formats. For example, the main structures' data can be fetched from Quebec datasets in different formats, including comma-separated values, and contains many attributes of different data types (e.g., numerical, categorical, and text) [23]. Such a variety of data types can impede further analysis and processing of data. In addition, it does not include any information about, e.g., crossing road class, bridge length or width, Annual Average Daily Traffic (AADT), and deterioration conditions or defects of different bridge components. On the other hand, some important information, including the aforementioned attributes, is provided on the Quebec Ministry of Transportation and Sustainable Mobility (MTQ) websites [24]. However, four challenges were encountered while trying to collect these pieces of information. First, the website is designed to show only a limited number of records at a time (i.e., 15 records out of 9,779 records), which cannot be downloaded or processed. Second, another page needs to be opened separately to reach specific information about a particular structure. These pages contain different types of unstructured non-downloadable data, meaning that collection of these data would be tedious and error-prone. Third, each structure has a different page to reach and download its inspection report, meaning more than nine thousand websites and download links should be accessed to download and store these inspection reports. Fourth, even more challenging, is how all these data will be filtered, merged, and compiled in one data repository that can be used later for further data analytics.

Furthermore, in addition to being time-consuming, manually extracting information from bridge inspection reports can be error-prone and challenging due to the large volume of unstructured text data. These reports often contain detailed information about the condition of

various bridge components and the extent of any defects or deterioration. However, due to the sheer volume of text data and the lack of standardized reporting formats, it is difficult to efficiently and accurately extract the relevant information from these reports. As a result, there is a need for automated tools and techniques that can efficiently and accurately extract information from bridge inspection reports and help identify any potential issues or areas for improvement.

4 Aim and Objectives

In the above context, the main goal of this paper is to create a structured yet comprehensive data repository that can be used for further processing, hence, developing innovative asset management tools for bridge infrastructures. This goal is broken down into the following objectives:

1. Automate the process of bridge-related data acquisition from different sources and formats, including the automatic retrieval of bridge inspection reports;
2. Analyse and pre-process the collected data to be ready for further processing steps;
3. Develop a rule-based method for information extraction from bridge inspection reports;
4. Use text mining to derive insights from text data buried, and not used, in inspection reports; and
5. Introduce how these collected data and insights can be used for future work.

5 Methodology

In order to achieve the objectives of this paper, the high-level methodology is depicted in Figure 1. As shown in Figure 1, the devised methodology comprises two phases. The first phase is a three-tier method designed for data acquisition and compiling. The output of this phase is a structured comprehensive data repository ready for further processing and modeling. The second phase intends for data processing and text mining of inspection comments buried in bridge inspection reports. This phase enables the analysis and visualization of the important information related to different types of defects in bridge decks, in addition to deriving insights from text data. It is worth pointing out that the second phase will continue in future studies and, for the scope of this paper, only text mining of inspection comments related to the bridge deck is considered. The three tiers of the first phase and the two phases are interconnected as indicated by arrows with letters a, b, and c, i.e., the output of one tier or phase can be used for the next tier or phase. The inputs, steps, and outputs of these phases are depicted in Figure 2 and Figure 3.

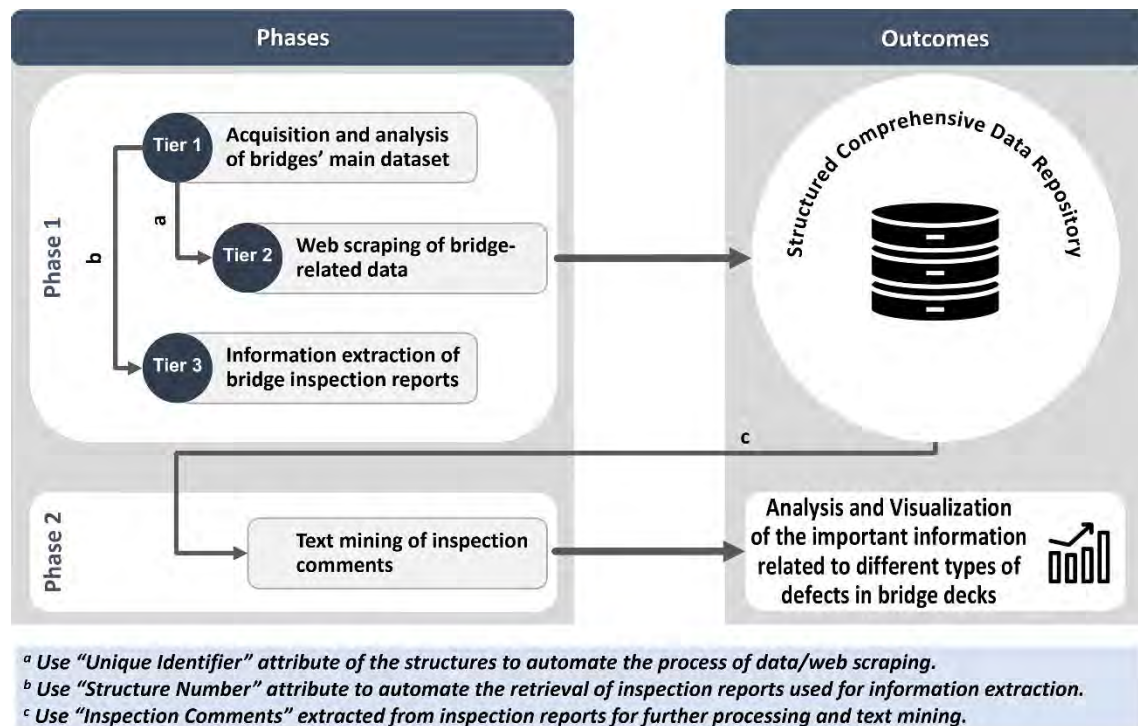


Figure 1. Automated two-phase methodology for bridge data acquisition and text mining of inspection reports

5.1 Phase 1: Data Acquisition and Compiling

As shown in Figure 2, the first stage is a three-tier phase. The first step involves obtaining the primary dataset of structures from the Quebec datasets website [23], which is then stored in a local data repository. Subsequently, an initial analysis is conducted on the data to gain a better understanding of its characteristics and identify any additional features that may need to be collected. The data is then subjected to preliminary preparation techniques, such as integer encoding, to make it suitable for subsequent processing and modeling. Finally, the dataset is filtered to include only bridges with reinforced concrete decks that are relevant to the scope of this study. The second tier of this phase involved web scraping of both the main page and separate pages of MTQ structures in order to collect additional data [24]. This task proved to be difficult due to several reasons. Firstly, the main page of MTQ structures only allows a limited number of records to be opened per page, which is also not accessible directly. Secondly, some pieces of information were stored separately for each structure on different pages with varying layouts. Extracting and manipulating data from over nine thousand structures required a systematic and well-defined approach. Accordingly, the code was designed to scrape each web page separately, merge, and manipulate the extracted data before adding them to the main data repository.

Tier three posed the greatest challenge in the project

as it involved handling text data from bridge inspection reports, which lacked any standard or structured format due to being written by different inspectors using different styles and language features. These text data contain information related to deterioration conditions and deficiencies of different bridge components. The inspection reports were initially automatically downloaded from web pages and subsequently analyzed and annotated to identify the necessary information for extraction. Then, a rule-based information extraction approach was adopted, where eighteen different rules were formulated to extract various information pieces from the text. These included the structure number, structure level, last and next general inspection dates, and inspectors' comments, among others. The integration between the Docparser platform [25] and the python programming language through REST API enabled the effective and correct extraction of information into a structured format. Finally, the data were stored in a comprehensive structured data repository. It is worth pointing out that, for the scope of this paper, only inspection comments related to different elements forming the bridge deck were considered for extraction. In the Quebec inspection program [1], the bridge deck system is divided into four elements based on load transmission: two principal elements (deck and exterior sides), and two secondary elements (road/driving surface and drainage system).

Additionally, although the filtering process resulted in 4,119 inspection reports eligible for information extraction, this paper's focus is limited to only 200 reports. To ensure that the information extraction process was performed accurately, the 200 reports were divided into 10-report samples. First, each sample was annotated for the required information, then uploaded to the Docparser to create rules. The extracted information was then verified, cleaned, and prepared. The following sample underwent the same procedure if the information was accurately extracted. Otherwise, the process is repeated on the previous sample until the extracted information is correctly obtained. While these detailed steps were tedious, they were necessary to ensure precise results. Importantly, these 200 reports will serve as a training set for the remaining reports.

5.2 Phase 2: Data Processing & Text Mining

After unifying and structuring all the data, further data analytics can be performed. This paper is a part of a larger research project that aims to use this data to develop bridge management tools. This paper focuses on text mining of inspection comments extracted from bridge inspection reports. Accordingly, various text mining tools and techniques were employed to get insights into these inspection comments, as depicted in Figure 3. The text mining output includes frequent

defects found on bridge decks, common comments made by inspectors, correlations between different defects, and their severity levels. This information could further inform maintenance and repair decisions and ultimately improve the safety and longevity of the bridge deck.

In Natural Language Processing (NLP), there are several steps to prepare text data for analysis. The first step is to remove stop words, which are commonly used words that do not add value to the analysis, such as "a," "an," and "the" in English. It is important to carefully select the list of stop words based on the project rather than relying on pre-built lists from libraries. Punctuation marks are also removed since they do not contribute to the analysis and may lead to incorrect results. Converting the text to the same case, preferably lowercase, is crucial to prevent different-case words from misleading the analysis. Tokenization is the process of dividing the text into token-sized pieces, which can be individual words, phrases, or complete sentences. Certain characters, such as punctuation marks, may be removed during tokenization. Typically, tokens are used as input in parsing and text-mining procedures. Lemmatization is applied to convert any word to its basic root mode and combine several word inflections with the same meaning into their root forms. Finally, the results are cleaned and visualized after each step to ensure the correct form of results is obtained since text analysis is very sensitive to changes and sometimes requires manual revision.

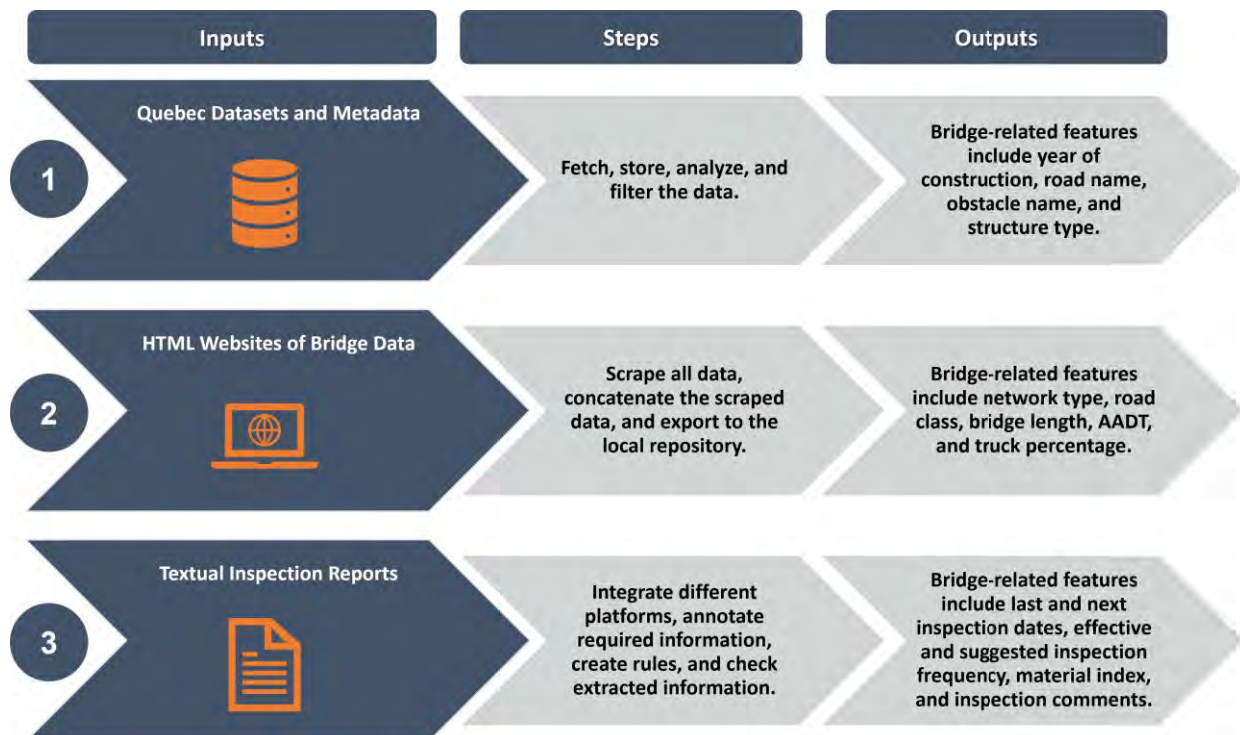


Figure 2. Inputs, steps, and outputs of the data acquisition and compiling phase and its three tiers

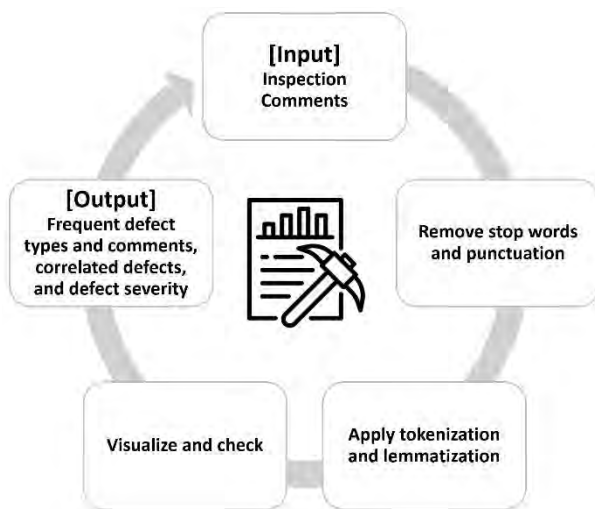


Figure 3. Inputs, steps, and outputs of the data processing & text mining phase

6 Results and Discussions

The results of the proposed approach can be summarized into two major outcomes. Firstly, a structured and comprehensive data repository is generated that is ready for further processing and modeling steps. Secondly, valuable insights into the inspection comments related to the bridge deck are obtained, including frequent defect types, common comments, correlations between different defects, and their corresponding severity levels. The first outcome involves consolidating various attributes related to bridge structures and crossing roads into a single repository. These attributes include, but are not limited to, structure number, year of construction, structure type, bridge geometry, road class, AADT, inspection frequency, and inspection comments. The repository is built upon the Statistical Package for the Social Sciences (SPSS) software, enabling effective organization, management, and data analysis. One of the most crucial features of the repository is the ability to view and modify variable properties within a dataset, including the attribute name and length; data type and measure (e.g., numeric, string/nominal, or date/time); descriptive labels for easier identification and interpretation; and the ability to specify values and assign corresponding labels similar to integer encoding. In addition to its ability to effectively import, manipulate, and analyze large datasets, this tool also offers features for identifying missing values, duplicates, and outliers. It also provides various statistical procedures, including descriptive statistics and inferential statistics. Various visualization tools, including charts, graphs, and tables, can explore and present the data meaningfully, aiding preliminary analysis before further advanced modeling.

The second outcome includes the results of the text mining of inspection comments. As shown in Figure 4, cracking, spalling, and delamination are the most common defects, followed by rust, efflorescence, corrosion, and scaling. Cracks have a significantly more absolute and relative frequency than other words. For more information about these defect types and their progression into concrete, the reader may refer to this reference [20]. Crack-related comments were further analyzed for a more thorough analysis of inspection comments, as depicted in Figure 5. Figure 5a presents the most common phrases inspectors use to describe defects of elements with cracks associated with their relative frequency. The comments also show the severity of the cracks, i.e., crack width, which ranges from “less than 0.80 mm” to “more than 15 mm,” with low severity cracks being the most frequent (relative frequency of 66%). In addition, these phrases can be transformed into information about defect severity and material condition, as shown in Figure 5b. The guidelines for classifying cracks based on their severity and associated material condition are provided in Table 1. The coexistence of cracks with another defect was examined by calculating the correlation of being in the same sentence. As shown in Figure 5c, cracks probably coexist with spalling (correlation of 67.32%) and reinforcement corrosion (correlation of more than 65%).

The created data repository can serve as a kick-off point for building innovative tools to support the optimization of maintenance and budget allocation of bridge structures. In addition, the information extracted from inspection comments can help develop probabilistic defect-based deterioration models and intervention strategies. For example, ongoing research is currently exploring the relationship between the severity levels of different defects, such as cracking, corrosion, delamination, scaling, and spalling, and the probability of a bridge deck being in a certain condition. This investigation is being accomplished through the use of a Bayesian-belief-network model, with the output of text mining being used to determine the marginal and conditional probability for the model. Moreover, other important attributes, such as the year of construction and AADT, will be included in the analysis to identify the most critical factors affecting bridge decks' deterioration.

Table 1. Material condition and degree of crack severity based on crack opening/width (adapted from [1])

Material Condition	Crack Opening (mm)	Degree of Severity
A	None	Slight
B	< 0.8	Moderate
C	≥ 0.8 & ≤ 3.0	Significant
D	> 3.0	Severe

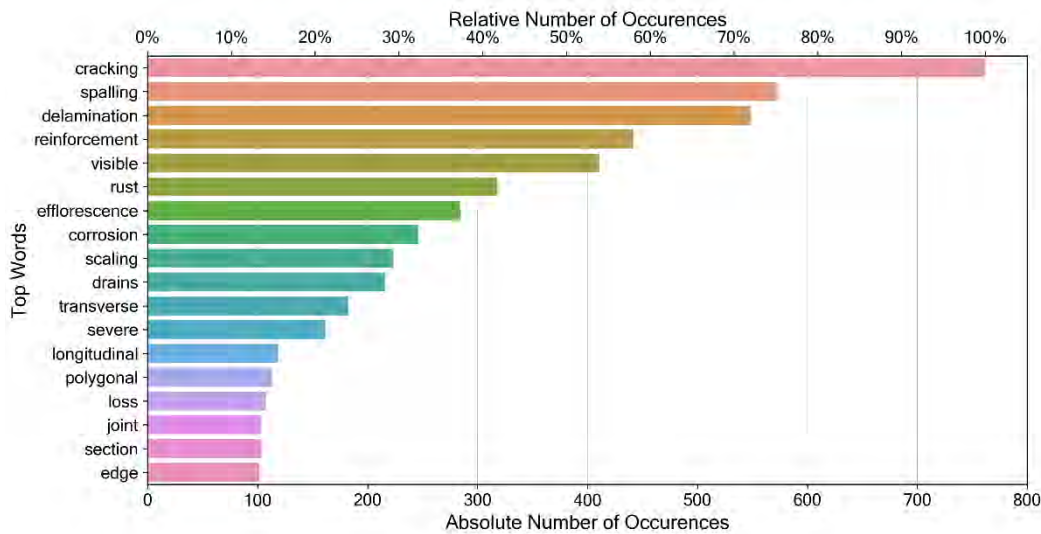


Figure 4. Absolute and relative frequencies of top words/defects appeared in inspection comments

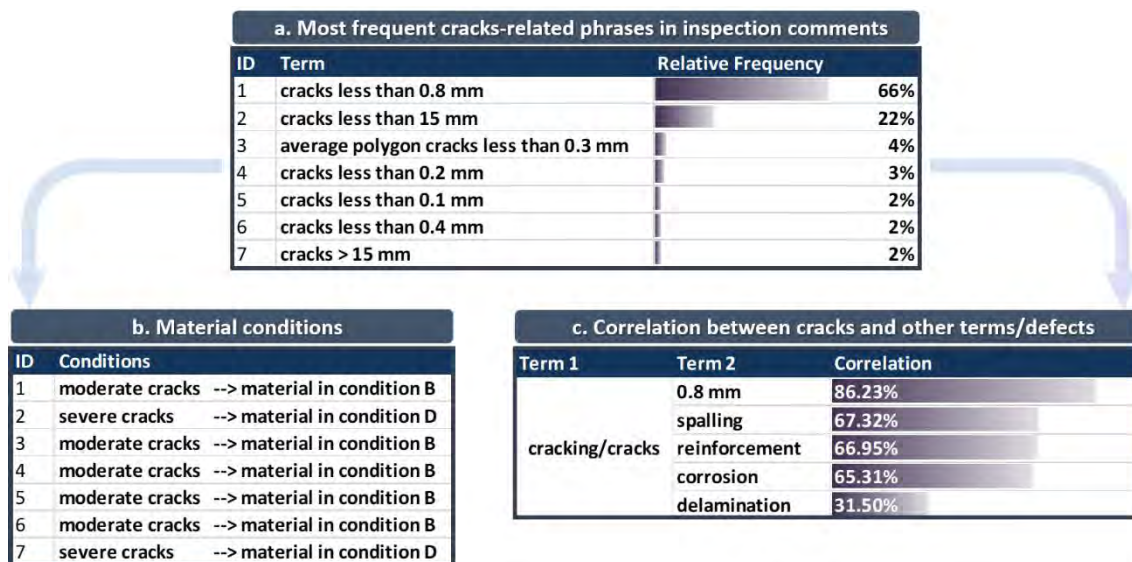


Figure 5. Analysis of cracks-related inspection comments

7 Conclusions

This study introduced an integrated approach for automatically collecting bridge-related data and deficiency evaluation. Transportation agencies' websites and unstructured textual bridge inspection reports were considered to gather information utilizing web scraping and information extraction techniques. The study enabled the creation of a structured data repository ready for further data analytics and the development of innovative asset management tools. In addition, text mining was used to get insights into the inspection comments buried in inspection reports and always overlooked. Text mining

results showed that cracking, spalling, and delamination are the most common defects in bridge decks. These inspection comments were also transformed into severity levels that can be used for developing probabilistic deterioration models. The contribution of this study lies in integrating different techniques and tools to facilitate the process of data acquisition besides creating a structured data repository that encompasses the most important bridge-related attributes. It also introduced the application of text mining of inspection comments for developing probabilistic deterioration models that, to the best of the authors' knowledge, never used before in that domain, besides laying the foundation for future work.

References

- [1] Ministry of Transport and Sustainable Mobility. *Structure Inspection Manual*. Quebec Government, National Library and Archives of Quebec, 2017.
- [2] Abdelkhalek S. and Zayed T. Comprehensive Inspection System for Concrete Bridge Deck Application: Current Situation and Future Needs. *Journal of Performance of Constructed Facilities*, 34(5): 03120001, 2020.
- [3] Liu K. and El-Gohary N. Ontology-based semi-supervised conditional random fields for automated information extraction from bridge inspection reports. *Automation in construction*, 81: 313-327, 2017.
- [4] Hooks J. M. and Frangopol D. M. LTBP bridge performance primer. On-line: <https://rosap.nfl.bts.gov/view/dot/26946>, Accessed: Jan 30, 2023.
- [5] Lubis V. How to Scrape Data from a Website using Python for Beginner. On-line: <https://medium.com/analytics-vidhya/how-to-scrape-data-from-a-website-using-python-for-beginner-5c770a1fbc2d>, Accessed: Jan 30, 2023.
- [6] Foo E. What is Web Scraping and How Does It Work. On-line: <https://www.datasciencecentral.com/what-is-web-scraping-and-how-does-it-work/>, Accessed: Jan 30, 2023.
- [7] Hiremath O. S. A Beginner's Guide to learn web scraping with python! On-line: <https://www.edureka.co/blog/web-scraping-with-python/>, Accessed: Jan 03, 2023.
- [8] Mamedli M. O. and Umnov A. V. Real estate valuation based on big data. *Voprosy Ekonomiki*, 2022(12): 118-136, 2022.
- [9] Uriarte J. I., Ramirez Muñoz De Toro G. R., and Larrosa J. M. C. Web scraping based online consumer price index: The "iPC Online" case. *Journal of Economic and Social Measurement*, 44(2-3): 141-159, 2020.
- [10] Vishwakarma D. K., Meel P., Yadav A., and Singh K. A framework of fake news detection on web platform using ConvNet. *Social Network Analysis and Mining*, 13(1), 2023.
- [11] Hobbs J. R. and Riloff E. *Information Extraction. HANDBOOK OF NATURAL LANGUAGE PROCESSING, SECOND EDITION*. Taylor & Francis Group, 2010.
- [12] Sarawagi S. Information extraction. *Foundations and Trends® in Databases*, 1(3): 261-377, 2008.
- [13] Zhang J. and El-Gohary N. M. Semantic NLP-based information extraction from construction regulatory documents for automated compliance checking. *Journal of Computing in Civil Engineering*, 30(2): 04015014, 2016.
- [14] Zhou P. and El-Gohary N. Ontology-based automated information extraction from building energy conservation codes. *Automation in Construction*, 74: 103-117, 2017.
- [15] Williams T. P. and Betak J. F. *Identifying Themes in Railroad Equipment Accidents Using Text Mining and Text Visualization*. International Conference on Transportation and Development 2016. 2016.
- [16] Lv X. and El-Gohary N. Text analytics for supporting stakeholder opinion mining for large-scale highway projects. *Procedia Engineering*, 145: 518-524, 2016.
- [17] Zhao D., McCoy A. P., Kleiner B. M., Du J., and Smith-Jackson T. L. Decision-making chains in electrical safety for construction workers. *Journal of Construction Engineering and Management*, 142(1): 04015055, 2016.
- [18] Mostafa K., Attalla A., and Hegazy T. Data mining of school inspection reports to identify the assets with top renewal priority. *Journal of Building Engineering*, 41: 102404, 2021.
- [19] Statistics Canada. Age of Public Infrastructure: A Provincial Perspective. On-line: <https://www150.statcan.gc.ca/n1/pub/11-621-m/11-621-m2008067-eng.htm>, Accessed: Mar 08, 2022.
- [20] Omar A. and Moselhi O. Condition Monitoring of Reinforced Concrete Bridge Decks: Current Practices and Future Perspectives. *Current Trends in Civil & Structural Engineering - CTCSE*, 8(4), 2022.
- [21] Crisis and Disaster Management Research and Training Initiative at Syracuse University. Collapse of Concorde Boulevard Bridge. On-line: <https://cdm.syr.edu/research/case-studies/>, Accessed: Jan 30, 2023.
- [22] Minnesota Legislature. Minneapolis Interstate 35W Bridge Collapse. On-line: <https://www.lrl.mn.gov/guides/guides?issue=bridges>, Accessed: Jan 30, 2023.
- [23] Quebec Data Partnership. Structures Dataset. On-line: <https://www.donneesquebec.ca/recherche/dataset/structure>, Accessed: Sep 16, 2022.
- [24] Ministry of Transport and Sustainable Mobility. Inventory and Inspection of Structures. On-line: <https://www.transports.gouv.qc.ca/fr/projets-infrastructures/structures/Pages/inventaires-structures.aspx>, Accessed: Sep 27, 2022.
- [25] docparser. Extract Data From Your Business Documents. On-line: <https://docparser.com/>, Accessed: Oct 31, 2022.

Coupling asphalt construction process quality into product quality using data-driven methods

Q. Shen^a, F. Vahdatikhaki^a, S.R. Miller^a, and A.G. Dorée^a

^a Department of Construction Management and Engineering, University of Twente, the Netherlands
q.shen@utwente.nl, f.vahdatikhaki@utwente.nl, s.r.miller@utwente.nl, a.g.doree@utwente.nl

Abstract –

The long-term quality of the asphalt layer is crucial for maintaining the functionality of roads. Despite extensive research on predicting pavement failure modes and the effect of design and road use on the quality of the asphalt layer, there is limited understanding of how the quality of road construction impacts the long-term quality of asphalt pavement. This paper presents a data-driven approach to studying the impact of construction process quality on the International Roughness Index (IRI) of roads. Two machine learning models (Random Forest and Gated Recurrent Unit) were compared in a case study, with the GRU model (R^2 of 0.8284) outperforming the RF model (R^2 of 0.5498). Results showed that construction process quality was the third most significant factor affecting IRI.

Keywords –

Asphalt construction; construction process quality; international roughness index (IRI); data-driven methods; regression; machine learning

1 Introduction

The demand for road infrastructure and longer guarantee periods has driven the asphalt construction industry to prioritize quality in order to remain competitive [1]. However, the industry is reliant on craftsmanship and experience-based decision-making, making quality assurance a challenge. To address this, the Process Quality Improvement (PQi) methodology was proposed by Miller [2] and has since been widely adopted as part of asphalt construction quality control methods in the Netherlands [3–5]. This methodology uses advanced sensing technologies in an integrated network, the Internet of Things (IoT), to monitor compaction efficiency/consistency and temperature homogeneity during the construction process. The collected data is used to evaluate process quality and provide feedback to contractors. While it is known that construction process quality impacts the long-term quality of asphalt pavement [6], the extent of this impact

remains unknown. Further investigation is needed to determine the effect of operational strategies on the quality of the asphalt pavement.

At present, the correlation between the process and product quality of the asphalt pavement is still treated implicitly and intuitively during the construction practices, primarily owing to the system's non-linearities. In the past few years, attempts have been made by various studies to develop data-driven empirical models regarding the long-term performance of asphalt pavement [7–10]. Various data-driven techniques, such as machine learning (ML), have been applied to extract valid patterns and knowledge. Particularly, the pavement condition regarding the roughness, which is represented by International Roughness Index (IRI), has received the most attention. However, although the data-driven techniques have been successfully applied to these studies, investigations in these studies were confined to correlating the pavement's long-term performance with indicators during the operational stage, such as traffic intensities, climate conditions, and previous inspections of the pavement conditions. To provide a more comprehensive understanding of the pavement performance it is essential to take the quality of the construction process into consideration.

On these premises, this research aims to explicitly investigate the correlations between the asphalt construction process quality (PQi data) and the long-term asphalt pavement quality, focusing primarily on IRI. A dataset covering the design, construction, and operation phases of road construction lifecycle was developed using data from two highway sections in the Netherlands, resulting in 62 samples. Considering the general performance of non-linear regression and the time-variant characteristic of the IRI data, Random Forest (RF) and Gated Recurrent Unit (GRU) were selected. The GRU model outperformed the RF model with an R^2 of 0.8284 compared to 0.5498. Permutation feature importance analysis revealed the construction process quality indicator as an important factor for pavement performance.

The remainder of the paper is structured as follows. First, the methodology of the research is presented. This

is followed by a case study demonstrating the validation of the proposed method. The paper ends with a discussion and a conclusion.

2 Methodology

Figure 1 provides an overview of the methodology applied in this research. In general, this methodology included the development of the dataset, ML model development, and evaluation and interpretation. Overall, the dataset development phase mainly focused on building a structured dataset that can be used for ML-based analysis. The second phase was dedicated to the development of ML models. An optimization algorithm was used to find the optimal configuration of the ML models. In the last phase, first, the developed ML models were evaluated based on the pre-defined metrics and then interpreted by analyzing the importance of the input features, i.e., how changes within the features influence the overall performance of the models. This can give more insights regarding the inner mechanism of the ML models, as well as a more intuitive representation of how to process quality indicators that contribute to certain product quality indicators. The following will provide a detailed explanation of each step.

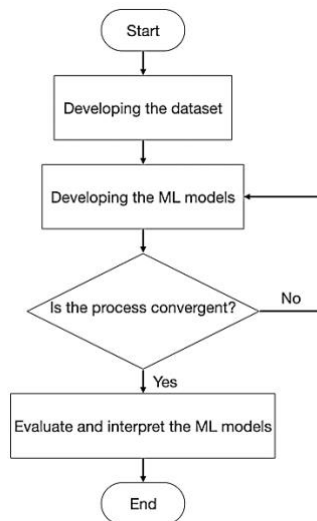


Figure 1. A schematic overview of the proposed modeling process

2.1 Dataset development

The proper input-output structure of a dataset is crucial for successful data mining. This involves understanding the cause-and-effect relationships that connect process quality indicators with the product quality indicator, in this case, the International Roughness Index (IRI). Three distinct types of parameters (i.e., features in the ML nomenclature) were considered in this research, namely design, construction,

and operation parameters (each pertaining to a phase in the lifecycle of the road).

As for the design-related parameters, this study considered the type of asphalt mix. While the design characteristics of the asphalt mix play a significant role in the long-term performance of the road, for the purposes of understanding the correlation between construction process quality and long-term pavement quality, a simplification was necessary. Instead of examining each individual design characteristic (such as bitumen content, aggregate type, etc.), only the mix type indicator was used. This choice was made because the focus of this research was not on exploring the individual impact of design characteristics on long-term performance, but rather on ensuring that the design phase was accurately represented in the ML model. This was achieved by consolidating all design parameters into the mix type indicator.

The definition of quality of the asphalt construction process was adopted from the previous work of the authors [3], where the process quality is defined as the degree to which the asphalt layer was compacted sufficiently (i.e., enough compaction passes) at the right temperature (i.e., avoiding the compaction of the asphalt layer when it is too hot or too cold). More specifically, the construction process quality is assessed using the Effective Compaction Rate (ECR) index proposed by [4], as indicated in Equation (1).

$$ECR_{p,k} = \frac{n_{p,k}}{N} \quad (1)$$

where $n_{p,k}$ refers to the number of cells that have received $\pm k$ passes (i.e., tolerance margin) of the target number of passes, and at least $p\%$ of received passes were within the defined compaction window. In this equation, N represents the total number of measurement cells.

In addition, the operation of the pavements during their service, such as the traffic intensity and weather, can also significantly influence the condition and performance of the pavements [8,11]. For the traffic loads, the author considered the average daily traffic and average daily truck traffic to reflect the daily intensity of the investigated highways. Therefore, in this study, the average hourly traffic intensities of three different types were considered, including passenger vehicles, heavy trucks, and medium trucks. When it comes to weather conditions, as pointed out in the literature [12], temperature variation and moisture change can have a great impact on the material properties of the pavement structure. It is shown that freeze-thaw cycles during pavement operation also contribute to the deterioration rate of the asphalt [13]. Therefore, this research considered the average annual temperature, average annual precipitation, and the number of freeze-thaw

cycles.

As for the labels in the dataset (i.e., the parameter about which the prediction is to be made), IRI is used as the sole metric. Although IRI is often recorded during regular inspections, it is a time-variant metric. To account for the complexity of changes in road usage, this study considers a rolling time window of 1 year instead of a long-term average of road use. This approach allows for a more accurate evaluation of the roads' condition by considering the most recent IRI measurement and the amount of use the road has seen since then. Table 1 below summarizes the identified input-output structure.

Table 1. The summary of the identified dataset structure

	Variable	Description
Input	ECR	The effective compaction rate, which was described in Equation 1
	Mixture type	The type of the asphalt mixture
	Age	The age of the pavement compared to the construction year
	Heavy truck intensity per workday	The mean intensity of the heavy trucks of a certain road section on the workday from the previous year
	Medium truck intensity per workday	The mean intensity of the medium trucks of a certain road section on the workday from the previous year
	Passenger car intensity per workday	The mean intensity of the passenger vehicles of a certain road section on the workday from the previous year
	Annual mean temperature	The mean value of the annual temperature of the road section from the previous year
	Annual mean precipitation	The mean value of the annual precipitation of the road section from the previous year
	Annual freeze-thaw cycle	The annual number of freeze-thaw cycles of the road section from the previous year
	IRI-1	The IRI value from the previous year
Output	IRI	International Roughness Index, which quantitatively reflects the roughness of the pavement

2.2 Machine learning model development

2.2.1 Selecting machine learning algorithms

Based on the problem context of the research, two types of ML algorithms were used, namely random forest (RF) and gated recurrent unit (GRU).

As a widely applied tree-based ML algorithm, random forest (RF) can solve both regression and classification problems using ensembled decision trees. An RF model is built by randomly ensembling various decision trees using the bagging method and obtaining the output(s) by voting [14]. As a powerful ML algorithm, RF can overcome the overfitting problem and improve the robustness against the outliers, without compromising the performance in handling non-linear classification and regression problems. The ensembling

technique and bootstrapping also allow RF to achieve potentially good performance on small datasets.

As previously mentioned, regression modelling faces great system non-linearities. To tackle the complexities of non-linear regression and provide better performance with time-series data, GRU was also selected. GRU is a special form of recurrent neural network (RNN) that can describe the dynamic behaviour of time-series data by circulating states in the networks. However, the conventional architecture of RNN soon showed its limits, because of problems such as the gradient's vanishing and explosion, and the difficulty in learning long-term patterns. To tackle the aforementioned challenges, long short-term memory (LSTM) and gated recurrent unit (GRU) was developed and introduced as extensions of conventional RNN [15].

Previous studies found that GRU has comparable or even surpassed the performance of LSTM [16]. In addition, although the structure of the GRU unit is similar to LSTM, the architecture of the GRU cell will require fewer external gating signals. Therefore, fewer parameters are needed, and the training process will be more efficient. Therefore, in this research, GRU was used.

However, when applying GRU, one issue is that apart from the time-variant variables, such as IRI-1, traffic intensities, and climate conditions, other input features including ECR and mixture types cannot be processed by the default GRU layer, because these input features are time-invariant. Therefore, these time-variant features were converted into vectors using affine transformation as the internal state of the GRU architecture. This transformed initial state is then added to the hidden state of the GRU when calculating the output [17–19]. In addition, to further tackle the complexities and non-linearities of the problems, a hybrid network can be used by adding more dense layers behind the GRU layer, thus increasing the depth of the network to boost its performance [9,10].

2.2.2 Hyperparameter optimization

To obtain optimal performance of developed ML models, it is essential to fine-tune and optimize the model configurations. Table 2 presents the list of optimized hyperparameters from RF and GRU.

A widely applied approach for hyperparameter optimization in ML is to use meta-heuristic methods, e.g., genetic algorithm (GA) or particle swarm optimization (PSO). This research used GA-based optimization of the ML models as proposed in the literature [20]. Figure 2 represents the flowchart of the GA-based hyperparameter optimization framework.

The developed dataset was first divided into 80% training and 20% testing subsets. Subsequently, the k -fold cross-validation was applied to the training subset by

further dividing the subset into k non-repeating sections. During the training process, the model was trained k times, using $k-1$ sub-training sets each time. The remaining sub-training set was then used for the evaluation of the model. By averaging the evaluation of the model k times, the fitness score was calculated. By using k -fold cross-validation, it can be ensured that all the samples of the training subset are involved in both the training and testing process. Therefore, this method reduces the sensitivity of the models' performances to how the training subset will be further split. Considering the trade-off in terms of computational time and accuracy, the value of k was set to 10.

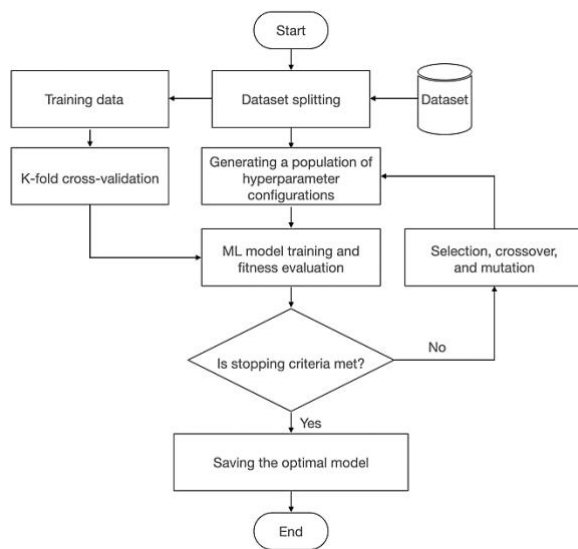


Figure 2. The GA-based hyperparameter optimisation framework

Table 2. The summary of the selected hyperparameters required to be optimized

ML algorithm	Hyperparameter	Description
RF	n_estimators	The number of decision trees in the RF structure.
	max_depth	The allowed maximum depth of each decision tree.
	min_samples_split	The minimum number of samples needed to split an internal node.
	min_samples_leaf	The minimum number of samples required to be at a leaf node.
GRU	n_layers	The number of the hybrid dense layer.
	n_neurons	the number of neurons within each hybrid dense layer.
	units	The number of GRU units.
	epochs	The number of epochs for the model training.

At the beginning of the optimization process, a random set of hyperparameter arrays are generated and used to develop the first generation of ML models. The

performances of each model are assessed and through a ranking process, the best models are identified. By applying crossover and mutation on the top-ranking solutions, the subsequent generation of models is generated. The optimization process will continue until the stopping criteria are met.

2.3 Model evaluation and interpretation

Finally, the developed ML models were validated using the data outside the range of the training dataset. Several metrics were used to represent the regression performance of developed ML models, including R-squared (R^2), mean squared error (MSE), and mean absolute error (MAE). The equations of these three metrics were given below.

$$R^2 = 1 - \frac{\sum_{i=1}^n (\hat{y}_i - \bar{y})^2}{\sum_{i=1}^n (y_i - \bar{y})^2} \quad (2)$$

$$MSE = \frac{\sum_{i=1}^n (y_i - \hat{y}_i)^2}{n} \quad (3)$$

$$MAE = \frac{\sum_{i=1}^n |\hat{y}_i - y_i|}{n} \quad (4)$$

where n refers to the total number of samples, y_i refers to the true value, \hat{y}_i refers to the prediction, and \bar{y} refers to the mean value of the sample.

Additionally, among these metrics, R^2 was also used as the fitness function in the GA-based model optimization process to represent the fitness of each examined chromosome. To explicitly represent the correlations between various process quality indicators and product quality indicators, the obtained regression models were interpreted in the form of feature importance, which was through a sensitivity analysis. The feature importance reflects how important the features are for the regression. Therefore, the feature importance analysis can provide explicit insights into the models, as well as the hidden correlations between inputs and outputs. For this purpose, the model with the highest predictive performance was used. To ensure that the feature importance interpretation can be applied to both ML algorithms, this research adopted the permutation importance as the interpreting approach, which randomly shuffles a certain input feature and re-evaluates the model performance. By comparing the performance changes with the baseline performance, the importance of a certain input feature can be obtained.

3 Case study

To validate the proposed framework, a case study was conducted. Two Dutch highway sections (A58 and A4) with a total length of 4.1 km, were selected. For both sections, PQi measurements and regular IRI inspections were available. The historical PQi measurements (i.e.,

construction process quality indicator) were retrieved

Table 3. An example of the developed dataset

Samples	Input features										IRI
	ECR	Mixture	Age	Annual Mean Temp.	Annual Mean Preci.	Annual Freeze/Thaw Cycles	Passenger Cars/Day	Med. Trucks/Day	Heavy Trucks/Day	IRI-1	
1	0.1792	ZOAB-1	3	10.7713	2.2784	55	47318	3406	3476	1.32	0.93
2	0.1372	ZOAB-1	3	10.7713	2.2784	55	47318	3406	3476	1.20	0.64
⋮	⋮	⋮	⋮	⋮	⋮	⋮	⋮	⋮	⋮	⋮	⋮

from the database of the Dutch research network ASPARi [21]. The IRI data were retrieved from the IVON database and yearly inspectional records held by the Ministry of Infrastructure and Water Management of the Netherlands (Rijkswaterstaat). Regarding the data about the operation phase of the roads, two databases were used. For the traffic intensity, data were extracted from the INTensiteit op WEGVakken (INWEVA) database of Rijkswaterstaat. This database covers the entire Dutch highway network and registers the historical traffic intensity of each hectometer section with specified BPS locations. Besides, the weather data were derived from the Koninklijk Nederlands Meteorologisch Instituut (KNMI) database. Table 3 provides an example of the developed dataset.

Several parameters for the GA-based hyperparameter optimization were also defined including the size of the population, the size of offspring, crossover and mutation rates, and the total number of generations, as shown in Table 4. In this case study, the number of generations is the stopping criterion.

Table 4. Pre-defined GA-parameters

GA parameter	Value	Description
Population size	100	The total number of individuals contained in one population.
Offspring size	100	The total number of individuals that will be generated after each iteration.
Crossover rate	0.8	The probability of the occurrence of crossover between two individuals.
Mutation rate	0.2	The probability of the occurrence of mutation within one individual.
Generation number	100	The number of iterations

3.1 Results

As explained in section 2.2.1, two ML algorithms were selected and used, namely RF and GRU. Table 5 presents the comparison of the two models in terms of MSE, MAE, and R^2 . Also, Figure 3 demonstrates the regression plots of each model, including both the training and testing processes. Additionally, Table 6 also summarizes the results of the optimization of the hyperparameters.

Based on Table 5 and Figure 3, the developed GRU model significantly outperformed the RF model, where

the latter is considerably underfitting, due to the high training and testing errors. This underfitting issue will be further discussed in the following section. The GRU model achieved a promising result regarding R^2 , with a value of 0.8284. Besides, the errors of the predictions compared to the true values, which are reflected by MSE and MAE, were well-controlled. The results between the training process and testing process are close, meaning that the developed GRU model has reasonable generality.

Table 5. The summary of the results of the model validations

Model	R^2	MSE	MAE
RF	0.5498	0.0123	0.0847
GRU	0.8284	0.0050	0.0600

As mentioned earlier, only the best-performing model (i.e., GRU model) was used for the feature importance. MAE was used as the metric to evaluate the impact of each feature on the overall model performance.

Table 6. The summary of the optimization results regarding hyperparameter configurations

ML algorithm	Hyperparameter	Value
RF	n_estimators	100
	max_depth	None
	min_samples_split	20
GRU	min_samples_leaf	1
	n_layers	2
	n_neurons_first_layer	14
	n_neurons_second_layer	8
	units	18
	epochs	210

Figure 4 shows the permutation importance of each input feature. Based on the results, the feature IRI-1 has the highest importance. By changing the values of this feature, the model performance reduces dramatically reduced. Compared to other features, features including the mean annual temperature and ECR also have rather higher importance, ranking second and third respectively. The feature importance of the rest of the features is quite lower, while the differences are not considerable. However, the feature representing the characteristics of the mixtures ranks the lowest among all the features.

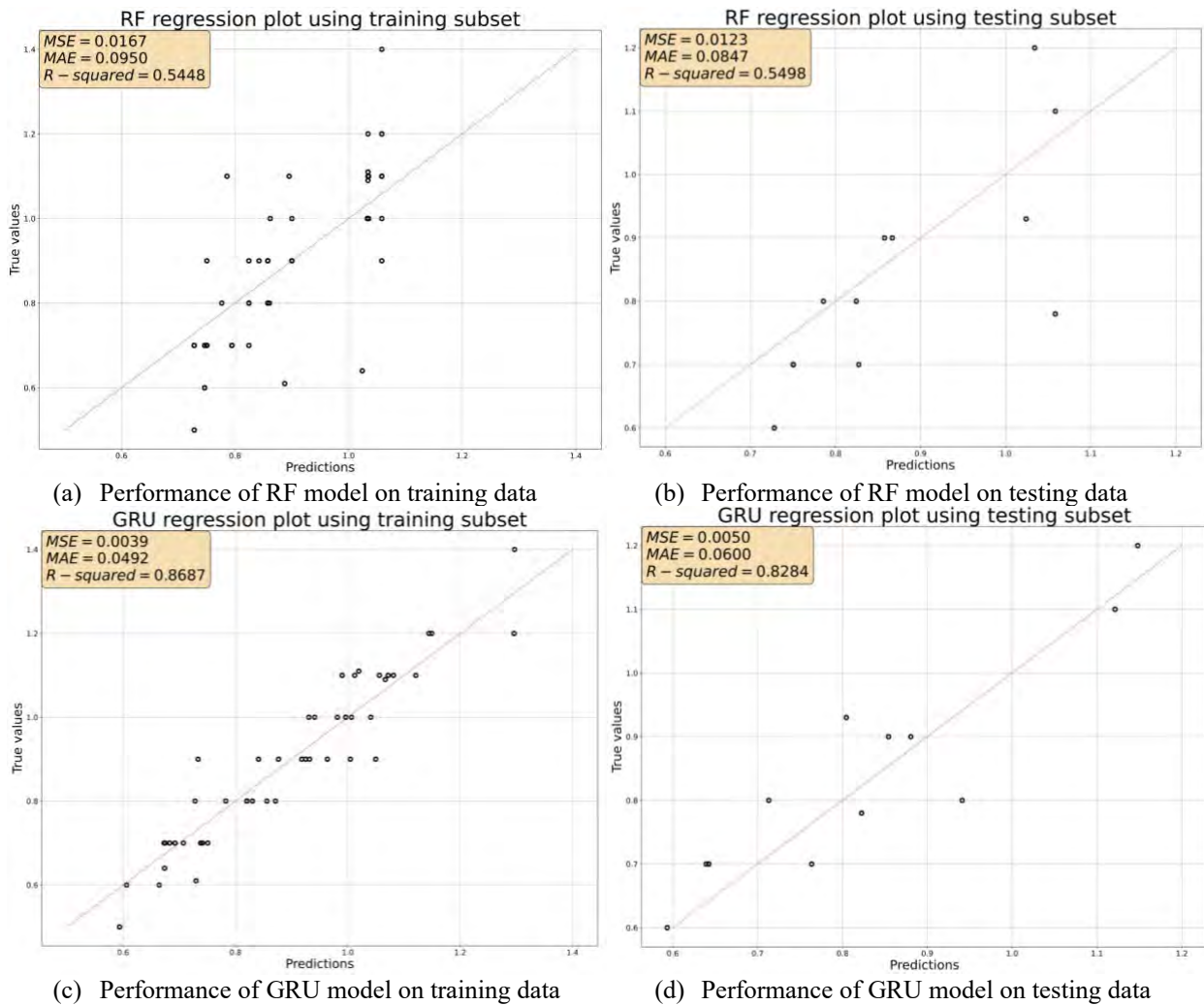


Figure 3. Regression plots of the developed models

4 Discussion

The main contribution of the presented research is to systematically investigate the correlation between process quality and product quality in asphalt construction. Asphalt is a highly complex material, where the quality in each phase of the lifecycle is influenced by various factors and also how the previous phases unfolded [22]. Therefore, this study provides an opportunity to scale up the regression task from the focus on one phase of the asphalt construction lifecycle to multiple phases. This would be significantly beneficial in the highly competitive environment of the asphalt construction sector. For instance, to the contractors, the explicit correlation between process and product quality can eventually help further justify the efforts to improve and optimize the planning and implementation of the on-site operational strategies.

The GRU model performed well despite the small dataset. The size of the dataset is essential in drawing reliable conclusions; however, the consideration of other factors such as the quality of the data and the model's ability to identify significant features and relationships is also crucial to the reliability and validity of the conclusions derived from data analysis.

Essentially, unlike conventional ML algorithms, algorithms such as GRU will have a much higher level of abstraction, thus prone to be greedy to the amount of the data to prevent the overfitting problem. However, a previous study suggests that the high reliability of the model can be achieved even with small datasets [7]. In this study, the R^2 of developed models reached 0.9941 and 0.9893 on two different datasets. Besides, in the presented study, RF was also utilized. Compared to GRU, RF has a rather simpler architecture and less complexity. However, in the represented study, the developed RF model suffered from the underfitting problem with the

small amount of data. This could potentially mean that the data used in this study is insufficient to support conventional ML algorithms, such as RF. On the other hand, the developed GRU model showed outstanding capability regarding feature extraction.

Lastly, the previous measurements of the IRI outranked the other features. This is in line with various studies which also applied time-series regression to the IRI data [8,10]. Representing the construction process quality, ECR ranked third, which indicates a rather high impact of construction process quality on product quality. This further highlights the importance of investigating the asphalt product quality from the life-cycle perspective. In addition, the feature representing the properties of the asphalt mixtures ranked the lowest. This is in line with the findings of the previous studies [23].

5 Conclusion and future work

This research aimed to investigate the correlations between asphalt construction process quality and product

quality, using data-driven techniques. In this research, the IRI was selected as the output and representation of the pavement product quality indicator.

A GA-based ML model development framework was designed, where RF and GRU were selected as the algorithms. For the validation, a case study was conducted. Based on the collected data, the developed GRU model significantly outperformed the RF model, with an R^2 of 0.8284. After interpreting the permutation importance, ECR achieved the third highest importance, revealing the rather high correlation between process quality and product quality in asphalt construction.

For future work, because the case study in this research was performed on a small dataset, the authors would like to expand the scope of the dataset. Besides, the presented research only focused on the IRI, while in the further study, more product quality indicators concerned with both in-place pavement properties (i.e., density, thickness, etc.) and long-term pavement performance (i.e., raveling, cracking, rutting, etc) can be considered.

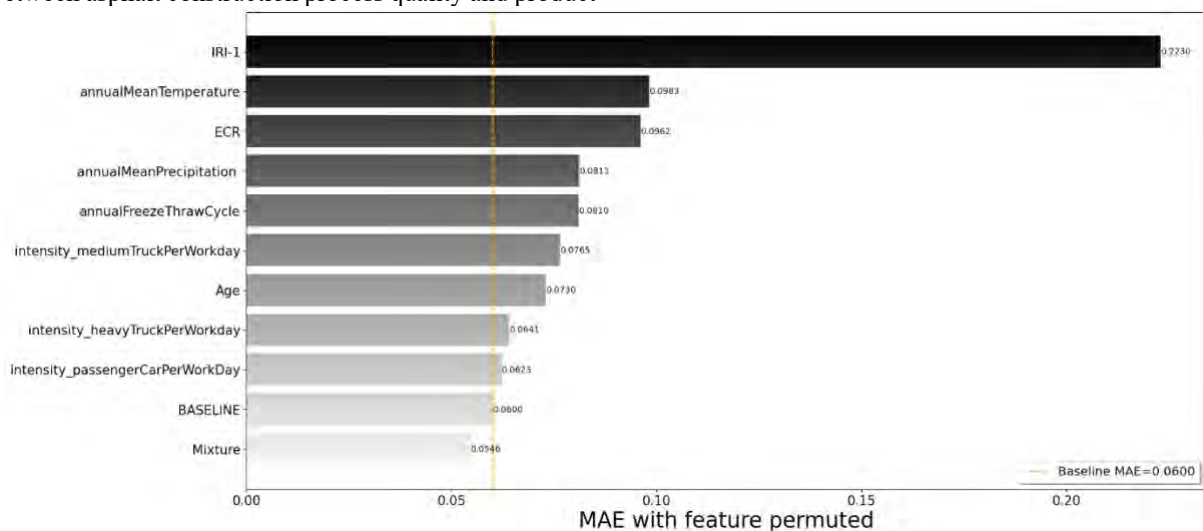


Figure 4. The permutation feature importance

References

- [1] S.R. Miller, H.L. ter Huerne, A.G. Doree, Towards understanding asphalt compaction: An action research strategy (in special issue for the IPRC), Built & Human Environment Review. 1 (2008) 11–24. <https://research.utwente.nl/en/publications/towards-understanding-asphalt-compaction-an-action-research-strat> (accessed February 10, 2021).
- [2] S.R. Miller, Hot mix asphalt construction : towards a more professional approach, University of Twente, 2010. <https://doi.org/10.3990/1.9789036531283>.
- [3] F.R. Bijleveld, S.R. Miller, A.G. Dorée, Making Operational Strategies of Asphalt Teams Explicit to Reduce Process Variability, J Constr Eng Manag. 141 (2015) 04015002. [https://doi.org/10.1061/\(ASCE\)CO.1943-7862.0000969](https://doi.org/10.1061/(ASCE)CO.1943-7862.0000969).
- [4] D. Makarov, F. Vahdatikhaki, S. Miller, A. Jamshidi, A. Dorée, A framework for real-time compaction guidance system based on

- compaction priority mapping, *Autom Constr.* 129 (2021) 103818.
<https://doi.org/10.1016/J.AUTCON.2021.103818>.
- [5] D. Makarov, S.R. Miller, F. Vahdatikhaki, A. Doree, A Generic Framework for Automating the Asphalt Construction Process, in: 12th Conference of Asphalt Pavements for Southern Africa (CAPSA), Sun City, South Africa, 2019: pp. 1227–1241.
<https://research.utwente.nl/en/publications/a-generic-framework-for-automating-the-asphalt-construction-proce> (accessed April 21, 2021).
- [6] S. Sørungård, G. Sindre, Aspects of process quality, in: *Proc. 4th Software Quality Conference*, Dundee, Scotland, 1995: pp. 318–326.
- [7] M. Mazari, D.D. Rodriguez, Prediction of pavement roughness using a hybrid gene expression programming-neural network technique, *Journal of Traffic and Transportation Engineering (English Edition)*. 3 (2016) 448–455.
<https://doi.org/10.1016/J.JTTE.2016.09.007>.
- [8] H. Gong, Y. Sun, X. Shu, B. Huang, Use of random forests regression for predicting IRI of asphalt pavements, *Constr Build Mater.* 189 (2018) 890–897.
<https://doi.org/10.1016/J.CONBUILDMAT.2018.09.017>.
- [9] J. Li, G. Yin, X. Wang, W. Yan, Automated decision making in highway pavement preventive maintenance based on deep learning, *Autom Constr.* 135 (2022) 104111.
<https://doi.org/10.1016/J.AUTCON.2021.104111>.
- [10] J. Li, Z. Zhang, X. Wang, W. Yan, Intelligent decision-making model in preventive maintenance of asphalt pavement based on PSO-GRU neural network, *Advanced Engineering Informatics*. 51 (2022) 101525.
<https://doi.org/10.1016/J.AEI.2022.101525>.
- [11] F. Alharbi, Predicting pavement performance utilizing artificial neural network (ANN) models, Iowa State University, 2018.
<https://dr.lib.iastate.edu/entities/publication/ae0e177-bebe-4cd4-b7ae-3c82c4a024fb> (accessed September 28, 2022).
- [12] L. Žiliūte, A. Motiejūnas, R. Kleiziene, G. Gribulis, I. Kravcovas, Temperature and Moisture Variation in Pavement Structures of the Test Road, *Transportation Research Procedia*. 14 (2016) 778–786.
<https://doi.org/10.1016/J.TRPRO.2016.05.067>.
- [13] B.S. Smith, *Design and Construction of Pavements in Cold Regions: State of the Practice*, Brigham Young University, 2006.
<https://scholarsarchive.byu.edu/etd/1111/> (accessed March 31, 2023).
- [14] L. Breiman, Random forests, *Mach Learn.* 45 (2001) 5–32.
<https://doi.org/10.1023/A:1010933404324>.
- [15] A. Sherstinsky, Fundamentals of Recurrent Neural Network (RNN) and Long Short-Term Memory (LSTM) network, *Physica D*. 404 (2020) 132306.
<https://doi.org/10.1016/J.PHYSD.2019.132306>.
- [16] J. Chung, C. Gulcehre, K. Cho, Y. Bengio, Empirical Evaluation of Gated Recurrent Neural Networks on Sequence Modeling, (2014).
<https://doi.org/10.48550/arxiv.1412.3555>.
- [17] A. Karpathy, L. Fei-Fei, Deep Visual-Semantic Alignments for Generating Image Descriptions, *IEEE Trans Pattern Anal Mach Intell.* 39 (2014) 664–676.
<https://doi.org/10.48550/arxiv.1412.2306>.
- [18] O. Vinyals, A. Toshev, S. Bengio, D. Erhan, Show and Tell: A Neural Image Caption Generator, *Proceedings of the IEEE Computer Society Conference on Computer Vision and Pattern Recognition*. 07-12-June-2015 (2014) 3156–3164.
<https://doi.org/10.48550/arxiv.1411.4555>.
- [19] philipperemy/cond_rnn: Conditional RNNs for Tensorflow / Keras., (n.d.).
https://github.com/philipperemy/cond_rnn (accessed January 24, 2023).
- [20] Q. Shen, F. Vahdatikhaki, H. Voordijk, J. van der Gucht, L. van der Meer, Metamodel-based generative design of wind turbine foundations, *Autom Constr.* 138 (2022) 104233.
<https://doi.org/10.1016/J.AUTCON.2022.104233>.
- [21] HOME | Aspari, (n.d.). <https://www.aspari.nl/> (accessed January 25, 2023).
- [22] C. Han, F. Tang, T. Ma, L. Gu, Z. Tong, Construction quality evaluation of asphalt pavement based on BIM and GIS, *Autom Constr.* 141 (2022) 104398.
<https://doi.org/10.1016/J.AUTCON.2022.104398>.
- [23] Perera, R. W., Byrum, C., Kohn, S. D., & Soil and Materials Engineers, Inc. (1998). Investigation of Development of Pavement Roughness.
<https://rosap.nrl.bts.gov/view/dot/42761> (accessed March 31, 2023).

BIM-GIS integration and crowd simulation for fire emergency management in a large, diffused university

Silvia Meschini¹, Daniele Accardo², Mirko Locatelli¹, Laura Pellegrini¹, Lavinia Chiara Tagliabue³ and Giuseppe Martino Di Giuda²

¹ Department of Architecture, Built Environment and Construction Engineering, Politecnico di Milano, Italy

² Department of Management, University of Turin, 10134 Turin, Italy

³ Department of Computer Science, University of Turin, 10149 Turin, Italy

silvia.meschini@polimi.it, daniele.accardo@unito.it, mirko.locatelli@polimi.it, laura1.pellegrini@polimi.it, laviniachiara.tagliabue@unito.it, giuseppemartino.digiuda@unito.it

Abstract

The integration of BIM (Building Information Modeling) and GIS (Geographic Information System) is promising to develop Asset Management Systems (AMS) for complex assets such as university building stocks. The potential lies in the ability to connect and contextualize data from several domains and at different scales, considering the relationship between buildings and surroundings, and paving the way towards the definition of Digital Twins (DTs) for proactive AMS. In a previous work, an AMS-app was developed through BIM-GIS integration in a web platform aimed at optimizing the Operational and Maintenance (O&M) phase of the large and diffused university of Turin's asset. The main objective was to provide an accessible and integrated database, supporting decision-making and improving user experience, enhancing resources use in both ordinary and emergencies scenarios. The paper presents the application of such a BIM-GIS platform and AMS-app for fire emergencies management through a case study. It illustrates the crowd simulation methodology developed, replicable to analyse the current fire safety level of the whole university asset and display it through the AMS-app and interactive dashboards. It describes how this is key to identify non-compliances and intervention priorities, in addition to the tailored data needed for each building. Furthermore, its importance for the long-term objective of developing DTs and active wayfinding systems useful for rescuers and users during fire emergencies is illustrated, identifying useful data which should be provided from on field sensors.

Keywords –

BIM, GIS, Asset Management, Operation and Maintenance, data integration, crowd simulation, fire emergency, Digital Twins

1 Introduction

The smart city concept recently was borrowed at campus scale to define digital AMS aimed at providing optimal resources use and a more satisfactory user experience during the low digitalized and investigated O&M phase [1-3].

BIM-GIS integration (i.e. GeoBIM) provides numerous advantages when applied together with Artificial Intelligence (AI) and Internet of Things (IoT), leading to buildings able to react to environmental changes autonomously and dynamically. Indeed, GeoBIM is promising to develop DTs and smart campuses [4], simulating buildings behaviour in the actual conditions of both the interior and surrounding, providing contextualized data and promptly decisions. At this aim, an accessible, well-structured, centralized, and scalable database is needed [5,6].

Thus, the first phase of the research, illustrated in a previous work [7], dealt with the definition of a holistic information management approach. It was core to provide an AMS-app, based on BIM-GIS integration, for the O&M phase of the University of Turin (i.e. UniTO) asset. UniTO has one of the largest and diffused Italian campuses with a vast catchment area. Nonetheless, its management system is still strongly document-based and fragmented, preventing awareness of its exact consistency and use. Over the past five years, enrolled students increased, amounting to approximately 83,000 in 2022. Together with teaching, administrative, and technical staff, it represents a quite complex system with a yearly expense of 1,3 million euros. Therefore, even a little improvement in the AM system can provide significant savings.

The research is part of a wider project, the short-term objective consisted in providing administrators with a digital AMS aimed at optimizing resources use and space occupancy [7]. The long-term objective concerns the

development of a smart campus through interconnected DTs aimed at several purposes (e.g. management of energy use, mobility, emergency, facility and so forth) with buildings autonomously optimizing their performance based on real-time, historical, internal, and external contextualized data [8]. The first objective was provided through an AMS-app which enabled the asset visualization through an interactive 3D map, based on BIM-GIS integration [7]. Such an app collects all the data currently handled by several Directorates through a centralized database, key for the second long-term aim of developing future consistent DTs both for ordinary and emergency scenarios.

The most probable emergency in university campuses is fire emergency, still low investigated with respect to energy and facility management [9-10]. Thus, a crowd simulation methodology was developed and here presented through its implementation on a case study to check the current building fire risk level based on actual space occupancy and conditions. First results are presented, showing how this methodology could be replicated to cover the whole UniTO asset and provide a quick visualization of its current fire risk level through tailored analytics dashboards connected to the AMS-app. Required data which should be stored in the centralized database and gathered in real-time through future IoT systems were also identified. Providing administrators with such an AMS could enable to identify priority intervention, accordingly optimizing resources use and better programming of punctual enhancements. Finally, it's discussed how future implementation of AI, IoT, DTs and Virtual Reality (VR) could enable active wayfinding systems useful for rescuers and users during fire emergencies, also identifying useful data which should be provided from on field sensors.

2 Background and motivation

2.1 BIM and GIS integration

The recent wide diffusion of IoT networks and digital technologies in construction industry is finally shaping the concept of smart buildings, and that of the smart city accordingly. BIM-GIS integration and DTs promise to facilitate their development and to provide cognitive buildings, autonomously reacting to environmental changes toward more resilient, proactive, and sustainable environments [6]. GeoBIM is a trend research topic, promising to reach data integration, strategic decision-making, and urban management with many advantages and applications [11]. Indeed, BIM enables to handle information at the scale of the building and its elements, while GIS at the macro-level of its surroundings [12]. Thus, the strength of such an integration consists in enabling digital AM from the micro-scale of the single

component to the macro-scale of the territory. Nonetheless, BIM and GIS are not fully interoperable domains, and many issues must be overcome for their integration [13]. [14] identified three possible paths to convert and integrate data in a GeoBIM system, from BIM to GIS was recognised as the optimal one, with data extracted from BIM and imported into GIS. ESRI ArcGIS Pro® paired with Autodesk Revit® represents the most agreed and diffused authoring solution, easily providing BIM-GIS interoperability and data integration through a visualization platform. Numerous studies agree that the greatest benefits of BIM-GIS integration during the O&M phase can be found in AM and crowd simulation with a focus on risks, energy, facility, and security management [1, 3, 11, 14]. BIM improves route planning with its specific geometrical and semantic information about building interior and components. GIS provides spatial statistical methods for analysis, modelling data, in addition to localization data [27]. BIM-GIS provides the ability of creating a comprehensive scenario and enabling valuable simulations to identify optimal evacuation paths. One of the biggest issues in managing emergency scenarios.

Nevertheless, [3] illustrated how GeoBIM is still rarely investigated in the AM field, despite the great results in data collection, visualization, and analysis, providing enhanced decision-making. Mostly due to the challenges in collecting and storing a big amount of heterogeneous data with various granularity levels.

Finally, BIM-GIS integration is usually closely related to DTs and smart cities development and [1,3] highlighted how GeoBIM will be further improved to respond to the growing demand of DTs, significantly boosting the development of smart cities and smart campuses. [4]. GIS not only provides an immediate data contextualization, but it also enables data integration and DTs interconnection [15]. This is challenging but could result in great added value for university AM with a broader decision-making context in economic, social, and environmental perspectives. Indeed, it is needed the visualization of unknown and dynamic contextualized information for decentralized management based on a single source of truth. This is key in managing standard O&M scenarios but even more in emergency ones.

2.2 Smart campuses and university AM

Hardly accessible, and fragmented databases often struggle universities AM which is still strongly document based. This results in incomplete information leading to ineffective decisions. Particularly during the O&M phase which is already complicated [1] due to the need of comprehensive data exchanges among various stakeholders. A digital and dynamic AMS based on the principles of information management can support decision-making, providing a more comfortable

environment, reduced costs, and resources waste [1, 3, 16]. A holistic information management system across several databases is still missing [1,3], even if could be particularly significant in smart campuses.

Several universities are borrowing the smart city concept at campus scale, mostly to provide more satisfactory user experiences and optimal resources use during the still low investigated O&M phase [1,2]. Indeed, university assets are characterized by a variety of services (e.g., courses, lecturers, and seminars) and users (e.g., professors, students, researchers, administrative staff, external people, and facility managers), resulting in a highly dynamic and changeable environment, complex to be managed [9, 17]. Ordinary management scenarios are characterized by a high level of unpredictability due to several heterogeneous users with different aims and schedules, representing a relevant causality source. During emergencies, panic stresses user behaviour and worsens unpredictability [9], especially in complex systems with crowded spaces such as smart campuses.

An agreed definition of smart campuses is still missing, even though many studies tackled their development with interesting results [10]. [18] identified six main features: context-aware, data-driven, forecasting, immersive, collaborative, and ubiquitous, highlighting the key role of data and their contextualization to provide consistent information and decision-making [1, 15]. The same key features are needed to develop valuable DTs for universities AM [1]. Thus, a switch from fragmented document-based approaches to digital collaborative ones is strongly needed [19]. Smart campuses with digital data-driven, user-friendly, analytical tools demonstrated to enable a holistic information management approach, needed to consider heterogeneous but interlinked data, influencing several ordinary AM activities (e.g., cleaning, maintenance, space optimization and occupancy monitoring). This enables to optimize information exchanges among several stakeholders throughout the complex university asset lifecycle, providing the best value and the optimal environment for users and owners.

Most cases developed so far started from a pilot building and its BIM model, only later georeferenced through BIM-GIS integration and then extending the procedure to the whole asset [12]. While this works for minor-sized assets, in the case of large and diffused ones would require years of development, preventing enhancement to the environmental footprint and to reach higher resilience and sustainability. Few examples exploited the reverse “macro to micro” approach [3], preferable to gain a quick overview of the asset in order to check its overall consistency, needed interventions and optimization opportunities. Indeed, there is not a unique and correct approach, the choice depends on the purpose. The “macro to micro” approach should be preferred when

a strategic management tool for large assets is urgently needed and accordingly the analysis of its consistency and distribution [12]. Especially, when forecasting the development of smart campuses and future DTs.

One of the most interesting features unlocked by DTs consists in the ability to manage emergencies, that is complex scenarios due to their rapid evolution and variability [9, 20]. Particularly, in smart cities and smart campuses which requires crowd management due to many users carrying out various activities. DTs and VR can enhance quick decisions and crowd coordination through active wayfinding or alerting systems.

3 Methodology

The methodology is split in two parts: the first one, focused on the development of the web-based AMS-app with analytics dashboards using Business Intelligence (BI) tools. It dealt with the structuring of a centralized database, digitalization and georeferentiation of the whole UniTO asset through BIM-GIS integration [7]. The second part illustrates the significant potentials of such an AMS-app in one of its possible applications. The methodology defined for crowd simulation in fire emergencies is described and applied on a complex building, exploited as a demonstrator of its replicability to map the whole UniTO asset fire risk.

3.1 Data integration and AMS-app

The first step of the wider UniTO research project dealt with the definition of a methodology to develop the AMS-app, illustrated in [7] and following reported with a brief description of each step implemented.

1. Data acquisition and analysis of building stock and management processes: it dealt with the analysis of UniTO building stock and its management system to identify already available data, existing databases and platforms, in addition to the administrations involved in the AM. Useful missing data were unveiled and collected from the UniTO accessible communication channels or the several Directorates;
2. Data structuring to develop the integrated database: this was a key step concerning the identification and structuration of data previously collected, enriched with missing data about spaces and their functional attributes, providing a centralized, comprehensive relational database for the O&M phase. It was defined a tailored encoding system which uniquely identifies spaces and related data throughout the database, overcoming existent redundancies and duplicated codes, leading to multiple assignments. The data structure is flexible, enabling to insert additional fields whenever new data are needed;
3. BIM-based information modelling: BIM models

were developed and enriched with both spatial and functional semantic data. Buildings were modelled as masses, floors, and rooms to obtain an adequate level of information able to represent the whole diffused UniTO asset, without overburdening the AMS-app. Then, spatial and functional data previously acquired and collected in the centralized database were assigned to the related category of elements created (masses, plants, and environments) through Visual Programming Language (VPL).

4. Information models georeferentiation through the BIM-GIS web-based platform: the information models were implemented into the web-based BIM-GIS environment, providing UniTO asset and its attributed real-time visualization in an interactive 3D digital map (i.e., AMS-app). BIM-GIS interoperability was checked and achieved through the “BIM to GIS” approach exploiting ESRI ArcGIS Pro® and Autodesk Revit®, currently representing the most suitable approach, as literature states. A tailored BIM-GIS integration workflow was used to model and georeferencing the whole UniTO asset, providing the AMS-app. The BIM models of the whole asset were imported in the GIS platform as georeferenced building masses, with geometric and semantic attributes;
5. Interactive analytics dashboards development: BI technology was exploited, enabling both the analysis of large amounts of data and interactive dashboard development aimed at facilitating information visualization and understanding. This is key to support AM and decision making, especially through future DTs. Several analytic dashboards were developed to provide information visualization at different scales, ranging from the macro level of the whole building or groups of buildings to the room micro level.

3.2 Crowd simulation for fire emergency

The steps afore-outlined involved information models integration in a web-based queryable AMS-app with their spatial and functional attributes. The further step concerned the definition of a replicable methodology for crowd simulations in case of fire (Figure 1), exploiting data stored in the centralized database.

The methodology aims at visualizing user reaction and movements in a fire emergency scenario, checking spaces and escape routes crowding levels, in addition to measuring and comparing the escape time with the regulatory reference one. It enables to analyse dangerous circumstances with high-density moving crowds at critical points of a building, such as stairs or fire exits. Crowding and emergency evacuations during hazardous events impeding to use one or more escape routes at a selected building floor can be assessed.

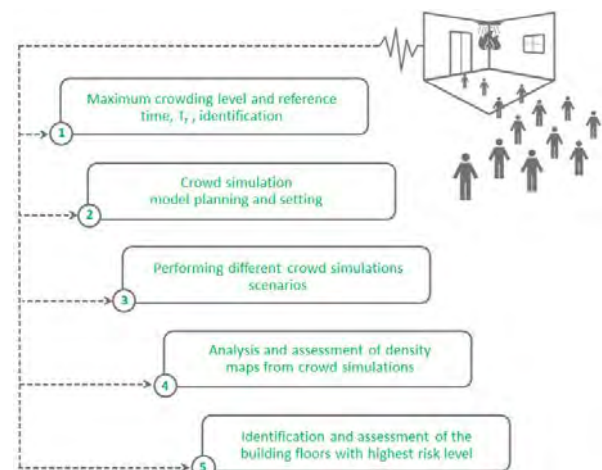


Figure 1. Methodology path for crowd simulation.

Previous studies identified the maximum crowding level, that is the maximum density of moving crowds over which high risk situations might arise, at five people per square meter (i.e., 5 p/smq) [21]. National prescriptive regulations (Italian M.D. 10/03/1998) define the reference escape time (T_R) as the effectiveness maximum time for the safety measures required. Thus, the actual safety of the building floors can be investigated considering high-risk levels of moving crowds and comparing the measured escape time with the prescriptive regulations' threshold.

The second step concerned crowd simulation model planning and setting (Figure 1). A microscopic approach [22] was applied to analyse the casual crowd [23]. Literature identifies four factors influencing crowd simulations, among which space layout and users behaviour. The former can be considered by modelling the whole building or just a relevant portion, including all spaces and user flows exploiting the same safe place, escape routes and stairs, ensuring simulation reliability. Furthermore, the model should consider limitations on escape route or space access for predefined user groups. The users are represented as agents able to identify the best escape route according to crowd behaviours and the least effort principle thanks to an AI system. The model exploits a collision avoidance algorithm based on vision-based cognitive models [24], enabling agents to perceive their mutual position and movements and acting accordingly. Consequently, field of view (FoV) angle, user speed, avoidance preference direction, and avoidance range are defined. In order to simulate the worst possible evacuation scenario, agents are modelled considering the maximum building, building section, or occupancy capacity. Further scenarios are simulated introducing a hazardous event preventing the use of one or more escape routes on a selected building floor with agents able to use only free escape routes. The proposed crowd simulations aim to assess the safety of space distribution and occupancy besides the effectiveness of

escape routes and exits.

The third methodology step (Figure 1) performed crowd simulation scenarios. The first scenario considered the whole building, or the section analysed as in the selected demonstrator. The agents are triggered to leave their personal spaces and evacuate through any possible escape routes and exits. Then, a hazardous event in one or more escape routes is introduced, preventing agents from their use during the evacuation.

The fourth step (Figure 1) involved the density map analysis resulting from performing crowd simulation. It is the maximum density of moving crowds reached during the whole simulation in each point of the building. As literature highlight, it is key to verify density values at critical points (i.e., fire exits, stairs access, and corridors), where different user flow intersections can provide overcrowding and accidents. In addition, scenario simulations enable the identification of the building floors with high risk levels of moving crowds, (i.e., density values greater 5 p/sqm) in non-safe areas, selected to be analysed in the next step. While safe areas are the protected and external stairs and the safe places identified by fire emergency plans, non-safe areas are spaces and corridors.

In the fifth step (Figure 1), the building floors which showed high-risk levels of moving crowds are further analysed, and for each selected floor, the escape time is measured (T_1, T_2, \dots, T_n). It starts when the first agent of the floor is triggered to leave the building and continues until the last agent has reached the safe place or the floor exit, which leads directly to the protected or external stairs. The measured escape time is then compared with the reference one. If $T_n < T_R$, the escape time is comparable or inferior to the one defined by prescriptive regulations, safety measures are defined based on it, and the check is satisfied. Otherwise, if $T_n > T_R$, the check is not satisfied, and the actual building layout, escape routes, exits, and other safety measures are not sufficient to ensure user safety during an emergency.

4 Case study

UniTO asset represents a large widespread campus, the third largest Italian university with a huge catchment area and users' number, resulting in a hard management and usability. It counts 112 buildings for an amount of almost 629,000 net square meters, mixed in style and destination, with a huge heterogeneity. UniTO's buildings host various activities, often open to the public such as seminars, exhibitions, and cinema; together with administrative, teaching, and technical staff, it represents the management of a small town with a high level of complexity and unpredictability. Nonetheless, the current UniTO AMS is fragmented and poorly digitized, preventing awareness of its consistency, use, and

distribution over the territory. The prompt perception of these features is needed by administrators, as well as an AMS strongly connected with the urban space.

The selected demonstrator represents a significant case study, chosen due to its spatial and management complexity (Figure 2), worsened by the strong crowding. The building is Palazzo Nuovo and houses the school of humanities with five departments, 33 degree courses, and about 965 study courses, amounting to 22,641 students in the last academic year, that is the 27.7% of the total university population, showing a positive growing rate of 14.8%. It is composed by seven floors above ground and three basement floors, in addition to three huge classrooms separate from the main body with a net area of 6787 sqm (Figure 2). It counts 5000 seats between classrooms, study rooms and degrees spaces, in addition it holds places in other external buildings for a total availability of almost 7,475.

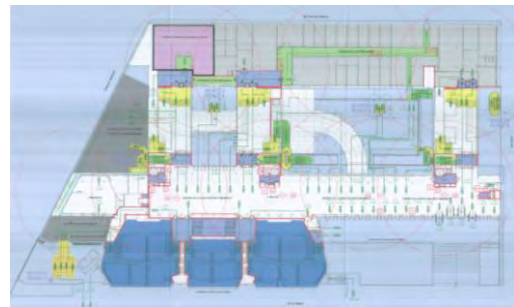


Figure 2. Standard floor plan showing the complex spatial articulation of Palazzo Nuovo.

Hence, current places can't cover Palazzo Nuovo demand and its complex management makes it a suitable case study to apply the crowd simulation methodology defined for fire emergency. Recently it undergone major renovations to minimize asbestos-related and to improve space and fire safety. All the staircases and escape routes were isolated to fulfil national standards and lead to a safe place according to the requested escape time.

5 Results and discussion

In the aim of testing the AMS-app and centralized database application potential, crowd simulations have been conducted on Palazzo Nuovo, investigating its actual level of safety in case of fire. The methodology defined enabled to simulate different evacuation scenarios compliant with fire and safety prescriptive standards. Traditional approach limitations were discussed, exploring improvements achievable through dynamic simulations and DTs during evacuations.

First and foremost, the reference escape time (T_R) for each floor was identified through the analysis of national fire regulations. T_R is defined as the maximum escape

time from each single floor, enabling users to reach the nearest fire exit, leading either to fire protected or external stairs. Italian Government M. D. 10/03/1998 provides prescriptions and limitations both for existing and new buildings, identifying three buildings fire risk level: high, medium, or low. Palazzo Nuovo is classified as a university facility hosting more than 1,000 occupants with a high fire risk level, thus the simulation T_R is equal to 1 min for escape routes between 15 and 30 m long. According to the literature, the maximum moving crowds density to be considered is equal to 5 p/sqm. The crowd simulation model includes the six floors above the ground, counting a full capacity of 1,765 users using the same escape routes, stairs, and exits to reach the only two safe places at the ground floor. The six stairs represent the escape routes, placed two by two in the centre and on the two opposite sides of the building (Figure 3, top side). The basement floors were excluded as have dedicated exits and escape routes with less worrying crowd phenomena. The ground floor also was excluded as most of the exits lead directly to safe places. The simulation model involved the following parts:

- The ground floor with two safe places;
- The six floors above the ground and their spaces;
- The expected maximum occupants' number in each space from fire emergency plans, their walking speed, avoidance range, FoV angle, and avoidance preference. User speed is defined as a triangular distribution function of three speed values: low value of 0.8 m/s, medium value of 1.35 m/s, and high value of 1.75 m/s [25]. Avoidance range and FoV angle were set equal to 10 m and 75° as the default settings of the simulation software, and the avoidance preference was set on right;
- The six staircases representing the escape routes (i.e., three external and three protected).

Then, crowd simulations in two evacuation scenarios were performed. The first one considering the entire building section defined, while the second one with a hypothetical hazardous event on the first floor which hosts the greatest number of users. It was located in front of the two staircases on the left, preventing access to the two stairs for the first floor (Figure 3, top side). The next step tackled the density map analysis during the simulation for the two crowd scenarios (Figure 3, bottom side), at each floor of the building. Density above 5 p/sqm were considered dangerous when detected in non-safe areas, that is areas different from safe places and protected or external stairs.

In the first scenario (Figure 3), only the first floor shows high risk levels of moving crowds, becoming significantly more crowded in relation to other floors. The same results in the second scenario (Figure 3).



Figure 3. First floor with the hazardous event (Top side) and density maps from the first and second simulated scenario (Left and right bottom side respectively).

Comparing the two first-floor density maps, in the second scenario non-safe place area with density over 5 p/sqm is 14.23% greater than in the first one. Finally, each floor of the two scenarios with a detected density over 5 p/sqm has been analysed. T_n is defined for each floor as the time at which the first agent of the floor is triggered by the emergency alarm. It ends when the last agent of the floor reaches the fire exit, leading to a safe place or to the protected or external stairs. T_n was then compared to the previously defined T_R (1 min) in the two scenarios. The escape time of the first floor, in the first scenario, T_1 , and in the second scenario, T_2 , is:

- $T_1 = 12 \text{ min } 52 \text{ s} > T_R (1 \text{ min})$; 12.86 time greater than T_R
- $T_2 = 15 \text{ min } 48 \text{ s} > T_R (1 \text{ min})$; 15.80 times greater than T_R
- The comparison shows $T_2 > T_1$ with T_2 22.79% greater than T_1 .

The results pointed out the limits of prescriptive regulations to ensure building fire safety. Despite the escape routes maximum length, defined according to regulations (i.e., between 15 and 30 m with high fire-risk level, corresponding to a T_R of 1 min), should ensure the correct evacuation to all users, at all the building levels, the dynamic simulation highlighted criticalities due to user flows. This results in overcrowding and an escape time far superior to prescribed values, T_R , in both scenarios. Furthermore, the great negative impact that a hazardous event can have on the occurrence of dangerous phenomena and on the evacuation were pointed out.

The crowd simulations enabled also to define the set of significant data, which should be found in the database (e.g., T_R , T_n , density values, walking speed, FoV angle, avoidance range, expected occupants, and avoidance preference). It will be key both for future dynamic simulations aimed at mapping the current asset fire-risk level through the AMS-app and defining “fire emergency DTs”. The actual occupation was individuated as the first, crucial data which should be provided in real-time through IoT networks. In the future, the current data set

should be enriched and completed. Such as, all the possible crowd evacuation routes at each floor should be simulated and stored in the AMS-app. Thus, an AI algorithm could be integrated to analyse and optimize them as simulations progress, teaching the DTs better behaviours. They should also be loaded into a VR system connected to the AMS-app to provide active wayfinding [26]. Finally, a tailored dashboard was developed and connected to the AMS-app for fire safety analysis of each floor of the building, (Figure 4).

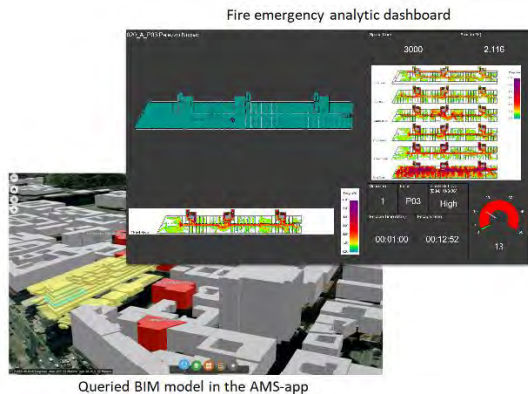


Figure 4. Example of queried BIM model in the AMS-app and related fire emergency dashboard.

It shows:

- the floor plan with occupancy levels,
- the floor plan with crowd simulation,
- the level of fire risk with respect to the regulations,
- the maximum escape time and the effective one deriving from the simulation.

6 Conclusion and future work

The paper is part of a wider research with the short-term objective of developing an AMS-app based on BIM-GIS integration to improve the O&M phase management of the large and diffused UniTO asset. This was accomplished in a previous work, briefly summarized, providing a centralized and flexible database. Then, the paper focused on the first steps toward the second long-term objective: the definition of the UniTO smart campus through DTs aimed at several purposes. This will enable to resolve or prevent deviations from expected behaviors in ordinary scenarios but especially in fire emergency. At this aim, a replicable crowd simulation methodology was presented and tested through a complex case study. The results highlighted the limitations posed by current prescriptive regulations and the need to integrate them with dynamic simulations based on updated data about the building and its occupancy. Required data which should be available from the centralized database and provided also through the IoT networks were identified.

In the future development, the crowd simulation methodology will be replicated throughout the whole UniTO asset, providing an overall “fire risk map” in the AMS-app, able to highlight interventions’ priorities. In the aim of providing a consistent smart campus, it will be also investigated how AI and VR systems could enable the cognitive features required by DTs. Thus, buildings will promptly react and adapt their behavior to environmental changes, improving performances simulation by simulation. Additionally, active wayfinding for fire scenarios could be provided and drive users evacuation through audio-based systems or lighting signals, according to data gathered from IoT networks and the actual occupancy. Users can be real-time guided through the safest and shortest evacuation routes, exploiting paths loaded in the AMS-app and displayed through digital devices. The app can be exploited also to alert rescuers and guide them with indications to reach life in danger or fire outbreak point in the shortest possible path and time.

The AMS presented could overcome current still document-based and fragmented management issues, providing a suitable database to develop consistent DTs. It could provide effective decisions and management based on complete, contextualized, and real-time data, stored in a centralized and flexible database. Through synthetic dashboards and BI tools linked to the AMS-app, useful strategic data and graphs could be displayed. Thus, a better management of UniTO’s financial and spatial resources will be enabled, with cost savings and waste reduction. There will be several challenges in IoT and AI implementation through the AMS-app, besides the development and interconnection of several DTs and overcoming stakeholders’ hesitance in adopting the new collaborative approaches.

References

- [1] Lu, Q., Parlikad, A. K., Woodall, P., Don Ranasinghe, G., Xie, X., Liang, Z., Konstantinou, E., Heaton, J. & Schooling, J. Developing a Digital Twin at Building and City Levels: Case Study of West Cambridge Campus. *Journal of Management in Engineering*. ASCE, 2020
- [2] Ward, Y., Morsy, S., & El-Shazly, A. GIS-BIM data integration towards a smart campus. In *Design and Construction of Smart Cities: Toward Sustainable Community* (pp. 132-139). Springer International Publishing, 2021.
- [3] Moretti, N., Ellul, C., Re Cecconi, F., Papapesios, N. & Dejaco, M. C. GeoBIM for built environment condition assessment supporting asset management decision making. *Automation in Construction*. Elsevier, 130, October, p. 103859, 2021.
- [4] Zaballos, A., Briones, A., Massa, A., Centelles, P.,

- & Caballero, V. A smart campus' digital twin for sustainable comfort monitoring. *Sustainability*, 12(21), 9196, 2020.
- [5] Villegas-Ch, W., Palacios-Pacheco, X. & Luján-Mora, S. Application of a Smart City Model to a Traditional University Campus with a Big Data Architecture: A Sustainable Smart Campus., 2019
- [6] Deng, T., Zhang, K. & Shen, Z. J. (Max) A systematic review of a digital twin city: A new pattern of urban governance toward smart cities. *Journal of Management Science and Engineering*. Elsevier Ltd, 6(2), pp. 125–134, 2019.
- [7] Meschini, Silvia, et al. "Data integration through a BIM-GIS web platform for the management of diffused university assets." *EC3 Conference 2022*. Vol. 3. University of Turin, 2022.
- [8] Yitmen, I., Alizadehsalehi, S., Akiner, İlknur & Akiner, M. E. An Adapted Model of Cognitive Digital Twins for Building Lifecycle Management, 2021.
- [9] Naticchia, B., Messi, L. & Carbonari, A. BIM-based Holonic System for Real-Time Pathfinding in Building Emergency Scenario. Proceedings of the *European Conference on Computing in Construction*, 1 pp. 117–124, 2019
- [10] Chagnon-Lessard, N., Gosselin, L., Barnabe, S., Bello-Ochende, T., Fendt, S., Goers, S., Silva, L. C. P. Da, Schweiger, B., Simmons, R., Vandersickel, A. and Zhang, P. Smart Campuses: Extensive Review of the Last Decade of Research and Current Challenges. IEEE, pp. 124200–124234, 2021.
- [11] Shkundalov, D. & Vilutienė, T. Bibliometric analysis of Building Information Modeling, Geographic Information Systems and Web environment integration. *Automation in Construction*. Elsevier, 128, p. 103757, 2021.
- [12] Wang, H., Pan, Y. & Luo, X. Integration of BIM and GIS in sustainable built environment: A review and bibliometric analysis. *Automation in Construction*. Elsevier, 103, July, pp. 41–52. 2019
- [13] Noardo, F., Arroyo O., K., Biljecki, F., Ellul, C., Harrie, L., Krijnen, T., Kokla, M. & Stoter, J. THE ISPRS-EUROSDR GEOBIM BENCHMARK 2019. In *International Archives of the Photogrammetry, Remote Sensing and Spatial Information Sciences*, pp. 227–233, 2019.
- [14] Ma, Z. & Ren, Y. Integrated Application of BIM and GIS: An Overview. *Procedia Engineering*. No longer published by Elsevier, 196, January, pp. 1072–1079, 2017.
- [15] Centre for Digital Built Britain National Digital Twin Programme | Centre for Digital Built Britain. Online: <https://www.cdbb.cam.ac.uk/what-we-do/national-digital-twin-programme>, 2022.
- [16] Lytras, M. D. & Visvizi, A. Information management as a dual-purpose process in the smart city: Collecting, managing and utilizing information. *International Journal of Information Management*, 56, 2021.
- [17] Abdullah, A., Thanoon, M. & Alsulami, A. Toward a smart campus using IoT: Framework for safety and security system on a university campus. *Advances in Science, Technology and Engineering Systems*, 4(5), pp. 97–103, 2019.
- [18] Dong, Z. Y., Zhang, Y., Yip, C., Swift, S. & Beswick, K. Smart campus: definition, framework, technologies, and services. *IET Smart Cities*, 2(1), pp. 43–54, 2020.
- [19] Moretti, N., Xie, X., Merino, J., Brazauskas, J. & Parlikad, A. K. An openBIM Approach to IoT Integration with Incomplete As-Built Data. *Applied Sciences*, Vol. 10, Page 8287. Multidisciplinary Digital Publishing Institute, 10(22), p. 8287, 2020.
- [20] Selamat, H., Khamis, N. & Ghani, N. M. (2020) Crowd modeling and simulation for safer building design. *International Journal of Electrical and Computer Engineering Systems*, 11(2), pp. 77–88.
- [21] Still, K. G., Papalexi, M., Fan, Y. & Bamford, D. Place crowd safety, crowd science? Case studies and application. *Journal of Place Management and Development*, 13(4), pp. 385–40, 2020.
- [22] Klügl, F., Klubertanz, G. & Rindsfuser, G. Agent-Based Pedestrian Simulation of Train Evacuation Integrating Environmental Data. In Mertsching, B., Hund, M., and Aziz, Z. (eds) *KI 2009: Advances in Artificial Intelligence*. Berlin, Heidelberg: Springer Berlin Heidelberg, pp. 631–638.
- [23] Berlonghi, A. E. Understanding and planning for different spectator crowds. *Safety Science*, 18(4), pp. 239–247, 1995.
- [24] Hughes, R., Ondřej, J. & Dingliana, J. DAVIS: Density-adaptive synthetic-vision based steering for virtual crowds. In *Proceedings of the 8th ACM SIGGRAPH Conference on Motion in Games*, MIG 2015, pp. 79–84, 2015.
- [25] Bohannon, R. W. & Williams Andrews, A. Normal walking speed: A descriptive meta-analysis. *Physiotherapy*. *The Chartered Society of Physiotherapy*, 97(3), pp. 182–189, 2011.
- [26] Zhu, Yiqing, and Nan Li. "Virtual and augmented reality technologies for emergency management in the built environments: A state-of-the-art review." *Journal of Safety Science and Resilience* 2., 1-10, 2021.
- [27] Atyabi, S., Kiavarz Moghaddam, M., & Rajabifard, A. (2019). Optimization of emergency evacuation in fire building by integrated BIM and GIS. *The International Archives of the Photogrammetry, Remote Sensing and Spatial Information Sciences*, 42, 131-139.

Transformation of Point Clouds to Images for Safety Analysis of Scaffold Joints

Jeehoon Kim¹, Sunwoong Paik¹, Yulin Lian¹, Juhyeon Kim¹, and Hyoungkwan Kim¹

¹Department of Civil and Environmental Engineering, Yonsei University, Korea

E-mail: john101010@yonsei.ac.kr, tjsdnd4066@yonsei.ac.kr, yulin.lian@yonsei.ac.kr, kah5125@yonsei.ac.kr,
hyoungkwan@yonsei.ac.kr

Abstract –

Structural flaws in scaffolds can lead to fatal accidents on construction sites, and the installation status of scaffold joints is crucial for the safety of scaffolds. However, manual inspection of scaffold joints can be challenging due to their small size and large quantity. This paper presents a scaffold joint inspection mechanism using a Terrestrial Laser Scanner (TLS) to address the challenge of inspecting large numbers of scaffold joints for structural flaws. Scaffold members are first extracted from the TLS-acquired point clouds using a 3D segmentation model to generate scaffold joint image sets. Then, a rule-based classifier is used on the image sets to identify the installation status of each joint. Our experiment showed 82.1% accuracy in scaffold joint safety analysis and successfully localized the unsafe joints on the 3D point cloud data.

Keywords –

Deep learning; Scaffold; Point-to-Image; Safety analysis; Terrestrial Laser Scanning

1 Introduction

Point cloud data obtained through Terrestrial Laser Scanner (TLS) is more accurate than that obtained through photogrammetry due to its high sensor accuracy and the simplicity of static scan registration. Furthermore, depending on the scanner, it is also possible to obtain RGB or intensity information, allowing for the acquisition of texture information as well. Due to the advantages of TLS-acquired data, TLS is frequently used in construction site quality control research. Wang et al. [1] extracted information for rebar quality assessment by performing automated rebar position estimation using the (x, y, z) coordinate information and (r, g, b) color information of the point clouds obtained by TLS. Erkal and Hajjar [2] used texture-mapped 3D data obtained with a camera-integrated TLS to detect damages on building surfaces.

The unstable state of scaffolds is a major cause of

fatalities at construction sites. According to the Korean Ministry of Employment and Labor [3], 53% (341 cases) of occupational fatalities occurred in the construction industry in 2022. Among them, 208 fatalities were related to accidents that occurred in temporary structures; the statistic shows the importance of monitoring the safety condition of temporary structures. Typical causes of scaffold incidents include lack of fall protection, instability of the scaffold structure, overloading, and being struck by falling tools [4].

A previous study [5] investigated the detachment status of various components of scaffolds by directly processing the point clouds obtained by TLS. In the case of attached scaffold components, joint inspection is required to ensure proper installation. However, with large-scale construction site data, determining the presence of extremely small objects like the pins of a ringlock scaffold through direct processing of point clouds is computationally inefficient. On the other hand, Paik et al. [6] were able to efficiently solve the joint safety analysis task through the use of UAV-acquired images. However, since the image data do not include location or depth information, the automatic localization of the detected joint is challenging.

Various studies have utilized the fusion of 3D point clouds and 2D images. Nguyen et al. [7] employed images to effectively detect small features such as cracks in 3D data. They concatenated the image pixel features with low-density point clouds of the crack area and performed upsampling. Yang et al. [8] proposed Mem3D for effective 3D object reconstruction using a single-view image. For training Mem3D, the correspondence of the image-voxel pair of the dataset was used, including the memory network.

Motivated by the limitations of previous studies, we propose a methodology that combines the advantages of 3D point cloud data and 2D image data. The proposed method involves generating images from point cloud data, processing the generated images, and re-projecting the information processed from the image onto the 3D point clouds. This method allows us to use the rich data quality of point clouds and the efficiency of image processing to

effectively locate the unsafe joints in the scaffold.

2 Methodology

In this research, the semantic segmentation through RandLA-Net [9] and then post-processing for the desired information were based on the method proposed in [5]. Therefore, this paper describes the three parts after the semantic segmentation: Point-to-Image translation, object detection, and joint safety analysis. The overall framework is shown in Figure 1.

2.1 Point-to-Image

By using the algorithm from [5], we can obtain representative (x, y, z) coordinates of the “upright” and the “guard rail” in a scaffold. Combining these two information resulted in the intersection points of “upright” and “guard rail,” which is equal to the center coordinate of every joint. Afterwards, each joint coordinate is used as a center to crop a 20×20×20 (cm) sized bounding box from the point clouds, in order to extract the point cloud data for each joint. The joint extraction framework is shown in Figure 2. Then, the open-source library Open3D’s [10] Visualizer function is utilized to save the compressed appearance in the required viewpoint vector direction as an image for each joint point clouds. The required viewpoint vector varies depending on the type of joint. As shown in Figure 3, parallel joint (Figure 3(b)) generates one image from one viewpoint, while corner joint (Figure 3(c)) generates two images from two viewpoints.

2.2 Object detection

Images generated through the Point-to-Image

algorithm are fed into the YOLOv5 [11] model trained to detect “ledger end” and “tail” of the joint (Figure 4). The generated images are in the form of a white background with “upright” passing in the middle and “ledger end” and “tail” on sides of the “upright.” The two components’ information is sufficient to inspect the safety status of a joint. “Ledger end” indicates that there is a joint that should be inspected in that location, and “tail” is only visible when the pin is properly inserted into the corresponding “ledger end.”

2.3 Joint safety analysis and localization

The safety status of each joint is inspected through the information of “ledger end” and “tail” detected through YOLOv5 in each image. If “ledger end” does not exist in an image (Figure 5(c)), the image is excluded from inspection because it does not have a joint. If “ledger end” exists, it indicates that a joint exists in the image and the number of detected “tail” and that of “ledger end” are compared. If the number of detected “tail” is less than that of “ledger end,” it is judged as unsafe because the “tail” is not visible (Figure 5(b)); there is a risk of accident due to incorrect insertion of pins and loose joints. In the case of a corner joint, if either of the two images of a single joint is classified as unsafe, then the joint is considered unsafe. The scenarios of safe, unsafe, and no joint are presented in Figure 5. The flowchart of the rule-based joint safety classifier is shown in Figure 6.

In order to localize the unsafe joint images onto the point cloud map, we included the index of the corresponding joint in the file name format generated during the Point-to-Image algorithm. Through the index number, we were able to easily determine the (x, y, z) coordinates of the detected joint.

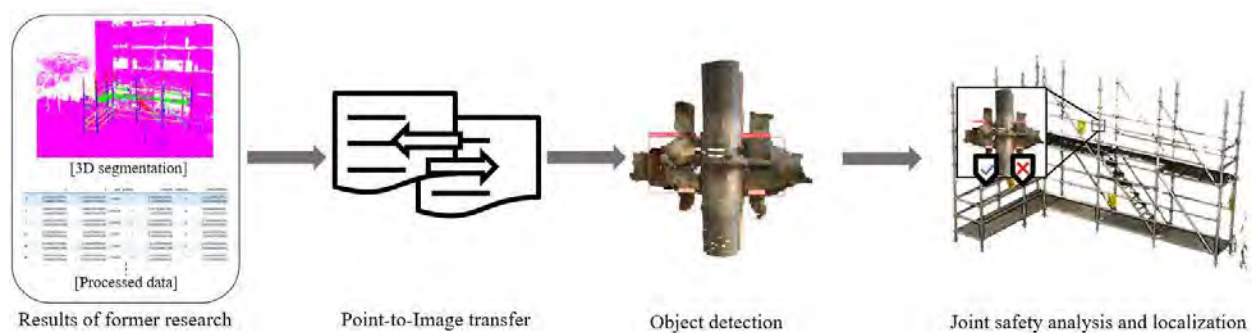


Figure 1. Overall framework.

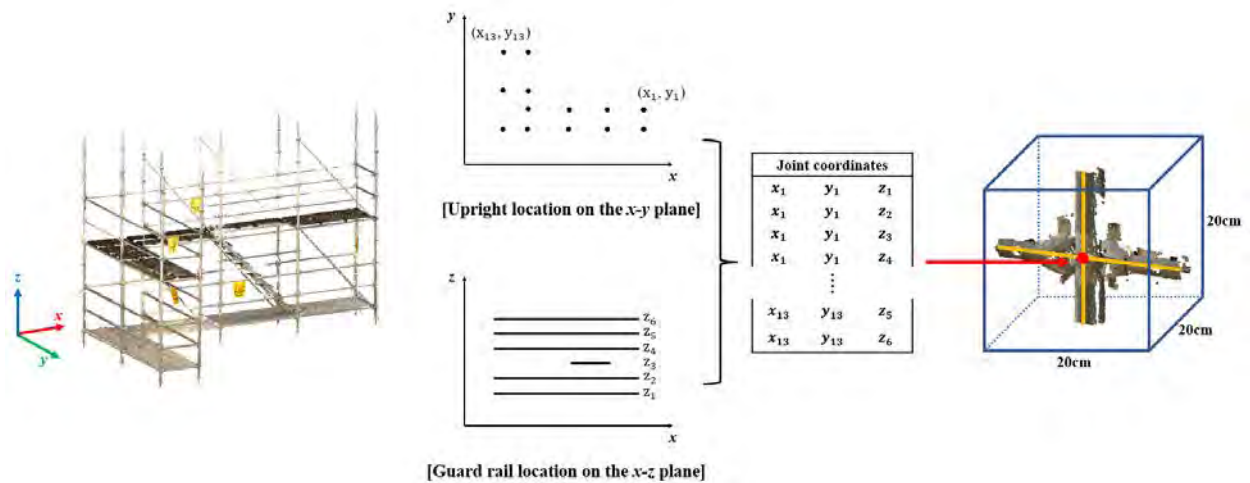


Figure 2. Joint extraction framework.

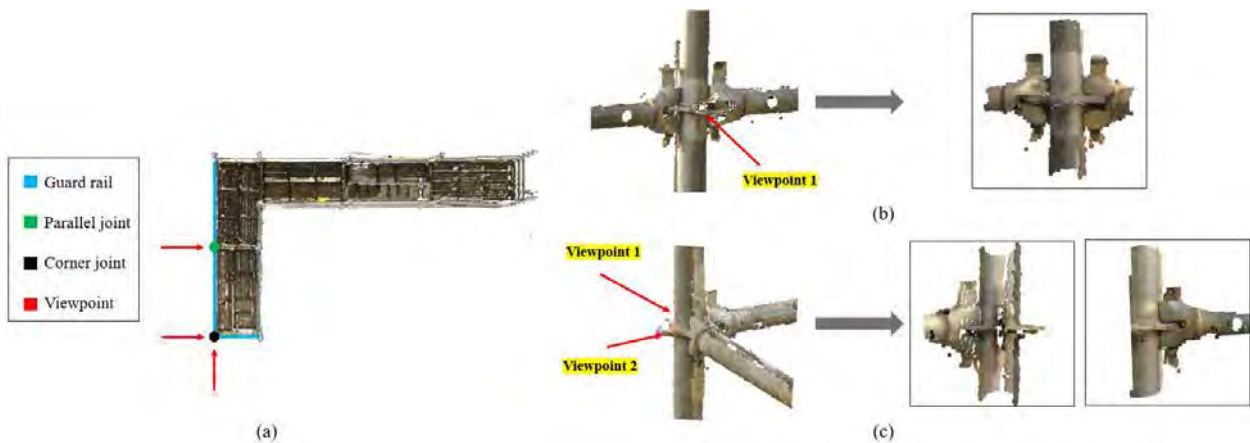


Figure 3. Two types of joints and the images generated from each type; (a) bird-eye view of a scaffold, (b) an example of parallel joint (left: point clouds, right: generated image), (c) an example of corner joint (left: point clouds, right: generated image).

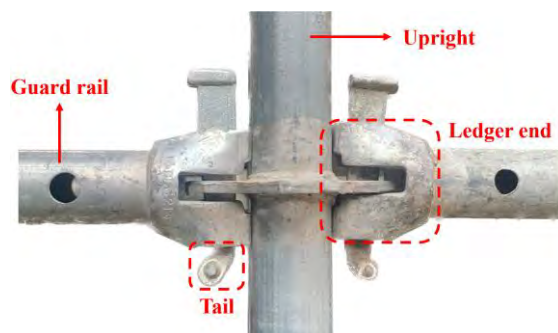


Figure 4. Image of a scaffold joint.

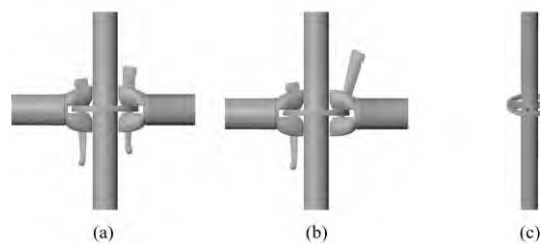


Figure 5. Scenario of joint safety status; (a) safe, (b) unsafe: tail is not visible on the right pin, (c) no joint: ledger end is not visible.

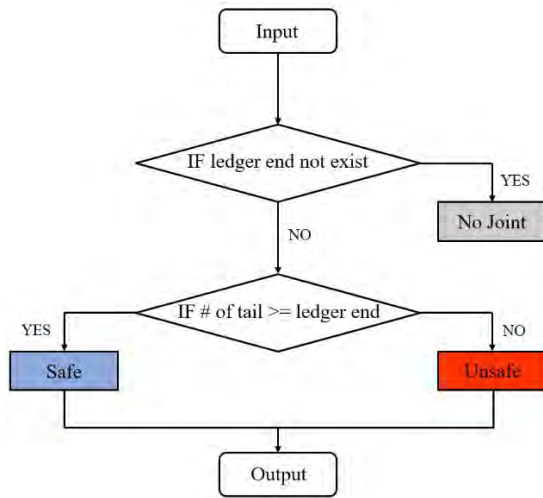


Figure 6. Rule-based joint safety classifier.

3 Experiments and Results

In this section, we present detailed information about the data used in the experiments and the evaluated results. We also discuss the current limitations and challenges revealed through the results of the experiments.

3.1 Dataset specification

The data used in this study were acquired from a total of three construction sites with ringlock scaffolds. In the point cloud data of site A shown in Figure 7, 239 joint images were acquired. These 239 images were augmented to 478 images by applying the gaussian blur method; to smoothen the variation in the images made by point size difference without breaking the geometry of the joint. In site B, a total of 90 joint images were acquired from the point cloud data. This study targets to inspect the structural safety of the scaffold after it is erected and before it is disassembled. Therefore, image data were acquired at the upper part of the scaffold without safety nets at site B. The images obtained from site A were used as the training dataset for YOLOv5, while the images obtained from site B were used as the validation dataset for YOLOv5. Point cloud data acquired from site C were used as test data.

All sites did not have actual unsafe joints. Therefore, a total of three unsafe joints were manually created by cropping and removing the scaffold joint pins from the point cloud data acquired from site C.

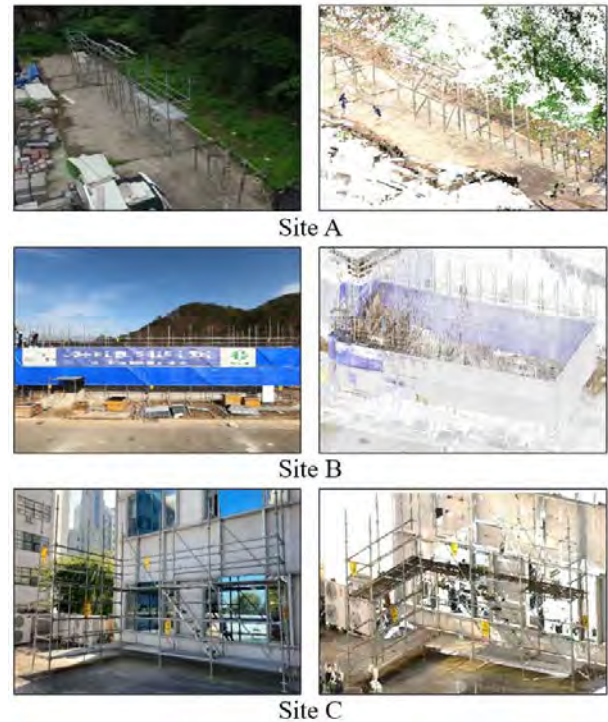


Figure 7. Image (left) and acquired point clouds (right) of data acquisition sites.

3.2 Results

Applying the methodology of [5] to the site C data yields 3D segmentation results that are divided by scaffold entities (results of former research in Figure 1). The segmented point cloud data of site C were fed into the Point-to-Image algorithm, producing 114 images from 78 joints (42 parallel joints and 36 corner joints) in 12m 53s. Object detection, joint safety analysis, and localization performed on the generated images took 1.74 seconds in total. Our methodology resulted in a per image accuracy of 74.6% and a per joint accuracy of 82.1% for site C. The results are summarized in Table 1.

Table 1. Joint safety analysis results

	Accuracy (%)
Per Image (114 images)	74.6
Per Joint (78 joints)	82.1

As explained in Section 2.3, unsafe joints can be automatically localized on the point cloud map. In order to visually display the locations, we created a



Figure 8. Localization & visualization of unsafe joints; (a) Prediction (red box), (b) Ground truth (blue box).

visualization algorithm that generates a red box around the unsafe joint. Figure 8(a) is the localization result of predicted unsafe joints.

3.3 Discussion

As shown in Figure 9, the proposed method successfully inspected a total of 78 joints in site C with a per joint accuracy of 82.1%. The 14 joints that were incorrectly predicted include one case that predicted an unsafe joint as “no joint” and two cases that predicted a safe joint as unsafe. These 14 misclassifications were mainly divided into two reasons; when the joint is occluded by obstacles such as work platforms or work ropes (Figure 10(a)), and when the object detection model fails to detect the joint (Figure 10(b)).

Safety analysis is a field that requires perfect predictions. False negative predictions are particularly important to avoid; an unsafe object predicted to be safe is vulnerable to accidents. Our model had one false negative error (red box in Figure 9), which occurred when the joint was occluded by a work rope.

4 Conclusion

This study presented a methodology for automating scaffold joint safety analysis by generating 2D image data from 3D point cloud data; thereby combining the advantages of both data types. The framework of this study is divided into three parts including Point-to-Image transformation, object detection, and rule-based joint safety analysis and localization. An accuracy of 82.1% was obtained for the joint safety status of a ringlock scaffold on a construction site. In contrast to previous image-based studies, the proposed method was able to easily localize the identified unsafe joints.

In future studies, the limitations mentioned in section 3.3 should be addressed. The scanning method should be optimized to minimize occlusion of data. The training dataset of the detection model should be supplemented to increase the accuracy of the detection model. Additionally, the joint analysis method should be developed and tested to be applicable to various sizes and types of scaffolds.

		Ground Truth		
		Unsafe	Safe	No joint
Prediction	Unsafe	2	2	1
	Safe	0	50	0
	No joint	1	10	12

● True predictions
● False negative predictions (regarding class “Unsafe”)

Figure 9. Confusion matrix of the safety analysis results. Numbers represent the number of joints.

Acknowledgment

This work was supported by the National Research Foundation of Korea (NRF) grant funded by the Ministry of Science and ICT (No. 2021R1A2C2004308) and the Ministry of Education (No. 2018R1A6A1A08025348).

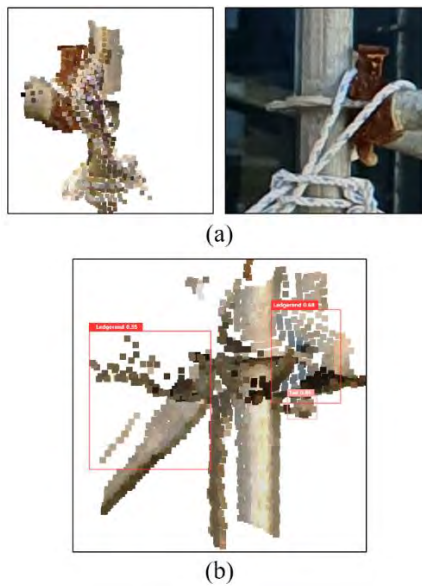


Figure 10. Misclassified image example; (a) occlusion by work rope, (b) detection failure of YOLOv5.

References

- [1] Wang Q, Cheng JC, and Sohn H. Automated estimation of reinforced precast concrete rebar positions using colored laser scan data. *Computer-Aided Civil and Infrastructure Engineering*, 32(9):787-802. 2017.
- [2] Erkal BG and Hajjar JF. Laser-based surface damage detection and quantification using predicted surface properties. *Automation in Construction*, 83:285-302. 2017.
- [3] Korean Ministry of Employment and Labor. Announcement of additional statistics on industrial accidents in 2022, status of fatalities subject to accident investigation. On-line: https://www.moel.go.kr/news/eneews/report/eneews_View.do?news_seq=14546, Accessed: 29/03/2023.
- [4] United States Department of Labor. Scaffolding: Overview. On-line: <https://www.osha.gov/etools/scaffolding/>, Accessed: 29/03/2023
- [5] Kim J, Kim J, Koo N, and Kim H. Automated checking of scaffold safety regulations using multi-class 3d segmentation. In *Proceedings of the International Symposium on Automation and Robotics in Construction*, Vol. 39, pages 115-119, Bogota, Colombia, 2022.
- [6] Paik S, Kim J, Kim Y, and Kim H. Automated analysis of scaffold joint installation status of UAV-acquired images. In *Proceedings of the 9th International Conference on Construction Engineering and Project Management (ICCEPM)*,

- Las Vegas, Nevada, USA, 2022.
- [7] Nguyen NH, Perry S, Bone D, Le Thanh H, Xu M, and Nguyen TT. Combination of Images and Point Clouds in a Generative Adversarial Network for Upsampling Crack Point Clouds. *IEEE Access*, 10:67198-209. 2022.
- [8] Yang S, Xu M, Xie H, Perry S, and Xia J. Single-view 3D object reconstruction from shape priors in memory. In *Proceedings of the IEEE/CVF Conference on Computer Vision and Pattern Recognition*, pages 3152-3161, 2021.
- [9] Hu Q, Yang B, Xie L, Rosa S, Guo Y, Wang Z, Trigoni N, and Markham A. Randla-net: Efficient semantic segmentation of large-scale point clouds. In *Proceedings of the IEEE/CVF conference on computer vision and pattern recognition*, pages 11108-11117, Seattle, WA, USA, 2020.
- [10] Zhou Q, Park J, and Koltun V. Open3D: A modern library for 3d data processing, *arXiv:1801.09847*, 2018.
- [11] Jocher G. YOLOv5 by Ultralytics. On-line: <https://github.com/ultralytics/yolov5>, Accessed: 23/03/2023.

Occlusion-free Orthophoto Generation for Building Roofs Using UAV Photogrammetric Reconstruction and Digital Twin Data

Jiajun Li¹, Frédéric Bosché¹, Chris Xiaoxuan Lu² and Lyn Wilson³

¹School of Engineering, University of Edinburgh, UK

²School of Informatics, University of Edinburgh, UK

³Historic Environment Scotland, UK

J.Li-301@sms.ed.ac.uk, f.bosche@ed.ac.uk, xiaoxuan.lu@ed.ac.uk, lyn.wilson@hes.scot

Abstract -

Building roofs are a primary barrier of the building fabric to protect building interiors and their occupants from the effects of the weather. Effectively monitoring their condition and maintaining them is thus critical, and even more so in light of the increasing risks induced by climate change. Ideally, this requires frequent and careful surveying, as well as recording of the results in a way that facilitates monitoring over time. Traditional manual data collection and defect detection and recording methodologies have been used mainly on building facades. Orthophotos are commonly used for recording. However, (1) current approaches to generate orthophotos cannot ensure the photos are occlusion-free; and (2) the results cannot be efficiently recorded in a structured, digital way with semantic relationship to the corresponding elements in the building Digital Twin (DT). In this paper, a method is proposed to automatically generate high-resolution orthophotos of roof panels from UAV data, given an existing building DT. The resulting orthophotos have high-resolution (e.g. 5mm per pixel). They are occlusion-free and linked semantically to the building elements in the DT. The method is demonstrated using a real case study of a complex pitched slated roof of a traditional building.

Keywords -

Roof; UAV; Orthophoto; Photogrammetry; Occlusion; Projection.

1 Introduction

As a key building element, a roof is one of the most exposed elements to the environment. Elevated temperature, moisture, material soiling can result in staining, weathering and even damage to different materials [1]. Over time, this gradually leads to roof fragility, component failure, and load redistribution, which can create further risks to the building and its occupants [2]. Extreme climate events, such as frequent high summer temperatures, heavier winter precipitation, unpredictable wind speed, intense storms, etc, will aggravate and accelerate deterioration to all kinds of buildings. For traditional buildings, prevent-

ing failure and conservation measures have become prime considerations [3]. Therefore, building roofs should be routinely monitored, so that defects can be detected and remedied promptly.

The first difficulty of maintaining building roofs is capturing roof data, which is commonly undertaken manually. However, with the development of digital photography, Unmanned Aerial Vehicles (UAV) is increasingly used, as it reduces the cost of access provision and the risks to surveyors [4]. Meanwhile, digital photogrammetry has been an active topic for generating 3D models of buildings due to its high level of automation and the fact that it can generate 3D data at low cost [5]. The combination of these two approaches, *UAV-based photogrammetry*, has been applied to several contexts, such as archaeology, disaster monitoring, construction monitoring, building surveying, or land mapping [6].

In the Facility Management (FM) industry, Digital Twins of building assets — derived from Building Information Modelling (BIM) models — can help facility managers make and record decisions related to operation and maintenance [7]. To ease the generation of semantically-rich 3D models which are commonly the basis of Digital Twins, Scan-to-BIM methodologies can be applied to survey data acquired by laser scanning or photogrammetry. For example, Rocha et al. [8] employ a manual modelling workflow based on photogrammetry and laser scanning data to develop a BIM model of a historic house in Lisbon for conservation and restoration. In [9], Adán et al. present an integrated system to reconstruct large scenes at five semantic levels, addressing issues of automated data collection, to architectural building element modelling, to small accessory component recognition. And, Valero et al. [10] propose a Terrestrial Laser Scanning (TLS) data-processing pipeline for producing semantic 3D models of furnished office and home interiors.

Orthophoto imagery has been used for many decades in FM, most commonly in the context of (traditional) building facade surveying. The advantage is that they provide a uniform scale across the entire image, which makes them measurable (with dimensions comparable across the or-

thophoto) and more suitable for detecting, reporting and assessing building defects [11]. The generation of orthophotos is achieved by an orthographic projection on vertical planes [12, 13]. Recently, high-resolution orthophotos of facades have been used as input data for automated detection of facade defects [14, 15, 16]. These examples show that orthophotos are convenient for monitoring buildings, and accessible for actual surface measurement and (automated) analysis.

However, compared to building facades, roofs are more easily occluded by other building elements, such as chimney, dormers, aerials, satellite dishes, etc [17]. As a result, building facade orthophotos may not enable a full view of roofs. Figure 1 shows an example of orthophoto commonly generated for a whole building. One can see that, while the stone facade(s) appear(s) fully, the middle roof panel is occluded by the balustrades and chimneys. These problems challenge the generation of clear orthophotos (without occlusion and with limited blur), and ultimately the development of automatic defect detection models, as the models need to be agnostic to different image acquisition situations (e.g. angle, distance).



Figure 1. Orthophoto for the entire front elevation of Duff House.

Therefore, in this study, a method is proposed for the generation of orthophotos of pitched building roofs based on Scan-vs-BIM context afforded by an existing building DT. The approach generates vertical orthophotos that are free of occlusions from other building elements and with reduced blur.

2 Methodology

The ortho-projection method realises transformation from a dense set of images taken by UAV and the DT of the building to a set of orthophotos corresponding to all

roof panels defined in the DT.

This method contains 3 steps: 1. As-is 3D reconstruction; 2. Roof panel mask generation; 3. Orthophoto generation.

2.1 Use Case

The methodology is simultaneously explained and validated using data from Duff House, a traditional building located in Banff, Aberdeenshire, Scotland. Duff House is a category A listed, early Georgian mansion under the care of Historic Environment Scotland (HES)¹. Note that this methodology is in fact generic, and not specific to Duff House.

2.2 Step 1: Reconstructing building's as-built 3D model

Duff House was fully surveyed using a UAV equipped with a Sony ILCE-7R digital camera, with a fixed focal length of 35 mm. The UAV survey acquired 859 images containing the roof, and with over 75% overlapping, enabled a detailed and accurate 3D reconstruction of the roof (and upper parts of the facades). A full 3D reconstruction of the house exterior (facades, entrance stair case, etc.) was also obtained by merging the UAV reconstruction with a Terrestrial Laser Scanning (TLS) point cloud. The complete 3D model of Duff House is shown in Figure 2, while the roof reconstruction from the UAV data only is shown in Figure 3. The UAV data reconstruction contains 2,104,179 points registered in the world coordinate system. The roof is 34.2m in length and 25.7m in width. Therefore, the average point cloud density is approximately 2,400 points/m².



Figure 2. Duff House complete 3D reconstruction.

¹<https://www.historicenvironment.scot/archives-and-research/publications/publication/?publicationId=d752300f-2266-4574-8334-a57000ca8ed8/>

The complete roof contains 36 slated panels, 20 of which are planar and 16 are curved. Aside from the slated roof panels, there is also significant leadwork surrounding the panels, as well as chimneys and decorative components nearby, like stone ornaments and balustrades, which can cause shadow and occlusions when taking images with UAV. Panel '4' in Figure 3 will be used to illustrate the processing for occlusion handling, while all four representative panels highlighted in the figure will be shown in the section reporting the final results.

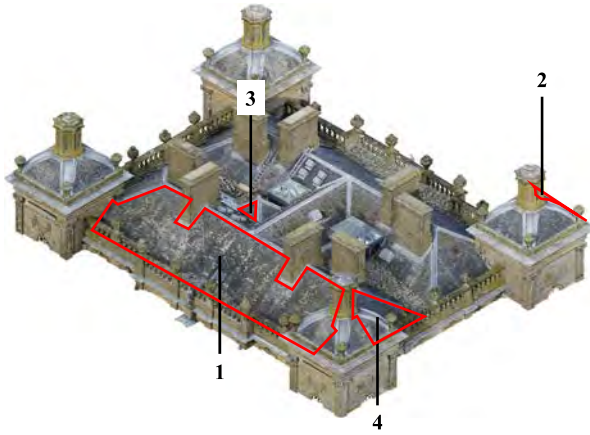


Figure 3. Reconstructed 3D point cloud of Duff House's roof. Four representative roof panels are highlighted that are used to illustrate and validate the proposed method.

Based on the input DT, a more granular model was built with an Industry Foundation Classes (IFC) object for each roof panel. This model simply needs to contain the geometry and location of each roof. As shown in Figure 4, all the panel models were built for representing only the slate part, without components such as leadwork and windows — for a reason that falls outside the scope of this paper. The geometry of each panel is defined as panel boundary with extrusion. As input to the proposed process, geometries of each roof were then defined as triangle meshes.

2.3 Step 2: Generating roof panel masks

The purpose of this step is to define, for each input UAV image, the parts of the image corresponding to a given roof panel. The boundary of each roof panel model is defined in world coordinate system. According to the input image camera external calibration in this world coordinate, this boundary can be transferred into the camera's 3D coordinate system, using equation 1.

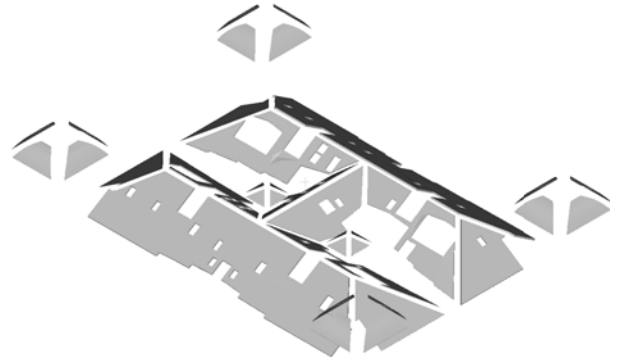


Figure 4. Roof panel models.

$$\mathbf{P}_c = \begin{bmatrix} X_c \\ Y_c \\ Z_c \end{bmatrix} = [\mathbf{R} \quad \mathbf{t}] \begin{bmatrix} \mathbf{P}_w \\ 1 \end{bmatrix} = [\mathbf{R} \quad \mathbf{t}] \begin{bmatrix} X_w \\ Y_w \\ Z_w \\ 1 \end{bmatrix} \quad (1)$$

where \mathbf{P}_c and \mathbf{P}_w are the point coordinates in camera system and world system respectively. \mathbf{R} represents the 3×3 rotation matrix in the world system, defined by the three camera rotation angles around x , y , and z axes. \mathbf{t} represents the 3×1 camera translation vector.

Some camera system would contain a polynomial distortion transformation, which is optional and varies with different camera settings. Such processing should be applied to normalize \mathbf{P}_c by dividing its first two components, X_c and Y_c , by its last one Z_c .

Next, each 3D point \mathbf{P}_c can be projected to the 2D image coordinate system, where the origin is the image centre, using equation 2. The output results u and v , in range $[-0.5, 0.5]$, are relative coordinates in the image system (centre as the origin).

$$\begin{bmatrix} u \\ v \\ 1 \end{bmatrix} = \frac{1}{Z_c} \mathbf{K} \mathbf{P}_c \quad (2)$$

where \mathbf{K} is the 3×3 camera's internal calibration matrix, containing focal length, camera skew, aspect ratio, and principle point offset. Finally, the above output results, u and v , should be scaled to the image pixels and transformed to where the top left corner is the origin of image coordinate system, as defined in Equation 3.

$$\begin{cases} \text{scale} = \max(w, h) \\ x = \text{scale} * u + w/2 \\ y = \text{scale} * v + h/2 \end{cases} \quad (3)$$

where w and h are the width and height pixels of the image. x and y compose the pixel coordinate in the image.

With this process, the boundary polygon of the target roof panel can be projected onto the image. The mask image for the input UAV image and for the given roof panel is then generated by setting the RGB value of all the pixels outside the polygon as $[0, 0, 0]$, and those inside the polygon as $[1, 1, 1]$.

By applying this process to all UAV pictures, the subset of pictures that captures at least part of a given roof panel is identified and, for each of those pictures, the set of pixels corresponding to that panel are also identified.

2.4 Step 3: Generating orthophotos

After generating all the mask images containing the given target roof panel, the masked UAV images can be converted into an orthophoto. For this, all the pixels in the masked area are projected on the model of the panel boundary in the world coordinate system, and these projections are then projected on the pre-defined orthophoto.

The plane of projection of each orthophoto is defined by computing the principal axes of the roof panel using Principal Component Analysis (PCA) [18]. A rotation matrix \mathbf{R}_{PCA} derived in this process defines the projection plane of the orthophoto in the world coordinate system of the reconstructed DT mesh data. As illustrated in Figure 5, the plane YOZ is the orthophoto projection plane for the roof panel '4'.

The orthophoto generation process then includes 3 steps: 1. (2D-3D) All the coloured 2D pixels in original masked image are firstly projected to the DT mesh data, with corresponding 3D points as output; 2. (3D-2D) All the 3D points derived are then projected onto the orthophoto plane. 3. The orthophoto boundary in the projection plane is then set based on the projection of the panel geometry and the resolution of the orthophoto is set to the required value — we use $5mm \times 5mm$ per pixel.

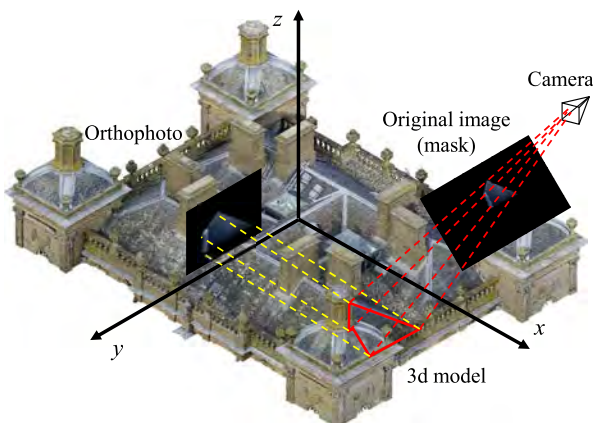


Figure 5. Orthophoto generation.

The outcome of the above process is an orthophoto

generated from each of the input UAV picture and for each given roof panel. These orthophotos can be used as-is for analysis. However, because of the fact that the original UAV images were taken from different angles and locations, pixels from occluders still exist and resolution artefacts can appear. The orthophoto in Figure 6a is a typical example: some pixels remain black because no original pixel reprojects on them, because the input image was too far and oblique. Also, the orthophoto contains occlusions by a nearby chimney.

We address these issues by merging all orthophotos for one roof panel into one. The images can be merged into one, by calculating the median value of the RGB for each orthophoto pixel. If, as we have observed, occlusions appear in fewer than 50% of the images, merging the orthophotos could help eliminate occlusions. Figure 6b shows the result of merging the 45 orthophotos obtained from the 45 UAV images in which roof panel '4' appears.

As can be seen, the resulting orthophoto is free of pixels from occluders and also does not contain any hole (i.e. empty pixel) in the roof panel area. However, careful observation shows that these merged images often contain significant amount of blur, which is attributed to small errors from the photogrammetric process.

To reduce the influence of these errors, the small shifts between images are detected and a correction applied. For this, Scale-Invariant Feature transform (SIFT) features are detected and matched across images [19]. Figure 7 shows the SIFT feature matching between two orthophotos. The green lines show SIFT matches between them two. Based on this, the homography can be computed and applied to the right orthophoto before merging it with the left one. This process is applied by selecting one orthophoto as the baseline, and shifting all the other ones to align them to it. The baseline orthophoto is ideally the one with best visual quality, and is selected by choosing the smallest values of the filtering parameters introduced below.

Afterwards, the median value for each pixel can be calculated taking into account all shifted orthophotos, to generate a merged orthoimage. As can be seen in Figure 6c, the resulting median orthophoto has less blur than that of the initial median orthophoto.

However, due to the fact that images were taken from various distances and with various incidence angles, not all the images contribute well to the merged orthophoto. Therefore, image filtering should first be carried out based on the angle and distances in order to remove those images that are just taken from too far or with angles that are too oblique. As illustrated in Figure 8, we define the ray shot from the pinhole camera O_i through the image centre C_i , and the intersection point with the roof plane is named as C'_i . Let's call C_p the centre of the target panel, and \vec{n}_p its normal. Therefore, the first filtering parameter in

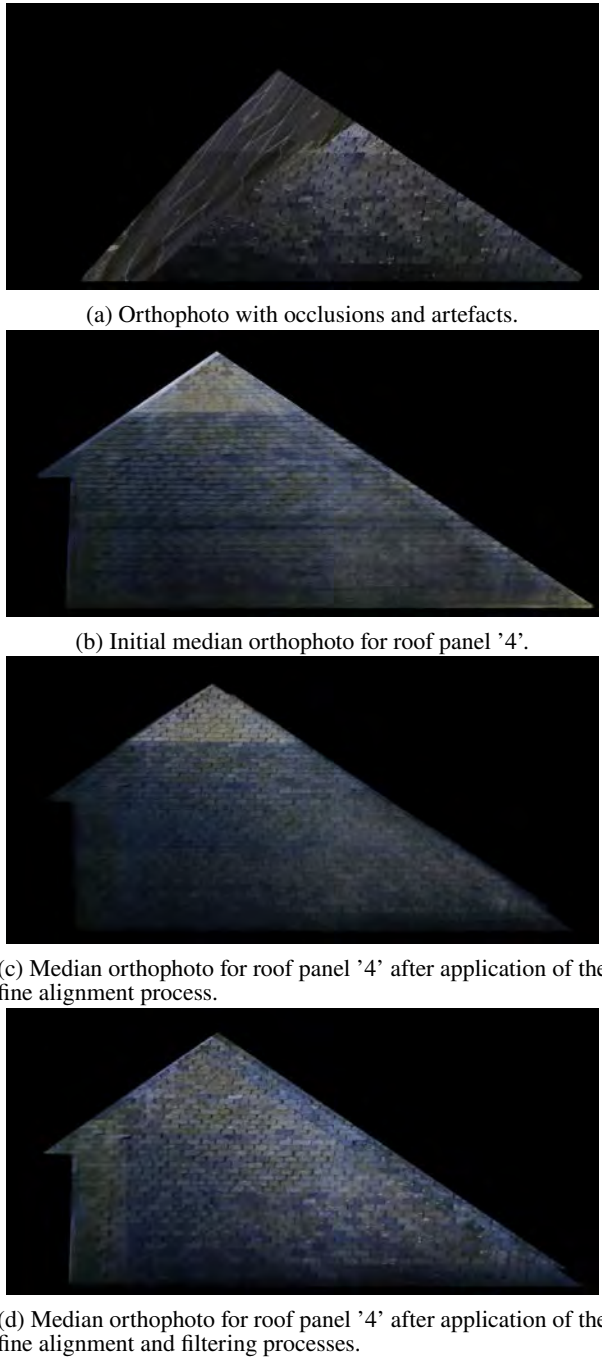


Figure 6. Merging result comparison between different datasets.

this study is the angle α_{pi} between $\overrightarrow{C'_i O_i}$ and \vec{n}_p , which captures the picture incidence angle between respect to the roof panel. The second filtering parameter d_{pi}^1 is the distance $\|\overrightarrow{O_i C'_i}\|$, which broadly captures the distance from the camera to the roof panel along the view direction. Finally, the third filtering parameters d_{pi}^2 is the distance

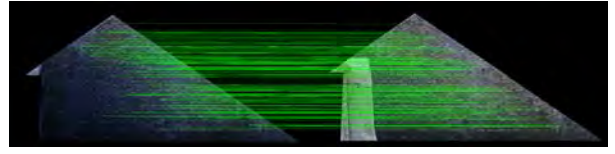


Figure 7. Pixel shifting.

$\|\overrightarrow{C_p C'_i}\|$ normalised by the maximum dimension of this panel d_p^{max} , which can be used to measure whether the camera is pointing at the target panel or away from it. The smaller α_{pi} , d_{pi}^1 and d_{pi}^2 are, the better the capture of the roof panel in the image should be.

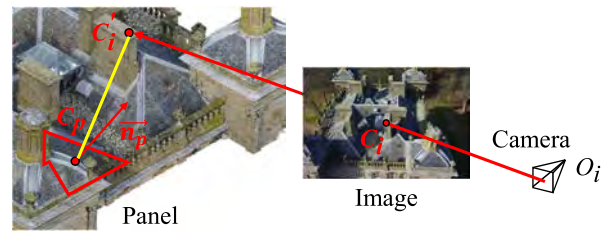


Figure 8. Explanation of different parameters for screening.

In the Duff House example, as mentioned earlier, initially 45 images contain the target roof panel '4'. Their α_{pi} , d_{pi}^1 and d_{pi}^2 values are presented in the 3D scatter plot in Figure 9. For the target panel here, the thresholds for α_{pi} , d_{pi}^1 and d_{pi}^2 are: 45° , 34m and 2. The angle 45° is defined somewhat arbitrarily but is set because beyond that images would be too oblique. The distance 34m is set as twice the value of the average UAV flying height from the roof. The relative distance 2, means twice the value of the largest dimension of the roof. In this case, 12 images simultaneously meet all these three requirements. Figure 6d shows the median orthophoto obtained using only the filtered set of images.

The final orthophoto in Figure 6d presents significantly less blur than the median orthophoto in Figure 6c obtained without image filtering. Furthermore, the proposed image dataset filtering appears to help balance the lighting condition in the whole image, with Figure 6b and Figure 6c both showing a brighter section at the top of the panel, while Figure 6d does not show it.

3 Further Results

The application of the proposed method to four representative panels in Figure 3 are reviewed here. Panel '1' is the largest panel within the whole roof, placed on the front and back side of the house (easily occluded by balustrades, chimneys and towers in some images, it doesn't appear

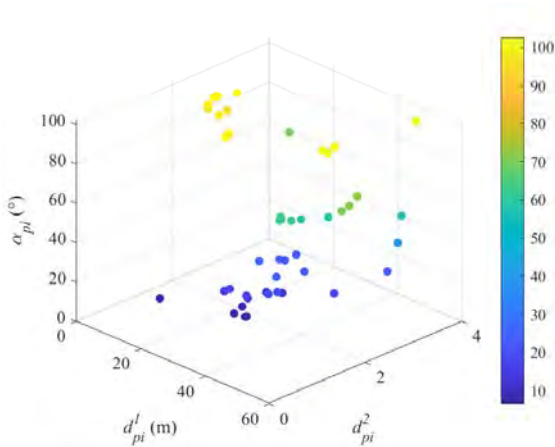


Figure 9. α_{pi} , d_{pi}^1 and d_{pi}^2 in different images.

completely in any single image). Panel '2' is a curved panel placed on the one of the towers of the house (easily occluded by stone ornaments). Panel '3' is one of the triangular panels placed near the middle of the roof with almost no occlusion. Finally, Panel '4' is one of the panels placed on the side of the house (easily occluded by the towers and balustrades on the edges).

The results obtained for panel '1' to '3' are shown in Figure 10. The results are evaluated qualitatively and quantitatively, considering: 1. whether the occlusions from other components have been removed; 2. the general level of blur the orthophoto presents (which can be evaluated by assessing the sharpness of the boundary of each slate); and 3. the mean percentage of matched features \bar{a} described below.

To quantify the quality of the final merged orthophoto for each panel, we propose to use the *mean percentage of matched features*, \bar{a} , calculated as:

$$\bar{a} = \frac{\sum_{i \in \mathcal{O} \setminus \{b\}} |\mathcal{F}_i^b|}{|\mathcal{F}_b|} \quad (4)$$

where \mathcal{O} is the set of orthophotos associated to the given panel, b is the baseline orthophoto, and \mathcal{F}_i^b is the set of SIFT features from orthophoto i matched to the baseline orthophoto, and \mathcal{F}_b is the set of SIFT features from orthophoto b .

Panel '1' presents the worst result, with the most significant and uneven level of blur. For this panel, $\bar{a} = 5\%$, which is the lowest among all the panels. This is likely due to the large size of the panel, which results in the whole panel not being seen completely in any single image meeting the acquisition minimum requirements in terms of the parameters α_{pi} , d_{pi}^1 and d_{pi}^2 . As a result, the alignment process described in Section 2.2 starts with one image that only covers a part of the roof. Notwithstanding, in comparison to Figure 1, all the potential occlusions for this

panel are successfully removed. The result for the curved Panel '2' is better, with $\bar{a} = 16\%$. This is likely because it is smaller and not as occluded, so that the baseline orthophoto has more matches with the other orthophotos have the most matches with the baseline. In the smallest Panel '3', the details are more clear under magnification: defects like the shallow organic growth appear very clearly. In this case again, $\bar{a} = 12\%$. Note that, for Panel '4', $\bar{a} = 10\%$. In general, The \bar{a} values of panel '2' to '4' are high.

The orthophoto examples in Figure 6d and Figure 10 illustrate two advantages: the slated roofs are clearly and precisely extracted and may thus be well suited for the application of automated defect detection models (e.g. deep learning based models). Besides, no matter which angle was the image taken or where the panel is located, the final orthophotos are all vertical, with the slates appearing as parallel horizontal rows in all images. This should further ease the development and application of robust automated defect detection models — and such representation also remains suited for manual defect annotation using current manual methodologies.

4 Discussion

The novel method for generating vertical orthophotos free of occlusions shows good results. Occlusions are currently handled by analysing the frequency of RGB and selecting the median value. While the method works reasonably well in the four representative examples presented, in some extreme cases, occlusions could appear in a large(r) number of images, which would defeat the proposed approach and cause shadows in the final merged orthophotos. For example, when some decorative components are placed right above or too close to the target panel, only when the UAV is flown exactly at the right location can the entire panel be captured without occlusion, which would require great skills as well as meticulous planning by the operator.

An alternative, more robust approach to deal with occlusions is to use depth information to refine the image masks (see section 2.3). Indeed, if the panel view is unobstructed, the depth associated to a pixel should be the range of the ray going through the pixel and intersecting the roof panel plane. But, if the ray intersects the overall reconstruction mesh (see Figure 2) at an occluding point, then the range will be significantly shorter, and the pixel should be labelled occluded and added to the mask. The remaining steps of the proposed process would then be applied as described.

From the final orthophoto of the curved panel, the slates closer to the top appear narrower than the ones near the bottom, due to the curvature of the panel. This illustrates the limitation of using vertical orthophotos. To solve such

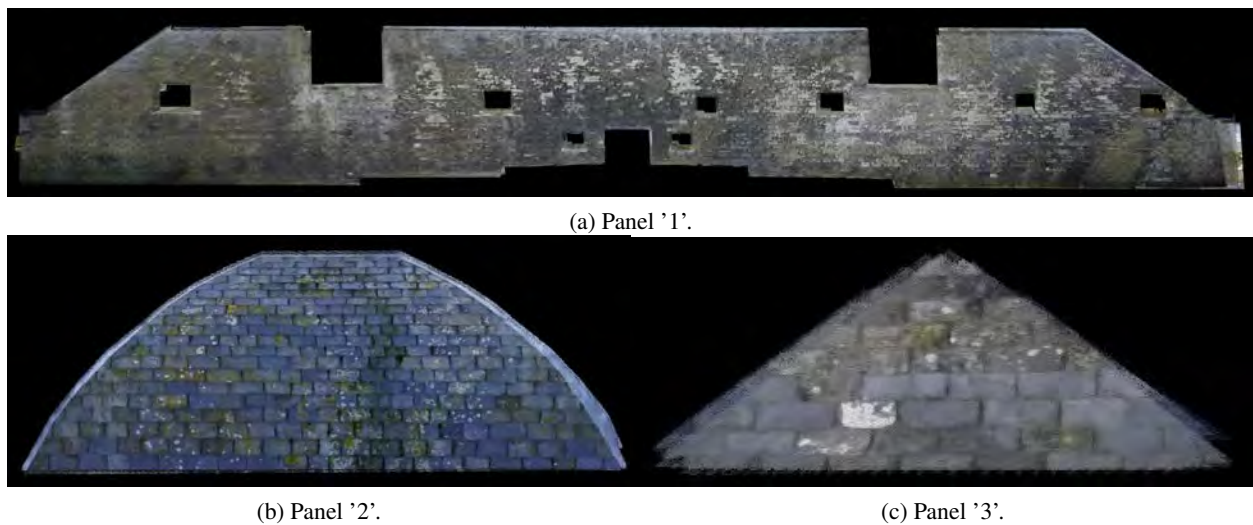


Figure 10. Generated orthophotos of typical panels.

a problem, an alternative approach to create orthophotos could be to define the projection plane perpendicular to the mean normal of the roof panel, i.e. along the two principal axes of the panel. Note that this would benefit the generation of orthophotos of planar roof panels as well. The reason why we have focused on generating vertical orthophotos is that this is in line with current practice by surveying professionals (as shown in Figure 1).

5 Conclusion

Current approaches to generate orthophotos for entire building facades have two main limits: lacking semantic link to the BIM model, and unavoidable occlusions in specific building area. To deal with these problems, this study proposes a new approach that generates an orthophoto for each building element, and illustrates the method specifically in the challenging context of roofs. The proposed method combines building reconstruction, camera projection, and orthophoto image generation with occlusion removal. The main benefits of the proposed approach are:

1. Orthophotos contain data for all parts of the roof elements and occlusions by other building elements are eliminated through the proposed merging mechanism that calculates the median orthophoto.
2. By introducing image filtering parameters (i.e. incidence angle and distances), the quality of the final merging orthophoto is further improved, with less blur and seemingly improved colour balancing.
3. Given a 3D model, the orthophoto generation process is fully automatic, and could bring convenience to current surveying practice, as well as emerging digitalised and automated methodologies, with the orthophotos (and any result that would be obtained

from their analysis) semantically linked to elements in the Digital Twin or Digital Logbook — of the building.

4. The proposed method can be applied to drone survey data acquired (at frequent intervals in the case of pro-active maintenance schemes) over the life of the building. The orthophotos acquired at each epoch can be used to detect defects and the comparison of the results across epochs be used to assess the evolution of defects over time.

6 Acknowledgements

This paper was made possible thanks to research funding from Historic Environment Scotland (HES) and the Engineering and Physical Sciences Research Council (EPSRC) [grant reference EP/W524384/1]. The views and opinions expressed in this article are those of the authors and do not necessarily reflect the official policy or position of HES and EPSRC. The authors would also like to acknowledge the HES Digital Documentation team for providing us with both the image and point cloud data used in the experiments reported in this paper. The authors appreciate the help from members of Cyberbuild group, including Dr Martin Bueno, Dr Shirin Malihi and Mr Boan Tao. For the purpose of open access, the authors have applied a Creative Commons Attribution (CC BY) licence to any Author Accepted Manuscript version arising from this submission.

References

- [1] Paul Berdahl, Hashem Akbari, Ronnen Levinson, and William A. Miller. Weathering of roofing materials – An overview. *Construction and Building*

- Materials*, 22(4):423–433, 2008. ISSN 0950-0618. doi:10.1016/j.conbuildmat.2006.10.015.
- [2] Mark G. Stewart, John D. Ginger, David J. Henderson, and Paraic C. Ryan. Fragility and climate impact assessment of contemporary housing roof sheeting failure due to extreme wind. *Engineering Structures*, 171:464–475, 2018. ISSN 0141-0296. doi:10.1016/j.engstruct.2018.05.125.
- [3] C. H. Sanders and M.C. Phillipson. Uk adaptation strategy and technical measures: the impacts of climate change on buildings. *Building Research & Information*, 31(3-4):210–221, 2003. doi:10.1080/0961321032000097638.
- [4] Anna Banaszek, Sebastian Banaszek, and Anna Cellmer. Possibilities of use of uavs for technical inspection of buildings and constructions. *IOP Conference Series: Earth and Environmental Science*, 95(3):032001, dec 2017. doi:10.1088/1755-1315/95/3/032001.
- [5] Anestis Koutsoudis, Fotis Arnaoutoglou, and Christodoulos Chamzas. On 3D reconstruction of the old city of Xanthi. A minimum budget approach to virtual touring based on photogrammetry. *Journal of Cultural Heritage*, 8(1):26–31, 2007. ISSN 1296-2074. doi:10.1016/j.culher.2006.08.003.
- [6] J. Unger, M. Reich, and C. Heipke. Uav-based photogrammetry: monitoring of a building zone. *The International Archives of the Photogrammetry, Remote Sensing and Spatial Information Sciences*, XL-5:601–606, 2014. doi:10.5194/isprsarchives-XL-5-601-2014.
- [7] De-Graft Joe Opoku, Srinath Perera, Robert Osei-Kyei, and Maria Rashidi. Digital twin application in the construction industry: A literature review. *Journal of Building Engineering*, 40:102726, 2021. ISSN 2352-7102. doi:https://doi.org/10.1016/j.jobe.2021.102726.
- [8] Gustavo Rocha, Luís Mateus, Jorge Fernández, and Victor Ferreira. A scan-to-bim methodology applied to heritage buildings. *Heritage*, 3(1):47–67, 2020. ISSN 2571-9408. doi:10.3390/heritage3010004.
- [9] A. Adán, B. Quintana, S.A. Prieto, and F. Bosché. An autonomous robotic platform for automatic extraction of detailed semantic models of buildings. *Automation in Construction*, 109:102963, 2020. ISSN 0926-5805. doi:10.1016/j.autcon.2019.102963.
- [10] Enrique Valero, Antonio Adán, and Frédéric Bosché. Semantic 3d reconstruction of furnished interiors using laser scanning and rfid technology. *Journal of Computing in Civil Engineering*, 30(4):04015053, 2016. doi:10.1061/(ASCE)CP.1943-5487.0000525.
- [11] Ayman F Habib, Eui-Myoung Kim, and Chang-Jae Kim. New methodologies for true orthophoto generation. *Photogrammetric Engineering & Remote Sensing*, 73(1):25–36, 2007. doi:https://doi.org/10.14358/PERS.73.1.25.
- [12] Gary S Smith. Digital orthophotography and gis. In *Proceedings of the 1995 ESRI User Conference*, pages 22–26, 1995.
- [13] Yu Liu, Xinqi Zheng, Gang Ai, Yi Zhang, and Yuqiang Zuo. Generating a high-precision true digital orthophoto map based on uav images. *ISPRS International Journal of Geo-Information*, 7(9), 2018. ISSN 2220-9964. doi:10.3390/ijgi7090333.
- [14] Enrique Valero, Alan Forster, Frédéric Bosché, Ewan Hyslop, Lyn Wilson, and Aurélie Turmel. Automated defect detection and classification in ashlar masonry walls using machine learning. *Automation in Construction*, 106:102846, 2019. ISSN 0926-5805. doi:https://doi.org/10.1016/j.autcon.2019.102846.
- [15] Koubouratou Idjaton, Xavier Desquesnes, Sylvie Treuillet, and Xavier Brunetaud. Stone-by-stone segmentation for monitoring large historical monuments using deep neural networks. In *Pattern Recognition. ICPR International Workshops and Challenges*, pages 235–248, Cham, 2021. doi:10.1007/978-3-030-68787-8_17.
- [16] Koubouratou Idjaton, Xavier Desquesnes, Sylvie Treuillet, and Xavier Brunetaud. Transformers with yolo network for damage detection in limestone wall images. In *Image Analysis and Processing. ICIAP 2022 Workshops*, pages 302–313, 2022. doi:10.1007/978-3-031-13324-4_26.
- [17] Philipp Meixner, Franz Leberl, and Mathieu Brédif. 3d roof details by 3d aerial vision. In *2011 IEEE International Conference on Computer Vision Workshops (ICCV Workshops)*, pages 212–218, 2011. doi:10.1109/ICCVW.2011.6130245.
- [18] Chi Yuan, Xiaoqing Yu, and Ziyue Luo. 3d point cloud matching based on principal component analysis and iterative closest point algorithm. In *2016 International Conference on Audio, Language and Image Processing (ICALIP)*, pages 404–408, 2016. doi:10.1109/ICALIP.2016.7846655.
- [19] David G. Lowe. Distinctive image features from scale-invariant key points. *International Journal of Computer Vision*, 60(2):91–110, 2004. doi:10.1023/B:VISI.0000029664.99615.94.

Geometric control of short-line match casting using Computational BIM

¹Nandeesh Babanagar, ¹Ashwin Mahalingam, ¹Koshy Varghese, and ²Vijayalaxmi Sahadevan

¹Department of Civil Engineering, Indian Institute of Technology Madras, India

²Center for Product Design and Manufacturing, Indian Institute of Science Bangalore, India
nandeesh.babanagar@gmail.com, mash@civil.iitm.ac.in, koshy@iitm.ac.in, svijaya16@gmail.com

Abstract

Short-line match casting is a method of producing segmental pre-cast concrete bridges. This segment production process is centralized, repetitive, compact, and is easily adaptable to geometry variations such as plan, vertical, and transition curves. But the main challenge is the complexity of geometry control and the need for high accuracy. The complexity arises due to the changing coordinate system and the accumulation of errors for each segment. Although the method can adapt geometries involving transition curves, it is susceptible to geometric errors that accumulate over the entire span resulting in significant deviation from the alignment. This calls for rigorous geometry control during the casting process. The current work proposes a framework/workflow, called the Geometric Error Minimization for Bridge Segment Casting (GEMBSC), for minimizing geometric errors in segmental casting alignment in real-time. It involves the formulation of an iterative geometric control algorithm using the least-square method and a software tool to manage the geometric control workflow. Dynamo, a computational BIM tool, was used to extract the coordinates from the BIM model and perform coordinate transformations that feed to the surveying instruments. Subsequently, the tool compares the as cast data with the planned geometry data and runs the error minimization algorithm to output the corrected coordinates for the casting of subsequent segments. The algorithm was validated based on past real-world data by the results obtained for the same data through a proprietary software application. The results indicated that GEMBSC is effective in minimizing errors along with providing other benefits such as savings in time and effort involved in error corrections with existing software use.

Keywords –

Computational BIM, Short-line match casting, Dynamo Visual Programming

1 Introduction

Segmental pre-casting of prestressed concrete bridges is a technique that offers many benefits to bridge construction in terms of time savings and quality of construction. The casting of all the segments of the bridge takes place in the casting yard thereby ensuring quality control of the segments [1]. One of the key components of the segments is the shear keys that need to interlock accurately during the erection process. Improper joints between segments coupled with high post-tensioning forces could lead to cracking and subsequent collapse of the final structure. Hence, accuracy in geometries of the segments during the casting is crucial to the process.

The casting of segments in the yard typically takes place either using the long line method or the short line method. In the Long line method, the moulds of the whole span are aligned as per the required geometry and the segments are cast one by one in their respective positions. However, long-line casting elevation has limitations when casting spans with large horizontal and vertical curvature due to space requirements [2].

On the other hand, in the short line method, one segment is cast at a time. As shown in Figure 1, the segment which is cast earlier acts as a formwork on one side whereas a fixed formwork is present at the other end.

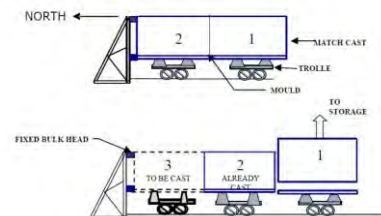


Figure 1: Schematic of Short-line match casting

After the segment is cast the previously cast segment is moved to the stacking yard and the current segment is moved to the position of the previous segment. This process is repeated till all the segments are cast. Hence, the short line approach is preferred over the long line

method in projects with space restrictions and spans with higher curvatures [3].

Although the method can adapt geometries involving intricate transition curves [4], it is susceptible to geometric errors that accumulate over the entire span resulting in significant deviations from the plan [5]–[8]

- Misalignment while translation from wet cast to match cast position
- Sliding of the segment in the match cast position from its fixed position due to the expansion of iron rails on which the whole assembly moves
- Movement of form mounted on rails during concreting due to vibrations
- Movement/ settling of jacks on which the segment is supported.
- Movement of dry segments due to horizontal pressure from wet concrete.
- Mistakes/errors in surveying
- Other human errors like positioning of punch plates.

This calls for rigorous geometric control during the casting process. Several proprietary geometry control software is available to streamline and simplify the surveying operations. These geometry control procedures are based on surveying of elevations combined with the double measurement with a tensioned tape of the sides and diagonals of rectangular top slabs [6]. In addition to the cost incurred in the procurement of such software and its utilization in correcting geometric errors, the casting personnel must often spend enormous amounts of time and effort in calculating these errors and minimizing them in the casting process. Therefore, there is a need for a framework/workflow for automatically minimizing geometric errors in segmental casting alignment in real time [9].

The geometric control process, if implemented with BIM, would lead to real-time updating of the BIM model which could further provide several other advantages. Hence, the current work aims to develop a model/framework for automated elimination of geometric errors and updating of the BIM model.

Towards this end the objective of the current work was to formulate a workflow for the real-time geometrical error minimization during segment casting called the Geometric Error Minimization for Bridge Segment Casting (GEMBSC). The formulation of the workflow mainly involved the formulation of a mathematical solution and its translation to visual programming script. The framework consists of four modules: Coordinates exporter from Revit model, Starter Segment Setup, Typical Segment Setup, and Generation of As Cast Model. The model was tested using past real-world data of segment casting. The results were compared with the results obtained from proprietary software.

This paper is organized into six sections. The second section discusses the existing studies in geometric error minimization in bridge segment casting. The third and fourth sections discuss the formulation of the mathematical solution and the description of the various modules of the GEMBSC. The final two sections comprise of the Results and the Summary and Conclusion.

2 Related Work

The geometric control must start from the conceptual design phase and be kept in mind throughout the design, detailing the casting curve, preparing production plan, and shop drawings phases [10]. Researchers have discussed techniques for geometric control in segmental match casting. Among the earliest works, [11] provided guidelines and steps to minimize geometrical errors caused solely due to twists. Although the suggestions are useful in preventing geometrical errors, they do not provide real-time predictions of errors during the casting process. A researcher [6] proposed a procedure that could be utilized in geometrical control software. However, the study does not consider a few types of errors and therefore has limitations. Also, the correction of the errors in the proposed software occurs in a single step which could lead to sharp changes in the bridge alignment. Similarly, [8] proposed a new MATLAB based platform for geometric corrections of bridge segments and implemented it using a case study. Similar studies have been conducted by researchers such as [4], [12], [13]. Most of the above-mentioned techniques do not focus on BIM integration for monitoring and correction of geometric errors. Further, several of the existing studies have been conducted using proprietary software.

A researcher [14] has proposed a BIM and 3D laser scanning framework to produce an automated and reliable dimensional and surface quality assessment for precast concrete elements which is more specific to the surface defect identification. A similar method can be applied to automate the process of collecting the data of the precast segments. However, for the purpose of geometric control of a bridge segment, which is governed by six control coordinates, processing of point cloud of entire segment may be computationally expensive at this point in time.

From the review of literature on the existing techniques in geometric corrections, it is evident that different techniques focusing on geometrical error minimization for bridge segment casting have been explored. However, most of the techniques have limitations in terms of effectiveness and implementation and could also have cost and time implications. Further, currently available BIM related tools and interfaces could

facilitate simpler geometrical formulations for the automation of the workflow on geometric correction and revision of BIM as cast models.

3 Geometric error compensation:

There are two strategies to compensate for the geometric errors in the casting of any segment, single step and progressive nullifying of errors. To avoid the sharp changes and kinks in bridge alignment that could result from single step nullifying of errors, progressive minimization of errors was adopted. This strategy involves gradual correction of errors by converging the fore joint coordinates of the succeeding few segments toward the planned alignment.

The Least Square Method is a popular method used by researchers for correction of geometric errors. The least squares method is applicable for adjustment of the basic measurements made in surveying, including observed differences in elevation, horizontal distances, and horizontal and vertical angles. The principle of least square is that if the sum of the squares of the errors in a system are minimized, the points will fit best in the system.

3.1 Mathematical Solution Formulation

The logic used in error correction using Least Square method is demonstrated in Figure 2.

In Figure 2, S1 is the span of first segment
S(last) is the last segment of the span

S(n-1) is the previous segment in which error has occurred

S(n) is the current segment for which the corrected coordinates need to be calculated

Fc = Coordinates of the first segment at the center

Lc = Coordinates of the last segment at the center

Pe, Pc, and Pw = Planned Coordinates of the previous segment at East, Center and West side

Pae, Pac, and Paw = Actual coordinates of the previous segment at East, Center and West side

Ce, Cc, and Cw = Planned coordinates of the current segment at East, Center and West side

As shown in Figure 2, the distance between Pe and Ce represents the width of the segment and the distance between Ce and Cw represents the length of the segments. The aim of the geometry correction exercise here is to find the revised coordinates of the points Ce, Cc and Cw. Figure 2 also illustrates the network of relationships between segment coordinates and errors.

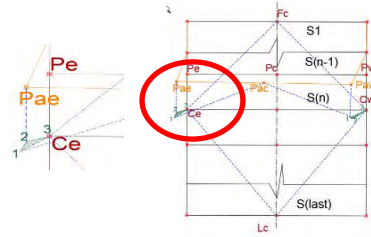


Figure 2: Network of relationship between segment coordinates and errors

A relationship between actual coordinates of the previous segment (Pae) and the succeeding segments (Ce) is set up such a way that it represents the same relationship that existed between the planned coordinates (i.e., between Pe and Ce). This relationship indicates a new position for point Ce. Since the system is over-determined, a unique point for Ce is not obtained but three different points 1,2,3 as shown in the figure are obtained. Applying least square principle we will find a point within the boundaries of the three different points suggested (a hatched region in the figure) that has the least sum of squares from all the boundary points (1,2 and 3).

Hence, the corrected coordinates of point Ce and Cw are obtained by considering them as floating points. The solution which is the best fit is obtained after the rigorous iterative procedure of minimizing the errors. The point Cc will then be computed as a midpoint between Ce and Cw. The error which occurred in segment S(n-1) is not nullified yet, but the error has reduced, and the alignment is tending towards the planned alignment. When the same calculation procedure is repeated for the succeeding segments S(n+1) and S(n+2) and so on, the error gradually reduces, and the actual alignment converges with the planned alignment.

Since the horizontal alignment of the bridge is governed by the center coordinates and the elevation is governed by the outer four coordinates the X, Y coordinates and Z coordinates are calculated separately. Hence two networks of relationships are set up, one for horizontal adjustment and another for leveling adjustment. In the horizontal network, the X and Y coordinates of Ce and Cw must be determined. Therefore, there are four unknowns present in the horizontal network. In the vertical network, there are two variables, the Z coordinates of the points Ce and Cw.

Setting up relationship between points: The relationship between the points can be modeled in different ways such as position, distance, and direction using method of triangulation or using only position and distance in method of trilateration. Trilateration network is much easier and is adequate for this case as the measurement of errors are in terms of distances.

Any Linear distance between i and j can be written as:

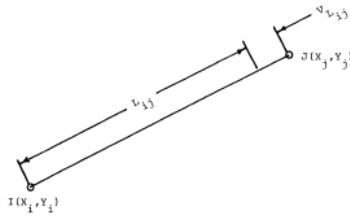


Figure 3: Error in measurement between points two points

$$L_{ij} + V_{ij} = F(X_i, Y_i, X_j, Y_j) \text{ (figure 3)}$$

$$F(X_i, Y_i, X_j, Y_j) = \sqrt{(X_i - X_j)^2 + (Y_i - Y_j)^2}$$

Here, L_{ij} is the observed length of the line IJ , V_{ij} is the error in the observation. X_i, Y_i, X_j and Y_j are the X and Y coordinates of the point I and J respectively.

Applying Taylor's series approximations and neglecting the higher order terms, the following equations were derived.

$$\begin{aligned} X_i &= X_{i0} + dX_i & Y_i &= Y_{i0} + dY_i \\ X_j &= X_{j0} + dX_j & Y_j &= Y_{j0} + dY_j \end{aligned}$$

By evaluating the partial derivatives of the function F , and solving we get

$$K_{L_{ij}} + V_{ij} = \left[\frac{X_{i0} - X_{j0}}{I_{j0}} \right] (dX_i) + \left[\frac{Y_{i0} - Y_{j0}}{I_{j0}} \right] (dY_i) + \left[\frac{X_{i0} - X_{j0}}{I_{j0}} \right] (dX_j) + \left[\frac{Y_{i0} - Y_{j0}}{I_{j0}} \right] (dY_j)$$

$$\begin{aligned} \text{Where } K_{L_{ij}} &= L_{ij} - I_{j0} \\ I_{j0} &= \sqrt{(X_{j0} - X_{i0})^2 + (Y_{j0} - Y_{i0})^2} \end{aligned}$$

Based on the above result, the trilateration relationship between points $F_c - C_e$ and F_c to C_w is setup considering C_e and C_w as floating points with planned coordinates as initial approximations. Since the error are present, the actual distance between F_c and C_e will be $L1'$ instead of $L1$. The relationships can be represented in the form of a matrix. Since there are relationships containing error values (from point P_{ac}), the least square method mainly involves finding a fit for the points C_e and C_w which will minimize the error of the whole system of relationships. Since this method finds the difference that needs to be added to the initial approximations of the points C_e and C_w , it is called the method of variation of coordinates.

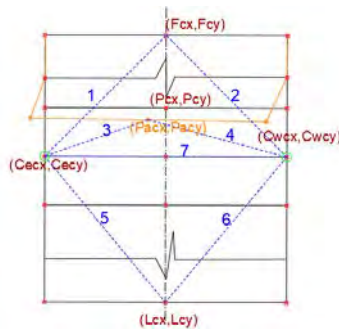


Figure 4: Horizontal network relationships

The matrix of relationships can be represented as:

$$AX = K + V$$

Where,

$$A = \begin{pmatrix} \frac{C_{ecx} - F_{cx}}{L1} & \frac{C_{ecy} - F_{cy}}{L1} & 0 & 0 \\ 0 & 0 & \frac{C_{wcx} - F_{cx}}{L2} & \frac{C_{wcy} - F_{cy}}{L2} \\ \frac{C_{ecx} - P_{acx}}{L3} & \frac{C_{ecy} - P_{acy}}{L3} & 0 & 0 \\ 0 & 0 & \frac{C_{wcx} - P_{acx}}{L4} & \frac{C_{wcy} - P_{acy}}{L4} \\ \frac{C_{ecx} - L_{cx}}{L5} & \frac{C_{ecy} - L_{cy}}{L5} & 0 & 0 \\ 0 & 0 & \frac{C_{wcx} - L_{cx}}{L5} & \frac{C_{wcy} - L_{cy}}{L5} \\ \frac{C_{ecx} - C_{wex}}{L7} & \frac{C_{ecy} - C_{ocy}}{L7} & \frac{C_{wcx} - C_{ex}}{L7} & \frac{C_{wcy} - C_{ocy}}{L7} \end{pmatrix}$$

$$X = \begin{pmatrix} dX_e \\ dY_e \\ dX_w \\ dY_w \end{pmatrix} \quad K = \begin{pmatrix} L1 - L1' \\ L2 - L2' \\ L3 - L3' \\ L4 - L4' \\ L5 - L5' \\ L6 - L6' \\ L7 - L7' \end{pmatrix}$$

Where,

$$\begin{aligned} L1 &= \sqrt{(C_{ex} - F_{cx})^2 + (C_{ey} - F_{cy})^2} \\ L1' &= \sqrt{(C_{ecx} - F_{cx})^2 + (C_{ecy} - F_{cy})^2} \\ L2 &= \sqrt{(C_{wx} - F_{cx})^2 + (C_{wy} - F_{cy})^2} \\ L2' &= \sqrt{(C_{wex} - F_{cx})^2 + (C_{wcy} - F_{cy})^2} \end{aligned}$$

Similarly, $L3$ to $L7$ and $L3'$ to $L7'$ can be computed between other points shown in the image 4

A is the matrix of relationships

X is the matrix of variation of coordinates $X_e, Y_e, X_w,$ and Y_w

K is the matrix of the difference between planned and actual distances.

V is the matrix containing the errors.

Upon solving for the matrix X , we get the correction factor which needs to be applied to the planned coordinates of subsequent segments to be cast.

The same logic was utilized for the vertical error adjustment. The above mathematical operations were modelled using visual programming tools.

3.2 The GEMBSC framework

The Figure 5 shows the flow chart of the complete operation of the Geometric correction algorithm. As shown in Figure 5 the solution framework consists of four main components: 1. Coordinate Exporter, 2. Starter segment Set-up, 3. Typical Segment correction, and 4. As cast model generator.

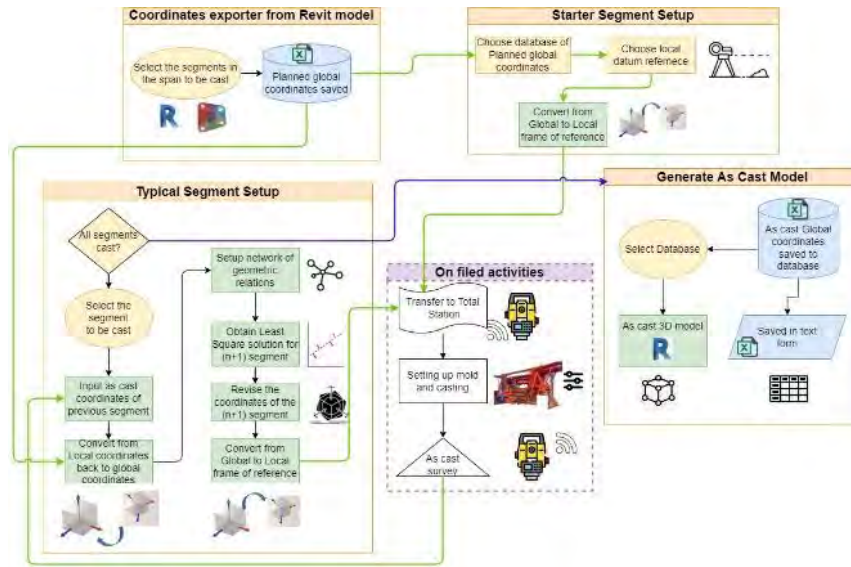


Figure 5: Solution framework

3.2.1 Module-1: Coordinate Exporter

The steps corresponding to Module-1 shown in Figure 5 are discussed below.

1. The model elements selected are filtered based on the Family type of “Control Points”.
2. The Control points which are marked in order of East, centre and west for each joint by the designers. These are extracted and sorted based on the index number of the point in the list.
3. Each joint has three control coordinates, hence the points at index 0,3,6,9 and so on are stored in a list of East control points, Points at index 1,4,7,10, etc. are stored in Center control points list and the remaining points are stored in the West control point list.
4. These lists are combined in a standard format in a multilevel list
5. The data is written to an Excel file, from the path which will be chosen by the user.

Figure 6 shows the interface of coordinator exporter module whereas Figure 7 shows the screenshot of the output of the coordinate exporter module.



Figure 6: Coordinate Exporter module

Joint	XE	YE	ZE	XC	YC	ZC	XW	YW	ZW
0	-248.5	-8.52673	10.66026	-246.6	-8.52673	10.66026	244.1	-8.52673	10.66026
1	-244.1	-0.85228	10.66026	-241.2	-8.52673	10.66026	-241.2	-8.5132	10.66026
2	-241.2	8.82206	10.66012	-238.3	-8.52673	10.66026	-238.3	-8.5038	10.66026
3	-238.3	8.82202	10.66026	-235.4	-8.52678	10.66026	-235.4	-8.5197	10.66026
4	-235.4	8.82246	10.66026	-232.5	-8.52673	10.66026	-232.5	-8.5296	10.66026
5	-232.5	8.82183	10.66026	-229.6	-8.52673	10.66026	-229.6	-8.5208	10.66026
6	-229.6	8.82205	10.6602	-226.7	-8.52672	10.66026	-226.7	-8.5182	10.66026
7	-226.7	8.82097	10.66026	-223.8	-8.52665	10.66024	-223.8	-8.5142	10.66026
8	-223.8	8.82217	10.66016	-219.8	-8.52673	10.66026	-219.8	-8.5182	10.66026
9	-219.8	8.82241	10.66026	-215.8	-8.52673	10.66026	-215.801	-8.5182	10.66026
10	-215.8	8.822154	10.66021	-211.8	-8.52673	10.66026	-211.8	-8.5182	10.66026
11	-211.8	8.822196	10.66021	-207.8	-8.52696	10.66026	-207.8	-8.5182	10.66026
12	-207.8	8.822056	10.66026	-203.8	-8.52673	10.66026	-203.799	-8.5182	10.66026
13	-203.8	8.822355	10.66026	-199.8	-8.52653	10.66026	-199.801	-8.5182	10.66026
14	-199.8	8.822143	10.66023	-195.8	-8.5267	10.66026	-195.801	-8.5182	10.66026
15	-195.8	8.822524	10.66026	-191.8	-8.52624	10.66026	-191.799	-8.5182	10.66026

Figure 7: Output of the coordinate Exporter module

3.2.2 Module-2: Starter Segment Setup

The steps corresponding to Module-2 shown in Figure 5 are discussed below.

1. From the extracted global coordinates, the control coordinates of the starter segment are filtered out.
2. The joint which should match cast with the second segment should be on the bulkhead side (Figure 8). Therefore, the center coordinate of this edge is made the origin of the newly created local coordinate system.
3. The X, Y and Z axes are defined for the newly created coordinate system. The X axis is the vector between the created origin (center coordinate) and the East control point of the same edge. The Z axis is defined by creating a point with the same X and Y coordinate of the Origin with an arbitrary high Z coordinate value (say 1000) and defining a vector between this point and origin.

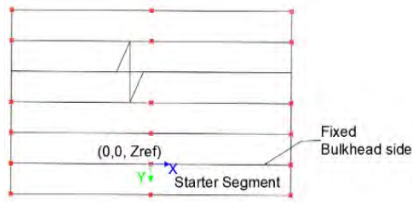


Figure 8: Starter segment Local coordinates

4. The Y axis is defined as the cross product between these vectors of the Z-axis and X-axis, to satisfy the left-hand rule of the coordinate system.
5. The other points which are filtered out from the list in step-1 are read relative to this coordinate system, to obtain the X and Y local coordinates of all the points in the starter segment.
6. The Z coordinates depend on the user input Z-reference, Therefore the Z coordinates of the points are calculated relative to this value.

Figure 9 shows the interface of the starter segment setup module whereas Figure 10 shows the screenshot of the output starter segment setup module.



Figure 9: Starter segment setup module

Station	NORTHING	EASTING	ELEVATION
SE	2.58042	6.82873	10.00000
SC	1.90880	5.05138	10.00000
SW	1.02510	2.71278	10.00000
NE	8.20410	0.00000	10.00000
NC	0.00000	0.00000	10.00000
NW	7.17990	-2.71312	10.00000

Figure10: Output of Starter segment setup module

3.2.3 Module-3: Typical Segment Correction:

The steps corresponding to Module-3 shown in Figure 5 are discussed below.

1. From the extracted as-planned global coordinates, the control coordinates of the currently selected segment and the previous segments are filtered out.
2. The as-cast local coordinates of the previous segment are obtained from the total station input, now this must be converted to global coordinates to know the errors in casting. But the local origin of these coordinates lies at the fixed bulkhead center. Since the bulkhead is rigid and fixed, any deviations that have happened would be on the other edge of the segment.
3. To convert the local to global coordinates, the

edge/joint, which is on the match cast side, whose coordinates are known should be taken as reference (Fig.11). The East coordinate of the match cast joint is taken as reference and its coordinates are equated to the as-cast global coordinates of the same edge which was formed during casting of the previous segment. With this point as a reference, the transformation of other points is made with the help of translation and rotation matrix to convert the as-cast local coordinates to global coordinates. Fig11 illustrates this logic.

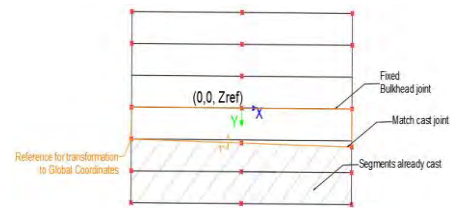


Figure 11: Logic of conversion transformation from local to Global coordinates

4. Based on the as-cast global coordinates and planned global coordinates, the matrix of relationships is set-up and solved using least squares criteria. The corrections to be applied to the planned coordinates of the current segment is obtained. Similarly, the elevation network is also set-up and solved to get the corrected Z-coordinates.
5. From the corrected coordinates obtained, the new local coordinate system is defined at the joint which will be on the bulkhead side. This method is similar to the method followed to convert the global coordinates to local coordinates in starter segment setup.
6. The output of the corrected local coordinates is obtained in excel file which can then be transferred to total station for staking out the operation.
7. Also, the as-cast global coordinates obtained by transformations as explained in earlier steps is then stored in the database. This data can later be used to generate the as-cast model of the bridge.

Figure 12 shows the interface of typical segment correction module whereas Figure 13 shows the screenshot of the output of the coordinate exporter module.

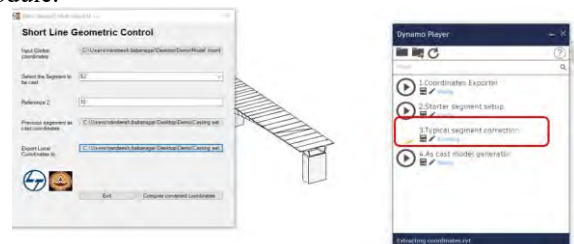


Figure 12: Typical segment correction module

B	C	D	E	A	B	C	D
-244.1	-8.52673	10.66026	Left	Station	Northing	Easting	Elevation
-246	-8.52673	10.66026	centre	NE'	-7.675	2.900	100.000
-248.5	-8.52673	10.66026	Right	NC'	0.000	2.900	100.000
-248.5	-8.52228	10.66026	Left	NW'	7.674	2.900	100.000
-251.4	-8.52673	10.66026	centre	NE	7.674	0.000	100.000
-251.4	-0.85132	10.66026	Right	NC	0.000	0.000	100.000
				NW	-7.674	0.000	100.000
				SE'	-7.675	5.800	100.000
				SC'	-0.004	5.800	100.000
				SW'	7.674	5.800	100.000

Figure 13: As cast global coordinates and local coordinates output from Typical Segment correction

3.2.4 Module-4_As cast model generator:

The steps corresponding to Module-4 shown in Figure 5 are discussed below.

1. The adoptive family type of the cross section is imported to Dynamo
2. From the as-cast global coordinates data, the Left, centre, and Right corridor points of the bridge are plotted as a spline.
3. Based on the number of segments, parameters are defined to place the generic Cross sections along the centreline corridor 3D polyline.
4. The parameters of the box girder are adjusted as desired by the user
5. To 'Left Lane width', 'Right lane width', 'Zleft' and 'Zright' Instance parameters are adjusted for each cross-section placed along the 3D polyline based on the Left and Right corridor points.
6. After the cross sections placed along the curve are 'Loft' to create a solid. The solid thus formed represents the as-cast geometry of the bridge.

Figure 14 shows the interface of as cast model generator module whereas Figure 15 shows the screenshot of the output of the coordinate exporter module.



Figure 14: As-cast model generation module



Figure 15: Output of As-cast model generator

4 Model Validation

The aim of the validation step in the current work was to determine the degree to which the suggested model for finding the corrected coordinates is close to the results obtained from a proprietary software used in a real-world project. The validation was performed in a user defined custom function which was developed using excel macro.

The comparison of the results obtained from the custom logic and proprietary software was made with respect to the global coordinate system, because of its ease of analysis. For testing the framework, first the site data of the planned coordinates and actual coordinates were obtained. The planned coordinates were input in both the custom application and MC3D software. The as-cast data of a segment is input in both MC3D and GEMBSC. The GEMBSC computes the corrected coordinates and hence the error in each segment for any error introduced assuming the corrected coordinates as the as-cast data for the downstream segments, but the MC3D requires inputs of the as-cast data at each step. The setup coordinates obtained from MC3D for each segment is entered as the as-cast data for the succeeding downstream segments.

The report of the global as cast joint coordinates are obtained from MC3D after the above step is repeated until the last segment. The coordinates obtained from the report are arranged in the required format to make the comparison. The results of validation are discussed in the following section.

5 Results

The following observations were made from the comparison of the outcomes of the validation steps.

Figure 16 shows an instance of the comparison for east side plan deviation. Similar plots were obtained for centerline plan, west side plan, CL elevations, and centerline alignment deviations.

The errors that occurred during casting of any segment were reduced in the succeeding segment/s and converged to zero after the casting of subsequent set of segments. However, with increase in the magnitude of the error the convergence took place over a greater number of segments. From this observation it can be inferred that the logic applied is effective, however the pattern of convergence may differ when compared to other methods of error correction.

It was further observed that the convergence of plan deviations made by MC3D is more rapid than the GEMBSC. In most cases, MC3D reduces the error in a single step. Whereas the custom software reduces errors in a more gradual manner, which is a more practical solution where the geometric constraints of the bridge are not violated. The same pattern is seen with respect to vertical alignment also.

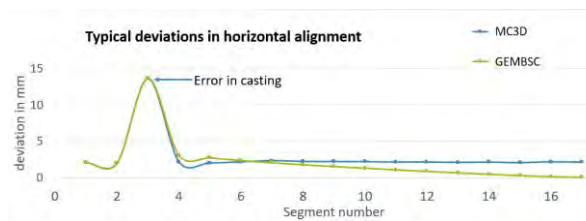


Figure 16: Plot typical deviation in horizontal alignment

6 Summary and Conclusion

In this work, a BIM-based application is developed for Geometric control of Short-line match casting of bridge segments. An algorithm for finding the corrected coordinates using the least square method is used in developing the application. The results from the solution algorithm was compared with the results of the commercially available software called MC3D. The GEMBSC gave better results as the error that occurred during the casting of any segment was corrected in the succeeding segments in a gradual manner with smaller corrections spread over a larger number of segments.

Future work could involve incorporation of 3D model creation with GEMBSC, that could be useful for quality management purpose through capturing data such as actual transverse pre-stressing force applied to the segment, date of casting of segment, the Engineer-in charge who conducted inspection, concrete strength used for the segment etc. Further, the application of linear actuators coupled with servos to adjust moulds, use of LiDAR based scanning methods coupled with BIM for automated data collection, and the use of Self-Propelled Modular Vehicle (SPMVs) needs exploration.

With the power of data analytics, the geometric control process can be explored to be made more proactive, by predicting the possibility of error based on various parameters and adjusting the moulds so as to nullify the errors.

7. References

- [1] S. Sengupta, "Fast track construction of 9.5 km long elevated expressway by largescale, prefabrication of superstructure," *Proc. Int. FIB Symp. 2008 - Tailor Made Concr. Struct. New Solut. our Soc.*, p. 208, 2008, doi: 10.1201/9781439828410.ch157.
- [2] A. J. Moreton and H. H. Janssen, "Casting box girder segments," *Aberdeen's Concr. Constr.*, vol. 40, no. 1, 1995.
- [3] J. E. Kristensen, "Precast Segmental Bridge Construction - An Introduction," in *Suncam Online Publication*, 2012, pp. 1–15.
- [4] X. Dai, X. Wu, and T. Zhang, "Research on the Precision Control Technology of Short - Line Segmental Prefabricated Assembly Bridge," *IOP Conf. Ser. Earth Environ. Sci.*, vol. 128, no. 1, 2018, doi: 10.1088/1755-1315/128/1/012088.
- [5] G. Hermann, "Geometric error correction in coordinate measurement," *Acta Polytech. Hungarica*, vol. 4, no. 1, pp. 47–62, 2007.
- [6] K. Kumar, K. Varghese, K. S. Nathan, and K. Ananthanarayanan, "Automated geometry control of precast segmental bridges," *ISARC 2008 - Proc. from 25th Int. Symp. Autom. Robot. Constr.*, pp. 88–94, 2008, doi: 10.3846/isarc.20080626.88.
- [7] S. Matupayont, "Precast Segmental Box-Girder Construction Technology," no. June, 2015.
- [8] X. H. He, X. L. Meng, and L. J. Li, "Design and construction of the bridges on Guangzhou metro line 4," *Procedia Eng.*, vol. 14, pp. 126–133, 2011, doi: 10.1016/j.proeng.2011.07.014.
- [9] Y. Huang, H. Zheng, M. Wang, and X. Wu, "Geometry control technology of transition curve section in cross-sea bridge erected by precasting segment girder," *Appl. Mech. Mater.*, vol. 256–259, no. PART 1, pp. 1548–1553, 2013, doi: 10.4028/www.scientific.net/AMM.256-259.1548.
- [10] B. F. Bender, "Geometry Control of Precast Segmental Concrete Bridges.," *J. - Prestress. Concr. Inst.*, vol. 27, no. 4, pp. 72–86, 1982, doi: 10.15554/pcij.07011982.72.86.
- [11] J. E. Breen, "Controlling Twist in Precast Segmental Concrete Bridges.," *J. - Prestress. Concr. Inst.*, vol. 30, no. 4, pp. 86–111, 1985, doi: 10.15554/pcij.07011985.86.111.
- [12] M. Rohani, G. Shafabakhsh, A. Haddad, and E. Asnaashari, "Operation planning of concrete box girder bridge by 4D CAD visualization techniques," *Int. J. Civ. Environ. Eng.*, vol. 10, no. 6, pp. 805–811, 2016.
- [13] B. Jia, Y. Yang, B. Xie, and X. Yu, "Novel Geometric Control Technology for Precast Segmental Bridges," *J. Constr. Eng. Manag.*, vol. 147, no. 4, pp. 1–14, 2021, doi: 10.1061/(asce)co.1943-7862.0002006.
- [14] M. K. Kim, J. C. P. Cheng, H. Sohn, and C. C. Chang, "A framework for dimensional and surface quality assessment of precast concrete elements using BIM and 3D laser scanning," *Autom. Constr.*, vol. 49, pp. 225–238, 2015, doi: 10.1016/j.autcon.2014.07.010.

A pre-trained language model-based framework for deduplication of construction safety newspaper articles

Abhipraay Nevatia¹, Soukarya Saha², Sundar Balarka Bhagavatula³ and Nikhil Bugalia^{3*}

¹Department of Mechanical Engineering, Indian Institute of Technology Madras, India

²Department of Engineering Design, Indian Institute of Technology Madras, India

³Department of Civil Engineering, Indian Institute of Technology Madras, India

E-mail: me20b007@smail.iitm.ac.in, ed20b062@smail.iitm.ac.in, ce18b103@smail.iitm.ac.in,

*nikhilbugalia@gmail.com

Abstract –

The unavailability of Occupational Health and Safety (OHS) statistics for the construction sector is a systemic hurdle in improving safety, particularly for developing countries. Alternatively, online newspaper articles are deemed a potential source for OHS statistics. Machine Learning (ML) approaches for text-mining are essential for the otherwise resource-intensive processing of news articles. However, the previous literature applying ML for newspaper articles has been scarce, and tasks, such as removing duplicate reports, have not been addressed satisfactorily. The current study develops and evaluates a novel framework based on pre-trained language models for the deduplication tasks for construction safety-related news articles to address the research gap. The study relies on the Question and Answering (QA) ability of the Longformer model pre-trained on Stanford QA Dataset (SQUAD) to identify the date and location of the construction accidents from the news articles. A combination of date and location is used as a key for deduplicating news articles that refer to the same accidents. The comparative performance of the developed framework is evaluated on 141 accident articles systematically extracted from 7 months of construction-relevant news articles in India. With an accuracy of more than 90%, the proposed method outperforms other methods for date identification. The performance of the deduplication process based on Longformer, i.e., F1 score of 0.79, is comparable to the Cosine similarity-based approaches. However, compared to the commonly adopted Cosine similarity-based method, the newly developed method in this study is reliable and consistent for periodically processing large quantities of unlabeled datasets.

Keywords –

Construction safety, News Articles, Machine Learning, BERT, Longformer, Deduplication

1 Introduction

For developing countries such as India, the construction sector remains one of the worst-performing sectors for Occupational Health and Safety (OHS) matters [1]. For policymakers wishing to solve the issue, one of the essential ideas to improve safety performance is to collect and analyze data on accidents, injuries, and near-miss reports and utilize the learning from these reports to enable sector-wide safety measures [2]. However, the unavailability of robust OHS statistics for the construction sector in developing countries is a systemic hurdle facing academia and practitioners [3], where government agencies have no formal mechanisms to collect and publish such statistics.

Without formal databases, online newspaper articles have been recognized as a potential source of information for developing OHS statistics [3,4]. However, previous attempts to leverage large-scale online news data for developing such safety statistics for the construction sector have been scarce, and the challenges faced in such analysis have not been well-addressed [4]. For example, only a handful of previous studies have addressed the resource-intensiveness-related problem related to processing large quantities of text data [5], as generally found in news articles [4]. A few of them have relied on efficient data processing approaches such as Machine Learning (ML) and text-mining for construction-related news items [6,7]. Even within these ML studies on construction news articles, issues such as identifying duplicate news articles have not been addressed appropriately. Current studies typically rely on text-similarity-based approaches to compare news articles and detect duplicates [6]. However, such text-similarity-based approaches lack consistency in creating a database of accident articles synthesized through large quantities of news articles that can be updated periodically (see section 2 for details).

The essential motivation for this paper is to develop a novel approach that can accurately and consistently

identify the duplicates in construction safety-related news articles. Consequently, the current study aims to develop and test a novel duplicate identification approach relying on state-of-the-art pre-trained language models, similar to Bidirectional Encoder Representations from Transformers (BERT). The study makes essential contributions to advancing the usage of ML approaches in developing reliable trends on OHS statistics using newspaper articles, especially in countries where industry-wide reporting on OHS data is non-existent.

The study is structured as follows. Section 2 provides an overview of the literature and identifies the essential gaps to where the study contributes. Section 3 describes the essentials of BERT-based language models and the analytical methodology adopted in the current study. Results have been summarized in section 4, followed by discussions in section 5. Conclusions have been outlined in section 6.

2 Literature Review

One of the most comprehensive analyses of fatal accidents in the construction sector using newspaper data has been presented in [4]. Using statistical approaches such as cluster analysis and principal component analysis, they obtained key statistics related to accidents, such as the date and time of the fatal accidents. Overall, the study provides comprehensive ideas on processing newspaper reports; however, the manual data collection and entity extraction processes adopted were resource intensive. Only a handful of previous studies have relied on automated ML and text-mining approaches to analyze newspaper data for construction safety. For example, Feng & Chen [8] proposed a natural language data augmentation-based framework for automatic information extraction using deep neural networks. However, the articles used for their study were handpicked, and their framework can only be applied to small datasets extracted manually. They emphasize the necessity of a robust automatic information extraction model capable of handling large volumes of data [8]. The challenge of automatically extracting large quantities of construction safety data from newspapers has been partially addressed in [9]. They relied on a keyword-based extraction technique to collect news articles. Their data helped identify factors and interrelationships affecting fire-related accidents in construction.

However, even Kim et al. [9] do not address some fundamental challenges facing the widespread usage of ML approaches for generating OHS statistics in the construction sector [6]. For example, the keyword-based extracted data on newspaper articles may contain duplicates. The duplicates are of different types. Examples include - the same accident being reported in print and online format, multiple media houses reporting

the same construction accidents, and a piece of news referring to a previously reported construction safety event [6]. Removal of duplicates, also known as the deduplication process, is essential to avoid obtaining overestimated OHS statistics [4].

The commonly adopted deduplication approaches rely on using vector space techniques such as Cosine similarity, Jaccard similarity, and Euclidean distances to calculate the text similarity [10]. However, such models are inherently limited. Specifically, the news articles sparsely contain the target safety-relevant words, and most of the textual information is generic [6]. In such conditions, text-match-based scores may not be precise. One of the most significant limitations of vector space models for deduplication tasks is their lack of trainability and consistency. Vector space models make a pair-wise comparison of articles and generate a text-similarity score. Afterward, the analysts must set a threshold value, and articles above the threshold value are considered duplicates. Such a threshold value is optimized using an annotated dataset for identifying duplicates. However, Barbera et al. [6] note a significant variability in the data distribution obtained through keyword extraction-based approaches across different periods. Furthermore, it is implausible that two sub-sets of the same extensive data will follow a similar distribution. Such data limitations make it challenging to set the vector-space model's threshold values for deduplication tasks that can be consistently applied to the whole dataset. Hence, alternative ML and text-mining methods for the deduplication process must be explored. However, such explorations have been rare in the existing literature.

Sitas et al. [11] provided a framework for designing a deduplication process. They recommend identifying relevant "fields" in the data. Such *fields* should be relatively stable constructs despite the variability in the overall information in multiple records. A combination of multiple such fields can then be used to create "keys," which can be used for deduplication. For negative consequence-related information in news articles, the date of the event and the broad region or locality of the adverse event is most-commonly described. Hence, the accident's date and location are potential candidates to be used as *fields*, and a combination of them can serve as a potential *key* for the deduplication process [12].

For extracting the date and location-related information from the textual data, many previous studies have utilized different text-mining approaches broadly under the category of tasks known as Named Entity Recognition (NER). The NER tasks are either Rule-Based approaches or Supervised ML approaches. However, all the above methods are resource-intensive, requiring manual efforts to identify patterns or annotate the data. On the other hand, natural language processing has witnessed a significant paradigm shift since the

introduction of the BERT method. BERT is a language model pre-trained on large volumes of unlabelled texts. BERT representations can achieve state-of-the-art results on several language processing tasks. For example, recent studies have also shown that BERT based model can outperform conventional methods even in the NER tasks [13]. While such work is commendable, the tagged text phrases still need to be manually interpreted to identify the date and the location of a construction-related accident, as often there can be mentions of multiple dates and places in a single news article. In recent years, significant progress has been made in the BERT-based models across various language processing-related tasks such as summarization and question-answering [14]. Some of these advancements have the potential to make the overall process of date and location identification in newspaper articles efficient and less resource intensive.

However, to the authors' knowledge, none of the existing studies have utilized the BERT-based language models to analyze construction safety-related news articles. An efficient and resource-effective process for deduplication based on BERT will significantly advance the body of knowledge. It will pave the way for leveraging readily available news articles for developing safety-related OHS statistics.

3 Methodology

The overall analytical process adopted for the current study has been summarized in Figure 1. The focus of the analysis has been to understand the comparative performance of the BERT-like pre-trained language models in deduplication tasks with conventional text-similarity-based methods and manual estimation.

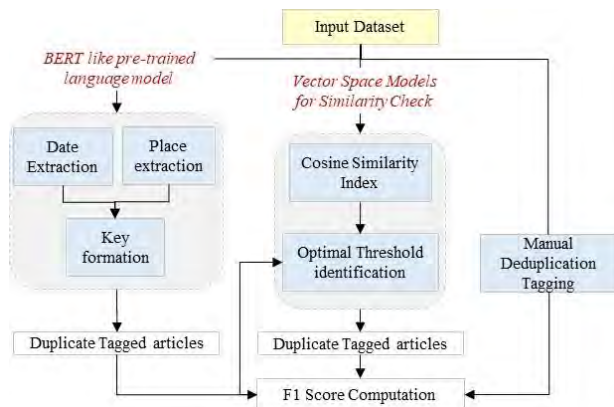


Figure 1. The analytical process of the study

3.1 Input Dataset and Manual Deduplication

The current study relied on the services of a news media analytics company, which has access to digital news articles from all major news agencies in India to

obtain data. Consistent with the recommendations of the literature, a keyword-based search was used to extract relevant news articles. The keywords used for extraction are 'Construction', 'Accident', 'Injur*', 'Fall', 'Collapse', 'Struck', 'Dead', 'Worker'. The 'Construction' keyword is mandatory in the given keywords. This way, 11,208 articles reported between July 2021 and January 2022 were obtained. Multiple safety experts manually examined the text of each article to identify the articles describing construction accidents. Despite such an extensive manual effort, only 141 articles (1.26% of the total) contained information on actual construction accidents.

Three authors then implemented a pair-wise comparison scheme to tag the duplicate articles. Such information was stored in a 141*141 matrix, where the cell (i,j) was marked as "1" if the article in i^{th} row was found to duplicate the article on the j^{th} column. Otherwise, a value of "0" was assigned to cell (i,j) . The manual deduplication matrix thus created is the *Truth Matrix* and has been used to evaluate the performance of the other algorithms. Such a process revealed the significant extent of deduplication in the news articles, where 77 out of 141 articles had at least one duplicate. On the other hand, 1 single accident also matched with 26 other articles.

3.2 Vector-Space model for similarity check

Consistent with the previous literature, the current study also develops a Cosine similarity-based text-match score to estimate the duplicates. The purpose of including the results from the Vector-space model is to provide a comparative assessment of the proposed model. Like the steps described above for the *Truth Matrix*, a 141*141 matrix containing a cosine similarity score from a pair-wise comparison of the articles is first developed. Then, a threshold value is selected, and any score above the threshold represents duplication in the articles and is marked as "1". Similarly, scores below the threshold are marked as "0".

The optimal cosine similarity threshold is identified through a sensitivity analysis approach. The results between the *Truth Matrix* and the cosine-similarity matrix are compared for generating F1 statistics for any arbitrarily selected threshold value. F1 statistics is a common approach to evaluate the various ML algorithm's performances compared to the truth data on binary classification tasks [1]. F1 score ranges between 0 and 1, and a higher F1 score represents a better performance for any algorithm. The threshold values are identified such that the F1 score is maximized.

3.3 Pre-trained language model-based novel deduplication framework

Consistent with the recommendations from the

previous work on deduplication, accident date, and location are considered the two *fields* commonly reported in news articles. Combining the two *fields* can be a unique *key* to help identify duplicate articles [12].

3.3.1 Date identification

Transformer-based pre-trained language models like BERT are among the most significant breakthroughs in text-mining and natural language processing. However, even BERT cannot process long text sequences (more than 512 tokens). Longformer has been developed as an alternative. Longformer's architecture is like BERT's architecture but has a different self-attention mechanism [14]. Literature has also shown that Longformer outperforms the BERT-based models for long text sequences in NER tasks [14]. Many news articles obtained in the current study are longer than 512 tokens; hence, Longformer implementation is deemed more suitable.

The Longformer model is primarily efficient in Question and Answering (QA) tasks [14]. The QA ability of the Longformer allows the user to ask questions in natural language, for which answers are sought from the target article, even if the exact sequence of the words present in the questions is not present in the target text being searched [14]. Considering these advantages, the current study uses Longformer for QA pre-trained on Stanford QA Dataset (SQUAD), mainly comprising of information from Wikipedia [15]. The QA query aimed to get an output that could readily help estimate the date of the accident. The exact question has been fine-tuned with several trials. Once the news articles are parsed through the Longformer, the output is a string. The information in this string is converted to an exact date using a reference for the *article publishing date* mentioned in the online article. The *Datetime* library in Python is used for such implementation. The *Datetime* library recognizes the "on <weekday>" format and not just "<weekday>." Therefore, in the *Datetime* function, the term "on" has been inserted before the <weekday>. The accuracy of the Longformer formulation is measured by comparing the manually extracted dates. In some instances, such a process also returns a NULL value.

3.3.2 Location identification

Like the date identification task described above, the current study uses Longformer for location identification tasks. However, in many cases, Longformer's output was insufficient to identify the accidents' location suitably. Hence, additional efforts for location identification are needed. Another pre-trained NER algorithm, [Locationtagger](#), can identify all the places in the articles. Further, even when NER models are ineffective, the whole article was parsed as a string. Combined output is obtained by concatenating the output of each of the three methods to detect location, i.e., Longformer, NER-tagger,

and the whole article parsing (See Figure 2). Each term in this combined string is then compared against a database containing names of Indian cities and places. The first term in the concatenated string that exactly matches with the database is estimated as the location of the accident. In such a manner, the highest priority is given to the location identified through Longformer, as the method is expected to capture the context of the description very well. The process for location identification is also summarized in Figure 2. The accuracy of the above formulation is measured by comparing the location of the accident manually extracted by the authors.

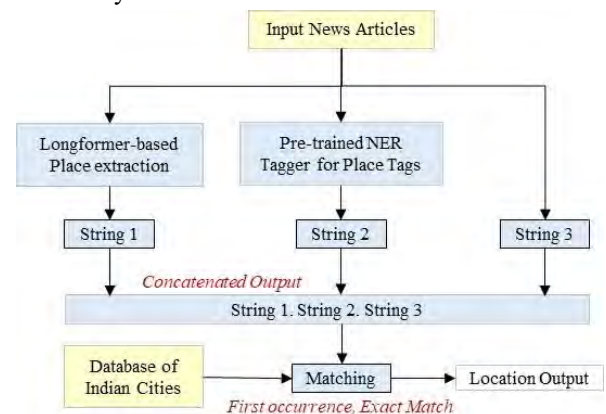


Figure 2. Location identification process

3.3.3 Key Formation

The output of the date and the location identification is concatenated to develop a *Key* that can serve as a unique identifier for a construction accident reported across multiple news reports. However, this approach's efficacy depends on the cases when both date and location are suitably identified from a news report. However, a NULL output may sometimes be possible from either date or location identification processes. Hence, two scenarios have been conceptualized to incorporate the possible NULL output for developing the *Key*.

Scenario 1: If either date or place is NULL, the study assumes the article is unique and does not compare it with any other article.

Scenario 2: If either date or place is NULL, the study removes the article from its dataset and further comparison.

Similar to the approaches defined above, a pair-wise comparison matrix is developed to predict two articles as duplicates when their *Key* matches (marked as 1). If the *Key* does not match, the articles are predicted as unique (marked as 0). The matrix thus generated is then compared with the *Truth Matrix* to compute the F1 score, an indicator of the deduplication process's efficiency.

3.4 Implementation

All algorithms have been developed using the Python programming language. The Longformer model pre-trained on SQUAD dataset is readily available in the *Huggingface* library of Python and does not require any other modifications for processing news articles. The reference library and Longformer implementation can be referred to from the following [LINK](#).

4 Results

4.1 Accuracy of the date identification

Table 1 shows the results of different questions asked to the Longformer model and the corresponding accuracy in identifying dates compared to manually extracted true dates. The results demonstrate that the QA method for Longformer is highly efficient and can successfully identify the date of accidents in 124 articles out of 129 articles where the accident date was present in the original text. Similarly, the Longformer correctly returns a NULL output in 8 out of 12 cases where the accident date was absent in the original data. Although the results from the QA model are also a function of the QA query, which requires fine-tuning is essential to get good results.

Table 1. Date identification accuracies for Longformer

QA for Longformer	Number of articles Original Data (Correctly Predicted by the Longformer)	
	With Dates	With No Dates
“What day of the week did the accident take place”	129 (124)	12 (8)
QA – “When did the accident take place”, returned the time of the accident if the time is mentioned. But is not able to detect the day in many cases. Correctly predicts the results in 82/141 cases. QA – “What Day did the accident take place”. Returns the time in some cases. Correctly predicts the 117 instances out of the total 141.		

4.2 Accuracy of Location Identification

For the query “Which city did the accident take place in” the Longformer-based QA method can correctly identify the locations in only 62 out of 141 articles. The results demonstrate that identifying the location in the news articles is challenging. The accuracy of location identification improved significantly when the

Longformer’s output was further combined with the output of the other models, as shown in Figure 2—such combined model results in the correct location prediction for 112 articles out of 141.

4.3 Deduplication Results

Table 2. Comparative performance of various methods on Deduplication efficiency

Results	Scenario 1	Scenario 2
Key (Date and Location), Location – Combined Model		
Null articles Removed	-	27
Accuracy	0.97	0.99
Precision	0.95	0.95
Recall	0.34	0.68
F1 Score	0.50	0.79
F1 Score (Cosine)	0.72	0.80
Threshold (Cosine)	0.20	0.24
Key (only date)		
Null articles Removed	-	12
Accuracy	0.98	0.99
Precision	0.91	0.91
Recall	0.68	0.88
F1 Score	0.78	0.90
F1 Score (Cosine)	0.72	0.77
Threshold (Cosine)	0.20	0.21

Table 2 shows the comparative analysis of deduplication efficiency between the proposed Longformer-based model and the Cosine similarity. Comparative analysis is also performed for both Scenario 1 and Scenario 2. Results from two different types of Keys have also been shown in Tables 2 and 3. The first Key relies on both fields, i.e., date and location. The second Key relied only on the date as the *field*. For comparison, results from Cosine similarity and the optimal cosine thresholds have also been included in Table 2. The results thus obtained have been discussed in detail in the next section.

Table 3. Confusion Matrices for various methods and scenarios

Results	TP	FP	FN	TN
Key (Date and Location), Location – Combined Model				
Longformer Scenario 1	161	8	311	9390
Longformer Scenario 2	161	8	77	6195
Cosine Scenario 1	325	105	147	9293
Cosine Scenario 2	181	31	57	6172
Key (only date)				

Longformer Scenario 1	319	30	153	9368
Longformer Scenario 2	319	30	43	7864
Cosine Scenario 1	325	105	147	9293
Cosine Scenario 2	268	68	94	7826
TP – True Positives, FP – False Positives, FN – False Negatives, TN – True Negatives. The number represents the count of duplicates (1) and non-duplicates (0) in the matrix.				

5 Discussions

5.1 Effectiveness of Longformer model in Date and Location extraction

Long-term spatial and temporal trends for OHS issues are essential in policymakers' decision-making. Hence, automatically identifying the date and the location of a given accident from newspaper articles is also a crucial problem to be solved. The pre-trained Longformer models adopted in the current study have shown promising date and location identification results. Notably, for date identification, the Longformer model can achieve an accuracy of 90% and outperforms the contemporary NER models on date identification by a significant margin [16]. The effectiveness of the Longformer model is further demonstrated by its ability to provide the correct accident date for a complex example of a news article shown below.

*“The contractor's failure to follow safety measures led to the death of a worker engaged in the lifting of a concrete girder for the elevated highway on New Natham Road here **on Saturday**. Public Works Minister E.N. Velu said **on Sunday**. After inspecting the site along with Finance Minister Palanivel Thiaga Rajan, Mr. Velu said a team of experts from the National Institute of Technology, Tiruchi, would hold an inquiry. The construction of the elevated highway, stretching 7.3 km from Chokkikulam to Chettikulam, began **in November 2018**.”*

In the above example, three instances that could indicate the date of an event are present (indicated in bold). One of these dates is related to the occurrence of the accident. The other date refers to a statement made by the regulatory authority on the accident. Nevertheless, another date refers to the event when the structure's construction began. The Longformer-based date detection model can distinguish these three dates and provide a correct output. Such a contextual interpretation of the dates is generally impossible, even for the pre-trained NER models relying on supervised ML approaches.

However, despite the excellent performance in date

detection, even a Longformer-based formulation faces challenges in location identification. A quick analysis of the prediction errors provides an overview of some common reasons for poor location prediction performance. One of the primary reasons is that often, in news articles, the locations mentioned refer to streets, names of the localities, or residential colonies within a city. However, the database for comparison only contains information on the city. In such cases, a possibility of an exact match between the Longformer prediction and the matching database reduces significantly, leading to an overall poor performance of location prediction. Such error analysis also provides essential ideas for further improving the algorithm's performance on location identification. These ideas have been summarized in section 5.3 of the current study.

5.2 Effectiveness of Longformer-based deduplication process

Overall, several advantages of the Longformer-based deduplication process can be observed from the results obtained in the current study. The foremost advantage of the Longformer-based model, compared to the conventional Cosine similarity-based process, is the expected generalizability of the method. As shown in Table 3, the optimal threshold value for Cosine similarity can change significantly even for a subset of the same dataset. Results in Table 3 demonstrate how different the number of True Positives is when the Cosine similarity method is applied to a smaller subset of the larger dataset. Because of such fluctuations in the results of the cosine similarity, it cannot be considered a reliable method for the deduplication process for large quantities of unlabeled data. However, such challenges are absent in the Longformer-based pre-trained language models used for deduplication. The models are robust (even for a smaller subset, as shown in Table 3) and can be readily used consistently without retraining across different prediction issues.

Nonetheless, the current study identifies many areas where even the proposed Longformer-based model requires improvement. First, the Cosine similarity-based method still outperforms the novel Longformer-based model for deduplication tasks. In many cases where either the date and location are not present in the online article or the Longformer face difficulties in detecting the date and the location, the proposed Longformer-based approach suffers. For such cases, the efficiency of the Cosine similarity method for the deduplication process is significantly better (See Scenario 1 results in Table 2). In other cases (See Scenario 2 results in Table 2), the performance of the Longformer is like the Cosine similarity-based methods. However, in such cases, a few articles have been excluded from being considered in the deduplication process. At the same time, the cosine

similarity-based method can predict all articles.

The result from the study also demonstrates that the efficiency of the Longformer-based deduplication process is significantly hampered due to the combination of multiple *fields*. For the sample of news articles considered in the current study, a “date” only *key* leads to a significant improvement in the efficiency of the deduplication process is observed. Such results indicate that stricter criteria requiring exact matches between multiple *fields* to detect duplicates reduce the effectiveness of the duplication process. Hence, the study results would indicate that a straightforward solution could be to reduce the number of *fields* included in the deduplication process. However, such a solution may not be human-intuitive. For example, despite the enhanced performance of the only date-based deduplication process, it is not practical to expect that only one accident is expected in one day for a construction industry as large as it is in India.

5.3 Ideas for improving the performance of the deduplication process

The comparative assessment of the two methods highlights the complexities of the deduplication tasks for news articles. The conventional Cosine similarity-based deduplication process is simple and can be done on the whole corpus of the dataset. However, the approach is unreliable, especially when a large quantity of unlabeled data must be checked for duplication periodically. In contrast, the Longformer-based pre-trained language model is potentially generic and can work on the unlabeled dataset. However, its limitations in identifying dates and locations based on exact match criteria for each article pair pose significant challenges for their usage in the deduplication process. The Longformer method can be improved in two significant directions to solve the abovementioned challenges.

First, efforts should be made to enhance the Longformer’s prediction efficiency for particular *fields*. The output from multiple QA queries can be combined to identify the date and location. Similar efforts could also be made to enhance the Longformer’s predictive capability of accident location at a city level. For example, Longformer’s model can be assessed to identify the text phrases which contribute most towards the outcome of the Longformer, i.e., access the Longformer’s attention matrix. The NER-based search for locations only on these high-attention text phrases can potentially improve the prediction capabilities of the Longformer for locations.

Second, efforts could also be made to shift from an “exact match” paradigm to a “partial match” paradigm. For example, an approximate search for accident locations at a city level can also be done by correlating the multiple locations mentioned in the article. The

article’s publishing location could also be used as a reference point. However, such an effort will require understanding the spatial information-based libraries specifically for India. Further, the partial match paradigm could also be extended to develop a clustering approach based deduplication process. For example, Longformer can further extract more features about the accident, such as the number of people affected and the gender of those affected. Type of construction activities where accidents were reported, such as bridges, roads, and buildings, or type of construction accidents, such as falls from a height, among others, could also serve as features. Then various clustering techniques that can simultaneously leverage the multiple features could be used to identify duplicate articles. The clustering techniques are versatile and can also be trained therefore maintaining the generalizability benefits of the Longformer-based models compared to the Cosine similarity methods.

5.4 Study limitations and future scope

The advantages of the Longformer-based deduplication process developed in this study have been shown only for a small dataset of 141 news articles. The availability of such a small sample set was not intentional but was due to the sparseness of the construction accident news in the whole dataset searched for relevant keywords. Although the preliminary results from handpicked news articles from the USA processed through the proposed method show a good performance in date, place, and duplication identification (see [Link](#)). However, the generalizability of the method should also be explored for large datasets of articles comprising multiple geographic regions. Despite the advances shown in the paper here, it is expected that in a multi-lingual country such as India, only a fraction of the construction accidents will feature in English news articles. India features more than 20 major vernacular languages. The scope of the analysis should be extended to include articles from these vernacular languages in future studies. In principle, the BERT-based models efficiently develop work processes that simultaneously assimilate data from multiple languages. However, the deduplication tasks for information featured in multiple languages will be an academically exciting extension of the current work.

6 Conclusions

The current study develops and evaluates a novel framework based on pre-trained language models for deduplication tasks for construction-related news articles. The study relies on the QA ability of the Longformer model pre-trained on SQUAD to identify the date and location of the construction accidents from the news articles. A combination of date and location is used as a key to detecting duplicate news articles that refer to the

same accidents featured in multiple news reports. The proposed method outperforms other methods by correctly identifying the date of accidents in more than 90% of the articles. Although, detecting the location of the accident through Longformer continues to be challenging. Overall, the Longformer-based model outperforms the traditional Cosine similarity-based method in the deduplication tasks when only accident date is used as a key. However, for a more realistic Key involving date and location, the Longformer's performance is comparable to the Cosine similarity-based method. The foremost advantage of the Longformer-based model, compared to the conventional Cosine similarity-based models, is the expected generalizability of the method. The prediction based on Longformer models are robust (even for a smaller subset, as shown in Table 3) and can be readily used consistently across different prediction issues. The study contributes to the scarce body of knowledge on scarce ML applications for analyzing construction safety statistics using newspaper articles. The study's findings pave the way to automate the process of extracting and processing large quantities of news articles and use them to prepare reliable trends in OHS statistics. The unavailability of OHS statistics for the construction sector is a systemic hurdle in improving safety, particularly for developing countries.

References

- [1] N. Bugalia, V. Tarani, J. Kedia, H. Gadekar, Machine learning-based automated classification of worker-reported safety reports in construction, *Journal of Information Technology in Construction*, 27:926–950, 2022. <https://doi.org/10.36680/j.itcon.2022.045>.
- [2] N. Bugalia, Y. Maemura, K. Ozawa, A system dynamics model for near-miss reporting in complex systems, *Saf. Sci.*, 142:105368, 2021. <https://doi.org/10.1016/j.ssci.2021.105368>.
- [3] D.A. Patel, K.N. Jha, An estimate of fatal accidents in Indian construction, in: *Proceedings of the 32nd Annual ARCOM Conference*, 1: 577–586, 2016.
- [4] Y.-H. Chiang, F.K.-W. Wong, S. Liang, Fatal construction accidents in Hong Kong, *J Constr Eng Manag*, 144: 4017121, 2018. [https://doi.org/10.1061/\(ASCE\)CO.1943-7862.0001433](https://doi.org/10.1061/(ASCE)CO.1943-7862.0001433).
- [5] H. Gadekar, N. Bugalia, Automatic classification of construction safety reports using semi-supervised YAKE-Guided LDA approach, *Advanced Engineering Informatics*, 56: 101929, 2023. <https://doi.org/10.1016/j.aei.2023.101929>.
- [6] P. Barberá, A.E. Boydstun, S. Linn, R. McMahon, J. Nagler, Automated text classification of news articles: A practical guide, *Political Analysis*, 29:19–42, 2021.
- [7] J. Ninan, Construction safety in media: an overview of its interpretation and strategic use, *International Journal of Construction Management*, 1–9, 2021. <https://doi.org/10.1080/15623599.2021.1946898>.
- [8] D. Feng, H. Chen, A small samples training framework for deep Learning-based automatic information extraction: Case study of construction accident news reports analysis, *Advanced Engineering Informatics*, 47: 101256, 2021. <https://doi.org/10.1016/j.aei.2021.101256>.
- [9] J. Kim, S. Youm, Y. Shan, J. Kim, Analysis of Fire Accident Factors on Construction Sites Using Web Crawling and Deep Learning Approach, *Sustainability*, 13:11694, 2021. <https://doi.org/10.3390/su132111694>.
- [10] R. Singh, S. Singh, Text similarity measures in news articles by vector space model using NLP, *Journal of The Institution of Engineers (India): Series B*, 102: 329–338, 2021. <https://doi.org/10.1007/s40031-020-00501-5>.
- [11] A. Sitas, S. Kapidakis, Duplicate detection algorithms of bibliographic descriptions, *Library Hi Tech.*, 26:287–301, 2008. <https://doi.org/10.1108/07378830810880379>.
- [12] A. Abid, W. Ali, M.S. Farooq, U. Farooq, N.S. Khan, K. Abid, Semi-Automatic Classification and Duplicate Detection From Human Loss News Corpus, *IEEE Access*, 8:97737–97747, 2020. <https://doi.org/10.1109/ACCESS.2020.2995789>.
- [13] S. Almasian, D. Aumiller, M. Gertz, BERT got a Date: Introducing Transformers to Temporal Tagging, *ArXiv Preprint ArXiv:2109.14927*, 2021.
- [14] I. Beltagy, M.E. Peters, A. Cohan, Longformer: The long-document transformer, *ArXiv Preprint ArXiv:2004.05150*, 2020.
- [15] P. Rajpurkar, J. Zhang, K. Lopyrev, P. Liang, Squad: 100,000+ questions for machine comprehension of text, *ArXiv Preprint ArXiv:1606.05250*, 2016.
- [16] I. Jayaweera, C. Sajeewa, S. Liyanage, T. Wijewardane, I. Perera, A. Wijayasiri, Crime analytics: Analysis of crimes through newspaper articles, in: *2015 Moratuwa Engineering Research Conference*, IEEE, 277–282, 2015. [10.1109/MERCon.2015.7112359](https://doi.org/10.1109/MERCon.2015.7112359).

Development of a BIM-based spatial conflict simulator for detecting dust hazards

L. Messi ^a, A. Carbonari ^a, A. Corneli ^a, S. Romagnoli ^a, and B. Naticchia ^a

^aUniversità Politecnica delle Marche (UNIVPM), Faculty of Engineering, DICEA Department, Ancona, Italy
E-mail: l.messi@staff.univpm.it, alessandro.carbonari@staff.univpm.it, a.corneli@staff.univpm.it, s.romagnoli1996@gmail.com, b.naticchia@staff.univpm.it

Abstract –

In construction management, a spatial conflict between two activities is generally identified as the intersection between related workspaces. Such assumption works well for detecting the majority of conflicts. Nevertheless, in certain dynamic scenarios, a spatial interference between two activities may occur even if the related workspaces do not intersect each other. This study, being construction sites one of the major responsible for creating particulate matter (PM), focuses on spatial interferences related to dust hazard, still representing an open issue. In fact, although the correlation between PM concentration and health diseases dates back several decades, no study has addressed yet spatial interferences caused by PM-creating activities under the effect of meteorological and seasonal factors.

In order to cover these gaps, this study proposes a BIM-based spatial conflict simulator that, framed within a workspace management framework, spatially checks future construction work plans according to atmospheric phenomena based on weather forecast data. The resulting prototype, developed within Unity3D™ and tested through sensitivity analysis, has been applied on a real construction site scenario. Experiments results has confirmed the possibility to virtually simulate construction activities and atmospheric phenomena in order to support project managers in adopting countermeasures against dust hazards.

Keywords –

Workspace Management; Spatial Conflict; Dust Hazard; Particulate Matter; BIM; Game Engine.

1 Introduction

In construction projects, each activity requires a specific workspace to be executed, defined as the suitable occupational volume occupied by the involved crew and/or equipment [1], [2]. The space in construction sites must be considered as a limited but renewable resource,

similar to workers, equipment, and materials [3]. Identifying a spatial conflict as two activities sharing the same workspace generally works well for detecting the majority of conflicts affecting construction works. Nevertheless, in certain dynamic scenarios (e.g., dust hazard in windy conditions), a spatial interference may occur even if activities' related workspaces do not intersect each other. An example is represented by PM-creating activities (e.g., sawing and smoothing operations of wooden formworks for concrete placing) that in windy conditions may interfere with other ones, hence resulting incompatible, even if related workspaces do not interfere.

This study, being construction sites one of the major responsible for creating PM [4], [5], focuses on spatial interferences related to dust hazard. The relevance of this topic is confirmed by sector studies showing that atmospheric particle pollution may have adverse effects on human health. In fact, PM is believed to contribute to cardiovascular and cerebrovascular diseases and researches show that long term exposure is responsible for significantly high cardiovascular incident and mortality rate [4]. In order to dampen this trend, a workspace management framework, aimed to reduce dust hazards by integrating spatial analysis with the construction work planning phase, has been proposed by this study. A BIM-based spatial conflict simulator that spatially checks future working days, according to the work plan and atmospheric phenomena based on weather forecast data, has been developed in Unity3D™.

The rest of this paper is structured as follows. In Section 2, the scientific background is presented. Section 3 reports the methodology adopted for the prototype development, described in Section 4. In Section 5, experiments design on a real use case is presented, whereas obtained results are discussed in Section 6. Finally, Section 7 is devoted to conclusions.

2 Scientific Background

Nowadays, the need to consider the spatial dimension to ensure schedule feasibility and avoid critical issues,

such as safety, productivity, and constructability, is unanimously accepted by field experts. Stemming from this assumption, researchers have spent many efforts on the topic of workspace management. A 4D CAD system prototype, based on a micro-level discretization (i.e., building component space, labor crew space, equipment space, hazard space, protected space, and, finally, temporary structure space), has been developed in [6] to detect spatial interferences. Complementarily, the authors in [7] have introduced the concepts of macro-level (e.g., storage areas) and paths (e.g., equipment's and crews' paths) discretization. Macro- and micro-level discretizations have been extended in [2] by differentiating labor crew workspaces into static and dynamic ones, depending respectively on their full or partial usage across time. In [8], a micro-level discretization plus the space for material handling path have been defined and adopted for collecting and reusing historical activity-specific workspace information for congestion identification and safety analysis in BIM. In [3], workspaces defined by aforementioned studies have been grouped into two main categories: entity (i.e., laborers, mechanical equipment, and building components) and working spaces (i.e., spaces required to ensure smooth operation and tasks). The workspaces classification adopted in [9], inherited from the manufacturing industry, includes, in addition to workspaces occupied by building elements and reserved as safety distance, a discretization depending on the value added by activities. A "Main Workspace" is required by activities that add tangible value to the project (e.g., building a wall), whereas a "Support Workspace" is required by preparatory activities (e.g., transferring materials) supporting the first category. The authors have applied the described taxonomy to develop a construction workspace management tool using the XNA game engine. The same workspace taxonomy has been adopted in [10]–[12] to develop, using the serious game engine Unity3D™, spatial conflict simulators able [12] to detect interferences due to moving crews [10, 11] and falling objects. Numerous commercial 4D modeling software solutions are available in the market. A comparison between the two most popular ones, namely Autodesk Navisworks and Synchro Pro, has pointed out that, although both of them implements clash detection functionalities, the second one is more indicated for checking spatial interferences during the construction process [13], [14]. In addition, in order to carry out dynamic simulations, both the tools, not embedding any physics engine, require to define objects animations manually one by one.

The literature review has pointed out that existing studies, although assuming different workspace taxonomies and technological solutions, detect spatial conflicts based on – mostly static [2], [3], [6]–[9] – geometrical intersection tests among workspaces. Although this approach, stemming from detecting space resource overloads,

has provided significative contributions in automating the workspace management domain, spatial interferences strictly dependent from construction site dynamics still remain largely uncovered. An example is represented by dust-producing activities (e.g., sawing and smoothing operations of wooden formworks for concrete pouring) that in windy conditions may interfere with other ones, hence resulting incompatible, even if related workspaces do not intersect each other. Despite correlations between PM concentration and health diseases dates back several decades [5], to the best of the authors knowledge, no past study has addressed so far spatial interferences caused by PM-creating activities. In addition, no tool supporting projects managers in managing workspaces and dust hazards during the works planning phase exists yet. Technical difficulties in implementing a similar tool are related to the need to consider also meteorological and seasonal factors affecting PM concentration in construction sites [15].

In order to cover these gaps, this study proposes a workspace management framework aimed to reduce dust hazards by integrating spatial analysis with the construction work planning phase. A BIM-based spatial conflict simulator that spatially checks future working days, according to the work plan and atmospheric phenomena based on weather forecast data, has been developed. The resulting prototype has been developed in Unity3D™ and tested on a real construction site scenario.

3 Methodology

3.1 Air quality requirements for construction activities

PM is a group of polluting agents consisting of dust, smoke, and all types of solid and liquid materials that remain suspended in the air because of their small size [16]. In general, particulate matter is identified by the wording PM plus its size in μm . For example, PM100 indicates PM particles having a diameter of 100 μm . Past studies have shown as pollutants concentration tend to exceed regulations limits in construction sites. Some studies have confirmed that PM generated by construction activities has a certain degree of impact on the air throughout the city due to meteorological (e.g., wind, rainfall, etc.) and seasonal factors [15].

In this study, wood processing (e.g., sawing and smoothing operations) to produce formworks for concrete placing has been assumed as the reference activity generating PM. Even if wood is not a carcinogenic material, its dust can be, as potential harmful effects on health are determined by the penetration and deposition of particles in the first respiratory tract [17]. This is confirmed by the European Directive 2017/2398 [18] that sets the occupational exposure limit (OEL), measured over an 8-

hour period as the inhalable fraction, equal to 2 mg/m^3 . The inhalable fraction is defined by the UNI-EN 481/1994 standard [19] as the mass fraction of total airborne particles that can be inhaled by nose and mouth (i.e., particles having a 50 % size cut-off equal to an aerodynamic diameter of $100 \mu\text{m}$ corresponding to diameters between $10 \mu\text{m}$ and $100 \mu\text{m}$).

3.2 Workspace management framework for managing dust hazards

In order to cover the gaps identified in Section 2, the authors have proposed a workspace management framework that integrates the construction scheduling phase (Figure 1, top lane) with the contribution given by a spatial conflict simulator (Figure 1, bottom lane). The latter, developed by adopting the serious game engine technology (e.g., Unity3D™), can detect eventual incompatibilities between activities based on both the geometric and semantic information provided by BIM (Figure 1, green nodes) and the construction process data included in the construction schedule (Figure 1, blue nodes). To this purpose, workspaces must be generated in the gaming environment. In the state of the art of workspace management, a spatial conflict is detected between two given workspaces assigned to different crews only if their boundaries intersect each other. This study tries to go over by carrying out physics simulation of spreading dust under the effect of atmospheric phenomena based on weather forecast data. The latter must be retrieved for the desired temporal horizon and provided, along with workspaces,

as an input to physics simulations and geometric computations (Figure 1, red nodes). As a result, the list of detected spatial conflicts is generated and delivered to the reasoner that, once set according to regulations in force, can be applied to filter non-critical scenarios and avoid conflict overestimations (Figure 1, orange tasks). Afterwards, the construction management team, made aware of likely future incompatible activities, can adjust (Figure 1, blue nodes) or confirm (Figure 1, violet node) the workplan.

4 Prototype development

In this study, a prototype of spatial conflict simulator that, based on weather forecast data, carries out physics simulations in order to detect incompatible activities has been developed. The reasoner, instead, aiming to automatically discard negligible spatial conflicts related to under-threshold PM concentrations will be implemented in future studies according to PM limits [19] and fractions distributions [20] defined by regulations [18], [19].

4.1 Defining 4D model and workspaces

The spatial conflict simulator proposed by this study has been developed within the serious game engine Unity3D™. As shown in Figure 1 (bottom lane), the BIM model and the construction work schedule are provided as input to define the 4D model. BIM models can be imported into the gaming environment through several methods, involving different file formats (e.g., .ifc, .gltf, .fbx, etc.). In this study, the one involving

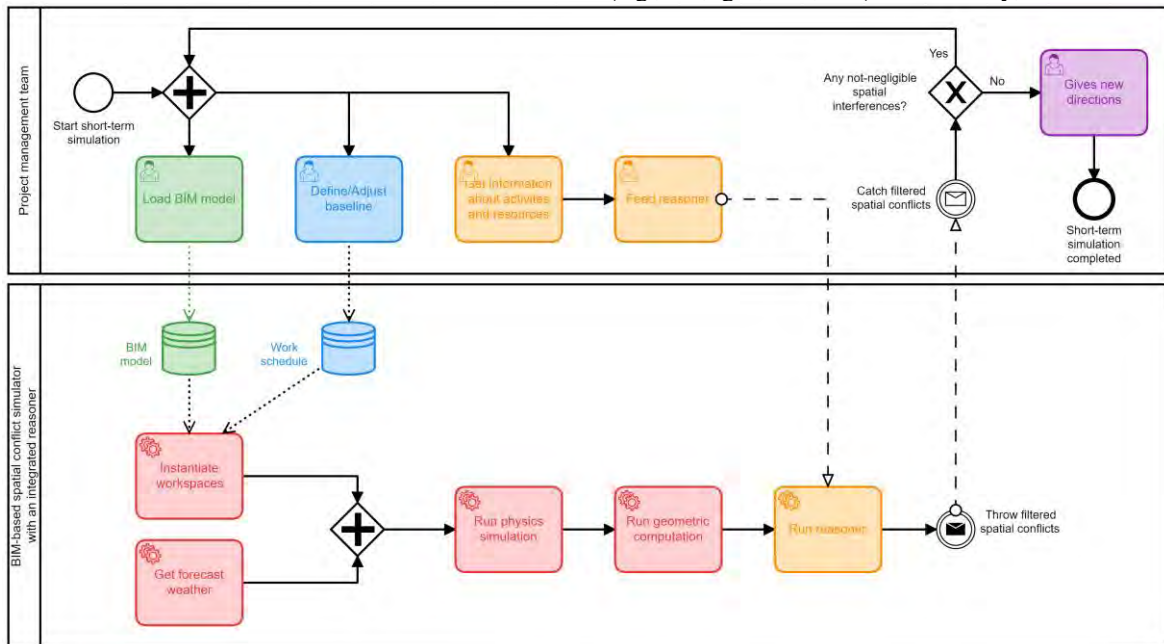


Figure 1. Proposed workspace management framework for managing dust hazards.

the .fbx (i.e., FilmBox) format has been adopted due to the smoother importing workflow, which only requires re-associating material through a computer graphics software (e.g., 3D Studio Max). In fact, contrarily to the other file formats requiring dedicated importers (e.g., “IFC importer” [20] or “Piglet: glTF Importer” [21]), an .fbx file can be directly added to the Unity3D™ scene as a prefab. Construction schedules are then imported into the serious gaming tool in .csv format using a C# script developed by the authors. Based on the 4D model information, another C# script developed by the authors generates main workspaces in the virtual gaming environment as “Cube” game objects, each one with an attached “Box collider” component enabling collision detection. The process of generating a main workspace has been fully described by the authors in [10], [12].

4.2 Retrieving forecast weather data

In order to identify any interference caused by dust-producing activities, PM spreading must be virtually simulated according to atmospheric phenomena replicated according to weather forecast data. The latter must be retrieved for the days the simulation is planned for. To this purpose, the Unity3D™ tool Real-Time Weather has been adopted. Such tool enables to retrieve weather forecast data up to several days into the future via “Tomorrow.io mode” or “OpenWeatherMap mode”. The only required inputs are the geographical coordinates of the construction site and an Api Key, available on tomorrow.io [22] and OpenWeathermap.org [23] web portals, respectively.

At this point, weather forecast data (e.g., wind speed and direction), required for dynamically simulate atmospheric phenomena, have been accessed. Such data can be displayed on a 24-hours or 7-days base by clicking on the dedicated information panel of the Real-Time Weather tool. The wind speed is expressed in m/s, whereas its direction in counter-clockwise radians from due north.

4.3 Running physics simulations and geometric computations

The serious game engine Unity3D™, embodying mechanical physics, enables to (i) virtually mirror likely weather conditions affecting the considered construction site and (ii) virtually simulate dust-producing activities during a specific time interval of the work plan.

About virtually mirroring likely weather conditions, this study focuses on replicating windy conditions (e.g., speed and direction) affecting PM spreading around the construction site. To this purpose, a virtual agent replicating the action of the wind spreading PM according to retrieved weather forecast data (Section 4.2) amongst construction site workspaces (Section 4.1) must be defined. To make this possible, a “Wind Zone” game object

[24], defining a virtual wind agent with its speed (i.e., “Main” field, expressed in unit of space per unit of time, assumed as m/s) and direction (i.e., “Rotation” Vector3 fields, expressed in degrees) within Unity3D™, has been used. In order to apply weather forecast data to simulate wind dynamics, the following two C# scripts have been defined by the authors:

- “ProcessWindData.cs”: for each simulation frame, it continuously processes wind speed and direction, provided by the Real-Time Weather tool, to make them readable by the “Wind Zone” game object. In particular, it converts the wind direction from radians to degrees.
- “GetWindData.cs”: for each simulation frame, it continuously gets wind data, processed by the previous C# script, and update speed (i.e., “Main” field) and direction (i.e., “Rotation” fields) of the “Wind Zone” game object.

About virtually simulating PM-creating activities, this study focuses on wood processing (e.g., sawing and smoothing operations) to produce formworks for concrete placing. To determine the amount of dust emitted by each piece of equipment, a report carried out by Veneto region [25], providing samplings for the production of wooden furniture and fixtures, has been assumed as a reference. Specifically, such report collects dust concentrations emitted by various pieces of equipment, measured during 2.5-hours samplings and expressed in mg/m³. In order to virtually simulate activities producing dust particles in Unity3D™, the “Particle System” effect [26] has been used. Such component requires the user to set the number of particles emitted per seconds. In order to determine such value, the following assumptions have been made:

- The particles volume has been computed by assuming diameters included between 10 μm and 100 μm, since wood particles within this range (i.e., inhalable fraction), if inhaled, produce carcinogenic effects [17]. In the absence of more detailed information, a uniform size distribution of 10 % for each 10-μm-interval between 10 μm and 100 μm has been assumed. The resulting 10 intervals exhaustively describe how the wind differently affects dust particles according to their size;
- The weight of a particle for each 10-μm-interval fraction has been computed by multiplying its volume by fir wood’s specific gravity;
- The number of emitted particles for each 10-μm-interval fraction has been computed by dividing the total weight of dust aspirated during samplings, provided by [25], by the weight of each particle size.

Furthermore, the “Particle System” effect has been defined by setting a spheric shape and the related volume.

In addition, such effect has been set by checking the “External Forces” and “Collision” features. The first one enables the movement of dust particles according to the wind speed and direction. The second one enables physical collisions against whole world’s game objects. This setting is required to quantify the amount of dust within a workspace, determined by monitoring the number of particles that impact against workspaces through the “OnParticleCollision” function [27]. By calling such function through a C# script assigned to each workspace game object, the number of collided particles is returned. The total weight of collided particles is computed as the sum of contributions obtained by multiplying the number of collided particles, uniformly distributed for each interval between 10 μm and 100 μm , by the weight of the corresponding particle size. Finally, the amount of dust within a workspace is computed as dust concentration by dividing the total weight of collided particles, computed assuming the same aforementioned size distribution of 10 % for each 10 μm -interval between 10 μm and 100 μm , by the workspace volume.

4.4 Sensitivity Analysis

The reason why a sensitivity analysis has been carried out is checking the realistic responsiveness of the developed spatial conflict simulator prototype. In fact, reasonable variations of dust in the considered workspaces should correspond to variations of dust in the amount of emitted particles and wind directions. To prove this, six different scenarios, reported by Table 1, have been defined by varying the number of emitting equipment (i.e., multiples of circular saws and orbital sanders), that produce a different amount of particles, and the wind direction (i.e., directions 1, 2, and 3). Figure 2 depicts the positions of emitters and workspaces and the assumed wind directions.

Results of sensitivity analysis, reported by Table 2, confirm what was expected. In fact, in scenario 2, which assumes the double the particles emitted in scenario 1 and wind blowing towards direction 1 like in scenario 1 (i.e., orthogonal to workspaces) (Table 1), the double the dust concentration of scenario 1 has been registered within workspaces (Table 2). In scenarios 3 and 4, as the wind

direction change into direction 2 (i.e., oblique to workspaces) (Table 1), dust concentration radically decreases within workspaces (Table 2). Even further, in scenarios 5 and 6, as the wind direction change into direction 3 (i.e., parallel to workspaces) (Table 1), dust concentration becomes zero within workspaces (Table 2). It must be noted that, for all scenarios, dust concentrations registered for workspace 3 are lower than the ones registered for the other workspaces. This is due to the fact that workspace 3 is located at a lower level than dust emitters and, hence, only marginally involved in particles uptake. Finally, results of sensitivity analysis are comparable to the limit of 2 mg/m^3 imposed by [18]. In scenarios 1 and 2, dust concentrations registered respectively for workspace 1 and workspaces 1 and 2 exceed such limit.

Table 1. Overview of sensitivity analysis’s scenarios.

Scenario	No. of dust emitters		Wind direction
	Circular saws	Orbital sander	
1	2	1	1
2	4	2	1
3	2	1	2
4	4	2	2
5	2	1	3
6	4	2	3

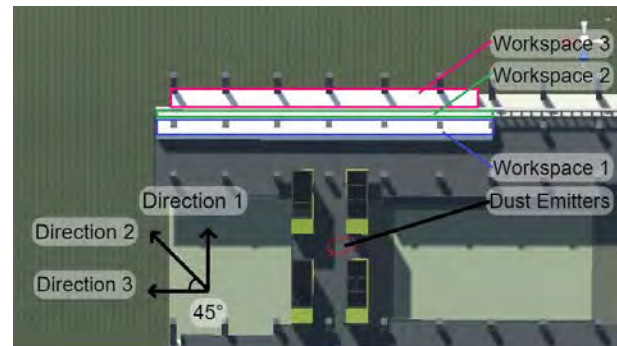


Figure 2. Sensitivity analysis’s set up indicating positions of emitters and workspaces and wind directions.

Table 2. Results of sensitivity analysis.

Workspaces	Volume [m^3]	Dust concentration [mg/m^3]					
		Scenario 1	Scenario 2	Scenario 3	Scenario 4	Scenario 5	Scenario 6
Workspace 1	350,63	1,160	2,320	0,190	0,380	0,000	0,000
Workspace 2	175,31	2,080	4,170	0,220	0,430	0,000	0,000
Workspace 3	645,00	0,003	0,006	0,004	0,009	0,000	0,000



Figure 3. Construction site use case with workspaces and dust emitters.

5 Use Case and Experiments Design

The proposed spatial conflict simulator, once its functioning has been confirmed by sensitivity analysis, has been tested on a real construction site scenario. To this purpose, the construction process of the Eustachio Building, a public building hosting the Faculty of Medicine of the Polytechnic University of Marche, has been selected as an example for validation purposes (Figure 3). The Eustachio Building is located in the extra-urban area of Ancona (Italy), close to the main regional hospital. The mixed-use building is arranged on six floors above ground and has a total area of 16,900 m². For simplicity and paper length constraints, only two working days (i.e., January 30th and 31st, 2023) of the construction work schedule, highlighted by a red box in Figure 4, have been taken into account for experiments design.

The experiments, carried out in this study, consist in applying the developed spatial conflict simulator, according to the workspace management framework presented in Section 3.2, for detecting eventual spatial interferences due to dust hazard in the two considered working days. The experiments start with loading the BIM model and the work schedule within the gaming environment in order to generate workspaces (Section 4.1). Afterwards, weather forecast data will be retrieved as described in Section 4.2 and, finally, physics simulations of selected working days with related wind conditions will be carried out. Each working day has been assumed including 8 working hours, from 8 am to 4 pm.

Task name	Duration	Start	Finish	
Install west side stairwells formworks	2 days	Mon 30/01/23	Tue 31/01/23	
Install 3rd level north wing E alignment pillars	2 days	Mon 30/01/23	Tue 31/01/23	
Install 3rd level north wing north facades	4 days	Mon 30/01/23	Thu 02/02/23	
Place ground level north wing part ovest industrial flooring	2 days	Mon 30/01/23	Tue 31/01/23	

Figure 4. Excerpt of the overall construction schedule reporting the activities scheduled for the selected working days (i.e., January 30th and 31st, 2023).

The four activities, scheduled for these days, are shown in Figure 4. They include the installation of pre-cast façade (3rd level, north-west wing), the installation of precast pillars (3rd level, north-west wing), the placing of the industrial flooring (ground floor, north-west wing), and the installation of stairwells formworks (3rd level, west block). The latter activity, responsible for creating and spreading PM into the environment, involves sawing and smoothing operations of the wooden formwork. They take place in the area among the four stairwells, highlighted in yellow in Figure 3. The cutting operation has been assumed to be done by using two circular table saws, while the smoothing operation by using an orbital sander. A reasonable construction site layout has been assumed in this study. Although temporary construction structures (e.g., scaffoldings) may affect dust spreading, they have not been considered in this first implementation. This is justified by the fact that this paper, presenting a proof of concept of the proposed spatial conflict simulator, focuses on the prototype development and testing.

6 Results and Discussion

Experiment results, obtained by carrying out spatial conflict simulations for the working days January 30th and 31st, 2023, have been reported in Table 3. Experiments results for the selected working days (i.e., January 30th and 31st, 2023).. Dust concentrations in the three workspaces are very low for both days and do not exceed the threshold of 2 mg/m³ imposed by [18]. These results can be explained by considering that on January 30th, the weather forecast data indicates low wind speeds (i.e., between 3,33 m/s to 3,38 m/s) and a North-East direction, that is oblique to workspaces. Hence, workspaces have been only partially affected by dust spreading. On January 31st, the weather forecast data indicates low wind speeds (i.e., between 3,45 m/s to 4,19 m/s) and a East direction, that is parallel to workspaces. Hence, workspaces have not been affected by dust spreading. In these cases, since dust concentration complies with the aforementioned regulation limit, the reasoner would return no incompatibilities among scheduled activities, meaning that the work plan can be confirmed by the project manager and delivered as it is to the construction site. Contrarily,

Table 3. Experiments results for the selected working days (i.e., January 30th and 31st, 2023).

Workspaces	Volume [m ³]	Dust concentration [mg/m ³]	
		30 th Jan	31 th Jan
Install 3 rd level north wing E alignment pillars	350,63	0,024	0,000
Install 3 rd level north wing north facades	175,31	0,020	0,000
Placing ground level north wing west part industrial flooring	645,00	0,000	0,000

in case registered dust concentrations exceed the regulation limit [18], the application of mitigation actions to the workplan should be evaluated by the project manager. An example of mitigation action could be giving directions to wear PPE (e.g., face masks) to who is working in workspaces close to the emitters and affected by above-threshold dust concentrations. Another example of mitigation action could be moving backward or forward the PM-emitter and/or the PM-receiving activities.

7 Conclusions and outlook

This study, being construction sites one of the major responsible for emitting PM whose long exposure may cause health diseases, has focused on spatial interferences related to dust hazard, still representing an open issue. In fact, to the best of the authors knowledge, no study has addressed yet spatial interferences caused by dust-producing activities under the effect of meteorological and seasonal factors. In addition, no tool supporting projects managers in managing workspaces and dust hazards during the works planning phase exists yet. In order to cover these gaps, this study proposes a workspace management framework aimed to reduce dust hazards by integrating spatial analysis with the planning phase. A BIM-based spatial conflict simulator that spatially checks future construction work plans according to atmospheric phenomena based on weather forecast data has been developed. The resulting prototype has been implemented in Unity3DTM and its functioning confirmed through sensitivity analysis before to be applied on a real construction site scenario. Experiments results confirmed the possibility to virtually simulate construction activities and atmospheric phenomena in order to support project managers in adopting countermeasures against interferences due to dust hazards.

Limitations of this study can be summarized as follows. First, in this study, the reasoner has not been imple-

mented yet. Hence, the compliance of dust concentrations, registered during spatial conflict simulations carried out by the developed prototype, to the regulation limit has been assessed manually. In addition, dust spreading has been simulated within the gaming environment under the effect of only wind speed and direction. In future implementation, more atmospheric phenomena (e.g., rainfall), seasonal factors, and particles size distributions will be considered. Sensitivity analysis, virtually carried out within the gaming environment, will be extended with real world experiments in order to assess the consistency of simulation results to reality. Finally, future studies will investigate on the possibility to integrate (e.g., through a Functional Mock-up Unit) the proposed spatial conflict simulator with an external co-simulator, supporting advanced fluid dynamics simulations of dust spreading.

Acknowledgments

This research has been partially funded by the EU research project entitled “Encore” (Project Number 820434) and the Italian Ministry of Education, University and Research PRIN 2017 research project entitled “A Distributed Digital Collaboration Framework for Small and Medium-Sized Engineering Enterprises” (prot. 2017EY3ESB).

References

- [1] A. Hosny, M. Nik-Bakht, and O. Moselhi, “Workspace planning in construction: non-deterministic factors,” *Autom Constr*, vol. 116, no. March, 2020, doi: 10.1016/j.autcon.2020.103222.
- [2] A. Mirzaei, F. Nasirzadeh, M. Parchami Jalal, and Y. Zamani, “4D-BIM Dynamic Time-Space Conflict Detection and Quantification System for Building Construction Projects,” *J Constr Eng Manag*, vol. 144, no. 7, p. 04018056, 2018, doi: 10.1061/(asce)co.1943-7862.0001504.
- [3] H. Ma, H. Zhang, and P. Chang, “4D-Based Workspace Conflict Detection in Prefabricated Building Constructions,” *J Constr Eng Manag*, vol. 146, no. 9, p. 04020112, 2020, doi: 10.1061/(asce)co.1943-7862.0001883.
- [4] S. Ahmed and I. Arocho, “Emission of particulate matters during construction: A comparative study on a Cross Laminated Timber (CLT) and a steel building construction project,” *Journal of Building Engineering*, vol. 22, pp. 281–294, Mar. 2019, doi: 10.1016/j.jobeb.2018.12.015.
- [5] J. S. Kinsey and C. Cowherd, “Particulate emissions from construction activities,” *J Air Waste Manage Assoc*, vol. 55, no. 6, pp. 772–783, 2005, doi: 10.1080/10473289.2005.10464669.

- [6] B. Akinci, M. Fischen, R. Levitt, and R. Carlson, "Formalization and Automation of Time-Space Conflict Analysis," *Journal of Computing in Civil Engineering*, vol. 16, no. 2, pp. 124–134, 2002, doi: 10.1061/(asce)0887-3801(2002)16:2(124).
- [7] N. Dawood and Z. Mallasi, "Construction workspace planning: Assignment and analysis utilizing 4D visualization technologies," *Computer-Aided Civil and Infrastructure Engineering*, vol. 21, no. 7, pp. 498–513, 2006, doi: 10.1111/j.1467-8667.2006.00454.x.
- [8] S. Zhang, J. Teizer, N. Pradhananga, and C. M. Eastman, "Workforce location tracking to model, visualize and analyze workspace requirements in building information models for construction safety planning," *Autom Constr*, vol. 60, pp. 74–86, 2015, doi: 10.1016/j.autcon.2015.09.009.
- [9] M. Kassem, N. Dawood, and R. Chavada, "Construction workspace management within an Industry Foundation Class-Compliant 4D tool," *Autom Constr*, vol. 52, pp. 42–58, 2015, doi: 10.1016/j.autcon.2015.02.008.
- [10] L. Messi, B. Garcia de Soto, A. Carbonari, and B. Naticchia, "Spatial conflict simulator using game engine technology and Bayesian networks for workspace management," *Autom Constr*, vol. 144, p. 104596, Dec. 2022, doi: 10.1016/j.autcon.2022.104596.
- [11] L. Messi, B. G. de Soto, A. Carbonari, and B. Naticchia, "Intelligent BIM-based spatial conflict simulators: A comparison with commercial 4D tools," *Proceedings of the 39th ISARC*, p. pp 550-557, 2022, doi: 10.22260/ISARC2022/0078.
- [12] L. Messi, B. Garcia de Soto, A. Carbonari, and B. Naticchia, "Addressing COVID-19 Spatial Restrictions on Construction Sites Using a BIM-Based Gaming Environment," *Proceedings of the 38th ISARC*, no. Isarc, pp. 521–528, 2021, doi: 10.22260/isarc2021/0071.
- [13] Y. Nechyporchuk and R. Bašková, "The conformity of the tools of selected software programs for 4D building modeling," *IOP Conf Ser Mater Sci Eng*, vol. 867, no. 1, 2020, doi: 10.1088/1757-899X/867/1/012034.
- [14] SYNCHRO Construction, "15 Minute Fridays: Using Synchro PRO for Workspace Clash Detection," 2015. <https://www.youtube.com/watch?v=x0fv3So5Rkc> (accessed Nov. 27, 2021).
- [15] R. J. B. de Moraes, D. B. Costa, and I. P. S. Araújo, "Particulate Matter Concentration from Construction Sites: Concrete and Masonry Works," *Journal of Environmental Engineering*, vol. 142, no. 11, Nov. 2016, doi: 10.1061/(asce)ee.1943-7870.0001136.
- [16] United States Environmental Protection Agency (USEPA), "Particulate Matter (PM) Pollution," 2017. <https://www.epa.gov/pm-pollution> (accessed Jan. 28, 2023).
- [17] INAIL, "Esposizione lavorativa a polveri di legno," 2012. [Online]. Available: www.inail.it
- [18] European Union, "Directive (EU) 2017/2398 of the European Parliament and of the Council of 12 December 2017 amending Directive 2004/37/EC on the protection of workers from the risks related to exposure to carcinogens or mutagens at work," 2017. <https://eur-lex.europa.eu/legal-content/EN/TXT/?uri=CELEX%3A32017L2398> (accessed Jan. 29, 2023).
- [19] UNI-EN, "UNI EN 481:1994 - Atmosfera nell'ambiente di lavoro. Definizione delle frazioni granulometriche per la misurazione delle particelle aerodisperse," 1994. <https://store.uni.com/uni-en-481-1994> (accessed Jan. 29, 2023).
- [20] Arcventure, "IFC importer." 2022. <https://assetstore.unity.com/packages/tools/utilities/ifc-importer-162502> (accessed Jan. 28, 2023).
- [21] Awesomesauce Labs, "Piglet: glTF Importer," 2022. <https://assetstore.unity.com/packages/tools/utilities/piglet-gltf-importer-173425> (accessed Jan. 28, 2023).
- [22] The Tomorrow Companies Inc., "tomorrow.io API key," 2022. <https://app.tomorrow.io/development/keys> (accessed Jan. 28, 2023).
- [23] OpenWeather, "OpenWeathermap API key," 2022. <https://openweathermap.org/api> (accessed Jan. 28, 2023).
- [24] Unity Technologies, "Wind Zones," 2021. <https://docs.unity3d.com/Manual/class-WindZone.html> (accessed Jan. 28, 2023).
- [25] Direzione Regionale per la Prevenzione, "Linee Guida per l'applicazione del Titolo VII del D.Lgs. 626/94, come modificato dal D.Lgs. 66/2000, alle attività comportanti esposizione a polveri di legno," 2000.
- [26] Unity Technologies, "ParticleSystem," 2023. <https://docs.unity3d.com/ScriptReference/ParticleSystem.html> (accessed Jan. 28, 2023).
- [27] Unity Technologies, "OnParticleCollision," 2023. <https://docs.unity3d.com/ScriptReference/MonoBehaviour.OnParticleCollision.html> (accessed Jan. 28, 2023).

MN-Pair Contrastive Damage Representation and Clustering for Prognostic Explanation

Takato Yasuno¹, Masahiro Okano¹ and Junichiro Fujii¹

¹Yachiyo Engineering, Co.,Ltd. Research Institute for Infrastructure Paradigm Shift, Japan.

{tk-yasuno, ms-okano, jn-fujii}@yachiyo-eng.co.jp

Abstract – For infrastructure inspections, damage representation does not constantly match the predefined classes of damage grade, resulting in detailed clusters of unseen damages or more complex clusters from overlapped space between two grades. The damage representation has fundamentally complex features; consequently, not all the damage classes can be perfectly predefined. The proposed MN-pair contrastive learning method helps to explore an embedding damage representation beyond the predefined classes by including more detailed clusters. It maximizes both the similarity of M-1 positive images close to an anchor and dissimilarity of N-1 negative images using both weighting loss functions. It learns faster than the N-pair algorithm using one positive image. We proposed a pipeline to obtain the damage representation and used a density-based clustering on a 2-D reduction space to automate finer cluster discrimination. We also visualized the explanation of the damage feature using Grad-CAM for MN-pair damage metric learning. We demonstrated our method in three experimental studies: steel product defect, concrete crack, and the effectiveness of our method and discuss future works.

Keywords –

Damage Representation; Density-Based Spatial Clustering; Damage Importance Explanation.

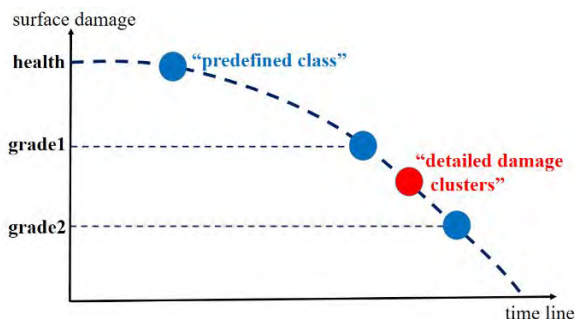


Figure 1. Predefined classes and finer clusters for prognostic damage understanding

1 Introduction

1.1 Objective and Pipeline

1.1.1 Damage Inspection and Clustering Problem

It is crucial for infrastructure managers to maintain high standards, to ensure user satisfaction during daily operations. Surveillance cameras and drone inspections have enabled progress toward automating the inspection of damaged features and assessing the deterioration of infrastructure. By providing a pair of raw images and damage class labels, we can train the supervised learning to identify a predefined grade of damage and displacement. However, such a damage representation does not constantly match the predefined classes of damage grade, hence, there may be some detailed clusters from the unseen damage spaces or more complex clusters from overlapped spaces between two damage grades, as shown in Figure 1. Damage representations have fundamentally complex features; consequently, not all the damage classes can be perfectly predefined.

In practice, some grades of damage that includes complex features may be occasionally scattered for human annotators to consistently categorize. Furthermore, there are rare occurrences of minor classes of deterioration, making it difficult to establish predefined classes that encompass all possible damage types based solely on our prior knowledge. Contrastive learning methods present an opportunity to explore the embedding damage representations beyond these predefined classes, allowing for the identification of more detailed clusters.

1.1.2 Contrastive Damage Metric Learning

Deep metric learning has been extensively investigated using shared-parameter networks, such as Siamese and triplet networks [1]. Since 2013, various contrastive loss function minimizations have been proposed for learning representations from pairs of similar/dissimilar samples [2]. For face recognition, verification, and clustering, several deep convolutional networks have been used to map from facial images onto

a compact Euclidean space, where the distance points indicates the degree of facial similarity [3][4]. The usefulness of deep metric learning for recognizing the target of damaged surface similarity in infrastructure, in the construction domain, has still not been sufficiently understood.

During the lifecycle of a deterioration process, the damaged surface of infrastructures frequently exhibits complex representations. While inspecting against the surface on the parts of a structure using vision-based technology, predefined qualitative grading classes are used to recognize and record any damage observed. Despite the possibility of encountering unseen circumstances and ambiguous statuses that fall outside of predefined classes, further experience may be necessary. Furthermore, complex defects can include multiple types of damages and a mixture of defects that are not typically observed in real-world structural monitoring.

Measuring the similarity of damage in high-dimensional visual images requires the learning of an embedding in a lower-dimensional damaged space. Once such a damage-embedding space has been produced, vision-based inspection tasks such as damage recognition, diagnosis, and prognostic clustering can be easily implemented as standard techniques with damage embedding as feature vectors.

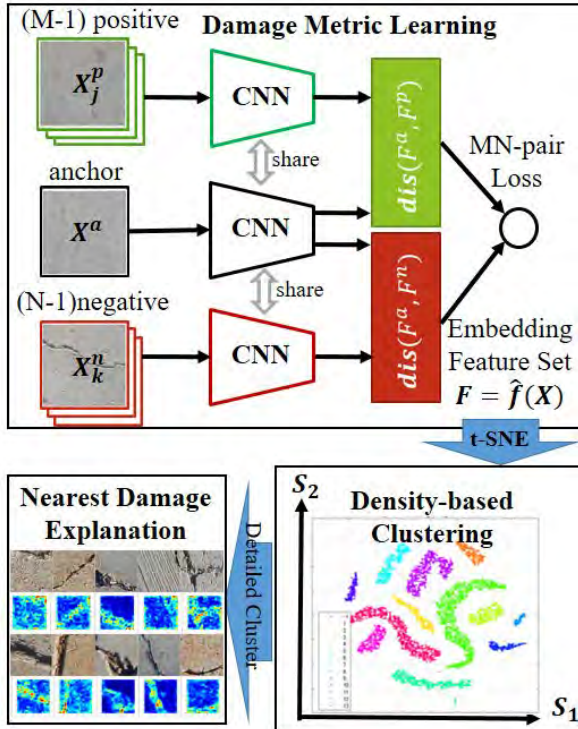


Figure 2. Our pipeline for damage representation learning, embedded clustering, and explanation

1.1.3 Damage Representation Clustering Pipeline

As shown in Figure 2, we proposed a damage representation pipeline for learning damage features and for clustering more detailed heterogeneous damages. The first training stage involved developing a damage metric learning. Our proposed MN-pair contrastive learning method maximizes both the similarity of M-1 positive images to an anchor and the dissimilarity of N-1 negative images, using a weighting MN-pair loss function. Triplet networks share the parameters under a convolutional neural network (CNN). The outputs of the damage-embedding feature set with 16 elements were reduced to two dimensions using the t-SNE algorithm. The second stage was density-based clustering toward more detailed damage clusters with an outlier option using the density-based spatial clustering application with noise (DBSCAN) algorithm. The third explanation stage involved sorting the nearest feature scores and visualizing the tiles of the ten nearest images. Furthermore, each image enabled us to compute heat maps using an adapted Grad-CAM algorithm for the metric learning of MN-pair damage.

2 Damage Representation Learning

2.1 MN-pair Damage Contrastive Learning

Let \mathbf{x} denote the set of inspected input images with predefined deterioration classes. Let $\mathbf{e}_i = f(\mathbf{x}_i; \boldsymbol{\theta}) \in R^L$ be the i -th damage embedding of input $i \in \{1, \dots, n\}$ that preserves the damage semantic aspects. Here, n is the number of input images. Furthermore, $\boldsymbol{\theta}$ is a shared parameters under a CNN for damage metric learning, and L is the dimension of the damage embedding space. Let $\mathbf{F}_i = \mathbf{e}_i / \|\mathbf{e}_i\|_2$ be the l_2 -normalized version. The damage similarity can be measured from the distance between the two images i_1 and i_2 using the normalized cosine similarity:

$$s_{\theta}(\mathbf{x}_{i_1}, \mathbf{x}_{i_2}) = (\mathbf{F}_{i_1})^T \mathbf{F}_{i_2} \quad (1)$$

where larger values indicate greater similarities. Here, the suffix T denotes the transposed operation.

The N-pair loss approach [5] creates a multiclass classification in which we create a set of N-1 negative $\{\mathbf{x}_k^-\}_{k=1}^{N-1}$ and one positive \mathbf{x}_j^+ for every anchor image \mathbf{x}_i . We define the following N-pair loss function for each set:

$$L_{N\text{-pair}}(\boldsymbol{\theta}; \mathbf{x}_i, \mathbf{x}_j^+, \{\mathbf{x}_k^-\}_{k=1}^{N-1}) = \log \left(1 - \exp(s_{\theta}(\mathbf{x}_i, \mathbf{x}_j^+)) + \sum_{k=1}^{N-1} \exp(s_{\theta}(\mathbf{x}_i, \mathbf{x}_k^-)) \right) \quad (2)$$

For simple expression, we denote cosine similarities as:

$$s_{i,j}^{a,+} = s_{\theta}(\mathbf{x}_i, \mathbf{x}_j^+) / \tau, \quad s_{i,k}^{a,-} = s_{\theta}(\mathbf{x}_i, \mathbf{x}_k^-) / \tau \quad (3)$$

Here, this is divided by a normalized temperature scale τ . This scale enhances small values, to ensure that N-pair loss is able to train efficiently, for example, we can set the scale $\tau=0.3$. Thus, the N-pair loss in (2) can be expressed as follows:

$$= -\log \frac{\exp(s_{i,j}^{a,+})}{\exp(s_{i,j}^{a,+}) + \sum_{k=1}^{N-1} \exp(s_{i,k}^{a,-})} \quad (4)$$

The N-pair loss is identical to the InfoNCE loss [6][7]. However, N-pair loss is a slow starter, because of the presence of only one positive image toward N-1 negative images. A positive signal is important to bond the inner embedding space around the same class of each anchor.

Thus, we propose an MN-pair weighting loss instead of (2)-(4), in which we create a set of N-1 negative $\{\mathbf{x}_k^-\}_{k=1}^{N-1}$ and M-1 positive $\{\mathbf{x}_j^+\}_{j=1}^{M-1}$ for every anchor \mathbf{x}_i :

$$L_{MN-pair}(\boldsymbol{\theta}; \mathbf{x}_i, \{\mathbf{x}_j^+\}_{j=1}^{M-1}, \{\mathbf{x}_k^-\}_{k=1}^{N-1}) = -\log \frac{v \sum_{j=1}^{M-1} \exp(s_{i,j}^{a,+})}{v \sum_{j=1}^{M-1} \exp(s_{i,j}^{a,+}) + w \sum_{k=1}^{N-1} \exp(s_{i,k}^{a,-})} \quad (5)$$

where v is a positive weight, and w is a negative weight constrained by that $v + w = 1$, for example, $v = 0.15$. To train the parameters $\boldsymbol{\theta}$ under a CNN for damage metric learning, we can minimize the MN-pair loss function $L_{MN-pair}$ using a standard optimizer, such as, the Adam.

2.2 Density-Based Damage Clustering

Using the damage-embedded feature \mathbf{F}_i , with $i \in \{1, \dots, n\}$ and the dimension L , we can reduce its dimension into two axes of scores using the t-SNE algorithm [8]. Several different concepts exist for clusters of damage representation, including, 1) well-separated clusters, 2) center-based clusters within a specified radius, and 3) density-based clusters. Under a two-dimensional damage-embedding space, we can use either a center-based or a density-based approach. The former is based on the distance from neighboring points to the center, such as the K-means [9], and k-nearest neighbor [10]. To provide an effective approach for representing a heterogeneous subdivided region of damage beyond the predefined classes, we used the density-based clustering algorithm (DBSCAN) [11]. The points of the embedded damage features were classified into 1) *core points* in the interior of a dense region, 2) *border points* on the edge of a dense region, and 3) *noise points* in a sparsely occupied region (a noise or background). The DBSCAN algorithm is formally expressed as

1. Label all points as core, border, or noise points.
2. Eliminate noise points.

3. Put an edge between all core points that are within a user-specified distance parameter ϵ of each other.
4. Make each group of connected core points into a separate cluster.
5. Assign each border point to one of the clusters of its associated core points.

Because we used a density-based definition of a cluster, it is relatively resistant to noise and can handle clusters with arbitrarily damaged shapes. Therefore, DBSCAN can determine numerous damage clusters that cannot be identified using a center-based algorithm, such as k-means. For damage representation clustering, we can set a distance parameter (for example, $\epsilon=3$) and a minimum number of neighbors for core points (for example, 10).

2.3 Nearest Damage Explanation

CNN models with millions of shared parameters achieve satisfactory performance in contrastive deep metric learning. The reasons for this remain unclear despite the impressive performance. Visualization techniques are mainly divided into a masked sampling and an activation mapping approaches. The former includes the occlusion sensitivity [12] and the local interpretable model-agnostic explanations (LIME) [13]. The merits of this approach is that it does not require in-depth knowledge of the network's architecture, and the disadvantage is that it requires iterative computations per image a significant amount of running time for local partitioning, masked sampling, and output prediction. To represent damage metric contrastively, this output is not an image-based prediction output, but an embedding damage feature \mathbf{F}_i , $i \in \{1, \dots, n\}$ extracted from a CNN output layer for contrastive damage metric learning. Therefore, we selected an activation map approach such as the class activation map (CAM) [14] or gradient-based extension (Grad-CAM) [15]. The weighting feature map of the CAM is ineffective because it limits the global average pooling (GAP) and fully-connected (FC) at the concluding layer of a CNN.

Inspired by the work of [16], we proposed a gradient-based visualization technique for damage metric learning. The final layer of our proposed MN-pair contrastive learning is a damage-embedding space FC sized $1 \times 1 \times L$. Unlike a classification model, we cannot specify any pair of similarities between the anchor, positive, and negative because of the numerous combinations of their pairs. Practically, we proposed a *reduced similarity score* as a *reduction function* to enhance the average powered similarity for a damage explanation as follows:

$$y^S(\mathbf{U}) = \sum_{m=1}^K (U^m)^2 \quad (6)$$

where $\mathbf{U} = (U^1, \dots, U^K)$ is an embedded damage feature

with K dimensions before the final output layer with a size of $1 \times 1 \times K$ and serves as the *reduction layer*; for example, FC $1 \times 1 \times 128$. To obtain the similarity contrastive localization map $G_{Grad-CAM}^S \in R^{W \times H}$, we can compute the gradient of the reduced similarity score $y^S(\mathbf{U})$ with respect to feature map activations $A^m(x, y)$ of the convolutional or ReLU layer serving as a *feature layer*, that is, $\partial y^S / \partial A^m$. Here, A^m has the size of the array $W \times H \times K$, for example, ReLU $20 \times 20 \times 128$. These gradients flowing back are global averages pooled over the width x and height y , respectively to obtain the similarity importance weights.

$$\alpha_m^S = \frac{1}{WH} \sum_x \sum_y \frac{\partial y^S}{\partial A^m(x, y)}, m = 1, \dots, K. \quad (7)$$

Thus, this weight α_m^S represents partial linearization of the CNN downstream from feature map activations A^m , and captures the similarity importance. We can use a weighted combination of forward activation maps for damage similarity representation learning.

$$G_{Grad-CAM}^S = ReLU \left(\sum_{m=1}^K \alpha_m^S A^m \right). \quad (8)$$

3 Applied Results

We conducted experimental studies using our method and applied it to three damage datasets of damage.

3.1 Damage Dataset and Training Setup

We implemented experiments using open-accessed datasets of steel product defects (11,638 samples from steel defect detection [17]) and concrete cracks on decks and pavements (12,633 samples from SDNET2018 [18]). Table 1 illustrates each dataset for the experimental studies containing the target damage, the number of predefined classes, and the partitions of the training and test images, respectively.

Table 1. Datasets for experimental studies

Target damage	Predefined Classes	Number of training/test
Steel product defect	5	8,148 / 3,490
Concrete crack	4	8,844 / 3,789

Table 2. Summarizes the sizes of input damage images and the number of clusters from the results of DBSCAN clustering under the damage embedding space with two dimensions reduced by the t-SNE. Surprisingly, our contrastive damage representation learning provided two or more multiplied clusters toward the number of

predefined classes in Table 1.

Table 2. Training image size and clustering results

Target damage	Input Image Size [h,w]	Density-Based Output of Clusters
Steel product defect	[256, 256]	10
Concrete crack	[256, 256]	13

As listed in Table 3, we set the layer type and output shape of the CNN architecture for our experiments. We set up a simple but practical network with 15 layers containing convolution-ReLU-max pooling, and FC. The architecture had neither batch normalization nor skip connections. We set the mini-batch to 128 and the number of iterations to 2,000–5,000 while training the CNN network to obtain a stable loss curve. We used the Adam optimizer with a learning rate of 0.0001, and set the gradient decay factor to 0.9, and set the squared gradient decay factor to 0.99. We used image augmentation with random erasing [21][22]. Ablation studies were conducted on 128, 144, 160, 180, and 200 pixels, the input size was set to $160 \times 160 \times 3$. We also set the output dimensions of the damage-embedding space to 16 after conducting ablation studies on 8, 16, and 32. Furthermore, we set the temperature scale to 0.3, compared with the ablation studies of 0.1, 0.2, 0.3, and 0.5. Finally, we set the hyperparameters of the MN-pair damage contrastive learning $M=N$ to 4 and 5, which corresponds to the number of classes in the target dataset. We also set the positive weight to $v = 0.15$, after testing values of 0.1, 0.15, 0.2, and 0.3. For written space restriction, we eliminated these ablation studies where the evaluation index was the overall accuracy from the damage-feature-based classification trained to test the dataset. To compute the gradient-based activation map Grad-CAM, we set the feature layer to Relu4 and set the reduction layer to FC1, as listed in Table 3.

Table 3. Layer type and shape of CNN architecture

Layer type	Output Shape (S,S,C)	Params #
Conv1-Relu1	160,160,8	224
Maxpool1	80,80,8	--
Conv2-Relu2	80,80,32	2,336
Maxpool2	40,40,32	--
Conv3-Relu3	40,40,64	18,496
Maxpool3	20,20,64	--
Conv4-Relu4	20,20,128	73,856
FC1-Relu5	1,1,128	6,553,728
FC2	1,1,16	2,064
total	Learnables	6.6M

3.2 Steel Defect Representation Results

3.2.1 Steel Defect Embedding Clustering

Figure 3 illustrates the results of steel defect clustering using five colors under the damage-embedding space using the t-SNE. The predefined 1st normal class (red), 3rd inclusion (light green), and patch defect (magenta) were subdivided into two or three regions.

Figure 4 shows the results for the density-based 11 clusters using the HSV-based colors from 1 to 11. Note that an outlier exists in the predefined 4th scratch class. We found that the steel damage representation using damage metric learning did not match the predefined five classes of steel defects, as shown in Figure 3. These results analyze 11 clusters in detail; thus the calibrated clusters were density-based and separated independently, as shown in Figure 4.

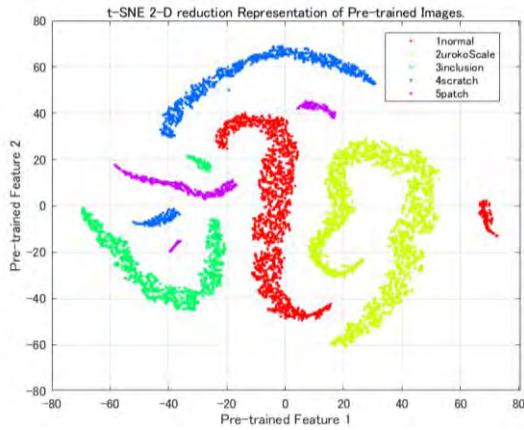


Figure 3. t-SNE visualization of 2-D reduced outputs obtained through training 5 classes of steel defects

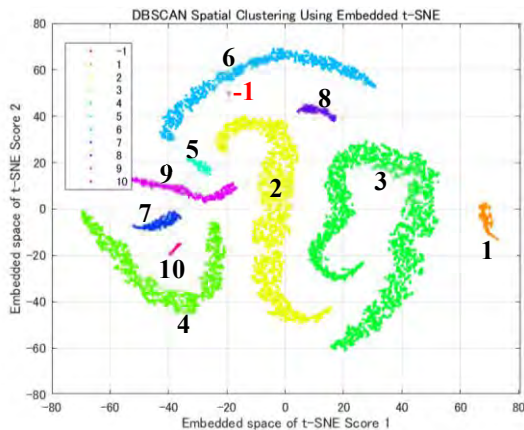


Figure 4. Density-based clustering of Steel product defects into ten using the DBSCAN

3.2.2 Steel Defect of Each Cluster Nearest Images

Figure 5 depicts the density-based ten steel clusters in each row of images, where the first column is sampled, and the nine right images have the nearest similarity

score. The numbers on the left-hand side denotes each group shown in Figure 4. The clustered outputs were obtained using a density-based clustering method on a steel dataset.

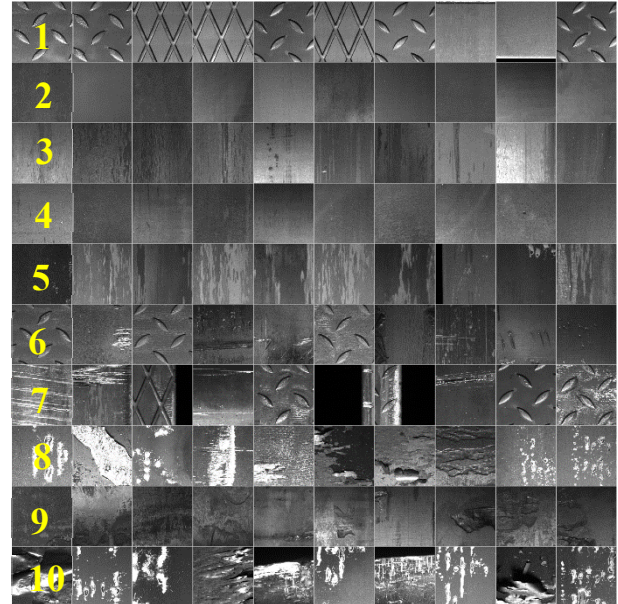


Figure 5. Density-based ten clusters in each row of images, the first column is sampled, and the right nine images have nearest similarity scores

3.2.3 Steel Product Defect Explanation

Figure 6 illustrates the results of the steel defect explanation by computing the gradient-based activation map using Grad-CAM for contrastive damage metric learning. The order of the rows and columns is the same as that shown in Figure 5. The heat maps illustrate the damage features of the steel defect clusters.

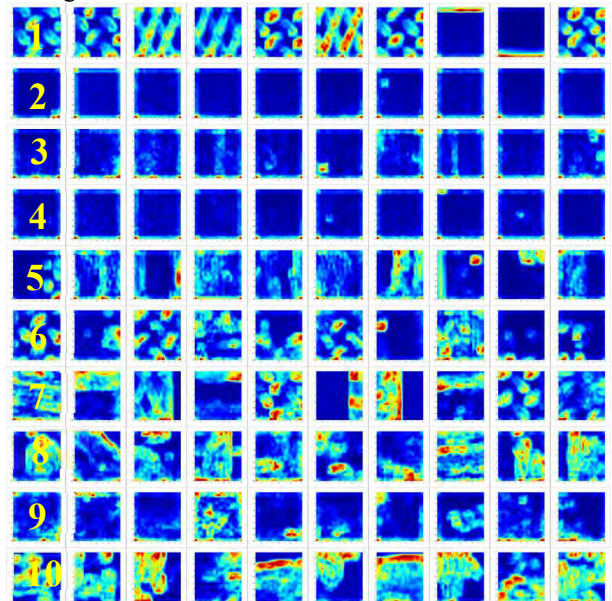


Figure 6. Steel defect of damage explanation

3.3 Concrete Crack Representation Results

3.3.1 Concrete Crack Embedding Clustering

Figure 7 illustrates the results of crack clustering using the four colors under the damage-embedding space using t-SNE. The predefined 1st deck-crack class (red), 3rd pavement-crack (light green), and pavement-non-crack (magenta) classes were subdivided into three or four regions.

Figure 8 shows the results for the density-based 14 clusters using HSV-based colors numbered from 1 to 14. Note that one outlier exists in the fourth class of pavements-non-crack. We found that the concrete damage representation using damage metric learning did not match the predefined four classes of cracks, as shown in Figure 7. These results analyze 14 clusters in detail; thus, the calibrated clusters were density-based and separated independently, as shown in Figure 8.

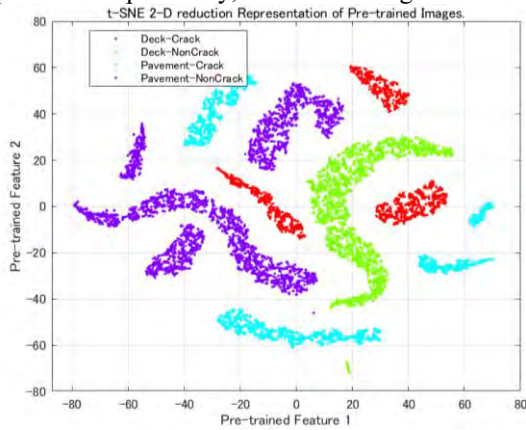


Figure 7. t-SNE visualization of 2-D reduced outputs obtained through training 4 classes of concrete damage

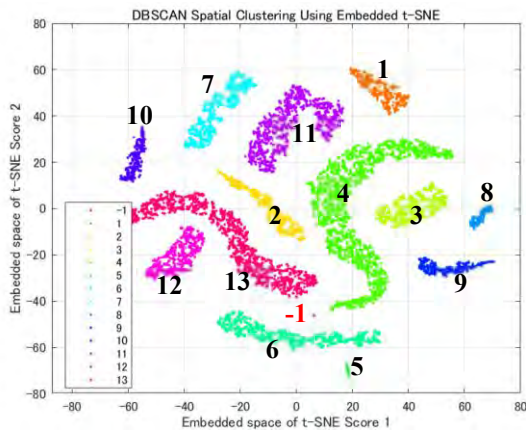


Figure 8. Density-based clustering of Concrete damage into 13 using the DBSCAN

3.3.2 Concrete Crack Clusters Nearest Images

Figure 9 shows the 13 density-based crack clusters in each row image, with the first column sampled and the

nine images to the right having the nearest similarity score. Subsequently, the deck and the pavement subgroups were divided.

3.3.3 Concrete Crack Explanation

Figure 10 illustrates the results of the crack explanation by computing the gradient-based activation map using Grad-CAM for contrastive crack metric learning. The arrangement of the rows and columns is consistent with that shown in Figure 9. The heat maps explain the damage features of the crack clusters, and discriminate each background texture between the deck and pavement surfaces. The numbers on the left-hand side denote each group shown in Figure 8. The clustered outputs were obtained using a density-based clustering method on a concrete damage dataset.



Figure 9. Thirteen density-based clusters in each row of images, the first column is sampled, and the right nine images have nearest similarity scores

4 Concluding Remarks

4.1 Experimental Results

We proposed a contrastive learning and clustering pipeline for damage representation. Specifically, we introduced the MN-pair damage-embedding space formulation, which includes an anchor and M-1 positive

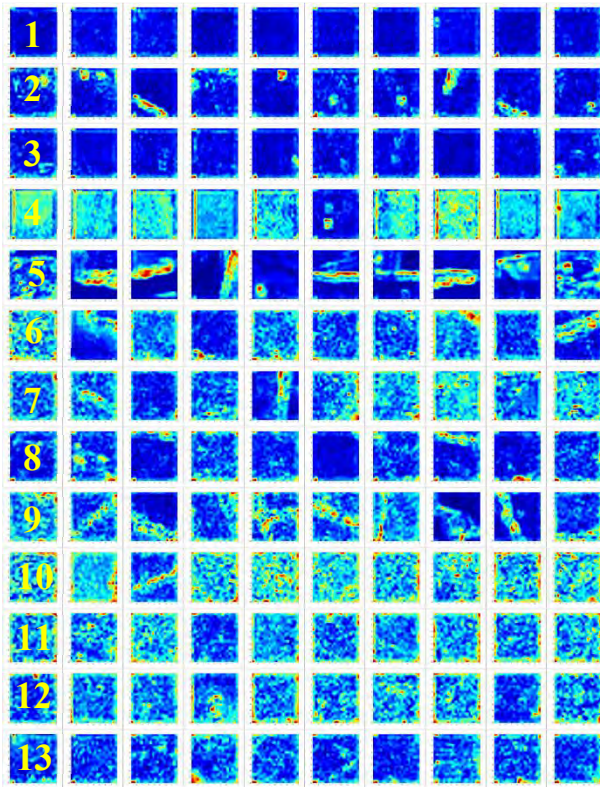


Figure 10. Concrete crack of damage explanation

and $N-1$ negative images. The shared network architecture was a simple but practical convolutional network with 15 layers. Furthermore, we proposed a clustering method using the output of an MN-pair damage-embedding space after two-dimensional-reduction by the t-SNE and density-based DBSCAN clustering. Furthermore, we presented a gradient-based damage explanation to adapt to the final activation map from a convolutional network trained by MN-pair contrastive damage representation learning.

We found that the damage features exhibited considerable heterogeneous variation compared to the predefined classes determined by human inspection. The damage-embedding space exhibited an unexpected increase in the number of detailed clusters. We demonstrated our method in three experimental studies using the open-access datasets, such as steel products with surface defects, concrete cracks of decks and pavements. We confirmed the efficacy of the proposed method using surface damage datasets.

4.2 Limitations and Future Works

We attempted to address the sewer pipe defect dataset, but were hindered by the certain limitations that affected the clarity of the obtained results. Each inspection image was significantly different in terms of the distance and angle toward the damaged region. Simultaneously, the

sizes of images were significantly low resolution, with dimensions of 768×576 , to clearly visualize the damage region. We believe that a unified distance and angle condition is critical for acquiring inspection images of at least HD quality, that is, 1280×720 .

There are more practical problems with *co-defect* representation, where one image has a multiple labels and bordered regions between damaged pairs of classes. To address this issue, a hard-negative sampling scheme was used. For *robustness* against heterogeneous damage, a mixture and erasing augmentation would improve the performance. An MLP-based network is an option for *faster* computation. For *applicability*, other trials should include water quality, disaster scenes, and LCZ built-up/natural classes.

Acknowledgment We gratefully acknowledge the constructive comments of the anonymous referees. We wish to thank Takuji Fukumoto (MathWorks Japan) for providing helpful MATLAB resources to pace up.

References

- [1] Kaya, M. Bilge, H.S. Deep Metric Learning: A Survey, *Symmetry*, MDPI, 2019.
- [2] R. Karsten, Milbich T. et al. Revisiting Training Strategies and Generalization Performance in Deep Metric Learning, *Proceedings of 37th International Conference on Machine Learning, PMLR*, 2020.
- [3] Schroff, F. Kalenichenko, D. FaceNet: A Unified Embedding for Face Recognition and Clustering, *2015 IEEE Conference on Computer Vision and Pattern Recognition*, IEEE Xplore, 2015.
- [4] Chopra, S. Hadsell, R. Learning a Similarity Metric Discriminatively with Application to Face Verification, *CVPR* 2005.
- [5] Sohn K. Improved Deep Metric Learning with Multi-class N-pair Loss Objective, *30th Conference on Neural Information Processing Systems*, 2016.
- [6] Khosla, P. Teterwak P. et al. Supervised Contrastive Learning, *34th Conference on Neural Information Processing Systems, NeurIPS*, 2020.
- [7] Oord, A. Li, Y. and Vinyals, O. Representation Learning with Contrastive Predictive Coding, *arXiv:1807.03748v2*.
- [8] Linderman, G.C., Steinerberger, S. Clustering with t-SNE, Provably, *Society for Industrial and Applied Mathematics*, Vol.1, No.2, pp313-332, 2019.
- [9] Hartigan J. A., Wong M.A., A K-Means Clustering Algorithm, *Journal of the Royal Statistical Society. Series C*, Vol. 28, No. 1, pp. 100-108, 1979.
- [10] Comak, E., Arslan, A. A New Training Method for Support Vector Machines: Clustering k-NN SVM, *Expert Systems with Applications* 35, pp564–568, 2008.

- [11] Evangelos, S. Jiawei, H. et al. A Density-Based Algorithm for Discovering Clusters in Large Spatial Databases with Noise, *Proceedings of the Second International Conference on Knowledge Discovery and Data Mining (KDD-96)*, 1996.
- [12] Zeiler, M.D., Fergus, R., Visualizing and Understanding Convolutional Networks, *arXiv:1311.2901v3*.
- [13] Ribeiro, M.T., S. Sameer Why Should I Trust You? Explaining the Predictions of Any Classifier, *Knowledge Discovery and Data Mining, KDD 2016*.
- [14] Zhou, B., Khosla, A., Lapedriza A. et al. Learning Deep Features for Discriminative Localization, *2016 IEEE Conference on Computer Vision and Pattern Recognition, NV*, 27-30, 2921-2929, 2016.
- [15] Selvaraju, R.R., Cogswell M. et al. Grad-CAM: Visual Explanations from Deep Networks via Gradient-based Localization, *ICCV*, 2017.
- [16] Zhu, S., Yang T. et al., Visual Explanation for Deep Metric Learning, *IEEE Transactions on Image Processing*, 30:7593-7607, 2021.
- [17] Severstal: Steel Defect Detection, Kaggle public, <https://github.com/zdaiot/Kaggle-Steel-Defect-Detection>, Data Accessed at March 26, 2023.
- [18] Dorafshan, S., Thomas, R.J. et al. SDNET2018: An Annotated Image Dataset For Non-contact Concrete Crack Detection Using Deep Convolutional Neural Networks, *Data in Brief*, Vol.21, 1664-1668, 2018.
- [19] C. Shorten, T.M. Khoshgoftaar A Survey on Image Data Augmentation for Deep Learning”, *Journal of Big Data*, 6:60, 2019.
- [20] Zhongyix, Z. Zheng, L. et al. Random Erasing Data Augmentation, *Proceedings of the AAAI Conference*, Vol.34 No.7:AAAI-20 Technical Tracks 7, 2017.

Indoor Defect Region Identification Using an Omnidirectional Camera and Building Information Modeling

Yonghan Kim¹ and Ghang Lee¹

¹Department of Architectural Engineering, Yonsei University, Republic of Korea

cgv03109@yonsei.ac.kr, glee@yonsei.ac.kr

Abstract –

An omnidirectional (i.e., 360°) camera is an efficient device that can capture the status of a room with a single shot. To detect objects in a spherical image captured by a 360° camera, the image should be flattened and divided into patches reflecting normal fields of view (NFoV). However, detecting indoor defects in omnidirectional camera images is difficult because they are relatively small and span multiple patches. Another challenge is to set the appropriate size for an NFoV patch. To overcome these challenges, this paper proposes a method to locate possible regions of indoor defects using building information modeling (BIM). The core idea is to subtract a 360° camera image from a photorealistically rendered BIM model image of the same location. Bounding boxes are generated around the areas where differences are detected. The proposed method was tested in a single room with artificially implanted cracks. In the experiments, two different omnidirectional cameras were used. The image classification algorithm was trained on open crack datasets. The results showed that the proposed method improved the F1-score from 0.15 to 0.39 and recall from 0.16 to 0.87. The proposed method could detect more cracks while reducing the number of patches needed for indoor crack inspection compared to the traditional method.

Keywords –

Defect Inspection; Omnidirectional Camera; Crack Detection; BIM.

1 Introduction

Indoor defect inspection is a crucial task for construction companies to ensure customer satisfaction and maintain the quality of work. Since a unit's condition directly impacts residents, defects in the interior can result in numerous complaints, claims, and even litigation [1]. These conflicts have negative impacts on

construction companies' brand images, leading to financial damage [2]. Therefore, in industry and academia, methods for efficiently managing defects have been continuously required.

The methods of inspecting for indoor defects keep advancing, from visual inspection to increased reliance on low-cost, high-performance, easy-to-use devices and advanced technology. These technologies provide opportunities to tackle the challenges associated with the laborious, time-consuming, and error-prone methods of physical visual inspection [3–6]. However, detecting indoor defects in an equirectangular image is still difficult because indoor defects are relatively small compared to general objects.

This study proposes a method to identify indoor defect regions using pixel-wise subtraction of the on-site image from the photorealistically rendered building information modeling (BIM) image. Cracks were selected as the target defect type for inspection. The proposed method was validated through an experiment that involved implanting cracks of various sizes in a single room while capturing indoor scenes using two different off-the-shelf omnidirectional cameras. The results of detection performance and time for inference using the traditional method and the proposed method were compared.

2 Background and Related Studies

The omnidirectional (i.e., 360°) camera is an efficient and easy-to-use device that can capture a comprehensive view of an area in one shot. As such, 360° cameras are utilized for inspecting enclosed spaces, such as tunnels, pipes, and culverts [7–9], as well as collecting indoor scene data for real estate advertising purposes [10].

The 360° camera has also been used to capture facility conditions and to detect indoor defects by leveraging advanced image-processing technologies that can detect objects and classify patches. Humpe [11] has shown the captured visual feature from a 360° camera can be also utilized for autonomous crack inspection with similar

results to a standard high-definition camera when it is captured close enough. Chow et al. [4] used the 360° camera to capture defects on concrete surfaces and classify extracted patches with a deep learning-based image classification model. Luo et al. [12] proposed customized object detection models to detect defects on steel surfaces from extracted patches.

Equirectangular images, another form of a spherical image from a 360° camera, is the format used to not only store and transmit a spherical image but also widely adopted as an input format in related studies. There are three general approaches to detecting objects from the equirectangular image. Some studies [13–16] proposed methods to input the whole equirectangular image into the trained object detector. Other approaches [17,18] are to input cropped patches with a flat grid into the object detector or image classifier. The other approaches [4,13] are to input the normal field of view (NfoV) patches, which are divided based on a spherical grid and flattened. These studies have shown that the third approach presents a promising performance in detecting objects from a spherical image, including defects.

However, the major challenge in detecting indoor defects from equirectangular images using the third approach lies in determining the appropriate size for a NfoV patch. The conventional method of segmenting an equirectangular image into NfoV patches involves dividing the entire image into overlapping patches, with the size determined arbitrarily by the developer based on the target size. Moreover, indoor defects are relatively small compared to target objects in related studies, resulting in an excessive number of patches. Despite advances in computing capacity that allow for the inspection of numerous image patches, suitable patch sizes must still be identified to minimize redundancy and

improve analysis speed. Consequently, a region identification method is required to localize defects and reduce the number of image patches that need to be examined by a trained classification model.

Therefore, this study aims to identify and localize the region of defects from equirectangular images to reduce the number of image patches that need to be examined by a trained classification model, thereby ensuring efficient automated indoor defect inspection.

3 Methods and Implementations

A defect region is identified from the equirectangular images based on the proposed sequence of modularized processing methods as shown in Figure 1. The proposed method aims to improve the traditional method of extracting NfoVs, which uses a spherical grid for classification. The detailed implementation process consists of eight steps, as depicted and described in the following sub-sections. Most methods were implemented using Python with the OpenCV library.

3.1 View Generation

Revit, which was used to generate a BIM model, did not support viewpoint generation on exactly designated coordinates using a graphical user interface (GUI). Therefore, an application programming interface (API) that could generate a view of the exactly designated coordinates in the BIM model was used. In this study, the central coordinates of the target room and the height of each omnidirectional camera were used as parameters for view generation.

Enscape was plugged into Revit to generate 3-dimensional photorealistic rendering images directly

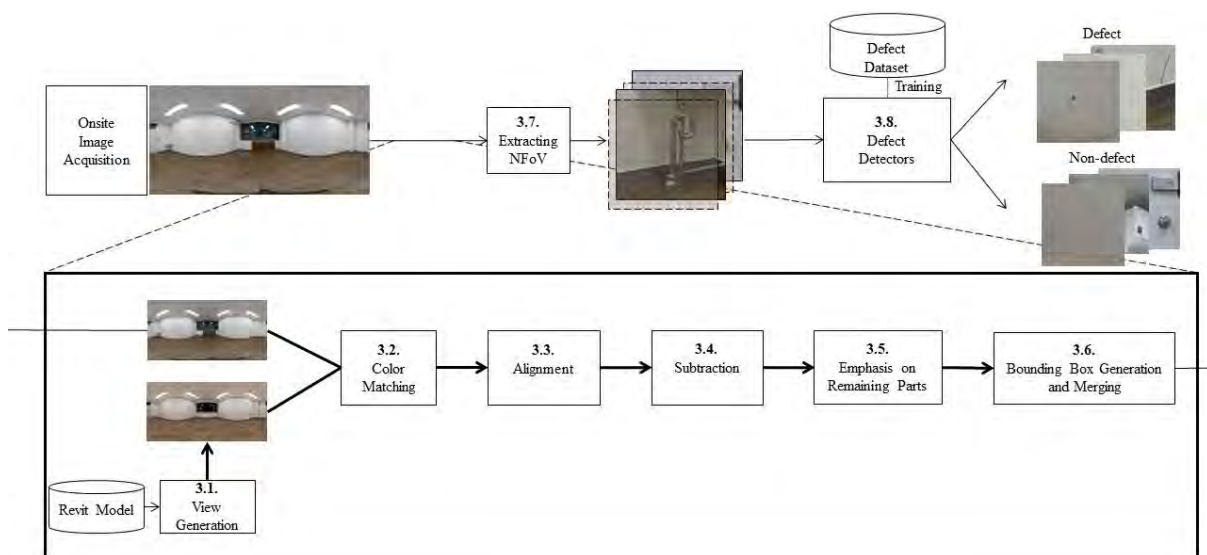


Figure 1. Overview of the proposed method.

from a Revit model. As Enscape was plugged into Revit, viewpoints from the Revit and Enscape environments were automatically synchronized. Enscape provides a feature for generating spherical images in equirectangular form by capturing multiple images at designated locations and stitching them.

3.2 Color Matching

Two images from different sources, regardless of how realistic and similar they are, inevitably have different distributions of pixel values because of different conditions, such as lighting and reflections. Therefore, color-matching methods were applied to reduce the gap between each pixel value. The pixel values of the original images were adjusted. Intensity refers to the pixel value distribution of the source image and was used to efficiently discard similar regions and emphasize distinct regions.

3.3 Alignment

Another merit of a 360° camera is that generated image can stand upright regardless of the pose of the device because of the inertial measurement unit (IMU) sensor. This, combined with the robust tripod, allows an on-site image to be easily aligned with the image from Enscape. However, the camera could be mislocated slightly away from the center of the target room or misdirected by errors from the sensors and a slanted floor.

To mitigate these problems, an image alignment module was implemented. This module calculated the average of the subtracted pixel values and defined them as a target for minimization. The parameters to be optimized were pitch, yaw, and roll. The parameters could rotate on-site spherical images to align with the rendered images to minimize the difference between the two sets of images. The SciPy [19] library was utilized to implement the optimization process.

3.4 Subtraction

This section discusses the pixel-wise subtraction of two spherical images in equirectangular form. The normal subtraction operation, which subtracts the rendering image from the on-site image to negate visually similar parts, resulted in negative pixel values outside the valid range of 0 to 255. To handle negative pixel values, a unique operation was required. In this research, the absolute difference operation was used, which involves taking the absolute values of the subtracted pixel values. This operation ensured that the final values for the pixels were all positive and within the valid range. Using the absolute difference operation was particularly important because normal subtraction

methods could result in different outcomes depending on the order of the minuend and subtrahend. By using the absolute values of the subtracted pixel values, a consistent measure of the differences between the rendered image and the on-site images, regardless of which was the minuend.

3.5 Emphasis on Remaining Parts

In ideal cases, the different parts will have high pixel values after subtraction while the same parts would have pixel values of approximately (0, 0, 0). Pixels that have values less than 5 are neglected by the thresholding operation. To emphasize the remaining features and denoise the subtracted result, canny edge detection was utilized [20]. Then, the parameter values of the low and high threshold for canny edge detection were heuristically set to 80 and 160 respectively.

3.6 Bounding Box Generation and Merging

The minimum bounding boxes of the emphasized edges can be generated using contour features from OpenCV. However, too many bounding boxes overlapped and were close to each other. Therefore, a distance-based bounding box merging algorithm was implemented with the expectation that each bounding box would cover a single object to be inspected. The distance between the bounding boxes was calculated based on the center coordinates of each box.

3.7 Extracting the Normal Field of View

Every pixel from an equirectangular image could be mapped on the spherical coordinate system based on the corresponding longitude and latitude. Therefore, considering the coordinates corresponding to the centers of the bounding boxes and the sizes of each box, the NFoV patches were extracted using flattening methods.

3.8 Defect Detector and Training Datasets

A module that can distinguish images with cracks and images without cracks was also implemented to validate the usage of the proposed method. The detector can be an object detection model, semantic segmentation model, or image classification model. Although segmentation models excel at detecting cracks, creating a dataset for indoor defects in the form of a segmentation or object detection task can be challenging due to the diverse range of defect shapes and sizes. Thus, this study chose an image classification model as a detector, which significantly reduced data preparation time and effort.

In this research, the image classification model VGG-19, a convolutional neural network (CNN)-based image classification algorithm that has demonstrated promising

performance for various classification tasks, was trained using open crack datasets [21,22]. The datasets for training were secured from publicly open datasets [21,23,24]. The main reason for selecting these datasets was to produce crack features for various backgrounds based on the on-site crack features.

4 Experiment

An experiment was conducted to determine the validity of the proposed and implemented methods in a controlled environment. In this section, the specifications of the 360° cameras, the as-designed BIM model, and the implanted cracks are discussed.

4.1 Devices Used to Acquire On-Site Images

A single room with artificially implanted cracks was inspected by two off-the-shelf omnidirectional cameras. Devices less than \$600 were intentionally selected for their price, considering the accessibility and generalizability of each device. The Insta One X2 from Insta 360 was around \$430, and the QooCam 8K was around \$590. Two fish-eye lenses were applied to both devices to acquire more than each 180° scene and to stitch the two images together as one spherical image. The major difference between the two devices is the maximum resolution of the footage. The QooCam 8K can generate an image with an 8K (7680 × 3840) resolution, while the other can generate a 5.7K (6080 × 3040) resolution.

4.2 BIM Model Generation

The experiment was conducted in a real building, where a BIM model was generated using the as-designed conditions of the target room in real world. The BIM model was used to generate a reference spherical image, which was subtracted from an on-site image. Objects that were not described in the corresponding plan but exist in the physical room, such as the air conditioner, sink, pipes, and radiator, were neglected in the model. The detailed model featured objects such as power sockets, lights, windows, skirting, and a door. To create a photorealistic rendering as close to reality as possible, material mapping was conducted using manually acquired material libraries. Finally, in order to adjust the color and geometrical differences between the rendered image and

the on-site image, ‘color matching’ and ‘aligning’ algorithms were utilized.

4.3 Implanting Cracks

Since the target room did not have cracks that could be detected by the trained classifier, 19 cracks of various sizes were manually implanted. The sizes of the implanted cracks were intentionally determined based on the width and length of each crack from small to large. The small cracks were less than 100 mm², the medium-sized cracks were less than 1,000 mm², and the large-sized cracks were over 1,000 mm².

5 Results

Following the traditional method, an image from each device generated 1,028 extracted NfV patches, meaning each patch overlapped approximately 30% of the neighboring image. The QooCam, which can generate images with a higher resolution, had the best detection results, securing an F1 score of 0.218 by detecting the largest number of cracks.

After applying the proposed methods, the number of patches to be inspected decreased from 1,028 to 187 and 118 patches, respectively, leading to increased recall and precision values, indicating a reduction in the number of false positive and false negative detection cases. The actual number of detected cracks using Insta One X2 footage increased from 4 to 7 but decreased from 9 to 7 in the case of the QooCam images. The reason for the decreased number of detected cracks is that the traditional method gives a model multiple opportunities to classify the same cracks from a different perspective, while the proposed method only provides a single opportunity. Another reason is that even though overall detection performance was high with the high-resolution camera, some crack features are neglected through the ‘emphasis on remaining parts’.

Considering the effectiveness that can be quantified as F1-score, the results indicate that the proposed method is valid, even though it sacrifices some number of true positive detection results. The detailed detection results are shown in Table 1. Processing time refers to the overall duration taken for classifying the extracted patches. With the VGG-19 model, 1028 patches from the traditional method were processed in 14 seconds while the reduced number by the proposed method lead to decreasing

Table 1. Overall Experimental Results

Condition	Device (Resolution)	No. of patches	Processing Time (Sec)	F1 Score	Detected Cracks (detected/total)
Traditional method	QooCam (8K)	1028	13.82	0.218	9/19
	InstaOne X2 (5.7K)	1028	8.81	0.145	4/19
Proposed method	QooCam (8K)	187	2.51	0.263	7/19
	InstaOne X2 (5.7K)	118	1.59	0.387	6/19

processing time to 3 seconds on an RTX 3090 GPU. The result signifies a substantial decrease in processing time, with the total time for processing reduced to approximately 18% of the processing time incurred by the traditional method.

Five types of cracks that could not be detected before could be detected using the proposed methods. However, small cracks, shorter than 100 *mm*, could not be detected by any device using any of the methods.

Figure 2 and Figure 3 show the samples of true positive cases, while the red boxes indicate the cracks that were not detected by the traditional method but detected when adjusting the proposed method.

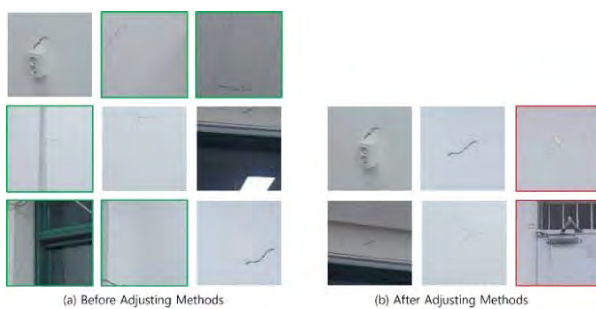


Figure 2. True positive cases and after adjusting the methods based on InstaOne X2 images.

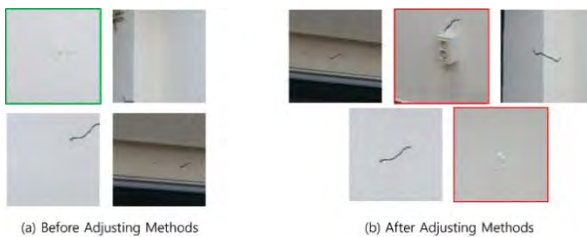


Figure 3. True positive cases before and after adjusting the methods based on Qoocam images.

6 Discussion

The main purpose of this research, to reduce the number of redundant patches, was achieved using the proposed method. Even though it primarily inspected single patches for one crack feature, the proposed method could detect new crack features that formal methods could not detect. This phenomenon happens because the patches' sizes and locations were determined to have similar visual features based on the training datasets. The major parts of the training images had centralized crack features.

Unlike the traditional methods, the proposed method could also extract the region that is different from the clean image from the as-designed BIM model. The patches generated using traditional methods consist of many meaningless patches from floor and ceiling images,

but the proposed methods can generate a suspected region that is different from the as-design image.

Despite the achievements of this research, the results have several limitations. First, the trained classifier showed that the proposed method cannot be applied for practical defect inspection. Even though the detector was trained using numerous crack images with various backgrounds, the crack images from the indoor spherical images were unseen data. Therefore, future research is needed to find an appropriate detector that can distinguish real indoor defects on a practical level with securing real indoor defect datasets.

Second, small crack features could be neglected by the proposed method. For example, green boxes in Figure 2 and Figure 3 indicate cases where the traditional method successfully detected defects that the proposed method could not detect. These small crack features were neglected while thresholding or emphasizing the remaining parts after image subtraction, depending on user-defined parameters for the canny edge detection algorithm. Therefore, the optimal parameters for each indoor scene condition must be determined in future research.

Third, the location of the camera for on-site image acquisition may not have been in the exact center of the target room. Although several modules were devised to mitigate this issue, images acquired from a completely misplaced device cannot be assessed using this method. In future research, the center points must be accurately secured by leveraging additional methods, such as simultaneous localization and mapping (SLAM).

This method was developed aiming at detecting cracks and other types of defects during construction or the pre-occupancy inspection before furniture, home appliances, and electrical fixtures are installed. However, any visual inspection using cameras has a disadvantage in that it can only work on visible things. The proposed vision-based method has this inherited limitation.

7 Conclusion

An omnidirectional camera is an efficient device for the inspection of rooms because it can capture the whole scene of the target space at one time. However, traditional methods for detecting defects using spherical images have been difficult to implement because a crack occupies a small portion of an image and because there is ambiguity regarding the appropriate size of the NfoV patches. Therefore, a method to extract regions suspected of having defects was proposed as a sequence of modules. The proposed method was validated through a lab-conditioned experiment. The results showed that the proposed method could effectively reduce the number of NfoV patches to be inspected while ensuring the same or even better detection performance than the traditional

method. This method is expected to decrease the number of false positive cases and reduce the overall inspection time. Ultimately, the proposed method is expected to offset the time and effort required to create a rendering image when it applied to defect inspection of numerous units of identical housing types, such as apartment units.

Our future research will focus on determining proper detectors and ways to train them to identify patent indoor defects. Additional methods must be applied to ensure that the camera is in the correct location and position. Finally, experiments for validation must be conducted at a site featuring real defects.

References

- [1] Kim, D.-H., Lee, D., Lee, H.-J., Min, Y.-G., Park, I., Cho, H. Analysis of importance by defect type in apartment construction. *Journal of the Korea Institute of Building Construction*, 20, 357–365, 2020. <https://doi.org/10.5345/JKIBC.2020.20.4.357>.
- [2] Othman, A.A.E. An international index for customer satisfaction in the construction industry. *International Journal of Construction Management* 15: 33–58, 2015. <https://doi.org/10.1080/15623599.2015.1012140>.
- [3] Perez, H. and Tah, J.H.M. Deep learning smartphone application for real-time detection of defects in buildings. *Structural Control and Health Monitoring*, 28: e2751, 2021. <https://doi.org/10.1002/stc.2751>.
- [4] Chow, J.K., Liu, K., Tan, P.S., Su, Z., Wu, J., Li, Z., Wang, Y.-H. Automated defect inspection of concrete structures. *Automation in Construction* 132: 103959, 2021. <https://doi.org/10.1016/j.autcon.2021.103959>.
- [5] Filgueira, A., Arias, P., Bueno, M., Lagüela, S. Novel inspection system, backpack-based, for 3D modelling of indoor scenes. *International Conference on Indoor Positioning and Indoor Navigation*, page 4, 2016.
- [6] Du, H., Henry, P., Ren, X., Cheng, M., Goldman, D.B., Seitz, S.M., Fox, D. Interactive 3D modeling of indoor environments with a consumer depth camera. *Proceedings of the 13th International Conference on Ubiquitous Computing*, pages 75–84, 2011. <https://doi.org/10.1145/2030112.2030123>.
- [7] Li, D., Xie, Q., Gong, X., Yu, Z., Xu, J., Sun, Y., Wang, J. Automatic defect detection of metro tunnel surfaces using a vision-based inspection system. *Advanced Engineering Informatics* 47: 101206, 2021. <https://doi.org/10.1016/j.aei.2020.101206>.
- [8] Meegoda, J.N., Kewalramani, J.A., Saravanan, A. Adapting 360-degree cameras for culvert inspection: Case study. *Journal of Pipeline Systems Engineering and Practice* 10: 05018005, 2019. [https://doi.org/10.1061/\(ASCE\)PS.1949-1204.0000352](https://doi.org/10.1061/(ASCE)PS.1949-1204.0000352).
- [9] Karkoub, M., Bouhali, O., Sheharyar, A. Gas pipeline inspection using autonomous robots with omni-directional cameras. *IEEE Sensors J*, 21: 15544–15553, 2021. <https://doi.org/10.1109/JSEN.2020.3043277>.
- [10] Sulaiman, M.Z., Aziz, M.N.A., Bakar, M.H.A., Halili, N.A., Azuddin, M.A. Matterport: Virtual tour as a new marketing approach in real estate business during pandemic COVID-19. *Atlantis Press*, 221–226, 2020. <https://doi.org/10.2991/assehr.k.201202.079>.
- [11] Humpe, A. Bridge inspection with an off-the-shelf 360° camera drone. *Drones* 4: 67, 2020. <https://doi.org/10.3390/drones4040067>.
- [12] Luo, C., Yu, L., Yan, J., Li, Z., Ren, P., Bai, X., Yang, E. Liu, Y. Autonomous detection of damage to multiple steel surfaces from 360° panoramas using deep neural networks. *Computer-Aided Civil and Infrastructure Engineering*, 36, 1585–1599, 2021. <https://doi.org/10.1111/mice.12686>.
- [13] Chou, S.-H., Sun, C., Chang, W.-Y., Hsu, W.-T., Sun, M., Fu, J. 360-Indoor: Towards learning real-world objects in 360° indoor equirectangular images. *IEEE Winter Conference on Applications of Computer Vision (WACV)*, pages 834–842, 2020 <https://doi.org/10.1109/WACV45572.2020.9093262>.
- [14] Wang, K.-H., Lai, S.-H. Object Detection in Curved Space for 360-Degree Camera. *International Conference on Acoustics, Speech and Signal Processing (ICASSP)*, pages 3642–3646, 2019 <https://doi.org/10.1109/ICASSP.2019.8683093>.
- [15] Coors, B., Condurache, A.P., Geiger, A. SphereNet: Learning spherical representations for detection and classification in omnidirectional images. *ECCV 2018*. 518–533.
- [16] Lee, Y., Jeong, J., Yun, J., Cho, W., Yoon, K.-J. SpherePHD: Applying CNNs on 360 Images With Non-Euclidean Spherical PolyHeDron Representation. *IEEE Trans. Pattern Anal. Mach. Intell.*, pages 834–847, 2022 <https://doi.org/10.1109/TPAMI.2020.2997045>.
- [17] Turečková, A., Tureček, T., Janků, P., Vařacha, P., Šenkeřík, R., Jašek, R., Psota, V., Štěpánek, V., Komínková Oplatková, Z. Slicing aided large scale tomato fruit detection and counting in 360-degree video data from a greenhouse. *Measurement*. 204: 111977, 2022

- <https://doi.org/10.1016/j.measurement.2022.111977>.
- [18] Hirabayashi, M., Kurosawa, K., Yokota, R., Imoto, D., Hawaii, Y., Akiba, N., Tsuchiya, K., Kakuda, H., Tanabe, K., and Honma, M. Flying object detection system using an omnidirectional camera. *Forensic Science International: Digital Investigation* 35, 301027, 2020 <https://doi.org/10.1016/j.fsidi.2020.301027>.
- [19] SciPy 1.0: Fundamental algorithms for scientific computing in Python. *Nature Methods*, (n.d.). Online: <https://www.nature.com/articles/s41592-019-0686-2>.
- [20] Canny, J. A computational approach to edge detection. *IEEE Transactions on Pattern Analysis and Machine Intelligence. PAMI-8* 679–698, 1986. <https://doi.org/10.1109/TPAMI.1986.4767851>.
- [21] Äzgenel, Ä.F. and SorguÄ§, A.G. Performance comparison of pretrained convolutional neural networks on crack detection in buildings, *ISARC Proceedings*, 693–700, 2018.
- [22] Xu, H., Su, X., Wang, Y., Cai, H., Cui, K., Chen, X., Automatic Bridge Crack Detection Using a Convolutional Neural Network, *Applied Sciences*. 9 2867, 2019. <https://doi.org/10.3390/app9142867>.
- [23] Dorafshan, S., Thomas, R.J., and Maguire, M. SDNET2018: An annotated image dataset for non-contact concrete crack detection using deep convolutional neural networks. *Data in Brief*, 21: 1664–1668, 2018. <https://doi.org/10.1016/j.dib.2018.11.015>.
- [24] Elhariri, E., El-Bendary, N., and Taie, S.A. Historical-crack18-19: A dataset of annotated images for non-invasive surface crack detection in historical buildings. *Data in Brief*, 41: 107865, 2022. <https://doi.org/10.1016/j.dib.2022.107865>.

Subword Tokenization of Noisy Housing Defect Complaints for Named Entity Recognition

Kahyun Jeon¹ and Ghang Lee²

¹Department of Architecture and Architectural Engineering, Yonsei University, Republic of Korea
jeonkh0310@yonsei.ac.kr, glee@yonsei.ac.kr

Abstract –

In domain-specific named entity recognition (NER), the out-of-vocabulary (OOV) problem arises due to linguistic features and rare vocabulary. OOV problem is particularly challenging in agglutinative languages such as Korean. The irregular decomposition of morphemes makes it difficult to represent all of them in language model dictionaries, resulting in poor NER performance. Subword tokenization which segments a word into atomic tokens that are no longer divided can be one of the possible solutions. In the construction industry, existing NER methods do not effective on housing defect complaints which contain many rare words, including jargon, slang, and typos. To address this challenge, we propose subword tokenization algorithms that can mitigate OOV problems based on considering linguistic features and pre-trained language models (PLMs). The primary objective of this study is to identify the optimal NER performance by comparing different subword tokenization methods depending on the language models used. For domain-specific NER, we defined and used 23 defect-specific named entity tags for dataset labelling. We then experimented with a total of three state-of-the-art language models: one SentencePiece-based and two WordPiece-based subword tokenization models. The results demonstrate that the SentencePiece-based Korean Bidirectional Encoder Representations from Transformers (KoBERT) outperformed the two WordPiece-based language models (multilingual-BERT and Korean Efficiently Learning an Encoder that Classifies Token Replacements Accurately (KoELECTRA)) with an F1 score of 84.7%. The proposed method is expected to improve not only NER but also other downstream tasks that involve using Korean documents in the construction industry.

Keywords –

Out of vocabulary (OOV), Subword tokenization; WordPiece; SentencePiece; Named entity recognition (NER); Construction defect management

1 Introduction

In natural language processing (NLP), many studies have shown that the out-of-vocabulary (OOV) problem degrades the performance of downstream tasks, such as named entity recognition (NER), speech recognition, and neural machine translation [1–4]. OOV occurs because domain-specific terms, non-standard words, or typos in a test dataset do not exist in the vocabulary of a training corpus [5].

A representative example of unstructured noisy text data is housing defect complaints, which include numerous non-standard words and words that rarely appear in construction text. When defect complaints are automatically analyzed, such non-standard and rarely used words are often divided into unintended ways, and consequently, the original meaning is lost. Moreover, these incorrectly tokenized characters are recognized as ‘*unknown*’ tokens, tagged as ‘[UNK]’ in the NER task results. The ‘[UNK]’ token refers to the failure to decode corresponding tokens based on the embedded vocabulary sets in each pre-trained language model (PLM). Therefore, the OOV problems become more serious as non-standard words used only in specific domains, as well as typos and syntax errors, increase.

Among many previous efforts to reduce OOV, subword tokenization is one of the promising solutions [3,6–8]. Subword tokenization refers to the segmentation of words into smaller tokens that can be aggregated or decomposed based on the principles of subword tokenization algorithms [9]. According to these principles, frequently appearing terms should not be segmented, but rarely used combinations of characters should be decomposed [10].

The most widely used subword tokenization methods in transformer-based PLMs are the WordPiece and SentencePiece algorithms [11,12]. While WordPiece tokenizes input text by finding the sequence of characters that can make the longest word, SentencePiece tokenizes input text by predicting the most common token that appears after the previous token [12]. Thus, WordPiece is sensitive to the wordlist of a given language while

SentencePiece is language-independent [13].

In this study, we investigated the effect of the difference between WordPiece and SentencePiece algorithms on NER performance. Three pre-trained language models—Multilingual Bidirectional Encoder Representations from Transformers (mBERT), Korean Efficiently Learning an Encoder that Classifies Token Replacements Accurately (KoELECTRA), and Korean BERT (KoBERT)—were fine-tuned using a defect complaint corpus through transfer learning. Each pre-trained model has its own embedded tokenizer with two different subword tokenization algorithms, either WordPiece or SentencePiece. To perform NER based on housing defect complaints, we also defined defect-specific named entity tags in the pre-processing step. The NER performance was evaluated using the F1 score and accuracy.

The paper is organized as follows. In Section 2, related works on solutions to OOV problems and subword tokenization methods are reviewed. In Section 3, the research methods are described in detail. In Section 4, the results are presented with some discussion, and in Section 5, study limitations and suggestions for future work are provided.

2 Related Work

2.1 OOV Problems and Solutions

Fundamentally, OOV problems occur because a language model is dependent on a training dataset [14]. During the language model training process, if the words do not appear in the training dataset, the language model cannot learn the embedding vectors. Consequently, OOV problems degrade the system performance. More severe OOV problems occur in low-resource languages (e.g., non-alphabetical languages) or web-generated text, including slang, coinage, and emojis [4]. To overcome these problems, several solutions have been proposed.

The easiest and simplest method is to eliminate OOV as noise [14]. However, this method is rarely used, owing to the risk of losing important words. Another solution is to use spell-check algorithms, such as the Peter Norvig algorithm [15] and the Levenstein distance [16]. However, spell-check algorithms cannot solve semantic OOV problems caused by jargon or slang.

Previous studies have proposed deep learning-based typo embedding methods [17] or language-independent architecture of robust word vectors [18]. However, these methods were not able to separate irregular morphemes of agglutinative words into meaningful units. Consequently, they could not be applied to solve OOV problems in agglutinative languages, such as Korean.

Some studies focused on dealing with OOV problems considering the linguistic features of Korean [14,19–21].

One of the specific linguistic features of Korean that previous studies mainly focused on is a sub-character, called ‘jamo’, which consists of 14 consonants and 10 vowels. However, although those studies have proposed high performance on tokenization regarding sub-characters, the proposed methods are limited to use for the tokenizer the existing transformer-based language models. A comparison of the previous efforts to mitigate OOV problems is shown in Table 1.

Table 1. Comparison of the existing methods that mitigate OOV problems

Previous methods	Advantage	Disadvantage	Ref.
Remove OOV	Easy	Losing information	[14]
Spell-check	Easy, Accurate	Not effect for semantic errors	[15,16]
Deep-learning-based	Robust on typos	Not effect for rich-morpheme languages	[17,18]
Language-specific OOV handling	Specific to language features	Limited to transformer-based language models	[14,19–21]

To overcome the previous methods’ limitations, and solve the OOV problem while utilizing most state-of-the-art (SOTA) language models based on the transformer architecture, subword tokenization—a method for segmenting words into smaller units—has emerged [4]. The smaller units can be Unicode or characters, which can no longer be divided based on the specific algorithm [22]. Various subword tokenization algorithms that have been used by integrating transformer-based language models are described in the following section.

2.2 Subword Tokenization Algorithms

There are several types of subword tokenization methods, such as byte pair encoding (BPE) [3], unigram language model (ULM) [6], WordPiece [4], and SentencePiece [13].

BPE is a basic subword tokenization algorithm, which finds pairs of characters that appear the most sequentially and combines them into one word [3]. BPE was originally introduced to compress data [23], after which the algorithm was proposed as an OOV solution for neural machine translation [3]. In the iterative process of BPE, a set containing a pair or token and a token’s frequency is generated. Then, each token is divided into character levels by a pre-tokenizer according to the space. In each iteration, the most frequent character pair is

merged until the desired or pre-defined vocabulary size is reached. The core idea of BPE is to consider text as a sequence of bytes rather than a sequence of characters. Therefore, BPE can be applied to any type of character [3].

The WordPiece model is an expanded BPE algorithm. An ideal subword tokenizer divides low-frequency or morphologically complex words into smaller subword units, otherwise keeping high-frequency words as they are. The WordPiece tokenizer is used in BERT, DistillBERT, and ELECTRA [4]. The WordPiece model merges pairs of characters that increase the likelihood of a corpus, which is different from BPE, which uses word frequency. In other words, WordPiece algorithms choose to divide or preserve words depending on the direction that increases the probability of the language model the most.

A unigram language model (ULM) was proposed based on a subword tokenization algorithm that outputs multiple subword tokenization with probabilities [6]. The ULM supposes that each subword occurs independently, and consequently. Therefore, each subword occurrence probability can be estimated by maximizing the expected likelihood. A ULM is usually used with SentencePiece in transformer-based language models to increase system performance.

SentencePiece is an unsupervised subword tokenizer and detokenizer [13,24], and was developed based on ULM [6] and BPE [3] subword regularization algorithms. Unlike all other algorithms, which require pre-tokenization based on whitespace, SentencePiece directly processes the input text without pre-tokenization. Instead of pre-tokenization, SentencePiece can be trained using raw sentences that include whitespace. In addition, the original whitespace can be preserved by replacing it with an underscore ('_'; represented by U+2581 in Unicode) in the subword tokenization stage. Conversely, the subword tokens can be detokenized without any ambiguity caused by whitespace. For example, the complaint 'wall paper torn' can be segmented as ['_w', 'all', '_p', 'ap', 'er', '_t', 'or', 'n'] by the SentencePiece tokenizer. This shows that SentencePiece considers a sentence as a Unicode sequence rather than characters. This principle makes SentencePiece work on non-space or space-free languages. This is the most significant difference from other subword tokenization algorithms because it makes the SentencePiece language independent. As SentencePiece supports on-the-fly processing through Python and Tensorflow Library API, it can be easily integrated and customized with other frameworks. SentencePiece has been widely adopted in many SOTA language models, such as ALBERT [25], XLNet [26], and T5 [27]. A comparison of subword tokenization methods is shown in Table 2.

After conducting a thorough review of previous

efforts, we have identified several research gaps. First, there exist multiple effective subword tokenization algorithms that are dependent on the linguistic features of a given language. The language-dependent tokenizer requires separate training for every language it may not perform as well in cross-lingual tasks. Second, the choice of subword tokenization algorithm is determined during the pre-training process of the internal tokenizer of the PLMs. Third, the various subword tokenization approaches employed by different PLMs can have a significant impact on the performance of downstream tasks.

Table 2. Comparison of subword tokenization methods

Cate gory	BPE [3]	ULM [6]	Word Piece [4]	Sentence Piece [13]
SA	Char, Unicode	Char	BPE	BPE, ULM
FP	Word frequency	Likeli- hood	Likelihood	BPE- dropout
VS	Enlargeme nt	Pre- defined	Enlarge- ment	Pre- defined
PT	Require	Require	Require	No
OS	Yes	Yes	Google internal	Yes
PL	No	No	N/A	Yes
HT	Yes	Yes	Yes	Yes

* SA: Supported algorithms; FP: Functional principle; VS: Vocab-Size; PT: Pre-tokenization required; OS: Open source; PL: Python library available; HT: HuggingFace tokenizer available.

In light of these research gaps, it is crucial to consider the linguistic features, such as the agglutinative nature of the Korean language, when performing NER using transformer-based PLMs. Fourth, NER tasks with domain-specific text data and their respective subword tokenization algorithm have been rarely studied. Therefore, this study aims to identify the most effective PLM and subword tokenization algorithm for domain-specific NER tasks for construction defect management.

3 Research Methods

The research flow is depicted in Figure 1. For this study, over 90,000 defect complaints were collected from several collective housing construction sites in South Korea. After performing deduplication and removing abnormal data, a dataset of 69,750 complaints was used for training and validation. Additionally, we created a separate ground truth test dataset consisting of 4,566 complaints gathered from different construction sites. The test dataset was constructed through cross-validation

by three researchers, who possess extensive defect inspection experience at construction sites.

After pre-processing and tokenizing, the collected data were labeled with defect named entity tags for NER. Labeling was performed on a rule basis using a dictionary of defective object names that corresponded to 23 tags defined in advance. The first labeling results were cross-validated by three researchers who perform defect inspections at construction sites.

Subsequently, the labeled dataset was divided into a training dataset for transfer learning and a testing dataset for the NER performance evaluation at a ratio of 9:1. Before transfer learning, the PLM uses each tokenizer to perform subword tokenization of the input text. In the test phase of the fine-tuned language model, the same subword tokenization was applied. The NER results are compared with the F1 score and accuracy as evaluation indices.

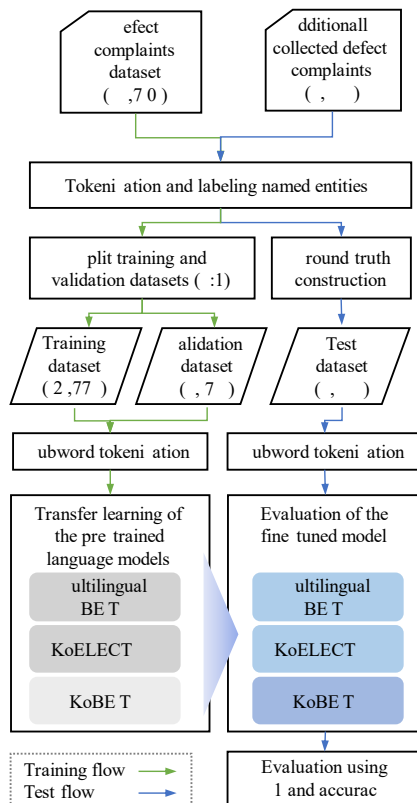


Figure 1. Research flow

3.1 Tokenization and Labeling Dataset

As Korean is an agglutinative language, most Korean words consist of ‘a stem of the word (a meaning part)’ and ‘a particle or an ending (a grammatical part).’ For example, ‘물이 새는(water leak)’ can be decomposed to the following combination: ‘물(water: stem)’+

‘ㅇ](particle)’ + ‘새(-다)(leak: stem)’+ ‘(ending)’. The morpheme analysis-based tokenization method is required to separate and process the meaning parts and the grammatical function parts.

To achieve this, we used Korean-specific NLP libraries, including MeCab-Ko [28], a Korean version of the original MeCab [29], for morpheme analysis and tokenization. In the first pre-processing step, the date or time expressions, ‘07/07/2021’ and ‘07:37’, were processed and extracted using regular expression rules, and other punctuation and symbols were removed. Then, the rest of the pure text part was tokenized using the MeCab-Ko tokenizer. The pure text part of the defect complaints was tokenized, and the part of speech (POS) was tagged. We extracted not only nouns but also verbs, adjectives, and adverbs because they also represent defect phenomena: for example, ‘skew(-ed)’ or ‘tilt(-ed)’.

After tokenization, all tokens should be labeled with an NE tag, information that we want to extract. Moreover, it is necessary to label the entire dataset to construct the training dataset and the ground truth. Before labeling the NE tags, we need to define defect-related NE categories. Unlike existing NER methods that have general NE tags, such as the name of the country, city, or person, domain-specific NE tags should be defined to recognize the specialized terms in a certain domain. In this study, 17 tags were defined based on Omniclass Table 22 [30]. The categories include structure work (STR), waterproofing (WPF), electrical work (ELC), door and window (DNW), cabinet work (FUR), stonework (STM), paper hanging work (PAP), flooring (FLR), painting and finishing (FNS), tiling (TLE), masonry (MSN), home appliance work (APL), mechanical systems (MEC), gas fitting work (GAS), fire protection work (FIR), miscellaneous (MIS), and elevator work (ELV). In addition, five meta-data categories were defined to identify the date and time (TME), the name of the room or space (SPC), a specific part of the space, such as ‘above’ or ‘left side’ (LOC), the type of request (REQ), the name of person or organization in charge of the repair work (WHO) and expressions that describe defect phenomena (DFT).

To label the dataset using 23 NE tags, we checked the tokenization error cases, which means a series of words that should not be decomposed are tokenized. For example, a multi-token entity consists of more than one word, such as ‘poor horizontal and vertical alignment’, which is tokenized as five words: ‘poor/ horizontal/ and/ vertical/ alignment’. If this multi-token entity is decomposed, the original meaning will be lost, and it cannot be properly recognized as a defect NE. As a solution, we performed tokenization and NE labeling according to the ‘inside-outside-beginning2 (IOB2) scheme’. The IOB2 scheme is a popular tagging scheme for recognizing a multi-token NE in an NER task [31]. ‘I’ indicates that the token is inside the NE, and ‘B’ indicates

the start token of the NE. ‘O’ indicates that the token belongs to none of the NE. ‘I’ and ‘B’ are joined in front of each NE tag (i.e., B-DFT, B-SPC, and I-SPC), and ‘O’ is used alone. The dataset was labeled based on the rule-based method, and then the automatically labeled dataset was cross-validated by three researchers who have defect inspection experience.

3.2 Pre-trained Language Models with Different Subword Tokenization Algorithms

The PLM has a substantial number of context vectors and vocabularies. Thus, it is easy to shift and use efficiently for specific tasks by fine-tuning based on the transfer learning rather than training the whole neural architecture from scratch. For specific domains (e.g., medical or construction), fine-tuning a PLM with a domain-specific corpus is recommended to achieve higher performance [32]. Therefore, we chose three PLMs and implemented them for NER transfer learning.

Three PLMs with different subword tokenizers were used to transfer learning for NER. The mBERT developed by Google and KoELECTRA have a WordPiece tokenizer, while KoBERT uses a SentencePiece tokenizer. As the dataset is Korean, we first selected mBERT [33] as the baseline model. We also selected KoBERT, a specifically trained BERT with the Korean dataset KoWiki composed of 54 million words [34]. KoELECTRA [35] was chosen to compare the performance of different language model algorithms between BERT and ELECTRA, which is known for exceeding BERT’s performance in terms of training speed with less data. The specifications of the three pre-trained language models are described in Table 3.

Table 3. Details of the pre-trained language models

Category	KoBERT	mBERT	Ko-ELECTRA
Tokenizer Algorithm	SentencePiece	WordPiece	WordPiece
Pre-trained Language	Korean	104 languages	Korean
Parameter	92M	110M	110M
Layers	12	12	12
Reference	[34]	[36,37]	[38,39]

3.3 Experiment Design

Subword tokenization was performed as a previous step for fine-tuning PLMs. The input text data are tokenized by the pre-trained tokenizer designated by each language model. In this process, the label of each token

was also expanded to the same number of subword tokens. Then, subword tokens and labels were converted to a numerical format using a pad sequence, and the attention mask was generated at the same time. We observed the subword tokenization results in the middle of the experiment process to determine how subword tokenization affects the final NER performance. To compare this with the case without subword tokenization, a deep neural network model, a bi-directional long-short-term-memory (bi-LSTM) network, was performed as a baseline.

All input texts were fit into the same fixed length of the 0.985 quantile value (top 1.5%) of the entire training dataset, because all the text lengths of the input data are different. In this process, the 0.985 quantile value was defined as the maximum length, one of the hyperparameters that determines the input vector shape. The same value of the 0.985 quantile of the input text length was applied to the input of the testing dataset in the evaluation.

In the experiments, all three PLMs were fine-tuned to only three epochs with a batch size of 32, an ‘adam’ optimizer with a learning rate of 2.E-05, and ‘parseCategoricalCrossentropy’ as for a loss function. It is important to note that batch size refers to the number of data points used to update the model’s parameters during a single forward/backward pass. The ‘adam’ optimizer, which stands for ‘adaptive moment Estimation’ is commonly used in deep neural networks for its training efficiency. Despite the default learning rate value of 1.E-03, we opted for a smaller value of 2.E-05 for enhancing generalization efficiency.

3.4 Evaluation Metrics

Accuracy and the F1 score were employed to evaluate the NER performance considering each performance of the NE tags. The total number of NE tags is 46, which is twice the unique 23 tags owing to the addition of ‘I’ and ‘B’ of the IOB2 scheme. Similar to the multi-class classification with imbalanced data distribution, the F1 score, a harmonic mean of precision and recall, is widely used for evaluating NER performance [40]. Accuracy refers to the ratio of the number of correctly predicted samples over the number of all samples regardless of class. Therefore, we measured both F1 score and accuracy to consider the imbalanced distribution of each NE tag. The evaluation metrics for integrating NER tags can be automatically obtained with a Python library for sequence labeling evaluation named ‘seqeval’ [41].

4 Results and Discussion

The NER performance results depending on the three PLMs with different subword tokenization algorithms are shown in Table 4.

Table 4. NER performance results for the deep neural network-based model and three PLMs with different subword tokenization methods

NER Models	SW-T*	F1 (%)	Acc. (%)
(Baseline) bi-LSTM	-	23.0	49.0
mBERT	WP	72.0	86.6
KoELECTRA	WP	72.4	86.3
KoBERT	SP	84.7	89.3

*SW-T: Subword tokenization algorithm; WP: WordPiece; SP: SentencePiece

For the NER performance, the KoBERT model using the SentencePiece algorithm as a subword tokenizer had the best F1 score (84.7%) and an accuracy of 89.3%. There was little difference in performance between the BERT and ELECTRA models using the WordPiece algorithm, but a significant difference in the F1 score, which was 11.7% lower than that of the KoBERT model. For the baseline, the bi-LSTM showed a very low performance even with the same training and test datasets except for the subword tokenization step.

Table 5. Subword tokenization results (translated into English from the original Korean words)

Word Tag	KoBERT	mBERT	KoELECTRA
Zendai	_Zendai	Zen###da###i	Zen###dai
	B-STN	○	B-STN
Osai	_Osai	O###sa###i	Osa###i
	B-DNW	○	B-DNW
Ventilating Fan	_Ventilating	[UNK]	Ventilating
	_Fan		###Fan
	B-SYS/ I-SYS	○	B-SYS/ I-SYS
Floating	_Float_ing	Flo###[UNK]	Floating
	B-DFT/ I-DFT	○	B-DFT
Horizontal Defect	_Horizontal	Horizon###tal#	Horizontal
	_defect	#de###fect	###defect
	B-DFT/ I-DFT	B-DFT	B-DFT/ I-DFT

To compare the subword tokenization results of three language models, we selected five words—zendai, osai, ventilating fan, floating, and horizontal defect—that frequently lead to tokenization errors when a morpheme-based tokenizer is used.

The results for subword tokenization with the corresponding NER tag relying on three PLMs are shown in Table 5. KoBERT with SentencePiece correctly

tokenized all words, but mBERT and KoELECTRA showed different results although they used the same WordPiece algorithm. In mBERT, the defect-related tokens were incorrectly tagged with the ‘O’ tag because the segmented tokens were recognized as [UNK].

The subword sequences tokenized by mBERT showed a smaller segmentation pattern similar to KoELECTRA. This result can be interpreted as KoELECTRA was trained one more time in Korean, and naturally, its vocabulary is larger; thus, the probability of preserving a word is greater than the probability of splitting a word.

5 Conclusion

The OOV problem deteriorates the overall NER performance because invalid tokens recognized as ‘unknown’ fail in named entity tagging. And this problem occurs more often in agglutinative language such as Korean due to its complex morphological feature. To mitigate this problem, subword tokenization methods have been widely used, which either decompose the word into subword units or aggregate in reverse based on the maximization of probability or likelihood between the sequence of the subword units. Based on these principles, most state-of-the-art transformer-based language models adopt WordPiece or SentencePiece, the representative subword tokenization algorithms, as their tokenizer.

In this study, we investigated differences in NER performance when we suggested that the different subword tokenization methods affect the overall downstream task. To validate this hypothesis, mBERT and KoELECTRA using WordPiece and KoBERT using SentencePiece were selected. In NER, each subword tokenization was applied before the fine-tuning and testing steps. This means that each language model obtains a different shape of the sequence of the tokens as an input, depending on the subword tokenization method.

As a result, this study confirmed that the KoBERT model using the SentencePiece tokenizer showed the best performance based on the F1 score (84.7%), as well as the most accurate tokenization results. In addition, SentencePiece showed more robust tokenization results in Korean than WordPiece. Although this study has limitations in not controlling for other factors that can affect performance, such as parameter optimization during transfer learning or skewed distribution of NE tags, they will be further investigated and adjusted to deliver more robust results in future studies. Another future study will include further validation of whether the direct training of SentencePiece using a domain-specific corpus improves downstream tasks.

Acknowledgements

This work was supported by a National Research Foundation of Korea (NRF) grant (No. 2021R1A2C3008209) and an Institute for Information and Communications Technology Promotion (IITP) grant (No. 2019-0-01559-001), both funded by the Ministry of Science and ICT (MSIT) of Korea.

References

- [1] N. Garneau, J.-S. Leboeuf, L. Lamontagne, Predicting and interpreting embeddings for out of vocabulary words in downstream tasks, (2019). <https://doi.org/10.48550/arXiv.1903.00724>.
- [2] Y. Goldberg, Neural Network Methods for Natural Language Processing, *Synthesis Lectures on Human Language Technologies*. 10 (2017) 1–309. https://doi.org/10.2200/S00762ED1V01Y201703_HLT037.
- [3] R. Sennrich, B. Haddow, A. Birch, Neural Machine Translation of Rare Words with Subword Units, (2016). <https://doi.org/10.48550/arXiv.1508.07909>.
- [4] M. Schuster, K. Nakajima, Japanese and Korean voice search, in: 2012 IEEE International Conference on Acoustics, Speech and Signal Processing (ICASSP), 2012: pp. 5149–5152. <https://doi.org/10.1109/ICASSP.2012.6289079>.
- [5] Y. Pinter, R. Guthrie, J. Eisenstein, Mimicking Word Embeddings using Subword RNNs, (2017). <https://doi.org/10.48550/arXiv.1707.06961>.
- [6] T. Kudo, Subword Regularization: Improving Neural Network Translation Models with Multiple Subword Candidates, (2018). <https://doi.org/10.48550/arXiv.1804.10959>.
- [7] S. Moon, N. Okazaki, PatchBERT: Just-in-Time, Out-of-Vocabulary Patching, in: Proceedings of the 2020 Conference on Empirical Methods in Natural Language Processing (EMNLP), Association for Computational Linguistics, Online, 2020: pp. 7846–7852. <https://doi.org/10.18653/v1/2020.emnlp-main.631>.
- [8] S. Moon, N. Okazaki, Jamo Pair Encoding: Subcharacter Representation-based Extreme Korean Vocabulary Compression for Efficient Subword Tokenization, in: Proceedings of the 12th Language Resources and Evaluation Conference, European Language Resources Association, Marseille, France, 2020: pp. 3490–3497. <https://www.aclweb.org/anthology/2020.lrec-1.429> (accessed March 23, 2021).
- [9] J. Devlin, M.-W. Chang, K. Lee, K. Toutanova, BERT: Pre-training of Deep Bidirectional Transformers for Language Understanding, in: Proceedings of the 2019 Conference of the North American Chapter of the Association for Computational Linguistics: Human Language Technologies, Volume 1 (Long and Short Papers), Association for Computational Linguistics, Minneapolis, Minnesota, 2019: pp. 4171–4186. <https://doi.org/10.18653/v1/N19-1423>.
- [10] Summary of the tokenizers, (n.d.). https://huggingface.co/docs/transformers/main/tokenizer_summary (accessed January 4, 2023).
- [11] A. Nayak, H. Timmapathini, K. Ponnalagu, V. Gopalan Venkoparao, Domain adaptation challenges of BERT in tokenization and sub-word representations of Out-of-Vocabulary words, in: Proceedings of the First Workshop on Insights from Negative Results in NLP, Association for Computational Linguistics, Online, 2020: pp. 1–5. <https://doi.org/10.18653/v1/2020.insights-1.1>.
- [12] R. Ma, Y. Tan, X. Zhou, X. Chen, D. Liang, S. Wang, W. Wu, T. Gui, Q. Zhang, Searching for Optimal Subword Tokenization in Cross-domain NER, (2022). <https://doi.org/10.48550/arXiv.2206.03352>.
- [13] T. Kudo, J. Richardson, SentencePiece: A simple and language independent subword tokenizer and detokenizer for Neural Text Processing, *ArXiv:1808.06226 [Cs]*. (2018). <http://arxiv.org/abs/1808.06226> (accessed August 20, 2021).
- [14] O. Kwon, D. Kim, S.-R. Lee, J. Choi, S. Lee, Handling Out-Of-Vocabulary Problem in Hangeul Word Embeddings, in: Proceedings of the 16th Conference of the European Chapter of the Association for Computational Linguistics: Main Volume, Association for Computational Linguistics, Online, 2021: pp. 3213–3221. <https://doi.org/10.18653/v1/2021.eacl-main.280>.
- [15] P. Norvig, How to Write a Spelling Corrector, (2007). <http://norvig.com/spell-correct.html> (accessed December 2, 2021).
- [16] K. Kukich, Techniques for automatically correcting words in text, *Acm Computing Surveys (CSUR)*. 24 (1992) 377–439.
- [17] B. Edizel, A. Piktus, P. Bojanowski, R. Ferreira, E. Grave, F. Silvestri, Misspelling Oblivious Word Embeddings, (2019). <https://doi.org/10.48550/arXiv.1905.09755>.
- [18] V. Malykh, V. Logacheva, T. Khakhulin, Robust Word Vectors: Context-Informed Embeddings for Noisy Texts, in: Proceedings of the 2018 EMNLP Workshop W-NUT: The 4th Workshop on Noisy User-Generated Text, Association for Computational Linguistics, Brussels, Belgium, 2018: pp. 54–63. <https://doi.org/10.18653/v1/W18-6108>.

- [19] S. Lee, H. Shin, The Korean Morphologically Tight-Fitting Tokenizer for Noisy User-Generated Texts, in: Proceedings of the Seventh Workshop on Noisy User-Generated Text (W-NUT 2021), Association for Computational Linguistics, Online, 2021: pp. 410–416. <https://doi.org/10.18653/v1/2021.wnut-1.45>.
- [20] S. Eo, C. Park, H. Moon, H. Lim, Research on Subword Tokenization of Korean Neural Machine Translation and Proposal for Tokenization Method to Separate Jongsung from Syllables, Journal of the Korea Convergence Society. 12 (2021) 1–7. <https://doi.org/10.15207/JKCS.2021.12.3.001>.
- [21] K. Park, J. Lee, S. Jang, D. Jung, An Empirical Study of Tokenization Strategies for Various Korean NLP Tasks, ArXiv:2010.02534 [Cs]. (2020). <http://arxiv.org/abs/2010.02534> (accessed January 11, 2021).
- [22] T. Mikolov, I. Sutskever, A. Deoras, H.-S. Le, S. Kombrink, J. Cernocky, Subword language modeling with neural networks, Preprint (<http://www.fit.vutbr.cz/Imikolov/Rnnlm/Char>. Pdf). 8 (2012). <http://www.fit.vutbr.cz/Imikolov/rnnlm/char.pdf>.
- [23] P. Gage, A new algorithm for data compression, C Users Journal. 12 (1994) 23–38.
- [24] SentencePiece, (2023). <https://github.com/google/sentencepiece> (accessed January 3, 2023).
- [25] Z. Lan, M. Chen, S. Goodman, K. Gimpel, P. Sharma, R. Soricut, ALBERT: A Lite BERT for Self-supervised Learning of Language Representations, ArXiv:1909.11942 [Cs]. (2020). <http://arxiv.org/abs/1909.11942> (accessed May 21, 2021).
- [26] Z. Yang, Z. Dai, Y. Yang, J. Carbonell, R. Salakhutdinov, Q.V. Le, XLNet: Generalized Autoregressive Pretraining for Language Understanding, ArXiv:1906.08237 [Cs]. (2020). <http://arxiv.org/abs/1906.08237> (accessed May 21, 2021).
- [27] C. Raffel, N. Shazeer, A. Roberts, K. Lee, S. Narang, M. Matena, Y. Zhou, W. Li, P.J. Liu, Exploring the Limits of Transfer Learning with a Unified Text-to-Text Transformer, (2020). <https://doi.org/10.48550/arXiv.1910.10683>.
- [28] Y. Lee, Y. Yoo, Eunjeon / mecab-ko — Bitbucket, (2013). <https://bitbucket.org/eunjeon/mecab-ko-dic/src/master/> (accessed August 9, 2021).
- [29] T. Kudo, Mecab: Yet another part-of-speech and morphological analyzer, SourceForge. (2006). <https://sourceforge.net/projects/mecab/> (accessed August 9, 2021).
- [30] C. OmniClass, OmniClass Table 22- Work Results approved, (2013). www.omniclass.org.
- [31] H.-C. Cho, N. Okazaki, M. Miwa, J. Tsujii, Named entity recognition with multiple segment representations, Information Processing & Management. 49 (2013) 954–965. <https://doi.org/10.1016/j.ipm.2013.03.002>.
- [32] J. Li, A. Sun, J. Han, C. Li, A Survey on Deep Learning for Named Entity Recognition, ArXiv:1812.09449 [Cs]. (2020). <http://arxiv.org/abs/1812.09449> (accessed February 2, 2021).
- [33] J. Devlin, BERT-Base: Multilingual Cased, GitHub Repository. (2019). <https://github.com/google-research/bert/blob/master/multilingual.md>.
- [34] H. Jeon, SKT-KoBERT: Korean BERT pre-trained cased, GitHub Repository. (2020). <https://github.com/SKTBrain/KoBERT>.
- [35] J. Park, KoELECTRA: Pretrained ELECTRA Model for Korean, GitHub Repository. (2020). <https://github.com/monologg/KoELECTRA>.
- [36] J. Devlin, M.-W. Chang, K. Lee, K. Toutanova, BERT: Pre-training of Deep Bidirectional Transformers for Language Understanding, in: Proceedings of the 2019 Conference of the North American Chapter of the Association for Computational Linguistics: Human Language Technologies, Volume 1 (Long and Short Papers), Association for Computational Linguistics, Minneapolis, Minnesota, 2019: pp. 4171–4186. <https://doi.org/10.18653/v1/N19-1423>.
- [37] J. Devlin, BERT-Base: Multilingual Cased, GitHub Repository. (2019). <https://github.com/google-research/bert/blob/master/multilingual.md>.
- [38] K. Clark, M.-T. Luong, Q.V. Le, C.D. Manning, ELECTRA: Pre-training Text Encoders as Discriminators Rather Than Generators, ArXiv:2003.10555 [Cs]. (2020). <http://arxiv.org/abs/2003.10555> (accessed August 11, 2021).
- [39] J. Park, KoELECTRA: Pretrained ELECTRA Model for Korean, GitHub Repository. (2020). <https://github.com/monologg/KoELECTRA>.
- [40] P. Hühthwohl, R. Lu, I. Brilakis, Multi-classifier for reinforced concrete bridge defects, Automation in Construction. 105 (2019) 102824. <https://doi.org/10.1016/j.autcon.2019.04.019>.
- [41] H. Nakayama, seqeval: A Python framework for sequence labeling evaluation, (2018). <https://github.com/chakki-works/seqeval>.

A Framework of Reconstructing Piping Systems on Class-imbalanced 3D Point Cloud Data from Construction Sites

Yilong Chen¹, Seongyong Kim¹, Yonghan Ahn², and Yong K. Cho¹

¹School of Civil and Environmental Engineering, Georgia Institute of Technology, U.S.A
ychen3339@gatech.edu, skim3310@gatech.edu, yong.cho@ce.gatech.edu

²Department of Architecture and Architectural Engineering, Hanyang University, South Korea
yhahn@hanyang.ac.kr

Abstract –

In construction environments, modifications to the dimensions, positioning, and trajectory of plumbing infrastructure within edifices are frequently necessitated by on-site conditions and pragmatic installation procedures. Recent advancements in Scan-to-BIM technology have streamlined pipe construction processes by monitoring development through a 3D model. However, existing 3D point cloud processing methods rely heavily on given local geometric information to distinguish pipes from adjacent components. Furthermore, point clouds originating from construction environments are mostly class-imbalanced data which could negatively impact the data-driven approach. This paper proposed a novel framework for segmenting and reconstructing piping systems utilizing raw 3D point cloud data acquired from construction sites, addressing the aforementioned challenges. The data firstly undergoes preprocessing, including the elimination of redundant points, rotational adjustments, and sampling procedures. Subsequently, a point cloud semantic segmentation network is trained to predict the per-point class labels after adding local features and mitigating the class imbalance issues. Finally, Efficient RANSAC is employed to identify cylinder-shaped pipes based on the prediction outcomes. The proposed framework shows superior performance compared to existing semantic segmentation methods and exhibits considerable promise for piping system reconstruction.

Keywords –

Point cloud segmentation; pipe reconstruction; construction sites; deep learning

1 Introduction

Mechanical, electrical, and plumbing (MEP) system makes up a large amount of construction cost and asset value. Recent advances in laser scanning and Building Information Modeling (BIM) technologies have demonstrated the great potential of Scan-to-BIM application for MEP systems. However, compared with visible structural and architectural components like columns, walls, floors, ceilings, windows, and doors in an as-built interior environment, pipes and ducts are less frequently extracted, analyzed, and reconstructed [1]. The workflow for extracting MEP systems directly from raw point cloud data with architectural and structural components in close proximity remains to be discussed [2].

3D point cloud data applications in the construction field, such as geometry quality inspection and semantic model reconstruction, are limited by requiring the existence of a BIM model as a precondition. Construction sites are ideal places to capture the point cloud data before pipes are covered by other structural components to record the size, location and route [1]. However, only a partial scan of the pipe surface might be available due to the space limitation for scanning [3].

Machine learning and deep learning are fast-growing techniques in 3D point cloud reconstruction. Current state-of-the-art deep learning model, like PointNet [4], uses no local structure information within neighboring points [5] and thus cannot correctly separate pipes from neighboring contexts, like ceilings and walls, in terms of semantic segmentation. There are other works focusing on classifying point cloud data, including pipes by traditional machine learning methods like Support Vector Machine (SVM) [6], AdaBoost [7], Conditional Random Field and Markov Random Field [2], which do not directly feed raw point cloud data into the neural network but instead calculate and use predefined geometric features to train the classifier.

This paper proposes a framework to segment and reconstruct a pipe model using raw 3D point cloud data from construction sites with architectural and structural components in close proximity. An overview is shown in Figure 1. The onsite raw scans are first preprocessed by removing redundant information, applying rotation to align data to the x-axis and y-axis directions and sampling points for training from evenly divided blocks. Then the training data sets containing six classes of structural components are passed to the proposed neural network. The backbone network is robust to semantic segmentation tasks on pipes by adding local features like intensity and normal, modifying the classifier such as adding weight for loss function and using a threshold for prediction, and using ROC AUC as alternative evaluation metrics. The output of the deep learning model is then processed with Efficient RANSAC algorithms to detect cylinder shapes with heavy noise in a constrained time. The obtained cylinder's parameters could then be used to create a potential BIM model. Finally, the proposed framework is verified by comparing reconstruction results using ground truth data collected from a laser scanner on a construction site with the prediction result made by the neural network. The key contributions of this work can be delineated as follows: (a) the study summarized research related to reconstruction of piping systems and extended them to be generally applicable as a framework, (b) the research proposes an procedure to modify and tune a deep learning model suitable for partially scanned objects, highly imbalanced, and over-noisy datasets, and (c) the experiment explored and assessed the proposed semantic segmentation and shape detection framework by empirically employing real-world construction site dataset.

2 Related Work

2.1 3D Models in Construction Field

There are mainly two kinds of 3D model reconstruction based on the information contained in the model: (1) geometry model reconstruction and (2) semantic model reconstruction [8]. The difference is that the latter includes the geometric information and the object's semantic information. Both two categories depend heavily on the implementation of computer vision algorithms such as Structure from Motion (SfM) [9] and random sample consensus (RANSAC) [10]. The semantic information for point clouds acquired from the construction field refers to building components such as ceilings, walls, and MEP systems. Instance-wise or point-wise object classification has been widely studied to reconstruct the as-built model with the purpose of comparing it with an pre-design 3D model. Given existing BIM models, 3D point clouds can be used for

geometry quality inspection and construction process monitoring [11]. Even if not, as-built 3D model reconstruction can still be helpful for facility management, such as renovation [12], maintenance [13], and energy analysis [14]. As the 3D BIM model is beneficial for various applications in the whole life cycle of a building, there still lacks a general framework for segmentation and reconstruction of the as-built building, where onsite 3D point cloud data would be practical for constructing a workflow.

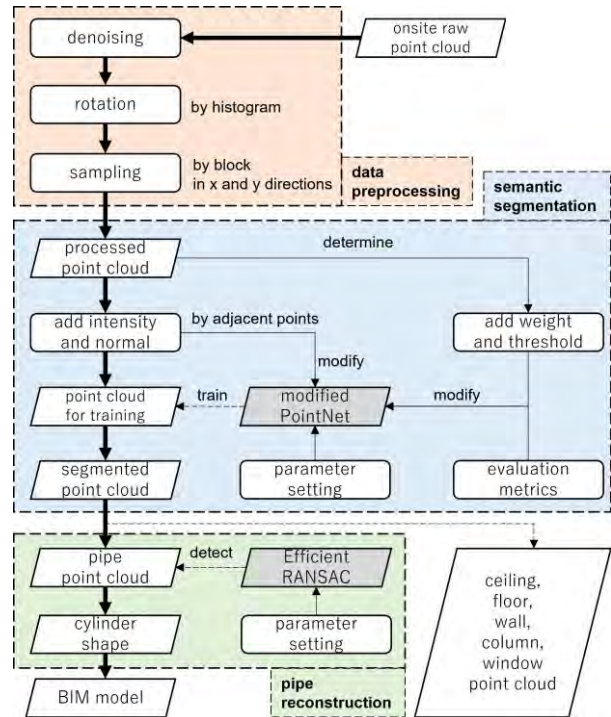


Figure 1. Overview of pipes segmentation and reconstruction process

2.2 3D Semantic Segmentation

Semantic segmentation of 3D point clouds is to generate semantic information for every point. It is usually considered supervised learning methods, including traditional machine learning techniques and state-of-the-art deep learning approaches [5]. Supervised machine learning techniques are further divided into two groups: (1) feature based on every single point, such as Support Vector Machine [6], AdaBoost [7] and (2) feature based on contextual information in graphical models, such as Conditional Random Field and Markov Random Field [2]. Compared with traditional machine learning methods, deep learning approaches feed training data directly into a neural network to acquire high-dimensional features without specific knowledge for feature design and extraction. The deep learning approaches can then be divided into three categories

based on the format in which the point cloud is fed into the neural network: (1) Multiview [15], (2) voxel, and (3) raw point cloud. Since Multiview and voxel forms need to convert 3D point cloud data to 2D images or low-resolution forms, directly binding transformation in the neural network and performing on point cloud data have advantages in controlling computational overhead and maintaining original information of feature space. However, these deep learning approaches deal with only single-shape recognition problems or lack local structure information to correctly separate certain target classes from neighbor structural components in close proximity. A refinement for the architecture of the current neural network used in 3D point cloud semantic segmentation on construction sites needs to be further explored.

2.3 Plumbing Pipe Reconstruction

There has been extensive interest in research on the reconstruction of pipes by 3D point cloud data in computer vision and construction management. Ahmed et al. [16] use Hough-transform and domain constraints to develop an effective approach to locating and reconstructing 3D pipes. Dimitrov et al. [17] introduce a new region-growing method with a single parameter, which accounts for the desired level of abstraction for context-free segmentation of building point clouds, including MEP systems. Due to a large number of noises and different sizes of pipelines that cannot be directly used by traditional methods such as region-growing, RANSAC and Hough transformation, Liu et al. [18] proposed a simpler method to find circles in 2D space rather than finding cylinders in 3D space. Since most of the above research targets are pipes in scenes where there are dominantly planar or non-planar surfaces, Perez-Perez et al. [2] presented a Markov Random Field learning method to assign semantic labels to point cloud segment where MEP systems are close to building components. Studies also use neural networks to reduce the time-consuming and labor-intensive process of pipe recognition and segmentation. Kim et al. [19] showed an automatic pipe and elbow recognition method, including CNN, to filter falsely classified points against occlusion between pipes and elbows. Cheng et al. [20] utilized PointCNN [21] to learn the point cloud feature and classify points into 6 different classes and no-part for later clustering and aggregation. Kim et al. [22] tested the performance of MCVNN [15] and PointNet [4] on retrieving piping component types from an already segmented point cloud. In most of the research, the MEP system data has already had a high resolution before classification or shape detection, while the point cloud data from the construction site is usually a partial scan due to the obstructions. There is also little discussion about evaluating reconstruction results using the original ground truth data with reconstruction results by the

prediction result.

2.4 Imbalanced Classification

While the convolutional neural network is gaining significance in perception fields, one big challenge is that, some classes in the data set have a remarkably higher portion than other classes; it's also referred to as class imbalance. The class imbalance would affect convergence during training and a model's generalization while testing. [23] Strategies for addressing the class imbalance problem are mainly divided into two categories [24]: (1) data-level sampling methods and (2) classifier-level weight methods. The main idea of oversampling is replicating samples from minority classes, while undersampling refers to removing examples from majority classes. Both methods would address the problem to some extent, but there are also shortcomings: while oversampling may cause an overfitting problem, undersampling would lose specific valuable data. Cost-sensitive learning [25] assigns different weights for wrong predictions from different classes. One way to implement it in a neural network is to pass the weighted loss to the backpropagation process. Another classifier-level weight method is tantamount to adjusting the threshold for the last layer of the neural network. Usually, the output is divided by its prior probability, which equals the ratio of the corresponding instances in the same class. These strategies are mainly proposed for 2D image classification tasks, and the effectiveness of 3D point cloud semantic segmentation on data from construction sites remains to be tested.

3 Datasets

For this study, the datasets were acquired by a LiDAR scanner at the student center construction site at Georgia Institute of Technology. They are manually labeled into 10 classes: ceiling, column, floor, pipe, wall, window, noise, and others. The numbers of points for the first 6 classes (Figure 2) in total 4 scans were shown in Table 1.

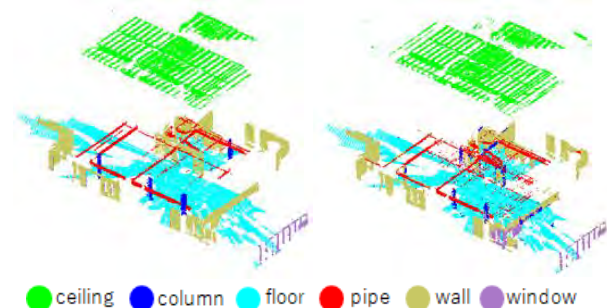


Figure 2. Example of ground truth (left) and segmentation result (right). The ceiling is moved upwards for better visualization for other classes.

4 Data Preprocessing

4.1 Denoising

Raw point cloud data from construction sites contain redundant information that should be removed before preprocessing. Except for six structural components, including ceilings, columns, floors, pipes, walls and windows, other movable onsite components such as workers, tools, materials, and noise are removed to keep the data specialized, clean, and distinct. We use statistical outlier removal to remove noise that deviate from their neighbors compared with the average of the point cloud. There are primarily two benefits to denoise raw point cloud data. The first one is that movable data like workers, tools, and materials occupy only a small percentage of the total data; however, the amount can vary largely across different sites, aggravating the imbalanced-classification problem and influencing the accuracy of other desired structural components. The second reason is that those movable data do not have regular geometric shapes; thus, the normal for small local faces can differ even on the same object. In Table 2, we calculate and add the normal of small faces formed by local points to the backbone network. Removing these irregular components would improve the model's performance by making the cylinder shapes more distinguishable from the plane context, since the normal of cylinders and planes are more consistent on a local surface than movable objects.

4.2 Point Transformation

In the PointNet framework, an affine transformation matrix is used for the input and feature transformations in the model, and it is claimed that combining both the regularization and transformations can achieve its best performance [4]. In our implementation of raw point cloud data from construction sites, we found that higher accuracy can be achieved by applying a rotation on the point cloud data to align most walls to the x-axis and y-axis before feeding it into the neural network. Raw point cloud data from construction sites have more complicated shapes and contain more outlier points than the indoor environment, so alignment to x-axis and y-axis would help each block have a more reasonable distribution of different categories of points in the afterward sampling process. In actual practice, we

divided the angle from -45° to 45° by small intervals. For each small angle, we calculated the histogram of the distribution of the x-axis and y-axis for the point cloud data. Then we operate max pooling on the number of points in each bin by step size 3 and sum up the top 20 results in the x-axis and y-axis. By maximizing the density of bins in this way, we could acquire an angle by which most of the walls are rotated in x and y directions. For the four datasets we used for training and evaluating, the angles are, respectively -33.44° , -42.48° , 3.86° and -15.29° .

4.3 Point Sampling

We apply the same sampling method used in [4] for indoor environments. We divide the area of construction sites in x and y directions with a block size of 2 meters. In every single block, we sample 1024 points randomly through the z direction and use stride size 1 meter in x and y directions to overlap part of the sampling space. The training result determines these numbers that a sparser sampling would not likely provide enough neighbor points for later normal calculation, thus harming the accuracy of prediction, while a denser sampling would significantly increase the number of points as well as the time used for training and computing. Note that in this study, we do not apply any sampling methods such as oversampling or undersampling. Further research involves using other sampling strategies to improve prediction accuracies of minor classes such as window and column.

5 Semantic Segmentation

5.1 Backbone Network

PointNet is a neural network framework that can consume point cloud data directly to perform 3D recognition tasks, such as object classification, part segmentation, and semantic segmentation, efficiently and effectively without transforming the data to 3D voxel grids or 2D images. The detailed design of the network structure uses the max pooling layer, global feature combined with the local feature, and transformation matrices to deal with the three main properties of point cloud data, unordered, interaction among points, and invariance under transformations.

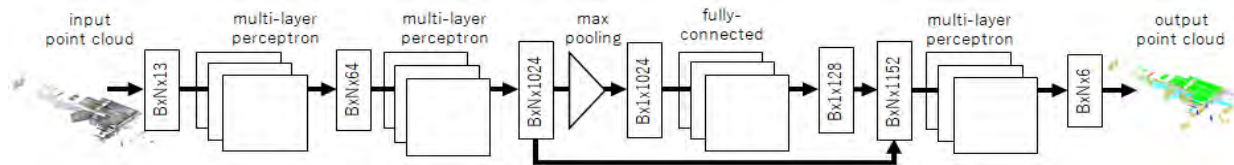


Figure 3. The architecture of the modified PointNet

In our implementation, we use a similar neural network structure to the PointNet paper for indoor semantic segmentation, except for increasing input data dimension from 9 to 13. The architecture of our backbone network is shown in **Error! Reference source not found.**

5.2 Intensity and Normal

In the original PointNet framework, the 9 features of the point cloud used in the neural network are, respectively local x, y, z coordinates, global x, y, z coordinates, and normalized R, G, B values of color. Although local coordinates combined with global coordinates provide certain knowledge for point segmentation, in practice, this information is still insufficient for extracting pipe systems with structural components like ceilings in proximity for semantic segmentation.

Therefore, we consider adding other features such as intensity and normal. Intensity is a feature that we could get directly from raw point cloud data from construction sites. Since it records the return strength of the beam, it has been used in recent research to help recognize the material information of construction sites [26]. However, since additional factors such as scan angle, range, and moisture content can also affect the intensity, it does not always lead to a consistent result. Indeed, in our experiment, we expected intensity could help us recognize columns and windows apart from walls, but the result was not promising. We investigated the specific intensity field of the data and learned that the intensity of columns is relatively stable, but there are also such values in the same range for walls. Considering the close spatial relationship, it makes sense that the intensity of these structural components would be similar, especially for raw point cloud data from construction sites.

On the other hand, normal is beneficial for distinguishing pipes from ceilings. We use a K-d Tree with dimension three to search neighbor points for each point and then calculate the normal vectors of the plane constructed by those points. We set the radius to 1 meter and the maximum number of neighbors to be searched as 30. Since pipes have cylindrical shapes and ceilings have plane shapes, the direction and the distribution of normal vectors of pipes and ceilings should be distinct even in a small close proximity. The result shows that by adding normal and combining with other proposed methods, we can largely improve the accuracy of pipes without affecting the accuracy of other major classes such as ceiling, wall, and floor.

5.3 Weight and Threshold

The class imbalance has been a big problem in convolutional neural networks. For point cloud data from construction sites, this problem is more severe than

indoor environments. The ratios of each class to the total number of points of our data are respectively 35.84% for ceiling, 3.13% for column, 26.93% for floor, 9.30% for pipe, 23.28% for wall and 1.52% for window. Major classes like ceiling, floor and wall make up over 86% of the whole dataset, while the smallest minority class only contains 1.52% of the total points, which causes the ratio of imbalance reaches to over 23 [23]. What makes the problem worse is that those categories occupying a larger percentage of the total data have relatively simple shapes compared with the remaining categories. This would make the model redundant to change once it finds a straightforward relationship between certain features and corresponding labels, say the z-axis and floor, and reach high accuracy. To mitigate the negative influence of class imbalance, we try to apply weight while calculating loss and threshold while making a prediction. Before adding the loss together, we assign a different weight w_i for wrong predictions from different classes by multiplying $(1/r_i)/\sum(1/r_i)$ for each class, where r_i is the prior probability of each class, equalling the ratio of each class, calculated by the total number of points n_i for each class (**Error! Reference source not found.**). Note here that we roughly use each class's ratio in the whole dataset instead of each training batch; we defer this exploration to future work. The other strategy we try is to adjust the decision threshold of the output layer in the test phase by multiplying the equivalent weight we use for calculating loss. We found that weight for training combined with a threshold for testing would improve the accuracy for minor classes like pipe, column, and window, although it might make accuracy for other major classes lower. Since recall might not fully reflect the correctness of prediction, we further investigate the IoU of each class before and after applying weight and threshold. The result is shown in **Error! Reference source not found.** For pipes, from the 4th configuration to the 5th configuration, the accuracy increases while IoU decrease means that both true positive points and false positive points increase. This result is favorable for later shape fitting since little more false positive outlier points for pipes should not affect cylinder fitting too much because RANSAC algorithm uses normals to detect shape.

Table 1. Number of points (million) and weight (threshold) for six classes.

	ceiling	column	floor	pipe	wall	window
1	2.33	0.07	2.74	0.82	2.20	0.04
2	2.63	0.45	2.17	0.53	2.71	0.19
3	3.39	0.07	1.30	0.51	1.65	0.17
4	3.02	0.40	2.34	1.09	0.83	0.09
n_i	11.37	0.99	8.54	2.95	7.38	0.48
r_i	0.36	0.03	0.27	0.09	0.23	0.02
w_i	0.02	0.27	0.03	0.09	0.04	0.55

5.4 Evaluation Metrics

Since overall accuracy favors over-represented majority classes, leading to a highly misleading assessment of both training and evaluating [23], we use the area under the receiver operating characteristic curve, ROC AUC [27], to determine when to stop while training. ROC AUC is essentially a plot of the false positive rate to the true positive rate for different prediction thresholds. While the area under the curve depicted by plots of false positive rate and true positive rate pairs gets larger and near to 1, the model’s ability to distinguish two different classes becomes better. Usually, ROC AUC is used for binary classification, but it can also be extended to multiple classes. Here we utilize the One-vs-rest algorithm to compute the AUC of each class against the rest classes [28] to let the model understand the whole scene and achieve better performance than binary classification. We save the model with the highest ROC AUC score for testing during training and use this model for further evaluation.

5.5 Results and Analysis

We set the number of sampling points in each block as 1024, block size as 2 meters, stride size as 1 meter, batch size as 24, learning rate as 0.001 and stop training in 20 epochs. We use cross-validation across all four datasets, training on three datasets while testing on the remaining dataset four times before averaging the results, and our modified backbone network (5th configuration in **Error! Reference source not found.**) results in 89.83% average overall training accuracy, 99.08% training ROC AUC score with 84.54% average overall validation accuracy, 91.10% validation ROC AUC score on the semantic segmentation task. **Error! Reference source not found.** shows an example of a prediction result.

From Table 2, we can safely conclude that we have found a better way to solve issues caused by partially imbalanced noisy data sets. Firstly, comparing the result for the first 5 configurations, by utilizing rotation and adding intensity, normal, and weight, the average

accuracy and IoU for pipes would increase from 70.32% and 50.88% to 86.26% and 66.42%, while the average accuracy and IoU for all 6 classes would increase from 61.75% and 51.03% to 77.92% and 61.78%. This means data preprocessing, adding local features, and dealing with class imbalance problems are useful for recognizing plumbing pipes from other structural components. Secondly, comparing the result for last 3 configurations, we found that minority classes like column and window would benefit from weight for loss calculation and threshold for the testing phase. For pipes, the accuracy would increase while the IoU would decrease a little, which means some points of the ceiling are recognized as pipes. However, this fact should not affect the cylinder fitting process too much because RANSAC uses normal to detect the shape, and the normal for cylinder and plane are different. Finally, we discovered that using weight combined with the threshold proposed in the last configuration is not as effective as using them separately. This might be because we have already compensated weight to the loss function through backpropagation in the training process. The repeating threshold in the test phase would conversely hurt the prediction results.

6 Pipe Reconstruction

6.1 Cylinder Shape Detection

RANSAC is a non-deterministic algorithm to estimate the parameters of a mathematical model among noisy data. [10] It has been extensively used in reverse engineering, like point cloud reconstruction, with its favorable properties such as generality, simplicity, and robustness. Efficient RANSAC is a variation of the original RANSAC algorithm that uses a lazy cost evaluation function with a structured sampling strategy for candidate shapes like planes, spheres, cylinders, and other additional primitives. [29] This method is suitable and efficient for automatically acquiring raw point cloud data under relatively adverse conditions, such as heavy noise in constrained processing time.

Table 2. Result of semantic segmentation.

configuration	ceiling	column	floor	pipe	wall	window	average
	acc/IoU	acc/IoU	acc/IoU	acc/IoU	acc/IoU	acc/IoU	acc/IoU
Base PointNet [4]	77.9/70.2	31.3/22.0	98.3/95.6	70.3/50.9	78.7/60.5	15.2/7.0	62.0/51.3
Ours (w/ rotation)	85.3/78.0	33.7/23.9	96.7/93.6	68.9/51.6	77.5/61.2	32.9/18.5	65.8/54.5
Ours (w/ rotation & intensity)	90.0/78.8	24.4/17.4	97.9/95.0	69.2/55.6	80.2/64.9	43.0/25.3	67.5/56.2
Ours (w/ rotation & intensity & normal)	94.6/85.2	23.7/12.1	98.7/97.6	80.3/ 68.3	79.8/65.0	54.7/25.1	72.0/58.9
Ours (w/o threshold)	86.0/80.4	53.3/26.8	98.1/97.1	86.3/66.4	76.3/ 66.4	67.5/33.5	77.9/61.8
Ours (w/o weight)	88.0/81.5	33.9/17.6	99.2/98.1	83.6/64.8	72.2/64.0	74.7/ 34.8	75.3/60.1
Ours (w/ full condition)	82.3/78.3	48.9/15.4	95.3/94.5	89.3/61.3	45.5/38.4	81.0/22.5	73.7/51.7

For the shape to estimate, a cylinder is generated from two points with normals and then verified by the two free parameters: max distance to primitive ϵ and max normal deviation α .

6.2 Experiment Results

Since there is no common rule for setting distance threshold ϵ and normal deviation threshold α , we found their optimal values as well as other parameters from the experiments. We set the distance threshold ϵ as 0.15 and 10 for normal deviation threshold α . For the minimum support points for each primitive, we set the value as 200. We use a uniform sampling method like we used in the training process. We also use cross-validation across all four datasets and make predictions for each area. **Error! Reference source not found.** shows the detection result on the ground truth point cloud and prediction result. The error rate for cylinders' center coordinates, radius r , and length h are listed in **Error! Reference source not found.**.

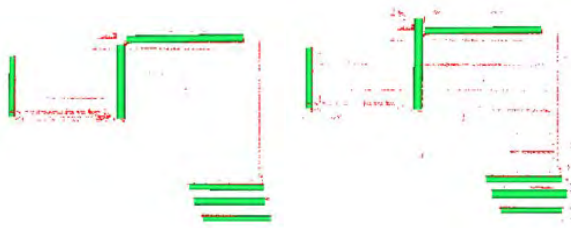


Figure 4. Example of reconstruction result of pipes by ground truth (left) and prediction result (right).

The outcome of cylinder shape detection on the prediction result is very satisfactory. The error rates for x , y , z coordinates of cylinders' centers are mostly under 1%, while the error rates for the radius r and length h of detected cylinders are under 10% and 5%, respectively. Although visibly, some leftover points could not be detected as cylinders under the current algorithm and parameter settings, either due to the unified distance and minimum support points we chose or the fact that some point clouds from other classes are mislabelled as pipes, these results do indicate the potential for directly using semantic segmentation prediction result from our framework to reconstruct plumbing pipes if the shape detection method itself reaches to a sufficient accuracy.

Table 3. Error rate for RANSAC estimation of cylinder parameters.

		x	y	z	r	h
error rate	mean	0.40	0.57	0.54	9.60	4.70
	(%)					
	stdev	0.00	0.01	0.01	0.06	0.05

7 Conclusion

The proposed framework shows a novel approach that employs class-imbalanced point cloud data from construction sites to segment and reconstruct piping systems. The proposed techniques and enhanced backbone network exhibit robust performance in semantic segmentation of partially scanned, highly imbalanced, and noisy point cloud data. Moreover, the comparison with the ground truth demonstrates the feasibility of shape detection.

Despite the experiment results indicating robust segmentation performance, further improvements will be investigated by leveraging alternative sampling methods and computing weight and threshold values per each batch training step. Also, ablation studies such as parameter selection will be considered to optimize the piping reconstruction performance across varying plumbing pipe dimensions.

Acknowledgments

This research was supported by the National Science Foundation under Grant no. (2222723) and the Ministry of Science and ICT through the National Research Foundation of Korea (NRF-2022H1D3A2A01093584).

References

- [1] F. Bosché, A. Guillemet, Y. Turkan, C. Haas and R. Haas. Tracking the built status of MEP works: Assessing the value of a Scan-vs-BIM system. *Journal of Computing in Civil Engineering*, 28(4), pages 1-28, 2014.
- [2] Y. Perez-Perez, M. Golparvar-Fard and K. El-Rayes. Segmentation of point clouds via joint semantic and geometric features for 3D modeling of the built environment. *Automation in Construction*, 125, 2021.
- [3] H. Son, C. Kim and Changwan Ki. Fully Automated As-Built 3D Pipeline Extraction Method from Laser-Scanned Data Based on Curvature Computation. *Journal of Computing in Civil Engineering*, 29(4), 2015.
- [4] C. R. Qi, H. Su, K. Mo and L. J. Guibas. PointNet: Deep Learning on Point Sets for 3D Classification and Segmentation. In *Proceedings of the IEEE conference on computer vision and pattern recognition*, pages 652-660, 2017.
- [5] Y. Xie, J. Tian and X. Zhu. Linking Points With Labels in 3D: A Review of Point Cloud Semantic Segmentation. *IEEE Geoscience and Remote Sensing Magazine*, 8, pages 38-59, 2020.
- [6] Q. Wang and M.-k. Kim. Applications of 3D point cloud data in the construction industry: A fifteen-

- year reveiwo from 2004 to 2018. *Advanced Engineering Informatics*, 39, pages 306-319, 2019.
- [7] M. Westoby, J. Brasington, N. Glasser, M. Hambrey and J. Reynolds. 'Structure-from-Motion' photogrammetry: A low-cost, effective tool for geoscience applications. *Geomorphology*, 179, pages 300-314, 2012.
- [8] M. A. Fischler and R. C. Bolles. Random sample consensus: a paradigm for model fitting with applications to image analysis and automated cartography. *Commun. ACM*, 4(6), pages 381-395, 1981.
- [9] F. Bosché, M. Ahmed, Y. Turkan, C. T. Haas and R. Haas. The value of integrating Scan-to-BIM and Scan-vs-BIM techniques for construction monitoring using laser scanning and BIM: The case of cylindrical MEP components. *Automation in Construction*, 49, pages 201-213, 2015.
- [10] C. C. Aydin. Designing building façades for the urban rebuilt environment with integration of digital close-range photogrammetry and geographical information systems. *Automation in Construction*, 43, pages 38-48, 2014.
- [11] E. Valero, F. Bosché and A. Forster. Automatic segmentation of 3D point clouds of rubble masonry walls, and its application to building surveying, repair and maintenance. *Automation in Construction*, 96, pages 29-39, 2018.
- [12] C. Wang, Y. K. Cho and C. Kim. Automatic BIM component extraction from point clouds of existing buildings for sustainability applications. *Automation in Construction*, 56, pages 1-13, 2015.
- [13] J. Zhang, X. Lin and X. Ning. SVM-Based Classification of Segmented Airborne LiDAR Point Clouds in Urban Areas. *Remote Sensing*, 5(8), pages 3749-3775, 2013.
- [14] Z. Wang, L. Zhang, T. Fang, P. T. Mathiopoulos, X. Tong, H. Qu, Z. Xiao, F. Li and D. Chen. A Multiscale and Hierarchical Feature Extraction Method for Terrestrial Laser Scanning Point Cloud Classification. *IEEE Transactions on Geoscience and Remote Sensing*, 53(5), pages 2409-2425, 2015.
- [15] H. Su, S. Maji, E. Kalogerakis and E. G. Learned-Miller. Multiview convolutional neural networks for 3d shape recognition. In *Proceedings of the IEEE international conference on computer vision*, pages 945-953, 2015.
- [16] M. Ahmed, C. T. Haas and R. Haas. Autonomous Modeling of Pipes within Point Clouds. In *2013 Proceedings of the 30th ISARC*, pages 1093-1100, 2013.
- [17] A. Dimitrov and M. Golparvar-Fard. Segmentation of building point cloud models including detailed architectural/structural features and MEP systems. *Automation in Construction*, 51, pages 32-45, 2015.
- [18] Y.-J. Liu, J.-B. Zhang, J.-C. Hou, J.-C. Ren and W.-Q. Tang. Cylinder Detection in Large-Scale Point Cloud of Pipeline Plant. *IEEE TRANSACTIONS ON VISUALIZATION AND COMPUTER GRAPHICS*, 19, pages 1700-1707, 2013.
- [19] Y. Kim, C. H. P. Nguyen and Y. Choi. Automatic pipe and elbow recognition from three-dimensional point cloud model of industrial plant piping system using convolutional neural network-based primitive classification. *Automation in Construction*, 116, 2020.
- [20] L. Cheng, Z. Wei, M. Sun, S. Xin, A. Sharf, Y. Li, B. Chen and C. Tu. DeepPipes: Learning 3D pipelines reconstruction from point clouds. *Graphical Models*, 111, 2020.
- [21] Y. Li, R. Bu, M. Sun and B. Chen. PointCNN: Convolution On X-Transformed Points. *Proceedings of the 32nd International Conference on Neural Information Processing Systems*, pages 828-838, 2018.
- [22] H. Kim, C. Yeo, I. D. Lee and D. Mun. Deep-learning-based retrieval of piping component catalogs for plant 3D CAD model reconstruction. *Computers in Industry*, 123, 2020.
- [23] M. Buda, A. Maki and M. A. Mazurowski. A systematic study of the class imbalance problem in convolutional neural networks. *Neural Networks*, 106, pages 249-259, 2018.
- [24] H. He and E. A. Garcia. Learning from Imbalanced Data. *IEEE Transactions on Knowledge and Data Engineering*, 21, pages 1263-1284, 2009.
- [25] C. Elkan. The foundations of cost-sensitive learning. *International joint conference on artificial intelligence*, 17(1), pages 973-978, 2001.
- [26] J. Park and Y. K. Cho. Point Cloud Information Modeling: Deep Learning-Based Automated Information Modeling Framework for Point Cloud Data. *Journal of Construction Engineering and Management*, 148, 2022.
- [27] A. P. Bradley. The use of the area under the ROC curve in the evaluation of machine learning algorithms. *Pattern Recognition*, 30, pages 1145-1159, 1997.
- [28] F. Provost and P. Domingos. Well-trained PETs: Improving probability estimation trees. *CeDER Working Paper #IS-00-04, Stern School of Business, New York University*, 2000.
- [29] R. Schnabel, R. Wahl and R. Klein. Efficient RANSAC for Point-Cloud Shape Detection. *Computer Graphics Forum*, 26(2), pages 214-226, 2007.

Information Modelling Guidelines for the Mining Sector

Jyrki Salmi¹ and Rauno Heikkilä¹

¹University of Oulu, Finland

jyrki.salmi@oulu.fi, rauno.heikkila@oulu.fi

Abstract –

Mining is rapidly digitalizing and big data surrounds mines in their everyday activities and processes. Building Information Modelling (BIM) has long since taken an indispensable role in the design and management of buildings and infrastructures and is currently widely used as a standard for information management. Based on the results of the workshop series organized by the University of Oulu, a proposal is presented for further development of the concept of Mining Information Modelling (MiningBIM or MIM for short). The purpose of the workshops was to present, prepare and lay the foundation for the development of modelling guidelines for the mining sector. From the participants' point of view BIM is seen as a megatrend that there is no point in trying to stop, and the idea of standardizing BIM in the mining and tunnelling sector is strongly supported. The results of the workshops showed that BIM is already a widely recognized tool and it is worth starting to study and develop further towards MIM and TIM concepts, including also international standardization work.

Keywords –

BIM; MIM; TIM; Modelling Guidelines

1 Introduction

Mining Information Modelling (MIM) enables efficient information management and big data visualization throughout the mining project life cycle. In mining, there has traditionally been an inability to recognize the value of all available information in different parts of the production and processing chain.

1.1 Background

1.1.1 Big data

Digitalization is everywhere in different industries and also in our private lives. Barnewold and Lottermoser [1] describe that “digitalization in the mining industry refers to the use of computerized or digital devices, systems and digitized data that are to reduce costs, improve business productivity, and transform mining

practices.”

The mining world is rapidly digitalizing and big data, or mass data, surrounds mines everywhere in their everyday activities and processes. “With big data, the key to success is to turn a huge repository of data into a functional intelligence and get value from it. The mining industry can significantly benefit from implementing big data and real-time data analysis” [1].

1.1.2 From data to information models

Data, that is, facts and statistics collected for some reference, must always be presented somehow. Raw data itself is worthless, but it is important and worth refining. “In a mine, the entire tunnel design information”, according to Koch et al. [2], “is traditionally available in the form of independent, dispersed, and heterogeneous data files, and since data sources are barely linked in practice, unilateral decisions are made that do not consider all relevant aspects”. So when structured or unstructured data exists, it often needs to be shared and combined with other data sources to enable data fusion. “The project data, that is typically shared among the team members of organization, varies also in terms of type, scale, format, and life cycle phase” [2]. Figure 1 shows the authors' view of the trajectory from raw data to advanced target setting.

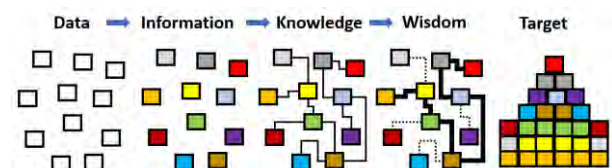


Figure 1. Trajectory from raw data to advanced target setting

The use of data makes it possible to make future actions smarter. The true value of data is determined only when decisions are made based on the information, i.e. when some given data or learned data is put into practice or passed on in some form. All relevant information collected from the mining process lays the foundation for the mine's decision-making process as knowledge, i.e. data, information and skill combined with an understanding of the topic. The wisdom gained after that can be used to achieve the goals set. Analyzing and real-

time utilizing the relevant information accumulated with the help of big data is a key part of the mine's information management process. Likewise, "stable, economical, and sustainable design and construction of all underground facilities requires reliable knowledge regarding the expected impacts of the used construction method on the built environment" [2].

Huang et al. [3] state, that "when semiautonomous or autonomous mining platforms, used for data acquisition are combined with machine learning, and especially with deep learning, information of the built environment can be managed to build knowledge forward and create values". According to Willmott [4], "the future for mining in which many assets are operated by machines that run automatically or autonomously means, that the only capability that will matter, is going to be the ability to make decisions based on the information those assets provide. Having the right data at the right time and the tools and capabilities to understand and manage the data is becoming absolutely fundamental to business success". This means that in the future, all relevant industrial information must be structured, modelled, and visualized in information models in order to process and manage it efficiently in the human-machine interaction process. Figure 2 shows the authors' view of the pursuit of desired values based on the benefits of utilizing information modelling and automation.

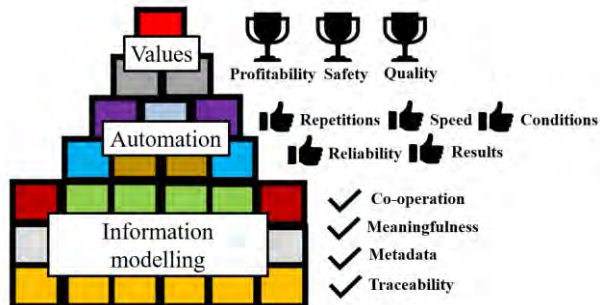


Figure 2. The benefits of information modelling support the benefits of automation to achieve the desired values

According to Slansky [5], "big data can be used especially in information modelling to support advanced analytics applications to discover the flaws and to achieve continuous process improvements and determine best practices across the whole design or build lifecycle".

1.1.3 BIM

The information model is described by Li et al. [6] so that it is a "3D information integration technology based on Computer Aided Design (CAD). It is a digital and visual expression of the physical and functional information produced in the engineering construction and management process. Information modelling includes

two main aspects: information integration and 3D geometrical modelling".

There are numerous options for describing BIM. The definition of BIM varies in different contexts and also from different perspectives. Australasian authors of the National Guidelines for Digital Modelling [7] defined BIM in 2009 as "a three-dimensional representation of a facility based on objects including some information about the objects beyond the graphical representation".

In building construction, BIM has long played an indispensable role in the design and management of buildings, where it has been widely used as a standard for information management [8]. In practice, BIM has been widely applied in design and construction phases, while applications in the facility management and operation phases are still at a very early stage [9][10].

According to Hegemann et al. [10] it is important to "include only those data in the BIM model that are required for evaluations to avoid overloading the model and, thus, losing the clarity that makes a BIM model so valuable". A collaborative process of information modelling is defined as OpenBIM that shares process information and supports seamless collaboration for all process participants throughout the process lifecycle, implementing open, neutral data exchange formats [11].

62 research articles related to BIM and 171 case studies have been reviewed, and it has been found that BIM plays a much less role in underground tunnelling than in building construction. Only very few applications focus on maintenance and much less on tunnel maintenance [9]. To achieve the benefits of BIM also in underground tunnelling (Tunnelling Information Modelling, TIM), approaches have been proposed to extend the BIM concept to underground infrastructure projects as well, in order to facilitate design and analysis tasks and thus increase the productivity in design, construction, and operation [12][13]. In the same way, this paper now provides a built infrastructure information modelling (InfraBIM/I-BIM) approach to increase the potential of the mining sector to further develop the concept of Mining Information Modelling (MIM) for mining as well.

1.2 Mining Information Modelling (MIM)

Fraser [14] states, that "issues related to communications in mining like data exchange and interoperability, need to be overcome in future mines and industry-wide standards need to evolve. Then ultimately, transformational productivity gains will be realized by combining an enhanced knowledge of the resource with the improved control of mining and milling systems, and an ability to optimize or tailor all mine activities as a whole-of-business, end-to-end process".

In Australia CSIRO [15] has stated that "a standard for data communication and data base architecture must

be agreed among the mining and tunnelling community before information exchange is practical between different data sources of the mine's production processes. When instruments and communications comply with the standard, then the industry will access the benefits of maximum interoperability allowing machines and mining systems to model and react to changing conditions in real time". CSIRO has named this overall concept as The Common Mine Model™. Also, according to CSIRO [16] the "first of the seven fundamental components for the successful operation of the future mine is a knowledge driven database model that is common and accessible across all activities of the mining operation".

In China, the term Digital Mine is used instead of BIM, and its essence is Mining Information Model to store all mine-related information [17]. MIM in that context is a "digital expression of the mining resources, mining environment and mining engineering objects and a digital re-engineering of the mine life cycle's business processes to realize information interoperability, information sharing and collaboration of various business entities and to solve the problem of information islands in the mining industry and to improve the efficiency and quality of the participants" [17].

According to Wang J. et al. [18], "hardware and software products in the whole life cycle of mines, lack uniform data standards and specifications and therefore each system has its own data format and storage file and the phenomenon of "information islands" is serious. Therefore, a theoretical framework of Mining Technology Collaboration Platform (MTCP) has been proposed. Under the guidance of the BIM idea, the information island problem, as well as information loss, redundancy, duplication, inconsistency, and other issues can be well resolved". Du et al. [19] also suggest that "for creating high yield and high efficiency mining production, mining companies should develop the formerly mentioned Digital Mine concept rapidly".

However, the target functionality of most BIM tools designed for architecture and building modelling is not very well suited for mining projects. Editing custom parameter objects and object families becomes inevitable. "While still pending full standardization, the application of BIM in tunnel projects requires customized solutions for many aspects of design and construction phases. Ground characterization and geospatial location information are vital to the establishment of as-designed underground BIM model. The inclusion of ground conditions and geotechnical data into the BIM model also improve the quality and the usefulness of the mining model, not only during the design phase but also, and in particular, during the construction and the lifecycle management of the infrastructure, as a support to decision making process. Geological and geotechnical

issues are thus the most important part of underground infrastructures design" [20].

In the course of this research, it has become clear to the author that there is already a fairly well-established description of TIM in the tunnelling sector. But it has also become clear that for the mining sector the overall picture of MIM, and therefore of the real research gap, is not at all so mature. In mining, certain elements of BIM already exist, for example, 3D models are widely used, but very rarely any information is associated with these model structures.

The route from traditional construction BIM and GeoBIM domains to InfraBIM and TIM development, the BIM path is leaning towards more precise MIM definitions. Based on existing examples and very good experiences of developing the InfraBIM domain in Finland since 2013, the need to start further research on MIM and find out its benefits for the mining sector is highlighted. Figure 3 shows the authors' view of the development path of BIM technology towards MIM and its potential for utilization, especially in machine control (MC).



Figure 3. The development path of BIM technology towards MIM and its utilization possibilities in MC

One of the great advantages of MIM conceptualization is an open digital model-based operating environment (ecosystem) that enables the efficient use of semi-automated, automatic and autonomous machines and swarms of machines. In the mining and tunnelling sectors, it would therefore enable knowledge-driven and model-based production.

1.2.1 MIM prerequisites

Currently, there are no specific BIM guidelines or other related specifications available for the mining sector. However, the basic modelling idea of MIM is the same as that of InfraBIM based on the OpenBIM concept. The OpenBIM concept is built on the idea that is three basic prerequisites for a successful BIM process: 1) Modelling guidelines, 2) Information classification, and

3) Data transfer formats, see below Figure 4. These key elements must primarily be sound and consistent for BIM management and practice to work. In Finland, the success of the InfraBIM concept implementation is strongly based on this setup.

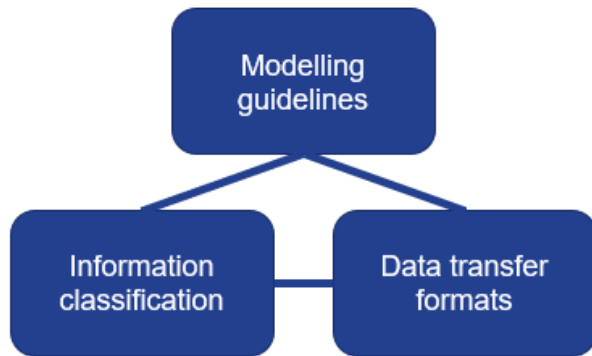


Figure 4. Three key elements in the development and implementation of the BIM process

In this paper, modelling guidelines are discussed mainly because they make up the bulk of the whole. Modelling guidelines tell designers what and how to model. In Finland, these InfraBIM guidelines are called “Common Infra Model Requirements” (YIV-ohjeet in Finnish) [21]. They were prepared in the InfraFINBIM project in 2013 together with companies in the field of infrastructure construction.

Information classification defines the common language on which modelling is based on. “Different stakeholders may use several different data standards and if no common information classification is used, it can result in huge amounts of unusable data and difficulties with exchanging data between different data systems and databases. For tunnelling sector there already exists several different coding systems, one also presented especially for tunnel facility management” [10].

“Common and standard data transfer formats make work machines in the field and computers to talk with central IT systems. Data interoperability is enabled in tunnelling projects with Industry Foundation Classes (IFC) format, which allows data exchange between several BIM software” [2]. Because “IFC provides a well-organized kernel and contains information rich objects used in the construction industry, it is logical to apply to the development of the information modelling in mining, too” [6]. However, there are also many other common data transfer formats available. For example, the IM-format (Infra Model) is used in Finland, where efforts have been made to ensure that all machine control systems support this common and open form of data transfer for earthworks. In USA, the Open Mining Format (OMF) is being developed as an open-source file definition format that supports the transfer of geological and topological data between software systems.

1.3 Aim of the research

The aim of the research is

- to discuss about the challenges of management of relevant data and information in mines,
- to present the potential of BIM based information modelling concepts and propose the idea of applying InfraBIM and TunnellingBIM concepts into the mining sector, and
- to present the results of the MIM development workshop series on modelling guidelines in Finland and propose the next steps for implementing MIM in the mining sector.

This research paper proposes the introduction of InfraBIM and TunnellingBIM methods in the mining environment, either in underground (UG) or open cast (OC) mines. The idea of creating such a new BIM-based information ecosystem for the entire mining and tunnelling sector is ideally based on the rapid growth of the number of automated and autonomous machines in mines and tunnel construction sites. Therefore, translating physical mining infrastructure into digital infrastructure for machine control purposes is increasingly necessary to enable automation of both single machine and a swarm of machines.

2 Materials and methods

In 2021, an extensive Next Generation Mining (NG Mining) research project funded by Business Finland and Finnish industry was launched in Finland. The project focused on enabling the safe, sustainable and productive use of autonomous and networked non-road mobile machinery in underground mining environments. As part of the research project, which also included the conceptualization of the digital twin, the need to start exploring the OpenBIM concept suitable for the entire mining and tunnelling sector was identified and suggested.

During 2022, the University of Oulu organized a series of workshops series of a total of six special, three-hour-long, online workshops, both for all participants in the NG Mining project and for all key Finnish representatives of the mining and tunnelling sector. The workshops were chosen as a research method in order to create the widest possible discussion of a new topic among specialists from different fields.

2.1 Workshop series

The main goal of the workshop series was to create a consensus-based starting point for the development of new and open Mining & Tunnelling Information Modelling (MIM&TIM) concepts in Finland. In addition, goals were to present BIM and its advancements and

opportunities in the mining and tunnelling sectors, to evaluate the experience and best practices already accumulated in InfraBIM and other domains, to stimulate discussion on the needs and objectives of MIM&TIM development, and to explore the possibilities, capabilities and general will to start drafting the development steps of MIM&TIM concepts.

The workshops were carried out, processed, and reported by the University of Oulu, Research Unit of Civil Engineering and Civil Engineering, Digital Construction and Mining Research Area. The workshop series covered six main topics, such as 1) Modelling Guidelines, 2) Information Classification, 3) Data Transfer Formats, 4) The use of building information models in work machine automation, 5) The real-time cloud services of the MIM&TIM process and 6) Organizing models of MIM&TIM future development.

A total of 107 people participated in at least one of the six workshops out of a total of 235 invited people. A total of 54 companies or organizations participated out of a total of 84 invited companies. Throughout the workshop series, online and email surveys were utilized as the most important research tools. A total of 52 BIM-related orientation presentations and numerous group assignments were held in the workshops. Each workshop was recorded and reported in writing with all the results. For the research results, as much as possible of the opinions and experiences of the participants were collected from the workshops, which were then analyzed and summarized by the authors.

3 Results

In the first workshop, the main theme was modelling guidelines and the main topic was the definition of the need for further research and development of the MIM and TIM concepts in Finland.

The main research method was surveys that were conducted before, during and after the actual workshop. The preliminary survey was carried out several days before the workshop using an on-line Webropol software tool, which included five (5) questions related to the main topics of the workshop.

In the actual workshop, the workshop participants gave six (6) well-prepared orientation presentations, which presented all workshop participants with ideas for general BIM and InfraBIM modelling guidelines. After these presentations, a groupwork section was organized with 22 questions using an online Mentimeter software. A total of 53 people from 30 different companies or organizations participated in the workshop. After the workshop, the feedback survey was carried out a few days later using an online Webropol software tool, which included two (2) questions related to the main topics of the workshop.

A total of 29 questions were asked about the main topics and a total of 569 responses were given to these questions. The results obtained from the participants' contribution to these questions were carefully analyzed and compiled in a separate workshop report. The results are summarized by the author in the following sections 3.1-3.3.

3.1 BIM concept in mining

The workshop participants were asked how well the BIM concept would be suitable for mining. The following types of responses were derived and compiled from the participants' responses.

"In Finland, the mining and tunnelling sectors lack a uniform BIM modelling approach. Only minor examples of the implementation of BIM in tunnelling can be found. In the global scale, the tunnelling sector has a maturing BIM approach, but a similar one has not yet been found in the mining sector."

Here are some of the participants' comments on the further development of the MIM concept in the mining sector.

- "BIM is a megatrend – a trend that is pointless to try to stop."
- "Digital tools and systems developed for BIM enable the further development of many other areas."
- "Now is just the right time to move forward with MIM in the mining and tunnelling sectors."
- "There is strong support for the idea of standardizing BIM in the mining and tunnelling sectors."

3.2 Current MIM status

The workshop participants were asked what kind of capabilities are in the MIM implementation. The following types of responses were derived and compiled from the participants' responses.

"The level of BIM expertise may not yet be very extensive in the mining and tunnelling sector in Finland. The mining and tunnelling sector definitely has an interest in starting preparations and research activities in this area. The possibilities and capabilities of BIM have already been clearly identified."

"The use of BIM in other domains has mainly focused only on the first stages of the entire process chain 1) Initial data, 2) Design and planning and 3) Construction. The implementation has not yet had time to extend extensively to the latter part of the process chain, like 4) Maintenance, 5) Production, 6) Termination of operations and 7) Aftercare. The Initial data and Design and planning process stages are strengths in the current Finnish InfraBIM modelling guidelines. The identified specificities of the mining and tunnelling sectors indicate

that there are significant needs for change and development towards the end of the process compared to the current guidelines.”

“There are already some preliminary and very limited guidelines for the mining and tunnelling sectors, but they are not widespread. There are no actual uniform or common model naming conventions. There are some specifications for geological rock type and characteristics, data produced and processed in the mine’s production process and machine utilization, and rock support data. The mining and tunnelling sectors are characterized by longer time horizons and lower, not millimeter scales, accuracy requirements compared to other BIM domains.”

“From a software perspective, national capabilities for BIM-based information management work have already been developed to reasonable level in other BIM domains. The number of suitable software applications remains very limited in the tunnelling sector, and in particular in the mining sector.”

3.3 Expectations for the MIM

The workshop participants were asked what their expectations are for MIM development. The following types of responses were derived and compiled from the participants’ responses.

“The potential of different BIM solutions is perceived as significant. BIM is seen to be needed in many different mining and tunnelling solutions, which enables savings and brings added value to all parties. MIM is seen as an opportunity for high-quality mining, where geological data can be utilized by mining machines in different work phases smoothly together with the material flow, ensuring all interfaces and specifications along the way to the concentrator. It is seen to be useful, especially when looking for a new direction and taking advantage of new opportunities.”

“Expectations for MIM development are emphasized by the importance and relevance of cooperation in order to achieve a better outcome through common specifications and established standards. The general need for additional knowledge and learning related to MIM is great. The potential of various BIM solutions in the mining and tunnelling sector is considered to be very high.”

“Current modelling guidelines for the building construction and InfraBIM sector can also be applied to the mining and tunnelling sectors. However, due to the peculiarities of mining and tunnelling, the need for changes is estimated to be quite large. Creating new modelling guidelines, and at the same time coordinating old practices in the existing operations will be a challenge. The mining and tunnelling sectors are also likely to need two modelling guidelines, one for each sector separately. However, it may be worth evaluating this in more detail during the actual phase of creating the guidelines and also

possibly making use of modularity, for example. In the mining sector itself, two separate guidelines may also be required, considering UG and OC mining. The mining and tunnelling sectors should develop modelling guidelines that are as consistent as possible. Expertise may already exist in other BIM domains and especially in the construction and built infrastructure sectors, and this know-how must be utilized.”

4 Next steps

Suggestions of the author of this paper for the next steps MIM development are presented in the following sections 4.1-4.2.

4.1 MIM development

The InfraBIM domain has already reached a high level of BIM maturity in Finland. However, the information classification in the mining sector is quite specific, and therefore the current terminology in the InfraBIM sector should be revised very closely if necessary. The current GeoBIM references would also be useful in defining, for example, solid modelling of ores and other formation rocks, as they are not included in the InfraBIM guidelines.

Further development of MIM’s modelling guidelines may be based on the existing InfraBIM guidelines. Where necessary, they should only be adapted to the specific needs of the mining and tunnelling sectors. It is also clear that GeoBIM guidelines must be included in the overall picture of this future BIM domain.

The actual preparation of MIM guidelines should take place in a separate development project. One good possibility would be a co-innovation project involving key experts and actors from different fields. Similarly, development trends in international BIM domains must be taken into account as part of the creation of new guidelines and classifications.

It would also be important to start general international standardization work and/or creation of a White Paper on MIM development. Significant advances in information modelling in mining are most likely to be developed and implemented through a collaborative, multi-party approach and coordinated by an industry-centric steering group. Industrial cooperation is very critical because the technical challenges are extensive and outside any single entity to be solved.

4.2 MIM guidelines

In Finland, the buildingSmart Finland organization is the controlling unit of all specifications related to BIM. The InfraBIM sector has had very good modelling guidelines since 2013.

The author of this paper made a rapid study and a

preliminary proposal to assess the need to make possible changes to the current outline of these guidelines if they were applied and implemented in the mining and tunnelling sectors. The proposal was presented and discussed among the workshop participants. It was found that, in fact, little change is needed to the current outline in order to be better suited and to fill in the gaps in the needs of the mining sector. A preliminary proposal for modelling guidelines for the mining sector is presented in Figure 5.

Original table of contents of the built infrastructure modelling guidelines	Proposed table of contents adapted for the mining sector
General inframodel requirements	General mining model requirements
1. General matters	1. General matters
2. Initial data	2. Initial data
3. Design and planning	3. Design and planning
4. Construction	4. General preparatory tunnelling
	5. Excavation and production
	6. Mine closure and afterwork

Figure 5. The main content of the MIM modelling guidelines

The first three headings, which include 1) General matters, 2) Initial data and 3) Design and planning, are also very suitable for the mining sector. The fourth heading in the InfraBIM guideline, Construction, should be looked at in more detail. In the mining sector, it should be opened up more widely 4) General preparatory tunnelling, which would also cover all other tunnelling work in the mine. Also, for the production phase of the actual mine, 5) Excavation and production section, would include all issues related to mining. Finally, 6) Mine closure and afterwork section, would describe all the necessary details of the post-production period. Similar comparisons and suggestions were also made to all subtitles of the InfraBIM guidelines to make them more suitable for the mining sector. However, the results of these are not presented in this paper but are available from the author.

5 Conclusion

Mines and tunnelling work sites need to work with enormous amounts of data, coming from many different sources like humans, machines, and surrounding environment. Data can be located in many different places at the same time. In the mining sector, 3D-modelling, data management and mine automation are still mainly handled separately. Both the mining and tunnelling sectors lack a unified information modelling methodology for converting physical mining infrastructure into digital infrastructure for machine control.

Various BIM domains have developed very rapidly in recent years and clear benefits have been reported from

many industries. InfraBIM, GeoBIM and TIM domains have been continuously developed internationally. The mining sector does not yet have a common OpenBIM derived approach.

Numerous questions were asked in the workshops held in Finland, and the author has analyzed and summarized the results obtained from the contribution of the participants. Based on the results, it was concluded that now is the right time to move forward with MIM in the mining and tunnelling sector. The potential of various BIM solutions was considered significant. BIM is seen to be needed in many different mining and tunnelling solutions, which enables savings and brings added value to all parties. However, specific features have been identified in the mining and tunnelling sectors which indicate that the current guidelines need to be further developed significantly.

A preliminary proposal for the main outline of the MIM guidelines was presented and discussed. Further development of MIM's modelling guidelines could well be based on the existing InfraBIM guidelines. There is strong support for the idea of standardizing BIM in the mining and tunnelling sectors. The need to start researching and further developing the MIM concept in future development projects was identified. It would also be important to start general international standardization work on MIM.

CRedit authorship contribution statement

Jyrki Salmi: Conceptualization, Methodology, Writing, Review & Editing. **Rauno Heikkilä:** Conceptualization, Methodology, Writing, Review & Editing.

Declaration of Competing Interest

The authors declare that they have no known competing financial interests or personal relationships that could have appeared to influence the work reported in this paper.

Acknowledgments

The presented work has been supported by the Next Generation Mining project, funded by Business Finland and led by Sandvik and Nokia. The authors thank you gratitude for your support.

References

- [1] Barnewold L. and Lottermoser B.G. Identification of digital technologies and digitalisation trends in the mining industry. *International Journal of Mining Science and Technology*, 30:747–757, 2020.

- <https://doi.org/10.1016/j.ijmst.2020.07.003>
- [2] Koch C., Vonthron A. and König M. A tunnel information modelling framework to support management, simulations, and visualisations in mechanised tunnelling projects. *Automation in Construction*, 83:78-90, 2017. <https://doi.org/10.1016/j.autcon.2017.07.006>
- [3] Huang M.Q., Ninic J and Zhang Q.B. BIM, machine learning and computer vision techniques in underground construction: current status and future perspectives. *Tunnelling and Underground Space Technology*, 108:103677, 2021. <https://doi.org/10.1016/j.tust.2020.103677>
- [4] Willmott A. Accenture mounts case for mining's digital shift. *Mining Journal*, Staff reporter interview 2016. On-line: <https://www.mining-journal.com/leadership/news/1171901/accenture-mounts-mining%E2%80%99-digital-shift>. Accessed: 13/01/2023.
- [5] Slansky D. Sight Machine Enables Operational Intelligence with the Digital Twin, ARC Advisory group, ARC view, 2017. On-line: <https://www.arcweb.com/blog/sight-machine-enables-operational-intelligence-digital-twin>. Accessed: 13/01/2023.
- [6] Li W., Li S., Lin Z. and Li Q. Information modeling of mine working based on BIM technology. *Tunnelling and Underground Space Technology*, 115:103978, 2021. <https://doi.org/10.1016/j.tust.2021.103978>
- [7] Mitchell J. and Parken D. National Guidelines for Digital Modelling, CRC Construction Innovation. On-line: http://www.construction-innovation.info/images/pdfs/BIM_Guidelines_Book_191109_lores.pdf, 2009. Accessed: 13/01/2023.
- [8] Eastman C.M., Jeong Y.-S., Sacks R. and Kaner I. Exchange model and exchange object concepts for implementation of national BIM standards. *Journal of Computing in Civil Engineering*. 24 (1), 2010. DOI: 10.1061/(ASCE)0887-3801(2010)24:1(25)
- [9] Chen L., Shi P., Tang Q., Liu W. and Wu Q. Development and application of a specification-compliant highway tunnel facility management system based on BIM, *Tunnelling and Underground Space Technology*, Volume 97, 103262, 2020. <https://doi.org/10.1016/j.tust.2019.103262>
- [10] Hegemann F., Stascheit J. and Maidl U. As-built documentation of segmental lining rings in the BIM representation of tunnels, *Tunnelling and Underground Space Technology*, 106:103582, 2020. <https://doi.org/10.1016/j.tust.2020.103582>
- [11] Borrmann A., König M., Koch M. and Beetz J. *Building Information Modeling: Technology Foundations and Industry Practice*. Springer, 2018. <https://doi.org/10.1007/978-3-319-92862-3>
- [12] Smith S. Building information modelling – moving forward Crossrail, UK, forward. *Proceedings of the Institution of Civil Engineers – Management, Procurement and Law*, 167(3):109-159, 2014. <https://doi.org/10.1680/mpal.13.00024>
- [13] Daller J., Zibert M. Exinger C. and Lah M. Implementation of BIM in the tunnel design – Engineering consultant's aspect. *Geomechanics and Tunnelling* 9(6):674-683, 2016. <https://doi.org/10.1002/geot.201600054>
- [14] Fraser S. Beyond Mine Automation: The Rock Factory and The Common Mine Model. *First International Conference on Minerals in the Circular Economy*, 2014. On-line: https://publications.vtt.fi/pdf/technology/2014/T19_2.pdf. Accessed: 13/01/2023.
- [15] Cunningham J., Fraser S.J., Gipps I.D., Widzyk-Capehart E., Ralston J.C. and Duff E.F. Development and future directions in mine-site automation. *AusIMM Bulletin*, April 2012. On-line: https://www.researchgate.net/publication/260340912_Development_and_future_directions_in_mine-site_automation. Accessed: 13/01/2023.
- [16] Gipps I., Cunningham J., Fraser S. and Widzyk-Capehart E. Now to the Future – A Path Toward the Future Mine. In *proceedings of the Second International Future Mining Conference*, pp 157-162, Melbourne, Australia, 2011. <http://hdl.handle.net/102.100.100/105341?index=1>
- [17] Wang L. and Zhang H. Discussion on Lifecycle Management of Mine Construction Based-On Mining Information Model. *International Conference on Internet Technology and Applications*, pp. 1-4, 2010. DOI: 10.1109/ITAPP.2010.5566392
- [18] Wang J., Bi L., Wang L., Jia M-T., Mao D. A Mining Technology Collaboration Platform Theory and Its Product Development and Application to Support China's Digital Mine Construction. *Applied Sciences* 9(24):5373, 2019. <https://doi.org/10.3390/app9245373>
- [19] Du X., Yi L, Lu X and Ji J. Overview of Digital Mine, *Information Technology Journal*, 9(6):1241-1245, 2010. DOI: 10.3923/itj.2010.1241.1245
- [20] Fabozzi S., Biancardo S.A., Veropalumbo R. and Bilotta E. I-BIM based approach for geotechnical and numerical modelling of a conventional tunnel excavation, *Tunnelling and Underground Space Technology*, 108:103723, 2021. <https://doi.org/10.1016/j.tust.2020.103723>
- [21] Yleiset Inframallivaatimukset YIV. On-line: <https://drive.buildingsmart.fi/s/9mFGPHLx49KaM24?dir=undefined&path=%2F2021&openfile=5738>. Accessed 13/01/2023.

Automated Layout Zoning: A Case of the Campus Design Problem

Vijayalaxmi Sahadevan¹, Kane Borg², Vishal Singh¹, and Koshy Varghese³

¹Center for Product Design and Manufacturing, Indian Institute of Science Bangalore, India
²Department of Civil Engineering, Indian Institute of Technology Madras, India
³Department of Civil Engineering, Aalto University, Finland
vijayalaxmi@iisc.ac.in, kane.borg@aalto.fi, smghv@iisc.ac.in, koshy@iitm.ac.in

Abstract –

Layout zoning is the foremost and crucial step in the design of large-scale greenfield construction projects. While it is known that early design decisions have significant impact on the social and environmental value of the completed facility, much of the relationship between design attributes and values are tacit knowledge. In addition to the challenges, such as the number of design alternatives that can be evaluated in a limited time, traditional methods of design generation and evaluation do not focus on capture of stakeholder defined values and their quantification for effective evaluation of design alternatives. Computational design tools provide several benefits that can be leveraged in automated design generation to overcome the limitations of conventional methods of design. However, the translation of stakeholder defined value to parametric form in automated design generation is not adequately explored in existing works. In this work, generation and evaluation is formulated in a visual programming environment -Grasshopper. The ‘growth algorithm’ discretizes the available area into numerous land parcels and allocates the parcels to seed nodes until the area requirement is satisfied. The implementation in the case of a real-world campus layout revealed that the script was able to generate layout alternatives with different configurations of zones. Further, from the case study, a set of values and their relationship with design attributes were derived. Using parametric scripting, it was illustrated how the value-based design objectives can be quantified by utilizing the layout solutions produced by the growth algorithm-based script.

Keywords –

Visual Programming; Parametric design; Computational design

1 Introduction

The social, economic, and environmental value of a built facility are significantly influenced by proper

planning and design. In addition to addressing the functional and site related requirements, the significance of incorporating stakeholder values in built facility design has been emphasized by researchers [1][2]. However, the traditional methods of design generation and evaluation do not pay adequate attention to value and values in design. This is mainly because they are perceived as intangible design criteria that are difficult to quantify [3]. In the pursuit of theorizing the various types of design values a previous study by the authors derived the following set of ten Architectural Design Values (ADVs) for campus projects. The ten ADVs include Functional, Environmental, Constructability, Design quality, Schedule, Social, Cost, Flexibility, Iconic, and Aesthetic value [4]. A subsequent study showed that the relationship between design attributes and stakeholder values are explicable [5] and hence quantifiable. Additional investigation is needed to investigate the viability of employing such relationships for the evaluation of design options.

Design generation and their evaluation is a challenging task particularly in the layout design phase due to the ill-defined nature of the design problem. Hence, design generation requires significant effort and expertise from the designer. As a result, typically using traditional methods only a limited number of design alternatives can be generated.

The advent of digitization in design has led to an increase in automation of design activities, creation of newer ways of interacting with design, and improvements in the efficiency of the design process through innovative workflows. This study utilizes two closely related concepts, parametric design and generative design, that has gained significant traction in design generation and creative architecture in recent years. Parametric design deals with the generation of design variants using fixed and variable entities [6]. While parametric design has been around even before the invention of computers, generative design is a relatively new concept. As per [7], “Generative Design (GD) is the process of defining high-level goals and constraints and using the power of computation to automatically explore a wide design space and identify the best design options.”

A key aspect of GD is the explication and representation of domain knowledge [8]. It is expected that the explicated relationship between design attributes and value can be leveraged in GD frameworks to facilitate automated design evaluation.

Layout design is a necessary first step in the design of a built facility. Several authors have investigated techniques for the automated generation of layout alternatives. These include techniques for locating facilities [9], exhaustive generation of design alternatives [10], topology and geometry representation methods [11]-[15], and learning-based methods [16][17]. Most of the existing works in automated layout design have limitations in terms of constrained geometries. Further, the existing works utilize tangible objectives for evaluation of design alternatives such as energy [19]-[21], daylight [18][19] and structural performance [19][20]. Also, the proposed techniques are more relevant in the detailed design stage of building design. In the current work, the authors conducted an exploratory study on the design evaluation process of a public university campus in India to empirically understand the layout zoning problem. From the detailed observation of the various stages of the evaluation process, the zoning requirements, and the design attributes to ADVs relationship were identified. In the current problem, the layout was characterized by the presence of uneven or irregular boundaries which is a common feature in large-scale greenfield projects. Since standard methods of layout generation typically rely on rectangular geometries, these methods cannot be directly applied in the current problem.

Hence, the current work attempts to address the need for a method for the automated generation of layout alternatives with various zoning configurations for layouts with irregular boundaries. Secondly, the work explores if the layout alternatives can be evaluated against ADVs. The study was conducted using the real-world case of a greenfield campus design project. Towards this end, a ‘growth algorithm’ for the automated zoning of a layout was formulated. Further, based on the case study, a set of rules defined by the stakeholders for the quantification of value-based design objectives were derived. The rules were translated to parametric form in a visual programming environment and incorporated with the layout generation script. Based on the results of the script the findings of the study were derived.

Zoning decisions are based on limited design criteria such as distances between the zones and are based on limited information available to the designers at that stage. The other types of values such as cost, flexibility, and design quality could be modelled as the designers are

provided with more details. In the later stages, when the design is more detailed and as additional data becomes available, the other relevant factors can be incorporated. While the current work is limited to zoning, it is an exploration regarding the effectiveness and utility of mapping the values-design attributes relationship and their translation to parametric form that will be a future investigation through the detailed design stage using the case of the same project.

This paper is organized into five sections. The second section of the paper gives an overview of the existing works related to layout generation techniques. The third section discussed the layout zoning problem and its evaluation based on the campus development case study. This is followed by the discussion section. The final section of the paper is the Conclusion section.

2 Related works

Various approaches have been used to investigate automated layout design generation and evaluation. The seminal works in layout exploration viewed it as a ‘location problem’ and focused on the costs associated with moving between locations [9]. Other studies utilized mathematical approaches for generation of layout alternatives such as Quadratic Assignment problems [22] and General Space Planner [23]. However, the above techniques consider only a limited number of architectural aspects such as adjacency, sight, distance, and access in layout generation.

Several investigations on layout design have utilized representation techniques for addressing automated layout generation. These representation techniques include the use of graphs [11][15] and the bubble diagram [12]. Another method that has been popular in layout representations is the shape grammar [13][14]. The main feature of shape grammar is that it generates floor plans through shape rules. However, the definition of rules to reflect the relationship between design components in terms of geometries is challenging, let alone the evaluation of more complex architectural value. The application of each of the representational techniques in automated design generation has specific advantages and limitations with respect to automated building design generation as discussed by [8].

Other methods investigated in floor planning include exhaustive generation of floor plans [10], Expert Systems that provides solutions to a design problem by considering criteria and constraints based on the enumerated solutions in the system [24], constraint-based systems which involves conversion of architectural constraints into mathematical model to determine the placement of a room [25], and physics-based method

which utilizes spring-damper forces for defining topology logic [26]. Evaluation of quality of plans based on value in design is not given any attention in the above studies.

Recent studies in automated layout generation utilize learning-based techniques. [27] applied a modified Generative Adversarial Network (GAN), the pix2pixHD, for generating new architectural plans from a set of 100 existing plans. Similarly, [28] developed a GAN based framework for generating new layouts by using 45 plans from the work of Le Corbusier. Optimization techniques such as neuroevolution of augmenting topologies (NEAT) [16][17] and graph convolutional networks (GCN) [25] have been used for translating initial inputs in terms of spatial configurations or design criteria to final optimized floor plans. Most of the above studies focus on building design. Further, there are limitations of these approaches. For instance, in case of NEAT the final layout depends on the initial configurations and at the inputs given at the various iterations of the genetic algorithm whereas in case of GAN the results depend on the characteristics of the training data set [17].

There are a number of studies that deal with the placement of site facilities on the site to address objectives such as material movement cost as discussed in the review paper by [31]. Most of the studies utilize rectangular geometries to represent various facilities. The division of layout to address area requirements of different facilities is explored by researchers. For instance [32] discussed an approach for allocation of layout facilities to satisfy area requirements and evaluate it based on safety and other functional requirements. Similarly, [33] proposed an approach for utilizing freeform geometries in layout facilities planning. In both the studies the approaches did not focus on generation of various design alternatives but to arrive at an optimum solution to satisfy the proximity and area requirements. There are limited studies with respect to the site layout zoning that can be applied to the current problem of layout planning for largescale projects.

In most of the studies reviewed in this section, the geometry of the layouts and their components were restricted to rectangular shapes hence geometrically constrained. Further, the scale of the problems was limited to housing or industrial units. In the existing literature, there is little focus on zoning of large-scale layout such as campus design. Furthermore, it could be challenging to apply the strategies to site layouts with uneven boundaries. The criteria used in the evaluation of layouts are easily quantifiable and relevant to advanced stages of building design and therefore not applicable to the layout zoning problem.

3. Research Methodology

The main activities of the current work are summarized in Figure 1.

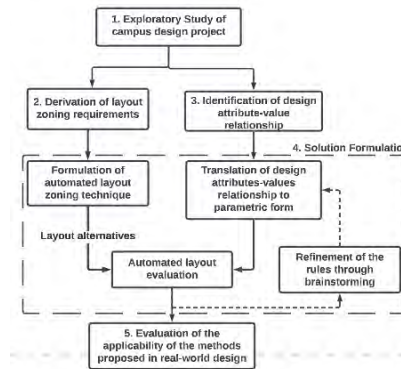


Figure 1: Steps in the current research
Each of the activities shown in Figure 1 are discussed in detail below.

3.1 Exploratory study of campus design project

This section discusses the details of the exploratory case study. In this work, the design evaluation process of a greenfield campus project was studied to empirically understand the requirements of the campus layout zoning problem and to identify the design attribute-stakeholder value relationship. Figure 2 shows the site location plan of the project.

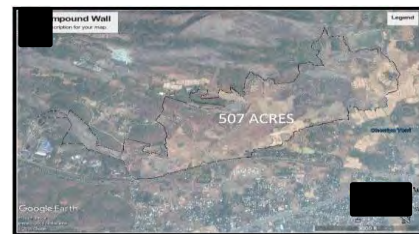


Figure 2: Site location plan

As shown in Figure 2, the total area of the site was 507 acres. The scope of work included development of master plan for the campus. The master plan needed to address a capacity of 20,000 students and was to be developed in three phases over a span of 20 years. Qualitative techniques of data collection were employed as shown in Figure 1 to identify the design requirements and the evaluation criteria.

Figure 3 illustrates the various methods that were used in the exploratory study. Participatory and non-participatory observations of the evaluation of the design concepts provided the main sources of data. In

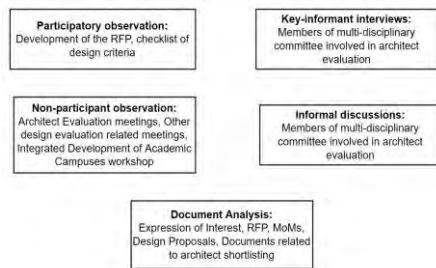


Figure 3: Data collection techniques adopted in the exploratory study

In addition, semi-structured in-depth interviews and informal discussions were conducted with eleven key informants who were part of the committee that was the decision-making body in the architect selection process. The duration of the interviews ranged from one to two hours. The key informants included committee members who are experts in the field of Engineering, Architecture, and Construction Management, and the directors of the respective institutes, whose experience ranged from 30 to 50 years in their respective fields. The interviews were audio recorded and transcribed for further analysis. The researcher further had access to project-related documents such as the Expression of Interest, Request for Proposal (RFP), and Minutes of Meetings which were also analysed.

The data analysis process was conducted in two stages. The first stage involved identifying themes and patterns relating to design values in the qualitative data. This analysis led to broad categorization of values which was refined in the second stage of the analysis. In the second stage, the data from participant and non-participant observations was used to map the value categories with the design attributes. The researcher bias was addressed by using multiple sources of data and presenting the results to 2-3 experts who participated in the design evaluation process. The outcomes of the data analysis are discussed in the following sections.

Table 2: ADV and their relationship with design attributes

No.	ADV	Description	Relationship of ADV with design attributes
1	Environmental	Travel carbon footprint	Length of route connecting academic and residential zones
2	Aesthetics	Vegetation /waterbody exclusion Academic zone needs to occupy the central position in the campus layout symbolizing the significance of the academic zone while also maintaining the proximity to the entrance of the layout to minimize the view of other zones for visitors	Areas with vegetation/ waterbody Distances between the centroids of the academic zone and the layout; Distance between the entrance point of the layout and the closest point of the academic zone
3	Social	Proximity between academic, hostel zone, and faculty residential zone to improve social interactions between students and faculty	Distance between the centroids of the three zones

3.2 Derivation of layout zoning requirements

As shown in Figure 2, the layout is characterised by uneven boundaries. The total area of 507 acres needed to be allocated to five zones. The five zones include administrative, academic, hostel, residential, and sports. Based on the proportion of the population that would utilize the five zones the respective approximate areas for each of the zones were calculated. The area requirements were calculated based on the estimate of built up area required for the various buildings in the five zones to meet the target number of users. The estimate was derived based on the data of existing campus projects. The area requirements for the various zones are summarized in Table 1.

Table 1: Zoning requirements

No.	Zone	Area requirement (sq. m)	Number of sub-zones
1	Administration	93104	1
2	Academic	764426	5
3	Hostels	495316	2
4	Residential	626780	2
5	Sports	44690	1

3.3 Layout zoning requirements and the evaluation criteria

As the second objective of the paper was to illustrate how ADV associated with zoning can be converted to parametric form and employed in the evaluation of layout alternatives. The data analysis resulted in the identification of three ADV and their relationship with design attributes relevant to the zoning problem. Table 2 summarizes the ADV and design attribute relationship.

In contrast to the current level, the computation of the various values in the advanced stages of the design will require features that go beyond simple geometrical attributes and are more difficult to quantify.

3.4 Solution Formulation

Figure 4 illustrates the tools used in the solution formulation to translate the design problem to parametric form using the visual programming script.

As shown in Figure 4, there are three main components in the solution framework. The various components were developed in the modelling software, the Rhinoceros [29] and the visual programming software, the Grasshopper [30]. The components are described below.

While the effectiveness of the ‘growth algorithm’ could be based on the ability of the script to generate layout alternatives, the accuracy of the rules and their translation to parametric form needed verification. As shown in Figure 1, the implementation and the refinement of the rules relating values and design attributes was conducted iteratively through brainstorming with the stakeholders of the project.

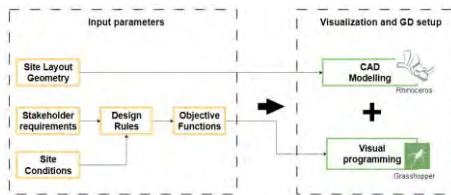


Figure 4: Data collection techniques adopted in the study

Input parameters: The input parameters consist of the following information: the site layout geometry, the stakeholder requirements, and other site related information.

Visualization and GD setup: The site layout geometry was visualized in the modelling environment whereas the design objectives were modelled in the visual programming environment. The logic of translation of the design objectives to parametric form in the visual programming language is described below.

Formulation of automated layout zoning script: The current problem deals with the division of site into five zones while satisfying the area requirements of the zones. In the current work, this was achieved by formulating a ‘growth algorithm’ using python code within the visual programming environment. Figure 5 illustrates the logic of the ‘growth algorithm’ and Figure 6 shows the snapshot of the python code used for its execution.

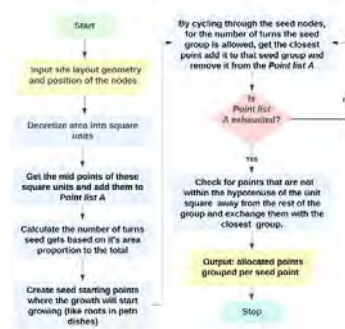


Figure 5: Logic of the ‘growth algorithm’



Figure 6: Snapshot of the python code within the visual programming script

In the ‘growth algorithm’, a change in the position of the nodes will result in a different layout alternative. Figure 7 illustrates the instance of discretization of the layout. As shown in Figure 7 the layout is divided into land parcels. These land parcels are allocated to the closest seed node representing a zone. Figure 8 illustrates the zoning alternatives with the use of different node positions for initiation of the ‘growth algorithm’.



Figure 7: Layout discretization

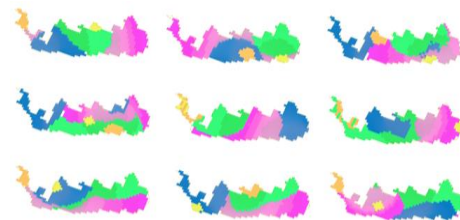


Figure 8: Examples of layout zoning alternatives
As shown in Figure 8, based on different node positions the script generates different layout zoning configurations. However, the formation of a small percentage of land parcels in a different zone in the layouts that were generated by the script.

Translation of design attributes-ADV relationship to parametric form: The translation of the three ADV discussed in Table 2 to parametric form using the visual programming script is discussed below.

Environmental value:

This value mainly deals with the preservation of the natural environment by minimizing the impact of human activities. This value was addressed using two objectives: The measurement of the travel carbon footprint and the areas with natural vegetation. While the measurement of travel carbon footprint could further facilitate its minimization, the vegetation and waterbodies could be preserved by avoiding development activities in the identified areas. The rules for the two evaluations are discussed below.

The travel carbon footprint is linked with the distance between the academic zone (green) and the residential zone (purple). The visual programming script quantified this criterion by generating graphs from the centroids of the zones. The script identifies the longest path of travel between the predetermined zones as shown in Figure 9.



Figure 9: Longest route based on radial graphs

Vegetation/ waterbody exclusion: As summarized in Table 2, the vegetation /waterbody areas can be represented in the layout in terms of geometry. To illustrate the evaluation of this value, a script for the automated allocation of building layouts was first developed. The script automatically creates building layouts in areas other than the vegetation exclusion areas as shown in Figure 10.



Figure 10: Illustration of vegetation areas exclusion
As shown in Figure 10, the script will automatically avoid creating buildings in areas that are covered with vegetation or waterbody.

Aesthetic value:

This value deals with the overall view that a visitor will get when entering the campus. The value focuses on placement of the academic zone at the center of the campus signifying that it is core of the facility while minimizing the distance from the entrance to avoid a visitor viewing other zones while entering the campus. This value consists of two rules. The quantification of the value is based on the distance between the centroid of the academic zone and the centroid of the layout. In this way, the script gives a measure of how far the zone is from the center of the campus. Secondly, shortest distance between the academic zone and a predefined entrance

point helps in determining the proximity of the zone from the entrance of the layout. Figure 11 illustrates academic zone location evaluation measurement using the visual programming script.



Figure 11: Centrality of the academic zone and its proximity to entrance measure by distances

In Figure 11, the black line shows the distance between the centroid of the academic zone (pink region) and the centroid of the layout. It also shows the shortest distance between the pre-determined entrance point and the academic zone.

Social value:

The social value aims at improving the proximity of three zones: the academic, the hostel, and the faculty residential zones. This value is based on the belief that the closeness of the zones will improve the social interactions between the users of the zones. The distance between the three zones gives an indication about their proximity. The script for measuring the social value computes the proximity of zones by measuring the centroid-to-centroid distances of the set of identified zones.

3.5 Evaluation of the applicability of the solution framework

The applicability of the solution frameworks in the current case study was evaluated through a presentation and discussion session with the architects' group that were involved in the design of the current project. The participants were experts in campus design and had experience ranging from four years to thirty years. The session followed the Focused Group Discussion guidelines. Overall, the group gave a strong agreement regarding the applicability of the methods used in the study in real-world design process.

Architect 1 articulated the benefit of utilizing the methods used in the current work in exploratory study. Architect 1: *Design is a continuous process. You work something on the paper you translate it on the computer then you keep working on it. The technology helps to produce faster results, you tend to work out many options at one time.*

While emphasizing on the relevance of the quantification of values Architect 2 made the following statement. Architect 2: *What is very critical is how you evaluate it (design alternatives) and although it is very easy to quantify certain things but there are certain things such*

as the feeling that a person would have in this space which gets very difficult to quantify.

Architect 3 further discussed how the methods used in the study could be useful in utilizing design criteria that are quantifiable along with the criteria that are intangible in nature.

Architect 3: It cannot be denied it (the methods) is very essential because it must give us the optimal use of resources like space and money. And again, very critical at the same time is that you don't miss out on those factors which might come to you intuitively when you design but you forget when you are actually evaluating them altogether.

From the discussion it was evident that design exploration activities could benefit from using the methods used in the current work.

4 Discussion

In the current work a technique was formulated for generating zoning alternatives for layout with irregular boundaries and script for the integration of three categories of values was formulated to illustrate the automated evaluation of design alternatives against values. A 'growth algorithm' was proposed for the zoning of layout for a campus design project. The results obtained from the 'growth algorithm' based script showed that to a great extent the script was able to produce different options for zoning of the layout. However, one of the limitations of the 'growth algorithm' was the creation of land parcels of a different zone within a zone. While the algorithm incorporated a mechanism for eliminating the land parcels, a small percentage of it persisted.

The study further illustrated how the generated layouts can be evaluated against a set of ADV. In the current work, the derived logic of ADV evaluation for layout design was translated to parametric form. The presence of land parcels led to inaccurate evaluation results in some instances of evaluation in the current study. However, the work provided evidence that values evaluation can be translated to parametric form. This could be further utilized in automated evaluation of layout alternatives and for arriving at high-performing design solutions.

In the current work, the effectiveness of the "growth algorithm" was evaluated by generating several design alternatives. Based on the design variants generated by the "growth algorithm" through visual examination it was observed that it was capable of generating numerous unique design solutions. To establish evidence for the effectiveness of the "growth algorithm" and the ADV

computation, additional empirical investigation may be required.

The algorithms used in the facility layout planning cannot be directly applied to the current work as the current work deals with the zoning of largescale site layout with irregular boundaries for greenfield campus projects. Hence, it is difficult to compare the performance of the existing algorithms to the current work.

The current work discusses the problem of layout zoning automation and their evaluation using the case of campus layout design. The study was based on the recognition that there are several such projects under development globally. The authors believe that the "growth algorithm" and the values evaluation approaches that is discussed in the paper could be applied to any type of AEC project that require zoning of irregular boundaries. Evidence regarding the effectiveness of algorithm to other type of projects will require empirical investigation of the application of the algorithm to other types of projects.

5. Conclusion and Future Work

The current study is based on the need for an approach for automated zoning of layouts with irregular boundaries and further evaluating the zoning alternatives using values-design attributes relationships identified through empirical study of a campus project. The work proposed a 'growth algorithm' based approach for generating zoning alternatives for layouts with irregular boundaries. The work further illustrated that values-design attribute relationship can be utilized for evaluating the alternatives. The study thus demonstrates the feasibility of automating the zoning of layouts and their evaluation against values.

The work provides an approach for stakeholder teams to quickly generate design alternatives for layout zoning and exploring design alternatives through visualization of the layout alternatives and their performance in terms of values. In the current work, the ADV were limited to three as the study focused on illustrating the quantification of the value-based objectives. Further, the design attributes were limited to geometrical aspects. Future study could focus on adopting more rigorous methods for the identification of the comprehensive set of value-based objectives and incorporation of site conditions data. Further, the weightages for the various objectives can be elicited from the stakeholders and incorporated in the automated evaluation process. The use of site constraints could give insights regarding the effectiveness of the method in real-world design. Genetic Algorithm based techniques could be incorporated to provide more controlled generation of high performing design alternatives.

6. References

- [1] Thomson, D. S., S. A. Austin, H. Devine-Wright, and G. R. Mills. Managing value and quality in design. *Build. Res. Inf.* 31 (5): 334–345. 2003. <https://doi.org/10.1080/0961321032000087981>.
- [2] Lera, S. G. Empirical and theoretical studies of design judgement: A review. *Des. Stud.* 2 (1): 19–26. 1981.
- [3] Macmillan, S. Added value of good design. *Build. Res. Inf.* 34 (3): 257–271. 2006.
- [4] Sahadevan, V., and K. Varghese. 2018. Stakeholder value evolution, capture and assessment in AEC project design. In *Proc., 26th Annual Conf of the Int. Group for Lean Construction*, 549–559. 2018.
- [5] Sahadevan, V., & Varghese, K. A Framework to Identify Stakeholder Values for Building Layout Design. *Journal of Architectural Engineering*, 28(3), 04022019, 2022.
- [6] Hernandez, C. R. B. Thinking parametric design: Introducing parametric Gaudi. *Des. Stud.*, 27 (3), 309–324. 2006. <https://doi.org/10.1016/j.destud.2005.11.006>.
- [7] Villaggi, L. and Nagy, D. Generative Design for Architectural Space Planning: The Case of the Autodesk University 2017 Layout. 2019.
- [8] Singh, V. and N. Gu. Towards an integrated generative design framework. *Design studies*, 33(2), 185–207, 2012.
- [9] Weber, A. *Über den Standort der Industrien*, 1. Teil: Reine Theorie des Standortes, 1901. English Translation: on the Location of Industries. University of Chicago Press, Chicago, IL. Translation published in 1929.
- [10] Galle, P. An Algorithm for Exhaustive Generation of Building Floor Plans. *Commun. ACM*, 24 (12): 813–825, 1981. <https://doi.org/10.1145/358800.358804>.
- [11] Steadman, J. P. Graph theoretic representation of architectural arrangement *Architectural Research and Teaching* 2 161–172, 1973.
- [12] Korf, R. E. A shape independent theory of space allocation. *Environment and Planning B: Planning and Design*, 4(1), 37–50, 1977.
- [13] Stiny, G., and Gips, J. Shape grammars and the generative specification of painting and sculpture. In *IFIP congress (2)*. Vol. 2, No. 3, pp. 125–135, 1971
- [14] Mitchell W. J. *The Logic of Architecture: Design, Computation, and Cognition*, MIT Press, Cambridge, MA, 1990. Martin, J. Procedural House Generation: A method for dynamically generating floor plans. *ACM Trans. Graph.*, 1–2, 2006.
- [15] Martin, J. Procedural House Generation: A method for dynamically generating floor plans. *ACM Trans. Graph.*, 1–2, 2006.
- [16] Simon, J. Evolving floorplans. On-line: https://www.joelsimon.net/evo_floorplans.html, Accessed: 19-01-2023
- [17] Carta, S. Self-Organizing Floor Plans. *Harvard Data Sci. Rev. HDSR*. 2021
- [18] Caldas, L. Generation of energy-efficient architecture solutions applying GENE_ARCH: An evolution-based generative design system. *Adv. Eng. Informatics*, 22 (1): 59–70. 2008. <https://doi.org/10.1016/j.aei.2007.08.012>.
- [19] Janssen, P. Dexen: A scalable and extensible platform for experimenting with population-based design exploration algorithms. *AI EDAM*, 29(4), 443–455, 2015.
- [20] Flager, F., Welle, B., Bansal, P., Soremekun, G., & Haymaker, J. Multidisciplinary process integration and design optimization of a classroom building. *Journal of Information Technology in Construction (ITcon)*, 14(38), 595–612, 2009.
- [21] Caldas, L. GENE_ARCH: an evolution-based generative design system for sustainable architecture. In *Workshop of the European Group for Intelligent Computing in Engineering* (pp. 109–118). Springer, Berlin, Heidelberg, 2006.
- [22] Liggett, R. S., & Mitchell, W. J. Optimal space planning in practice. *Computer-Aided Design*, 13(5), 277–288, 1981.
- [23] Eastman, C. M. Preliminary report on a system for general space planning. *Communications of the ACM*, 15(2), 76–87, 1971.
- [24] Flemming, U. A generative expert system for the design of building layouts: version 2, 1988.
- [25] Li, A., Tian, R., Wang, X., & Lu, Y. PlanGCN Team. *Graph to Plan*, 2020.
- [26] Arvin, S. A., & House, D. H. Modeling architectural design objectives in physically based space planning. *Automation in Construction*, 11(2), 213–225, 2002.
- [27] Huang, W., & Zheng, H. Architectural drawings recognition and generation through machine learning, 2018.
- [28] Newton, D. Generative deep learning in architectural design. *Technology| Architecture+ Design*, 3(2), 176–189, 2019.
- [29] <https://www.rhino3d.com/>
- [30] <https://www.grasshopper3d.com/page/download-1>
- [31] Sadeghpour, F. & Mohsen A. The constructs of site layout modeling: an overview. *Canadian Journal of Civil Engineering*. 42(3): 199–212, 2015. <https://doi.org/10.1139/cjce-2014-0303>
- [32] Abotaleb, I., Nassar, K. and Hosny, O. Layout optimization of construction site facilities with dynamic freeform geometric representations. *Automation in Construction*, 66, pp.15–28, 2016.
- [33] Elbeltagi, E., Hegazy, T., & Eldosouky, A. Dynamic layout of construction temporary facilities considering safety. *Journal of construction engineering and management*, 130(4), 534–541, 2004.

Deep learning for construction emission monitoring with low-cost sensor network

Huynh A.D. Nguyen¹, Trung H. Le¹, Quang P. Ha¹ and Merched Azzi²

¹Faculty of Engineering Technology and IT, University of Technology Sydney, Australia,

²Department of Planning and Environment, New South Wales, Australia

{HuynhAnhDuy.Nguyen; Hoang.T.Le; Quang.Ha}@uts.edu.au,
Merched.Azzi@environment.nsw.gov.au

Abstract -

Emissions from construction activities, particularly in metropolitan areas, are carefully monitored to prevent health problems and environmental degradation. The data quality of low-cost wireless sensors in construction sites remains a challenge for pollution predictive models due to uncertainties of measurement and volatile environment. In this study, we propose a hybrid model using a Long short-term memory integrated with a Bayesian neural network to infer the probabilistic forecasts of particulate matters (i.e., $PM_{1.0}$, $PM_{2.5}$, and PM_{10}) emitted from construction activities. The training data are fused by two sources: (1) our developed low-cost wireless sensor network (LWSN) monitoring at a construction site located in Melrose Park, Sydney, Australia, and (2) air-quality stations (AQSS) in four suburbs nearby that monitoring site. The proposed model (LSTM-BNN) is compared with other deep learning methods, namely Gated recurrent unit (GRU), Bidirectional long short-term memory (BiLSTM) and One-dimension convolution neural network (1D-CNN), commonly used for time-series forecast. The experimental results indicate the outperformance of our model to all benchmark models and display a significant improvement at 56.3%, 27.9% and 37.9% in MAEs forecast for all three types of particles compared to a deterministic LSTM model.

Keywords -

Forecast; Time series; Deep Learning; Wireless sensor network; Dust monitoring

1 Introduction

Emission from construction sites is a common problem that adversely impacts on the health of workers, residents, and environment. The concentration levels of invisible particles (e.g., $PM_{1.0}$, $PM_{2.5}$ and PM_{10}) generated by a variety of construction activities, such as drilling, blasting, demolishing or earth moving need to be monitored and controlled [1, 2]. Recently, the development of IoT-enabled technology has improved the operational robustness of a low-cost wireless sensor network (LWSN) to stream reliable information in volatile conditions of the construction industry [3]. However, real-time data are insufficient for contractors to ensure compliance with governmental regulations over the environmental policy related to construction activities, of which noise and emissions often exceed the standards [4]. As such, an accurate forecast of the particle concentrations on the sites allows them to plan efficient activities and enable appropriate measures for minimizing dust emissions [5].

From a recent survey, despite the promising applications of machine learning (ML) and deep learning (DL) models in various tasks (e.g., site supervision, building inspection, safety detection and intelligent management [6]), there are only a few publications in predicting particles emitted from construction activities using on-site monitoring data. For example, a study from the UK proposed a deep neural network (DNN) in a scalable framework for highway air-quality monitoring [7], and in [8], the Bayesian optimization method was used to tune the hyperparameters of a long short term memory (LSTM) network trained by IoT-based data to predict $PM_{2.5}$ in subway construction. These studies used deterministic models of which the performance relies on only stationary data. Hence, to improve the prediction performance, a probabilistic approach appears promising to be explored for DL models in this area.

The estimation accuracy of DL models is determined by multiple components including but not limited to the modeling data, the choice of algorithm, model architectures and hyperparameters [9]. During the optimization process, intrinsic uncertainties of these components are required to be identified and mitigated by iterative training with updated data, especially to tackle a formidable task of forecasting particulate matter (PM) using LWSN data. Uncertainties involved in the process are aleatoric due to random noise in data as well as epistemic uncertainty arising from a lack of knowledge or information about the model or the process being modeled [9]. As such, addressing these uncertainties is crucial for creating reliable models that can make accurate predictions.

In fact, data gathered from LWSNs at construction sites are subject to inevitable noise, climatic factors and instability of physical systems [1, 10], resulting in significant aleatoric uncertainties. Additionally, on-site measurements are typically taken over a short period of time and often subject to information loss or missing, as determined by the project's duration and location. This limitation of data leads to epistemic uncertainty [9]. Therefore, a key question is how to handle uncertainties presented in LWSN data and model in order to improve the accuracy of DL algorithms for forecasting fine particles emitted from construction activities. This study proposes a DL model

applying the long short term memory - recurrent neural network (LSTM-RNN) for modeling the time-series profiles of PM measured by LWSN fused with AQS data. An approximation of Bayesian neural network (BNN) for quantifying and mitigating uncertainties of model's inference is integrated with LSTM network to formulate a hybrid probabilistic model (LSTM-BNN) to improve the accuracy and reliability of the estimation.

The main contribution of this work rests with the capability of the proposed DL hybrid model in accurate and reliable prediction of emissions from construction sites in suburban areas by using the fusion of low-cost wireless sensor networks (LWSN) and air quality stations (AQS), by overcoming the two challenging factors: (1) limited amount of on-site data of air pollutants to train a forecast model and (2) reliability of the data collected due to random noise of the low-cost sensors.

The paper is organized as follows. After the Introduction, Section 2 presents the system framework including sequential steps from data collection to probabilistic inference of forecast values. Section 3 is devoted to model structures of LSTM and BNN approximation. The experimental results and benchmark with other deterministic DL models (i.e., LSTM, GRU, BiLSTM, and CNN) will be shown by important evaluation metrics in Section 4. Finally, a conclusion is drawn in Section 5.

2 System framework

The system framework is presented in Figure 1 comprising five sequential procedures, namely data collection, data processing, data preparation, model training and predictive inference.

2.1 Data collection

In this study, we used two sources of air-quality monitoring data to train and validate the performance of our proposed LSTM-BNN model. The first data source was from a developed LWSN implemented practically with a reliable sensing scheme, namely Wireless Dependable Sensing (W-DepS) networks published in our previous study [3]. This sensor network including 15 sensor motes was deployed at fixed locations within the construction site of Melrose Park in the state of New South Wales (NSW), Australia. Each device was equipped with sensors for measuring continuously air temperature, relative humidity and air-pollutant parameters such as particulate matters ($PM_{1.0}$, $PM_{2.5}$ and PM_{10}). The second data source was obtained from the AQS managed by the NSW government at four suburbs within a 10-km radius of the construction site, namely Parramatta North, Macquarie Park, Lidcombe and Rozelle [11]. Next, the crucial steps of processing data will be conducted before training model.

2.2 Data processing

Since the values from LWSN are asynchronized due to the latency of the wireless communication with the measured period of 15 minutes, the sensory data are firstly aligned in the same time stamp t for all values recorded within the interval of $(t - 7.5 \text{ min}, t + 7.5 \text{ min}]$ [3]. Besides, the hourly-averaging values of AQS are resampled and interpolated to the same 15-minute interval with the re-aligned sensory data. Next, the data noise and outliers are removed by a moving-average filter and the Cook's distance method expressed in the Equations 1 and 2:

$$x_{filter} = \frac{1}{n} \sum_{i=-\frac{n-1}{2}}^{\frac{n-1}{2}} x_i, \quad (1)$$

where x_{filter} is the output of the filter, x_i is a range of values being averaged, and n is the range of centered samples (an odd number).

$$D_i = \frac{\sum_{j=1}^n (\hat{x}_j - \hat{x}_{(j)i})^2}{c \cdot MSE}, \quad (2)$$

where D_i is the Cook's distance of the observation i^{th} , x_i and $x_{(j)i}$ are respectively the fitted values when including and excluding samples i^{th} , MSE is the mean square error of two datasets, and c is the number of coefficients of the fitting model. Here, those samples were selected at least 3 times the means of the outliers' values [3].

Finally, the Min-Max normalization is applied to assure a synchronized scale for all variables. This step also contributes to faster optimization as the converging time of model parameters is reduced significantly during model training. The formula of normalizing data in a range of [0-1]:

$$x_{scaled} = \frac{x_{raw} - X_{min}}{X_{max} - X_{min}}, \quad (3)$$

where x_{scaled} is a normalized value, x_{raw} is a raw value to be normalized, X_{max} and X_{min} are respectively the maximum and minimum values of the whole dataset.

2.3 Data preparation

Before training an RNN model in a supervision approach, we divide the time series D into sequences including pairs of an input sequence (X_i) and an output sequence (Y_i) which formulate a training sample $D_i(X_i, Y_i)$. These pairs of samples are split in a walk-forward fashion to attain the dynamics of time series ($D = \{D_1(X_1, Y_1), D_2(X_2, Y_2), \dots, D_n(X_n, Y_n)\}$) as presented on the top right of Figure 1. In addition, this approach also enhances the number of samples for training the LSTM-BNN model presented in the next section.

Finally, the total processed data are approximately 15000 samples per variable over a period of 6 months

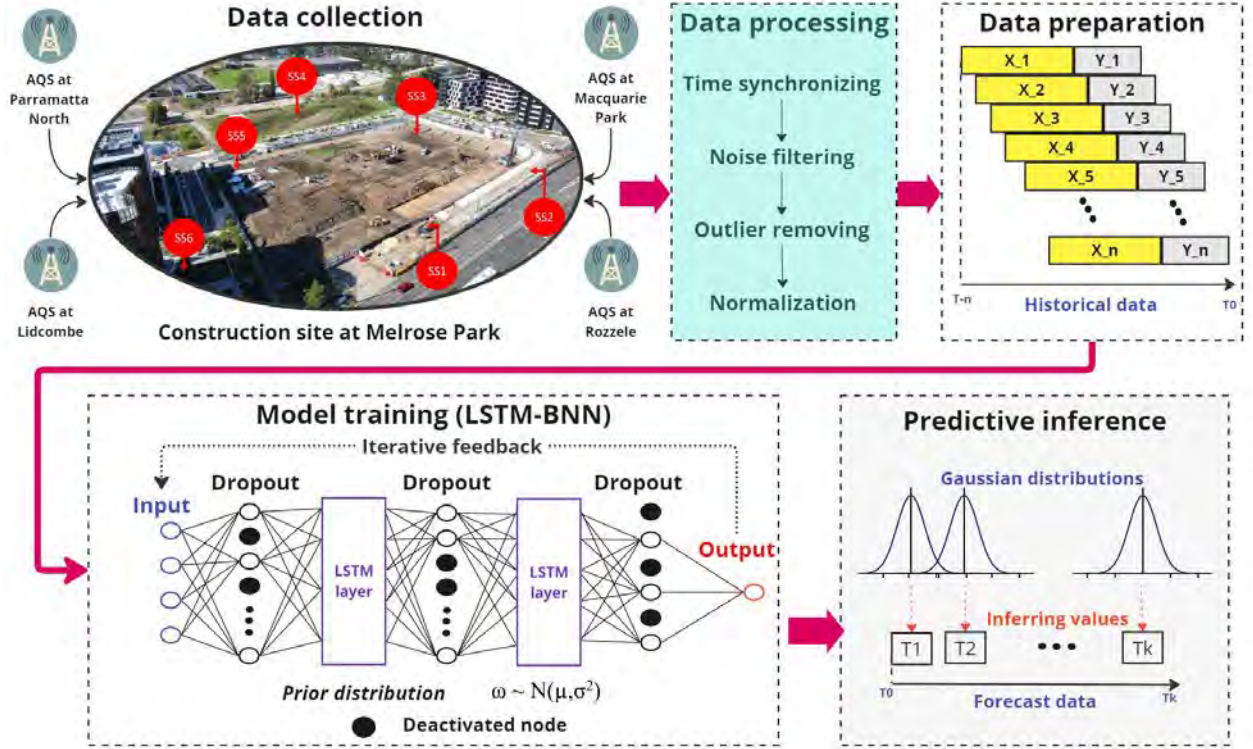


Figure 1. System framework for particles forecast with LSTM-BNN using LWSN (red nodes) located at a construction site at Melrose Park and AQS data from four nearby suburbs

(from November 2019 to May 2020). Here, three types of dust ($PM_{1.0}$, $PM_{2.5}$ and PM_{10}) measured by 15 low-cost sensors and two main particles ($PM_{2.5}$ and PM_{10}) from 4 neighbor AQSs are accounted for input variables.

During the monitoring period, there were two environmental incidents directly affecting the concentration levels in NSW, Australia: bushfires (Nov. 2019 - Feb. 2020) [12] and COVID-19 lockdown (from Mar. 2020) [3]. Hence, we partition 80% of the prepared data into the training set to ensure that the proposed model can capture the underlying patterns and generalize the data distributions over these events [8]. The remaining 20% of samples (i.e., equivalent to 36 days of observation) is divided equally into validating and testing sets to tune and evaluate the model performance.

3 Proposed learning model

3.1 LSTM-BNN network

The LSTM network is a variant of RNN proposed by Hochreiter and Schmidhuber in 1997 [13]. The key innovation of LSTM is the introduction of memory cells with three inputs of data x_t , the cell state C_{t-1} , and the hidden state h_{t-1} of the previous cell. As such, the long-term dependencies of time series are modeled well to adapt to periodic patterns and trends in air-quality forecast problems. The following equations express the flow of information

into and out of the LSTM cells:

$$C_t = f_t * C_{t-1} + i_t * \tilde{C}_t, \quad (4)$$

where f_t and i_t are respectively the forget and input gates:

$$f_t = \sigma(W_f \cdot [h_{t-1}, x_t] + b_f), \quad (5)$$

$$i_t = \sigma(W_i \cdot [h_{t-1}, x_t] + b_i), \quad (6)$$

$$\tilde{C}_t = \tanh(W_C \cdot [h_{t-1}, x_t] + b_C). \quad (7)$$

The hidden state h_t is determined as a function of the cell state C_t :

$$h_t = o_t * \tanh(C_t), \quad (8)$$

where the output gate o_t is determined as:

$$o_t = \sigma(W_o \cdot [h_{t-1}, x_t] + b_o), \quad (9)$$

σ and \tanh represent respectively sigmoid and hyperbolic activation functions:

$$\sigma(x) = \frac{1}{1 + e^{-x}}, \quad (10)$$

$$\tanh(x) = \frac{e^x - e^{-x}}{e^x + e^{-x}}. \quad (11)$$

The learnable parameters W_f , W_i , W_C , and b_f , b_i and b_C are respectively the weights and biases of the three

gates. The cell state C_t is updated by an element-wise product ($*$) of the forget gate with the previous state ($f_t * C_{t-1}$) to skip the unimportant features and add up with the new feature from the input gate ($i_t * \tilde{C}_t$).

In this work, one input layer, two hidden LSTM layers (256 and 128 units), and one output layer formulate the proposed network with Rectified Linear Unit (ReLU) activation functions attached to both hidden layers [14].

$$ReLU(x) = \begin{cases} x & \text{if } x > 0, \\ 0 & \text{otherwise.} \end{cases} \quad (12)$$

The drop-out layers are inserted between the above-mentioned layers, taking the responsibility of a regularizer for reducing overfit problem [15]. This technique deactivates randomly the layer's nodes with a predefined probability p to force model learning multiple independent representations of the data, and hence it approximates the Gaussian process of BNN [16], and forms a hybrid network that we call the LSTM-BNN model.

Some other configurations for training the LSTM-BNN model include (i) Adam optimizer with mean square error metrics, (ii) the learning rate ($\lambda = 3e-4$), and (iii) an early-stopping function which terminates the learning process at a certain training iteration (epoch) when the model begins to overfit [17]. After training model, the next step will be inferring the prediction values. To quantify the uncertainties from data of LWSN and the model's configurations, an approximation of Bayesian inference is applied with the drop-out method to produce the predictive distributions at each forecast time step.

3.2 Bayesian inference approximation

In a BNN [18], the distribution of model's parameters ω are updated given the training data X_{train} following Bayesian theorem:

$$p(\omega|X_{train}) = \frac{p(X_{train}|\omega)p(\omega)}{p(X_{train})}, \quad (13)$$

where $p(X_{train}|\omega)$ is the likelihood of input values given ω with the prior $p(\omega)$, and $p(X_{train})$ is the marginal likelihood for the input distribution. The prior is initialized model's weights updated from the previous batches of data in each training epoch, sampled from parameters ω , assumed to follow the Gaussian distribution ($\omega \sim \mathcal{N}(\mu_\omega, \sigma_\omega)$).

When inferring outputs, the BNN model produces a predictive distribution from the weight distribution ω given a new input X_{new} :

$$p(y_{out}|X_{new}) = \int p(y_{out}|\omega)p(\omega|X_{new})d\omega. \quad (14)$$

Since the posterior of weights $p(\omega|X_{new})$ is intractable, its approximation can be sought via (i) sampling the model

parameters with Markov Chain Monte Carlo (MCMC) inference [19] or (ii) variational inference (VI) method to find an equivalent distribution $q(\omega)$ by minimizing the divergence between this approximation and the true posterior $p(\omega)$ [16]. However, the number of weights and biases are large that the former approach (MCMC) will be computationally expensive in a DL neural network for air-pollutant forecast. Regarding to the latter method, Gal and Ghahramani have mathematically proved that the drop-out regularization during inference can approximate Bayesian inference in deep Gaussian processes [16]. As such, we apply the drop-out inference to formulate the proposed LSTM-BNN model for uncertainty quantification and accuracy enhancement for dust forecast.

Procedure 1 Forecast distribution inference

Input: Input sequences ($x_i \in X_{new}$),
 1: Pretrained model $f(p(\omega|X_{train}))$
 2: Initialize $Training_{Dropout} = True$
 3: Initialize $Y_{forecast} = \emptyset$
 4: Define forecast length: $Timesteps \in \mathbb{Z}$
 5: Define distribution samples: $Samples \in \mathbb{Z}$
 6: **repeat**
 7: **for each** $i \in Samples$ **do**
 8: $y_i^j = f(\omega_{i-Dropout}, x_i)$
 9: **end for**
 10: $y^j = Concatenate(y_i^j)$
 11: **until** $j = Timesteps$
Output: $Y_{forecast} = Concatenate(y^j)$

Procedure 1 explains the distribution inference of model forecast for a number of future *Timesteps* based on Bayesian approximation with the drop-out method. The key point of this method is to set the training status of drop-out layers to be active (*True*) to randomly vary the model's configuration (i.e., active nodes of each layer) and sample weights ($\omega_{i-Dropout}$) when making a prediction. The *Samples* variable defines a number of iterative predictions y_i^j produced from the model $f(\omega_{i-Dropout})$ for an input sequence x_i . Then, all predictions are concatenated to form a distribution (y^j) of the forecast time step j^{th} . The model repetitively predicts until the final time step ($j = Timesteps$) and combines all the outputs to a sequence of the forecast distributions $Y_{forecast}$.

We practically find the forecast distributions of our data are converged to Gaussian distributions from at least 50 predictions. Hence, the value of *Samples* is selected at 50 for all *Timesteps*. Then, the mean of Gaussian distributions can be inferred to a forecast value at each time step.

4 Results and discussion

This section presents the experiment results for the prediction of particulate matters $PM_{1.0}$, $PM_{2.5}$ and PM_{10} emitted on a construction site in Melrose Park

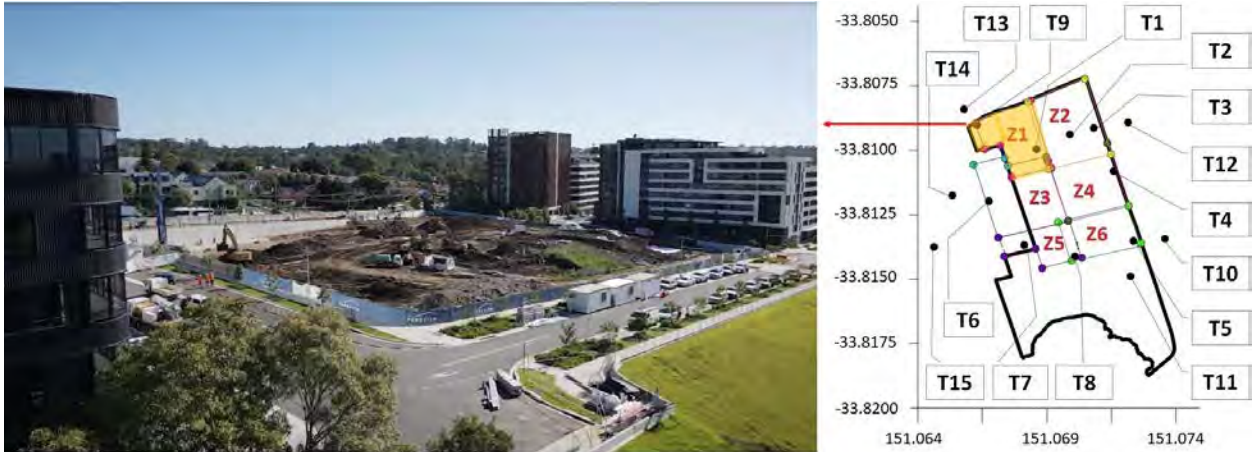


Figure 2. Construction site in Zone 1 (left) and the locations of 15 sensor nodes for emission monitoring in Melrose Park and residential areas (right) [20, 3]

of the NSW suburb Paramatta North of coordinates ($33^{\circ}49'11''S$; $151^{\circ}4'38''E$). The site is shown in Figure 2, where low-cost sensors are installed on the site as well as in residential areas surrounding it [3].

The forecast results are validated with ground-truth values in the early period of May 2020. Then, the performance of the proposed model (LSTM-BNN) will be compared with advanced DL models commonly used for time-series forecasts by popular statistical metrics.

4.1 Evaluation metrics

We use two error and two correlation metrics to evaluate the model's performance including:

- The mean absolute error (MAE):

$$MAE = \frac{1}{n} \sum_{i=1}^n |y_i - \hat{y}_i|, \quad (15)$$

- The root mean square error (RMSE):

$$RMSE = \sqrt{\frac{1}{n} \sum_{i=1}^n (y_i - \hat{y}_i)^2}, \quad (16)$$

- The Pearson's correlation (r):

$$r = \frac{\sum (x_i - \hat{x}_i)(y_i - \hat{y}_i)}{\sqrt{\sum (x_i - \hat{x}_i)^2 \sum (y_i - \hat{y}_i)^2}}, \quad (17)$$

- The coefficient of determination (R^2):

$$R^2 = 1 - \frac{\sum (y_i - \hat{y}_i)^2}{\sum (y_i - \bar{y})^2}, \quad (18)$$

where y_i and \hat{y}_i here are respectively the measured observations and forecast values of variable y at the i^{th} instant, (similarly to variable x), and n is the number of inspected samples. The lower values of $RMSE$ and MAE or higher values of r and R^2 indicate better performances.

4.2 Benchmark models

In order to validate the robustness of the proposed model, we benchmark LSTM-BNN with three popular models used to forecast time series:

- Gated recurrent unit (GRU) is considered as a lightweight version of LSTM with only two gates (update and reset gates). Both LSTM and GRU are robustly implemented for time series forecasting, but LSTMs are generally considered to be more powerful and better at capturing long-term dependencies in the data, while GRUs are considered to be faster and more computationally efficient [21].
- Bidirectional long short-term memory (BiLSTM) network is a variation of the LSTM network that processes the input sequence in two directions (i.e., forward and backward). The two LSTM layers are then concatenated and the output from both layers is combined to form the final output of the network [22].
- One-dimension convolution neural network (1D-CNN) model is recently implemented to forecast time series [23]. Although CNN models are popular in computer vision due to its robust capacity of feature extraction by 2D convolutional layers [17], special patterns of time series are also learned well with 1D convolutional filters. The deeper layers can learn more features of data and then can be reconstructed at the fully connected layer in the output of CNN models.

Both two RNN models (GRU and BiLSTM) share the same configuration with our proposed model (i.e., number of layers, nodes/units, drop-out proportion, learning rates, etc.) for a fair comparison. The CNN model is configured

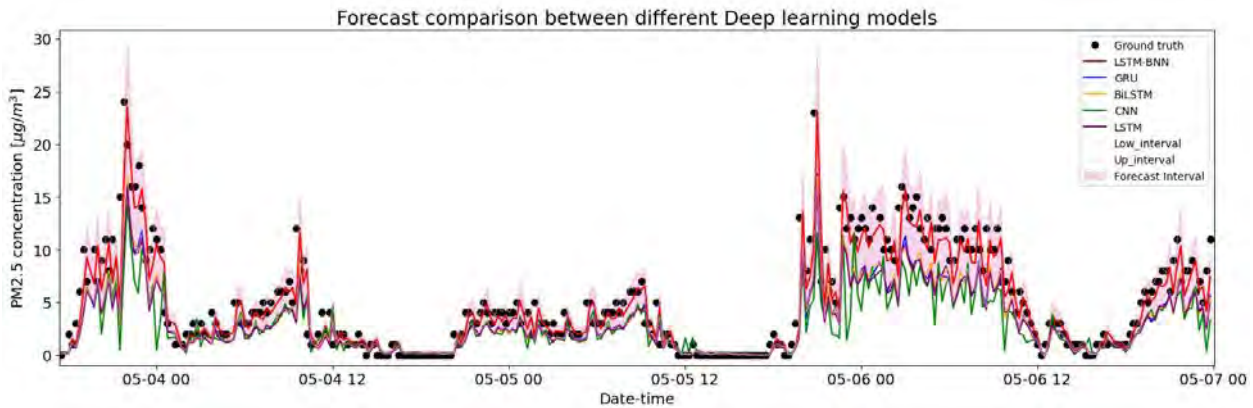


Figure 3. Forecast comparison between proposed model (LSTM-BNN) and benchmark models

by one 1D-CNN layer concatenated with a Flatten layer and two fully connected layers. Besides, the LSTM deterministic model will be accounted as the fourth benchmark model.

4.3 Experimental results

Table 1. Compared metrics of $PM_{1.0}$ forecasts

Models	MAE	RMSE	Pearson_r	R^2
GRU	1.573	2.894	0.929	0.287
BiLSTM	1.379	2.553	0.931	0.445
CNN	1.677	2.838	0.928	0.314
LSTM	1.508	2.839	0.927	0.314
LSTM-BNN	0.658	1.320	0.929	0.852

Table 2. Compared metrics of $PM_{2.5}$ forecasts

Models	MAE	RMSE	Pearson_r	R^2
GRU	1.211	2.335	0.891	0.703
BiLSTM	1.196	2.312	0.921	0.708
CNN	1.488	2.917	0.829	0.536
LSTM	1.229	2.378	0.915	0.692
LSTM-BNN	0.886	1.731	0.946	0.837

Table 3. Compared metrics of PM_{10} forecasts

Models	MAE	RMSE	Pearson_r	R^2
GRU	3.010	4.971	0.855	0.253
BiLSTM	3.065	5.077	0.849	0.220
CNN	3.138	4.988	0.835	0.244
LSTM	3.059	5.063	0.852	0.225
LSTM-BNN	1.899	3.270	0.855	0.677

Figure 3 depicts the comparison of $PM_{2.5}$ forecasts of all involved models with the ground truth over the period from 3rd to 7th of May 2020. In general, all models learn and follow well the patterns of fine particles. Presented in the red line, the means of forecast distributions from the LSTM-BNN model significantly fit to the ground truth (black dots) with the forecast interval (pink) covering most of measured values. GRU, BiLSTM and LSTM have similar forecast accuracies, while CNN model (green line) demonstrates strong fluctuations with the worst performance. There are underpredictions produced by all benchmark models at high concentrations. These results are probably caused by the volatile dynamics of particle

concentrations, and the quality of sensory data is challenging the learning capacity of deterministic models. It indicates our hybrid LSTM-BNN model handles quite well aleatoric uncertainty. Besides, the quantity of training data in this case are quite limited to train DL models compared to other similar studies [7, 8]; hence, the robustness of LSTM-BNN reduces the epistemic uncertainty as lack of information.

Tables 1, 2 and 3 present the quantified error metrics of all models forecasting $PM_{1.0}$, $PM_{2.5}$ and PM_{10} , respectively. LSTM-BNN outperforms all benchmark models over all studied metrics. The significant improvements are recorded upto 56.3%, 27.9% and 37.9% in MAE for three particles compared to its deterministic model (LSTM). Although Pearson's r values are similar for all models, the coefficient of determination (R^2) of LSTM-BNN is nearly triple those calculated by all benchmark models for PM_{10} forecast (e.g., 0.677 as opposed to 0.225).

4.4 Estimation of missing information

Since missing data of LWSN operating in construction sites is inevitable [10], we conduct another experiment to verify the imputation capacity of the proposed model for recreating the continuous information. Here, a period of 02nd - 05th January 2020 in the Black Summer (Nov. 2019 - Jan. 2020) with a severe bushfire in Australia is selected for this experiment. The rationale for this choice is the significant levels of concentrations were measured in this period over the whole NSW state [12]. Hence, it would be impossible to evaluate the net emission from construction activities by using inferred values from the neighbor AQSS. Being confirmed by the Weather bureau of the Australian government, this was also the nation's hottest and driest summer, which disrupted the normal operation of some on-site sensors [3].

As shown in Figure 4, the full data (black line) are randomly removed some values with a defined proportion called the missing ratio to simulate the missing prob-

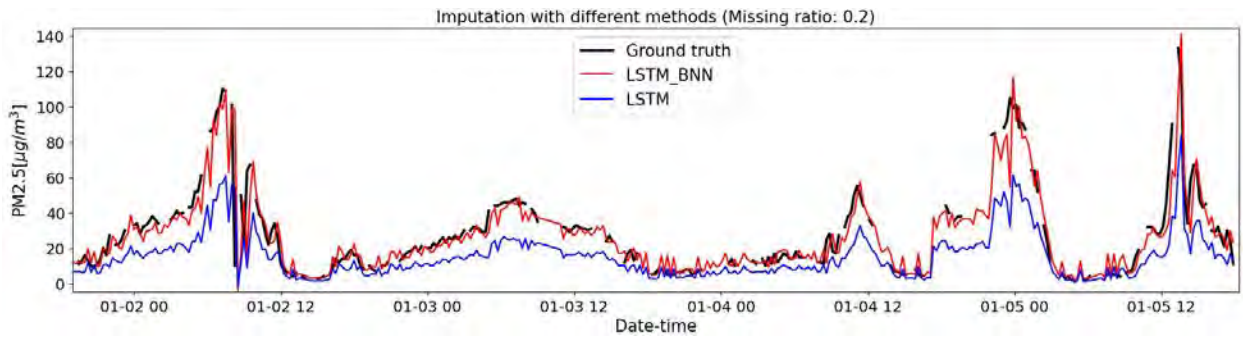


Figure 4. Imputations with LSTM-BNN and LSTM models for 20% randomly missing values of $PM_{2.5}$ over a period of 02nd - 05th January 2020

Table 4. Imputation capacity of LSTM-BNN compared with LSTM model with different missing ratios for $PM_{2.5}$

Missing ratios	MAE ($\mu\text{g}/\text{m}^3$)			R^2		
	LSTM-BNN	LSTM	Improvement (%)	LSTM-BNN	LSTM	Improvement (%)
0.1	6.261	12.723	50.8%	0.773	0.315	59.2%
0.2	6.521	12.627	48.4%	0.760	0.305	59.9%
0.3	8.324	13.175	36.8%	0.588	0.165	71.9%
0.4	9.032	13.353	32.4%	0.592	0.163	72.5%
0.5	9.668	13.544	28.6%	0.570	0.128	77.5%

lem. At a missing ratio of 0.2 (i.e., 20% of data being removed randomly), the imputation results for both probabilistic LSTM-BNN (red line) and deterministic LSTM (blue line) depict the trend of $PM_{2.5}$ being learned well by the remaining values of the LWSN and the data from AQSS. The LSTM-BNN model outperforms with smaller errors than the deterministic LSTM model over the whole studied period. We can see the estimated fluctuations of the LSTM-BNN model at the missing points due to less information from inputs, representing high epistemic uncertainty. When there are a higher number of absent values, more fluctuations are recorded. The performances of the two models at different missing ratios ranging from 0.1 to 0.5 are presented in Table 4. The statistical values in this table show huge improvements when imputing with the probabilistic LSTM-BNN model from 28.6% to 50.8% and from 59.2% to 77.5% for MAE and R^2 , respectively.

5 Conclusion

We have presented a hybrid deep learning model for estimating dust emissions of construction sites by using LSTM and BNN with drop-out regularization during probabilistic inference. This model has merits of uncertainty quantification and mitigation for highly uncertain and limited data of LWSN, which addresses challenging issues of limited amount of on-site data and reliability of the data collected due to sensor noise [6]. The experimental results show significant improvements for important evaluation metrics in forecasting three types of particulate matters emitted during construction activities in a residential suburb. Since inferring the forecast values by the means of predictive Gaussian distributions requires sam-

pling a high number of predictions in each future time step, the cost of computation will be more expensive than deterministic models. This will be our future work to develop a new inference method for reducing the number of predictive samples by estimating the practical distributions of model outputs. Besides, construction schedules are also one potential input to the proposed model that can be considered to further improve the prediction accuracy for on-site emissions concentrations.

References

- [1] Huynh A.D. Nguyen, Lanh V. Nguyen, and Quang P. Ha. Iot-enabled dependable co-located low-cost sensing for construction site monitoring. In *Proc. 37th Int. Symposium on Automation and Robotics in Construction (ISARC)*, pages 616–624, Kitakyshu, Japan, 2020. doi:10.22260/ISARC2020/0086.
- [2] Huynh A.D. Nguyen and Quang P. Ha. Robotic autonomous systems for earthmoving equipment operating in volatile conditions and teaming capacity: a survey. *Robotica*, pages 1–25, 2022. doi:10.1017/S0263574722000339.
- [3] Huynh A.D. Nguyen and Quang P. Ha. Wireless sensor network dependable monitoring for urban air quality. *IEEE Access*, 10:40051–40062, 2022. doi:10.1109/ACCESS.2022.3166904.
- [4] Denis Clement, Amir A Aliabadi, Jennifer Mackey, Jesse Thé, and Bahram Gharabaghi. Dust emissions management model for construction sites. *Journal of Construction Engineering and Management*, 147

- (8):04021092, 2021. doi:10.1061/(ASCE)CO.1943-7862.0002121.
- [5] NSW-DPE. Air quality guidance note - construction sites. On-line: www.environment.nsw.gov.au/resources/air/mod3p3construc07268.pdf, Accessed: 01/01/2023.
- [6] Yayin Xu, Ying Zhou, Przemyslaw Sekula, and Lieyun Ding. Machine learning in construction: From shallow to deep learning. *Developments in the Built Environment*, 6:100045, 2021. ISSN 2666-1659. doi:10.1016/j.dibe.2021.100045.
- [7] Taofeek D. Akinosho, Lukumon O. Oyedele, Muhammad Bilal, Ari Y. Barrera-Animas, Abdul-Quayyum Gbadamosi, and Oladimeji A. Olawale. A scalable deep learning system for monitoring and forecasting pollutant concentration levels on uk highways. *Ecological Informatics*, 69:101609, 2022. ISSN 1574-9541.
- [8] Xiaohui Guo, Yuanfeng Wang, Shengqi Mei, Chengcheng Shi, Yinshan Liu, Lei Pan, Kai Li, Boqun Zhang, Junshan Wang, Zhiwu Zhong, and Minzhong Dong. Monitoring and modelling of pm2.5 concentration at subway station construction based on iot and lstm algorithm optimization. *Journal of Cleaner Production*, 360:132179, 2022. ISSN 0959-6526. doi:10.1016/j.jclepro.2022.132179.
- [9] Moloud Abdar, Farhad Pourpanah, Sadiq Hus-sain, Dana Rezazadegan, Li Liu, Mohammad Ghavamzadeh, Paul Fieguth, Xiaochun Cao, Abbas Khosravi, U. Rajendra Acharya, V. Makarenkov, and S. Nahavandi. A review of uncertainty quantification in deep learning: Techniques, applications and challenges. *Information Fusion*, 76:243–297, 2021.
- [10] Santanu Metia, Huynh A. D. Nguyen, and Quang P. Ha. Iot-enabled wireless sensor networks for air pollution monitoring with extended fractional-order kalman filtering. *Sensors*, 21(16), 2021. ISSN 1424-8220. doi:10.3390/s21165313.
- [11] Matthew Riley, John Kirkwood, Ningbo Jiang, Glenn Ross, and Yvonne Scorgie. Air quality monitoring in nsw: From long term trend monitoring to integrated urban services. *Air Quality and Climate Change*, 54(1):44–51, 2020. doi:10.3316/informit.078202598997117.
- [12] Friends of the Earth Australia. Australia’s black summer. On-line: www.foe.org.au/australia_black_summer, Accessed: 02/01/2023.
- [13] Sepp Hochreiter and Jürgen Schmidhuber. Long short-term memory. *Neural computation*, 9(8): 1735–1780, 1997. doi:10.1162/neco.1997.9.8.1735.
- [14] Abien Fred Agarap. Deep learning using rectified linear units (relu). *arXiv preprint arXiv:1803.08375*, 2018. doi:10.48550/arXiv.1803.08375.
- [15] Stefan Wager, Sida Wang, and Percy S Liang. Dropout training as adaptive regularization. *Advances in neural information processing systems*, 26, 2013. doi:10.48550/arXiv.1307.1493.
- [16] Yarın Gal and Zoubin Ghahramani. Dropout as a bayesian approximation: Representing model uncertainty in deep learning. In *ICML*, pages 1050–1059. PMLR, 2016.
- [17] Qiuchen Zhu, Hiep T. Dinh, Duong M. Phung, and Quang P. Ha. Hierarchical convolutional neural network with feature preservation and autotuned thresholding for crack detection. *IEEE Access*, 9:60201–60214, 2021. doi:10.1109/ACCESS.2021.3073921.
- [18] Igor Kononenko. Bayesian neural networks. *Biological Cybernetics*, 61(5):361–370, 1989. doi:10.1007/BF00200801.
- [19] Adam D Cobb, Atılım Günes Baydin, Ivan Kiskin, Andrew Markham, and Stephen J Roberts. Semi-separable hamiltonian monte carlo for inference in bayesian neural networks. In *Advances in Neural Information Processing Systems Workshop on Bayesian Deep Learning*, 2019.
- [20] Melrose Park. Melrose park village construction update. On-line: <https://melrosepark.com.au/news/melrose-park-village-construction-update>, Accessed: 28/03/2023.
- [21] Peter T Yamak, Li Yujian, and Pius K Gadosey. A comparison between arima, lstm, and gru for time series forecasting. In *Int. Conf. on Algorithms, Computing and Artificial Intelligence*, pages 49–55, 2019. doi:10.1145/3377713.3377722.
- [22] Zhendong Zhang, Yongkang Zeng, and Ke Yan. A hybrid deep learning technology for pm 2.5 air quality forecasting. *Environmental Science and Pollution Research*, 28:39409–39422, 2021.
- [23] Narendra Chaudhary, Sanchit Misra, Dhiraj Kalamkar, Alexander Heinecke, Evangelos Georganas, Barukh Ziv, Menachem Adelman, and Bharat Kaul. Efficient and generic 1d dilated convolution layer for deep learning. *arXiv preprint arXiv:2104.08002*, 2021.

Restructuring Elements in IFC Topology through Semantic Enrichment: A Case of Automated Compliance Checking

Ankan Karmakar¹ and Venkata Santosh Kumar Delhi¹

¹Department of Civil Engineering, Indian Institute of Technology Bombay, India
204046006@iitb.ac.in, venkatad@iitb.ac.in

Abstract –

The current trends exhibit that the construction industry is focusing on implementing the Building Information Model (BIM) to improve visual analyses, cost estimation, and information exchange. Though standards, requirements, and development control rules (DCR) govern the construction project lifecycle, only a few applications have been developed to investigate BIM's capability in automated code compliance checking (ACCC). A significant amount of the existing application limits its checking capabilities to direct parameter values, easily extractable from a Building Information Model (BIM). On the other hand, a few clauses require implicit information to be extensively expressed in machine language for automated checking. Industry Foundation Classes (IFC) derived from BIM models lacks the relational connections of building elements required for extracting property values for automated checking. This study develops a model to restructure a topologically complex element relationship (i.e., sunshade projection width) in an IFC schema. Different categories of semantic enrichment tasks are performed for restructuring and to represent the required clause test values explicitly. The model's performance was assessed on a test case concerning the clause requirements of the Unified Development Control and Promotion Regulations (UDCPR) code for Maharashtra, India. The compliance check method identified the sunshades in the developed model through simple if-then conditions. The method adopted in the study can be applied to similar code requirements to reduce the manual data preprocessing effort required from the architects and modelers, leading to enhanced penetration of ACCC in the industry.

Keywords –

Automatic Code Compliance Checking; Building Information Modeling; Industry Foundation Class; Semantic Enrichment; Artificial Intelligence

1 Introduction

The architectural, engineering, and construction (AEC) industry is increasingly becoming information intensive with the increased complexity of projects being executed in shorter timeframes. A direct implication is that the industry processes diverse information across projects. Such information is often encapsulated in a BIM model. BIM is now being used for but not limited to, data sharing, retrieval, cost estimation, energy consumption calculations, visual analyses, and building regulatory compliance checking [1]. Modern BIM tools successfully address most of these capabilities, except for automated code compliance checking (ACCC) [2].

Regulations, requirements, and standards administer a building project's lifecycle progress. For any new or extension to an existing project, the design has to go through code compliance requirements verification. This process is manual, time-consuming, and error-prone for local governing authorities in many countries [3]. Past research has been conducted in the domain of ACCC to improve its productivity. However, the currently available automatic code compliance checking systems remain restricted to a limited amount of code requirements, specifically to explicitly defined model attributes or numerical constraints accessible through direct rule-interfacing [4].

Further, with the increase in the industrial acceptance of BIM systems, the requirement for a standard data exchange format emerged. When models are exported from native BIM authoring tools to the open file format of Industry Foundation Class (IFC) [5], according to ISO 16739-1:2018, it loses the associational topological relationships. As a result, generic model review systems are unable to process complex code requirements that involve data processing through aggregations, connections, or physical topological structures.

The topological structure of IFC is illustrated in 'Figure 1'. The 3D object geometries, and their spatial connections are classified as the physical topology. The logical connections between the object classes are termed as the associative topology. Combination of both

associative and physical topology creates relational topology of the IFC schema. Nodes represent the physical topology and edges signify the associative topology in 'Figure 1'. IFC models exported from BIM models suffer due to misclassification of object classes or logical connections. Such examples include internal walls tagged as 'IsExternal' [6], 'Skylight' tagged as 'Window' despite a presence of its predefined type, in the IFC schema. In such instances, the information is implicit in the model, even though the topological relationships are incorrect. These relationships can be re-structured the Semantic enrichment (SE) process.

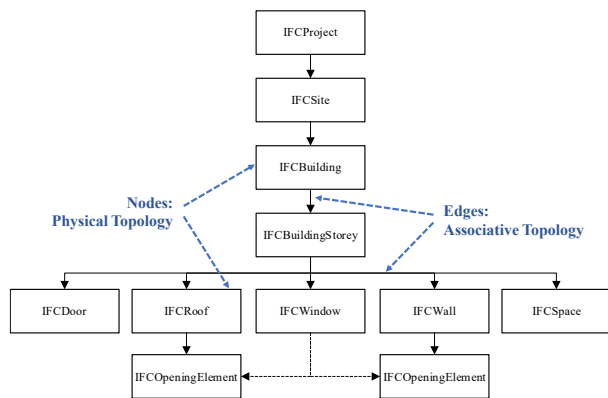


Figure 1. Topological relationships in IFC schema

SE automatically normalizes the implicit information to an explicit representation, thus supplementing BIM models for domain-specific applications [1]. Automatic data augmentation reduces the manual preprocessing effort required by the architects and modelers while submitting the model for verification. SE reinforces the automatic verification process and lays the path for the industry's digital transformation through enhanced transparency and information transfer [7]. Through a test case, this study explores the data enrichment process for compliance checking of topologically complex model elements. An Indian DCR code clause for Maharashtra was used to identify the semantic enrichment tasks and steps involved in the ACCC process.

2 Literature Review

Fenves first ideated the concept of automated rule checking for structural design checks through a logic table in 1966 [8]. 'DesignCheck' brought the next revolution in the ACCC domain by using IFC as a bridging tool between CAD systems [9]. Thereafter IFC started marking its presence in the open-building model schema.

2.1 IFC in ACCC

The object-oriented data schema for building product modeling was first envisioned by Eastman [10] in 1999. Object-oriented modeling (OOM) was established as an essential function for digitally representing building components, their function, and forms. Guiding principles for modeling space and space boundaries were originated by Bjork [11]. Further, these concepts were enriched through the 'RATAS' project model [12] and 'CIMSteel' model for constructional steelwork [13]. As a result of these developments, the thrust towards open building model schema resulted in IFC. The current format addressed in this paper is IFC4, according to ISO 16739-1:2018 [14].

The academic and automated model-checking applications developed chiefly depend on the information extracted from the IFC model. The first significant tool officially used in compliance checking was the Singapore e-CORENET project, with enriched IFC through the FORNAX engine [15]. Table 1 shows a plethora of code compliance checking applications developed subsequently based on the IFC schema.

Table 1. ACCC tools developed based on IFC schema

Name	Input Data Format	Subject of Compliance
CORENET e-PlanCheck [15]	IFC model enriched with FORNAX engine	Fire, water, and energy design for Singapore
LiCA [24]	Process Converted IFC	Water distribution system
Melzner [25]	IFC	Site Safety
RegBIM [26]	RASE-based IFC	UK building regulations
Dimyadi [27]	IFCOwl	New Zealand building code
Bus [28]	IFCOwl	French fire safety and accessibility
Zhong [29]	NLP and IFC	Environmental check
Nawari [30]	IFCXml	Florida building code
Messaoudi [31]	IFC	Permits for the state of Florida
Solibri Model Checker [19]	IFC	Rules for accessibility and intersections
BIMDCR [32]	Enriched IFC	Indian building code and DCR
EDMmodel-Checker [18]	IFC	None

2.2 Requirement for Semantic Enrichment

Automated compliance checking for complex code clauses requires explicit representation of enriched semantic information [16]. The existing automated code-checking applications face challenges in retrieving essential information in its proper representation [17]. Current ACCC applications like EDMmodelchecker [18] and Solibri [19] use hard-coded rule sets to evaluate test values. The explicit requirement of information requires manual preprocessing of data. A spectrum of semantic enrichment for code-checking strategy was proposed by Sacks et al. [20]. Complete enrichment through rule-inferencing is at one end of the spectrum [21], whereas the other end directs toward the application of deep learning. As per Bloch et al., the classification of a pass or fail for each class can be achieved by feeding a complete building model directly to the model-checking deep learning algorithm [4]. However, the idea of replacing the requirement of semantic enrichment entirely through ML is an unexplored territory. The SE is used in two areas of ACCC, i.e., pre-processing of data before submission of the IFC model for verification, and automatic verification stage. As shown in 'Figure 1' currently the pre-processing task are done manually, and model verification is done for a few rules that require explicit information. SE is a multi-layered process requiring ordered steps of concept development, which leads to acquiring desired property values from the information model [22]. Additional steps of classification and geometric calculations are sometimes required to develop the missing concepts in an IFC model, as explained in their study by Bloch et al. [4]. The task sequence depends on the characteristics and structures of the semantic enrichment problems. When missing topological relationships are understood, it is preferable to create a rule-based solution as ML-based solution provide false positive and false negative results. Specially in the case of ML-based verification, the incorrect results can lead to legal and authorization issues. However, where the topology identification is difficult and a pattern exists among the semantic entities, ML-based approaches perform better in such cases.

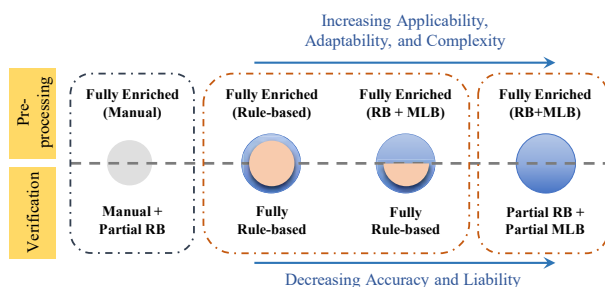


Figure 2. Hybrid approach of SE for ACCC

A test case of topologically complex code requirements is considered in this paper to identify the intertwined relationship between the semantic enrichment task types proposed by Bloch [23]. The application of these tasks is tested on elements misplaced in the IFC Schema. The topological connection restructuring is illustrated through SE tasks on the code requirements for a chajja (sunshade) projection according to an Indian DCR.

3 Chajja Projection Code Requirements

A chajja means a horizontal or sloping structural overhang, usually provided over windows and openings on external walls with the purpose of protecting from sun and rain. In a few cases, it is used for architectural appearance as well. Due to weather conditions, chajja is generally provided in every apartment building in India. According to clause 6.7 (a) of UDCPR, Maharashtra, the external marginal open spaces of a building should be kept free from any erection. Therefore, the maximum permissible width for chajja is 0.75 m over the open space. However, the chajja provided over a balcony is permitted up to balcony projections at a horizontal level [33].

The difficulty in solving this clause requirement arises as the IFC does not have any specific class dedicated to chajja elements. Further, the current modeling practices show the use of slab elements to create chajja projection. As slabs can have any arbitrary shape in a plan view, the width parameter of chajja cannot be explicitly extracted from the model. Hence, several semantic enrichment tasks are executed before the automated code compliance checking.

3.1 Semantic Enrichment Task Types

An automated code-checking process requires understanding all such objects' relations and attributes, which might be used during compliance checking. The IFC format is a standard representation for collecting these properties from a BIM model. The process aims to enrich a model to the extent that a chajja object explicitly contains its width value. This requirement dictates the semantic enrichment steps.

According to Bloch and Sacks [22], semantic enrichment tasks are categorized under broad heads of properties and concepts. The tasks defined for concept development are creation and association, whereas the final properties of an object are extracted through classification and clustering. Among these, the classification task can be addressed through a machine learning (ML)-based approach. Whereas the other three are better solvable through rule inferencing. However, these tasks are not independent and are intertwined for complex code requirements like chajja identification.

As architectural projection does not have any specified class in the IFC, it is created with a slab element. Therefore, the chajja classification of 'IFCSlab' elements is necessary for further calculation tasks. A model consists of numerous slab elements such as floors, stair landings, sunshades, cornices, and lofts. Thus, a slab must satisfy the conditions for chajja as defined in section 3, according to the UDCPR rulebook. However, an 'IFCSlab' element does not contain any inverse relationship between connected walls and associated windows in those walls. For classification through ML, a feature vector must be generated for every slab element. Among these features, two key features are the proximity relationship of the slab with the nearby window and the slab should be placed in an external space. Due to these features' absence, an association task is required to develop the relationship between 'IFCSlab' and 'IFCWindow'. Further, the association task was conducted depending upon the creation of an abstract bounding box element. The steps followed to ensure a successful enrichment of the test case for code requirements are as follows –

1. Identify all windows with precisely one related space, and mark those as external windows.
2. Create a bounding box around the window and create an upwards and outwards buffer to filter 'IFCSlab' elements intersecting with the developed bounding box.
3. Mark the slab element filtered as chajja if it is not at the structural slab level and is above the window.
4. Calculate the max perpendicular projection of the chajja from the associated wall.

Finally, the test value acquired for each chajja is checked against the permissible limit in the compliance checking step. The semantic enrichment stages from this case are explained in detail in the following sections.

3.1.1 Association Stage

In this stage, the windows of the model are filtered, and the association of the window with related spaces is checked. If more than one case of space boundary is found, the window is tagged as an external window. However, IFC4 needs to be created from the model with second-level space boundaries for this relationship to work properly. Second-level space boundaries are generated by walls, doors, windows, and slabs associated with an abstract entity, i.e., space. 'Figure 3' illustrates an example of an external window associated with a single space boundary. Having more than one space boundary associated with a window means there is room on both sides of the room. This case is only possible for internal windows.

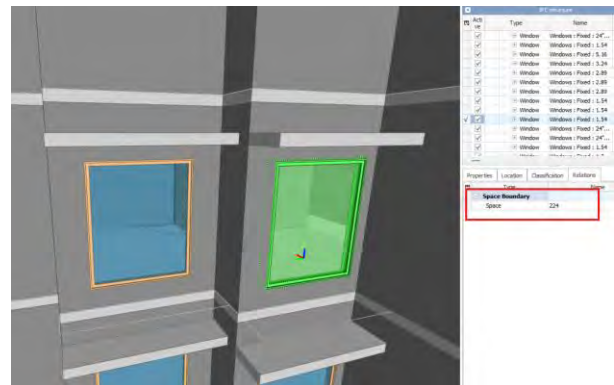


Figure 3. Example of an external window associated with a single Space Boundary

3.1.2 Creation and Classification Stage

Once the external windows are identified, a bounding box for each window is generated. According to the definition, a chajja should be placed above the window. Hence, a buffered bounding box is created, with upwards and outward extensions of 0.5 m. Next, any slab elements are filtered that intersect with the buffered bounding box. The subsequent test checks whether the slab bottom elevation is higher than the window top elevation.

Further check ensures that these slabs are not on the structural floor level. If a chajja is designed at the structural floor level, it is considered a slab projection or cornice, not a sunshade. Once a slab passes all the checks, it is classified as a chajja. 'Figure 4' depicts a buffered bounding box created around an external window and an 'IFCSlab' element (marked in red) intersecting with the bounding box.

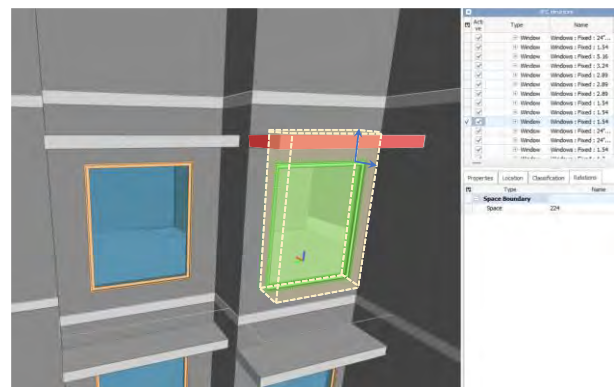


Figure 4. Creation of a buffered bounding box to identify any overlapping slab element in the box

3.1.3 Calculation Stage

The next step is to calculate the width of the chajja projection. First, the host wall of a window is identified for this computational task. Next, the shape representation of the chajja element is checked. If the

chajja is rectangular, the X and Y dimensions of the slab are extracted. The dimension perpendicular to the host wall line is considered the chajja width. On the other hand, if the slab is L-shaped or of any arbitrary polygon shape, the edge line properties of the slab polygon are extracted. The straight-line properties slope (m) and intercept (c) are generated. Edge lines that are nearest and parallel to the wall line are considered the baseline. For parallelity check, the slope 'm' of both lines is compared, and the difference between the intercept 'c' of the lines is used for finding the nearest distance. 'Figure 5' highlights the associated wall line and the nearest parallel chajja edge considered as a baseline for width computations. The shortest distance of other parallel edges from the baseline is calculated in the next step. The maximum value acquired among the perpendicular distances calculated is returned as the maximum width of the chajja. 'Figure 6' illustrates the parallel dimensions computed from the baseline for width calculation.

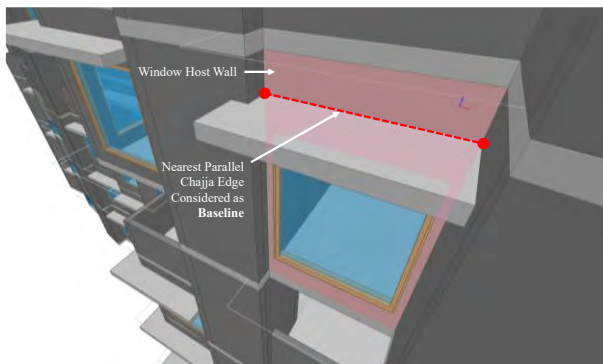


Figure 5. Host identification and Chajja baseline marking for perpendicular distance calculation

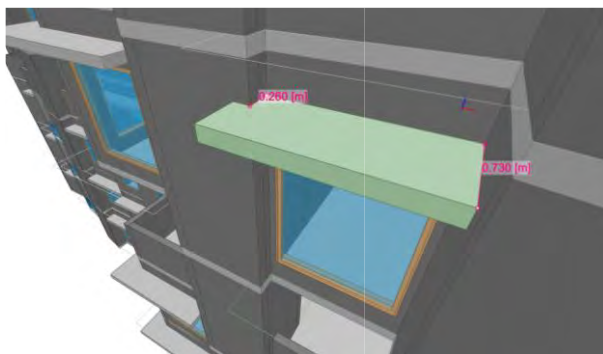


Figure 6. Shortest distance computation between chajja edges. The maximum computed value is returned as the optimal result.

3.2 Code Compliance Checking

As the semantic enrichment task is conducted to contain a single explicit width value of the chajja projection, a single rule check is conducted to check if

the projection is greater than 0.75 m. The current result is returned in the form of a dictionary that contains 'Pass' or 'Fail' outcomes under the unique GUID (Global ID) of chajja elements as the key values.

```

IF
  object X is a IFCSlab AND
  object X tag = "Chajja" AND
  perpendicular dist. P for object X ≤ 0.75
THEN
  object X flag = "Pass"
ELSE
  object X flag = "Fail"

```

4 Test Implementation

The semantic enrichment and compliance checking process was applied to a model of an existing residential building project in Mumbai to validate the correctness of outcomes. As the model was taken from a real-life project, all the chajja widths were expected to meet the code clause. Hence, a few changes were introduced in the model to simulate cases where the compliance check will fail. The modified building contained seven floors with seventy chajja slabs. The fourth floor of the building consisted of a refuge area, leading to only six windows on the specified floor. The model was exported as an IFC4 design transfer view for further processing. 'Figure 7' shows an overview of the sample building model in an IFC viewer software.

The code compliance check was conducted on a python-based platform. As expected, the code evaluated the chajjas correctly that were compliant with the code requirements. Five L-shaped chajjas were reported as a violation of the 0.75 m maximum permissible width. 'Figure 8' illustrates the case where one dimension (0.6 m) of the chajja satisfies the requirements. However, the check fails due to higher width (0.78 m) along another direction. A compliance report view with "Pass" and "Fail" results, along with the reported maximum width of chajja, is demonstrated in 'Figure 9'.



Figure 7. Perspective view of developed model

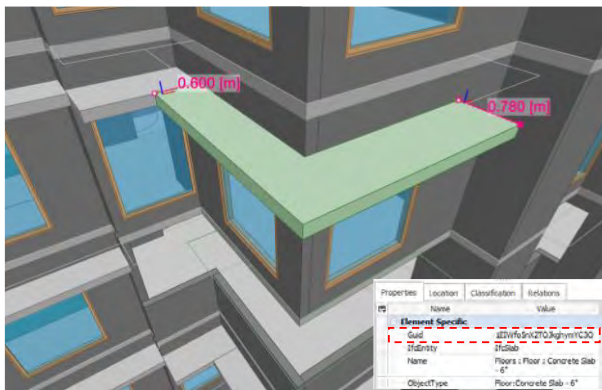


Figure 8. A view of an L-shaped chajja that violated code requirements in one direction

Key	Value
1EIIwfo5nX2TOJkghymYAsD	[0.75, 'Pass']
1EIIwfo5nX2TOJkghymYC30	[0.78, 'Fail']
1EIIwfo5nX2TOJkghymYC55	[0.73, 'Pass']
1EIIwfo5nX2TOJkghymYC8t	[0.57, 'Pass']

Figure 9. A view of the compliance report window with "Pass" and "Fail" tags

A similar approach can be adopted for identification of external walls, and dead walls on the building depending on the semantic relationships among IFC classes. The location of walls, connectivity to habitable and non-habitable spaces, window and door locations are correct in such an example. However, the due to absence of correct logical connections in IFC schema, information required for rules related to such objects cannot be directly extracted. Similar SE steps can be used in combinations to restructure the relational topology.

5 Discussion and Conclusion

In this study, semantic enrichment tasks were performed through a set of rules performed in sequence for checking code compliance requirements of chajja projections. This task required the evaluation of topologically complex model elements. The task stages involved identifying objects with no pre-defined IFC Class and performing geometrical calculations on these objects. The challenge faced while tackling this problem is to generate the associative topology among building objects. In BIM, the model consists of relational topologies among building elements. Relational topologies consist of associative topology and physical topology. Physical topology refers to the physical layout of the building, including the arrangement of its components and systems, focusing on the position and

location of elements in the physical space. Associative topology refers to how different objects or elements in a building model are related or connected. The physical layout and logical connections together produce logical relationships, which is the essence of the relational topology. Even though there are relationships like walls terminating below a structural slab in BIM authoring tools (Revit 2023), the intelligent constraints are not transferred while exported as an IFC file. As a result, the IFC file lacks enrichment beyond the physical topology of the objects. Hence, an automated semantic enrichment was required to replace the necessity of manual preprocessing of data.

The semantic enrichment steps are composed of a progressive chain of rule-based calculations. The entire cycle of rules works on every element of the models that satisfy the eligibility criteria. The object classification task can be solved through an ML-based approach. However, notice that the classification task of Chajja identification was performed solely through rule inferencing in this example. The ML-based approach was not used as the relationship between wall and slab objects is missing in the IFC environment. Once the associational relationship data is established, the chajja classification task is reduced to simple IF-THEN rule evaluation. However, a challenge might arise during identifying chajja through the 'IFCSlab' method. As no standardized BIM modeling practice is imposed in the industry, the feasibility of purely rule-based classification can raise questions [22]. In the cases of architectural awning sunshades, the objects can be modeled through the generic model-in-place function of Revit. Thus, this work's future scope includes checking the machine learning model's capabilities for dealing with diverse object compositions in the case of chajja classification.

Once the classification task is completed, the code requirement values for width are generated through geometric computational methods. The final rule evaluation was conducted for a single test case value generated through semantic enrichment. This result emphasizes the importance of mixed multi-method enrichment processes on IFC models exported from BIM. Through the combination of creation and association (concepts) alongside classification and computational (properties) methods, implicit model data can be expressed as a single explicit data point for enhanced machine readability.

The concept and property type tasks are performed in alternate sequences to achieve the final attribute data. Defining concepts can be classified as a high-level task, as it converts implicit information to explicit data through relational topologies. Once the relations are established, property tasks generate the final single test value for verification. In complex code requirements, property tasks might be required first to generate an associative

relationship between the undefined class of objects in the IFC schema. However, as we progress toward the "no semantic enrichment" end of the spectrum [20], the alternate semantic task sequences can be merged and skipped through the application of ML algorithms. In a recent research on room type classification, the classification task of occupancy type identification and association type task of apartment room clustering was performed in a single step through the graph neural networks [34].

The adaptation of SE can be through both rule-based and ML-based approaches. However, the rule-based approach illustrated in the paper may face limitations due to complex relationship among building elements. When the required relationships are not defined in the DCR rulebooks, and rules are subjected to reviewer's discretion, in such scenarios ML-based SE approaches may perform better. It is important to understand the optimum complexity level of the relational restructuring required, to decide on the most suitable approach. Future work in this domain will focus on understanding the advancements in the relationships of semantic task types layers through ML applications. Also, a research work is under progress to identify the level of 'relational restructuring complexity' for application of rule-based and ML-based methods. These levels will inform the concerned authority (ULBs) about the trade-off to consider between adaptability and accuracy of the ACCC systems. Finally, from a comprehensive stakeholder's perspective, the adaptation of AI/ML-based semantic enrichment removes the additional efforts required from the end users, leading to an organic growth of Automatic code compliance checking in the industry.

References

- [1] M. Belsky, R. Sacks, and I. Brilakis, "Semantic Enrichment for Building Information Modeling," *Comput. Civ. Infrastruct. Eng.*, vol. 31, no. 4, pp. 261–274, Apr. 2016, doi: 10.1111/mice.12128.
- [2] R. Sacks, C. Eastman, G. Lee, and P. Teicholz, *BIM Handbook: A Guide to Building Information Modeling for Owners, Designers, Engineers, Contractors, and Facility Managers*, 3rd ed. John Wiley & Sons, 2018.
- [3] W. Solihin and C. Eastman, "Classification of rules for automated BIM rule checking development," *Autom. Constr.*, vol. 53, pp. 69–82, May 2015, doi: 10.1016/j.autcon.2015.03.003.
- [4] T. Bloch, M. Katz, R. Yosef, and R. Sacks, "Automated Model Checking for Topologically Complex Code Requirements – Security Room Case Study," in *European Conference on Computing in Construction*, 2019, pp. 48–55. doi: 10.35490/EC3.2019.157.
- [5] buildingSMART, "Industry Foundation Classes (IFC)." <https://www.buildingsmart.org/standards/bsi-standards/industry-foundation-classes/> (accessed Jul. 10, 2022).
- [6] H. Ying and S. Lee, "A rule-based system to automatically validate IFC second-level space boundaries for building energy analysis," *Autom. Constr.*, vol. 127, no. August 2020, p. 103724, 2021, doi: 10.1016/j.autcon.2021.103724.
- [7] A. Karmakar and V. S. K. Delhi, "Construction 4.0: what we know and where we are headed?," *J. Inf. Technol. Constr.*, vol. 26, no. July, pp. 526–545, 2021, doi: 10.36680/j.itcon.2021.028.
- [8] S. J. Fenves, "Tabular Decision Logic for Structural Design," *J. Struct. Div.*, vol. 92, no. 6, pp. 473–490, Dec. 1966, doi: 10.1061/JSDEAG.0001567.
- [9] L. Ding, R. Drogemuller, M. Rosenman, D. Marchant, and J. Gero, "Automating code checking for building designs -DesignCheck," *Fac. Eng. - Pap.*, Jan. 2006, Accessed: Mar. 21, 2022. [Online]. Available: <https://ro.uow.edu.au/engpapers/4842>
- [10] C. M. Eastman, *Building Product Models: Computer Environments, Supporting Design and Construction*. Boca Raton: CRC Press, 1999. doi: 10.1201/9781315138671.
- [11] B. C. Björk, "A conceptual model of spaces, space boundaries and enclosing structures," *Autom. Constr.*, vol. 1, no. 3, pp. 193–214, Dec. 1992, doi: 10.1016/0926-5805(92)90013-A.
- [12] B. Björk, "RATAS Project Developing an Infrastructure for Computer Integrated Construction," *J. Comput. Civ. Eng.*, vol. 8, no. 4, pp. 401–419, Oct. 1994, doi: 10.1061/(ASCE)0887-3801(1994)8:4(401).
- [13] A. J. Crowley and A. S. Watson, "Representing Engineering Information for Constructional Steelwork," *Comput. Civ. Infrastruct. Eng.*, vol. 12, no. 1, pp. 69–81, Jan. 1997, doi: 10.1111/0885-9507.00047.
- [14] ISO, *ISO 16739-1:2018 Industry Foundation Classes (IFC) for data sharing in the construction and facility management industries — Part 1: Data schema*. 2018.
- [15] B. H. Goh, "E-Government for Construction: The Case of Singapore's CORENET Project,"

- IFIP Adv. Inf. Commun. Technol.*, vol. 254 VOLUME 1, pp. 327–336, 2007, doi: 10.1007/978-0-387-75902-9_34.
- [16] W. Solihin, N. Shaikh, X. Rong, and L. K. Poh, “Beyond Interoperability of Building Model: A Case for Code Compliance,” in *Proceedings of the BP-CAD Workshop*, 2004, no. July.
- [17] C. Preidel and A. Borrmann, “Automated code compliance checking based on a visual language and building information modeling,” *32nd Int. Symp. Autom. Robot. Constr. Min. Connect. to Futur. Proc.*, 2015, doi: 10.22260/isarc2015/0033.
- [18] Jotne, “Jotne IT.” <https://jotneit.no/> (accessed May 13, 2022).
- [19] “Solibri | Solibri Office.” <https://www.solibri.com/solibri-office> (accessed Mar. 23, 2022).
- [20] R. Sacks, T. Bloch, M. Katz, and R. Yosef, “Automating Design Review with Intelligence and BIM: State of the Art and Research Framework,” *Comput. Civ. Eng.*, no. Mvd, pp. 353–360, 2019.
- [21] C. Eastman, J. min Lee, Y. suk Jeong, and J. kook Lee, “Automatic rule-based checking of building designs,” *Automation in Construction*, vol. 18, no. 8. Elsevier, pp. 1011–1033, Dec. 01, 2009. doi: 10.1016/j.autcon.2009.07.002.
- [22] T. Bloch and R. Sacks, “Clustering Information Types for Semantic Enrichment of Building Information Models to Support Automated Code Compliance Checking,” *J. Comput. Civ. Eng.*, vol. 34, no. 6, pp. 1–11, Nov. 2020, doi: 10.1061/(ASCE)CP.1943-5487.0000922.
- [23] T. Bloch, “An Evaluation of Computational Approaches for Semantic Enrichment of BIM models,” Technion - Israel Institute of Technology, 2020.
- [24] J. P. Martins and A. Monteiro, “LicA: A BIM based automated code-checking application for water distribution systems,” *Autom. Constr.*, vol. 29, pp. 12–23, Jan. 2013, doi: 10.1016/j.autcon.2012.08.008.
- [25] J. Melzner *et al.*, “A case study on automated safety compliance checking to assist fall protection design and planning in building information models,” <https://doi.org/10.1080/01446193.2013.780662>, vol. 31, no. 6, pp. 661–674, Jun. 2013, doi: 10.1080/01446193.2013.780662.
- [26] T. H. Beach, Y. Rezgui, H. Li, and T. Kasim, “A rule-based semantic approach for automated regulatory compliance in the construction sector,” *Expert Syst. Appl.*, vol. 42, no. 12, pp. 5219–5231, Jul. 2015, doi: 10.1016/J.ESWA.2015.02.029.
- [27] J. Dimyadi, P. Pauwels, and R. Amor, “Modelling and accessing regulatory knowledge for computer-assisted compliance audit,” *J. Inf. Technol. Constr.*, vol. 21, no. July, pp. 317–336, 2016, [Online]. Available: <https://www.itcon.org/2016/21>
- [28] N. Bus, F. Muhammad, B. Fies, and A. Roxin, “Semantic topological querying for compliance checking,” in *eWork and eBusiness in Architecture, Engineering and Construction*, CRC Press, 2018, pp. 459–464. doi: 10.1201/9780429506215-57.
- [29] B. Zhong, C. Gan, H. Luo, and X. Xing, “Ontology-based framework for building environmental monitoring and compliance checking under BIM environment,” *Build. Environ.*, vol. 141, no. December 2017, pp. 127–142, 2018, doi: 10.1016/j.buildenv.2018.05.046.
- [30] N. O. Nawari, “A Generalized Adaptive Framework (GAF) for Automating Code Compliance Checking,” *Build. 2019, Vol. 9, Page 86*, vol. 9, no. 4, p. 86, Apr. 2019, doi: 10.3390/BUILDINGS9040086.
- [31] M. Messaoudi and N. O. Nawari, “BIM-based Virtual Permitting Framework (VPF) for post-disaster recovery and rebuilding in the state of Florida,” *Int. J. Disaster Risk Reduct.*, vol. 42, p. 101349, Jan. 2020, doi: 10.1016/J.IJDRR.2019.101349.
- [32] SoftTech Engineers Limited, “BIMDCR.” <https://softtech-engr.com/bimdcr/> (accessed May 13, 2022).
- [33] Government of Maharashtra Urban Development Department, *Unified Development Control and Promotion Regulations for Maharashtra State*. 2020.
- [34] Z. Wang, R. Sacks, and T. Yeung, “Exploring graph neural networks for semantic enrichment: Room type classification,” *Autom. Constr.*, vol. 134, no. October 2021, p. 104039, Feb. 2022, doi: 10.1016/j.autcon.2021.104039.

Towards Automation in Steel Construction: Development of an OWL Extension for the DSTV-NC Standard

V. Jung^a, L. Kirner^a and S. Brell-Cokcan^a

^aChair of Individualized Production (IP), RWTH Aachen University, Campus-Boulevard 30, 52074 Aachen, Germany

E-mail: jung@ip.rwth-aachen.de, kirner@ip.rwth-aachen.de, brell-cokcan@ip.rwth-aachen.de

Abstract –

The automation of steel construction requires new possibilities to link process data, measured deviations and tolerances. Our current research in robotic steel fabrication aims to address this challenge by developing an adaptive information model interface that can seamlessly integrate the cross-process considerations necessary for precise and efficient fabrication. The objective is to further develop existing information interfaces and to increase the use of flexible and partially automated robot concepts in steel construction. Our approach builds on existing standards and product interfaces e.g., DSTV-NC in steel construction and focuses on converting and extending them with help of an ontology including tolerances and process parameters. The results provide a contribution to the development of automated systems in construction and promote small and medium-sized enterprises in steel construction to deal with current challenges of skill shortages, productivity, and occupational safety.

Keywords –

Domain Ontology, Robotic Steel Construction, Linked Data, Semantic Web

1 Introduction

In today's construction industry, (partially) automated production systems are used almost exclusively for prefabrication processes. However, in steel construction, several characteristics make the widespread integration of automated production systems difficult [1]. The main challenges include geometric tolerances, material variations, component size and weight, as well as small batch sizes of complex assemblies. In comparison to other industries, steel construction has significantly higher component and manufacturing tolerances [2–5]. This hampers the integration of robots because path planning is usually based on ideal component dimensions. For the widespread use of robots, there is a lack of a transparent and continuous information process as well as a standard for the storage of the deviation and process

information of the real component deviations in an adaptive information model. Currently, some machines are already capable of measuring the real dimensions of single parts but there is no defined place to feedback the information to the virtual information model. In addition, a connection between planning and fabrication data is missing, which would also increase the possibility to optimize and analyze the processes based on real data.

Full robotic processes require access to machine readable data, resulting in a demand to digitalize steel tolerance norms. An efficient interface would enable machines to exchange tolerance and process information and could therefore help to implement concepts according to Industry 4.0 [6].

Therefore, the motivation of this research is the development of an ontology (see chapter 2.2) which enables the use of semantic web technologies for the description of steel construction information. This includes process information needed for robotic processes, manufacturing process metadata such as tolerances and data feedback including quality measurements. Identifying and capturing critical deviations as well as resource-bound process parameters could raise efficiency and enable robotic workflows. In addition, further opportunities for process optimization can be developed.

The approach of using semantic web technologies to describe and link plan data with real fabrication and process information in steel construction was chosen because the technology promotes a continuous flow of information and allows all stakeholders to be connected, regardless of their software or machines. The concept will be verified in a real demonstrator to show the feasibility.

2 Related Work

The manufacturing process of steel construction is predominantly carried out in individual and small series production [7]. It is divided into planning, production and assembly. In practice, there is a spatial separation

between the three process steps mentioned. Due to the lack of back documentation, there is no central information model that combines the data of all involved actors. In principle, graphic or product interfaces can be used to transmit information about components. Graphic interfaces describe the products in geometric form; however, a description of how these can be produced is not included. The product interface DSTV-NC format was developed by "bauforumstahl" and is currently the most widely used data format [8, 9].

2.1 DSTV-NC standard as a base for robotic manufacturing

The DSTV-NC standard in steel construction represents a fundamental interface between design, production planning and machine control. It functions as an interface between CAD/CAM applications and NC production in steel construction. The DSTV-NC standard allows the control of various NC machines via the respective postprocessing. In particular, subtractive manufacturing processes using sage drilling machines, flame-cutting and punching machines as well as 5-axis CNC machining are used. Based on that format a prototypical interface for the control of an industrial robot was implemented by developing an independent plugin for Grasshopper3d. Programming itself represents a great barrier in using robots for individual tasks and small batches as knowledge and special skills are required to adapt the path planning to the current task. To overcome this problem, an efficient task-oriented approach was chosen for the implementation of the interface, in which a task corresponds to a machining step according to DSTV-NC. For these tasks, a strategy was stored in the interface, with which robot code is automatically generated. For collision-free machining of several sides of a component, a rule-based global path planning was developed and implemented [10].

During the validation it was highlighted that the DSTV-NC format does not contain real part information, as the information refer to the planned geometry. Due to the specific characteristics of steel and the large part sizes there are deviations from the planned geometry to the real dimensions of the steel part. This information is missing so far in the DSTV-NC format, consequently the path plan must be manually adapted to avoid any collision of the robot with the part. The modular structure of this format could allow the extension with additional information. So far, however, it is only used as a manufacturing instruction with ideal geometries, without the possibility of feedback of real values or updating values [11].

Currently, another group is focusing on transferring the information from the DSTV-NC standard into the Industry Foundation Classes (IFC), which is the common

exchange format for the Building Information Modelling (BIM) data. The objective is to be able to operate and generate machine code based on an IFC description of the desired work piece. IFC could be an alternative for storing additional tolerance and process information to enable a robotic process for steel construction. IFC forms the basis for an open, neutral and standardized data format and, in addition to the 3D data model, contains extensive data structures for describing objects from almost all sectors [11, 12].

2.2 Ontologies as a base for robotic manufacturing

Ontologies seem to be a promising solution for semantic interoperability problems [13–16]. In Computer Science an ontology is defined as "an explicit specification of conceptualization for a domain of interest" [17]. Typically, a logical theory written in a particular language formalizes the conceptualization within an ontology. Ontologies also provide reasoning capabilities that can be used to infer new knowledge. Ontologies contain explicit and unambiguous data semantics, and thus enable semantic interoperability, because they contain a formal representation of concepts, individuals and the relationships between these concepts, data and entities [18].

In recent years, many ontologies have already been developed for the domain of construction. Most approaches are based on the translation of already existing models [19, 20] or the development of new mapping techniques [21]. The previous achievements in this area mostly do not describe steel construction processes but approaches for the mapping of general geometric and topological information or the description of product and component information [21, 22].

In various research projects such as Digitizing Construction Workflows (DiCtion) or the Internet of Construction (IoC) ontologies for describing general construction processes have been developed [23, 24].

The concept of the IoC ontology is built around the core concept of `ioc:process`. This top level ontology is meant to create an interconnection to different sub-domains of construction, such as steel construction [24]. Previous works that focused to form domain ontologies for the steel construction are scarce. To enable a global optimization of the overall steel production value chain, Zillner et al. aimed to address the challenges of the information exchange between boarders, locations and companies [25]. There are also specific ontologies for robotics, such as OCRA [26] but they do not focus on the domain of steel construction and are therefore not in scope of this paper. In the future, it may function as a top-level ontology for approaches such as the *DSTV* ontology.

However, the advantages of using ontologies for process data have not yet been addressed nor developed. Established concepts like DSTV-NC format can be easily integrated into the Semantic Web stack. This enables to link heterogenous and unstructured data and includes various sources of information, such as BIM or scheduling data.

3 Methodology

This section describes the workflow which was executed to transfer the existing information from the DSTV-NC standard to an ontology created in Web Ontology Language (OWL), including the extension of specific information which are not yet defined in the DSTV format but required for a robotic manufacturing process. The ontology is referenced in the following as “DSTV ontology” (*dstv*) with the Base URI set to <http://ip.rwth-aachen.de/dstv#>.

3.1 Ontology Design

Unlike the conventional methods of ontology creation [27], the DSTV ontology was initially developed by aligning the structure of the XML-based standard with the concepts and properties in OWL. Table 1 shows an excerpt of the DSTV Classes (BFS-RL 03-105) [9].

Table 1. Extract tolerances for position of screw holes

DSTV Class	Description, “german description”
hljob	hole job, “Durchgangsloch”
stjob	screw thread, “Gewinde”
bhjob	blind hole, “Sackloch”
shjob	sink hole, “Senkung”
ohjob	oblong hole, “Langloch”
pmjob	punchmark, “Einzelkörnung”

The information contained in the DSTV-NC was restricted to workpiece information and details related to drilling processes, specifically those defined as *hl*, *hljob*, etc. As a result, the corresponding OWL ontology comprised 258 classes and 1583.

Based on the analysis which information, processes and resources are required for the robotic manufacturing process, new concepts, and classes for the extension of the current DSTV-NC model are defined. These concepts focus on the tolerance information defined in DIN-norms, measurement concepts for different steel profiles as well as models for storing process and machine data. Alignments to the IoC ontology as well as the ifcOWL and Linked Building Data (LBD) ontologies are added. As seen in fig 1, this enables to link design and fabrication data-sources as well as dynamic process information.

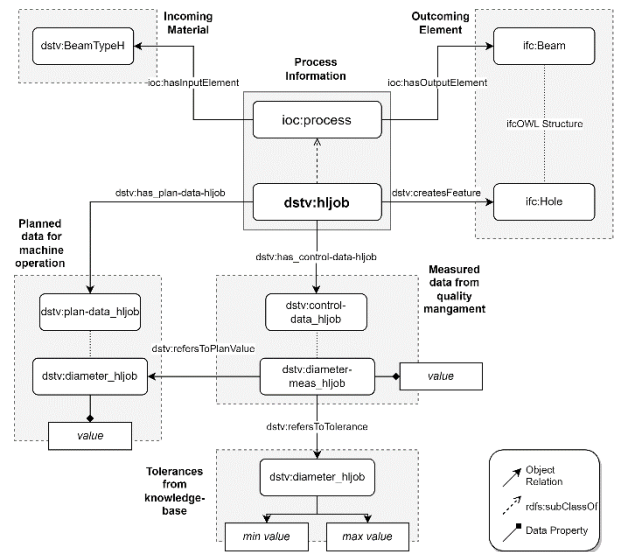


Figure 1: Abstract overview over the DSTV ontology with aligning concepts of ifcOWL and ioc ontology

By facilitating the alignment of planning data from DSTV-NC to IFC, the suggested ontology can ensure that both formats are consistent with each other. This alignment is particularly important for data such as diameter, as illustrated in Figure 1, which must match in both formats.

The proposed ontology can be utilized even in the absence of an IFC file, which is especially crucial when domain-specific software generates DSTV-NC but cannot be integrated with IFC. As the depicted structures are overly intricate to be represented coherently in the graphic, the object properties within the boxes have been simplified.

3.2 Extension of tolerance information

To display and collect all the relevant information for the steel construction process an extensive research and personal discussion with steel fabrication experts have been undertaken. Besides the status quo of the current information flow processes and the used data formats it was identified that some machines are already capable of measuring the part before and/or after it was processed. It is lacking a place to store the measured data and integrate defined tolerances. Tolerances are essential in defining the allowable variations in dimensional and geometric parameters of steel components such as beams, columns and connections. They are used to ensure that the different parts of a structure fit together correctly during assembly to provide the desired function, stability and performance under load conditions.

Manufacturing tolerances of steel sections describe the accepted deviations of the steel element itself, such as

profile height, flange width, web thickness or flange thickness. Depending on the steel section, the standardized values for these tolerances can be found in relevant building codes, standards and specifications. In particular, DIN EN 10034 (I and H beams), DIN EN 10279 (U beams), DIN EN 10219-2 (cold-rolled hollow sections) and DIN EN 10210-2 (hot-formed hollow sections).

At present, the tolerance specifications for the various processes in steel construction are only human readable.

The process of integrating these tolerances into an ontology started with an Excel spreadsheet to collect the information from the various standards. This included all relevant tolerance types, the standard to which they belong, the values and the conditions under which they can be applied. For transfer into the ontology, manufacturing tolerances are first distinguished by steel sections, which then list all relevant tolerances for a specific steel section. Process tolerances are similarly subdivided with the drilling process as the central class for all tolerances associated with that process. Table 2 displays an extract of the defined tolerances for a bore process, here the position of a screw hole according to DIN EN 1090-2.

Table 2. Extract tolerances for position of screw holes

Parameter	Basic tolerance	Extending tolerance class 1	Extending tolerance class 2
Deviation of the center line	+2,0/-2,0 [mm]	+2,0/-2,0 [mm]	+1,0/-1,0 [mm]
Deviation of the distance "a" between a single hole with diameter "d" and the edge of a sheet metal			
if $a < 3d$	+0,0/-0,0 [mm]	+3,0/-0,0 [mm]	+2,0/-0,0 [mm]
if $a \geq 3d$	+3,0/-3,0 [mm]	+3,0/-3,0 [mm]	+2,0/-2,0 [mm]

In the case of determining the tolerance for the position of a screw hole, the *dstv:hljob* is linked to a measured value for the *vertex-x* and *vertex-y* on the relevant surface through *dstv:has_control-data-hljob* and its subcategories. Subsequently, these values are matched against the applicable tolerance value, which varies depending on the relevant tolerance classes defined in specific DIN standards. The tolerance node is connected to the *control-data-hljob* by the object property *dstv:refersToTolerance*. Once these values are aligned, the modeled tolerances can be easily connected to every

process that belongs to the *dstv:* classes such as *dstv:hljob*.

3.3 Extension of process information

In addition to tolerance information, process data must also be stored. This is mainly done via *ioc:process* and its aligned concepts. Certain concepts in the proposed ontology have areas of overlap with the general process concepts outlined in DSTV-NC. This is the case for attributes such as the machine name, manufacturer, process speed, and the tool used, along with its respective properties. However, by utilizing the relevant ontologies, the proposed framework also enables the management of dynamic information that emerges during the robotic process execution. Consequently, feedback data pertaining to the starting and ending times of various manufacturing steps, in the form of timestamps, can be incorporated into future datasets.

4 Use-Case

This section provides an illustration of how the created capabilities can be leveraged to map manufacturing data in steel construction, using the DSTV ontology as a guide. (see fig. 2).

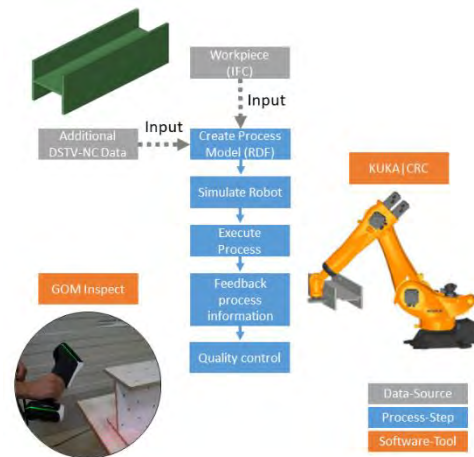


Figure 2: Coarse depiction of the use case including data sources, process steps and software tools.

We propose an approach using an IFC file as the source material and existing approaches for Linked Building Data [28]. For the robotic process, tools and interfaces are used that are developed by robots in architecture [29] and are available to us as WIP - in development versions.

4.1 Model conversion

The example manufacturing process is based on an

IPE 300 profile that is to be drilled with two holes. The model of the profile has been created and provided by an ad-hoc workgroup for ongoing research into the implementation of the DSTV-NC logic in the IFC data model.

The supplied file is converted to Resource Description Framework (RDF) using the IFC2LBD [30] converter which also includes conversion via the ifcOWL ontology (IFC4_ADD2_TC1) [31]. For storing the created triples, an instance of the Stardog triple store is installed on the university server. The triple store provides a SPARQL endpoint that can be used to add, modify and query the linked data in the graph. The original IFC4 file, which is 48KB in size, corresponds to approximately 6100 triples.

4.2 Process data modeling

In a next step, the processes for the robotic fabrication are instantiated using the *ioc* process ontology (<http://w3id.org/ioc#>). The ontology is subject to unpublished research as part of the Internet of Construction project [24]. The processes consist of a parent process that link the input element (IPE300) with the information of the output element (the specific profile including two drilled bores). The detailed child processes correspond to the intended robot movements. As example five movements were created, that are initialized with the following statements:

```
inst:safeto_hljob_01 a ioc:Process. (1)
inst:hljob_01 a ioc:Process, dstv:hljob. (2)
inst:traveltohljob_02 a ioc:Process. (3)
inst:hljob_02 a ioc:Process, dstv:hljob. (4)
inst:safetoEndpos a ioc:Process. (5)
```

The processes are then put in a sequence via *ioc:hasSuccessor* and *ioc:hasPredecessor* statements. The drilling processes in (2) and (4) are belonging to both the *ioc:Process* and *dstv:hljob* class. For the cause of better readability, the prefixes are not stated here. The example is further shown via a detailed description of the first drilling process (2).

```
inst:hljob_01 a ioc:Process, dstv:hljob; (6)
ioc:hasPredecessor inst:safeto_hljob_01; (7)
ioc:hasSuccessor inst:traveltohljob_02; (8)
ioc:hasMethod inst:iocMethod_02; (9)
dstv:has_control-data-hljob (10)
inst:hljob_01_control-data;
dstv:has_fab-data-hljob inst:hljob_01_fab-data; (11)
dstv:has_plan-data-hljob inst:hljob_01_plan-data; (12)
dstv:has_drilling_tolerances (13)
inst:drilling_tolerances_diameter_01;
dstv:refersToIfcElement (14)
inst:IfcVoidingFeature_195.
```

The developed processes serve as a means of

integration, enabling the incorporation of information extracted from the DSTV-NC standard, as well as supplementary metadata, including tolerances and deviations. The drilling processes are classified as *rdf:type dstv:hljob* (6), a classification that stems from the original process descriptions outlined in the DSTV-NC standard. Using the object property *dstv:refersToIfcElement* (14), the processes are connected to the *IfcVoidingFeature* that they generate. Planning, fabrication, and quality control data related to DSTV-NC are linked with object properties *dstv:has_plan-data-hljob*, *dstv:has_fab-data-hljob*, and *dstv:has_control-data-hljob*, respectively (10-13). Generating data for some of these nodes requires manual input since the IFC File does not include all of the necessary parameters, although data such as hole diameter and position can be sourced from the IFC file. For specific control parameters, such as diameter tolerances, the corresponding nodes are linked to the modeled values via object properties *dstv:refersToTolerance* and *dstv:refersToPlanValue*.

In this stage, tolerances are simply modeled by inserting limit sizes and value ranges. For the diameter tolerance, the values were chosen from DIN standards such as DIN EN 10034 and described as min and max value via data properties.

4.3 Path planning

For the shown exemplary implementation, the automated path planning for the robot was done in Rhino / Grasshopper with the KUKA | crc plugin. To retrieve the data, a WebSocket was used to query the database. For this, three SPARQL queries retrieve planes, the geometric information of the IPE profile and the geometric information of the holes. Besides advanced logic to prevent collisions between the robot and the workpiece, only the query for the planes is strictly needed to generate the path. In (15-17) excerpts from the SPARQL query for retrieving planes are shown. The full query consists of 54 lines including prefixes. The shown part of the script solely queries the cartesian plane-basepoint.

```
?void ifc:predefinedType_IfcVoidingFeature (15)
ifc:HOLE.
?void ifc:objectPlacement_IfcProduct ?place. (16)
?place ifc:coordinates_IfcCartesianPoint ?carts. (17)
```

Querying the geometry was added as it is a convenient way to supervise the algorithms in the Rhino Environment as 3D geometry can be rebuild from it. To do this simple python scripts were implemented in ghpython. These recreate the geometry from the query response which is given in the SPARQL 1.1 Query Results JSON Format recommended by the W3C.

Semantic description of the required planes has a benefit that enables the robot's movements to correspond to specific commands based on the process class. With IoT connectivity, tools can automatically trigger specific actions (in this case, drilling) when a particular plane is connected to a *dstv:hljob*. Related research describes workflows to accomplish this task. [32]. The use of this logic enables the generation of a path planning that includes tool control. KUKA|crc stores this in a JSON object (18), which can be added to the database via SPARQL UPDATE.

```
(18)
{
  "id": "a3c478c8",
  // Unique Command Identifier for Information
  Flow Tracing
  "cmd": "MovePtp",
  // Basic Command Typ or Skill Class Name
  "dev": "robotid",
  // Executing Device the Command is Forwarded
  to
  "sync": false,
  // Synchronization Flag for Inter-device
  Synchronization
  "tcpPose": {
    "X": 500.0,
    "Y": 500.0,
    "Z": 420.0,
    "A": -180.0,
    "B": 0.0,
    "C": 180.0
  },
  /* Command Class Specific Parameters such as
  * TCP Target Position, Axis Target Position
  etc.
  */
  "meta": {
    "status": "010",
    "redAxis": 45.0,
    "speed": 80.0
  }
}
```

The objects that comprise all the necessary information for the robotic process are linked to the modeled processes in the graph through a *ioc:hasMethod* and a *schema:value* property.

4.4 Robotic manufacturing

When production is due, a simple python script running on a WebServer, automatically queries the database to check if all necessary information are available, as well as checking the status of robot and tool. If ready, the JSON object, which includes the robot control information, gets send to a KUKA|crc instance connected to the robot. This is done via the MQTT protocol. The robot then interprets the commands and starts the process sequence. The test setup is shown in fig. 3.

After every process (-step), the robot sends a command to the WebServer to adjust the process status of the given process. The timestamps generated can later be used to optimize the movement and thus time consumption of the process.

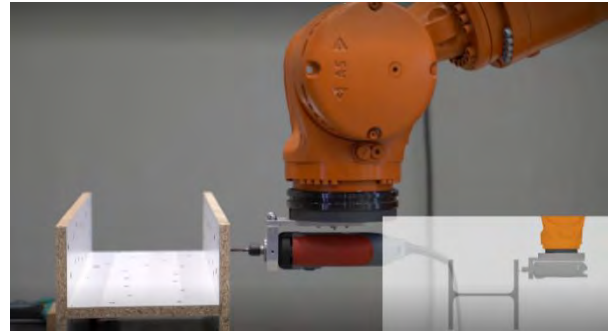


Figure 3: Robotic fabrication test with a wooden dummy IPE 300 profile. Process parameters are described by the DSTV ontology and accessed via MQTT.

4.5 Quality control and feedback of information



Figure 4: Hand held 3D scanner which was used to capture deviations

After the bore holes were robotically drilled, the part was scanned with a 3D hand-held laser scanner (see fig. 4). The scanned point cloud was analyzed with the GOM Inspect software.

The measured data can be added to the overall semantic web description via the python interface of GOM and a SPARQL UPDATE Query. In the modeled graph the data is connected via the *dstv:has_control-data-hljob* object property. As the model has also access to the defined tolerances of the drilled hole and the planned geometry data a comparison between these values can be executed. The result of the used query returns a JSON object. It shows that the control value for the x-vertex is 15.24mm (19) while the plan value is 15.0mm (20)

```
"controlvertex_x": {
  "datatype":
  "http://www.w3.org/2001/XMLSchema#float",
  "type": "literal",
  "value": "15.24"
} (19)
```

```

    }
    "planvertex_x": {
      "datatype":
        "http://www.w3.org/2001/XMLSchema#float",
      "type": "literal",
      "value": "15.0"
    }
  }
}

```

(20)

The resulting graph of the whole use-case consists of 6400 Triples. Figure 5 shows the resulting interconnected data model, based on the *ioc:process* in the center, which links the IFC based data (incoming material and created features – here *ifcHOLE*) and the specific DSTV extension data. It is visible that the DSTV extension consist of three branches which are the planned and measured data as well as the pre-defined tolerances.

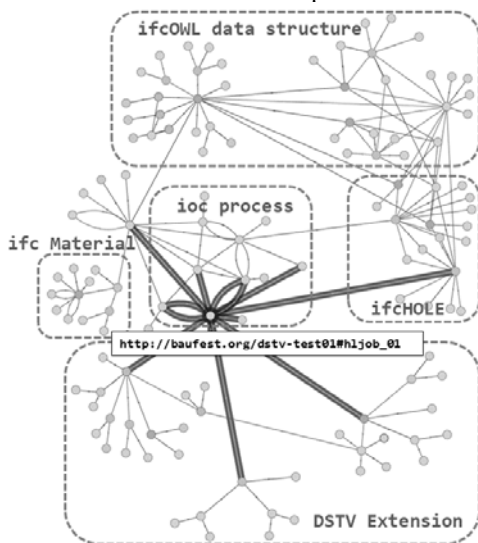


Figure 5: The resulting graph of the use-case

5 Outlook

The DSTV ontology allows the use of semantic web technologies for the description of steel construction information. It enables the description of robotic process and overall steel construction information and connects all the relevant information of different fabrication processes, including manufacturing process metadata such as tolerances and data feedback. The additional information can be used to automate the evaluation of the measured data, as well as to analyze which tools cause which deviations from the planned geometry. Optimization of processes based on real data is feasible and promotes more efficient steel construction processes.

The first draft of the DSTV ontology was able to demonstrate that the concept is feasible and easy to implement, as it follows the structure of the DSTV-NC from which it originates, extending it only where necessary. However, future research should evaluate the ontology further to optimize and simplify it. It should also address the limitations and prerequisites of this work

such as the required digital data and modeling expertise or solutions to current disadvantages of using the IFC data model such as data loss or version conflicts.

6 Acknowledgements

The project (BauFeSt 4.0) (21690 N/FE1) is being carried out in cooperation with the industrial partners and financially supported by the Federal Ministry for Economic Affairs and Energy (BMWi) via the German Federation of Industrial Research Associations (AiF). This work is also part of the research project Internet of Construction (funding number 02P17D081).

7 References

- [1] Kuntze, P.; Mai, C.-M.: Arbeitsproduktivität - nachlassende Dynamik in Deutschland und Europa. In: WISTA - Wirtschaft und Statistik 72 (2020), Heft 2, S. 11-24.
- [2] Sikstrom, F.; Ericsson, M.; Nylén, P. et al.: 3D-Scanning for Weld Distortion Measuring. In: : Proceedings of the 23rd IEEE Instrumentation and Measurement Technology Conference – IMTC/06 ; Sorrento, Italy - 24-27 April 2006. IEEE Instrumentation and Measurement Society. Inst. of Electrical and Electronics Engineers, Sorrento, Italy, 2006, S. 2132-2137.
- [3] Wilmsmeyer, H.; Flasskamp, M.; Schierenberg, M.-O.: Intelligente Korrektur eines Schweißroboters. In: Jasperneite, J.; Lohweg, V. (Hrsg.): Kommunikation und Bildverarbeitung in der Automation, Technologien für die intelligente Automation. Springer Berlin Heidelberg, Berlin, Heidelberg, 2018, S. 283-294.
- [4] DIN EN 1090-2: Ausführung von Stahltragwerken und Aluminiumtragwerken - Teil 2: Technische Regeln für die Ausführung von Stahltragwerken. Norm, Ausgabe 2018.
- [5] H. Wilmsmeyer; M. Flasskamp; T. Jungeblut et al.: Intelligenter Schweißroboter: Selbständige Reaktion eines Schweißroboters auf große Toleranzen. In: wt Werkstattstechnik online (2016), Heft 106, S. 595-599.
- [6] Plattform Industrie 4.0: Digitale Ökosysteme global gestalten – Leitbild 2030 für Industrie 4.0 (2019).
- [7] R. Fischer: Prozess- und Modellorientierung des Stahlbaus: Ein Beitrag aus der Praxis. In: Motzko, C. (Hrsg.): Praxis des Bauprozessmanagements – Termine, Kosten und Qualität zuverlässig steuern. Ernst & Sohn, Berlin, 2013, S. 193-212.
- [8] bauforumstahl e.V.: Standardbeschreibung von Stahlbauteilen für die NC-Steuerung (ASCII), 2003.

- [9] *bauforumstahl e.V.*: Standardbeschreibung von Stahlbauteilen für die NC-Steuerung (XNC), 2006.
- [10] *Jonas Hippe*: Entwicklung einer prototypischen Schnittstelle zur Ansteuerung von Industrierobotern über den DSTV-NC. Aachen, RWTH, Masterarbeit, 2021.
- [11] *bauforumstahl news*. In: *Stahlbau* 87 (2018), Heft 2, S. 173-190. <https://doi.org/10.1002/stab.201870214>.
- [12] DIN EN ISO 16739-1 (2021-11-00): Industry Foundation Classes (IFC) für den Datenaustausch in der Bauwirtschaft und im Anlagenmanagement - Teil 1: Datenschema. Norm, Ausgabe 2021.
- [13] *Sabou, M.; Biffl, S.; Einfalt, A. et al.*: Semantics for Cyber-Physical Systems: A cross-domain perspective. In: *Semantic Web* 11 (2020), S. 115-124. <https://doi.org/10.3233/SW-190381>.
- [14] *Wong, A.; Ray, P.; Parameswaran, N. et al.*: Ontology mapping for the interoperability problem in network management. In: *IEEE Journal on Selected Areas in Communications* 23 (2005), Heft 10, S. 2058-2068. <https://doi.org/10.1109/JSAC.2005.854130>.
- [15] *Gyrard, A.; Zimmermann, A.; Sheth, A.*: Building IoT based applications for Smart Cities: How can ontology catalogs help? In: *IEEE internet of things journal*, Vol. 5 (2018), Iss. 5, pp. 3978-3990. <https://doi.org/10.1109/jiot.2018.2854278>.
- [16] *Cao, Q.; Giustozzi, F.; Zanni-Merk, C. et al.*: Smart Condition Monitoring for Industry 4.0 Manufacturing Processes: An Ontology-Based Approach. In: *Cybernetics and Systems* 50 (2019), Heft 2, S. 82-96. <https://doi.org/10.1080/01969722.2019.1565118>.
- [17] *Gruber, T.R.*: A translation approach to portable ontology specifications. In: *Knowledge Acquisition* 5 (1993), Heft 2, S. 199-220. <https://doi.org/10.1006/knac.1993.1008>.
- [18] *Patil, L.; Dutta, D.; Sriram, R.*: Ontology-Based Exchange of Product Data Semantics. In: *IEEE Transactions on Automation Science and Engineering* 2 (2005), Heft 3, S. 213-225. <https://doi.org/10.1109/TASE.2005.849087>.
- [19] *buildingSMART Technical: ifcOWL - buildingSMART Technical*, 2023, <https://technical.buildingsmart.org/standards/ifc/ifc-formats/ifcowl/> [Zugriff am: 05.01.2023].
- [20] *Mathias Bonduel; Jyrki Oraskari; Pieter Pauwels et al.*: The IFC to Linked Building Data Converter-Current Status. In: , 2018.
- [21] *BOT: the Building Topology Ontology of the W3C Linked Building Data Group*: swj2224.
- [22] *Wagner, A.; Sprenger, W.; Maurer, C. et al.*: Building product ontology: Core ontology for Linked Building Product Data. In: *Automation in Construction* 133 (2022), S. 103927. <https://doi.org/10.1016/j.autcon.2021.103927>.
- [23] *Zheng, Y.; Törmä, S.; Seppänen, O.*: A shared ontology suite for digital construction workflow. In: *Automation in Construction* 132 (2021), S. 103930. <https://doi.org/10.1016/j.autcon.2021.103930>.
- [24] *Kirner, L.; Lublasser, E.; Brell-Cokcan, S.*: Internet of Construction: Research Methods for Practical Relevance in Construction. In: *Technology|Architecture + Design* 5 (2021), Heft 2, S. 146-152. <https://doi.org/10.1080/24751448.2021.1967053>.
- [25] *Zillner, S.; Ebel, A.; Schneider, M.*: Towards intelligent manufacturing, semantic modelling for the steel industry. In: *IFAC-PapersOnLine* 49 (2016), Heft 20, S. 220-225. <https://doi.org/10.1016/j.ifacol.2016.10.124>.
- [26] *Olivares-Alarcos, A.; Foix, S.; Borgo, S. et al.*: OCRA – An ontology for collaborative robotics and adaptation. In: *Computers in Industry* 138 (2022), S. 103627. <https://doi.org/10.1016/j.compind.2022.103627>.
- [27] *Natasha Noy*: *Ontology Development 101: A Guide to Creating Your First Ontology* (2001).
- [28] The Linked Building Data Community Group, 2022, <https://w3c-lbd-cg.github.io/lbd/> [Zugriff am: 31.01.2023].
- [29] Association for Robots in Architecture – making robots accessible to the creative industry, 2023, <https://robotsinarchitecture.org/> [Zugriff am: 31.01.2023].
- [30] *M. Bonduel; J. Oraskari; P. Pauwels et al.*: The IFC to linked building data converter - current status (2018).
- [31] *Pieter Pauwels; walter.terkaj@itia.cnr.it*. OWL ontology for the IFC conceptual data schema and exchange file format for Building Information Model (BIM) data [online], 2019 [Zugriff am: 31.01.2023], https://standards.buildingsmart.org/IFC/DEV/IFC4/ADD2_TC1/OWL/index.html.
- [32] *Dai, R.; Kerber, E.; Reuter, F. et al.*: The digitization of the automated steel construction through the application of microcontrollers and MQTT. In: *Construction Robotics* 4 (2020), 3-4, S. 251-259. <https://doi.org/10.1007/s41693-020-00042-9>.

Quality monitoring of Concrete 3D Printed elements using computer vision-based texture extraction technique

Shanmugaraj Senthilnathan¹ and Benny Raphael^{2*}

^{1,2}Civil Engineering Department, Indian Institute of Technology Madras, India
¹ce20d005@smail.iitm.ac.in, ^{2*}benny@civil.iitm.ac.in

Abstract –

Concrete 3D Printing (3DP) has the potential to reduce construction time and the usage of labor and material in the construction industry. However, many parameters are found to influence the output of 3DP, and consequently, the variations in the quality of output are high. To fully realize the advantages of 3DP and to develop it into a technology for large-scale construction, a focus on quality monitoring and control is required. The workability of concrete is found to reduce with time, impacting the extrudability and buildability properties. This can be seen in 3DP elements, where the bottom layers are found to have a smooth textural finish while the top layers have cracks, voids, and defects. To quantify the extrudability changes in the concrete, a new computer-vision-based methodology is proposed in this paper using a modified Histogram of Oriented Gradients (HOG) texture extraction method. Different levels of texture variations are extracted to quantify both minor and major textural changes. Weighted texture and normalized weighted texture metrics are introduced to have a combined single measure for minor and major textural variations. Further, a temporal textural change study is proposed to indirectly assess the buildability properties of concrete 3DP. This paper contributes to developing a non-intrusive autonomous quality monitoring and assessment technique for concrete 3D printed elements.

Keywords –

Concrete 3D printing; Computer Vision; Histogram of Oriented Gradients; Extrudability; Quality monitoring

1 Introduction and background

Concrete 3D printing (3DP) is an emerging free-form-based digital construction technology that has the potential to improve automation in the construction industry. 3DP increases productivity by reducing construction time while also reducing material and labor usage. Though there are many advantages, employing the

technology on a larger scale requires maturity in terms of repeatability and quality control [1]. But the number of studies on quality control in concrete 3DP is limited, and many industry experts consider it a critical topic [2].

Since concrete 3DP depends on many input parameters, the quality of printed extrudates varies drastically [3]. Effective quality control systems help to avoid re-work and material wastage. The output quality of the concrete 3DP elements varies with the reduction in the material's workability and moisture content. The bottom layers are seen to have a smooth surface texture finish, and the top layers have a more granular finish, ultimately leading to voids/discontinuities. The changes in workability are found to affect the extrudability and buildability properties of concrete [4]. Extrudability is the ability of the concrete to pass with a high shear through a nozzle and maintain the liquid properties. Buildability is the ability of concrete to maintain its shape without much deformation under the influence of the weights of successive layers. There have been studies that use mechanical tests to quantify workability over time [5], but they cannot be used for real-time monitoring [6].

Computer vision (CV) has gained significant importance in additive manufacturing[7] and slowly getting traction in concrete 3DP [8][9]. Hence there are very few studies in concrete 3DP using CV for quality assessment and using it for real-time feedback to control the quality of 3D printing.

This study proposes the use of images and videos of 3D printed elements to evaluate the surface textural variations. CV-based texture extraction helps to obtain surface textural variations within each printed layer image to detect defects like voids and discontinuities. It is a continuation of the previous work [6], which utilized a different two-bin Local Binary Pattern (LBP) algorithm that only captured texture variation in the horizontal direction. A novel approach to capture texture in three directions with a method to categorize minor and major textural variations is developed in this study to assess the quality of the printed layers. Also, a temporal textural variation study is introduced to assess the buildability properties.

1.1 Objective

The main objective of this study is to develop a non-intrusive autonomous quality monitoring and assessment methodology using a CV-based texture extraction method.

1.2 Methodology

An overview of the methodology is shown in Figure 1. It involves collecting images or videos of 3D-printed layers during the printing process. Pre-processing is done to crop the individual layers into separate images, which are used in textural analysis to extract the variations within each layer. A novel method is proposed to capture both minor and major textural variations.

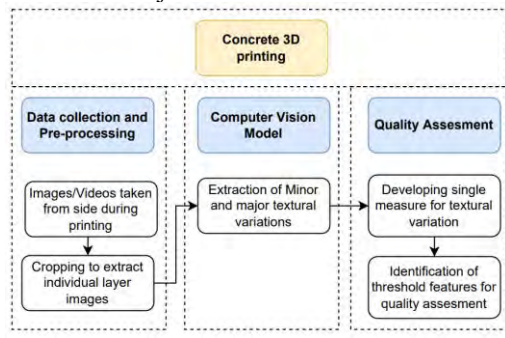


Figure 1 - Methodology of quality assessment using computer vision

A single metric is developed to capture all the minor and major textural variations. And a threshold for the metric is identified for assessing the quality of the printed layers.

2 Materials and Methods

2.1 Materials used

For this study, sample 3D printed elements were printed with a recently developed Limestone Calcined Clay (LC2) mix composed of OPC cement and Limestone Calcined Clay as the binder materials [10]. The aggregate used was 4.75mm size Manufactured Sand. Super-plasticizers and powder-based Viscosity Modifying Admixtures (VMA) were used to achieve optimum rheological properties of the mix to print.

A gantry-based robotic printer is used in this study. For evaluating the newly developed methodology, two specimens were used. One circular cross-section element was printed for a height of 1000 mm. Another circular 3D-printed element of height 700 mm was printed with a chemical-based super-plasticizer. Since it was a chemical-based super-plasticizer, there were many voids, and the printing was stopped at 700 mm as it may lead to the clogging of pipes.

2.2 Image Data Collection and Pre-processing

Since the current study is focused on extracting the texture variations in all the layers, image/video data is collected by keeping a camera perpendicular to the printed element. The camera is positioned 1.5 m horizontally from the printed elements, such that all the side layers are visible in a single shot of the 3D-printed element. Since a single picture containing all the layers was used for the analysis, the influence of differential illumination on different images is avoided.



Figure 2 - Printed element A (left), bottom section of Element A taken for analysis - Section A1 (middle), Top section of Element B taken for analysis - Section A2 (right)

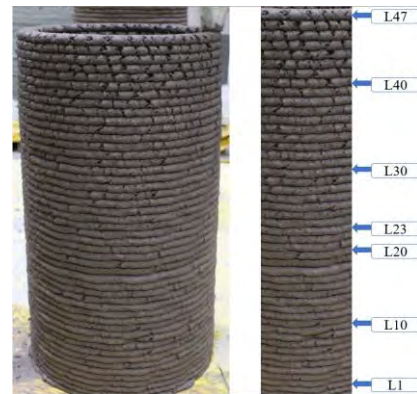


Figure 3 - Printed Element B (left), Section considered for analysis and the layer designations of Element B (right)

The camera used in the study is a Canon EOS 1300D DSLR camera with an 18 MP resolution. Since the printed elements are of circular cross-sections, images/videos taken from the sides will have the impact of curvature. The central one-third of the image is used in this study to avoid the curvature effects on the analysis.

The individual layers of the printed element are cropped to create the input images for analysis. The individual layer elements are designated as L1 for the bottom layer and numbered sequentially for the top layers. The two printed elements-Element A and B, and their layer designations are given in Figure 2 and Figure 3,

respectively. The cropping of individual layers was done manually in this study, but it can be automated using computer vision techniques like image segmentation. It is a part of ongoing research and is proposed as a part of future work.

2.3 Texture extraction – Histogram of Oriented Gradients (HOG)

The layer images were analyzed using a texture extraction algorithm written in Python language. Multiple texture extraction algorithms were evaluated for their capability to identify quality defects in 3DP concrete specimens. A custom-designed version of the Histogram of Oriented Gradients (HOG) approach was found to give the best results.

The Histogram of Oriented Gradients (HOG) was first conceptualized in 1986. It is a popular feature extractor that can extract useful information from the given image and eliminate unwanted information. HOG uses the gradients of pixel values in the images [11]. The gradient measures the pixel intensity variation in a particular direction. The gradient can be computed in one or many directions.

In this study, a new version of the HOG feature extractor is designed to extract gradients in three different directions using masks, as shown in Figure 4, namely, Horizontal, Vertical, and Diagonal masks. The masks were designed based on Robert's filter to detect the edges in images. Application of each mask at a pixel position involves taking an inner product of the matrix with the corresponding pixel values in the neighborhood of the pixel position.

Horizontal Mask		Vertical Mask		Diagonal Mask	
-1	0	-1	1	-1	0
1	0	0	0	0	1

Figure 4 - Gradient masks used for texture extraction

These masks are convoluted across the input images; the inner product is calculated at each pixel position. To consider both minor and major texture variations, a range of thresholds is used to calculate the number of pixels that have large gradients. A window size of 4 image pixels (2x2) is chosen for the study.

The individual pixel windows are convoluted with the horizontal, vertical, and diagonal masks to get the output gradients. The output of the HOG operator is taken as the number of pixels having gradient changes in any one of the directions after converting the images into grayscale.

The HOG algorithm developed in this work is different from the conventional HOG algorithm in the following aspects: the histogram is computed using the count of pixels having gradient greater than different

threshold values; that is, it computes the gradient in horizontal, vertical, and inclined directions and counts the number of pixels where the gradient exceeds the threshold.

Since the count of the HOG gradient variations gives the textural variations within the printed element, the output of the HOG operator shall be called as texture in this study.

2.4 Weighted mean calculation

From the HOG analysis, different outputs are obtained for a single-layer image for different threshold values. The smaller threshold outputs will capture all the minor gradient changes, and the larger threshold captures only the major textural variations like voids and discontinuities.

The voids/discontinuities in the printed layers contribute to the major textural changes. Hence maximum weightage is given for large threshold values; that is, the threshold of 128 is given the maximum weightage and the threshold of 4 the minimum. Then the weighted mean is computed for each of the “i” threshold values, as per the following equation,

$$\text{Weighted mean of the image} = \sum(w_i * x_i) / \sum(w_i)$$

Where, w_i – the weight given for the threshold value “i”, x_i – HOG output of the image for the threshold value “i”. The weighted mean is computed for each of the individual layer images and then tabulated. The weighted mean gives the weighted values of the textural pattern seen in the individual printed layer image, which shall be designated as weighted texture in this study.

2.5 Normalized weighted mean calculation

Though the weighted mean gives a fair representation of the textural variations within the printed elements, the impact of brightness/illumination changes will influence the output. To eliminate the variabilities due to illumination, the mean and standard deviation of weighted mean values are computed for all the layers in the different printed elements separately. Then, each of the weighted HOG mean outputs of individual layer “i” of the printed element “j” is normalized using the following formula,

$$\text{Normalized weighted mean for each layer image} = (x_{i,j} - \mu_j) / \sigma_j$$

$x_{i,j}$ – HOG weighted mean of the individual layer “i” of printed element “j”, μ_j – Mean value of all the individual layer’s HOG weighted mean values of printed element “j”, σ_j – Standard deviation value of all the individual layer’s HOG weighted mean values of printed element “j”. Normalized weighted mean values of the textural variation shall be identified as Normalized weighted texture in this study for ease of understanding.

2.6 Entropy value calculation

Another measure of textural variations generally used is information entropy by Shannon. It is used in this study, given by the formula,

$$\text{Entropy} = -\sum P_i * \log_2 P_i$$

Where, P_i – Ratio of the number of HOG pixel outputs for a threshold value “i” to the total number of pixels found (textural variations) in all the threshold value outputs. Entropy represents the distribution of pixel brightness/intensities within a given image. It indirectly measures the changes within a layer, like thickness variations due to the buildability properties of 3DP concrete material.

3 Results

3.1 Surface textural variation within a printed element – texture extraction

The individual layer images are processed using a CV-based HOG textural extraction algorithm for different threshold values. The output will be the number of pixels/points having textural variations beyond the specified threshold. For example, the HOG textural variation output of a few different threshold value outputs for layer L19 of printed element B is shown in Figure 5. Different positions/points in the image where textural variations exist are marked as black pixels. The output with a threshold value of 4 captures all the minor

variations in the printed layers, leading to a higher density of black pixels. It captures both the minor variations within the printed layer and the major variations at the layer edges. In contrast, for the 128-threshold output, only the major textural variations that happen only at the layer edges and voids are captured. It is seen that the number of black pixels reduces and concentrates only on the layer edges as the threshold value increases.

32 different values for each layer image corresponding to different threshold values are shown in Figure 6. The outputs are for the bottom ten layers of the 3D-printed element B. From the results, it is evident that beyond the 128-threshold value, the output of the HOG algorithm is minimal. Hence the analysis was not done beyond the 128-threshold value.

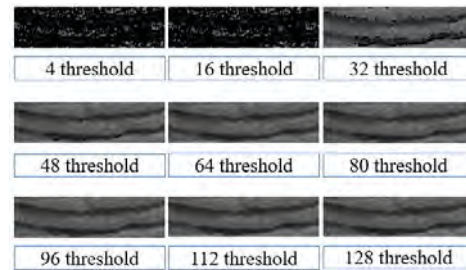


Figure 5 - HOG output for different threshold pixel values for individual layer - L19 of Element B

Layer Number	4 Threshold	8 Threshold	12 Threshold	16 Threshold	24 Threshold	32 Threshold	36 Threshold	40 Threshold	44 Threshold	48 Threshold	52 Threshold	56 Threshold	60 Threshold	64 Threshold	68 Threshold	72 Threshold	76 Threshold	80 Threshold	84 Threshold	88 Threshold	92 Threshold	96 Threshold	100 Threshold	104 Threshold	108 Threshold	112 Threshold	116 Threshold	120 Threshold	124 Threshold	128 Threshold		
L1	2340	1872	1437	1075	776	584	451	349	301	280	254	228	208	190	181	157	149	137	122	109	98	91	84	79	62	52	40	22	2	0	0	
L2	2613	2058	1491	1027	685	419	247	147	103	66	39	27	17	14	14	12	12	12	11	9	9	8	8	6	6	4	4	2	2	2	0	0
L3	2643	1986	1442	1023	697	421	249	126	53	27	14	6	3	1	0	0	0	0	0	0	0	0	0	0	0	0	0	0	0	0	0	0
L4	2320	1617	1087	735	457	258	136	45	9	1	0	0	0	0	0	0	0	0	0	0	0	0	0	0	0	0	0	0	0	0	0	0
L5	2788	2039	1361	914	578	317	156	66	20	2	1	0	0	0	0	0	0	0	0	0	0	0	0	0	0	0	0	0	0	0	0	0
L6	2884	2111	1541	1104	748	456	256	114	47	17	10	3	1	1	0	0	0	0	0	0	0	0	0	0	0	0	0	0	0	0	0	0
L7	2538	1806	1246	858	563	357	191	78	32	13	5	0	0	0	0	0	0	0	0	0	0	0	0	0	0	0	0	0	0	0	0	0
L8	2111	1492	987	623	424	257	122	51	18	4	0	0	0	0	0	0	0	0	0	0	0	0	0	0	0	0	0	0	0	0	0	0
L9	2972	2152	1474	1049	741	470	261	147	72	34	14	6	1	0	0	0	0	0	0	0	0	0	0	0	0	0	0	0	0	0	0	0
L10	2967	2185	1575	1139	829	497	375	200	93	46	23	10	4	1	0	0	0	0	0	0	0	0	0	0	0	0	0	0	0	0	0	0

Figure 6 - HOG outputs for different threshold values for Element B (first ten layers)

3.1.1 Weighted mean variation – weighted texture calculation

The weighted texture is taken as a single measure of texture variation representation. A weightage of 32 is given to the 128-threshold output and reduced by one for every 4-pixel point reduction in the threshold value. Since the primary focus of this study is to identify layers with defects/voids, higher weightage is given to major textural variation outputs (128 threshold), and lesser weightage is given to minor textural variation outputs (4 threshold).

The outputs of the weighted texture for Element A and B are plotted in Figure 7. The weighted texture values obtained for Element B are higher than Element A. It is due to the presence of more voids and discontinuities in the printed layers. It confirms that Element A is a relatively good quality print in comparison to Element B.

3.1.2 Normalized weighted texture calculation

Further, a normalized weighted mean is computed from the weighted texture to evaluate the print quality, as shown in Figure 8. The standard deviation and mean of all the individual layer’s HOG weighted texture output in

each printed element are calculated, and each data point is normalized in terms of mean and standard deviation within its printed element. It eliminates the influence of illumination and brightness variation during the different times of printing Elements A and B. The normalized values will be easy to compare and evaluate the effectiveness of the print quality. Also, this step eliminates the subjectivity in selecting weights for the weighted texture calculation. Making the technique more robust in terms of evaluation.

The results indicate that the normalized weighted texture values of Element B are generally higher than Element A. This means that the textural variations within the individual layers of Element B are higher than Element A. It indicates the presence of more granular texture and voids/defects in the individual layers. The evolution of normalized weighted texture for Elements A and B is explained in detail as follows,

Element A: From Figure 8, the normalized weighted texture values of the bottom layers of Element A are less than zero. The variations of values are also low, which can be directly correlated to the smooth textural finish of the bottom printed layers found in Figure 2. Beyond L20, higher value spikes were found (beyond the value of zero) in the normalized weighted texture values that can be directly related to the voids present in the individual layers of Element A. Beyond L20, some layers are not found to have any voids, which can be identified by the lower values of the normalized weighted texture. However, other layers having voids are characterized by higher normalized weighted texture values making the variation of values erratic. It can be visually understood that higher value spikes are found for individual layer elements having voids/deformities. And beyond L20, the concrete has lost significant value of moisture content requiring external interference to get good quality prints.

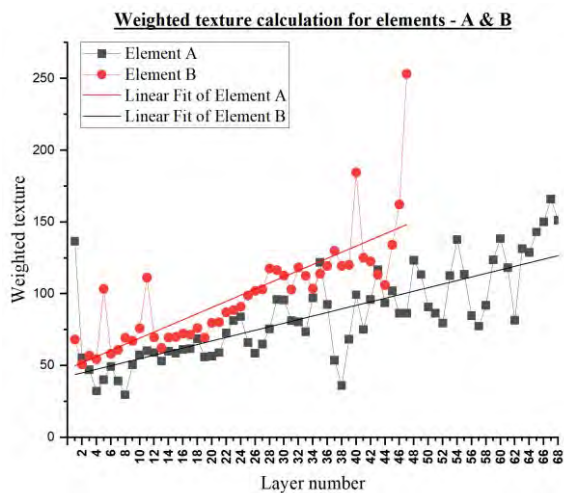


Figure 7 - Weighted texture output for the individual layer images of Element A and B

Element B: In contrast to Element A, Element B's normalized weighted texture values started to vary drastically and reach higher values (more than zero) in the initial layers. It can be correlated with voids/defects present in the initial few layers of Element B, as shown in Figure 3. But in the other bottom layers, due to sufficient workability, a smooth texture can be found, which is indicated by lower values of normalized weighted texture until L20. But, beyond L20, the values are always higher than zero and increasing, indicating the granular texture and the presence of voids/defects in every layer. Higher spikes in normalized weighted texture values beyond the value zero match with the layers having voids/deformities.

Further, the linear fit obtained on the normalized weighted texture values of elements A and B indicates a steep increase in the values for Element B compared to Element A. Hence, the slope of the linear fit of the normalized weighted texture values can also indicate the quality of the 3D printed elements.

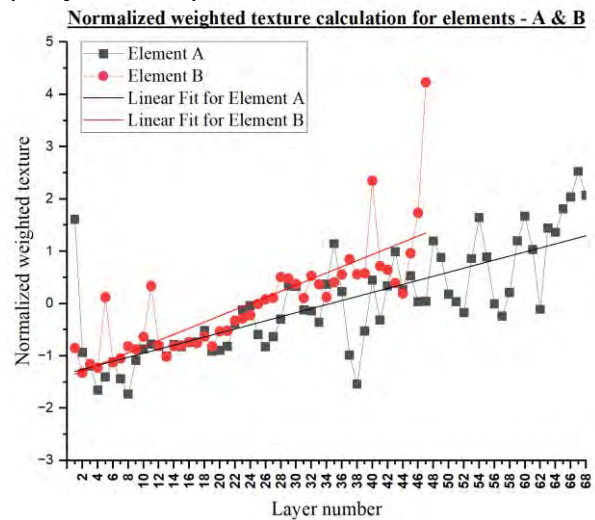


Figure 8 - Normalized weighted texture output of individual layer images of Element A and B

3.2 Temporal textural variation of a single printed layer

A temporal texture variations study is proposed to assess the buildability properties using surface texture analysis. To achieve this, temporal textural variation for a single layer of a printed element is extracted at different instances of printing to understand the variations happening on the individual layer due to the weight of the layers printed above it.

For a better-quality print, the thickness variations in the bottom layers due to the weight of the layers printed above should be minimum so that the final printed element will satisfy the dimensional and geometrical accuracy.

For this analysis, a video of the entire printing process is captured, and a single fixed crop window is selected for an individual layer of a printed element. The HOG textural variations are extracted at every instance a layer is printed above it. During this period, the target layer under study changes in dimension and textures. A single crop window consisting of layer L6 of Element A is considered, and images at different instances after the printing of every layer above it are shown in Figure 9. Similarly, crop windows were set for other layers like L7, and L8 of Element A and layers L21, L22, and L23 of Element B.

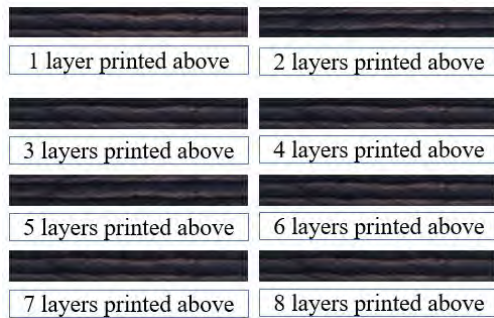


Figure 9 - Image of layer L6 of Element A after the number of layers printed above it

HOG textural values are extracted for each image for different threshold values, and the output is generated similar to that shown in Figure 6. To have a single output value, an entropy calculation is performed. The entropy values are obtained for the same layer at different instances after subsequent layers are printed above them. Entropy variations for the layers considered for analysis in Element A and Element B are plotted and shown in Figure 10 and Figure 11, respectively.

Element A – The entropy variation indicates the textural variations happening within the printed layer at that instance. First, the case of only one printed layer above the target layer is taken. The single layer above will not impart much weight on the layer below and will not cause a major reduction in the layer thickness. Hence, the printed layer is of its original printing height, and minor texture variations within the layers are predominant in the image. But as the number of layers printed above increases, the bottom layer compresses and makes the layer boundary more prominent visually. This results in the image consisting of predominantly dark pixels and causes a reduction in textural variations. The same is brought out in Figure 10, showing the reduction of entropy values as the number of printed layers increases. Beyond the four layers printed above, the thickness variation of the layer is reduced as the concrete reaches sufficient early strength to support the weight of the layers printed above, which is reflected with almost a flat curve in Figure 10.

Element B – In the case of Element B, it was difficult

to study the temporal texture changes in the bottom layers as there were undulations and major voids. Hence, layers L21, L22, and L23 are considered where there are smaller voids. The layers' HOG entropy values are plotted in Figure 11. Layer L23 is found to exhibit similar trends, as shown in Figure 10. But in the case of layers L21 and L22, due to the presence of minor voids, the entropy values are found to vary drastically.

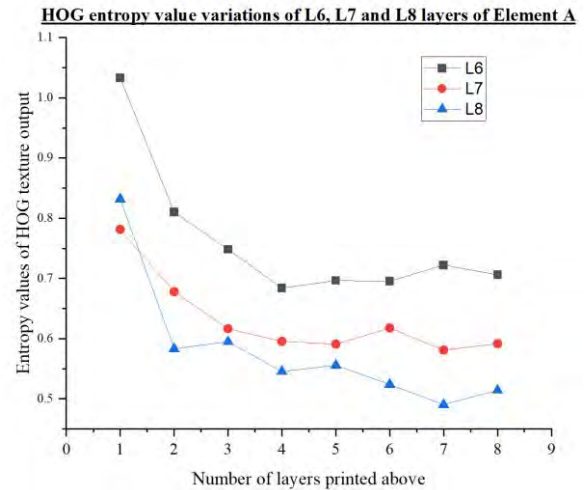


Figure 10 - Entropy value variations of HOG outputs for layers L6, L7, and L8 of Element A

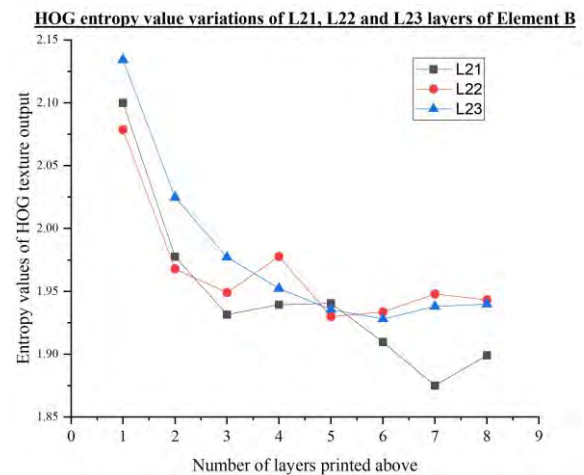


Figure 11 - Entropy HOG outputs for layers L21, L22, and L23 of Element B

4 Analysis and Discussion

4.1 Quality assessment of printed layers

From the previous section, it is plausible that the normalized weighted texture calculation is a valid representative of the textural variations within printed layers. Higher values were found for layers with

voids/defects, which can help classify the layers as bad quality.

Since the HOG texture extractor was designed to quantify textural variations in horizontal, vertical, and inclined directions, gradient variations in all directions are considered. The usage of different threshold values helps in capturing both minor and major textural variations, making it an end-to-end quality assessment technique for 3D printed elements.

This study analyzed two different elements printed at two different times and lighting conditions. The illumination changes and distance of the camera will have minimal effect on the results due to the following reasons: All the computations involve a relative comparison of output values obtained from the different layers of the same image. Further, a normalization technique is introduced, which allows for all the output values to be normalized in terms of the mean and standard deviation obtained over the entire image of the printed element. Due to this normalization procedure, the results are not very sensitive to the weighting scheme used for the weighted texture computation.

But in the case of off-site 3D printing, where the printing process is undertaken in a closed environment, a single trial 3D printed element can be printed and analyzed with the proposed technique to obtain the mean and standard deviation values. And using them, the quality of newly 3D printed elements during their printing can be assessed. Care should be taken to keep the camera position and printing material mix design constant.

Comparing the weighted texture values and the normalized weighted texture in Figure 7 and Figure 8, both graphs have a similar evolution of values (slope of the linear fit of values), matching the voids in the printed elements. Hence even the weighted texture values of the HOG feature extraction can be used as an effective quality assessment tool. But the normalized weighted texture measure is considered to significantly eliminate the impact of brightness/illumination changes, thereby making a robust controlled setup.

Overall, the normalized weighted texture values obtained from the HOG texture extractor prove to be a better-quality assessment metric for concrete 3D printed elements. It can further be used as a quality assessment tool for already printed layers after the printing process is completed.

4.2 A measure of workability and extrudability

The observed results from the computer vision model can be used to quantify the workability of the 3D printing concrete. The change in workability of the mix used for printing Element A was studied and found to be reducing with time, as shown in Figure 12 [10]. A flow table test

was conducted to quantify the workability change with time for the material matching the mix used for this study, LC2-MS-0.6SP (Limestone Calcined Clay mix with Manufacture Sand and Super Plasticizer).

It is to be noted that the spread diameter from the flow table test keeps on reducing every half an hour, indicating a reduction in workability.

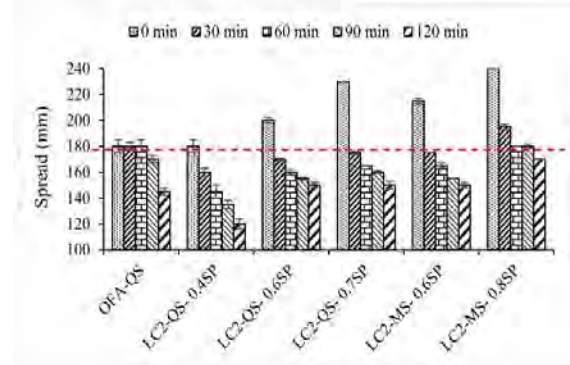


Figure 12 - Evolution of workability of 3DP concrete with time-based on flow table test [10]

Characterization of workability for every 5 to 10 minutes is not considered in the scope of this study, but the graph indicates the reduction in workability with time. There is a reduction in workability with time, whereas there is an increase in the normalized weighted texture values from HOG. Hence an inverse correlation can be obtained, which helps in indirect non-intrusive quantification of workability. The workability can be directly related to the extrudability properties of the 3DP concrete. Hence the developed methodology can be used to indirectly quantify the extrudability and workability properties of concrete 3D printing.

4.3 An Assessment of Buildability Properties

In section 3.2, HOG entropy values are found to be high in the initial instance when only one layer is printed above it. But as the number of layers printed above increases, the bottom layer has sufficient time to gain early strength. This phenomenon was captured in this analysis; the HOG entropy values are found to stabilize and flatten after the printing of four layers above any target layer. But in the case of layers L21 and L22 of element B, the HOG textural variations are not found to stabilize even after the printing of four layers above it. It is due to the presence of minor voids in the layers. Hence, if the HOG textural variations are not found to stabilize within a few printed layers, then it indicates the presence of voids or the failure of buildability properties. A detailed study of buckling is outside the scope of this study. The developed methodology is intended to provide early indications of buildability issues. This study can be used to monitor and assess the buildability properties of 3DP concrete during the printing process.

5 Conclusion

A quality control and assessment technique for concrete 3D printed elements based on computer vision has been developed in this study. Using continuous monitoring, several possible defects leading to wastage in terms of cost, materials, and time are avoided, reinforcing the sustainability aspects of concrete 3D printing technology. The variations in the surface texture of the concrete due to the reduction in workability or moisture content are analyzed using 2D images taken through a camera. The main contribution of this study is the introduction of a new algorithm for texture extraction based on the concept of Histogram of Oriented Gradients (HOG). This algorithm uses multiple threshold levels to capture minor and major textural variations. Also, the normalized weighted texture value of the distribution is found to be an appropriate metric to quantify the textural variations. This metric is found to have higher values for layers having voids. Also, the values increase as the granularity of the layers increases resulting in a reduction in workability. Further, a temporal changes study is also conducted for an individual layer to understand the variations within the layer due to the buildability properties. The significant conclusions obtained from this study are as follows,

- A continuous, non-intrusive method to monitor the temporal changes in the extrudability properties of 3D printing concrete has been achieved.
- The newly developed method is less sensitive to variations in illuminance levels. The normalized weighted texture minimizes the influence of differential brightness/illumination changes.
- Results show that the defects and voids present in the 3DP layers can be autonomously detected.
- An inverse correlation is observed between the normalized weighted texture value and the workability over time. This means that the workability properties of concrete can be indirectly quantified using texture data.
- Temporal textural variation study helps in indirectly assessing the buildability properties. The changes in layer thickness can be correlated to the changes in the textural variations.

Results prove the feasibility of using computer vision-based texture extraction methods for quality monitoring of 3D printed elements. Further, the quality assessment obtained can be used as feedback to the printing system to control the printing parameters like extrusion and printing speed to achieve a better-quality print. Increasing the extrusion speed will help in making the concrete material shear and flow continuously without voids and discontinuities. As a result, a change in the normalized weighted texture value can be used as

feedback to the printing system for taking corrective actions to avoid material wastage and achieve high-quality output. The study opens many opportunities to extract useful information from non-intrusive based sensor data collected to help the sustainability aspects of 3D printing technology.

References

- [1] M. Hoffmann, S. Skibicki, M. Techman, Automation in the Construction of a 3D-Printed Concrete Wall with the Use of a Lintel Gripper, (2020). <https://doi.org/10.3390/ma13081800>.
- [2] R. Buswell, P. Kinnell, J. Xu, N. Hack, H. Kloft, M. Maboudi, M. Gerke, P. Massin, G. Grasser, R. Wolfs, F. Bos, Inspection Methods for 3D Concrete Printing, RILEM Bookseries. 28 (2020) 790–803. https://doi.org/10.1007/978-3-030-49916-7_78.
- [3] A. Kazemian, X. Yuan, O. Davtalab, B. Khoshnevis, Automation in Construction Computer vision for real-time extrusion quality monitoring and control in robotic construction, Autom Constr. 101 (2019) 92–98. <https://doi.org/10.1016/j.autcon.2019.01.022>.
- [4] Y. Zhang, Y. Zhang, W. She, L. Yang, G. Liu, Y. Yang, Rheological and harden properties of the high-thixotropy 3D printing concrete, Constr Build Mater. 201 (2019) 278–285. <https://doi.org/10.1016/j.conbuildmat.2018.12.061>.
- [5] S. Ahmed, S. Yehia, Evaluation of Workability and Structuration Rate of Locally Developed 3D Printing Concrete Using Conventional Methods, Materials. 15 (2022). <https://doi.org/10.3390/ma15031243>.
- [6] S. Senthilnathan, B. Raphael, Using Computer Vision for Monitoring the Quality of 3D-Printed Concrete Structures, Sustainability (Switzerland). 14 (2022). <https://doi.org/10.3390/su142315682>.
- [7] A. Oleff, B. Küster, M. Stonis, L. Overmeyer, Process monitoring for material extrusion additive manufacturing: a state-of-the-art review, Progress in Additive Manufacturing. (2021) 23–27. <https://doi.org/10.1007/s40964-021-00192-4>.
- [8] O. Davtalab, A. Kazemian, X. Yuan, B. Khoshnevis, Automated inspection in robotic additive manufacturing using deep learning for layer deformation detection, J Intell Manuf. (2020). <https://doi.org/10.1007/s10845-020-01684-w>.
- [9] R. Rill-García, E. Dokladalova, P. Dokládál, J.-F. Caron, R. Mesnil, P. Margerit, M. Charrier, Inline monitoring of 3D concrete printing using computer vision, Addit Manuf. 60 (2022) 103175. <https://doi.org/10.1016/j.addma.2022.103175>.
- [10] B. Shantanu, J. Smrati, S. Manu, Criticality of binder-aggregate interaction for buildability of 3D printed concrete containing limestone calcined clay, Cem Concr Compos. 136 (2023) 104853. <https://doi.org/10.1016/j.cemconcomp.2022.104853>.
- [11] L. Armi, S. Fekri-Ershad, Texture image analysis and texture classification methods - A review, 2 (2019) 1–29. <http://arxiv.org/abs/1904.06554>.

Digital twins of bridges: notions towards a practical digital twinning framework

Kamil Korus¹, Marek Salamak¹ and Jan Winkler²

¹Department of Mechanics and Bridges, Silesian University of Technology, Poland

²Digital Engineering Solutions, Poland

kamil.korus@polsl.pl, marek.salamak@polsl.pl, j.winkler@de-solutions.info

Abstract

Digital twins, the virtual counterparts of objects throughout their life cycle, are a crucial component of ongoing digitization. While the civil engineering community has already recognized the advantages of utilizing digital twinning, there is still a lack of comprehensive research in the field, resulting in uncertainties. This article proposes a set of notions regarding digital twins of bridges – structures of logistic and strategic importance and high demands of resilience. By stating the principles for comprehensive digital twinning, the notions can guide practical applications of digital twins of bridges and other civil engineering facilities.

Keywords –

Digital twins, Digitization, Bridges, Building Information Modeling

1 Introduction

Digital twins are virtual counterparts of objects throughout their life cycle. First implemented by NASA, today are contributing to multi-industrial digitization, reported as a crucial component of Industry 4.0. The benefits of digital twinning have been spotted by many industries, including civil engineering. It resulted in increasing research interest and work by practitioners [1]. Although ongoing works are promising, the digital twinning concept is still nascent in civil engineering practice. Both theoretical principles and practical use cases are required to push the concept of civil engineering digital twins.

1.1 Digital twins in civil engineering

At the current stage of digital twinning development, the research is double-track, also in civil engineering. Some activities focus on theoretical frameworks and principles for applying digital twins ([2], [3]); others on practical use cases.

The first civil engineering applications of digital

twins utilize modern techniques like BIM (Building Information Modeling), SHM (Structural Health Monitoring), 3D reconstruction, and AI (Artificial Intelligence). The techniques are often integrated to provide additional benefits. BIM models can be used to visualize SHM sensor data [4]. FEM models can be synthesized with monitoring data to reconstruct unmonitored structure responses [5]. Artificial intelligence helps in managing the fatigue of steel bridges [6]. Point clouds can be a source for the automated generation of semantic models [7].

The use of these techniques is a positive trend. Due to the fast development (in the field of, e.g., computer vision and data acquisition equipment [8], automated model generation [9], and machine learning [10]), the techniques are increasingly popular and useful. The current applications make a foundation for complex digital twinning. Nonetheless, still more activities are required for applying complete digital twins in the form of intelligent management systems coexisting with real facilities through their entire life cycle and cooperating with other instances in the digital space.

1.2 Research motivation: the need for digital twins of bridges

Activities on digital twins of bridges are motivated by both requirements and opportunities of the nowadays world and challenges in bridge engineering. The following sections discuss why this area should be a subject of thorough research.

1.2.1 Digital twins as the enabler of effective functioning

Industries must adapt to the requirements and demands of the nowadays world to function effectively both in the business and technological sense. The process of adaptation forces applying new techniques to benefit from technical innovations. Adopting digital twinning is challenging. However, as a worldwide trend, it connects its adopters to multi-industrial cooperation, giving instant and long-term profits.

The digital era facilitates collaboration. Industries have become more interdisciplinary, adapting foreign practices and tools. The trend also leads to multi-industrial standardization. Cross-sectoral written standards and versatile data exchange formats (e.g., JSON, XML) are already used. As industries become more interdisciplinary, models of different assets will collaborate more, similar to their physical counterparts. Cooperation between digital twins will be based on standardized data exchange interfaces. The collaboration will open opportunities for the adapted – and exclude technical laggards.

Modern techniques increase the effectiveness of whole industries but are also beneficial on a smaller scale. BIM is already proven to provide commercial advantages for contractors. BIM is expected to provide “new markets, new services, new business models, new entrants. [11]” BIM, a technical innovation, is seen as an export product, increasing the competitiveness of the national market. The same reasoning, on the interdisciplinary scale, applies to digital twinning.

1.2.2 The impact and challenges of bridge engineering

Bridges, similar to other objects, have specific factors, characteristics, requirements, and context of operation. These should be regarded in conceptualizing specified frameworks, including the digital twinning framework. This section analyzes the features of bridges and the challenges of bridge engineering.

The first factor is the strategic role of bridges. Infrastructure systems provide essential services for the proper functioning of societies [12]. As links between the infrastructure, bridges are indispensable for logistics. Historically, they have also been crucial from a military perspective. Due to these, bridges have always been a strategic component of societies’ wealth. This wealth is not easy to assess, but some numbers are helping in the realization of scale. Only in the USA are there 619 thousand bridges [13]. One of them, the San Francisco Oakland Bay Bridge, appears in the Guinness Book as the most expensive bridge. Just the restoration in 2002 is estimated at 6.3 billion USD.

Safety is – or should be – an indispensable characteristic of bridges. Bridges need to be resilient due to their strategic role and the impact of their malfunctions, which can have a direct influence on people’s lives and an indirect influence on economies. The infamous catastrophes of Ponte Morandi in Genua in 2018 (with 43 killed), the Mexico City Metro overpass in 2021 (with 26 killed), and the Julto Pul pedestrian bridge in Morbi, India, in 2022 (with 135 killed) convince that bridges’ collapses are not just an imaginary black scenario.

A nontrivial part of the civil infrastructure is aging

and suffering from alarming deterioration [12]. It also regards bridges. Of the mentioned USA bridges, 224 thousand require major repair work or replacement [13]. Due to the need for safety, bridges must be adequately monitored and maintained. Nonetheless, bridges’ condition assessment still relies mostly on periodic human inspections. The aging bridges require holistic management solutions, especially given their assumed lifespan: many bridges are designed for 100 years.

The modern world aims at new goals; one of them is ecology. The construction and operation of buildings were responsible for 36% of global energy demand and 37% of energy-related CO₂ emissions in 2020 [14]. The ecological factors already influence civil engineering – advanced Life Cycle Assessment (LCA) regarding economic, social, and environmental costs are already being required.

Civil engineering makes up around 15% of the world’s Gross Domestic Product [15]. Although of high impact, civil engineering is ineffective compared to other sectors: since World War II, productivity in manufacturing, retail, and agriculture has grown by around 1500%, but productivity in civil engineering has nearly not changed [16]. As estimated, civil engineering productivity can be increased by 50-60% [16]. This margin is a business motivation for the implementation of modern solutions.

Bridges are complex and unique. The need for liaison with the environment results in various structural, material, and manufacturing solutions. Even if bridges are of typical structure, their uniqueness comes from the different conditions in which they operate – the same structure influenced by different phenomena throughout its life cycle can have noticeably different characteristics. The uniqueness and complexity of bridges demand thorough monitoring and analysis.

1.3 Scope of the article

Activities on digital twins of bridges must be based on principles regarding the general concepts of digital twins and the specificity of bridges and civil engineering. Therefore, this article proposes a set of notions regarding digital twins of bridges. By stating the principles for comprehensive digital twinning, the notions can guide practical applications for bridges and other civil engineering facilities. The notions have been formulated based on the literature study, as well as the original research and experience of the authors. The studied articles regard general concepts of digital twins and their practical applications in various fields, with a particular focus on civil engineering and bridges. The studied articles also regard accompanying techniques (e.g., computer vision, artificial intelligence, data analysis, Internet of Things). The study also comprised reports of industrial companies and associations.

2 Notions towards digital twinning of bridges

2.1 Digital twins' frameworks should be object-specific

Digital twinning encompasses various industries and types of objects – such different as bridges and livers [17]. Various industries have different requirements and aims; various objects have different characteristics. Digital twins need to be based on general standards to enable cooperation. At the same time, the standards must be flexible enough to enable reflecting the specificity of the twinned object. It resulted in the specified digital twinning frameworks for, e.g., shop floors [18], air force [19], and cities [20].

The frameworks are attempts to adapt digital twinning principles to serve specific objects. The frameworks also discuss the strategy of implementation. The strategy is crucial because digital twins need to be industry applicable to develop as a concept (section 2.10). Therefore, the digital twin frameworks should regard not only the specificity of the object but also its industrial environment – for example, the industry's ability and willingness to implement new techniques. All industries, including civil engineering, must declare dedicated digital twinning frameworks based on general principles but suited to the specificity.

The specificity of frameworks should also be considered on a more granular level. Bridges can be classified regarding many features, e.g., structural solution (e.g., beam, arch, suspension), material (e.g., concrete, steel, timber), and function (e.g., road, rail, pedestrian). These aspects influence the bridge's response to loads, resilience to environmental factors, risks, damages, and maintenance during its life cycle. A bridge's complexity, costs, and logistic importance also influence its management. Therefore, the digital twinning frameworks should be flexible to enable attaching functionalities serving particular needs (e.g., complex numerical analysis for bridges under dynamic loads, extended maintenance planning for bridges of high costs and logistics importance). This is especially important in the initial stage of implementing digital twins when, due to practical obstacles and implementation costs, instances are not fully-functional digital twins but have selected functionalities.

Many current digital twin applications focus on bridges of high complexity (e.g., cable-stayed bridges with a span of 950 m length [21]) or under unusual conditions (e.g., strong earthquakes [22]). This is a positive trend. Nonetheless, also the structures of common types can benefit from digital twinning. Additionally, the idea of smart cities demands the virtualization of most infrastructure. Therefore, creating

frameworks for typical structures (like concrete beam and slab bridges (one of the most popular solutions for existing and planned bridges [23]) should be a priority.

2.2 Ultra-high fidelity is not always required

The early digital twins' definitions envisioned "ultra-high fidelity" [24] simulations of the physical counterpart; the physical object was to be reflected starting from the "micro atomic level" [25]. The definitions were established when digital twin was just an idea, unable to be implemented due to technical limitations. More recent definitions are less strict, orienting on practice.

Undoubtedly, micro-atomic fidelity opens new scientific possibilities; e.g., the simulations regarding the micro-atomic structure of a material, instead of its averaged properties, may clarify unexplainable phenomena. But current modeling techniques are not prepared for such fidelity, nor simulation tools to consume such data. BIM methodology describes model accuracy with the Level of Detail or Level of Development (LOD). BIM projects in practice are in LOD 200-350, frequently starting on a lower level to gradually increase during the project. It would be hard – and unproductive – to demand the highest LOD 500 if a lower one enables effective performance.

"A digital twin must represent a physical reality at a level of accuracy suited to its purpose [11]." Ultra-high fidelity is the ultimate aim for the future. However, the approach of gradually increasing the fidelity of digital twins, following the abilities of modeling and simulation tools, is practically beneficial today.

2.3 Data synchronization does not need to be perfect

Similarly to "ultra-high fidelity", the early digital twin visions demanded "real-time synchronization" [26]. Indeed, latency is crucial in some cases, but others may operate properly with a lower synchronization rate. In practice, the synchronization rate should be established regarding how dynamically the decisions based on in-time data must be made.

Consider examples of an autonomous car and a bridge. The car is continually affected by its environment: the temperature affects tire pressure and the windshield misting. The environment also drives the car's operating parameters: the weather and road conditions are factors for setting the driving speed. Most importantly, for the car, dynamic changes in the environment require dynamic decision-making. When a pedestrian unexpectedly enters the road, the one-second latency between registering the event and making a decision can result in a crash. The bridge is also continually affected by its environment. Although the

changes are typically not observable with a bare eye, bridges continually respond to the loads from vehicles, wind, or temperature. However, the bridge is not adjusting its parameters to the dynamic events – decisions about bridges are typically not made in an in-time fashion. Thus, synchronization latency can be higher.

A digital twin comprises different sources of data, e.g., SHM sensors and point clouds. These sources of data vary in their acquisition rate. The sensors can collect data almost continually, so the digital twin can be continually updated with its data. On the other hand, acquiring point clouds is a periodical task – given the pace of geometry changes in civil engineering facilities, typically, annual actualization is sufficient. The source and type of data affect the synchronization rate.

Undoubtedly, the lower latency, the better since it gives new opportunities. Considering the future communication between digital twins, an approaching car sends an introductory data package to the bridge; if the car is suspected of causing damage to the structure, the bridge may obstruct the car's passage. In-time decision-making, possible with in-time data, is beneficial for all kinds of objects. But, in some cases, it is not essential. The synchronization rate affects the digital twin's implementation costs. High upfront costs of in-time synchronization may result in neglecting the digital twinning concept. Therefore, starting with lower synchronization is acceptable from a practical perspective.

2.4 Digital twin should not neglect any data freely

After two notions lightening the strict rules (“ultra-high fidelity is not always required” and “data synchronization does not need to be perfect”), this one is to balance into complex implementations.

Data is the raw material of the XXI century [27] and gives advantages to its possessors. Data-driven techniques have vast applications in business and industrial practice. In science, they complement or displace traditional calculating theories. The data-driven algorithms need data to be trained and tuned. But not only the amount and quality of data affect algorithms operation – also the diversity of data features. GPT-3, a natural language processing algorithm, is based on 175 billion input features [28]. Many AI practitioners are even stating that proper data from various sources and of various characteristics are more important for the effectiveness of the AI systems than the algorithms architectures [29] (i.e., a weak algorithm trained on strong data is preferred from a strong algorithm trained on weak data).

Existing calculating theories enable engineering practice, but it is arrogant to think that we already have

understood the majority of phenomena. Perhaps new calculating theories based on data-driven techniques will disclose new, currently omitted patterns. Perhaps the new theories will be based on data that today seem useless.

Digital twinning prepares to solve engineering tasks in the future phases of the object life cycles. Due to stored data and learned patterns, the questions can be of a type that has not been initially thought of [30]. Therefore, data prepares for the expansibility of digital twins' features to match future industrial requirements.

Storing all data is practically not possible, but continually cheaper storage and new filtering algorithms help in extensive data-collecting. In the design of the digital twins' systems, data should not be neglected freely – if it is possible to collect additional data with the designed methods, it should be done.

2.5 Digital twin should provide interfaces to work with the data

The multitude of data is beneficial for data-driven algorithms but can be overwhelming for humans. The famous Buckminster Fuller's knowledge-doubling curve predicted the increasing pace of knowledge production, eventually leading to knowledge doubling every 12 hours [31]. Humans are not adapted to that pace. The “drowning in data” [32] syndrome affects people's effectiveness.

Digital twins are data-rich models. The multitude of data is utilized by the algorithms, but people also should have access to the insights. It should be provided with proper user interfaces.

Interfaces are essential in industrial practice. They are the linkers between users and complicated systems. User interfaces perform various roles: on commercial websites, they attract visitors to convert them into customers; in specialized systems, they provide access to operation details and enable management. In digital twins, the interfaces should present historical, current, and predicted performance in an easily interpretable way. Due to data-processing techniques, the performance can be presented not as raw data but as more consumable information or knowledge. Based on the data, intelligent algorithms may even suggest a decision – this is the ultimate step of automating data interpretation.

Also, data interfaces allow segregating data access. Different users of digital twins are focused on different areas, e.g., not the same data should be provided for designers, construction site workers, managers, or users of bridges. This is important both for security and productivity.

A digital twin is a data-rich system that must provide benefits from data rather than just store it. Therefore, properly designed user interfaces – in various forms –

are essential in digital twinning.

2.6 Digital twin includes processes

Models are typically expected to store data about objects. The data-richness depends on the model type: CAD models store geometric data, while BIM models also include semantics. The semantics enable advanced analysis but are insufficient for a thorough description of a reflected object. For civil engineering facilities, knowledge about the expected response to loads or environmental factors is crucial for management. But just like the behavior of a person cannot be predicted based merely on his/her appearance, the response of an object cannot be predicted based only on semantic data. To utilize its potential, a digital twin must include not only semantics but also processes.

Digital twins include past processes by storing historical performance data. The data is processed by machine learning algorithms to distill patterns. The patterns represent the object's behavior and act as the "process knowledge" – based on that, the algorithms predict future performance.

The historical performance of a bridge is driven not only by explicit parameters (e.g., geometry, materials) but also by elusive factors (e.g., environment) – the one-object-dedicated patterns implicitly comprise also this elusive data. Such a dedicated approach leads to more accurate predictions than those based on generalizations [33]. Eventually, the developing sensing techniques will enable measuring the today-elusive factors and implement them as explicit features of global machine learning algorithms, perhaps displacing the dedicated solutions. However, even then, the dedicated patterns will be beneficial to understand the responses of an object. Processes – both historical performance, represented by data, and future expectations, represented by patterns - are indispensable components of digital twins.

2.7 Digital twin is intelligent, autonomous

Artificial intelligence is becoming a standard automation solution, also in civil engineering [10]. Digital twins are compatible with various machine learning algorithms. As a big data system, the digital twin allows the training of supervised algorithms, the most common type of ML algorithms so far. As a simulation environment, the digital twin also allows the development of unsupervised algorithms, e.g., reinforcement learning types, that are increasingly more popular and powerful.

With intelligent algorithms, the digital twin gains autonomy. Autonomy can be on various levels. The first is giving suggestions. A digital twin can analyze physical counterpart conditions and present improving

suggestions, e.g., a bridge digital twin may report a need for additional inspection or maintenance works. On this first level, the suggestions enhance human decision-making. On the next autonomy level, the suggestions are transformed into executable decisions. A digital twin of an autonomous car interprets data from its physical counterpart's sensors. The decisions resulting from actual conditions must be executed instantly and autonomously, with no human operator confirmation.

The digital twinning concept reveals an additional level of autonomy. A digital twin cooperates with other digital twins (Social Internet of Things [34], Web-of-things [35], or Social Internet of Vehicles [36] attempt to establish rules for this cooperation). With such partnership abilities, intelligent algorithms may consider the actual conditions of the collective, not only a single instance. This is beneficial for the whole group – if two cars spot a danger, but both choose the same escape path, the crash is inevitable. Therefore, digital twins communicate to make shared decisions. This is another level of autonomy when a digital twin, besides managing itself, influences others.

2.8 Digital twin is a system

A digital twin is often perceived as a single model. In civil engineering, this perception may emerge from BIM. BIM shares many features with digital twinning, so the digital twin is sometimes incorrectly perceived as a more advanced version of the BIM model. But although the model is the center of the digital twinning concept, a digital twin is more than a model – it is a system. This statement is validated on various levels.

Modularity is one of the digital twins' characteristics. The digital twin's modules are chosen regarding the specificity of the object and technical maturity. The modules may require specific submodels to perform analyses (e.g., a bridge structural response module may need a FEM model). The submodels derive from the central model and data storage, so they are based on concise, actual data. The submodels are used for specific tasks (e.g., structural analysis, scheduling, cost estimations, visualization) and, therefore, expand the abilities of the whole digital twin. The digital twin is a system of modules, while the central model and its derivatives form a complementary system of models.

Digital twins operate on data beyond the typical model-stored type (e.g., big data from SHM sensors is likely to be stored in dedicated databases). Digital twins also include interfaces (section 2.5). Digital twins' submodels cooperate with themselves and the central model. All of these factors lead to extensive infrastructure orchestrating digital twins functioning. The infrastructure links the digital twinning components and establishes the digital twin system.

Digital twins, with their interoperable abilities,

establish systems with other digital twins. The cooperation can be at parallel or subordinate levels. A digital twin can represent an object big as a planet [37] or small as a microchip. The complex digital twins comprise subordinate digital twins: a digital twin of a smart city may contain a bridge digital twin, which may contain digital twins of its sensors. The complexity of these connections transforms a digital twin into a system of systems.

2.9 Digital twins enable dedicated approaches

Currently, data about bridges' behavior (e.g., load responses) is rarely collected in their normal state; monitoring is usually applied when a structure already shows signs of malfunctioning. Having insufficient data about the particular object, we cannot establish dedicated patterns – the object's state is assessed based on a generalization determined by other objects' data. But the normality of one object does not necessarily match the normality of the other. This statement is a basis for the digital twinning approach of personalized medicine: discovering individual patterns, varying with biophysical and lifestyle factors, allows determining optimal ranges of health indicators (e.g., blood pressure), which may differ from standard population-based values [38]. Bridges, even of similar parameters (geometry, materials), are affected by different conditions (environment, climate, soil, loads). Relying on generalizations may lead to omitting factors and dependencies affecting the particular object.

Digital twinning establishes unique big-data systems for every object. It enables a dual approach. Individualized intelligent algorithms, looking for dependencies and patterns of the particular object, enable analyzing and forecasting. Global algorithms, operating on multiple objects' data, are an additional layer of security. If the normality of one object strongly differs from the global pattern, it will be detected; it can be an indicator of the initial malfunction. Digital twinning enables learning objects empirically – observing how inputs affect outputs and understanding better the processes.

2.10 Digital twins must provide practical benefits

Siemens's report on digital twins in buildings' life cycle states: "a pressing concern for possibly any company that starts on the journey to digitization could be the clear ability to show benefits and realize value from its investment in creating a digital twin [1]." The report focuses on the importance of the transparent benefits resulting from the implementation of digital twins. The ways to provide benefits must be addressed in establishing digital twinning frameworks.

Digital twins have been born and raised in the scientific environment [25], but only wide industrial applications can reveal their full potential. Digital twinning frameworks should address scientific requirements (e.g., proper fidelity and synchronization rate) while also balance them with implementation costs. Indeed, there is no point in demanding ultra-high detailing if it will lead to only scientific applications and neglecting the digital twinning concept in industrial practice.

Digital twinning frameworks must show clear premises of returns on implementation investment. The returns can be in various forms: limiting economic and social costs in the life cycle; automating design, manufacturing, and maintenance; increasing the effectiveness of management. Also, the human factor should be considered: digital twinning will be demanded if it will enhance the day-to-day tasks of designers, construction site workers and engineers, and managers. Therefore, besides theories and standards, digital twinning research – both scientific and industrial – must provide practical use cases, e.g., advanced simulation and modeling, automation of manufacturing, and effective management decision-making. This bottom-up approach fuels the practical development of the digital twinning concept.

3 Conclusions

Technical advances come from demand and opportunities. Digital twins originated as a concept for handling the pressing requirements of digitization, but initially, due to technological limitations, the concept was impossible to implement. Today, however, technical advances open gates for digital twinning practice. It requires thorough digital twinning research. This article states notions towards digital twinning focusing on bridges, applicable also to other civil engineering facilities. The notions form foundations for establishing frameworks for civil engineering digital twins.

Civil engineering is still in the early stages of digital transformation. Nonetheless, BIM, one of the main civil engineering transformation representatives, is already utilized. BIM implementation comes from both top-down and bottom-up approaches. In top-down, BIM is required by national laws (often for public investments, as in the United Kingdom, Norway, or Singapore), and companies must adapt. In the bottom-up approach, BIM is not required, but its benefits are spotted by commercial companies and implemented to increase effectiveness. This trend is increasingly popular. Potentially, technological possibilities coming from digital twinning may convince practitioners to complex digital twinning and fuel digital twins' implementations.

The need for the technological step – from BIM to digital twins – has been spotted by countries leading in civil engineering digitization. Centre for Digital Built Britain announced the idea of National Digital Twin [11], an ecosystem of digital twins connected to share data. The motivation for The National Digital Twin are expected benefits: data-sharing in construction will save 20-30% industrial costs; holistic management will strengthen infrastructure resilience; an increase in innovations will open new markets. Centre for Digital Built Britain forecasts almost 100 million IoT (Internet of Things) connections in the infrastructure sectors by 2024; these devices will need to cooperate based on multi-industrial standards, like digital twinning.

Civil engineering needs digital twinning to not stay a technical laggard. Digital twinning will open civil engineering to the best multi-industrial practices and enables the digital partnership of civil engineering facilities and other objects. This is especially important for bridges that in the smart cities will act as connectors of smart infrastructure. Therefore, it is the right time to research possibilities, form practices, and establish frameworks for civil engineering digital twinning.

3.1 Limitations and resulting future work

The proposed notions regard the foundations for the digital twinning of bridges but do not resolve all the issues of practical implementations. It leads to the identification of future work paths. Future research should aim to concretize the recommendations to answer specific questions. What should be synchronization rates for various data sources? How should the user interfaces be designed? Which new and emerging technologies should be integrated? Digital twinning encompasses broad multi-domain areas; every aspect requires thorough, interdisciplinary research. The next step is the creation of practical use cases based on the proposed principles to induce designers, engineers, and managers of infrastructure to adopt digital twinning.

Acknowledgments

The work was supported by the European Social Fund (POWR.03.05.00-00-Z305).

References

- [1] Siemens, Digital twin - Driving business value throughout the building life cycle, 2018. [Online].
- [2] Sacks R.Brillakis I.Pikas E.Xie H. S.and Girolami M., Construction with digital twin information systems, *Data-Centric Engineering*, vol. 1, no. December, 2020,
- [3] Boje C.Guerriero A.Kubicki S.and Rezgui Y., Towards a semantic Construction Digital Twin: Directions for future research, *Automation in Construction*, vol. 114, no. January, 103179, 2020,
- [4] Ye C. *et al.*, A digital twin of bridges for structural health monitoring, *Structural Health Monitoring 2019: Enabling Intelligent Life-Cycle Health Management for Industry Internet of Things (IIOT) - Proceedings of the 12th International Workshop on Structural Health Monitoring*, vol. 1, no. September, 1619–1626, 2019,
- [5] Yu S.Li D.and Ou J., Digital twin-based structure health hybrid monitoring and fatigue evaluation of orthotropic steel deck in cable-stayed bridge, *Structural Control and Health Monitoring*, vol. 29, no. 8, 7–13, 2022,
- [6] Jiang F.Ding Y.Song Y.Geng F.and Wang Z., An Architecture of Lifecycle Fatigue Management of Steel Bridges Driven by Digital Twin, *Structural Monitoring and Maintenance*, vol. 8, no. 2, 187–201, 2021,
- [7] Lu R. and Brillakis I., Digital twinning of existing reinforced concrete bridges from labelled point clusters, *Automation in Construction*, vol. 105, no. May, 102837, 2019,
- [8] Spencer B. F.Hoskere V.and Narazaki Y., Advances in Computer Vision-Based Civil Infrastructure Inspection and Monitoring, *Engineering*, vol. 5, no. 2, 199–222, 2019,
- [9] Czerniawski T. and Leite F., Automated digital modeling of existing buildings: A review of visual object recognition methods, *Automation in Construction*, vol. 113, no. July 2019, 103131, 2020,
- [10] Paresh Chandra Deka, *A Primer on Machine Learning Applications in Civil Engineering*. CRC Press, 2019. doi: <https://doi.org/10.1201/9780429451423>.
- [11] Bolton A, Enzer M S. J. et al., The Gemini Principles, *Centre for Digital Built Britain: University of Cambridge*, 15, 2018,
- [12] Broo D. G. and Schooling J., Digital twins in infrastructure: definitions, current practices, challenges and strategies, *International Journal of Construction Management*, vol. 0, no. 0, 1–10, 2021,
- [13] ARTBA, Bridge Report 2022, 2022. [Online].
- [14] Global Alliance for Buildings and Construction, Global Status Report 2021 For Buildings and Construction: Towards a Zero-emission, Efficient and Resilient Buildings and Construction Sector, 2021.
- [15] Pan Y. and Zhang L., Roles of artificial intelligence in construction engineering and management: A critical review and future trends, *Automation in Construction*, vol. 122, 103517,

- 2021,
- [16] Barbosa F. *et al.*, Reinventing Construction: A Route To Higher Productivity, *Mckinsey Global Insititute*, no. February, 20, 2017,
- [17] Subramanian K., Digital Twin for Drug Discovery and Development—The Virtual Liver, *Journal of the Indian Institute of Science*, vol. 100, no. 4, 653–662, 2020,
- [18] Tao F. E. I. and Zhang M., Digital Twin Shop-Floor: A New Shop-Floor Paradigm Towards Smart Manufacturing, *IEEE Access*, vol. 5, 20418–20427, 2017,
- [19] Kraft E. M., The US air force digital thread/digital Twin – life cycle integration and use of computational and experimental knowledge, *54th AIAA Aerospace Sciences Meeting*, vol. 0, no. January, 1–22, 2016,
- [20] Deng T.Zhang K.and Shen Z. J. (Max), A systematic review of a digital twin city: A new pattern of urban governance toward smart cities, *Journal of Management Science and Engineering*, vol. 6, no. 2, 125–134, 2021,
- [21] Sofia H.Anas E.and Faiz O., Mobile mapping, machine learning and digital twin for road infrastructure monitoring and maintenance: Case study of mohammed VI bridge in Morocco, *Proceedings - 2020 IEEE International Conference of Moroccan Geomatics, MORGEO 2020*, 2020,
- [22] Lin K.Xu Y. L.Lu X.Guan Z.and Li J., Digital twin-based collapse fragility assessment of a long-span cable-stayed bridge under strong earthquakes, *Automation in Construction*, vol. 123, no. September 2020, 103547, 2021,
- [23] Kim M. K.McGovern S.Belsky M.Middleton C.and Brilakis I., A Suitability Analysis of Precast Components for Standardized Bridge Construction in the United Kingdom, *Procedia Engineering*, vol. 164, no. June, 188–195, 2016,
- [24] Reifsnider K. and Majumdar P., Multiphysics stimulated simulation digital twin methods for fleet management, *Collection of Technical Papers - AIAA/ASME/ASCE/AHS/ASC Structures, Structural Dynamics and Materials Conference*, 1–11, 2013.
- [25] Grieves M. and Vickers J., Digital twin: Mitigating unpredictable, undesirable emergent behavior in complex systems, *Transdisciplinary Perspectives on Complex Systems: New Findings and Approaches*, no. August, 85–113, 2016,
- [26] Negri E.Fumagalli L.and Macchi M., A Review of the Roles of Digital Twin in CPS-based Production Systems, *Procedia Manufacturing*, vol. 11, no. June, 939–948, 2017,
- [27] Alcácer V. and Cruz-Machado V., Scanning the Industry 4.0: A Literature Review on Technologies for Manufacturing Systems, *Engineering Science and Technology, an International Journal*, vol. 22, no. 3, 899–919, 2019,
- [28] Brown T. B. *et al.*, Language models are few-shot learners, *Advances in Neural Information Processing Systems*, vol. 2020-Decem, 2020.
- [29] Chip Huyen, *Designing Machine Learning Systems: An Iterative Process for Production-Ready Applications*. O’Reilly Media, 2022.
- [30] Boschert S. and Rosen R., Digital Twin - The Simulation Aspect, in *Mechatronic Futures: Challenges and Solutions for Mechatronic Systems and Their Designers*, Springer International Publishing, 2016, 59–74. doi: 10.1007/978-3-319-32156-1.
- [31] Fuller B., *Critical Path*. St. Martin’s Press, 1981.
- [32] Remund D. and Aikat D. “Deb,” Drowning in Data: A Review of Information Overload within Organizations and the Viability of Strategic Communication Principles, in *Information Overload*, Hoboken, NJ, USA: John Wiley & Sons, Inc., 2012, 231–250. doi: 10.1002/9781118360491.ch11.
- [33] Gkouskou K.Vlastos I.Karkalousos P.Chaniotis D.Sanoudou D.and Eliopoulos A. G., The “virtual Digital Twins” Concept in Precision Nutrition, *Advances in Nutrition*, vol. 11, no. 6, 1405–1413, 2020,
- [34] Atzori L.Iera A.Morabito G.and Nitti M., The social internet of things (SIoT) - When social networks meet the internet of things: Concept, architecture and network characterization, *Computer Networks*, vol. 56, no. 16, 3594–3608, 2012,
- [35] Guinard D.Fischer M.and Trifa V., Sharing using social networks in a composable Web of Things, *2010 8th IEEE International Conference on Pervasive Computing and Communications Workshops, PERCOM Workshops*, 702–707, 2010,
- [36] Alam K. M.Saini M.and El Saddik A., tNote: A Social Network of Vehicles under Internet of Things, in *Internet of Vehicles – Technologies and Services*, 2014, 227–236. doi: 10.1007/978-3-319-11167-4_23.
- [37] Bauer P.Stevens B.and Hazeleger W., A digital twin of Earth for the green transition, *Nature Climate Change 2021 11:2*, no. 2, 80–83, 2021,
- [38] Bruynseels K.de Sio F. S.van den Hoven J.Sio F. S. Deand Hoven J. Van Den, Digital Twins in health care: Ethical implications of an emerging engineering paradigm, *Frontiers in Genetics*, vol. 9, no. FEB, 1–11, 2018,

Marker-based Extrinsic Calibration for Thermal-RGB Camera Pair with Different Calibration Board Materials

Bilal Sher, Xuchu Xu, Guanbo Chen, and Chen Feng

Tandon School of Engineering, New York University, USA

bas9876@nyu.edu, xx762@nyu.edu, gc2720@nyu.edu, cfeng@nyu.edu

Abstract -

UAVs are used to rapidly and safely collect site data for engineering purposes. Thermal and RGB imagery are often captured for building envelope inspections. On large sites, the data produced can be cumbersome to process, especially if taken in a video format. This paper presents a way to perform image registration, or low-level data fusion, on thermal and RGB images that were simultaneously captured from rigidly fixed cameras - the same type as those found on commercial RGB-Thermal UAVs. The intention is to convert raw captured data into RGB-Thermal tensors that can be used in deep learning applications. Current techniques of geometrically calibrating a thermal camera can include complicated setups that make calibration at extreme angles difficult. Three calibration boards were involved in testing this image registration method: a cardboard and acrylic board, a wood and vinyl board, and a metal and vinyl board. Of the three, only the metal and vinyl calibration board yielded a consistent image, regardless of the time passed between the first and last captured image. This proves that calibration can be conducted cheaply and in any open area without obstructions.

Keywords -

UAVs; Thermal Imagery; Building Envelopes; Data Preparation;

1 Introduction

Thermal cameras are valuable tools for building envelope energy analysis, but they frequently produce distorted images that must be geometrically calibrated before use in computer vision applications like deep learning segmentation networks (See Figure 1).

Image segmentation can be done in multiple ways, including using a deep learning model that accepts two uncalibrated tensors as input. However, this approach requires significant training data to generalize to other drones and camera setups. The workaround is to undistort and align the images into a single tensor with the same field of view. Undistortion is necessary to ensure accurate recognition of shapes across different camera types and different areas of the image. Distortion affects different parts of the image differently; with fisheye lens distortion significantly affects the edges more than the center. Accounting for information from all portions of the image is crucial when automating computer vision tasks.

Geometric calibration determines the intrinsic properties of the camera that can be used to undistort the camera

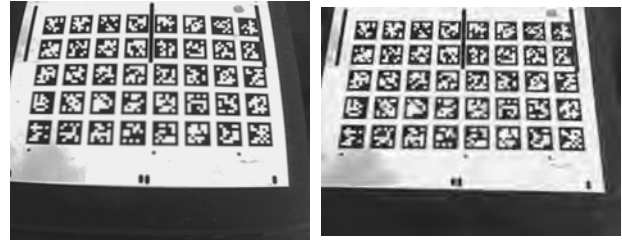


Figure 1. Raw and Processed Thermal Images

image. To learn the camera's calibration matrix and distortion coefficients, a scene with known coordinates is necessary. In RGB photos, the most common method of achieving this is through a checkerboard or a chessboard (See Figure 2). The alternating light-dark pattern identifies a common corner between the squares, and the OpenCV library finds the checkerboard points and performs camera calibration and undistortion based on the corner's screen location.

This paper examines various techniques for geometrically calibrating both thermal and RGB images taken by a drone for use in building envelope energy analysis using deep learning segmentation networks. We explore materials for the easy and simple calibration and image alignment for drones. Additionally, it proposes a method to combine them into a 4D tensor for deep learning network use. Our findings will benefit building energy analysts, engineers, and researchers who employ drones and deep learning segmentation networks for building envelope energy analysis and sustainability.

2 Related Works

2.1 Thermal Camera Calibration

There have been a number of successful attempts to geometrically calibrate a thermal camera. Ursine et al. [1] attempted to geometrically calibrate a thermal camera by creating a checkerboard calibration grid. This grid was constructed with a copper plate that had a painted checkerboard calibration pattern. The problem with such a set up is that multiple calibration rigs would be susceptible to a level of error based on the human painters skills. The

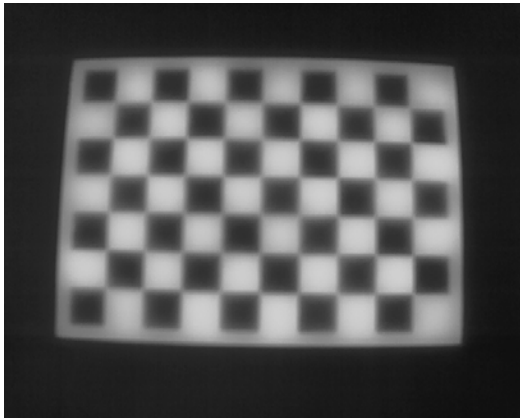


Figure 2. Uncalibrated and distorted thermal image of a checkerboard - corners of the checkerboard are known to lie on straight lines

process of making and manufacturing these calibration grids limits industrial reproducibility.

Shibata et al. [2] are able to ensure industrial reproducibility through the use of an offset grid. While they use a checkerboard pattern and the size of the checkers can be ensured to be consistent within a level of machine error, the offset they introduce can result in poor calibration if a camera calibration image is taken at a somewhat large angle. Furthermore, Shibata et al recognize that it is difficult to produce thermal images of checkerboard patterns with a quality and contrast high enough for corner detection and camera calibration. They introduce a novel tone mapping technique to adaptively increase the contrast of their images. The drawback of their method is that they require active heating of their calibration grid this means that camera calibration can only be performed in labs with specific equipment. Producing their set-up is also labour intensive and cannot be easily shipped from one location to another.

Hou et al. [3] were able to achieve results similar to those achieved by Ursine et al. They used a cardboard with square tin foil cut outs to create an emissivity difference that could be create a checkerboard pattern in thermal images. They were able to find the corners in the checkerboard pattern, but they required lab scale conditions to calibrate their thermal camera. Additionally, the calibration kit they have is not robust enough for commercial applications and could easily be damaged in transportation.

Previous papers either use a complicated set up involving active heating [4], resistors [5], or offset plates [2] that make calibration at extreme angles difficult. Other papers use image processing techniques to improve the detectability of points and lines on a thermal image. This paper uses

Apriltags ensuring that it requires no further image processing and can be used to easily calibrate the cameras on a UAV that's flown above and around the board.

2.2 RGB & Thermal Image Alignment

There are a number of successful attempts to combine and register thermal and RGB images. Istenic et al. [6] used a Hough transform to register thermal and RGB images. They required a structured environment with many lines and were not able to accurately account for scale between images in all cases. Knyaz and Moshkantsev [7] developed a technique that created a 3D scene using RGB and thermal information and combined the two 3D scenes to find the transforms between associated RGB and thermal images. Dlesk et al. [8, 9] researched the use of homography to align images with detectable feature points and went on to perform experiments that create RGBT imagery through combining RGT, TBG and RTB imagery.

3 Method

3.1 Cardboard and Acrylic Calibration Board

Initial calibration experiments involved creating a calibration kit with a spatially offset calibration board and heating up protruding parts of the board to create an observable thermal difference between black and white checks in a thermal image. The calibration board was made of black acrylic laser cut squares glued on to a cardboard backing/substrate. Paper with a printed 6 x 8 checkerboard pattern was pasted onto the cardboard sheet and acrylic squares were glued onto the paper. Black sections of the paper were covered by acrylic squares. The cardboard of size 12.5 inches (317.5 mm) x 11.5 inches (292.1 mm). Acrylic squares had a side length of 1.1 inches (27.94 mm) and the printed checkerboard pattern had checks of the same size.

3.2 Wood and Vinyl Calibration Board

A calibration board for thermal imaging was made by spray painting a 300 mm x 420 mm x 3.175 mm thick wood board white and laser cutting it to have 40 mm squares. The squares were connected with 0.1 mm connections to keep them together and prevent falling out. A black vinyl substrate was taped to the back. The board was heated by placing it on a warm surface (40 C to 50 C) to create a temperature difference between the surface of the substrate and the surface of the wood, and images were captured indoors at 23 C to 25 C. The drone flew indoors to hover over the board placed on indoor carpeting, and images were captured over 6 minutes. After the calibration kit had cooled off, it was reheated, and additional images were taken. The connection between the squares was small

enough to not be detected by an RGB corner detection algorithm.

3.3 Metal and Vinyl Calibration Board

A metal Apriltag calibration board was created using a large metal board and vinyl. The metal was 3/8 inches thick and made of unpolished oxidized aluminum, while the vinyl was cut using a Cricut Maker in the NYU Makerspace. The vinyl was applied onto transfer paper, then carefully placed over the metal substrate board, making sure to reduce the chance of bubbles being captured under it. The transfer paper was carefully removed to leave only the vinyl on the metal substrate. Tests were conducted both heated and unheated, indoors and outdoors. In the first qualitative test, the vinyl side of calibration board was heated indoors to produce a thermal differential between the vinyl and the metal substrate, resulting in a strongly visible image. The drone was flown indoors to hover over the calibration board which was put onto carpeted ground and images were captured over a span of 2 minutes and 36 seconds. Noise in the non-covered metal captured in the thermal image became more apparent as the plate lost heat (See Figure 3).

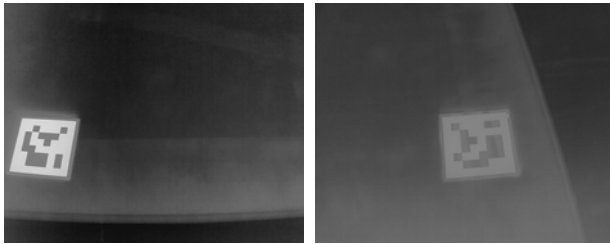


Figure 3. Thermal reflections are more easily visible in the metal portions of the calibration board

In the second test, conducted outdoors on an overcast day, the kit was placed on the concrete ground with an unobstructed view of the sky; the outside temperature on that day was approximately 8 C. The sky emits thermal energy from space which is minimal if the sun doesn't reflect on the calibration board. Overcast clouds helped diffuse the sun's energy and reduce its effect on the board. This minimal, passive, diffuse thermal energy reflected differently on the metal than the vinyl and created a sharp clear image that needed no additional heating. In order to calibrate the images, the pyAprilTag library was used to calculate the distortion coefficients and the camera calibration matrix of the two cameras. RGB images that were too large and had to be reduced in size to accurately find the AprilTags. Raw captured thermal images needed to have their color scheme inverted, but no sharpening or filtering was done otherwise.

4 Results

4.1 Thermal Camera Calibration

4.1.1 Cardboard Calibration Kit

Attempts to detect checker corners on thermal images were hindered by uneven heating of the calibration board, resulting in unclear corners. Image processing techniques were employed to improve contrast between acrylic and cardboard, as seen in Figure 4).

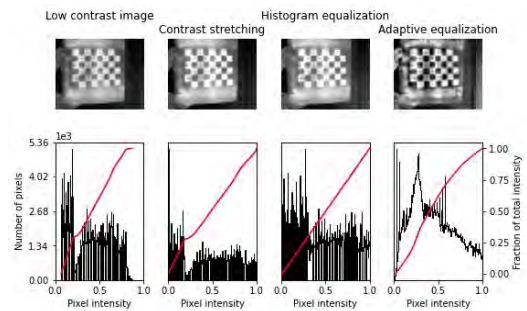


Figure 4. Image enhancement techniques were not able to improve the checker detection on the cardboard and acrylic calibration board due to uneven heating and cooling over the board.

Despite using various image processing techniques, it was not possible to get useful calibration information out of this technique. Although the acrylic squares were able to heat up evenly, the corner detection algorithm failed due to the uneven heating of the cardboard substrate. A better calibration kit was needed with a thinner substrate that would cool off more rapidly than the overlaid checker pattern. 0 corners were detected and 0 images could be used for calibration.

4.1.2 Wood and Vinyl Calibration Board

This calibration board required reheating every 6 minutes. Although some thermal images showed a checkerboard pattern, the raised corners made it difficult for the corner detection algorithm to determine the actual corner, resulting in subpar calibration (See Figure 5).

The only solution was to capture images from a distance, which caused excessive blur and made the algorithm ineffective. This experiment highlighted the need for a planar calibration surface, passive heating for capturing a large number of calibration images, and accurate detection of corners/feature points for precise alignment of RGB and thermal images. 0 corners were consistently detected and 0 images could be used for calibration.

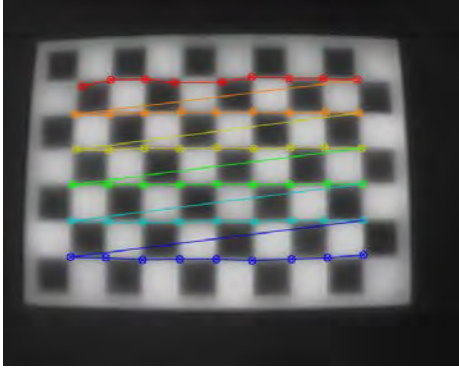


Figure 5. Corner detection issues on calibration boards with spatial offsets

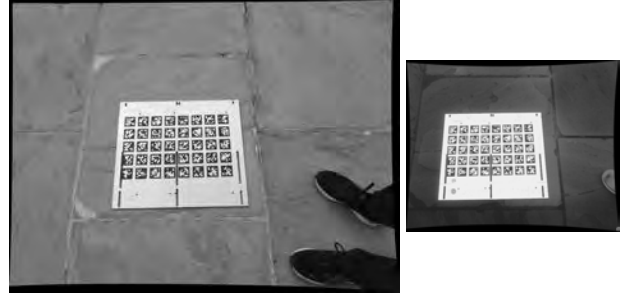


Figure 6. An example of an undistorted image pair

4.1.3 Metal and Vinyl Calibration Board

Passively heating the calibration board and orienting it towards the sky negated the need for active heating ensured consistency in the captured images, making the calibration process inexpensive and easily deployable in open areas. The use of vinyl AprilTags on a metal substrate improved the robustness of feature point detection, creating a clear contrast between high-emissivity vinyl and low-emissivity metal. Additionally, the AprilTags helped in finding common points in both RGB and thermal images, although not all AprilTags could be detected in both. Two AprilTags were consistently undetectable due to holes in the metal board, and were thus not used in analysis. Nearly 5500 points were detected using this method.

4.2 RGB & Thermal Image Alignment

4.2.1 AprilTag Detection after Image Reduction

Images were first undistorted using the distortion coefficients and the calibration matrix obtained in the previous step (See Figure 6).

Once images were undistorted, an RGB and thermal image pair was created from the RGB and thermal images taken at the same time of the same scene.

$$\text{Image Pair} = (P_i^{RGB}, P_i^{Th}) \quad (1)$$

Each image in the image pair was individually run through the AprilTag detection algorithm to create two sets of detected tag coordinates, X .

$$f(P_i^{RGB}) = \{X_{i,1} \dots X_{i,n}\} = \mathbb{S}_{RGB} \quad (2)$$

$$f(P_i^{Th}) = \{X_{i,1} \dots X_{i,n}\} = \mathbb{S}_{Th} \quad (3)$$

The intersection of the two sets of detected tag coordinates creates a new set of tag coordinate pairs.

$$\mathbb{S}_{RGB} \cap \mathbb{S}_{Th} = \mathbb{S}_{TCP} \quad (4)$$

$$\mathbb{S}_{TCP} = \{(X_{i,1}^{RGB}, X_{i,1}^{Th}) \dots (X_{i,n}^{RGB}, X_{i,n}^{Th})\} \quad (5)$$

Each of the Euclidean coordinate pairs is then homogenized into a vector of homogeneous coordinates. At this point, all the coordinates in an image pair could be normalized and all of the detected coordinates in an image of an image pair could be represented as a coordinate matrix:

$$(P_i^{RGB}, P_i^{Th}) \rightarrow (C_i^{RGB}, C_i^{Th}) \quad (6)$$

The first normalization step is centralization – all coordinates are translated via a translation matrix T such that they are all collectively centered around the origin. The second normalization step is scaling to reduce the average distance from the origin of all centralized points to 1 via a scaling matrix S .

$$\tilde{C}_i^{RGBc} = S^{RGB} \cdot T^{RGB} \cdot C_i^{RGB} \quad (7)$$

$$\tilde{C}_i^{Thc} = S^{Th} \cdot T^{Th} \cdot C_i^{Th} \quad (8)$$

The normalized points can now be used to assemble an A matrix that will be used to solve a homogeneous linear least squares problem, $Ax = 0$.

$$g(\text{Image Pairs}) \rightarrow A \quad (9)$$

After assembling the complete A matrix, singular value decomposition can be used to calculate the homography from normalized RGB image AprilTag coordinates to normalized thermal image AprilTag coordinates.

$$A = U\Sigma V^T \quad (10)$$

The rightmost column of V can be reshaped into a 3×3 \tilde{H} matrix that is the homography matrix between normalized coordinates. In order to establish a baseline level of error for this algorithm, the tag coordinates in the RGB image were transformed into tag coordinates in the thermal image using the following algorithm:

$$C_i^{Th,RGB} = T^{Th^{-1}} \cdot S^{Th^{-1}} \cdot \tilde{H} \cdot S^{RGB} \cdot T^{RGB} \cdot C_i^{RGB} \quad (11)$$

This could also be represented by the general homography from RGB to thermal images:

$$H = T^{Th^{-1}} \cdot S^{Th^{-1}} \cdot \tilde{H} \cdot S^{RGB} \cdot T^{RGB} \quad (12)$$

The X, Y, and overall reprojection error between the thermal image and the transformed RGB image was calculated and compared. The thermal images were taken as the ground truth. RGB images needed to be resized smaller in order for the AprilTags to be detected. This analysis was carried out on RGB images that were resized to be 90% to 10% of the original size in 5% increments. This was done to maximize the number of AprilTags detected and increase the accuracy of the homography between the image pairs. Reprojection error results are summarized in Figure 7.

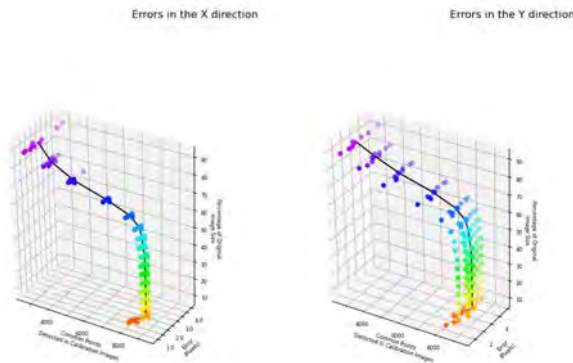


Figure 7. Image Registration Error for homographies between RGB and Thermal images calculated at various RGB image sizes

This general homography could now be applied to overlap an RGB image and a thermal image given a set of corresponding points seen in both images. However, thermal and RGB images often don't share enough features to allow for making correspondences. The differently sized thermal and RGB images meant that a different general homography would be needed to transform RGB images to thermal images for data fusion. An overall flow chart of the process is seen in Figure 8

4.2.2 Homography Calculation

Although a different general homography was required, the normalized homography between all images remained the same. The field of view of the RGB camera was larger than the thermal camera and so there was a portion of the RGB image that would consistently cross over the portion

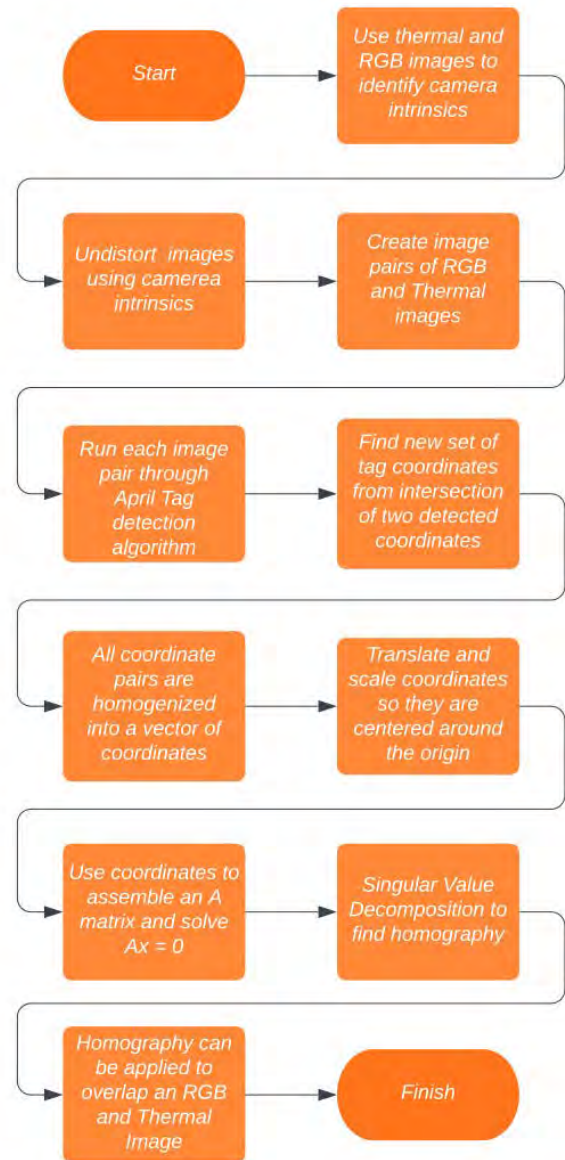


Figure 8. Homography Process Flow Chart

of the thermal image. To calculate the general homography for images between the two cameras, new normalization transforms were calculated. These transforms would not normalize AprilTags corners and centers or some other features observable within both images in an image pair. These would require the following general normalization transforms:

$$T_G^{Th} \rightarrow \text{General centralizing normalization matrix for thermal images}$$

T_G^{RGB} → General centralizing normalization matrix for RGB images

S_G^{Th} → General scaling normalization matrix for thermal images

S_G^{RGB} → General scaling normalization matrix for RGB images

These thermal image transformations would normalize the thermal image corners and the corresponding points in the RGB image. The normalization points in the thermal image are defined to be based on the image size.

$$P_{N G}^{Th} = \begin{bmatrix} 0 & 0 \\ 0 & Height(Th_i) \\ Width(Th_i) & 0 \\ Width(Th_i) & Height(Th_i) \end{bmatrix} \quad (13)$$

However, the normalization points within the RGB image are not precisely known. T_G^{Th} , T_G^{RGB} , and S_G^{Th} can be directly calculated from the size of the RGB and thermal image by using the RGB and thermal image corners. We do not know the precise corresponding normalization points within the RGB image, so we cannot directly calculate the S_G^{RGB} . Instead we must use a Hadamard quotient to relate the S_G^{RGB} and S_G^{Th} . In the previous normalization step, the RGB and thermal images in each image pair were normalized by the scaling normalization matrices S_i^{RGB} and S_i^{Th} that were unique to the images in each image pair. The Hadamard quotient, or the element-wise division, of these two matrices results in a relative scaling matrix that is related to the level of normalization scaling performed for the RGB and thermal images [10].

$$S_i^{RGB} \oslash S_i^{Th} = S_i^{HMD} \quad (14)$$

Given a set of image pairs with corresponding feature points, we could extract a set of scaling normalization matrices for each image pair and this would allow us to obtain a set of Hadamard quotients between the scaling normalization matrices.

$$\{P_i^{RGB}, P_i^{Th}\} \rightarrow \{S_i^{RGB}, S_i^{Th}\} \rightarrow \{S_i^{HMD}\} \quad (15)$$

The set of Hadamard quotients could be averaged to produce a general Hadamard quotient.

$$S_G^{HMD} = \frac{1}{n} \sum_{i=1}^n S_i^{HMD} \quad (16)$$

The general Hadamard quotient and the general scaling normalization matrix for thermal images could be used to generate a pseudo general scaling normalization matrix for RGB images.

$$S_G'^{RGB} = S_G^{HMD} \odot S_G^{Th} \quad (17)$$

With $S_G'^{RGB}$, a new general homography could be calculated to transform all RGB images to the thermal image space so that they could be merged into 4 channel RGBT tensors.

$$H_G = T_G^{Th^{-1}} \cdot S_G^{Th^{-1}} \cdot \tilde{H} \cdot S_G'^{RGB} \cdot T_G^{RGB} \quad (18)$$

This general transformation homography was applied to all the RGB images in the set of RGB and thermal image pairs to produce a new set of warped RGB image and thermal image pairs.

$$\{H_G(P_i^{RGB}, P_i^{Th})\} \quad (19)$$

An AprilTag detection algorithm was used on every image in the new set of image pairs to detect AprilTag corners and center pixel locations. The detected points in the thermal images were used as the ground truth to assess the detected points in the RGB images. Figure 9 shows the pixel errors seen for all detected points in the image pair dataset.

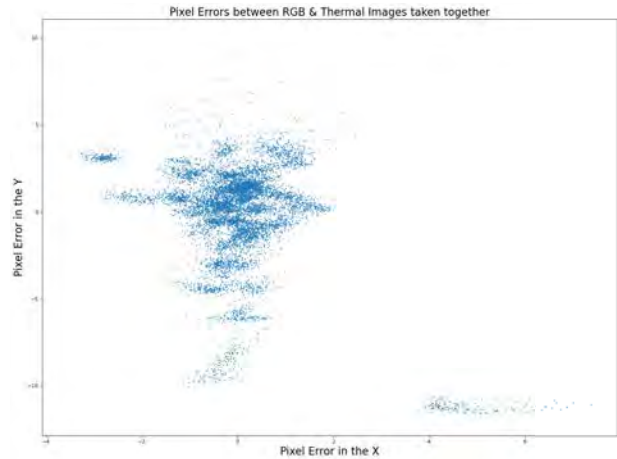


Figure 9. Image Registration Errors between Simultaneously Captured RGB and Thermal Images

5 Discussion

5.1 AprilTag Detection after Image Registration

As the images were downsized from 100% to 80% of their original size, baseline registration accuracy improved until 5500 feature point pairs were available. The experiment revealed that downsizing the RGB image to 50% of its original size was ideal to detect the maximum number of AprilTag points – just under 8000 feature point pairs. Although this didn't improve accuracy, it reduced the impact of outliers on \tilde{H} . This study also established a baseline error rate for the method. Sky-facing plates with

AprilTags and vinyl can be used to create common feature points in RGB and thermal images of the same scene. Metal plates can be placed around a building to improve

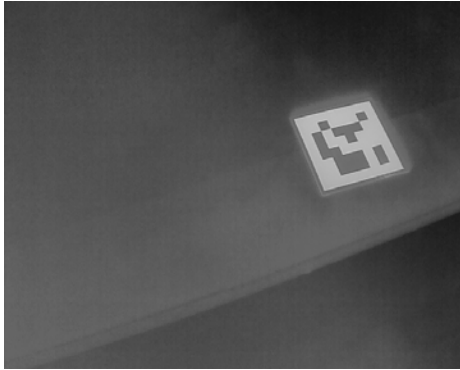


Figure 10. Thermally observed AprilTag marker that could be used to provide common feature points in RGB and thermal images

the algorithm's image registration if the general homography transform yields subpar results. This is depicted in Figure 10.

This study focuses on calibrating and aligning individual RGB and thermal images from a DJI Mavic 2 Enterprise Advanced drone. Processing and analyzing thermal video footage posed difficulties due to lost frames, loss of information, and blur caused by drone movement. To obtain accurate calibration and alignment, thermal footage needs significant pre-processing, making video analysis impractical for this study. As a result, thermal camera calibration with video clips is not within the scope of this paper.

5.2 Homography Calculation

This experiment showed that thermal and RGB images could be aligned despite differences in distortion and field of view between cameras.

One of the major limitations of how well the RGB and thermal images can be aligned is the relative closeness of the scene to the camera taking the image. Figure 11 shows how the overlap between RGB and thermal images improves as the camera is moved further away from the scene. The nature of building envelope photography is such that drones will always be a large distance away from the scene they are surveying and as a result will not suffer from issues of poor overlap.

This is because as the distance between the 3D location of the AprilTags and the cameras, (X^{Th}, X^{RGB}) , increases, the ratio between the distance between the 3D location of the AprilTags and the cameras and the baseline distance between the two cameras gets progressively

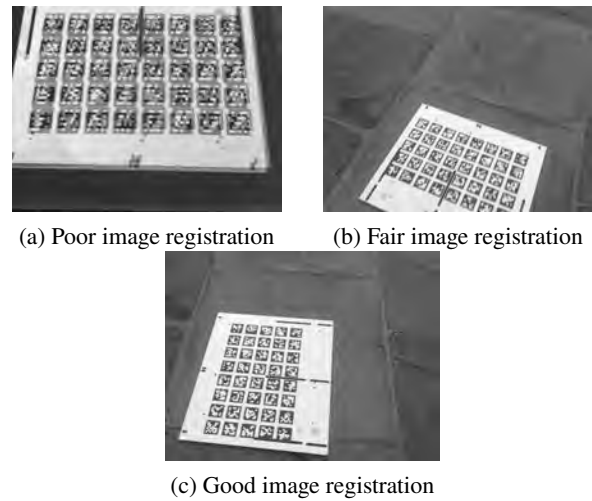


Figure 11. Image registration results showing examples of poor, medium, and fair image registration

smaller and begins to approach 0. Therefore the angle between the two cameras and the world point changes less as the depth of the world point increases. Figure 12 shows how the 3D to 2D projection of a world point onto the camera image plane changes significantly based on the distance of the world point to the cameras and the baseline distance between the cameras.

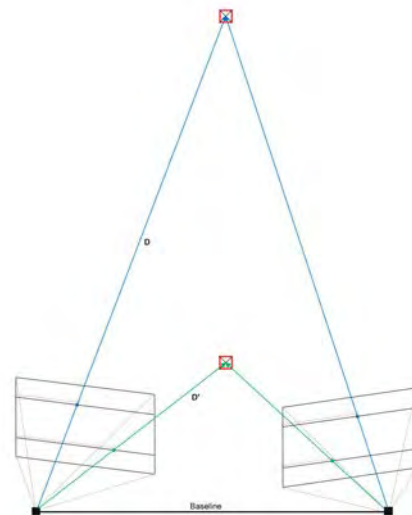


Figure 12. The effect of near-depth objects on image registration via the homography approximation method.

Another limitation is that images taken too closely to-

gether have an influence on the alignment homography and this could result in a less-than-optimal alignment homography. This could be solved through an iterative approach that discards any images from the homography calculation that are far outside the general cluster of errors, this can be visually seen in Figure 9. The image registration algorithm could be further improved by having a better S_G^{HMD} estimation. This estimation can be improved by using RANSAC to filter out images that required an S_G^{HMD} that was significantly different from other images.

6 Conclusion

Using a calibration board made of machine-cut vinyl overlaid onto a metal plate creates a robust calibration rig. Calibration images of this rig aren't affected by spatial offsets and when placed in an open field during the daytime, it does not require active heating. Thermal cameras can be calibrated robustly using vinyl AprilTags and metal plates.

The alignment algorithm is an approximation based on the assumption that the two cameras are positioned relatively close and the image that they are viewing is relatively far away, which is accurate for UAV photography of buildings and building envelopes.

In general, the image registration algorithm had a pixel error of ± 5 pixels in the y direction and ± 2 pixels in the x direction. These images are fairly well aligned and this algorithm can be used to create custom thermal and RGB image datasets of building envelopes.

Acknowledgment. This work is supported by NSF CNS-2228568 and TI-2232494, and DOE E-ROBOT challenge.

References

- [1] W. Ursine, F. Calado, G. Teixeira, H. Diniz, S. Silvino, and R. De Andrade. Thermal / Visible Autonomous Stereo Visio System Calibration Methodology for Non-controlled Environments. In *Proceedings of the 2012 International Conference on Quantitative InfraRed Thermography*. QIRT Council. doi:10.21611/qirt.2012.261. URL <http://qirt.org/archives/qirt2012doi/papers/QIRT-2012-261.pdf>.
- [2] Takashi Shibata, Masayuki Tanaka, and Masatoshi Okutomi. Accurate joint geometric camera calibration of visible and far-infrared cameras. 2017(11): 7–13.
- [3] Yu Hou, Rebekka Volk, Meida Chen, and Lucio Soibelman. Fusing tie points' RGB and thermal information for mapping large areas based on aerial images: A study of fusion performance under different flight configurations and experimental conditions. 124:103554.
- [4] Philip Saponaro, Scott Sorensen, Stephen Rhein, and Chandra Kambhamettu. Improving calibration of thermal stereo cameras using heated calibration board. In *2015 IEEE International Conference on Image Processing (ICIP)*, pages 4718–4722, 2015. doi:10.1109/ICIP.2015.7351702.
- [5] Michael Gschwandtner, Roland Kwitt, Andreas Uhl, and Wolfgang Pree. Infrared camera calibration for dense depth map construction. In *2011 IEEE Intelligent Vehicles Symposium (IV)*, pages 857–862, 2011. doi:10.1109/IVS.2011.5940515.
- [6] R. Istenic, D. Heric, S. Ribaric, and Damjan Zazula. Thermal and visual image registration in hough parameter space. In *2007 14th International Workshop on Systems, Signals and Image Processing and 6th EURASIP Conference Focused on Speech and Image Processing, Multimedia Communications and Services*, pages 106–109. IEEE. ISBN 961-248-036-2.
- [7] V. A. Knyaz and P. V. Moshkantsev. JOINT GEOMETRIC CALIBRATION OF COLOR AND THERMAL CAMERAS FOR SYNCHRONIZED MULTIMODAL DATASET CREATING. XLII-2/W18:79–84. ISSN 2194-9034. doi:10.5194/isprs-archives-XLII-2-W18-79-2019. URL <https://www.int-arch-photogramm-remote-sens-spatial-inf-sci.net/XLII-2-W18/79/2019/>.
- [8] Adam Dlesk, Karel Vach, and Karel Pavelka. Transformations in the Photogrammetric Co-Processing of Thermal Infrared Images and RGB Images. 21(15):5061, . ISSN 1424-8220. doi:10.3390/s21155061. URL <https://www.mdpi.com/1424-8220/21/15/5061>.
- [9] Adam Dlesk, Karel Vach, and Karel Pavelka. Photogrammetric Co-Processing of Thermal Infrared Images and RGB Images. 22(4):1655, . ISSN 1424-8220. doi:10.3390/s22041655. URL <https://www.mdpi.com/1424-8220/22/4/1655>.
- [10] Roger A Horn. The hadamard product. In *Proc. Symp. Appl. Math*, volume 40, pages 87–169, 1990.

Online Safety Risk Management for Underground Mining and Construction Based on IoT and Bayesian Networks

Milad Mousavi¹, Xuesong Shen¹ and Binghao Li²

¹ School of Civil and Environmental Engineering, The University of New South Wales (UNSW), Australia

² School of Mineral and Energy Resources Engineering, The University of New South Wales (UNSW), Australia
milad.mousavi@unsw.edu.au, x.shen@unsw.edu.au, binghao.li@unsw.edu.au

Abstract –

Management of environmental hazards in underground mining and construction sites has always been a challenging task for project managers and site engineers. Poor ventilation, the production of hazardous gases, dust, and considerable heat and humidity are some of the inherent characteristics of these ecosystems. Most conventional underground risk management methods are static and overly simplistic, making it almost impossible to predict and control these complex hazards. This paper aims to develop an online safety risk management system for underground mining and construction environments that enables dynamic and remote monitoring, analysis, and control of safety risks in underground space. The proposed system benefits from an automated combination of Internet of Things (IoT) wireless sensors as an environmental perception layer and Bayesian networks (BNs) as a powerful risk modelling engine. Using an open-source dataset collected in a real underground coal mine, a proof-of-concept example is presented to demonstrate the applicability of the proposed system. The proposed system will enable real-time and remote monitoring of underground ecosystems and enhance worker safety upon implementation.

Keywords –

Online Safety Risk Management; Internet of Things; Bayesian Networks; Underground Mining and Construction

1 Introduction

Recent years have seen a considerable amount of volatility in the international economy. Aside from political and economic instability, the mining and construction industries are also facing decreasing productivity, skills shortages, and social and environmental concerns [1]. The rapid exhaustion of near-surface coal seams and the growing demand for mineral resources has led underground mining activities

to move deeper into the earth to extract coal deposits. Consequently, the environmental condition of mines located at greater depths deteriorates due to poor ventilation and the production of hazardous gases, dust, and a significant amount of heat [2]. Particularly, there are many risks associated with underground coal mining, including high temperatures, high humidity, and the release of destructive gases. Reviews of historical coal mine accidents reveal that, despite technological advancements, major explosions have been ineffectively controlled, and adequate safety measures have failed to be implemented [3, 4]. As these risks are complex in nature, it is often difficult to predict and control them. It is, therefore, imperative to implement innovative solutions, best practices, and additional safety precautions to overcome these challenges and reap substantial economic benefits.

In many regions worldwide, mining and construction companies still use manual methods to assess the risks [5]. On the other hand, the more advanced risk assessment methods are generally offline and static, whereas the risks in underground spaces tend to be dynamic [6]. It has been demonstrated that traditional methods of analysis are insufficient for quantitative evaluation, dynamic control, and uncertainty management [7]. Most studies fail to represent the dynamic nature of coal mining adequately. Additionally, traditional methods cannot examine the non-linear relationships between safety data [8]. Due to the high risks and high costs associated with the experimental analysis of large-scale, complex gas explosions, it is impossible to reproduce the large-scale explosion evolution process through experimental techniques. The Computational Fluid Dynamics (CFD) simulation models are also ineffective since they are computationally intensive and incapable of incorporating dynamic information related to emergency rescues [9]. It is common practice in coal mines to have monitoring, supervision, and dispatching systems well integrated with machinery, devices, and transportation systems. Moreover, systems are designed to monitor natural hazards such as methane concentrations, seismicity, and

fires. Even so, the collected data is typically used only for visualization purposes, when deeper analysis could significantly improve many coal mining processes [10].

This paper aims to develop an online safety risk monitoring and management system for underground mining and construction environments that enables real-time, dynamic, and remote monitoring, analysis, and control of safety risks. The study benefits from the powerful risk assessment capabilities of Bayesian Networks (BNs) to represent the probabilistic and complicated nature of safety risks in underground mining and construction environments. The online data streams of the Internet of Things (IoT) sensors provide input to the BNs to enable the real-time monitoring of safety risks.

2 Background Review

This section reviews the state-of-the-art methods and technologies commonly used in the underground environment to manage safety risks.

2.1 Underground Safety Risk Management

Risk analysis methods in underground engineering can be divided into qualitative and quantitative approaches. Among the former are safety testing lists, Delphi's technique, interviews, brainstorming, the comprehensive fuzzy evaluation method, etc. Quantitative approaches include event tree analysis, Fault Tree Analysis (FTA), decision trees, support vector machines, neural networks, etc. [7]. In the mining industry, there has been an increasing interest in risk assessment and management, as evidenced by a significant number of publications and reports focused on these issues. Intensive mining, which results in large-scale production, is associated with numerous risks related to mining operations and the interaction between the mining system and the environment. Therefore, it is particularly important to conduct research on risk analysis, assessment, and management for this sector, especially concerning ecological, social, and economic factors. Risks should not only be evaluated in terms of their professional implications (human factor) but also in terms of their strategic implications (environmental impact) and operational concerns (safety, equipment, and the correctness of the mining process) [11].

2.2 Bayesian Network Applications in Underground Safety

Since their first adoption in the late 1990s, BNs have been extensively used in risk and reliability assessment, accident modelling, diagnostics, and prognostics [6]. Tong et al. [9] developed a BN to study the factors influencing mine gas explosions. The authors used expert knowledge and the Delphi method to determine

conditional probabilities. According to the authors, BN offers several advantages, such as multi-scale node variables representing diverse types of influential factors, representing uncertain factors during disaster evolution, and dynamic probability updates. In addition to representing various gas accumulation sources and influences, the proposed model would also incorporate dynamic explosion impacts on ventilation systems and roadways and emergency rescue or intervention measures in the process of successive gas explosions. The BN is generally established by learning the network's structure and the model's parameters based on sufficient data. Nevertheless, collecting enough data in some research fields may be difficult. Expert knowledge can also be used to determine the BN in this case. Despite its ability to structure safety and control knowledge, the proposed method deals with gas explosion accidents passively. It allows the personnel only a minimal time to evacuate the site.

It is also a hot topic in research to learn the structure and relationships in BNs from data. BNs were used by Li et al. [12] to predict rockburst risks in underground spaces. BN was constructed utilizing the Tree augmented Naïve Bayes classifier with five parameters, namely the buried depth of the tunnel, maximum tangential stress of surrounding rock, the uniaxial tensile strength of rock, the uniaxial compressive strength of rock, and elastic energy index. A dataset of rockburst case histories was studied to learn conditional probabilities. The database contained 135 case histories, of which 83 were rockburst cases, and 52 were non-rockburst cases. In addition to the 8-fold cross-validation, the model was also validated with another group of 15 incomplete case histories that were not used during training. The Bayesian approach was utilized by Rusek et al. [13] to create a decision support system for assessing the risk of damage to prefabricated reinforced concrete buildings exposed to the industrial environment of mines that can cause subsidence and tremors. To learn the structure of the BN from data, the authors used two types of score-based methods. The Tabu-search algorithm was used as the first method to search iteratively for potential solutions. Second, a stochastic search algorithm was used based on the global optimization algorithm Simulated Annealing. Analyses were conducted in R using the *catnet* and *bnlearn* packages. The study data was collected from a database of 129 prefabricated reinforced concrete buildings in a copper mining area in Poland. A total of eight damage intensity indices were used to analyze the risk of structural and finishing elements being damaged.

Li et al. [14] used a Fuzzy Bayesian Network (FBN) to analyze the risk factors of ignition in mines. The expert group decision-making method was used to construct risk topological and structural models of ignition sources. Experts were weighted using a FAHP. The technique can

be used to calculate the probability of occurrence of potential risk events and the probability distribution of risk factors using causal reasoning, logical reasoning, and sensitivity analysis. Historical data of 215 major gas explosion accidents in China from 2000 to 2017 were studied to characterize possible accidents. Netica software produced by Norsys was used to create the BN. Wu et al. [15] presented a Dynamic Bayesian Network (DBN) to analyze dynamic road surface damage caused by tunnelling over time. In order to construct the DBN and its relationships, the authors consulted standards, technical reports, expert experience, as well as some qualified fault trees. The BN parameters were derived from 786 monitoring records regarding tunnel-induced road surface settlement and its influential variables. This was accomplished by employing the K2 algorithm, a well-known algorithm for BN structure learning. The dynamic nature was determined by expert estimation. In order to demonstrate the feasibility and applicability of the proposed system, a case study was conducted for the Wuhan Yangtze Metro Tunnel in China.

2.3 IoT-Enabled Underground Safety

IoT technology has been applied in a wide array of applications to provide solutions to manufacturing and transportation [16]. In recent years, IoT has also found its way into underground safety applications, helping to improve the safety and efficiency of underground operations. Zhou and Ding [16] proposed an IoT-based hazard energy monitoring system for underground construction sites, which involves identifying hazard energy, collecting data, and analyzing safety barriers. The authors discussed technical, operational, and organizational safety barrier systems and compiled a checklist of hazard energy sources. IoT technologies were employed to gather information about hazardous energy on the underground construction site.

Zhang et al. [17] proposed an Artificial Intelligence Internet of Things (AIoT) system for real-time monitoring of tunnel construction. The authors categorized tunnel information into three groups: tunnel geometric factors, geological parameters, and shield operational parameters. A database of 12 parameters was created, including the above parameters, and measured settlement data. IoT sensors were used to capture real-time shield data parameters. Geometric and geological parameters were determined prior to tunnel construction. Random Forest models were employed to predict operational parameters for successive rings and the resulting settlement with high accuracy.

Dey et al. [18] proposed a hybrid CNN-LSTM model to improve the safety and productivity of underground coal mines using IoT-enabled sensors. In this study, IoT sensors installed in the underground mine transmitted

data wirelessly to the control room on the ground. The CNN-LSTM model extracted spatial and temporal features from mine data to predict the miner's health quality index (MHQI) for working faces and gas concentration levels in goaf areas. The predicted results were displayed in the control room using the graphical user interface developed for the digital mine software. The proposed prediction model achieved an accuracy of 89.2% for MHQI and 99.3% for methane prediction.

3 Methodology

Figure 1 provides an overview of the proposed research framework. There are three interrelated parts to the framework. The first part is associated with the physical underground mining and construction environment. Here, a network of IoT sensors will be deployed according to a predesigned layout to collect data about environmental factors, such as wind speed, temperature, atmospheric pressure, and methane concentration. The measurements will be transferred to data storage for later use in the data pre-processing module. The time-series data will be cleaned and labelled according to the requirements of the BN inputs. A BN will be created that considers the cascading causes and effects of safety accidents in the underground environment. Real-time IoT measurements will then be fed into the BN. Once the BN is activated, the probability distribution of accidents and their consequences will be immediately updated. Different parts of the proposed framework are explained in the following sections.

3.1 Environmental Perception

In the first module of the proposed framework, IoT sensors are used to collect real-time environmental data on underground space. Different types of sensors are utilized for measuring gas concentration levels, wind speed, air pressure, temperature, and humidity. Among the existing gases in underground mines that can potentially increase the risk of safety accidents, such as explosions, are methane and oxygen. These sensors must be installed in various locations within the underground space according to an appropriate deployment strategy to provide a comprehensive view of the environmental status. The working face, ventilation systems, and tunnels are among the critical locations that may require continuous environmental monitoring in underground environments. The data collection interval can differ from seconds to hours based on the type of potential hazard being investigated, the specific environmental factors being monitored, regulatory requirements, the type of underground environment, and the nature of the environment. It must be carefully planned in the deployment strategy. The collected data must then be

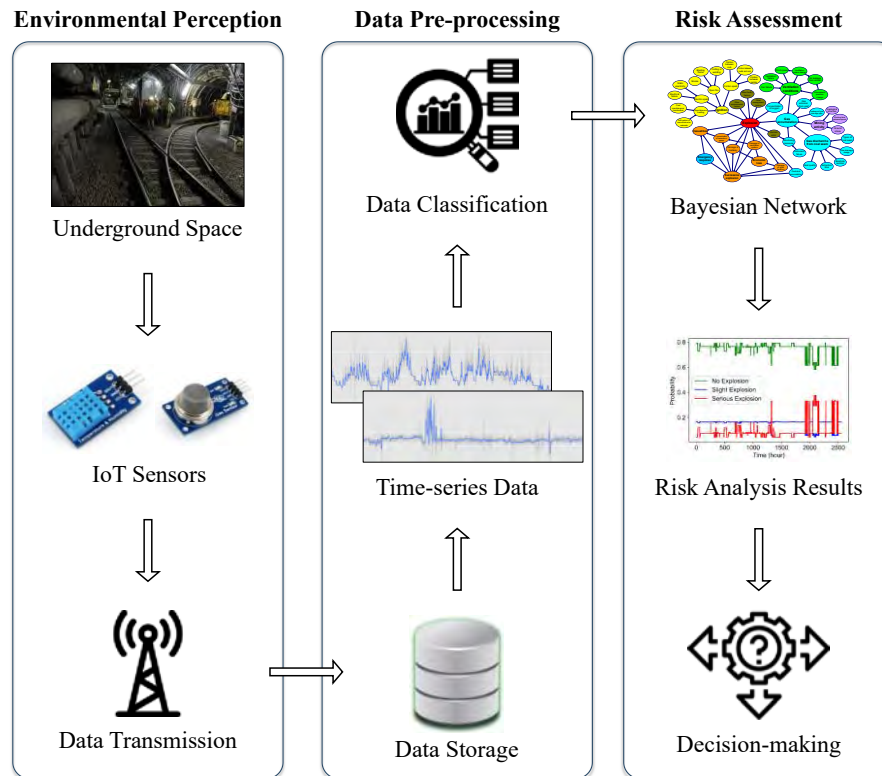


Figure 1. Proposed online safety risk management framework.

transmitted to data storage for later use in the following modules of the proposed framework. Based on industry standards and common practices, Wi-Fi is the most commonly used technology for data transmission in coal mining applications, followed by LTE and 5G [19]. Therefore, these wireless technologies should be considered when selecting data transmission tools.

3.2 Data Pre-processing

The raw data collected from the IoT sensors are in the form of numerical time-series data. In contrast, the input data to the BN must typically be in the form of categorical data. Therefore, a data cleaning and classification process on the raw data is necessary to prepare them for the risk assessment module. If the sensors are installed and calibrated correctly, the possibility of generating flawed data would be minimal. Any missing data or outliers should be cleaned in the pre-processing module. Next, the clean data must be classified and labelled according to the requirements of the Bayesian network. In this step, safety experts must define appropriate thresholds for categorising the data. For example, when the gas concentration in coal mines exceeds the one per cent limit, the mining operation will be subject to potential interruptions, and panic might be inflicted on the workers [20]. As a result, the one per cent limit can be defined as the threshold for classifying the gas concentration level

as serious in coal mines. Concentration values below this threshold will be labeled as slight concentration, while values exceeding this threshold will be classified as serious discharge. These discrete categories will then be utilized as evidence in the BN model to update the risk of other nodes within the network. This logic can also be applied to the raw environmental data generated by the other types of sensors.

3.3 Risk Assessment

The BN is used in the proposed framework as a robust risk assessment tool. BNs are directed acyclic graphs that represent probabilistic relationships among variables. A BN consists of nodes representing random variables. A causal relationship is indicated by an arrow connecting two nodes, while the absence of an arrow indicates conditional independence between two variables. BN modelling begins with identifying the network structure to analyze the conditional independence and dependency relationships between the input variables. Following the definition of the BN structure, it is necessary to describe the intensity of the relationship, that is, the conditional probability of one variable given another. Assuming that a BN has n nodes, the joint probability of the BN's random variables would be defined as:

$$P(U) = P(X_1, \dots, X_n) = \prod_{i=1}^n P(X_i | \pi(X_i)) \quad (1)$$

Where X_i denotes the i^{th} random variable, and $\pi(X_i)$ represents the set of parent nodes of X_i .

In the case of discrete variables, Conditional Probability Tables (CPTs) can be used, which determine how likely it is that the "end node" will be in one of its possible states if the "origin node" will be in one of its possible states as well. A BN has the additional feature of being updated as new evidence is acquired, a process referred to as belief updating [12]. Regarding safety and disaster risk management, each node in the BN can represent one of the causes or consequences of the accident [21]. A similar definition was taken in this framework for identifying the structure of the BN.

After developing the BN, the real-time data pre-processed in the previous module are fed into it as new evidence. The BN then initiates the belief updating process to calculate the new probability of the accident node, along with the probabilities of all its causes and consequences. The result will be an online and real-time risk assessment chart for the critical nodes, which can be used to assist the decision-makers and safety managers in foreseeing the occurrence of any safety accidents, tracing the most likely causes of the accident, and taking preventive measures to control the accident and its consequences. In the next section, a case study is conducted to illustrate the details of implementing the different steps of the proposed framework.

4 Case Study

A proof-of-concept example of a case coal mine in Poland was taken to illustrate the applicability of the proposed methodology. The following sections explain

the different parts of the method implementation for the proof-of-concept example.

4.1 Open-source Methane Dataset

This study simulated live streams of IoT data using an open-source dataset from a coal mine in Poland. The data were collected from 28 different sensors located at various locations within the case coal mine between 2 March 2014 and 16 June 2014. A total of 9,199,930 samples are included in this dataset. The measurements are taken at intervals of one second. The dataset contains no missing values. Kozielski et al. [22] first published the dataset, but it was previously used by Słezak et al. [10] to train a forecasting model to predict near-future methane concentration levels in coal mines. Table 1 describes the characteristics of the sensors and the other features used to collect the open-source dataset.

4.2 Bayesian Network of Methane Explosion Accidents

A preliminary BN was developed for methane explosion accidents in underground coal mines as part of the case implementation. The network has eight categories of nodes: methane accumulation, ignition, mining properties, ventilation, accidents, consequences, mitigation measures, and human error. In Figure 2, each category is represented by a different color. A review of relevant literature was conducted to determine the structure of the network and the probability of each root node. The conditional probabilities of intermediate nodes were estimated using reasonable assumptions and an analysis of the general relationship discussed in the literature. BNs were developed using BayesFusion's GeNIe Modeler [23].

Table 1. Characteristics of sensors used for collecting the open-source methane dataset.

Category	Sensor/Feature	Number of Sensors/Features
Climatic condition	Anemometer	3
	Temperature	2
	Humidity	2
	Barometer	2
	Methane meter	7
	High-concentration methane meter	1
The activity of the longwall shearer	Pressure difference on the methane drainage flange	1
	The pressure inside the methane drainage pipeline	1
	The temperature inside the pipeline	1
	Methane delivery	1
	Current meter	5
	Driving direction	1
	Cutter loader speed	1

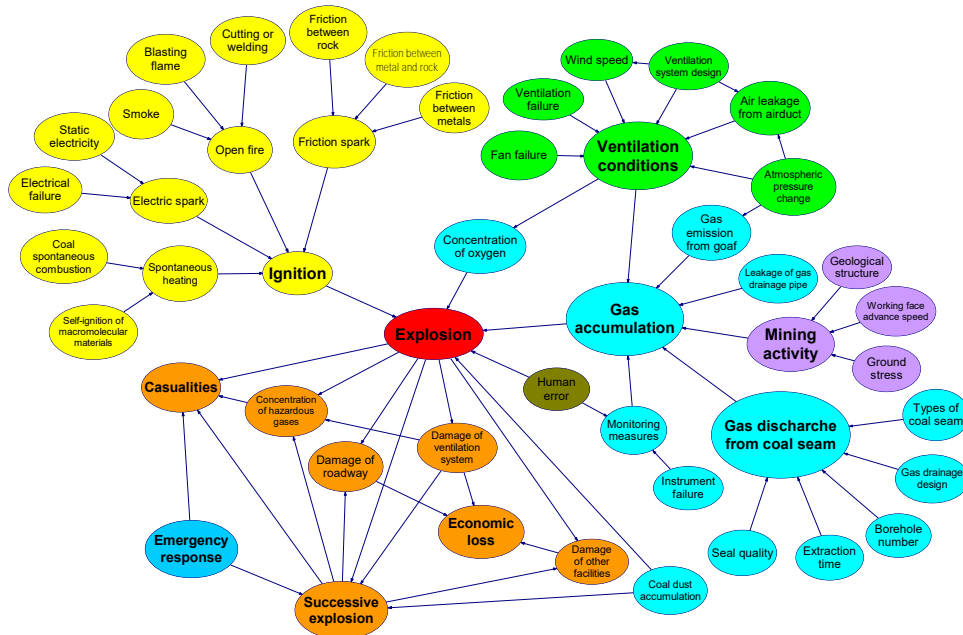


Figure 2. Bayesian network of methane explosion accidents in underground coal mines.

4.3 Live Risk Monitoring System

In the third part of the case study, a simple algorithm was developed to link IoT data streams to the Bayesian network. It was accomplished by using the Python wrapper for the SMILE Engine. The SMILE library is a set of C++ classes that manage the Genie Modeler from different software [24] via an Application Programming Interface (API). In the first step, the size of the dataset was reduced by taking the average of measurements every 600 seconds as the representative of each ten minutes. This resulted in 15,334 samples, each representing ten minutes rather than 9 million samples, each representing one second. For this purpose, an algorithm was developed using the Pandas package in Python [25]. Afterwards, a separate algorithm was designed to incorporate the pieces of evidence into the preliminary BN and calculate the evolution of the explosion risk. This was achieved using the SMILE wrapper in Python.

In this case study, the values of only two sensors were selected as an example to update the BN in real time. The first selected sensor was one of the most critical methane meter sensors installed close to the longwall. This sensor's values were used as evidence to update the Gas discharge from the coal seam node (see Figure 2). The methane concentration levels above one per cent were considered serious gas discharge, and the levels below this threshold were labelled as slight gas discharge [20]. The other selected sensor was the closest anemometer to the longwall, which was used to update the ventilation

conditions through the wind speed node (see Figure 2). Here, the values above 0.3 m/s were considered adequate wind speed, between 0.15 m/s and 0.3 m/s were considered ordinary, and those below 0.15 m/s were regarded as inadequate wind speed. Figure 3 displays the evolution of the explosion risk at each interval.

Reviewing the open-source dataset, the wind speed in the case coal mine was consistently adequate, but the gas concentration reached above the one per cent limit during the data collection. As seen in Figure 3, the effect of this phenomenon was reflected in the evolution diagram of the explosion risk. Generally, it can be stated that, in the data collection period, the case coal mine was a safe environment in terms of the methane explosion. Other researchers can conduct a similar analysis to assess the safety risks in underground space.

5 Conclusions

An online underground safety risk assessment framework was proposed in this paper. The framework benefits from the mutual benefits of IoT sensors to generate real-time environmental data and BNs, as a robust risk assessment engine. A case study was conducted on an open-source dataset of methane concentration in an underground coal mine in Poland. The results indicate that the proposed framework is capable of assisting safety managers in underground mines to monitor the risks of safety accidents on a real-time basis and take appropriate measures as necessary.

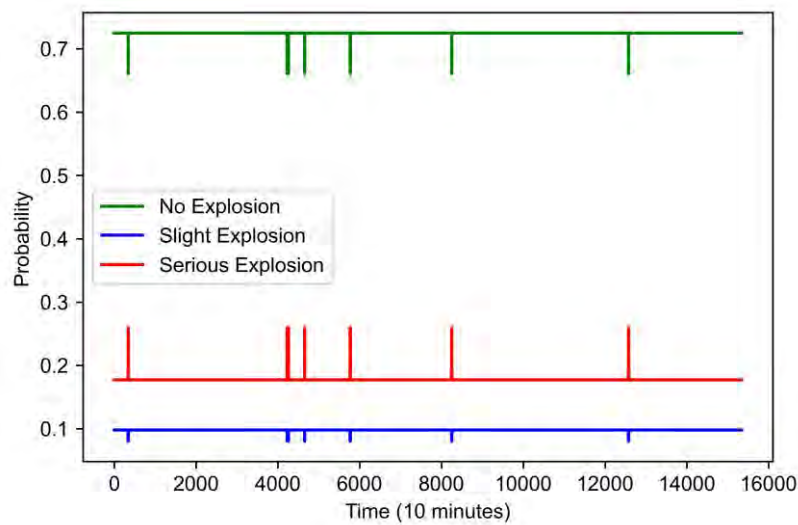


Figure 3. The explosion risk evolution diagram.

The proposed framework yields two important deliverables that can contribute to the field of safety in underground environments. Firstly, developing a Bayesian network enables the capture and retention of tacit knowledge within the underground environment from safety experts. Due to its implicit nature, this knowledge is often difficult to transfer to others, but it can be effectively captured and applied to improve safety practices in underground mining and construction by means of the developed BN. Second, implementing the framework will lead to the development of an online system that allows for real-time monitoring and assessment of safety risks in underground environments. Through this system, safety measures can be continuously evaluated and improved, as well as potential risks can be identified and addressed before they escalate into more serious incidents.

One of the limitations of the current study is that the structure and the conditional probabilities of the developed BN were derived based on the data and information available in the literature. Future studies can use historical data, expert knowledge, or a combination of these two to create a more accurate BN. Further research can also explore the use of additional sensors to provide a more comprehensive understanding of the framework and generate more accurate results.

References

- [1] H. Jang and E. Topal, "Transformation of the Australian mining industry and future prospects," *Mining Technology*, vol. 129, no. 3, pp. 120-134, 2020/07/02 2020, doi: 10.1080/25726668.2020.1786298.
- [2] S. He, Y. Lu, and M. Li, "Probabilistic risk analysis for coal mine gas overrun based on FAHP and BN: a case study," *Environmental Science and Pollution Research*, vol. 29, no. 19, pp. 28458-28468, 2022/04/01 2022, doi: 10.1007/s11356-021-18474-3.
- [3] T. Porselvi, C. S. Sai Ganesh, B. Janaki, K. Priyadarshini, and S. Shajitha Begam, "IoT Based Coal Mine Safety and Health Monitoring System using LoRaWAN," in *2021 3rd International Conference on Signal Processing and Communication (ICSPC)*, 13-14 May 2021 2021, pp. 49-53, doi: 10.1109/ICSPC51351.2021.9451673.
- [4] Y. Wu, M. Chen, K. Wang, and G. Fu, "A dynamic information platform for underground coal mine safety based on internet of things," *Safety Science*, vol. 113, pp. 9-18, 2019/03/01/ 2019, doi: <https://doi.org/10.1016/j.ssci.2018.11.003>.
- [5] A. Janusz, M. Grzegorowski, M. Michalak, Ł. Wróbel, M. Sikora, and D. Ślęzak, "Predicting seismic events in coal mines based on underground sensor measurements," *Engineering Applications of Artificial Intelligence*, vol. 64, pp. 83-94, 2017/09/01/ 2017, doi: <https://doi.org/10.1016/j.engappai.2017.06.002>.
- [6] R. Moradi, S. Cofre-Martel, E. Lopez Droguett, M. Modarres, and K. M. Groth, "Integration of deep learning and Bayesian networks for condition and operation risk monitoring of complex engineering systems," *Reliability Engineering & System Safety*, vol. 222, p. 108433, 2022/06/01/ 2022, doi: <https://doi.org/10.1016/j.res.2022.108433>.
- [7] M. Li, H. Wang, D. Wang, Z. Shao, and S. He, "Risk assessment of gas explosion in coal mines

- based on fuzzy AHP and bayesian network," *Process Safety and Environmental Protection*, vol. 135, pp. 207-218, 2020/03/01/ 2020, doi: <https://doi.org/10.1016/j.psep.2020.01.003>.
- [8] M. You, S. Li, D. Li, and S. Xu, "Applications of artificial intelligence for coal mine gas risk assessment," *Safety Science*, vol. 143, p. 105420, 2021/11/01/ 2021, doi: <https://doi.org/10.1016/j.ssci.2021.105420>.
- [9] X. Tong, W. Fang, S. Yuan, J. Ma, and Y. Bai, "Application of Bayesian approach to the assessment of mine gas explosion," *Journal of Loss Prevention in the Process Industries*, vol. 54, pp. 238-245, 2018/07/01/ 2018, doi: <https://doi.org/10.1016/j.jlp.2018.04.003>.
- [10] D. Słęzak *et al.*, "A framework for learning and embedding multi-sensor forecasting models into a decision support system: A case study of methane concentration in coal mines," *Information Sciences*, vol. 451-452, pp. 112-133, 2018/07/01/ 2018, doi: <https://doi.org/10.1016/j.ins.2018.04.026>.
- [11] A. Tubis, S. Werbińska-Wojciechowska, and A. Wroblewski, "Risk Assessment Methods in Mining Industry—A Systematic Review," *Applied Sciences*, vol. 10, no. 15, 2020, doi: 10.3390/app10155172.
- [12] N. Li, X. Feng, and R. Jimenez, "Predicting rock burst hazard with incomplete data using Bayesian networks," *Tunnelling and Underground Space Technology*, vol. 61, pp. 61-70, 2017/01/01/ 2017, doi: <https://doi.org/10.1016/j.tust.2016.09.010>.
- [13] J. Rusek, K. Tajduś, K. Firek, and A. Jędrzejczyk, "Score-based Bayesian belief network structure learning in damage risk modelling of mining areas building development," *Journal of Cleaner Production*, vol. 296, p. 126528, 2021/05/10/ 2021, doi: <https://doi.org/10.1016/j.jclepro.2021.126528>.
- [14] M. Li, D. Wang, and H. Shan, "Risk assessment of mine ignition sources using fuzzy Bayesian network," *Process Safety and Environmental Protection*, vol. 125, pp. 297-306, 2019/05/01/ 2019, doi: <https://doi.org/10.1016/j.psep.2019.03.029>.
- [15] X. Wu, H. Liu, L. Zhang, M. J. Skibniewski, Q. Deng, and J. Teng, "A dynamic Bayesian network based approach to safety decision support in tunnel construction," *Reliability Engineering & System Safety*, vol. 134, pp. 157-168, 2015/02/01/ 2015, doi: <https://doi.org/10.1016/j.ress.2014.10.021>.
- [16] C. Zhou and L. Y. Ding, "Safety barrier warning system for underground construction sites using Internet-of-Things technologies," *Automation in Construction*, vol. 83, pp. 372-389, 2017/11/01/ 2017, doi: <https://doi.org/10.1016/j.autcon.2017.07.005>.
- [17] P. Zhang, R.-P. Chen, T. Dai, Z.-T. Wang, and K. Wu, "An AIoT-based system for real-time monitoring of tunnel construction," *Tunnelling and Underground Space Technology*, vol. 109, p. 103766, 2021/03/01/ 2021, doi: <https://doi.org/10.1016/j.tust.2020.103766>.
- [18] P. Dey, S. K. Chaulya, and S. Kumar, "Hybrid CNN-LSTM and IoT-based coal mine hazards monitoring and prediction system," *Process Safety and Environmental Protection*, vol. 152, pp. 249-263, 2021/08/01/ 2021, doi: <https://doi.org/10.1016/j.psep.2021.06.005>.
- [19] Global Mining Guidelines Group (GMG), "Underground Mine Communications Infrastructure Guidelines Part III: General Guidelines," in *Underground Mine Communications Infrastructure guideline suite: Global Mining Guidelines Group (GMG)*, 2019.
- [20] P. Lyu, N. Chen, S. Mao, and M. Li, "LSTM based encoder-decoder for short-term predictions of gas concentration using multi-sensor fusion," *Process Safety and Environmental Protection*, vol. 137, pp. 93-105, 2020/05/01/ 2020, doi: <https://doi.org/10.1016/j.psep.2020.02.021>.
- [21] A. Tohidifar, M. Mousavi, and A. Alvanchi, "A hybrid BIM and BN-based model to improve the resiliency of hospitals' utility systems in disasters," *International Journal of Disaster Risk Reduction*, vol. 57, p. 102176, 2021/04/15/ 2021, doi: <https://doi.org/10.1016/j.ijdr.2021.102176>.
- [22] M. Kozielski, M. Sikora, and Ł. Wróbel, "Data on methane concentration collected by underground coal mine sensors," *Data in Brief*, vol. 39, p. 107457, 2021/12/01/ 2021, doi: <https://doi.org/10.1016/j.dib.2021.107457>.
- [23] BayesFusion. "GeNIe Modeler: Complete Modeling Freedom." <https://www.bayesfusion.com/genie/> (accessed 20 July 2022).
- [24] BayesFusion. "SMILE: Structural Modeling, Inference, and Learning Engine." <https://www.bayesfusion.com/smile/> (accessed 20 July 2022).
- [25] W. McKinney, *Python for data analysis: Data wrangling with Pandas, NumPy, and IPython*. O'Reilly Media, Inc., 2012.

Evaluating Road Segmentation Performance in Participatory Sensing: Investigation into Alternative Metrics

Jeongho Hyeon¹, Minwoo Jeong¹, Giwon Shin¹, Wei-Chih Chern², Vijayan K. Asari², and Hongjo Kim¹

¹Yonsei University, Republic of Korea
hyeon9404@yonsei.ac.kr, 2016144045@yonsei.ac.kr, giwone1330@yonsei.ac.kr, hongjo@yonsei.ac.kr ²University of Dayton, OH, United States
chernw1@udayton.edu, vasari1@udayton.edu

Abstract

For road condition assessment, participatory sensing has been proposed in literature utilizing a normal vehicle equipped with a dashboard camera. In such environment, the main technical challenge is not only the recognition performance on target classes such as cracks, but also the preparation of training and test datasets with high quality annotations. This study found that the annotation quality presents a unique problem in the performance test of participatory sensing-based road condition assessment. To address the problem, this study explores the adequacy of most commonly-used evaluation metric, the Intersection over Union (IoU), and suggest alternative metrics for road segmentation models in the context of participatory sensing. Experiments were conducted on the AIM crack dataset collected from urban road environments using dashboard cameras on normal vehicles. This study provides new insights into the importance of considering proper evaluation metrics in participatory sensing-based infrastructure monitoring.

Keywords –

Participatory sensing, road crack segmentation, performance evaluation metric, convolutional neural network, semantic segmentation

1 Introduction

The expenses for the maintenance and repair (M&R) of road networks in South Korea have increased significantly, recording \$2 billion in 2015 to \$2.9 billion in 2021 [1]. Previous research has shown that proactive M&R of road damages can significantly reduce M&R costs compared with reactive M&R [2]. To facilitate proactive M&R, it is essential to monitor road damages in a timely manner. However, limited budgets and monitoring resources in governmental agencies

responsible for managing road infrastructure often make it difficult to identify road surface damages promptly.

A previous study suggested an alternative monitoring method for road surfaces through participatory sensing, which leverages the data collection capabilities of citizens [3,4]. The previous study [3,4] utilized deep CNN to identify surface cracks, demonstrating the applicability of AI-based recognition systems. Most recent studies have used object detection models to find road surface damages [5]. However, to make data-informed decisions in road M&R, damage information in a bounding box format could be insufficient as it cannot provide the length and shape of cracks, which are crucial for selecting proper treatment methods.

Semantic segmentation models are advantageous for road M&R as they can recognize target classes, such as cracks, at the pixel-level. The segmentation results naturally facilitate the quantification of crack ratios in road sections, which can help make M&R decisions based on real-inspection data in a timely manner. However, participatory sensing environments presents a unique challenge in preparation of training and test datasets with accurate annotations due to poor image quality. Poor image quality is attributed to the low specification of dashboard camera image sensors, car motions, external lighting conditions, and weather effects. Therefore, annotated images often have erroneous annotations as shown in the right-hand side of Fig. 1. This problem is not only caused by human error, but also poor image quality with excessive noise as shown in Fig. 2. With such image quality, annotators are hard to differentiate cracks from road surfaces. Additionally, as shown in Fig. 1, the large field of view captured by a dashboard camera leads to objects in the distance appearing smaller and narrower, making the annotation task challenging.

When it comes to making decisions for proactive M&R of road networks, critical information is the ratio and length of cracks in a road unit. Although there is a widely used road condition indicator such as the international

roughness index (IRI), proactive M&R activities do not need such level of details. Therefore, in the context of participatory sensing, the required level of details for road conditions includes the shape of cracks, not the width of them. Considering this, the current evaluation metric, the IoU, could mislead the interpretation of experimental results of semantic segmentation models, as it checks how accurately the model predicts crack regions in pixels. Fig. 1 illustrates this problem. From a road manager's perspective, the prediction result is acceptable as it can provide the current status of road cracks, but the IoU score is low recording 0.28. Few pixel differences in location, thickness, and length between the predicted results and ground truth have little effect on road M&R judgment.

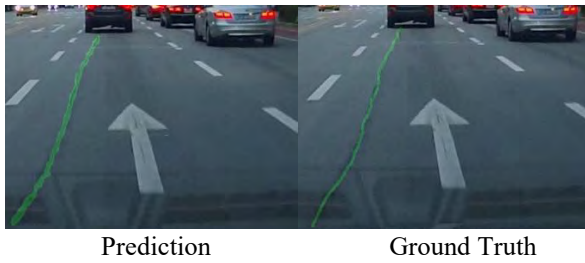


Fig. 1. An example of the segmentation results (left) and the ground truth (right). The IoU Score is 0.28.

To address this issue, this study investigates alternative performance evaluation metrics for participatory-sensing based road M&R decision making. The first evaluation method is composed of a morphological operation and a buffer method to yield performance scores for evaluation metrics such as 'completeness', 'correctness', and 'quality'. The buffer method is a simple matching procedure in which any portion of the prediction pixel within a defined pixel distance from the ground truth (GT) pixels is considered as a correct match. The second method, the keypoint matching method, evaluates the distance between the prediction and ground truth keypoints. The proposed evaluation metrics can be useful for road monitoring in the context of participatory sensing as the goal of crack recognition is identifying the ratio and length of cracks in certain road units to facilitate proactive M&R for road networks.

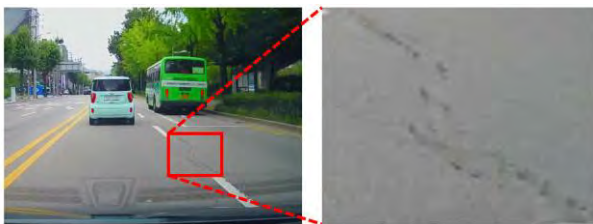


Fig. 2. Poor image quality due to harsh imaging conditions using a dashboard camera in a moving car.

2 Evaluation metrics for participatory sensing-based road monitoring

New evaluation metrics for participatory sensing-based road monitoring are designed to achieve the following goals:

- The performance of road crack segmentation is evaluated by the crack shape and length.
- The segmentation results should be meaningful to make decisions for proactive M&R of road networks.

To achieve the goals, this study designs and examines two evaluation metrics.

2.1 Shape-based evaluation of crack segmentation

The first evaluation method is named as 'shape-based evaluation of crack segmentation', as it focuses on the integrity of crack shapes. That is, the metric evaluates whether a segmentation model correctly recognize the crack shapes, with the tolerance on the difference between the pixel thickness of prediction results and the ground truth. For example, if a prediction result is a straight crack line with the pixel width of 5 and length of 100, and the ground truth is also a straight crack line with the pixel width of 1 and length of 100, then the metric should give 100% score.

To realize the above idea, this study adopts CCQ metric which utilizes the concept of 'completeness', 'correctness', 'quality', and the buffer [6]:

'Completeness' represents the proportion of the predicted cracks that lies within the buffer around the ground truth cracks. It is expressed as a percentage and defined by equation (1).

'Correctness' refers to the proportion of the predicted cracks that lie within the buffer of the ground truth network, as quantified by equation (2).

'Quality' of the result, which takes into account both completeness and correctness, is a measure of how well the final outcome has been achieved. It is quantified by equation (3) and it is equivalent to IoU.

"F1 score" is the harmonic mean of completeness and correctness, and it is defined by equation (4).

$$\text{Completeness} = \frac{TP_{buffer}}{TP_{buffer} + FN_{buffer}} \quad (1)$$

$$\text{Correctness} = \frac{TP_{buffer}}{TP_{buffer} + FP_{buffer}} \quad (2)$$

$$\text{Quality} = \frac{TP_{buffer}}{TP_{buffer} + FP_{buffer} + FN_{buffer}} \quad (3)$$

$$F1score = \frac{2 * Completeness * Correctness}{Completeness + Correctness} \quad (4)$$

The term "True Positive" (TP) refers to the correct identification of a crack segment by the model. A "False Positive" (FP) refers to a pixel that the model falsely identified as a crack, while a "False Negative" (FN) refers to a real crack pixel that the model failed to identify as such.

Fig. 3 illustrates the buffer concept. Based on GT, it is defined as TP if the prediction is included in the buffer width, and FP if not. If GT is not included in the buffer width based on the prediction, it is defined as FN. In this study, the buffer width was defined as 5 pixels. In other words, if the predicted result is included within GT and 5 pixels, it is determined that the prediction is successful.

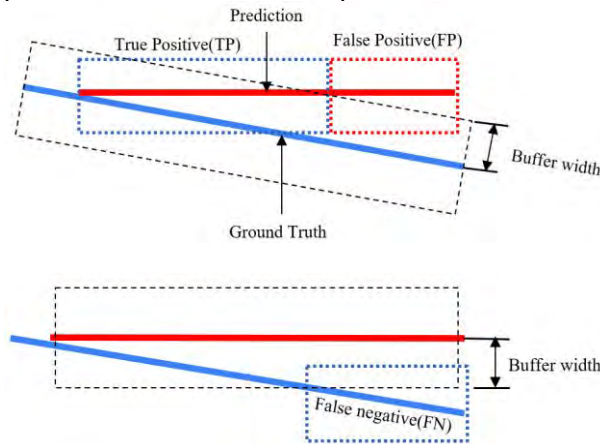


Fig. 3. Illustration of TP, FP, and FN of cracks using CCQ metric with the buffer

Skeletonization is also applied to predicted and ground truth masks of cracks to examine the segmentation performance focusing only on the crack shape. Skeletonization is a morphological operation in image processing that aims to produce the skeletal structure or the thinned version of a binary image, preserving only the essential structures of the image. The goal of using skeletonization is to obtain a simplified representation of road cracks while retaining their shape and topology.

2.2 Keypoint-based evaluation metric

The second evaluation metric examines the keypoint matching between predictions and ground truth, to mitigate the sensitivity to pixel thickness. To this end, this study employed the GFTT (Good Features to Track) concept, introduced by Shi and Tomasi in 1994. Their objective was to determine which features are appropriate for tracking in a feature-based vision system, as the identification and tracking of good features is crucial for its operation (Shi and Tomasi 1994). By

adopting this features, the shape-based evaluation is possible for crack segmentation results. The GFTT detector was originally designed to extract features such as corner points, similar to the key point extraction method of Harris and Stephens [5]. The coordinates of the keypoints were obtained from the segmentation results and ground truth images. If a keypoint of the segmentation results is within 5 pixels of a keypoint of the ground truth, it was considered a True Positive ($TP_{prediction}$). If a keypoint of the ground truth is within 5 pixels of a keypoint of the segmentation results, it was considered a True Positive (TP_{GT}). Prediction, GT, and Keypoint scores are defined by equation (5), (6), (7).

$$\begin{aligned} \text{Prediction score} &= \frac{TP_{prediction}}{\# \text{ of keypoints in Prediction}} \quad (5) \end{aligned}$$

$$GT \text{ score} = \frac{TP_{GT}}{\# \text{ of keypoints in GT}} \quad (6)$$

$$\begin{aligned} \text{Keypoint score} &= \frac{2 \times \text{Prediction score} \times GT \text{ score}}{\text{Prediction score} + GT \text{ score}} \quad (7) \end{aligned}$$

3 Experiment

The experiments were conducted on the AIM crack dataset [3], collected by multiple normal vehicles equipped with dashboard cameras. The dataset consisted of 327, 100, and 100 images for training, validation, and test, respectively. The dataset provides polygon annotations for road cracks. DeepLabv3+ [8] and FPN [9] were used as a segmentation model. In the implementation, DeepLabv3+ has been trained for 50 epochs with the encoder part of mit_b5, which was SegFormer [10] pre-trained on ImageNet. The mini-batch had 6 images, the learning rate of 0.0001 before 25 epochs and 0.00001 after, and the optimizer of Adam were set to train the model. For comparison, FPN was trained for 50 epochs with the encoder part of Efficientnet_b5[11], which was pre-trained on ImageNet. The mini-batch had 16 images, the learning rate of 0.0001 before 25 epochs and 0.00001 after, and the optimizer of Adam were set to train the model.

3.1 CCQ metric experiment

To count TP, FP, and FN, this study produced the crack masks on the test images (see examples in Figs. 1, 8 and Table 1). As shown in Fig 4, the location and shape of the cracks were accurately predicted. However, the presence of FP suggests that the model's prediction of crack thickness is wider than the ground truth. This result yields a low IoU score of 0.49. In Fig 5, for the same reason,

IoU score was only 0.29. As the correct prediction of crack thickness is less critical in making proactive M&R decisions for road networks, the shape-based evaluation using the CCQ score and the skeletonization was conducted, as shown in Fig 6, 7. The CCQ score provides insight into the model's ability to produce results that are similar to human cognitive evaluation in the context of participatory sensing, by using the buffer method.



Fig. 4. Segmentation mask visualization of IoU (top) and the proposed metrics (bottom) using DeepLabV3+. TP is blue, FP is green, FN is red.

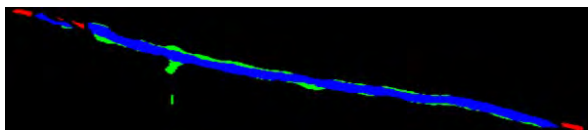
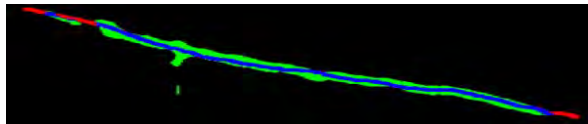


Fig. 5. Segmentation masks produced by FPN, with the IoU (top) and proposed metrics (bottom). TP is blue, FP is green, FN is red.

To further reduce errors due to the crack thickness difference, this study performed skeletonization on both prediction and ground truth masks, and measured CCQ again. Skeletonization is a critical preprocessing step for crack segmentation models, as it can mitigate errors arising from differences in prediction and ground truth crack thickness. For instance, if a crack is labeled with a thickness of one pixel in the ground truth, an accurate prediction of the crack's location with a thickness of four pixels would yield an IoU score of only 0.25. By skeletonizing both prediction and ground truth mask, the thickness is reduced to one pixel (Fig 8), thereby enabling better correspondence with the ground truth and improving the accuracy of the segmentation model. Skeletonization was performed using the Python package called scikit-image. Using this package, the skeletonization algorithm iteratively removes peripheral pixels of the image data, while preserving the connectivity of the objects of interest. This operation is

performed iteratively until the desired level of a one-pixel thick skeletonization is achieved.

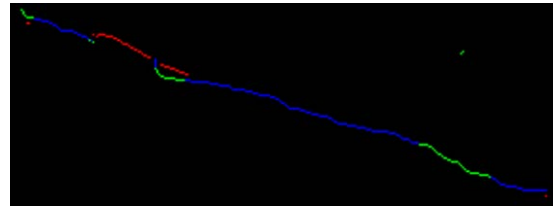
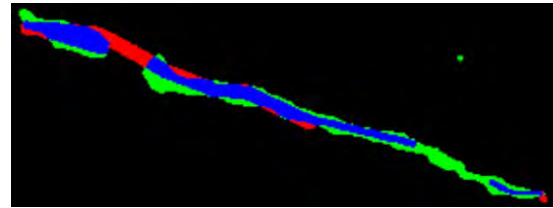


Fig. 6. Segmentation mask visualization of IoU (top) and the CCQ metric after skeletonization (bottom) using DeepLabV3+. TP is blue, FP is green, FN is red.

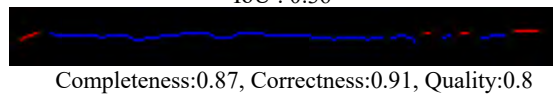
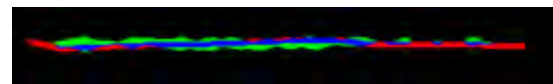


Fig. 7. Segmentation masks produced by FPN, with the IoU (top) and the CCQ metric after skeletonization (bottom). TP is blue, FP is green, FN is red.

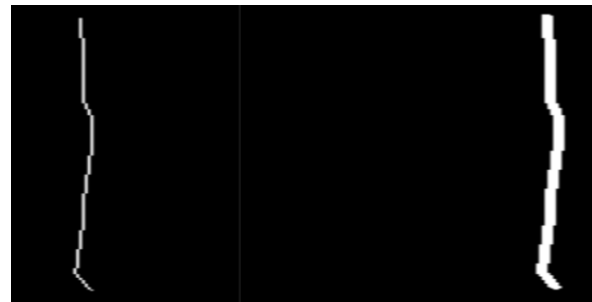


Fig. 8. Example of Skeletonization

3.2 Keypoint metric experiment

Key point extraction was performed on both the prediction and ground truth masks, and the extracted key points can be seen in Fig. 9. Key points were generated throughout the crack, and matching was performed based on the distance between the key points of the prediction and ground truth. Key points within 5 pixels were assumed to be matched, so the score can be adjusted to compensate for the position and thickness difference of the cracks in the prediction and ground truth mask.

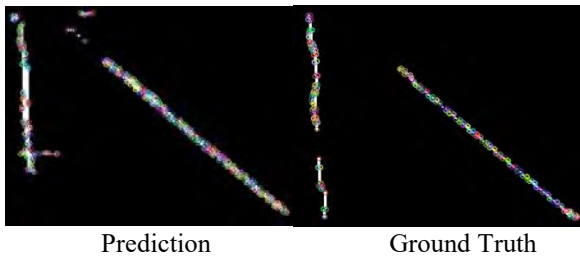


Fig. 9. An example of keypoint matching results. (IoU = 0.33, keypoint matching score = 0.6)

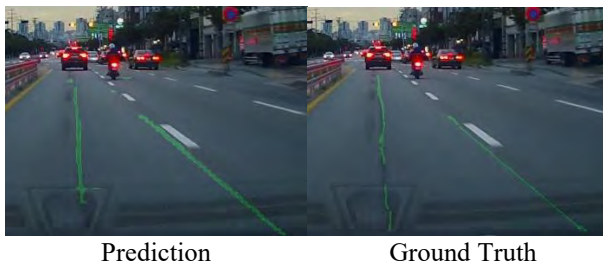


Fig. 10. Visualization of the predicted masks versus the ground truth masks. Despite correct predictions in crack shapes, the IoU score is low as shown in Table 1.

Table 1. Model performance evaluation in each metric for Fig. 10

Row	IoU	Comp.	Corr.	Qual.	Keypoint
First	0.33	0.92	0.73	0.81	0.6
Second	0.35	0.84	0.78	0.81	0.79
Third	0.24	0.69	0.69	0.69	0.69
Fourth	0.32	0.88	0.89	0.88	0.68

Table 2. Model evaluation

	S*	IoU	Comp.	Corr.	Qual.	Keypoint
Score (Deep LabV3+)		0.22	0.71	0.54	0.43	0.44
	✓	0.06	0.73	0.55	0.44	0.45
Score (FPN)	S*	0.24	0.74	0.67	0.53	0.44
	✓	0.07	0.69	0.73	0.53	0.45

S*: Skeletonization

4 Limitation & Future study

In this study, we present a metric that is capable of assessing the predictive capabilities of a road crack segmentation model in participatory sensing environments. The effectiveness of this metric was demonstrated through the experiments. However, the prediction results for fatigue cracks, as shown in Fig. 11, is relatively difficult to handle using the proposed metric. Although the prediction result seems plausible to the naked eye, evaluating the model's performance using the CCQ metric with and without skeletonization was not successful in the case of fatigue cracks, as shown in Fig. 13 and Table 3.

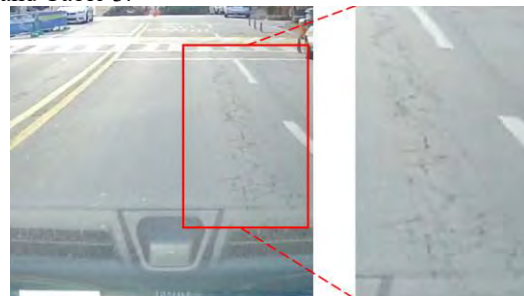


Fig. 11. Example of fatigue crack

Future research is needed to develop a suitable approach for evaluating the model's performance in fatigue cracks. The proposed metric can be applied exclusively to non-fatigue cracks by using object detection models which identify fatigue cracks. If suitable evaluation metrics are

applied for each type of crack, it will be possible to more accurately evaluate the model's predictive ability.

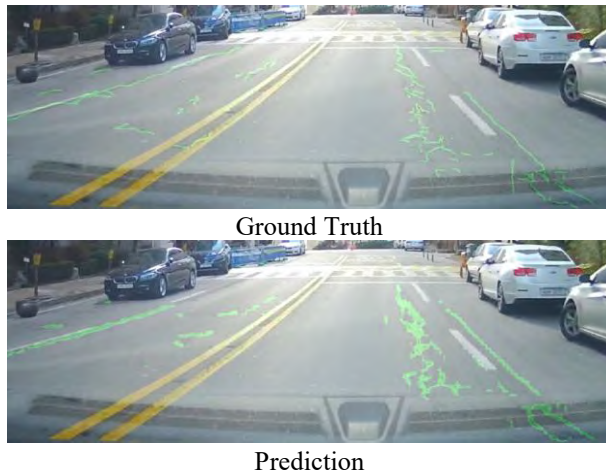


Fig. 12. The ground truth and the prediction results were overlaid on the raw images.

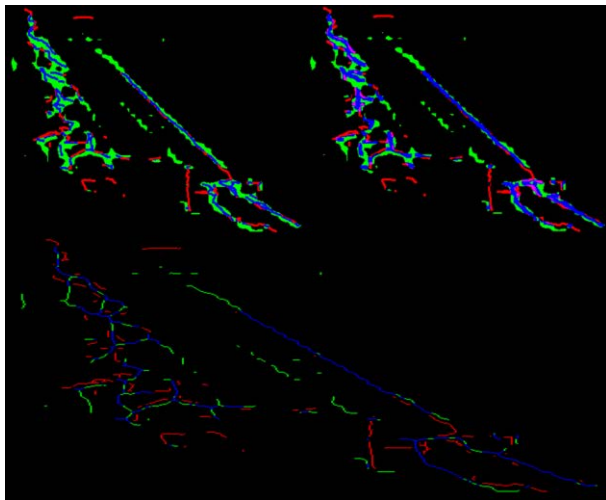


Fig. 13. IoU (Top Left), CCQ (Top Right), CCQ after Skeletonization (Bottom). TP is blue, FP is green, FN is red.

Table 3. Model performance evaluation for fatigue cracks shown in Fig. 13

	S*	IoU	Comp.	Corr.	Qual.
Score		0.26	0.62	0.53	0.4
	✓	0.05	0.49	0.56	0.35

5 Conclusion

This study investigated alternative segmentation performance evaluation metrics for road crack segmentation in the context of participatory sensing. As inaccurate annotations are inevitable due to poor image quality of a dashboard camera, the proposed evaluation metric allow users to examine the segmentation performance with a criterion that the predicted masks are useful for decision-making in proactive M&R for road networks. The experimental results imply the use of IoU score is disadvantageous in participatory sensing, as it is highly sensitive to the width of cracks rather than the predicted crack shape which can provide the crack ratio and length information. Rather than IoU, the CCQ score or keypoint based assessment is more preferable. This study highlights the importance of using appropriate performance evaluation metric to assess road crack segmentation models focusing on crack shapes, thereby facilitating the accurate performance evaluation for participatory sensing-based road monitoring results.

Acknowledgements

This research was conducted with the support of the “2022 Yonsei University Future-Leading Research Initiative (No. 2022-22-0102)” and the “National R&D Project for Smart Construction Technology (RS-2020-KA156488)” funded by the Korea Agency for Infrastructure Technology Advancement under the Ministry of Land, Infrastructure and Transport, and managed by the Korea Expressway Corporation. This work was also supported by K-water Grant funded by the Korean Government (Innovative talent nurturing project in the digital water industry). Any opinions and findings in this paper are those of the authors and do not necessarily represent the funding agencies listed above.

References

- [1] Korea Institute of Civil Engineering and Building Technology. Road Statistics and Maintenance Information System. On-line: http://www.rsis.kr/maintenance_summary.htm, Accessed: 30/01/2023
- [2] Federal Highway Administration. Pavement Performance Measures and Forecasting and The Effects of Maintenance and Rehabilitation Strategy on Treatment Effectiveness (Revised). U.S. Department of Transportation: Research, Development, and Technology Turner-Fairbank Highway Research Center, 6300 Georgetown PikeMcLean, VA 22101-2296, 2017
- [3] Bang, S., et al., Encoder–decoder network for pixel-level road crack detection in black-box images.

- Computer-Aided Civil and Infrastructure Engineering*, 34(8): p. 713-727, 2019.
- [4] Somin Park, Seongdeok Bang, Hongjo Kim, and Hyoungkwan Kim., Patch-based Crack Detection in Black Box Images using Convolutional Neural Networks. *Journal of Computing in Civil Engineering*, 33(3), 04019017, 2019.
- [5] Cao, M.-T., et al., Survey on performance of deep learning models for detecting road damages using multiple dashcam image resources. *Advanced Engineering Informatics* 46: 101182, 2020.
- [6] Wiedemann, Christian, et al. Empirical evaluation of automatically extracted road axes. *Empirical evaluation techniques in computer vision*, 12: 172-187, 1998.
- [7] Zhu, Zhenhua, and Khashayar Davari. Comparison of local visual feature detectors and descriptors for the registration of 3D building scenes. *Journal of Computing in Civil Engineering* 29.5: 04014071, 2015.
- [8] Chen, L.-C., et al., Rethinking atrous convolution for semantic image segmentation. *arXiv preprint arXiv:1706.05587*, 2017.
- [9] Lin, Tsung-Yi, et al. Feature pyramid networks for object detection. *Proceedings of the IEEE conference on computer vision and pattern recognition*. 2017.
- [10] Xie, E., et al., SegFormer: Simple and efficient design for semantic segmentation with transformers. *Advances in Neural Information Processing Systems*, 2021. 34: p. 12077-12090.
- [11] Tan, Mingxing, and Quoc Le. Efficientnet: Rethinking model scaling for convolutional neural networks. *International conference on machine learning*. PMLR, 2019.

Microservice-Based Middleware for a Digital Twin of Equipment-Intensive Construction Processes

Anne Fischer¹, Yuling Sun¹, Stephan Kessler¹, and Johannes Fottner¹

¹Chair of Materials Handling, Material Flow, Logistics, TUM SoED, Technical University of Munich, Germany

anne.fischer@tum.de, yuling.sun@tum.de, stephan.kessler@tum.de, j.fottner@tum.de

Abstract -

Following the example set by Industry 4.0, digitization is being proven as a vital tool in equipment-intensive construction processes. Telematics data from equipment is sent to platforms. The profitable use of this data is part of today's research regarding digital twins. This paper shows the conformity to Industry 4.0 terminology and digital twin components in construction. It reveals the need for data transformation and integration to cope with the diversity of equipment fleets. Thus, this paper introduces middleware systems based on different microservices, each with a different functionality, and shows their implementation at the special foundation engineering project.

Keywords -

Middleware; Microservice architecture (MSA); Digital twin in construction (DTC); Discrete-event simulation (DES)

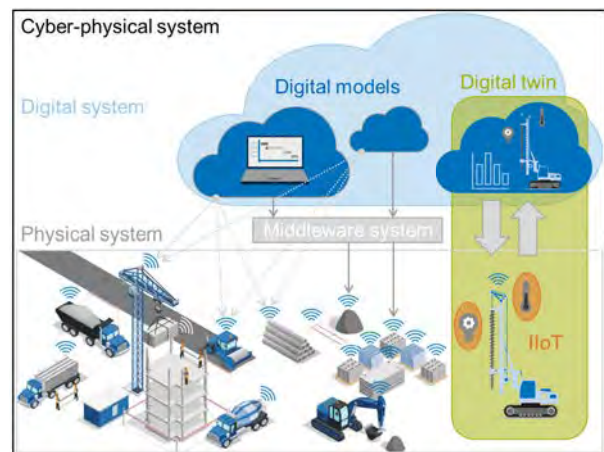


Figure 1. Overview of Industry 4.0 terms in the context of equipment-intensive construction processes

1 Introduction

Pushed by the achievements of the Industry 4.0 movement, first mentioned in Germany's high-tech strategy plan for 2020 [1], the construction industry is trying to emulate it as it has yet to profit from productivity growth following digitization [2]. The Industry 4.0 objective is to give every asset an identification understandable at any time to anyone [3]. This identification helps to digitize the physical asset as a digital twin (DT), see Figure 1.

It is hard to simply adopt the DTs of Industry 4.0 - even though the degree of digitization is increasing, as several systematic literature studies show, e.g., [4]. Limitations arise from construction-specific requirements [5]: (1) The unique character of each individual construction site; (2) Transient processes; (3) Dependence on location and weather conditions; (4) The use of different (often inoperable) technologies; (5) Strong fragmentation of the construction industry; (6) Segmentation along the product life cycle or process chain. In this context, the exchange of heterogeneous data in a construction project's life cycle must be managed before DTs are adopted [6].

As a first step, this paper introduces a middleware system as a layer to centralize data exchanges, see dotted

vs. straight arrows in Figure 1. The paper clarifies the terms relating to DTs to understand the need and the requirements for middleware. It shows the implementation of a specially developed microservice-based middleware for DT of equipment-intensive construction processes. Its verification and validation show the need for data management and also point out middleware's weaknesses regarding proprietary interfaces. The paper ends with a summary and presents an outlook.

2 Background

2.1 Digital twins in the construction industry

The interest in digital technology has increased exponentially over the last decades [7]. In a discussion of DTs, it is essential first to clarify the terms and definitions [8].

Cyber-physical system (CPS): A DT is part of a cyber-physical system (CPS) [9], see Figure 1. A CPS "links real (physical) objects and processes with information-processing (virtual) objects and processes via open, partly global and always interconnected information networks" [10]. A common description for scaled CPS is, therefore,

a “system of system” [11]. Cross-linking various physical assets implies an increasing standardization effort [12], e.g., RAMI 4.0 [3].

Industrial internet of things (IIoT): The term internet of things (IoT) or industrial internet of things (IIoT) is one part of the CPS, see Figure 1. It concentrates on the connectivity of the assets [13]. The IIoT enables bidirectional data flow within and between DTs [14]. Various reliable protocols are available for networking IIoT devices [15, 6]. Fuller et al. [14] conclude that it is one of the significant technical aspects of a DT.

Digital twin (DT): According to Kritzinger et al. [16], the degree of integration between the digital and physical model increases from digital model (DM) to digital shadow (DS) to digital twin (DT). The last allows bidirectional communication between the models to use real data, on the one hand, and to influence the real model directly, on the other hand (gray arrows in Figure 1).

Digital twin in construction (DTC): In line with the efforts in the manufacturing and health sectors, DTs have high potential in the construction industry [14]. Building information modeling (BIM) can potentially be used as a digital twin in construction (DTC) for information storage and process modeling and monitoring [17]. Fundamentally, BIM is a 3D construction project description. Fed with more than geometrical data, such as time and costs, and described in a standardized format, like IFC (industry foundation classes), BIM evolved into a DTC [18]. Sacks et al. [19] strengthen the term digital twin by differing between the construction digital twin (CDT) according to Boje et al. [18] and the digital twin in construction (DTC). They thereby emphasize that DTC is more than a technology. A DTC implies a workflow. It can be classified as a dynamic model of a construction site that monitors construction in real time to generate added value from the site data [20]. However, criticism arises as BIM has weaknesses in handling big data with the help of Artificial Intelligence (AI) [19]. Furthermore, BIM is very popular in high-rise building construction but not in heavy civil engineering, where Geographic Information System (GIS) is more appropriate [21, 22]. Visual forms of representation and interaction based on web interfaces, AR/VR technologies, artificial intelligence (AI), or simulation are necessary to process the information provided and to make it available to the people on-site [4]. Sacks et al. [19] strengthen the term construction digital twin (CDT) according to Boje et al. [18] to the term DTC implying a workflow.

2.2 Components of a DTC

According to Feng et al. [23], DTCs are basically composed of five parts: (1) data acquisition, (2) data transmission, (3) data model, (4) data integration, and (5) data service.

Data acquisition: For the identification of the assets and the recording of the construction progress, sensors can be divided into three classes according to [24]: (1) Vision-based, e.g., laser scanning [25], image recognition [26]; (2) Audio-based, e.g., microphones [27]; (3) Kinematic, e.g., inertial measurement unit (IMU) [28], equipment sensors such as for hydraulic pressure or forces [29, 30], or radio-frequency identification (RFID) tags [31].

Digital models and service: Besides BIM, discrete event simulation (DES) models are digital models for predicting construction processes [32]. Data-driven DES has the benefit of being more efficient and the results have a better quality [33]. Regarding real-time simulation, studies exist using DES and data from construction equipment without describing data exchange [34]. However, as mentioned above, data exchange is one key challenge of the digital twin. Some authors tried to adapt the high-level architecture (HLA) from IEEE standard 1516 [35] [36, 37]. HLA helps running simulation models in a distributed network environment. However, to the authors’ best knowledge, the standard is not further extended.

Data transmission and integration: From a manufacturer’s point of view, Ghosh et al. [38] emphasize the need for IIoT but also data storage, management, and an analyzing system to arrange different DTs in a CPS fully. Feng et al. [23] come to the same conclusions for applying DTCs: Solutions to transmit and integrate heterogeneous data in the construction industry are lacking. Especially, in equipment-driven construction processes, an appropriate tool for linking heterogeneous data sources is required. However, today’s construction equipment manufacturers offer their proprietary fleet management systems integrating clients’ different equipment types from different manufacturers. The ISO standard 15143-3 [39] faces standards for telematics data exchange.

Will and Waurich [40] therefore give an overview of proprietary and typical data space approaches, and middleware systems, such as open platform communications unified architecture (OPC-UA). Existing commercial middleware solutions have been used for DTs [41] but there exist reservations on data security [14]. Ravi et al. [41] show the implementation of a DTC in robotics, using commercial services from Amazon and Rhino to store and analyze data. Fuller et al. [14] name other commercial middleware

systems provided by Google or Microsoft, but emphasize data security challenges in the context of DTCs.

The construction industry has realized the need for a middleware system, but there exist only few approaches to specially developed middleware for DTC. In the following, we want to clarify this term and its specification from the viewpoint of software development.

2.3 Middleware systems

A middleware domain manages the integration and linkage of data to distributed applications or services [42]. In contrast to the common point-to-point topology where data is exchanged directly between the services, middleware serves as a translator layer, so that different services can communicate with each other [43], see Figure 1.

Communication protocols: A middleware uses different communication protocols. The transmission control protocol (TCP) is straightforward and fast. It transports data via a stream of bytes [44]. In contrast to continuous data streaming, the hypertext transfer protocol (HTTP) sends messages from a client to a server for response [45]. The communication interface for applications is the application programming interfaces (API). If the interfaces follow the design principles of the representational state transfer (REST), they are called REST-APIs, enabling, e.g., a uniform interface and layered system architecture [46]. Thus, the middleware is also a specific protocol [47].

Middleware architectures: According to Ungurean et al. [42], the following are relevant middleware systems: Distribute device data for real time systems (DDS), message queuing telemetry transport (MQTT), advanced message queuing protocol (AMQP), and extensible messaging and presence protocol (XMPP). These middleware systems are all limited to specific layers, e.g., MQTT is used only for device-to-server communication, and DDS is used for a single system. An IIoT-specific middleware is missing. Today, OPC-UA [48] is the standard middleware system to enable the real-time implementation of Industry 4.0 technologies [49, 8, 47]. OPC-UA is historically developed for the collaboration among manufacturing robots (of different robotic producers). Thus, it is interoperable among different systems.

Service oriented architecture (SOA): In recent years, there has been a lot of research into the computing paradigm of service oriented architecture (SOA) [50]. In SOA, distributed applications are built using services as the main component. These services are autonomous and platform-independent so that they can be discovered and used by service consumers dynamically. There are three

components in SOA: (1) the service provider, (2) the service requester, and (3) the broker registry [51].

Microservice architecture (MSA): Microservice architecture (MSA) is similar to SOA but with some differences [52]. SOA focuses more on enterprise or even cross-enterprise software systems, which have certain requirements, e.g., being protocol-agnostic. In contrast, the application of MSA is restricted to smaller applications without the claim of scalability or generic protocol transformations. Thus, it is less complex and, therefore, easier to implement.

A microservice is a small application with only a single task, or there is only a single reason for it to change. The advantages of microservices [53] are that they can be deployed, scaled, and tested independently. However, as an application grows, it becomes more challenging to make changes, so it becomes unmaintainable.

2.4 Research gap and objective

The literature review shows that the application of digital technologies to DTCs is not yet realistic. As a critical challenge, the authors identified that the interoperable connection of the components of a DTC in a CPS. A microservice-based middleware is suitable to fulfill these requirements. It orchestrates protocols and interfaces from different services in one centralized layer. Further services can be easily added as they are decoupled, allowing for independent development and maintenance. In DTC, research needs to focus on this data transmission and integration problem. In the following, we introduce the implementation of a microservice-based middleware system for the equipment-intensive construction industry.

3 Methodology

3.1 Framework

Regarding the construction industry, the authors are working on a DTC in heavy civil engineering. More precisely, their use case is pile production according to the Kelly drilling method, which is used to build deep foundations to transfer loads into the ground, e.g., for high-rise buildings or bridges. Figure 2 shows the DTC in a feedback control system. Based on the definition above, the physical asset is the equipment for drilling these piles, called a Kelly drilling rig (scheme on the right). The digital asset is the DES for project scheduling and process simulation (left two clouds). We developed a hybrid deep learning model to recognize the telematics data from the Kelly drilling rig (cloud on the bottom). The data exchange among the equipment, the DES, and the activity recognition is orchestrated by the following middleware (green arrow).

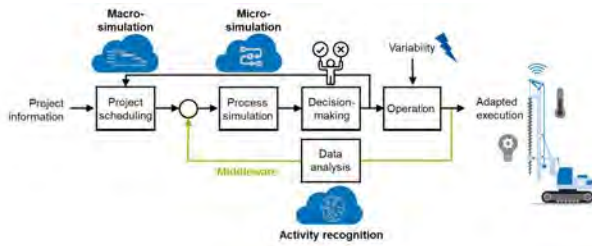


Figure 2. Feedback control system from Fischer et al. [54] including the functionality of the middleware

3.2 Implementation

Figure 3 shows the middleware architecture. It is implemented in Java 11 using the Spring Boot framework [55] and Apache Maven [56] as a build management tool on an Ubuntu system.

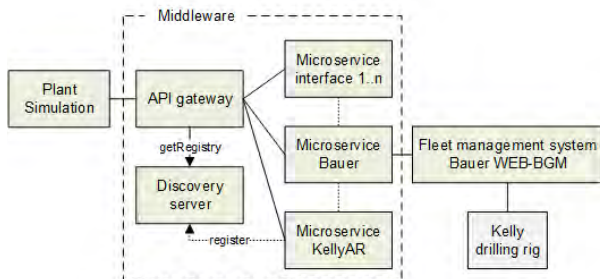


Figure 3. Middleware architecture adapted from [57]

Communication protocols: The middleware uses HTTP for internal and external communication with machine data systems via REST requests. Communication with users is handled either by HTTP or TCP.

API gateway and discovery server: The middleware consists basically of two components: (1) an API gateway and (2) a discovery server. They allow communication between the user and the microservices, see Figure 4 (left). The API gateway is the single entry point to the middleware. It provides a REST API and a TCP-based API for requesting all data from the different fleet management systems or other applications. In addition, it can translate between TCP and HTTP messages for requests and responses. The API gateway needs the discovery server to know the addresses of the microservices to transmit the requested data then. We therefore implemented a client-side server discovery using the Spring Eureka service registry and Eureka Discovery Client. Figure 4 (left) shows the components and the sequence of the API gateway: (1) The TCP requests are received and translated into HTTP

requests; (2) The HTTP requests are transferred to the REST endpoint; (3) From there, they are forwarded to the implemented microservices using the locations from the discovery server.

Microservices: The middleware includes several microservices responsible for communicating with fleet management systems. Their job is to bring the different kinds of data from the construction site into a single format, i.e., hide the differences in authentication, communication formats, or from the user. Two microservices are required to realize the DTC: Bauer and KellyAR, see Figure 4 (right). The Bauer microservice connects to the proprietary fleet management system from our industry partner Bauer Maschinen GmbH in Germany. This platform receives and stores data from their Kelly drilling rigs via TC3G data modules [58]. The requests follow ISO standard 15143-3 [39]. The KellyAR microservice pre-processes the telematics data for the DES because the model requires the duration of the steps in the single construction process for production optimization [30].

3.3 Validation

Before validation, we verified the code of the middleware by the API Postman [59]. The validation of the described framework is then split into two test set-ups including a virtual and a real Kelly drilling rig. The first test-set up is used to test standardized data transfer via ISO 15143-3. The second test set up is used to test the DTC framework including the update of the DES with the current production time. In both cases, the DES is conducted with the Tecnomatix Plant Simulation software from Siemens [60].

The DES model for the first test follows the Plant Simulation guideline for exchanging data via a network socket [61]. It includes a client socket object to enable a TCP connection to the middleware (server socket), a method object to program the way messages are sent, and string variables to monitor the requested and sent TCP messages. The required OAuth 2.0 identification within ISO 15143-3 first requires the authentication request, and then, finally, the received token is used for requesting fleet information. We received the 20 data points, according to ISO 15143-3, from a virtual drilling rig from Bauer, including o.a., header information, last known location, operating hours, and cumulative fuel used.

However, this data does not include the construction process step duration. We therefore developed the KellyAR microservice to recognize the equipment's activities based on sensor data and calculate the duration. These sensor data could not send to the fleet management system. As a result, the implemented microservice was not needed for communication.

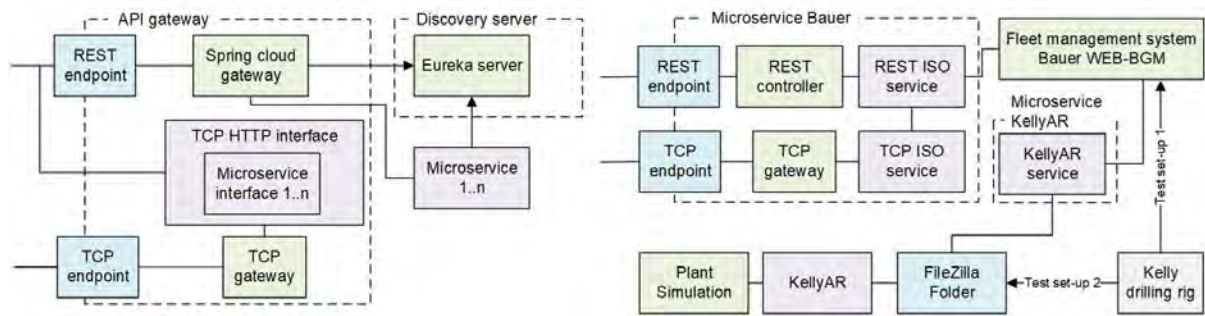


Figure 4. Middleware components and data flow adapted from [57]

Instead, we used a simple bidirectional data exchange via the open-source server FileZilla. FileZilla enables direct TCP exchange. To log into the wifi of the drilling rig and transmit the data directly to a local folder from the application, see Figure 4 right. The KellyAR microservice interprets the data and transfers it to the Plant Simulation.

4 Results and discussion

Limitations arise on the middleware verification due to a missing manufacturer API, so only data exchange via ISO standard 15143-3 [39] was tested. Further studies are needed to address the optimization of the data exchange performance, the security aspects, and the system bandwidth and connectivity on site. However, these aspects were essential for the practical and effective use of DTCs in real-world construction settings.

The validation of the middleware is further limited to a specific use case. As mentioned in Section 2, there will be various systems in a system in the future. Although proprietary APIs exist, a single implementation and validation are time-consuming. The standardization effort is highly relevant for DTCs. For commercial purposes, it is further mandatory to ensure data access, e.g., by data trustees, such as Gaia-X [62] in the automotive industry or the agrirouter [63] in the agricultural industry.

To finally achieve a DTC, the equipment sends data and receives data from the simulation model. It is not for automating the construction process by controlling the construction equipment but forecasting the construction process. The results from the simulation model, such as the remaining construction progress [64] or a cost-benefit comparison of alternative process execution [65], are therefore transferred by the people on-site to optimize the construction process.

Overall, the application of DTCs in the future requires that on-site personnel have enhanced skills to use the simulation model or to integrate new equipment. The construction industry needs to think of new job profiles in order to benefit from the Industry 4.0 technologies.

5 Conclusion

DTC is one buzzword increasingly used in the construction industry to talk about digitization. A common understanding of the terms and definitions is mandatory to push DTC further toward realization. Different relevant Industry 4.0 technologies exist to realize a DTC. Middleware is, therefore, required to orchestrate the data exchange between the physical and the digital assets of the DTC. The DTC framework described in this paper aims to support the decision-makers on-site with simulation models cyclically updated by information on the production equipment, here the drilling rig for pile production. This paper presents and discusses the implementation of specially developed microservice-based middleware. The work presented in this paper is limited as the validation of the middleware is not conducted on a real use case.

6 Acknowledgment

This research was funded by the German Federal Ministry of Education and Research through the research project “Bauen 4.0” (02P17D230). We thank our industry partner for the cooperation.

References

- [1] H. Lasi, P. Fettke, H.-G. Kemper, T. Feld, and M. Hoffmann. Industry 4.0. *B&I Syst. Eng.*, 6(4): 239–242, 2014. doi:10.1007/s12599-014-0334-4.
- [2] McKinsey Global Institute. Reinventing construction: A route to higher productivity, 2017. Online: https://www.mckinsey.com/-/media/mckinsey/business_functions/operations. Accessed: 12/14/2022.
- [3] DKE. RAMI 4.0, 2019. URL <https://www.dke.de/de/arbeitsfelder/industry/rami40>. Accessed: 12/19/2022).
- [4] T.D. Oesterreich and F. Teuteberg. Understanding the implications of digitisation and

- automation in the context of Industry 4.0. *Computers in Industry*, 83:121–139, 2016. doi:10.1016/j.compind.2016.09.006.
- [5] W. Günthner and A. Borrmann. *Digitale Baustelle- innovativer Planen, effizienter Ausführen [Digital Construction Site - Innovative Planning, Efficient Execution]*. Springer-Verlag Berlin Heidelberg, Germany, 2011. ISBN 978-3-642-16485-9.
- [6] C.J. Turner, J. Oyekan, L. Stergioulas, and D. Griffin. Utilizing Industry 4.0 on the construction site: Challenges and opportunities. *IEEE Trans. on Ind. Inform.*, 17(2):746–756, 2021. doi:10.1109/TII.2020.3002197.
- [7] R. Al-Sehrawy and B. Kumar. Digital twins in architecture, engineering, construction and operations: A brief review and analysis. In *Proc. 18th Int. Conf. Comp. in Civil & Build. Eng.*, volume 98, pages 924–939. 2021. doi:10.1007/978-3-030-51295-8_64.
- [8] M. Perno, L. Hvam, and A. Haug. Implementation of digital twins in the process industry: A systematic literature review of enablers and barriers. *Computers in Industry*, 134:103558, 2022. doi:10.1016/j.compind.2021.103558.
- [9] A. Akanmu and C.J. Anumba. Cyber-physical systems integration of building information models and the physical construction. *Eng., Constr. & Arch. Mgmt.*, 22(5):516–535, 2015. doi:10.1108/ECAM-07-2014-0097.
- [10] The Assoc. of Germ. Eng. (VDI). Industrie 4.0 – Begriffe/Terms, 2021. URL <https://www.vdi.de/ueber-uns/presse/publikationen/details/industrie-40-begriffeterms>. Accessed 12/19/2022.
- [11] S.K. Khaitan and J.D. McCalley. Design techniques and applications of cyberphysical systems: A survey. *IEEE Systems J.*, 9(2):350–365, 2015. doi:10.1109/JSYST.2014.2322503.
- [12] A.J.J. Braaksma, W. Klingenberg, and P.W.H.M. van Exel. A review of the use of asset information standards for collaboration in the process industry. *Computers in Industry*, 62(3):337–350, 2011. ISSN 01663615. doi:10.1016/j.compind.2010.10.003.
- [13] H. Boyes, B. Hallaq, J. Cunningham, and T. Watson. The industrial internet of things (IIoT): An analysis framework. *Computers in Industry*, 101:1–12, 2018. doi:10.1016/j.compind.2018.04.015.
- [14] A. Fuller, Z. Fan, C. Day, and C. Barlow. Digital twin: Enabling technologies, challenges and open research. *IEEE Access*, 8:108952–108971, 2020. doi:10.1109/ACCESS.2020.2998358.
- [15] B. Vogel-Heuser, E. Trunzer, D. Hujo, and M. Sollfrank. (Re-)deployment of smart algorithms in cyber-physical production systems using dsl4hdncs. *Proc. of the IEEE*, page 12, 2021. doi:10.1109/JPROC.2021.3050860.
- [16] W. Kritzinger, M. Karner, G. Traar, J. Henjes, and W. Sihn. Digital twin in manufacturing: A categorical literature review and classification. *IFAC-PapersOnLine*, 51(11):1016–1022, 2018. doi:10.1016/j.ifacol.2018.08.474.
- [17] A. Borrmann, M. König, C. Koch, and J. Beetz, editors. *Building Information Modeling: Technologische Grundlagen und industrielle Praxis [Technology Foundations and Industry Practice]*. Springer Vieweg, Wiesbaden, Germany, 2015. ISBN 978-3-658-05605-6.
- [18] C. Boje, A. Guerriero, S. Kubicki, and Y. Rezgui. Towards a semantic construction digital twin: Directions for future research. *Automation in Construction*, 114, 2020. doi:10.1016/j.autcon.2020.103179.
- [19] R. Sacks, I. Brilakis, E. Pikas, H.S. Xie, and M. Girolami. Construction with digital twin information systems. *Data-Centr. Eng.*, 1, 2020. doi:10.1017/dce.2020.16.
- [20] M. Shahinmoghadam and A. Motamedi. Review of BIM-centred IoT deployment: State of the art, opportunities, and challenges. *Proc. 36th Int. Symp. on Autom. & Robot. in Constr., ISARC 2019*, 2019. doi:10.22260/ISARC2019/0170.
- [21] X. Liu, X. Wang, G. Wright, J. Cheng, X. Li, and R. Liu. A state-of-the-art review on the integration of building information modeling (BIM) and geographic information system (GIS). *ISPRS Int. J. of Geo-Inf.*, 6(2):53, 2017. doi:10.3390/ijgi6020053.
- [22] R. Fosse, L. Spitler, and T. Alves. Deploying BIM in a heavy civil project. In *24th Ann. Conf. of the Int. Group for Lean Constr.*, Boston, MA, USA, 2016.
- [23] H. Feng, Q. Chen, and B. Garcia de Soto. Application of digital twin technologies in construction: An overview of opportunities and challenges. In *Proc. 38th Int. Symp. on Autom. & Robot. in Constr. (ISARC)*, pages 979–986, Dubai, UAE, 2021. IAARC. doi:10.22260/ISARC2021/0132.

- [24] B. Sherafat, C.R. Ahn, R. Akhavian, A.H. Behzadan, M. Golparvar-Fard, H. Kim, Y.-C. Lee, A. Rashidi, and E. R. Azar. Automated methods for activity recognition of construction workers and equipment. *J. of Constr. Eng. & Mgmt.*, 146(6), 2020. doi:10.1061/(ASCE)CO.1943-7862.0001843.
- [25] M. Breitfuß, M. Schöberl, and J. Fottner. Safety through perception: Multi-modal traversability analysis in rough outdoor environments. *IFAC-PapersOnLine*, 54(1):223–228, 2021. doi:10.1016/j.ifacol.2021.08.026.
- [26] M. Bügler, G. Ogunmakin, J. Teizer, P. A. Vela, and A. Borrmann. A comprehensive methodology for vision-based progress and activity estimation of excavation processes for productivity assessment. In *21st Int. Workshop: Intl. Comp. in Eng. 2014*, 2014.
- [27] C.F. Cheng, A. Rashidi, M.A. Davenport, and D.V. Anderson. Evaluation of software and hardware settings for audio-based analysis of construction operations. *Int. J. of Civ. Eng.*, 17(9):1469–1480, 2019. doi:10.1007/s40999-019-00409-2.
- [28] K.M. Rashid and J. Louis. Automated activity identification for construction equipment using motion data from articulated members. *Frontiers in Built Env.*, 5, 2020. doi:10.3389/fbuil.2019.00144.
- [29] A. Fischer, M. Liang, V. Orschlet, H. Bi, S. Kessler, and J. Fottner. Detecting equipment activities by using machine learning algorithms. In *17th IFAC Symp. on Inform. Ctrl. Probl. in Manufact.*, Budapest, Hungary, 2021. INCOM. doi:10.1016/j.ifacol.2021.08.094.
- [30] A. Fischer, A. Bedrikow Beiderwellen, S. Kessler, and J. Fottner. Equipment data-based activity recognition of construction machinery. *IEEE Int. Conf. on Eng., Tech. & Innov. (ICE/ITMC)*, 2021. doi:10.1109/ICE/ITMC52061.2021.9570272.
- [31] S. Rinneberg, S. Kessler, and W. A. Günthner. Attachment identification on excavators – recommendations and a guide on the use of RFID technology. *Building Constr. Machinery*, 2015.
- [32] A. Kargul, W.A. Günthner, M. Bügler, and A. Borrmann. Web based field data analysis and data-driven simulation application for construction performance prediction. *J. Inf. Tech. in Constr.*, 20:479–494, 2015.
- [33] R. Akhavian and A.H. Behzadan. Construction equipment activity recognition for simulation input modeling using mobile sensors and machine learning classifiers. *Adv. Eng. Inform.*, 29(4):867–877, 2015. doi:https://doi.org/10.1016/j.aei.2015.03.001.
- [34] K.M. Rashid and J. Louis. Integrating process mining with discrete-event simulation for dynamic productivity estimation in heavy civil construction operations. *Algorithms*, 15(5):173, 2022. doi:10.3390/a15050173.
- [35] IEEE Standard for Modeling and Simulation (MS) High Level Architecture (HLA) - Framework and Rules. *IEEE Std 1516-2010*, pages 1–38, 2010. doi:10.1109/IEEESTD.2010.5553440.
- [36] S. AbouRizk, D. Halpin, Y. Mohamed, and U. Hermann. Research in modeling and simulation for improving construction engineering operations. *J. Constr. Eng. & Mgmt.*, 137(10):843–852, 2011. doi:10.1061/(ASCE)CO.1943-7862.0000288.
- [37] A.H. Behzadan, C.C. Menassa, and A.R. Predhan. Enabling real time simulation of architecture, engineering, construction, and facility management (AEC/FM) systems: A review of formalism, model architecture, and data representation. *J. Inform. Techn. in Constr.*, 20:1–23, 2015.
- [38] Angkush Kumar Ghosh, A. SharifM.M. Ullah, Roberto Teti, and Akihiko Kubo. Developing sensor signal-based digital twins for intelligent machine tools. *J. Ind. Inf. Integr.*, 24:100242, 2021. ISSN 2452414X. doi:10.1016/j.jii.2021.100242.
- [39] Int. Org. for Standard. (ISO). Earth-moving machinery and mobile road construction machinery — worksite data exchange — Part 3: Telematics data. Standard ISO/TS 15143-3:2020, January 2020.
- [40] F. Will and V. Waurich. The role of construction machinery on an automated and connected construction site. *4th Int. VDI Conf. Smart Constr. Equipmt.*, 2020.
- [41] K.S. Ravi, M.S. Ng, J. Medina, and D.M. Hall. Real-time digital twin of robotic construction processes in mixed reality. In *Proc. 38th Int. Symp. on Autom. & Robot. in Constr. (IS-ARC)*, pages 451–458, Dubai, UAE, 2021. IAARC. doi:10.22260/ISARC2021/0062.
- [42] I. Ungurean, N.C. Gaitan, and Gaitan V.G. A middleware based architecture for the industrial internet of things. *KSII Trans. on Internet & Inform. Syst.*, 10(7):2874–2891, 2016. doi:10.3837/tiis.2016.07.001.
- [43] S. Yun, J.-H. Park, and W.-T. Kim. Data-centric middleware based digital twin platform for dependable cyber-physical systems. In *9th Int. Conf. on Ubiquitous & Future Netw. (ICUFN)*, pages 922–926. IEEE, 2017. doi:10.1109/ICUFN.2017.7993933.

- [44] M. Seyedzadegan, M. Othman, S. Subramaniam, and Z. Zukarnain. The TCP fairness in WLAN. In *Proc. Int. Conf. Telecomm. Malaysia Int. Conf. Comm.*, pages 644–648. IEEE, 2007. ISBN 978-1-4244-1093-4. doi:10.1109/ICTMICC.2007.4448564.
- [45] IBM Corp. TCP/IP TCP, UDP, and IP protocols. Online: <https://www.ibm.com/docs/en/zos/2.2.0?topic=internets-tcpip-tcp-udp-ip-protocols>, Accessed: 12/14/2022.
- [46] IBM Cloud Education. REST APIs. Online: <https://www.ibm.com/cloud/learn/rest-apis>, Accessed: 12/14/2022.
- [47] S. Profanter, A. Tekat, K. Dorofeev, M. Rickert, and A. Knoll. OPC UA versus ROS, DDS, and MQTT: Performance evaluation of industry 4.0 protocols. In *IEEE Int. Conf. on Industr. Techn. (ICIT)*, pages 955–962, 2019. doi:10.1109/ICIT.2019.8755050.
- [48] IEC International Electrotechnical Commission. OPC unified architecture - Part 1: Overview and concepts (iec/tr 62541-1:2010), 2010.
- [49] H. Arnarson, B. Solvang, and B. Shu. The application of open access middleware for cooperation among heterogeneous manufacturing systems. In *3rd Int. Symp. Sm.-Sc. Intell. Manufact. Syst. (SIMS)*, 2020.
- [50] V. Issarny, M. Caporuscio, and N. Georgantas. A perspective on the future of middleware-based software engineering. In *Future of Softw. Eng. (FOSE '07)*, pages 244–258, 2007. doi:10.1109/FOSE.2007.2.
- [51] L. Qilin and Z. Mintian. The state of the art in middleware. In *2010 Int. Forum on Inform. Techn. & Appl.*, volume 1, pages 83–85, 2010. doi:10.1109/IFITA.2010.118.
- [52] F. Rademacher, S. Sachweh, and A. Zündorf. Differences between model-driven development of service-oriented and microservice architecture. In *IEEE Int. Conf. on Softw. Arch. Workshops (ICSAW)*, pages 38–45, 2017. doi:10.1109/ICSAW.2017.32.
- [53] J. Thönes. Microservices. *IEEE Software*, 32(1): 116–116, 2015. doi:10.1109/MS.2015.11.
- [54] A. Fischer, G. Balakrishnan, S. Kessler, and J. Fottner. Begleitende Prozesssimulation für das Kellybohrverfahren [Accompanying process simulation for the kelly drilling process]. In *8. Facht. Baum.-technik*, pages 215–234, Dresden, Germany, 2020.
- [55] Inc. VMware. Spring boot. Online: <https://spring.io/projects/spring-boot>, Accessed: 12/14/2022.
- [56] Maven. Apache maven project. Online: <https://maven.apache.org/>, Accessed: 12/14/2022.
- [57] Yuling Sun. *Extension of a middleware by IoT systems and additional machine systems*. Interdisciplinary project at Department of Informatics, Technical University of Munich, Garching, Germany, 2022.
- [58] Sensor-Technik Wiedemann GmbH. TC3G. URL <https://www.stw-mobile-machines.com/en/products/connectivity-gateways/tcg-data-modules/>. Accessed March 25, 2023.
- [59] Postman API. Online: <https://www.postman.com/>, Accessed: 12/18/2022.
- [60] Siemens Product Lifecycle Management Software Inc. Siemens Digital Industry Software Products Tecnomatix. Online: <https://www.plm.automation.siemens.com/global/en/products/tecnomatix/>, Accessed: 12/18/2022.
- [61] Siemens Product Lifecycle Management Software Inc. Tecnomatix Plant Simulation Help. Online: https://docs.plm.automation.siemens.com/content/plant_sim_help/15/plant_sim_all_in_one_html/en_US/tecnomatix_plant_simulation_help/step_by_step_help/importing_data_for_the_simulation/exchanging_data_via_a_network_socket.html, year = Accessed: 03/12/2023.
- [62] Federal Ministry for Economic Affairs and Climate Action. The Gaia-X Hub Germany. Online: <https://www.bmwk.de/Redaktion/EN/Dossier/gaia-x.html>, Accessed: 12/14/2022.
- [63] DKE-Data GmbH Co. KG. Agrirouter. Online: <https://agrirouter.com/>, Accessed: 12/14/2022.
- [64] A. Fischer, Z. Li, F. Wenzler, S. Kessler, and J. Fottner. Cyclic update of project scheduling by using equipment activity data. In *17th IFAC Symp. on Inform. Ctrl. Probl. in Manufact.*, Budapest, Hungary, 2021. INCOM. doi:10.1016/j.ifacol.2021.08.025.
- [65] A. Fischer, Z. Li, S. Kessler, and J. Fottner. Importance of secondary processes in heavy equipment resource scheduling using hybrid simulation. In *Proc. 38th Int. Symp. Autom. & Robot. in Constr. (ISARC)*, pages 311–318, Dubai, UAE, 2021. IAARC. doi:10.22260/ISARC2021/0044.

BIM-SLAM: Integrating BIM Models in Multi-session SLAM for Lifelong Mapping using 3D LiDAR

M. A. Vega Torres¹ & A. Braun¹ & A. Borrmann¹

¹Chair of Computational Modeling and Simulation, Technical University of Munich, Munich, Germany

miguel.vega@tum.de, alex.braun@tum.de, andre.borrmann@tum.de

Abstract -

While 3D Light Detection and Ranging (LiDAR) sensor technology is becoming more advanced and cheaper every day, the growth of digitalization in the Architecture, Engineering and Construction (AEC) industry contributes to the fact that 3D building information models (BIM models) are now available for a large part of the built environment. These two facts open the question of how 3D models can support 3D LiDAR long-term Simultaneous Localization and Mapping (SLAM) in indoor, Global Positioning System (GPS)-denied environments. This paper proposes a methodology that leverages BIM models to create an updated map of indoor environments with sequential LiDAR measurements. Session data (pose graph-based map and descriptors) are initially generated from BIM models. Then, real-world data is aligned with the session data from the model using multi-session anchoring while minimizing the drift on the real-world data. Finally, the new elements not present in the BIM model are identified, grouped, and reconstructed in a surface representation, allowing a better visualization next to the BIM model. The framework enables the creation of a coherent map aligned with the BIM model that does not require prior knowledge of the initial pose of the robot, and it does not need to be inside the map.

Keywords -

BIM, Multi-Session SLAM, Pose-Graph Optimization, Localization, Mapping, 3D LiDAR.

1 Introduction

The ability to align, compare, and manage data acquired at different times that could be spaced apart by long periods, also known as long-term map management, is crucial in real-world robotic applications.

Since the real world is permanently evolving and changing, long-term map management is essential for autonomous robot navigation and users who want to use the map to understand the current situation and its evolution. In particular, in an emergency, an up-to-date map can serve first responders to increase situational awareness and support decision-making to save lives efficiently and safely [1].

Maps are usually created with mobile robots equipped with sensors and leveraging SLAM algorithms to enable fast and automated workflows. However, these maps are commonly disconnected from any preliminary information, creating a map that may suffer from significant drift and does not allow change detection or comparison with a prior map. However, these maps are commonly disconnected from any preliminary information, creating a map that may suffer from significant drift and does not allow change detection or comparison with a prior map.

Nonetheless, a georeferenced BIM model is available for most contemporary buildings and can be used as a reference map to enable accurate LiDAR localization and mapping.

In addition, the robot's pose in the coordinate system of the BIM model could be retrieved with a localization algorithm [2]. Given this pose, the BIM model could support autonomous robotic tasks. For example, path planning, object inspection [3] or maintenance and repair [4].

As will be discussed in Section 2, several researchers have investigated the use of Building Information Modeling (BIM) for robot localization [2]. However, only a few aim to create an accurate, updated map aligned with the information from the BIM model.

Furthermore, most of them also require a perfect estimation of the robot's initial position, which must be inside the prior map. On top of that, almost no method considers discrepancies between the reference BIM model and the real world (Scan-BIM deviations). While we allow Scan-BIM deviations, we also assume that the model still represents a reliable map suitable for localization, i.e., the BIM contains enough features that coincide geometrically with the real world.

To address this challenge, we propose a novel framework that allows the improvement of a map created with mobile 3D LiDAR data. The map is corrected as it is aligned with a BIM model, allowing a better understanding of the scene and change detection for long-term map management.

First, we create session data from BIM models. Session data (SD) represent data collected from the exact location at various periods. These data are very convenient for performing offline operations between sessions, e.g., inter-session alignment [5] or place recognition [6].

A proposed ground-truth multi-session anchoring uses these Session Data (SD) to align and rectify another query SD with a reference BIM model.

Finally, the aligned data is compared against the BIM model, and positive differences are represented as reconstructed surfaces, enabling a better understanding of the current environment.

Overall, the proposed technique aims to contribute to accurately mapping indoor GPS-denied environments and posterior long-term map management.

The remainder of this paper is organized as follows. Section 2 describes related work on BIM-based LiDAR localization and mapping. Section 3 introduces our modular **BIM-SLAM** framework, which is divided into three main steps: **1.** Generation of SD from BIM models, **2.** Alignment of new session data with the reference BIM model and **3.** Positive change detection and segmentation of new elements. Section 4 presents the experimental settings and implementation details. Finally, section 6 summarizes our contributions and concludes our work.

2 Related research

Besides having the potential to support robot localization, a 3D BIM model can be used as a prior map to create accurate, updated 3D maps and allow fast autonomous navigation.

This section will overview state-of-the-art methods, which used prior building information, i.e., BIM models or floor plans, to support robot localization and also methods that support mapping.

2.1 BIM-based 2D LiDAR localization and mapping

Follini et al. [7] demonstrate how the standard Adaptive Monte Carlo Localization (AMCL) algorithm may be used to obtain the transformation matrix between the robot's reference system and a map that was extracted from the BIM model.

The same algorithm was used by [8], [4], and [3] to localize a wheeled robot in an Occupancy Grid Map (OGM) generated from the BIM model. The main difference between these approaches relies on how they create the OGM from the BIM model.

Hendrikx et al. [9] proposed an approach that, instead of using an OGM, applies a robot-specific world model representation extracted from an Industry Foundation Classes (IFC) file for 2D-LiDAR localization. In their factor graph-based localization approach, the system queries semantic objects in its surroundings (lines, corners, and circles) and creates data associations between them and the laser measurements. More recently, in [10], they improved and evaluated their method for global localization, achieving better results against AMCL.

Instead of using a BIM model, [11] use a CAD-based architectural floor plan for 2D LiDAR-based localization. In their localization system, they implement Generalized ICP (GICP) for scan matching with a pose graph SLAM system. Later, they proposed an improved pipeline for long-term localization and mapping in dynamic environments performing better than Monte Carlo Localization (MCL) in the pose tracking problem [12].

In our previous work [2], besides proposing a method to create an OGM from a multi-story IFC Model, we demonstrated that the widely used AMCL is not that robust to deal with changing and dynamic environments, as compared to Graph-based Localization (GBL) methods, like Cartographer and SLAM Toolbox. Based on these findings, and in an effort to facilitate the transition from Particle Filter (PF) to GBL methods, we also contributed with an open source method that converts OGM to Pose Graph-based Maps (PGBM) for robust robot pose tracking. [2].

2.2 BIM-based 3D LiDAR localization and mapping

Other methods have explored 3D LiDAR localization with BIM models.

A high-accuracy robotic building construction system was proposed by [13]. Besides a robust state estimator that fuses Inertial Measurement Units (IMU), 3D LiDAR, and Wheel encoders, they use ray-tracing with three *laser-distance sensors* and a 3D Computer-aided Design (CAD) model to localize the end-effector with sub-cm accuracy. To accomplish this, they took several orthogonal range measurements while the robot was stationary.

In [14] and [15], the 3D LiDAR scan is aligned with the BIM model using the Iterative Closest Point (ICP) algorithm. Whereas in [14], the alignment is constrained to a few selected reference-mesh faces to overcome ambiguities, [15] use image information to filter foreground and background in the point cloud and use only the background for registration. Later the pipeline was reconfigured to create a self-improving semantic perception method that can better handle clutter in the environment [16].

[17] propose a technique to create *.pbstream* maps from BIM models and achieve localization using Cartographer. This method is very convenient; however, since they use Cartographer in localization mode, the robot must have its initial pose inside the boundaries of the prior map to be localized and create an aligned map.

[18] propose Reference-LOAM (R-LOAM), a method that leverages a joint optimization incorporating point and mesh features for 6 degrees of freedom (DoF) Unmanned Aerial Vehicle (UAV) localization. Subsequently, in [19], they improved their method with pose-graph optimization to reduce drift even when the reference object is not visible.

Recently, [20] introduced a semantic ICP method that can leverage the 3D geometry and the semantic informa-

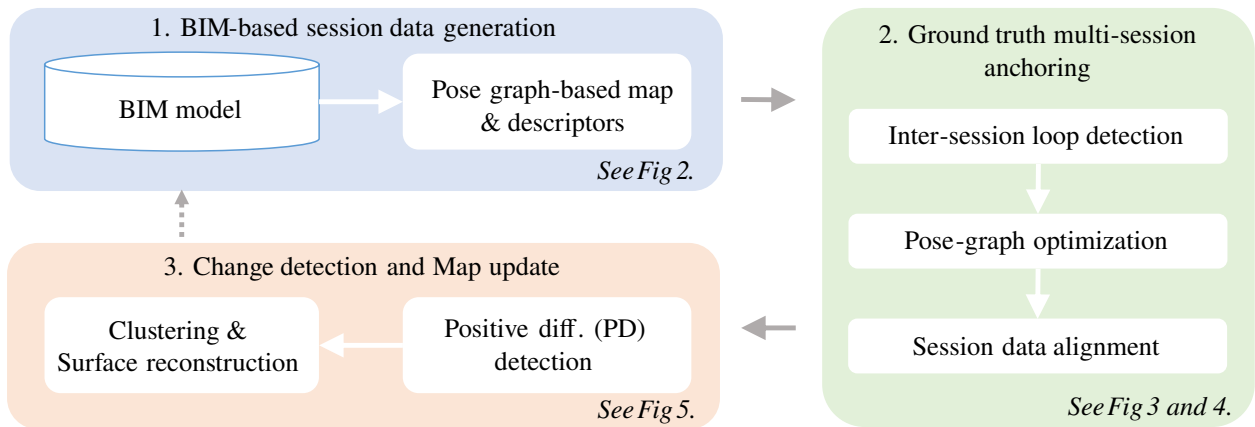


Figure 1. Overview of **BIM-SLAM**. The pipeline consists of three steps: BIM-based session data generation, Multi-session anchoring, and Map update.

tion of a BIM model for data associations achieving a robust 3D LiDAR localization method. Their framework proposes a BIM-to-Map conversion, converting the 3D model into a semantically enriched point cloud. Their experiments show that they can achieve effective 3D LiDAR-only localization with a BIM model.

[21] proposed another relevant approach; here, instead of using object semantics for localization, they use geometric and topological information in the form of walls and rooms. With this information, they create Situational Graphs (S-Graphs), which are then used for accurate pose tracking. Later, they enhanced their method allowing the creation of a map prior to localization and posterior matching and merging with an A-graph (extracted from BIM models). The final merged map was denoted as an informed Situational Graph (iS-Graph) [22].

In [23], the authors introduced direct LiDAR localization (DLL), a fast direct 3D point cloud-based localization technique using 3D LiDAR. They employ a registration technique that does not require features or point correspondences and is based on non-linear optimization of the distance between the points and the map. The approach can track the robot's pose with sub-decimeter accuracy by rectifying the expected pose from odometry. The method demonstrated better performance than AMCL 3D.

While numerous strategies aiming to leverage BIM models for LiDAR localization and mapping have emerged. Most of them have focused on real-time localization without allowing a better estimation of previous poses with pose-graph-based optimization techniques.

Moreover, almost all must have a good initial pose inside the given map. Without this initial pose and if the robot starts from a point where the BIM model is not visible, there is no possibility for localization or the creation of an aligned map. Furthermore, most focused on something

different than automatically identifying the environmental discrepancies.

In this paper, we propose a method that handles these issues, demonstrating that it is possible to retrieve an accurate, aligned, updated, optimized map close to the ground truth and identify positive differences. The method also works if the robot's starting position is not inside the map.

3 Methodology

3.1 Overview

Our method can be divided into three main steps, as illustrated in Figure 1: **Step 1:** Automatic generation of ground truth SD from an IFC model employing OGM to Pose Graph-based map (Ogm2Pgbm) [2] and Gazebo simulator. **Step 2:** Multi-session anchoring with a BIM model as ground truth. **Step 3:** 3D aligned map construction and change detection.

3.2 BIM-based session data generation

Using parts of our previous contribution [2], 3D LiDAR SD with ground truth poses can be created from the BIM model. As a first step, an OGM is created from the model, which is then used to determine the path where a robot will be simulated. The generation of SD from an OGM is performed with the open source Ogm2Pgbm package [2], with a slight modification. Instead of simulating 2D laser scan Robot Operating System (ROS) messages with ray casting, we leverage the Gazebo physics simulation engine [24] to simulate the complete 3D LiDAR scans. This simulation is done by sending navigational goals to a simulated robot and leaving it to navigate autonomously with the ROS Navigation Stack through the estimated path

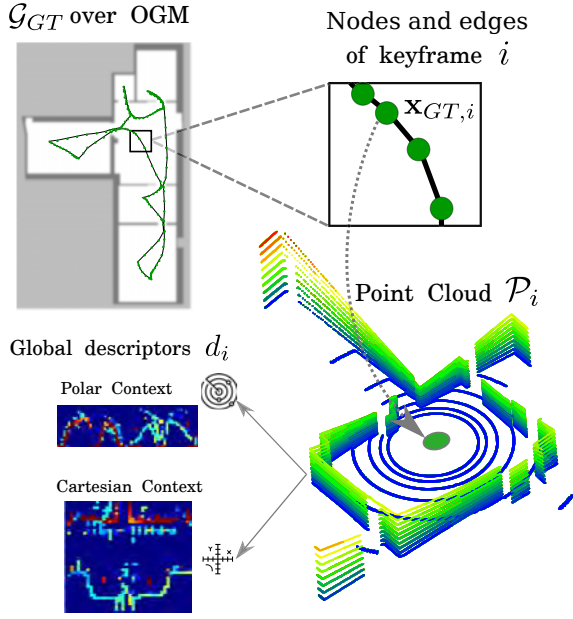


Figure 2. Generated SD from the BIM model. In the top left, the ground truth pose graph-based map \mathcal{G}_{GT} , with its nodes and edges (the result of odometry constraints). Besides having position and orientation, each node $\mathbf{x}_{GT,i}$ has its corresponding laser scan \mathcal{P}_i and global descriptors d_i . In this research, we use only polar context descriptors.

provided by the Wavefront Coverage Path Planner (PP) of Ogm2Pgbm.

The navigational goals are found by retrieving only one waypoint out of 20 in the list of generated waypoints from the PP. In this way, the waypoints are separated by a considerable distance but still allow the robot to navigate the complete path without skipping any region. Then the selected waypoints are passed as navigational goals (with pose and orientation) to Gazebo only when the simulated robot is at a certain distance to the next selected waypoint. These navigational goals are necessary to allow the robot to execute the whole exploration smoothly without unnecessary stops or skipping previous navigational goals.

It is necessary to recall that in this step, the semantics of the BIM model are leveraged, extracting only permanent structures (for example, walls, ceilings, and floors) and excluding spaces, non-permanent or LiDAR-invisible objects (like doors, windows, or curtain walls). Please, refer to [2] for more details about this step.

Once the 3D LiDAR data is simulated with ground truth odometry, we implement a *keyframe information saver* [5] to generate *session data* from it. A session \mathcal{S} is defined as

$$\mathcal{S} := (\mathcal{G}, \{(\mathcal{P}_i, d_i)\}_{i=1, \dots, n}), \quad (1)$$

where \mathcal{G} is a pose-graph text file with pose nodes, odometry edges, and optionally recognized intra-session loop edges.

The (\mathcal{P}_i, d_i) are the 3D point cloud and the global descriptor of the i^{th} keyframe, and n is the total number of equidistantly sampled keyframes. Figure 2 illustrates the elements of the SD.

3.3 Ground-truth multi-session anchoring

Given the SD from the real-world data \mathcal{S}_Q , denoted as *query*, and the SD from the BIM model $\mathcal{S}_{\mathcal{G}\mathcal{T}}$, denoted as *ground truth session*, our goal is then to align \mathcal{S}_Q with $\mathcal{S}_{\mathcal{G}\mathcal{T}}$ and retrieve a globally consistent map.

To align these maps, we use anchor node-based inter-session loop factors, as described in [5], [25], [26], [27]. Instead of optimizing the poses of the two sessions, we do not allow modifications of the ground truth session created from the model. This step is based on the assumption that, while there can be Scan-BIM deviations, the model still represents a reliable map suitable for localization.

In order to avoid alterations to the current session in $\mathcal{S}_{\mathcal{G}\mathcal{T}}$, we add its poses as *prior factors* with a very low variance (i.e., 1×10^{-100}) in its noise model, to the pose-graph optimization problem.

Anchor nodes represent the transformation from the local frame of each session graph to a standard global reference frame. Once the poses of each session are transformed into the global frame (via the anchor nodes), a comparison of the measurements between sessions is possible.

As outlined in Kim et al. [25], the anchor node can successfully approximate the offset between sessions. Besides allowing faster convergence to the least-squares solvers, anchor nodes allow each session to optimize their poses before global constraints are observed [27].

This characteristic is beneficial for long-term mapping since it allows the creation of a first consistent map in the state of the environment at the time the data was collected. Once a map is created with a new session, the anchor nodes allow finding the transformation that aligns that session with another reference one. In our case, the reference session is extracted from the BIM model.

To add the anchor node to the pose graph optimization problem, we only need to add the following factor:

$$\begin{aligned} & \phi(\mathbf{x}_{Q,j}, \Delta_Q) \\ & \propto \exp\left(-\frac{1}{2} \left\| ((\Delta_{GT} \oplus \mathbf{x}_{GT,i}) \ominus (\Delta_Q \oplus \mathbf{x}_{Q,j})) - c \right\|_{\Sigma_c}^2 \right), \end{aligned} \quad (2)$$

Here \mathbf{x} is a SE(3) pose; c is an encounter [25], i and j are pose indexes; \oplus and \ominus are the SE(3) pose composition operators. Δ indicates an anchor node, which is also a SE(3)

pose variable. Whereas the query session's anchor node Δ^Q has a relatively high covariance, the ground truth's Δ^{GT} has an insignificant value (very close to zero).

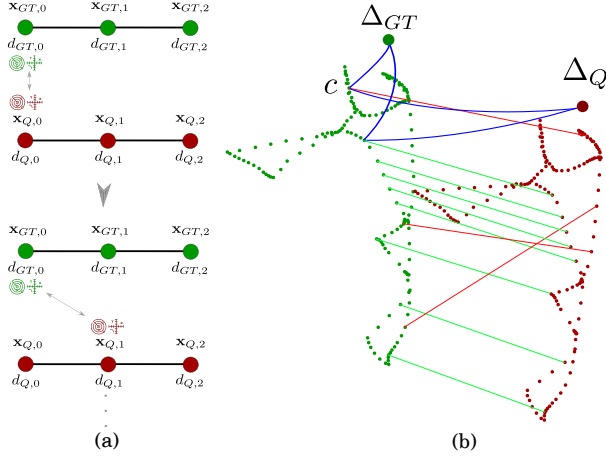


Figure 3. Loop closure detection between sessions. (a) the descriptors of each session data are compared against each other to find correspondences. (b) Some correctly and wrongly detected loop closures are shown in green and red, respectively. In blue, two encounters c linked to the trajectories' respective anchors. The trajectory's offset concerning a common global frame is specified by the anchors Δ .

To identify loop-closure candidates between sessions, we use Scan Context (SC) [28] and the pose proximity-based radius search loop detection. Figure 3 exemplifies the inter-session loop closure detection process. Once loops are detected, a 6D relative constraint between two keyframes is determined by registering their respective laser scan point clouds $\mathcal{P}_{GT,i}$ and $\mathcal{P}_{Q,j}$ with ICP. As in [5], only loops with adequate low ICP fitness ratings are allowed, and the score is used to calculate an adaptive covariance Σ_c in (2).

Once the values of the anchor nodes and the poses on the local coordinate system of \mathcal{S}_Q are optimized, as shown in Figure 4, all the poses in the pose-graph can be converted from the local (denoted as ${}^Q\mathcal{G}_Q^*$) to the global coordinate system ${}^W\mathcal{G}_Q^*$ by applying the following transformation to each pose \mathbf{x} in a graph:

$${}^W\mathbf{x}_Q^* = \Delta_Q^* \oplus^Q \mathbf{x}_Q^*,$$

where W is the global coordinate system.

3.4 Aligned map construction and Change detection

With the calculated poses on the same coordinate system, a map can be created by placing the respective laser scans $\mathcal{P}_{Q,i}$ in the estimated poses ${}^W\mathbf{x}_{Q,i}^*$, which are now in the BIM coordinate system.

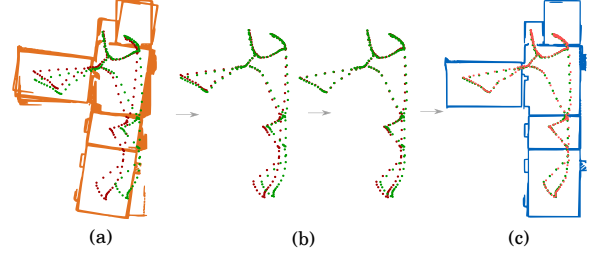


Figure 4. Pose graph optimization with multiple sessions. (a) In orange is the drifted map created by a SLAM system (exaggerated for illustrative purposes); in red is the respective trajectory; in green is the ground truth trajectory (b) Each pose graph optimization iteration tries to create a consistent global map placing the scans closer to the ground truth. (c) The final map is correctly aligned with the BIM model.

Once the 3D map of the current state of the environment is aligned with the BIM model, a comparison of the two maps is possible. A distance threshold is set to differentiate between objects present in the model and the new objects in the updated environment, also known as *Positive Differences (PD)*.

A signed distance computation lets us determine which points are close to and far from the mesh. Close points allow confirming BIM model elements, and far points are considered new elements, i.e., elements not present in the model.

In the next step, a density-based clustering algorithm (DBSCAN) is used to split the point cloud of detected PDs into segments of points that are close to each other and might represent single objects. This results in better visualization of the new objects in combination with the model, allowing a better scene understanding.

Finally, each cluster of the PDs is converted to a mesh representation created using cubes from a Voxel Grid (VG) of the point cloud.

Compared with other surface reconstruction methods, voxels represent the actual geometry of the objects visible in the scene. A final result is visible on 5.

4 Experiments and results

The data used for evaluating the proposed strategies are presented in this section, together with implementation and evaluation details. Both simulated and real environments were used for the experiments.

4.1 Simulated experiments

We used Gazebo [24] to simulate the experimental data.

The robot used for the simulated experiments was the Robotnik SUMMIT XL, equipped with a Velodyne VLP-

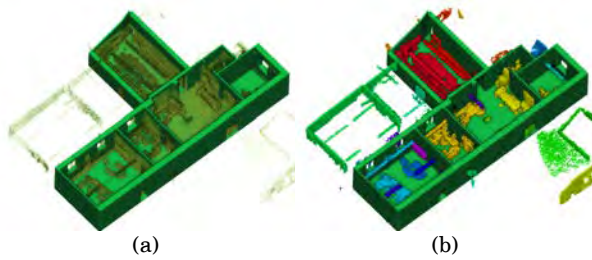


Figure 5. Detected positive differences in the point cloud and the BIM model. (a) The original aligned corrected point cloud (b) Only voxelized clustered new objects in the scene. The ceiling was removed for better visualization.

16 3D LiDAR. Table 1 presents the results on the simulated sequence.

Table 1. Quantitative comparative results.

Method	Trans. Error (cm)		Rot. Error (deg)	
	RMSE	Max	RMSE	Max
SC-A-LOAM	12,439	24,015	2,316	5,276
BIM-SLAM	10,594	20,175	2,074	4,841

4.2 Real-World experiments

The real-world data was collected in the same environment as the simulated one with an Ouster OS1-32 LiDAR. The sensor was mounted with a mini-PC and batteries in a mapping system. This system can be used as a handheld or above a robotic platform as depicted in 6. The legged robot Go1 was the robot platform we utilized for these tests. This data was used to generate the results shown in Figure 5.

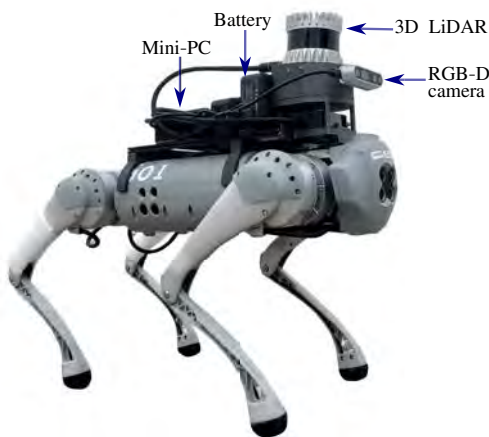


Figure 6. Portable mapping system developed to acquire real-world data. Here it is placed over the Go1 quadruped robot.

4.3 Implementation details

While the *Step 1* and *3* were implemented in Python, *Step 2* was written in C++ using ROS noetic.

Ogm2Pgbm [2], Scan Context [28], and LT-SLAM [5] were sources that we used that are freely available online. The parameters of SC were adjusted for indoor environments; for example, we use a maximum radius of 10 m and a cosine similarity threshold between descriptors of 0.6.

Whereas in *Step 2*, the pose-graph optimization is done with GTSAM using iSAM2, in *Step 3*, the process is done with Trimesh and Open3D.

The generation of the SD was done with SC-A-LOAM [6] an enhanced version of A-LOAM with loop closure and key-frame information saving capabilities (i.e., for SD generation).

5 Discussion

While in terms of drift reduction, our method performs only slightly better than state-of-the-art SLAM algorithms, as shown in Table 1. The main advantage of the proposed technique relies on the alignment of the acquired sensor data with the BIM model. The method also allows the creation of a map without the sensor being inside the prior map (as localization algorithms would require) or knowing its initial position.

We also show how the aligned sensor data can improve situational awareness (see Figure 5). Moreover, once the data is aligned, the model can be leveraged to identify new and missing components and clean the point cloud, removing unnecessary noisy points from the surroundings. These features would enable robust long-term map data management, using less memory than needed and saving all the information in one reference coordinate system.

However, our pipeline still presents some limitations. For example, in the case of significant levels of Scan-BIM deviations, the minimal overlap between the scan and the BIM, or symmetric environments, the correct alignment may not be possible with our method. Adjustments in creating the point cloud descriptors or the corresponding matching process might be necessary to address this issue.

Nonetheless, the method is not restricted to Manhattan-world environments with enclosed rooms, like in [22], nor does it require manual input of the robot's initial position in the map like the one proposed in [19].

Avenues for future research include enhancements in the place recognition algorithm (here, we use SC); leveraging topological and semantic information from the BIM model to make most robust the alignment and optimization process; and improvements on the extraction of SD from BIM models, in terms of speed and feature extraction, perhaps with a faster rendering method.

6 Conclusions

This paper presents a modular pipeline to allow 3D LiDAR data alignment and change detection with a BIM model as a reference map. Contrary to several other approaches, we aim to create an accurate, consistent map of the current state rather than focusing on real-time performance. The method does not need to know the robot's initial position, nor does the robot need to start inside the given map. In this way, our framework allows map alignment and extension even if the reference BIM model is no longer visible or if only a part of the model is scanned.

In the future, we would like to test the method on SD with more environmental changes and to enhance the change detection module to handle negative differences, i.e., when parts of the original BIM model are no longer present in the environment.

7 Acknowledgement

The presented research was conducted in the frame of the project “Intelligent Toolkit for Reconnaissance and assessment in Perilous Incidents” (INTREPID) funded by the EU's research and innovation funding programme Horizon 2020 under Grant agreement ID: 883345.

References

- [1] Pierre Alliez, Fabien Bonardi, Samia Bouchafa, Jean-Yves Didier, Hicham Hadj-Abdelkader, Fernando Ireta Muñoz, Viachaslau Kachurka, Bastien Rault, Maxime Robin, and David Roussel. Real-time multi-slam system for agent localization and 3d mapping in dynamic scenarios. In *2020 IEEE/RSJ International Conference on Intelligent Robots and Systems (IROS)*, pages 4894–4900. IEEE, 2020.
- [2] M.A. Vega Torres, A. Braun, and A. Borrmann. Occupancy grid map to pose graph-based map: Robust BIM-based 2d- lidar localization for lifelong indoor navigation in changing and dynamic environments. In Sujesh F. Suján Eilif Hjelseth and Raimar Scherer, editors, *eWork and eBusiness in Architecture, Engineering and Construction: ECPPM 2022*. CRC Press, Sep 2022. ISBN 978-1-003-35422-2. URL https://publications.cms.bgu.tum.de/2022_ECPPM_Vega.pdf.
- [3] Kyungki Kim and Matthew Peavy. BIM-based semantic building world modeling for robot task planning and execution in built environments. *Automation in Construction*, 138:104247, 2022. ISSN 09265805. doi:10.1016/j.autcon.2022.104247.
- [4] Sungjin Kim, Matthew Peavy, Pei-Chi Huang, and Kyungki Kim. Development of BIM-integrated construction robot task planning and simulation system. *Automation in Construction*, 127:103720, 2021. ISSN 09265805. doi:10.1016/j.autcon.2021.103720.
- [5] Giseop Kim and Ayoung Kim. Lt-mapper: A modular framework for lidar-based lifelong mapping. In *2022 International Conference on Robotics and Automation (ICRA)*, pages 7995–8002. IEEE, 2022.
- [6] Giseop Kim, Seungsang Yun, Jeongyun Kim, and Ayoung Kim. Sc-lidar-slam: A front-end agnostic versatile lidar slam system. In *2022 International Conference on Electronics, Information, and Communication (ICEIC)*, pages 1–6, 2022. doi:10.1109/ICEIC54506.2022.9748644.
- [7] Camilla Follini, Valerio Magnago, Kilian Freitag, Michael Terzer, Carmen Marcher, Michael Riedl, Andrea Giusti, and Dominik Tobias Matt. BIM-integrated collaborative robotics for application in building construction and maintenance. *Robotics*, 10(1):2, 2020. doi:10.3390/robotics10010002.
- [8] Samuel A. Prieto, Borja Garcia de Soto, and Antonio Adan. A methodology to monitor construction progress using autonomous robots. In Hisashi Osumi, editor, *Proceedings of the 37th International Symposium on Automation and Robotics in Construction (ISARC)*, Proceedings of the International Symposium on Automation and Robotics in Construction (IAARC). International Association for Automation and Robotics in Construction (IAARC), 2020. doi:10.22260/ISARC2020/0210.
- [9] R. W. M. Hendriks, P. Pauwels, E. Torta, H. J.P. Bruyninckx, and M. J. G. van de Molengraft. Connecting semantic building information models and robotics: An application to 2d lidar-based localization. In *2021 IEEE International Conference on Robotics and Automation (ICRA)*, pages 11654–11660. IEEE, 2021. ISBN 978-1-7281-9077-8. doi:10.1109/ICRA48506.2021.9561129.
- [10] RWM Hendriks, HPJ Bruyninckx, J Elfring, and MJG Van De Molengraft. Local-to-global hypotheses for robust robot localization. *Frontiers in Robotics and AI*, page 171, 2022.
- [11] Federico Boniardi, Tim Caselitz, Rainer Kummerle, and Wolfram Burgard. Robust lidar-based localization in architectural floor plans. In *2017 IEEE/RSJ International Conference on Intelligent Robots and Systems (IROS)*, pages 3318–3324. IEEE, 2017. ISBN 978-1-5386-2682-5. doi:10.1109/IROS.2017.8206168.

- [12] Federico Boniardi, Tim Caselitz, Rainer Kümmerle, and Wolfram Burgard. A pose graph-based localization system for long-term navigation in cad floor plans. *Robotics and Autonomous Systems*, 112:84–97, 2019. ISSN 09218890. doi:10.1016/j.robot.2018.11.003.
- [13] Abel Gawel, Hermann Blum, Johannes Pankert, Koen Krämer, Luca Bartolomei, Selen Ercan, Farbod Farshidian, Margarita Chli, Fabio Gramazio, Roland Siegwart, et al. A fully-integrated sensing and control system for high-accuracy mobile robotic building construction. In *2019 IEEE/RSJ International Conference on Intelligent Robots and Systems (IROS)*, pages 2300–2307. IEEE, 2019.
- [14] Selen Ercan, Hermann Blum, Abel Gawel, Roland Siegwart, Fabio Gramazio, and Matthias Kohler. Online synchronization of building model for on-site mobile robotic construction. In *37th International Symposium on Automation and Robotics in Construction (ISARC 2020)(virtual)*, pages 1508–1514. International Association for Automation and Robotics in Construction, 2020.
- [15] Hermann Blum, Julian Stiefel, Cesar Cadena, Roland Siegwart, and Abel Gawel. Precise robot localization in architectural 3d plans. *arXiv preprint arXiv:2006.05137*, 2020.
- [16] Hermann Blum, Francesco Milano, René Zurbrügg, Roland Siegwart, Cesar Cadena, and Abel Gawel. Self-improving semantic perception on a construction robot. *CoRR*, abs/2105.01595, 2021. URL <https://arxiv.org/abs/2105.01595>.
- [17] Mateus Sanches Moura, Carlos Rizzo, and Daniel Serrano. BIM-based Localization and Mapping for Mobile Robots in Construction. *2021 IEEE International Conference on Autonomous Robot Systems and Competitions, ICARSC 2021*, pages 12–18, 2021. doi:10.1109/ICARSC52212.2021.9429779.
- [18] Martin Oelsch, Mojtaba Karimi, and Eckehard Steinbach. R-LOAM: Improving LiDAR Odometry and Mapping with Point-to-Mesh Features of a Known 3D Reference Object. *IEEE Robotics and Automation Letters*, 6(2):2068–2075, 2021. ISSN 23773766. doi:10.1109/LRA.2021.3060413.
- [19] Martin Oelsch, Mojtaba Karimi, and Eckehard Steinbach. Ro-loam: 3d reference object-based trajectory and map optimization in lidar odometry and mapping. *IEEE Robotics and Automation Letters*, pages 1–1, 2022. doi:10.1109/LRA.2022.3177846.
- [20] Huan Yin, Zhiyi Lin, and Justin K.W. Yeoh. Semantic localization on BIM-generated maps using a 3d lidar sensor. *Automation in Construction*, 146:104641, 2023. ISSN 0926-5805. doi:https://doi.org/10.1016/j.autcon.2022.104641.
- [21] Muhammad Shaheer, Hriday Bavle, Jose Luis Sanchez-Lopez, and Holger Voos. Robot localization using situational graphs and building architectural plans. *arXiv preprint arXiv:2209.11575*, 2022.
- [22] Muhammad Shaheer, Jose Andres Millan-Romera, Hriday Bavle, Jose Luis Sanchez-Lopez, Javier Civera, and Holger Voos. Graph-based global robot localization informing situational graphs with architectural graphs, 2023.
- [23] Fernando Caballero and Luis Merino. Dll: Direct lidar localization. a map-based localization approach for aerial robots. In *2021 IEEE/RSJ International Conference on Intelligent Robots and Systems (IROS)*, pages 5491–5498. IEEE, 2021.
- [24] Nathan Koenig and Andrew Howard. Design and use paradigms for gazebo, an open-source multi-robot simulator. In *2004 IEEE/RSJ International Conference on Intelligent Robots and Systems (IROS)(IEEE Cat. No. 04CH37566)*, volume 3, pages 2149–2154. IEEE, 2004.
- [25] Been Kim, Michael Kaess, Luke Fletcher, John Leonard, Abraham Bachrach, Nicholas Roy, and Seth Teller. Multiple relative pose graphs for robust cooperative mapping. In *2010 IEEE International Conference on Robotics and Automation*, pages 3185–3192. IEEE, 2010.
- [26] J. McDonald, M. Kaess, C. Cadena, J. Neira, and J.J. Leonard. Real-time 6-dof multi-session visual slam over large-scale environments. *Robotics and Autonomous Systems*, 61(10):1144–1158, 2013. ISSN 0921-8890. doi:https://doi.org/10.1016/j.robot.2012.08.008. Selected Papers from the 5th European Conference on Mobile Robots (ECMR 2011).
- [27] Paul Ozog, Nicholas Carlevaris-Bianco, Ayoung Kim, and Ryan M Eustice. Long-term mapping techniques for ship hull inspection and surveillance using an autonomous underwater vehicle. *Journal of Field Robotics*, 33(3):265–289, 2016.
- [28] Giseop Kim and Ayoung Kim. Scan context: Ego-centric spatial descriptor for place recognition within 3d point cloud map. In *2018 IEEE/RSJ International Conference on Intelligent Robots and Systems (IROS)*, pages 4802–4809. IEEE, 2018.

A Review of Computer Vision-Based Techniques for Construction Progress Monitoring

Shrouk Gharib¹ and Osama Moselhi²

¹Department of Building, Civil and Environmental Engineering, Concordia University, Canada

²Centre for Innovation in Construction and Infrastructure Engineering and Management (CICIEM), Department of Building, Civil and Environmental Engineering, Concordia University, Canada

shrouk.gharib@mail.concordia.ca, moselhi@encs.concordia.ca

Abstract –

Monitoring the progress of construction operations on site is crucial to keep an up-to-date schedule. In the past, manual methods were used for that purpose, which lead to errors and delays in generating up-to-date schedules. Current practices and research lines have been studying different methodologies to reach a fully automated progress-monitored construction.

Automated progress monitoring and tracking are important to avoid delays and cost overruns resulting from a lack of timely management decisions. Manual reporting and human intervention on site are error-prone, time-consuming, and can negatively impact productivity. Recently, computer vision techniques are proving to be cost and time efficient for monitoring and progress reporting of construction operations.

This paper investigates the required steps and technologies used to have an automated tool for progress monitoring. The paper also provides a review of the common methodologies used, previous practices, limitations, and future directions for the evolution of automated construction progress monitoring.

Keywords –

Progress Monitoring; Automation in Construction; Sensing Technology; Computer Vision; Data Acquisition

1 Introduction

Construction progress monitoring is crucial aspect of construction projects, as it plays a key role in ensuring process control and the success of the project [1, 2]. Failure to monitor construction progress accurately has been found to result in cost overruns in more than 66% of the projects and schedule delays in more than 53% of the projects[2]. The pressure of monitoring the budget and adhering to the schedule can also have an impact on the quality of work during the progress of the project [1]. Therefore, it is essential to select an efficient data

acquisition tool that can measure construction progress in an accurate and efficient manner. Various studies have investigated different technologies commonly used on construction sites for daily monitoring, reviewed data acquisition methodologies, and evaluated methods of storing, and reviewing data [2, 3].

Computer vision (CV) is an artificial intelligence branch that leverages images to obtain visual data that resembles human visualization. In the recent times, CV has attracted significant interest from researchers due to its impressive capabilities of automation in construction. CV can be applied in different fields, such as quality control, progress monitoring, and quality management [4–6]. Several CV technologies, including Laser scanning, photogrammetry, and videogrammetry, have been studied for data acquisition. Additionally, several startups, such as OpenSpace, Smartvid.io, and HoloBuilder have emerged in recent years.

Laser scanning is widely regarded as the most accurate method of data acquisition. However, this method is also known to be very expensive and requires a long data-acquisition time [7]. In contrast, taking daily images using cameras has gained popularity due to their cost-effectiveness and ease of accessibility. This development has led to extensive research on data acquisition and construction site monitoring using various forms of media [8].

The objective of this study is to provide a systematic review of recent developments and necessary steps to reach automated progress monitoring using computer vision-based technologies, recent studies, challenges, and future directions.

2 Research Methodology

In this research, a systematic literature review methodology was used to gather most research on the use of computer vision-based technologies in construction progress monitoring. The literature was collected through the following databases and search engines; google scholar, Web of Science, and Scopus. The keywords that

were used in this study include: “automated project monitoring”, “construction project updating”, “construction progress tracking”, “construction progress detection”, “construction progress recognition”, “progress monitoring”, “progress tracking”, “computer vision”, “image processing”, “3D scene reconstruction”, “building information modelling”, “deep learning”, and “as built 3d reconstruction”. The papers were scanned and filtered to include only the related papers from review papers, peer-reviewed conference proceedings and journal papers. Another further filtration was processed to include only papers in English and papers that were published from 2013 to 2022. After the screening and filtration, a total of 156 papers were selected and reviewed. The papers were then configured according to the year of publication and were categorized into “Journal Technical papers”, “Review papers”, and “Conference Technical Papers” as shown in Figure 1 and further details about technologies used, mounting method, whether indoor or outdoor and they key focus of these studies shown in Table 1.

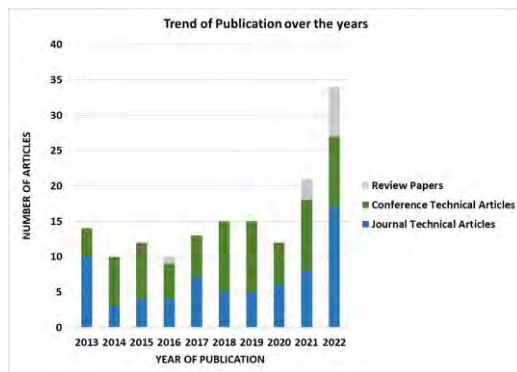


Figure 1. Papers Distribution and categorization

3 Overview of vision-based monitoring of construction progress

Based on literature review, the process of monitoring construction progress using computer vision in any construction site can be divided into three main steps. These steps are illustrated in Figure 2 and provide

an overview of the framework for computer vision-based construction progress monitoring (CV-CPM).

In the following sections, each of these steps will be discussed in detail. Specifically, Section 3.1, will cover the data acquisition technologies and the various methodologies used for mounting cameras or other data acquisition devices. Section 3.2 will describe the 3D reconstruction process, including the methods and algorithms used to generate a three-dimensional model of the construction site. Finally, 3.3 will address the last step in the process, which involves generating an as-built model from the 3D reconstruction and comparing it with the as-planned model.

By following these steps, construction project managers and stakeholders can use computer vision-based monitoring to track and manage construction progress more efficiently and accurately. This approach can provide valuable insights into the construction process, facilitate decision-making, and help identify potential issues or delays.

3.1 Data Acquisition

Data acquisition is the first and most important step in the CV-CPM process. The method used will determine how well the construction site can be monitored and how subsequent steps can be developed. To successfully manage a construction site, the acquired data must be accurate and reliable, covering all aspects of the site and updated regularly to reflect changes in the schedule and to generate an as-built model [9].

The Architecture, Engineering, and Construction (AEC) industry leverages various imaging devices to acquire data, such as monocular/binocular cameras, Unmanned Aerial Vehicles (UAVs) with cameras or video cameras, video cameras, laser scanners, depth cameras, and others. The key performance indices of these devices are presented in Table 2 [10]. For competent project management and control, the team must acquire an accurate data collection methodology in order to be able to compare it later with the as-planned data and stay up-to-date with the actual progress to deliver a time and cost-efficient project [11]. There are different types of technologies used for data acquisition,

Table 1 Review of papers used vision-based progress monitoring.

Paper	Technology	Mounting Method	Indoor/Outdoor	Key Focus
[12]	Camera	Fixed	Outdoor	Bridge
[13]	Laser Scanner	Manual	Outdoor	4 story building
[14]	Digital Camera + Laser Scanner	Fixed / Manual	Outdoor	Structural work for a residential building
[15]	Lidar	Manual	Outdoor	Bridge
[1]	Camera	UAV	Outdoor	Columns

[16]	Camera	Manual	Indoor	Plastering
[17]	Camera	UAV	Outdoor	Building structure
[18]	Depth Camera	Manual	Indoor	Building Elements
[19]	Camera	Manual	Both	Walls
[20]	Laser Scanner	Manual	Both	Rectangular Columns

but the types of technologies used for data acquisition, but the type of data extracted from them doesn't only depend on the type of technology but also on the method of mounting these technologies.[21]

Table 2. Device performance comparison

Technology	Mounting Method	Data Type	Cost	Technical Threshold	Resolution
Camera	Fixed	Photos	Low	Low	High
	UAV/UGV	Photos	Medium	Medium	High
Video Camera	Fixed	Video	Low	Low	Low
	UAV/UGV	Video	Medium	Medium	Low
Laser Scanner	N/A	Point Cloud	High	High	High
Depth Camera	N/A	Point Cloud	Medium	Low	High

The data generated by these instruments can be categorized into two types: image and point cloud. The laser scanner, which produces point cloud data, exhibits feature such as high equipment costs and technical requirements, rendering it unviable for most construction companies. Consequently, images, including photographs and videos, are employed as a feasible substitute. Multiple devices can be used to obtain images, with most of them being low-cost, possessing low technical demands, portable, and high-resolution. As a result, image-based 3D reconstruction is a critical technology for automated progress monitoring [10].

Various studies have investigated the use of different acquisition technologies and their combinations for vision data acquisition. Digital cameras [12, 14], video camera [22], laser scanner [23], and range imaging (RGB-D camera)[24, 25] are commonly used technologies. These technologies can be mounted in different ways, such as being fixed in a location with minimal movement, handheld, or mounted on unmanned ground or aerial vehicles, including drones equipped with optical sensors or digital cameras [26].

Unmanned aerial vehicles (UAVs) have gained popularity in the construction industry due to their low cost, speed, and ability to collect data in areas that may be difficult to reach for humans or ground-based vehicles [11]. However, operating UAVs requires expertise and careful planning of flight paths with various data capturing angles. Modern UAVs now allow pre-planned flight paths to be programmed [11, 27, 28].

Handheld devices such as mobile phones, small digital cameras, or video cameras are also widely used on construction sites to collect daily photologs and record construction updates due to ease of access and availability. [26, 29]. The visual data captured by these devices can be used to create 3D as-built models in various studies.

Other studies have explored the benefits of mounting digital cameras on fixed cranes, camera mounts [25] and using surveillance cameras for progress monitoring and reporting instead of installing an additional video cameras [30]. Additionally, sensors can be mounted on unmanned ground vehicle (UGV) using robotic systems or unmanned aerial vehicles (UAV) [22, 31, 32]

3.2 3D Reconstruction

Three-dimensional (3D) reconstruction techniques have been increasingly used in construction engineering to obtain the 3D representations of objects, such as point cloud models, mesh models and geometric models. Among these, point cloud models are the most commonly used [3]. 3D models can be generated from 2D and 3D visual data, and this step involves generating 3D models (mesh models, geometric models and point clouds) from the output of cameras, video cameras, laser scanners, or range cameras [10]. The main objective is to transform the output of each of sensing technology into an as-built point cloud model [3, 10]. The data collected can be either monocular, stereo, RGB-depth images, or video frames.

After the data acquisition step, the next step is to process 3D reconstruction algorithms to generate the point cloud model. Laser scanner output already generates point cloud models and does not require further processing. However, digital camera images and video frames do not include any location information, accordingly, the SfM (Structure from Motion) approach is used to add depth information for sparse 3D reconstruction.

Depth images generated from depth cameras (RGB-D) contain three coordinate information (XYZ coordinates) along with color information (RGB). This information is used for mapping and executing 3D reconstruction using extrinsic and intrinsic camera factors [33].

This paper presents the basic concept of Structure

from Motion (SfM) as a technique for photogrammetric 3D reconstruction from multiple image frames. SfM combines algorithms for feature extraction, feature matching, camera motion estimation, sparse 3D reconstruction, and model parameter correction [10, 34]. The quality and sequence of the image frames obtained are crucial for feature matching of image pairs. However, SfM can work with unordered image frames, making it suitable for construction sites that collect images from multiple location-aware sensors. Visual SfM and Open SfM [35] are popular implementations of SfM.

3.2.1 SfM (Structure from Motion)

Structure from Motion (SfM) is a photogrammetric technique used to reconstruct a 3D model/point clouds from 2D images of a scene or object. SfM requires at least two or more images of the same scene taken from different viewpoints to triangulate the 3D positions of points in the scene. It belongs to the quantification photogrammetric techniques, which involves collecting real-life measurements from 2D image dataset [36]. SfM automatically detects and matches features from an image dataset of varying scales, angles, and orientations, and collects feature points that reflect the primary formation of the scene. The inputs are in the form of image data with recommended 60% side overlap and 80% forward overlap between images to achieve high-quality and detailed 3D models/point clouds as outputs [37].

The technique has been applied in several studies that exploit images taken from construction sites for productivity analysis, quality control, progress monitoring, and safety. These applications allow project management teams to visualize as-built data and exercise better control over the project [1, 19].

The next step after feature point collection and camera position estimation is absolute scale recovery and dense 3D reconstruction. This is necessary because the output from the initial step is sparse.

3.2.2 Absolute Scale Recovery

After processing images and video frames captured by cameras and video cameras using SfM, the resulting outputs are typically sparse and non-scalar point clouds that require absolute scale recovery and dense 3D reconstruction. Absolute scale recovery is the process of determining the real-world size and distance of the reconstructed 3D scene. While laser scans do not require this step, determining the absolute scale of the sparse point cloud is achieved using local coordinates. This typically involves manual techniques, such as using pre-measured objects or georegistration, although the latter can be automated by sensing the camera parameters rather than relying on manual measurements and ground truth.

3.2.3 Dense 3D Reconstruction

Dense 3D reconstruction involves recovering the actual scene with all its details, which is done using various algorithms such as SGM (semi-global matching), CMVS (clustering views for multi-view stereo), MVS (multi-view stereo). This step is essential as the point clouds reconstructed from monocular or stereoscopic images or video frames are sparse. On the other hand, the reconstruction output from the depth images is dense enough and does not require dense 3D reconstruction. After generating the dense point cloud, the next step is pre-processing, which includes registration, noise filtering, down-sampling, and outlier removal [21].

3.3 Model Generation

To assess the current state of progress, determine whether it is behind schedule, ahead of schedule, or on track, and potentially take corrective action, it is necessary to compare the as-built model data obtained from the previous step with the as-planned data.

This step, illustrated in Figure 2, involves generating the as-planned model and identifying its features. By comparing the two models, it is possible to identify any discrepancies and assess the level of conformity with the original plan.

3.3.1 As-planned model

As planned models are the baseline plans for a project, typically created during the design phase. To monitor progress accurately and ensure functionality, as-planned models are essential for comparing against the as-built models. As-planned model, or 4D models, combine a 3D BIM model with the project's time schedule. As-built models are then overlaid onto the 4D BIM to facilitate comparison between the two models.

3.3.2 As-built model

The creation of accurate as-built models involves several essential steps. The first step is to acquire a point cloud generated from the previous stage or obtained from laser scanners. The main step in generating as-built models is point cloud pre-processing, which involves eliminating outliers and noise points from the acquired point cloud [38]. Outliers and noise points are unnecessary points from the surroundings that can be removed using outlier removal and noise filtering processes [39]. Common algorithms used for both processes include manual point removal from the surrounding [40] and RANSAC [39].

Moreover, the process of overlapping the point cloud during registration makes the model dense and requires down sampling to avoid reducing the efficiency of the subsequent processing. A point spacing strategy algorithm, typically used for down sampling [41],

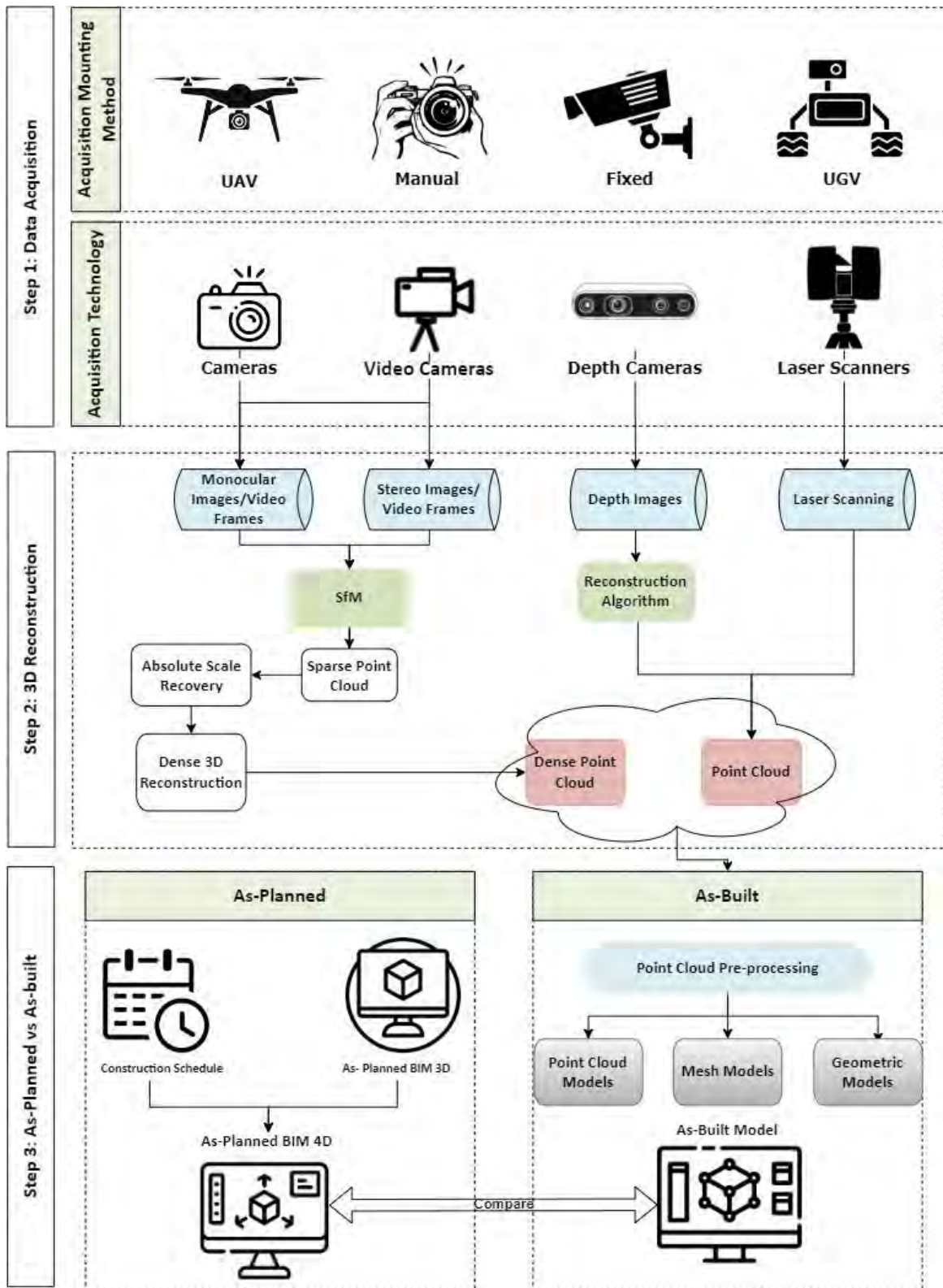


Figure 2 Framework for computer vision-based construction progress monitoring (CV-CPM)

organizes the point cloud into a 3D grid cell with equivalent portions. Points in each single 3D grid cell, including at least one point, are reduced until they meet the requirements [42].

Previous studies have identified three main types of as-built models: point cloud models, mesh models [24], and geometry models. The level of progress monitoring proposed for a project plays a vital role in deciding the type of as-built model to be generated.

3.4 Visualization & Quantification

The literature has discussed various methods of visualization, including color labels, Augmented Reality (AR) [43, 44], 3D model Viewers, Virtual Reality (VR) Environments [18] and Mixed Reality (MR) Environment [24]. Visualization plays a crucial role in enabling the continuous monitoring of construction sites and is considered a predominant method for sites implementing Computer Vision-based Construction Progress Monitoring (CV-CPM) methodology.

Quantification, on the other hand, is primarily useful for contractors, owners, and other stakeholders for reporting and tracking progress on the site. It involves quantifying the completed work tasks, which helps in understanding the overall progress of the project.

4 Discussion

The present research study addresses the crucial role of automated progress monitoring in construction projects, which can significantly improve project management and enhance project outcomes. In particular, the study aims to shed light on the potential benefits and techniques of implementing computer vision technologies for automated progress monitoring.

To achieve this aim, the study provides an overview of various computer vision technologies that can be used for automated progress monitoring. This includes a detailed exploration of the different techniques for mounting these technologies and integrating them into the construction process.

Moreover, the study explains the process for creating a 3D as-built model, which is a critical component of the automated progress monitoring system. The model is generated by following a sequence of steps that include data acquisition, registration, and integration, which are described in detail.

Finally, the study describes the algorithm used for estimating progress based on the data collected, which is the final step in the automated progress monitoring system. The algorithm considers various factors, such as the current state of the project, the expected completion time, and the rate of progress, to provide an accurate estimate of the project's status.

In summary, the present study contributes to the

growing body of research on automated progress monitoring in construction projects. By providing a comprehensive understanding of the potential benefits and techniques of implementing computer vision technologies, the study can assist construction professionals in improving project management and enhancing project outcomes.

A systematic review was conducted to identify applications of digital images and computer vision techniques for construction progress monitoring and reporting, as well as integrated frameworks utilizing Building Information Modeling (BIM) and computer vision. Challenges in 3D reconstruction within the construction industry were also documented, emphasizing the need for future research to improve the accuracy and efficiency of algorithms used to produce point clouds. Furthermore, the study identified opportunities for automated integration of computer vision activities with BIM for as-built modeling. Our research aims to develop a real-time building progress monitoring framework that leverages sensor technology and enhances algorithms to further advance the field.

References

- 1 Braun, A., Tuttas, S., Borrmann, A., Stilla, U.: 'Improving progress monitoring by fusing point clouds, semantic data and computer vision' *Automation in Construction*, 2020, **116**, p. 103210.
- 2 Alaloul, W.S., Qureshi, A.H., Musarat, M.A., Saad, S.: 'Evolution of close-range detection and data acquisition technologies towards automation in construction progress monitoring' *Journal of Building Engineering*, 2021, **43**, p. 102877.
- 3 Ma, Z., Liu, S.: 'A review of 3D reconstruction techniques in civil engineering and their applications' *Advanced Engineering Informatics*, 2018, **37**, pp. 163–174.
- 4 Shamsollahi, D., Moselhi, O., Khorasani, K.: 'Construction Progress Monitoring and Reporting using Computer Vision Techniques – A Review' 2022, p. 9.
- 5 Feng, X., Jiang, Y., Yang, X., Du, M., Li, X.: 'Computer vision algorithms and hardware implementations: A survey' *Integration*, 2019, **69**, pp. 309–320.
- 6 Xu, S., Wang, J., Shou, W., Ngo, T., Sadick, A.-M., Wang, X.: 'Computer Vision Techniques in

- Construction: A Critical Review' *Arch Computat Methods Eng*, 2021, **28**, (5), pp. 3383–3397.
- 7 Wang, Z., Zhang, Q., Yang, B., *et al.*: 'Vision-Based Framework for Automatic Progress Monitoring of Precast Walls by Using Surveillance Videos during the Construction Phase' *J. Comput. Civ. Eng.*, 2021, **35**, (1), p. 04020056.
 - 8 Hamledari, H., McCabe, B., Davari, S.: 'Automated computer vision-based detection of components of under-construction indoor partitions' *Automation in Construction*, 2017, **74**, pp. 78–94.
 - 9 El-Omari, S., Moselhi, O.: 'Data acquisition from construction sites for tracking purposes' *Engineering, Construction and Architectural Management*, 2009, **16**, (5), pp. 490–503.
 - 10 Xue, J., Hou, X., Zeng, Y.: 'Review of Image-Based 3D Reconstruction of Building for Automated Construction Progress Monitoring' *Applied Sciences*, 2021, **11**, (17), p. 7840.
 - 11 Sami Ur Rehman, M., Shafiq, M.T., Ullah, F.: 'Automated Computer Vision-Based Construction Progress Monitoring: A Systematic Review' *Buildings*, 2022, **12**, (7), p. 1037.
 - 12 Kim, C., Kim, B., Kim, H.: '4D CAD model updating using image processing-based construction progress monitoring' *Automation in Construction*, 2013, **35**, pp. 44–52.
 - 13 Kim, C., Son, H., Kim, C.: 'Development of a System for Automated Schedule Update Using a 4D Building Information Model and 3D Point Cloud', in 'Computing in Civil Engineering' ASCE International Workshop on Computing in Civil Engineering, (American Society of Civil Engineers, 2013), pp. 757–764
 - 14 Kim, C., Son, H., Kim, C.: 'Automated construction progress measurement using a 4D building information model and 3D data' *Automation in Construction*, 2013, **31**, pp. 75–82.
 - 15 Puri, N., Turkan, Y.: 'Bridge construction progress monitoring using lidar and 4D design models' *Automation in Construction*, 2020, **109**, p. 102961.
 - 16 Wei, W., Lu, Y., Zhong, T., Li, P., Liu, B.: 'Integrated vision-based automated progress monitoring of indoor construction using mask region-based convolutional neural networks and BIM' *Automation in Construction*, 2022, **140**, p. 104327.
 - 17 Ibrahim, A., Golparvar-Fard, M., El-Rayes, K.: 'Multiobjective Optimization of Reality Capture Plans for Computer Vision-Driven Construction Monitoring with Camera-Equipped UAVs' *J. Comput. Civ. Eng.*, 2022, **36**, (5), p. 04022018.
 - 18 Pour Rahimian, F., Seyedzadeh, S., Oliver, S., Rodriguez, S., Dawood, N.: 'On-demand monitoring of construction projects through a game-like hybrid application of BIM and machine learning' *Automation in Construction*, 2020, **110**, p. 103012.
 - 19 Mahami, H., Nasirzadeh, F., Hosseinineveh Ahmadian, A., Nahavandi, S.: 'Automated Progress Controlling and Monitoring Using Daily Site Images and Building Information Modelling' *Buildings*, 2019, **9**, (3), p. 70.
 - 20 Maalek, R., Lichti, D.D., Ruwanpura, J.Y.: 'Automatic Recognition of Common Structural Elements from Point Clouds for Automated Progress Monitoring and Dimensional Quality Control in Reinforced Concrete Construction' *Remote Sensing*, 2019, **11**, (9), p. 1102.
 - 21 Reja, V.K., Varghese, K., Ha, Q.P.: 'Computer vision-based construction progress monitoring' *Automation in Construction*, 2022, **138**, p. 104245.
 - 22 Bognot, J.R., Candido, C.G., Blanco, A.C., Montelibano, J.R.Y.: 'BUILDING CONSTRUCTION PROGRESS MONITORING USING UNMANNED AERIAL SYSTEM (UAS), LOW-COST PHOTOGRAMMETRY, AND GEOGRAPHIC INFORMATION SYSTEM (GIS)' *ISPRS Ann. Photogramm. Remote Sens. Spatial Inf. Sci.*, 2018, **IV-2**, pp. 41–47.
 - 23 Bosché, F., Ahmed, M., Turkan, Y., Haas, C.T., Haas, R.: 'The value of integrating Scan-to-BIM and Scan-vs-BIM techniques for construction monitoring using laser scanning and BIM: The case of cylindrical MEP components' *Automation in Construction*, 2015, **49**, pp. 201–213.
 - 24 Kopsida, M., Brilakis, I.: 'Real-Time Volume-to-Plane Comparison for Mixed Reality-Based Progress Monitoring' *J. Comput. Civ. Eng.*, 2020, **34**, (4), p. 04020016.

- 25 Pučko, Z., Šuman, N., Rebolj, D.: 'Automated continuous construction progress monitoring using multiple workplace real time 3D scans' *Advanced Engineering Informatics*, 2018, **38**, pp. 27–40.
- 26 Rehman, M.S.U., Shafiq, M.T.: 'Identifying the Process for Automated Vision- based Construction Progress Monitoring.' 2021.
- 27 Nex, F., Remondino, F.: 'UAV for 3D mapping applications: a review' *Appl Geomat*, 2014, **6**, (1), pp. 1–15.
- 28 Melo, R.R.S. de, Costa, D.B., Álvares, J.S., Irizarry, J.: 'Applicability of unmanned aerial system (UAS) for safety inspection on construction sites' *Safety Science*, 2017, **98**, pp. 174–185.
- 29 Golparvar-Fard, M., Peña-Mora, F., Savarese, S.: 'Automated Progress Monitoring Using Unordered Daily Construction Photographs and IFC-Based Building Information Models' *J. Comput. Civ. Eng.*, 2015, **29**, (1), p. 04014025.
- 30 Ahmadian Fard Fini, A., Maghrebi, M., Forsythe, P.J., Waller, T.S.: 'Using existing site surveillance cameras to automatically measure the installation speed in prefabricated timber construction' *ECAM*, 2022, **29**, (2), pp. 573–600.
- 31 Adán, A., Quintana, B., Prieto, S.A., Bosché, F.: 'An autonomous robotic platform for automatic extraction of detailed semantic models of buildings' *Automation in Construction*, 2020, **109**, p. 102963.
- 32 Asadi, K., Kalkunte Suresh, A., Ender, A., *et al.*: 'An integrated UGV-UAV system for construction site data collection' *Automation in Construction*, 2020, **112**, p. 103068.
- 33 Wang, Q., Tan, Y., Mei, Z.: 'Computational Methods of Acquisition and Processing of 3D Point Cloud Data for Construction Applications' *Arch Computat Methods Eng*, 2020, **27**, (2), pp. 479–499.
- 34 Yang, M.-D., Chao, C.-F., Huang, K.-S., Lu, L.-Y., Chen, Y.-P.: 'Image-based 3D scene reconstruction and exploration in augmented reality' *Automation in Construction*, 2013, **33**, pp. 48–60.
- 35 Han, K.K., Golparvar-Fard, M.: 'BIM-Assisted Structure-from-Motion for Analyzing and Visualizing Construction Progress Deviations through Daily Site Images and BIM', in 'Computing in Civil Engineering 2015' 2015 International Workshop on Computing in Civil Engineering, (American Society of Civil Engineers, 2015), pp. 596–603
- 36 Mostafa, K., Hegazy, T.: 'Review of image-based analysis and applications in construction' *Automation in Construction*, 2021, **122**, p. 103516.
- 37 Golparvar-Fard, M., Peña-Mora, F., Savarese, S.: 'D4AR – A 4-DIMENSIONAL AUGMENTED REALITY MODEL FOR AUTOMATING CONSTRUCTION PROGRESS MONITORING DATA COLLECTION, PROCESSING AND COMMUNICATION' no date.
- 38 Sun, Y., Paik, J.K., Koschan, A., Abidi, M.A.: '3D reconstruction of indoor and outdoor scenes using a mobile range scanner', in 'Object recognition supported by user interaction for service robots' 16th International Conference on Pattern Recognition, (IEEE Comput. Soc, 2002), pp. 653–656
- 39 Liu, Y.-F., Cho, S., Spencer, B.F., Fan, J.-S.: 'Concrete Crack Assessment Using Digital Image Processing and 3D Scene Reconstruction' *J. Comput. Civ. Eng.*, 2016, **30**, (1), p. 04014124.
- 40 Lee, J., Son, H., Kim, C., Kim, C.: 'Skeleton-based 3D reconstruction of as-built pipelines from laser-scan data' *Automation in Construction*, 2013, **35**, pp. 199–207.
- 41 Son, H., Kim, C., Kim, C.: 'Fully Automated As-Built 3D Pipeline Extraction Method from Laser-Scanned Data Based on Curvature Computation' *J. Comput. Civ. Eng.*, 2015, **29**, (4), p. B4014003.
- 42 Li, Y., Wu, H., Xu, H., An, R., Xu, J., He, Q.: 'A gradient-constrained morphological filtering algorithm for airborne LiDAR' *Optics & Laser Technology*, 2013, **54**, pp. 288–296.
- 43 Golparvar-Fard, M., Peña-Mora, F., Savarese, S.: 'Integrated Sequential As-Built and As-Planned Representation with D4AR Tools in Support of Decision-Making Tasks in the AEC/FM Industry' *J. Constr. Eng. Manage.*, 2011, **137**, (12), pp. 1099–1116.
- 44 Zollmann, S., Hoppe, C., Kluckner, S., Poglitsch, C., Bischof, H., Reitmayr, G.: 'Augmented Reality for Construction Site Monitoring and Documentation' *Proc. IEEE*, 2014, **102**, (2), pp. 137–154.

A corpus database for cybersecurity topic modeling in the construction industry

Dongchi Yao^{1,2} and Borja García de Soto^{1,2}

¹S.M.A.R.T. Construction Research Group, Division of Engineering, New York University Abu Dhabi (NYUAD), Experimental Research Building, Saadiyat Island, P.O. Box 129188, Abu Dhabi, United Arab Emirates

²Tandon School of Engineering, New York University (NYU), United States
dy2037@nyu.edu, garcia.de.soto@nyu.edu

Abstract –

In the digitalized era of Construction 4.0, ensuring the confidentiality, availability, and integrity of digital assets through cybersecurity is crucial for the construction industry. Although more than 75% of respondents from a Forrester survey who are in the construction, engineering, and infrastructure industries reported to have experienced a cyber-incident in the past 12 months, only 0.25% of cybersecurity publications focus on the construction industry until Jan 2023. Considering the significance of ensuring cybersecurity in construction, this study uses Latent Dirichlet Allocation (LDA) Topic Modeling technique to identify potential research directions in cybersecurity in the construction industry, based on various text sources collected, including news, articles & blogs, academic publications, books, standards, and company reports. The results of the study identify eight topics for future research: Perform Risk Analysis, Prevent the Increasing Cyber Incidents, Detect Ransomware, Strengthen Management Process, Protect Network Devices, Regulate Information Storage and Sharing, Protect Privacy, and Improve Authentication Process. Additionally, the corresponding action is proposed for addressing each topic. These findings can be used by researchers, practitioners, and policymakers in the construction industry to address the challenges and opportunities in cybersecurity.

Keywords –

Cybersecurity; Topic Modeling; Deep Learning; Natural Language Processing; Construction Industry

1 Introduction

The construction industry is shifting towards digitalization, known as Construction 4.0, which involves the use of digital technologies such as digital twins, drones, robotics, cloud computing, and virtual reality [1]. These technologies have the potential to

improve the speed, cost, and quality of construction, operation, and maintenance of assets [2]. Protecting the data generated in construction projects, such as blueprints, bidding documents, sensor data, and maintenance parameters, is critical to ensure the smooth implementation of these technologies and prevent data breaches that can cause damage to data and physical spaces, disrupting business operations and compromising safety [3].

Several cybersecurity incidents have been reported in the construction industry recently, such as the theft of floorplan files from the Australian intelligence headquarters [4], identity theft resulting in a loss of 17.2 million euros for a Finnish crane maker [5], exposure of private information of employees in a data breach at Turner Construction [6], theft of trade secrets from ThyssenKrupp (a construction escalator manufacturer) due to a data breach [7], ransomware attack at the federal construction firm called Bird Construction [8]. The construction industry was the third largest target of ransomware attacks in 2020, following government agencies and manufacturing, with AEC companies being more than twice as likely to be targeted. Many businesses in the industry fail to develop a protection plan for their digital assets, which can lead to significant losses in the event of a cyberattack [9]. These incidents highlight the importance of prioritizing cybersecurity in the construction industry. However, cybersecurity in the construction industry presents unique challenges compared to general cybersecurity. This is due to the dynamic nature of construction projects, which involves frequent changes in teams, varying levels of cybersecurity knowledge among employees, scattered and frequent communications within the supply chain, frequent exchange of digital information among stakeholders, and the overlapping of different projects. As a result, standard frameworks and methodologies for general cybersecurity designed for more static industries, like the manufacturing industry, may not be adequate for addressing the specific needs of the construction industry. Instead, tailored and industry-specific approaches are

required to effectively address the cybersecurity challenges in the construction sector.

In the last few years, some studies have addressed cybersecurity in the construction industry, the purpose of which can be classified into general discussions, review papers and specific solutions. General discussions on cybersecurity topics in construction include works by Bello and Maurushat [10], El-Sayegh et al. [11], García de Soto et al. [1], Mantha and García de Soto [4], to name a few. Review papers include works by Pärn and Edwards [12], Sonkor and García de Soto [13]. Specific technical solutions cover blockchain technology [12] [14], machine learning and deep learning algorithms [15][16], threat modeling [7][17], framework proposal [5], and CVSS score [3]. Despite these efforts, the search in the Web of Science database with query words “cybersecurity” and “construction industry” only resulted in a total number of no more than 62 in the past 5 years, among which there is no unified framework to help practitioners who are not computer science experts to implement cybersecurity measures handily. In this context, this study proposes to synthesize existing content that has been published online, screen and organize it into a corpus database (a corpus is simply a list of sentences), and implement a topic modeling technique on the corpus that can be used to identify future research directions in the field of cybersecurity in the

construction industry. Compared to previous works [2] [4] [18], this study is the first to analyze content from such extensive sources, including news, articles & blogs, LexisNexis database, academic publications, books, standards, and company reports, which provides a more concrete foundation and a more comprehensive information integration for topic identification.

The rest of the paper is organized as follows: Section 2 introduces the steps and methods for collecting, processing, and screening the text and illustrates how the topic modeling is implemented. Section 3 demonstrates the experiments of semantic screening, lists the statistical information of all the corpora established and demonstrates how to decide the input variable for topic modeling. Section 4 discusses and summarizes the topics. Finally, Section 5 concludes the paper, identifies the existing limitations of the paper and proposes future work.

2 Steps and methods

Figure 1 illustrates the overall process of this study. It can be seen that there are 6 main steps leading to the final purpose of topic modeling, during which 4 intermediate corpora are formed and stored. The steps are explained in detail in Sections 2.1 to 2.6.

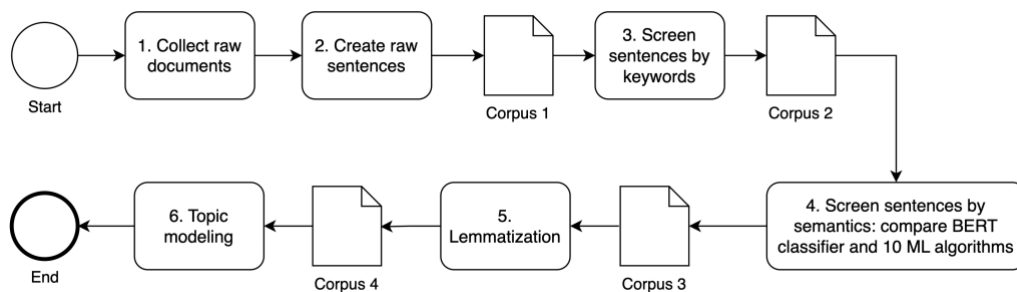


Figure 1. Overview of the main steps used in this study

2.1 Collect raw documents

As much relevant text as possible was collected to perform topic modeling in the field of cybersecurity in the construction industry. The text was collected from six sources to cover most of the necessary data.

(1) News articles and blogs are useful sources of domain-specific text as they provide detailed information about contemporary cyber incidents, including their causes, procedures, and impacts. In this study, we used the Octoparse software to crawl over 70 websites. From each website, we extracted the title, URL, and content of each piece of text. Search criteria: “cyber*” and “construction industry”.

(2) LexisNexis is a reputable provider of online legal, business, news, and public records information, which includes documents dating back decades and adding about 54 million new documents each month. This study utilized the free API service provided by New York University (NYU) to request relevant documents using the Python query code. Through this process, we obtained and saved nearly 4,000 pieces of text in CSV form. Search criteria: “cyber*” and “construction industry”.

(3) Academic peer-reviewed publications are important data sources on cybersecurity in the construction industry due to the high quality and relevance of their professional knowledge. We conducted

searches using the same query words as above in the Google Scholar, Web of Science, and Scopus databases to identify the most relevant publications on this topic. Search criteria: “cyber*” and “construction industry”.

(4) Books and book chapters related to our topic. Although we could only find a small number of relevant books and book chapters, we could use relevant information from those sources. Search criteria: “cyber*” and “construction industry”.

(5) Specifications and standards are important sources as they contain complete statements of legal or industry requirements related to cybersecurity. In this study, we collected 37 documents for text extraction, including PAS 1192-5:2015, ISO/IEC 27001 etc. Search criteria: “cyber*” and “construction industry”.

(6) Reports from companies, such as slides and manuals, can be useful sources of text, although the text may be scattered throughout the document and require manual compilation. We used Google Search to locate PDF files of company reports. Search criteria: “cyber*” and “construction industry”.

The collected raw documents are open-sourced on the GitHub page [19].

2.2 Create raw sentences (Corpus 1)

In this step, we organized the raw documents into a list of sentences. There are four types of raw documents: CSV, PDF, JSON, and TXT. We used open-sourced or self-created Python scripts and libraries to extract the texts from these documents. This resulted in Corpus 1 (summarized in Section 3.1), which is a list of sentences. The Python scripts and libraries used are summarized as follows: (1) The Slate3k library was used to extract text from one-column PDF files of books, standards, and reports; (2) The Pyesseract library is used to extract text from PDF files of papers that have two columns; (3) The Pandas library was used for processing CSV and JSON files and text handling; (4) Mysentences, a self-created Python script, was used to preliminarily clean and split the texts into sentences.

2.3 Screen sentences by keywords (Corpus 2)

Not all sentences were relevant to this study. Sentences containing noisy or irrelevant information were removed. To do this, the authors have created a list of 76 keywords to screen out related sentences, including “cyber”, “threat”, “vulnerab”, “internet”, “secur”, “safe”, “information”, “cloud”, etc. Some of the keywords are partial words, as there are different variations of the word, and some are abbreviations commonly used in the cybersecurity field. This process resulted in Corpus 2 (summarized in Section 3.1).

2.4 Screen sentences by semantics (Corpus 3)

To ensure that all sentences in our study were meaningful and relevant, we used a semantic screening process that involved training a deep learning model. We randomly selected and manually labeled 2,000 pieces of sentences with the label “0” indicating “Exclusion” and the label “1” indicating “Inclusion.” The criteria for inclusion of sentences in the training corpus are as follows: (1) the sentence should have a good format and structure, and (2) the sentence should be directly relevant to the construction industry or cybersecurity. These two criteria are clear and not ambiguous and should effectively screen out useful texts for training the model.

The 2,000 sentences were then randomly split into a training set with 1,660 samples and a test set with 340 samples (~80:20 data split). The training set was fed into a deep learning model for classification tasks, which was composed of a pre-trained BERT model [20] and a linear layer. We experimented with different sets of hyperparameters and configurations for fine-tuning the model and ultimately selected the set of hyperparameters that achieved the highest performance on the test set. This model was trained using the Hugging Face’s Transformers library [21].

For comparison to the BERT classifier, we also trained and tested 10 traditional statistics-based machine learning algorithms [22] as baselines: Naive Bayes (NB), Support Vector Machine (SVM), Logistic Regression (LR), Random Forest (RF), K-Nearest Neighbors (KNN), Gradient Boosting Decision Tree (GBDT), eXtreme Gradient Boosting (XGBoost), Stochastic Gradient Descent (SDG) Classifier, Decision Tree (DT), and Light Gradient Boosting Machine (LGBM) Classifier. To do this, we used the lemmatized version of Corpus 2 (see Section 2.5 for the explanation of lemmatization) to create Term Frequency-Inverse Document Frequency (TF-IDF) features and fed them into these machine learning algorithms. The training of these 10 algorithms was implemented using the scikit-learn library [23].

After comparing the performance of the 11 models (1 BERT classifier and 10 ML algorithms), we selected the model with the highest test performance to screen all sentences in Corpus 2. The resulting sentences labeled with “Inclusion” formed Corpus 3 (summarized in Section 3.1).

2.5 Lemmatization (Corpus 4)

Once the samples in Corpus 3 were cleaned in terms of semantics, we established a corpus that integrates information and knowledge about cybersecurity in the construction industry. In order to perform topic modeling, we need to create a lemmatized version of Corpus 3. Lemmatization involves removing inflectional endings from a word and returning it to its base or dictionary form,

known as the lemma. Lemmatization can reduce the number of tokens while maintaining the same level of information, improving the performance of NLP tasks. The lemmatization process consists of the following steps: lowercasing each sentence, tokenizing each sentence into words using the NLTK library, removing stop words and punctuations and lemmatizing the words.

A Python script named “myRaw2Lemmatized.py” [24] was developed to perform the entire lemmatization process in an integrated way, resulting in Corpus 4 (summarized in Section 3.1).

2.6 Topic modeling

Topic modeling is a technique for identifying the key themes or topics in a collection of texts. It is performed using the Latent Dirichlet Allocation (LDA) method [25]. To optimize the results of the LDA model, we must first determine the input variable, which represents the number of topics to be generated. To achieve this, we experimented with input variables ranging from 5 to 30 and evaluated the models based on their perplexity and coherence scores. Perplexity scoring measures the accuracy of a probabilistic model in predicting a sample, while coherence scoring measures the relatedness of the top words in a topic. A low perplexity score and high coherence score indicate that the model is more accurate and the topics are more coherent, respectively. A Python script called “topic_modeling.py” [26] was developed to run the entire process. Section 3.3 describes the experimentation process and indicates how we ultimately chose 8 as the input variable (i.e., the number of topics), which means that eight topics will be summarized. The eight topics identified and summarized can provide insights into future directions for research on cybersecurity in the construction industry.

3 Experiments and Results

In Section 3.1, we present the experiments and results of screening sentences by semantics (corresponding to Section 2.4) and then present an overview of the statistical information for the four corpora established. Section 3.2 describes the experiment process for deciding the input variable for topic modeling and presents the preliminary results of the eight topics (corresponding to Section 2.6).

3.1 Corpora establishment

Sections 2.1 and 2.2 are for collecting related text or documents and tokenizing them into individual sentences, which result in Corpus 1. Table 1 shows statistical information on Corpus 1. Sections 2.1 through 2.3 outline the process of collecting raw sentences and filtering them using keywords, resulting in the creation of Corpora 1

and 2. Although these steps require significant effort, they are relatively straightforward to implement. In contrast, Section 2.4, which involves screening sentences based on semantics, requires extensive experimentation to determine the most effective model. Therefore, in this section, we provide a detailed explanation of the experimentation process.

Table 1. Statistics of Corpus 1 (Raw Documents)

Text source	Tools	# of document	# of sentence	Total number
News articles and blogs	Octoparse crawling tool	75 websites	71 K	
LexisNexis databases	LexisNexis API through NYU	3,968 pieces of news	596 K	
Academic papers	Google Scholar, Web of Science, and Scopus	78 pieces	26 K	802 K
Books (chapters)	Google search	13 files	73 K	
Specifications/Standards	Google search	37 files	22 K	
Company reports	Google search	46 files	14 K	

3.1.1 Screen sentences by semantics

In Section 2.4, we used Corpus 2 as input for the BERT classifier; at the same time, we compared the BERT classifier with 10 ML algorithms. A total of 1,660 examples were used for training and 340 for testing. The training and experimenting of the BERT classifier were conducted on the Google Colab. A total of 10 experiments using the BERT classifier were conducted. The hyperparameter settings and training results are presented in Table 2. In these experiments, the main variables were the batch size for gradient accumulation, learning rate, class weights, and dropout rate. We set the total number of training epochs to 6, the optimizer with scheduler to Adam with decoupled weight decay (AdamW), and the loss function to CrossEntropy. Note that in the 2,000 sentences, the number of label ‘Exclusion’ is 1,381 while that of ‘Inclusion’ is 619. To make the training dataset more balanced for training, we set different class weights when computing the loss, respectively 1:3, 1:2 and 1:1.4. Any ratio between 1:3 and 1:1 should be fine for experimentation.

We found that both Setting 7 and Setting 9 achieved the highest testing accuracy of 0.903, demonstrating the BERT model’s strong ability to fit training examples and its superiority in semantic understanding. This validates our labeling process on the 2,000 random samples and subsequent training on the entire Corpus 2. In comparison, we also applied 10 statistic-based ML algorithms (in Section 2.4) to predict labels on the 340 test samples. The results indicate that the performance of

statistic-based ML algorithms is generally lower than that of the BERT model, with the highest accuracy being 0.797 from the XGBoost and GBDT models.

Table 2. BERT classifier experiments

Setting number	Batch size	Learning rate	Class weights	Dropout rate
1	4	5e-5	1:3	0.2
2	8	5e-5	1:3	0.2
3	4	5e-5	1:2	0.4
4	8	5e-5	1:2	0.4
5	4	5e-5	1:1.4	0.2
6	8	5e-5	1:1.4	0.2
7	4	4e-5	1:3	0.2
8	8	4e-5	1:3	0.2
9	4	4e-5	1:1.4	0.4
10	8	4e-5	1:1.4	0.4

Therefore, we selected the BERT classifier as our final model, which was configured with Setting 7 in Table 2. We then used this trained model to automatically label all sentences in Corpus 2, resulting in the creation of Corpus 3. For example, the 2nd sentence in Corpus 3 is “For some construction companies, recent ransomware attacks have led to the loss of confidential data or a systems shutdown”, and the BERT classifier labels it as “Inclusion” with probability 0.998, meaning that this sentence should be included in our corpus with a high confidence score. The 189th sentence is “Innovative building firms employ Building Information Modeling (BIM) as a central database for blueprints, designs, and other assets”, and the BERT classifier labels it as “Inclusion” with a probability of 0.687, meaning that this sentence can only be included in our corpus with a low confidence score. Sentences with probabilities lower than 0.5 should be excluded from our corpus. From our result, more than 90% of the final sentences have a probability of over 0.85, which demonstrates the effectiveness of our labeling process. These high probabilities also indicate that the BERT classifier is highly confident in its judgments.

3.1.2 Statistical information of the four corpora

The statistical information (number of sentences, number of words, number of unique words, and storage size) for Corpora 1 through 4 are summarized below.

- Corpus 1: 802K sentences, 23,753K words, 905K vocabulary items, 163 MB
- Corpus 2: 238K sentences, 9,224K words, 447K vocabulary items, 66 MB
- Corpus 3: 66K sentences, 2,227K words, 121K vocabulary items, 15 MB
- Corpus 4: 66K sentences, 1,305K words, 34K vocabulary items, 11 MB

Each step significantly reduces the number of sentences, words, vocab size, and storage size, with some

reductions exceeding 50%. This results in a more content-rich and semantically useful corpus for our study. We will use Corpus 4 to perform topic modeling.

3.2 Decide the input variable for topic modeling

In Section 2.6, we used Corpus 4 for topic modeling through the LDA method. To determine the optimal input variable for the LDA model, we evaluated different numbers (5 to 30) using perplexity and coherence scores as metrics [25]. Figure 2 shows how the perplexity score decreases with an increase in the input variable while the coherence score fluctuates, generally decreasing. Out of the three candidate input variables (8, 15, and 30) that reach a peak respectively in the fluctuating line, we chose 8 as it results in more focused topics. Therefore, the final number of topics derived is 8, with a perplexity score of -8.68 and a coherence score of 0.48.

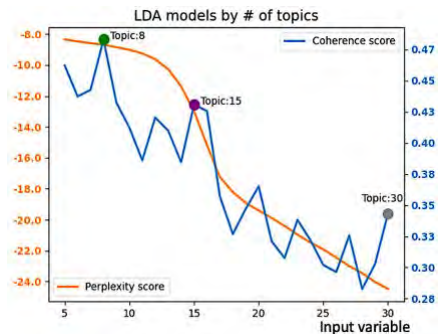


Figure 2. Perplexity and coherence scores

The LDA model then uses 8 as the input variable for topic modeling. The results are visualized in Figure 3 as a 2D mapping of the 8 topics grouped into clusters. The distances between the clusters indicate their correlation, with topics 1, 2, 3, and 8 being closely related and topics 4, 5, 6, and 7 being more independent. The size of the bubble represents the prevalence of each topic, with topics 1, 2, and 3 being the most prevalent and thus to be prioritized.

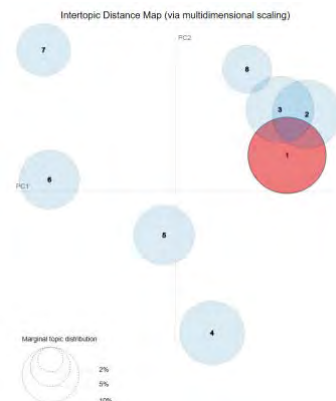


Figure 3. 2D mapping of eight topics

4 Discussions on summarizing topics

Once the number of topics was selected, in this case, eight, they were summarized based on two elements: (1) keywords associated with each topic, which were identified by the LDA model as the 10 keywords with the highest weights, and (2) representative original sentences for each topic, which were selected from the 3 most meaningful sentences out of a pool of 10 sentences with the highest contribution percentage, calculated using the Gensim library [27]. The 3 most meaningful sentences from a pool of 10 sentences with the highest percentage of contribution for each topic were selected.

For example, for the 1st topic, the top 10 keywords with the highest weights were: 0.05: security; 0.04: cybersecurity; 0.03: safety; 0.02: risk, training, may; 0.01: area, provide, private, ensure. The chosen three representative sentences are as follows: (1) Construction companies need to conduct comprehensive and frequent third-party cyber security assessments so they can identify and remediate vulnerabilities; (2) Cyber security is not just an IT issue. Cyber risk should not be seen as an issue solely for your IT department or provider; (3) Many construction firms also lack awareness regarding cyber security. Their percentages of contribution are 0.96, 0.92, and 0.92, respectively. By combining the 10 keywords and the 3 representative sentences, we can infer and summarize the topic: *Increase awareness of construction firms by providing training and contact periodic risk analysis.*

A similar process for Topic 1 was used to determine the remaining topics. The results are summarized in Table 3. In general, the 8 topics can be described as Perform Risk Analysis, Prevent the Increasing Cyber Incidents, Detect Ransomware, Strengthen Management Process, Protect Network Devices, Regulate Information Storage and Sharing, Protect Privacy, and Improve Authentication Process. The action to take to address these topics is also proposed in Table 3. These 8 identified topics and corresponding suggested actions can serve as a reference for researchers interested in studying future research directions in cybersecurity within the construction industry. Based on the topic prevalence (the size of the bubble) shown in Figure 3, we recommend prioritizing research on risk analysis and specific solutions to threats, such as ransomware, corresponding to Topics 1, 2, and 3.

5 Conclusions and outlooks

This study employs topic modeling to uncover potential research directions in cybersecurity in the construction industry. We gathered 6 types of raw text sources, which were transformed into 802K raw sentences. Through a process of keyword and semantic

screening, the data was reduced to 66K sentences, forming the corpus (Corpus 4) for our topic modeling analysis. We utilized the LDA method and tested input variables ranging from 5 to 30, evaluating and selecting the model based on perplexity and coherence scores. Our analysis revealed that 8 was the most suitable number of topics. The results of our analysis identified 8 potential topics for future research, and corresponding actions to take are also proposed.

Some of the limitations of this study include (1) the corpus was not as clean as it could have been, as some samples contained irregular characters and signs from the original crawled websites due to semantic screening only considering the meaning of sentences and ignoring their format, and (2) the number of specific studies on cybersecurity in the construction industry is limited, which inevitably impacted the comprehensiveness of our final corpus.

To address these limitations, the authors are adding a new corpus and comprehensively cleaning up selected texts. Additionally, the resulting corpus can be used for other purposes, such as training large language models to create question and answer systems (like the ChatGPT dialogue system released in Nov 2022 [28]), which can provide relevant people with preliminary consulting advice on cybersecurity management and will also be the focus of our future research.

Acknowledgments

The authors want to thank the Center for Cyber Security at New York University Abu Dhabi (CCS-AD) for the support provided.

References

- [1] García de Soto B., Agustí-Juan I., Joss S., and Hunhevicz J. Implications of Construction 4.0 to the workforce and organizational structures, *International Journal of Construction Management*, 22(2): 205-217, 2022.
- [2] Kayan H., Nunes M., Rana O., Burnap P., and Perera C. Cybersecurity of Industrial Cyber-Physical Systems: A Review, [Online]. Available: <http://arxiv.org/abs/2101.03564>, 2021.
- [3] Mantha B. R. K., and García de Soto B. Assessment of the cybersecurity vulnerability of construction networks, *Engineering, Construction and Architectural Management*, 28(10): 3078–3105, 2021.
- [4] Mantha B. R. K., and García de Soto B. Cyber security challenges and vulnerability assessment in the construction industry, in *Proceedings of the Creative Construction Conference 2019*, pages 29–37, Budapest, Hungary, 2019.

Table 3. Summarized topics and actions to take

Topic No.	Keywords	Three representative sentences for each topic	Topic summarized	Some actions to take
1	security, cybersecurity, safety, risk, may, training, area, provide, private, ensure	<ul style="list-style-type: none"> Construction companies need to conduct comprehensive and frequent third-party cyber security assessments so they can identify and remediate vulnerabilities. Cyber security is not just an IT issue. Cyber risk should not be seen as an issue solely for your IT department or provider. Many construction firms also lack awareness regarding cyber security. 	Perform Risk Analysis	Researchers should take the lead to develop frameworks first.
2	cyber, security, standard, sector, industry, technology, development, dimension, report, impact	<ul style="list-style-type: none"> Regardless of the industry, there is a worrying shift in the mindsets of security professionals. Rising cyber-attacks 75% of respondents reported an increase in cyber-attacks in the last 12 months. We are undoubtedly in a changing world, and cyber security is an ever-changing industry. 	Prevent the Increasing Cyber Incidents	Industry practitioners should share the incident data.
3	threat, infrastructure, national, critical, attack, cyber, government, public, measure, communication	<ul style="list-style-type: none"> You don't want to get ransomware, and the government also doesn't want you to accept ransomware. Phishing emails have increased by 20%, while malware soared by 423%. For example, supply-chain-based attacks, such as the SolarWinds SUNBURST attack, are not simple system vulnerabilities. 	Detect Ransomware and Malware	Software providers must constantly update their algorithms.
4	construction, risk, project, building, design, system, management, build, personnel, may	<ul style="list-style-type: none"> These risks can be physical and directly affect the insurance business, or they may be more transitional and affect insurers. Stakeholder-associated life cycle risks in the construction supply chain. Due to known and unknown risks, the Company's results may differ materially from its expectations and projections. 	Strengthen Management Process	Companies should adopt strict policies and train employees effectively.
5	system, http, use, control, security, network, secure, access, internet, device	<ul style="list-style-type: none"> The Internet of Things (IoT) is a system where devices are connected wirelessly with the help of unique identifiers. Access to the software is not properly controlled. Centralized visibility allows organizations to control access for any device, connecting from any network. 	Protect Network Devices	Hardware manufacturers should integrate advanced security features.
6	information, data, asset, personal, include, use, level, access, specific, person	<ul style="list-style-type: none"> Besides proprietary employee data, other potentially vulnerable information includes sensitive client data, and tenant personally identifiable information (PII). Are any assets (e.g., web server, web application) Internet-facing? What information is being shared, and what is the purpose of sharing it? 	Regulate Information Storage and Sharing	Governments must establish strict data protection laws.
7	data, protection, activity, policy, breach, require, state, privacy, key, manage	<ul style="list-style-type: none"> The attacked data was encrypted, and ransom payments were demanded in the Bitcoin cryptocurrency. After that, both processing and privacy should be determined before clarifying the requirement of granularity of trajectory data. They are triggered if: (1) there is a breach of contract, and (2) the penalty for breach is stated in the contract. 	Protect Privacy	Users should be educated on best practices, and developers should prioritize privacy by design.
8	cybersecurity, develop, strategy, response, incident, framework, security, number, practice, plan	<ul style="list-style-type: none"> Here are some strategic approaches: Deploy Multi-Factor Authentication. Implementing cyber security strategies to fortify endpoints and IT/OT integration while establishing a robust incident response plan will go a long way toward delivering peace of mind. Choose a good, strong password: passwords are the weakest cybersecurity link. 	Improve Authentication Process	Companies should implement multi-factor authentication or biometrics.

- [5] Turk Ž., García de Soto B., Mantha B. R. K., Maciel A., and Georgescu A. A systemic framework for addressing cybersecurity in construction, *Automation in Construction*, 133: 103988, 2022.
- [6] Infosec, Phishing Attacks in the Construction Industry, Infosec, On-line: <https://resources.infosecinstitute.com/topic/phishing-attacks-construction-industry/>, Accessed: 14/03/2022.
- [7] Mantha B., García de Soto B., and Karri R. Cyber security threat modeling in the AEC industry: An example for the commissioning of the built environment, *Sustainable Cities and Society*, 66: 102682, 2021.
- [8] Glamoslija Katarina. Ransomware Facts, Trends & Statistics for 2021, *Safety Detective*, On-line: <https://www.safetydetectives.com/blog/ransomware-statistics/>, Accessed: 08/01/2023.
- [9] Salami Pargoo N., and Ilbeigi M. A Scoping Review for Cybersecurity in the Construction Industry, *Journal of Management in Engineering*, 39(2), 2023.
- [10] Bello A., and Maurushat A. Technical and Behavioural Training and Awareness Solutions for Mitigating Ransomware Attacks, in *Advances in Intelligent Systems and Computing*, 1226(AISC): 164-176, 2020.
- [11] El-Sayegh S., Romdhane L., and Manjikian S. A critical review of 3D printing in construction: benefits, challenges, and risks, *Archives of Civil and Mechanical Engineering*, 20(2), 2020.
- [12] Pärn E. A., and Edwards D. Cyber threats confronting the digital built environment: Common data environment vulnerabilities and block chain deterrence, *Engineering, Construction and Architectural Management*, 26(2), 2019.
- [13] Sonkor M. S., and García de Soto B. Is Your Construction Site Secure? A View from the Cybersecurity Perspective, in *Proceedings of the 38th International Symposium on Automation and Robotics in Construction (ISARC)*, pages 864-871, Dubai, United Arab Emirates, 2021.
- [14] Shemov G., Garcia de Soto B., and Alkhzaimi H. Blockchain applied to the construction supply chain: A case study with threat model, *Frontiers of Engineering Management*, 7(4): 564-577, 2020.
- [15] Goh G. D., Sing S. L., and Yeong W. Y. A review on machine learning in 3D printing: applications, potential, and challenges, *Artificial Intelligence Review*, 54(1): 63-94, 2021.
- [16] Yao D., and García de Soto B. A preliminary SWOT evaluation for the applications of ML to Cyber Risk Analysis in the Construction Industry, *IOP Conference Series: Materials Science and Engineering*, 1218(1): 012017, 2022.
- [17] Mohamed Shibly M. U. R., and García de Soto B. Threat Modeling in Construction: An Example of a 3D Concrete Printing System, in *37th International Symposium on Automation and Robotics in Construction*, pages 625-632, Kitakyushu, Japan, 2020.
- [18] Sonkor M. S., and García de Soto B. Operational Technology on Construction Sites: A Review from the Cybersecurity Perspective, *Journal of Construction Engineering and Management*, 147(12), 2021.
- [19] Yao D. Data for topic modeling, GitHub repository, On-line: <https://github.com/Daniel-Yao-Chengdu/NLP-project/blob/master/Data%20for%20topic%20modeling>, Accessed: 16/03/2023.
- [20] Devlin J., Chang M.-W., Lee K., and Toutanova K. BERT: Pre-training of Deep Bidirectional Transformers for Language Understanding, [Online]. Available: <http://arxiv.org/abs/1810.04805>, 2018.
- [21] Jain S. M. Hugging Face, Introduction to Transformers for NLP, pages 51–67. CA: Apress, Berkeley, 2022.
- [22] Giuseppe B. Machine Learning Algorithms. Packt Publishing Ltd, Birmingham, 2017.
- [23] Kramer O. Scikit-Learn, Machine Learning for Evolution Strategies, pages 45–53. Springer, Cham, Oldenburg, 2016.
- [24] Yao D. myRaw2Lemmatized, GitHub repository, On-line: <https://github.com/Daniel-Yao-Chengdu/NLP-project/blob/master/myRaw2Lemmatized.py>, Accessed 07/01/23.
- [25] Blei D. M., Ng A. Y., and Edu J. B. Latent Dirichlet Allocation, *Journal of Machine Learning Research*, 3: 993-1022, 2003.
- [26] Yao D. Topic Modeling, GitHub repository, On-line: https://github.com/Daniel-Yao-Chengdu/NLP-project/blob/master/Topic%20modelling/topic_modeling.py, Accessed 07/01/2023.
- [27] Rehurek R., and Sojka P. Gensim-python framework for vector space modelling, NLP Centre, Faculty of Informatics, Masaryk University, Brno, Czech Republic, 3(2), 2011.
- [28] OpenAI ChatGPT: Optimizing Language Models for Dialogue, OpenAI, On-line: <https://openai.com/blog/chatgpt/>, Accessed: 07/01/2023.

Lessons Learned from ‘Scan to BIM’ for Large Renovation Projects by the U.S. Army Corps of Engineers

Tony Cady¹, Anoop Sattineni² and Junshan Liu³

¹United States Army Corps of Engineers, USA

^{2,3}McWhorter School of Building Science, Auburn University, USA

¹Anthony.E.Cady@usace.army.mil, ²sattian@auburn.edu, ³liujuns@auburn.edu

Abstract –

The U.S. Army Corps of Engineers (USACE) Savannah District recently invested in the adoption of a process of transferring 3D Light Detection and Ranging (LiDAR) scan data into a Building Information Model (BIM), a process commonly known as Scan to BIM. This research explores the challenges and benefits of adopting and using this technology for large renovation projects in USACE. Two buildings were evaluated as part of the study. The BIM for one building was developed using traditional methods of physically capturing dimensions. In the second building, data captured from LiDAR scanners were used to develop the BIM. Lessons learned from the development of Scan to BIM process and a comparison of how this is accomplished in USACE is discussed. Key issues identified from interviews with stakeholders include reduced labor for documenting existing conditions and improved accuracy of the data captured. Participants also identified the cost of equipment, cost of training and development of organizational standards as being important for future use of Scan-to-BIM technologies.

Keywords –

USACE, Laser Scanning, LiDAR, Scan-to-BIM, Renovation Projects

1 Introduction

The U.S. Army Corps of Engineers (USACE or the “Corps”) is the design and construction agent for all U.S. Army and U.S. Air Force facilities and infrastructure worldwide. As such, the Corps is one of the largest construction owners in the world and frequently undertakes the development of designs for large renovation and repair projects (greater than \$3 million estimated construction cost) using “in-house” design teams. This paper will investigate a technological approach of capturing the existing conditions of facilities to develop architectural Building Information

Models (BIM) which are then used as the basis for the renovation design. Recently the USACE Savannah District invested in adopting the process of transferring 3D ‘Light Detection and Ranging’ (LiDAR) scan data into BIM, a process commonly known as Scan to BIM [1]. This research will explore the challenges and benefits of adopting this methodology more widely for large renovation projects within the organization.

Since 2013, Building Information Modeling (BIM) has been required on all vertical construction projects by the Corps (US Army Corps of Engineers, 2013). The requirement was renewed and refined in 2018 under Engineering and Construction Bulletin 2018-7, Advanced Modeling Requirements on USACE Projects. That document requires the use of BIM on all projects which exceed 5000 gross square feet or a construction cost of \$3 million or greater [2]. BIM is a shared knowledge resource for information about a facility forming a reliable basis for decisions during its life cycle [3].

LiDAR scanning technology has the capability to efficiently capture the 3D geometry of a facility in the form of “point clouds” [4]. These point clouds can then be used to construct digital 3D models or a BIM of a facility. And since a laser scanning process is the fastest method of 3D data acquisition for existing buildings [5], a review of the potential benefits and challenges associated with the adoption of the Scan to BIM process by the Savannah District to develop the architectural BIM for large renovation projects is a test case within the US Army Corps of Engineers.

LiDAR, laser, or 3D scanning is a means of using a laser scanner to map an area with high accuracy (Ellis, 2020). It has emerged as a useful tool in documenting existing conditions of buildings and has been referred to as a “mantra” to solve the issue of developing and analyzing existing facilities for renovations [6]. Integrating laser scanning with BIM can yield significant advantages over traditional approaches by facilitating fast and accurate data acquisition of existing conditions [7].

2 Literature Review

According to Bortoluzzi and his co-authors, most of the research regarding BIM generation for existing buildings focuses on three areas: 1. Laser Scanning and Photogrammetry; 2. Translation of 3D point clouds to BIM; and 3. Automated conversion of 2D plans to BIM [8]. The process of converting point cloud data into an 'as-is' BIM is known as "Scan-to-BIM" [8] [6] [1]. This process has become an established and widely used method of acquiring the geometry of a building to generate 'as-built' or 'as-is' building models in the AEC industry. Geometric surfaces or volumetric primitives are fitted to a 3D point cloud to model walls, floors, ceilings, columns, beams, and other structures of interest. The modeled primitives are annotated with semantic information including identity labels (e.g., wall) and meta-data, such as the surface material (e.g., concrete), and spatial and functional relationships between nearby structures and spaces are established [9]. It is basically a practice of creating a digital representation of existing conditions of the building with its physical and functional characteristics in a BIM. A laser scanner is used to capture an accurate 3D point cloud which is ultimately imported into 3D BIM software (e.g., Autodesk's Revit, Graphisoft's ArchiCAD, Vectorworks, etc.) to create accurate as-built models [10].

2.1 Increased Use of Scan to BIM

Scan to BIM has been in use since the 1980s [11]. Since then, developments in the technology and workflow processes have resulted in more widespread use of the process to gather in situ geometric data [12] [13] and improvements in the reliability of that data [14]. The sheer amount of current research on the topic illustrates its increased use for numerous facility management activities including, 'reverse engineering' [15], energy efficiency and sustainability [14] [5] [16] [17] [6], material reuse/recycling [16], cost estimating and control [8] [6], structural analysis [18] [14], historical building information modeling (HBIM) [19] [14] [20] [21], safety, decommissioning, and renovation designs [18].

In their journal article "A Survey of Applications with Combined BIM and 3D Laser Scanning in the Life Cycle of Buildings" Liu and his co-authors compared current methods of integrating 3D laser scanning with BIM, applications in a building's life cycle, and impacts of the continued development of the technology [17]. They found that more and more researchers are focusing on Scan to BIM applications. The researchers went on to state laser scanning has become "common technology" to acquire point clouds due to its high precision and accuracy. This finding was also supported

by others who claim that laser scanning is used in most cases to obtain an existing building's geometry [22]. One clear reason for this is the intrinsic value of geometric and spatial information upon which to base renovation designs [6].

2.2 Benefits of Scan to BIM

Current literature clearly documents the reductions in the amount of time it takes and the costs of collecting 'as-is' conditions of existing facilities as a primary benefit of the Scan to BIM process. Not only is the process faster but it also reduces the cost of data collection over manual methods, e.g., multiple architects physically measuring and sketching the facility. The reduced time and/or cost to collect existing condition data is cited frequently in the current literature [5] [6] [15] [13] [1]. In a systematic literature review of 194 papers discussing HBIM it was concluded the use of laser scanners accelerated data collection and decreased errors and claimed it would result in cost and time savings not only during data collection, but also during design, and construction [22]. Skrzypczak et al. also found that laser scanning is more efficient and reduces time and costs of data collection over conventional or manual methods [11]. Additionally, recent advances in laser technology have made acquisition of point clouds even faster and more effective [18].

The other clear advantage of laser scanning is the accuracy of the data collected. Antova and Tanev state manually measuring a facility with measuring tapes is accurate to 25 – 75mm (approximately 1 – 3 inches) [18]. This level of accuracy is clearly not suitable for large renovation planning and design. On the other hand, Terrestrial LiDAR Scanning (TLS) can achieve accuracy within several millimeters [17]. Mellado and his co-authors concluded laser scanners can produce models with + 2mm accuracy at 250 meters [6]. Skrzypczak and his colleagues analyzed the accuracy of three different buildings and found that scanning significantly enhanced the accuracy of the BIM and had a level of error of + 1cm [11]. Hossain and Yeoh also claim the degree of accuracy is within 1cm to 1mm [23]. And Sanhudo and colleagues conclude accuracy up to 0.6mm at a 10m range [13].

Safety is another benefit of the use of laser scanning to capture existing conditions because capturing data in hard to reach or inaccessible areas can be accomplished without the need to expose personnel to unnecessary risks [11] [24].

Laser scanning provides 3D documentation of a facility and access to images and photos during design development [11] and it can be used in low light conditions [23] [12]. Another benefit is the facilitation of design development in an efficient manner,

evaluating various design alternatives, decision making, and cost estimating [6] [13]. Laser scanning also allows a wider range of measurements at higher resolutions than photogrammetry techniques [12] and it offers the potential of some degree of automation in the BIM development [13]. Perhaps the most fundamental statement regarding the value of Scan to BIM was provided by Merckx who stated, “Laser scanning is the best way to document the indoor environment of a building” [25].

2.3 Challenges with Laser Scanning

The primary challenges identified in the literature reviewed are the time and cost to develop the BIM from point clouds, the modeler’s skill and experience, and the insufficiency of automated or semi-automated modelling to identify and record semantic information.

Developing BIM for existing buildings from a point cloud is “complex, tedious, time consuming, and costly” [30]. This observation is shared and articulated by numerous researchers [18] [26] [5] [24] [16] [17] [26] [27] [15] [13] [12] [1]. One survey stated setbacks during BIM development are common and 80% of respondents to a survey agreed that the modeling step is the most time consuming in the Scan to BIM process [15]. And as one would expect, the complexity, time, and costs increase with an increase in the level of detail (LOD) required and the model’s intended use; for example, BIM for a renovation project will require a much higher level of detail than a model to be used strictly for operations and maintenance or facility management requirements [23]. Higher quality and more accurate models involve a higher cost of development. Therefore, a tradeoff should be made to balance the model’s reliability and development costs [1].

Despite advances in automated modeling, creating BIM from point clouds is often subjective and requires skilled modelers with specific expertise [28], [23]. Moreover, modeler qualifications have a large impact on the quality of the BIM developed [24] and different modelers will create different models using the same software and data [12]. Researchers provided a quantitative analysis of the accuracy of 25 modelers and demonstrated the benefit of training as well as the use of semi-automated methods to develop the BIM [28]. The training alone produced dramatic results decreasing the standard deviation by 330% and average absolute modeling error by 260%. The paper concluded that standardizing manual modeling techniques can provide significant value regarding the accuracy and precision of BIM developed from laser scanning.

Automatic modeling is currently being used for common building elements including structural, mechanical, electrical, and plumbing components as

well as the exterior facades of buildings [17]. Many advanced algorithms have been developed to automate portions of the modeling step although the process is still semi-automated at best [28]. A thorough summary of research to advance automated modeling over the past 10 years was completed by others [29]. They discussed software designed to automate geometric modeling including Edgewise, CloudWorx, Faro Scene, Autodesk Recap, and RealWorks. Despite the vast amount of research on the topic of automating the process researchers points out additional work is needed as noise and occlusions in their case study proved challenging for the semi-automated process [22]. Wang et al. [1] stated “although numerous studies are reported for semi-automatic or automatic ‘as-is’ BIM reconstruction from laser scan data, the existing techniques still have room for improvement regarding accuracy, applicability, and automation”, concluding it is difficult to achieve high accuracy and high levels of automation.

3 Methodology

A qualitative methodology was chosen for the purpose of this study. This methodology allowed the researchers to probe implementation issues in detail. Interviews with design and construction professionals within the USACE and industry designed to assess and understand their experience and opinions regarding existing condition data collection and BIM development for large renovation projects. Profile of the interview participants is shown in Table 1. All participants are employees of the Corps except one private owner who is the principal at a private firm. Participants included chiefs of engineering, construction, and design branches from five USACE districts. From an organizational standpoint, USACE is comprised of nine divisions with multiple districts under each division.

Table 1 Interview Participant Profile

#	Position, Title and Experience
1	Chief of Engineering - 31 Years
2	Chief of Construction - 25 Years
3	Chief of Design Branch - 19 Years
4	Senior Architect, Design - 20 Years
5	Senior Architect, Design- 13 Years
6	Chief of Design Branch - 37 Years
7	Chief, of QA Branch - 24 Years
8	Chief of Architecture & Design - 15 Years
9	Chie of Engineering - 35 Years
10	GIS Analyst - 14 Years
11	Chief of Research, CAD/BIM - 13 Years
12	Researcher, CAD/BIM - 3 Years
13	Owner (Private Industry) - 13 Years

4 Results and Discussion

Each year the Savannah District develops multiple architectural BIM models as the basis of design for large renovation projects. These designs are then used to procure construction contracts with private industry. For the purposes of comparison, the researcher limited information on the time and cost necessary to develop BIM to two nearly identical projects at Ft. Gordon, GA. In 2021, the design branch completed the design and specifications for a barrack renovation project at Ft. Gordon, Building 315. In 2022, a similar design was done for barrack Building 317 at Ft. Gordon. The existing conditions of both buildings were captured using manual methods of ‘as-is’ building data collection. However, the existing conditions for Building 317 were later also captured using LiDAR scanners as part of an initial training curriculum developed specifically for the Savannah District by educators from an accredited institution of higher learning. Preparing these designs in the shortest amount of time, at the lowest cost, and as free of errors or omissions as possible, is one of the organization’s primary goals. The workflow adopted to capture existing data and develop design documentation for buildings 315 and 317 is shown in figure 1. In the case of Building 315, designers needed to return to the site obtain missing information that was not captured during the original site visit, whereas that was not required in the case of Building 317.

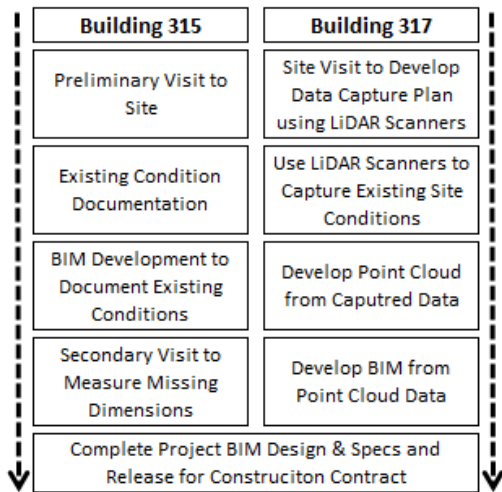


Figure 1: Project Workflow for Building 315 and 317 BIM Development

In late September 2021, the existing as-built conditions of Building 315 were manually measured, and an architectural BIM was prepared to complete the renovation design. Building 315 is a 41,165 gross square foot, 3-story building that houses 136 Soldiers.

In February 2022, the existing as-built conditions of Building 317 were captured using laser scanners. Building 317 is a 68,851 gross square foot, 3-story building that houses 224 Soldiers. The buildings have nearly identical floor plans, the primary difference is Building 317 has two additional ‘stacks’ of barrack rooms as can be seen in Figure 2 below.



Figure 2. Buildings 315 and 317, Ft. Gordon, GA

In October 2021, face-to-face interviews were held with the Savannah District Engineering Division Design Branch Chief, Architectural Team Chief, BIM Manager, and a senior Project Architect Engineer (PAE). The results are presented in Table 2. The purpose of the discussion was to determine current processes, costs, challenges, and the amount of time it takes to develop an architectural BIM model for large renovation projects. This data was used later to contrast to compare thoughts of key personnel upon conclusion of the study after using laser scanners.

Table 2 Preliminary Interviews Summary

Question	Response Summary
<ul style="list-style-type: none"> What procedure is currently used to record existing conditions and develop architectural BIM for renovation designs? 	Four (4) architects spend four (4) days at the building site manually measuring and recording the ‘as-is’ conditions of the facility.
<ul style="list-style-type: none"> What are the challenges with this method? 	Missing or omitted data identified after the team returns and completion of the architectural model frequently requires one or more personnel to return to the site to capture the missing data. Exterior elements require lift

- capability to measure.
- How much time is required to develop the architectural BIM? It takes one architect approximately 8 hours per day for 5 days: 40 hours total.
 - What is the cost of developing the BIM? The approximate cost using \$125/hour as a standard hourly rate is \$5000.
 - How accurate is the data collected? The final model is considered accurate enough to use as a baseline for renovation design and construction contract award with unknowns minimized to the maximum extent possible. Unknowns are in inaccessible spaces or missed measurements.
 - What are the challenges? The primary challenge is compiling measurements from multiple sources and in various formats. Wall widths are often 'backed in to' by using exterior overall dimensions and room widths. The width of utility chases is estimated. A great deal of professional judgement is used when developing the model and the accuracy of these assumptions varies based on the employee's experience and expertise.

Laser scanning data collected in February 2022 was used to develop the BIM model for building 317, as shown in figure 3. Upon completion of the process a second round of interviews were held with a wider group of stake holders, as identified in Table 1. Interviews consisted questions designed to elicit responses regarding the respondent's level of experience with large renovation project designs, current 'as-is' data collection methods and associated challenges, familiarity with other data collection techniques (e.g., Scan to BIM, photogrammetry) anticipated benefits of Scan to BIM, and their thoughts on the future use of Scan to BIM in the USACE. A summary of the issues identified from the interview data is presented below.

4.1 Current Data Collection Methods and Challenges

Nearly all the respondents (92%) identified labor

and manpower as a primary challenge with current data collection techniques. Personnel from five different USACE districts were interviewed and asked about their current data collection techniques for gathering 'as-is' building conditions for large renovation projects.



Figure 3. Laser Scanned Model of Building 317 at Ft. Gordon, GA

All districts included requesting any available scanned paper or CAD files from the installation's Directorate of Public Works (DPW) or Base Civil Engineer (BCE). As-built drawings received often included numerous additional drawings reflecting the renovations completed since the building was built (in some cases, more than 20 years of minor renovations). After the drawings are coordinated, a field investigation is conducted to verify the accuracy of the as-built drawings. This process involved varying numbers of personnel in various design disciplines. Most frequently, the team collecting as-built conditions included architects, and electrical, mechanical, and structural engineers. The duration for data collection varies according to the size of the building and district processes but can range from 1 day to weeks. 85% of respondents discussed the availability and accuracy of as-built drawings as an issue. In all but one case, respondents uniformly agreed current as-built drawings are generally out of date, inaccurate, and often very challenging to secure. Multiple respondents also mentioned that hidden building features were not captured and many also mentioned the amount of data that is missed during these field investigations. One respondent shared that often during design the building owners want additional items added to the renovation project scope and invariably that data would not have been collected during the initial site visit and a return trip would be required.

4.2 Challenges of Using Scan to BIM

Nearly two thirds of respondents identified challenges with the actual LiDAR scanning including the inability to capture hidden or occluded items such as pipe networks above the ceiling and behind walls. Many of them noted these features would not be identified

using manual methods of data collection either. One respondent highlighted the value of having architects physically on-site to see and tour the facility and become familiar with the materials. Over half of the respondents identified challenges with BIM development from the point cloud generated from LiDAR scanning. Specifically, they mentioned the inability of Autodesk Revit to model deflections and the necessity for a conscious decision to be made by the designers to determine deflections which could be ignored such as the undulation in non-load bearing walls, and those which needed to be identified and addressed in the renovation design, e.g., structural deflection of floors or ceilings. The lack of semantic data automatically modeled by the software used to convert the point cloud into a format which can be imported into Autodesk Revit was also mentioned. Although, as the literature review discovered, software manufacturers are making progress on the inclusion of automated modeling capabilities in their products, and this is anticipated to continue. Nearly 40% of respondents discussed data management as a challenge as well. This included the computing power necessary to process the raw point cloud and cybersecurity requirements. Those requirements are of particular importance to USACE because of the stringent security standards software and any cloud-based programs must meet to be allowed on the organization's network. The initial and maintenance costs of adopting Scan to BIM were also mentioned by roughly 1/3 of respondents. Concerns included the initial investment and budgeting for future upgrades in scanner technology and software improvements. It should be noted here that several respondents also believed the benefits will far outweigh the costs.

4.3 Benefits of Using Scan to BIM

100% of respondents highlighted the advantage of the data collection process as a primary benefit of the use of Scan to BIM for large renovation projects. The efficiency of data collection, the sheer amount of data collected, and the accuracy of the data were of particular importance. Reduced opportunity costs were an additional benefit mentioned frequently. This allows design engineers and architects to continue to complete design work on other projects while data is being collected. This goes hand in hand with the reduced manpower requirements to capture existing 'as-is' conditions. For example, the Savannah District sends up to four (4) architects and mechanical, electrical, civil, and structural engineers to a facility to collect existing information for multiple days to collect as much data as possible about the building. It is anticipated that the use of Scan BIM would allow manpower needs to be reduced to one architect and a scanning technician for a

day or two, depending on the size of the facility. This obviously results in reduced labor and travel costs. Time savings during data collection and BIM development was considered another primary benefit by those interviewed. One respondent provided an example of capturing existing conditions of a 160,000 square foot facility in one week and estimated it would have taken a team of architects up to six (6) weeks to manually measure and record the building and its features and develop an initial BIM. Data management, particularly 3D documentation and information sharing, were identified as benefits of the process as well. The 3D documentation was considered particularly important because the scope of renovation projects frequently changes after original data collection is completed. The point cloud will have a record of everything captured and interview respondents considered it to be of value to refer to during design development. The ease of use and relative effectiveness of the various software used to register, clean, trim, and import the point clouds into Autodesk Revit was also considered a benefit by some. Only one quarter of interviewees mentioned a potential reduction in unforeseen and differing site conditions during construction because of the use of Scan to BIM.

4.4 Future Uses of Scan to BIM

Respondents discussed their thoughts on the future use of Scan to BIM and resulted in several use cases being identified. Use cases included renovations, civil works projects, damage assessments, and one respondent discussed its value for aircraft hangar and powerhouse renovations. Scan to BIM on these types of projects was of value because the structure is normally open, and piping networks, duct work, and other building systems are generally visible and not hidden behind walls or drop ceilings. Damage assessments, structural evaluations, scanning during construction to develop true as-built BIM, and the use of Scan to BIM to develop as-built drawings were also identified by the respondents as potential future uses of the Scan to BIM technology and workflow. A point cloud's contribution to the development of a 'digital twin' was also mentioned by one interview participant.

5 Conclusions

Large project renovations within the military programs of the USACE are a large portion of the work the organization executes. In many cases, it is most of the work performed and is anticipated to continue to be. This is especially true given the recent focus on the living conditions for the nation's soldiers and airmen that reside in barracks and dormitories. Initiatives to improve the execution of design development and construction for those and other projects is a continual

process and goal. Based on this research, interviews, and case study, it is clear the adoption of Scan to BIM will improve the Savannah District's efficiency and ability to deliver successful renovation projects to the U.S. Army and Air Force. The authors believe it is reasonable to assume similar benefits may be realized in other USACE districts. The literature review identified the extensive use of Scan to BIM and the rapidly advancing state of the technology and workflows to continue to improve the process. The key advantages of developing BIM from laser scans include the efficiency of data capture, the accuracy of the data captured, improved safety during data collection, and the facilitation of design development. All these benefits were also identified by subject matter experts interviewed particularly within the sub-theme of data collection. Without exception, the interviewees touted the benefits of data collection efficiency realized using Scan to BIM. This includes the amount of data collected, the accuracy of that data, the 3D documentation the point cloud provides during the entire project lifecycle, and the reduced manpower, labor and opportunity costs associated with the use TLS to capture 'as-is' building conditions. In the case of building 315 and 317, participants acknowledged that certain risks of unforeseen site conditions remained due to assumptions made by the problem of occlusion.

The main contributions of this research include the following:

- This research has shown yet again that challenges to scan-to-BIM identified in the literature review such as the lack of semantic information in the resultant point cloud, the ability to capture occluded, hidden, or hard to reach building features, the digital file size of the point cloud, and the lack of quality and accuracy standards continue to hinder design and construction professionals. USACE professionals identified the need for investment in equipment and training at the organizational level and the development of standard operating procedures
- Despite the challenges presented by the use of point cloud data, the study has shown that seasoned industry professionals agree that it has significantly improved accuracy of the BIM developed from the data, as shown in Building 317.
- In the case of USACE, participants agreed that investment in scan-to-BIM technology will improve the organization despite the high adoption cost and potentially reduce data collection costs and minimize design changes after the award of contracts.

- Point cloud data can identify physical features that are easily missed by manual data collection, as shown in the excessive floor deflection found in Building 317, which was missed in Building 315.

References

- [1] Q. Wang, J. Guo, and M.-K. Kim, "An Application Oriented Scan-to-BIM Framework," *Remote Sensing*, vol. 11, no. 3, Art. no. 3, Jan. 2019, doi: 10.3390/rs11030365.
- [2] US Army Corps of Engineers, "US Army Corps of Engineers Engineering and Construction Bulletin No. 2018-7. Advanced Modeling Requirements on USACE Projects." Jun. 06, 2018.
- [3] "Frequently Asked Questions About the National BIM Standard-United States | National BIM Standard - United States," Oct. 16, 2014. <https://web.archive.org/web/20141016190503/http://www.nationalbimstandard.org/faq.php#faq1> (accessed Oct. 11, 2021).
- [4] T. Gao, B. Akinci, S. Ergun, and J. Garrett, "Full paper: Constructing as-is BIMs from progressive scan data," presented at the Gerontechnology, Dec. 2012, vol. 11. doi: 10.4017/gt.2012.11.02.500.00.
- [5] A. Borodinecs, J. Zemitis, M. Dobelis, and M. Kalinka, "3D scanning data use for modular building renovation based on BIM model," in 6th International Scientific Conference on Integration, Partnership and Innovation in Construction Science and Education, IPICSE 2018, November 14, 2018 - November 16, 2018, Moscow, Russia, 2018, vol. 251, p. The Foundation for the Development of Construction Education and Science. doi: 10.1051/mateconf/201825103004.
- [6] F. Mellado, P. F. Wong, K. Amano, C. Johnson, and E. C. W. Lou, "Digitisation of existing buildings to support building assessment schemes: viability of automated sustainability-led design scan-to-BIM process," *Architectural Engineering and Design Management*, vol. 16, no. 2, pp. 84–99, Mar. 2020, doi: 10.1080/17452007.2019.1674126.
- [7] Z. Ding, S. Liu, L. Liao, and L. Zhang, "A digital construction framework integrating building information modeling and reverse engineering technologies for renovation projects," *Automation in Construction*, vol. 102, pp. 45–58, Jun. 2019, doi: 10.1016/j.autcon.2019.02.012.
- [8] B. Bortoluzzi, I. Efremov, C. Medina, D. Sobieraj, and J. J. McArthur, "Automating the creation of building information models for existing buildings," *Automation in Construction*, vol. 105, p. 102838, Sep. 2019, doi: 10.1016/j.autcon.2019.102838.

- [9] X. Xiong, A. Adan, B. Akinci, and D. Huber, "Automatic creation of semantically rich 3D building models from laser scanner data," *Automation in Construction*, vol. 31, pp. 325–337, May 2013, doi: 10.1016/j.autcon.2012.10.006.
- [10] P. Doshi, "The Ultimate Guide to Scan to BIM." <https://www.united-bim.com/ultimate-guide-of-scan-to-bim/> (accessed Oct. 16, 2021).
- [11] I. Skrzypczak, G. Oleniacz, A. Leśniak, K. Zima, M. Mrówczyńska, and J. K. Kazak, "Scan-to-BIM method in construction: assessment of the 3D buildings model accuracy in terms inventory measurements," *Building Research & Information*, pp. 1–22, Jan. 2022, doi: 10.1080/09613218.2021.2011703.
- [12] C. Wang, Y. K. Cho, and C. Kim, "Automatic BIM component extraction from point clouds of existing buildings for sustainability applications," *Automation in Construction*, vol. 56, pp. 1–13, Aug. 2015, doi: 10.1016/j.autcon.2015.04.001.
- [13] L. Sanhudo et al., "A framework for in-situ geometric data acquisition using laser scanning for BIM modelling," *Journal of Building Engineering*, vol. 28, p. 101073, Mar. 2020, doi: 10.1016/j.jobe.2019.101073.
- [14] F. Banfi, R. Brumana, G. Salvalai, and M. Previtali, "Digital Twin and Cloud BIM-XR Platform Development: From Scan-to-BIM-to-DT Process to a 4D Multi-User Live App to Improve Building Comfort, Efficiency and Costs," *Energies*, vol. 15, no. 12, Art. no. 12, Jan. 2022, doi: 10.3390/en15124497.
- [15] G. Rocha and L. Mateus, "A Survey of Scan-to-BIM Practices in the AEC Industry—A Quantitative Analysis," *ISPRS International Journal of Geo-Information*, vol. 10, no. 8, Art. no. 8, Aug. 2021, doi: 10.3390/ijgi10080564.
- [16] N. A. Haron, A. Hizami, and T. H. Law, "Investigating Approaches of Integrating BIM, IoT, and Facility Management for Renovating Existing Buildings: A Review," *Sustainability*, vol. 13, no. 7, p. 3930, 2021, doi: 10.3390/su13073930.
- [17] J. Liu, D. Xu, J. Hyppa, and Y. Liang, "A Survey of Applications with Combined BIM and 3D Laser Scanning in the Life Cycle of Buildings," *IEEE Journal of Selected Topics in Applied Earth Observations and Remote Sensing*, vol. 14, pp. 5627–5637, 2021, doi: 10.1109/JSTARS.2021.3068796.
- [18] G. Antova and V. Tanev, "Creation of 3D Geometry in Scan-to-CAD/BIM Environment," *IOP Conf. Ser.: Earth Environ. Sci.*, vol. 609, p. 012085, Dec. 2020, doi: 10.1088/1755-1315/609/1/012085.
- [19] G. Bartoli et al., "From TLS data to FE model: a workflow for studying the dynamic behavior of the Pulpit by Giovanni Pisano in Pistoia (Italy)," *Procedia Structural Integrity*, vol. 29, pp. 55–62, Jan. 2020, doi: 10.1016/j.prostr.2020.11.139.
- [20] S. S. Bastem and A. Cekmis, "Development of historic building information modelling: a systematic literature review," *Building Research & Information*, vol. 50, no. 5, pp. 527–558, Jul. 2022, doi: 10.1080/09613218.2021.1983754.
- [21] R. Hellmuth, "Update approaches and methods for digital building models – literature review," *ITcon*, vol. 27, pp. 191–222, Feb. 2022, doi: 10.36680/j.itcon.2022.010.
- [22] M. Honic, I. Kovacic, I. Gilmudinov, and M. Wimmer, "Scan to BIM for the Semi-Automated Generation of a Material Passport for an Existing Building," 2020, p. 346. doi: 10.46421/2706-6568.37.2020.paper024.
- [23] M. A. Hossain and J. K. W. Yeoh, "BIM for Existing Buildings: Potential Opportunities and Barriers," *IOP Conf. Ser.: Mater. Sci. Eng.*, vol. 371, p. 012051, Jun. 2018, doi: 10.1088/1757-899X/371/1/012051.
- [24] "GSA_BIM_Guide_Series_03.pdf." Accessed: Aug. 27, 2022. [Online]. Available: https://www.gsa.gov/cdnstatic/GSA_BIM_Guide_Series_03.pdf
- [25] R. Merckx, "The utilisation of aerial photography and laser scanning in BIM modelling," 2020. <http://www.theseus.fi/handle/10024/340528> (accessed Aug. 20, 2022).
- [26] M. Bassier, M. Vergauwen, and B. Van Genechten, "Automated Semantic Labelling of 3D Vector Models for Scan-to-BIM," in *Proceedings of the 4th Annual International Conference on Architecture and Civil Engineering (ACE2016)*, 20160425, pp. 93–100. doi: 10.5176/2301-394X_ACE16.83.
- [27] J. Park et al., "Deep Learning-Based Automation of Scan-to-BIM with Modeling Objects from Occluded Point Clouds," *Journal of Management in Engineering*, vol. 38, no. 4, p. 04022025, Jul. 2022, doi: 10.1061/(ASCE)ME.1943-5479.0001055.
- [28] M. E. Esfahani, C. Rausch, M. M. Sharif, Q. Chen, C. Haas, and B. T. Adey, "Quantitative investigation on the accuracy and precision of Scan-to-BIM under different modelling scenarios," *Automation in Construction*, vol. 126, p. 103686, Jun. 2021, doi: 10.1016/j.autcon.2021.103686.
- [29] T. Czerniawski and F. Leite, "Automated digital modeling of existing buildings: A review of visual object recognition methods," *Automation in Construction*, vol. 113, p. 103131, May 2020, doi: 10.1016/j.autcon.2020.103131.

Demonstration of LiDAR on Accurate Surface Damage Measurement: A Case of Transportation Infrastructure

Nikunj Dhanani¹, Vignesh V P², Senthilkumar Venkatachalam³

^{1,2,3}Department of Civil Engineering, Indian Institute of Technology, Palakkad - 678623, India
¹102013002@smail.iitpkd.ac.in, ²102214002@smail.iitpkd.ac.in, ³senthil@iitpkd.ac.in

Abstract

Accurate damage measurements of the transport infrastructure facilities during their maintenance/service life are characterized by their higher cost, safety hazards, historical data loss etc. Conventional techniques such as active sensing equipment and manual visual inspection have limitations on their longevity and sustainability. To overcome this, many non-contact measurement technologies such as photogrammetric techniques, LiDAR etc., are demonstrated in various measurement-related applications. However, measurement accuracy in these photogrammetric techniques is affected by many external factors, which discourage their wider usage as preferable measurement techniques. Many of these factors cannot be controlled by the surveyor/operator on the ground, but the scanner location plays a significant role in the accuracy of the collected point cloud data. Also, there exist minimal guidelines on the scanner placement with respect to the accuracy of measurements. Hence, there is a need for a guiding method to appropriately place the LiDAR towards achieving the targeted accuracy level. With this background, the study developed mathematical equations to understand the variation of point cloud density with respect to the location of LiDAR from the target surface. An interaction diagram is developed to accurately predict the effective scan area, with anticipated point cloud density/point spacing. A non-contact LiDAR-based measurement framework has been developed as part of this research. However, this paper only has the scope to elaborate on the evaluation of the developed framework's accuracy through a case study on an old bridge structure with surface damage. The study was carried out on a straight and curved surface of the piers by placing the LiDAR at appropriate guiding locations from the target surfaces, with varying orientations to the scan surface. Upon post-processing the collected point cloud data, it is concluded that the proposed scan area planning framework using LiDAR can detect surface damages as little as 3mm on the highway bridge components accurately.

Keywords – LiDAR; Scan area planning; Surface damage assessment.

1 Introduction

Damages due to environmental and human factors are inevitable to any structural component that causes distress to the whole structural system. According to a report by Indian Bridge Management System (IBMS), more than 137 bridges were classified as distressed, which emphasizes the importance of timely maintenance and early damage detection intervention to extend the life and serviceability of the structural system [1,2]. Traditionally, periodic monitoring of the bridge is done by employing conventional diagnostic methods which include the active strain gauge or through the inspector's visit. Relatively, all the above-mentioned distressed bridge structures are constructed a long time ago, the effectiveness of the active devices on the bridge members is not capturing the damages and hence the inspectors visit the site periodically and perform visual inspections. Based on the inspector's subjective assessment of damages, various Non-Destructive Tests (NDT) such as the ultrasonic pulse velocity test, rebound hammer test, penetration method, and many other tests are performed [3]. Despite high accuracy, these methods require the deployment of costly special types of equipment, such as an 'under-bridge inspection truck' to access the damages. Due to this reason, the assessment is performed only on the critically damaged areas instead in an exhaustive, periodic, and proactive manner. In addition, it is a challenge to inspect and measure the progressive damages in the same area over a period of time, as there are no accurate historical data to compare with, but the subjective assessment statements by the experts. Therefore, employing a digitalised non-contact proactive monitoring method may overcome the limitations associated with these traditional inspection-based assessments and monitoring [4,5].

Evidently, Digital imaging and Three-dimensional (3D) laser scanning or otherwise LiDAR is considered as most effective non-contact measurement technologies for rapid and precise detection of preliminary structure damages [6]. In both Photogrammetry and LiDAR, the structure is captured as a 3D point cloud data, which is

generally defined in a cartesian coordinate system (X, Y, and Z) along with RGB colour values. Image-based acquisition of 3D point clouds using robotic equipment such as UAVs/drones has created vast new prospects for rapid and detailed 3D point cloud generation. These point cloud data are then utilized for structural damage detection through Multiview-Stereo (MVS), Structure-from-Motion (SfM) and other photogrammetry-based algorithms [7,8,9]. However, in the case of photogrammetry, for large-scale structures such as bridges, the image quality is influenced by many factors such as the surrounding environmental conditions, distortion, etc., and it is time-consuming [10]. But the deployment of 3D laser scanning technology shows advantages in terms of processing time and data quality [11]. LiDAR technology is demonstrated to monitor large-scale non-moving structures such as bridges, tunnels, etc., on a temporal basis [12], however, its wider application has not been realized due to many reasons. It collects data over time to detect structural changes due to events like seasonal variations, accidental impact, and natural calamities such as earthquakes, landslides, heavy rain, etc. The laser scanner units are primarily classified based on their data-capturing modes, such as aerial, mobile, and terrestrial. Although each of these LiDAR data collection methods has its own advantages and limitations, the terrestrial is more common and widely adopted in collecting data on structures and their components such as cracks and deformations over a period of time [13].

As seen in Figure 1, Terrestrial Laser Scanner (TLS) scans the surface by locating millions of points in vertical parallel lines. It rotates by an angle $\Delta\theta$ along a horizontal plane to cover the vendor-specified scan area along the plane and, then it rotates along the vertical plane by an incremental angle of $\Delta\theta$ to cover the specified coverage range. The distance covered by rotating the angles $\Delta\theta$ and $\Delta\theta$ is known as interpoint spacing which is denoted by a_h and a_v as shown in Figure 1. In order to detect structural damages on a millimetre scale, it is necessary to obtain interpoint spacing of the point cloud in a similar range. The interpoint spacing variations depend on many factors such as point cloud density, target surface distance from the scanner location, scan resolution, atmospheric conditions, object surface properties, scanning geometry, instrument mechanism etc., [14]. Among these factors, the scanner position and orientation are the only factors that can be controlled by the operator in the field.

Further, the scanning geometry is significantly influenced by the distance and orientation of the scanned surface concerning the scanner position, 'D' in Figure 1(A). Therefore, the location of the scanner plays a significant role in the point cloud density. Therefore, the

main aim of this study is to obtain a sufficiently denser point cloud, to detect surface damages of desired accuracy with an appropriate scanner location from the scan target surface. The proposed-scan area planning task in this study is divided into two steps. The first step is the determination of the Field of View (FOV) calculation from a particular TLS location. Second, the calculation of interpoint spacing variation within the estimated FOV. In this regard, Anil et al. [15] conducted several lab experiments to identify the limits of laser scanners for damage assessment of reinforced concrete buildings. Also, Anil et al. demonstrated their study using vendor-provided post-processing tools and guidelines. In a related context, Chen et al. [16] and Frasc et al. [17] developed a 2-D model-based scan planning approach to estimate the horizontal FOV of an existing building using vendor-provided post-processing tools. Furthermore, Biswasa et al. [18] and Wakisaka et al. [19] developed a 3-D model-based scan planning approach to estimate the horizontal as well as vertical FOV of a structure.

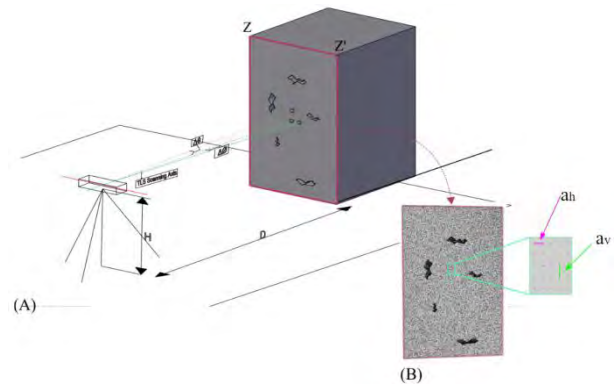


Figure 1: (A) Scanning of pier front side ZZ' using TLS. (B) Scanned point cloud of side ZZ'

From the literature, it is evident that most of the previous studies were primarily focused on FOV determination without much emphasis on the accuracy of the collected data. However, to accurately capture minor damages on the surface of the structural components, it is necessary to have the appropriate interpoint spacing in the collected point cloud data. In addition to this, most of these past studies have validated the developed FOV approach in a lab environment. Thus, in this paper authors attempted to validate the developed framework through a field experiment to ascertain the accuracy of the proposed framework. The research adopted three steps procedures viz. 1) Development of the scanning FOV framework through mathematical equations and guiding interaction diagrams to the field operators. 2) An experiment in a controlled/lab environment. 3) A field experiment to validate the developed framework. Since the first two steps of this research were published in a

previous article [20] and due to the limitations on the length of the manuscript, the explanation of the same is not included within the scope of this paper. The readers are strongly recommended to refer to the article in case more explanation is needed to understand the first two steps adopted in this research. The paper is organized as follows. The following section discusses the brief about the first two steps of the developed scan area planning framework for surface damage assessment. Section 3 outlines the methodology adopted for conducting the field experiment. Further sections describe the details of the case study and the experiment. The manuscript ends with the inferences from the obtained results, discussions, and conclusions.

2 Development of framework and Validation in a Controlled Environment

The interpoint spacings (a_h , a_v) increment depends upon the length of the scan plane from the scanning axis (i.e. L_x , L_z), scanner's horizontal and vertical angular increment capability (i.e., $\Delta\theta$, $\Delta\phi$), and its distance from the surface (D) as depicted in Figure 2.

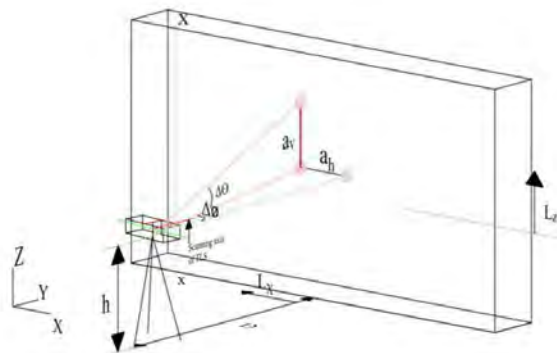


Figure 2. Scanning the surface perpendicular to the scanning axis of the TLS

The following equations are derived for a straight scanning surface perpendicular to the scanning axis using a simple trigonometrical relationship,

$$L_{x'} = [(\tan(\tan^{-1}(L_x/D) + \Delta\theta)) \times D] \dots\dots\dots (1)$$

$$a_h = (L_{x'} - L_x) \dots\dots\dots (2)$$

$$R = \sqrt{(L_{x'})^2 + D^2} \dots\dots\dots (3)$$

$$a_v = [(\tan(\tan^{-1}(L_z/R) + \Delta\phi)) \times R] - L_z \dots\dots\dots (4)$$

Similarly, a total of 19 mathematical equations are formulated for scanning the straight and curved surfaces by locating TLS parallel and perpendicular to them. Also, the interaction diagrams as shown in Figures 3 and 4 for all the above-mentioned combinations are also generated to guide the surveyor/operator in fixing the FOV and for

identifying the appropriate scanner location to obtain the required interpoint spacing.

From the graphs in Figures 3 and 4, it has been inferred that the TLS can be located anywhere between 3m to 10m from the target surface to cover a scanning area of 5.4m x 4.9m ($L_x \times L_z$) with a interpoint spacing as little as 2mm.

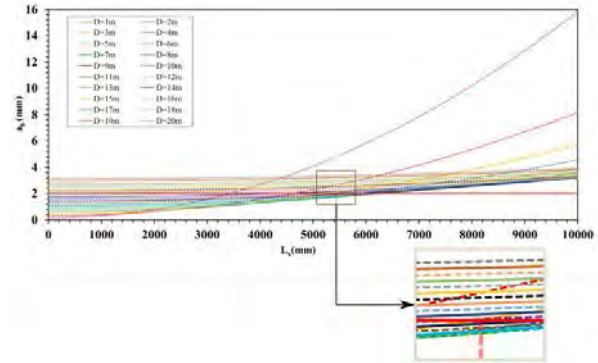


Figure 3. Variation of interpoint spacing a_h along the horizontal length (L_x) with different TLS distance (D) at 0.009° TLS incremental angle ($\Delta\theta$)

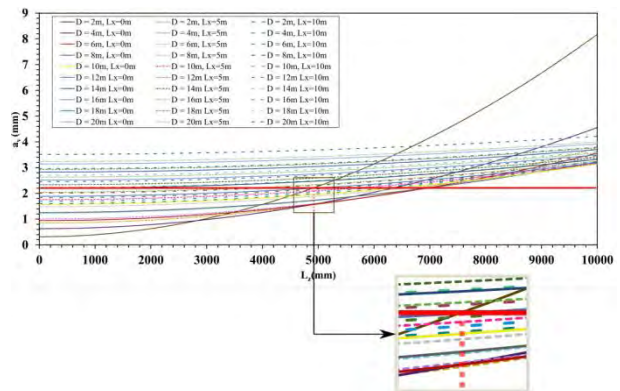


Figure 4. Variation of inter-point spacing a_v along the vertical length (L_z) with different TLS distance (D) at 0.009° TLS incremental angle ($\Delta\theta$)

For validating the developed Scan Area Planning framework, experiments were conducted in a controlled/lab environment. Using interactive graphs, it was found that for a scan perpendicular to the target surface, to cover an area of about 5.4m x 4.9m ($L_x \times L_z$), the TLS shall be placed anywhere between 3m to 10m from the scanning surface. Average interpoint spacing differs by approximately 0.04mm from the measured value from the experiment and the predicted value based on the formula developed. Similarly, for other cases also, with the help of interactive graphs, the scan area and location of TLS can be predicted for aimed accuracy. The obtained results' accuracy motivated the authors to experiment with the same in a real-world setup, with all the other external factors.

3 Field Experiment Methodology

After the controlled environment experiments, the field experiment location was identified. The authors visited many bridge sites in and around the institute and with the help of a local public works organization identified the Velanthavalam bridge site shown in Figure 5.

This bridge was constructed in 1986 over a river (Kumittipathi). It was located on the border connecting two states (Kerala and Tamil Nadu) in India. The bridge has round-nosed rectangle piers. Therefore, it is possible to demonstrate the framework's accuracy on both vertical straight and curved surfaces of planned scan area exercises. In addition, the bridge is accessible from most of the sides and has identifiable surface damages of varying sizes (many cracks of varying sizes on the straight and curved surfaces). Hence this site was selected to validate the crack detection accuracy for various distances of scanner locations from the surface.



Figure 5. Velanthavalam bridge site

For this field experiment, TLS specifications with horizontal and vertical angle increment of 0.009° and specifications of, range 0.6m to 350m, Field of view (horizontal/vertical): $360^\circ / 300^\circ$, Min angular increment (horizontal/vertical): $0.009^\circ / 0.009^\circ$, Laser wavelength: 1550nm and Measurement speed (pts/sec): 976,000 was used. The same scanner was also used for the controlled experiments. The field experiment has the below objectives.

1. To predict the distance and orientation of the scanner from the damaged surface using the proposed framework, which includes the TLS location calculated using the developed mathematical equation and interactive graphs.
2. To validate the interpoint spacing and measurement accuracy using the collected point cloud data of the vertical straight and curved surfaces of the damaged bridge pier.

The unit of analysis for this validation exercise is the crack width, length, etc., obtained from the point cloud data. The data collection includes scanning the vertical

straight and curved surfaces while locating the scanner perpendicular to the damaged surface.

Based on the interaction diagram developed from the developed mathematical equations, it is suggested to place the scanner between 2 to 8 m distances to obtain an accuracy of more than 3 mm. The horizontal and vertical angle increment is assumed to be set as 0.009° during the experiment.

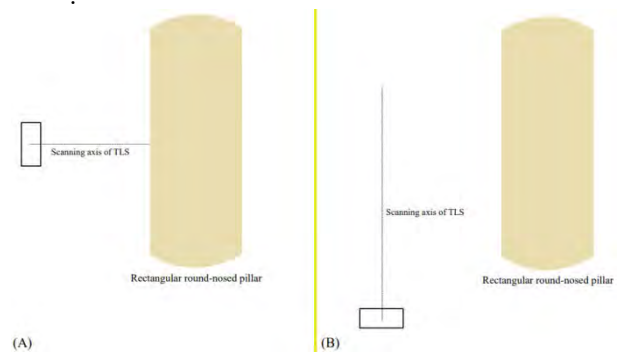


Figure 6. (A) TLS positioned perpendicular to the surface. (B) TLS positioned parallel to the surface

4 Validation of the scan area planning on Vertical Straight surfaces

Depending on accessibility, there were two possible locations for TLS placement towards scanning the pier's vertical straight surfaces. If the scanning surface is accessible, the scanner can be placed perpendicular to it (Figure 6 (A)). If not, it needs to be placed parallel to the surface (Figure 6 (B)).

As shown in Figure 7, the scanning is performed by placing the TLS at a 5m distance from the damaged surface. To validate the variation of the interpoint spacing, the value of a_h and a_v are measured at various points in the damaged surface (i.e., mentioned as A, B, C etc. in Fig. 7) along the horizontal and vertical axis (L_x and L_z).

The interpoint spacing values calculated from the mathematical equations (C_v) and the measured interpoint spacing values (M_v) from the post-processing software are tabulated in Table 1. The difference between them is noticed in the range of 0.1 to 0.2 mm.

To validate the accuracy on measuring various damages, a comparison analysis is carried out in which each damage is measured using a vernier scale as shown in Fig. 8 and scanned point cloud data of the crack width and length. Table 2 compares the crack width value measured using the Vernier scale and the crack width value measured using scanned point cloud data.

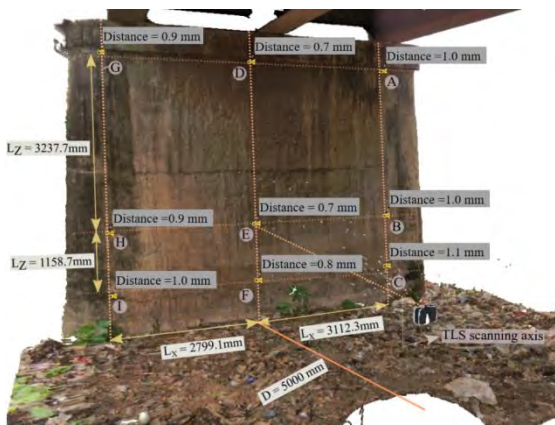


Figure 7 Measurement of point cloud spacing a_h , a_v along L_x & L_z

Similarly, the verification exercise is carried out for the scanner placed along the parallel plane of the scan axis. The same steps which are explained in the previous experiment, scanner placement on perpendicular to the scan surface are followed. Firstly, the value of a_h and a_v is measured at different sections along the length L_y and L_z (see Figure 9). Subsequently, a comparison table is prepared (see Table 1). Here also, the maximum difference between calculated (C_v) and measured values (M_v) of interpoint spacing was noticed in the range of 0.1mm to 0.2mm. Similarly, the crack width was measured using the post-processing tool and the Vernier scale (see Table 2), and the accuracy attained was around 2 mm which is better than, the targeted accuracy set before the field experiment (i.e., 3 to 5mm).



Figure 8. (A) Scanned cracks using TLS
(B) Measurement of crack 1 using Vernier scale



Figure 9 Measurement of point cloud spacing a_h , a_v along L_y & L_z

Table 1 Comparison of Interpoint Spacing in Field Environment

Interpoint Spacing Value on a Plane Perpendicular to the Scanning Axis of TLS							Interpoint Spacing Value on a Plane Parallel to the Scanning Axis of TLS					
a_h along lengths L_x and L_z				a_v along lengths L_x and L_z			a_h along lengths L_y and L_z			a_v along lengths L_y and L_z		
S_N	M_V	C_V	D_F	M_V	C_V	D_F	M_V	C_V	D_F	M_V	C_V	D_F
A	1	1.1047	0.1047	1.2	1.2192	0.0192	0.9	0.7854	0.1146	1.2	1.1131	0.0869
B	1	1.1047	0.1047	0.9	0.9456	0.0456	0.9	0.7854	0.1146	0.8	0.7568	0.0432
C	1.1	1.1047	0.0047	0.9	0.9807	0.0807	1	0.7854	0.2146	0.8	0.7435	0.0565
D	0.7	0.8091	0.1091	1.2	1.129	0.071	1.6	1.5141	0.0859	1.3	1.271	0.029
E	0.7	0.8091	0.1091	0.8	0.8094	0.0094	1.5	1.5141	0.0141	1.2	1.0145	0.1855
F	0.8	0.8091	0.0091	0.9	0.8504	0.0496	1.6	1.5141	0.0859	1.1	1.0048	0.0952
G	0.9	1.1048	0.2048	1.3	1.2019	0.0981	3.1	3.0996	0.0004	1.7	1.6019	0.0981
H	0.9	1.1048	0.2048	0.9	0.9211	0.0211	3.1	3.0996	0.0004	1.6	1.4227	0.1773
I	1	1.1048	0.1048	0.9	0.9571	0.0571	3.2	3.0996	0.1004	1.6	1.4161	0.1839

Note: S_N , M_V , C_V , D_F - Name of intersection points, Measured value, Calculated value, and their Difference respectively. All the values are in mm

Table 2 Accuracy comparison of crack width

S _N	TLS perpendicular to the surface		TLS parallel to the surface	
	W _{PCD}	W _{VS}	W _{PCD}	W _{VS}
Crack 1	23.3	24	22.3	24
Crack 2	55.6	55	55.2	55
Crack 3	36.7	35	35.2	35

Note: S_N, W_{PCD}, and W_{VS} – The name of cracks, measured of crack width using scanned point cloud and using Vernier scale respectively. All values are in mm

5 Validation of the scan area planning on Curved surfaces

From the earlier study [20] it was found that TLS can cover at least 90° of Pier 1’s FOV (Visible quarter) and 45° of Pier 2’s FOV as shown in Fig. 10 and 11. A similar FOV behavior is observed when scanning the curved portions of the piers at a distance of 3m perpendicular to the surface (see Figure 10).

As shown in Figure 11, the circular surface of the Pier is having varying diameters. Therefore, two sections (Section 1 at the bottom and Section 2 at the top) are selected to validate interpoint spacing variation behavior. At each section, the interpoint spacing value is checked at two locations (represented in blue and orange lines respectively in Fig.11). In Table 3, a comparison is made between the measured (M_V) and calculated values (C_V) at multiple locations and sections.

From the experiment, it was found that in Pier 1, some minor cracks were found, and its sizes range in mm. According to the developed model, if the scanner was placed 3m away, it would be able to detect cracks up to 1mm around the 0° location of the 1st pier. As seen in Figure 12, all minor cracks are captured accurately, and also the width captured by the TLS point cloud is compared with the Vernier scale measurement (Table 4). It is noticed that the difference between the calculated (W_{PCD}) and measured (W_{VS}) is in a fraction of a mm.



Figure 10: Scan coverage area while locating TLS perpendicular to the first pier

Table 3 Comparison of interpoint spacing a_h at different sections of Pier 1 & 2

	S _N	N _L	M _V	C _V	D _F
Pier 1	Section 1	0° Location	0.4986	0.4953	0.0032
		90° Location	1.7111	1.8954	0.1843
	Section 2	0° Location	0.5511	0.4953	0.0557
		90° Location	2.4125	2.9681	0.5557
Pier 2	Section 1	0° Location	2.6032	2.5433	0.06
		90° Location	13.754	14.3866	0.6326
	Section 2	0° Location	2.677	2.5759	0.1011
		90° Location	13.574	13.6395	0.0655

Note: S_N, N_L, M_V, C_V and D_F -The sections name, location name, measured value, calculated value and Difference between two points respectively. All values are in mm



Figure 11. Measurement of point cloud interpoint spacing a_h, at each location of the pier section

Table 4 Accuracy comparison of crack width measured at Section 2 of Pier 1 (Fig. 11 and 12)

S _N	W _{PCD}	W _{VS}
Crack 1	2.7	3
Crack 2	2.9	3
Crack 3	34.6	33.3

Note:

S_N, W_{PCD}, and W_{VS} – the name of cracks, measured crack width using scanned point cloud and using Vernier scale respectively. All values are in mm

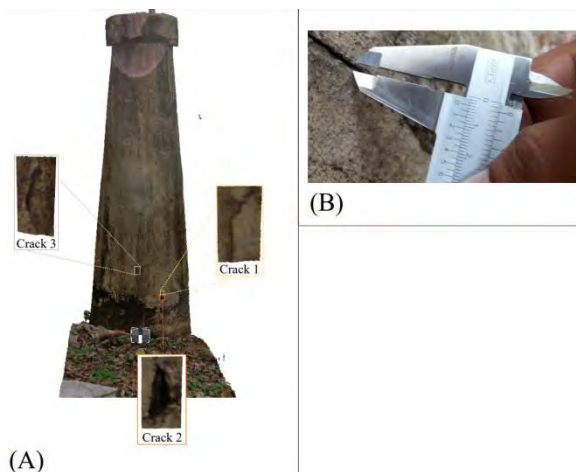


Figure 12 (A) Scanned cracks using TLS (B) Measurement of crack 1 using Vernier scale

6 Discussions

The point cloud interpoint spacing variations between the measured and calculated values in this experiment ranges between 0.0004mm to 1.7mm. The maximum variation occurs while locating TLS parallel to the surface at a 2m distance. It is advisable to keep the TLS as close and perpendicular as to the cracks. The height of the TLS can be limited between 1.2m to 1.6m for better ergonomic operations. The field experiment conducted during this study, chose a conducive external environment such as light, accessibility, etc., however, collecting data during less visibility and adverse weather conditions may reduce the data and measurement accuracy. Further, the study was conducted when there was no water in the causeway, however, the water in the causeway may affect the data collection about the submerged surfaces. The existing deformities and irregular geometrics have not been considered in this study. However, the same becomes insignificant when the temporal variations on the surface damages are assessed. The study may also demand fixing standard station points to obtain the data temporally over a period of time regularly. Furthermore, this study did not consider any economic or time benefit analysis, future experiments may include the same in order to compare with the conventional methods over the LiDAR-based technologies for their benefits.

7 Summary and Conclusions

This study developed a Scan Area Planning framework to collect point cloud data with the desired level of accuracy in identifying surface damages. The study aims to accurately collect minor structural damages using LiDAR technology. This paper summarizes the significant role of scanner location in obtaining point

cloud data with the desired level of accuracy. The developed mathematical equations and generated interaction diagrams can be utilized as a guiding ready reckoner for the field surveyors/operators to fix the scanner location and orientation for collecting the appropriately suitable and accurate point cloud data. This paper further demonstrated validation methodology for the developed framework (reported in the previous study [20]) and concluded that the location and orientation of the scanner to the target surface itself could be controlled to obtain accurate surface damage measurement using the LiDAR point cloud. The experiments were aimed to capture the surface damages ranging from 3mm to 5mm. Nevertheless, the validation results indicate that around 1mm cracks were also captured using the developed models. The study has some limitations as the accuracy hasn't been checked with varying scanner positions and longer-range distances from the target surface. The interaction diagram was developed only up to 20m distance from the target in this study. Further, working under extreme weather conditions and temporal variations are not captured to claim the applicability with a wider scope. However, the authors are of the opinion to obtain similar results and are willing to experiment with the same in the near future. Collecting and storing this accurately measured point cloud data during the life cycle of the structural members may lead to capturing the progressive damages that the structural members may undergo and warrant a timely retrofitting which may increase and improve the life span and serviceability of the infrastructure facility.

Acknowledgement

The authors would like to acknowledge KHRI and Kerala PWD for their support to access the bridge site and funding for this research work.

References

- [1] N. De Belie and E. Gruyaert, HEALCON-Conference-Self-Healing Concrete for Prolonged Lifetime, Delft, Nederland, 2016, pp. 1–5.
- [2] Joshi, S. and Raju, S.S., 2018. Indian Bridge Management System-Overview and Way Forward. Maintenance, Safety, Risk, Management and Life-Cycle Performance of Bridges, pp.205-205.
- [3] E. Niederleithinger, S. Gardner, T. Kind, R. Kaiser, M. Grunwald, G. Yang, B. Redmer, A. Waske, F. Mielentz, U. Effner et al., arXiv preprint arXiv:2008.07251, 2020.
- [4] J. Thomas, A. Kareem and K. W. Bowyer, IEEE Transactions on geoscience and remote sensing, 2013, 52, 3851–3861.
- [5] M. Abdo, A review book. Open Science, 2014.

- [6] Truong-Hong, L., Falter, H., Lennon, D. and Laefer, D.F., 2016, January. Framework for bridge inspection with laser scanning. In EASEC-14 Structural Engineering and Construction, Ho Chi Minh City, Vietnam, 6-8 January 2016.
- [7] S. Ullman, Proceedings of the Royal Society of London. Series B. Biological Sciences, 1979, 203, 405–426.
- [8] A. Alfonso-Torreño, Á. Gómez-Gutiérrez, S. Schnabel, J. F. L. Contador, J. J. de Sanjosé Blasco and M. S. Fernández, Science of the Total Environment, 2019, 678, 369–382.
- [9] D. Giordan, Y. Hayakawa, F. Nex, F. Remondino and P. Tarolli, Natural hazards and earth system sciences, 2018, 18, 1079–1096.
- [10] C. Axel and J. A. van Aardt, Journal of Applied Remote Sensing, 2017, 11, 046024.
- [11] D. Skarlatos and S. Kiparissi, 2012.
- [12] S.-E. Chen, Laser Scanner Technology, 2012, 71.
- [13] B. Riveiro, M. DeJong and B. Conde, Automation in Construction, 2016, 72, 258–268.
- [14] S. Soudarissanane, R. Lindenbergh, M. Menenti and P. Teunissen, Proceedings ISPRS Workshop Laserscanning 2009,1-2 Sept 2009, Paris, France, Paris, France, 2009, pp. Vol. XXXVII, Part 3/W8.
- [15] E. B. Anil, B. Akinici, J. H. Garrett and O. Kurc, ISARC. Proceedings of the International Symposium on Automation and Robotics in Construction, Montreal, Canada, 2013.
- [16] M. Chen, E. Koc, Z. Shi and L. Soibelman, Automation in Construction, 2018, 93, 165–177.
- [17] E. Frías, L. Díaz-Vilariño, J. Balado and H. Lorenzo, Remote Sensing, 2019, 11, 1963.
- [18] H. K. Biswasa, F. Boschéa and M. Suna, Symposium on Automation and Robotics in Construction and Mining (ISARC 2015), Waterloo, Canada, 2015.
- [19] E. Wakisaka, S. Kanai and H. Date, ISARC. Proceedings of the International Symposium on Automation and Robotics in Construction, Waterloo, Canada, 2019.
- [20] N. Dhanani and S. Venkatachalam, CIB - Conference-Smart Built Environment, Dubai, United Arab Emirates, 2021, pp. 101–110

DeepGPR: Learning to Identify Moisture Defects in Building Envelope Assemblies from Ground Penetrating Radar

Bilal Sher and Chen Feng

Tandon School of Engineering, New York University, USA

bas9876@nyu.edu, cfeng@nyu.edu

Abstract -

Conventionally used moisture detection equipment such as infrared scanners and capacitance meters require a trained interpreter to understand moisture issues on rooftops. Additionally, conventional sensors can only provide reliable results in specific environmental conditions. In this paper, we will discuss the various methods used for roof moisture scans and their limitations. We will then provide an in-depth analysis of GPR paired with deep segmentation neural networks for roof moisture scans, including its advantages, limitations, and potential applications. We will also present a case study demonstrating the effectiveness of this approach in detecting moisture damage in a real-world scenario. Our preliminary experiments find that deep neural networks are effective in segmenting GPR radargrams and finding moisture, with particular neural networks more effective than others.

Keywords -

Ground penetrating radar; moisture detection; building envelope analysis; rooftop moisture survey

1 Introduction

Roof moisture scans are essential for maintaining the structural integrity of buildings by identifying moisture damage to the roof. Traditional methods such as visual inspection, infrared thermography, nuclear moisture gauges, and capacitance meters have limitations that can affect the accuracy and reliability of results. However, Ground Penetrating Radar (GPR) paired with Artificial Intelligence (AI) has emerged as a promising solution for conducting roof moisture scans.

GPR is a non-destructive testing technique that uses electromagnetic waves to detect and image subsurface features of materials. The integration of GPR and AI enables a comprehensive and accurate assessment of moisture levels in the roof structure. GPR provides high-resolution imaging of the subsurface, while AI can process the data and identify patterns that may not be visible to the human eye. This combination allows for early detection of moisture damage, reducing repair costs and increasing the lifespan of the roof.

GPR technology captures data by measuring the dielec-

tric properties of materials, making it an effective tool for detecting moisture within building envelopes and roofs [1, 2]. The Proceq GP8800 SFCW handheld GPR sensor is a popular device for capturing GPR data, recording data at a fixed distance interval of 1 cm [3]. However, interpreting the data can be challenging, which has limited its widespread adoption [4].

To overcome this challenge, a deep segmentation neural network was tested to pair with GPR for moisture detection applications on building envelopes, particularly roof assemblies. The preliminary experiments found that deep neural networks are effective in segmenting GPR radargrams and finding moisture, with particular neural networks being more effective than others. By leveraging deep learning techniques, GPR can provide more accurate and reliable results in detecting moisture, enhancing its potential for building maintenance and inspection.

The potential benefits of GPR for detecting moisture issues on rooftops and building facades are significant. By identifying moisture issues early on, building owners and maintenance professionals can address them before they become costly problems. Additionally, GPR can help ensure the safety and longevity of structures by detecting potential structural issues caused by moisture. While more research is needed to fully realize the potential of GPR in this application, it is clear that the technology offers a valuable tool for enhancing building maintenance and inspection.

2 Related Works

Researchers have explored the use of artificial intelligence (AI) and neural networks in analyzing ground penetrating radar (GPR) scans. This has included using AI to assess moisture content in various materials, such as concrete and soil. One example is Kilic and Unluturk [5], which used a simple artificial neural network to analyze a GPR scan and classify it as wet or dry. Others, such as Zhang et al. [6], have used more advanced techniques, like Resnet and YoloV2, to draw bounding boxes around areas of suspected moisture. Researchers have also attempted to estimate soil moisture content using GPR scans, such as with Qiao et al. [7]'s radial basis function neural net-

work. Zheng et al. [8] improved on this method by using a convolutional neural network (CNN) connected to a fully connected layer to analyze soil moisture content. Other authors have used similar CNN and fully connected layer set-ups to find object representations within GPR scans [9, 10, 11, 12, 13]. Hou et al. [14] implemented a Mask R-CNN to segment hyperbolic signatures of rebar in GPR scans of a bridge deck. Our work improves upon these methods in a number of ways. First, it presents a new approach to simulating moisture in building envelope assemblies. Second, it tests various segmentation models equipped with a line scan conversion block to determine if a portion of the GPR scan is wet or dry. Finally, it adds five additional data channels for analysis, including a max-amplitude normalization channel, a time-gain channel, and three additional channels that are power spectral density images based on the raw GPR scan channel, the max amplitude normalized channel, and the time-gain channel.

3 Preparation and Data Collection

3.1 GPR Technology

GPR is a non-destructive testing technique that uses electromagnetic waves to detect and image subsurface features of materials. It works by measuring the dielectric properties of materials, making it an effective tool for detecting moisture within building envelopes and roofs, as the dielectric constant of water is much higher than other materials commonly used in construction [15, 16, 17, 18, 19]. The GPR technology can be captured using different methods, with impulse and stepped frequency continuous wave (SFCW) being the most common. In impulse GPR, a fixed frequency pulse is sent into a medium, and the reflected signal is detected [4]. SFCW GPR, on the other hand, sends a continuous signal with a modulated frequency into the medium and listens for the reflectances from various wavelengths. Some studies have shown that SFCW is the superior configuration for capturing data of smaller, shallow targets, which is particularly relevant in the structural and building analysis use case of GPR [20, 4].

3.2 Data Collection in Lab Setting

A novel testbed was created to test building assemblies with simulated moisture contents (See Figure 1). The base of the test bed had a 5/16" thick 4' x 8' standard-size OSB sheathing board. Moisture was simulated by placing moistened paper towels inside a plastic Ziploc bag on various portions of the test bed. The base of the test bed had a standard-size OSB sheathing board. Normal OSB moisture content can vary from 11.5% to 12.5% in New York City [21]. A base moisture content of 11.7% was assumed, and the amount of water needed to be added

to the paper towels was calculated accordingly. Due to size and spacing requirements on the test kit as well as the range of moisture content required to cause mold growth, the following breakdown in tests was chosen:

Due to size and spacing requirements on the test kit as well as the range of moisture content required to cause mold growth, the following breakdown in tests was chosen:

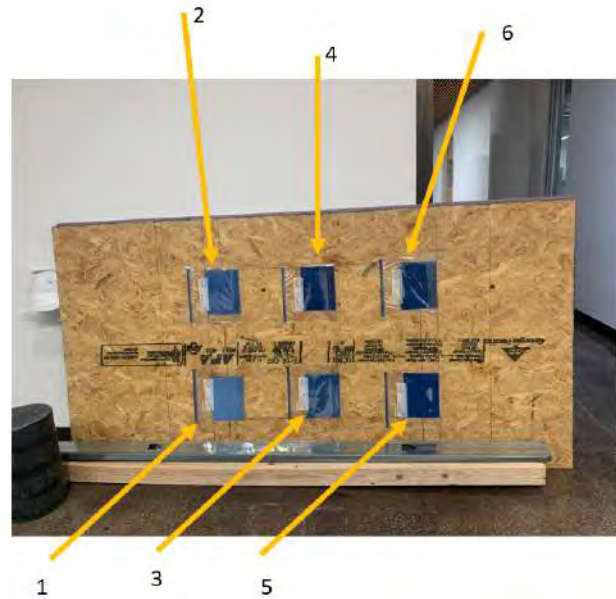


Figure 1. Moisture Testbed

Packet	1	2	3	4	5	6
MC (%)	11.7	18.7	25.8	32.8	39.8	46.8

Various building materials were added to create a dataset of GPR scans (See Figure 2). 48 different combinations of building material were captured, with each configuration producing 6 different scans. Each configuration produced 6 different scans making it equivalent to 288 different GPR scans conducted with varying moisture content and different superimposed building envelope materials. The building materials superimposed onto the testbed included:

1. $\frac{7}{16}$ in OSB sheet
2. 1in Rigid Foam Insulation
3. Timber 2 x 4 studs
4. Metal 2 x 4 studs
5. 8in x 4in x 2in clay masonry wall bricks
6. 4in x 16in x 8in hollow concrete blocks
7. R19 Batt Insulation

Thin materials like vapor barriers, air barriers, and waterproofing membranes were not included in the test as



Figure 2. Various testbed configurations

they don't affect GPR readings. The test simulated moisture condensing on both exterior and interior sides of a wall assembly, depending on the climate and time of year. Research from other authors confirms that moisture is not evenly distributed throughout a wall or roof assembly, and it is more concentrated at either the interior or exterior side of the assembly [22]. This test was also designed based on research that shows that moisture content at or above 19% will catalyze mold growth [23]. Figure 3 shows the testbed set up with layers of interior and exterior insulation to simulate an EIFS assembly. The test bed was simply supported over two tables, and the tables were placed at least 30 cm from the edges of the moisture areas to ensure that the table legs did not affect the GPR readings. Overall, the test bed provided a comprehensive dataset of GPR scans conducted with varying moisture content and different building envelope materials, which can help researchers and practitioners in developing effective moisture control strategies for building assemblies.



Figure 3. Testbed configuration for multiple layers of insulation

3.3 Pre-Processing of the Collected GPR Data

During the GPR testing process, data was collected by moving the Proceq GPR 8800 unit over the moist sections of the testbed, which were premarked to ensure ease of testing. As the wheel attached to the GPR unit moves, it records data. However, discontinuities may occur in the radargram when the unit gets caught on surfaces being scanned. To address this, scans were redone more

slowly when the unit was caught on a brick. In some cases, the GPR unit was raised slightly to allow it to clear obstacles such as slightly protruding bricks. The scans were recorded on the Proceq GPR Live app and uploaded to the Proceq servers, where they were exported as SEG-Y files. Different GPR manufacturers have different data exporting methods, but the benefit of using equipment that exports data in an SEG-Y format is that we can easily process it in Python through the SEG-Y-SAK python library. The Software Underground community routinely performs machine learning and deep learning on GPR-acquired datasets. The SEG-Y file is processed with the SEG-Y-SAK API to extract a numpy array of the raw, unfiltered GPR scan data. Each column in the numpy array represents a trace. This library is supported by the Software Underground community, which routinely performs machine learning and deep learning on GPR-acquired datasets.

$$\mathbf{G}_{i,j} = \begin{bmatrix} t_{r_{1,1}} & \cdots & t_{r_{1,n}} \\ \vdots & \ddots & \vdots \\ t_{r_{m,1}} & \cdots & t_{r_{m,n}} \end{bmatrix} = [\mathbf{T}_{r_1} \quad \cdots \quad \mathbf{T}_{r_n}] \quad (1)$$

The data obtained from the GPR was raw radargram data, which was then processed by maximum amplitude normalizing the data. This is a noise removal technique that is valid on flat/level surfaces or surfaces where the GPR unit is a constant distance from the surface being measured. Maximum amplitude trace normalization finds the average peak amplitude across all traces and scales each trace so that its maximum amplitude is now the average peak amplitude.

$$A_p = \frac{1}{n} \sum_{i=1}^n \max(\mathbf{T}_{r_i}) \quad (2)$$

$$\tilde{\mathbf{G}}_{i,j} = \begin{bmatrix} t_{r_{1,1}} \cdot \frac{A_p}{\max(\mathbf{T}_{r_1})} & \cdots & t_{r_{1,n}} \cdot \frac{A_p}{\max(\mathbf{T}_{r_n})} \\ \vdots & \ddots & \vdots \\ t_{r_{m,1}} \cdot \frac{A_p}{\max(\mathbf{T}_{r_1})} & \cdots & t_{r_{m,n}} \cdot \frac{A_p}{\max(\mathbf{T}_{r_n})} \end{bmatrix} \quad (3)$$

In addition to applying maximum amplitude trace normalization, a temporal signal gain was also applied to the images. There are many ways of applying a temporal signal gain, but the linear and exponential methods were used in the tests below. For linear signal gains, $\mathbf{G}n_{m \times n}^l$ later signals are enhanced by multiplying the traces with a linearly increasing gain vector that is the same length as the trace. For exponential signal gains, $\mathbf{G}n_{m \times n}^e$, the signal can be enhanced by multiplying the traces with an exponentially increasing gain vector.

$$Gn_{m \times n}^l = C \cdot \begin{bmatrix} 1 & \dots & 1 \\ \vdots & \ddots & \vdots \\ m & \dots & m \end{bmatrix} \quad (4)$$

$$\tilde{G}'_{i,j} = G_{i,j} \odot Gn_{m \times n}^l \quad (5)$$

$$Gn_{m \times n}^e = \begin{bmatrix} 1^c & \dots & 1^c \\ \vdots & \ddots & \vdots \\ m^c & \dots & m^c \end{bmatrix} \quad (6)$$

$$\tilde{G}'_{i,j} = G_{i,j} \odot Gn_{m \times n}^e \quad (7)$$

This resulted in 3 different GPR scans: the raw data scan $G_{i,j}$, the maximum amplitude trace normalized scan $\tilde{G}_{i,j}$, and the temporal signal gain scan $\tilde{G}'_{i,j}$. These were further enhanced by finding a power spectral density image associated with each scan. The power spectral density image was generated by finding the PSD of each individual trace and then concatenating them into a 2D image.

$$PSD(G_{i,j}, \tilde{G}_{i,j}, \tilde{G}'_{i,j}) = P_{i,j}, \tilde{P}_{i,j}, \tilde{P}'_{i,j} \quad (8)$$

There are other GPR scan normalization techniques that are not applicable to our current scanning data set and would not produce additional usable information. As a result, each GPR scan could be represented as a 6 channel tensor $I^{(m \times n \times 6)} = [G_{i,j}, \tilde{G}_{i,j}, \tilde{G}'_{i,j}, P_{i,j}, \tilde{P}_{i,j}, \tilde{P}'_{i,j}]$. This 6 channel tensor served as the input to the deep learning network. Data was annotated by denoting sections, i.e., multiple consecutive whole traces, of the radargram as being either moist or dry. The locations of the simulated moisture in the test bed was used as a guide because there were minor changes in the starting or ending position of the GPR scan from run to run. This was used to produce a 2D image mask, $M_{1 \times n}$, with a pixel height of 1 and a width that represented the distance the GPR moved.

4 GPR Segmentation by Deep Learning

Data augmentation is a technique used to increase the diversity of data in a dataset for training machine learning models. In this study, random horizontal flips and random resizing were used for data augmentation. Horizontal flipping had a 50% chance of occurring while resizing had a 75% chance of occurring. Resizing involved expanding or shrinking the horizontal portions of the scans by up to 40% compared to the original horizontal scan length. After resizing, the binary 0 or 1 representation of the masks would no longer hold, and any mask value above 0 was set to 1.

To ensure that the scans could be easily processed by deep learning segmentation algorithms, the height and width of the batches were fixed to 672 and 128, respectively. Scans were top-padded by copying the first row of

the input tensor. If the scan width was less than 128, scans were left-padded, and if the scan width was greater than 128, scans were left-cropped. The left padding was a copy of the leftmost trace.

Every segmentation model had a line scan conversion head at the end. This conversion head was a block consisting of a 2D convolutional layer with a 3x3 kernel and 1x1 padding, a 2D bilinear upsampling layer that brought the output size back up to the original input size followed by ReLU activation, and a 2D convolutional layer with a kernel of input height x 3 and padding applied width-wise, but not height-wise, and a channel reduction to 1.

A series of experiments were conducted to determine the optimal model for accurately segmenting a raw GPR scan. Various hyperparameters and model configurations were tested. The results of these tests will be used to guide future tests on data obtained from real-world field tests.

A number of hyperparameters were kept the same during all tests. Each individual input in the batch was standardized per channel using the following formula:

$$I_{std}^{(m \times n \times 6)} = \begin{bmatrix} \dots & \left[\frac{C_{**k} - \text{mean}(C_{**k})}{\text{std}(C_{**k})} \right] & \dots \end{bmatrix} \quad (9)$$

For all tests, the learning rate started off at 1e-4 and was reduced to 5e-5 after 125 epochs. All tests were run for 250 epochs.

Three metrics were used to evaluate the success of the model:

1. Intersection of Union
2. Dice Score
3. Pixel Accuracy (Accuracy)

IoU and dice score are crucial metrics for evaluating line scan segmentation algorithms, with IoU being the most important as this is a segmentation problem.

Deep Supervision: UNet is a widely used image segmentation model, with nearly 60,000 citations as of April 2023. [24] However, it struggles with segmenting fine details, which can represent a problem for GPR scans as they can contain finer details than typical images. To address this, Zhou et al created UNet++, which adds dense skip connections from higher and lower levels of the segmentation encoder and includes deep supervision. This helps to train earlier layers and ensure that finer details are detected. The effectiveness of UNet++ was tested to evaluate whether it can improve segmentation accuracy.

Encoder Type: Segmentation models have an encoder and decoder. The encoder converts data into a form that the decoder can process. VGG16 is the standard encoder for UNet and UNet++. Other encoder networks like ResNets and Inceptionv4 can be used instead of VGG16. Different

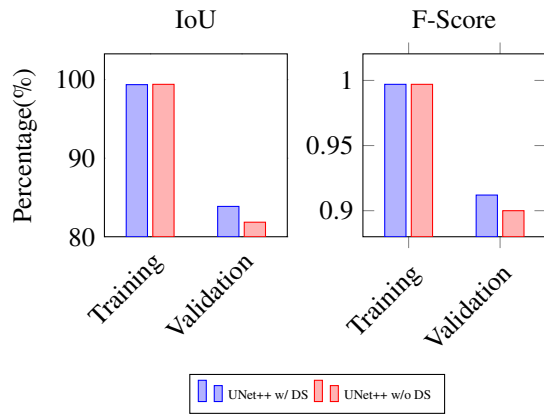


Figure 4. Effect of Deep Supervision on Model Accuracy

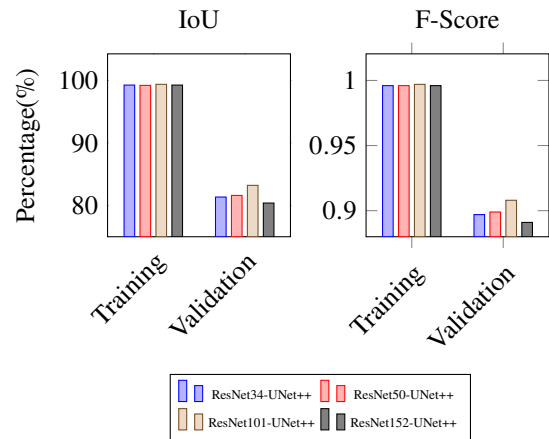


Figure 6. Effect of Encoder Depth on Model Accuracy

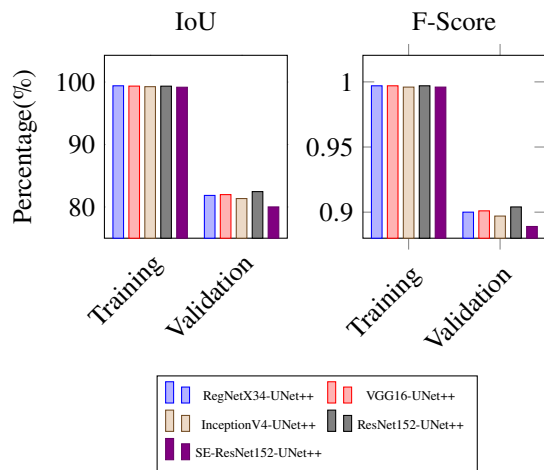


Figure 5. Effect of Encoder Type on Model Accuracy

networks have different capabilities. A test was conducted to see the effect of different encoder types on segmentation.

Encoder Depth: Deep Learning Encoders extract features from images to create a feature map, with deeper encoders extracting more features up to a limit. Using deeper encoder networks can improve models. To test encoder depth effects, increasingly deep ResNet encoders were added to a UNet++ decoder.

Decoder Type: Various segmentation decoders exist beyond the standard UNet and UNet++ algorithms, including Feature Pyramid Networks, DeepLabV3, DeepLabV3+, and Pyramid Attention Networks. Feature Pyramid Networks are similar to UNets but use skip connections and lateral connections passed through a 1x1 convolution. DeepLabV3 concatenates dilated convolutions over

an encoded feature map to obtain global features, while DeepLabV3+ is an improved version of this model. Pyramid Attention Networks combine high and low level features using a feature pyramid attention module and global upsampling attention module. To evaluate the effectiveness of these decoders in segmenting GPR scans, tests were conducted using different encoder types. A ResNet34 encoder was used in the first set of tests, followed by an InceptionV4 encoder in the second set, and a RegNetX32 encoder in the third set. These tests aimed to determine the most effective decoder for the GPR scan segmentation task, while also ensuring that the encoder did not significantly affect the model’s accuracy.

Decoder Depth: The UNet and UNet++ models use a VGG16 network as their standard decoder. This network decodes by progressively lowering the number of channels within layers in each consecutive block of the decoder network until eventually it the number of channels has been reduced to the number of output channels. To train a CNN to detect more features, the decoder can be modified to have significantly more channels. In testing, a UNet++ algorithm was trained with various encoders and different decoder depths to evaluate their performance.

Type 1 (T1) Decoders had a [16, 32, 64, 128, 256] channel structure. Type 2 (T2) Decoders had a [32, 64, 128, 256, 512] channel structure.

ROC Curves & False Positive vs. False Negative Rate To assess the performance of moisture detection models, select models were analyzed using receiver operating characteristic (ROC) curves (See Figure 9). Current moisture detection methods are criticized for high false positive rates, which can be addressed by thresholding, but this increases false negatives. Detection error tradeoff (DET)

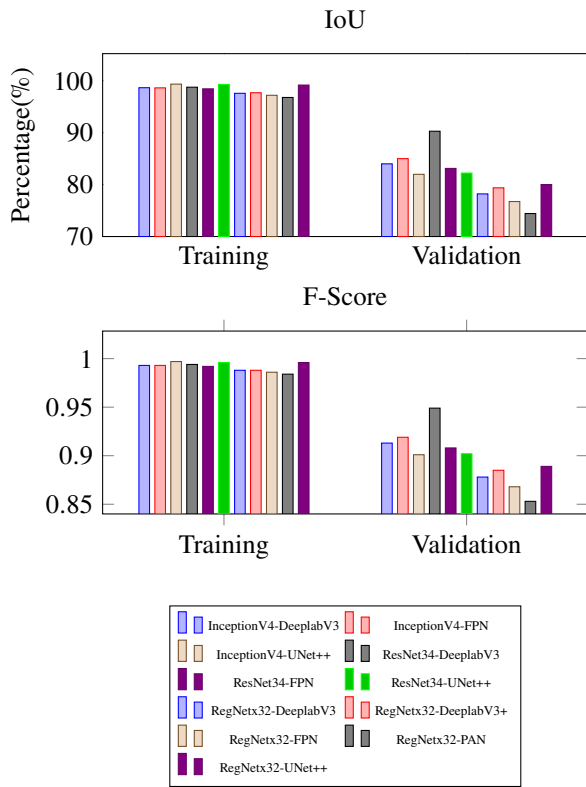


Figure 7. Effect of Decoder Type on Model Accuracy

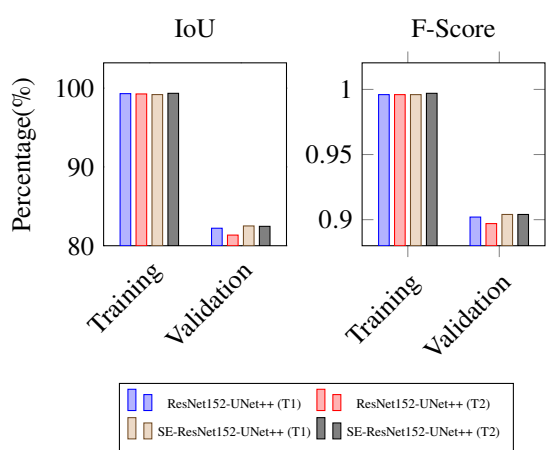


Figure 8. Effect of Decoder Depth on Model Accuracy

curves explore this trade-off and provide insight into segmentation models' performance at different scales.

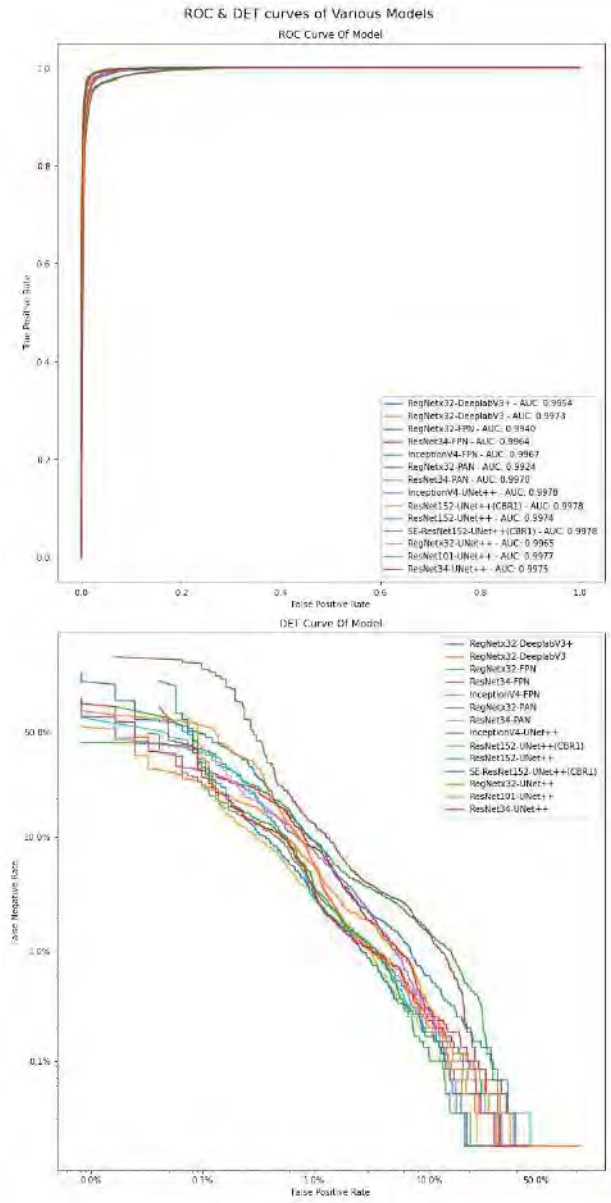


Figure 9. ROC & DET curves of various evaluated models

5 Conclusion

5.1 Testbed

The testbed simulates moisture in building envelopes using various construction materials. The conditions simulated are in some aspects more rigorous than real-world

non-destructive testing for moisture intrusion. Moisture is located under multiple dry layers of building material, making electrical impedance testing and IRT the only viable testing methods. Additionally, scanning was conducted when moisture was at a depth of up to 2 feet, which is beyond the range of non-destructive moisture testing methods.

Future works to improve upon this testbed would be to:

1. Soak various materials to artificially increase their internal moisture content.
2. Add additional building materials such as different kinds of rigid and non-rigid insulation, conductive waterproofing membranes like EPDM, and exterior wall finishings like stucco.
3. To conduct tests at various temperatures

However, the current testbed setup establishes a standard protocol for conducting future tests. Field testing will further confirm the efficacy of this testbed setup.

5.2 Data Analysis

Providing a six-channel tensor containing scans and PSD images gave the network additional data. Another data point could be a 3D tensor created from converting GPR traces into a spectrogram or a Mel-spectrogram. Combining the 2D and 3D data could present a problem, but it can be fused within the model.

5.3 Deep Learning Experiments

The ResNet34 encoder with DeeplabV3 decoder network achieved the highest validation IoU while maintaining high training accuracy. The InceptionV4-FPN model also performed well in terms of validation IoU. UNet++ decoders achieved the highest AUC scores but underperformed on validation tests, indicating overfitting. The best model had the smallest discrepancy between training and validation accuracies and achieved over 9% pixel accuracy on the validation set. However, the model struggled to classify the edges of moisture as wet or dry. The relatively small size of the training and validation dataset may have impacted the model's performance.

6 Future Work

The predicted line scan mask could then be fused with the path of the GPR to create a moisture survey map over a rooftop. This allows for the creation of automated moisture survey maps using robotics, SLAM, and deep learning.

Acknowledgment. This work is supported by NSF CNS-2228568 and TI-2232494, and DOE E-ROBOT challenge.

References

- [1] Andrew Horsley and David S. Thaler. Microwave detection and quantification of water hidden in and on building materials: Implications for healthy buildings and microbiome studies. 19 (1):67. ISSN 1471-2334. doi:10.1186/s12879-019-3720-1. URL <https://doi.org/10.1186/s12879-019-3720-1>.
- [2] Iván Garrido, Mercedes Solla, Susana Lagüela, and Norberto Fernández. IRT and GPR Techniques for Moisture Detection and Characterisation in Buildings. 20(22):6421. ISSN 1424-8220. doi:10.3390/s20226421. URL <https://www.mdpi.com/1424-8220/20/22/6421>.
- [3] Proceq GP8800 Structural imaging and inspection with SFCW ground penetrating radar technology. URL www.screeningeagle.com/en/products/proceq-gp8800-ultraportable-concrete-gpr-radar.
- [4] Erica Carrick Utsi. *Ground Penetrating Radar: Theory and Practice*. Elsevier Science & Technology. ISBN 978-0-08-102217-7. URL <http://ebookcentral.proquest.com/lib/nyulibrary-ebooks/detail.action?docID=4844133>.
- [5] Gokhan Kilic and Mehmet S. Unluturk. Performance evaluation of the neural networks for moisture detection using GPR. 29(4):283–296. ISSN 1058-9759. doi:10.1080/10589759.2014.941839. URL <https://doi.org/10.1080/10589759.2014.941839>.
- [6] Jun Zhang, Xing Yang, Weiguang Li, Shaobo Zhang, and Yunyi Jia. Automatic detection of moisture damages in asphalt pavements from GPR data with deep CNN and IRS method. 113:103119. ISSN 0926-5805. doi:10.1016/j.autcon.2020.103119. URL <https://www.sciencedirect.com/science/article/pii/S0926580519311537>.
- [7] Xu Qiao, Feng Yang, and Xianlei Xu. The prediction method of soil moisture content based on multiple regression and RBF neural network. In *Proceedings of the 15th International Conference on Ground Penetrating Radar*, pages 140–143. doi:10.1109/ICGPR.2014.6970402.
- [8] Jing Zheng, Xingzhi Teng, Jie Liu, and Xu Qiao. Convolutional Neural Networks for Water Content Classification and Prediction With Ground Penetrating Radar. 7:185385–185392. ISSN 2169-3536. doi:10.1109/ACCESS.2019.2960768.

- [9] Jun Sonoda and Tomoyuki Kimoto. Object Identification from GPR Images by Deep Learning. In *2018 Asia-Pacific Microwave Conference (APMC)*, pages 1298–1300. doi:10.23919/APMC.2018.8617556.
- [10] Zhongming Xiang, Abbas Rashidi, and Ge (Gaby) Ou. An Improved Convolutional Neural Network System for Automatically Detecting Rebar in GPR Data. In *Computing in Civil Engineering 2019*, pages 422–429. American Society of Civil Engineers. ISBN 978-0-7844-8243-8. doi:10.1061/9780784482438.054. URL <http://ascelibrary.org/doi/10.1061/9780784482438.054>.
- [11] Lance E. Besaw and Philip J. Stimac. Deep convolutional neural networks for classifying GPR B-scans. In *Detection and Sensing of Mines, Explosive Objects, and Obscured Targets XX*, volume 9454, pages 385–394. SPIE. doi:10.1117/12.2176250.
- [12] Takahiro Yamaguchi, Tsukasa Mizutani, and Tomonori Nagayama. Mapping Subsurface Utility Pipes by 3-D Convolutional Neural Network and Kirchhoff Migration Using GPR Images. 59(8):6525–6536. ISSN 1558-0644. doi:10.1109/TGRS.2020.3030079.
- [13] F. Ponti, F. Barbuto, P. P. Di Gregorio, F. Frezza, F. Mangini, R. Parisi, P. Simeoni, and M. Troiano. GPR radargrams analysis through machine learning approach. 35(12):1678–1686. ISSN 0920-5071. doi:10.1080/09205071.2021.1906329. URL <https://doi.org/10.1080/09205071.2021.1906329>.
- [14] Feifei Hou, Wentai Lei, Shuai Li, Jingchun Xi, Mengdi Xu, and Jiabin Luo. Improved Mask R-CNN with distance guided intersection over union for GPR signature detection and segmentation. 121:103414. ISSN 0926-5805. doi:10.1016/j.autcon.2020.103414. URL <https://www.sciencedirect.com/science/article/pii/S0926580520309948>.
- [15] Stanislav Stefanov Zhekov, Ondrej Franek, and Gert Frolund Pedersen. Dielectric Properties of Common Building Materials for Ultrawideband Propagation Studies [Measurements Corner]. 62(1):72–81. ISSN 1558-4143. doi:10.1109/MAP.2019.2955680.
- [16] Yosef Pinhasi, Asher Yahalom, and Sergey Petnev. Propagation of ultra wide-band signals in lossy dispersive media. In *2008 IEEE International Conference on Microwaves, Communications, Antennas and Electronic Systems*, pages 1–10. doi:10.1109/COMCAS.2008.4562803.
- [17] M. Uematsu and E. U. Frank. Static Dielectric Constant of Water and Steam. 9(4):1291–1306. ISSN 0047-2689, 1529-7845. doi:10.1063/1.555632. URL <http://aip.scitation.org/doi/10.1063/1.555632>.
- [18] Qingqing Cao and Imad L. Al-Qadi. Effect of Moisture Content on Calculated Dielectric Properties of Asphalt Concrete Pavements from Ground-Penetrating Radar Measurements. 14(1):34.
- [19] Goran Stojanović, Milan Radovanović, Mirjana Malešev, and Vlastimir Radonjanin. Monitoring of Water Content in Building Materials Using a Wireless Passive Sensor. 10(5):4270–4280. ISSN 1424-8220. doi:10.3390/s100504270. URL <https://www.ncbi.nlm.nih.gov/pmc/articles/PMC3292119/>.
- [20] Guido Tronca, Isaak Tsalicoalou, Samuel Lehner, and Gianluca Catanzariti. Comparison of pulsed and stepped frequency continuous wave (SFCW) GPR systems. In *2018 17th International Conference on Ground Penetrating Radar (GPR)*, pages 1–4. doi:10.1109/ICGPR.2018.8441654.
- [21] W. T. Simpson. Specific gravity, moisture content, and density relationship for wood. URL <https://www.fs.usda.gov/treesearch/pubs/5914>.
- [22] Andre Desjarlais. A New Look at Moisture Control in Low-Slope Roofing. In *Fourth International Symposium on Roofing Technology*. URL <https://nrcawebstorage.blob.core.windows.net/files/TechnicalLibraryNRCA/5855.pdf>.
- [23] Daniela Tudor, Sara C Robinson, and Paul A Cooper. The influence of moisture content variation on fungal pigment formation in spalted wood. 2:69. ISSN 2191-0855. doi:10.1186/2191-0855-2-69. URL <https://www.ncbi.nlm.nih.gov/pmc/articles/PMC3577483/>.
- [24] [1505.04597] U-Net: Convolutional Networks for Biomedical Image Segmentation. URL <https://arxiv.org/abs/1505.04597>.

Using AI for Planning Predictions – Development of a Data Enhancement Engine

Ashwath.K¹, Vikas Patel², Viranj Patel³, Bhargav Dave⁴

¹Post Graduate Student in Construction Engineering and Management, Faculty of Technology, CEPT University, Ahmedabad, Gujarat

²Technical Support Specialist, VisiLean, Ahmedabad, Gujarat

³Product owner, VisiLean, Ahmedabad, Gujarat

⁴CEO, VisiLean, Ahmedabad, Gujarat

ashwath2917@gmail.com, vikas.patel@visilean.com, viranj.patel@visilean.com, bhargav@visilean.com

Abstract

The construction industry is prone to cost overruns, time overruns, and quality issues. These are all caused by several factors, among which improper planning resulting from unreliable assumptions and unpredictable risks plays a significant role. This could be overcome if the planning-related issues are well predicted, and the risks are accounted for appropriately. Prediction of the various aspects of planning could be enabled by identifying the trend in past data and making it useful for current and future planning. Also, the data being semantic is significant to perform decisive predictions. This could be done by leveraging growing technology like Machine Learning, and Natural Language Processing which are all a part of Artificial Intelligence. Hence, as a starting point for building a robust prediction engine, this research focuses on building a data enhancement engine that would link the plan and model automatically, enabling seamless correlation of the data in the two silos and making it semantic. An engine has been developed as part of this research, and it performs well with respect to the existing data set. Several suggestions to improve the engine have been given as part of the future scope.

Keywords

Artificial Intelligence, Machine Learning, Planning predictions, BIM, Data Enhancement, Sustainability.

1 Introduction

The construction industry is a sector that has the capacity to massively impact the economic and social development of any country. It has grown tremendously in the past years and is also expected to grow steadily in the upcoming years. It determines a country's technological and technical advancement and regulates

the growth of the country's infrastructural development, often directing to its advancement with respect to its sustainability assurance [1]. But the challenges related to cost, time, and quality are predominant in the construction industry [2] and are caused by improper planning, which is a significant determinant of the success of any construction [3],[4]. Planning includes proactive identification and resolution of day-to-day issues, make-ready process, linking short-term and long-term planning, proper duration estimation, proper resource planning, prediction of quality issues and establishing control over them, proper design management, etc. These factors vary based on the scale of a project, its nature, region, etc. These factors are highly interdependent, making it difficult for planners to identify potential risks and make reliable assumptions during the planning process. This risk can be averted if the planners are familiar with these aspects of planning by exposing themselves to the past information corresponding to these factors [5]. Planners need to understand them by correlating the data corresponding to the various factors involved in planning.

The data we are talking about here is not obtained from a single source. It is extracted from several components of the construction industry like the material and equipment sector, consultancy, site execution, investment and developer database, and databases linked to technology like BIM, etc as shown in Figure 1. However, reviewing the data in an isolated manner would not give a broad picture of any situation leading to improper assumptions. These data do not become information unless correlated, streamlined, and made reliable for the planned project. The more reliable the information, the higher would be the accuracy of predictions leading to proper planning.

It is nearly impossible for planners and construction managers to manually assess the enormous reserves of past data and draw parallels between them and the current projects and remember the inferences from such mass

data. Unless there is a mechanism to use the past data effectively, the decision taken by the manager based on their experience would be subjective [6].

Artificial Intelligence (AI) enables Machine Learning (ML) and Natural Language Processing (NLP) which could be leveraged to effectively collect, organize, and derive effective inferences from existing and past data. [7]. They are capable enough to establish hidden patterns among the data [6] and effectively pull out the interdependencies among them. This would help deriving insight from the existing data thereby converting data into information.

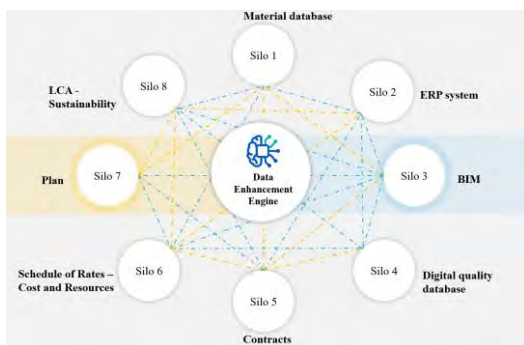


Figure 1: Data sources and correlation

Among the several sources of data mentioned, this research focusses on the plan (i.e., schedule integrated with resource information) and data-rich model (i.e., BIM-based 3D model) which are predominant in the industry. The engine to be developed would effectively link the two silos automatically, creating vast reserves of interlinked data, which would be the base for performing predictions. AI, ML, and NLP-based technologies have been explored concerning the data available, and solutions have been arrived at to perform automatic linkage of the plan and model. The outcome would be a novice engine that could predict the linkage between the plan and model to a certain extent.

1.1 Complexity in existing data extraction

Vast contextual data is available in the BIM models and project plans. This data being in two silos would be less valuable and would not open the opportunity to several use cases like 4D, 5D, planning predictions, etc. unless the data from the silos are linked and correlated with each other. The linking of the model elements and the tasks is not done precisely because of the difficulties in the existing linkage methods. The existing methods to link tasks are as follows:

- Manual linking by selecting the task and the model element
- Linking based on any common ID defined in both the task and the model element

The first method makes the planning process difficult for the last planners. It would even delay the planning process. The second method makes the modeler's work difficult since grouping and labeling the model elements with an ID is time-consuming. Once these difficulties are overcome, the resulting data which could be extracted would be richer in context.

1.2 Aim and Objective

The aim is to develop an AI-driven engine to link the schedule activities and model elements automatically.

The objectives to be achieved to achieve the main goal involve the following.

- Develop a suitable BIM model and relevant plan/schedule for the selected projects
- Leverage the model, schedule, and the AI-ML technology to prepare a proof of concept
- Validate the POC based on relevant metrics and improve the engine accordingly

1.3 Scope

For this research purpose, the scope for data includes three projects. 2nd and 3rd projects are for validating the effectiveness of the POC.

- Project 1: This is for developing the POC. This is a multistorey commercial cum residential complex
- Project 2: This is a multistorey commercial cum building
- Project 3: This is a museum building with RCC and steel structural elements.

2 Research methodology

This research involves active participation in an organization development of an engine that would solve the mentioned problems in the industry. The objectives to develop this engine have been laid down; the engine would be developed, experimented to provide a solution for certain instances of the problem, evaluated based on relevant metrics, and the development would be iterated for perfection ending up in generalizing the perfected engine to the industry. Based on this, the design science approach seems to be the best suitable framework to base the research rather than the other existing research approaches. [8] have given six steps that make the constructive research approach and the research has been carried out until the fifth step i.e., development, demonstration, and evaluation of the engine. Further, several optimizations to the solution have been suggested, which would be carried out through iterations as a part of future scope which is the sixth step of the design science approach.

A digital platform that enables the linking of a plan and a BIM model is necessary for the research. Several platforms like Navisworks, Synchro, VisiLean etc., are available to do the same. Apart from conventional information included in a plan like schedule, cost, and resource data, more Last Planner System (LPS) based information like constraints, reasons for variance, etc., could be added in VisiLean. This makes the data more contextual and useful for predicting planning issues. Hence, VisiLean has been chosen to be the platform for linking the plan and model and retrieving the necessary data related to the linked plan and model for the research.

3 Data Collection and Processing

3.1 Collection and Preparation

Data collection and preparation involves preparing the model data, relevant schedule data, and the linkage data necessary to teach the machine for automatic linkage. These are as explained below.

3.1.1 Preparation of model, schedule and extraction of data

Model corresponding to Project 1 has been obtained from the organization. Model data are obtained through the VisiLean system by using a certain API program. Data regarding both the structural and architectural models have been obtained in such a way.

The schedule corresponding to the model has been prepared in Primavera. The schedule is then imported into VisiLean and the entire schedule related information can be extracted from the software.

3.1.2 Linking and extracting linkage data

The linkage of the activity and model elements has been done manually in VisiLean. The columns, beams, and floors from the structural model and the architectural model's masonry walls were linked to the respective activities. There are no separate elements for shuttering or reinforcement in the model, and hence the activities related to shuttering and reinforcement are also linked to concrete elements. Staircase, Lift and Finishing work related activities are not linked because of absence of relevant elements in the model.

After the linkage, two files corresponding to the linkage i.e., one for the structural model and other for the architectural model have been obtained. These files mainly consist of the information regarding the activity and element which are linked together. It doesn't have the information related to those activities and elements which are not linked.

3.1.3 Data Summary:

Model, schedule, and linkage data have been obtained

by the end of the data collection and preparation process.

3.2 Data Processing

The data obtained cannot be used directly for the ML algorithm. The data should be processed and brought to the necessary format to proceed further. The various processing steps followed are as explained further.

3.2.1 Dimensionality reduction

The reduction of features is referred to as dimensionality reduction in ML terms. Features mean the columns representing the several model, schedule, and linkage parameters. Dimensionality reduction can be done using ML-related coding, but it has been done manually here. The data available is huge enough and misleading because of the presence of unwanted and useless data. Using Power BI, each column has been analysed, empty columns and columns with very minimal and repetitive data have been removed before combining the data.

The data corresponding to string datatype i.e., only text is considered for the initial trials. The data corresponding to several other datatypes would add complexity to the algorithms to be applied. Hence, the parameters corresponding to the float data type have been eliminated for the initial trials of algorithm and the corresponding pre-processing. Certain parameters would be not necessary, and some would be repetitive. For example: Parameters like 'Omni class title' in the BIM model convey the same information as the parameter 'Name' which tells name of the element. Hence, such repeated info conveying parameters should be removed to reduce the noise in the data.

3.2.2 Combining data

Currently there are several files corresponding to schedule, model and linkage. These files have to be combined into a single file based on some common parameters in these files. The base for combining these files will be the linkage file data. It has the GUID of the activities and the BIM Model IDs of the elements which are linked together and this can be done using PowerBI.

3.2.3 Labelling data

The linkage data contains only the linked activities and model elements, and hence the label corresponding to linkage would be 'Yes' to all the rows. Whereas false data should also be present to teach the machine. False data means the data corresponding to the activities and elements which do not link. Hence, the data corresponding to 'No' linkage must be extracted.

3.2.4 Dimensionality reduction

3.2.5 Pre-processing of text

Since only text data is considered for the initial trials, text pre-processing is an important step before applying any ML-based algorithm. The parameters mentioned in Table 1 represent the data considered for the initial trials. The presence of text data necessitates the use of NLP along with ML-based algorithms. Several NLP based construction sector related projects were analyzed with respect to the methodology which has been followed and the pre-processing techniques followed in those projects.

Based on the review of the NLP based projects, several pre-processing techniques have been identified, which are essential to make the text suitable enough for the machine to analyze and run any ML algorithm on them [9],[10],[11],[12]. The pre-processing technique carried out are like punctuation removal, filling of blank cells, lowercasing, removal of stop words, tokenizing, lemmatization and vectorization.

3.2.6 Vectorization with Word2Vec and DocVec

Word2Vec is a method used to represent words as vectors, i.e., numbers in an N-dimensional vector space, i.e., it helps to obtain contextual word embeddings. The words would be placed in the vector space based on their combination and frequency of occurrence. This method indirectly considers the semantic relationship between the words since the combination of their occurrence plays a vital role in vectorization and not only the frequency.

The process involves feeding the right combination of words into the Word2Vec algorithm. After feeding them and running the model, a 2D graph could be generated to visualize the placement of words as shown in Figure 2.

The main limitation of using the Word2Vec algorithm alone is that only the individual words could only be vectorized and not sentences. To compare the plan and model data, we have several sentences that are to be compared and not only individual words. DocVec algorithm has been found to be useful to obtain the sentence vectors. Hence, the DocVec model combined with the Word2Vec model seemed to give the required results.

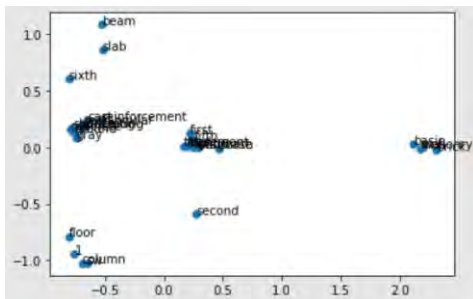


Figure 2: 2D graph output of Word2Vec model

4 Development of POC

The aim of this study is to develop an engine that would automatically link the model elements to the schedule activities to reduce the massive consumption of human resources and time required to perform the linkage process. This issue is also supported by [13] and they have devised a method to do the same. They have proposed a mapping solution with a learning loop that can adapt itself to the different activities and element categories of projects of varying nature. The mapping has been done based on three attributes namely Building, Level and Discipline.

There exist numerous other parameters in the plan obtained from VisiLean and the model. Several of these parameters would also be relevant to the linkage, which can be added to the mapping process. Although several parameters have been eliminated to reduce the complexity of the initial trials of pre-processing and application of algorithms, they can be added on further after a preliminary engine is made, which shows promise for automatic linkage. This preliminary engine is termed the 'Proof of Concept', and it is one of the main objectives of this research.

4.1 Layers to be scrutinized for mapping

From the plan, we can get the task's name, location data, and even the trade-related details. Unlike the task information, model elements have numerous parameters. All these parameters would contribute to the linkage in one way.

With respect to the data, we have for the initial trials of pre-processing and application of algorithms, from the information corresponding to plan, the task name, trade and location details can be identified. To associate these details to the model, we need similar details from the model information which we have. From the model, the element name, location details and material details could be used to relate to the plan information.

Table 1: Layers considered

Parameters	Layer
Task name and Element name	Name
Task location and Element location	Location
Task name and Element material	Trade

4.2 Application of algorithms and evaluation

A combination of the layers mentioned in Table 1 have been experimented with several algorithms to achieve the best performance.

The study is focused on supervised Machine Learning.

Based on the data and the kind of prediction we have to do, algorithms that can do effective classification are preferred to those which do regression.

Several algorithms have been used based on the problem to be addressed. The most recurrently used algorithms are Decision tree, Support Vector Machine, and Naïve Bayesian. But there is no clear distinction on which algorithm is best because the performance depends on the kind of data and purpose of prediction. Based on interaction with certain AI experts, three algorithms, namely Random Forest Classifier (RFC), Support Vector Machine (SVM), and XG Boost, were considered for the initial trials. RFC and SVM are single algorithms, whereas XG Boost is a decision tree-based ensemble algorithm.

Before the data is passed on to any algorithm, the pre-processing steps mentioned earlier must be performed. After the pre-processing is done, the similarity between the sentence vectors obtained from the Word2Vec and DocVec model will be identified. These similarities would be passed as the input to the algorithms and the ‘Yes’ or ‘No’ linkage data would be given as the output to these algorithms. Based on the input and output, the algorithms would be trained.

4.3 Combination of layers and tests

Five different combinations of the layers have been tried out to get the optimum result. This can be seen in Table 2.

Table 2: Trials and relevant details

Trial	No of layer s	Layers used	Remarks
1	2	Name, Trade	-
2	2	Name, Location	-
3	3	Name, Location, Trade	-
4	3	Name, Location, Trade	In this case, the unwanted words like ‘level’, ‘floor’, ‘pour’ etc., were removed from location data.
5	3	Name, Location, Trade	In this case, after removing unwanted words, the locations were categorized into numbers. Ex: ‘First’=1.

While applying each algorithm, the training data is split into 70% and 30% among which the 70% portion

would be used for training and the remaining 30% would be used by the algorithm to test itself. This testing will be termed ‘self-test’ from now on in this report. Apart from this testing, five different combinations of plan parameters have been provided (combinations of words which are not a part of the self-test data set – different words and different combinations), and the predictions have been evaluated manually. This testing will be termed ‘external-test’ from now on in this report. The trials performed with the varying combination of the layers and the performance evaluation of the algorithms for the self-test and external-test have been discussed in detail in the following sections.

4.4 Evaluation of the tests

The performance measurement indices corresponding to the confusion matrix are predominantly being used to evaluate ML-based algorithms. Such indices referred from the literature such as Precision (P), Recall (R), F1 score (F1) and Accuracy (A) have been considered for evaluation. Higher Accuracy, Recall and Precision are preferred for a better performance.

5 Results and Discussions

The values of the indices mentioned earlier have been compared among the several trials. All these analyses correspond to the self-test performed by the algorithms based on a part of the training data set.

Parallel to the self-test performed, external testing has been carried out by providing five sets of plan data, and the predicted model data has been manually analyzed for performance. Comparing the results of the self-test and external testing results, the combination of layers was experimented with until the most optimum combination was achieved.

5.1 Performance evaluation

The legend in Figure 3 conveys the information regarding the trial, the combination of layers used and the algorithms having high performance. In some trials there are distinct difference between the performance of the algorithms and in those cases the respective single algorithm is mentioned. In the cases where the performance of algorithms varies minorly (i.e., + or – 1 or 2), multiple algorithms have been taken into consideration for high performance, and the highest value under each performance index is taken for the graph.

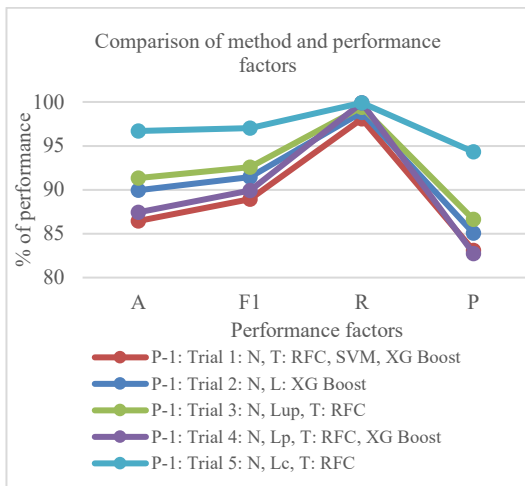


Figure 3: Trial 1-5 self-test performance indices

5.1.1 Performance of algorithms with respect to self-test as per confusion matrix related indices

In Trial-1, all the three algorithms have similar performance. In Trial-2, the performance of XG Boost is distinctly higher than the other two, and hence it is considered for high performance. In the case of Trial-3 and Trial-5, RFC shows the best performance, followed very closely by XG Boost, and the SVM shows lower performance compared to them both. In the case of Trial-3, RFC performance is distinctly higher than others. In Trial-4, the performance of all the algorithms varies minutely from each other, whereas with respect to 'Recall', XG Boost performs distinctly better than the other three, and hence we could say XG Boost performed better overall in Trial-4.

```

Accuracy: 85.37186246663107
F1 Score: [81.12947658 88.05579773]
Recall: [68.32946636 99.90188803]
Precision: [99.83050847 78.72174591]

Total instances: 1873

Confusion matrix:
[[ 589 273]
 [ 1 1010]]

```

Figure 4: Confusion matrix and relevant performance metrics corresponding to RFC algorithm in Trial 1

5.1.2 Evaluation of Trial

From Figure 3 we can infer that the performance increases gradually while the layers are being added one by one. All the performance factors of Trial-3 > Trial-2 > Trial-1. But, if we compare this to the performance in case of external tests, the location category has not been predicted by any of the algorithms in any of the Trials. But the prediction of location is a must, and hence the location parameter must be optimized in such a way to get good results. The reason behind the location being not predicted might be the availability of very less

vocabulary with respect to the location data and the confusion created by the unnecessary words like 'floor', 'level' etc., in the location data.

Hence, Trial-4 is tried out with processed location parameters free from words which do not add much value for linking purpose. This trial will help us to understand whether removing such unwanted words increase the performance. Figure 3 shows a decrease in performance with respect to all the performance indices when compared with the first three Trials. But when we compare the previous trials with this trial, some improvement has been seen with respect to location predictions. But still, the location predictions are not satisfactory, and hence further optimization has to be done in case of the method used.

Since the lesser vocabulary in location data makes it difficult for the engine to make a clear distinction between the several locations, the available locations can be categorized into numerical values and then taught to the engine, which will help to make a clear differentiation between the locations. This categorization has been done to location data in the case of Trial-5 combined with the similarity method for name and trade-related data.

From Figure 3 we can infer that the performance of Trial-5 is much better than the first 4 trials in the case of all performance measurement indices, and this high performance corresponds to the RFC algorithm. XG Boost is the next high performing, whereas SVM is low performing compared to these algorithms.

5.1.3 Performance measurement indices

With respect to all the indices, Trial-5 scores the highest. In the case of Recall, although all the trials performed well, the Precision of Trial-5 is distinctly higher than the others. Having 100% Recall value and 94% Precision value in Trial-5, we can say that the engine would seldom predict a 'Yes' linkage as 'No' whereas it may predict a 'No' linkage as 'Yes'. But there are high chances for the engine corresponding to the other trials to predict the 'No' linkage as 'Yes', which would not be desirable.

5.1.4 Outcome

By comparing the performance of the best performing algorithms among the different trials, Trial-5 is found to be better. Name and Trade are predicted to a good extent but none of the algorithms perfectly achieved the prediction of location for all the external test instances.

The outcome of Trial-5, RFC and Brick Work activity in Second level has been highlighted in model and is as shown in Figure 5. This outcome corresponds to the results from the prediction. The rightly predicted element ID's have been obtained and used for highlighting in the model.

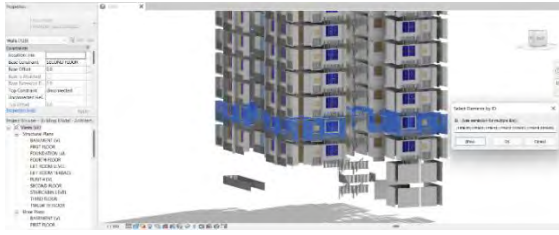


Figure 5: Right wall elements highlighted in model

We can see that all the predicted elements are correct, i.e., all are wall elements corresponding to brick material and second level. The bad performance with respect to location prediction could be oriented to the following reason. For elements like columns and walls, the location provided by the planner would match with the base levels of the model elements whereas in case of slabs and beams the locations in model would be one level ahead of the location mentioned by the planner. This is because the beam or slab of a particular floor would be placed at the base of the next floor.

5.2 Testing of POC with additional project, its results and evaluation

The second and third project data have been obtained, processed and added to the existing project data and then the machine has been taught and tested similar to the previous case. Layers corresponding to Trial-5 are considered for the combination of 1st and 2nd project as Trial-5 gave the best results in the previous case whereas layers corresponding to Trial-4 are considered for the combination of 1st, 2nd and 3rd project as the location data in the 3rd project is more specific to the nature of the project and cannot be categorised. Both self-test and external test with new plan data as input have been performed and the results have been compared to the previous case results.

The self-test results were good and similar to the previous case as shown in Figure 6 but the external test results were not satisfying and poorer than the previous case. Several instances which were predicted rightly in the previous case are not predicted properly in the case of the combined project data. In the case of the external tests run with respect to single project data, the predictions of Name and Trade were right for even new activities. Several reasons for the non-satisfactory performance are like

- The vast transformation in the Word2Vec model because of the addition of several new vocabulary and its implication on the existing combination of words.
- Insufficiency and inconsistency in data points, i.e., in general, the data points used for training are very less for a NLP-based project and comparatively,

Project-1 has more data points with respect to ‘Yes’ and ‘No’ linkage compared to Project-2.

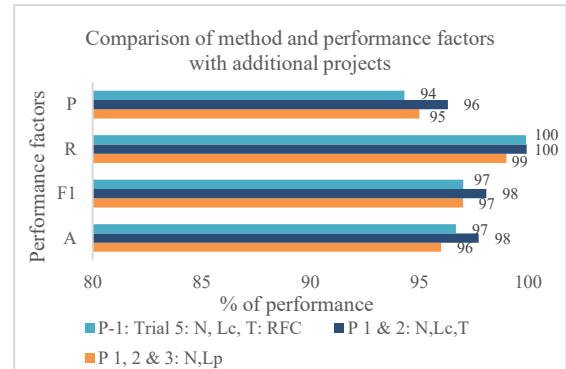


Figure 6: Self-test results of additional projects

5.3 Limitations of the engine

Several limitations are associated with the usage of AI based techniques which is applicable to this engine [7]. They are as follows.

- Biased outputs based on nature of data fed
- Uncertainty in the functionality since past data would not be available to train the system for all possible situations. This scarce nature of data availability limits the engine’s scalability
- Difficulty in finding the root cause for any errors in the output since huge reserves of data is involved

5.4 Future scope: Learning loop and extended use cases

The engine can be perfected by providing it with ample data and by enabling self-learning. As the users plan through VisiLean, even though if the machine predicts wrongly, they could link the right task and element from which the engine would learn the right path of linkage and such continued learning would result eventually in the perfection of the engine. This method of continuous improvement through dynamic interaction of the planner with the system during the planning process would address the limitation of data scarcity, scalability, and in-built data bias to a considerable extent. This is a combination of edge computing and AI which is in line with the principle of Edge AI.

Once the engine is perfected, it poses ‘n’ number of use cases. It can be used to perfect the planning process by predicting the uncertainties with respect to duration, quality etc., with more accuracy, it can also predict sustainability parameters by accessing the existing sustainability databases as represented in Figure 1 and also by making use of the learnings from the user input

sustainability factors etc.

6 Conclusion

The engine which has been developed shows good performance concerning the self-tests performed on a portion of the training data. The external test performance is comparatively not satisfactory.

It has been identified that pre-processing of data is a vital process in developing the engine. The engine developed can predict the element and trade, i.e., material to a reasonable extent but the prediction of location is not satisfactory. Main reasons identified for unsatisfactory performance are like insufficient relevant sample size, insufficient labelled data, inconsistency in the vocabulary used across the projects considered etc. Several limitations have been identified at several phases of the research. The areas to be mainly focused on are such as enlargement of sample size, effective pre-processing and the method to assess the similarity. These can be taken as a part of future scope.

If the limitations are overcome, and the engine is optimized it would provide huge reserves of contextual data essential for predictions. This engine could be used to collate and correlate data from several databases such as contract documents, standard manuals, quality related digital databases, sustainability related databases etc. This would be helpful for the various stakeholders in the construction industry to plan effectively to overcome the challenges thereby reducing the wastage with respect to materials, process, time, cost etc. and also to dynamically monitor the project sustainability. Thus, the proposed AI based engine could automate the data enrichment thereby making construction sustainable.

References

- [1] Chaudhery, Mustansar Hussain, Mosae Selvakumar Paulraj, S. N. (2022). Source Reduction and Waste Minimization. Elsevier. <https://doi.org/https://doi.org/10.1016/C2020-0-01110-2>
- [2] Ibrahim, A. R. Bin, Roy, M. H., Ahmed, Z. U., & Imtiaz, G. (2010). Analyzing the dynamics of the global construction industry: Past, present and future. *Benchmarking*, 17(2), 232–252. <https://doi.org/10.1108/14635771011036320>
- [3] Hamzah, N., Khoiry, M. A., Arshad, I., Tawil, N. M., & Che Ani, A. I. (2011). Cause of construction delay - Theoretical framework. *Procedia Engineering*, 20(Kpkt 2010), 490–495. <https://doi.org/10.1016/j.proeng.2011.11.192>
- [4] Johnson, R. M., & Babu, R. I. I. (2020). Time and cost overruns in the UAE construction industry: a critical analysis. *International Journal of Construction Management*, 20(5), 402–411. <https://doi.org/10.1080/15623599.2018.1484864>
- [5] Asadi, A., Alsubaey, M., & Makatsoris, C. (2015). A machine learning approach for predicting delays in construction logistics. *International Journal of Advanced Logistics*, 4(2), 115–130. <https://doi.org/10.1080/2287108x.2015.1059920>
- [6] Ayhan, M., Dikmen, I., & Talat Birgonul, M. (2021). Predicting the Occurrence of Construction Disputes Using Machine Learning Techniques. *Journal of Construction Engineering and Management*, 147(4), 04021022. [https://doi.org/10.1061/\(asce\)co.1943-7862.0002027](https://doi.org/10.1061/(asce)co.1943-7862.0002027)
- [7] Harvard Business Review. (2019). Artificial Intelligence: Insights you need from Harvard Business Review. Harvard Business Review Press.
- [8] Peffers, K., Tuunanen, T., Rothenberger, M. A., & Chatterjee, S. (2007). A design science research methodology for information systems research. *Journal of Management Information Systems*, 24(3), 45–77. <https://doi.org/10.2753/MIS0742-1222240302>
- [9] Hassan, F. ul, & Le, T. (2020). Automated Requirements Identification from Construction Contract Documents Using Natural Language Processing. *Journal of Legal Affairs and Dispute Resolution in Engineering and Construction*, 12(2), 04520009. [https://doi.org/10.1061/\(asce\)la.1943-4170.0000379](https://doi.org/10.1061/(asce)la.1943-4170.0000379)
- [10] Jallan, Y., Brogan, E., Ashuri, B., & Clevenger, C. M. (2019). Application of Natural Language Processing and Text Mining to Identify Patterns in Construction-Defect Litigation Cases. *Journal of Legal Affairs and Dispute Resolution in Engineering and Construction*, 11(4), 04519024. [https://doi.org/10.1061/\(asce\)la.1943-4170.0000308](https://doi.org/10.1061/(asce)la.1943-4170.0000308)
- [11] Jung, N., & Lee, G. (2019). Automated classification of building information modeling (BIM) case studies by BIM use based on natural language processing (NLP) and unsupervised learning. *Advanced Engineering Informatics*, 41(September 2018). <https://doi.org/10.1016/j.aei.2019.04.007>
- [12] Moon, S. M., Lee, G., Chi, S., & Oh, H. (2019). Automatic Review of Construction Specifications Using Natural Language Processing. *Computing in Civil Engineering*, 105–113. <http://toc.proceedings.com/49478webtoc.pdf>
- [13] Vaidyanathan, K., Raphael, B., Kumar, A., S, M., & Patil, Y. (2021). Seamless integration of site data for planning and monitoring of construction projects.pdf. *Proceedings of the Indian Lean Construction Conference - ILCC 2021*.

Lessons Learned from the “Hack My Robot” Competition and Considerations for Construction Applications

Muammer Semih Sonkor¹, and Borja García de Soto¹

¹S.M.A.R.T. Construction Research Group, Division of Engineering, New York University Abu Dhabi (NYUAD), Experimental Research Building, Saadiyat Island, P.O. Box 129188, Abu Dhabi, United Arab Emirates
semih.sonkor@nyu.edu, garcia.de.soto@nyu.edu

Abstract –

The construction industry is going through a digital transformation where automation and robotics are slowly making their way into construction projects. This change brings numerous benefits, such as cost and time efficiency and higher accuracy and quality. At the same time, it raises cybersecurity concerns. Since most construction environments are far from being human-free in the near future, the importance of providing robust cybersecurity when utilizing cyber-physical systems such as robots is augmented. The use of robotics in construction processes has long been under academia’s and industry’s spotlight, but the cybersecurity aspects have not received the attention they deserve. Several surveys have shown low awareness among construction stakeholders about cybersecurity, which increases the need for further studies on this topic.

This study provides an overview of the first academic-driven cybersecurity competition in the construction context, Hack My Robot (HMR), as part of CSAW’22, the most comprehensive student-run cybersecurity event in the world. HMR was held for the first time at New York University Abu Dhabi (NYUAD). The competition had two main rounds: the qualification round and the final round, where students presented their ideas to compromise the provided robotic system’s functionality and the collected information. The system used in the competition imitated a construction progress monitoring robot that utilizes Robotic Operating System (ROS). This paper presents how this competition aims to contribute to construction cybersecurity efforts, what main outcomes were obtained, and how it will be improved in the upcoming editions.

Keywords –

Construction 4.0; Cybersecurity; Competition; Robotics

1 Introduction

Construction has long been an industry that relies on conventional equipment and traditional methods to perform most tasks. In a report by McKinsey in 2016, construction was listed as the least digitized industry after agriculture and hunting [1]. However, this has been rapidly changing with the integration of new technology in recent years. In a 2021 report, construction was indicated as the second industry with the highest potential for productivity growth from 2019 to 2024 as a result of digital construction, industrialization, and operational efficiency [2]. Cyber-physical systems (CPSs), such as robots, have a significant role in the expected productivity growth since they are an integral part of industrialization and digitization in almost every sector.

Digital transformation of the construction industry is often called Construction 4.0. This transformation, which includes the use of robotics and automation, increases productivity, improves the quality and accuracy of the handled tasks, improves safety on construction sites, and decreases the inclusion of humans, who are, by nature, prone to make mistakes. Examples of robots used in construction include progress monitoring robots [3], autonomous machinery to handle repetitive tasks such as earthworks material loading [4] and overhead drilling [5], and drones to inspect structures for damage or defects during the operations and maintenance (O&M) phase [6]. Construction robotics holds significant potential for improving cost and safety while reducing time; it also introduces cybersecurity risks that must be considered to ensure the secure operation of these systems.

Attacks against construction companies and projects can lead to serious safety issues and financial losses due to disrupted operations and damaged reputation. Some cyberattacks in the construction industry had significant impacts, supporting this statement. For example, confidential design documents of the Australian Intelligence Service’s headquarters building were stolen by hackers in 2013 during the construction phase [7]. A study published by Trend Micro Research in 2019

included testing radio frequency (RF) remote controllers for cranes supplied by 17 vendors. The results showed that all tested controllers were vulnerable to cyberattacks [8]. Considering the close human-machine interaction in construction environments, potential attacks against the control systems of robots, which could result in the manipulation of functions, can cause serious safety issues. Since automated and robotic systems are starting to become a part of construction tasks in recent years, there have not been any known cyberattacks against construction projects that caused physical damage. However, examples from other sectors have proved the criticality of robust cybersecurity for safety. For example, a cyberattack against a steel mill in Germany caused the malfunction of a furnace and led to significant physical damage [9]. Also, sensitive data collected and transmitted by robots could be vulnerable to data breaches if proper security measures are not in place. Zhu et al. [10] emphasized that modern robotic systems are susceptible to various cyberattacks since most companies are targeting to get their products ready for the market quickly, which leads to overlooking cybersecurity mechanisms. Therefore, construction companies need to implement robust security measures to protect against these risks and ensure the safe and secure operation of robots on site.

Hack My Robot (HMR), held in 2022 to address the mentioned concerns, can be considered the first academic-driven cybersecurity competition in the construction context. It was a part of Cyber Security Awareness Week (CSAW), the world's most extensive student-led cybersecurity event. It took place at New York University Abu Dhabi (NYUAD), which hosted the Middle East and North Africa (MENA) region competitions of CSAW'22 on November 9-12, 2022. The students were challenged to generate ideas to compromise the data and operations of a progress monitoring robot, considering the characteristics of construction sites.

This study presents an overview of HMR and its preliminary results. The HMR competition and this paper do not aim to make a technical advancement in construction automation and robotics. Instead, the goals are to achieve a raised awareness about the cybersecurity aspects of digitalized construction environments with a particular focus on robotics, bringing the attention of the cybersecurity community to the construction sector, and utilizing the cybersecurity knowledge of students to discover potential problems raised with the use of robotics in construction projects. As mentioned by Salami Pargoo and Ilbeigi [11], construction cybersecurity studies have mostly focused on building information modeling (BIM), while issues related to construction robots have been considered for future work. To address this gap in the literature, this paper derives

conclusions based on the initial results of the HMR event and tries to answer the question, "Is it possible to identify cybersecurity vulnerabilities of construction robots through a competition?"

The rest of this paper is structured as follows. Section 2 explains the significance of cybersecurity in construction by showing the previous efforts and some examples of cyberattacks against construction companies. Section 3 gives an overview of HMR, presenting an overview of the robotic system, different rounds of the competition, and lessons learned. Finally, Section 4 discusses the conclusions of this study and presents the planned future work.

2 The Importance of Cybersecurity in Construction

Cybersecurity concerns in construction have been augmented as the industry increasingly relies on technology to produce and store information, handle tasks on-site, and connect stakeholders. Previous incidents showed that hackers could cause financial losses, disruption of operations, and reputational damage. The construction industry is no different from the other sectors regarding the potential consequences of cyberattacks. Therefore, construction companies must prioritize cybersecurity and take the necessary actions before any adverse event occurs.

The first aspect to consider is the cybersecurity of information generated and stored throughout the lifecycle of construction projects since the digitalization of information has been running ahead of the digitalization and automation of physical tasks in the industry. BIM technologies such as design authoring software and online collaboration tools allow planning, designing, and managing projects in digital environments. As a result of this change in projects, from paper to digital, the amount of valuable and sensitive data increases, which creates potential vulnerabilities that hackers can exploit. Some studies addressed these issues and proposed solutions. For example, Zheng et al. [12] proposed a context-aware access control for BIM data environments to replace the mainstream role-based access control. Boyes [13] emphasized the need for change in the construction companies' security practices and the security policies by governments.

Since the digital transformation of physical tasks and the use of operational technologies (OT) in construction projects has been relatively slow compared to the digitalization of information, there have not been many studies focusing on OT cybersecurity in construction so far. One of the studies on this topic has been conducted by Sonkor and García de Soto [14]. They performed a bibliometric analysis to scrutinize the OT, construction, and cybersecurity literature. Their study revealed a

research gap regarding the cybersecurity of automation and robotics in the construction industry, which is one of the motivations of the HMR competition presented in this paper.

Previous cyberattacks against the construction industry raised cybersecurity concerns and alerted construction decision-makers and policymakers. For example, a British construction company, Interserve, has recently been fined £4.4 million by the Information Commissioner's Office due to its failure to prevent a cyberattack in May 2020 and caused leakage of more than 110 thousand employees' personal data [15]. An employee of Interserve forwarded a phishing email to a colleague who opened the email and downloaded the malicious file, which resulted in the leakage. Even though most cyberattacks against construction companies targeted information systems, similar patterns of attacks can be seen impacting OT as it becomes more pervasive in construction. Therefore, the industry should learn from past incidents of attacks and take action to provide a secure environment for robots as they make their way into construction projects.

Finally, it is essential to understand the level of cybersecurity awareness in the industry since small human mistakes are mostly the reason for falling victim to severe attacks. An academic survey [16] conducted among construction professionals and academics from May to September 2020 revealed the extent to which the construction industry is ready for the upcoming cyber threats. The survey—with the participation of 281 people—showed that nearly half of the respondents had never heard of the cybersecurity standards and frameworks provided to them. Thirty-five percent of the participants did not know whether or not their company had a cybersecurity plan. On the other hand, most of the respondents (84%) indicated that they were concerned about cybersecurity in the construction industry.

3 Hack My Robot

HMR is the first academic-driven cybersecurity competition in the construction context. It was organized by the S.M.A.R.T. Construction Research Group at NYUAD. The competition was a part of the 19th edition of Cyber Security Awareness Week (CSAW). CSAW 2022 took place in five regions (i.e., Europe, India, MENA, Mexico, US-Canada) with more than 3,000 competitors. HMR happened only in the MENA region (i.e., CSAW'22 MENA) and was open to all undergraduate and graduate students registered in MENA universities. HMR will be held annually in the upcoming years with different challenges and construction robots as a part of CSAW.

The competition had two rounds: the qualification round and the final round. Students were asked to submit

ideas to compromise the collected data and the functionality of the robot during the qualification round and implement their ideas in front of the judges in the final round. The most successful teams in the final round, determined by the group of judges, were awarded cash prizes. The provided robotic system and its functionality simulated an autonomous progress monitoring task on a construction site. The data collection task in the challenge consisted of the robot autonomously moving across different predefined positions, capturing images on each of them, and returning to the initial position to start transmitting the collected data to another computer in the network, which would act as the server. The following subsections provide an overview of the competition and detail the different rounds.

3.1 Overview of the Robotic System

The robotic system used in the competition performs autonomous data acquisition to simulate a fully functional construction progress monitoring robot. Figure 1 shows different components of the robotic system divided into five levels based on their functionalities and the communications between them. This diagram was created based on the autonomous site monitoring system diagram presented in [17]. Further details of each level and the communication between the components can be found in [17]. Therefore, this section only provides a brief overview of the different levels.

Level 0 includes the physical components of the robotic system, including the robotic platform that houses all peripherals and the cameras and sensors that acquire data from the surrounding environment. Level 1 shows the network that connects all the elements of Level 0, the computer embedded in the robot (i.e., robot computer) that controls all the functionalities, the router that enables wireless communications, and the external computer that acts as the data server. Level 2 involves the Robot Operating System (ROS) [18] network, which is a widely used system in the robotics sector [19]. ROS 1, which has much fewer security features than ROS 2 [19], was chosen to show the cybersecurity vulnerabilities more clearly. In the ROS network, the robot computer functions as the ROS master, and the external computer connects to the ROS network to communicate with it. The ROS nodes can receive and publish information in the direction of ROS topics and give and receive commands in ROS services. Level 3 shows the autonomous control function of the robot. The robotic platform can autonomously communicate via ROS with all the actuators and sensors.

Finally, Level 4 demonstrates the human-machine interaction. Several graphical user interfaces provided by ROS enable visualizing the information collected by the sensors and cameras of the robot.

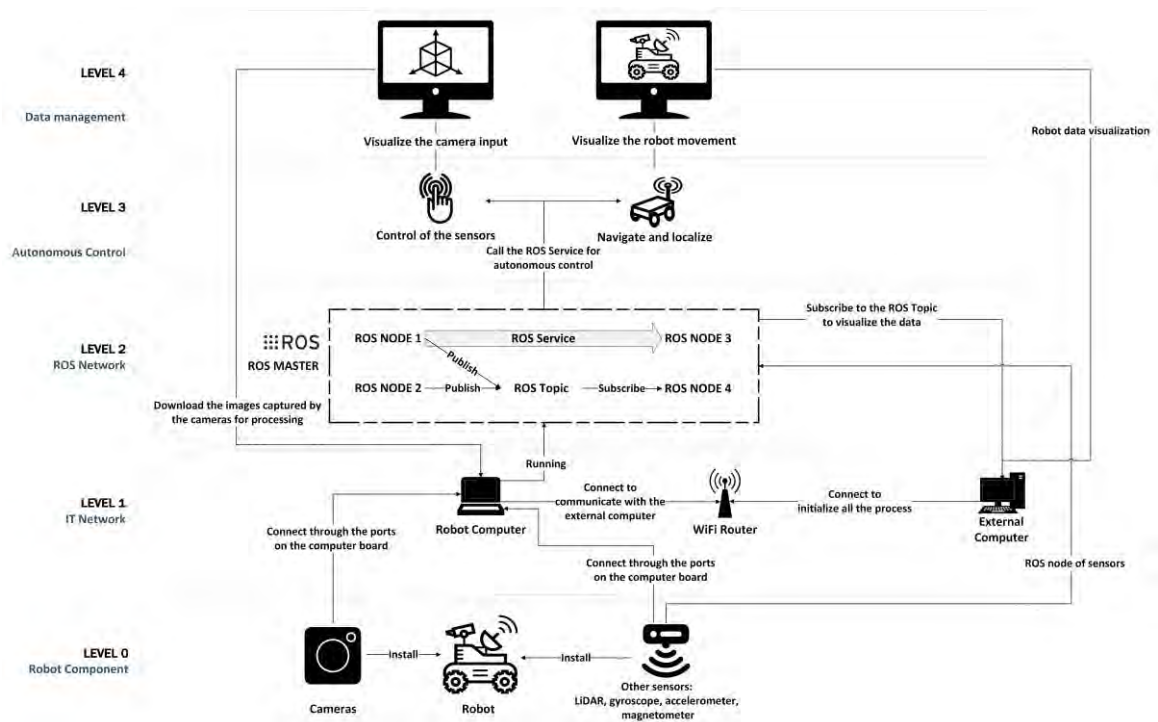


Figure 1. Diagram of the robotic system used in HMR (adapted from [17])

3.2 Qualification Round (Round 1)

The first round (i.e., qualification round) challenged the participating teams to generate ideas to compromise the provided robotic system (see Section 3.1) and find ways to improve its security level to mitigate the vulnerabilities they mentioned. They were also asked about their motivation to compromise such a system considering the construction context. They were given a Google Form to answer five open-ended questions for the qualification round and several other questions (e.g., team name, email addresses, university name) for registration purposes. The registration and the first round were open for one and a half months (from August 15 to September 30, 2022). The open-ended questions for the qualification round were as follows:

1. Considering the robotic system in the provided challenge document, what would you do to compromise the data collected?
2. Considering the robotic system in the provided challenge document, what would you do to compromise the operation?
3. In your opinion, what are the most vulnerable components? Why?
4. What modifications would you suggest to make the system less vulnerable? In other words, what would you change to reduce the vulnerabilities you identified in Question 3?
5. What would be your motivation to compromise the

described robotic system? Consider the characteristics of the environment where the robot operates and the potential impacts of such compromise on the business processes/continuity.

Six teams, including 19 students, registered and answered the questions in the qualification round. The answers from the participating teams were evaluated considering their technical knowledge, the feasibility of their ideas, the relevance of the answers in the given context, and the breadth of the responses. Based on the evaluation, five teams, including 18 students, were selected for the final round. Four finalist teams were from NYUAD, and one was from King Abdullah University of Science and Technology (KAUST), Saudi Arabia.

3.3 Final Round (Round 2)

3.3.1 Overview of the Final Round

Shortly after announcing the qualification round results, the finalist teams were provided with the robots (i.e., TurtleBot 3 Burger RPi4 4GB) and the peripherals (i.e., fisheye lens camera and camera frame) that they were going to use in the final round. The assembled robot can be seen in Figure 2. They were also provided with instructions (see the GitHub repository [20] for more details) to set up their robots and an IMG (.img) file with which they could flash the SD cards of their robots. The provided IMG file included a ROS system (ROS Noetic), including the ROS nodes, similar to the one used in the

final round. They had one month (from October 12 to November 11, 2022) to set up the robot and the ROS system to get familiar with them, research more on the given challenges, detail their ideas, and test their feasibility.



Figure 2. The robot provided to the finalist teams to be used in the final round

The final round took place on November 11, 2022, at NYUAD (see Figure 3 for the final round setup, including the arenas for the robots), with the attendance of four teams (16 students) since one of the finalist teams withdrew from the competition. The robots were collected from the teams one day before the competition and reset by the organizing team to have the final round system and settings. Moreover, an individual Wi-Fi network for each team was set up to prevent any interruptions among the teams while performing their attacks. The finalists had to bring their personal computers to the final round to perform their attacks. The final round took four hours, including 30 minutes for preparation/set up, two and a half hours for competition and judging, and one hour for poster presentations and judges' deliberations. Each team had to make a 10-minute poster presentation to summarize what they intended to do and what they could achieve.



Figure 3. The final round setup, including the different groups and arenas (square boxes) for the robots

The final round consisted of six judges, including one from the organizing team. The other five judges had different backgrounds to cover the robotics, cybersecurity, and construction aspects of the competition. One of the judges was a post-doctoral researcher specializing in robotics, another judge was a cybersecurity research engineer, two were from construction companies based in the UAE, and the fifth judge was a consultant working on forensic technology. The judges determined the winners based on the evaluation criteria explained in the following subsection.

3.3.2 Evaluation Criteria

The evaluation criteria (see [20] for the details) aimed to test the extent to which finalist teams are able to compromise the given system while being creative and thinking outside the box. The criteria were designed in consultation with the researchers from the Center for Cybersecurity (CCS) at NYUAD based on their expertise in the field and experiences in organizing cybersecurity competitions. There were seven criteria totaling 100 points and a bonus of up to 15 points. Therefore, the team scoring the highest out of 115 points (100 + 15) was chosen as the first-place team. The first five criteria were based on the targets that the teams were supposed to achieve during the competition and did not depend on the judges' personal opinions. However, each team was responsible for proving the achieved targets to the judges to receive the corresponding points. Moreover, each of these five criteria had sub-criteria to achieve a more detailed scoring. The teams could have physical access to the robot, Wi-Fi router, and external computer; however, half of the regular score was given if the team achieved a goal by utilizing a physical attack.

The last three criteria, including the bonus points (totaling 40 points), depended on the judges' opinions based on the teams' performances and poster presentations. Therefore, the poster presentations and the teams' ability to explain what they targeted and what they could achieve had an essential role in the final scores. All criteria—without including the sub-criteria—are as follows:

1. Did the team need the Wi-Fi password to proceed with the competition? (10 Points)
2. Is the team able to acquire/access the data collected by the robot and stored in the temporary or final storage? (15 Points)
3. Is the team able to alter/modify the data collected by the robot? (20 Points)
4. Is the team able to alter the predefined path or the functionality (i.e., preventing it from taking images) the robot should follow? (15 points)
5. Is the team able to compromise the availability of the robot? (15 Points)
6. Technical difficulty/sophistication of the utilized

- techniques (15 points)
7. Creativity (wow factor) (10 points)
 8. Other/bonus points (15 points)

3.3.3 Main Outcomes of the Final Round

During the final round, each team tried to implement their ideas from the qualification round and achieve the targets provided in the list of evaluation criteria by utilizing different techniques. While all the teams achieved some of the targets, others remained unachieved. For example, the first criterion required the teams to proceed with the competition without asking for the Wi-Fi password to achieve the maximum score. If the team asked for a list of possible passwords, they received a partial score. Finally, they did not receive any points if they asked for the correct password. All teams received a partial score for this criterion since all asked for the list of possible passwords. Most of them asked for it after a long duration of trying, utilizing dictionary attacks and brute force attacks. It shows that the level of difficulty for achieving the maximum score for this criterion was too high, considering the resources and time the teams had.

The second and third criteria that required teams to access and alter the collected data (i.e., photos taken by the robot's camera) could not be achieved by any teams. The main reason for this is the long duration spent on the first criterion that delayed the successful completion of the remaining targets. This showed the organizers that reducing the first criterion's difficulty could give the teams more time to spend on the other targets, or the teams would benefit from asking for the list of possible Wi-Fi passwords earlier at the competition. The fourth criterion (i.e., altering the predefined path or functionality) was achieved by two teams; however, both teams could achieve it by having physical access to the robot. For this reason, both teams received half of the standard score for this criterion. The only target fully achieved by all the teams was compromising the availability of the robot (i.e., the fifth criterion). Most teams used deauthentication attacks to disconnect the robot from the network and make it unavailable.

3.4 Results

Five out of six teams that attended the qualification round provided answers to the open-ended questions. These answers were analyzed using the qualitative data analysis software, MAXQDA, to find the most frequently mentioned words and word combinations. The words, such as determiners (e.g., the, this, each), pronouns (e.g., she, they), and auxiliary verbs (e.g., am, is, are) that do not have a contribution in the analysis were removed before analyzing the word frequencies. The result showed that the most commonly used word was "robot" (n=66). Other frequently used words include "attack(s)" (n=60), "access" (n=39), "attacker(s)" (n=28), "data"

(n=25), "ROS" (n=20), "master" (n=18), "network" (n=18), and "information" (n=17). None of these words are unexpected, considering the competition's context and the robotic system provided. Some frequently used words, such as "network", "ROS", "authentication" (n=13), "communication" (n=11), "router" (n=11), "sensors" (n=10), and "firmware" (n=10), show the most commonly targeted elements and functionalities of the robotic system by the participants. Besides the individual words, frequently used word combinations were identified as well. The most frequently mentioned ones were "robotic agent" (n=6), "construction site" (n=5), "direct access" (n=5), "information about" (n=5), and "access point" (n=4). Having "construction site" as a commonly used word combination shows that the participants considered the described construction environment while drafting their responses.

The finalist teams included the attacks and techniques they planned to use in their final poster presentations. These attacks and techniques planned to be conducted in the final round were categorized using the CIA Triad, which stands for Confidentiality, Integrity, and Availability [21], based on the security aspect that the attack mainly aims to compromise. Most cyberattacks affect more than one principle of the CIA triad. For this reason, this categorization intends to show the main focus of the attacks rather than covering all the impacted principles. This categorization can be seen as follows:

- **Confidentiality:** Packet sniffing, targeted packet sniffing, brute-force cracking, backdoor attack.
- **Integrity:** Packet modification attack, steganography.
- **Availability:** SYN-ACK flood denial of service (DoS) attack, deauthentication attack, ARP poisoning attack.

The attacks categorized above are mostly generic, not particularly targeting ROS-based systems and robots. Some examples of sophisticated attacks targeting ROS, which were partially presented by a finalist team, were suggested by Dieber et al. [22]. These attacks include the following:

- **Stealth Publisher Attack:** The mode of communication in ROS is based on a publish-subscribe pattern [10]. This attack targets injecting incorrect data into a running ROS application and tricking another ROS node into using the falsified data from this node. The subscriber is isolated from the regular publishers and forced into receiving data from the exploited publisher.
- **Action Person-in-the-Middle Attack:** One of the communication patterns in ROS is actions [10]. ROS actions are used for long-running and preemptable tasks, such as taking a laser scan. This attack utilizes the traditional Person-in-the-Middle attack to compromise ROS actions. The attacker aims to intercept the communication between the action client and the action server to publish malicious messages.

- **Service Isolation Attack:** ROS uses a client-server / request-reply way of communication as well, using services [10]. In this attack, the attacker aims to isolate a ROS service from the rest of the network and call it later for malicious purposes.
- **Malicious Parameter Update Attack:** Parameter API in ROS networks manages global configuration parameters [10]. One of the methods for a ROS node to get a parameter's value is to subscribe to a particular parameter, which requires the node to store the value in a local variable [22]. This attack exploits this method by maliciously updating the parameter value locally and not making any changes in the globally accessible parameter server.

3.5 Contributions to Construction Cybersecurity

The HMR competition is intended to (1) raise awareness about the increasing cybersecurity problems in the construction industry, (2) attract the cybersecurity community's attention to construction, and (3) utilize the cybersecurity skills and knowledge of students to solve construction-related problems while contributing to their learning process.

Considering the feedback from the judges of the competition from the construction industry, they agreed that this event helped point out some of the cybersecurity issues that are not always well-considered (or known) in construction projects. Although it is beyond the scope of this paper to assess the effectiveness of the event in improving cybersecurity awareness in the construction industry in general, it is reasonable to assume that this and future publications related to the competition and future editions of the HMR events will contribute to achieving that goal. Organizing the event as part of the world's most comprehensive student-led cybersecurity event helped achieve the second goal. Even though HILTI organized a construction cybersecurity event in 2022 [23], HMR was the first academic-driven event with the same focus, making it an important milestone in making the construction industry a part of cybersecurity efforts. The event included cybersecurity experts as judges and was prepared in collaboration with the CCS at NYUAD, contributing to the second goal. Finally, the third goal was achieved by challenging the students to tackle real-life cybersecurity issues related to robotics. The robots in the competition used ROS, which is a commonly used middleware suite. It helped students gain knowledge about ROS and discover potential security problems. The feedback from the students also showed that the competition helped them develop their skills and learn more about cybersecurity and robotics.

The research question of this study was "Is it possible to identify cybersecurity vulnerabilities of construction robots through a competition?", as presented at the

beginning of the paper. Based on the presented preliminary results from the competition and the feedback from the judges, collaborating cybersecurity experts, and attending students, it is possible to identify such vulnerabilities through a cybersecurity competition, such as HMR, which gathers large groups of people to solve an industry-specific problem. However, there are many areas for improvement and future work to achieve this target, which will happen in the following editions of the event.

4 Conclusions and Future Work

A crucial part of the digital transformation in the construction industry includes using robots to handle repetitive, labor-intensive, time-consuming, or dangerous tasks on construction sites. Even though construction robots are still not ubiquitous in projects, there have been considerable efforts from the industry and academia. Besides the benefits of robotics, such as increased productivity, improved safety, and higher accuracy, cybersecurity concerns are raised by the construction community. To address these concerns, the first student-led and academic-driven cybersecurity competition in the construction context, HMR, was organized by the S.M.A.R.T. Construction Research Group at NYUAD as a part of CSAW'22 MENA. The competition had two rounds, where students were initially challenged to generate ideas to compromise the data and functionality of an autonomous construction progress monitoring robot. The finalist teams chosen based on their answers in the first round were required to implement their ideas on a small-scale robot (i.e., TurtleBot 3 Burger) equipped with a camera that simulates a real progress monitoring robot. This paper presents an overview of the competition, its motivation, and its contributions.

Construction is still not a part of cybersecurity studies, and cybersecurity is still not the focus of construction studies. Therefore, one of the significant contributions of HMR was bringing the attention of the cybersecurity community to the construction sector while raising cybersecurity awareness within the construction community. Since HMR was the first robot hacking competition of CSAW, it also gave students a chance to learn more about robotics and the cybersecurity aspects of robotic platforms and ROS. They were required to think about cybersecurity in the construction context, which offered them an additional perspective.

As a part of future work, this paper will be extended to a journal article to include detailed analyses of the data collected during the competition. The collected data consists of the responses from the participants in the qualification round, the poster presentations (i.e., the content of the poster and the transcription of the presentation), and the responses of the finalist teams to

the follow-up questionnaire. Another significant future work is to improve the competition, considering the lessons learned and areas for improvement—including the suggestions from the finalists—and organize it annually with new challenges and robotic systems. The competition will focus on a different robot every year to draw attention to the cybersecurity aspects of automating different construction tasks.

Acknowledgment

The HMR competition was organized by the S.M.A.R.T. Construction Research Group with the support and collaboration from the Center for Cybersecurity (CCS) at NYUAD and the Center for AI and Robotics (CAIR) at NYUAD, which provided technical and financial support for the event. Special thanks are given to Prof. Ramesh Karri, Prof. Ozgur Sinanoglu, Prof. Mihalís Maniatakis, Prof. Farshad Khorrami, and Dr. Prashanth Krishnamurthy. The organizers of the HMR competition included the authors of this paper and two other researchers from the S.M.A.R.T. Construction Research Group: Xinghui Xu and Dr. Samuel A. Prieto. The authors would also like to thank them for their efforts in organizing the event. Finally, the authors thank all the competitors for their interest and all the judges of HMR—Nader Kayali from Accuracy, Sabyasachi Jana from ALEC, Dr. Daniel Feliu Talegon from Khalifa University, Christoforos Vasilatos from NYUAD's CCS, and Ebrahim Hamed from Aldar—for their valuable contributions to the event.

References

- [1] Agarwal R., Chandrasekaran S., and Sridhar M. Imagining construction's digital future. *McKinsey&Company*, (Exhibit 1), 2016.
- [2] McKinsey&Company. Highlights from McKinsey's 2021 sector research. 2021.
- [3] Prieto S. A., García de Soto B., and Adan A. A Methodology to Monitor Construction Progress Using Autonomous Robots. In *Proceedings of the 37th International Symposium on Automation and Robotics in Construction (ISARC 2020)*, pages 1515-1522, Kitakyushu, Japan, 2020.
- [4] Zhang L. *et al.* An autonomous excavator system for material loading tasks. *Science Robotics*, 6(55):3164, 2021.
- [5] Xu X., Holgate T., Coban P., and García de Soto B. Implementation of a Robotic System for Overhead Drilling Operations: A Case Study of the Jaibot in the UAE. In *Proceedings of the 38th International Symposium on Automation and Robotics in Construction (ISARC 2021 Online)*, pages 661-668, Dubai, UAE, 2021.
- [6] Ciampa E., De Vito L., and Rosaria Pecce M. Practical issues on the use of drones for construction inspections. *Journal of Physics: Conference Series*, 1249(1):12016, 2019.
- [7] Watson S. Cyber-security: What will it take for construction to act? *Construction News*. On-line: <https://www.constructionnews.co.uk/tech/cyber-security-what-will-it-take-for-construction-to-act-22-01-2018/>, Accessed: 07/01/2023.
- [8] Andersson J. *et al.* A Security Analysis of Radio Remote Controllers for Industrial Applications. 2019. On-line: https://documents.trendmicro.com/assets/white_papers/wp-a-security-analysis-of-radio-remote-controllers.pdf, Accessed: 07/01/2023.
- [9] BBC News. Hack attack causes “massive damage” at steel works. *BBC News*. On-line: <https://www.bbc.com/news/technology-30575104>, Accessed: 17/03/2023.
- [10] Zhu Q., Rass S., Dieber B., and Mayoral-Vilches V. Cybersecurity in Robotics: Challenges, Quantitative Modeling, and Practice. *Foundations and Trends in Robotics*, 9(1):1–129, 2021.
- [11] Salami Pargoo N. and Ilbeigi M. A Scoping Review for Cybersecurity in the Construction Industry. *Journal of Management in Engineering*, 39(2):3122003, 2023.
- [12] Zheng R., Jiang J., Hao X., Ren W., Xiong F., and Zhu T. CaACBIM: A context-aware access control model for BIM. *Information*, 10(2):47, 2019.
- [13] Boyes H. Security, Privacy, and the Built Environment. *IT Professional*, 17:25–31, 2015.
- [14] Sonkor M. S. and García de Soto B. Operational Technology on Construction Sites: A Review from the Cybersecurity Perspective. *Journal of Construction Engineering and Management*, 147(12):4021172, 2021.
- [15] Prior G. Interserve hit with £4.4m fine after cyber attack. *Construction Enquirer*. On-line: <https://www.constructionenquirer.com/2022/10/24/interserve-hit-with-4-4m-fine-after-cyber-attack/>, Accessed: 05/01/2023.
- [16] García de Soto B., Turk Ž., Maciel A., Mantha B. R. K., Georgescu A., and Sonkor M. S. Understanding the Significance of Cybersecurity in the Construction Industry: Survey Findings. *Journal of Construction Engineering and Management*, 148(9):4022095, 2022.
- [17] Sonkor M. S., Xu X., Prieto S. A., and García de Soto B. Vulnerability Assessment of Construction Equipment: An Example for an Autonomous Site Monitoring System. In *Proceedings of the 39th International Symposium on Automation and Robotics in Construction (ISARC 2022)*, pages 283-290, Bogotá, Colombia, 2022.
- [18] Quigley M. *et al.* ROS: an open-source Robot Operating System. In *ICRA workshop on open source software*, 3(3.2), 2009.
- [19] Mayoral-Vilches V., White R., Caiazza G., and Arguedas M. SROS2: Usable Cyber Security Tools for ROS 2. In *2022 IEEE/RSJ International Conference on Intelligent Robots and Systems (IROS)*, pages 11253–11259, Kyoto, Japan, 2022.
- [20] S.M.A.R.T. Construction Research Group. Hack My Robot. *GitHub*. On-line: https://github.com/SMART-NYUAD/hack_my_robot/tree/hmr_2022, Accessed: 07/01/2023.
- [21] ISO/IEC. ISO/IEC 27001:2013 - Information technology - Security techniques - Information security management systems - Requirements. 2013. On-line: <https://www.iso.org/standard/54534.html>, Accessed: 17/03/2023.
- [22] Dieber B. *et al.* Penetration Testing ROS in Robot Operating System (ROS) - The Complete Reference (Volume 4), 183–225, A. Koubaa, Ed. Springer International Publishing, Cham, 2020.
- [23] HILTI. Hilti IT Competition 2022. *HILTI*. On-line: <https://itcompetition.hilti.group/2022/index.html>, Accessed: 20/03/2023.

HLE-SLAM: SLAM for overexposed construction environment

Xinyu Chen¹ and Yantao Yu¹

¹Department of Civil and Environmental Engineering, Hong Kong University of Science and Technology

xchengl@connect.ust.hk, ceyantao@ust.hk

Abstract -

One of the main challenges in the visual simultaneous localization and mapping (V-SLAM) of construction robots is robustness to overexposure conditions. The main difficulties arise from sensor exposure limitations that cause images to lose information. In addition, construction robots can hardly track enough points in overexposure conditions due to the assumption of constant brightness in SLAM. We propose a High and Low Exposure SLAM (HLE-SLAM) system to recover missing information in overexposed frames. Our method uses frame exposure fusion to generate globally well-exposed frames. It uses exposure, contrast and information entropy as indicators to select the best part of brightness and information in high and low exposed frames. We adopt the Shi-Tomasi and Kanade-Lucas-Tomasi (KLT) sparse optical flow algorithms to improve the ability to detect and track feature points in the overexposed environment. Experimental results on data sets and real environments show that HLE-SLAM can effectively solve the overexposure problem.

Keywords -

Overexposure; Frames fusion; Simultaneous Localization and Mapping; Construction robots

1 Introduction

The construction industry in industrialized countries has faced severe labor shortages in recent years. Improving the automation of construction projects can solve these challenges[1]. As a result, the development of autonomous robotics and vehicles is increasing for a variety of construction applications. Nowadays, SLAM systems are mainly divided into LiDAR SLAM and V-SLAM systems. The V-SLAM system is more suitable for low-cost construction robot platforms due to its low price, low computational complexity, and rich visual information. Although these V-SLAM algorithms have achieved impressive results in a controlled laboratory environment, the robustness of V-SLAM in real-world construction scenarios is a major challenge[2]. In an indoor scene with direct sunlight or when moving from a dimly lit scene to a highly lit scene, overexposure problems occur due to the dynamic limitations of the visual camera.

The dynamic range of a camera is usually determined by fixed parameters or proprietary algorithm. The built-in control algorithms are generally suitable for situations where lighting conditions are constant or change only slowly. For scenes with changing lighting conditions, the automatic exposure camera will result in poorer exposure

images. The algorithms of V-SLAM are set for certain ideal environments, such as constant light intensity and rich textures. In other words, construction robots lose their localization and recognition capabilities in overexposed scenes. Complex lighting scenario on construction site is a major challenge for robot path planning. Nowadays, there are three solutions to reduce the impact of overexposed images on the V-SLAM. The first method relies on the post-processing of overexposed images to reduce variations in light intensity. The second approach uses the invariability of luminance changes in object detection for feature detection and matching. These methods can improve the performance of visual navigation to some extent. However, they cannot compensate for the loss of information caused by overexposed images, and these methods involve additional computational overhead. The third method is to adjust the image exposure parameters using an automatic exposure algorithm[3]. However, adjusting the camera response parameters is still a complex problem given different scenes. Improper exposure parameter settings can also result in low-light images.

In this paper, we propose a High and Low Exposure SLAM (HLE-SLAM) system to recover the overexposed images, which helps construction robots in localization and mapping. We use two cameras with different exposure settings to record videos simultaneously and repair the overexposed by exposure fusion. We calculate the exposure, contrast and information entropy values of different exposure images to generate the fusion weight. Then, we use fusion weight to retain rich frame information in different exposure pictures. After image fusion, we use the Shi-Tomasi[4] method for corner detection and uniformly assign feature points to track in ORB-SLAM2[5]. Finally, we test the HLE-SLAM system in EuRoc[6] dataset and construction environment. Experiments show that our proposed method has better location performance in both simulated overexposed environment datasets and real indoor overexposed construction environments.

2 Methodology

The flow of the proposed method is shown in Figure1. The HLE-SLAM system mainly consists of three parts: dual camera frame acquisition and alignment, frame ex-

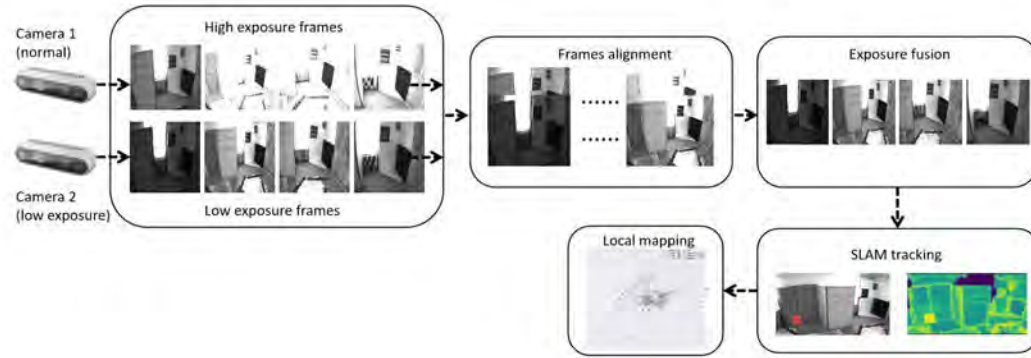


Figure 1. Architecture of the proposed HLE-SLAM.

posure fusion, feature extraction, tracking and local mapping.

A. Dual camera frame acquisition and alignment

We use two Intel RealSense Depth D435 cameras for synchronous data acquisition, and the acquisition frequency is both 20Hz. One uses built-in program parameters, and the other controls the overall brightness of the image by limiting the maximum exposure time of the camera. Since the two cameras are arranged vertically, there is a difference of several pixel values in the vertical direction. We achieve the overall alignment of the image by removing the non-overlapping pixel values in the top and bottom frames.

B. Frame exposure fusion

Frame exposure fusion produces globally well-exposed images by preserving the best-displayed parts of the high and low-exposed sequences. The frame contains colourless areas due to underexposure and overexposure. These areas should be weighted less, while areas containing good light intensity and picture information should be retained. We select the best brightness part of the two pictures using three index parameters: exposure, contrast, and information entropy. The final image is determined using an average weighting method.

Exposure: By calculating the intensity of the gray image, the exposure of the pixel value can be judged. We want to keep frame intensities that are not near zero (underexposed) or one (overexposed). We use the following Gaussian curve:

$$\exp\left(-\frac{(i-0.5)^2}{2\sigma^2}\right) \quad (1)$$

to set the weight of each pixel according to how close its intensity i is to 0.5. The σ equals 0.2 in our implementation. In this way, we can get the E representing the exposure value.

Contrast: We apply the Laplace filter to each grayscale image and take the absolute value of the filter response.

The Laplace filter is defined as:

$$\nabla^2 f(x, y) = \frac{d^2 f}{dx^2} + \frac{d^2 f}{dy^2}, \quad (2)$$

where $f(x, y)$ is a two-dimensional image. This results in a simple contrast indicator C . It tends to assign high weights to important elements like edges and textures.

Information entropy value: The one-dimensional entropy of the image represents the information contained in the aggregated features of gray distribution in an image. P_i represents the proportion of pixels whose gray value is i in the image, and then the unary gray entropy is defined as:

$$H = \sum_{i=0}^{255} P_i \cdot \log P_i, \quad (3)$$

Where H is the unary gray information entropy, and P_i is the proportion of grey value i . When the image is overexposed/dark (white or black), there is only one grey value. Then the entropy is the minimum, $H = 0$. The rich information of images is conducive to feature extraction of V-SLAM. We divide the whole image into 16×16 blocks and calculate the information entropy of each block. Then, we assign the calculated information entropy value of each block to all pixels within that block, representing their information entropy value. On this basis, we generate the corresponding weight value and save the larger information entropy part. By using multiplication, we combine the information from the different index parameters into a scalar weight map. The linear combination weighting method is used to control the influence of each measure part, and the weight of each picture is generated by the following formula:

$$W_{i,j,k} = \omega_c(C_{i,j,k}) \cdot \omega_e(E_{i,j,k}) \cdot \omega_h(H_{i,j,k}), \quad (4)$$

where C , E and H are contrast, exposure and information entropy. The ω_c , ω_e , ω_h represent the corresponding weight. The subscript i and j , refers to pixel (i, j) in

k(high/low) exposure images. We use equally weighted quality measures ($\omega_c=\omega_e=\omega_h=1$). In extreme lighting situations, such as a large area facing direct sunlight, we adjust the parameters based on field tests.

The fusion image R can then be obtained by a weighted blending of the input high/low exposure images:

$$R_{ij} = \sum_{high-exposure}^{low-exposure} W_{ij,k} \cdot I_{ij,k}, \quad (5)$$

where W means weight map, I means input images.

C. Feature extraction, tracking and local mapping

In this paper, ORB-SLAM2 is selected as a navigation algorithm for construction robots. The ORB-SLAM2 system is based on feature point extraction and matching, but in an overexposed environment, feature points are hardly detected and matched. Therefore, position and pose tracking will fail in a construction site scene with low texture and overexposed scenes. We adopt the Shi-Tomasi and Kanade-Lucas-Tomasi (KLT) sparse optical flow algorithms to solve these problems. The average distribution of feature points in an overexposed environment reduces feature point matching requirements. New points are added if there are not enough points left after the uniform procedure to reach the required 200. The next frame is considered a new keyframe if the difference between the parallaxes of the two frames is significant.

3 Experiments and results

Our work focuses on the visual navigation of construction robots to work reliably in overexposed environments. Therefore, we experiment with the EuRoc MAV dataset and real construction scenes.

A. Public Dataset

In EuRoc MAV datasets, there are some overexposed scenes. These indoor lighting problems are similar to overexposed problems in construction scenes, so they are used to test algorithms in overexposed environments. We artificially increased the exposure value in the MAV to create more obvious overexposure frames. In the dataset experiment, we use the original dataset as the low-light video stream and enhance it to simulate the overexposed video stream.

Therefore, our HLE system use the original and overexposed datasets as input. As shown in Figure 2, we use the HLE method to recover the overexposed frames in MAV datasets. To verify the availability of our method in overexposure, we compare the HLE with original and overexposure frames in SLAM feature point extraction and gradient calculation, as shown in Figure 3. Our method enhances the gradient information of frames and enables the algorithm to detect more feature points.

Table 1 compares the performance of the HLE in



Figure 2. The results of image fusion in MAV datasets.

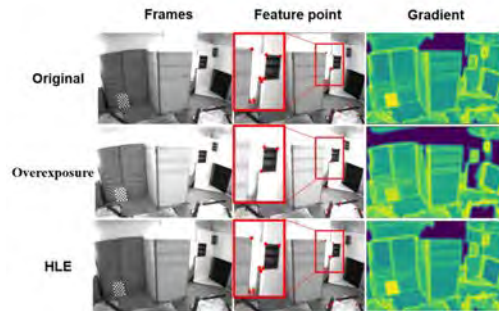


Figure 3. The gradient and feature point results of original, overexposure and HLE method.

Table 1. Performance comparison in the EuRoc MH datasets (Root mean square error in m).

Sequence	Original	Overexpose	HLE
V101	0.055	0.143	0.058
V102	0.064	0.155	0.061
V103	0.096	0.151	0.097
V201	0.046	0.121	0.074
V202	0.057	0.118	0.059

monocular sensors with original and overexposed; all tests are based on the KLT ORB-SLAM2. As shown in the table, raising the exposure value makes the overexposed frames show a more significant estimated error. Our method can reduce the interference caused by overexposure and restore image information to reduce errors. In the V102, the HLE shows better results than the original. Because some low-light images exist in the V102, it is difficult to locate them in the dark environment. The overexposed frames are fused with low-light frames to enhance the low-light frames in the original video. The HLE method outputs frames with stable and continuous brightness and more information, which makes the robot position with smaller error results.



Figure 4. High and low exposure frames captured by the Intel Realsense 435 camera and processed frame in the HLE method.

B. Real-World Experiment

We use the Intel Realsense 435 camera to conduct real experiments in overexposed indoor construction scenes. In our real-world experiment, we capture overexposed images in a direct sunlight environment using an auto-exposed camera, while we use a camera with a shorter exposure time to capture the low-exposure images. Low-exposure frames are difficult to initialize and map. So we only compare the HLE method with the original overexposure frames in the real-world experiment. In Figure 4, we compare the overexposed image with the HLE image. The camera produces some overexposed frames because of the intense light. In frames, overexposure is shown in the balcony doors and windows, and much information is missing. The HLE fuses overexposure frames with low-exposure frames to recover missing information. In order to further verify the performance of our algorithm, we conduct location estimation and mapping experiments. As shown in Figure 5, in the left part of the navigation, the original frames cannot provide enough feature points for tracking and matching, so we cannot locate them effectively in this part. In addition, there is a large deviation in the right corner part.

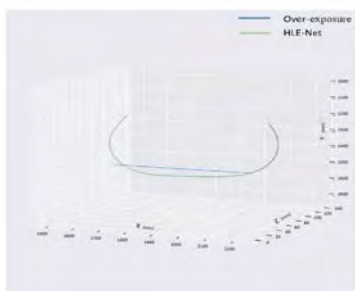


Figure 5. 3D pose graph. The green line is the HLE-SLAM. The blue line is the original overexposure frame.

4 Conclusions

In this paper, an exposure fusion-based construction robot SLAM system is proposed for overexposure problems. The exposure fusion method based on contrast, exposure and information entropy can recover missing information and help the construction robot track the feature points in the overexposed environment. We validate our HLE-SLAM in public datasets and real construction scenes. The results show that our method can effectively solve the problem of location errors caused by overexposed light. Our method can run in real-time on mobile computers and is suitable for various overexposed construction scenarios.

5 Acknowledgement

This work was financially supported by the HKUST-BDR Joint Research Institute Fund, No. OKT23EG01.

References

- [1] Sungjin Kim, Soowon Chang, and Daniel Castro-Lacouture. Dynamic modeling for analyzing impacts of skilled labor shortage on construction project management. *Journal of Management in Engineering*, 36(1):04019035, 2020.
- [2] Xinyu Chen and Yantao Yu. Image illumination enhancement for construction worker pose estimation in low-light conditions. In *Computer Vision—ECCV 2022 Workshops: Tel Aviv, Israel, October 23–27, 2022, Proceedings, Part VII*, pages 147–162, 2022.
- [3] Zichao Zhang, Christian Forster, and Davide Scaramuzza. Active exposure control for robust visual odometry in hdr environments. In *2017 IEEE international conference on robotics and automation (ICRA)*, pages 3894–3901. IEEE, 2017.
- [4] Jianbo Shi et al. Tomasi. good features to track. In *1994 Proceedings of IEEE Conference on Computer Vision and Pattern Recognition*, pages 593–600. sn, 1994.
- [5] Raul Mur-Artal and Juan D Tardós. Orb-slam2: An open-source slam system for monocular, stereo, and rgb-d cameras. *IEEE transactions on robotics*, 33(5):1255–1262, 2017.
- [6] Michael Burri, Janosch Nikolic, Pascal Gohl, Thomas Schneider, Joern Rehder, Sammy Omari, Markus W Achtelik, and Roland Siegwart. The euroc micro aerial vehicle datasets. *The International Journal of Robotics Research*, 35(10):1157–1163, 2016.

AprilTag detection for building measurement

Kepa Iturralde^a, Juncheng Shen^a, Thomas Bock^a

^aChair of Building Realization and Robotics, School of Engineering and Design, Technical University of Munich, Germany

E-mail: kepa.iturralde@br2.ar.tum.de

Abstract

Building façade renovation with prefabricated panels requires the installation of supporting connectors. Obtaining the exact locations and angles of the connectors is currently a time-consuming activity. The new method presented in this paper uses AprilTag markers as targets on the wall and measures them based on a photogrammetry concept. The 3D coordinates of the targets are estimated by our algorithm, and then we can obtain the location and direction of each connector. Current results are promising but still need some improvement. Our goal is to measure the exact position and angle of each marker, and the error should not exceed 1mm at about 10m away from the building. This objective is not reached in this paper, but latest advances show very close results.

Keywords –

AprilTags, detection, measure

1 Introduction

When placing prefabricated modules with solar panels on existing buildings, it is important to know the location of the connectors or anchors so the modules fit them with high accuracy. Measuring the location of connectors with Total Station is a time consuming process. Therefore, visual or photograph based methods can be a solution to capture the location of the connectors in an automated manner.

Visual fiducials are artificial landmarks designed to be easy to recognize and distinguish from one another. Although related to other 2D barcode systems such as QR codes [1], they have significantly goals and applications. With a QR code, a human is typically involved in aligning the camera with the tag and photographs it at fairly high-resolution obtaining hundreds of bytes, such as a web address. In contrast, a visual fiducial has a small information payload (perhaps 12 bits) but is designed to be automatically detected and localized even when it is at very low resolution, unevenly lit, oddly rotated, or tucked away in the corner of an otherwise cluttered image.

Unlike 2D barcode systems in which the position of the barcode in the image is unimportant, visual fiducial systems provide camera-relative position and orientation of a tag. Fiducial systems also are designed to detect multiple markers in a single image [2]. Visual fiducial systems are perhaps best known for their application to augmented reality, which spurred the development of several popular systems including ARToolkit [3] and ARTag [4]. Real-world objects can be augmented with visual fiducials, allowing virtually generated imagery to be super-imposed. Similarly, visual fiducials can be used for basic motion capture [5]. AprilTag is a kind of fiducial marker as a black-and-white square tag with an encoded binary payload. Usually, those fiducial markers are placed in the space, and a camera takes photos of them. The photos can tell the pose information relative to the camera, while the ids of different tags can be recognized [6]. One paper compared the performance of various fiducial markers including ARTag, ArUco, Stag and AprilTag [7] AprilTag performs well in terms of position, orientation, and detection rate. Therefore, we chose AprilTag as the positioning marker for our project. This research is part of the ENSNARE project [8].

2 Research Gaps and Approach

When it comes to detection of visual fiducials, it is important to have a technique that is not only efficient but also consumes less time than current target measurement with, for instance, Total Stations. The Research Gap found in this field is that there are no existing methods to detect AprilTags using stereo vision. The rest of the paper provides in detail solutions to help tackle these research gaps.

The AprilTag detection process can be described as the following steps as also described in Figure 1:

- Camera and markers preparation
- Image pre-processing
- Geometry extraction
- Marker localization

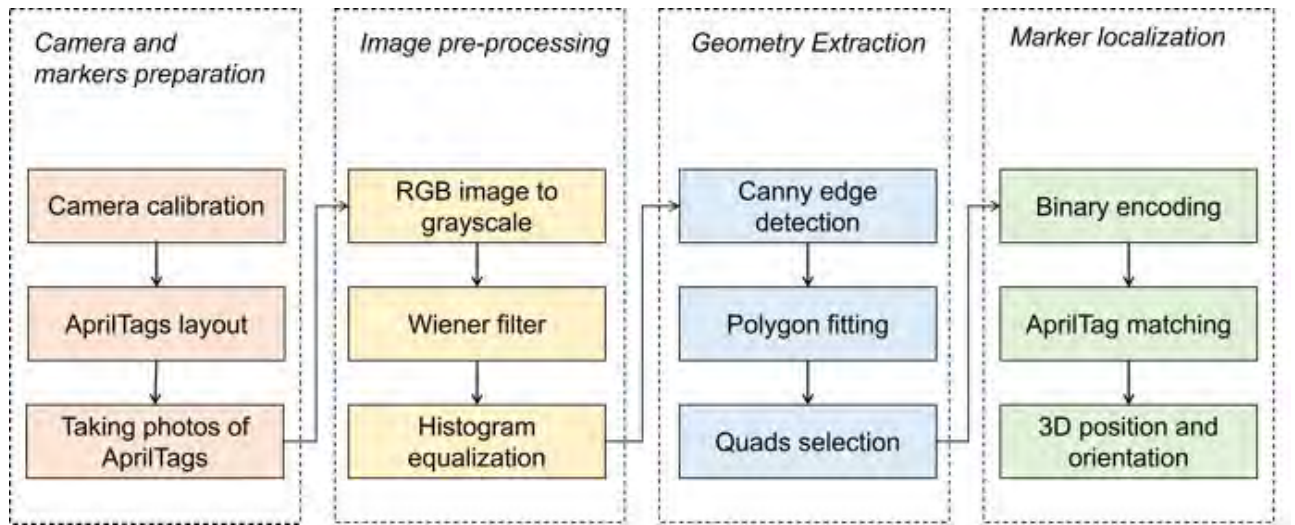


Figure 1. The process flow chart for AprilTag detection

Four steps are employed in the AprilTag detection:

- The color photos of targets are converted to grey.
- Noises are reduced by using an adaptive low pass Wiener filter.
- Contrast is enhanced using Histogram equalization [9]] to ensure the images are of the ideal brightness.
- Canny edge detection algorithm is used to get the edges, fit the edges into several closed polygons and filter out the unqualified polygons, leaving only the quads.

The candidate quads are binary encoded and if they match successfully with the AprilTag library, their IDs, and the pixel positions of the 4 corners can be output. Finally, SolvePnP [10] (perspective-n-point) method is used to solve the 3D position and orientation of each marker according to the 4 corners, marker size, and the camera calibration matrix.

The recognition distance d of Apriltag is related to many factors [11]:

$$d = \frac{f \times h_r \times I_p}{h_p \times S_s \times c} \quad (1)$$

where f is the focal length of the camera in mm, h_r is the real height of the AprilTag in mm, I_p is the height of image sensor in pixels, h_p is the AprilTag height in pixels and S_s is the image sensor's height in mm. c is a constant to change the unit scale. After a comprehensive reference to the formula and considering the need to measure outdoors, we decided to use a full-frame digital camera Sony A7R4 with different lens for target detection.

We can obtain translation matrix t and rotation matrix R of each Apriltag based on four corner coordinates in the image. Written as a transformation matrix in the form of

$$T = \begin{bmatrix} R_{11} & R_{12} & R_{13} & t_1 \\ R_{21} & R_{22} & R_{23} & t_2 \\ R_{31} & R_{32} & R_{33} & t_3 \\ 0 & 0 & 0 & 1 \end{bmatrix} \quad (2)$$

Suppose there are two targets, and their transformation matrices are T_A and T_B , then the transformation matrix of the latter in the former coordinate system is

$$T_{B \text{ in } A} = T_A^{-1} * T_B \quad (3)$$

Initially, the center of the bottom left target (id: 1) is chosen as the origin and convert the coordinates of the rest of the targets to the world coordinate system. The problem is that once there is a small deviation in the position and angle of the world coordinate system, the deviation will increase after the remaining coordinates are converted into it. The solution is that we use 4 AprilTag (1 to 4) as a big origin.

There are 16 corner points in total, and we know the exact position between them, then we can use SolvePnP to get their pose matrix more precisely. Figure 2 depicts the method of using AprilTags to form a big origin.

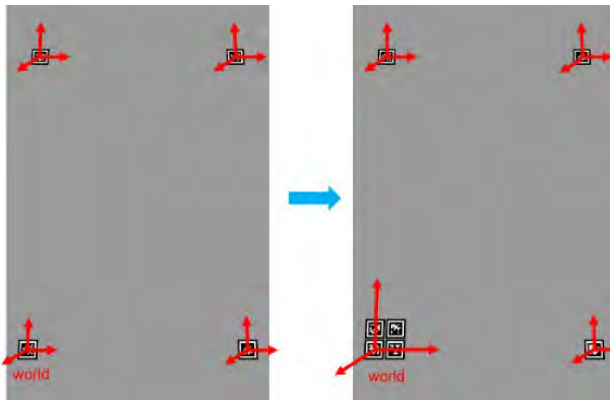


Figure 2. AprilTag to form a big origin

In the real test, one very serious factor that affects accuracy is the size of the AprilTag in the image. When we photographed a 15m building, our 200mm x 200mm AprilTag was very small and unclear in the frame. Therefore, we take photos from different angles, one image contains only 4 adjacent AprilTags and all images cover the entire facade. The advantage of this method is that each target in the photo is as large as possible Figure 3 depicts shooting local targets.



Figure 3. Shooting local targets

The camera needs to be calibrated after each shot because the focal length changes when shooting.

Image pre-processing is performed with the python OpenCV. Noise is reduced from the read images, and all AprilTags are detected from the different images. The transformation matrix, id and 2D coordinates of the corners of each AprilTag are obtained. If the image contains the big origin ($id \leq 4$), the exact transformation matrix is got with SolvePnP. When this is not the case, the coordinate system of the rest of the AprilTags is converted to the coordinate system of the bottom left AprilTag of the current image. All coordinate systems are then unified into the world coordinate system. The 3D coordinates, as well as the Euler angles from the rotation matrix, are acquired from the transformation matrix. Figure 4 explains the process of the algorithm employed:

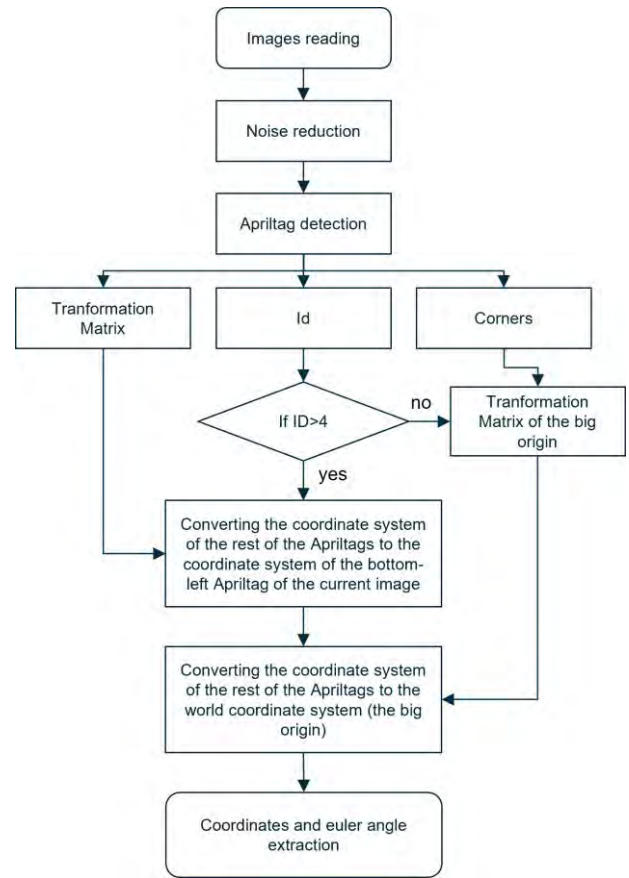


Figure 4. AprilTag position extraction process

After extensive testing, the accuracy of the method is as follows. The accuracy is fair in the case of low floors and decreases with the height of the floor as explained in Table 1.

Table 1. The accuracy of the algorithm

Target height	Translation deviation	Angle deviation
2.8m	2mm to 3mm	0.05°
6.1m	2mm to 5mm	0.1°
8.9m	7mm to 9mm	0.2°
12.1m	20mm	0.6°
15.1m	50mm	1°

These results are still optimal but open the way for further development.



Figure 5. Experimental setup for AprilTag detection

An experiment was conducted to verify the AprilTag detection algorithm as seen in Figure 5.

3 Conclusion

The algorithm to detect the AprilTags precisely was described in the paper. Experimental validation was also provided. The new detection algorithm includes to adjust the 2D detection algorithm and external environment to solve the problem of instability. Calibration was done and was combined with calibration algorithms to get the pose of markers.

The amount of AprilTags that needs a building in order to be measured, depends on the complexity and size of the building. Besides, if the building is covered by vegetation, traffic signals, or other objects, the approach would need to consider taking more and closer range pictures. This problem is common to other data acquisition techniques.

Currently the method is being improved and the results are already better and the main objective (1mm in 10m) is getting close under certain light conditions.

Acknowledgements



This project has received funding from the European Union's Horizon 2020 research and innovation programme under grant agreement No. 958445.

References

- [1] C.-H. Chu, D.-N. Yang, and M.-S. Chen, "Image stabilization for 2D barcode in handheld devices," in *Proceedings of the 15th ACM international conference on Multimedia*, Sep. 2007, pp. 697–706. doi: 10.1145/1291233.1291394.
- [2] E. Olson, "AprilTag: A robust and flexible visual fiducial system," in *2011 IEEE International Conference on Robotics and Automation*, 2011, pp. 3400–3407. doi: 10.1109/ICRA.2011.5979561.
- [3] D. Wagner, G. Reitmayr, A. Mulloni, T. Drummond, and D. Schmalstieg, "Pose tracking from natural features on mobile phones," in *2008 7th IEEE/ACM International Symposium on Mixed and Augmented Reality*, 2008, pp. 125–134. doi: 10.1109/ISMAR.2008.4637338.
- [4] M. Fiala, "ARTag, a fiducial marker system using digital techniques," in *2005 IEEE Computer Society Conference on Computer Vision and Pattern Recognition (CVPR'05)*, 2005, vol. 2, pp. 590–596 vol. 2. doi: 10.1109/CVPR.2005.74.
- [5] A. C. Sementille, L. E. Lourenço, J. R. F. Brega, and I. Rodello, "A Motion Capture System Using Passive Markers," in *Proceedings of the 2004 ACM SIGGRAPH International Conference on Virtual Reality Continuum and Its Applications in Industry*, 2004, pp. 440–447. doi: 10.1145/1044588.1044684.
- [6] J. Wang and E. Olson, "AprilTag 2: Efficient and robust fiducial detection," in *2016 IEEE/RSJ International Conference on Intelligent Robots and Systems (IROS)*, 2016, pp. 4193–4198. doi: 10.1109/IROS.2016.7759617.
- [7] M. Kalaitzakis, S. Carroll, A. Ambrosi, C. Whitehead, and N. Vitzilaios, "Experimental Comparison of Fiducial Markers for Pose Estimation," in *2020 International Conference on Unmanned Aircraft Systems (ICUAS)*, 2020, pp. 781–789. doi: 10.1109/ICUAS48674.2020.9213977.
- [8] "ENSNARE," <https://www.ensnare.eu/>, Jan. 24, 2023.
- [9] M. Abdullah-Al-Wadud, Md. H. Kabir, M. A. Akber Dewan, and O. Chae, "A Dynamic Histogram Equalization for Image Contrast Enhancement," *IEEE Transactions on Consumer Electronics*, vol. 53, no. 2, pp. 593–600, 2007, doi: 10.1109/TCE.2007.381734.
- [10] A. Kriegler and W. Wöber, "Vision-based Docking of a Mobile Robot," Jan. 2020. doi: 10.3217/978-3-85125-752-6.
- [11] S. M. Abbas, S. Aslam, K. Berns, and A. Muhammad, "Analysis and Improvements in AprilTag Based State Estimation," *Sensors*, vol. 19, no. 24, 2019, doi: 10.3390/s19245480.

UAV for target placement in buildings for retrofitting purposes

Kepa Iturralde^a, Wenlan Shen^a, Tao Ma^a, Soroush Fazeli^a, Weihang Li^a, Hünkar Suci^a, Runfeng Lyu^a, Jui Wen Yeh^a, Phillip Hübner^a, Nikhita Kurupakulu Venkat^a, Thomas Bock^a

^aChair of Building Realization and Robotics, School of Engineering and Design, Technical University of Munich, Germany

E-mail: kepa.iturralde@br2.ar.tum.de

Abstract

The use of UAVs in the construction industry is a rather novel concept whose applications are not widespread yet. This research aims to develop a UAV with an end effector used to fix targets on a building façade. With the use of this application, the use of manual force and cranes can be eliminated. The UAV also can reach places with complicated geometry and greater heights which is difficult to be performed manually. The finite element analysis was performed before manufacturing and the flight simulation was performed using ROS. Results are still ongoing but promising.

Keywords –

UAV, end effector, simulation, ROS

1 Introduction

The use of drones in various industries has been on the rise in recent years, and the technology is continuing to evolve and improve. One area of drone technology that has seen significant advancements is the use of 3D printing in the manufacturing of drones. The ability to 3D print drones allows for greater customization, faster production times, and cost savings. The traditional approach used for synthesizing, implementing, and validating a flight control system in [1], [2] for manned aircrafts is time consuming and resource intensive. Applying the same techniques to the small UAVs is not realistic. To reduce the cost and time to market, small UAV systems make use of low cost commercial-off-the-shelf autopilots [3]. These autopilots are often classical Proportional–integral–derivative (PID) controllers and ad-hoc methods are used to tune the controller gains in flight [4]. In this research article, a UAV with an end effector is developed and manufactured. The components of the UAV are manufactured using 3D printing with PLA. The hardware is assembled, and flight simulations is done using ROS. This research is part of the ENSNARE project [5].

2 Research Gaps

UAVs are still not prominently used in the construction industry. This research aims to tackle the following Research Gaps (RGs):

- To place the targets, a heavy operating machine like a crane should be employed, but with the use of a UAV, this can be eliminated. In principle, the UAV is planned to perform with lightweight targets.
- Using a UAV is also time and cost effective than using heavy machinery. According to first simulations, the placement of a target would take about 20 seconds, while with the use of a mobile platform and operators, this would take much longer.

The Apriltag needs to be stuck to the building. We have used a double side tape that performs correctly in the preliminary phases. The rest of this paper aims to provide a solution to develop an unarmed aerial vehicle (UAV) that tackles the above-mentioned RGs.

3 Approach and Results

The UAV was designed with an end effector which is used to place AprilTags on building façades. UAV was designed to be compact, light and have a stable center of gravity. Finite Element Analysis was performed on the body to make sure the material does not undergo fracture during its collision with the building façade as shown in Table 1.

Table 1. Displacement simulation results at various velocities

Velocity (m/s)	Force (N)	Maximum displacement (mm)
1	0.4	0.01668
2	0.8	0.0325
5	2	0.0814

Moreover, in the preliminary studies, the weight of

the end-effector was balanced with the weight of the hardware devices of the UAV, mainly with the battery. This aspect should be further considered in the next steps.

The UAV was manufactured using 3D printing [6]–[9] with PLA [10] as shown in Figure 1. The UAV hardware consists of a battery, brushless motors, rotors, raspberry pi 4 and a Navio2 Flight Controller.



Figure 1. Right, Manufactured UAV model.

Various tests were performed on the end effector to ensure it is efficient in attaching targets on building facades. Tests were also performed to calibrate the hardware of the drone in order to attain a stable center of gravity.

3.1 Flight control

The flight control can be divided into three divisions: Software, Middleware, and hardware.

The main Component of software structure is the controller as seen in Figure 2. To be able to make the drone stable during flight, its necessary to use a controller. As it can be seen in the figure the controller has two inputs, Desired state which comes from a human side with RC controller or from a mission planner, that calculates the desired state in order to accomplish the mission autonomously. On the other hand, Controller tries to calculate the errors and decide required actions that needs to be taken. In our case, controller sends the calculated rpm (rotations per minute) to motors. During flight testing we tried three different controllers:

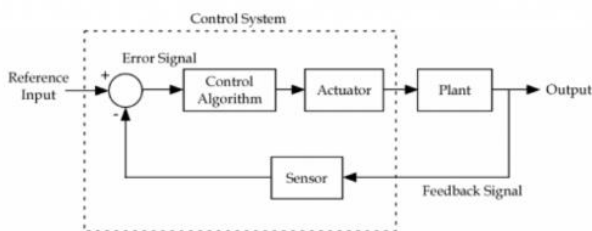


Figure 2. A general flight controller

- Geometric Controller:** This controller as seen in Figure 3 for the quadrotor is generally based on the principle of solving control problems with the geometry of the state space.

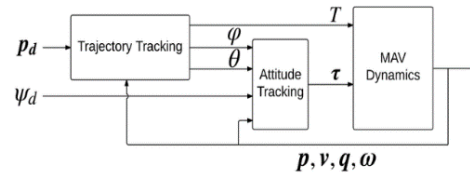


Figure 3. A geometric controller

- PID Controller:** A proportional–integral–derivative controller (PID controller or three-term controller) is a control loop mechanism employing feedback that is widely used in industrial control systems and a variety of other applications requiring continuously modulated control. A PID controller continuously calculates an error value $e(t)$ as the difference between a desired setpoint (SP) and a measured process variable (PV) and applies a correction based on proportional, integral, and derivative terms (denoted P, I, and D respectively). Figure 4 shows the framework of a PID controller

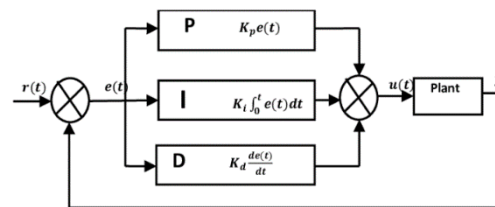


Figure 4. A PID controller

- ArduPilot:** ArduPilot is an open source, unmanned vehicle Autopilot Software Suite, capable of controlling autonomous drones. The ArduPilot software suite consists of navigation software (typically referred to as firmware when it is compiled to binary form for microcontroller hardware targets) running on the vehicle (either Copter, Plane, Rover, AntennaTracker, or Sub), along with ground station controlling software including Mission Planner, APM Planner, QGroundControl.

Robot Operating System (ROS) is an open-source robotics middleware suite. Although ROS is not an operating system (OS) but a set of software frameworks for robot software development, it provides services designed for a heterogeneous computer cluster such as hardware abstraction, low-level device control, implementation of commonly used functionality,

message-passing between processes, and package management. Figure 4 shows the framework of ROS.

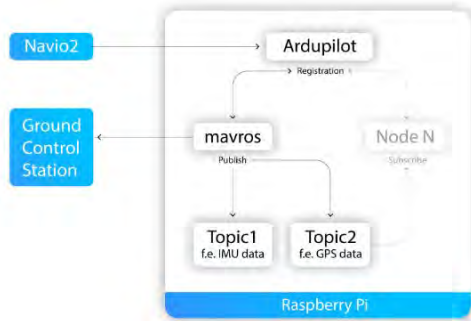


Figure 5. ROS framework

ROS makes communication processes, known as nodes, extremely easy using ROS topics which can be published and subscribed to. Each topic has a certain message type that tells the publisher or subscriber what kind of data can be sent and received from over a topic. In this case it would be possible for the software to communicate with the hardware components such as actuators and sensors.

3.2 Hardware

Every drone has essential hardware components in order to fly, such as flight controller, on-board computer, ESC, Motors, Propellers and Battery.

Flight Controller: The main function of the Flight Controller is to provide control for the Electronic Speed Controller (ESC) to direct the rpm of motors based on inputs from the on-board computer. It has sensors on the board so it can understand how the craft is moving. Using the data provided by these sensors, the FC uses algorithms to calculate how fast each motor should be spinning for the craft to behave

- **On-Board Computer:** Raspberry Pi is a micro-computer at the size of an average credit card for data processing. With the General-Purpose Input Output (GPIO) pins, the Raspberry Pi has high processing capability to run functions like flying a drone. All the algorithms and middleware software are implemented on raspberry pi. Also, on-board computer is connected to flight controller in order to getting the sensor data and sending commands.
- **ESC:** An ESC is a device that interprets signals from the flight controller and translates those signals into phased electrical pulses to determine the speed of a brushless motor. The ESC is graded with the maximum amount of current that it allows to pass through. In this project, a 4-in-1 ESC has been used. A 4 in 1 brushless ESC allows you to move ESCs from the arms of your quadcopter into the center

stack with your flight controller. Compact builds can benefit, as they make wiring a lot simpler, removing the need for a power distribution board and separate BEC in some cases.

- **Motors:** The motors are the main drain of battery power on your quad, therefore getting an efficient combination of propeller and motor is very important. Motor speed is rated in kV, generally a lower kV motor will produce more torque and a higher kV will spin faster
- **Propellers:** Propellers for Drones and UAVs. Propellers are devices that transform rotary motion into linear thrust. Drone propellers provide lift for the aircraft by spinning and creating an airflow, which results in a pressure difference between the top and bottom surfaces of the propeller.
- **Battery:** LiPo batteries are the power sources of the quadcopters. LiPo is used because of the high energy density and high discharge rate. LiPo batteries are rated by their nominal voltage (3.7V per cell), cell count in series, capacity in mAh (ie.1300mAh) and discharge rate (ie. 75C).

3.3 Simulation

The simulation software aims to reproduce the idea we want to realize in the real world with real UAV. The code designing principles follow the idea from [11]. Figure 6 depicts the simulated building with targets on ROS. Figure 7 is the framework of UAV functions.

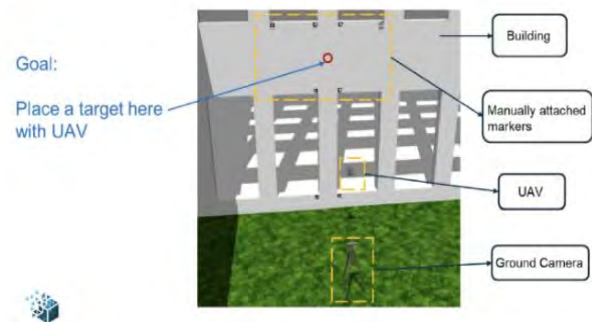


Figure 6. Simulated TUM building with placed target

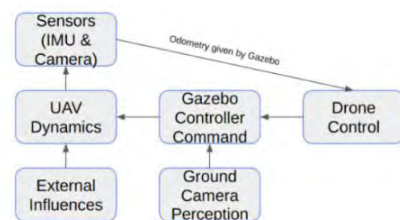


Figure 7. Framework of the UAV functions

The flight simulation on ROS is performed in the following steps.

1. Simulated TUM building environment with placed target.
2. Simulated UAV with the same physical property with design team.
3. Fine-tuned geometry controller to stabilize the drone to a specific position.
4. AprilTag detection algorithm [12] with real-time localization ability.
5. Simulated ground camera with possible extension for accurate target localization.
6. Simulated with real-world joystick.

It was observed through flight simulation that the drone remained stable under various flight conditions.

4 Conclusion

This research paper presents the development of an unmanned aerial vehicle (UAV) with an end effector specifically designed for use in the construction industry. The UAV is equipped with an advanced manipulator arm, which allows for the precise handling of the targets. The UAV and end effector were tested under various scenarios and the end effector has been effective in attaching the targets. The flight control has been calibrated to obtain a good precision. Using the FEM method and 3D printing for the parts has optimized the capabilities of the UAV.

Acknowledgements



This project has received funding from the European Union's Horizon 2020 research and innovation programme under grant agreement No. 958445.

References

- [1] B. L. Stevens 1939-, *Aircraft control and simulation* / Brian L. Stevens, Frank L. Lewis. New York: Wiley, 1992.
- [2] R. W. Pratt, *Flight Control Systems: practical issues in design and implementation*. Institution of Engineering and Technology, 2000. doi: 10.1049/PBCE057E.
- [3] H. Chao, Y. Cao, and Y. Chen, "Autopilots for Small Fixed-Wing Unmanned Air Vehicles: A Survey," in *2007 International Conference on Mechatronics and Automation*, 2007, pp. 3144–3149. doi: 10.1109/ICMA.2007.4304064.
- [4] Y. C. Paw and G. J. Balas, "Development and application of an integrated framework for small UAV flight control development," *Mechatronics*, vol. 21, no. 5, pp. 789–802, 2011, doi: <https://doi.org/10.1016/j.mechatronics.2010.09.009>.
- [5] "ENSNARE," <https://www.ensnare.eu/>, Jan. 24, 2023.
- [6] S. A. M. Tofail, E. P. Koumoulos, A. Bandyopadhyay, S. Bose, L. O'Donoghue, and C. Charitidis, "Additive manufacturing: scientific and technological challenges, market uptake and opportunities," *Materials Today*, vol. 21, no. 1, pp. 22–37, 2018, doi: <https://doi.org/10.1016/j.matod.2017.07.001>.
- [7] Z.-X. Low, Y. T. Chua, B. M. Ray, D. Mattia, I. S. Metcalfe, and D. A. Patterson, "Perspective on 3D printing of separation membranes and comparison to related unconventional fabrication techniques," *J Memb Sci*, vol. 523, pp. 596–613, 2017, doi: <https://doi.org/10.1016/j.memsci.2016.10.006>.
- [8] M. A. Caminero, J. M. Chacón, I. García-Moreno, and G. P. Rodríguez, "Impact damage resistance of 3D printed continuous fibre reinforced thermoplastic composites using fused deposition modelling," *Compos B Eng*, vol. 148, pp. 93–103, 2018, doi: <https://doi.org/10.1016/j.compositesb.2018.04.054>.
- [9] X. Wang, M. Jiang, Z. Zhou, J. Gou, and D. Hui, "3D printing of polymer matrix composites: A review and prospective," *Compos B Eng*, vol. 110, pp. 442–458, 2017, doi: <https://doi.org/10.1016/j.compositesb.2016.11.034>.
- [10] "Francofil – ECO PLA Filament - Filamentworld," https://www.filamentworld.de/shop/pla-filament-3d-drucker/francofil-pla-kaffee-filament-1-75-mm/?dTribeID=veXm51HUzdJXNn9Pq1qOOU0FPzvXxjTD%7Cadtribes%7C103307&utm_source=Google%20Shopping&utm_campaign=Google%20Feed%202&utm_medium=cpc&utm_term=103307&gclid=103307, Jan. 24, 2023.
- [11] F. Furrer, M. Burri, M. Achtelik, and R. Siegwart, "RotorS – A Modular Gazebo MAV Simulator Framework," in *Studies in Computational Intelligence*, vol. 625, 2016, pp. 595–625. doi: 10.1007/978-3-319-26054-9_23.
- [12] E. Olson, "AprilTag: A robust and flexible visual fiducial system," in *2011 IEEE International Conference on Robotics and Automation*, 2011, pp. 3400–3407. doi: 10.1109/ICRA.2011.5979561.

BIM Implementation Strategy- A proposal for KMRL

Dona James¹, Berlin Sabu² and Dyna James³

^{1,2,3}Mar Athanasius College of Engineering, Kothamangalam

donamariajames22@gmail.com, berlinsabu@mace.ac.in, dynamargretjames@gmail.com

Abstract –

The implementation of Building Information Modelling (BIM) is a widely adopted pattern of revolution in the construction sector and the results gained through BIM adoption in multidisciplinary projects are well pronounced. Even though BIM is a widely accepted technique, its adoption in Kerala, especially for Kerala government projects is rare.

Kochi Metro Rail Limited (KMRL) is one of the rapid transit systems serving the city of Kochi in Kerala and now its 2nd phase has obtained approval. Taking advantage of its current status, this research aims to develop an effective implementation strategy for BIM adoption in the 2nd phase of the Kochi Metro Rail project. This research also focuses to develop the key contents of the BIM Execution Plan (BEP) - which sets the standard for BIM execution by defining how, when and by whom the BIM processes should be carried out. The surveys conducted with KMRL project team members and BIM professionals for the smooth adaptation of BIM and framing BEP contents based on survey results are included in this study.

Keywords –

BIM implementation strategy, Kochi Metro Rail project, BEP contents.

1 Introduction

Building Information Modelling (BIM) is a process which enables the development, use, and transfer of a digital information model of a building project to improve its design, construction, and operations. BIM also contribute to construction documentation with its potential for sharing and managing information with project participants. The advantages of BIM usage are more utilised in multidisciplinary projects as its sharing requirements of information are high.

Even though large multidisciplinary infrastructure projects are taking place in Kerala, the adoption of BIM in Kerala government projects is very less. This means the complexities which are offered to be overcome with BIM usage still exist as a future achievement in such projects. A revolutionary strategy is still required for the actualisation of BIM in Kerala government projects.

Kochi Metro Rail project is one of the large infrastructure projects in Kerala and now it has obtained its approval for 2nd phase with 11.2 km Pink Line and 11

stations. From this perspective, there exists an opportunity for proposing a BIM culture in this new venture. Given this situation, this research aims for developing an effective implementation strategy for BIM in the Kochi Metro Rail project. At the same time, it is also important to understand the significance of the challenges behind its effective implementation. This paper also works on overcoming these challenges.

2 Related Research Studies

For the purpose of identification of implications behind BIM adoption, several case studies and journals that are associated with BIM and its implementation strategies have been referred to. From those references, it was evident that the process of implementing BIM requires significant adjustment to the current practice followed in the organization [3]. All members of the team must understand the project goals and the eventual end-uses of the BIM model in order to set it up properly to allow the end uses [5]. Also, BIM-enabled practice requires construction professionals to interact frequently through a common information-sharing platform [3]. The weakening of this collaboration in BIM-based working could lead to design clashes, omissions, and errors [3].

When it comes to BIM standards, a BIM Execution Plan (BEP) is one of the powerful tools in providing a standardized workflow and general guidance for strategic BIM implementation in a holistic approach for a particular project or a group of projects [1]. Developing a strategic framework for BEP is thus important for the successful implementation of BIM in any construction project [1] [5] [6]. About BEP or any standards, one of the common misconceptions is that all projects are the same, and the same methods can be used for all of them, but every project is unique. i.e., construction projects involve people with varying degrees of knowledge and expertise, and project managers with different levels of sophistication; some projects are predictable, others are complex and risky, and so on [4]. This implies one standard doesn't fit all. Also, the involvement of all parties such as design, construction and Operation & Management (O&M) teams is necessary for the preparation of BEP [5]. When it comes to BEP contents, its elements include- Project goals- Roles and Responsibilities- BIM process design- Collaboration Procedures- Model structure- Model Quality Control and

Project Deliverables [1]. Among these, the most important key element is the identification of Project Goals/BIM Objectives since BEP is set for meeting those goals [1] [6].

Based on the studies conducted, the importance of BEP in a BIM project was a clear knowledge and thus this research reached the objective of developing the implementation process by proposing the key BEP contents which set guidance for introducing BIM in the Kochi metro rail Project.

3 Methodology

3.1 Discussion with KMRL Project Team

Prior to structuring the BIM Execution Plan contents, it was necessary to conduct discussions with the KMRL project team. For this purpose, a questionnaire was prepared in the form of unstructured interviews and discussions, and their answers were found.

As the studies suggested, if the roles of the sociotechnical elements (i.e., actors, tasks, technology, and structure) are more fully understood, then BIM deployment and the encompassing process change can better be managed [3]. Thus, the identification of the current organisation structure was the first preference. The source and destination of each piece of information throughout the construction process were also other key factors that need to be identified. When it comes to BIM, Why BIM? Was crucial to get an answer. For that, the problems associated with the traditional way of practice in KMRL and the needs and expectations of KMRL through BIM adoption at different stages of construction within this project were also expected to get clarified.

From the responses of KMRL project team members the background of the team was outlined as, the project organization structure and workflow commences with the in-house team from where the concept of the design starts. This conceptual design will then be developed into detailed design with the involvement of a detailed design consultancy. Once the detailed design is completed, the drawings will then be transferred to the execution team which will be a project management consultancy comprising of a project manager with the crew members comprising of engineers of different departments, architects, and interface manager and so on for executing their part of the work.

At present, there is no team for conducting coordination of all the disciplines. The identification of coordination issues and its corrections are carried out at the site itself. Based on this workflow, the organisation structure was framed out with the responsibilities of appointing party (the client) and appointed parties (the design team and the execution team). Apart from the information exchange pattern, the level of information

produced at each stage (conceptual design stage, detailed design stage, construction stage) of the project was also another concern. Combination of all these aspects of information was crucial to frame out the BIM overview map and process map which contains the high level of information exchanges that occur throughout the project lifecycle [6]. As described in the studies related to BIM implementation, the introduction of BIM should not result in a sudden change in the usual practice as it creates a reluctance towards its acceptance. In the preparation of BEP also, one of the key contents is defining the roles and responsibilities of everyone involved in the process. So, through the questionnaire session, it was able to compare the task associated with each team member in the current organisation (other than the BIM team), before and after BIM implementation and thus enabling a smooth transition for the process.

Besides this, the next intention was to find the needs and expectations of KMRL with BIM implementation. For that, identification of the issues associated with the current practice was crucial. Based on the responses, delays affecting the work progress were found to be the more frequent issue and they are listed along with the other issues affecting smooth project execution,

- Drawing mismatches.
- Delay due to lack of information at the site.
- Lack of coordination between the execution team.
- Delay caused due to delayed work of one party.
- Delay in obtaining approval for a design change.
- Lack of accurate estimate of materials in accordance with timely changes.
- Material unavailability at the time of procurement.
- Lack of proper visualization for design review, etc.

When it comes to estimation of Bill Of Quantities (BOQ) and their by the cost, lots of inaccuracies are prevailing as the existing way of practice proceeds by taking measurements manually from CAD drawings. Apart from the incompetence of this traditional method, inaccuracy exists in terms of lack of coordination. For example, the length of any mechanical pipe or duct obtained in terms of a manual CAD based calculation will be different from that of a measurement from a well-coordinated clash free BIM model. Besides, this prevailing method of quantity takeoff does not incorporate design changes happening in a timely manner.

Furthermore, the unavailability of materials at the time of procurement can be avoided by the proper monitoring of procurement status of materials. The need of visualization of construction sequence is emulated here.

3.1.1 BIM Uses/BIM Goals

The findings obtained from this questionnaire session were taken for the development of the BIM process. The

first and most important key content in a BEP is defining BIM uses/ BIM goals. The characteristics of the BIM process depend mainly on the purpose for which it is created as the adjustment of the project management approach varies as per the needs of each project. The identified BIM uses are listed below.

- Clash detection and coordination
- Design review
- 4D construction sequencing
- BOQ along with cost estimates

3.2 Questionnaire Survey with BIM Professionals

Once after finalising the BIM use/ BIM goals, it was necessary to conduct a survey with BIM professionals specifically based on the contents of BEP. As they have the knowledge and real-time work experience with BIM projects, they can suggest the most relevant and effective BIM techniques. Responses were collected from 30 BIM professionals consisting of BIM Managers, BIM Coordinators, BIM modellers, BIM engineers and certain IT specialists. A set of 15 questions were prepared with the expectation to get answers regarding roles of responsibilities played by each person in a BIM-based project. In addition, the level of information required and information exchanges at different stages of the BIM execution process, the relevance of BEP, software and hardware requirements, the relevance of following international standards for the BIM project execution along with the type of Common Data Environment (CDE) adopted for data sharing in the respective projects were the other necessary questions to get answered. The responses were categorised based on the level of experience and level of knowledge about BEP.

4 Results and Discussions

From the responses obtained from the survey, the results are categorised and sorted for formulating the other contents of BEP.

4.1 BEP Contents Based on Survey Results

4.1.1 Roles and Responsibilities

- BIM Manager: Develops BEP standard, participates in the decision-making process, standardize workflow, manage BIM models, works on quality assurance process, Track and control information resources, provides training session, attends client meetings, design review meetings and coordination meetings, develops and implement more precise work process to achieve quality with controlled time under budget.
- BIM Coordinator: Submit RFI reports and clear

coordination issues, attends coordination meeting, design review meeting and BIM team meetings, attend decision-making processes, timely submit discipline models, creates modelling and shop drawing templates, Assures quality of BIM models, confirms naming standards for document management, maintains information exchange logs.

- BIM Modeller: Works on BIM modelling and shop drawing generation, identification of issues and preparation of RFI reports, confirms BIM model and shop drawing quality with clash checks and checklist.

By analyzing the current workflow pattern and BIM goals and expectations of KMRL, the need for certain roles was skipped to avoid the sudden accommodation of a huge team.

4.1.2 BIM Overview map

BIM Overview Map shows the relationship of Model uses on the project throughout the project lifecycle [6]. Based on the responses of BIM professionals about the stages of BIM execution and comparing them with project stages of KMRL, the BIM overview map was prepared for the identified BIM uses/goals that to be expected from BIM implementation in this particular project as shown in Figure 1. An overview of the information required and exchanged is also represented in the BIM overview map.

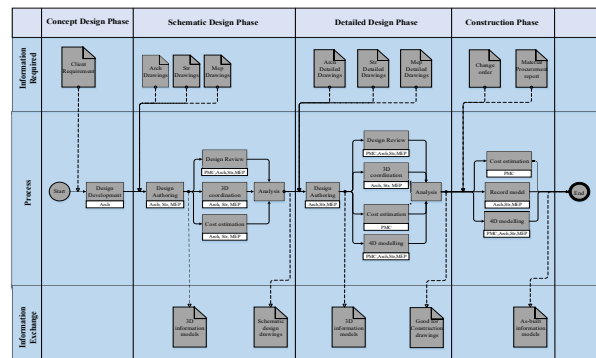


Figure 1. BIM overview map

4.1.3 BIM Process map

BIM Process Maps were created for each identified BIM use on the project to clearly define the sequence of various processes to be performed [6]. The tasks performed by each individual from the start to end of each BIM use with information exchanges taking place in between each task are indicated in the map. Both the overview map and process map are prepared as BPMN diagrams. The process map for one of the identified BIM use, clash detection and coordination is shown in Figure 2. The BIM team was constituted of one BIM manager, BIM coordinators for each discipline (Architecture,

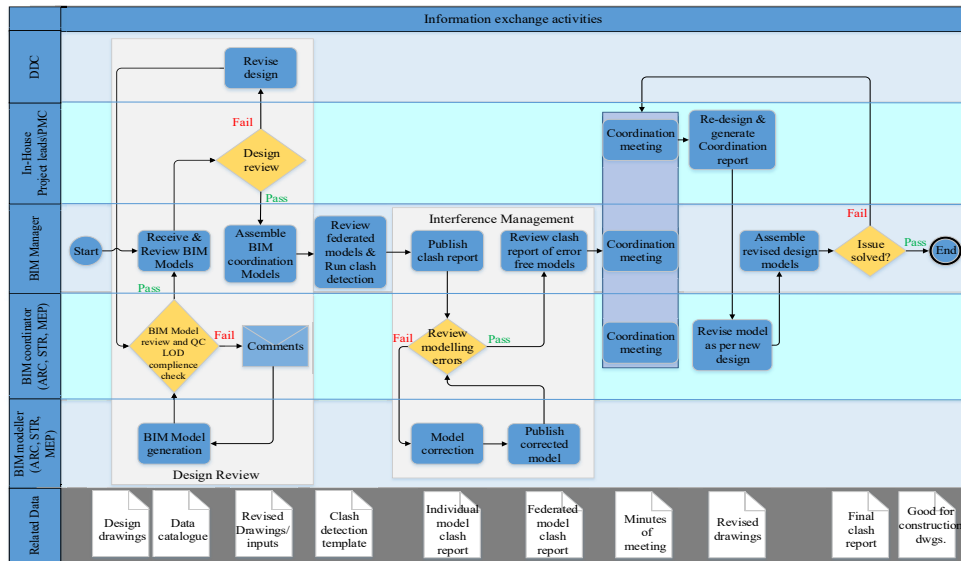


Figure 2. Process map for clash detection and coordination

Structure and MEP) and BIM modellers working with each BIM coordinator. While preparing the process map, one fact i.e., BIM should connect everyone was very important. So, connecting the BIM team with the currently existing project team in KMRL, including in-house project leads, detailed design consultancy and a project manager in the execution team was very crucial. In the process map, provisions for design review and interference management were also included, confirming the model's accuracy and output.

4.1.4 Collaboration Process

Collaboration indicates how communication and information sharing are managed between the responsible parties in the BIM process. Based on survey responses, even though folder structure as per ISO-19650 is enough for internal communication, BIM Collaboration Pro, which is the latest version of BIM 360 was proposed for non BIM team to conduct cloud-based design review.

5 Conclusion

BIM is a revolutionary trend in construction management. Based on the survey and its findings, this paper proposes a BIM implementation strategy by considering the current culture followed in the organization to formulate the key contents of the BIM execution plan such as BIM uses, Roles and responsibility, BIM overview map, Process map, Quality assurance technique and Collaboration process. Since the participants selected for the survey was currently working and experienced BIM professionals, their valid

responses can contribute to the effectiveness of the implementation process.

Meanwhile, the main factor depends on the mentality of the staff members of the organization for accepting the current trend. Since the proposed plan of action is incorporated with the current practices of project participants, the difficulty in acceptance can probably be minimized.

Future expansion for this study is possible for formulating additional contents of BEP.

References

- [1] Ahmad Ridzuan Abu Bakar, Ahmad Tarmizi Haron and Rahimi A. Rahman. *Building Information Modelling Execution Plan (BEP): A Comparison of Global Practice*, 2020.
- [2] University of South Florida. *BIM Project Execution Plan Template*.
- [3] E. Sackey, M. Tuuli, Ph.D and A. Dainty, Ph.D. *Sociotechnical Systems Approach to BIM Implementation in a Multidisciplinary Construction Context*, 2015.
- [4] Iason Tzanakakis. *A study on the customization of the BIM Execution Plan based on project characteristics*. 2021.
- [5] J. J. McArthur & X. Sun. *Best practices for BIM Execution Plan development for a Public-Private Partnership Design-Build-Finance-Operate-Maintain project*, 2015.
- [6] John Messner, Chimay Anumba, Craig Dubler, Sean Goodman et al. *BIM Project Execution Planning Guide, Version 3.0*.

Object detection in construction department

Pralipa Nayak

Machine learning Developer
pralipan@vconstruct.in

Abstract:

The capability to automatically identify shapes and objects from the image content through direct and indirect methodologies has enabled the development of several civil engineering related applications that assist in the development of construction projects. This paper shows how this automation process has been made possible using Machine Learning techniques to reduce the time and effort consumed in the field of construction industry. Also how technology has helped to transform the construction industry. Manually where various objects like doors, beams and columns were detected throughout an architectural plan by counting and recording, this process used to take many hours to work on a single plan. Automating this process with the help of Object detection and Machine learning has helped to reduce the time and effort consumption by a huge margin.

Introduction:

In the construction industry, most of the work, from verifying an architectural plan to detecting various objects in the plan, are done manually. This in turn takes a lot of time and effort.

Object detection is a computer vision technique that can be used to automate this process which in turn, will reduce time and effort to a great extent. It basically has a series of instructions for a computer to transform input data into desired output. Instructions are mostly based on an IF-THEN structure: when conditions are met, the program executes a specific action.

Machine learning techniques like Image processing can be used to further enhance this process and perform object detection with better accuracy and speed. It enables machines to solve problems with little

or no human input., and take actions based on past observations. This approach will help to automate detecting various objects in an architectural plan and various other work and help us save time and effort.

Background:

We are surrounded by different types of beautiful architecture around us. And the basis for any architecture is the architectural plan. For any architecture to stand firmly for ages, the plan should be perfect with negligible to no flaws.

Object detection helps to a great extent in recognizing designs according to existing data and extracting data from them for further investigations like finding flaws or whether any section needs changes, detecting changes in revised plans in accordance with old plans and quantifying elements in a plan.

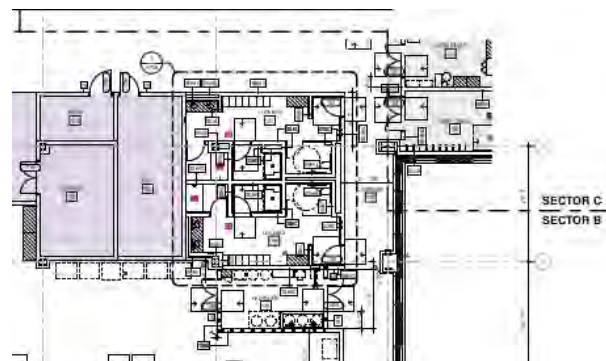


Figure 1. Image of an architectural plan from which doors and water closets are to be recognized.

The above given figure is an architectural plan, based on which construction will be made. Our goal was to detect various objects like doors, water closets, columns, beams etc.

Approach:

On-Screen Takeoff is a construction estimating and takeoff solution for contractors and construction professionals. It is widely used to mark items on a 2d plan and add properties to the items. Once the relevant items are marked, it can extract the desired quantities as required. But this is a manual process and is repetitive in all projects. On an average, it requires nearly a day for a single plan. Another tool called Autodesk Takeoff also does the same thing, however it also takes a similar amount of time.



Figure 2. Image showing details of a page in On-screen Takeoff.

Figure 2 shows the details of the architectural pan in an indexed way. Using OST(On-screen Takeoff) formulas are prepared to mark different objects like doors, water closets, etc one by one. The objects are then marked throughout all the pages as per the formulas manually. This method takes up lots of time and effort.



Figure 3. Image showing marked doors in the architectural plan.

As per figure 3, we can see the doors have been marked as per the formulas created however it was done one by one for all the objects. All the similar objects will be marked the same way.

The next approach was to use machine learning techniques to make the process automated. This way we were able to get the data in a very less amount of time as compared to the manual approach. Machine learning helped us to get the data within an hour which saved us lots of time. We had a pdf which has multiple pages of architectural plans. Machine learning techniques like pdf mining and image processing were used to achieve the results. Pdf mining helped in reading and extracting details from every page.

Challenges:

The first approach for ML was using OpenCV. The challenges faced were:

1. This approach detects images exactly the same as template images.
2. This approach does not support rotation and resizing of objects so to solve the rotation issue the template image was rotated 90 degree clockwise, 180 degree and 90 degree counterclockwise then all the rotated template images were matched to the input image and the output was found, however the size of the object in input image has to be exact with the template image size and if one object in input image is rotated by 95 degree, then OpenCV won't consider this as a match.
3. Accuracy was extremely low and it did not support overlapping.

The next approach was using Tensorflow. The challenges faced were:

1. The accuracy was very good (above 95%), however it did not work with larger images(2-4 MB) which did not satisfy the requirement.

The next approach was Custom-Vision. The challenges faced were similar to the former approach.

1. Though it supports overlapping and accuracy was also very good (above 95%), it did not work with large images (2-4MB) which did not satisfy the requirement.

Solution:

Then we moved towards using YoloV5 (You Only Look Once).

As per machine learning standards, first train and test datasets were prepared by splitting in 80-20 ratio and labelled using Labelling library.

After labelling, the model was trained using YoloV5 (You Only Look Once) and we got the trained model for detecting doors.

Then we converted the pdf page to an image file in which object (door) detection was performed.

As a 2-d architectural plan is way too large, we used a library called SAHI to detect objects in large images. SAHI stands for Small object detection by slicing Aided Hyper Interface. It is a vision library for large scale object detection and instance segmentation. What SAHI basically does is, it slices large images into smaller segments and performs object detection on those segments so it easily picks almost all the objects in a large image.

We created a script written in python3 that loads the trained model, takes up the pdf file as an input parameter, reads each page as an image, then uses SAHI to slice the image and perform object detection on the image with pretty good accuracy.

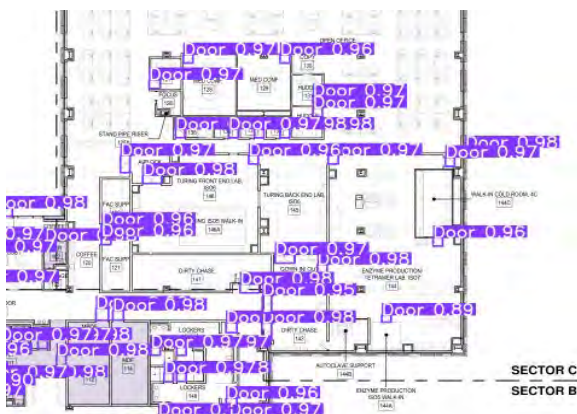


Figure 4. Image with detected doors and labeled accordingly.

The above image is one of the results we got after performing object detection on a given pdf file. The detected doors haven't been labelled as doors at their respective coordinates. This gives us a clear idea of which of the elements present in the image (a page in pdf) are doors or any other elements.

Similar process was followed for detecting other objects. Model was trained accordingly using related datasets and prediction was made based on the trained model.

Another scenario popped where we needed written textual data from pdf files consisting of tables. This seemed easy as there are lots of packages like Camelot, PyPdf that deal with such scenarios. However, they are limited to text pdfs. The need was to extract those data from image/ scanned pdfs. Image processing helped here too. Pytesseract or Python-tesseract was used to get the results. Pytesseract is an Optical Character Recognition tool for python. It reads and recognizes text in images.

The challenge now was to provide the coordinates or the location from where pytesseract will perform the recognition. Since in a table, the data are separated to groups using vertical and horizontal lines, those lines were extracted first. It was done by inverting the image first to monochrome. Then the vertical line and horizontal lines were extracted from the table, which helped us get the coordinates from the image. The co-ordinates were then used to verify the locations from where we needed the data and were given to pytesseract, which read and recognized the text from those locations and gave us the data. This flow was achieved by bundling pytesseract with some data structure logic, used for manipulating the data in required structure.

The above mentioned flow is also used to extract data from the earlier mentioned 2d architectural plans like beams and columns data. Since they are also made as horizontal and vertical lines, this algorithm helps extract data like the length, angles, and thickness of the parameters. Which is required for major

calculations while moving with a construction project.

Pdf files with data stored in the form of tables but where pages are images instead of plain texts are used. Here the image was processed with pytesseract to extract the data from it. First it was inverted to monochrome format and horizontal lines were extracted from the inverted image. Then from the inverted image, vertical lines were extracted. Both extracted images were then merged which gave us an inverted image of the whole table.

After the horizontal and vertical lines were merged to get the whole table in inverted format, the resulting image was then used to contour the image, Figure 5.

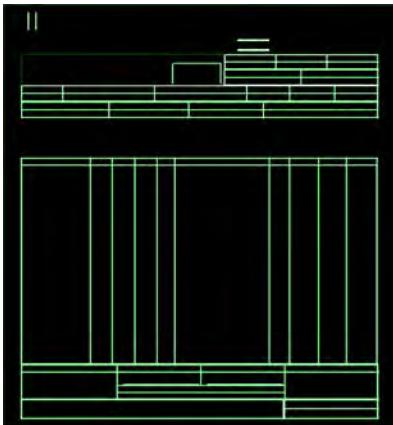


Figure 5. Table after contouring.

The coordinates were then used to recognise the smaller rectangles. And then from those rectangles, the data from the table were extracted based on some keywords like the column names. Thus data was successfully extracted from the image pdf with zero errors.

Conclusion:

The algorithms created were tested rigorously on various types of data. Which in turn gave us lots of error and opportunity at the same time to resolve them and get the algorithms ready for use with negligible to zero failures or error results.

The manual approach, using OST, gave results while taking a longer period of time,

almost more than 15 hours, with involvement of human resources. This problem was solved using Machine learning where the process took just some minutes also without requiring any human efforts. This paper shows how this automated process can save us a huge amount of time and effort as compared to manual approaches. If implemented on a larger scale, this process can save a lot of time and effort, which in turn can save a lot of funds.

References:

- [1] Fitz
<https://pymupdf.readthedocs.io/en/latest/module.html>
<https://github.com/pymupdf/PyMuPDF/blob/master/fitz/fitz.i>
- [2] LabelImg
<https://github.com/heartexlabs/labelImg>
<https://towardsdatascience.com/how-to-label-images-for-object-detection-step-by-step-7ee317f98583>
<https://medium.com/deepquestai/object-detection-on-training-preparing-your-custom-dataset-6248679f0d1d>
- [3] YoloV5
<https://github.com/ultralytics/yolov5>
<https://learnopencv.com/custom-object-detection-on-training-using-yolov5/>
<https://stackabuse.com/object-detection-inference-in-python-with-yolov5-and-pytorch/>
- [4] SAHI
<https://github.com/obss/sahi>
<https://medium.com/codable/sahi-a-vision-library-for-performing-sliced-inference-on-large-images-small-objects-c8b086af3b80>
<https://analyticsindiamag.com/small-object-detection-by-slicing-aided-hyper-inference-sahi/>

Pralipa Nayak
Machine learning Developer
pralipan@vconstruct.in

Online Modelling and Prefab Layout definition for building Renovation

Kepa Iturralde^a, Sathwik Amburi^a, Sandhanakrishnan Ravichandran^a, Samanti Das^a, Danya Liu^a, Thomas Bock^a

^aChair of Building Realization and Robotics, School of Engineering and Design, Technical University of Munich, Germany

E-mail: kepa.iturralde@br2.ar.tum.de

Abstract

This paper introduces a powerful semi-automated tool that efficiently creates detailed 3D building models and layouts of prefabricated modules with solar panels from building images and Open Street Map floor plans. The tool permits the generation of the existing building model and the layout of the prefabricated panels in an average of 25 minutes, depending on the complexity of the building geometry. The shape of the building and the number of solar panels that can fit on the building envelope are determined using the generated 3D models and layouts. With the use of prefabricated modules and solar panels, building upgrades can be made more affordable and energy-efficient.

Keywords –

Building model, renovation, prefabrication, semi-automated

1 Introduction

In building renovation, the use of prefabricated modules for energy saving and generation is often less competitive compared to manual procedures because of the need for more detailed and thorough planning. Among other aspects, building owners, promoters, or engineers should have a comprehensive understanding of the building's capabilities for generating solar energy, the costs of investment, and the need for insulation in the early stages of the project. To achieve this, it is necessary to have a geo-located 3D model of the building that can accurately depict the building's shape and structure and the ability to fit the prefabricated modules and solar panels on top of the building. This is where the layout of the prefabricated walls and solar panels comes into play. A proper layout can give a clear idea of how many solar panels can fit on the building envelope, how much insulation is needed, and how much investment is required.

This paper explains the latest updates on a tool that

allows for semi-automated online building modelling and the layout of prefabricated modules with solar panels using a Python plugin for FreeCAD [1]. This tool generates a detailed 3D building model and layout of the prefabricated modules by using building images and Open Street Map floor plans [2]. In other words, the tool generates a building model (an .ifc file) without the need for on-site measurements. Moreover, the tool generates the layout of the prefabricated modules with solar panels. With this input, in the next step (that the authors haven't developed), it is possible to estimate costs and energy savings for building upgrades with prefabricated modules and solar panels. This tool is an effort to continue to explore and improve the efficiency and cost-effectiveness of building renovation within the ENSNARE project [3].

2 Research Gaps

Economic feasibility [4]-[7] is an important factor for the efficient marketability of robotics and automated solutions in construction. According to the authors, there is a need for a faster and more detailed Building Modeling during the first stages of the project. An estimation is needed so the different stakeholders (building owner, engineers, contractors...) can decide if the project is feasible technically and economically before any relevant investment (material or services) is made. For that purpose, a building model is needed in the first stages. But it is necessary to avoid an on-site measurement of the building in order to diminish recurrent (travel) costs. For this reason, an online Building Modelling tool is necessary. Moreover, the tool must permit the automated layout definition of the prefabricated insulated modules that include the solar panels.

Previous research shows that the semi-automated solar panel grid generation was defined [8]-[9]. However, in these experiences a regular grid for roofs and with no insulation is generated. In the ENSNARE project, the idea is to cover facades (with windows, balconies...),

with waterproof and air-tight prefabricated modules that include solar panels which is more complex than the aforementioned solution.

In previous stages of the ENSNARE project [10], the tool was able to generate a Level of Detail (LOD) 3 model. The updated tool can generate models that include a wide range of features such as windows, doors, balconies, and roofs, all with a LOD 4 [11] and generate the layout of the new added façade.

By using the tool described in this paper, building owners, promoters, and engineers can make informed decisions about the installation of prefabricated modules with solar panels and make sure that the renovation project is economically viable and energy efficient.

3 Approach and Results

The tool is based on a Python plugin for FreeCAD that allows users to generate detailed 3D BIM/IFC building models quickly and easily from images of the

building. Utilizing pyside2 GUI's and automating the information workflow for all phases of building renovation (data acquisition, generation of the layout, CAM generation for prefabricating the modules, and on-site marking of the connectors), this plugin streamlines the data acquisition process and reduces associated costs and time by up to 90% because it avoids the preliminary visit on-site.

The development process for the plugin involves the following steps. The Python plugin for FreeCAD was developed using a range of tools and technologies like: OpenCV, Python, Pyside2, PyTorch, ArcGIS, scikit-learn (sklearn), Timm, fastai, NumPy, SciPy [12]–[21].

These are some of the key libraries and technologies used in the development of the Python plugin for FreeCAD. Other libraries and tools were also used to provide a range of functionality and facilitate the data acquisition and processing process for building renovations.

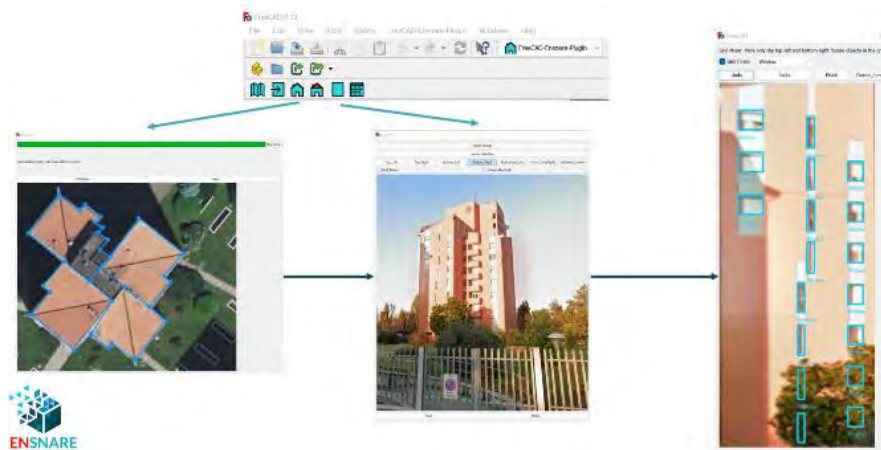


Figure 1. Corner and window detection by the plugin in the demo building in Milan (ENSNARE project)

Our plugin has a range of features as seen in Figure 1 that allow users to gather and analyze data for building renovations. These features include:

1. **Facade selections:** With this feature, users can upload images of a building and can either manually select its corners from the image or let the plugin do it for them. The image is then subjected to a perspective transformation by the plugin to obtain the right aspect ratio for additional processing, which includes the automatic detection of facade objects like windows, doors, and balconies. It's important to remember that automatic corner detection may not always be accurate.
2. **BuildingEdit:** With the help of the aerial view of the building, users can modify the OSM data. This is

helpful if the OSM data is not always accurate or correct.

3. **Floors:** This feature enables users to add floor slabs to the structure, giving them a more accurate and detailed view of the building. The plugin now can add roofs and façade elements like doors and balconies. Additionally, it can detect objects and approximate objects.

Overall, these features provide a range of functionality for gathering and analyzing data for building renovations, allowing users to create detailed and accurate 3D BIM/IFC models of the building.

The following features can now be added on the plugin:

- Pitched roofs

- Windows
- Doors, Balconies (both inside and outside)
- Floors

Given a FreeCAD building model, the plugin extracts

relevant information (position, orientation of walls, roofs, windows, doors, and balconies) as JSON files. Then, it projects each facade in 2 dimensions. This is illustrated in Figure 2.

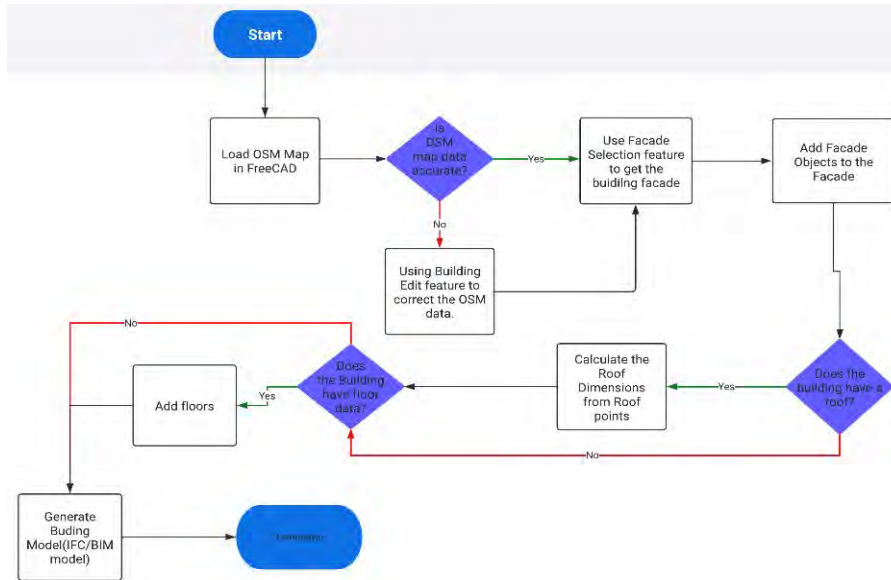


Figure 2. Process Map of the plugin application

After applying the algorithm, the optimum distribution of solar panels in each facade is generated as shown in the figure below in Figure 3. The 2D distribution of solar panels is then projected back to 3 dimensions and placed on the existing building models.



Figure 3. Left, Demo Building model in Milan. Right, building in Milan with added prefabricated façade with solar panels (ENSNARE project)

It is important to note that the Python plugin for FreeCAD has some limitations and issues that may affect its functionality and accuracy. These include errors or inconsistencies in OpenStreetMap (OSM) data which can affect the accuracy of the 3D BIM/IFC model generated

by the plugin, automatic corner detection and facade object detection may not be perfect due to limitations in computational resources or data, and the current user interface is not very user-friendly. It is crucial to be aware of these limitations when using the plugin for building renovations.

4 Conclusion

The Python plugin for FreeCAD is a tool for gathering and analyzing data for building renovations, providing a cost-effective and efficient way to create detailed 3D BIM/IFC models of buildings. The plugin has several key features, including the ability to load OSM map data, perform facade selections and automatic detection of facade objects, make corrections to the OSM data using BuildingEdit, and add floor slabs to the building model. The average time for defining the building model and the layout is about 25 minutes, which reduces considerably the amount of time in the first stages, especially if travel time to the site is considered. There are a few known limitations and issues with the current version of the plugin, including the potential for incorrect OSM data, tricky roof implementations, difficult angles for perspective transformation, and

limitations in the accuracy of automatic corner detection and facade object detection.

Several areas for further research and discussion could enhance the functionality and accuracy of the Python plugin for FreeCAD:

1. Development of wall extrusions and adding facade objects to them: One potential area for further research is the development of algorithms or techniques for creating wall extrusions and accurately placing facade objects on them. This could improve the realism and detail of the 3D BIM/IFC models generated by the plugin.
2. Web app for better user experience: Another possibility is the development of a web app version of the plugin, which could provide a more convenient and user-friendly interface for gathering and analyzing data for building renovations.
3. Improved perspective transformation algorithms: Improving the algorithms used for perspective transformation could enhance the accuracy of the 3D BIM/IFC models generated by the plugin, especially in cases where the client takes pictures of the building at difficult angles.
4. Improved building modelling accuracy: Further research and development of techniques for improving the accuracy of the 3D BIM/IFC models generated by the plugin could make it an even more valuable tool for building renovations and related projects.

Overall, these are just a few examples of the potential directions for further research and discussion that could enhance the capabilities of the Python plugin for FreeCAD.

Acknowledgements



This project has received funding from the European Union's Horizon 2020 research and innovation programme under grant agreement No. 958445.

References

- [1] "FreeCAD Your own 3D parametric modeler," <https://www.freecadweb.org/>, Jan. 24, 2023.
- [2] VA, "OSM," <https://osmbuildings.org/documentation/data/> (accessed Jul. 25, 2022).
- [3] "ENSNARE," <https://www.ensnare.eu/>, Jan. 24, 2023.
- [4] M. Skibniewski and C. Hendrickson, "Analysis of Robotic Surface Finishing Work on Construction Site," *J Constr Eng Manag*, vol. 114, no. 1, pp. 53–68, 1988, doi: 10.1061/(ASCE)0733-9364(1988)114:1(53).
- [5] C. Balaguer and M. Abderrahim, "Trends in Robotics and Automation in Construction," 2008. doi: 10.5772/5865.
- [6] A. Warszawski, "Economic implications of robotics in building," *Build Environ*, vol. 20, no. 2, pp. 73–81, 1985, doi: [https://doi.org/10.1016/0360-1323\(85\)90001-0](https://doi.org/10.1016/0360-1323(85)90001-0).
- [7] R. Hu *et al.*, "A Simple Framework for the Cost-Benefit Analysis of Single-Task Construction Robots Based on a Case Study of a Cable-Driven Facade Installation Robot," *Buildings*, vol. 11, no. 1, 2021, doi: 10.3390/buildings11010008.
- [8] Z. Awwad, A. Alharbi, A. H. Habib, and O. L. de Weck, "Site Assessment and Layout Optimization for Rooftop Solar Energy Generation in Worldview-3 Imagery," *Remote Sens (Basel)*, vol. 15, no. 5, p. 1356, Feb. 2023, doi: 10.3390/rs15051356.
- [9] "Automatic planning of solar systems," <https://dida.do/de/projekte/solaranlagen-planung>, Apr. 03, 2023.
- [10] K. Iturralde *et al.*, "Solution Kits for automated and robotic facade upgrading," in *Proceedings of the 39th International Symposium on Automation and Robotics in Construction*, T. Linner, B. de Soto, R. Hu, I. Brilakis, T. Bock, W. Pan, A. Carbonari, D. Castro, H. Mesa, C. Feng, M. Fischer, C. Brosque, V. Gonzalez, D. Hall, M. S. Ng, V. Kamat, C.-J. Liang, Z. Lafhaj, W. Pan, M. Pan, and Z. Zhu, Eds., International Association for Automation and Robotics in Construction (IAARC), Jul. 2022, pp. 414–421. doi: 10.22260/ISARC2022/0057.
- [11] M.-O. Löwner, B. Joachim, G. Gröger, and K.-H. Häfele, "New Concepts for Structuring 3D City Models - an Extended Level of Detail Concept for CityGML Buildings," Jan. 2013, pp. 466–480. doi: 10.1007/978-3-642-39646-5_34.
- [12] "Python," <https://www.python.org/>, Jan. 24, 2023.
- [13] "OpenCV," <https://opencv.org/>, Jan. 24, 2023.
- [14] "Pyside2," <https://doc.qt.io/qtforpython/>, Jan. 24, 2023.
- [15] "PyTorch," <https://pytorch.org/>, Jan. 24, 2023.
- [16] "ArcGIS," <https://www.esri.com/en-us/arcgis>, Jan. 24, 2023.
- [17] "scikit-learn," <https://scikit-learn.org/stable/>, Jan. 24, 2023.
- [18] "Timm," <https://github.com/rwightman/pytorch-image-models>, Jan. 24, 2023.
- [19] "fastai," <https://www.fast.ai/>, Jan. 24, 2023.
- [20] "NumPy," <https://numpy.org/>, Jan. 24, 2023.
- [21] "SciPy," <https://www.scipy.org/>, Jan. 24, 2023.

Overview of robotic shotcrete technologies with basalt reinforcement

Thomas Bock¹, Viacheslav Aseev² and Alexey Bulgakov^{2,3}

¹Technical University Munich, Germany

²Southwest State University, Russia

³Central Research and Development Institute of the Ministry of Construction of Russia, Russia

thomas.bock@br2.ar.tum.de, swsu_aseev@mail.ru, a.bulgakov@gmx.de

Abstract –

The article provides an overview of current developments in the technology of shotcrete surfaces of building elements, examples of construction robots that provide robotization of such technologies are presented. The article also presents the shotcrete technology, which will improve the quality of building structures and automate the shotcrete process using basalt fiber as reinforcement. Also, a model of reinforcement of the processed building structure according to the proposed technology is given.

Keywords –

Shotcrete; Basalt; Robotization; Reinforcement

1 Introduction

During the reconstruction of historical buildings and structures, it becomes necessary to strengthen and interface individual structural elements or the entire building as a whole. The key point in carrying out such work is the preservation of architectural expressiveness. Basalt fiber is one of the materials used to replace the metal components of structures, equipment and products, being inexpensive, lightweight and affordable, as well as resisting corrosion. These facts are also evidenced by modern studies [1,2,3].

Preservation of architectural forms can also be achieved by shotcrete technology, which has proven itself as a technology that provides a process of reinforcement when working in conditions of negative temperatures, minimal water absorption due to the compaction of the solution, resistance to aggressive environments, sudden changes in temperature/moisture, as well as laying without the need for installation formwork.

When investigating shotcrete, it is also necessary to consider the use of traditional reinforcement or the possibility of reinforcing structures with metal or non-metal fiber components. This is relevant in the production of work related to the construction, repair or restoration of load-bearing and enclosing building

structures of buildings and structures.

Modern methods of shotcrete today include technologies such as "dry" and "wet" application. "Dry" gunning is characterized by the possibility of applying thick layers of material, as well as high productivity [3]. In turn, "wet" gunning has such advantages as the uniformity of the composition of the material and the ability to work in cramped conditions. Analysis and generalization of the advantages and disadvantages of these technologies reasonably set the task of using an effective innovative, mobile, low-budget technology that allows combining the advantages of shotcrete methods and leveling the disadvantages.

2 Shotcrete technology

Speaking of modern shotcrete technology, it is assumed that it combines as many positive characteristics of existing technologies as possible, and also includes a new equipment configuration. So, a group of engineers led by Chelpanov V.G. the technology of the "semi-dry" method of concrete spraying was developed and implemented [4] (fig. 1).



Figure 1. Mobile equipment and technology for applying semi-dry sprayed concrete

This technology occupies an intermediate position between dry and wet shotcrete, using the advantages of

both. In the proposed technology, the solution is supplied through the material hose in portions with air gaps, which increases the efficiency of the supply due to the piston action of the portion. This allows you to easily hold the sleeve and barrel in your hands, as it is semi-empty and light. Trial equipment for applying sprayed concrete by the semi-dry method was created and tested, which significantly expands the possibilities of using the technology to solve various engineering problems.

However, the technology of applying semi-dry shotcrete involves the use of equipment of a special configuration. The modern development of barrel modification (shotcrete nozzle) was developed by Russian researchers (fig. 2) [5, 6].



Figure 2. Shaft modification for semi-dry shotcrete

The resulting process of semi-dry shotcrete using a modified barrel allows you to apply a layer of up to 250 mm on a vertical surface [4].

As a result of improvement, large-scale testing and implementation of this technique and equipment at the leading enterprises of Russia on various shotcrete equipment, using various dry mixes, effective production results were obtained. A cardinal reduction in the rebound of dry mixes is achieved by 5 times and dust content in the workplace by more than 6 times, which makes it possible to obtain a significant economic, environmental and social effect (fig. 3). Positive results were also established when applying fiber-reinforced concrete [7].

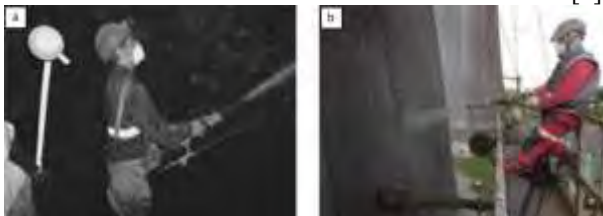


Figure 3. Shotcrete using a modified shaft configuration in the shaft (a) and at a height (b)

At the same time, materials and equipment for the implementation of this technology are significantly cheaper than those offered on the market, which ultimately reduces the cost of the product and allows you to successfully compete in the market for services for this type of work.

However, in case of buildings with higher criticality rating we need to minimize the human factor, the reliability of the operations performed, and often increase the speed of work, which indicates the natural need for robotization of the shotcrete process.

3 Shotcrete robotic technologies

The use of programmable robots in the construction process certainly has its advantages, but it should be borne in mind that in order to implement this idea, it is first of all advisable to conduct a comparative analysis of existing robots. For the introduction of robotics in the shotcrete process, it would be advisable to give examples of the successful use of installations similar in type of work. One such construction of a mortar applicator is shown in fig. 4.

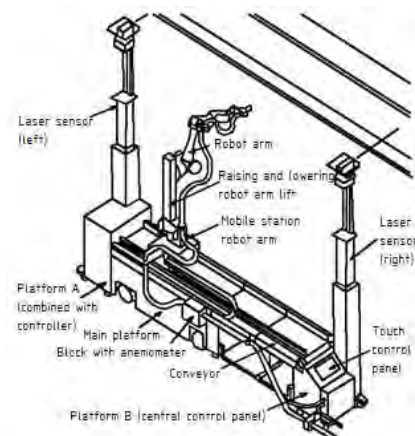


Figure 4. Configuration of a modern robot for outdoor finishing works

The main purpose of a modern robot for outdoor finishing work is spraying decorative coatings and applying paint compositions. The robot arm is placed on the lifting platform and moves along it, which significantly expands the capabilities of the seven-link manipulation system. The manipulator is the basis of the spray mechanism equipped with a nozzle. The positioning device of the robot is equipped with laser sensors, which allow you to control the distance to the main beam, on which the painting robot is suspended, with great accuracy. The platform is equipped with a control device that controls all links and components of the robot. The use of an active display to control the robot made it possible to easily set the parameters of the robot's

movement. The presented design is cumbersome and requires significant refinement.

In contrast to the considered robot configuration, in fig. 5 shows an improved design of the manipulator, designed for applying solutions by spraying with compressed air. The wall surface robot is mounted on a light platform moved by a winch along the wall surface. This robot can also clean walls, or be used to check the quality of tiles on a wall surface.

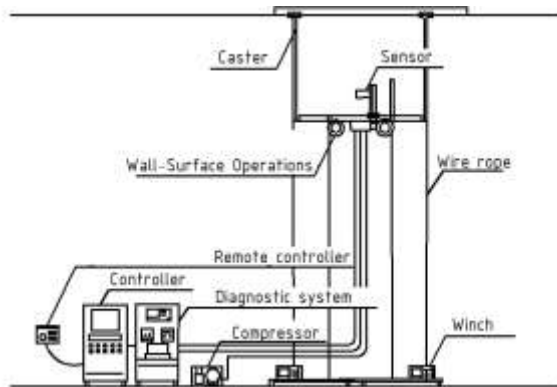


Figure 5. Design of improved manipulator

An analysis of construction robot designs shows that it is advisable to create specialized manipulators and robots for the robotic application of cement compositions, which provide the preparation of vertical and horizontal surfaces. Among the various solutions for such robots, one can distinguish mobile and mounted on a lifting platform manipulators. Moreover, for the movement and orientation of the processing tool, 5 degrees of freedom are sufficient, while it is advisable to use a block-modular design.

The calculation of concrete structures by the finite element method convincingly proves that where there is no active ingress of moisture, the destruction of concrete occurs due to forced natural vibrations of the structure. The first cracks in the structure appear simultaneously with the start of its operation. The design initially contains concrete zones, which during operation either crack or tear off part of the concrete. And only in the process of further operation, chlorides appear, corrosion of the reinforcement due to the initial power cracks. As a conclusion: the application of non-fiber-reinforced materials to a locally damaged surface leads to the appearance of cracks and rejection of materials, since these materials do not work in tension.

4 Reinforcement technology

Given the need for reinforcement, a solution was developed that provides an easy installation of reinforcement, which can be integrated into the workflow

of construction robots. Below is one of the solutions for reinforcing with basalt fiber rods using the example of shotcrete work on the load-bearing column of a building (fig.6).

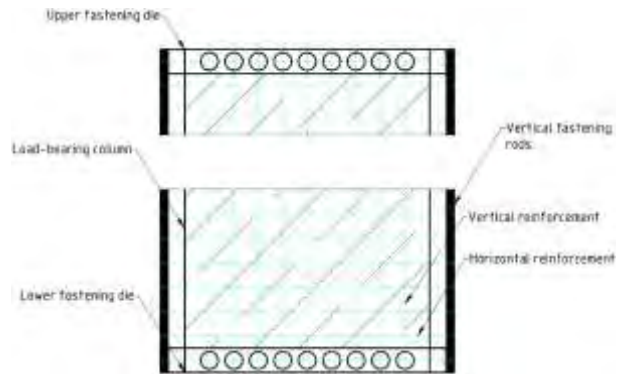


Figure 6. An example of reinforcement with basalt fiber of a load-bearing column before the shotcrete process

A fastening die is attached to the column being processed along the upper and lower faces, the design of which is shown in fig.7. The function of the fastening die is that it serves as an attach-point for tensioning the basalt rod, which, in its turn, reinforces the required volume of concrete. Such a solution makes it possible to robotize the process of strengthening the shotcrete, since the robot installation is implicitly capable of reading information about the location of the fastening die and the features of its location and configuration. After the installation of the structure, vertical fastening rods are also attached to such dies, which serve as an attach-point for tensioning the basalt rod of horizontal reinforcement. After mounting the fixing dies and bandaging the basalt reinforcement along it, the shotcrete process takes place. The dismantling of such dies is not necessary, but rather even undesirable, since, by adhering to the column, they provide the reinforcement with a better connection with the structural element being processed.

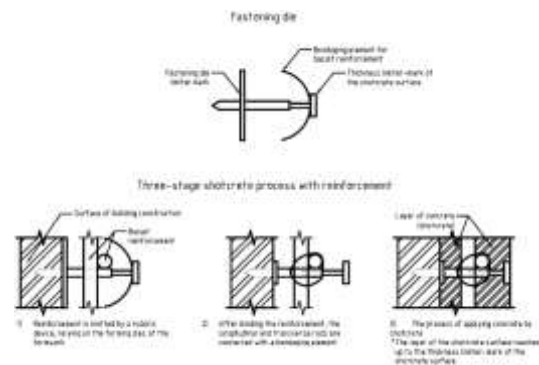


Figure 7. The algorithm of the shotcrete process using basalt rebar rods

5 Discussion

In addition, it is also worth considering that in order to perform shotcrete with basalt fiber reinforcement, it is necessary to take into account the fact that some structural elements can be spherical and other non-planar configurations. Uniform application of solutions over such structures requires modification of existing technologies for robotic shotcrete. Also, to quickly stop shotcrete at the end of the wall or when moving to the ledges of walls and niches, it is still not enough to set the pump alone, because due to the residual pressure in the hose, the solution is still supplied by inertia to the executive body of the plastering tool. Therefore, it is required to have a controllable shut-off valve that can immediately stop the flow of material. There is also a need to ensure the alignment of large irregularities, so the flow of material must be regulated in accordance with their geometric dimensions. This can be realized through the variable productivity of the shotcrete robot, for example, with the help of an adjustable pump or by changing the speed of the plastering tool with its constant productivity.

The analysis of shotcrete robots shows that kinematic schemes with a polar base coordinate system, despite their compact construction, are the least suitable for such robots due to the spherical shape of the working area. More suitable in this case are kinematic schemes with swing axes, due to its great flexibility and compactness. Technical control costs and limited accuracy due to kinematic errors for this scheme are the main disadvantages. Kinematic schemes with a cylindrical base coordinate system, as well as with a rectangular one, are well suited for shotcrete robots, but still with some disadvantages regarding the working area and accuracy. Kinematic schemes with a rectangular coordinate system are best suited for plastering work, which is explained by the good consistency of the rectangular working area of the robot with the usually flat surface of the surfaces being reinforced and increased accuracy due to the ease of orienting the kinematic axes along the given motion trajectories. The costs for the technical implementation of such systems due to simple kinematic links are significantly lower compared to other options. The disadvantage is the large overall dimensions, due to the use of such a scheme for constructing kinematics.

6 Conclusion

Based on the methods described above, it can be concluded that modern technologies naturally lead the process of strengthening the structures of buildings and structures to robotization. The above reinforcement technology also implies the robotization of the process,

which will solve a number of existing problems that accompany shotcrete surfaces. It is also worth noting that the use of rebar or fiber as part of the concrete mixture during the shotcrete process is extremely appropriate, given the need to eliminate the shortcomings of this technology for the rehabilitation of facades and surfaces of buildings and structures. Further research involves the analysis and selection of the most optimal of the considered options for shotcrete technology with the further development of a shotcrete installation together with reinforcement with basalt fiber.

References

- [1] Letova T. and Tilinin Y. Improvement of technological processes of concreting and reinforcing monolithic structures. *Colloquium-journal*, (25 (49)), pages 34-38, 2019.
- [2] Okolnikova G., Tikhonov G., Bronnikov D. and Vasiliev I. Application of the basalt and carbon network during reconstruction of buildings and constructions. *System technologies*, no. 2 (31), pages 14-18, 2019.
- [3] Yakovlev G., Galinovsky A., Golubev V., Saraikina K., Politaeva A., and Zykova E. Nanostructuring as a method of adhesion properties increase of the «cement stone - basalt fiber reinforcement». *News of the Kazan State University of Architecture and Engineering*, no. 2 (32), pages 281-288, 2015.
- [4] Volchenko G., Chelpanov V. and Fryanov V. Improving the technique and technology of sprayed concrete to expand the scope in emergency situations. *Bulletin of the Siberian State Industrial University*, no. 4 (22), pages 36-44, 2017.
- [5] Volchenko G., Fryanov V., Prib V., Volchenko N. Non-standard approach to improving the efficiency and resource saving of low-budget technology of sprayed concrete when fixing mine workings. *Science-intensive technologies for the development and use of mineral resources: Collection of scientific articles*, pub. SibSIU, pages 133-137, 2015.
- [6] Volchenko G., Seryakov V., Fryanov V. and Volchenko N. Technique and technology of sprayed concrete Termiton® for fixing mine workings in difficult conditions. *Science-intensive technologies for the development and use of mineral resources: Collection of scientific articles*, pub. SibSIU, pages. 82-93, 2016.
- [7] Volchenko G., Isakharov B., Fryanov V., Volchenko N., Volkov E. and Prib V. Industrial tests of the shaft of dedusting sprayed concrete Termiton X4. *Vestnik SibSIU* No. 1 (11). pages. 32-35, 2015.

Automatic Design of various Reinforced Concrete Structures based on AutoCAD AutoLISP

Dharani V P¹, Parvatham Vijay²

¹Department of Civil Engineering, Thiagarajar College of Engineering, Madurai, India. ²Department of Electronics and Communication Engineering, Sri Sai Ram Institute of Technology, Chennai, India.

¹dharanivp@student.tce.edu, ²parvathamvijay_73@yahoo.co.uk

Abstract –

The objective of this paper is to develop different automatic designs for building construction using a new tool called AutoCAD AutoLISP. One-way slab, Reinforced Cement Concrete pipe, straight stairs spanning horizontally, Circular tank over the ground and a Square Column Footing. These are the designs developed using AutoLISP software. Five Library functions are developed to get the 3D model for these designs. After getting the input parameters from the user, the required design structure will be generated automatically. The advantage of this tool is that since the library is created, the import of drawings in the structural analysis will be easy; it will shorten the design period compared to other software. Developing all types of slabs, stairs and tanks using this software will be more beneficial to improve the design efficiency and quality.

Keywords –

Automatic; Design; Reinforced; Concrete; structures; AutoCAD; AutoLISP.

1 Introduction

Software has been developed for the design and drafting of reinforced concrete structures. The reinforcement sketches given by many of such software are of a standard fixed format. Therefore, structural designers could not modify its format as per their requirements. Preparing drawings manually is a tedious and time-consuming work and may also have manual errors. Hence, there is a need for a program that can be easily customized as per the individual's choice and generates the required design in the form of intuitive 3D design automatically.

Automation in design has been used in modern industries and design enterprises. In chemical industry applications, with the help of AutoCAD Visual Basic Applications, a program has been developed which can

automatically generate the 3D model of trough-type liquid distributor as per design parameter input [1]. In manufacturing industry applications, with the help of AutoCAD customization, the automatic generation of a model of milling of a gear wheel has been developed, where the impact of cutting parameters on the tooth form of a manufactured wheel is examined. [2]

For computer aided drafting, AutoCAD is widely used. Therefore, a program that can customize AutoCAD rather than an independent package is needed as all other drawings are prepared in AutoCAD, such as Layout plans, schedules, Notes etc. AutoLISP can be used to write customized programs which control virtually every aspect of drawing and database [3]. AutoLISP program is used to automatically generate geometrically accurate computer 3D models of gear drives and hob cutters [2]. AutoLISP program is used in the Simulation of the Processing of a Helical with the aid of a frontal-cylindrical milling tool. [4]

2 About AutoLISP

AutoLISP is a unique language specially designed for AutoCAD automation [5]. AutoLISP programs perform functions by connecting points in the 3D graph by objects. For example, adding length to the X-coordinate of a point and then adding width to the Y-coordinate of the formed point forms an L shape. Simple mathematical operations and loop functions can be incorporated into AutoLISP programs. Using AutoLISP, programs can be written to generate the automatic 3D designs of any structural member or even a complete structural design of a building like a security cabin. The following sections explain the design automation process for one-way slab, RCC pipe, straight stairs spanning horizontally, circular tank over ground and square column footing.

2.1 Functioning of Program

Flowchart representation

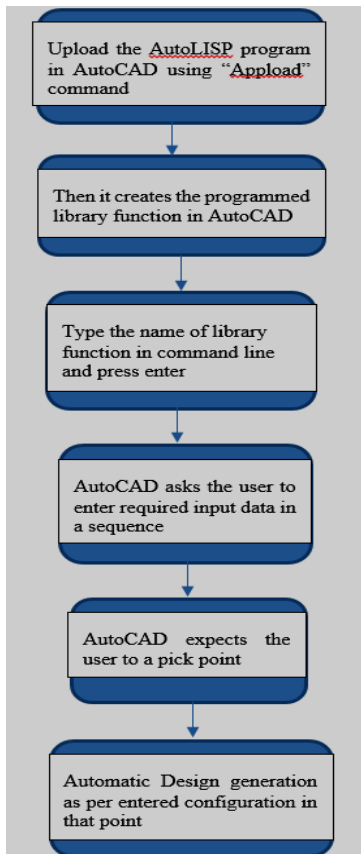


Figure.1. Flow chart

3 Automatic design of straight stairs

Straight stairs are provided in a long narrow stair case. It often consists of one flight. The library function created can generate a 3D design of single- flight straight stairs spanning horizontally as per the dimensional parameters provided by the user [6].

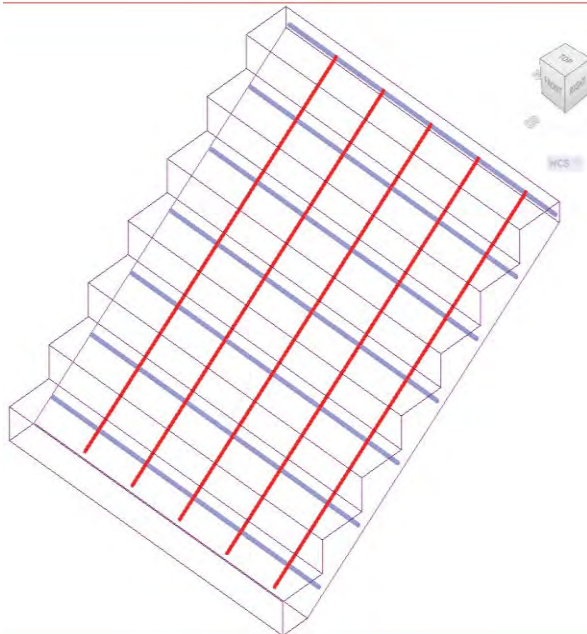


Figure 2. Design output for straight stairs

Table 1. Design parameters for straight stairs

serial number	Parameter	Values in millimeter
1	length of riser	Need input
2	length of thread	Need input
3	span of stair slab	Need input (<1500)
4	wall or beam thickness on either side of slab	Need input
5	Diameter of main bars	6
6	Diameter of distribution bars	10
7	Thickness of waist slab	80
8	Number of steps	Need input

4 Automatic design of one-way slab

Slabs form floors and roofs of buildings. Consider a slab panel supported on all four sides. If the ratio of the long span to the short span is greater than 2, such a slab is considered a one-way slab [7]. The library function created in AutoCAD can automatically generate the design of reinforcement detailing of the slab after giving all the input parameters.

Table 2. Design parameters for one-way slab

serial number	Parameter	Values in millimeter
1	Long span of slab	Need input
2	Short span of slab	Need input
3	Beam thickness	Need input
4	Clear cover distance for main bars	Need input
5	Diameter of main bars	Need input
6	Diameter of distribution bars	Need input
7	Length of crank in main bars	Need input
8	Centre to Centre spacing of main bars	Need input
9	Centre to Centre spacing of distribution bars	Need input

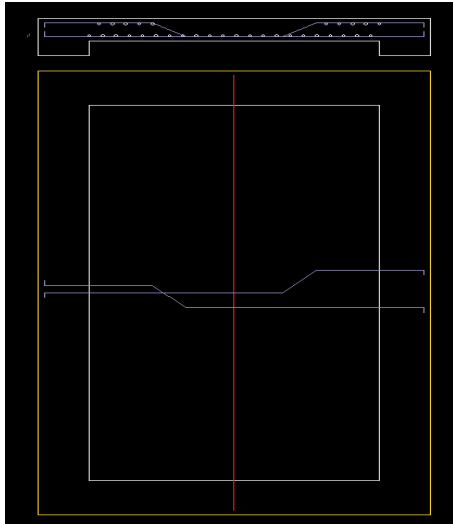


Figure 3. Design output for one-way slab (Cross section and plan of slab)

5 Automation in design of RCC pipe

Reinforced concrete pipes are generally used for carrying water in the water supply systems, carrying wastewater or storm water and conducting small streams or drains under embankments. This library function automatically generates the reinforcement detailing for the RCC pipe after getting input from the users (table 3).

Table 3. Design parameters for RCC pipe

serial number	Parameter	Values in millimeter
1	Diameter of pipe	Need input
2	Thickness of pipe	Need input
3	Diameter of bars in vertical reinforcement	Need input
4	Diameter of bars in hoop reinforcement	Need input
5	Pitch of hoop reinforcement	Need input
6	Length of pipe	Need input

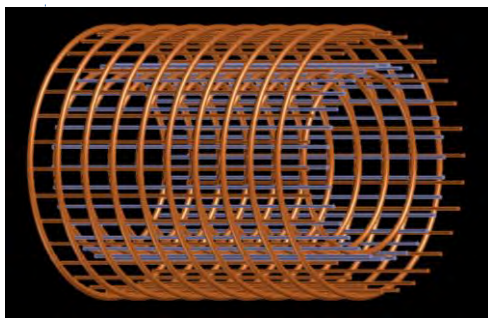


Figure 4. Design output of RCC pipe reinforcement

6 Automation in design of circular tank

A reinforced concrete tank is a very useful structure meant for storing water, for swimming baths, sewage sedimentation and similar purposes. This library function automatically generates the reinforcement detailing for a circular tank on the ground and open to the atmosphere after getting the required input from the users. The joint is flexible between the base and reinforcement. In base, the top and bottom mesh is designed and if the ring beam is required, its design is also generated automatically.

Table 4. Design parameters for circular tank having non-monolithic walls and base slab

serial number	Parameter	Values in millimeter
1	Diameter of tank	Need input
2	Diameter of bars in top and bottom mesh in base slab	10
3	Diameter of bars in vertical reinforcement	Need input
4	Thickness of wall	Need input
5	Thickness of base slab	Need input
6	Diameter of bars in hoop reinforcement	Need input
7	Centre to Centre spacing of bars in mesh	250
8	Pitch of hoops	Need input

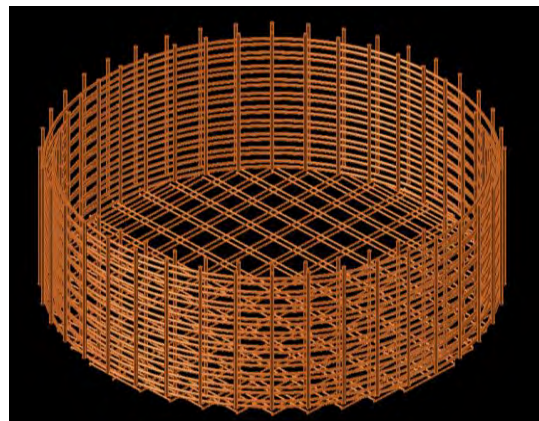


Figure 5. Design output of circular tank reinforcement

7 Automatic Design of Square Column Footing

Square column footing is a type of shallow foundation in which the base of a wall or column is sufficiently enlarged to act as individual support. The

widened base provides stability and is useful in distributing the load on sufficient soil area. This library function automatically generates the three-dimensional design of square column footing after getting the required input data from the users (Table 5). After giving all the inputs, the user has to pick a point for inserting the design. This action will plot the design in the AutoCAD window following the configurations provided by the user, as shown in Figure 6. This design can be easily edited by using AutoCAD drawing commands.

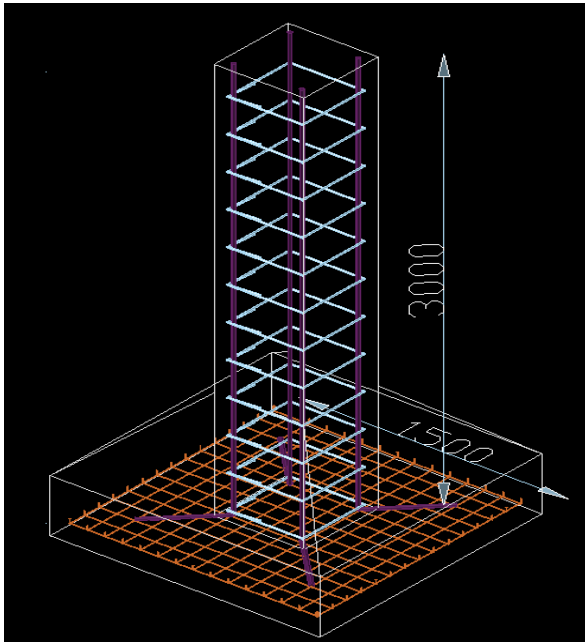


Figure 6. Design output for square column footing

Table 5. Design parameters for square column footing

serial number	Parameter	Values in millimeter
1	Side length of footing	Need input
2	Total depth of footing	Need input
3	Reduced depth of footing	Need input
4	Number of bars in footing reinforcement in principal direction	Need input
5	Diameter of bars in footing reinforcement	Need input
6	Diameter of longitudinal bars in column reinforcement	Need input
7	Pitch of lateral ties	Need input

8	Diameter of lateral ties	Need input
9	Side length of column	Need input
10	Clear cover for footing reinforcement	Need input
11	Clear cover for column reinforcement	Need input

8 Conclusion

This tool will be handy for structural and design engineers since the design gets generated automatically after feeding input parameters. The dimensional parameters gained after performing engineering calculations for specific structure has to be entered into this tool which has a set of library functions. Then, it generates the required 3D intuitive design within a minute. This tool helps to focus on more creative design, improving design efficiency and quality, shortening product design period. Being very useful in product design, it can be used for more and more specialized design and development. By developing all types of slabs, stairs, foundations and tanks using this software, perfection in design can be maintained in our day-to-day structural design of buildings.

References

- [1] Pengfei Zhang and Luojia Wan. 3D Parametric Design on Trough Type Liquid Distributor Based on AutoCAD VBA. In *international conference on information and computer application*, pages 524–530, Hong Kong, China, 2012.
- [2] Kheifetc A. L. Geometrically Accurate Computer 3D Models of Gear Drives and Hob Cutters. In *International Conference on Industrial Engineering*, pages 1098 – 1106, South Ural State University, Russia, 2016.
- [3] Poleshchuk N. *AutoCAD Developer's Guide to Visual LISP*, First Indian edition. Eswar Press, "Archana Arcade" No. 16/8, Natesan Street, T.Nagar, Chennai, India, 2003.
- [4] Sorin Cristian Albua. Simulation of Processing of a Helical with the aid of a frontal-cylindrical milling tool. In *The 12th International Conference Interdisciplinarity in Engineering*, pages 36–41, 2019.
- [5] George O. Head. *AutoLISP In Plain English*, Second edition. Galgotia Publications pvt. ltd, 5, Ansari Road, Daryaganj New Delhi, India, 1990.
- [6] Code of Practice for Plain and Reinforced Concrete, Bureau of Indian Standards, IS456:2000, Manak Bhavan, New Delhi.
- [7] Ramamrutham S. *Design of Reinforced Concrete Structures*, Seventeenth Revised and enlarged edition. Dhanpat Rai Publishing Company, New Delhi, India, 2010.

PEXCon: Design and Development of Passive Exoskeleton for Construction

Sachin Kansal, Ph.D.,¹ and Jiansong Zhang, Ph.D.²

¹Computer Science Engineering Department, Thapar Institute of Engineering Technology, Patiala, India

²Automation and Intelligent Construction (AutoIC) Lab, School of Construction Management Technology, Purdue University, Indiana, USA

sachin.kansal@thapar.edu, zhan3062@purdue.edu

Abstract –

The concept of teleoperation is crucial in modern and future construction workplaces, as it can be used in remote or challenging/hazardous environments such as workspace in a desert, close to a nuclear reactor, or underwater, among others. The success of teleoperation hinges on its interface, where passive exoskeleton with ergonomics considerations has shown great promise. In the literature, however, the ergonomic design of the passive exoskeleton and the 3-D environment for precise visual feedback is lacking. To address that, the authors target to design and develop an ergonomic inclined and light-weighted passive exoskeleton to support construction teleoperation activities.

Keywords –

Tele-operation; Manipulator; Construction Technology; Passive Exoskeleton; Sensors; Construction Education.

1 Introduction

With the workforce shortage prevalent in the construction industry, companies are picking up interest again in construction automation with robotics. While new robot design tailored for construction has been looked into, an alternative and potentially more cost-effective approach is to adapt industrial robots to the construction work context. One challenge faced in this approach is the more dynamic and uncertain environment of the construction sector compared to those in the manufacturing industry. Given that, the concept of teleoperation is crucial in modern and future construction workplaces, as it can be used in remote or challenging/hazardous environments such as workspace in a desert, close to a nuclear reactor, or underwater, among others.

The success of teleoperation hinges on its interface, where a passive exoskeleton with ergonomics considerations has shown great promise. In the literature, however, the ergonomic design of the passive

exoskeleton and the 3-D environment for precise visual feedback is lacking. To address that, the authors target to design and develop an ergonomic inclined and light-weighted passive exoskeleton to support construction teleoperation activities. By using a passive exoskeleton as a master unit in a teleoperation system, an operator can control a robotic arm that would otherwise be difficult to access, enabling smooth remote manipulation of the arm [1]. In this paper, we proposed a novel design of a passive exoskeleton for remote construction operations. A human operator will wear the passive exoskeleton to support the teleoperation activity useful in construction operations, such as in transferring heavy payload, screwing, etc., [2-6], which is to be carried out by an industrial arm manipulator. To ensure proper operation, the motion of the exoskeleton (master unit) is replicated in the arm manipulator (slave unit), with the power amplified according to the user's preferences. "Position-based teleoperation" is used, which refers to this particular mode of control where the developed exoskeleton's end-effector is mapped to the manipulator's end-effector. One challenge in this mapping is matching the movements at all degrees of freedom (DOF). As per the anatomy, a human arm has seven degrees of freedom, while the anthropometric exoskeleton only has six.

On the other hand, the arm manipulator adopted (KUKA) only has six DOFs. Specifically, there are three DOFs at the shoulder joint, two at the wrist joint, and two at the elbow joint. The exoskeleton has sensors mounted in seven distinct locations across its surface to detect the various joint angles. Potentiometers are utilized for the elbow joint's rotation and the shoulder joint's pronation and supination. The angle of rotation of adduction - abduction (outside - inside) and extension - flexion (backwards - forward) motions can be measured with the help of rotary potentiometers. The performance evaluation of sensor coupling and human motion tracking will be used. In addition, smooth control of the slave robot (KUKA) using the exoskeleton (PEXCon) as a master device will be pursued.

2 Methodology

2.1 Design and Development Steps

The design steps that are going to be incorporated are as follows:

- (a). Literature review of state of the art reported in design, control interfaces, power, actuation, communication networks, and 3-D immersive environments.
- (b). Biomechanics and ergonomic study based on the design optimisation.
- (c). Mechanical design of the proposed PExCon exoskeleton.
- (d). Kinematics analysis and workspace analysis.
- (e). Instrumentation process that includes fabrication of the sensor, noise-removing filters, Kalman estimation algorithms, and switching circuits.
- (f). Setting up of communication protocols, including Inter-Integrated Circuit (I2C), Transmission Control Protocol/Internet Protocol (TCP/IP) and User Datagram Protocol (UDP).
- (g). The design process involves analysing and fabricating the filtering circuits, such as Butterworth order five, median, and Kalman filters, to deal with the noise incorporated in the sensors while taking the reading.
- (h). Development of a 3-D immersive environment to enable teleoperations when looking at the 3-D rendering of the live-streamed scene and its integration with the PExCon exoskeleton.
- (i). Verification and validation of the PExCon exoskeleton. To assess the operation of remotely human-controlled systems, several techniques will be employed:
 1. Simulation-based testing (and training).
 2. Physical testing.
 3. User validation — interview operators about effectiveness, ease of use, and their preferences of the system.
 4. Formal verification, for example, as part of corroborative verification [7].
- (j). Deployment and repeatability test.

2.2 Arm Kinematics

The human arm, or upper limb, extends from the shoulder to the fingertips. It consists of three segments: the forearm, the arm (the region between the shoulder and elbow in a anatomy), and the hand, which are connected by three joints: the elbow, the shoulder, and the wrist. According to Figure 1, the upper limb is composed of the clavicle (which is attached to the trunk), the humerus in the arm, the scapula, the radius and ulna in the forearm, and the carpal bones, metacarpals, and phalanges of the hand and wrist [8].



Figure 1. Human upper limb prominent bones, elbow, and wrist joints

2.3 System Architecture based on UDP Protocol

UDP is used to communicate between the manipulator's KRC2 controller and the computer connected through which the robot is controlled using Robot Sensor Interface (RSI), as illustrated in Figure 2. For PExCon and KUKA manipulator integration, UDP transmits data between two computers, as both are connected to the KUKA KRC2 controller [9].

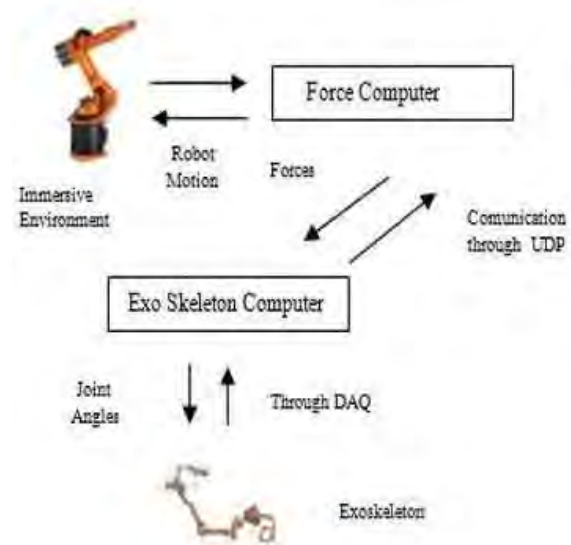


Figure 2. Communication between the KUKA manipulator and exoskeleton [10]

2.4 System Architecture Based on UDP Protocol

User Datagram Protocol (UDP) is the elementary Transport Layer protocol available within the Transmission Control Protocol/Internet Protocol (TCP/IP) protocol suite. There are few communication mechanisms involved [10]. Some consider UDP an unreliable protocol, but it employs IP services that provide a best-effort delivery mechanism, as illustrated in Figure 2. In UDP, the receiver does not send a packet acknowledgement, and the sender does not wait for a packet acknowledgement.

2.5 Ergonomic Design Reported in the PExCon

An aesthetic design of the exoskeleton will be implemented with the following features incorporated:

1. Modular fitment for sensors and accompanying electronics.
2. Jacket model for the stable base of the PExCon base.
3. Joystick design for the hand.

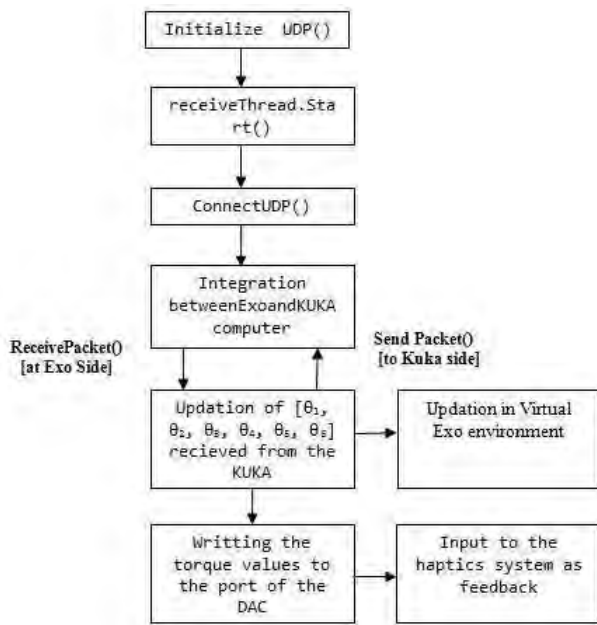


Figure 3. System architecture based on UDP protocol [3]

Table 1 Components of the PExCon

Implementation Modules	Description
Goniometry	7 joints
Kinematics	DH-parameters
Interface	PExCon -KUKA-3D immersive

Electronic components	environment
Haptics	Noise removing algorithms
Communication protocols	Yes
	TCP/IP + UDP

2.6 Design and Deployment Phases

The passive exoskeleton reported in [10] has limitations such as in weight, sensor alignment, sensor placement, and noise. We will target to resolve these concerned issues in the steps followed to achieve the design and deployment phases:

1. Design of low-weight framework for the PExCon.
2. Development of a simulation-based environment (integrating the KUKA robot with PExCon).
3. FEA-based analysis of the PExCon.
4. Development of a UDP-based communication channel for data sharing and updating.
5. Interfacing the developed PExCon with the KUKA robot in the real-time scenario.
6. Verification and validation of the developed environment.
7. Deployment of the PExCon in construction context and register the feedback (user-based, vision-based, and data log).

2.7 Construction Testbed

The PExCon will be implemented at the new construction lab located in the Dudley and Lambertus Hall (i.e., The Gateway Building) at Purdue University for testing in a real construction environment. The construction lab is a high-bay space with more than 430 square meters of floor area and an overhead gantry crane to help mobilize equipment and materials across the area (Figure 4) [10]. The construction lab can host multiple timber/steel construction projects in parallel.

In previous research at the Automation and Intelligent Construction (AutoIC) Lab at Purdue University, a workflow has been established that integrates building information modelling (BIM) and robotic simulation to investigate the feasibility of selected robotic systems in construction operations [11]. This workflow will be adapted to examine the feasibility of using the PExCon and KUKA robots (Figure 5) in helping with the operations of timber and steel

construction in the construction lab, prior to the physical test. This represents a closed-loop testbed that integrates modelling, simulation, and physical hardware testing. Furthermore, the successful testing of the PExCon will help tremendously in the accessibility of the construction lab to both residential and online learners by providing remote access to construction operations.

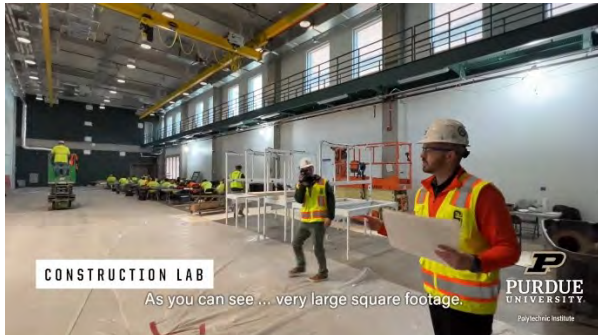


Figure 4. The new construction lab at Purdue University opened in 2023 [12]



Figure 5. The KUKA robot to be installed at the construction lab

3 Conclusion

This short paper gave a detailed overview of the development of the PExCon passive exoskeleton-based remote construction robotic operation system, where an arm exoskeleton was deployed for the teleoperation of the KUKA manipulator and preliminarily tested. The teleoperation will be carried out in our further test in a real construction environment to perform construction operations, such as carrying a heavy payload, unbolting, etc., to support closed-loop testing of construction operations and remote accessibility of the construction lab by both residential and online learners.

References

- [1] R. Gopura, D. Bandara, K. Kiguchi, and G. K. Mann, Developments in hardware systems of active upper-limb exoskeleton robots: A review, *Robotics and Autonomous Systems*, 75: 203-220, 2016.
- [2] P. Desbats, F. Geffard, G. Piola in, and A. Coudray, Force-feedback teleoperation of an industrial robot in a nuclear-spent fuel reprocessing plant, *Industrial Robot: An International Journal*, 2006.
- [3] S. Mukherjee, M. Zubair, B. Suthar, and S. Kansal, Exoskeleton for teleoperation of industrial robot, in *Proceedings of Conference on advances in robotics*, 2013, pages 1–5.
- [4] A. Schiele and G. Visentin, The ESA human arm exoskeleton for space robotics telepresence, in *Proceedings of the 7th International Symposium on Symposium on Artificial Intelligence, Robotics, And Automation in Space*, pages 19-23, 2003.
- [5] Z. Xie, G. Wu, Z. Jiang, J. Xia, and H. Liu, Teleoperation of a space robot experiment system, in *Proceedings of the IEEE International Conference on Robotics and Biomimetics (ROBIO)*, pages 2546-2550, 2013.
- [6] S. Cobos-Guzman, J. Torres, and R. Lozano, Design of an underwater robot manipulator for a telerobotic system, *Robotica*, 31(6): 945–953.
- [7] M. Webster, W. David, A. Dixon, E. Kerstin, F. Michael, A. Pipe, Corroborative Approach to Verification and Validation of Human–Robot Teams. *Int. J. Robot. Res.*, 39, pages 73–79, 2020.
- [8] J. Ponce, *Wearable robots: biomechatronic exoskeletons*, John Wiley & Sons Ltd, The Atrium, Southern Gate, Chichester, West Sussex PO198SQ, England, 2008.
- [9] A. Hayat, S. Chaudhary, R. Boby, A. Dayal, S. Roy, S. Saha, and S. Chaudhary, *Vision-Based Identification and Force Control of Industrial Robots*, *Studies in Systems, Decision and Control*, 404, Springer, Singapore, 2022.
- [10] S. Kansal, M. Zubair, B. Suthar, and S. Mukherjee, Tele-operation of an Industrial Robot by an Arm Exoskeleton for Peg-in-Hole Operation Using Immersive Environments, *Robotica*, 2021.
- [11] O. Wong Chong, J. Zhang, R.M. Voyles and B. Min, (2022). A BIM-based approach to simulate construction robotics in the assembly process of wood frames to support offsite construction automation, *Automation in Construction*, 137(May 2022): 104194.
- [12] Purdue Polytechnic Institute, *Construction Management Technology – Gateway Complex May 2022 Update – Purdue Polytechnic*, online: https://www.youtube.com/watch?v=g5zeY_aXLwY, accessed 15/01/2023.

The Analysis of Lean Wastes in Construction 3D Printing: A Case Study

Wassim AlBalkhy¹, Scott Bing¹, Saad El-Babidi¹, Zoubeir Lafhaj¹, Laure Ducoulombier²

¹ Centrale Lille, CNRS, UMR 9013-LaMcube, Lille, France

² Bouygues Construction, Lille, France

wassim.al-balkhy@centralelille.fr, scott.bing@centralelille.fr, saad.el-babidi@centrale.centralelille.fr,
zoubeir.lafhaj@centralelille.fr, L.Ducoulombier@bouygues-construction.com

Abstract –

One way to improve the construction sector is by paving the way toward adopting innovative technologies and practices that may contribute to improving efficiency and performance in this sector. During the last few years, lean construction and 3D printing have been considered compatible with this goal. Nevertheless, their integration together is still overlooked. The current study aims to fill this gap by analyzing the non-value-adding activities (waste) in 3D printing operations. To do so, two-phase 3D printing laboratory investigations were conducted and analyzed. The results showed room for efficiency improvements in 3D printing processes when integrated with lean thinking as the proportion of waste was reduced from 24% to 13.1% following the introduction of lean to the 3D printing system. The study offers researchers and practitioners an example of lean adoption in 3D printing operations that can be even adopted in other sectors.

Keywords –

Additive manufacturing, 3D printing, Lean, Lean construction, waste elimination.

1 Introduction

Additive manufacturing (AM), more commonly known as three-dimensional (3D) printing, is an innovative technology that is used to fabricate objects based on successive addition of materials [1]. Without using tools or fixtures, this successive process allows 3D printing to produce numerous on-demand complex structures and geometric shapes that are not easy to produce with other fabrication techniques [2]. This has made 3D printing one of the trendiest innovative technologies in the last few years. In 2021, the global revenue of the 3D printing sector exceeded 10 billion US dollars with expectations of growing to more than 50 billion US dollars in 2030 [3]. This was due to the growing level of maturity the sector is entering and the

higher demand for 3D-printed products due to the global logistics challenges that appeared after the COVID-19 pandemic [4-5].

The construction industry can benefit from 3D printing applications to face the challenges it encounters (e.g. poor productivity, delays, poor quality, and poor environmental performance) [6-7]. One example of how 3D printing can be advantageous in architecture and design is its ability to create customized structures that are not always possible with conventional construction methods. 3D printing is capable to fabricate complex structures with more design flexibility and easier ability to cope with design changes even after the pre-planning phase [7]; unlike the traditional construction methods where design changes have a significant impact on the time, cost, and even relationships between stakeholders in the projects [8-10]. Additionally, 3D printing contributes to saving a significant amount of time during the design and construction process, making it an ideal solution for constructing quick shelters in emergencies or wartime conditions [11]. In terms of the cost, despite the large capital needed for the initial investment due to the expensive 3D printing equipment, the overall cost of the projects can be decreased due to the savings in materials management (e.g. handling, delivery, acquiring), labor, framework, and costs resulted from design changes, overproduction, and human errors [6-7]. According to Mohd Tobi [12], the use of 3D printing in housing construction can help by saving up to 35% of the total house price in the UK. In regards to the sustainable impact, 3D printing offers opportunities to reduce the generation of waste, use more eco-friendly materials, and reduce greenhouse gas emissions (GHG) resulting from several sources such as materials production and transportation and machines use [6,13,14]. According to a report by market research company “Markets and Markets”, 30-60% of the generated waste during construction can be saved when using concrete 3D printing. Social sustainability factors such as the comfort of workers, safety, and healthy working conditions can also improve due to 3D printing



Figure 1. 3D printing and lean integration [6].

[11,13,15,17].

However, despite its many advantages, 3D printing has not yet significantly impacted the construction industry. While it is gaining popularity among professionals in this sector, it remains at an early stage of development and is only used in small-scale projects by a few teams [6,11,14].

According to Lafhaj et al [6], one of the main reasons that this technology has not been implemented at a wider scale is the fact that there has been no corresponding change in the system of building and there has not been enough work to link it with other managerial concepts and process optimization philosophies such as the philosophy of lean. Lean philosophy can help construction companies optimize their processes so that new technologies can be introduced smoothly and effectively. In their study, Lafhaj et al [6] pointed to a two-direction relationship between lean and 3D printing (as shown in Figure 1). Their study also listed a set of lean wastes that 3D printing can eliminate and other wastes that may appear during the 3D printing process. Based on this relationship, the performance in construction can be improved by benefiting from the two concepts. On one side, 3D printing can significantly contribute to eliminating various wastes and generating value for the client; which are core concepts of lean philosophy. On the other side, lean principles can help in improving the production system of construction 3D printing and achieving safer, faster, greener, and better printing.

Despite the existing potential to improve construction production systems through the integration of lean and 3D printing, the work in this field is still

insufficient. And generally speaking, this integration is still overlooked even in other sectors [18-19]. Therefore, the current study aims to shed the light on this area by investigating how lean principles can be applied in the construction 3D printing processes.

2 Lean Theory and 3D Printing

The theory of lean originated in Japan following the development of the Toyota Production System (TPS) [20]. Following World War II, Toyota faced various challenges such as the scarcity of raw materials, low productivity levels, and the need to meet the diversity in the demand by the Japanese customer. These challenges raised awareness toward achieving a zero-waste production system [21]. The new production system helped Toyota to benefit from the advantages of craft production and mass production at the same time without being affected by the high cost of the first and the rigidity of the second [22]. It also helped Toyota to achieve remarkable success to the limit that it was labeled as “The Machine that Changed the World” in the book of Womack et al [23]. This success was key to improving many production systems in various countries and several sectors including the construction sector [24].

Value creation based on the client’s need and requirement, value stream mapping, creating flow, establishing pull, and achieving continuous improvement are the main principles of the lean theory [25]. Creating flow means that the production process must flow smoothly and all the bottlenecks that hinder should be eliminated [26]. These bottlenecks are defined

as wastes. Taiichi Ohno; the developer of TPS presented seven categories for lean wastes in his book “Toyota production system: beyond large-scale production”. Recently, two categories were added (“non-utilized talents” and “crises”) [27-28]:

1. Defects: examples of defects include producing a defective product or component, failure to meet quality standards, or the need to rework.
2. Motion: this covers unnecessary movement on site or in the workspace.
3. Waiting: delays or wasted time due to waiting for a machine, product, labor, action, decision, information...etc.
4. Transportation: unnecessary movement of materials or equipment.
5. Over-processing: examples of over-processing cover the unnecessary steps in the production or producing something that is not valued or required by the client
6. Overproduction: this refers to producing more than the planned or needed items, producing a product or a component earlier than planned, or ordering too many materials than needed. too early/ ordering too many materials
7. Inventory: Excess storage of materials, Work-In-Progress (WIP), or unused tools
8. Non-utilized talents: Non-utilized crew and skills
9. Crisis: failure to benefit from crisis and opportunities

In construction, 3D printing can offer many opportunities to eliminate wastes when it is compared to traditional construction methods. Lafhaj et al [6] identified a group of factors that contribute to waste elimination due to the use of 3D printing in construction. The factors include:

1. Material management in 3D printing, which helps to reduce unnecessary inventory, WIP, waiting time, and areas for saving final products. This is due to the limited amount of needed materials and the possible direct integration of materials in production.
2. Additive process, which requires no formwork. Accordingly, it reduces the inactive time needed for curing concrete, and formwork time.
3. Automated process, which helps to reduce waiting for labor and unnecessary movement on-site. In addition to reducing rework due to the ability to notice defects earlier than it is in the conventional construction methods. The automated process helps also to avoid overproduction and excess processing wastes.
4. Stable production system, which offers less waiting for crew and logistics.

Nevertheless, similar to any production system,

various wastes can be found in the 3D printing processes [6,18-19]. Lafhaj et al [6] listed various possible examples of lean wastes in 3D printing systems such as errors in the design (defects), defects in the robotic system (defects), defective layer (defects), a non-optimal path of printing (motion), waiting for maintenance (waiting), transportation of materials (transportation), too early printing (overproduction), and others.

Apart from the conceptual study by Lafhaj et al [6] that aimed to provide possible examples of lean wastes in the construction 3D printing processes, the authors of this study did not find any study that tried to investigate the presence of wastes in construction 3D printing. Therefore, this study aims to fill this gap and provide an analysis of the found wastes in a conducted 3D printing test.

3 Research Methodology

The main aim of this study is to analyze the lean wastes that may appear during the 3D printing processes. Identifying and removing the wastes in these processes can help achieve improvements and optimize 3D printing.

To achieve this aim, the current study used the following methodology (as shown in Figure 2):

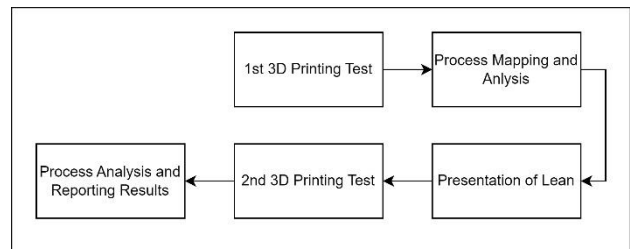


Figure 2. Research Methodology.

3.1 Conducting the first 3D printing test

The test was conducted in a laboratory environment. The team of researchers has previously conducted several 3D printing experiments in the laboratory; however, lean thinking had not been introduced before to these experiments.

As shown in Figure 3, the two tests were conducted to print the same shape. This was to ensure that the results from the tests are comparable.

The printed object has an initial layer in the shape of a hexagon and a final layer in the shape of a circle. Between the first and final layers, the trajectory twists from one shape to another, creating an object impractically constructed with traditional methods. The printed object has a diameter and height of 45 cm, a layer height of 1 cm, and a layer thickness of 5cm. The

overall printing time is supposed to be 15 minutes and 34 seconds and the overall volume of concrete is 132.32 Liters.



Figure 3. Printed object.

3.2 Process Mapping and Analysis

Process mapping aims to understand and register all the process steps and sub-tasks to understand the value-adding activities (VA) and the non-value-adding activities (i.e. wastes or NVA) [18]. The team divided the overall process based on 17 main steps starting from the preparation of the printing materials (following wearing personal protective equipment) to the end of the printing process.

Using video recording during the two tests, the process was mapped and analyzed in a standardized structure that is shown in Table 1. This structure was for the two parts of each test; the materials and robotic parts.

Using the mapping and analysis structure, each task was decided if it is necessary (VA) or unnecessary (NVA). The time of each task was defined and each NVA task was assigned to the waste category it belongs to. Following the mapping of the tasks, the analysis was conducted to identify the overall wasted time and the percentage of each waste category.

Table 1. Process mapping and analysis structure.

No.	Time	Task description	Type (VA/NVA)	Category (if NVA)
Task 1	t_1	Searching for a tool	NVA	Motion
Task 2	t_2
...
Task n	t_n

4 Results

4.1 The first test

The analysis of the first test revealed that the overall time to print the selected object was 2785 seconds and the total wasted time was 678 seconds. In other words, 24.34% of the printing process was wasted on non-value-adding activities.

The analysis also showed (as shown in Figure 4) that 45% of the overall wasted time was due to the occurrence of waiting activities, 22% was due to transportation activities, and 19% was because of the unnecessary movement or motion activities. For the robotics part, the percentage of the waiting activities was 55%, and then 14.53% and 13.70% for the transportation and motion activities, respectively. The highest percentage for the materials part was for the transportation activities (32.25%), then for waiting (29.22%), and then for motion (26.62%).

Examples of the NVA activities include waiting for information (waiting), searching for the design file (waiting), waiting due to technical error (waiting), searching for a tool (motion), searching for materials (motion), transportation of the mixer (transportation), redo weighing of materials (defects/rework).

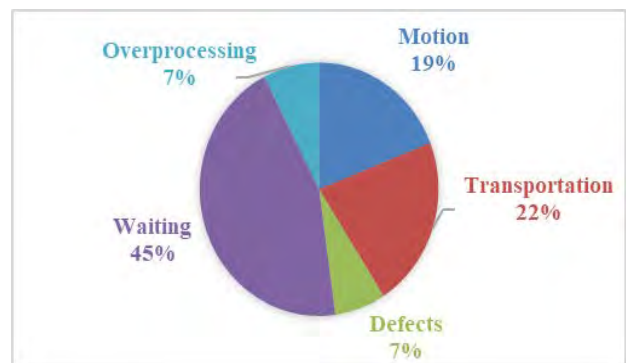


Figure 4. Percentages of waste categories activities to the overall NVA activities in the 1st test.

4.2 Presentation of lean

Following the analysis of the first test's results, lean principles and tools were introduced to the team. The presentation included introducing the principles of lean and lean construction and reviewing the wastes found in the first test. The presentation also covered some tools that can be helpful when trying to improve the 3D printing process and eliminate the found waste. The tools that were covered were:

- 5 Why: "is a systematic questioning process used to identify the root cause of a problem" [29]. This tool was used to explain the occurrence of lean wastes found in the first test.

- Value Stream Mapping (VSM): one of the main principles and tools of lean, where the process is mapped and visualized to show the value flow along the different activities, and as a result, finding rooms for eliminating wastes and optimizing adding value activities [29-30].
- 5S workplace organization: a structured method to achieve, maintain and improve workplace organization and standardization aiming to ensure having a safe work area and efficient processes with the least amount of waste [29]. 5S is based on five actions that start with the letter “S”, which are “Sort”, “Set”, “Shine”, “Standardize”, and “Sustain”.
- Plan-do-check-act for continuous improvement (PDCA): a four-step iterative structured method to achieve continuous improvement by testing gains in the process improvement when taking different actions. In this method, Plan refers to (set up a plan and expect results), Do refers to (execute the plan); Check refers to (verify anticipated result achieved); and Act (evaluate; do it again) [29-30].

In addition to discussing some solutions such as the supermarket solution, Visual Management (VM), predictive maintenance, error-proofing, and parallel processing.

4.3 The second test

Following the lean presentation, the team decided to take some measures to improve the 3D printing process such as the use of supermarket, workplace organization, and parallel processing. Other measures were decided to be adopted in the future due to the time limitation and the need to conduct more than one test to validate their use. Examples of these measures include visual management, error-proofing, and predictive maintenance.

The analysis of the results of the second test revealed that the total time was reduced by 152 seconds (total= 2633 seconds) in comparison to the first test. The total wasted time on NVA activities was 13.1% of the overall process time.

Figure 5 shows the percentages of the waste categories activities to the overall NVA activities. The figure shows that waiting activities remained to be the most frequent activities in the second test constituting 51% of the overall NVA. The percentage of the waiting wastes was mostly in the robotics (65.77%), while in the materials part was 16.6%. Following the waiting activities, motion (23%) and transportation (15%) remained to be the highest.

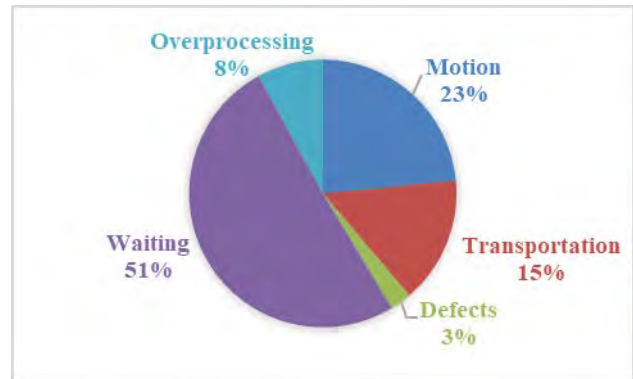


Figure 5. Percentages of waste categories activities to the overall NVA activities in the 2nd test.

Figure 6 shows a comparison between the number of NVA activities in the two tests. The Figure shows a decrease in all categories. The highest change was in the transportation activities and the defects/rework activities. This might be attributed to the workplace organization and parallel processing work that helped the team to avoid doing too many transportation activities or doing the same thing twice.

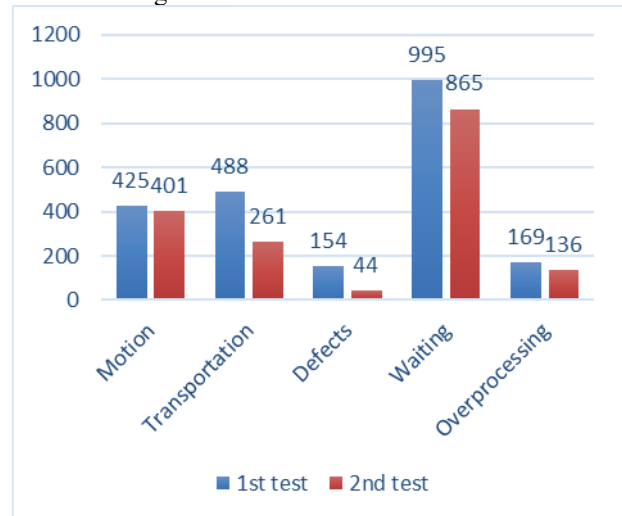


Figure 6. Percentages of waste categories activities to the overall NVA activities in the 2nd test.

Despite the decrease in the waiting and motion activities, there is a need for more work to ensure achieving the continuous improvement goals, delivering higher value, and eliminating more waste. This might be done by improving the planning of the process and workplace, use of visual management, and improving the coordination work.

5 Discussion

Lean thinking and 3D printing are two of the most

important concepts in the modern construction environment. This is because the two concepts have shown numerous potentials to revolutionize the construction sector in many ways including efficiency improvement, saving time of construction, improving quality, achieving client satisfaction, and achieving sustainability [31-33]. Nevertheless, the integration of the two concepts together has not been sufficiently covered. The current study, which is based on two-phase laboratory investigations tries to achieve this aim by analyzing the found lean wastes that affect the flow in the 3D printing processes.

The results of the first test showed that more than 24% of the 3D printing time was wasted on non-value-adding activities. According to Aziz and Hafez [34], the average wasted time in manufacturing operations is around 12%, while it is more than 57% in construction projects. Despite the need for many other investigations, the found ratio in this study may support the claim that 3D printing can help reduce wasted time in construction operations. However, this ratio is still high and calls the need of further thinking about possible ways to improve 3D printing operations' efficiency.

Following the presentation of lean, the ratio of waste was reduced to 13.1%. This showed a possible opportunity to improve the time and even the cost of 3D printing systems while maintaining the quality or even improving it, which is the essence of lean thinking.

In the two tests, the percentage of waiting wastes was the highest among the non-value-adding activities. The same behavior was reported in different cases in the traditional methods of construction [35-36]. As a result, similar to the traditional construction methods, 3D printing systems should be built over a high level of coordination and can benefit from different lean tools (e.g. JIT, VM, and pull planning) to eliminate as much waste as possible. It is worth mentioning here that as the current study was conducted in a laboratory environment with a known mixture and known test parameters, other sources of waste may appear while constructing a full-scale 3D printing building. One main example of these wastes is the "defects", which was not the highest in this study but according to Sini et al [12], it is the main reason why 3D printing is still immature enough to guarantee the quality of the 3D printed products. Accordingly, it is recommended to conduct similar investigations to answer the same research questions in a real project environment, where other factors such as supply chain and logistics management can be covered.

6 Conclusions

The current study presents an example of employing lean thinking to improve the performance of 3D printing

systems in construction. It also shows that the two concepts can be integrated to maximize productivity in this sector. This study tries to fill the gap in the literature that lies in the scarcity of resources about this integration. It also serves as an example of how to analyze and identify wastes in 3D printing operations. As a result, this study tries to provide practitioners and researchers with a way to investigate how to improve efficiency in the construction of 3D printing.

In addition to the lab investigation, the current study has the limitation of the number of tests. While continuous improvement is one of the core concepts of lean, the current study builds its results over a short period of investigations. As a result, there is a need for a larger number of tests and a longer period to ensure achieving greater improvement and eliminating the possible wastes that may appear over time. Other research areas can cover investigating the lean wastes or lean adoption opportunities in onsite and offsite construction 3D printing systems, exploring the challenges that face this adoption, examining the impact of lean on supply chain management and sustainability in the two types of systems, and using other construction 4.0 practices side by side with lean to improve the performance in 3D printing operations.

References

- [1] N. Shahrubudin, T. C. Lee, and R. Ramlan, "An Overview on 3D Printing Technology: Technological, Materials, and Applications," *Procedia Manuf.*, vol. 35, pp. 1286–1296, Jan. 2019.
- [2] X. Ning, T. Liu, C. Wu, and C. Wang, "3D Printing in Construction: Current Status, Implementation Hindrances, and Development Agenda," *Adv. Civ. Eng.*, vol. 2021, 2021.
- [3] M. Molitch-Hou, "Three Areas Holding Back The \$10.6B 3D Printing Industry," 2020. [Online]. Available: <https://www.forbes.com/sites/michaelmolitch-hou/2022/04/25/three-areas-holding-back-the-106b-3d-printing-industry/>. [Accessed: 20-Jan-2023].
- [4] Y. Y. C. Choong, H. W. Tan, D. C. Patel, W. T. N. Choong, C. H. Chen, H. Y. Low, M. J. Tan, C. D. Patel, and C. K. Chua, "The global rise of 3D printing during the COVID-19 pandemic," *Nat. Rev. Mater.* 2020 59, vol. 5, no. 9, pp. 637–639, Aug. 2020.
- [5] S. Ishack and S. R. Lipner, "Applications of 3D Printing Technology to Address COVID-19–Related Supply Shortages." *Am. J. Med.*, vol. 133, no. 7, p. 771, Jul. 2020.

- [6] Z. Lafhaj, W. Albalkhy, and D. Karmaoui, "Identification of Lean Waste in Construction 3D Printing Processes," in *The International Inorganic-Bonded Fiber Composite Conference (IIBCC)*, Hamburg, Germany, 2022.
- [7] L. Hou, Y. Tan, W. Luo, S. Xu, C. Mao, and S. Moon, "Towards a more extensive application of off-site construction: a technological review," <https://doi.org/10.1080/15623599.2020.1768463>, vol. 22, no. 11, pp. 2154–2165, 2020.
- [8] I. Abdel-Rasheed, M. A. El-Mikawi, and M. E.-S. A.-H. Saleh, "Empirical Model for Prediction the Impact of Change Orders on Construction Projects- Sports Facilities Case Study," *Int. Conf. Civ. Archit. Eng.*, vol. 10, no. 10th International Conference on Civil and Architecture Engineering, pp. 1–11, May 2014.
- [9] J. M. Assbeihat and G. Sweis, "Factors affecting change orders in public construction projects," *Int. J. Appl.*, vol. 5, no. 6, pp. 56–63, 2015.
- [10] G. Sweis, R. Sweis, A. Abu Hammad, and A. Shboul, "Delays in construction projects: The case of Jordan," *Int. J. Proj. Manag.*, vol. 26, no. 6, pp. 665–674, Aug. 2008.
- [11] S. J. Schuldt, J. A. Jagoda, A. J. Hoisington, and J. D. Delorit, "A systematic review and analysis of the viability of 3D-printed construction in remote environments," *Autom. Constr.*, vol. 125, no. February, 2021.
- [12] F. Sini, P. Chiabert, G. Bruno, and F. Ségonds, "A Lean Quality Control Approach for Additive Manufacturing," *IFIP Adv. Inf. Commun. Technol.*, vol. 594, pp. 59–69, 2020.
- [13] L. Romdhane, "3D Printing in Construction: Benefits and Challenges," *Int. J. Struct. Civ. Eng. Res.*, vol. 9, no. 4, pp. 314–317, 2020.
- [14] M. K. Dixit, "3-D Printing in Building Construction: A Literature Review of Opportunities and Challenges of Reducing Life Cycle Energy and Carbon of Buildings," *IOP Conf. Ser. Earth Environ. Sci.*, vol. 290, no. 1, 2019.
- [15] N. O. E. Olsson, A. Shafqat, E. Arica, and A. Økland, "3d-printing technology in construction: Results from a survey," *Emerald Reach Proc. Ser.*, vol. 2, pp. 349–356, 2019.
- [16] Z. Lafhaj, A. Z. Rabenantoandro, S. el Moussaoui, Z. Dakhli, and N. Youssef, "Experimental Approach for Printability Assessment: Toward a Practical Decision-Making Framework of Printability for Cementitious Materials," *Buildings*, vol. 9, no. 12, p. 245, Dec. 2019.
- [17] I. Krimi, Z. Lafhaj, and L. Ducoulombier, "Prospective study on the integration of additive manufacturing to building industry—Case of a French construction company," *Addit. Manuf.*, vol. 16, pp. 107–114, Aug. 2017.
- [18] H. Groneberg, R. Horstkotte, M. Pruemmer, T. Bergs, and F. Döpfer, "Concept for the reduction of non-value-adding operations in Laser Powder Bed Fusion (L-PBF)," *Procedia CIRP*, vol. 107, no. 2021, pp. 344–349, 2022.
- [19] H. Groneberg, J. Koller, A. Mahr, and F. DÖpper, "Development of a systematic approach to identify non-value-adding operations in the LBM process chain," *Procedia CIRP*, vol. 104, no. January, pp. 1613–1618, 2021.
- [20] W. Albalkhy, R. Sweis, and Z. Lafhaj, "Barriers to Adopting Lean Construction in the Construction Industry—The Case of Jordan," *Buildings*, vol. 11, no. 6, p. 222, May 2021.
- [21] T. Diekmann, J. E., Balonick, J., Stewart and S. Won, "Application of lean manufacturing principles to construction," 2004.
- [22] F. Innella, M. Arashpour, and Y. Bai, "Lean Methodologies and Techniques for Modular Construction: Chronological and Critical Review," *J. Constr. Eng. Manag.*, vol. 145, no. 12, 2019.
- [23] J. Womack, D. Jones, and D. Roos, *Machine That Changed the World*. New York: Simon and Schuster, 1990.
- [24] W. Albalkhy and R. Sweis, "Assessing lean construction conformance amongst the second-grade Jordanian construction contractors," *Int. J. Constr. Manag.*, vol. 22, no. 5, pp. 900–912, 2022.
- [25] J. Womack and D. Jones, "Beyond Toyota: How to root out waste and pursue perfection," *Harv. Bus. Rev.*, vol. 74, pp. 1–16, 1996.
- [26] A. Mossman, "Lean & the deployment of robots in construction," in *2nd Annual Architecture and Civil Engineering Workshop (ACE Workshop)*, Lille, France, 2020, no. January.
- [27] Z. Dakhli and Z. Lafhaj, *La révolution de la construction lean*. Auto-edition, 2018.
- [28] M. El Jazzer and H. Nassereddine, "Interactions Between Construction 4.0 and Lean Wastes," *Proc. Int. Symp. Autom. Robot. Constr.*, vol. 2021-Novem, pp. 971–978, 2021.
- [29] R. O'Connor and B. Swain, *Implementing Lean in construction: Lean tools and techniques-an introduction*. London, UK: CIRIA, 2013.
- [30] R. Hannis Ansah, S. Sorooshian, S. Bin Mustafa, and G. A. Duvvuru Leon Linton, "Lean Construction Tools," in *Proceedings of the 2016 International Conference on Industrial Engineering and Operations Management*,

- Detroit, Michigan, USA, 2016, pp. 784–793.
- [31] W. Albalkhy and R. Sweis, “Barriers to adopting lean construction in the construction industry: a literature review,” *Int. J. Lean Six Sigma*, vol. 12, no. 2, pp. 210–236, Mar. 2021.
- [32] M. Žujović, R. Obradović, I. Rakonjac, and J. Milošević, “3D Printing Technologies in Architectural Design and Construction: A Systematic Literature Review,” *Buildings*, vol. 12, no. 9, p. 1319, 2022.
- [33] N. Labonnote, A. Rønquist, B. Manum, and P. Rütther, “Additive construction: State-of-the-art, challenges and opportunities,” *Autom. Constr.*, vol. 72, pp. 347–366, 2016.
- [34] R. F. Aziz and S. M. Hafez, “Applying lean thinking in construction and performance improvement,” *Alexandria Eng. J.*, vol. 52, no. 4, pp. 679–695, Dec. 2013.
- [35] M. S. Bajjou, A. Chafi, and A. En-Nadi, “A Comparative Study between Lean Construction and the Traditional Production System,” *Int. J. Eng. Res. Africa*, vol. 29, pp. 118–132, 2017.
- [36] J. G. Sarhan, B. Xia, S. Fawzia, and A. Karim, “Lean construction implementation in the Saudi Arabian construction industry,” *Constr. Econ. Build.*, vol. 17, no. 1, pp. 46–69, 2017.

Exploring the Digital Thread of Construction Projects

Makram Bou Hatoum ¹, Hala Nassereddine ¹, Nadine AbdulBaky ², and Anwar AbouKansour ²

¹ Department of Civil Engineering, University of Kentucky, Lexington, KY, USA

² ProMission FZ LLC, Dubai, United Arab Emirates

mnbo229@uky.edu, hala.nassereddine@uky.edu, nadine.baky@promissionmcss.com, anwarak141@live.com

Abstract –

The construction industry is one of the most information-intensive industries where the success of projects depends on information being accurate, complete, timely, readily available, and understandable by different recipients. As projects become complex and processes become more digitized, the value of capturing, tracking, accessing, and sharing lifecycle-spanning data becomes critical for project stakeholders. One way to capitalize on the value of data is through the concept of Digital Thread. The Digital Thread breaks down the silos of information and makes it accessible to the right stakeholder at the right time, promoting high-fidelity collaboration among stakeholders, enabling richer stakeholder-driven analysis, enhancing decision-making, and increasing transparency and information exchange. With the concept being relatively new in the construction industry, research on Digital Threads remains limited. Thus, this paper addresses the gap by exploring the concept and its pillars. The paper proposes a comprehensive definition of the Digital Thread of the construction project and explores the interconnectivity between people, processes, and data (three pillars) along the construction project Digital Thread. The paper also presents a case study to further investigate the interconnections between the three pillars and proposes a three-Dimensional Digital Thread Infrastructure using the construction phase of the Design Bid Build project in the Middle East. Future work will build on the findings of this paper to create an interface for the Digital Thread schema for the construction project and build a platform to provide all stakeholders with the means to achieve full project lifecycle traceability.

Keywords –

Digital Thread; People; Process; Social Network Analysis; Topology

1 Introduction

Projects in the construction industry require the

involvement of a wide range of stakeholders throughout their lifecycle – from conceptual planning to decommissioning [1]. As such, project teams would therefore comprise multiple players employed by various organizations that conduct different businesses [2]. This makes projects both complex and dynamic, as completing project tasks would require information to be accurate, complete, timely, delivered promptly, and readily available in a clear format that can be understandable by different recipients [3,4].

Thus, the success of construction projects relies heavily on the management of the flow of data and information among key players as the project moves from one phase to another [5,6]. However, the multidisciplinary and fragmented nature of the construction industry creates a challenging environment for the seamless flow of data and information, and in return, hinders the successful implementation of the project [7]. This makes lifecycle-spanning data difficult to capture in the construction industry, and the value of such data usually remains unused [8].

1.1 Digital Transformation in Construction

Researchers have noted that the main reason for the inefficient exchange of data between stakeholders among projects is the absence of digitization of construction processes [8]. Advancements in technology driven by the fourth industrial revolution have led to numerous studies that focused on shifting the construction industry into the digital sphere [9,10]. Examples of such studies include investigating cyber-physical systems [11], enabling digital twins [12], exploiting artificial intelligence [13], adopting robotics [14], utilizing wireless and sensing technologies [15], and pushing cognitive and cloud computing across the project lifecycle [16]. Although construction companies are slow to adopt and adapt to digital change, such studies have paved the way for digitization in the construction industry, which in turn enables the digitalization of processes and moves the industry toward the eventual digital transformation and the digital twin of the project [17].

Digital transformation is essentially built on data [18]. While data is the ‘engine’ of digital transformation, the ‘Digital Thread’ is the ‘amplifier’ that capitalizes on the

value of data and enables this transformation [19,20]. To develop and achieve the digital twin of the construction project, a digital thread must be established [31]. The concept of Digital Thread has been leveraged in different industrial sectors [21], but the concept remains relatively new to the construction industry [17].

1.2 The Digital Thread

The Digital Thread introduces a unique solution to solve the problems with the information jungle, inconsistency, and disintegration associated with the traditional, fragmented nature of the construction industry. The Digital Thread breaks down the silos of information and makes it accessible to the right stakeholder at the right time, promoting high-fidelity collaboration among stakeholders, enabling richer stakeholder-driven analysis, enhancing decision-making, and increasing transparency and information exchange [17,21,22].

1.3 Research Gap and Objective

Building on the awareness of the construction industry of the Digital Thread potential, this paper aims to enable informed dialog about Digital Thread in the construction industry by achieving two objectives: proposing a comprehensive definition of the Digital Thread of the construction project and exploring the interconnectivity between people, processes, and data along the construction project Digital Thread. The paper is part of an ongoing effort to create an interface for the Digital Thread schema for the construction project and build a platform to provide all stakeholders with the means to achieve full project lifecycle traceability.

2 Research Methodology

To achieve the desired objectives, the authors began by reviewing the existing definitions of Digital Thread and then proposed a comprehensive definition of the Digital Thread for the construction project. Following the definition, the three main pillars of the construction project Digital Thread were discussed: people, processes, and data.

Next, a case study is conducted to further investigate the interconnections between the three pillars of the Digital Thread (data, people, and processes). The case study solely focuses on the digital thread of the construction phase of Design-Bid-Build projects executed in the Middle East. Three interviews were conducted with three subject matter experts with an overage of 12 years in the industry to collect data on 1) the processes that constitute the construction phase, 2) the stakeholders involved in every process, and 3) the sources of data that stakeholders need in each process.

The interview data is then organized and translated into a Digital Thread infrastructure and matrix to analyze the connections between the three Digital Thread pillars. A discussion section is then presented.

3 Digital Thread of the Construction Project

The Digital Thread concept emanated from the military aircraft industry as a game-changing opportunity to advance manufacturing and help the U.S. Air Force meet the need for more rapid development and deployment [23]. Digital Thread introduces the concept of digital linkage between materials, design, processing, and manufacturing to provide the agility and tailorability needed to support rapid development and deployment [23]. Following the emergence of Digital Thread in the *2013 Global Horizons: United States Air Force Global Science and Technology Vision report*, [24] referred later to Digital Thread at a National Institute of Standards and Technology (NIST) symposium as a “cross-domain, common digital surrogate of a material system that provides the analytical framework for organizing output from high-fidelity, physic-based model across the entire lifecycle.” A year later and during a National Defense Industrial Association (NDIA) Conference, [25] defined Digital Thread as “an extensible, configurable and Agency enterprise-level analytical framework that seamlessly expedites the controlled interplay of authoritative data, information, knowledge, and computer software in the enterprise data-information-knowledge systems, based on the Digital System Model template, to inform decision makers throughout a system’s life cycle by providing the capability to access, integrate and transform disparate data into actionable information”. [26] later put forth a refined definition stating that digital thread is “an extensible, configurable, and enterprise level framework that seamlessly expedites the controlled interplay of authoritative data, information, and knowledge to inform decisions during a system’s life cycle by providing the capability to access, integrate, and transform disparate data into actionable information”.

[27] then reviewed all existing Digital Thread definitions until the year 2015 and noticed that while the definitions vary, Digital Thread can be envisioned as the “single authoritative representation of a product”. Digital Thread becomes “the definitive repository of authoritative information containing everything about the system at that instant of time” which means that Digital Thread serves as the primary data and communication platform for an organization’s product at any time during the product lifecycle. [27] also noted that for Digital Thread to be the authoritative source of information, information has to be current and complete. [28] referred to Digital Thread as “the communication framework that

allows a connected data flow and integrated view of the asset's data throughout its lifecycle across traditionally siloed functional perspectives [enabling the delivery] of the right information to the right place at the right time.”

As interest in Digital Thread continued to grow among practitioners and academics, new definitions emerged. [29] provided a simple definition of the concept as “the flow of information about a product's performance and use from design to production, sale, use and disposal or recycling”. [30] stated that Digital Thread is “a data-driven architecture that links together information generated from across the product lifecycle and is envisioned to be the primary or authoritative data and communication platform for a company's products at any instance of time”. In a PTC article on *What is Digital Thread*, [31] noted that a Digital Thread creates a closed loop between the digital and physical worlds, documenting how products are engineered, manufactured, and serviced. This link between the phases enables simple, continuous universal access to data. Most recently, Digital Thread is defined by [32] as “a communication network that enables a connected flow of data as well as an integrated view of an asset's data across its lifetime through various isolated functional perspectives, thus promoting the transmission of the correct information, to the correct place, at the correct time.”

It can be noted from the synthesis of the existing Digital Thread that manufacturing is often the industry of interest. One of the first applications of Digital Thread in the construction industry is attributed to the United Kingdom's Building Safety Bill requiring a digital “golden thread of information”, which is both information about the facility to ensure its safe operation and the information management to ensure that the information is accurate, current, and accessible [33]. Beyond this application, the concept of Digital Thread remains a novice in the construction industry. Thus, there is a need to comprehensively define Digital Thread in the context of construction management.

3.1 Proposed Definition for the Digital Thread of a Construction Project

While the concept of Digital Thread is the same regardless of the industry, to understand how Digital Thread is relevant to an industry, the definition needs to be tailored to the application. Building off the existing definitions, the authors propose the following definition of the Digital Thread of a construction project: The Digital Thread is a data-driven architecture that links traditionally siloed *processes* into a connected flow of *data* that presents 1) a single authoritative source of current and complete data and 2) an integrated view of data gathered, used, and exchanged by the right *stakeholders* across the construction project lifecycle

phases at the correct time.

3.2 Pillars of Construction Project Digital Thread

The proposed definition highlights three main pillars for the Digital Thread of the construction project: people, processes, and data. *People* represent the internal and external stakeholders involved in the realization of the construction project from conception to decommissioning. *Processes* are the various steps or functionalities that constitute the various phases of the construction project lifecycle.

These three main pillars can be represented by the fundamental *who*, *when*, and *how* questions asked at each project phase:

- *Who* is involved? (people)
- *When* is the party involved? (process)
- *How* does the data flow between the people and across the processes? (data)

Quality data is what prevents a broken Digital Thread, and thus, the third question on *how* is a complex, multi-dimensional question that embodies the management of the data lifecycle. Proper data management depends on the understanding of how data is produced, obtained, and used, and transparency regarding data sources and uses is critical [34].

4 Case Study

Creating the schema for the construction project Digital Thread depends on understanding and mapping out the relationships between the three main pillars: people, processes, and data. To further investigate the dynamics between the three pillars, a case study is conducted for the construction phase of Design-Bid-Build (DBB) projects in the Middle East.

Three subject matter experts (SMEs) in Middle East construction projects with a total of 45 years of experience working for contractors and performing project management consulting services were asked to perform three tasks: (1) identify the main processes in the construction phase of a DBB project, (2) identify the stakeholders who are involved in each of those processes, and (3) identify the sources of data that the stakeholders need to successfully complete each process. The case study was limited to collecting data sources and did not get into the detail of the different data formats used by stakeholders. Moreover, the use of data was limited to simply stating the sources of data for a particular process and indicating all involved stakeholders. Future work will detail the relationships between the data sources, data format, and data users.

Once the data was gathered, a three-dimensional Digital Thread Infrastructure was developed to map the

three pillars of the Digital Thread: processes, stakeholders, and data source. The infrastructure and the interview data were then translated into a matrix which was later used to visualize a network topology of three pillars and perform social network analysis.

Thread were mapped in the three-dimensional Digital Thread Infrastructure which outlines the fundamental elements of the Digital Thread, as shown in Figure 1. The SMEs identified 21 processes in the pre and post-award phases of the construction phase; 39 stakeholders between contractors, engineers, subcontractors, employer(s), and other parties; and 37 sources of data.

4.1 Three-Dimensional Digital Thread Infrastructure

The three pillars of the construction project Digital

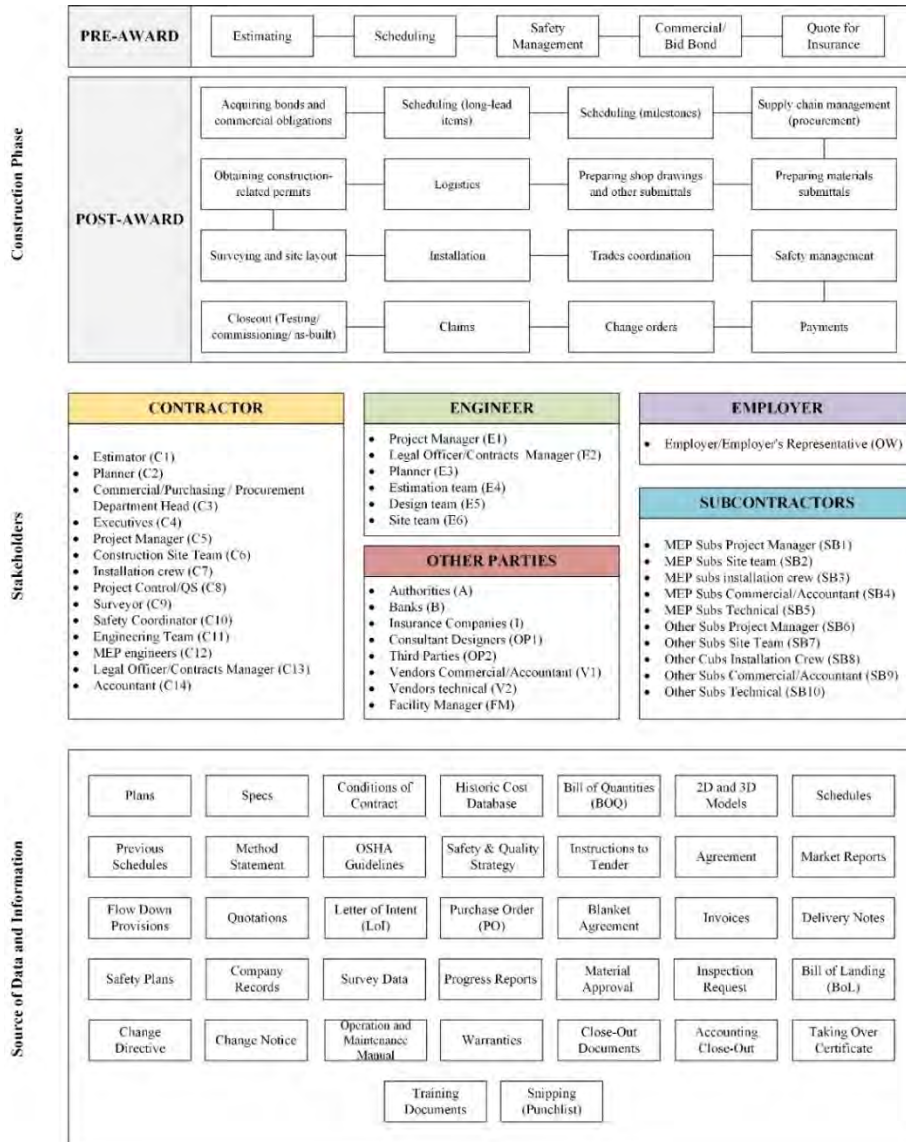


Figure 1. Case study fundamental elements of the digital thread.

4.2 Analysis Matrix

For every construction phase process, the SMEs were asked to select the stakeholders who are involved as well

as the sources of data that the process requires. The selections were then transformed into a binary analysis matrix where the rows represented the processes and the columns represented the stakeholders and the sources of

data. A value of “1” was given to selected stakeholders and sources of data, and a value of “0” was given to the stakeholders and sources of data that were not selected.

For example, for the “estimating” process, the SMEs selected eight sources of data and seven involved stakeholders. Thus, the columns representing the seven sources (plans; specs; conditions of the contract; historic cost database; BOQ; schedules; 2D and 3D models) and the 14 stakeholders (OW; E1; E4; E5; C1; C4; SB1; SB4; SB5; SB6; SB9; SB10; V1; V2) received a value of “1” while all remaining columns received a value of “0”. The rest of the processes followed the same procedure.

4.3 Results and Analysis

4.3.1 Network Topology

The analysis of the three pillars begins by first exploring the relationships between stakeholders at a high level (i.e., main entities), construction processes (pre- and post-ward), and data sources (i.e., what information stakeholders need to perform their tasks). A network topology (Figure 2) was constructed from the matrix to build connections between the high-level stakeholders, processes, and data sources. Results from the network topology show that:

- The engineer, contractor, and subcontractor are the high-level stakeholders that were most involved in the construction phase.
- The processes that require a high concentration of stakeholders’ involvement include acquiring bonds and commercial obligations, payments, claims, and close-out.
- The processes that involve various data sources include scheduling milestones, supply chain management (procurement), installation, payments, change orders, claims, and closeout.
- The most utilized data sources are plans, specs, conditions of contract, and bill of quantities (BOQ). These data sources flow across various processes and are needed by the majority of the stakeholders.

4.3.2 Social Network Analysis

Additional analysis was performed to understand the relationships and dynamics of stakeholders at a detailed level. Based on the preliminary matrix, **E1** (E-Project Manager), **C5** (C-Project Manager), **SB6** (Other Subs Project Manager), **SB1** (MEP Subs Project Manager), and **V1** (Vendors Commercial/Accountant) had the highest number of functions that they were involved in. To further understand the information sharing among stakeholders and collaboration, social network analysis (SNA) was performed on the matrix. The SNA networks consist of two elements: nodes represented by circles and

edges represented by straight lines. Nodes can vary in size depending on the SNA

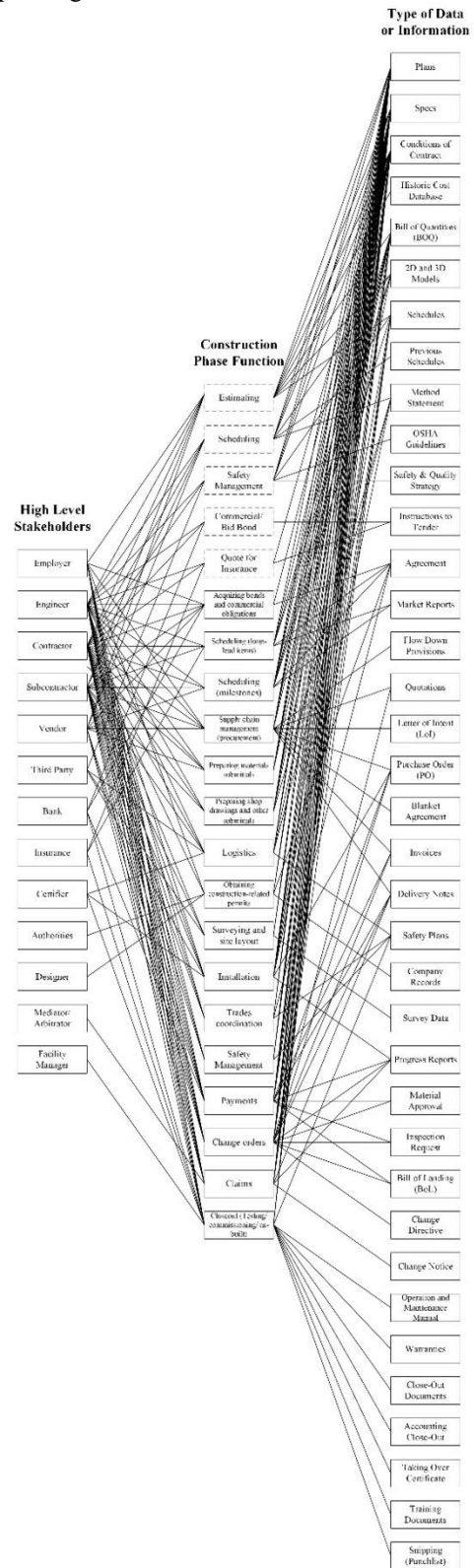


Figure 2. Network topology for the case study.

metrics used, while edges can vary in thickness based on the weight of the connection between two nodes. In this paper, two SNA metrics were used: 1) Degree Centrality (DC) – a normalized metric that represents the number of edges that one node possesses and the extent to which the node dominates the network [35], and 2) Closeness Centrality (CC) – a normalized metric that represents the extent to which a node is close to other nodes and the extent to which the close nodes are studied together [36].

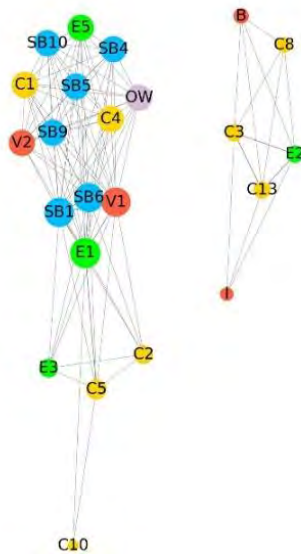


Figure 3. Pre-award network.

Two social networks were created: one for the pre-award (Figure 3) and one for the post-award (Figure 4). It can be observed in Figure 3 that the pre-award network is *disconnected* because the nodes are portioned into two subsets: one subset includes parties that engage in administrative processes at the organizational/institutional level (i.e., bank, insurance, legal office, etc.) and the second subset includes parties that get involved in the day-to-day processes at the project-level. A *disconnected* network indicates that there are two communication channels between some stakeholders. On the other hand, the post-award network is *connected* because there is a path between every pair of nodes in the graphs indicating that all involved stakeholders are connected and data flow from any stakeholder to any and/or every other stakeholder through the pairwise communication channels.

Based on the calculated centralities (both degree as well as closeness), the analysis of the pre-award shows that **E1** (E-Project Manager) is the most dominant stakeholder indicating that the Project Manager of the Engineering firm is a key player in the three project-level processes during pre-award. **E1** was followed by **SB1**

In this research, the nodes represent the stakeholders who are involved in the construction phase, while the edges represent the construction phase processes. The size of the node varies by degree centrality – i.e., the bigger the node, the more processes the stakeholder has collaborated on with other stakeholders. The thickness of the edges represents the number of processes that the two nodes that the edge connects have collaborated on – i.e., the thicker the edge, the more collaboration and data exchange is needed between the two stakeholders.

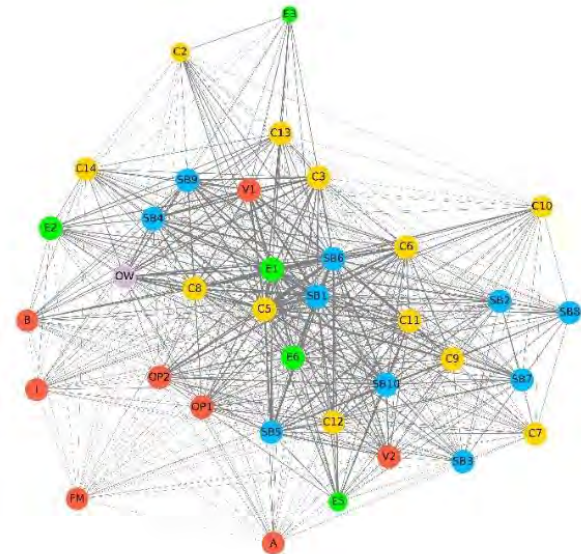


Figure 4. Post-award network.

(MEP Subs Project Manager), **SB6** (Other Subs Project Manager), and **V1** (Vendors Commercial/Accountant). It could be surprising that none of the contractor's internal stakeholders were highlighted in the centrality analysis, and this is justifiable because, at this phase of the project, the contractor has not selected their project manager.

The analysis of the post-award network shows that **E1** (E-Project Manager), **C5** (C-Project Manager), **C8** (C-Project Control/QS), **SB1** (MEP Subs Project Manager), and **SB6** (Other Subs Project Manager) are the most dominant stakeholders. Compared to pre-award, the contractor becomes a major player post-award and is represented by the Project Manager and Project Control/Quantity surveyor (QS).

4.4 Discussion

The results of the analysis of the pre and post-award highlight that there are key players that flow from one phase to another (such as E1, SB1, and SB6), there are major players that join the project at a later stage (such as C5 and C8), and there are supporting stakeholders whose role, although not dominant, is vital for supporting the

various processes. Understanding who is involved, when they are involved, and what sources of data they need is fundamental for advancing the application of Digital Thread in the industry.

As presented in the proposed definition, Digital Thread enabled the right person to access the right data, at the right time. The Digital Thread is thus a data problem and understanding how data flows between stakeholders and across processes throughout the construction project lifecycle is key to achieving Digital Thread-enabled decisions on the project.

The connections between these three pillars are often taken for granted in the construction industry. However, developing an efficient architecture for the Digital Thread of the construction project depends on a thorough analysis of the dynamics between people, processes, and data. Understanding what data is exchanged, between who, and when is essential for organizations to build the Digital Twin of the project using correct and accurate data. Having a well-established Digital Thread that holistically considers the entire construction project lifecycle and ecosystem is fundamental for the digital transformation of the industry. The data encompassed in the Digital Thread is important for all stakeholders and supports short- and long-term decisions and could lead to better project predictability and performance, greater collaboration and transparency between stakeholders, and more standardization of the industry.

The explicit discussion of the relationships between the stakeholders is also valuable to technology providers and provides them with the necessary information to develop integrative solutions that are congruent with the Digital Thread. Additionally, delineating the answers to each of the above-mentioned questions (who, when, and how) build the infrastructure needed to support AI-driven solutions. Moreover, the results could be used as an educational tool to train less experienced stakeholders about their role in the project, the stakeholders that they will engage with, and the sources of data that they will need.

The approach presented in this paper lays the foundation for this premise and for developing a Digital Thread schema for the construction project. By providing a generic model of who can be involved in the project, what processes they will engage in, and what sources of data they will need, supply chain traceability becomes a reality.

5 Conclusions

This paper provides the construction industry with a comprehensive definition of the Digital Thread of the construction project and explores the interconnectivity between people, processes, and data – the three pillars of the Digital Thread. A case study is performed to

investigate the connections between the three pillars during the construction phase of the DBB project in the Middle East. Network topology and SNA were employed to explore interconnections between people, processes, and data by presenting and analyzing a three-Dimensional Digital Thread Infrastructure.

This study does come with limitations. The interviews did not delve into the data formats used by stakeholders for the different data sources, the relationships highlighted in the networks are unidirectional, and the analysis was limited to the construction phase of a DBB project. Further studies will tackle the limitations by accounting for the flow of data to indicate the sender and recipient, analyzing the remaining phases of the project, and comparing networks across different project delivery systems. Future work will also leverage the findings of this paper to create an interface for the Digital Thread schema for the construction project and build a platform to provide all stakeholders with the means to achieve full project lifecycle traceability.

References

- [1] Bou Hatoum M, Piskernik M, Nassereddine H. A Holistic Framework for the Implementation of Big Data Throughout a Construction Project Lifecycle. In: *Proceedings of the 37th International Symposium on Automation and Robotics in Construction (ISARC)*, Kitakyushu, Japan: International Association for Automation and Robotics in Construction (IAARC), 1299–306, 2020
- [2] Newcombe R. From client to project stakeholders: a stakeholder mapping approach. *Construction Management and Economics* 21(8):841–8, 2003.
- [3] Bilal M, Oyedele LO, Qadir J, Munir K, Ajayi SO, Akinade OO, Owolabi HA, Alaka HA, Pasha M. Big Data in the construction industry: A review of present status, opportunities, and future trends. *Advanced Engineering Informatics* 30(3):500–21, 2016.
- [4] Abotaleb I, El-adaway IH. Managing Construction Projects through Dynamic Modeling: Reviewing the Existing Body of Knowledge and Deriving Future Research Directions. *Journal of Management in Engineering* 34(6):04018033, 2018.
- [5] Ammar A, Dadi G, Nassereddine H. Transportation Asset Data Management: BIM as a Holistic Data Management Approach. *Construction Research Congress 2022*, Arlington, Virginia, 208–17, 2022
- [6] Ramadan BA, Taylor TRB, Real KJ, Goodrum P. The Construction Industry from the Perspective of the Worker's Social Experience. *Construction Research Congress 2022*, 611–21, 2022

- [7] Alashwal A, Rahman HA, Beksin AM. Knowledge sharing in a fragmented construction industry: On the hindsight. *Scientific Research and Essays* 6(7):1530–6, 2011.
- [8] Brell-Cokcan S, Stumm S, Kirner L, Lublasser E. Transparency and Value of Data in Construction. In: Trauth D, Bergs T, and Prinz W, editors. *The Monetization of Technical Data: Innovations from Industry and Research*, Berlin, Heidelberg: Springer Berlin Heidelberg, 539–58, 2023
- [9] Boton C, Rivest L, Ghnaya O, Chouchen M. What is at the Root of Construction 4.0: A Systematic Review of the Recent Research Effort. *Archives of Computational Methods in Engineering* 28(4):2331–50, 2021.
- [10] Schober K-S, Hoff P. *Digitization in the Construction Industry: Building Europe's Road to "Construction 4.0."* Munich, Germany.
- [11] Klinc R, Turk Ž. Construction 4.0 - Digital Transformation of One of the Oldest Industries. *Economic & Business Review* 21(3):393–410, 2019.
- [12] Ammar A, Nassereddine H, AbdulBaky N, AbouKansour A, Tannoury J, Urban H, Schranz C. Digital Twins in the Construction Industry: A Perspective of Practitioners and Building Authority. *Frontiers in Built Environment* 8:834671, 2022.
- [13] Pan Y, Zhang L. Roles of artificial intelligence in construction engineering and management: A critical review and future trends. *Automation in Construction* 122:103517, 2021.
- [14] Aghimien DO, Aigbavboa CO, Oke AE, Thwala WD Mapping out research focus for robotics and automation research in construction-related studies. *Journal of Engineering, Design, and Technology*, 2019.
- [15] Hatoum MB, Ammar A, Nassereddine H, Dadi G, Tripathi A, Sturgill R. Wireless and Sensing Technologies in U.S. Highway Projects: Usage, Maturity, Challenges, and KPIs. *International Conference on Transportation and Development 2021*, Austin, Texas: American Society of Civil Engineers, 2023.
- [16] Gangwar H, Date H, Ramaswamy R. Understanding determinants of cloud computing adoption using an integrated TAM-TOE model. *Journal of Enterprise Information Management* 28(1):107–30, 2015.
- [17] Papadonikolaki E, Krystallis I, Morgan B. Digital transformation in construction-Systematic literature review of evolving concepts. *Proceedings of the Engineering Project Organization Conference (EPOC)*, Vail, Colorado, USA, 1–14, 2020.
- [18] Hinterhube A, Nilles M. Digital transformation, the Holy Grail and the disruption of business models. *Managing Digital Transformation*. 1st ed., Routledge, 261–5, 2021
- [19] Intercax. Digital Thread - The Foundation for Digital Engineering and Digital Transformation, 2022
- [20] Kniker C, Narsalay R, Roush W. A Digital Thread: Capitalize on Your Data's Value, 2021
- [21] Pang TY, Pelaez Restrepo JD, Cheng C-T, Yasin A, Lim H, Miletic M. Developing a Digital Twin and Digital Thread Framework for an 'Industry 4.0' Shipyard. *Applied Sciences* 11(3), 2021.
- [22] Mies D, Marsden W, Warde S. Overview of Additive Manufacturing Informatics: "A Digital Thread." *Integrating Materials and Manufacturing Innovation* 5(1):114–42, 2016.
- [23] United States Air Force. *Global Science and Technology Vision*. United States Air Force
- [24] Kraft E. Expanding the Digital Thread to Impact Total Ownership Cost, 2013
- [25] Christian T. Determining the Contents of the Digital System Model, 2014
- [26] Kraft ME, Baldwin K, Holland JP, Walker DE. The Digital System Model: The New Frontier in Aerospace & Defense Acquisition, 2015
- [27] West TD, Pyster A. Untangling the Digital Thread: The Challenge and Promise of Model-Based Engineering in Defense Acquisition. *INSIGHT* 18(2):45–55, 2015.
- [28] Leiva C. Demystifying the Digital Thread and Digital Twin Concepts. *Industry Week*, 2016.
- [29] Cognizant Digital thread. *Cognizant Glossary*, 2022.
- [30] Osofsky M. What is the Definition of a Digital Thread? *Jama Software*, 2020.
- [31] Hastings W. What Is a Digital Thread? *PTC*, 2021.
- [32] RGBSI. *Digital Engineering: Transformation of Product Innovation and Manufacturing*. RGBSI
- [33] Building Regulations Advisory Committee (BRAC). *Building Regulations Advisory Committee: golden thread report*. United Kingdom: Ministry of Housing, Communities and Local Government (MHCLG).
- [34] DAMA International *DAMA-DMBOK: Data Management Body of Knowledge*=. 2nd ed. Technics Publications
- [35] Assaad R, El-adaway IH. Enhancing the Knowledge of Construction Business Failure: A Social Network Analysis Approach. *Journal of Construction Engineering and Management* 146(6):04020052, 2020.
- [36] Nassereddine H, Hatoum MB, Musick S, El Jazzer M. Implications of Digitization on a Construction Organization: A Case Study. *Proceedings of the Creative Construction e-Conference*, Budapest, Hungary: Budapest University of Technology and Economics, 71–9, 2022

The impact of the combined innovations at the Hungarian National Athletics Stadium steel roof structure construction

Orsolya Heidenwolf¹, Márton István Juhász², András Balázs Kocsis², Dániel Gáncs³, Zoltán Kézsmárki⁴, Attila Kis⁴, Dr Ildikó Szabó¹

¹Corvinus University of Budapest, Doctoral School of Economics, Business and Informatics, Hungary
orsolya.nagy@uni-corvinus.hu, ildiko.szabo2@uni-corvinus.hu

²bimGROUP Ltd., Hungary
juhaszm@bimgroup.hu, kocsisa@bimgroup.hu

³GeoLink3D Ltd., Hungary
gancsdaniel@geolink3d.hu

Abstract –

The aim of the research is to discover the interrelation between Construction 4.0 technologies and Sustainable development Goals (SDG) in a complex project. The construction of the National Athletic Stadium in Hungary of the 25.000m² steel and cable membrane roofing structure demanded special innovations due to its uniqueness and its special geometry was used to explore these relationships. Construction 4.0 technologies such as Design for Manufacturing and Assembly (DfMA), Building Information Modelling (BIM), the combination of parametric-algorithmic design and large volume metrology (LVM) laser tracking have been applied to deliver the complex shape. Qualitative case study research methodology was applied to demonstrate that Construction 4.0 technologies can facilitate complex projects, increase collaboration, decrease risk and save significant time and money while contributing to the achievement of Sustainable Development Goals (SDG).

Keywords –

DfMA, sustainability, parametric-algorithmic design, laser tracking, construction 4.0, metrology, case study, SDG

1 Introduction

Industry 4.0 involves supporting relatively standardised processes with digital tools. However, in contrast to industrial production, a particular problem is that the type, location and size of construction projects vary with each investment by the companies involved, thus standardising processes is a particular challenge in the absence of modern technology and an unskilled workforce. The Construction Industry (CI) is

transforming into a new cyber-physical ecosystem called Construction 4.0 that facilitates this problem. This cyber-physical ecosystem includes technologies, methodologies and concepts and strong collaboration in order to build in a more sustainable way [1]. To achieve this, it is simply not enough to apply innovations on a large scale, the combined impact of related technologies must also be taken into account throughout the whole value chain [2].

Despite the fact that sustainability has become a pillar of the transformative industry, there is still a research gap in the relationship between new construction technologies and the SDGs. Thus, the aim of the research was to answer the question of how the technologies used in a complex project affect the quality, time and costs of the project and how these relate to the achievement of SDGs. The case study introduces the construction and applied innovations of the National Athletics Stadium in Hungary of the 25.000m² steel and cable net structure. The special roofing of the service area was built by the KÉSZ Group and its member companies with the assistance of innovation partners and experts.

The design-manufacture and assembly teams worked together early in the design phase to realise the complex structure. The design was facilitated by Building Information Modelling (BIM) and parametric-algorithmic design which together founded the concept of Design for Manufacturing and Assembly (DfMA). DfMA is the strategy that considers the building element in the design phase for manufacturability and buildability in order to speed up construction processes and optimises material usage [3,4].

DfMA in combination with parametric design can reduce waste during manufacturing [5] and enhance the use of tight quality control and can infuse more innovation offsite [6]. This is particularly important during the construction of a special steel structure that demands a geometrical accuracy of mm. For this, large-

volume metrology (LVM) laser tracking can provide a solution that can facilitate tens of mm over large objects. This technology has been successfully applied in many industries such as aerospace, automotive and shipbuilding in manufacturing processes [7–10].

The United Nations report shows that the CI is responsible for 37% of energy-related carbon emissions [12] due to its inefficiency and high-emission supply chain. Major changes are needed in the design and procurement phases also to achieve responsible consumption and production targets. Unfortunately, the most optimal solutions are still not brought to the design table [13]. Furthermore, the industry's raw material production 95% uses water [14] which has a great impact on the Earth's clean water. Technological infusion especially DfMA can directly support organisations to achieve SDGs [6]. Literature highlights sustainable cities and communities (SDG11), climate action (SDG13), responsible consumption and production (SDG12) and clean water (SDG6) as the four most important SDGs from the perspective of CI [11]. Climate action is the common goal for the whole society. [12][13][14]

2 Research Methodology

Qualitative research methodology was applied with a case study approach to prepare an explanatory case study. Explanatory case study aims to “*seek answer for presumed causal links in real-life interventions that are too complex for the survey or experimental strategies*” [15]. The preparation of the case study consisted of three different phases: the design of the case study, conducting the case study and analysis of the results [14]. A preliminary workshop was conducted with the KÉSZ Group management and project participants during the design of the case study. The workshop aimed to explore the innovations used in the construction of the Hungarian National Athletics Stadium. As a result of the workshop the participants agreed that the main innovation of the project was the application of the LVM technology. During this workshop, the sampling strategy was also agreed on how to conduct interviews for each phase of the project participants. In the second phase of the case study, further two workshops and four semi-structured interviews were conducted with a total of eleven people, each playing a different role in the four project phases to explore how the technologies were applied. The output of the second phase was the technologies effect for each project phase. Finally, in the third phase of the case study, the results were analysed in a matrix based on the project process to evaluate the results in terms of challenges, solutions and impacts of sustainability. At this stage, a literature review was conducted to clarify the sustainable impacts. The results were post-reviewed by the project participants. Table 1 illustrates each interviewee and their

main collaboration phase in the project.

Table 1 Interviewee participants and their role

Number	Role	Phase
Interviewee 1	Contractor	Assembly
Interviewee 2	Contractor	Assembly
Interviewee 3	Designer	Design
Interviewee 4	Designer	Design
Interviewee 5	Manufacturing	Manufacturing
Interviewee 6	Manufacturing	Manufacturing
Interviewee 7	Quality Control	Manufacturing
Interviewee 8	Quality Control	Manufacturing
Interviewee 9	Quality Control	Manufacturing
Interviewee 10	Contractor	Assembly
Interviewee 11	Consultant	Cable tension

3 Case study

The implementation of a complex cable-tensioned steel structure required innovations that overcame the complex challenges of design, manufacturing and construction. This case study aims to demonstrate through the construction of the roof structure of the Hungarian National Athletics Stadium the impact of innovations and their interrelation with the SDGs on the implementation of an entire project and its interconnected processes during the design, manufacturing and assembly (construction) phases.

3.1 The challenges of the steel structure

The varying geometry in different construction stages required high dimensional accuracy, which was only possible with a quality control (QC) method capable of sub-mm accuracy during the manufacturing process. In addition, the manufacturer sought to achieve the structure with the most optimal use of materials, as the technical problems were exacerbated by the emergence of the pandemic that generated further problems in the supply chain.

During the design, the biggest challenge was the complex geometry as the different phases of construction formed different geometrical shapes. Furthermore, the complexity of the structure had to be taken into account by choosing the manufacturing and construction technology. Thus, the plans had to be prepared for four different service conditions:

1. Manufactured steel structure
2. Assembled steel structure
3. Tensioned cable structure
4. As-built steel structure

The geometry and structural complexity induced the tight tolerance problem. For the appropriate functioning of the structure, the structural 3 mm tolerance between

the structural nodes, while the entire structure's 50 mm tolerance was specified for the entire length of the structure. In interpreting the tolerance specification, it is important to emphasise that tolerance was not defined as the tolerance of individual components, but as the sum of the tolerances of several manufactured components, which required quality control beyond the continuous inspection of manufactured components.

Thus, the steel structure was built with a higher execution class based on EN 1090 EU standard than required by the design. Execution class (EXC) refers to the level of quality and assurance controls needed to ensure a structure meets the engineer's design assumptions. KÉSZ Group has applied the highest execution class, EXC4 for the steel ring due to having as much optimisation as possible. Thus, the carbon footprint had been reduced and the pandemic and the fragile supply chain were taken into account. Although the EXC quality control system specifies a number of requirements, in this case study geometric dimensional accuracy will be discussed in detail.

The tolerances and size also needed to be considered during the baseplate assembly installation during the construction phase. Since the tolerance had to be provided together with the manufacturing and placement defects of the base assemblies, the result of the design evaluation had to be taken into account in all cases until the base assemblies were pinned. The complexity was further induced by the reinforced concrete structure as it was built in pre-shift to the steel structure installation. Cable installation required a structure built with precise geometry and cables cut to exact dimensions. Table 1 summarises the challenges of steel structure construction.

Table 2 The challenges of the steel structure construction

Phase	Challenges
Design	Complex geometry had to be followed in the different stages of construction
Manufacturing	Consideration of installation technology, feasibility, materials 3 mm tolerance between the structural nodes and 50 mm tolerance in the entire structure Temperature Pandemic and supply chain problems
Assembly	Baseplate assembly installation and size
Cable tension	Cable and geometry accuracy

3.2 The solution

The complex structure demanded a technological

solution for the problems of the design, manufacturing, assembly and cable tensioning processes together. In addition to the complexity, the feasibility was also a risk, therefore the concept of the technology was developed during the tender phase.

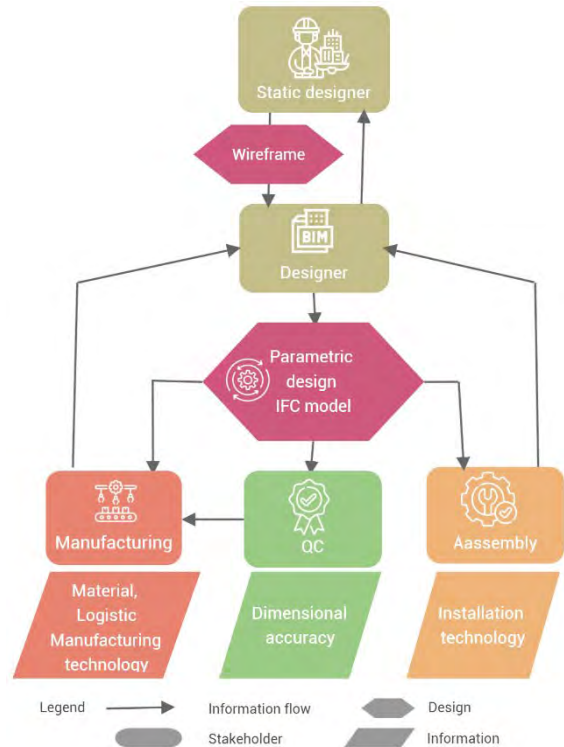


Figure 1 The design collaboration

This was facilitated by DfMA-oriented parametric-algorithmic design in combination with LVM laser tracking. The implementation of the four different geometries was facilitated by parametric design, which supported the design, manufacturing, quality control and assembly team collaboration in the design phase. Figure 1 illustrates this process.

The combination of Tekla Structure and Rhinoceros-Grasshopper software were the core tool for the parametric-algorithmic design. Based on the structural calculation, the steel structure's wireframe was created. Due to the change of sections and stiffness during the design process, and after counting in the material quality and availability, the possibilities of installation and quality control opportunities new structural calculations were made several times, which resulted in continuous changes to the wireframes. This continuous change was tracked by the Rhinoceros-Grasshopper algorithm, which generated automatically the 3D shop drawings of the entire steel structure in Tekla Structures. Finally, the model was converted to IFC to be able to use for all departments in Trimble Connect. The entire model of the compressing ring was regenerated in 1-2 hours and with final model checking was ready in 1-2 days due to the

parametric design algorithm. Figure 2 illustrates the concept of the project process.

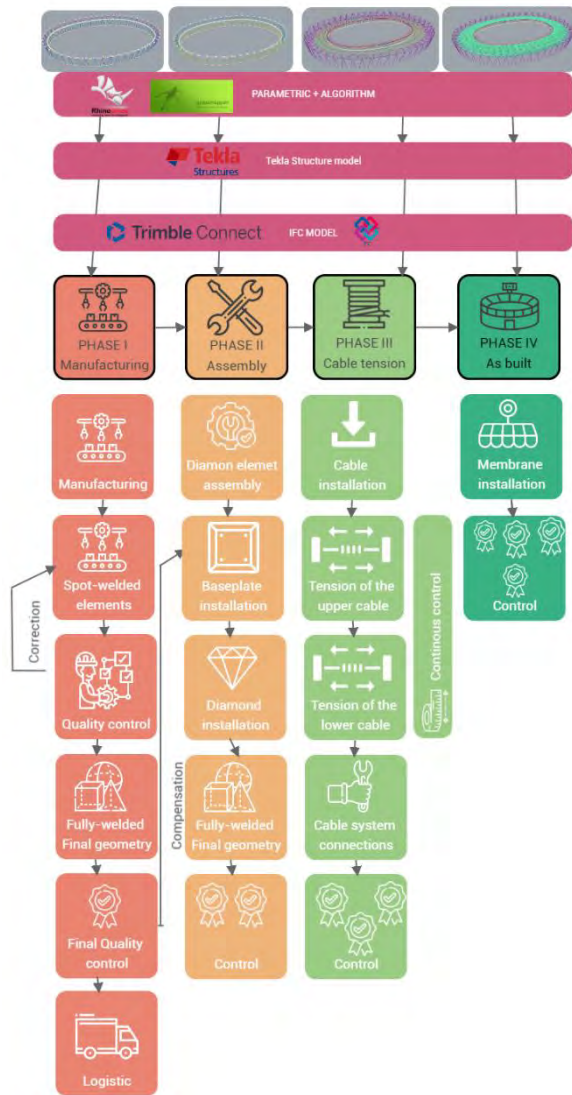


Figure 2 Concept of the project process

The entire process can be broken down into four main parts based on the geometry which represents the four service conditions: manufacturing, on-site assembly, cable tensioning and the built structure. These processes are described in detail in the following four subsections.

3.2.1 Phase I - Manufacturing

Based on the manufacturing, construction and logistical aspects, the steel structure has been divided into so-called diamond elements (Figure 3 red elements). The steel structure was made up of 48 diamonds, which were further broken down into manufacturing and logistical phases.

During manufacture, the required accuracy could only be ensured by LVM. Due to the dimensions of the structure, it was also necessary to take into account the

prevailing structural temperature during manufacture and to compensate for the theoretical mean value when setting the length dimensions. The data was provided by the design team in a variety of file formats (IFC, DXF, XML, NC) from the Tekla model, according to the manufacturer's machines, which were then used by the programming technologists to set up the machines. The communication between the teams was supported by Trimble Connect.



Figure 3 A selected diamond in the IFC model

The dimensional accuracy was facilitated by LVM laser tracking during the QC. The technological solution was developed based on a previous project where FARO® Quantum Faroarm® & Scanarm series was successfully applied by the innovation partner called Geolink3D. However, for elements of several metres and sometimes more than 10 tons, it became apparent that this tool would not be sufficiently precise. Thus, VantageS6 Max Laser Tracker was applied. This Laser Tracker was finally suitable to measure the approximately 10m length manufactured elements with a dimensional accuracy of 0.01mm.

QC worked closely with the design and manufacturing team. From the model, data were exported to FARO Cam2 software and the measurement criteria were recorded in the software. Finally, coordinate geometry was used to check each completed element against the geometric tolerances specified by the design team. Calibration was the first step in the LVM process. To achieve the correct dimensional accuracy of the machine needed to achieve equilibrium temperature which took about 30-80 minutes to compensate itself and a further 10 minutes were taken by the calibration. Each measurement was preceded by calibration to three points in a given area.

The first phase of the QC was the manufactured elements in spot welded condition. The 360-degree angle of view of the machine allowed to measure on both sides of the production area, therefore the QC and manufacturing teams could work together continuously to correct tenth of millimetre geometry instantaneous. The surfaces of the joined structures were machined using the data obtained by processing the measurement results

A joined element was typically assembled within three rounds of measurement and machining and within the tolerances allowed. The spot-welded elements were welded for their final geometry (Figure 4). Further dimensional variations could have occurred during the final welding hence all joined elements were post-qualified. The measurement results were recorded on a rolling basis per joined element; therefore, compensation could be made for the closure defect of the previously manufactured elements during the manufacture of the next element. Figure 4 shows a detail of a measurement protocol in an intermediate state. The total quality control process for a sole node element took approximately one hour, while for a compression ring node approximately 2-3 hours.

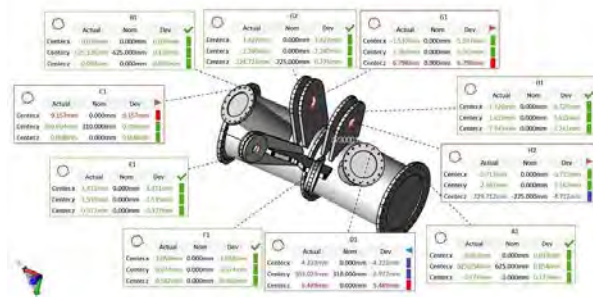


Figure 4 Compression ring node QC report

3.2.2 Phase II - Assembly

A diamond is made up of 10 sub-assemblies (c.f. Figure 3). Each diamond was thus assembled on site from 7 rods and a compression ring node and then inserted into 2 baseplate assemblies.

The baseplate node (Figure 5) was positioned and adjusted separately, as the vertical misalignment of the rods was compensated during the positioning of the baseplate. The positioning of the baseplates was a particular challenge due to the fact that each baseplate installation required the production of the connecting rods to be able to compensate their dimensional accuracy (final height coordinates), the accuracy of the reinforced concrete nest and the baseplate manufacturing defects. These challenges were solved by measuring from two positions during placement while taking each variable into account for the final compensation. During the alignment, the final compensation step was the correction of the baseplate node pin position, taking into account the resulting manufacturing defect of the connecting element series. The purpose of the baseplate node adjustment was to increase the geometrical accuracy of the compression rings on which the strained cables were loaded and to ensure that only forces in the direction of the actual rods

would occur, thus the two rigid compression rings would be as close as possible to the originally designed geometry.

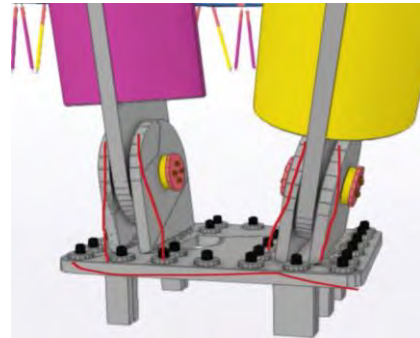


Figure 5 The base plate node in Tekla Structures

During this process, 3-4 baseplate assemblies were installed in one day and the 70 tons and 28m height diamond elements were assembled to this baseplate with the support of special crawler cranes that took further 3-4 hours per diamond. Assembly and installation were continuously carried out by two teams. The steel structure assembly followed the reinforced concrete structure in the compression ring direction.

3.2.3 Phase III – Cable tensioning

Computer controlled cable tensioning system was used to lift up the cable structure that spans 37 meters above the arena to cover the stadium. Once the cables were attached to the compression ring on-site (Figure 6) consisted of three steps.



Figure 6 The cables before the strain

In the first step, all the cables of the upper compression ring were prestressed by hydraulic jacks simultaneously, followed by the tensioning of the lower compression ring. The lifting process was controlled by a lifting sequence code, developed from finite element calculations of the lifting stages. This was a computer aided task. The goal of the process was to ensure a slide-free lift-off of the cable net from the scaffolding, as well

as to prevent the overstressing of the cables or the compression ring structure during the process (Figure 7).



Figure 7 The lifting process

The main input of the lifting process was the stroke sequence of the 96-strand jacking machines working simultaneously. The stroke distances were controlled by measuring the jack displacements as well as by direct distance measurements by a pull-wire system. As a third control instance, the forces in all cables were continuously measured from the oil pressure of the robot technology obtaining values within 2% of the design values during the lifting of the cable roof. Finally, the two-level cables were connected by the so-called flying columns. Flying column refers to the columns that were installed between two cables to keep the distance between the two levels (Figure 8). The final prestress applied by tensioning the lower radial cables to their pinning positions.



Figure 8 The flying columns

As a result, the surveyed deviations from the theoretical shape were of the order of mm (Figure 9). The force measurements were also a verification of the cable and compression ring system manufacturing processes, as their geometrical precision directly governs the achieved prestress state.

3.2.4 Phase IV – As built structure

To achieve the final steel membrane structure, the membranes were placed on the prepared "spider mesh" cable structure, which was strained to their final state on-site using hand tools and the structure achieved the final shape. The final shape was created by tangentially joining 3 arcs of different radii and then segmenting the

diamonds straight at their intersections.



Figure 9 The cable lifting final stage

3.3 Benefits of innovations

The world of Construction 4.0 is all about connecting technologies, methods and collaboration. The project team emphasised that feasibility could only be overcome and delivered on time and to the right technical standards through a combination of state-of-the-art technologies. Many research emphasises the isolated advantages of each technology however the authors here focus on the combined applications through the value chain.

First, in the tender and design phase, BIM created the opportunity for parametric, algorithmic design resulting in strong collaboration and more efficient solutions during the design, manufacturing and assembly phases than in the traditional solution. As a result, the team applied DfMA strategy during the project. The concept was developed during tender, therefore the costs of the technologies and the savings were taken into account in the quotation. Without a parametric design, the modelling phase would have taken at least four times longer and would have involved much more manpower, as the model was necessary for all four different service conditions. Thus, the design was significantly faster than without a parametric algorithm, leaving additional lead time for the manufacturing and assembly phases.

Second, as a result of the tight QC, the pre-assembly of the 48 diamonds in the factory was abandoned. The factory environment pre-assembly took two and a half days for the first diamond. The dimensional accuracy of this diamond has reached the required standards. For the further 47 diamonds this step was omitted, saving 47 times two and a half days. This equates to a total of 118 working days saving nearly six months. This time saving was particularly significant in the assembly phase to comply with the penalty period and to avoid another six months of project organisation costs on site.

Third, due to the detailed preparation the lifting of the cable net structure was completed in just over a month with the coordinated work of fewer than 20 people, and the forces measured during the lifting deviated on average by 1-2% from the preliminary calculations.

Last, according to the literature, the most important targets for the CI are SDG11-13, and SDG6 [11]. In addition to these objectives, this case study proves that

the application of Construction 4.0 technologies also contributes to the following goals: Decent work and economic growth (SDG8) and Industry, innovation and infrastructure (SDG9). Novel SDG indicators were guided to determine the technologies contribution to the SDGs [16]. The enhanced design of the roof structure reduced the amount of steel required by almost a fifth due to the cable-tensioned steel membrane structure. The DfMA-oriented parametric-algorithmic design combined with tight quality control (application of LVM laser tracking) further optimised the design and the materials left over from the production process (templates of cut-out elements) were recycled, thus contributing to the circular economy. These steps were significantly reduced the carbon footprint and directly contributed to SDG12 and SDG13. The reduced and optimised raw material decreased the necessary water needed for raw material production contributing to SDG6. SDG9 was facilitated by BIM combined with parametric-algorithmic design, DfMA, LVM laser tracking and a computer-controlled cable tensioning system. In addition, background calculation indicates that the technologies used during the project brought significant cost saving leading to economic growth contributing to SDG8.

4 Summary and conclusion

Hungary has been lagging far behind the digitisation of the CI since the 1980s and the challenge of promoting Construction 4.0 in this market is much greater than in Western countries [17]. Nevertheless, this case study demonstrated that market players can take significant steps in complex projects to embrace innovation in recent years and the construction of the steel roof structure of the Hungarian National Athletics Stadium is internationally outstanding. Challenges include the feasibility of the project, technology and construction risks, short deadlines, the complex shape of the structure, dimensional accuracy, different geometries, pandemics and the fragile supply chain.

In this case study, estimations were presented, showing that parametric-algorithmic design saved four times in modelling time in the design phase. DfMA-oriented parametric design in combination with tight QC (LVM laser tracking) reduced the manufacturing phase by eliminating pre-assembly that lead to avoid another six months of project organisation costs on site and finish the project on time. The case study presented a literature gap so far [18] on how LVM can contribute to BIM and DfMA. As a result of these combined technologies computer-controlled cable tensioning system was successfully applied and resulted in 1-2% force deviations compared to the designed condition. Finally, the final shape of the complete compression ring at 806m ended up at 21mm tolerance compared to the allowed 50

mm. Even though sustainability was not a primary consideration in the project, the results demonstrate that the combined use of technologies contributes to the following SDGs: SDG6, SDG8, SDG9, SDG12 and SDG13.

Among the many barriers of Construction 4.0, management attitude is critical due to the lack of risk and return on investment calculations in the technologies [19,20]. This case study presents a great example for industry practitioners to overcome these barriers and presents the bottlenecks of technology implementation. In addition, it contributes to areas of SDGs impacted by these technologies that require further in-depth research to measure these contributions through key performance indicators. Thus, the authors will use the results for the development of the Construction 4.0 Maturity Model Ontology to explore in detail how to measure the relationship between technologies and SDGs.

In summary, the case study demonstrated that Construction 4.0 technologies can facilitate complex projects, decrease risk, increase collaboration and save significant time while directly transforming the construction to a more sustainable industry, thus, contributing to the achievement of SDGs.

Acknowledgements

This research is part of the Construction 4.0 research and supported by the ÚNKP-22-3-II-CORVINUS-102 National Excellence Program of the Ministry for Culture and Innovation from the source of the National Research, Development and Innovation Fund. The research was further funded by the Hungarian Chamber of Engineers (MMK), BAMTEC Hungary Kft., ConTech Consulting Kft and ÉSZ Group. The authors gratefully acknowledge the collaboration with KÉSZ Group and with the professionals namely Róbert Barócsi, László Szalados, Péter Sörös, Attila Nagy, Máté Nagy, Ádám Kovács and Balázs Szuromi. Special thank you to Mihály Varga and László Polgár for their effort in the realisation of the research project. Any opinions, findings, conclusions or recommendations expressed in this material do not necessarily reflect the views of the companies mentioned in this article.

References

- [1] O. Nagy, I. Papp, R.Z. Szabó, Construction 4.0 Organisational Level Challenges and Solutions, Sustainability. 13 (2021) 12321. <https://doi.org/10.3390/su132112321>.
- [2] O. Nagy, R. Szabó Zs., Építőipar 4.0 • Construction 4.0, Magyar Tudomány. (2021). <https://doi.org/10.1556/2065.182.2021.1.13>.

- [3] Z. Yuan, C. Sun, Y. Wang, Design for Manufacture and Assembly-oriented parametric design of prefabricated buildings, *Autom Constr.* 88 (2018) 13–22. <https://doi.org/10.1016/j.autcon.2017.12.021>.
- [4] S. Bakhshi, M.R. Chenaghlo, F. Pour Rahimian, D.J. Edwards, N. Dawood, Integrated BIM and DfMA parametric and algorithmic design based collaboration for supporting client engagement within offsite construction, *Autom Constr.* 133 (2022). <https://doi.org/10.1016/j.autcon.2021.104015>.
- [5] S. Banihashemi, A. Tabadkani, M.R. Hosseini, Integration of parametric design into modular coordination: A construction waste reduction workflow, *Autom Constr.* 88 (2018) 1–12. <https://doi.org/10.1016/j.autcon.2017.12.026>.
- [6] P. Gallo, R. Romano, E. Belardi, Smart green prefabrication: Sustainability performances of industrialized building technologies, *Sustainability (Switzerland)*. 13 (2021). <https://doi.org/10.3390/su13094701>.
- [7] B. Muralikrishnan, S. Phillips, D. Sawyer, Laser trackers for large-scale dimensional metrology: A review, *Precis Eng.* 44 (2016) 13–28. <https://doi.org/10.1016/j.precisioneng.2015.12.001>.
- [8] D.A. Maisano, L. Mastrogiacomo, F. Franceschini, S. Capizzi, G. Pischetta, D. Laurenza, G. Gomiero, G. Manca, Dimensional measurements in the shipbuilding industry: on-site comparison of a state-of-the-art laser tracker, total station and laser scanner, *Production Engineering*. (2022). <https://doi.org/10.1007/s11740-022-01170-7>.
- [9] F. Franceschini, L. Mastrogiacomo, B. Pralio, An unmanned aerial vehicle-based system for large scale metrology applications, *Int J Prod Res.* 48 (2010) 3867–3888. <https://doi.org/10.1080/00207540902896220>.
- [10] J.E. Muelaner, B. Cai, P.G. Maropoulos, Large Volume Metrology Instrument Selection and Measurability Analysis, *Proceedings of the 6th CIRP-Sponsored International Conference on Digital Enterprise Technology*. 66 (2010) 1027–1041. https://doi.org/10.1007/978-3-642-10430-5_79.
- [11] W. Fei, A. Opoku, K. Agyekum, J.A. Oppon, V. Ahmed, C. Chen, K.L. Lok, The critical role of the construction industry in achieving the sustainable development goals (Sdgs): Delivering projects for the common good, *Sustainability (Switzerland)*. 13 (2021). <https://doi.org/10.3390/su13169112>.
- [12] 2021 GLOBAL STATUS REPORT FOR BUILDINGS AND CONSTRUCTION Towards a zero-emissions, efficient and resilient buildings and construction sector, n.d. www.globalabc.org.
- [13] R.A. Arcila Novelo, S.O. Álvarez Romero, G.A. Corona Suárez, J. Diego Morales Ramírez, Social sustainability in the planning, design, and construction in developing countries: Guidelines and feasibility for México, *Civil Engineering and Architecture*. 9 (2021) 1075–1083. <https://doi.org/10.13189/cea.2021.090410>.
- [14] Z. Liu, Q. Huang, C. He, C. Wang, Y. Wang, K. Li, Water-energy nexus within urban agglomeration: An assessment framework combining the multiregional input-output model, virtual water, and embodied energy, *Resour Conserv Recycl.* 164 (2021) 105113. <https://doi.org/10.1016/j.resconrec.2020.105113>.
- [15] P. Baxter, S. Jack, Qualitative Case Study Methodology: Study Design and Implementation for Novice Researchers, *The Qualitative Report*. (2015). <https://doi.org/10.46743/2160-3715/2008.1573>.
- [16] A.G. Olabi, K. Obaideen, K. Elsaid, T. Wilberforce, E.T. Sayed, H.M. Maghrabie, M.A. Abdelkareem, Assessment of the pre-combustion carbon capture contribution into sustainable development goals SDGs using novel indicators, *Renewable and Sustainable Energy Reviews*. 153 (2022). <https://doi.org/10.1016/j.rser.2021.111710>.
- [17] L. Polgár, The Hungarian construction industry needs to be put on a new level, XXIV. International Construction Science Online Conference. (2020) 142–147. <https://ojs.emt.ro/EPKO/article/view/237/194>.
- [18] A. Mehdipoor, I. Iordanova, Systematic Literature Review on the Combination of Digital Fabrication, BIM and Off-Site Manufacturing in Construction—A Research Road Map, in: *Lecture Notes in Civil Engineering*, Springer Science and Business Media Deutschland GmbH, 2023: pp. 283–296. https://doi.org/10.1007/978-981-19-0968-9_23.
- [19] R. Maskuriy, A. Selamat, P. Maresova, O. Krejcar, O.O. David, Industry 4.0 for the construction industry: Review of management perspective, *Economies*. 7 (2019). <https://doi.org/10.3390/economies7030068>.
- [20] R. Maskuriy, A. Selamat, K.N. Ali, P. Maresova, O. Krejcar, Industry 4.0 for the Construction Industry—How Ready Is the Industry?, *Applied Sciences*. 9 (2019) 2819. <https://doi.org/10.3390/app9142819>.

Generative Design for Prefabricated Structures using BIM and IoT applications – Approaches and Requirements

Veerakumar Rangasamy¹ and Jyh-Bin Yang¹

¹Graduate Institute Program of Construction Engineering and Management, Department of Civil Engineering, National Central University, Taiwan

sakthirgmv3@gmail.com, jyhbin@ncu.edu.tw

Abstract –

Building Information Modeling (BIM) has demonstrated a wide range of merits over traditional and modern constructions. The integration of generative design (GD) with BIM in the construction industry has become an interesting topic, even though the concept is not very new. Prefabricated construction (PC) offers several advantages over traditional construction and has recently advanced to a new level of study because of the usage of BIM. The synchronization of BIM with PC is becoming simpler to create automatic design solutions in its early phases, thanks to the current breakthroughs in the internet of things (IoT) and its applications. There has been an increase in research interests that are mostly focused on examining tools and applications. However, there are not many studies that have looked at methodological relationships and other factors, which has led researchers to focus more on GD-BIM-based investigations. This study provides a preliminary critical analysis of the software, skill, and methodological requirements for current GD-BIM integration methodologies. The publications are pulled from web of science platform and thoroughly examined in statistical and systematic methods to give a fresh viewpoint on objective-oriented and skill-driven GD-BIM development for PC. New guidance to improve skill learning for GD-BIM development is recommended in this study. The analysis and recommendations might aid the researchers and designers in comprehending the situation and paying attention to future requirements.

Keywords –

Generative Design, Building Information Modeling (BIM), Prefabricated Construction, IoT Applications.

1 Introduction

Prefabricated Construction (PC), a technologically advanced construction method, is regarded as the first

step toward industrialization in the construction industry following mechanization, automatic control, and production [1]. PC has merits over conventional construction methods, including the ability to build more quickly and cheaply, with better quality control, and with less material waste. PC promotes sustainability, and it has been the main concern in all engineering fields. Even though PCs have many benefits, adoption is hampered by factors like expensive design costs, significant capital expenditures, a lack of supply chain data, etc. [2]. Building Information Modeling (BIM) is frequently used as a potential solution to the sector's long-standing problems in architecture, engineering, and construction (AEC) [3]. Although Generative Design (GD) has been developed in the 1970s, it is currently integrated into BIM to increase its benefits for the building industry. The growing trend for GD-BIM integration can enhance BIM's ability to produce a wide range of design possibilities, which can lower the cost of PC design and also other hindrances [4-7].

GD-BIM integration in traditional construction has been attempted by several studies, but in PC, it has been found to be limited and there is no clear information on this. For example, some GD-BIM are produced and investigated to effectively address design difficulties, while other research examines software and programming techniques to compare developing tools [8-10]. To understand the methodological connection, skill requirements, and improvements to help designers, this study seeks to evaluate the present methods of GD-BIM in PC. To find the answer, the Web of Science (WoS) platform is used to search for publications relevant to this goal and conduct extensive analyses of those articles. The sections are organized as follows: GD-BIM integration, Methodology, Analysis & Discussions, and Conclusions & Recommendations. This study can provide comprehensive information regarding the adoption of GD-BIM in PC at this time.

2 GD-BIM integration

This section examines background information on

GD, its components, BIM, and GD-BIM integration to illustrate the need for and reasoning behind building GD in BIM.

2.1 Generative Design Elements

Generative design is a type of iterative design process. Using software and computational algorithms, generative design is a goal-oriented and simulation-driven design process that creates high-performance geometry based on user-defined technical requirements. Simply described, "GD systems" are systems that try to assist professional designers and/or automate portions of the design process using computational approaches [11]. Krish describes the GD components into three as follows: (1) "a design schema", (2) "a means of creating variations", and (3) "a means of selecting desirable outcomes" [12]. Marsh explains that GD requires three elements that are (1) "performance metric", (2) "configuration variation", and (3) "decision-making response" [13]. These studies help us to summarize the GD as three major elements in familiar terms, that are:

- (1) Parametric design (Generate);
- (2) Simulation (Evaluate); and
- (3) Optimization (Evolve).

GD development often follows several steps that are depending on the requirements of the problem. Among these, the algorithm development and the design goals/constraints setup constitute the key phase from which the parametric models are derived. Here, GD is decomposed into two major steps (1) algorithm and (2) design constraints.

2.1.1 Algorithm

An algorithm is a set of rules that a computer must follow to execute computations, carry out other problem-solving tasks, or create and optimize various models. Singh and Gu examined and outlined the most popular architectural design algorithms, which include cellular automata, genetic algorithms, L-systems, shape grammars, and swarm intelligence [11]. In terms of applications, the right algorithm selection is made based on the characteristics of the design goals. For instance, the Shape Grammars technique is probably chosen if the design goals are to haphazardly discover space arrangement or visual compositions. Alternatively, the genetic algorithm is typically used if the goal is design optimization or improvement.

2.1.2 Design Constraints

The design goals or constraints are related to scope of the projects. The same design objectives or limitations cannot be applied to every building project. For example, some projects might concentrate on design generations and optimization, others might concentrate on lighting

and ventilation, still others might concentrate on reducing embodied emissions, etc. The design constraints are a set of design criteria or motivations, such as dimensions restrictions, material choices, manufacturing processes, or even financial restrictions, etc. [14, 15]. At present, designers detail their design objectives in programming languages, and automated script development research is slowly growing, but there is still a long way to go. Figure 1 shows a basic flowchart of the generative design process.

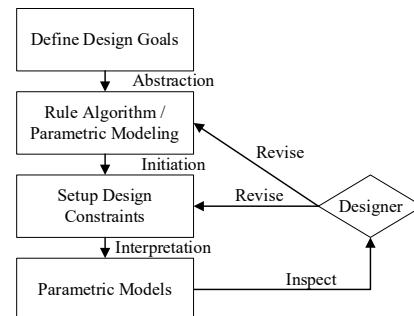


Figure 1 Generative Design Procedure

2.2 BIM in PC

BIM may assist PC in a variety of ways. BIM enables more precise material specification, which can lower over ordering and hence lower waste on the construction site. Fabricators and contractors can benefit from BIM by getting a 3D model of the element positions. To support building maintenance, subsequent demolition, and material recycling at the building's end of life, BIM can also store building information. When used wisely, BIM technologies can precisely describe the geometry, behavior, and characteristics of individual building components and objects, making it easier to incorporate them into standardized architectural parts or digitally accessible volumes [3].

BIM have shown greater improvements in design stage, cost calculations, supply chain and logistics and waste reduction in PC [1, 2, 5]. Currently various BIM software are available like Autodesk Revit, Tekla Structures, Graphisoft ArchiCAD, Bentley Microstation, Autodesk BIM 360 etc., that can be adopted based on the project requirements. It is more than just software because it makes it possible for all its users to manipulate and maintain shared data and information resources.

2.3 GD-BIM Integration

Although the implementation of BIM in PC has been widely discussed, most of it focuses largely on its later stages like fabrication, waste reduction, installation safety, supply chain and logistics. The BIM usage at the early stages like design development, structural design,

MEP design are relatively less in PC. The main hindrance is its inadequacy of capabilities, thus the integration of IoT applications like generative design, parametric modeling can enhance its implementation [16].

As a computer-aided design, geometric modeling is the focus of the GD to provide quicker design possibilities, but it is unable to preserve building information. As opposed to BIM, which allows for PC design with geometry and stores its information, design variants take longer to complete. Therefore, using this IoT method with well-known BIM software can increase PC use. Software like Revit currently supports Application Programming Interface (API), which enables users to add-on plugins and create their own tools through programming to optimize workflows.

3 Methodology

To remove the skewed conclusions, the review process uses a mixed review methodology that combines quantitative analysis and qualitative investigation. Since the Web of Science (WoS) database's rigorous peer review procedure sets a standard for published publications, it was chosen as the platform for article searching. For quantitative analysis, widely accepted VOSviewer software is used that can visualize the contemporary research status whereas the qualitative discussions focus on the objectives of GD-BIM implementation in PC and the relationship to the programming language, and skill requirements and learning paths of programming languages for GD-BIM development in PC.

GD is often related with Parametric Design (PD), Algorithm Design (AD) and geometric modeling, so all these terms including BIM, AI and IoT are used as initial keywords. The initial search generated 966 results but most of the papers focuses on conventional methods and out of the scope.

For precise results, the inputs are revised as "geometric modeling*" or "parametric design" or "generative design" or "algorithm design" or "DFMA" or "parametric modeling*" or "Design algorithm" or "algorithm" (Topic) AND "BIM" or "Building Information Model" or "Building Information Modeling" or "AI" or "artificial intelligence" or "IoT" or "Internet of Things" (Topic) AND "prefabrication" or "prefabricated buildings" or "prefabricated structures" or "prefabricated construction" or "modular Construction" or "precast construction" or "offsite construction" or "modular integrated construction" or "ppvc" (Topic) and Engineering Civil or Construction Building Technology (Web of Science Categories) produced 33 findings demonstrating the GD-BIM application in PC is in its initial phases. Figure 2 shows the flowchart for methodology adopted in this study.

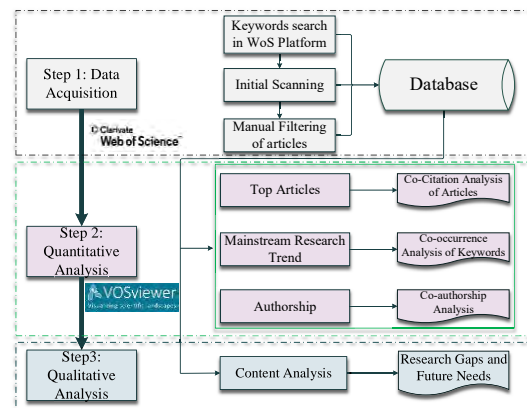


Figure 2 Methodology – Flowchart

4 Analysis and Discussions

As stated in the methodology section, the analysis of the retrieved materials is divided into two primary categories: quantitative and qualitative approach. The former study validates itself using numerical data, whereas the latter one offers more subjective conclusions.

4.1 Quantitative Analysis

To grasp the dominant research trends, top papers, and influential authors, the bibliometric software VOSviewer is used to analyze co-occurrence of keyword, article citations and journal citations which provide a quantifiable perspective of the subject area. The WoS platform's number of publications and the citations over the years is represented visually in Figure 3, which indicates that the GD-BIM implementation in PC took place in 2006 with one article but there is no article found in the successive years until 2011. Although articles scattered in 2012 and 2014 but there is no consistency in the publications. Notably, the number of publications and citations increased from 2018 until 2022 with 9 publications and 239 citations, describing that the subject's importance.

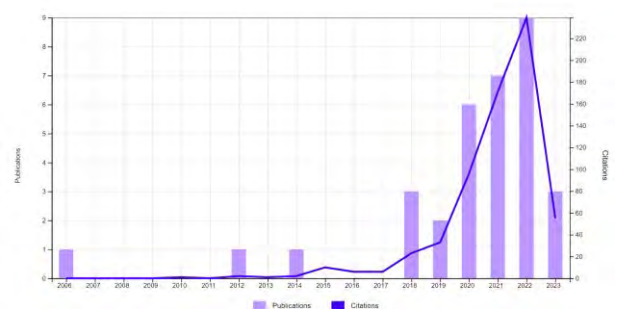


Figure 3 Year-wise publications in WoS

As illustrated in Figure 4, there are 30 original

research publications and 3 review articles among the published works, demonstrating the researchers' greater interest in understanding the subject matter.

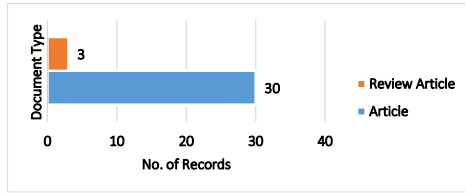


Figure 4 Type of published documents.

4.1.1 Co-occurrence of Keywords Analysis

The primary subject matter of published documents is represented by keywords, which also highlight the breadth of subject matter covered within any given domain. To illustrate the findings of the bibliometric analysis of the literature, the network of keywords was visualized. In the generated distance-based map, a greater distance often denotes a weaker association between the two objects. The size of the item label reflects the number of publications where the keyword was discovered, and the varied colors indicate the various knowledge domains that were grouped together using the clustering technique.

Since there are 33 publications, and Figure 3 clearly shows that the study area is in its early stages, the minimal number of occurrences was set to 2, making 47 of the 224 keywords meet the threshold. The network of related keywords is depicted in Figure 5 with 47 nodes, 360 linkages, and a total link strength of 84.50. The keyword occurrences and node strengths are summarized in Table 1.

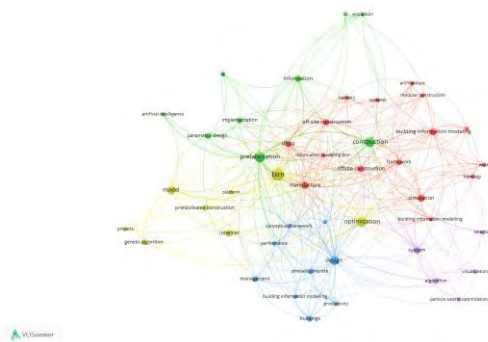


Figure 5 Bibliometric Network of keywords

According to Table 1, "BIM" including its abbreviation is the most frequently occurring keyword (24 times), with 83 links containing other keywords and a total link strength of 23. The successive keywords "prefabrication" & "construction" are found to be common with link strength as 10 & 9 respectively. The specific keywords like "optimization", "model", "internet" and "simulation" occurred more than 5 times

with at least 20 links with the other keywords and the reasonable link strength clarifies that the authors pay more importance in applying the IoT applications in their research. With minimum of 3 occurrences, the keywords such as "generative design", "algorithm", "parametric design" and "artificial intelligence" clearly supports the argument that the research area is in its inception level.

Table 1 List of top 10 keywords mapped

Keyword	Occurrences	Links	Total link strength
building information modeling (bim)	24	83	23
prefabrication	10	31	10
construction	9	31	9
optimization	9	30	9
design	8	30	8
model	7	20	7
internet	5	21	4
manufacture	5	26	5
simulation	5	20	4
dfma	4	24	4

4.1.2 Citation Analysis of Articles

By measuring the number of times that author, article, or publication has been cited by other people, citation analysis is a typical method for determining the relative relevance or impact of an author, an article, or a publication. It is a crucial tool for any literature study and aids researchers in determining how frequently a work has been cited in articles. Citation analysis is considered since the research field is in emerging stage that is more meaningful in understanding the most research contributions by the authors. VOSviewer generated citation network is shown in Figure 6 and Table 2 lists the top 7 documents with minimum of 25 citations and their links. The threshold is set up as minimum 3 citations that generated the network between 24 documents out of 33 as represented in Figure 6.

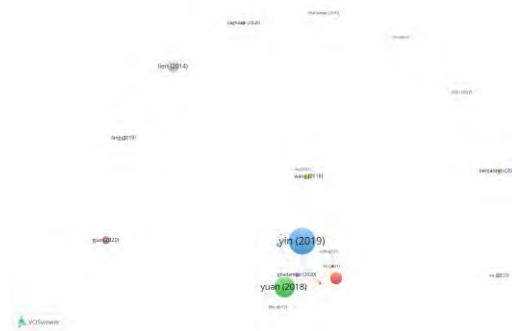


Figure 6 Document Citation Analysis Network

From the Table 2, Yin et al. (2019) [17] published a systematic review article cited 149 times followed by the article focusing on DFMA published by Yuan et al. (2018) [18] cited 110 times and the article which focus on optimizing tower crane layout by Lien and Cheng (2014) [19] cited by 60 articles. Interestingly, the Figure 6 clearly shows there are 9 articles that has citations but there is no connection with the others which directly represents the status the research topic as its initial level.

Table 2 Top 7 Cited Documents

Document	Citations	Links
<i>Yin (2019) et al</i> [17]	149	7
<i>Yuan (2018) et al</i> [18]	110	8
<i>Lien & Cheng (2014)</i> [19]	60	0
<i>Banihashemi et al (2018)</i> [20]	59	2
<i>Guo et al (2020)</i> [21]	37	0
<i>Benjaoran et al (2006)</i> [22]	33	0
<i>Wang et al (2018)</i> [23]	28	3

4.1.3 Citation Analysis of Journals

Journal citation analysis is carried out to understand the overall idea about the publications which pays interest in this research area. Interestingly there are only 11 journals found with the Automation in Construction holds maximum of 15 articles which is 45.5% of the total, Buildings and Journal of Construction Engineering and Management holds 15% & 9% with 5 & 3 articles respectively. The remaining 30% is shared by the other 8 journals. This indicates that most of the author intends to publish in journals with a high impact score.

Figure 7 shows the citation network of sources developed for a threshold of minimum 1 journal and 10 citations, which resulted 7 out of 11 journal sources. Table 3 lists the top 5 resulted journals and their respective number of articles and citation count.

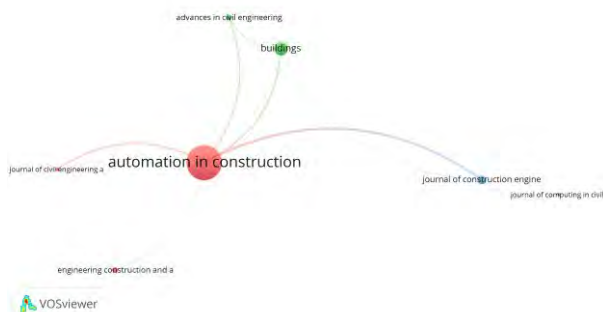


Figure 7 Journal Citation Network Analysis

Table 3 Top 5 List of Journals and their Citations

Journal Name	Articles	Citations
Automation in Construction	15	533
Buildings	5	11
Journal of Construction Engineering and Management	3	10
Engineering Construction and Architectural Management	2	24
Advances in Civil Engineering	2	13

4.2 Qualitative Analysis

This section examines the methodological linkages between the GD-BIM development objectives in PC, the applicability of programming languages, and the learning and development of programming abilities. Therefore, viewpoints of objective-oriented, and skill-driven GD-BIM adoption in PC are presented. The Co-occurrence of keywords analysis generated 5 clusters with 47 keywords as shown in Figure 5 is for subjective analysis to unfold more about the approaches and requirements.

4.2.1 Objective Oriented GD-BIM in PC

The two major objective of GD-BIM integration in PC are (1) solve specific design tasks and (2) support design process. While supporting design tasks are primarily used by researchers to enhance the overall design capabilities that are common to all projects, solving specific design tasks is typically project-based and is primarily developed by practitioners with the aim of solving individual design tasks creatively and efficiently. For instance Banihashemi et al. integrated parametric modeling PC to reduce construction waste using genetic algorithm through Rhinoceros 3D–Grasshopper platform resulted by 2% improvement [20]. Liu et al. used Symphony NET 4.6 to develop a simulation model in the Autodesk Revit software by inheriting its API in order to automatically generate the panelization design of manufacturing components [24]. In order to determine the best layout for PC drywall installation planning, Lobo et al. designed a framework with a decision support module that takes into account environmental, economic, and aesthetic factors [25]. This framework has shown to be beneficial. They used heuristic optimization algorithms and simulation-based design algorithms to choose the ideal.

Bakhshi et al. [26] used the framework proposed by Yuan et al. for supporting client engagement within offsite construction using Dynamo plugin in Revit software [18]. In order to restore the physical characteristics of PC components and support its informatics, Xu et al. reverse-modeled a PC component in Industry Foundation Class (IFC) using the equal-interval segmentation slice mapping approach [27].

Rest of the articles focuses on GD-BIM integration in

PC to support design process. For instance, Yuan et al. proposed a framework for Manufacture and Assembly Design (DFMA) [18], which is an organic combination of DFM and DFA. This framework instructs designers to fully consider the requirements from manufacture and assembly of PC at the design for better manufacturability and assemblability using Split design and DFMA analysis.

Similarly Bai et al. developed a common library for PC structural components using Graphic Media Mapping and EXPRESS language that can be used in Java tools [28]. Gan developed a graph data model and BIM-based geometric modeling in PC to support the overall design capabilities [29, 30]. In contrast to Textual Programming Languages (TPL) like Python, C#, or Java, Visual Programming Languages (VPL) like Dynamo and Grasshopper are easier to adopt and mimic the needs in.

4.2.2 Skill-driven GD-BIM adoption in PC

VPLs are simple to learn and use because they were created to facilitate simple computer interaction and were later used as teaching resources to train beginning programmers. TPLs are far more challenging to master, but once properly coded, they are capable of handling complex problems.

A user who is fluent in one TPL can design GD in several BIM environments using Rosetta/ HP ARIES without having to learn additional new programming languages. Rosetta serves as a conduit or converter, enabling users to program GD using specific TPLs (as front-end languages) and produce similar GD models across various applications (as back-end environments). Based on a thorough examination, designers at the entry level can utilize VPLs like Dynamo for Revit and Grasshopper for Rhino with ease due to their strong support for intuitive and novice users. Ma et al. suggested a path for skill development to improve GD-BIM integration based on the review process but it was not well described [31]. Thus, a modified new guidance to excel in GD-BIM integration for a newbie designer is shown in Figure 8, the same can be adopted for GD-BIM integration in PC. Consequently, to generate GD-BIM for simple designs, the designers must have at least a basic understanding of one programming language (either a VPL or TPL), but it is advised that they have a solid understanding of at least one TPL as well as AI approaches in order to build complicated designs and models.

GD is a process of using algorithms and computational tools to generate multiple design options that meet specific design criteria. Researchers are adopting various TPLs like Python [32], C#, JavaScript, Visual Basic based on their knowledge skills and requirements. Among which python is most widely used and easy to learn/use than other programming languages.

Regarding the algorithms, generative adversarial network (GAN) [33], genetic algorithm [34], particle swam algorithm [19], random forest [32] with TPLs that effectively improved the efficiency of generating large set of design variations and optimizes it to provide the best suited one for the design goals and constraints. The application of AI algorithms may aid in data analysis, problem solving for design challenges, predictive modeling, timetables and reporting, among other complicated tasks in the PC sector, in addition to design simulations and optimization. Although it is claimed that the complexity of the joints and connections in the PC design results in minimal variations, the integration of GD-BIM in the PC might be able to overcome this obstacle.

Thus, the selection of VPL/TPL and algorithms can be made based on the designers' skillset and the problem to be addressed. Ergo, the IoT and artificial intelligence technologies of today could greatly assist the designer in creating a variety of design solutions that take sustainability into account.

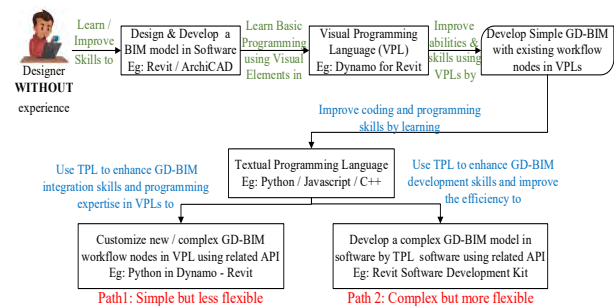


Figure 8 Guidance to improve skill learning for GD-BIM development

5 Conclusions and Recommendations

This section concludes the findings and offers suggestions for further research in the field based on the analysis and discussion of this study.

5.1 Conclusions

The main goal of this study is to review statistically and descriptively the status of GD-BIM integration in PC. This study has made it very evident what skills are needed to accomplish goal-oriented GD-BIM integration. Consequently, it is evident that the use of GD-BIM in PC is still in its infancy and that very few authors have made an effort to investigate it. The creation of generative design using BIM for PC can be made possible because of developments in AI and IoT applications. As a result, one obstacle, such as expensive design costs for design options, can be addressed. The employment of GD-BIM in PC research has produced effective results, and the

strategy for achieving its integration has improved, according to the conclusions of all the articles.

It is also observed that, like the development of GD-BIM in conventional construction design, only a small number of authors implemented the integration for specific problems, with the majority focusing on general design improvements. Additionally, it should be emphasized that the research topic does not examine many of the issues that must be considered during the early design stages, including spatial requirements, lighting and ventilation, MEP systems, quantity take-off, cost calculations, and more. In terms of the programming and skill needs, the designer or researcher should firmly hold at least one competence in either VPL like Dynamo, Grasshopper, Solibri Model Checker (SMC) or TPL like Python, C#, C++, or Java. The VPL/TPL can be interacted with 3D model BIM applications like Revit, ArchiCAD, and Tekla through its API. With the development of computing technologies like machine learning (ML), artificial neural networks (ANN), GAN, and various algorithms, including but not limited to genetic algorithms, evolutionary algorithms, and swarm algorithms, the potential for this research field is enormous in the current decade.

5.2 Limitations and Recommendations

Following a thorough examination, certain recommendations are made that might be very helpful for designers and researchers as they develop and apply generative design principles to the prefabricated construction technique. They are as follows:

1. Although GD have been tested for traditional construction methods while taking numerous elements into account, the same cannot be employed for PCs because of the different design process.
2. A strong potential to work either with VPL or TPL to effectively blend GD with BIM in PC.
3. The study theme is still in its early phases and has the potential to be explored in a variety of ways, as it is mentioned earlier.
4. By generating different design choices and optimizing them, GD, which focuses on early design stages, has the potential to reduce waste reduction and carbon emission while maximizing the PC benefits.
5. A GD framework that incorporates all design criteria can be created using BIM in PC and that can be used for every project.
6. To accommodate additional design processes, more sophisticated and organized GD-BIM could be developed.
7. It's indeed possible to conduct multidisciplinary research to ease the programming challenges.

This analysis on the approaches and requirements on GD-BIM integration in PC can help the researchers/

designers to understand and explore more on it. The study is an overview of the subject and also limited to the WoS database which covers the scholarly articles only rather than the conference and other sources.

References

- [1] Ay, I. &G.G. Ayalp. (2021). Factors Affecting the Design, Manufacturing, Storage, Transportation, and Construction Processes of Prefabricated Buildings. *Teknik Dergi*, 32(3):10907-10917.
- [2] Zhang, S.X., Z.F. Li, T.X. Li &M.Q. Yuan. (2021). A Holistic Literature Review of Building Information Modeling for Prefabricated Construction. *Journal of Civil Engineering and Management*, 27(7):485-499.
- [3] Abanda, F., J. Tah &F. Cheung. (2017). BIM in off-site manufacturing for buildings. *Journal of Building Engineering*, 1489-102.
- [4] Jung, J., S. Hong, S. Yoon, J. Kim &J. Heo. (2016). Automated 3D Wireframe Modeling of Indoor Structures from Point Clouds Using Constrained Least-Squares Adjustment for As-Built BIM. *Journal of Computing in Civil Engineering*, 30(4):
- [5] Malgit, B., U. Isikdag, G. Bekdas &M. Yucel. (2022). A generative design-to-BIM workflow for minimum weight plane truss design. *Revista De La Construccion*, 21(2):473-492.
- [6] Abrishami, S., J. Goulding &F. Rahimian. (2021). Generative BIM workspace for AEC conceptual design automation: prototype development. *Engineering Construction and Architectural Management*, 28(2):482-509.
- [7] Wu, S.A., N. Zhang, X.W. Luo &W.Z. Lu. (2021). Intelligent optimal design of floor tiles: A goal-oriented approach based on BIM and parametric design platform. *Journal of Cleaner Production*, 299
- [8] Quan, S.J., J. Park, A. Economou &S. Lee. (2019). Artificial intelligence-aided design: Smart Design for sustainable city development. *Environment and Planning B-Urban Analytics and City Science*, 46(8):1581-1599.
- [9] Ghannad, P. &Y.C. Lee. (2022). Automated modular housing design using a module configuration algorithm and a coupled generative adversarial network (CoGAN). *Automation in Construction*, 139
- [10] Aso, N., H. Yanami &M. Ogawa. (2022). Automatic Parametric Modeling Technique for Structural Design Standardization. *Ieee Access*, 1081031-81041.
- [11] Singh, V. &N. Gu. (2012). Towards an integrated generative design framework. *Design studies*, 33(2):185-207.

- [12] Krish, S. (2011). A practical generative design method. *Computer-Aided Design*, 43(1):88-100.
- [13] Marsh, A. *Generative and performative design: a challenging new role for modern architects*. in *The Oxford conference 2008*. 2008. WIT Press Oxford.
- [14] Buhamdan, S., A. Alwisy & A. Bouferguene. (2021). Generative systems in the architecture, engineering and construction industry: A systematic review and analysis. *International Journal of Architectural Computing*, 19(3):226-249.
- [15] Zhu, W.Z., Y.N. Hou, E.L. Wang & Y. Wang. (2020). Design of Geographic Information Visualization System for Marine Tourism Based on Data Mining. *Journal of Coastal Research*, 1034-1037.
- [16] Llatas, C., B. Soust-Verdaguer & A. Passer. (2020). Implementing Life Cycle Sustainability Assessment during design stages in Building Information Modelling: From systematic literature review to a methodological approach. *Building and Environment*, 182107164.
- [17] Yin, X.F., H.X. Liu, Y. Chen & M. Al-Hussein. (2019). Building information modelling for off-site construction: Review and future directions. *Automation in Construction*, 10172-91.
- [18] Yuan, Z.M., C.S. Sun & Y.W. Wang. (2018). Design for Manufacture and Assembly-oriented parametric design of prefabricated buildings. *Automation in Construction*, 8813-22.
- [19] Lien, L.C. & M.Y. Cheng. (2014). Particle bee algorithm for tower crane layout with material quantity supply and demand optimization. *Automation in Construction*, 4525-32.
- [20] Banihashemi, S., A. Tabadkani & M.R. Hosseini. (2018). Integration of parametric design into modular coordination: A construction waste reduction workflow. *Automation in Construction*, 881-12.
- [21] Guo, J.J., Q. Wang & J.H. Park. (2020). Geometric quality inspection of prefabricated MEP modules with 3D laser scanning. *Automation in Construction*, 11115.
- [22] Benjaoran, V. & N. Dawood. (2006). Intelligence approach to production planning system for bespoke precast concrete products. *Automation in Construction*, 15(6):737-745.
- [23] Wang, Y.W., Z.M. Yuan & C.S. Sun. (2018). Research on Assembly Sequence Planning and Optimization of Precast Concrete Buildings. *Journal of Civil Engineering and Management*, 24(2):106-115.
- [24] Liu, H.X., Y.X. Zhang, Z. Lei, H.X. Li & S. Han. (2021). Design for Manufacturing and Assembly: A BIM-Enabled Generative Framework for Building Panelization Design. *Advances in Civil Engineering*, 2021
- [25] Lobo, J.D.C., Z. Lei, H.X. Liu, H.X. Li & S. Han. (2021). Building Information Modelling- (BIM-) Based Generative Design for Drywall Installation Planning in Prefabricated Construction. *Advances in Civil Engineering*, 2021
- [26] Bakhshi, S., M.R. Chenaghlo, F.P. Rahimian, D.J. Edwards & N. Dawood. (2022). Integrated BIM and DfMA parametric and algorithmic design based collaboration for supporting client engagement within offsite construction. *Automation in Construction*, 133
- [27] Xu, Z., Y.Z. Liang, Y.S. Xu, Z.Z. Fang & U. Stilla. (2022). Geometric Modeling and Surface-Quality Inspection of Prefabricated Concrete Components Using Sliced Point Clouds. *Journal of Construction Engineering and Management*, 148(9):
- [28] Bai, S., M.C. Li, L.G. Song & R. Kong. (2021). Developing a Common Library of Prefabricated Structure Components through Graphic Media Mapping to Improve Design Efficiency. *Journal of Construction Engineering and Management*, 147(1):
- [29] Gan, V.J.L. (2022). BIM-based graph data model for automatic generative design of modular buildings. *Automation in Construction*, 134
- [30] Gan, V.J.L. (2022). BIM-Based Building Geometric Modeling and Automatic Generative Design for Sustainable Offsite Construction. *Journal of Construction Engineering and Management*, 148(10):
- [31] Ma, W., X.Y. Wang, J. Wang, X.L. Xiang & J.B. Sun. (2021). Generative Design in Building Information Modelling (BIM): Approaches and Requirements. *Sensors*, 21(16):
- [32] Xu, Z., Z. Xie, X.R. Wang & M. Niu. (2022). Automatic Classification and Coding of Prefabricated Components Using IFC and the Random Forest Algorithm. *Buildings*, 12(5):22.
- [33] Ghannad, P. & Y.C. Lee. (2022). Automated modular housing design using a module configuration algorithm and a coupled generative adversarial network (CoGAN). *Automation in Construction*, 13920.
- [34] Fang, Y. & S.T. Ng. (2019). Genetic algorithm for determining the construction logistics of precast components. *Engineering Construction and Architectural Management*, 26(10):2289-2306.

LeanAI: A method for AEC practitioners to effectively plan AI implementations

Ashwin Agrawal¹, Vishal Singh², and Martin Fischer³

¹Department of Civil and Environmental Engineering, Stanford University, Stanford, CA, USA

²Centre of Product Design and Manufacturing, Indian Institute of Science, Bangalore, India

³Department of Civil and Environmental Engineering, Stanford University, Stanford, CA, USA

ashwin15@stanford.edu, singhv@iisc.ac.in, fischer@stanford.edu

Abstract –

Recent developments in Artificial Intelligence (AI) provide unprecedented automation opportunities in the Architecture, Engineering, and Construction (AEC) industry. However, despite the enthusiasm regarding the use of AI, 85% of current big data projects fail. One of the main reasons for AI project failures in the AEC industry is the disconnect between those who plan or decide to use AI and those who implement it. AEC practitioners often lack a clear understanding of the capabilities and limitations of AI, leading to a failure to distinguish between what AI should solve, what it can solve, and what it will solve, treating these categories as if they are interchangeable. This lack of understanding results in the disconnect between AI planning and implementation because the planning is based on a vision of what AI should solve without considering if it can or will solve it. To address this challenge, this work introduces the LeanAI method. The method has been developed using data from several ongoing longitudinal studies analyzing AI implementations in the AEC industry, which involved 50+ hours of interview data. The LeanAI method delineates what AI should solve, what it can solve, and what it will solve, forcing practitioners to clearly articulate these components early in the planning process itself by involving the relevant stakeholders. By utilizing the method, practitioners can effectively plan AI implementations, thus increasing the likelihood of success and ultimately speeding up the adoption of AI. A case example illustrates the usefulness of the method.

Keywords –

Artificial Intelligence; Machine Learning; Technology management; Lean methodology; Last planner system; AI strategy; AI adoption; Technology adoption; Digital strategy

1 Introduction

Recent developments in Artificial Intelligence (AI) provide unprecedented automation opportunities in the Architecture, Engineering, and Construction (AEC) industry [1]. It offers the potential to significantly increase productivity, add enormous value, enhance competitive advantage, and increase economic welfare [2], [3]. This immense potential of AI has prompted many companies to invest in developing and adapting AI capabilities. In fact, Gartner expects 70% of organizations, including AEC, to invest and operationalize some form of AI capability by 2025 [4].

However, despite the enthusiasm regarding the use of AI, 85% of current big data projects fail [5]. In a recent survey by Boston Consulting Group and MIT, seven out of ten companies reported little or no impact of AI [6]. These constant failures result in wastage of time, money, and effort. It also risks AI adoption in the AEC industry since practitioners might reject AI as a hype [7].

One of the main reasons for AI project failures in the AEC industry is the disconnect between those who plan or decide to use AI and those who implement it [8]–[11]. [12], [13] notes that the process of implementing AI projects in engineering firms remains less understood. [11] reports from a survey of 3,000 business executives that there is a big disconnect between the ambitions and implementation of AI, and more than 60% firms do not have a concrete AI implementation strategy. Therefore, research addressing the disconnect between planning and implementation is crucial. Such research can provide valuable insights and lessons for organizations just beginning their AI journey and can help them navigate the complexities of implementation and increase their chances of success [14].

In this work, we introduce the LeanAI method to alleviate the disconnect between AI planning and implementation in the AEC industry. The LeanAI method delineates what AI should solve, what it can solve, and what it will solve, forcing practitioners to

clearly articulate and align these components early in the planning process itself by involving the relevant stakeholders. Based on our case studies data and practitioner feedback, it has been observed that the LeanAI method is highly valuable in facilitating better planning for AI implementations in the AEC industry (see Section 5 for details).

In the next section, the paper provides details about the research method used for developing the LeanAI method. This is followed by a brief background about the use of AI in AEC in Section 3, introducing the LeanAI method, detailing the steps on how it can be used and showcasing its usage in the context of an example in Section 4, and providing evidence for the usefulness of the method in Section 5. The paper is concluded with the discussions of the findings and their implications for the AEC industry in Section 6.

2 Research Method

The LeanAI method is built using an ethnographic-action research methodology [15], where the researchers helped AEC practitioners implement AI projects while simultaneously observing the challenges in AI implementation and formulating solutions. Ethnographic-action research has been popular for investigating the use of technology in construction projects [16], [17] because it allows the researchers to holistically understand the local context of AEC practitioners while building the solution, thereby increasing the likelihood of a solution that works in practice [18].

LeanAI-method development: The LeanAI method is built using data from two sources:

(1) An ongoing longitudinal study, which has investigated four case studies since 2018, has collected 50+ hours of interview data and conducted direct observations of AEC practitioners. The study focuses on Digital Twin and AI implementations that involve Machine Learning, Deep Learning, Computer Vision, and Natural Language Processing. This information has been documented in sources such as [8]-[10], [19], and [20].

(2) 12 graduate-level student case studies, each lasting for three months, involving AI implementations with industry partners in the USA, as part of a project-based class at Stanford University.

Each of the sixteen case studies involved an AEC company that wanted to implement some form of AI algorithm. The nature of the cases varied, with some being more exploratory in nature and others being very specific about the algorithm they wanted to implement.

The studies lasted an average of 3 to 6 months and involved three phases: ideation, AI algorithm development, and roadmap creation for future deployment. The authors were directly involved in at least one of these phases for each case study. Ethnographic techniques were used to collect data for all sixteen case studies.

Using above observations and hands-on experience of building AI projects with AEC professionals, the authors identified key components crucial to addressing the disconnect between AI planning and implementation. These included clearly defining the business needs the AI solution will address, outlining a specific problem statement for the AI to solve, identifying the required data and AI methods, and establishing metrics to measure the AI's performance. As the work progressed, the authors found that the Last Planner System [21] was effective in organizing these components in a simple, logical, and relatable structure for AEC practitioners, resulting in the development of the LeanAI method.

While the case studies demonstrated encouraging outcomes, it was crucial to conduct an independent validation of the efficacy of the LeanAI approach to ensure its robustness. This was necessary because the method was developed based on data from the case studies, and assessing its usefulness solely on those studies could introduce bias. Therefore, we conducted a workshop with practitioners as described below.

LeanAI-method's usefulness validation: Thirty practitioners from different companies used the LeanAI method to plan an upcoming/ongoing AI implementation in their companies. Their feedback about using the LeanAI method to plan their AI implementations was recorded and the results have been described in Section 5.

3 Background on Artificial Intelligence and its usage in AEC industry

AI is a rapidly growing field that encompasses a wide range of subdisciplines and application areas. Broadly, AI helps computers perceive, represent, reason, solve, and plan in an intelligent and adaptive manner, making them capable of dealing with complicated and ill-defined problems which were long thought to be the exclusive domain of humans [22].

Machine Learning (ML), a key area in AI research, involves the development of algorithms that allow computers to learn from data (and labels) to make predictions, decisions, and perform tasks for which they were not explicitly programmed. For example, Natural Language Processing (NLP), a sub-part of ML, involves development of algorithms that can understand, interpret,

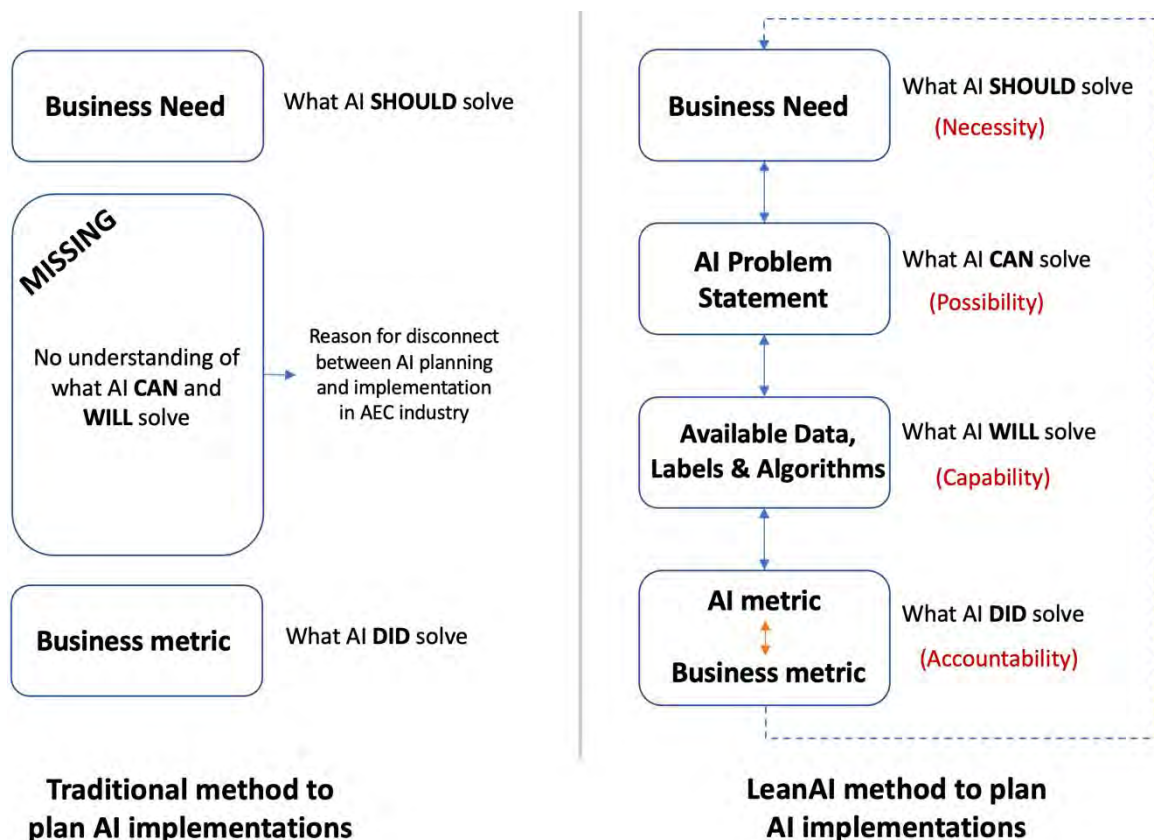


Figure 1 Comparison of traditional and LeanAI method to plan AI implementations

and respond to human language. NLP is used in a wide range of tasks such as language translation and text summarization for which writing an exhaustive set of rules to explicitly program the computer is nearly impossible. Another popular field within ML is Computer Vision. This field involves development of algorithms that can understand visual information, such as images and videos, like how humans use their eyes. Writing an explicit set of rules for computers to understand any image or video is, again, nearly impossible.

Owing to these exciting possibilities, AI has gained significant interest in the AEC industry [23]. Many pilot AI applications in the AEC industry have already been built to better manage planning of site logistics [24], plan safety on construction sites [25], monitor progress and productivity improvements [26], and plan building operations and maintenance [27].

Although the above pilot applications are encouraging, AI adoption is still in its very early stages in the AEC industry [28]. Limited studies exist that study the practical problems faced by practitioners [8], [29] while planning and deploying AI implementations. One possible reason for this might be that actual AI implementation span over several months or years, making it difficult to conduct a longitudinal study.

Furthermore, the limited interest of practitioners to collaborate and give access to information over such a prolonged period further complicates the issue. The authors of the paper are humbled and grateful for the positive reception they have received from practitioners, which allowed them to create the LeanAI method, which will be discussed in the following section.

4 LeanAI Method: An Introduction

When planning AI implementations, AEC practitioners often start by identifying the business needs that AI should address. These business needs, such as reducing maintenance costs for highways or speeding up projects by 20%, are the necessities that the project needs to address and thus drive the AI implementation and ultimately guide what the AI should aim to solve.

However, AI cannot directly solve these business needs. The AI problems need to be framed in an entirely different way as it concerns itself with learning a mathematical function from data. Bridging this gap between high-level business objectives and detailed properties of the implementation is often the key challenge to creating a successful AI project [30].

In our study, we found that AEC practitioners often use a traditional method of planning AI implementations

that does not clearly link high-level business objectives with detailed implementation properties (as shown on the left in Figure 1). Practitioners fail to distinguish between what AI should solve, what it can solve, and what it will solve, treating these categories as if they are interchangeable. While AEC practitioners may have a clear understanding of the pressing business needs and may wish that AI should solve certain problems, it is not always possible for AI to address these needs directly. Instead, AI can only solve a small part of the problem when properly formulated, with a direct or indirect impact on the business need. Additionally, just because AI has the capability to solve a problem does not guarantee that it will be able to do so for the practitioner's use case, as it depends on the data and labels available with them.

In fact, over 70% of the projects we observed either did not define a clear problem statement for AI or were unclear about it (e.g., only defining broad business objectives). A similar phenomenon is noted in [31], which states that many AI projects fail because they do not specify the exact problem that AI can solve and expect it to do everything. [30] notes that not defining the problem or success metric for an AI project is a sure way to waste time and money.

The LeanAI method (as shown on the right in Figure 1) clearly delineates what AI should solve, what it can solve, and what it will solve. This approach thus forces practitioners to clearly articulate these components clearly in the planning process itself by involving the relevant stakeholders (e.g., IT team who know about data and labels). Our data suggests that this approach, at least in part, ensures more robust planning of AI implementations.

The following paragraphs will describe the individual elements of the LeanAI method and provide steps for practitioners on how to use the method. We will also illustrate the use of the method through an example case study from our dataset.

Business need (Necessity that AI should solve): Defining the business need is an essential first step in planning AI implementations for AEC practitioners. It involves identifying areas where AI should make improvements in the current way of working. Examples of common business needs and necessities include reducing project costs, increasing safety on job sites, and speeding up construction schedules. Specifying a clear business need helps to guide the AI implementation and ensures that the correct problem is being addressed. It also helps to clarify the scope of the project and gain support from top management.

AI Problem statement (Possibility that AI can solve): The goal of AI is to address the defined business need,

but it cannot do so directly. Instead, the problem statement must be framed in a way that AI can solve it, and at the same time the formulated problem statement, at least partially, addresses the business need. For example, to address the business need of increasing safety on site, one of the problems that AI can potentially solve is to detect that safe distances are maintained between the crane and the workers using the camera image of the site. Another problem statement addressing the same business need can be to detect that workers are wearing protective gear on site. Based on the availability of current AI algorithms, each of these problem statements can be potentially solved by AI. Now, it is up to the practitioners to decide which solution will have the greatest impact for their use case, or to come up with a different AI problem statement altogether.

Available Data, Labels, and Algorithms (Capability that AI will require): Many contemporary AI and ML algorithms rely heavily on a large amount of data and labels for optimal performance. Therefore, just because a problem statement has been successfully addressed by AI in one context, it does not guarantee that it will be solved in another context as well. The ultimate determinant of what AI will solve will depend on the availability of suitable data, labels, and the expertise required to develop the algorithm.

Metrics [AI metric and Business metric] (Accountability of what AI did): Metrics are the way to measure how well AI did. This measurement process helps to ensure that the AI project stays on track and also provides feedback for continuous improvement in subsequent iterations of AI prototype development. As we have an AI specific problem statement (which is mathematical in nature) and a business need, we need two metrics, one for each, and a way to connect them. That is what we refer to an AI metric and a business metric.

The AI metric measures the performance of the AI algorithm on the problem statement, typically through mathematical measurements such as accuracy, F1 score, etc. which may or may not have a direct correlation to the business. On the other hand, the business metric directly measures the impact on the defined business need. Establishing the relationship between both metrics is a crucial step for practitioners to holistically evaluate AI. For example, in certain cases, 70% accuracy for AI algorithms might result in 25% cost savings and in other cases might not provide any substantial value to the business.

4.1 Steps for practitioners to use LeanAI method

While there is no "right" way to use the LeanAI method, we suggest the following steps as a starting point,

especially for the first-time users:

Step-1: Start by defining the business need: We have observed in our case studies that practitioners who do not think of the “bigger picture” (aka business need), often fail to get attention from the top management. This, ultimately, results in insufficient resources and lack of traction within the company even if the project is somewhat successful. Therefore, defining the business need is an essential first step. While defining the business need, we suggest practitioners to be as specific and precise as possible, because these business needs are the foundation on which the problem statements would build on later. For example, stating the need as “improving project performance” is not specific enough. It is important to clarify if the goal is to reduce cost, reduce time, improve safety, enhance worker's health, or something else. A more specific and precise business need would be “reduce the cost of the project” or, even better, “reduce the maintenance cost of the project.”

Step-2: Formulate multiple problem statements to address the business need: Once the specific and precise business need is identified, practitioners should brainstorm multiple ways in which AI can potentially address it. This would involve creating well-defined problem statements that AI can solve, and which will also fulfill the business need. For this step, it is, therefore necessary to involve two types of people: (1) those who are familiar with recent developments in AI and understand what it can and cannot do, and (2) those who know operational details of the business to connect where the capabilities of AI can be utilized.

Step-3: Evaluating if AI will be able to solve the formulated problem statements: In the next step, practitioners must determine if they possess the necessary data, labels, and expertise to construct an AI algorithm that can solve the formulated problem. To accomplish this, it is crucial to involve someone with experience in building AI algorithms as the data requirements for these algorithms can, sometimes, be substantial and may not be feasible for many companies. Therefore, it is crucial to obtain a realistic estimate of the data requirements and the performance of the AI algorithm from an expert, to ensure the feasibility of the project.

Step-4: Defining the metrics to track how well AI did: Next, practitioners need to define both the AI metric and the business metric and create a link between them. It is important to obtain input from AI experts at this stage to ensure that the metrics and targets set are realistic and achievable, given the data and algorithms at hand. For example, in one case study, the company required an AI

algorithm to achieve an accuracy of over 99% for it to have any value to the business. This unrealistic expectation from AI ultimately led to the failure of the AI project, which could have been avoided if the planning process had been done correctly.

Step-5: Keep iterating: Creating a successful AI algorithm is not a one-shot task. Practitioners need to continuously iterate and improve depending on how well the AI algorithm is performing on the AI and business metrics. This may sometimes involve revisiting and revising the business need and problem statement either partially or completely.

4.2 Example case study demonstrating the use of LeanAI method

In this section, we describe one of our case studies that required practitioners to use AI to improve highway maintenance. We will first explain how practitioners planned this AI implementation using the traditional method. We then illustrate how the LeanAI method helped them improve their planning.

Using traditional planning, we observed practitioners often defined broad and general goals on how AI can help improve highway maintenance, such as reducing the costs, decreasing rework, and increasing daily traffic capacity on highways. While these goals may be areas where AI should have an impact, they were not specific enough to guide the development team in determining how AI can be implemented to achieve them. This lack of specificity led to disconnects during the implementation phase as the AI development team struggled to understand how to apply AI to solve these problems. For example, one practitioner reported that despite top management’s push to implement AI on their highway maintenance projects, they have been struggling to find a use case for it. Another practitioner reported that his company’s AI project has been stalled for a few months due to a lack of labeled data which they did not account for in the planning phase.

In the LeanAI method, practitioners begin by identifying the business need, such as reducing costs. The next step is to identify the problem statement that AI can solve to address the business need. For example, in the context of highway maintenance, problem statements from practitioners included using AI to automate the detection of cracks on highways, predict crack growth and propagation, and predict traffic growth on the highway. These problem statements all aim to reduce costs by reducing the number of workers needed for maintenance or better planning for maintenance.

Although AI can potentially address all these problem statements, whether it will be able to do so or not will depend on the availability of data, labels, and algorithms. For example, when practitioners evaluated the

requirement of data and labels for the various formulated problem statements, they realized the lack of sufficient historical data for predicting crack propagation and growth. Therefore, they had to restrict themselves to either detecting cracks or predicting traffic growth on highways.

Practitioners then established the metrics to track AI and business performance. They determined that "accuracy" would be used to evaluate the AI's performance and the "amount of dollars saved in one year" would measure the business performance. However, upon further analysis, they found that even if the AI achieved the highest level of accuracy in predicting traffic, the financial savings would not justify the AI project. As a result, they decided to proceed with the problem statement of detecting cracks on highways and abandoned the predicting traffic problem statement.

In summary, using the LeanAI method in this case study, practitioners were able to clearly identify a use case for AI that had significant business impact and could be addressed with the available resources within the company, something that was difficult to achieve with the traditional method of planning AI implementations.

5 Validation of LeanAI method's usefulness

30 practitioners were divided into ten groups, each consisting of three members. These groups were given 90 minutes to plan an AI implementation project that they were either currently working on or planning to work on in the future, using the LeanAI method. The session ended with a collective reflection session, during which qualitative and quantitative feedback was gathered on the usefulness of the method.

Of the ten groups, seven found the LeanAI method to be very useful, while the remaining three found it somewhat useful. None of the groups found the method to be not useful at all. Practitioners particularly appreciated the simplicity of the method and its practicality, as well as the emphasis it placed on aligning all of the project's elements (business need, problem statement, data, and metrics) together. Participants stated that while each of these elements could be formulated individually, the real challenge was in aligning them, and the LeanAI method helped them achieve this.

Four out of the ten groups expressed interest in conducting more detailed workshops within their companies, indicating that they found the LeanAI method to be very useful.

6 Conclusion

The use of AI in the AEC industry presents great opportunity for automation. However, for a wide scale adoption of AI, it is crucial that practitioners have a clear understanding of what AI should solve, what it can solve, and what it will solve. The LeanAI method provides a starting point to address this challenge by encouraging practitioners to involve relevant stakeholders in the early stages of planning, ensuring that AI implementation is aligned with the business needs and goals. This approach can help to bridge the gap between planning and implementation, increasing the chances of success for AI projects in the AEC industry. Future research can further validate the robustness and usefulness of the LeanAI method in AEC and other industries.

References

- [1] A. Darko, A. P. C. Chan, M. A. Adabre, D. J. Edwards, M. R. Hosseini, and E. E. Ameyaw, "Artificial intelligence in the AEC industry: Scientometric analysis and visualization of research activities," *Autom. Constr.*, vol. 112, p. 103081, Apr. 2020, doi: 10.1016/j.autcon.2020.103081.
- [2] J. K.-U. Brock and F. von Wangenheim, "Demystifying AI: What Digital Transformation Leaders Can Teach You about Realistic Artificial Intelligence," *Calif. Manage. Rev.*, vol. 61, no. 4, pp. 110–134, Aug. 2019, doi: 10.1177/1536504219865226.
- [3] E. Brynjolfsson and A. McAfee, *The second machine age: Work, progress, and prosperity in a time of brilliant technologies*. WW Norton & Company, 2014.
- [4] L. Goasduff, "The 4 Trends That Prevail on the Gartner Hype Cycle for AI, 2021," *Gartner*, 2021. <https://www.gartner.com/en/articles/the-4-trends-that-prevail-on-the-gartner-hype-cycle-for-ai-2021> (accessed Dec. 19, 2021).
- [5] G. Satell, "How to Make an AI Project More Likely to Succeed," *Harvard Business Review*, Jul. 19, 2018. Accessed: Dec. 20, 2021. [Online]. Available: <https://hbr.org/2018/07/how-to-make-an-ai-project-more-likely-to-succeed>
- [6] S. Ransbotham, S. Khodabandeh, R. Fehling, B. LaFountain, and D. Kiron, "Winning with AI," *MIT Sloan Manag. Rev.*, vol. 61180, 2019.

- [7] P. Bosch-Sijtsema, C. Claeson-Jonsson, M. Johansson, and M. Roupe, "The hype factor of digital technologies in AEC," *Constr. Innov.*, vol. 21, no. 4, pp. 899–916, Jan. 2021, doi: 10.1108/CI-01-2020-0002.
- [8] A. Agrawal *et al.*, "Digital Twin in Practice: Emergent Insights from an ethnographic-action research study," in *Construction Research Congress 2022*, Arlington, Virginia, USA, 2022, pp. 1253–1260. doi: 10.1061/9780784483961.131.
- [9] A. Agrawal, M. Fischer, and V. Singh, "Digital Twin: From Concept to Practice," *J. Manag. Eng.*, vol. 38, no. 3, p. 06022001, May 2022, doi: 10.1061/(ASCE)ME.1943-5479.0001034.
- [10] A. Agrawal, R. Thiel, P. Jain, V. Singh, and M. Fischer, "Digital Twin: Where do humans fit in?," *Autom. Constr.*, vol. 148, p. 104749, Apr. 2023, doi: 10.1016/j.autcon.2023.104749.
- [11] S. Ransbotham, D. Kiron, P. Gerbert, and M. Reeves, "Reshaping business with artificial intelligence: Closing the gap between ambition and action," *MIT Sloan Manag. Rev.*, vol. 59, no. 1, 2017.
- [12] K. Hosanagar and A. Saxena, "The First Wave of Corporate AI Is Doomed to Fail," *Harvard Business Review*, Apr. 18, 2017. Accessed: Dec. 19, 2021. [Online]. Available: <https://hbr.org/2017/04/the-first-wave-of-corporate-ai-is-doomed-to-fail>
- [13] P. Hofmann, J. Jöhnk, D. Protschky, and N. Urbach, "Developing Purposeful AI Use Cases-A Structured Method and Its Application in Project Management.," presented at the *Wirtschaftsinformatik (Zentrale Tracks)*, 2020, pp. 33–49.
- [14] Y. Duan, J. S. Edwards, and Y. K. Dwivedi, "Artificial intelligence for decision making in the era of Big Data – evolution, challenges and research agenda," *Int. J. Inf. Manag.*, vol. 48, pp. 63–71, Oct. 2019, doi: 10.1016/j.ijinfomgt.2019.01.021.
- [15] T. Hartmann, M. Fischer, and J. Haymaker, "Implementing information systems with project teams using ethnographic–action research," *Adv. Eng. Inform.*, vol. 23, no. 1, pp. 57–67, Jan. 2009, doi: 10.1016/j.aei.2008.06.006.
- [16] D. Oswald and A. Dainty, "Ethnographic Research in the Construction Industry: A Critical Review," *J. Constr. Eng. Manag.*, vol. 146, no. 10, p. 03120003, Oct. 2020, doi: 10.1061/(ASCE)CO.1943-7862.0001917.
- [17] A. Mahalingam, A. K. Yadav, and J. Varaprasad, "Investigating the Role of Lean Practices in Enabling BIM Adoption: Evidence from Two Indian Cases," *J. Constr. Eng. Manag.*, vol. 141, no. 7, p. 05015006, Jul. 2015, doi: 10.1061/(ASCE)CO.1943-7862.0000982.
- [18] S. Azhar, I. Ahmad, and M. K. Sein, "Action Research as a Proactive Research Method for Construction Engineering and Management," *J. Constr. Eng. Manag.*, vol. 136, no. 1, pp. 87–98, Jan. 2010, doi: 10.1061/(ASCE)CO.1943-7862.0000081.
- [19] M. Fischer and A. Agrawal, "Digital Twin for Construction," *Center for Integrated Facility Engineering*, 2019. <https://cife.stanford.edu/Seed2019%20DigitalTwin> (accessed Oct. 01, 2021).
- [20] A. Agrawal, V. Singh, and M. Fischer, "A New Perspective on Digital Twins: Imparting Intelligence and Agency to Entities," *IEEE J. Radio Freq. Identif.*, vol. 6, pp. 871–875, 2022, doi: 10.1109/JRFID.2022.3225741.
- [21] H. G. Ballard, "The last planner system of production control," *d_ph*, University of Birmingham, 2000. Accessed: Jan. 21, 2023. [Online]. Available: <https://theses.bham.ac.uk/id/eprint/4789/>
- [22] D. Norman, "Design, Business Models, and Human-Technology Teamwork: As automation and artificial intelligence technologies develop, we need to think less about human-machine interfaces and more about human-machine teamwork," *Res.-Technol. Manag.*, vol. 60, no. 1, pp. 26–30, 2017.
- [23] N. Emaminejad, A. M. North, and R. Akhavian, "Trust in AI and Implications for the AEC Research: A Literature Analysis." arXiv, Mar. 07, 2022. Accessed: Jan. 21, 2023. [Online]. Available: <http://arxiv.org/abs/2203.03847>
- [24] A. Braun and A. Borrmann, "Combining inverse photogrammetry and BIM for automated labeling of construction site images for machine learning,"

- Autom. Constr.*, vol. 106, p. 102879, Oct. 2019, doi: 10.1016/j.autcon.2019.102879.
- [25] H. Baker, M. R. Hallowell, and A. J.-P. Tixier, "AI-based prediction of independent construction safety outcomes from universal attributes," *Autom. Constr.*, vol. 118, p. 103146, Oct. 2020, doi: 10.1016/j.autcon.2020.103146.
- [26] R. Sacks, M. Girolami, and I. Brilakis, "Building Information Modelling, Artificial Intelligence and Construction Tech," *Dev. Built Environ.*, vol. 4, p. 100011, Nov. 2020, doi: 10.1016/j.dibe.2020.100011.
- [27] J. López, D. Pérez, E. Paz, and A. Santana, "WatchBot: A building maintenance and surveillance system based on autonomous robots," *Robot. Auton. Syst.*, vol. 61, no. 12, pp. 1559–1571, Dec. 2013, doi: 10.1016/j.robot.2013.06.012.
- [28] Y. Pan and L. Zhang, "Roles of artificial intelligence in construction engineering and management: A critical review and future trends," *Autom. Constr.*, vol. 122, p. 103517, Feb. 2021, doi: 10.1016/j.autcon.2020.103517.
- [29] L. Rampini, A. Khodabakhshian, and F. Re Cecconi, "Artificial intelligence feasibility in construction industry," presented at the 2022 European Conference on Computing in Construction, Jul. 2022. doi: 10.35490/EC3.2022.189.
- [30] Geoff Hulten, *Building Intelligent Systems*. 2018. Accessed: Aug. 05, 2022. [Online]. Available: <http://link.springer.com/book/10.1007/978-1-4842-3432-7>
- [31] Erik Brynjolfsson and Tom Mitchell, "What can machine learning do? Workforce implications," *Science*, 2017. Accessed: Aug. 05, 2022. [Online]. Available: <https://www.science.org/doi/10.1126/science.aap8062>

Digital Twin as enabler of Business Model Innovation for Infrastructure Construction Projects

Sascha van der Veen¹, Elias B. Meusburger² and Magdalena Meusburger³

¹ Department of Digital Rail Services, Rhomberg Sersa Rail Group, Switzerland

² Department of Group Products and Innovation, Rhomberg Sersa Rail Group, Austria

³ Department of Business and Management, Vorarlberg University of Applied Sciences, Austria

sascha.vanderveen@rsrg.com, elias.meusburger@rsrg.com, magdalena.meusburger@fhv.at

Abstract

Emerging technologies and methods are becoming an important element of the construction industry. Digital Twins are used as a base to store data in BIM models and make use out of the data respectively make the data visible. The transparency in all phases of the lifecycle of building and infrastructure assets is crucial in order to get a more efficient lifecycle of planning, construction and maintenance. Whereas other industries increased performance in these phases by making use out of the data, construction industry is stuck in traditional methods and business models. In this paper we propose a concept that focuses on the digital production twin. The comparison of planning data with As-Is production data can empower a data driven continuous improvement process and support the decision-making process of future innovations and suitable business models. This paper outlines the possibility to use the data stored in a digital twin with regards to the evaluation of possible business models.

Keywords –

Digital Twin; Business Model Innovation; Infrastructure; Decision-Making

1 Introduction

Delays and cost overruns are frequent in infrastructure construction projects. Only around 25% of construction projects worldwide have come within the range of 10% of their original deadlines from 2012 to 2014 [1]. Globally, rail construction projects are frequently affected by budget and schedule overruns by an average of 44.7% [2]. Whereas other industries almost doubled their productivity over the past decades, the construction industry remained the same [3]. Research has shown that these 75 % of the projects that overrun schedule and costs end up 14 % above the estimated contract sum [4]. Considering railway construction projects, short durations for maintenance as well as new

instalments are crucial to avoid a breakdown of the railway network. Otherwise, time overruns are often fined with high penalties [5].

Traditionally, one of the biggest issues is the usage of static schedules that do not reflect real conditions on-site [6]. As a result, schedules become useless and coordination is based on improvisations. Furthermore, progress tracking is often based on rough estimations and thus schedule deviations are not known in detail. Scheduling is usually done according to the experience of the project or site manager and not based on the monitoring of the construction progress. Thus, it is very difficult to identify bottlenecks, as for example a machine that reduces speed and thus leads to a potential decrease of productivity of the following construction processes.

As a result of the previous mentioned issues, problems are often identified in a late stage making it difficult to implement appropriate improvement and innovation actions in time. Furthermore, infrastructure construction projects are loosely connected and improvements are not systematically stored or transferred to future projects [7]. Early identification of bottlenecks and a dynamic definition of improvement actions, innovation possibilities as well as their impact would decrease variability and thus reduce budget overruns. The infrastructure construction industry is seeking for answers to these problems to avoid time and cost overruns. New business models and innovation possibilities are necessary to empower future ways of creating revenue and decreasing variability on infrastructure construction projects.

Research and development are important areas for a company's future existence. Innovation is not only to be understood as the technical implementation of ideas, but the success of new products and system solutions must also include economic success on the market.

The use of digital twin-based approaches in infrastructure construction projects provides the opportunity to enhance efficiency and decision-making. The current focus lies on technical implementation, but in future a concept for value capturing is also needed in

the future. This paper proposes a concept of business model innovation for value capturing in infrastructure construction projects. This paper investigates the possibilities of using data from a digital twin to support the decision making process and business model creation.

2 Literature Review

To determine the current status quo of digital twin-based approaches in the context of business model innovation and value creation for infrastructure construction projects desk and literature research were conducted. A research definition for digital twin in infrastructure construction projects was created and the role of digital twin solutions in Business is described.

2.1 Digital Twin - Definition

In literature the term “digital twin” is subject to different definitions, which makes a uniform description difficult. For instance, Klostermeier [8] generally describes the digital twin as the virtual image of a real existing object. Grieves [9] describes three elements that constitute a digital twin: (a) the physical product, (b) the digital twin, (c) the connecting information in between. In a broader sense, the digital twin can include material objects as well as immaterial objects like products, systems, services and processes. Thus, based on these two authors, the definition of the Digital Twin arises as a virtual image of a physical object, product, system, process, or service, in which the connecting information is intelligently available for a wide variety of applications.

Concerning to the construction industry, there is often discussion about the distinction between BIM - 'Building Information Modelling' and Digital Twin. According to Tang [10] BIM can generally only provide static data. In combination with additional connected information, BIM inputs data to the digital twin. Deng [11] describes 5 levels of BIM evolution to Digital Twins:

- Level 1: BIM (Concept, Design, Construction Scheduling...)
- Level 2: BIM+Simulation (FM Operation, Estimation, Sim-Based Prediction ...)
- Level 3: BIM+Sensors (Real-Time Visualization, Real-Time Monitoring)
- Level 4: BIM+AI (Decision Making, Data-based Prediction)
- Level 5: Digital Twin (Control, Feedback, Optimization, Interaction)

In addition to the capabilities supported in Levels 1-4, the digital twin relies on the data connecting the physical object and the digital image and enables an intelligent feedback control system that allows optimised results and control strategies.

Deriving from this, this paper applies the following operational definition:

“A digital twin for infrastructure construction projects is a virtual image of the physical construction site with a link of the planning data in comparison to the construction site execution data, which is intelligently available for control feedback and further value creation”.

The planning data is a set of the BIM models, the construction progress plans, logistics plans, etc. The process data relates to the data during the construction process and the construction progress data from, for example, IoT sensors or cameras on the construction site.

At present, digital Twin technologies have their main purpose in real-time data capturing and monitoring, decision-making and maintenance [12].

In the future, digital twin approaches must be applied to infrastructure construction projects and will enable new business opportunities in the infrastructure sector.

2.2 Business Model Innovation with Digital Twins

When digital twins are investigated through the lens of innovation, two approaches can be used: innovation as a process and innovation as an outcome [13]. If seen as an innovation process, a digital twin enables value creation via collaboration through the value chain [14]. If the focus is placed on innovation as an outcome, the utilisation of a novel product, service, process or business model forms the hotspot. In literature product innovation, service innovation, process innovation and business model innovation are prevalent [14]. Herewith, innovation always refers to the development of new products/ services/ processes/ business models, the modification of existing products/ services/ processes/ business models, and the change from one product/ service/ process/ business model to another. Holopainen [14] states that the “Digital twins’ ability to synchronize the real and digital worlds also enables novel types of business model innovation, changing existing ways of operating”.

With these innovations, new types of revenue streams can be explored. However, the current focus of research and implementation is more on the technology rather than the impact on the construction projects business models. According to Spang [15] little has changed in the partnership for infrastructure projects and the bidding and contracting process in recent years. New business models therefore have high potential in this sector and will also have a high impact to the whole industry.

3 Concept / Proposal

In this paper we want to focus on the digital production twin which contains the scheduling data. The basis which is created in the work preparation phase will be the basis for real-time data that is being collected while construction phase. This concept aims to perform a data-driven continuous improvement process captured within a digital twin solution respectively environment. The focus is on construction processes on railway construction projects.

The concept is based on Lean Management, which focuses on the improvement of the processes by defining and evaluating the Value Stream with a focus on Value-Adding activities and the elimination of waste which is defined as 'any activity that does not add up to the products value' [16]. The analysis of the whole value chain leads to an efficient end-to-end process. However, the authors will focus on the construction phase since the main business of the Rhomberg Sersa Railgroup is the construction of railway assets.

The evaluation of production tasks is the basis in order to emphasize improvements respectively to support the business with less variability within the construction phase. A structured way to collect As-Is production data is crucial in order to compare it with planning data within a Digital Twin. In general both datasets need to be aligned with their units and metrics to collect valuable insights for further business models and decision making process.

The proposed concept consists of the following elements:

1. Planning

The planning of construction processes is being conducted in a site simulation software in which the BIM model is the basis for the planning. The construction machines are getting imported into the software and the tasks are planned according to the movement and processes of the machines. The speed of construction is defined by the productivity rates and the experience of the foreman. The planning data is the basis for the digital production twin and can be used for the comparison.

2. As-Is production data gathering

While the construction phase, a structured way to collect As-Is production data needs to be set up. The collected data needs to be aligned with the dataset of the planning phase. To run the comparison, an object-based throughput time needs to be captured and documented.

Since the technology of live image recognition has been difficult to implement on construction sites the first step will be the manual gathering of the data on site. E.g. the foremen will need to have a tool on which he can define the process as done at the moment when the object has been built. The timestamp within the tool will then

give the needed throughput time that is necessary for the further use.

3. Identification of deviations / waste processes

The comparison of the data needs to be handled in a Business Intelligence tool or in a software that is tailor made for the needs. The data must be compared and if certain threshold values are exceeded, the system highlights the processes that were delayed.

4. Problem categorisation

As previously described once a deviation that has exceeded the threshold value the system highlights the process that was delayed. The problem then needs to be categorised. Therefore an application is being developed in which the classification can be conducted and the data analysed for further improvement and analysis. As a structure to support the root cause analysis and thus the categorisation the 5 Why's can support in detecting the cause of the delay [17]. The tool is broadly being used as Lean methodology. The aim is to ask five times why to get deeper into the root cause and a more detailed picture of the problem.

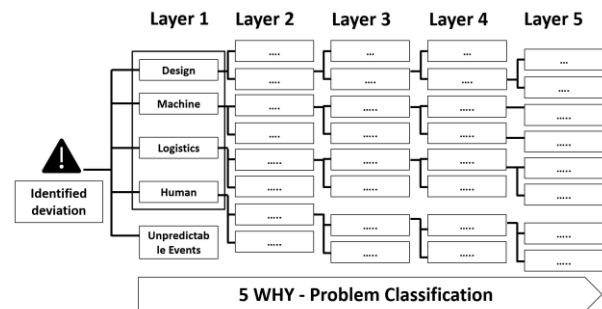


Figure 1. "5-Why" problem classification

A tree diagram (Figure 1) which will be the main structure for the approach will then grow with each problem identified. The different layers of the diagram represent different organisational target groups for decision-making. Whereas the first layer can support the C-Level respectively Top Management in making decisions by highlighting the overall areas in which improvements or innovations should be done, the Layer five can support for example, the machine maintenance department by showing the problems that lead to deviations on a detailed level.

The cross-project view of the diagram will support finding bottlenecks and the identification of innovations that will stabilise and improve processes along the value chain and support units such as maintenance.

5. Improvement and value creation opportunity

evaluation

The insights can then be used as a base for the decision of the innovations that need to be developed within the R&D portfolio. The dataset can be analysed in regards of construction bottlenecks and data-driven improvement actions and business model innovations taken. Different identified problems can be clustered into a improvement actions or initiatives.

6. Impact analysis of value creation and improvement

Once an innovation or improvement solution is developed the success of the decision and development can then be traced by tracking the decrease of the following problems respectively if the reason for deviation occurs again.

3.1 Demonstration Case

In this demonstration case we want to outline a possible case and its outcome regarding the evaluation of future improvements respectively business model creation. The case can be considered as an overall case that focuses on organizational decisions based on collected production data. The digital twin is being used for the data storage and the collected problems are connected to the object in the model.

The management of a company evaluates the digital twin data of the previously described concept for the annual report. The data shows that a major part of the deviations that occurred while construction was caused within the process of gravel tamping. The analysis also outlines that most of these deviations were caused by external subcontractors. The company doesn't have enough machines in order to handle all tamping processes with its own machine assets.

This knowledge gives the opportunity for a valid decision-making process. The company evaluates the opportunities and identifies the following options:

1. Investing in new tamping machines in order handle the processes inhouse.
2. Negotiate Performance-based contracts with the subcontractors.
3. Piloting a Revenue Sharing project on which the risk is shared with all project parties.

After some discussions the decision makers agree on performance-based contracts with their subcontractors that are responsible for the tamping processes. They also define that the year after they want to have a report of the success measure by the responsible manager in order to understand the impact and possible further actions if the decision didn't succeed. By evaluating the upcoming reasons for deviations it can be measured if the decision had the expected outcome respectively if the new

business model succeeded.

3.2 Impact on Industry/Projects/Companies

The proposed concept of collecting and analysing data in a digital twin can support in decision making on an organization and project level. For projects a digital production twin can support in short term decision making. That gives the opportunity to collect suggestions for improvements for further projects. Furthermore, that means that a data driven continuous improvement is established and the collected data can support the organization in identifying an overall view about their bottlenecks and thus a data supported basis for decision making of improvements, innovations and new business models. However, the industry needs to handle the needed transparency and align with emerging technologies as well as methodologies.

3.3 Concept: Business Model Innovation enabled by a Digital Twin

The described application of a digital twin in infrastructure projects enables business model innovation. To show which business mechanics are enabled, the concept of pattern adaptation according to the St. Galler Business Model Navigator is applied [18]. Gassmann, Frankenberger and Csik have compiled 55 successful business model patterns into a set of sample cards. According to the authors, more than 90% of successful business model innovations can be traced back to the recombination of these 55 basic patterns. In the following, the five most prospectus business mechanics applied to a digital twin have been chosen and will be described in detail.

3.3.1 Digitalization

A Digital Twin includes many aspects of the business model pattern Digitalization.

As the name suggests, the construction work will be made available to customers in digital form as a twin. The construction plans, the sequence planning and the cost planning are built up as digital models, such as BIM4D.

The construction work is digitally recorded utilizing sensors, and the data are processed and displayed. Other aspects are the digital overview of the entire construction site and the possibility of virtual site inspection. This and further possibilities in the sense of digitalization around the construction site can be additional services in the infrastructure industry.

3.3.2 Performance-Based Contracting

In this business model pattern, the price is based on the performance provided by a service or product. Customers do not buy the product directly, but the result of the service, with the product usually remaining in the

hands of the customer. The price is then based on the efficiency of the construction work, which is supported by the digital twin service. However, it must be identified which construction activity is significantly improved in its performance by an application of the digital twin. This allows a new structure of pricing in the infrastructure industry.

3.3.3 Revenue Sharing

In this business model pattern, revenue is shared with the involved stakeholders, such as subcontractors. The value-adding activities performed by the stakeholders are remunerated. This business model pattern promises the most potential for business model innovation out of a digital twin in infrastructure construction projects. With consideration to the added value of risk reduction, cost security and error avoidance as well as the increase in the efficiency of the construction process an increased value scaled to the construction volume and thus a business mechanics with revenue sharing according to turnover is enabled.

3.3.4 Make More of it

This business pattern describes that the available resources and knowledge are not only applied for the own company, but also sold as a service to others. The aim is to multiply the competencies outside the core business. In the thoughts on 'Make More of it', a digital twin enables to sell the results of successful construction projects, such as optimised construction processes or the the know-how of troubleshooting.

3.3.5 Leverage Customer Data

This business model pattern aims to collect customer data and use it profitably. This data can add value internally and/or is resold to external parties. Collecting and analysing data from construction sites can be useful for the current project itself, but also allows to use or sell it to other construction sites or other industries.

To consolidate the points discussed above, Figure 2 illustrates how the elements of a digital twin may influence the factors that typify digital twin innovation (product, service, process or business model) and in turn shows different types of enabled business models. The concept is based on authors' own thinking deduced from the literature described above.

4 Discussion

This study adds to the current understanding of how infrastructure construction projects may use a digital twin to enhance their business model innovation processes and enable their value creation processes.

The proposed concept provides a set of enabled business models for infrastructure construction projects which can evolve from an application of a Digital Twin. This type of business model innovation can have a fundamental impact on the way clients and construction companies work together. In addition, it could lead to an acceleration of infrastructure planning and awarding of contracts, as well as an efficiency increase in the construction phase which results in time and cost savings in the interest of public taxpayers.

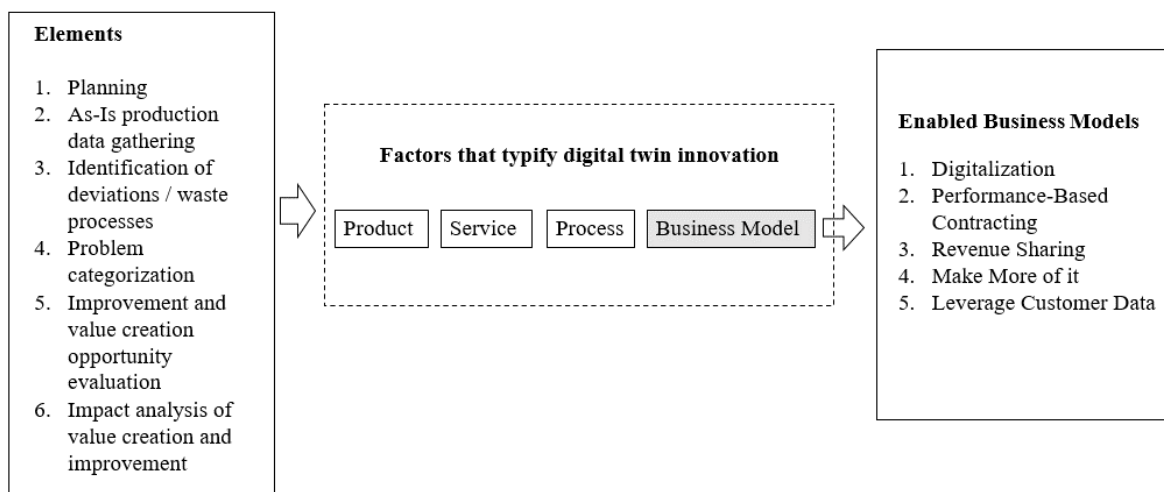


Figure 2. Digital Twin as enabler for Business Model Innovation in the field of infrastructure construction projects

5 Conclusion & Outlook

The use of As-Is data by comparing them with the planned and store them in a structured way in digital twin can support project, companies and the industry to support in their decision-making process regarding innovations and new business models. These decisions can be taken on valid datasets and the success of the decision measured. However, to be able to collect As-Is data and to use it for the proposed concept is a challenge for companies. Even though technology is up to date the use and implementation within the companies are still to overcome because of the lack of change in the last years.

Construction industry is in the middle of a big change and new business models can support in new revenue streams and a methodology that will not just change the future way of working but also the mindset of the whole industry. The concept can also be used for other construction projects respectively industries such as all linear construction projects or building construction. The impact of the improvements is very high on linear construction projects since the level of repetition is high. However the authors will follow up in the further development within railway construction projects.

References

- [1] KPMG (2015). Global Construction Survey Climbing the Curve: 2015 Global Construction Project Owner's Survey URL: www.kpmg.com/building. (accessed 16.12.2020).
- [2] Mc Kinsey Global Institute (2015). Megaprojects: The good, the bad and the better, URL: <https://www.mckinsey.com/business-functions/operations/our-insights/megaprojects-the-good-the-bad-and-the-better>. (accessed 19.12.2020)
- [3] McKinsey Productivity Sciences Center (2015). The construction productivity imperative, URL: <https://www.mckinsey.com/business-functions/operations/our-insights/the-construction-productivity-imperative>. (accessed 21.04.2021)
- [4] Dallasega, P., Marengo, E., & Revolti, A. (2020). Strengths and shortcomings of methodologies for production planning and control of construction projects: a systematic literature review and future perspectives. *Production Planning & Control*, 1-26. DOI: 10.1080/09537287.2020.1725170.
- [5] van der Veen, S., Dallasega, P., Hall, D. (2021). Data-driven Continuous Improvement Process framework for railway construction projects. 38th International Symposium on Automation and Robotics in Construction.
- [6] Dallasega, P., Rauch, E., & Frosolini, M. (2018). A lean approach for real-time planning and monitoring in engineer-to-order construction projects. *Buildings*, 8(3), 38. DOI: 10.3390/buildings8030038.
- [7] Tetik, M., Peltokorpi, A., Seppänen, O., & Holmström, J. (2019). Direct digital construction: Technology-based operations management practice for continuous improvement of construction industry performance. *Automation in Construction*, 107, 102910. DOI: 10.1016/j.autcon.2019.102910.
- [8] R. Klostermeier, S. Haag, and A. Benlian, *Geschäftsmodelle digitaler Zwillinge*. Wiesbaden: Springer Vieweg, 2019.
- [9] Grieves, M.; Vickers, J.: Digital Twin: Mitigating Unpredictable, Undesirable Emergent Behavior in Complex Systems. In: *Transdisciplinary Perspectives on Complex Systems*: Springer-Verlag, Berlin, Heidelberg 2017, S. 85–113
- [10] Tang S., Sheldon D.R., Eastman C.M., Pishdad-Bozorgi P. and Gao X. A review of building information modeling (BIM) and the internet of things (IoT) devices integration: Present status and future trends. *Automation in Construction*, 101:127-139, 2019.
- [11] Deng M., Menassa C.C. and Kamat V.R. From BIM to digital twins: a systematic review of the evolution of intelligent building representations in the AEC-FM industry. *Journal of Information Technology in Construction (ITcon)*, Special issue: 'Next Generation ICT- How distant is ubiquitous computing?', 26:58-83, 2021.
- [12] Zhao J., Feng H., Chen Q. and Garcia de Soto B. Developing a conceptual framework for the application of digital twin technologies to revamp building operation and maintenance processes. *Journal of Building Engineering*, 49, 2022.
- [13] Crossan M.M. and Apaydin M.A. Multi-Dimensional Framework of Organizational Innovation: A Systematic Review of the Literature. *Journal of Management Studies*, 47(6):1154–1191, 2010.
- [14] Holopainen M., Saunila M., Rantala T. and Ukko J. Digital twins' implications for innovation. *Technology Analysis & Strategic Management*, 2022.
- [15] Spang K. et al. *Projektmanagement von Verkehrsinfrastrukturprojekten*. 2016 2022.
- [16] Womack, J. P., & Jones, D. T. (1990). *The Machine That Changed the World*. New York: Simon and Schuster.
- [17] Mann, D. (2014). *Creating a Lean Culture: Tools to Sustain Lean Conversions*, Third Edition (3. Aufl.). Productivity Press
- [18] Gassmann O., Frankenberger K. and Csik M. *St. Galler Business Model Navigator*, 55 Musterkarten, On-line: <http://www.bmi-lab.ch>,

Using BIM to Facilitate Generative Target Value Design for Energy Efficient Buildings

Bhilare, Saurav¹, Khatri, Diya¹, Rangnekar, Salonee¹, Chen, Qian¹

¹ University of British Columbia, Okanagan Campus, Canada

E-mail: saurav15@student.ubc.edu

Abstract –

Buildings are one of the major energy consumers and the biggest producers of greenhouse gases, accounting for close to half of all energy emissions in construction industry. Construction stakeholders have been increasingly focusing on the broad idea of sustainable building design and construction technologies. The goal of sustainable design extends beyond project design development to take into account its significance at an early stage, before any detailed design, or even before a decision is taken to move forward with development. Although Building Information Modeling (BIM) and energy simulations have been integrated into early design processes, the integration method has not yet been further explored to enable multi-criteria design analysis (e.g., energy and solar performance) by varying design options to a defined energy target. This study proposes a BIM-based Target Value Design method to inform optimal energy-efficient building designs. The proposed methodology is primarily used for preliminary sustainability analysis such as solar and energy analysis. Campus building A is used as a case study to demonstrate the usefulness of the method and results showed a potential of 360 kWh/m²/yr reduction in annual energy consumption compared to the traditional sustainable design approach. The suggested new design workflows will substantially facilitate early design decisions of project clients, architects, civil engineers, and urban planners.

Keywords –

Generative Design; BIM; Building design; Target Value Design; Sustainable buildings; Energy Analysis; Solar Analysis

1 Introduction

The construction sector is one of the crucial contributors to Canada's economy. Construction activities account for around 6.5% of its Gross Domestic Product (GDP). Construction activities have a significant impact on all three pillars of sustainability; i.e. social, environmental, and economic. According to Industry Canada (2011), the built environment consumes 50% of

extracted natural resources and 33% of total energy use in Canada. In addition, buildings produce 25% of the landfill waste, 10% of airborne particles, and 35% of greenhouse gas emissions. The construction industry employed 1.2 million workers in 2010 which is 7.1% of the total workforce in the economy (Human Resources and Skills Development Canada, 2013). From 2000 to 2010 construction GDP in Canada increased by 42.7%, whereas GDP for all industries increased by 20.2%.

The building industry's inability to genuinely integrate sustainable practices is one of the biggest obstacles to the implementation of sustainable construction (Hollberg et al., 2019). A lack of knowledge or a lack of general awareness of sustainability can inhibit the development of sustainable structures. Designers generally exhibit trust in their capacity to access and apply knowledge, but this confidence wanes when sustainable construction challenges are brought up. There are other difficulties in stakeholder integration, including a lack of standard data protocols, lack of coherent information, and a lack of measurement instruments, among others (Chen et al., 2020). Instead, novel coordinating processes and role for building authorities and other public players in the construction industry are required. Efficient design and planning methods are desired to address the current challenges in improving sustainability in construction. This study proposes a target value design method to inform optimal energy-efficient building designs when adopting consistent BIM design workflows.

The remainder of this paper is structured as follows. Section 2 includes an overview of the relevant studies on Sustainable Design, Generative Design (GD) and Target Value Design (TVD). Section 3 introduces the methodology. Section 4 presents a case study. Section 5 provides the discussion related to the advantages and disadvantages of the proposed workflow, followed by the conclusions and future work in Section 6.

2 Literature Review

2.1 BIM-based sustainable design

The digital parametric data of building components in BIM offer an analysis and control function that may be

connected to sustainability building design. The capacity of BIM tools for energy modelling and sustainable material selection to reduce environmental effect illustrates the functional support of BIM for sustainable designs. Integrating BIM with sustainable design analysis tools (e.g., Energy plus) makes it easier to conduct thorough environmental trade-off analyses in the early phases of design (Kofi et al., 2020).

Building environmental performance assessments may be facilitated with the help of digital solutions based on BIM (Ilhan and Yaman, 2016). Recently, a number of technologies have been developed that base Life Cycle Assessment (LCA) on a BIM model for automatic quantity take-off (Azhar et al., 2011). Using the integrated BIM-LCA design processes, a real building's embodied global warming potential (GWP) may be assessed throughout the entire design process (Hollberg et al., 2019)

2.2 Generative Design for buildings

Generative Design (GD) is the process of inputting design goals, constraints and other data into software that evaluates all possible solutions. It has been extensively utilised in the manufacturing sector, and the architectural, engineering, and construction sector is paying more attention to it as it relates to space design, sustainability research, and urban planning.

The use of BIM in the design phase is primarily restricted to the latter design stages, despite the fact that it is relevant throughout the whole life cycle of the project. By filling in each other's shortcomings, the GD and BIM integration benefit each other by increasing their respective capabilities (Gan 2022). The integration enabled the buildability of these GD solutions, supports automatic and quick design explorations, and increases the utility of BIM during the early design stage. In order to implement the integration, the BIM API offers platforms and options.

2.3 Target Value Design

Target Value Design (TVD) is a management practice that drives the design to deliver customer values within project constraints. A project environment with advantageous features can provide value using the TVD. However, as cost is the TVD's main criterion for evaluation, the goal cost may be met while the project's full potential remains unrealized. This study uses a value analysis model to analyze the value generation of the project and applies the action research methodology to implement TVD in a housing project. It also studies the balance between cost and value fulfilment in the product and design process. It mostly focuses on value and cost aspect. There is the scope of work in TVD with respect to sustainability using Revit and Dynamo for GD of

buildings.

A team may offer the characteristics of a building that add value to the owner while staying under budget with the aid of TVD. Since its beginnings, TVD has made it possible to finish numerous institutional projects on time and on budget while also delivering more value to the client. Regarding their cost performance, several projects that explicitly used TVD have reported two consistent results: (1) The projects were completed below market cost, and (2) the estimated costs typically decrease as designs are developed.

2.4 Integration of GD and TVD

Researchers have identified the potential of GD and TVD in construction projects, but there has been lack of research regarding integrating these concepts. Study by Ng, C., & Hall, D (2021) shows how TVD can help in completing projects in a shorter time, with lower cost and higher profits without compromising design goals. Meanwhile, Schwartz et al. (2021) present a decision support tool that uses generative design to achieve the best possible design outcome. If these concepts are combined, it will help to streamline the design process and achieve high performance buildings that meet requirements of various stakeholders. This study is built on basis of the existing integrated GD and TVD processes and puts a focus on the *energy target*, instead of the cost target, to facilitate the sustainable designs.

3 Methodology

The aim of this work is to assess how GD analysis and TVD process can be combined to optimise and automate the building sustainability assessment in the early design stage. A problem-orientated approach will be used – developing a method that generates preliminary building design based on the target sustainability values. For this purpose, a proposed campus building will be considered as the case study and will be studied in order to evaluate the potential of GD for accessing sustainability criteria. Therefore, criteria such as window to wall ratio and orientation of the building will be considered for multi-criteria optimization using GD to find the best possible solution. The study will consider Autodesk Revit (version 2023) software since it is one of the most used BIM modeling software. In addition, GD analysis will be performed using ‘Autodesk Generative Design’ platform and Dynamo studio.

In the following stage, based on the result of the previous analysis, the applicability of Target Value based Generative Design (TVGD) to optimise the sustainability assessment process will be assessed. The suggested framework will define the workflow to automatically generate preliminary designs based on the targeted energy efficiency values.

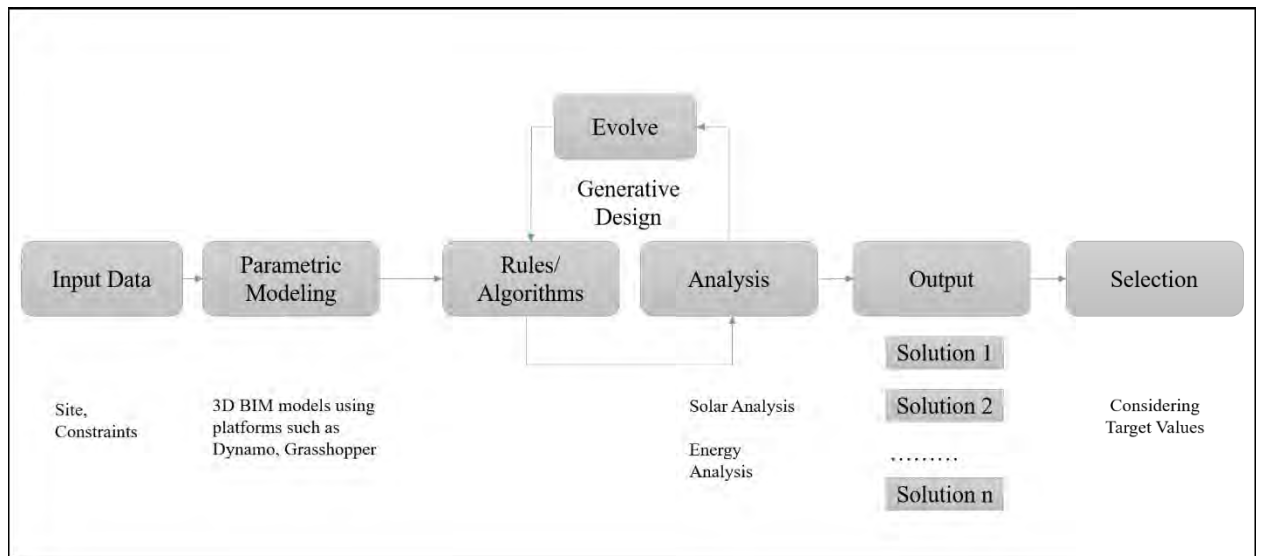


Fig 1: Generative Target Value Design Framework

The proposed framework includes the following components:

(1) Input data

For the GTVD, the first step is to create a BIM model of the site considering all the inputs such as location, surrounding buildings and site boundary for the project.

(2) Parametric modeling

The building structure was modeled using parametric design. Instead of considering fixed values, parameters and rules were used to determine the relationship between the design intent and response. In addition, algorithms were created for linking external sources for solar and energy analysis.

(3) Generative Design

In the GD analysis the parameters and rules from the Dynamo graph were analysed in cloud using AI and Machine Learning to generate a pool of design options.

(4) Target value consideration

The outputs of the GD analysis were filtered by energy target values according to the design goals.

4 Case study – Campus building A

The building considered for case study is a proposed institutional building in British Columbia. Four target value goals were considered for this case study: (1) Minimizing the annual energy consumption of the building, (2) Minimizing total solar incident radiation on the building façade, (3) Reducing the form factor of the building, (4) Increasing renewable energy generation by the roof top solar panels.

The proposed approach described above was used for the case study.

4.1 Model creation for analysis

Autodesk InfraWorks was used to model the 3D site using the GIS data layers from various online sources. This model was then imported in Revit to be used for sustainability analysis. The faces of the surrounding buildings were considered for the solar analysis as they will cast shadow on the proposed building and the weather conditions of the area were also considered.



Fig 2: 3D Site model

A parametric model was created in Dynamo Studio plugin for Revit. First, constraints were defined for the model creation:

a) Parcel restrictions: The plot boundary was created in Revit model, which acted as a restriction for the design options generated.

b) Floor height: For this analysis the floor height was considered as 4m and non-parametric.

c) Built-up area: The built-up area of the project was limited to that of the proposed building which was 14000 m².

Then parametric inputs were added, which provided flexibility to generate and analyse various design approaches. We considered the following parametric inputs:

a) Floor plan: We considered a floor plan consisting of 10 faces. Each face was first modeled as a line, thus forming a continuous polygon with 10 connecting points. Each point was given a range of values such that the lines do not intersect each other. This created various design options of the floor plan for analysis.

b) Number of floors: The overall built-up area is constant but the number of floors was considered variable which allowed for the variation in the floor area and form factor of the building.

c) Window-to-wall ratio: The window to wall ratio was considered between 0.4 to 0.8. This affects the overall energy consumption of the building.

d) Orientation of the building: The orientation of the building was considered as a variable because it affects the annual energy consumption as well as the average solar incident radiation on the surface of the building.

4.2 Target value calculations

4.2.1 Total annual energy consumption of the building

The Dynamo package ‘Energy predict ML’ was used for this workflow. The inputs for this calculation were surfaces of walls, windows, floors and shading. After providing inputs, the main node of the package uses an algorithm trained by machine learning on top of Autodesk Insight 360 database to predict energy performance.

4.2.2 Solar incident radiation on the building facade

The Dynamo package ‘Solar analysis for Dynamo’ was used for this workflow. The inputs for this calculation were weather conditions, analytical surfaces for walls, shading surfaces of surrounding building and duration of study (Jan 2023 to Dec 2023). This package makes external calls to a web service to get required data for the analysis.

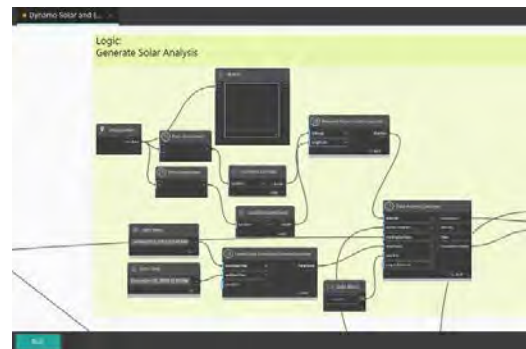


Fig 3: Dynamo graph for solar analysis

4.2.3 Form Factor of the building

Building envelope area and total volume is calculated. Form factor is calculated by dividing surface area by volume.

4.2.4 Renewable energy generated by the rooftop solar panels

The area of the analytical roof surface is variable which is calculated to find the renewable energy generation capacity of the building.

4.3 Generative Analysis

4.3.1 Data export

First the graph was validated by running the complete workflow once. Then the graph was exported for the GD analysis. All the dependency files required for the analysis were automatically generated by Dynamo.

4.3.2 Performing Generative Analysis

In the GD process the parameters and rules from the Dynamo graph are analysed in cloud using AI and Machine Learning algorithms to generate a pool of design options. We performed 5 iterations for the GD analysis while considering the following goals: Minimizing annual energy consumption, solar incident radiation on façade and Form Factor, while maximizing the surface area for rooftop solar panels.

As compared to our previous study, we increased the population size for the GD analysis and choose to maximize the built-up area¹. We increased the population size from 10 to 20. Population size is the initial number of individual options used by the genetic algorithm. Each individual option has a unique set of features that serve as the genes to evolve the design, so higher the population size, the more the design is optimized. Also, we choose to maximize the built-up area along with other target goals to increase the utilization of the building.

¹ For the Canadian Society of Civil Engineering (CSCE) Annual Conference, Moncton 2023, we performed GD analysis for our paper “BIM-based generative design processes for targeted value design of low-carbon

buildings.” Compared to that, our aim in this study was to specifically target energy performance optimization, so we made two changes to the GD analysis - increased population size and optimized rooftop solar panels).

4.4 Results of the analysis

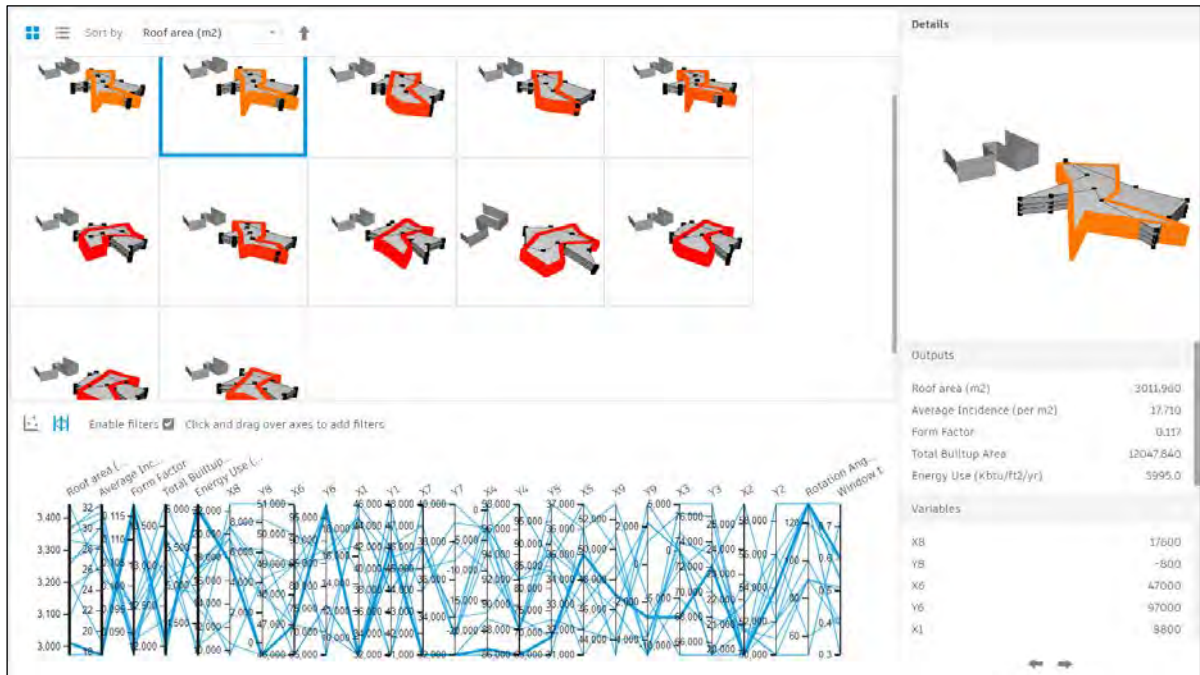


Fig 4: Outcomes generated after GD analysis

Table 1: Generative Design outputs

Sr. No.	Energy Use (kWh/m ² /yr)	Average Incident solar radiation (kWh/m ²)	Roof area (for rooftop solar panels) (m ²)	Form Factor	Total Built-up Area	Rotation Angle	Window to Wall Ratio
1	1561.98	19.11	3205.16	0.12	12820.64	130.00	0.77
2	1196.03	30.87	3345.96	0.09	13383.84	50.00	0.72
3	1427.50	28.22	3331.46	0.10	13325.84	90.00	0.39
4	1779.39	17.84	2972.86	0.11	11891.44	130.00	0.53
5	1436.87	26.34	3180.46	0.09	12721.84	130.00	0.30
6	1230.31	30.17	3252.56	0.09	13010.24	60.00	0.42
7	1378.27	28.29	3270.96	0.09	13083.84	130.00	0.54
8	1530.05	28.64	3084.06	0.09	12336.24	120.00	0.60
9	1501.92	25.27	3443.56	0.10	13774.24	100.00	0.40
10	1756.54	17.71	3011.96	0.12	12047.84	130.00	0.60
11	1523.31	31.53	3369.56	0.09	13478.24	90.00	0.50
12	1527.12	32.36	3361.46	0.09	13445.84	90.00	0.51

For each generated design options, the initial 3D model of the building is shown in grey colour and solar analysis is performed after considering various orientations.

client’s preference such as the shape of the building. We selected option 2 as it has the lowest annual energy consumption.

4.4.1 Optimized design options

Twelve design options were generated after the analysis. Each option can be selected to view all the input and output values for that option on the right side of the interface. Also, a graph showing all values for all the options is generated at the bottom of the interface, which can be used to understand the relationship between the variable inputs and outputs. There is an interdependency between all the target values calculated. Change in value of one parameter can positively affect one of the target values, while negatively impacting another value, so it is still challenging to improve all the target value outputs at the same time.

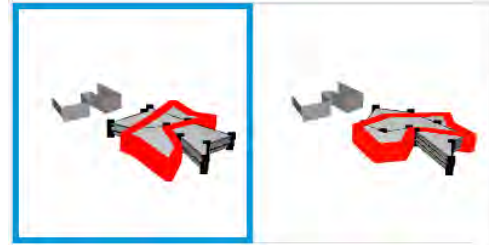


Fig 5: Filtering design options

4.4.2 Selection of preferred design options based on target values

We can select multiple combinations of the output values to select the optimal solutions. For this case study we selected two outputs: annual energy consumption and area for rooftop solar panels. The target values for annual energy consumption were considered to be below 1500 kWh/m²/yr and for area of rooftop solar panel the value was considered to be above 3300 m².

After adding the target values as filters, two design options were displayed as the optimal solutions (Option 2 and Option 3). Final selection can be done based on the

4.4.3 Comparison with original layout of the building

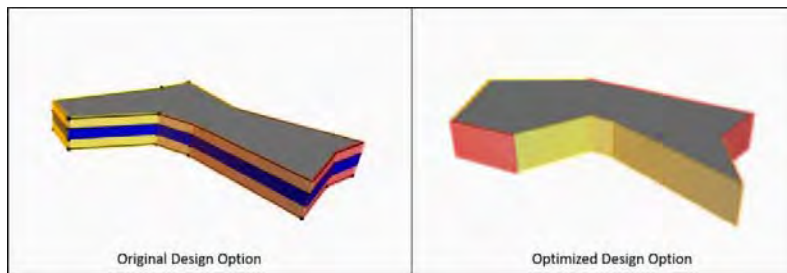


Fig 6: Comparison of original and optimized design option

Table 2: Comparison of target values of original and optimized design options

Sr. No.	Output	Original Design Option	Optimized Design Option
1	Annual energy consumption (kWh/m ² /yr)	1559.35	1196.03
2	Average incident solar radiation (kWh/m ²)	15.92	30.87
3	Roof area (m ²)	3192.52	3345.96
4	Form Factor	0.093	0.085
5	Total Built-up area (m ²)	13770.00	13383.84

The values shown in Table 2 were calculated in Dynamo Studio for both the options. It shows that there is a significant difference in energy consumption values. The optimized building consumes around 360 kWh/m²/yr less energy than the original building design.

4.4.4 Detailed Visualisation in Dynamo

The final selected option can be viewed in detail in Dynamo. For this study we selected the design option with the minimum annual energy consumption (i.e. option 2). In Dynamo we can view details such as the solar incident radiation value on a particular face of the building and also adjust the parameters such as duration of study to get outputs for a specific season.



Fig 7: Final output visualisation in Dynamo

Also, the design option can be viewed in Revit to give better perspectives with respect to the complete site.



Fig 8: Final output visualisation in Revit

5 Discussion

GD is a computer-aided design approach that has the ability to revolutionize the design process. It can generate new and innovative design solutions that may not have been considered by human designers, enabling designers to push the boundaries of what is possible. Moreover, GD has the capability to explore a wide range of design solutions, providing designers with a greater

understanding of different design possibilities, which in turn can lead to better design decisions and outcomes. With this technology, designers are able to experiment and explore more options, which can lead to a more efficient and effective design process.

Dynamo is a powerful tool for BIM that allows for the analysis and optimization of building systems. However, it has some limitations that need to be considered before implementing it [14]. One limitation is the limited ability to analyze complex building systems. Complex systems such as HVAC are made up of large number of interconnected components, which makes it difficult to accurately capture and represent all dependencies and interactions between the various elements using Dynamo. Another factor is the high cost of implementation, as BIM software and hardware can be expensive to purchase and maintain, and requires specialized training for users [15]. Additionally, the risk of errors is increased in Dynamo models due to their complexity and data-intensive nature, making proper management and maintenance crucial to ensure the accuracy and consistency of the models.

Manual output of energy efficiency is the traditional method of designing buildings for energy efficiency, which requires architects and engineers to manually calculate and analyze the energy performance of different design options. This approach can be time-consuming and may not result in the most efficient design. In comparison, Generative Target Value Design can help to increase the efficiency and speed of the design process and can also provide more accurate and efficient results than traditional energy efficiency calculations.

6 Conclusions and future work

The use of BIM tools such as the use of Dynamo scripting can facilitate Generative Target Value Design (GTVD) for energy efficient buildings through the proposed design framework/workflows. Different from traditional 2D or 3D design means, a visual programming tool allows for the automation of design processes, which can improve accuracy, speed, and efficiency in the design phase. The proposed workflows allow for the integration of various design elements and the ability to analyze and simulate different scenarios, which can help identify the most efficient and effective solutions for delivering an energy-efficient building. Additionally, the proposed workflows focus on the “energy target value” that allow for the integration of various simulation tools, which can help designers to evaluate the energy performance of the building and identify opportunities for improvement. The proposed workflows were demonstrated in a case study to show the potential in the design and construction of

energy-efficient buildings, and the use of GTVD could be considered in any type of project pursuing this goal. However, for this research, it was considered that all the stakeholders have collaborated to finalize the target values before the GD analysis. This does not take into consideration the continuous collaboration between the stakeholders for cost-based TVD. This scope can be added in future research.

GD used within a BIM environment helps to explore and optimize multiple design options for energy efficiency. This can be used to generate design options that meet specific energy performance criteria, such as reducing energy consumption or increasing renewable energy use. By using BIM in conjunction with Dynamo Revit and GD, architects, and engineers can more easily and effectively design buildings that are energy-efficient and optimized for performance. Canada is taking steps to ensure a clean energy future through investments in innovation that enhance the country's economy, create clean jobs, and help the citizens save on household energy costs. GTVD can contribute to this goal by significantly reducing the energy consumption of buildings and decreasing the carbon footprint

Acknowledgments

We would like to thank UBC Property Trust for providing the schematic design information about the case study building project.

References

- [1] Hollberg, A., Lützkendorf, T., & Habert, G. (2019). Top-down or bottom-up?—How environmental benchmarks can support the design process. *Building and Environment*, 153, 148-157.
- [2] Chen, Q., Hall, D. M., Adey, B. T., & Haas, C. T. (2020). Identifying enablers for coordination across construction supply chain processes: a systematic literature review. *Engineering, Construction and Architectural Management*, 28(4), 1083-1113.
- [3] Azhar, S., Carlton, W. A., Olsen, D., & Ahmad I. (2011). Building information modeling for sustainable design and LEED® rating analysis. *Automation in Construction*, 20(2), pp. 217-224.
- [4] Ilhan, B., & Yaman, H. (2016). Green building assessment tool (GBAT) for integrated BIM-based design decisions. *Automation in Construction*, 70, 26-37.
- [5] Touloupaki, E., & Theodosiou, T. (2017). Energy performance optimization as a generative design tool for nearly zero energy buildings. *Procedia engineering*, 180, 1178-1185.
- [6] Asare, K. A., Ruikar, K. D., Zanni, M., & Soetanto, R. (2020). BIM-based LCA and energy analysis for optimised sustainable building design in Ghana. *SN Applied Sciences*, 2, 1-20.
- [7] Hollberg, A., Genova, G., & Habert, G. (2020). Evaluation of BIM-based LCA results for building design. *Automation in Construction*, 109, 102972.
- [8] Ma W, Wang X, Wang J, Xiang X, Sun J. Generative Design in Building Information Modelling (BIM): Approaches and Requirements. *Sensors*. 2021; 21(16):5439.
- [9] Vermeulen, D., & El Ayoubi, M. (2020). Using generative design in construction applications. CS323296 Class Handout, Autodesk.
- [10] Kim, Y. W., & Alseadi, I. (2021). Identification and evaluation of the influencing factors in target value design process through an industry survey. *Journal of Civil Engineering and Construction*, 10(2), 75-83.
- [11] Ng, C., & Hall, D. (2021, July). Teaching target value design for digital fabrication in an online game: Overview and case study. In *Proceedings 29th Annual Conference of the International Group for Lean Construction (IGLC)* (Vol. 29, pp. 249-258). International Group for Lean Construction.
- [12] Schwartz, Y., Raslan, R., Korolija, I., & Mumovic, D. (2021). A decision support tool for building design: An integrated generative design, optimisation and life cycle performance approach. *International Journal of Architectural Computing*, 19(3), 401-430.
- [13] Gan, V. J. (2022). BIM-Based Building Geometric Modeling and Automatic Generative Design for Sustainable Offsite Construction. *Journal of Construction Engineering and Management*, 148(10), 04022111.
- [14] Chen, Q., Adey, B. T., Haas, C. T., & Hall, D. M. (2022). Exploiting digitalization for the coordination of required changes to improve engineer-to-order materials flow management. *Construction Innovation*, 22(1), 76-100.
- [15] Ng, M. S., Chen, Q., Hall, D. M., Hackl, J., & Adey, B. T. (2022). Designing for digital fabrication: An empirical study of industry needs, perceived benefits, and strategies for adoption. *Journal of Management in Engineering*, 38(5), 04022052.

Hardware/Software Solutions For an Efficient Thermal Scanning Mobile Robot

A. López-Rey¹, A. Ramón¹, and A. Adán¹

¹3D Visual Computing & Robotics Lab, University of Castilla-La Mancha, Spain
alejandro.lopezrey@uclm.es, amanda.ramon@uclm.es, Antonio.adan@uclm.es

Abstract –

The use of robotic platforms greatly facilitates the reconstructions of 3D models of buildings and automates tasks that would be tiring and inaccurate when carried out manually. In the specific area of thermal monitoring of buildings, robots can also develop an important role providing dense temperature information of envelopes and structural elements. However, the current robot-based systems that extract thermal models can work under serious restrictions that concern, among others, the complexity of the scene, autonomy, navigation, and computation. This article discusses the limitations and restrictions of the current mobile scanning robots for thermal mapping inside buildings and proposes a thermal scanning robot that solves some of these issues.

Keywords –

Robotic platforms; Thermal scanning; Thermal point clouds; FoV; Building sensing

1 Introduction

The use of robots and UAVs are being expanded in the AEC industry in recent years. Particularly, when it comes to the acquisition of geometry and characteristics of buildings, such automatic systems allow to reduce the time required for on-site work, as well as to improve the accuracy of the collected data. In the case of thermal digitization, the arrival of 3D thermal scanning systems is giving a new dimension to the thermal analysis of buildings as they provide larger amount of information than those that only work with 2D infrared cameras, thus showing a complete thermal representation of a building. In essence, the robot must capture points and temperature of the scene to generate a thermal point cloud (TPC) that can be later processed.

Although the thermal scanning platforms are evolving day-to-day with new functionalities in larger and complex environments, there are still many restrictions and limitations that must be overtaken in the next future. A comparison of the main mobile thermal

cloud acquisition platforms, including our systems, can be seen in [1] and [2]. In the next section, the most important limitations and issues regarding both hardware and software of the current thermal scanning platforms (TSPs) are described.

2 Limitations of the current thermal scanning platforms

In this section Hardware and Software limitations will be dealt with separately.

2.1 Hardware limitations (HL)

In the case of TSPs, the term “hardware” refers to the physical devices of the system, such as the robot base and sensors. There are several limitations in this matter that are still poorly addressed in the existing literature, which could be summarized as follows.

- HL1. Autonomy. Refers to whether the robotic platform navigates by itself, as in Adán et al. [3] and Borrmann et al. [4], or is commanded by a specialist technician, as the system presented by Hoegner et al. [5]. Besides, the possibility of carrying out a multi-session data campaign at different positions of the building, or at different times, also refers to an autonomy issue. Usually, an operator turns the system on and off at the appropriate times in case of multi-session processes. Most systems are therefore considered as semi-automatic.
- HL2. Scene. Refers to the characteristics of the scenario and their surroundings in which the platform navigates. We can differentiate between terrestrial TSP ([6], [7]) and UAV [8] systems. In the case of terrestrial platforms, some usual restrictions are flat floors with no stairs/steps and no multiple floor levels. In addition, there are also evident navigation problems in furnished indoors with few and small free spaces. For UAVs, there are also limitations when working in narrow spaces. Most of the current TSPs move

on wide spaces and unoccupied buildings, which signifies a serious restriction with respect to the type of scenes.

- HL3. Limited FoV. The reduction of the field of view in thermal cameras is an issue that has been discussed previously (Previtali et al. [9] or in Alba et al. [10]). The limited FoV of TIR makes the thermal point cloud be incomplete as it only assigns temperature to a part of the point cloud. Few TSPs have addressed and solved this issue.
- HL4. Batteries. All TSPs have power consumption restrictions on each one of their components. Usually, consumption is supported by batteries paired to one or more elements that make up the platform, so there is a restriction on the time of use depending on these power supplies. As a consequence of this, long data sessions and large scenarios should be avoided with poor power resources.
- HL5. Weight and dimensions. Heavy or large platforms are difficult to move from the lab to the environments where digitization is performed. Additionally, big platforms also make difficult to navigate in narrow environments or in passages between rooms, as in the case of the platform presented by Adán et al. in [3]. Other heavy platforms are on board of vehicles that navigate in outdoors of urban environments, such as the one of Hoegner and Stilla [11]. This limitation makes impossible to obtain thermal model of usual apartments and houses.
- HL6. Costs. The cost of a robotic platform is usually high, especially when considering an expensive terrestrial robot base and/or a sophisticated 3D sensor as a scanner. This is usually the case of UAVs, as it was previously addressed by Bulatov et al. [12] and Sun and Zhang in [13], or when using LIDAR technology, as in the system by Borrmann et al. [4]. Few low-cost TSPs can be found in literature.

2.2 Software limitations

Software limitations refer to the programming of the robot, as well as problems related to data transfer between different parts of the system or data storing.

- SL1. Robot programming. The bibliography shows that most of the robots used in the AEC industry are programmed under the Robotic Operating System framework (ROS), which can be limiting as it requires programmers and technicians specialized in this framework for its operation. ROS works under Linux operating system, while its operation with Windows is still under development today. This is also a

limitation in case of looking for interoperability between different systems and OSs. Kim and Peavy [14] show a retrieving method of building data using robots under this programming. Kyjanek et al. [15] describe a custom robot platform with ROS path planning for the human-robot collaboration in timber prefabrication. Meschini et al. [16] present a novel methodology on how to link ROS with a BIM model for automation in construction.

- SL2. Sensor programming. External sensors on board the robot base, such as cameras or scanners, must be programmed and integrated in ROS using compatible drivers. Additionally, it is very common to use a Software Development Kit (SDK) for each sensor. Therefore, specific programming tools for sensors are required.
- SL3. Multisession programming. There is hardly any bibliography that addresses performing multi-session data collection with robotic platforms, either performing data collection in the same place or using different sessions at different locations to obtain better coverage of the architectural space or thermal characteristics. Exceptions can be found in [17] and [18]. In Adán et al. [17] the system scans a wall in evenly spaced intervals of time to test its temperature evolution. In Rakha et al. [18] a drone is used to take 2D TIR pictures of the exteriors of a building during a determined period of time.
- SL4. Use of memory. For acquisition systems dealing with millions of points, there may be memory problems if the external storage system is not properly sized. In Xiong et al. [19] this problem is addressed by sub-sampling each scan. In López et al. [20] a sparse matrix instead of a fixed size matrix is used to represent a depth buffer in an optimized approach for thermal point clouds using an UAV platform.
- SL5. User interface. This is related to the framework used to manage a TSP, thus defining the proper planning and tracking the evolution of the data acquisition session. The use of efficient user interfaces in the AEC industry is essential. This facilitates the use of the TSP in multidisciplinary teams without experience in computer programming. None of the aforementioned papers presents a user interface to be used by construction workers.

3 MoPAD2: a reliable thermal scanning robot

In this section, a new thermal scanning platform is presented. MoPAD2 (Mobile Platform for Autonomous

Digitization) features some solutions for the earlier limitations and drawbacks. MoPAD2 is shown in Figure 1. MoPAD2 is a new platform that is a considerable improvement to the former version in terms of data collection, management, scope, and processing. For each item discussed, the contribution of MoPAD2 to limitations HL1-HL6 and SL1-SL5 will be pointed out in brackets.

3.1 Hardware solutions

- Robotic base (HL5, HL6, SL1). MoPAD2 is built on a TurtleBot 2 robot kit with a low cost and reduced size Kobuki robot base. This nonholonomic mobile robot can carry up to 5 kg and it is implemented in ROS.

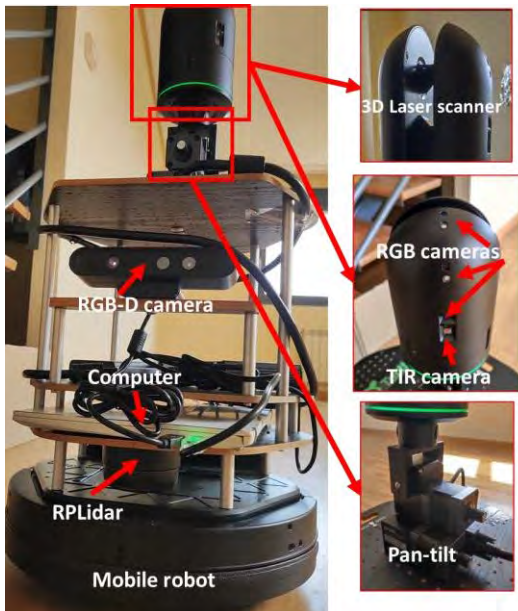


Figure 1. MoPAD2.

- Robot autonomous charging (HL1, HL4). The TurtleBot 2 includes a docking station (see Figure 2) that allows autonomous charging. Thus, multiple sessions can be carried out without human intervention. An example of autonomous charging can be seen in Section 4.



Figure 2. Docking station.

- 3D scanner (HL4, HL5, HL6). In our autonomous platform point clouds are captured using a mid-range 3D laser scanner (Leica BLK360). This small and lightweight scanner has a minimum range of 0.6 meters and a maximum range of 60 meters. Its field of view of $360^\circ \times 300^\circ$ (h x v) covers practically the entire visible space. It has three integrated RGB cameras that rotate with the scanner, capturing 30 images in one complete turn. The entire space is covered by the 15Mpx panoramic image obtained.

The scanner is powered by a removable battery, which enables 3 hours of continuous use. In order to extend the autonomy of the 3D scanner an external switch actuator is integrated.

- Thermal camera (HL3). The scanner also has an embedded thermal camera (FLIR IR camera) with a resolution of 160×120 pixels and a field of view of $71^\circ \times 56^\circ$ (v x h). It can work in a temperature range from -10°C to 65°C , and has a thermal sensitivity of 0.05°C . This camera obtains 10 overlapped thermal images as it rotates with the scanner. Thus, a panoramic image with a 71° vertical field of view can be generated. In order to solve this reduced FoV, a pan-tilt platform is integrated into MoPAD2.
- Pan-tilt platform. (HL3). The pan-tilt unit shown in Figure 3 (FLIR PTU E46) is incorporated to solve the lack of vertical range of the thermal camera. The FoV is increased by tilting the scanner. Pan movement is not used as the scanner rotates itself. As a consequence of this, an omnidirectional thermal image of the scene can be generated.

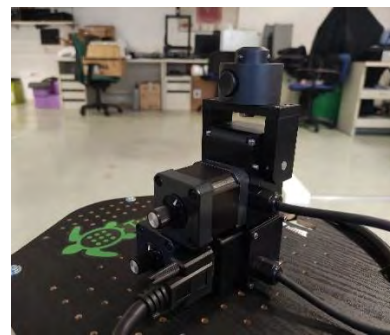


Figure 3. Pan-tilt platform.

- Switch actuator. (HL4, SL3) As a power saving measure, the 3D scanner needs to be switched off during idle periods, such as waiting time between sessions. For this reason, a switch actuator (see Figure 4) has been developed. This actuates the scanner button. This way, the power usage issue

is optimized, which increases the autonomy of the 3D scanner in case of a multi-session campaign.



Figure 4. Switch actuator.

- Computation and memory (SL4). MoPAD2 is controlled by a computer at 4.7 GHz. There is an external computer used by the operator to control the robot and define scanning sessions. It is also used as a data server in which point clouds and thermal images are stored to release memory from the computer in MoPAD2.
- Sensors for navigation (HL2). There are two sensors on board MoPAD2 that have been used depending on the type of the scenario. For textured and inhabited environments, the Orbbec Astra RGBD camera, with a range of 8 meters and a resolution of 1280 x 960, provides an efficient SLAM. The second sensor is the Slamtec RPLidar A2M8 laser rangefinder with a range of 6 meters. This is used in non-textured and uninhabited interiors. Therefore, robot location and navigation issues are efficiently covered for a variety of textured and non-textured environments.

3.2 Software solutions

- ROS integration. (SL1). All MoPAD2 components except the scanner and the switch actuator are implemented in ROS. The algorithms and functions are ROS-based as well. Even though ROS is a limiting factor for non-expert personal, this problem is solved with the addition of a user-friendly interface.
- Sensors and actuators programming. (SL2). The laser scanner and the TIR camera have been programmed using their own SDKs, which allows to customize data acquisition parameters. The switch actuator is controlled by a script running on a Raspberry Pi Pico microcontroller.
- Communication and data transference. (SL1). The different components of the system are connected via Wi-Fi. There are two networks: scanner network, which communicates the

scanner with the robot; and MoPAD2 network, which communicates the robot with the switch actuator and the control server. The communication and data transference are represented in the diagram in Figure 5. As all the acquisition and navigation processes are embedded in the robot computer, server connection is not required during data acquisition.

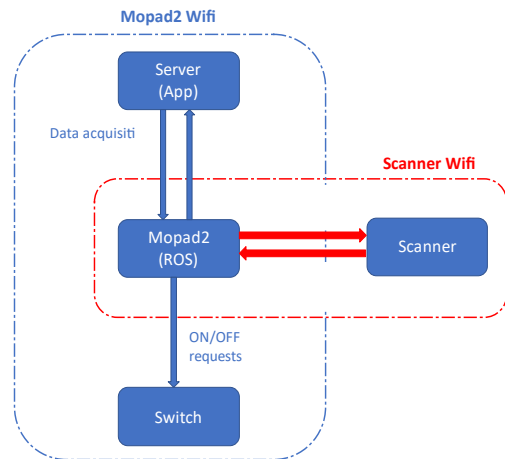


Figure 5. Communication and data transference.

- Multi-session programming. (SL3, SL4). Figure 6 shows the general scheme of a multi-session campaign. [A1] There is an offline phase (1) in which the scene's map is obtained. This map can be used in subsequent sessions if the scenario does not vary. At the session definition (2), some parameters are defined by the user such as: number of sessions, time between sessions, robot poses and scanning parameters. Data acquisition (3) for every defined session is then conducted. The robot navigates towards each previously stop point, where data is collected as planned beforehand. Data acquisition ends when the platform docks at the charging station. At this moment, point clouds and thermal images are sent to the server. Data is then deleted from memory in the robot and stored in a hierarchic database, which is structured in levels: day, session, zone, and position. In the data processing stage (4), various registration algorithms are carried out in order to obtain an omnidirectional thermal point cloud of the scenario ([21]). The point cloud registration problem is primarily solved by employing the localization data obtained from the mobile robot, and is later refined by applying the well-known ICP (Iterative Closest Point) technique ([22])

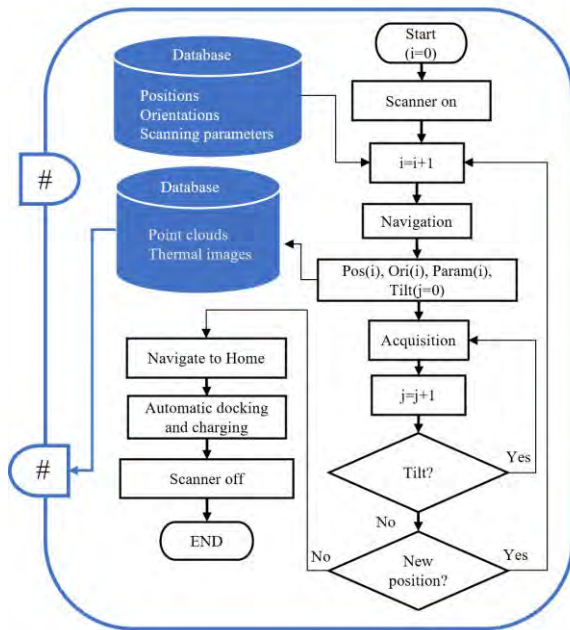
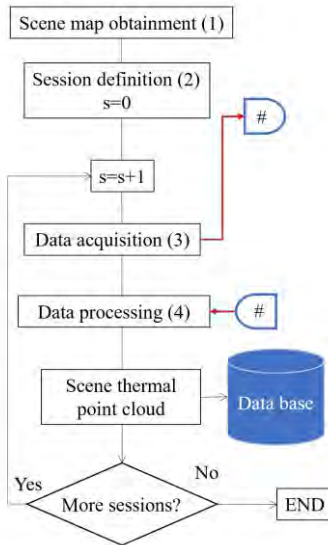


Figure 6. General scheme of a multi-session campaign.

- App. (SL5). MoPAD2 app has been developed to manage and control the robot during the data acquisition sessions (see Figure 7). Its interface includes an image of the scenario map with the current robot position and a set of buttons with different functionalities. Among others, the user can define the number of sessions, the time intervals between them, the type of data and specific the stop positions from which MoPAD2 will scan the scene. Moreover, the user can initialize components and manually command the robot. This app is therefore ready to be used by non-expert construction personal.

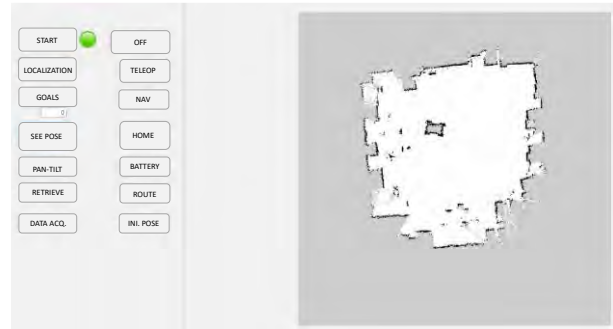


Figure 7. Interface of MoPAD2 control app.

4 Testing MoPAD2

MoPAD has successfully been tested for thermal digitization of interiors of buildings at floor scope, but there are some issues and restrictions that should be addressed in the future. First, the cost of MoPAD2 is still high and some of the sensors could be replaced or substituted by others, thus simplifying the whole platform. For example, the pan-tilt platform could be removed if a second thermal camera is coupled to the scanner set. In this way, the FoV issue would be solved. Second, the system which powers the scanner must be replaced if we want to tackle longer and larger-in-time single scanning sessions and, of course, larger multi-scanning sessions. Third, although the current MoPAD2's app is ready to be used by a multidisciplinary team, improvements in visualization and functionality aspects must be conducted.

Other limitations will remain in MoPAD2 without solution. These are: navigation in flat floors without stairs or steps and the still limited power supply capacity.

In this section, two experiments in different scenarios are presented.

The first experiment (see Figure 8) has been carried out in a part of an uninhabited conventional building with Manhattan structure. This scenario is composed of 4 rooms connected by doors. It has an area of 187 m² and a volume of 748 m³ (see Figure 9).

A total of 180 thermal images and 18 scans at 6 positions of the robot were needed for the thermal digitization. The omnidirectional thermal point cloud of the whole scene contains 88 million points. Two sessions were conducted on the same day with an interval of 5 hours (9 a.m. to 14 p.m.). Figure 10 shows the thermal point cloud of Zone 1 in both sessions using a colour palette range of [25°C, 35°C]. It is worth noting the evident increasing of the temperature (although with different degree) in walls, ceiling and floor in the second session.

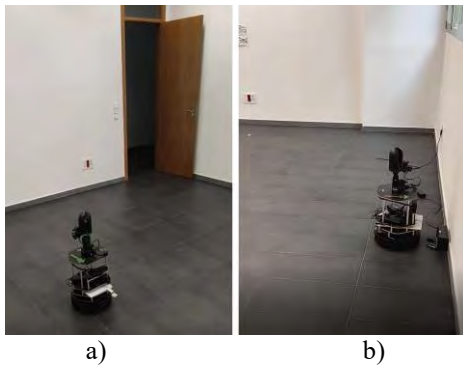


Figure 8. a) MoPAD2 in scenario 1. b) MoPAD2 docking in charging station.

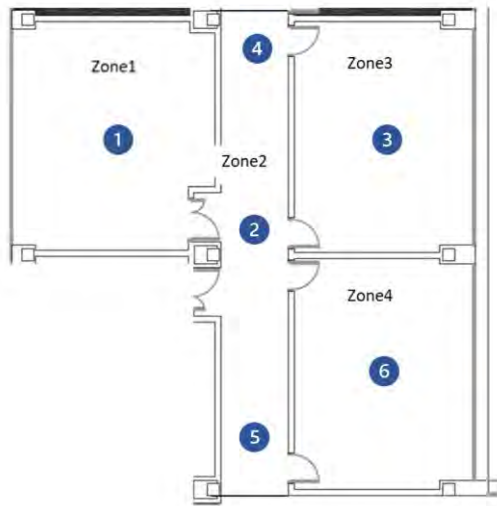
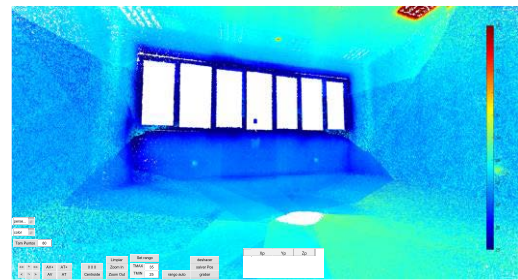
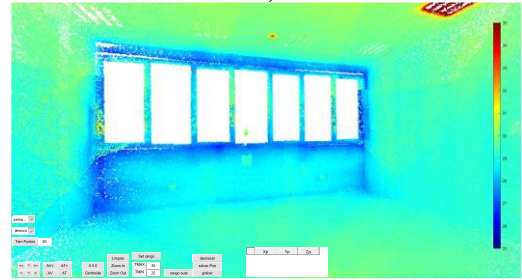


Figure 9. Floor plan of scenario 1 and stop locations in which the thermal scans have been taken. [A2]

The second validation test (see Figure 11) was carried out in an uninhabited apartment about 70 square metres, composed of 4 large rooms, 2 small rooms and a narrow corridor connecting them (see Figure 12). The scenario was digitized by taking 240 thermal images and 24 scans at 8 scanning positions. The total thermal point cloud of the scene contains 116 million points. Figure 13 illustrates several views of the final thermal point cloud in which it can be seen an evident temperature gradient between different structural parts of the scene. A significant increase in temperature is clearly observed in the window frames since the rooms receive significant solar radiation. Floor and ceiling have a small temperature gradient with respect to the walls which leads us to think that that the floor is in contact with an interior space conditioned at a temperature higher than that of the room, and the terraced upper exterior space has received a large amount of solar radiation throughout the daytime.



a)



b)

Figure 10. Indoor thermal view of scenario 1. a) TPC of Session 1. b) TPC of Session 2

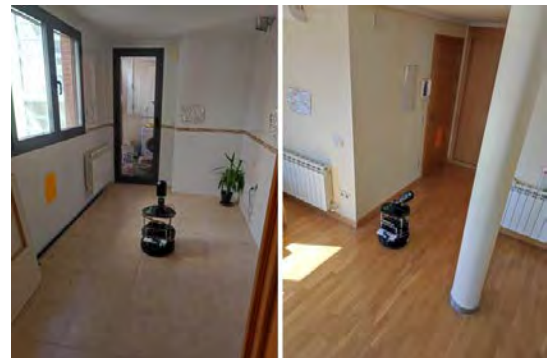


Figure 11. MoPAD2 in scenario 2.



Figure 12. Floor plan of scenario 2 and stop locations in which the thermal scans have been taken.

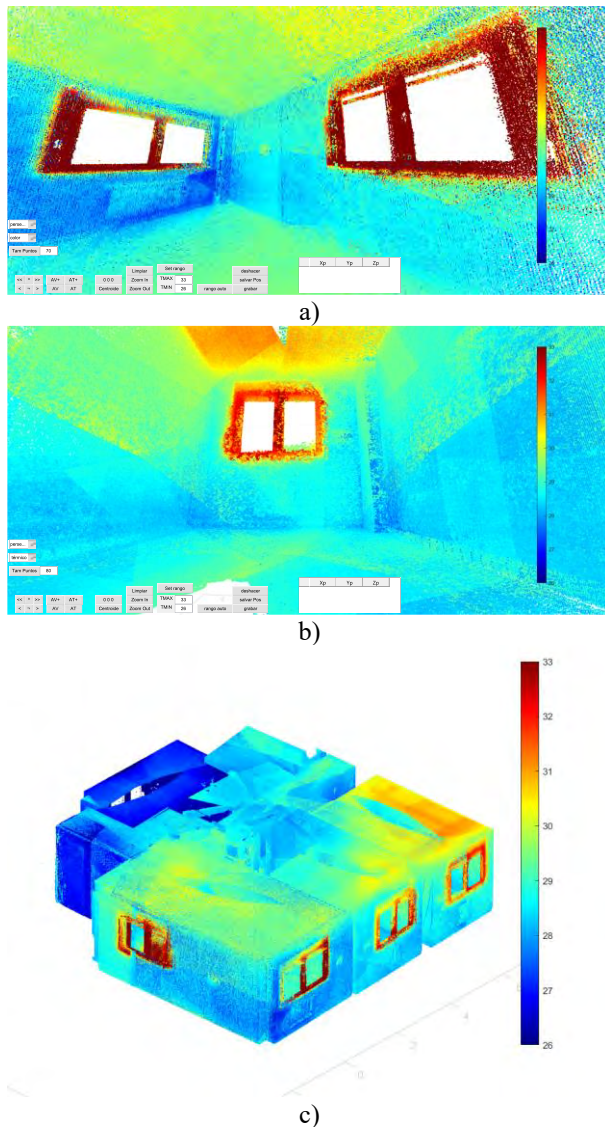


Figure 13. a) A view of the TPC from scanning position 3. b) A view of the TPC from scanning position 8. [A3] c) External view of the TPC of scenario 2.

5 Conclusions

MoPAD2 is a small size robotic platform that has been developed with the objective of obtaining thermal point clouds of indoors of buildings. This platform overcomes, or at least reduces, some of the principal restrictions and limitations of the current similar thermal scanning platforms. Specifically, there are clear improvements in matters regarding power consumption, mobility and translation, autonomy, point cloud completeness, scene size and environment. Apart from these, the issue of multi-session thermal clouds is particularly addressed, which is a topic that has not been

seen in much of the current bibliography, and in any case, only in 2D based approaches.

Programming and the integration issues have also been solved successfully under ROS and SDKs of different devices and sensors so that the platform is able to thermally digitize a wide variety of indoor scenarios. Thus, beyond a typical laboratory scene, MoPAD2 has been tested in various real-world environments such as official buildings and apartments.

In conclusion, it can be stated that a thermal point cloud of a building becomes a new monitoring tool that allows us quantitative and qualitative knowledge, and that the use of robotic platforms, such as MoPAD2, can be useful as a starting point for future improvements in this field of research.

References

- [1] A. Ramón, A. Adán, and F. Javier Castilla, "Thermal point clouds of buildings: A review," *Energy Build.*, vol. 274, p. 112425, Nov. 2022, doi: 10.1016/J.ENBUILD.2022.112425.
- [2] A. Adán, A. López-Rey, and A. Ramón, "Obtaining 3D Dense Thermal Models of Interiors of Buildings Using Mobile Robots," in *ROBOT2022: Fifth Iberian Robotics Conference, 2023*, pp. 3–14.
- [3] A. Adán, S. A. Prieto, B. Quintana, T. Prado, and J. García, "An Autonomous Thermal Scanning System with Which to Obtain 3D Thermal Models of Buildings," in *Advances in Informatics and Computing in Civil and Construction Engineering, 2019*, pp. 489–496. doi: 10.1007/978-3-030-00220-6_58.
- [4] D. Borrmann *et al.*, "A mobile robot based system for fully automated thermal 3D mapping," in *Advanced Engineering Informatics, 2014*, vol. 28, no. 4, pp. 425–440. doi: 10.1016/j.aei.2014.06.002.
- [5] L. Hoegner, S. Tutas, Y. Xu, K. Eder, and U. Stilla, "Evaluation of methods for coregistration and fusion of RPAS-based 3D point clouds and thermal infrared images," *Int. Arch. Photogramm. Remote Sens. Spat. Inf. Sci.*, vol. XLI-B3, pp. 241–246, Jun. 2016, doi: 10.5194/isprs-archives-xli-b3-241-2016.
- [6] J. Zhu, Y. Xu, Z. Ye, L. Hoegner, and U. Stilla, "Fusion of urban 3D point clouds with thermal attributes using MLS data and TIR image sequences," *Infrared Phys. Technol.*, vol. 113, p. 103622, Mar. 2021, doi: 10.1016/j.infrared.2020.103622.

- [7] M. Yamaguchi *et al.*, “Superimposing thermal-infrared data on 3D structure reconstructed by RGB visual odometry,” *IEICE Trans. Inf. Syst.*, vol. E101D, no. 5, pp. 1296–1307, May 2018, doi: 10.1587/TRANSINF.2017MVP0023.
- [8] P. Westfeld, D. Mader, and H. G. Maas, “Generation of TIR-attributed 3D point clouds from UAV-based thermal imagery,” *Photogramm. Fernerkundung, Geoinf.*, vol. 2015, no. 5, pp. 381–393, Oct. 2015, doi: 10.1127/1432-8364/2015/0274.
- [9] M. Previtali, L. Barazzetti, V. Redaelli, M. Scaioni, and E. Rosina, “Rigorous procedure for mapping thermal infrared images on three-dimensional models of building façades,” *J. Appl. Remote Sens.*, vol. 7, no. 1, p. 073503, Sep. 2013, doi: 10.1117/1.JRS.7.073503.
- [10] M. I. Alba, L. Barazzetti, M. Scaioni, E. Rosina, and M. Previtali, “Mapping infrared data on terrestrial laser scanning 3D models of buildings,” *Remote Sens.*, vol. 3, no. 9, pp. 1847–1870, Aug. 2011, doi: 10.3390/rs3091847.
- [11] L. Hoegner and U. Stilla, “Mobile thermal mapping for matching of infrared images with 3D building models and 3D point clouds,” *Quant. Infrared Thermogr. J.*, vol. 15, no. 2, pp. 252–270, Jul. 2018, doi: 10.1080/17686733.2018.1455129.
- [12] D. Bulatov, E. Burkard, R. Ilehag, B. Kottler, and P. Helmholz, “From multi-sensor aerial data to thermal and infrared simulation of semantic 3D models: Towards identification of urban heat islands,” *Infrared Phys. Technol.*, vol. 105, p. 103233, Mar. 2020, doi: 10.1016/j.infrared.2020.103233.
- [13] Z. Sun and Y. Zhang, “Using drones and 3D modeling to survey Tibetan architectural heritage: A case study with the multi-door stupa,” *Sustain.*, vol. 10, no. 7, p. 2259, Jun. 2018, doi: 10.3390/su10072259.
- [14] K. Kim and M. Peavy, “BIM-based semantic building world modeling for robot task planning and execution in built environments,” *Autom. Constr.*, vol. 138, 2022, doi: 10.1016/j.autcon.2022.104247.
- [15] O. Kyjanek, B. Al Bahar, L. Vasey, B. Wannemacher, and A. Menges, “Implementation of an augmented reality AR workflow for human robot collaboration in timber prefabrication,” in *Proceedings of the 36th International Symposium on Automation and Robotics in Construction, ISARC 2019*, 2019, pp. 1223–1230. doi: 10.22260/isarc2019/0164.
- [16] S. Meschini, P. Di Milano, K. Iturralde, T. Linner, and T. Bock, “Novel applications offered by integration of robotic tools in BIM-based design workflow for automation in construction processes,” no. April 2019, 2016.
- [17] A. Adán, J. García, B. Quintana, F. J. Castilla, and V. Pérez, “Temporal-Clustering Based Technique for Identifying Thermal Regions in Buildings,” *Lect. Notes Comput. Sci. (including Subser. Lect. Notes Artif. Intell. Lect. Notes Bioinformatics)*, vol. 12002 LNCS, pp. 290–301, Feb. 2020, doi: 10.1007/978-3-030-40605-9_25.
- [18] T. Rakha, Y. El Masri, K. Chen, E. Panagoulia, and P. De Wilde, “Building envelope anomaly characterization and simulation using drone time-lapse thermography,” *Energy Build.*, p. 111754, Dec. 2021, doi: 10.1016/j.enbuild.2021.111754.
- [19] X. Xiong, A. Adan, B. Akinci, and D. Huber, “Automatic creation of semantically rich 3D building models from laser scanner data,” *Autom. Constr.*, vol. 31, pp. 325–337, May 2013, doi: 10.1016/j.autcon.2012.10.006.
- [20] A. López, J. M. Jurado, C. J. Ogayar, and F. R. Feito, “An optimized approach for generating dense thermal point clouds from UAV-imagery,” *ISPRS J. Photogramm. Remote Sens.*, vol. 182, pp. 78–95, Dec. 2021, doi: 10.1016/j.isprsjprs.2021.09.022.
- [21] S. A. Prieto, B. Quintana, A. Adán, and A. S. Vázquez, “As-is building-structure reconstruction from a probabilistic next best scan approach,” *Rob. Auton. Syst.*, vol. 94, pp. 186–207, 2017, doi: 10.1016/j.robot.2017.04.016.
- [22] P. J. Besl and N. D. McKay, “A Method for Registration of 3-D Shapes,” *IEEE Trans. Pattern Anal. Mach. Intell.*, vol. 14, no. 2, pp. 239–256, Feb. 1992, doi: 10.1109/34.121791.

Construction Automation and Robotics for Concrete Construction: Case Studies on Research, Development, and Innovations

Rongbo Hu¹, Wen Pan¹, Kepa Iturralde¹, Thomas Linner² and Thomas Bock¹

¹Chair of Building Realization and Robotics, Technical University of Munich, Munich, Germany

²Faculty of Civil Engineering & Regensburg School of Digital Sciences, OTH Regensburg, Regensburg
rongbo.hu@tum.de, wen.pan@br2.ar.tum.de, kepa.iturralde@br2.ar.tum.de, thomas.linner@oth-regensburg.de,
thomas.bock@br2.ar.tum.de

Abstract –

The construction industry, supported by the materials industry, is a major user of natural resources. Automation and robotics have the potential to play a key role in the development of circular construction by increasing productivity, reducing waste, increasing safety, and mitigating labor shortages. Starting with a brief synopsis of the history of construction robotics and the concept of robot-oriented design, this article presents exemplary case studies of research projects and entrepreneurial activities in which the authors have participated that have contributed to the advancement of concrete construction. The activities of the authors have systematically led to spin-offs and start-ups, especially in recent years (e.g., CREDO Robotics GmbH, ARE23 GmbH, KEWAZO GmbH, ExlenTec Robotics GmbH, etc.), which shows that the use of construction robots is becoming an important part of the construction industry. With the use of automation and robotics in the built environment especially for concrete construction, current challenges such as the housing shortage can be addressed using the leading machinery and robot technology in Germany and other parts of the world. The knowledge and know-hows gained in these endeavors will lay the groundwork for the next frontier of construction robotics beyond the construction sites.

Keywords –

Automated Construction Machinery; Concrete Construction; Construction Robots; Infrastructure; Robot-Oriented Design

1 Background

The construction industry, along with the materials production sectors supporting it, is one of the largest exploiters of natural resources on the global stage, both

in physical and biological manners [1]. As the need of public housing due to the population explosion is continuously increasing [2], the material and labor costs are rising. The increased competition and shrinking profit margins are some further challenges facing the construction industry. According to McKinsey Global Institute, the construction industry has an intractable productivity problem. Furthermore, the report confirms that while sectors such as retail and manufacturing have reinvented themselves, construction seems stuck in a time warp. Global labor-productivity growth in construction has averaged only 1% a year over the past two decades, compared with growth of 2.8% for the total world economy and 3.6% in manufacturing [3]. Therefore, using innovative solutions to increase the productivity of the construction sector becomes critical to the sustainability of the construction industry.

Furthermore, the construction sector is responsible for 36% of the energy use and for producing 39% of the global carbon dioxide (CO₂) emissions including operational energy emissions and embodied emissions that are resulted from materials and construction processes along the whole life cycle [4]. Take concrete as an example: Invented more than 200 years ago, cement concrete continues to be the most frequently used building material. Its usage globally (in tonnage) is twice that of steel, wood, plastics, and aluminum combined [5]. The ready-mix concrete industry, the largest segment of the concrete market, is projected to surpass \$600 billion in revenue by 2025 [6]. In addition, concrete production uses substantial amount of energy and raw materials, which results in a large amount of total CO₂ emissions (around 7.0%) into the environment [7]. Lacking the use of recyclable materials, the construction sector is generating high levels of waste all around the world.

More importantly, labor safety in the construction sector is a major issue facing the industry today. The reduction in the number of onsite construction workers at height, through applying construction robots, can

substantially reduce the chance of fatal accidents and other injuries on the construction sites. According to Eurostat, there were 3552 fatal accidents at work in EU-28 states during 2017, of which one fifth happened in the construction sector [8]. In other words, more than 700 accidental deaths took place within the construction industry in EU countries just in 2017. Accordingly, many of these accidents are directly or indirectly related to concrete construction. The reduction in the number of onsite construction workers at height, through applying advanced technologies, can substantially reduce the chance of fatal accidents and other injuries on the construction sites.

In addition, as the global population is continuously aging, the construction industry is expected to bear the brunt for the years to come. In fact, many countries and regions have already experienced labor shortages in the construction sector, especially high-skilled ones [9-11]. The fact that the construction industry suffers from a bad public image (also known as “3D”: dangerous, dirty, difficult) also aggravates these shortages due to its lack of ability to attract younger workforce. Apparently, novel solutions are needed to mitigate these shortages.

Therefore, improving productivity, reducing waste, enhancing safety, as well as mitigating labor shortages in concrete construction will contribute significantly to the sustainable development of the construction sector, and automation and robotics can play a significant role in this process, just as it already did in the manufacturing industry. This paper will introduce the brief history of construction robotics and present exemplary case studies of research projects and entrepreneurial activities in which the authors have participated that have contributed to the sustainability of concrete construction.

2 The rise of construction robotics

The construction automation and robotics is a new yet flourishing research topic. Ever since the first stationary construction robotics' debut in the 1960s in Japanese modular prefabrication of the Sekisui Heim M1 that was designed by Dr. K. Ohno (see Figure 1), then from the late 1970s the first on-site construction robots (see Figure 2) were developed by Japanese general contractor Shimizu Corporation due to the lack of skilled labor, low construction quality, and bad public image, about 50 construction robot systems have been developed in the 1980s. Other catalysts also include high land prices, high interest rates, and high living cost which required rapid, on-time, high quality construction project delivery on site as planned as well as immediate return on investment. As a result, from the 1990s, on automated construction sites (e.g., the pioneering SMART System developed by Shimizu Corporation in 1992, see Figure 3) have also become a worldwide research topic [12].



Figure 1. Stationary construction robotics of the Misawa-Toyota Homes assembly line (photo: T. Bock)

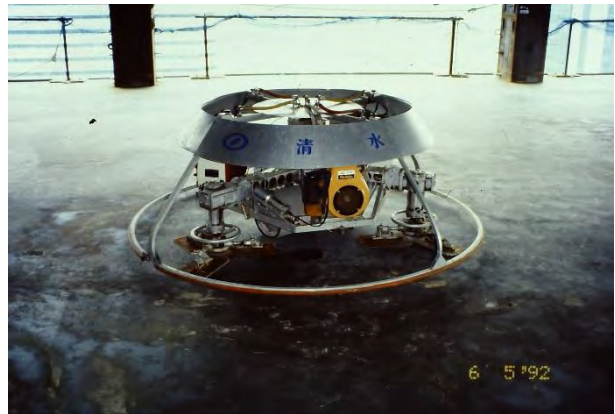


Figure 2. Concrete leveling robot developed by Shimizu Corporation (photo: T. Bock)



Figure 3. The pioneering automated construction site “SMART” developed by Shimizu Corporation (photo: T. Bock)

Further innovation push was triggered by earthquakes, landslides, volcano eruptions, and tsunamis where initially since 2000s, teleoperated construction robots (see Figure 4) and since 2010s, autonomous scrapers, graders, rollers, compactors, trucks, and excavator fleets for large infrastructure projects such as dams, roads, bridges and tunnels have been developed and applied (see Figure 5). For maintenance, inspection, and repair of buildings and infrastructure such as tunnels, roads, dams, and power plants, various maintenance robots were developed (see Figure 6). Most of these solutions are directly or indirectly related to cement or concrete construction.



Figure 4. Teleoperated construction robot for concrete tunnel construction (photo: T. Bock)



Figure 5. Autonomous heavy machinery fleet for large infrastructure projects (Photo: T. Bock)



Figure 6. Maintenance robot Enryu T-53 developed by TMSUK Co. Ltd. (photo: T. Bock)

As a national project on concrete construction, the Solid Material Assembly System (SMAS, see Figure 7) based on an earthquake-proof reinforced concrete block assembly and disassembly robot was successfully developed and tested at the Building Research Establishment (BRE) of Japan's Ministry of Construction from 1984 to 1988. During the project, the co-author T. Bock developed the notion of Robot-Oriented Design (ROD) [13], which was applied to the first automated construction site SMART (Figure 3) and to Obayashi's Automated Building Construction System (ABCS) from 1992 onwards, and also laid the foundation for the development of many construction robot systems.



Figure 7. The SMAS robot developed for the assembly and disassembly of reinforced concrete blocks using ROD concept (photo: T. Bock)

3 Case studies on the concrete processing construction robots developed by the authors' team

As mentioned above, construction robots are robots or automated devices that are developed primarily for tasks on the construction sites. It is a highly cross-disciplinary field which requires an integration of a variety of knowledge and expertise such as civil engineering, architecture, industrial design, construction management, robotics, mechanical engineering, electrical engineering, and informatics. Today, the application fields of construction robotics continue to expand. Bock and Linner summarized 200 existing construction robot systems into 24 categories based on their functions, many of which are directly or indirectly related to cement or concrete construction [14]. However, there is still a gap in the ubiquitous application of concrete processing robots due to various reasons, such as insufficient evidence of net economic benefits, lack of modularity and flexibility, lack of skilled labor for operation, incompatibility with other construction tasks, and time-consuming onsite setup [14]. Therefore, in the following sections, three exemplary case studies will be introduced on how Prof. Thomas Bock and his team attempted to bridge the gap in the field of concrete construction using construction robotics in a global context in recent years.

The endeavors in Europe began in the early 1990s. After the German reunification, there was an increased need for construction, especially for affordable housing - as is the case today. Together with SÜBA Bau AG, T. Bock developed the production system for the "x8 Haus" (see Figure 8) as part of his professorship for automation in construction operations at the civil engineering faculty of University of Karlsruhe (now Karlsruhe Institute of Technology) in 1990. It offered 100 m² of living space on two stories with a bathroom-toilet building service module, without a basement and can be prefabricated in 8 days by a specially developed multifunctional system with portal robots, assembled on site in 8 hours and sold for 80,000 German Marks (see Figure 9).

Since then, over the past three decades, T. Bock and his team from the Chair of Building Realization and Robotics at Technical University of Munich along with their start-ups and spin-offs such as CREDO Robotics GmbH, ARE23 GmbH, KEWAZO GmbH, ExlenTec Robotics GmbH have vigorously contributed to the automation and robotization of construction especially regarding concrete with several research and innovation projects in different regions around the world.

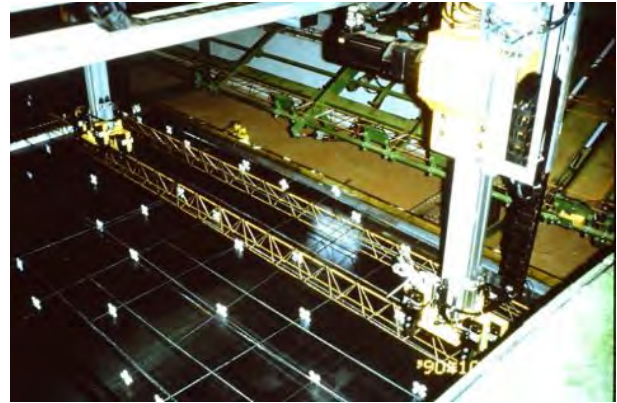


Figure 8. Robotic reinforced concrete parts production system for "x8 Haus" (Photo: T. Bock)



Figure 9. The built "x8 Haus" applying the ROD concept (Photo: T. Bock)

3.1 Case study 1: Consultancy on Investigating the Potential of Implementing Robotics and Automation in the Context of Large-scale Housing Development for Hong Kong SAR

The public housing construction industry in Hong Kong, predominantly using prefabricated concrete as the construction material, faces conspicuous challenges of high demands, safety, an ageing workforce, inconsistent quality and stagnant productivity. The consultancy project commissioned by the Construction Industry Council (CIC) of Hong Kong SAR evaluates the current on-site construction operation and identifies the existing bottlenecks that can be enhanced by implementing robotics and automation. In the current housing construction field, the systematic and scientific method to approach this type of undertaking, especially when closely associated with the industry and authorities, has not been comprehensively discussed.

Therefore, this project highlights the activities that signify these objectives using systems engineering, which include five key activities: literature review,

industry survey, on-site case study, co-creation workshops, and potential pilot project. As a result, a range of robotic applications that are tailor-made for Hong Kong's prefabricated public housing industry are recommended and hierarchically categorized [15]. In addition, as one of the most needed robotic applications, a semi-functional prototype of multifunctional façade-processing robot using specially-designed cartesian kinematics (e.g., painting, cleaning, grinding, inspection, marking, etc.) was designed, built and tested in laboratory as a proof of concept (see Figure 10 and Figure 11). The robot can work on the concrete façade of high-rise public housing buildings in Hong Kong and beyond in collaboration with workers. In summary, the above-mentioned learnings gained from this study will inspire the construction industry to initiate and explore innovative, compatible as well as feasible solutions to the implementation of the robotic application in specific regions in the world in the future [16].



Figure 10. The multifunctional façade-processing robot showcasing the painting function on the façade of public housing buildings in Hong Kong (image: R. Hu)



Figure 11. The semi-functional prototype of the multifunctional façade-processing robot exhibited in the Construction Innovation and Technology Application Centre in Hong Kong (photo: R. Hu)

3.2 Case study 2: HEPHAESTUS cable-driven façade installation robot in concrete structures

HEPHAESTUS stands for Highly Automated Physical Achievements and Performances Using Cable Robots Unique Systems. The HEPHAESTUS project explores the innovative use of robots and autonomous systems in construction, a field where the incidence of such technologies is minor to non-existent. The project aims to increase market readiness and acceptance of key developments in cable robots and curtain walls. The installation of curtain wall modules (CWMs) is a risky activity carried out in the heights and often under unfavorable weather conditions. CWMs are heavy prefabricated walls that are lifted normally with bindings and cranes. High stability is needed while positioning in order not to damage the fragile CWMs. Moreover, this activity requires high precision while positioning brackets, the modules, and for that reason, intensive survey and marking are necessary. In order to avoid such inconveniences, there were experiences to install façade modules in automatic mode using robotic devices.

In HEPHAESTUS, a novel system has been developed in order to install CWMs automatically. The system consists of two sub-systems: a cable driven parallel robot (CDPR, see Figure 12) and a set of robotic tools named as Modular End Effector (MEE, see Figure 13). The platform of the CDPR hosts the MEE. This MEE performs the necessary tasks of installing the curtain wall modules. There are two main tasks that the CDPR and MEE need to achieve: first is the fixation of the brackets onto the concrete slab, and second is the picking and placing of the CWMs onto the brackets. The first integration of the aforementioned system was carried out in a controlled environment that resembled a building structure. The results of this first test show that there are only minor deviations when positioning the CDPR platform [17]. In future steps, the deviations will be compensated by the tools of the MEE and the installation of the CWM will be carried out with the required accuracy automatically, which will be reported in upcoming publications.

Nevertheless, the initial on-site test results suggest that the robot can potentially boost productivity by 220% for an average construction job, compared to the conventional façade installation method. Furthermore, a study on the cost-benefit analysis (CBA) of construction robots estimates that the HEPHAESTUS cable-driven robot for facade installation is theoretically worth investing in the UK, as well as in the majority of G20 countries [18].



Figure 12. The HEPHAESTUS cable-driven façade installation robot on a testing site (photo: K. Iturralde)

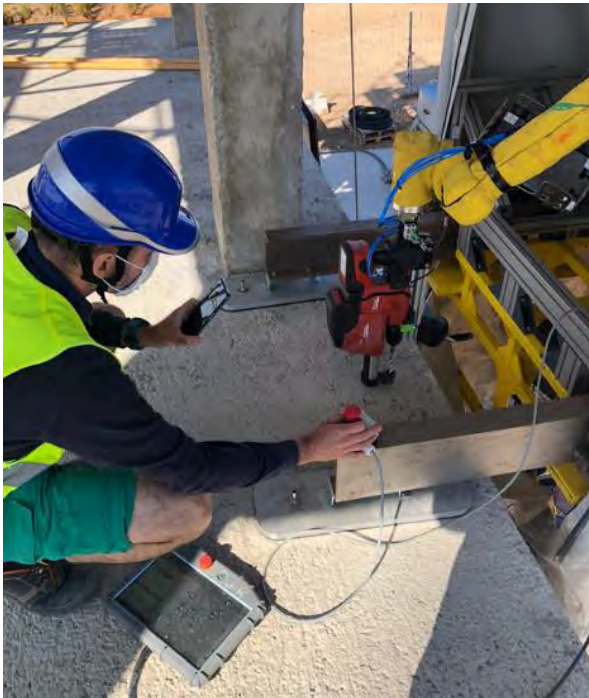


Figure 13. Co-author K. Iturralde checking the performance of the modular end-effector of the HEPHAESTUS robot (photo: S. Palencia Ludeña)

3.3 Case study 3: ARE23 wall painting robot

ARE23 GmbH was co-founded in 2020 in Germany, and the CEO, Dr.-Ing. Wen Pan is a researcher at the Chair of Building Realization and Robotics. It is an augmented robotics engineering company whose mission is to support laborers in the construction sector with artificial intelligence (AI) and robotics-driven technology. It automates the concrete coating industry and digitalizes the entire operational process with affordable solutions. Its products including small and large-scale spray coating robots for residential and commercial-sized projects complement human skills, improve productivity, and cut costs.

Providing the workforce with a catalogue of robotic spraying solutions will allow the industry to satisfy the increasingly growing labor demand while guaranteeing premium paint application quality. A 3-axis machine for an interior surface coating robot that can autonomously scan a surface, determine its optimal path, and spray hard-to-reach surfaces. Leveraging Vention's cloud-9 programming environment, they were able to write their own code and quickly merge it with their in-house operating system (ARE-OS). Next, the start-up aims at developing a range of robotic solutions for the painting, plastering and coating of the built environment.

For example, the "TITAN" range (Figure 14) is developed for larger commercial and industrial scenarios, while the "COMPACT" range (Figure 15) is suitable for residential, hotels, and offices. The initial test results suggest that both variants of the robot can potentially boost productivity by 250% compared to the conventional manual wall spraying method, with the same number of operators involved in both methods. The fully functional "COMPACT" product will be ready for the commercial pilot in Germany in early 2023. Although the technologies developed by ARE23 GmbH were primarily customized for the German market, their modularity and affordability ensure that they can be easily adapted for other regions in the world as well.



Figure 14. Prototype of the "TITAN" range on a pilot project (photo: ARE23 GmbH)



Figure 15. Proof-of-concept prototype of the “COMPACT” range (photo: ARE23 GmbH)

4 Conclusion

In summary, construction automation and robotics can potentially play a significant role in the sustainable development of the concrete construction industry by improving productivity, reducing waste, enhancing safety, as well as mitigating labor shortages. The research and innovation endeavors represented by several research projects and entrepreneur activities conducted by the Chair of Building Realization and Robotics at Technical University of Munich along with their in-house spin-offs and start-ups such as CREDO Robotics GmbH, ARE23 GmbH, KEWAZO GmbH, ExlenTec Robotics GmbH over the years have contributed significantly to the knowledge and know-hows in the construction industry, especially in the concrete construction sector.

In connection with new approaches from the field of human-centric use of robots, human labor can be perfectly supplemented in order to compensate for the shortage of skilled workers. Automated construction machinery for infrastructure construction offers highly efficient solutions for the expansion and renovation of roads, railroads, bridges, and tunnels. Advances in the field of digital connection and programming of robots increasingly facilitate the use of these solutions. Future research will be conducted on the universal simulation environment for customized robotic applications for a resource-efficient and human-centric construction industry. Furthermore, the knowledge and know-hows gained in these endeavors will lay the groundwork for the next frontier of construction robotics beyond the construction sites, such as dismantling concrete buildings and infrastructure (Figure 16) and constructing space architecture (Figure 17).



Figure 16. Concrete dismantling and concrete recycling robot Garapagos (Photo: T. Bock)

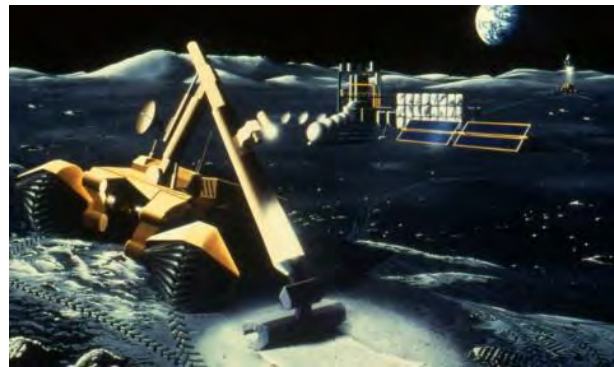


Figure 17. Next frontier for construction robotics: space stations and colonies (Photo: T. Bock)

Acknowledgment

The Consultancy on Investigating the Potential of Implementing Robotics and Automation in the Context of Large-scale Housing Development for Hong Kong was funded by the Construction Industry Council (CIC) in Hong Kong.

The HEPHAESTUS project has received funding from the European Union’s Horizon 2020 research and innovation programme under grant agreement No 732513.



ARE23 GmbH has received funding from the ESA BIC Bavaria Incubation Programme.

References

- [1] Spence, R. and Mulligan, H. Sustainable development and the construction industry. *Habitat International*, 19(3), 279–292, 1995. [https://doi.org/10.1016/0197-3975\(94\)00071-9](https://doi.org/10.1016/0197-3975(94)00071-9)
- [2] United Nations. World Population Prospects: the

- 2019 Revision, 2019. On-line: <https://population.un.org/wpp/Publications/>, Accessed: 21/01/2023.
- [3] McKinsey Global Institute. Reinventing Construction: A Route to Higher Productivity, 2017. On-line: <https://www.mckinsey.com/~media/mckinsey/business%20functions/operations/our%20insights/reinventing%20construction%20through%20a%20productivity%20revolution/mgi-reinventing-construction-executive-summary.pdf>, Accessed: 21/01/2023.
- [4] International Energy Agency. Global Status Report for Buildings and Construction 2019: Towards a zero-emissions, efficient and resilient buildings and construction sector. 2019 Retrieved from On-line: https://iea.blob.core.windows.net/assets/3da9daf9-ef75-4a37-b3da-a09224e299dc/2019_Global_Status_Report_for_Buildings_and_Construction.pdf, Accessed: 21/01/2023
- [5] Cockburn, H. Cleaner, greener, quicker, stronger: Is wood the building material of the future? Independent. On-line: <https://www.independent.co.uk/climate-change/news/wood-construction-concrete-steel-climate-b1796342.html>, Accessed: 21/01/2023.
- [6] Manjunatha, M., Seth, D., KVG D, B. and Chilukoti, S. Influence of PVC waste powder and silica fume on strength and microstructure properties of concrete: An experimental study. *Case Studies in Construction Materials*, 15, e00610, 2021. <https://doi.org/10.1016/j.cscm.2021.e00610>
- [7] Unis Ahmed, H., Mahmood, L. J., Muhammad, M. A., Faraj, R. H., Qaidi, S. M. A., Hamah Sor, N., Mohammed, A. S. and Mohammed, A. A. Geopolymer concrete as a cleaner construction material: An overview on materials and structural performances. *Cleaner Materials*, 5, 100111, 2022. <https://doi.org/10.1016/j.clema.2022.100111>
- [8] Eurostat. Accidents at work statistics. On-line: https://ec.europa.eu/eurostat/statistics-explained/index.php/Accidents_at_work_statistics/#Number_of_accidents, Accessed: 21/01/2023.
- [9] Mohd Rahim, F. A., Mohd Yusoff, N. S., Chen, W., Zainon, N., Yusoff, S. and Deraman, R. The challenge of labour shortage for sustainable construction. *Planning Malaysia*, 14(5 SE-Article), 2016. <https://doi.org/10.21837/pm.v14i5.194>
- [10] Ceric, A. and Ivic, I. Construction labor and skill shortages in Croatia: causes and response strategies. *Organization, Technology and Management in Construction: An International Journal*, 12(1), 2232–2244, 2020. <https://doi.org/10.2478/otmcj-2020-0019>
- [11] Ho, P. H. K. Labour and skill shortages in Hong Kong's construction industry. *Engineering, Construction and Architectural Management*, 23(4), 533–550, 2016. <https://doi.org/10.1108/ECAM-12-2014-0165>
- [12] Bock, T. and Linner, T. *Site automation: Automated/Robotic On-Site Factories*. Cambridge University Press, Cambridge, UK, 2016 <https://doi.org/10.1017/CBO9781139872027>
- [13] Bock, T. (1988). Robot-Oriented Design. In Proceedings of the 5th International Symposium on Automation and Robotics in Construction (ISARC) (pp. 135–144). International Association for Automation and Robotics in Construction (IAARC). <https://doi.org/10.22260/ISARC1988/0019>
- [14] Bock, T. and Linner, T. *Construction Robots: Elementary Technologies and Single-Task Construction Robots*. Cambridge University Press, Cambridge, UK, 2016. <https://doi.org/10.1017/CBO9781139872041>
- [15] Pan, W., Hu, R., Linner, T. and Bock, T. A methodological approach to implement on-site construction robotics and automation: a case of Hong Kong. In *Proceedings of 35th International Symposium on Automation and Robotics in Construction*, 362-369, Berlin, Germany, 2018. <https://doi.org/10.22260/ISARC2018/0051>
- [16] Linner, T., Hu, R., Iturralde, K., and Bock, T. A Procedure Model for the Development of Construction Robots. In S. H. Ghaffar, P. Mullett, E. Pei, & J. Roberts (Eds.), *Innovation in Construction – A Practical Guide to Transforming the Construction Industry*. Springer International Publishing, 321-352 2022. https://doi.org/10.1007/978-3-030-95798-8_14
- [17] Iturralde, K., Feucht, M., Illner, D., Hu, R., Pan, W., Linner, T., Bock, T., Eskudero, I., Rodriguez, M., Gorrotxategi, J., Izard, J.-B., Astudillo, J., Cavalcanti Santos, J., Gouttefarde, M., Fabritius, M., Martin, C., Henninge, T., Normes, S. M., Jacobsen, Y., ... Elia, L. Cable-driven parallel robot for curtain wall module installation. *Automation in Construction*, 138, 104235, 2022. <https://doi.org/10.1016/j.autcon.2022.104235>
- [18] Hu, R., Iturralde, K., Linner, T., Zhao, C., Pan, W., Pracucci, A. and Bock, T. A Simple Framework for the Cost–Benefit Analysis of Single-Task Construction Robots Based on a Case Study of a Cable-Driven Facade Installation Robot. *Buildings*, 11(1), 8, 2021. <https://doi.org/10.3390/buildings11010008>

3D Printing: An opportunity for the sustainable development of building construction

Christopher Núñez^a, Marck Regalado^a and Angela Gago^a

^aFaculty of Civil Engineering, National University of Engineering, Perú

E-mail: angela.gago.g@uni.pe, christopher.nunez.v@uni.pe, marck.regalado.e@uni.pe

Abstract

Traditional construction processes have certain shortcomings, due to waste generation, as well as quality, safety and environmental problems, etc. In this regard, there are some technological innovations that represent an acceptable alternative to improve said construction processes in a specific country. One of them is 3D concrete printing (3DCP), which requires a printer consisting of a nozzle that extrudes and disposes layers of concrete following a previously-designed trajectory. Keeping that in mind, it is necessary to identify the main barriers that could prevent the successful implementation of this technology in a country to better target national policies and encourage the participation of the private sector. One way to achieve this is to present the main opportunities offered by this technology in the construction industry. In this research, we started with a literature review that allowed us to identify 6 opportunities and 10 barriers of 3D printing technology for whole houses. Then, a survey was designed to rate and score them through expert judgment, using the Analytical Hierarchy Process (AHP) method and its simplified version, Best Worst (BW), respectively. To validate this procedure, Peru was taken as an example, and 20 professionals from the construction industry with extensive professional experience were interviewed. It was thereby identified that the main opportunities are greater on-site safety, construction quality, and social benefits, while the main barriers to the implementation of full-size 3D printing are the technology under development, printing material, and the skills required for using this new technology.

Keywords –

3D-printed construction; 3D concrete printing; Technology adoption; Sustainability; Concrete

1 Introduction

Concrete is the main material used in the global construction industry and the second most used mixture in the global market. However, it is also a major contributor to greenhouse gas emissions [1], [2]. In building construction, the traditional construction processes with this material have many shortcomings,

from the waste of resources [3], its high cost which makes it unaffordable [4], a high rate of occupational accidents [5], among others. In addition, there is a housing shortage in many countries, which is exacerbated by the steady global population growth [4].

Therefore, it is important to implement new technologies to overcome these problems and contribute to the sustainability of construction activities, being 3D concrete printing technology a great alternative which could be an important alternative [6]. This technology applies an automated process mainly based on the layered extrusion of concrete following a digital model, using a printhead or nozzle [7], [8].

Given that digital fabrication (DF) technologies have been being adopted in the construction industry in recent years, 3D concrete printing has become a focus of attention internationally due to the opportunities it offers, having begun to be implemented in some countries [9], [10]. These opportunities include, for example, greater freedom in architectural design, increased worker safety, time and cost savings, and reduced environmental impact [11], [12].

Although it presents different opportunities, in those countries where this technology has not yet begun to be investigated, let alone implemented, it is necessary to identify the main barriers that would exist for its optimal application. This evaluation of opportunities and barriers has already been carried out in other countries, based on a literature review, construction experts surveyed, and the identification of which opportunities and barriers would be the main ones to consider. In South Africa, its implementation was analyzed for low-cost sustainable housing, recognizing that the primary obstacle will be distributing the technology to the critical stakeholders of the construction sector [13]. In Europe, the main barriers are those related to stakeholder economic factors, technical and commercial factors, and traditional work culture [14]. In India, the main opportunity is their high speed of construction [15].

This research compiles the main opportunities and barriers for implementing full-scale 3D printing of concrete housing, which have been reported in recent research on this topic. Thus, those countries that wish to implement this technology and want to evaluate its potential main opportunities and barriers methodology

that is based on experts' opinions and analyzes them applying the hierarchical method AHP (Analytical Hierarchy Process) and the simplified method BW (Best Worst). For this research, Peru was taken as an example of how this evaluation would be carried out.

2 Bibliographic review process

First, many scientific papers related to the topic were collected to identify the opportunities and barriers for the implementation of full-scale 3D concrete printing in construction projects. Papers were collected considering keywords to make sure that the paper was important for the carrying out of the research (see Table 1).

Table 1. Keywords and complements

	Keyword	Complement
1	3D concrete printing	Challenge
2	Additive Manufacturing	Barriers
3	Robotic 3D printing	Issues
4	3D printing	Opportunities
5	-	Problems
6	-	Enables

Then, a combination of keywords and complements was tried to find all possible options in the following databases: Scopus, ASCE, IEEE, Web of Science, and previous versions of ISARC. Thus, a total of 359 papers were retrieved. Then, we applied filters to ensure that the selected papers are aligned with our research objective. We excluded applied research and studies focused on specific topics, and instead prioritized papers that made a comprehensive list of opportunities or barriers related to the implementation of 3D concrete printing. Following these criteria, we narrowed down our initial list of papers to a final selection of 65 (see Figure 1). From them, the list of opportunities and barriers was obtained, these were grouped and are shown in sections 3 and 4.

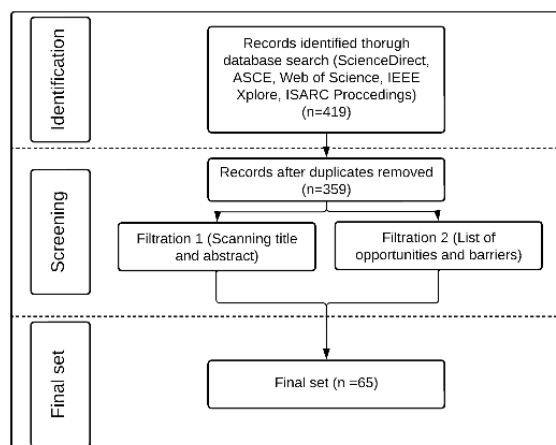


Figure 1. Bibliographic review flowchart

3 Opportunities of full-scale 3D concrete printing

The application of full-scale 3D concrete printing in the construction industry has multiple opportunities compared to conventional construction techniques. Based on the bibliographic study (see Table 2), we proceed to explain each of these opportunities.

3.1 Time saving and low cost

This includes, among others, the following:

- It generates a lower consumption of resources by not requiring formwork and steel reinforcement, and cancels any possible waste on site.
- Likewise, the geometry of the structure is optimized, requiring fewer materials (in volume) than in a traditional design. Approximately, construction time is reduced by up to 60% [48].
- In addition, the printing process is high-speed compared to traditional construction.
- Physical materials are also not required, thus eliminating the logistics associated with their purchase and placement on site.

3.2 Social benefits

This includes, among others, the following:

- It is ideal for the massive construction of affordable social housing, helping to reduce housing shortage in a country.
- It represents a market for the generation of new jobs.

3.3 Construction quality

This refers to the fact that, as the printing is automated, it improves the accuracy of the construction process, avoiding non-conforming products.

3.4 Freedom in architectural design

This includes, among others, the following:

- Complex architectural designs can be built without problems (such as curved walls), eliminating the design dependency of only replicated elements.
- It allows to generate eco-friendly designs, with better use of sunlight, ventilation, etc.

3.5 Increased safety at the construction site

Likewise, since printing is an automated process, the exposure of people to hazardous manual labor is reduced.

3.6 Environmental benefits during construction

This includes, among others, the following:

- It reduces energy footprint, carbon footprint and solid waste generation by requiring fewer resources and eliminating waste on site.
- It minimizes dust generation during construction work.

Table 2. Opportunities of 3D concrete printing

Item	Opportunities	Reference
O1	Time saving and low cost	[5], [10]–[13], [15], [17]–[40], [48]
O2	Social benefits	[4], [13], [17], [20], [21], [25], [30], [34]
O3	Construction quality	[12], [19]–[21], [24], [33], [41]
O4	Freedom in architectural design	[5], [7], [8], [10]–[12], [15], [17], [19]–[22], [24]–[27], [30], [33], [34], [37], [42], [43]
O5	Increased safety at the construction site	[10], [11], [13], [15], [17], [19]–[21], [23], [24], [27], [29]
O6	Environmental benefits	[7], [8], [11]–[13], [15], [17]–[25], [27]–[30], [33], [34], [41], [43], [44]

4 Barriers of full-scale 3D concrete printing

Similarly, the application of full-scale 3D printing in the construction industry has barriers that limit its successful implementation in a country. Based on the literature review (see Table 3), we proceed to explain each of these barriers.

Table 3. Barriers of 3D concrete printing

Item	Barriers	Reference
B1	Technology in development	[5], [8], [10], [12]–[15], [17], [19], [20], [22], [23], [26], [27], [29]–[32], [34]–[36], [39], [42]–[50]
B2	Printing material	[6], [12], [15], [19], [22], [23], [34], [43], [45], [46], [49]
B3	Social impact	[17], [22], [30], [44]
B4	Uncertainty about new technologies	[10], [30], [32], [35], [42], [43], [45]
B5	Environmental impact	[28]

B6	Cost of implementation and maintenance	[12]–[15], [17], [19], [44], [45]
B7	Dissemination of information	[10], [13]–[15], [17], [19], [34]
B8	Required capabilities	[5], [8], [10], [13]–[15], [17], [19], [29], [34], [51]
B9	Off-site manufacturing	[45]
B10	Operational failures	[12], [19], [30]

4.1 Technology in development

This barrier represents the following:

- There are no standards on mix design and quality testing for this type of concrete.
- There are no standards or software for its structural design, nor has the type of reinforcement it would include been defined (the mortar does not resist traction).
- There is a need to identify a wider variety of materials that can be used for printing.
- Its application is restricted to low-rise buildings.
- The project is limited to the dimensions of the terrain, the process required for printing, and the thickness and finish generated by the printed layers.

4.2 Printing material

This barrier represents the following:

- Cold joints caused between each layer of printed concrete, reducing its bonding strength.
- Printed material in a fresh state may deform.
- The print would suffer from cracking due to excessive shrinkage.
- The material would be sensitive to environmental conditions, especially extreme weather.

4.3 Social impact

Because the printer would perform most of the construction work, the demand for laborers would be decreased.

4.4 Uncertainty about new technologies

Being a new technology in the country, there is always uncertainty about its benefits and the risk of implementing it, despite foreign success stories.

4.5 Environmental impact

Printed buildings, being concrete-only, require greater use of cement, increasing carbon footprint.

4.6 Cost of implementation and maintenance

This barrier represents the following:

- There is a significant investment in the purchase of printers and the additional devices required, all of which are imported.
- Likewise, consider periodic maintenance for its proper operation.

4.7 Dissemination of information

This barrier represents the following:

- Low awareness of full-scale 3D concrete printing, its applications, and opportunities.
- It is not a subject that is taught in universities, nor are there local companies that provide training.

4.8 Required capabilities

This barrier represents the following:

- To have a professional who knows the technology, the optimal process to design the printing path, the cybersecurity of the equipment, its continuous monitoring, among others.
- Qualified technical personnel for the operation and maintenance of the equipment.
- To have suppliers that know the technology.

4.9 Off-site manufacturing

If 3D printing is used to manufacture components off-site, there will be an additional cost to transport them, and possible damage in transit.

4.10 Operational failures

This barrier represents the following:

- Nozzle clogging.
- Interruption in the flow of concrete, which could cause printing defects.

5 Survey design

After presenting the opportunities and barriers of this technology, if a country intends to implement it, then it should identify the order of importance of each of these to guide public policies and encourage private companies to invest in this technology.

First, it is necessary to validate the list of opportunities and barriers for a certain country to be studied. In this research, Peru was taken as an example case, to validate the procedure explained. The list of opportunities and barriers was validated by two experts in the Peruvian construction industry.

Then, to weight the importance of each one, the AHP and BW methods were chosen for the data analysis. The Analytical Hierarchy Process (AHP) is a decision-making method that involves multiple criteria and relies on expert pairwise comparisons, enabling the numerical quantification of the analyzed elements values. Unlike AHP, BW only compares references, which means that it only needs to determine the preference of the best criterion over all other criteria and the preference of all criteria over the worst criterion using a number between 1 and 9 [F, G].

5.1 Opportunities

After the literature review, 6 general opportunities were obtained in the implementation of full-scale 3D printing, which is why we chose to use the AHP method, which is a multi-criteria decision-making process based on pairwise comparisons made by experts, which in turn allows numerically measure the values of the elements analyzed [16], [52]. The survey asked 15 questions comparing opportunities based on established criteria (see Table 4).

Table 4. Importance criteria

Scale	Name	Description
1	Equal importance	Both alternatives are of equal importance.
3	Slight importance	One of the alternatives is slightly more favored.
5	Moderate importance	One of the alternatives is favored moderately more.
7	Strong importance	One of the alternatives is strongly favored.
9	Completely more important	One of the alternatives is strongly favored.

5.2 Barriers

In the case of barriers, the BW method was used, which is used to calculate the weights of criteria and alternatives based on pairwise comparisons with the least amount of data. Compared to other methods, fewer pairwise comparisons are made from which criteria weights are obtained [53], [54]. Unlike AHP used in opportunities, BW only compares benchmarks, which means that it only needs to determine the preference of the most important barrier over the rest of the barriers and the preference of all barriers over the least important barrier following the criteria already established (see Table 4). In this research, 18 questions were asked using the Best Worst method.

6 Data analysis

In total, 20 professionals with experience in the Peruvian construction industry were surveyed, asking them about their personal data and questions related to opportunities and barriers.

6.1 General data

Each respondent was asked about his or her academic degree and the following results were obtained (see Table 5).

Table 5. Academic degree

Academic degree	Percentage concerning total respondents
Graduate Engineer	90%
Magister	65%
Doctor	10%

Next, respondents were asked about their profession (see Table 6).

Table 6. Profession

Profession	Percentage concerning total respondents
Civil Engineer	85%
Architect	5%
Others	10%

In addition, each respondent was asked about his or her current job (see Table 7). Many had more than one job at the same time

Table 7. Current job

Work currently performed	Percentage concerning total respondents
Construction company	30%
Supervision	30%
Designer	5%
Supplier	0%
Consultant	35%
Laboratory	15%
Public Management	10%
Teaching	55%
Research	45%

The last question of the general data was about their professional experience, where the following results were obtained (see Table 8). Many had more than one type of experience.

Table 8. Professional experience

Professional experience type	1 to 5 years	6 to 10 years	More than 10 years
University teaching in courses related to construction processes and/or concrete technology.	15%	5%	30%
Construction of civil works in general, including supervisory and/or consulting work.	25%	25%	40%
Related to concrete technology: Research, materials laboratory and/or supplier.	15%	10%	20%

6.2 Qualification results

The AHP method was used for opportunities, where 15 questions were asked comparing them in pairs. In the case of barriers, the Best Worst method was used, obtaining 18 questions. Tables 9 and 10 present the results of the surveys, with the qualification obtained by each one.

Table 9. Qualification of opportunities

Item	Opportunity	Average rating	Ranking
O1	Time saving and low cost	0.186	4°
O2	Social benefits	0.190	3°
O3	Construction quality	0.208	2°
O4	Freedom in architectural design	0.061	6°
O5	Increased safety at the construction site	0.227	1°
O6	Environmental benefits	0.129	5°

Table 10. Qualification of barriers

Item	Barrier	Average rating	Ranking
B1	Technology in development	0.170	1°
B2	Printing material	0.113	2°
B3	Social impact	0.092	6°
B4	Uncertainty about	0.109	4°

	new technologies			
B5	Environmental impact	0.079	8°	
B6	Cost of implementation and maintenance	0.100	5°	[4]
B7	Dissemination of information	0.072	10°	
B8	Required capabilities	0.110	3°	
B9	Off-site manufacturing	0.081	7°	[5]
B10	Operational failures	0.074	9°	

7 Conclusions

After having evaluated 65 scientific papers related to the implementation of full-scale 3D printing technology for housing, 10 barriers that would limit its implementation in a country have been identified, as well as 6 opportunities for its successful implementation.

A survey based on the AHP method was designed to rank the barriers and advantages according to the opinions of experts in each country. Taking Peru as a case study, 20 professionals with experience in the Peruvian construction industry were surveyed, who have many years of experience related to university teaching in construction, construction projects and concrete technology.

The main opportunities for the implementation of full-scale 3D printing of houses in Peru were the increased safety at the construction site (22.7%), construction quality (20.8%), and social benefits (19%). This reflects the great benefits that this technology will have on national development, from the point of view of experts, which should reinforce state and private support.

The main barriers were technology in development (17%), printing material (11.3%), and required capabilities (11%). With this result, the country will be able to guide improvement actions to overcome these barriers.

References

- [1] M. Adaloudis and J. Bonnin Roca, "Sustainability tradeoffs in the adoption of 3D Concrete Printing in the construction industry," *J Clean Prod*, vol. 307, p. 127201, Jul. 2021, doi: 10.1016/J.JCLEPRO.2021.127201.
- [2] W. Li, X. Lin, D. W. Bao, and Y. Min Xie, "A review of formwork systems for modern concrete construction," *Structures*, vol. 38, pp. 52–63, Apr. 2022, doi: 10.1016/J.ISTRUC.2022.01.089.
- [3] P. Khandve and A. GULGHANE, "Management for Construction Materials and Control of Construction Waste in Construction Industry: A Review," *International Journal of Engineering Research and Applications*, ISSN : 2248-9622, vol. 5, p. 6, Apr. 2015.
- [4] V. Lojanica, V.-M. Colic-Damjanovic, and N. Jankovic, "Housing of the Future: Housing Design of the Fourth Industrial Revolution," in *2018 5th International Symposium on Environment-Friendly Energies and Applications (EFEA)*, 2018, pp. 1–4, doi: 10.1109/EFEA.2018.8617094.
- [5] R. Guamán-Rivera, A. Martínez-Rocamora, R. García-Alvarado, C. Muñoz-Sanguinetti, L. F. González-Böhme, and F. Auat-Cheein, "Recent Developments and Challenges of 3D-Printed Construction: A Review of Research Fronts," *Buildings*, vol. 12, no. 2, 2022, doi: 10.3390/buildings12020229.
- [6] L. Casagrande, L. Esposito, C. Menna, D. Asprone, and F. Auricchio, "Effect of testing procedures on buildability properties of 3D-printable concrete," *Constr Build Mater*, vol. 245, p. 118286, Jun. 2020, doi: 10.1016/J.CONBUILDMAT.2020.118286.
- [7] J. Xiao *et al.*, "Large-scale 3D printing concrete technology: Current status and future opportunities," *Cem Concr Compos*, vol. 122, p. 104115, Sep. 2021, doi: 10.1016/J.CEMCONCOMP.2021.104115.
- [8] N. Labonnote, A. Rønquist, B. Manum, and P. Rütther, "Additive construction: State-of-the-art, challenges and opportunities," *Autom Constr*, vol. 72, pp. 347–366, Dec. 2016, doi: 10.1016/J.AUTCON.2016.08.026.
- [9] H. Alhumayani, M. Gomaa, V. Soebarto, and W. Jabi, "Environmental assessment of large-scale 3D printing in construction: A comparative study between cob and concrete," *J Clean Prod*, vol. 270, p. 122463, Oct. 2020, doi: 10.1016/J.JCLEPRO.2020.122463.
- [10] T. Marchment and J. Sanjayan, "Mesh reinforcing method for 3D Concrete Printing," *Autom Constr*, vol. 109, p. 102992, Jan. 2020, doi: 10.1016/J.AUTCON.2019.102992.
- [11] S. Kristombu Baduge *et al.*, "Improving performance of additive manufactured (3D printed) concrete: A review on material mix design, processing, interlayer bonding, and reinforcing methods," *Structures*, vol. 29, pp. 1597–1609, Feb. 2021, doi: 10.1016/J.ISTRUC.2020.12.061.
- [12] S. Lim, R. A. Buswell, T. T. Le, S. A. Austin, A. G. F. Gibb, and T. Thorpe, "Developments in construction-scale additive manufacturing processes," *Autom Constr*, vol. 21, no. 1, pp. 262–268, Jan. 2012, doi: 10.1016/J.AUTCON.2011.06.010.
- [13] D. Aghimien, C. Aigbavboa, L. Aghimien, W. Thwala, and L. Ndlovu, "3D PRINTING FOR SUSTAINABLE LOW-INCOME HOUSING IN SOUTH AFRICA: A CASE FOR THE URBAN

- POOR,” *Journal of Green Building*, vol. 16, no. 2, pp. 129–141, Jun. 2021, doi: 10.3992/jgb.16.2.129.
- [14] J. M. Davila Delgado *et al.*, “Robotics and automated systems in construction: Understanding industry-specific challenges for adoption,” *Journal of Building Engineering*, vol. 26, p. 100868, Nov. 2019, doi: 10.1016/J.JOBE.2019.100868.
- [15] T. Anjum, P. Dongre, F. Misbah, and V. P. S. N. Nanyam, “Purview of 3DP in the Indian Built Environment Sector,” *Procedia Eng.*, vol. 196, pp. 228–235, Jan. 2017, doi: 10.1016/J.PROENG.2017.07.194.
- [16] D. Asmare, “Application and validation of AHP and FR methods for landslide susceptibility mapping around choke mountain, northwestern ethiopia,” *Sci Afr*, vol. 19, p. e01470, Mar. 2023, doi: 10.1016/J.SCIAF.2022.E01470.
- [17] R. García-Alvarado, A. Martínez, L. González, and F. Auat, “Proyecciones de la construcción impresa en 3D en Chile,” *Revista ingeniería de construcción*, vol. 35, pp. 60–72, 2020.
- [18] M. R. M. Saade, A. Yahia, and B. Amor, “How has LCA been applied to 3D printing? A systematic literature review and recommendations for future studies,” *J Clean Prod*, vol. 244, p. 118803, Jan. 2020, doi: 10.1016/J.JCLEPRO.2019.118803.
- [19] S. J. Schuldt, J. A. Jagoda, A. J. Hoisington, and J. D. Delorit, “A systematic review and analysis of the viability of 3D-printed construction in remote environments,” *Autom Constr*, vol. 125, p. 103642, May 2021, doi: 10.1016/J.AUTCON.2021.103642.
- [20] A. O. Afolabi, R. A. Ojelabi, I. O. Omuh, and P. F. Tunji-Olayeni, “3D House Printing: A sustainable housing solution for Nigeria’s housing needs,” *J Phys Conf Ser*, vol. 1299, no. 1, p. 012012, 2019, doi: 10.1088/1742-6596/1299/1/012012.
- [21] S. Bhattacharjee *et al.*, “Sustainable materials for 3D concrete printing,” *Cem Concr Compos*, vol. 122, p. 104156, Sep. 2021, doi: 10.1016/J.CEMCONCOMP.2021.104156.
- [22] G. de Schutter, K. Lesage, V. Mechtcherine, V. N. Nerella, G. Habert, and I. Agusti-Juan, “Vision of 3D printing with concrete — Technical, economic and environmental potentials,” *Cem Concr Res*, vol. 112, pp. 25–36, Oct. 2018, doi: 10.1016/J.CEMCONRES.2018.06.001.
- [23] M. Kaszyńska, S. Skibicki, and M. Hoffmann, “3D Concrete Printing for Sustainable Construction,” *Energies (Basel)*, vol. 13, no. 23, 2020, doi: 10.3390/en13236351.
- [24] M. Mahadevan, A. Francis, and A. Thomas, “A simulation-based investigation of sustainability aspects of 3D printed structures,” *Journal of Building Engineering*, vol. 32, p. 101735, Nov. 2020, doi: 10.1016/J.JOBE.2020.101735.
- [25] R. M. Mahdi, “Printed house as a model for future housing,” *IOP Conf Ser Mater Sci Eng*, vol. 1067, no. 1, p. 012035, 2021, doi: 10.1088/1757-899X/1067/1/012035.
- [26] T. D. Ngo, A. Kashani, G. Imbalzano, K. T. Q. Nguyen, and D. Hui, “Additive manufacturing (3D printing): A review of materials, methods, applications and challenges,” *Compos B Eng*, vol. 143, pp. 172–196, Jun. 2018, doi: 10.1016/J.COMPOSITESB.2018.02.012.
- [27] S. Pessoa and A. S. Guimarães, “The 3D printing challenge in buildings,” *E3S Web Conf.*, vol. 172, 2020, [Online]. Available: <https://doi.org/10.1051/e3sconf/202017219005>
- [28] M. Nodehi, T. Ozbakkaloglu, and A. Gholampour, “Effect of supplementary cementitious materials on properties of 3D printed conventional and alkali-activated concrete: A review,” *Autom Constr*, vol. 138, p. 104215, Jun. 2022, doi: 10.1016/J.AUTCON.2022.104215.
- [29] C. R. Rollakanti and C. V. S. R. Prasad, “Applications, performance, challenges and current progress of 3D concrete printing technologies as the future of sustainable construction – A state of the art review,” *Mater Today Proc*, vol. 65, pp. 995–1000, Jan. 2022, doi: 10.1016/J.MATPR.2022.03.619.
- [30] M. T. Souza, I. M. Ferreira, E. Guzi de Moraes, L. Senff, and A. P. Novaes de Oliveira, “3D printed concrete for large-scale buildings: An overview of rheology, printing parameters, chemical admixtures, reinforcements, and economic and environmental prospects,” *Journal of Building Engineering*, vol. 32, p. 101833, Nov. 2020, doi: 10.1016/J.JOBE.2020.101833.
- [31] Y. W. D. Tay, Y. Qian, and M. J. Tan, “Printability region for 3D concrete printing using slump and slump flow test,” *Compos B Eng*, vol. 174, p. 106968, Oct. 2019, doi: 10.1016/J.COMPOSITESB.2019.106968.
- [32] T. Wangler, N. Roussel, F. P. Bos, T. A. M. Salet, and R. J. Flatt, “Digital Concrete: A Review,” *Cem Concr Res*, vol. 123, p. 105780, Sep. 2019, doi: 10.1016/J.CEMCONRES.2019.105780.
- [33] J. Xu *et al.*, “Inspecting manufacturing precision of 3D printed concrete parts based on geometric dimensioning and tolerancing,” *Autom Constr*, vol. 117, p. 103233, Sep. 2020, doi: 10.1016/J.AUTCON.2020.103233.
- [34] G. H. Ahmed, N. H. Askandar, and G. B. Jumaa, “A review of largescale 3DCP: Material characteristics, mix design, printing process, and reinforcement strategies,” *Structures*, vol. 43, pp. 508–532, Sep. 2022, doi: 10.1016/J.ISTRUC.2022.06.068.
- [35] H. Kloft, M. Empelmann, N. Hack, E. Herrmann, and D. Lowke, “Reinforcement strategies for 3D-concrete-printing,” *Civil Engineering Design*, vol. 2, no. 4, pp. 131–139, Aug. 2020, doi: <https://doi.org/10.1002/cend.202000022>.

- [36] W. Lao, M. Li, and T. Tjahjowidodo, "Variable-geometry nozzle for surface quality enhancement in 3D concrete printing," *Addit Manuf*, vol. 37, p. 101638, Jan. 2021, doi: 10.1016/J.ADDMA.2020.101638.
- [37] V. Mechtcherine, V. N. Nerella, F. Will, M. Näther, J. Otto, and M. Krause, "Large-scale digital concrete construction – CONPrint3D concept for on-site, monolithic 3D-printing," *Autom Constr*, vol. 107, p. 102933, Nov. 2019, doi: 10.1016/J.AUTCON.2019.102933.
- [38] R. A. Buswell, R. C. Soar, A. G. F. Gibb, and A. Thorpe, "Freeform Construction: Mega-scale Rapid Manufacturing for construction," *Autom Constr*, vol. 16, no. 2, pp. 224–231, Mar. 2007, doi: 10.1016/J.AUTCON.2006.05.002.
- [39] N. O. E. Olsson, E. Arica, R. Woods, and J. A. Madrid, "Industry 4.0 in a project context: Introducing 3D printing in construction projects," *Project Leadership and Society*, vol. 2, p. 100033, Dec. 2021, doi: 10.1016/J.PLAS.2021.100033.
- [40] R. Buswell *et al.*, "Geometric quality assurance for 3D concrete printing and hybrid construction manufacturing using a standardised test part for benchmarking capability," *Cem Concr Res*, vol. 156, p. 106773, Jun. 2022, doi: 10.1016/J.CEMCONRES.2022.106773.
- [41] P. Bedarf, A. Dutto, M. Zanini, and B. Dillenburger, "Foam 3D printing for construction: A review of applications, materials, and processes," *Autom Constr*, vol. 130, p. 103861, Oct. 2021, doi: 10.1016/J.AUTCON.2021.103861.
- [42] L. Gebhard *et al.*, "Towards efficient concrete structures with ultra-thin 3D printed formwork: exploring reinforcement strategies and optimisation," *Virtual Phys Prototyp*, vol. 17, no. 3, pp. 599–616, Jul. 2022, doi: 10.1080/17452759.2022.2041873.
- [43] S. A. Khan, M. Koç, and S. G. Al-Ghamdi, "Sustainability assessment, potentials and challenges of 3D printed concrete structures: A systematic review for built environmental applications," *J Clean Prod*, vol. 303, p. 127027, Jun. 2021, doi: 10.1016/J.JCLEPRO.2021.127027.
- [44] A. O. Afolabi, R. A. Ojelabi, I. O. Omuh, and P. F. Tunji-Olayeni, "3D House Printing: A sustainable housing solution for Nigeria's housing needs," *J Phys Conf Ser*, vol. 1299, no. 1, p. 012012, 2019, doi: 10.1088/1742-6596/1299/1/012012.
- [45] F. Hamidi and F. Aslani, "Additive manufacturing of cementitious composites: Materials, methods, potentials, and challenges," *Constr Build Mater*, vol. 218, pp. 582–609, Sep. 2019, doi: 10.1016/J.CONBUILDMAT.2019.05.140.
- [46] F. Heidarneshad and Q. Zhang, "Shotcrete based 3D concrete printing: State of art, challenges, and opportunities," *Constr Build Mater*, vol. 323, p. 126545, Mar. 2022, doi: 10.1016/J.CONBUILDMAT.2022.126545.
- [47] S. Geetha, M. Selvakumar, and S. M. Lakshmi, "3D concrete printing matrix reinforced with Geogrid," *Mater Today Proc*, vol. 49, pp. 1443–1447, Jan. 2022, doi: 10.1016/J.MATPR.2021.07.212.
- [48] M. Tramontin Souza *et al.*, "Role of chemical admixtures on 3D printed Portland cement: Assessing rheology and buildability," *Constr Build Mater*, vol. 314, p. 125666, Jan. 2022, doi: 10.1016/J.CONBUILDMAT.2021.125666.
- [49] D. Lowke, E. Dini, A. Perrot, D. Weger, C. Gehlen, and B. Dillenburger, "Particle-bed 3D printing in concrete construction – Possibilities and challenges," *Cem Concr Res*, vol. 112, pp. 50–65, Oct. 2018, doi: 10.1016/J.CEMCONRES.2018.05.018.
- [50] N. Muhammad Salman, G. Ma, N. Ijaz, and L. Wang, "Importance and potential of cellulosic materials and derivatives in extrusion-based 3D concrete printing (3DCP): Prospects and challenges," *Constr Build Mater*, vol. 291, p. 123281, Jul. 2021, doi: 10.1016/J.CONBUILDMAT.2021.123281.
- [51] N. Ashrafi, S. Nazarian, N. A. Meisel, and J. P. Duarte, "Experimental prediction of material deformation in large-scale additive manufacturing of concrete," *Addit Manuf*, vol. 37, p. 101656, Jan. 2021, doi: 10.1016/J.ADDMA.2020.101656.
- [52] A. Radomska-Zalas, "The AHP method in the optimization of the epoxidation of allylic alcohols," *Procedia Comput Sci*, vol. 207, pp. 456–464, Jan. 2022, doi: 10.1016/J.PROCS.2022.09.100.
- [53] S. H. Hashemi Petrucci, H. Ghomi, and M. Mazaheriasad, "An Integrated Fuzzy Delphi and Best Worst Method (BWM) for performance measurement in higher education," *Decision Analytics Journal*, vol. 4, p. 100121, Sep. 2022, doi: 10.1016/J.DAJOUR.2022.100121.
- [54] R. Mahmoudi, S. N. Shetab-Boushehri, S. R. Hejazi, and A. Emrouznejad, "Determining the relative importance of sustainability evaluation criteria of urban transportation network," *Sustain Cities Soc*, vol. 47, p. 101493, May 2019, doi: 10.1016/J.SCS.2019.101493.

Crack Detection and Localization in Stone Floor Tiles using Vision Transformer approach

Luqman Ali ^{a,e,f}, Hamad Aljassmi ^{b,f}, Medha Mohan Ambali Parambil ^{c,e}, Muhammed Swavaf ^{a,e},
Mohammed AlAmeri ^d, Fady Alnajjar ^{a,f,*}

^aDepartment of Computer Science and Software Engineering, College of IT, United Arab Emirates University (UAEU), Al Ain 15551, UAE

^bDepartment of Civil Engineering, College of Engineering, UAEU, Al Ain 15551, UAE

^cDepartment of Information Systems and Security, College of IT, UAEU, Al Ain 15551, UAE

^dDepartment of Electrical Engineering, College of Engineering, UAEU, Al Ain 15551, UAE

^eAI and Robotics Lab (Air-Lab), UAEU, Al Ain 15551, United Arab Emirates

^fEmirates Center for Mobility Research, UAEU, Al Ain 15551, United Arab Emirates

E-mail: 201990024@uaeu.ac.ae; h.aljassmi@uaeu.ac.ae; medhamohanap@uaeu.ac.ae;
swavafup@uaeu.ac.ae; 201731009@uaeu.ac.ae; fady.alnajjar@uaeu.ac.ae

Abstract

Cracks are the initial indicators of the deterioration of any civil infrastructure. Structures are typically monitored manually by inspectors, which is time-consuming, laborious, costly, and easily prone to human error. To address these limitations this paper aims to present a vision transformer-based stone floor tiles crack detection and localization approach. The proposed model is trained on a custom dataset acquired from various stone tiles under various illumination conditions in the United Arab Emirates. The dataset consists of 5800 images having a resolution of 224×224 pixels. To assess the effectiveness of the proposed model, various evaluation metrics such as testing accuracy, precision, recall, F1 score, and computational time are employed to analyze its performance. The input patch size of the Vision Transformer (ViT) model is varied to investigate its effect on the performance of the model. The experimental results show that input patch size has a significant on the performance of the models. The ViT model trained on the lowest patch size of 14×14 pixels achieved the highest testing accuracy, precision, recall, and F1 score of 0.8612, 0.8840, 0.8304, and 0.8564 respectively. The inference time of the ViT model for a single patch is 0.092 sec. The crack localization is performed by combining the proposed trained ViT model with the sliding window approach. The model performed well in detecting and locating cracks in stone floor tiles, indicating its potential for practical use.

Keywords

Structural Health Monitoring; Crack Detection; Vision Transformer; Sliding Window Approach; Stone floor; automatic inspection.

1 Introduction

In structural health monitoring, it is important to detect and monitor surface cracks early for long-term maintenance and failure prediction. The structure's condition information can be collected manually by subjective human experts by visually inspecting and evaluating the structure or automatically by using various vision-based approaches. Manual Inspection techniques are laborious, time-consuming, inspector dependent, and easily vulnerable to the perspicacity of the inspector. In addition, numerous studies have demonstrated the inherent variability and inconsistency of visual inspection results [1], [2]. Inadequate inspection and condition assessment can result in various accidents, such as the Minneapolis Interstate 35W Bridge Collapse, which resulted in 13 fatalities and 145 injuries [3]. Another example is the November 28, 1999, incident involving a freight train in Japan's Reibunhama Tunnel, which occurred because shear cracks in the structure were not correctly detected [4]. Automatic inspection techniques provide an efficient solution by reducing subjectivity and providing a substitute for the human eye to circumvent the issues associated with manual inspection. The automatic vision-based crack detection approaches can be divided into traditional image processing, Machine Learning (ML), and Deep Learning (DL)-based approaches. The conventional image processing approaches include various edge detection [5], thresholding [6], and filtering approaches [7]–[10] however these approaches cannot show resilience to image illumination and require manual human efforts. Machine learning approaches have the capability to overcome the limitation associated with conventional crack detection approaches. Machine learning

approaches consist of feature extraction i.e., extracting useful features [11]–[13] from images, and classification i.e., classifying the feature into crack and non-cracks using classifiers [14]–[16]. The limitation of the machine learning approaches is the manual selection of feature extraction techniques which is not only challenging but sometimes the extracted features did not represent the actual cracks. These limitations can be addressed by using DL algorithms that are capable of automatic feature extraction and classification. DL algorithms are particularly effective in detecting features in images because they can automatically learn the feature representations from the data itself. Various works [17]–[21] have been presented in the literature using various DL based Convolutional Neural Network (CNN) models for crack detection in civil structures. However, these approaches suffer from localized receptive field problems in which the feature are not extracted in a global context. Vision transformers are a relatively new type of neural network that have shown promising results in image classification tasks, including crack detection. Several research studies have proposed using vision transformers to overcome the limitations of traditional methods in detecting and segmenting cracks [22]–[24]. Vision transformers are particularly effective due to their ability to capture long-range dependencies in images using self-attention mechanisms [25]. Therefore, this paper aims to present a vision transformer-based crack detection in stone floor tiles. The contribution of the proposed work is as follows:

1. A custom dataset of 5800 stone floor tiles with crack and non-crack images having a resolution of 224×224 is created.
2. A first ViT-based framework is proposed for crack detection in stone floor tiles.
3. The performance of the proposed ViT is compared based on various input patch sizes to select an optimum input patch size.

4. Based on the results, a detailed discussion is conducted to provide a reference to a researcher working in the same field.

The remainder of the paper is organized as follows. Section 2 explains the system overview. The experimental results are discussed in section 3 followed by a discussion and conclusion in the last section.

2 System Overview

The proposed ViT-based stone floor tile crack detection system is composed of three main phases, as shown in Figure 1. A dataset is constructed in the first phase, which is subsequently provided to ViT transformer for training. The final section phase of the proposed method involves testing the system after training and performing crack localization using a sliding window approach.

2.1 Dataset Creation

In the proposed work, the data is collected from a variety of stone floor tiles used in the United Arab Emirates. A mobile phone camera with a resolution of 4000×3000 pixels is used for the acquisition of images. The acquired images are divided into small patches of 224×224 pixels. In order to separate the acquired data into cracks and non-cracks, manual labeling is performed. A total of 5800 patches are distributed 50/50 between cracks and non-cracks. Figure 2 below shows sample images of the acquired dataset and patches. A data split of 60:20:20 is kept between the patches for training, validation, and testing of the proposed ViT model. The 60:20:20 split provides a balance between using enough data to train the model effectively, tune the hyperparameters of the model, while also ensuring that the model's performance is reliable on new data.

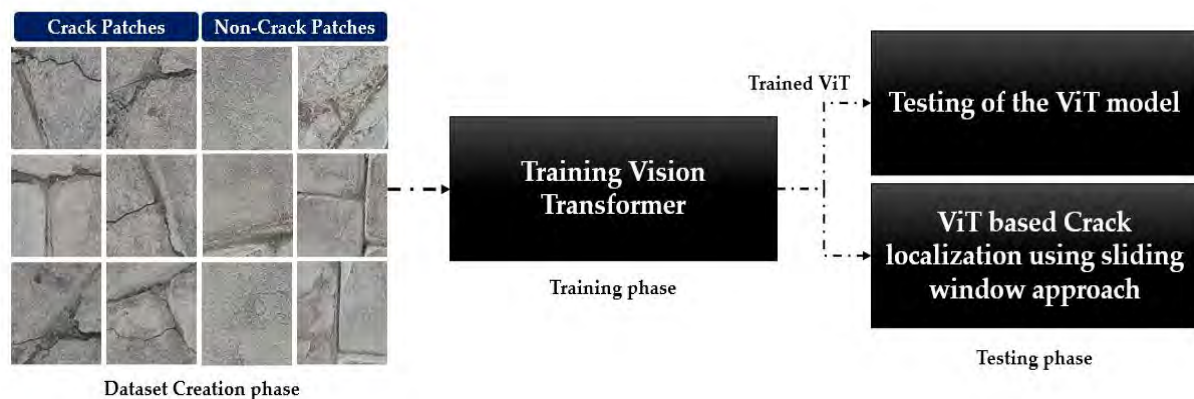


Figure 1. Overview of the proposed system

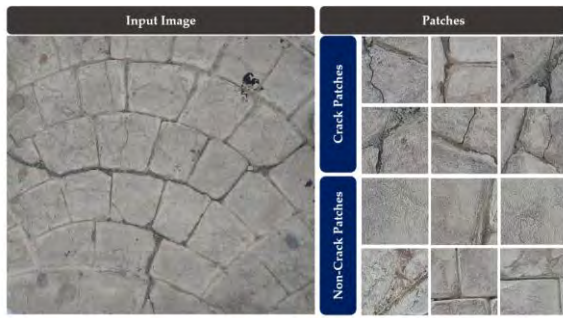


Figure 2. Sample of the acquired image and input patches (Crack and Non-Crack)

2.2 Training of the ViT Model

The data created in the previous phase is given to the ViT model for training purposes. The vision transformer model is first developed by [26] and can overcome the shortcoming of the DL approaches by considering the input images as a series of patches. The schematic diagram of the vision transformer is shown in Figure 03. ViT architecture consists of an embedding layer, an encoder, and a final head classifier. The embedding layers divide an image X from the training set into patches without overlap where each patch is considered a unique token. In the encoder part of the vision transformer, multi-head self-attention (MHSA) is used to extract and integrates information globally across multiple regions of the images whereas traditional CNN uses filters with a local receptive field. This acquired

information is encoded and fed into a multilayer perceptron classifier for classification purposes. Interested readers are referred to [26] for more information about the working of the vision transformer. In the proposed work, the ViT model is trained on various patch sizes i.e., 14×14 , 21×21 , 28×28 , and 56×56 to evaluate its effect on the crack detection performance of the ViT model. The hyperparameters are tuned based on trial and error basis. During the hyperparameters tuning stage of the model the learning rate, transformer layers, batch size, and the number of epochs is set to 0.001, 16, 16, and 40 respectively.

2.3 Testing of ViT classifier

The trained ViT classifier is tested with a new set of data that is not used in the training and validation phase of the model. The trained ViT model is also integrated with the sliding window approach to localize the crack region in the images. In the sliding window approach, a window size of 224×224 equal to the input patch size is considered. The single window patch is given to the trained ViT model to identify the crack and non-crack patches. The sliding window moves over 224 pixels horizontally and vertically until the whole image is covered. A red bounding box is drawn around the patch classified as a crack by the ViT model as depicted in Figure 4. Interested readers are referred to [27] for more information about the working of the sliding window approach.

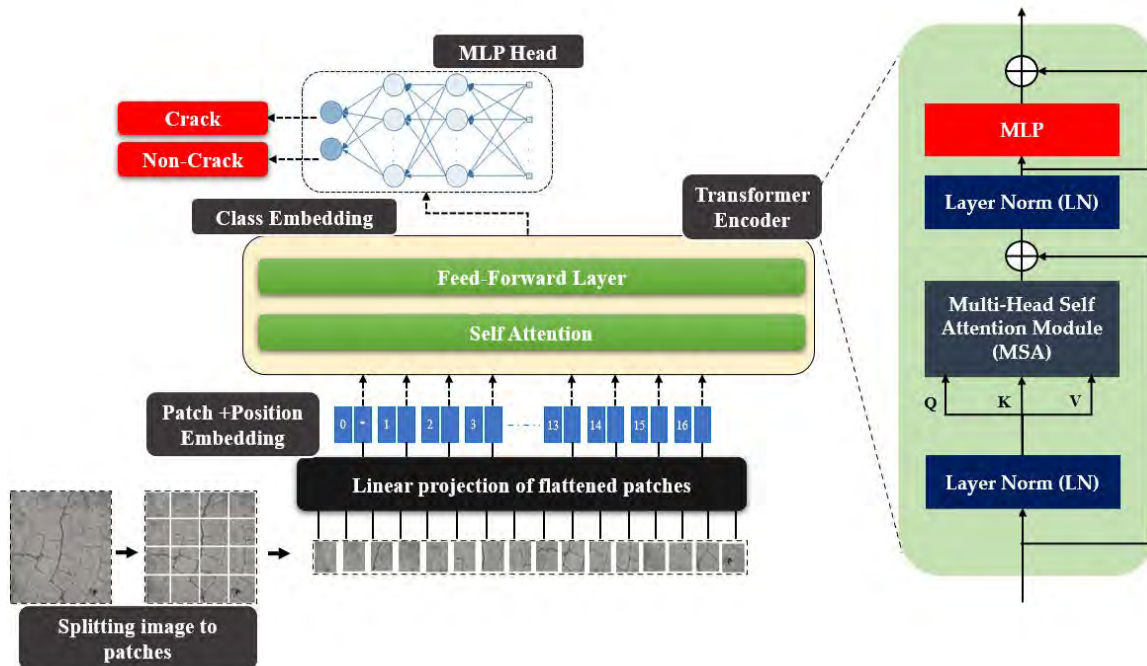


Figure 3. Schematic diagram of vision transformer.

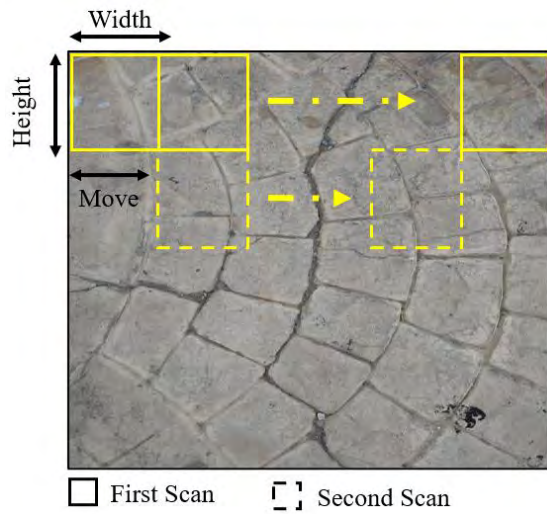


Figure 4. Representation of sliding window approach.

2.4 Evaluation Metrics

To evaluate the performance of the proposed crack detection model, several standard evaluation metrics, including accuracy, precision, recall, and F1 score (depicted in Equation 1, 2, 3, and 4 respectively) are used. Accuracy measures the proportion of correctly classified samples (both cracked and non-cracked) among all samples in the dataset.

$$\text{Accuracy} = \frac{(TP + TN)}{(TP + TN + FP + FN)} \quad (1)$$

Where TP, TN, FP, and FN represent the true positives, true negatives, false positives, and false negatives respectively. Precision measures the proportion of correctly classified cracked samples among all samples classified as cracked.

$$\text{Precision} = \frac{TP}{(TP + FP)} \quad (2)$$

Recall measures the proportion of correctly classified cracked samples among all true positive samples in the dataset.

$$\text{Recall} = \frac{TP}{(TP + FN)} \quad (3)$$

F1 score is the harmonic mean of precision and recall, and is often used to balance the trade-off between the two metrics.

$$\text{F1 score} = \frac{2 * ((\text{Precision} * \text{Recall}) / (\text{Precision} + \text{Recall}))}{1} \quad (4)$$

3 Experimental Results

The proposed ViT model is trained on Alienware Arura R8 core i9-9900k desktop system, CPU @3.60

GHz with 32 GB RAM and an NVIDIA GeForce RTX 2080 GPU. The performance of the model is evaluated on evaluation metrics i.e., ViT patch size, testing accuracy, precision, recall, and F1 score. The patch size of the ViT model is varied from smaller (14*14) pixels to larger (56*56) pixels to study its effect on the performance of the model. The number of epochs for training the model is considered 40 as there is no further increase in the accuracy and a decrease in the model loss after the 40th epoch. As shown in Table 1, the performance metrics of the ViT model are compatible and an accuracy of more than 80% is achieved for all patch sizes.

Table 1. Overall Results of the ViT model on various patch sizes

Patch Size	Testing Accuracy	Recall	Precision	F1 Score
14*14	0.8612	0.8840	0.8304	0.8564
21*21	0.8474	0.8613	0.8270	0.8438
28*28	0.8414	0.8518	0.8253	0.8383
56*56	0.8103	0.7896	0.8443	0.8161

Additionally, as shown in Figures 5, 6, 7, and 8, the training and validation curves (accuracy and loss) show slight divergence, which implies that the model has not been overfitted. Keeping the transformer patch size of 14*14, the ViT model achieved the highest testing accuracy, precision, recall, and F1 score of 0.8612, 0.8840, 0.8404, and 0.8564 respectively. Increasing the patch size to 21*21 pixels, the accuracy, precision, recall, and F1 scores decreased by 1.38, 2.27, 0.34, and 1.26% respectively. Further increasing the patch size to 28*28 pixels an accuracy of 0.8414, precision of 0.8518, recall of 0.8253, and F1 score of 0.8383 respectively. The lowest testing accuracy, precision, recall, and F1 score of 0.8103, 0.7896, 0.8443, and 0.8161 is recorded by the ViT model using the patch size of 52*52. The proposed model trained on a small patch size of 14*14 outperforms all the others in terms of all evaluation metrics. The confusion metrics of the model based on various patch size and number of parameters is depicted in Table 2.

The ViT model is then integrated with the sliding window approach for crack localization purposes in stone floor tiles. Testing images having a resolution of 1120*2240 acquired in various lightning conditions are taken. Using the sliding window approach, the test image is divided into 50 equal patches of size 224*224. Each patch is given to the trained ViT model to decide whether

it belongs to the crack class or not. The patch classified as a crack is represented by a red bounding box as shown in Figure 9. The whole image and single patch inference time of the ViT model are recorded to be 4.624 sec and 0.092 sec respectively. The black boxes in Figure 9 represent the False Positives. The False negative patches did not exist as the system has the capability to correctly identified the crack region however the greater number of FP is due to the similarity of the grout lines to crack regions. The number of FP can be decreased by increasing the number of training data.

Table 2. Patch size Vs No of parameters and Performance

PS	NOP (Millions)	Confusion Matrices		
		Class	Crk	N-Crk
14*14	36.51	Crk	480	98
		N-Crk	63	519
		Class	Crk	N-Crk
21*21	16.10	Crk	478	100
		N-Crk	77	505
		Class	Crk	N-Crk
28*28	11.44	Crk	477	101
		N-Crk	83	499
		Class	Crk	N-Crk
56*56	5.71	Crk	480	90
		N-Crk	130	452
		Class	Crk	N-Crk

*PS: Patch Size, *NOP: Number of parameters, *Crk: Crack, *N-Crk: Non-Crack

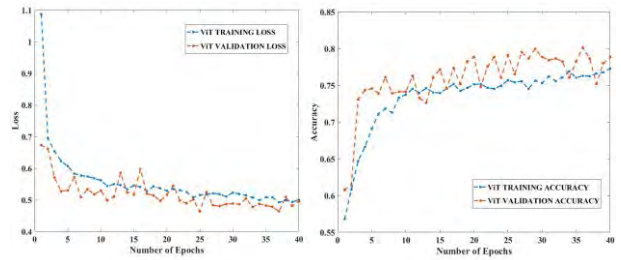


Figure 5. Training and validation (a) loss (b) Accuracy graphs of ViT model (14*14)

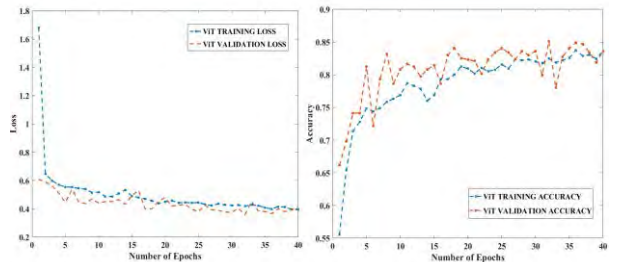


Figure 6. Training and validation (a) loss (b) Accuracy graphs of ViT model (21*21)

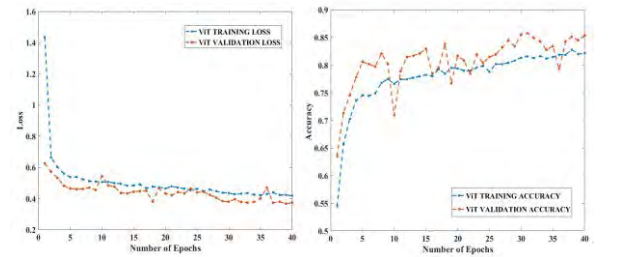


Figure 7. Training and validation (a) loss (b) Accuracy graphs of ViT model (28*28)

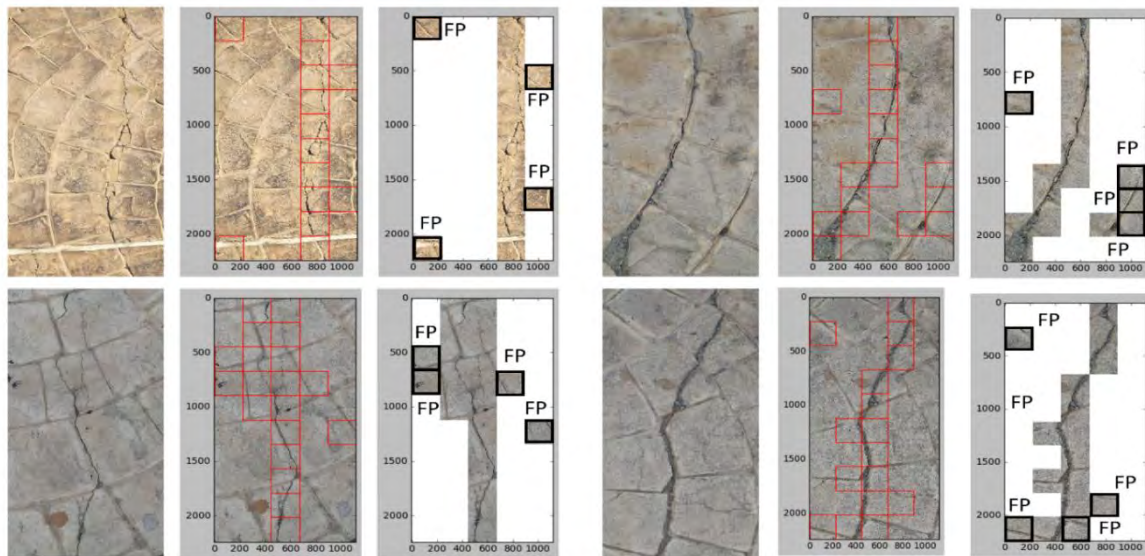


Figure 9. Crack localization and scanning for FP and FN using the sliding window approach.

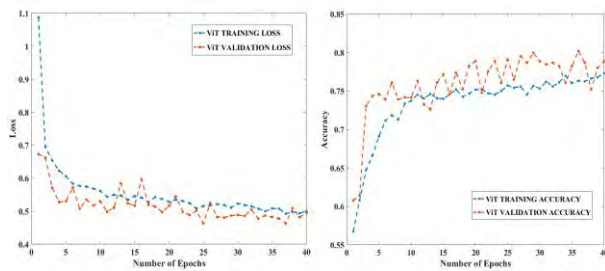


Figure 8. Training and validation (a) loss (b) Accuracy graphs of ViT model (56*56)

4 Discussion and Conclusion

This paper proposed a ViT-based framework for crack detection and localization in stone floor tiles. The performance of the proposed ViT model is compared to various input patch sizes. The experimental results showed that input patch size has a significant effect on the crack detection performance of the models. The model showed high crack detection performance on the lowest patch size. The performance of the model degraded as the patch size increased. It is also noted that decreasing the input patch increases the number of parameters of the ViT model which leads to an increase in the computational time and complexity of the model. The result of the crack localization in Figure 09 shows no FN and a small number of FP which shows that the model has the capability to localize the crack efficiently.

From the above discussion, it can be concluded that the ViT transformer integrated with the sliding window approach can be used to perform crack detection and localization in stone floor tiles. The ViT's ability to acquire global-scale features from the input image makes the task of crack detection. It can also be concluded that ViT transformers can be used for crack detection in various civil infrastructures i.e., pavement, concrete, bridges, and so on. Overall, the proposed ViT-based stone floor tiles crack detection method will enable Pavement inspection departments to automatically inspect the civil structure frequently. In the future, we are planning to add more data to the dataset to improve the accuracy of the proposed method.

References

[1] B. A. Graybeal, B. M. Phares, D. D. Rolander, M. Moore, and G. Washer, "Visual Inspection of Highway Bridges," *Journal of Nondestructive Evaluation*, vol. 21, no. 3, pp. 67–83, Sep. 2002, doi: 10.1023/A:1022508121821.

[2] B. M. Phares, G. A. Washer, D. D. Rolander, B. A. Graybeal, and M. Moore, "Routine Highway Bridge Inspection Condition Documentation Accuracy and Reliability," *Journal of Bridge*

Engineering, vol. 9, no. 4, pp. 403–413, Jul. 2004, doi: 10.1061/(ASCE)1084-0702(2004)9:4(403).

[3] "Minneapolis Interstate 35W Bridge Collapse - Minnesota Issues Resources Guides." <https://www.lrl.mn.gov/guides/guides?issue=bridges> (accessed Apr. 04, 2022).

[4] T. Asakura and Y. Kojima, "Tunnel maintenance in Japan," *Tunnelling and Underground Space Technology*, vol. 18, no. 2, pp. 161–169, Apr. 2003, doi: 10.1016/S0886-7798(03)00024-5.

[5] I. Abdel-Qader, O. Abudayyeh, and M. E. Kelly, "Analysis of Edge-Detection Techniques for Crack Identification in Bridges," *Journal of Computing in Civil Engineering*, vol. 17, no. 4, pp. 255–263, Oct. 2003, doi: 10.1061/(ASCE)0887-3801(2003)17:4(255).

[6] M. Kamaliardakani, L. Sun, and M. K. Ardakani, "Sealed-Crack Detection Algorithm Using Heuristic Thresholding Approach," *Journal of Computing in Civil Engineering*, vol. 30, no. 1, p. 04014110, Jan. 2016, doi: 10.1061/(ASCE)CP.1943-5487.0000447.

[7] S. K. Sinha and P. W. Fieguth, "Morphological segmentation and classification of underground pipe images," *Machine Vision and Applications*, vol. 17, no. 1, pp. 21–31, Apr. 2006, doi: 10.1007/s00138-005-0012-0.

[8] S. K. Sinha and P. W. Fieguth, "Automated detection of cracks in buried concrete pipe images," *Automation in Construction*, vol. 15, no. 1, pp. 58–72, Jan. 2006, doi: 10.1016/j.autcon.2005.02.006.

[9] S. Chambon, P. Subirats, and J. Dumoulin, "Introduction of a wavelet transform based on 2D matched filter in a Markov Random Field for fine structure extraction: Application on road crack detection," *Proceedings of SPIE - The International Society for Optical Engineering*, vol. 7251, Feb. 2009, doi: 10.1117/12.805437.

[10] Y. Fujita and Y. Hamamoto, "A robust automatic crack detection method from noisy concrete surfaces," *Machine Vision and Applications*, vol. 22, no. 2, pp. 245–254, Mar. 2011, doi: 10.1007/s00138-009-0244-5.

[11] I. Abdel-Qader, S. Pashaie-Rad, O. Abudayyeh, and S. Yehia, "PCA-Based algorithm for unsupervised bridge crack detection," *Advances in Engineering Software*, vol. 37, no. 12, pp. 771–778, Dec. 2006, doi: 10.1016/j.advengsoft.2006.06.002.

[12] X. Q. Zhu and S. S. Law, "Wavelet-based crack identification of bridge beam from operational deflection time history," *International Journal of Solids and Structures*, vol. 43, no. 7, pp. 2299–2317, Apr. 2006, doi: 10.1016/j.ijsolstr.2005.07.024.

- [13] X. Zhou, L. Xu, and J. Wang, "Road crack edge detection based on wavelet transform," *IOP Conf. Ser.: Earth Environ. Sci.*, vol. 237, no. 3, p. 032132, Feb. 2019, doi: 10.1088/1755-1315/237/3/032132.
- [14] L. Ali, F. Alnajjar, N. Zaki, and H. Aljassmi, "Pavement Crack Detection by Convolutional AdaBoost Architecture: 8th Zero Energy Mass Custom Home International Conference, ZEMCH 2021," *ZEMCH 2021 - 8th Zero Energy Mass Custom Home International Conference, Proceedings*, pp. 383–394, 2021.
- [15] L. Ali, S. Harous, N. Zaki, W. Khan, F. Alnajjar, and H. A. Jassmi, "Performance Evaluation of different Algorithms for Crack Detection in Concrete Structures," in *2021 2nd International Conference on Computation, Automation and Knowledge Management (ICCAKM)*, Jan. 2021, pp. 53–58. doi: 10.1109/ICCAKM50778.2021.9357717.
- [16] K. Chaiyasarn, W. Khan, L. Ali, M. Sharma, D. Brackenbury, and M. DeJong, "Crack Detection in Masonry Structures using Convolutional Neural Networks and Support Vector Machines," Jul. 2018. doi: 10.22260/ISARC2018/0016.
- [17] L. Ali, N. K. Valappil, D. N. A. Kareem, M. J. John, and H. A. Jassmi, "Pavement Crack Detection and Localization using Convolutional Neural Networks (CNNs)," in *2019 International Conference on Digitization (ICD)*, Nov. 2019, pp. 217–221. doi: 10.1109/ICD47981.2019.9105786.
- [18] L. Ali, F. Sallabi, W. Khan, F. Alnajjar, and H. Aljassmi, "A deep learning-based multi-model ensemble method for crack detection in concrete structures," *ISARC Proceedings*, pp. 410–418, Nov. 2021.
- [19] L. Ali, F. Alnajjar, W. Khan, M. A. Serhani, and H. Al Jassmi, "Bibliometric Analysis and Review of Deep Learning-Based Crack Detection Literature Published between 2010 and 2022," *Buildings*, vol. 12, no. 4, Art. no. 4, Apr. 2022, doi: 10.3390/buildings12040432.
- [20] L. Ali, F. Alnajjar, H. A. Jassmi, M. Gocho, W. Khan, and M. A. Serhani, "Performance Evaluation of Deep CNN-Based Crack Detection and Localization Techniques for Concrete Structures," *Sensors*, vol. 21, no. 5, Art. no. 5, Jan. 2021, doi: 10.3390/s21051688.
- [21] F.-C. Chen and M. R. Jahanshahi, "NB-CNN: Deep Learning-Based Crack Detection Using Convolutional Neural Network and Naïve Bayes Data Fusion," *IEEE Transactions on Industrial Electronics*, vol. 65, no. 5, pp. 4392–4400, May 2018, doi: 10.1109/TIE.2017.2764844.
- [22] E. Asadi Shamsabadi, C. Xu, A. S. Rao, T. Nguyen, T. Ngo, and D. Dias-da-Costa, "Vision transformer-based autonomous crack detection on asphalt and concrete surfaces," *Automation in Construction*, vol. 140, p. 104316, Aug. 2022, doi: 10.1016/j.autcon.2022.104316.
- [23] L. Ali, H. A. Jassmi, W. Khan, and F. Alnajjar, "Crack45K: Integration of Vision Transformer with Tubularity Flow Field (TuFF) and Sliding-Window Approach for Crack-Segmentation in Pavement Structures," *Buildings*, vol. 13, no. 1, Art. no. 1, Jan. 2023, doi: 10.3390/buildings13010055.
- [24] S. Wang, X. Chen, and Q. Dong, "Detection of Asphalt Pavement Cracks Based on Vision Transformer Improved YOLO V5," *Journal of Transportation Engineering, Part B: Pavements*, vol. 149, no. 2, p. 04023004, Jun. 2023, doi: 10.1061/JPEODX.PVENG-1180.
- [25] K. Han *et al.*, "A Survey on Vision Transformer," *IEEE Trans. Pattern Anal. Mach. Intell.*, vol. 45, no. 1, pp. 87–110, Jan. 2023, doi: 10.1109/TPAMI.2022.3152247.
- [26] A. Dosovitskiy *et al.*, "An Image is Worth 16x16 Words: Transformers for Image Recognition at Scale." arXiv, Jun. 03, 2021. doi: 10.48550/arXiv.2010.11929.
- [27] J. Lee, J. Bang, and S.-I. Yang, "Object detection with sliding window in images including multiple similar objects," in *2017 International Conference on Information and Communication Technology Convergence (ICTC)*, Oct. 2017, pp. 803–806. doi: 10.1109/ICTC.2017.8190786.

Integrating Building Information Modeling, Deep Learning, and Web Map Service for Sustainable Post-Disaster Building Recovery Planning

Adrianto Oktavianus¹, Po-Han Chen^{1,2} and Jacob J. Lin¹

¹Department of Civil Engineering, National Taiwan University, Taipei, Taiwan.

²Department of Building, Civil & Environmental Engineering, Concordia University, Montreal, Canada.
d09521030@ntu.edu.tw, pohan.chen@concordia.ca, jacoblin@ntu.edu.tw

Abstract

Building recovery is always a major issue after disasters due to the urgent need for efficient assessment of damaged buildings and effective management of required resources. At the same time, it is necessary that building recovery planning considers the impact of used materials on the environment as well as the proper allocation of budgets. In this paper, we propose a novel integrated post-disaster building recovery planning system that utilizes Building Information Modeling (BIM), Deep Learning (DL), and Web Map Service (WMS). BIM provides 3D models and detailed information for buildings; DL enhances the accuracy and efficiency of building assessment; WMS generates reliable data on locations and for route planning. The BIM-DL-WMS integration would contribute significantly to building recovery planning by automating building element assessment, cost estimation, and carbon emission analysis for repair/retrofit materials and material delivery. This developed system would make post-disaster building recovery planning more efficient, effective, and sustainable. The framework of the BIM-DL-WMS system is elaborated on in detail in this paper. The implementation of the system could be applied to not only single-building recovery planning but also the recovery planning of a district or even a town or city.

Keywords –

Building Information Modeling; Deep Learning; Web Map Service; Post-Disaster Building Recovery

1 Introduction and Background

The report published by the UN Office for Disaster Risk Reduction in 2020 [1] showed an increasing number of disasters in the past two decades, which led to more attention and efforts in pre- and post-disaster research. Building recovery is a post-disaster phase that requires

attention and is as important as other post-disaster phases like mitigation and emergency response. In the building recovery phase, various problems related to building assessment and building rehabilitation arise due to unintegrated data and poor management. These problems sometimes lead to delays in handling building damages and cause some of them to be abandoned in the end, for the government or building owners are unable to make timely decisions with adequate data. Therefore, it is necessary to develop an integrated post-disaster building recovery planning system to tackle these problems and help stakeholders resolve the problems.

At the same time, decarbonization has become a major concern nowadays in construction, due to an increasing awareness for sustainability. According to UNEP [2], the building and construction sector was responsible for over 34% of global energy consumption and 37% of global energy- and process-related CO₂ emissions in 2021, with building materials contributing to around 9% of overall energy-related CO₂ emissions. To meet the sustainability goal, minimization of carbon emission should be considered in the selection of rehabilitation methods, whether repair or retrofit, in post-disaster building recovery planning. The selection of materials, energy consumption of construction activities, and transportation means for material delivery should all be considered.

Building Information Modeling (BIM) could provide 3D models and relevant building elements data, and these data could be easily integrated with other data or software via an Application Programming Interface (API). Deep Learning (DL) has been proven to be an effective artificial intelligence tool, and has been used to classify building damages and recognize building element damages. The Geographic Information System (GIS)-based Web Map Service (WMS) could provide fairly reliable information on locations, distance calculation and transportation route planning, and the WMS API enables WMS to interoperate with other applications. In view of these advantages, this study integrates BIM, DL

and WMS to propose a sustainability-oriented post-disaster building recovery planning system. The framework of the proposed system and an example are presented in this paper. The application of the system could be a single damaged building, a damaged block, a district, or even a city.

2 Literature Review

The literature review in this paper covers four areas: (1) Post-disaster building recovery; (2) Decarbonization for sustainability in post-disaster building recovery; (3) Integration of Building Information Modeling (BIM) and Deep Learning (DL) in building assessment; and (4) Potential of BIM and Web Map Service (WMS) applications for decarbonization in building recovery. They are elaborated on in detail below.

2.1 Post-Disaster Building Recovery

In the post-disaster stage, building recovery is an important phase to be carried out as a continuation after the emergency response phase [3]. Building recovery has some functions, including identifying a disaster's physical impact and proposing a rehabilitation design [4]. Building assessment and rehabilitation design are essential activities of building recovery to support the decision-making for recovery execution strategies.

Some researchers divided damage assessment for buildings into three levels [5, 6]. The first level is a rapid assessment that evaluates the impact of damage based on the visual appearance of the exterior of a building and the condition of its surroundings. The second level is a detailed assessment that evaluates the damaged elements of the building from the exterior and interior of the building based on visual inspection parameters. At this level, moderate and light damages will be repaired. For severe damages or the third level, in-depth analysis is required and structural analysis will be conducted based on some tests of the existing strength of the building.

Building rehabilitation design focuses on repair and retrofit methods. The determination of repair and retrofit methods considers the damage conditions and building performance requirements based on design codes. The selection of materials for repair and retrofit, quantity take-off, and cost estimation are carried out under building rehabilitation design.

Several studies have developed several frameworks regarding the use of technology in post-disaster recovery. For example, Baarimah et al. [7] propose a comprehensive framework for integrating BIM adoption for post-disaster recovery projects by connecting the components with stakeholders. Meanwhile, several other studies have developed a BIM-based framework related to the virtual construction permitting process [8] and blockchain technology [9] in post-disaster recovery.

However, there needs to be a gap in developing a framework that integrates BIM with Web Map Service and uses deep learning in post-disaster building recovery.

2.2 Decarbonization for Sustainability in Post-Disaster Building Recovery

Sustainability during building construction refers to all construction activities and processes that have the least harmful environmental and social impacts [10]. Decarbonization is one way to achieve the sustainability goal, which represents an alternative way of working that reduces carbon emissions. In the building sector, decarbonization can be achieved through the production of more efficient building materials, the use of more environmentally friendly materials, and reduced energy consumption [11].

In the case of construction activities in buildings, the approach to analyzing the impact of carbon emissions uses the calculation of carbon emissions in materials, energy consumption, and transportation [12-14]. Calculation of carbon emissions in materials is done by calculating embodied carbon materials as a representation of material production. For activities on the construction site, the calculation of carbon emissions takes account of the use of tools in cleaning activities, installation of supporting equipment, repair and retrofit activities. Also, transportation carbon impact analysis is used as an approach to calculating carbon emissions produced for the delivery of materials and equipment by suppliers.

The above could be implemented in post-disaster building recovery planning. Building recovery planning should consider selecting lower-carbon repair and retrofit materials, using equipment that produces less energy, using supporting tools to strengthen structural elements more efficiently, and transporting materials using more environmentally friendly modes of transportation over shorter distances. Lu and Xu [15] asserted that post-disaster reconstruction could provide a unique opportunity to migrate to a low-carbon mode and move forward with sustainable development.

2.3 Integration of BIM and DL in Building Assessment

Deep Learning (DL) applications have become an interesting topic in the construction sector during the last few years. DL comes with the capability to automate tasks for object recognition, data processing and process monitoring [16]. This predictive capability also supports more accurate object detection, detection of possible impacts and decision-making. These DL capabilities have also been applied to building assessments to date.

In building assessment, DL can be applied for many purposes, e.g. to classify collapsed buildings, classify the

level of damage to buildings, classify the type of damage, identify building elements, and recognize areas of damage through images. Aerial images [17, 18] and street view images [19] are used as input to the deep learning process to detect collapsed buildings. Also, the use of more detailed images of building elements and certain areas of the building focuses on assessing elements and damage [20]. Some studies integrate DL with BIM due to the capability of BIM to provide detailed building data in 3D models and share information with other platforms.

In addition to 3D reconstruction using BIM 3D models, integration of BIM and DL is widely applied through the use of BIM data for inspection purposes [21], analysis of element conditions [22], automation data integration [23], and semantic analysis of building regulation [24]. In terms of using data integration, BIM can supply information about detailed elements used in analysis or recognition using DL processing. For example, the use of BIM data and DL networks can support infrastructure lifecycle management that monitors and assesses component condition [25].

2.4 The Potential of BIM and WMS Applications for Decarbonization in Building Recovery

Web Map Service (WMS) is an industry-standard protocol for delivering georeferenced map images generated by a map server from data provided by a GIS database via a web interface [26], such as Google Maps, OpenStreetMap, and Apple Maps. WMS provides the best service benefits in finding location points and planning routes in a free and interactive way. Route planning by WMS is considered comfortable to use on various platforms and very accurate since it is supported by actual maps provided by the GIS server system. In its application, the use of WMS can be integrated with other services and software through the API for transferring information.

Several studies have explored the use of WMS in the construction sector. Chen and Nguyen [27] integrated BIM and WMS as decision support tools for the source selection of sustainable construction materials. Chen and Nguyen [28] also developed a framework for location and transportation analysis in green building certifications using BIM-WMS integration. Li [29] integrated WMS and Dynamo BIM for assessment tools around possible construction sites. Farzad Jalaei [30] proposed an integrated methodology for a green building certification system at the initial design stage of a project based on BIM and WMS. Furthermore, Wen et al. [31] and Deng et al. [32] stated that the integration of BIM and GIS-based map services is very applicable to building design assessment and building recovery. In relation to research on the integration of BIM and GIS, such integration has decreased considerably in the last decade

compared to the previous one [31]. This condition encourages the need to further develop BIM-WMS integration research, especially in the post-disaster and sustainability fields, to support good management in the construction project cycle to respond to disasters.

3 The Approach of BIM-DL-WMS Integration for Post-Disaster Building Recovery

The application of technology for an integrated system in post-disaster building recovery remains a challenge. The latest developments in the application of technology in any sector, including construction, require truly interoperable data integration. Environmental differences in implementing these technologies require a bridge to transfer data and unify information in a platform. The maturity of each technology is the key in integrating these technologies.

Integration between BIM, DL, and WMS has the potential to provide significant added value in post-disaster building recovery. Consideration of sustainability through decarbonization efforts requires such integration in the same system. Thus, the idea of a sustainable integrated post-disaster building recovery system is to provide a building recovery system that considers sustainability in the rehabilitation of damaged elements with the support of DL for damage assessment, WMS to calculate sustainability parameters, and BIM as the data backbone at the element level. A BIM Level of Development (LOD) of 300 provides access to information for specific element types [33]. The use of information at the element level is suitable for post-disaster building recovery since both damage and rehabilitation also occur at the building element level.

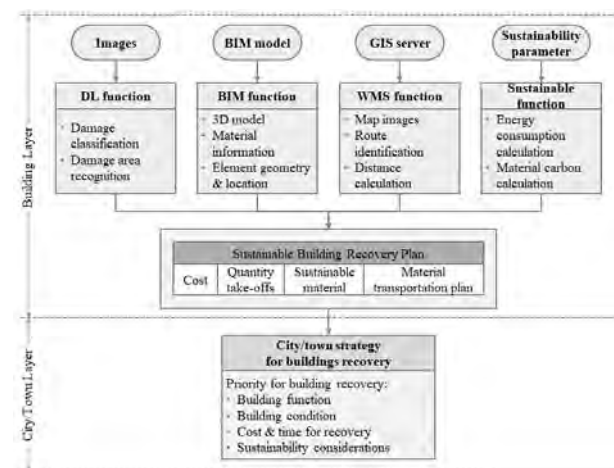


Figure 1. An Approach to Sustainable Integrated Post-Disaster Building Recovery

The approach to sustainable integrated post-disaster building recovery (Figure 1) comes from four main components: (1) DL for damage classification and damage area recognition; (2) BIM with 3D models, materials and element parameters; (3) WMS for map images, route identification, and distance calculation; and (4) sustainability-oriented carbon emission calculation for building elements and materials. The output of this system is a building recovery plan with information on design rehabilitation, quantity take-off, cost, carbon emission impact, and material transportation plan. Furthermore, at the city/town layer, recovery plans for buildings can assist the government or building owners in making building recovery priority decisions. Further benefits of this building recovery system can be applied for material efficiency, recovery execution optimization, and smart cities data support.

4 Sustainable Integrated Post-Disaster Building Recovery Plan

4.1 Framework

A developed flowchart for the proposed sustainable post-disaster building recovery planning system integrating BIM, DL, and WMS (Figure 2) shows how the concepts in Section 3 could be implemented. The flowchart depicts four main stages: (1) Building damage assessment; (2) Building damage analysis; (3) Recovery plan preparation; and (4) Sustainable material evaluation. The flowchart outlines the recovery planning process for a single building using low-carbon materials. The proposed framework is developed from an existing building recovery system by an authorized organization and has been verified by some professional engineers in earthquake and structural engineering.

Building damage assessment elaborates the BIM-data-based inspection process and damage assessment using the DL method. The framework requires the BIM model LOD 300, which facilitates object-level coordination. In addition, the BIM data supports the digital inspection form. Meanwhile, a building without a BIM model will make the framework application take longer to prepare the BIM model and can only do the inspection by manual form.

In the rapid assessment inspection, DL can assist in classifying collapsed and intact buildings. Meanwhile, in a detailed assessment, DL classifies the level of damage, type of damage, and damaged area of the elements. The building recovery system in this study focuses on buildings with elemental damages rather than collapsed buildings. The BIM-based inspection digital form allows the visual inspection results to connect to BIM data. Building damage analysis is a way to confirm the damage after a building damage assessment. Damage

classification at the severe level requires confirmation from engineers because of the potential global impact on the building structure. Building structural analysis helps calculate building strength performance through manual simulation by engineers. The proposed building damage analysis could facilitate engineers in conducting analyses through the support of 3D BIM models.

Recovery planning starts with preparing repair or retrofit methods, all the way to producing a building recovery plan. This stage automatically calculates quantity take-off and recovery costs, comprising components of materials, labor, equipment and other relevant items. The quantity calculation uses data from the BIM model and results of semantic segmentation from DL.

The sustainable material evaluation considers carbon emissions from three sources, namely, embodied material carbon, energy consumption in recovery activities, and carbon emissions in material delivery. The WMS module provides a map image for determining the site location and supplier location so that transportation planning and resulting carbon emission could be calculated automatically. The total carbon emission of a material can then be considered in the selection of materials. This system generates a sustainable building recovery plan with information on damaged elements, volume, recovery cost, carbon emission, and delivery transportation plan.

For the recovery planning of a district or a city, the system could provide information about the inspected building location, material repair needed volume, recovery cost, and transportation plan. The district recovery planning system opens the way to optimize the cost and decarbonized recovery plan by optimizing retrofit method selection, recovery execution schedule and material transportation plan. Moreover, the building recovery plan is essential to support the local government's decision-making in budget allocation and recovery priority strategies.

4.2 Demonstration

An example of the stages described in the flowchart in Figure 2 is given in Figure 3. The example shows the functions of BIM, DL, and WMS in a designed building recovery system. The example uses a real-case scenario from a building in Indonesia. The results show that the BIM-DL-WMS integration can support the output of a sustainable building recovery plan in the form of an alternative recovery planning scenario with technical, cost and environmental impact information.

Figure 3(A) shows the application of DL to the classification of images of damaged building elements and to semantic segmentation for identifying the damaged area in damaged building element images. The pixel amount for the damage and element is a basis for

calculating the material repair needed volume. In this example, EfficientNet is used as the image classification architecture, and UNet is selected as the semantic segmentation architecture. For image classification, the results show an accuracy of 89.23% with 800 images. For semantic segmentation, the intersection over union (IoU)

result is 49.8%, with 120 training images. This prediction still requires development, especially in the number of sample images and training efficiency, but the results obtained show that this method is capable of achieving the goal.

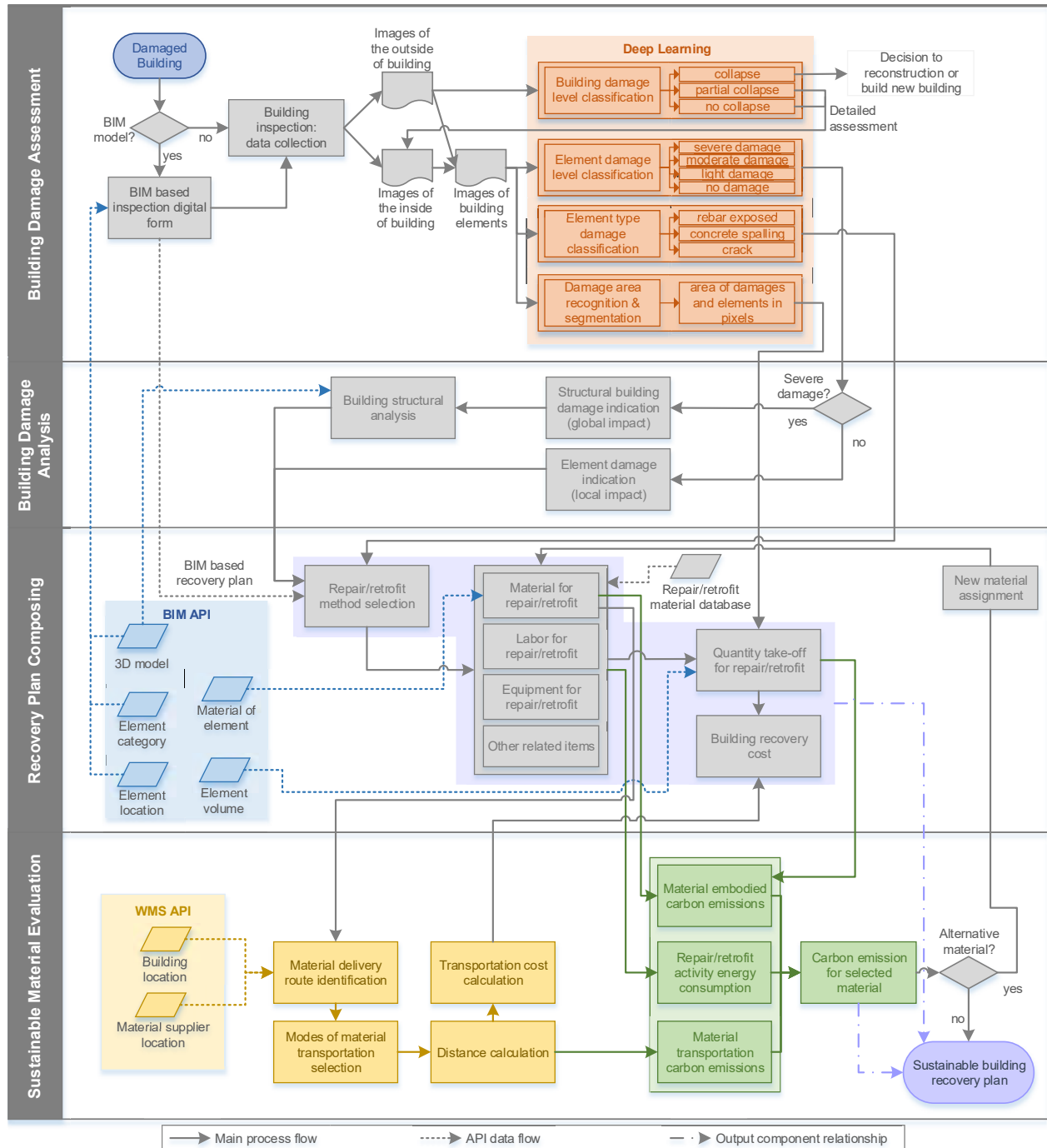


Figure 2. Flowchart of BIM-DL-WMS Integration for Sustainable Post-Disaster Building Recovery Planning

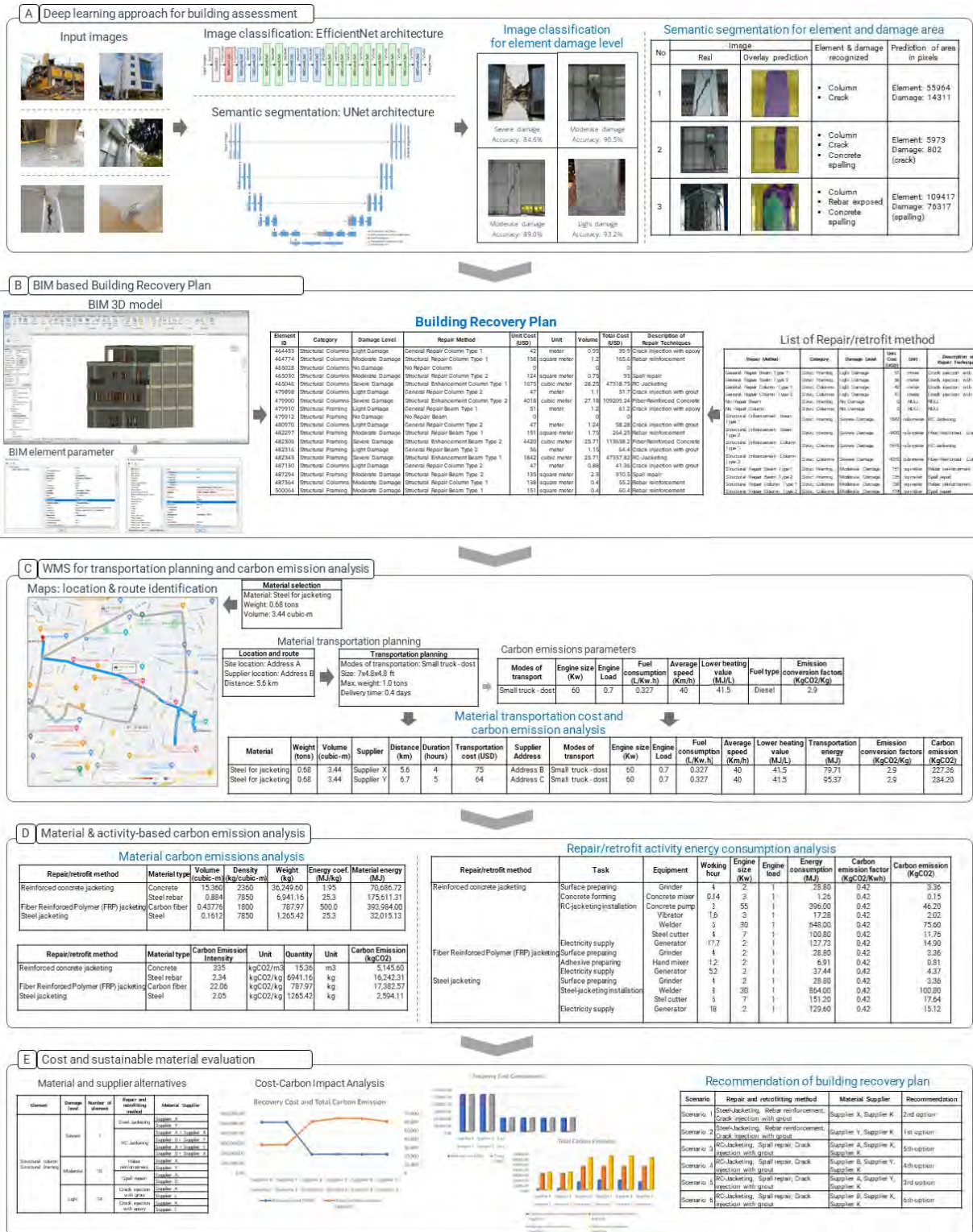


Figure 3. Implementation Example of Sustainable Post-Disaster Building Recovery Planning

Figure 3(B) shows the preparation of a building recovery plan through BIM data and a list of repair/retrofit methods. The first step is to create a 3D BIM model and access the parameter elements, followed by compiling a list of element rehabilitation methods (repair and retrofit) by engineers in the database. Afterwards, a building recovery plan is developed with data from the database and parameters from BIM, damage inputs from processed DL results, and a list of rehabilitation methods. API provides a way to access data in the BIM model, which is connected to WMS and the other parameter in a Windows Forms/Graphical User Interface (GUI) for a building recovery plan.

Material transportation planning and calculation of carbon emissions from transportation are presented in Figure 3(C). WMS provides map images and locations of sites and suppliers. The distance between the site and the supplier's location is used for transportation planning by determining the mode of transportation. The transportation plan and carbon emission parameters are inputs to material transportation cost and carbon emission analysis.

Figure 3(D) shows the calculation of the embodied carbon emissions for the materials selected for rehabilitation and the energy consumption calculation for the planned building recovery activities. Determination of new materials can be an alternative in order to obtain alternative costs and carbon emissions.

Figure 3(E) shows the results of a sustainable building recovery plan. The results obtained are alternative materials for repair/retrofit with technical information on rehabilitation, volume, cost, and carbon emissions. This building recovery plan provides BIM-based damaged element condition data with comprehensive recovery information to support decision-making. Furthermore, sustainable building recovery planning is able to provide an integrated system supported by BIM, DL, and WMS as a tool for decision-makers to set recovery priorities and allocate budgets with consideration of material impacts on the environment.

5 Conclusions and Recommendations

Post-disaster building recovery planning faces challenges in assessing building damages and producing rehabilitation plans in a timely manner, with unintegrated data, poor management, and unaware environmental impacts. Sustainability-oriented post-disaster building recovery planning aims to address these challenges by providing a decarbonized post-disaster building recovery planning system through the integration of the Building Information Model (BIM), Deep Learning (DL), and Web Map Service (WMS). The proposed BIM-DL-WMS-integrated system could achieve the goal of

decarbonization through the selection of low-carbon emission materials. The flowchart of the BIM-DL-WMS system was proposed, and an example is presented to demonstrate the implementation of the system. The proposed system offers an efficient and effective way for post-disaster building recovery planning that could be implemented either at a single building level or at a city/town/district level.

However, this study has several limitations related to limited datasets on the damaged element and detail of framework implementation on district recovery planning. Another issue is the availability of the BIM model before a disaster. In the future, it is hoped that more and more data and the real case would accommodate upgrading the system, while the BIM model also would be applied to all buildings.

References

1. Centre for Research on the Epidemiology of Disasters, U.N.O.f.D.R.R. *The Human Cost of Disasters: An overview of the last 20 years (2000-2019)*. 2020.
2. Programme, U.N.E., *2022 Global Status Report for Buildings and Construction: Towards a Zero-emission, Efficient and Resilient Buildings and Construction Sector*. 2022: Nairobi.
3. Alexander, D., *Principles of Emergency Planning and Management*. 2014: Dunedin Academic Press.
4. Lindell, M.K., *Recovery and Reconstruction After Disaster*, in *Encyclopedia of Natural Hazards*, P.T. Bobrowsky, Editor. 2013, Springer Netherlands: Dordrecht. p. 812-824.
5. Agency, F.E.M., *FEMA Post-disaster Building Safety Evaluation Guidance (FEMA P-2055)*. 2019, Washington, DC: Federal Emergency Management Agency, United States.
6. Maeda, M., K. Matsukawa, and Y. Ito, *Revision of guideline for post-earthquake damage evaluation of RC buildings In Japan*, in *10th U.S. National Conference on Earthquake Engineering: Frontiers of Earthquake Engineering, NCEE 2014*. 2014.
7. Baarimah, A.O., et al. *A Bibliometric Analysis and Review of Building Information Modelling for Post-Disaster Reconstruction*. *Sustainability*, 2022. **14**, DOI: 10.3390/su14010393.
8. Messaoudi, M. and N. Nawari, *BIM-based Virtual Permitting Framework (VPF) for post-disaster recovery and rebuilding in the state of Florida*. *International Journal of Disaster Risk Reduction*, 2019. **42**: p. 101349.
9. Nawari, N. and S. Ravindran, *Blockchain and Building Information Modeling (BIM): Review and Applications in Post-Disaster Recovery*. *Buildings*, 2019. **9**: p. 149.

10. Nizam, R.S., C. Zhang, and L. Tian, *A BIM based tool for assessing embodied energy for buildings*. Energy and Buildings, 2018. **170**: p. 1-14.
11. Mercader-Moyano, P. and P.M. Esquivias *Decarbonization and Circular Economy in the Sustainable Development and Renovation of Buildings and Neighbourhoods*. Sustainability, 2020. **12**, DOI: 10.3390/su12197914.
12. Karlsson, I., et al., *Roadmap for Decarbonization of the Building and Construction Industry-A Supply Chain Analysis Including Primary Production of Steel and Cement*. Energies, 2020. **13**: p. 4136.
13. Mehrvarz, N., K. Barati, and X. Shen, *Embodied Energy Modeling of Modular Residential Projects Using BIM*. 2021, IAARC Publications: Waterloo. p. 483-490.
14. Li, B., et al. *Life Cycle Carbon Emission Assessment of Building Refurbishment: A Case Study of Zero-Carbon Pavilion in Shanghai Yangpu Riverside*. Applied Sciences, 2022. **12**, DOI: 10.3390/app12199989.
15. Lu, Y. and J. Xu, *Low-carbon Reconstruction: A Meta-Synthesis Approach for the Sustainable Development of a Post-Disaster Community*. Systems Research and Behavioral Science, 2016. **33**(1): p. 173-187.
16. Khallaf, R. and M. Khallaf, *Classification and analysis of deep learning applications in construction: A systematic literature review*. Automation in Construction, 2021. **129**: p. 103760.
17. Wang, Y., A.W.Z. Chew, and L. Zhang, *Building damage detection from satellite images after natural disasters on extremely imbalanced datasets*. Automation in Construction, 2022. **140**: p. 104328.
18. Naito, S., et al., *Building-damage detection method based on machine learning utilizing aerial photographs of the Kumamoto earthquake*. Earthquake Spectra, 2020. **36**(3): p. 1166-1187.
19. Wang, C., S.E. Antos, and L.M. Triveno, *Automatic detection of unreinforced masonry buildings from street view images using deep learning-based image segmentation*. Automation in Construction, 2021. **132**: p. 103968.
20. Xu, Y., et al., *Automatic seismic damage identification of reinforced concrete columns from images by a region-based deep convolutional neural network*. Structural Control and Health Monitoring, 2019. **26**(3): p. e2313.
21. Tan, Y., et al., *Automatic inspection data collection of building surface based on BIM and UAV*. Automation in Construction, 2021. **131**: p. 103881.
22. Cheng, J.C.P., et al., *Data-driven predictive maintenance planning framework for MEP components based on BIM and IoT using machine learning algorithms*. Automation in Construction, 2020. **112**: p. 103087.
23. Koo, B., *Enhancing Deep Learning-based BIM Element Classification via Data Augmentation and Semantic Segmentation*, in *Proceedings of the 38th International Symposium on Automation and Robotics in Construction (ISARC)*. 2021, International Association for Automation and Robotics in Construction (IAARC). p. 227-234.
24. Lee, J.-K., *NLP and Deep Learning-based Analysis of Building Regulations to Support Automated Rule Checking System*, in *Proceedings of the 35th ISARC*. 2018, International Association for Automation and Robotics in Construction (IAARC). p. 586-592.
25. Jang, K., et al., *Infrastructure BIM platform for lifecycle management*. Applied Sciences (Switzerland), 2021. **11**(21).
26. Consortium, O.G. *WMS - Introduction*. 2017 January 2023]; Available from: <https://opengeospatial.github.io/e-learning/wms/>.
27. Chen, P.-H. and T.C. Nguyen, *A BIM-WMS integrated decision support tool for supply chain management in construction*. Automation in Construction, 2019. **98**: p. 289-301.
28. Chen, P.-H. and T.C. Nguyen, *Integrating web map service and building information modeling for location and transportation analysis in green building certification process*. Automation in Construction, 2017. **77**: p. 52-66.
29. Li, J., et al., *Integration of Building Information Modeling and Web Service Application Programming Interface for assessing building surroundings in early design stages*. Building and Environment, 2019. **153**: p. 91-100.
30. Jalaei, F., F. Jalaei, and S. Mohammadi, *An integrated BIM-LEED application to automate sustainable design assessment framework at the conceptual stage of building projects*. Sustainable Cities and Society, 2020. **53**: p. 101979.
31. Wen, Q.-J., et al., *The progress and trend of BIM research: A bibliometrics-based visualization analysis*. Automation in Construction, 2021. **124**: p. 103558.
32. Deng, Y., J.C.P. Cheng, and C. Anumba, *A framework for 3D traffic noise mapping using data from BIM and GIS integration*. Structure and Infrastructure Engineering, 2016. **12**(10): p. 1267-1280.
33. Administration, U.S.G.S. *BIM Approved Use Matrix*. 2022; Available from: <https://www.gsa.gov/real-estate/design-and-construction/3d4d-building-information-modeling/bim-software-guidelines/document-guides/level-of-detail/approved-use-matrix>.

Life cycle-oriented decision making based on data-driven building models

Niels Bartels^{1,2}, Josephine Pleuser^{1,3} and Timo Schroeder³

¹Faculty of Process Engineering, Energy and Mechanical Systems, University of Applied Sciences Köln, Germany

²Faculty of Civil Engineering and Environmental Technology, University of Applied Sciences Köln, Germany

³REHUB digitale Planer, Cologne, Germany

niels.bartels@th-koeln.de, josephine.pleuser@smail.th-koeln.de, ts@rehub.team

Abstract –

The integration of BIM and sustainability is a key success criterion for sustainable planning, construction and operation and maintenance. Actually, various research is conducted to integrate the economic, environmental and social aspects in the BIM method. Especially, Life Cycle Assessment (LCA) and Life Cycle Costing (LCC) are subjects of research. Although the integration of the various aspects has made significant progress in recent years, the complete life cycle is not regularly considered, but rather individual life cycle phases (such as design and construction). This is particularly due to the fact that building components consisting of different components are regularly included in the LCA and LCC calculation as a single component. The layered structure of the individual components (e.g. a wall with load-bearing elements, insulation, plaster and others) is thus not included in the respective calculations. However, it is a relevant criterion, since the conversion and renovation of buildings and the associated emissions and costs are strongly dependent on the layered structure and the deconstructability. Against this background, this paper presents a BIM- and data-based simulation of LCA and LCC to enable an optimized and realistic estimation of costs and emissions over the life cycle of building. The layered structure of building components is used to simulate the findings in a Proof-of-Concept (PoC). This paper shows, that BIM is a success criterion for the simulation of LCA and LCC and improves the construction and real estate industry's ability to implement sustainability concepts more effectively. It also indicates success factors for life cycle-orientated decision making as processes or definitions for the quality of information.

Keywords –

Building Information Modeling (BIM); Life Cycle Assessment (LCA); Life Cycle Costing (LCC); Data-driven Decision

1 Introduction

Sustainability defines a concept that aims to meet the present needs of a generation in a way that does not limit the opportunities of future generations [1]. In the current research and literature sustainability combines social, economic and environmental aspects [2,3]. In addition to that, the sustainability certification systems, as Leadership in Energy and Environmental Design (LEED), the Qualitätssiegel Nachhaltige Gebäude (QNG) or Deutsche Gesellschaft für Nachhaltiges Bauen (DGNB) combine these three aspects [4,5].

The combination of sustainability and digitization leads to new perspectives in the solution of current economic, social and environmental challenges [6]. Especially in the construction and real estate sector it is necessary to use all existing possibilities to solve sector-specific challenges, especially the reduction of costs and the carbon footprint of buildings [7]. 37% of global CO₂ emissions are due to the design, construction and operation & maintenance (O&M) of buildings [8]. To reduce the carbon footprint of buildings, the costs and benefits of new materials like wood (e.g. [9,10]), sustainable insulation materials (e.g. [11,12]) or carbon concrete (e.g. [13,14]) are researched. Furthermore, the technical equipment, like heating, cooling or ventilation, becomes more effective, e.g. due to big data analytics and the connection to the Internet of Things (IoT) [15].

To get a holistic view of efficiency and carbon footprint, it is necessary to collect, process, analyze and store all relevant data throughout the life cycle. With the help of a holistic and fully comprehensive data usage it is possible, to reduce waste, to minimize the energy consumption of buildings, to increase recycling and to support circularity [16–18]. In addition to that and due to new technologies, various data is generated by Building Automation Systems (BAS), sensor technologies and IoT devices. This data could also be used to identify actual usage, actual consumption and optimization potentials [19,20].

This large amount of data, new technologies and new

building materials leads to the fact, that structured data collection is necessary to manage the complex requirements for sustainability aspects. Building Information Modeling (BIM) is one essential component for structuring, analyzing and storing sustainability data throughout the whole life cycle and to make it usable for all relevant stakeholders [21,22].

This paper aims to combine economic and environmental sustainability aspects. It shows a solution to perform a BIM- and data-based simulation of LCA and LCC to enable a weighted and result-based decision for Design, Construction and O&M variants in early life cycle phases. Variables (e.g., a CO₂ tax) that may result in a change in LCA and LCC will also be included. The paper uses the layered structure of a wall as an example to illustrate the results.

2 Literature Review and related work

BIM as a method - that links various disciplines throughout the life cycle with the help of a digital building model enables transparent data exchange – also offers advantages to support sustainable design, construction and O&M [21,23]. Various research is actually conducted to combine BIM and sustainability aspects. Mostly, only one aspect of sustainability is focused (e.g. environmental criteria). A distribution of the research of BIM in the respective sub-aspects of sustainability is shown in Figure 1. Here, published papers on the sub-aspects are considered. Especially, the preparation for LCC, LCA, Simulations and Material Passports is supported by the integration of BIM and sustainability.

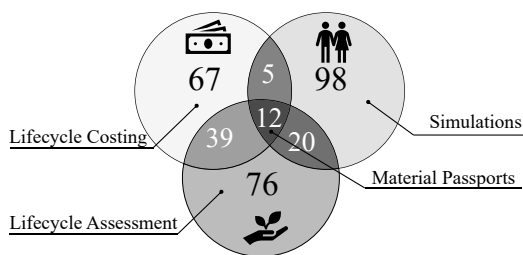


Figure 1. Application of the BIM method in the field of sustainable construction (number of publications mentioned) [24]

The analysis that forms the basis for Figure 1, serves as a basis for further literature analysis with regard to the link between BIM and sustainability. This further literature analysis considers in particular the integration of BIM with LCA and LCC, that are relevant research topics for the linking of BIM and sustainability. In this context, previous literature analyses were also included in the literature review (e.g. [25–29]). On the basis of these publications, a further literature analysis was carried out with three keywords “BIM AND LCA”, “BIM AND LCC” and “BIM AND LCA AND LCC”. These keywords were

searched in various research databases (e.g. SCOPUS, ScienceDirect, Springer, MDPI or google scholar). In this literature review, the years 2013 – 2023 were considered. In addition, attention was paid to the main focus of the publication, which means that publications that only mention a keyword in the text but do not have this as their focus were not included in the evaluation. Figure 2 shows the published papers during the years 2013 – 2022 (status as of 29 December 2022).

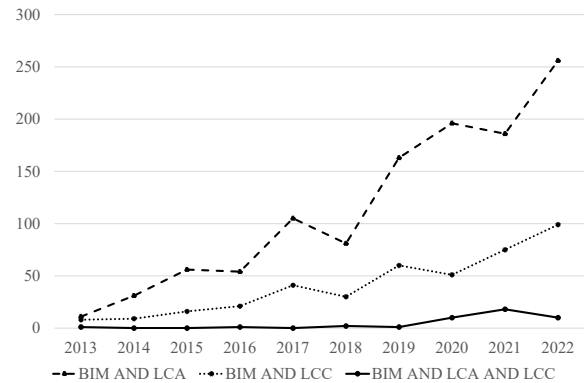


Figure 2. Literature review of the integration of BIM, LCA and LCC as of 29 December 2022.

As can be seen in Figure 2 most of the publications were published in the recent years. The main focus of the research was on papers about BIM and LCA. The research about the integration of BIM, LCA and LCC falls significantly in comparison to the other two research fields. The literature review also showed, that there is a lack of cross-life cycle comparison and thinking by using the BIM method for integrating LCA and LCC. The majority of the papers only focusses on one life cycle phase of the building. But to get a holistic view of the life cycle of a building, it is necessary to integrate various data and to get to know the relationship between the building components.

In particular, an evaluation of the layered structure of the individual components is rarely performed and is regularly incomplete. Instead, only the individual components (e.g. concrete, insulation) are considered. The layered structure, which leads to the fact that components can be deconstructed with different efficiency, is regularly not considered.

3 Integration of BIM-based LCA & LCC

For the integration of LCA and LCC it is necessary to consider all relevant cost and environmental aspects. Figure 3 shows the course of the developed method from uploading an IFC file to evaluating the results of the LCA and LCC. Based on the IFC-upload and a model check, three steps are passed through to calculate the LCA and LCC of the used materials, the building components and

finally of the entire building.

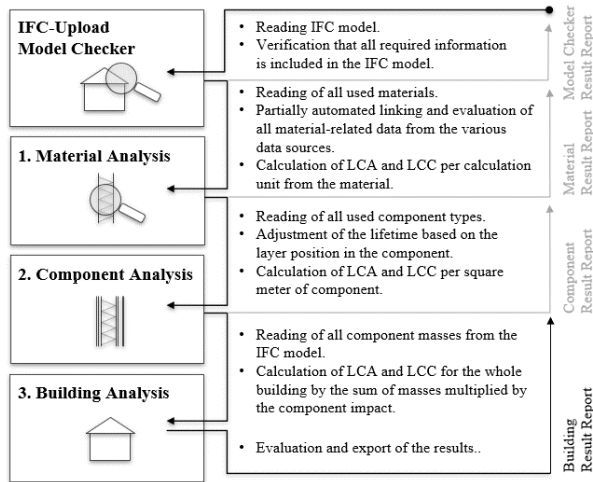


Figure 3. Course of the developed method

The following sections explain the steps 1-3 more in detail. Here this paper refers to the relevant databases (3.1), the calculation of the lifetime of building components (3.2), the calculation of LCA (3.3) and the combination of LCA and LCC (3.4). The upload and the model check are assumed to be established processes.

3.1 Relevant Databases

To calculate LCA and LCC it is necessary to use data bases. These databases have various purposes and may support by conducting LCA, Material Passports (MP), LCC or Simulations (Sim). An overview of German databases is shown in Table 1.

Table 1. Relevant German databases in sustainable construction [21]

Data base	LCA	MP	LCC	Sim
ÖKOBAUDAT	X	X		X
WECOBIS	X	X		X
EMMy	X	X		
Building material scout	X	X		X
IBU.data	X	X	X	X
Material library	X	X	X	X
DGNB Navigator	X	X	X	X
Cradle to Cradle certified	X		X	
BNB service lives	X	X	X	X

In addition to that, there are many more databases, as the data base of the Energy & Environmental Building Alliance (EEBA) [30]. Furthermore, it is necessary to integrate data of the lifetime of building components, what can be found in the data bases of the Informationsportal Nachhaltiges Bauen and the Bundesinstitut für Bau-, Stadt- und Raumforschung (BBSR). [31]

3.2 Calculation of the lifetime of building components

To evaluate the sustainability of a building structure or system (e.g. a Wall), it is necessary to calculate the lifetime of that component. Building components may consist of various layers (e.g. a wall consists of an Insulation layer, a reinforced concrete layer, plaster layers, etc.). In addition to the layer structure of the wall, the maintenance strategy of the building component in particular influences the life cycle costs. [32] Figure 4 shows that context using the example of a wall.

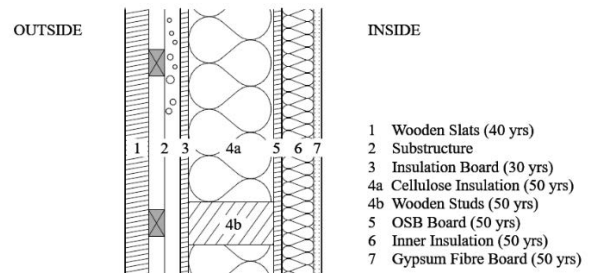


Figure 4. Lifetime of layers in a building component using the example of a wall (here: wall of a residential building in Cologne-Junkersdorf)

To calculate the sustainability of a building component, it is necessary to develop a concept for the visualization of the service life between the individual layers. Here, a distinction must be made between two variants:

1. If all component layers are detachable from each other, the components can be considered individually.
2. If the component layers cannot be detached from each other, the service life is limited by the lowest expected service life of the underlying layer groups [33]. This is to be considered as an attribute in the model

To model that, a function was developed to visualize and determine the course of the service life of the layer structure. Firstly, all multi-layer components (e.g. Ceilings, Walls) are detected using *IfcOpenShell*, a Python-based open source software library for working with Industry Foundation Classes. The *IfcRelAggregate* entity is used so that these can be read out from the IFC file previously uploaded to the browser app. With the help of the entity *IfcRelAssociatesMaterial*, which describes the relationship between components and their material components, the materials of the individual layers can be read out from the IFC file. [34] In the next step, the entity *IfcRelDefinesByProperties*, which allows the assignment of a property set to a single or multiple objects [35], is used to read all properties of the materials and filter them by "Component Properties". This property set stores information about the layer structure.

To structure the layers, a code is used to show whether the layer is a core layer or not. If it is a core layer, a “1” is appended to the list. If it is a non-core layer, a “0” is appended to the same list. (e.g. [0,0,1,0]). Afterwards, a layer number is assigned to each layer. Three different cases have to be differentiated. (e.g. [0,1,2,1]):

1. The first *IF*-loop considers the case that the component contains a core element. In that case, first the index of the core element is determined. Then, for each layer, it is checked whether its index is smaller than that of the core layer. In this case, the index can be kept. However, if it is larger, the numbering should decrease again, which is why one counter per layer is reduced by one.
2. In the second *IF*-loop the layers of components are numbered with an odd number of layers. First the number of layers must be determined for this. Then for each layer it is checked whether its index is smaller than half of the number of layers. In this case, the index can be kept. If the index of the layer is greater than or equal to half of the number of layers, the numbering should decrease again.
3. The *ELSE*-loop considers the remaining case, of a component without a core element with an even number of layers. This loop works in the same way as the one for the odd number of layers, except that the counter for counting down does not have to be reduced by one beforehand.

Figure 5 und Figure 6 show the results for two components. If the result is assigned with a “+”, the lifetime decreases from the core to the outside. If the result is assigned with a “-”, the lifetime increases from the core to the outside and adjustments might be required.

```

Component Typ 1
Layer:
- Wooden Slats
- Substructure
- Insulation Board
- Cellulose Insulation
- Wooden Studs
- OSB Board
- Inner Insulation
- Gypsum Fibre Board
Core element:      [0, 0, 0, 0, 1, 0, 0, 0]
Layer position:    [0, 1, 2, 3, 4, 3, 2, 1]
Lifetime of layers: [40, 'x', 40, 50, 50, 50, 50, 50]
Valuation for adjustment: ['+', '+', '+', '+', '+', '+', '+', '+']
Adjusted lifetime of layers: [40, 40, 40, 50, 50, 50, 50, 50]

```

Figure 5. Results of the lifetime of layers in a building component (lifetime decreases from the core to the outside)

```

Component Typ 2
Layer:
- Wooden Slats
- Substructure
- Insulation Board
- Cellulose Insulation
- Wooden Studs
- Insulation Board
- Inner Insulation
- Gypsum Fibre Board
Core element:      [0, 0, 0, 0, 1, 0, 0, 0]
Layer position:    [0, 1, 2, 3, 4, 3, 2, 1]
Lifetime of layers: [40, 'x', 30, 50, 50, 30, 50, 50]
Valuation for adjustment: ['+', '+', '-', '+', '+', '-', '+', '+']
Adjusted lifetime of layers: [30, 30, 30, 50, 50, 30, 30, 30]

```

Figure 6. Results of the lifetime of layers in a building component (lifetime increases from the core to the outside, adjustment might be required)

With the help of another function, the lifetime of the material is read out (e.g. by using databases as the BBSR tables [36]). By using the entity *IfcMaterialProperties* all PSets of a material can now be read out. In this way, the *IfcProperties* can also be identified with the unique IDs of the datasets of the databases. Using these IDs, information requests can be sent to the databases, connecting them to the browser app. In this way, the lifetime data of a material can be queried. In the next step, this function is applied to all materials of a component and all lifetime dates are stored in a list to compare these dates which each other. The consideration must always be made from the inside to the outside. Thus, it is started with the layer with the highest layer number, which represents the core layer of the component. In the next steps, it is checked whether the adjoining layers have a higher or lower lifetime. If the layer has a lower lifetime, it can be retained. If the layer has a higher lifetime than the lower layer, the lifetime must be adjusted to the lower layer.

3.3 Calculation of LCA

In order to be able to correctly offset the masses and life cycle assessments against the lifetime, the masses per component must be read out. In this case, all units are read from the IFC model so that the correct reference unit can be selected during LCA. If a bulk density for the material is stored in a database (e.g. ÖKOBAUDAT), this is used from the database rather than from the IFC file, because the bulk density and the LCA data belong to the same data set in this case and the building material data in the IFC model are often also very poorly maintained. As the bulk density is not mandatory in the case of the ÖKOBAUDAT database, the IFC model is used if it is not available. However, the building material masses are completely read out from the IFC model.

The following process was developed to integrate this data. First, all materials (of ceilings, roofs and walls) of the multi-layer components were determined by using the entity *IfcRelAssociatesMaterial* as already mentioned in 3.2. In the next step, all PSets of the materials can be identified by using the entity *IfcRelDefinesByProperties*, from which the PSet *Component Quantities* can now be filtered. In this PSet all data concerning the masses of the materials are stored. After that, the *IfcSingleValue* can be sorted by surface, volume and weight and attached to the corresponding property lists.

1. The volume has the entity *IfcQuantityVolume*.
2. The weight has the entity *IfcQuantityWeight*.
3. Since the Pset "Component Quantities" stores different surface areas, the component surface area cannot be filtered by the entity, but must be matched with the *Layer/Component Surface Area* label.

As this is done for each component layer, a list is obtained with all the square meters of the layer surfaces, all

the cubic meters of the material volumes and the weight in kilograms of each layer. To access the masses of a material in a component, only the index of the material is needed.

The last step is to link the material amounts of the IFC model to the databases by using a semi-automated process to connect the UUIDs. For this purpose, however, the materials must have a unique designation and be described and categorized as characteristically as possible. But the research showed that the connection between IFC and the databases regularly does not work properly. Especially a lack of standardization into the databases (e.g. ÖKOBAUDAT) complicates the connection. For this reason, a function was developed which creates a material preselection for the user. In this way there is at the same time a quality control by the user. For this purpose, in this function the columns "UUID", "Name (en)", "Category (original)" and "Raw density (kg/m³)" are first read out from the databases and stored in individual lists. In the next step, the database is reduced to the essential information for data processing, so that each material is no longer listed per life cycle phase but is reduced to one line. Based on the user's selection, the LCA can then be determined.

Figure 7 shows the example of a material selection parts of the developed interface for two exemplary materials. The interface displays all material-related data from the various data sources for the respective material.



Figure 7. Example for material evaluation and material selection (left: Insulation Board, right: Cellulose Insulation)

Only the LCA data still has to be linked to the material data using the drop-down menu manually.

3.4 Calculation of LCA and LCC

Based on the service life of the materials in each component, the manufacturing costs and LCA can be calculated for the entire life cycle of the building. With the help of that calculation, the best solution for the life cycle can be simulated. For this purpose, the LCA results from the different phases are calculated according to DGNB or QNG. Because of the partially insufficiently maintained databases, the focus here was placed on the manufacturing phase including raw material provision, transport and production (A1-A3), the replacement in the use phase (B4), in the disposal phase on waste treatment and land-filling (C3, C4) and finally on the recycling potential (D). The data basis of the manufacturing phase can be rated as quite good and since the replacement is calculated as new manufacturing according to DGNB, this phase is also covered by good data. The data for the disposal phase and the recycling potential, on the other hand, are partly incomplete. If the database does not provide a value for these phases, a "0" is set at this point, which is critical. While missing data for the recycling potential does not improve the value, missing values in the disposal phase even embellish it. Finally, the LCC can be calculated with the help of the cost parameters of the building materials. An example for the Global Warming Potential (GWP) is shown in Figure 8.

```
Global Warming Potential (GWP):
Material name:
- Wooden Slats
- Substructure
- Insulation Board
- Cellulose Insulation
- Wooden Studs
- OSB Board
- Inner Insulation
- Gypsum Fibre Board
calculation unit: ['m3', 'm3', 'm3', 'm3', 'm3', 'm3', 'm3', 'qm']
Production (A1-A3): [-721.74, -738.94, -198.4, -73.37, -654.77, -753.0, 40.31, 1.36]
Replacement (B4): [0, 0, 0, 0, 0, 0, 0]
Waste (C3,C4): [809.71, 796.78, 270.0, 99.08, 815.1, 967.0, 1.12, 0.13]
Recycling (D): [-351.38, -349.48, -184.5, -30.51, -288.65, -549.0, 0, 0]
DGNB: [-263.41, -291.64, -112.9, -4.8, -128.32, -335.0, 41.43, 1.49]
BMB: [87.98, 57.84, 71.6, 25.71, 160.33, 214.0, 41.43, 1.49]
```

Figure 8. Section of the calculation of the LCA per material of a building component (GWP)

Using the example of the wall, this can mean that a different wall construction, which at first glance appears to be more favorable in terms of LCA and LCC without considering the layered structure of the wall, has a worse life cycle balance in the life cycle due to the longevity of materials. In order to estimate the cost development for the LCC, figures from the Baukostenindex (BKI, German for Construction Cost Index) are used. The BKI represents the price development for construction projects in Germany and can be used as a basis here, as it allows an estimate of the price development for the future dismantling or replacement costs of components [37]. It is necessary to take into account not only complete components (e.g. a wall), but also the layered structure as described above, as this can lead to price differences. These price differences occur especially due to the fact, that the period of the adjustment of components is influenced by the

life time of its layers.

In addition, the cost parameters of the building materials must be differentiated into labor and material cost parameters for a correct calculation of the LCA and LCC. The distinction between labor and material cost is necessary, because the price increase rate differs for these parameters

4 Validation based on an example project

The concept presented in Section 3 was validated in a Proof-of-Concept (PoC) application to determine its practicality. For this PoC a residential building in Cologne was used. The building is located in Cologne-Junkersdorf, has a gross floor area of 410 m² and was designed by “Klara Architekten BDA”. This project is shown in Figure 9.



Figure 9. PoC – 3D model of the validation model by "Klara Architekten BDA"

To validate the findings of the previous sections, the building was modelled with BIM and without BIM to calculate the LCC and LCA. Especially due to the material selection, the LCC and LCA could be calculated easily and optimizations were evaluated. An example for the result of the calculation of the GWP and LCC for a wall are shown in Figure 10 and Figure 11.

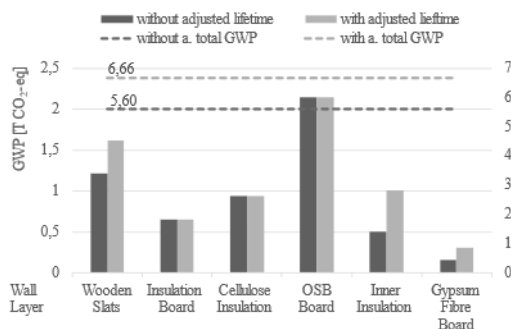


Figure 10. Effect of adjusting the lifetime on the GWP (calculation with BNB method).

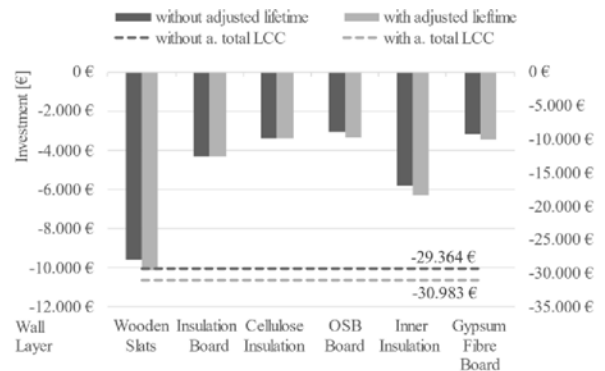


Figure 11. Effect of adjusting the lifetime on the LCC (calculation with the present value method)

Besides the results of the calculation of the LCC and the LCA, this validation shows especially five main factors that are relevant for successful implementation to integrate BIM and sustainability aspects:

1. All relevant data must be maintained even more precisely than in projects in which no application of LCA and LCC is carried out with the BIM method. In particular, data such as density (e.g. of the different concrete grades) must be maintained precisely, as they cannot always be retrieved unambiguously from the databases.
2. Furthermore, a differentiation of the materials for different types of building components is necessary. In the IFC model, for example, a different material should be used for mineral wool used as insulation between rafters than for mineral wool used in wall construction, since the expectation of its service life is different.
3. It is necessary that the user (e.g. the architect, technical equipment planner, construction management, sustainability planner) can intervene in the process via a user interface. The intervention is necessary because only a partially automated process is possible when linking the databases because of the missing standardizations. However, this also enables quality control by the user, as well as a high level of transparency and influence. In the test project Haus-Blu in Cologne-Junkersdorf by “Klara Architekten BDA”, for example, the quality classes of the concrete were not clearly marked, which is why manual linking became necessary.
4. Another point to consider is that the building components have to be built as a whole multi-layered building component. In the PoC, there was initially the problem that a differentiation was made between facade, shell and extension components. This is due to the construction process, tendering and the intersection of components. However, it is not possible to recognize the coherence of the component

and thus also not to adjust the service life on the basis of the position of the component layer in the component, since in this case façades, shell and extension components are considered individually instead of as one coherent component. To calculate the LCA and LCC of the component, it was necessary to remodel the wall construction in the PoC. In the future, it will therefore be necessary to ensure during modeling that the elements are classified as facade, shell and extension component and their layers can be assigned to a component via a parameter.

5. Components that are not modeled in the multi-layer component are neglected in the layer-by-layer analysis, e.g. timber frame, steel girders or profiles. In this case, it is also necessary to consider the corresponding parameters.

The findings from the PoC show that it is necessary to create clear processes and definitions regarding the relevant data. This requires clear Exchange Information Requirements (EIR) that map the requirements with regard to the calculation of LCA and LCC. Especially with regard to the layered structure of the components, a clear definition of the EIR, a high-quality modeling and an attribution of the relevant parameters is necessary.

5 Conclusion and Future Work

This paper presents a solution for calculating LCA and LCC that considers the layered structure of components. The validation carried out in the course of the research shows that the presented method offers a possibility to optimize the reliability of the calculations. Thus, the concept presented in this paper contributes to the construction and real estate industry's ability to implement sustainability concepts even more effectively, helping to reduce CO₂ emissions from the construction and real estate industry.

Although this paper takes various aspects into account, it considers only the service life of the materials due to the structure, which is considered the most favorable in design and construction. In the future, with regard to LCA and LCC, the costs for facility management must be priced in over the life cycle. For example, technical facilities that at first glance appear to be more costly and emission-intensive can become more cost-effective in the further life cycle if the facility management processes are optimally adjusted to these facilities.

In addition to that, it is necessary to specify the processes for the integration of BIM and sustainability regarding LCA and LCC. Especially the EIR needs to be specified by all technically involved people. These are two aspects that are being explored in the context of research at the University of Applied Sciences in Cologne.

References

- [1] Bundesministerium für wirtschaftliche Zusammenarbeit und Entwicklung. Nachhaltigkeit (nachhaltige Entwicklung). On-line: <https://www.bmz.de/de/service/lexikon/nachhaltigkeit-nachhaltige-entwicklung-14700>, Accessed: 12/01/2023.
- [2] Mota, B., Gomes, M. I., Carvalho, A., and Barbosa-Povoa, A. P. Towards supply chain sustainability: economic, environmental and social design and planning. *Journal of Cleaner Production*, 105:14–27, 2015.
- [3] Henriques, A., and Richardson, J. *The triple bottom line, does it all add up? Assessing the sustainability of business and CSR*. Earthscan Publications, London, Sterling, VA, 2004.
- [4] U.S. Green Building Council. LEED rating system. On-line: <https://www.usgbc.org/leed>, Accessed: 12/01/2023.
- [5] DGNB GmbH. Übersicht aller Kriterien für Gebäude Neubau. On-line: <https://www.dgnb-system.de/de/gebäude/neubau/kriterien/>, Accessed: 12/01/2023.
- [6] Jacob, M. *Digitalisierung & Nachhaltigkeit. Eine unternehmerische perspektive*, Springer Vieweg, Wiesbaden, 2019.
- [7] Braun, N., Hopfensack, L., Fecke, M., and Wilts, H. *Chancen und Risiken im Gebäudesektor für die Umsetzung einer klimaneutralen und ressourceneffizienten zirkulären Wirtschaft. Vorstudie im Rahmen des Verbundvorhabens Circular Economy als Innovationsmotor für eine klimaneutrale und ressourceneffiziente Wirtschaft* CEWI, Wuppertal, 2021.
- [8] UN Environment Programme. 2021 Global Status Report for Buildings and Construction. On-line: https://globalabc.org/sites/default/files/2021-10/GABC_Buildings-GSR-2021_BOOK.pdf, Accessed: 29/11/2023
- [9] Balasbaneh, A. T., and Sher, W. Comparative sustainability evaluation of two engineered wood-based construction materials: Life cycle analysis of CLT versus GLT. *Building and Environment*, 204:108–112, 2021.
- [10] Myllyviita, T., Soimakallio, S., Judl, J., and Seppälä, J. (2021) Wood substitution potential in greenhouse gas emission reduction—review on current state and application of displacement factors. *Forest Ecosyst. Epub*, 8(42): 2-18, 2021
- [11] Asdrubali, F., D'Alessandro, F., and Schiavoni, S. A review of unconventional sustainable building insulation materials. *Sustainable Materials and Technologies*, 4:1–17, 2015.
- [12] Siksnelyte-Butkiene, I., Streimikiene, D., Balezentis, T., and Skulskis, V. (2021) A Systematic Literature Review of Multi-Criteria Decision-Making

- Methods for Sustainable Selection of Insulation Materials in Buildings, *Sustainability*, 13(2):737, 2021.
- [13] Lee, J., Lee, T., Jeong, J., and Jeong, J. Sustainability and performance assessment of binary blended low-carbon concrete using supplementary cementitious materials. *Journal of Cleaner Production*, 280(1):124373, 2021.
- [14] Wasim, M., Abadel, A., Abu Bakar, B., and Al-shaikh, I. M. Future directions for the application of zero carbon concrete in civil engineering – A review, *Case Studies in Construction Materials*, 17:e01318, 2022.
- [15] Li, W., Koo, C., Hong, T., Oh, J., Cha, S. H., and Wang, S. A novel operation approach for the energy efficiency improvement of the HVAC system in office spaces through real-time big data analytics, *Renewable and Sustainable Energy Reviews*, 127:109885, 2022.
- [16] Lu, W., Yuan, L., and Xue, F. Investigating the bulk density of construction waste: A big data-driven approach. *Resources, Conservation and Recycling*, 169:105480, 2021.
- [17] Zhang, N., Zhang, C., and Wu, D. Construction of a smart management system for physical health based on IoT and cloud computing with big data. *Computer Communications*, 179:183–194, 2021.
- [18] Sprecher, B., Verhagen, T. J., Sauer, M. L., Baars, M., Heintz, J., and Fishman, T. Material intensity database for the Dutch building stock: Towards Big Data in material stock analysis. *Journal of Industrial Ecology*, 26:272–280, 2022.
- [19] Wang, Y., Ponnusamy, V., Zaman, N., Jung, L. T., and Amin, A. H. M. *Role of IoT in Green Energy Systems*, IGI Global, Hershey pennsylvania, 2021.
- [20] Bartels, N., and Weilandt, G. Erfolgsfaktor für Smart Buildings. Lebenszyklusorientierter Ansatz und durchgängige Nutzung von Daten. *Deutsches Ingenieurblatt*, 9:54–57, 2021.
- [21] Bartels, N., Höper, J., Theißen, S., and Wimmer, R. *Application of the BIM Method in Sustainable Construction. Status Quo of Potential Applications in Practice*, Springer Publishing, Cham, 2023.
- [22] Chong, H.-Y., Lee, C.-Y., and Wang, X. A mixed review of the adoption of Building Information Modelling (BIM) for sustainability. *Journal of Cleaner Production*, 142:4114–4126, 2017.
- [23] Bartels, N. *Strukturmodell zum Datenaustausch im Facility Management*, Springer Fachmedien, Wiesbaden, 2020.
- [24] Bartels, N., Höper, J., Theißen, S., and Wimmer, R. *Anwendung der BIM-Methode im nachhaltigen Bauen*, Springer Fachmedien, Wiesbaden, 2022.
- [25] Alasmari, E., Martinez-Vazquez, P., and Baniotopoulos, C. A Systematic Literature Review of the Adoption of Building Information Modelling (BIM) on Life Cycle Cost (LCC), *Buildings*, 12:1829, 2022.
- [26] Potrč Obrecht, T., Röck, M., Hoxha, E., and Passer, A. BIM and LCA Integration: A Systematic Literature Review. *Sustainability*, 12:5534, 2020.
- [27] Xue, K., Hossain, M. U., Liu, M., Ma, M., Zhang, Y., Hu, M., Chen, X., and Cao, G. BIM Integrated LCA for Promoting Circular Economy towards Sustainable Construction: An Analytical Review. *Sustainability*, 13:1310, 2021.
- [28] Safari, K., and AzariJafari, H. Challenges and opportunities for integrating BIM and LCA: Methodological choices and framework development. *Sustainable Cities and Society*, 67:102728, 2021.
- [29] Lu, K., Jiang, X., Yu, J., Tam, V. W., and Skitmore, M. Integration of life cycle assessment and life cycle cost using building information modeling: A critical review. *Journal of Cleaner Production*, 285:125438, 2021.
- [30] EEBA. Energy & Environmental Building Alliance. On-line: <https://eeba.ecomedes.com/>, Accessed: 13/20/2022
- [31] Bundesministerium für Wohnen, Stadtentwicklung und Bauwesen. Nachhaltig Planen und Bauen. On-line: <https://www.nachhaltigesbauen.de/>, Accessed: 12/12/2022
- [32] Ryll, F., and Freund, C. Grundlagen der Instandhaltung. In *Instandhaltung technischer Systeme* (Schenk, M., Ed.), pages 23–101, Springer, Heidelberg, 2010.
- [33] Ritter, F. *Lebensdauer von Bauteilen und Bauelementen. Modellierung und praxisnahe Prognose*, Technische Universität Darmstadt, Darmstadt, 2011.
- [34] buildingSMART International. IfcRelAssociates Material. On-line: https://standards.buildingsmart.org/IFC/DEV/IFC4_3/RC1/HTML/schema/ifcproductextension/lexical/ifcrelassociatesmaterial.htm, Accessed: 13/12/2022.
- [35] buildingSMART International. IfcRelDefines By-Properties. On-line: https://standards.buildingsmart.org/IFC/DEV/IFC4_3/RC2/HTML/schema/ifckernel/lexical/ifcreldefinesbyproperties.htm, Accessed: 13/12/2022.
- [36] Bundesministerium für Wohnen, Stadtentwicklung und Bauwesen. Nutzungsdauern von Bauteilen. On-line: <https://www.nachhaltigesbauen.de/austausch/nutzungsdauern-von-bauteilen/>. Accessed: 13/12/2022.
- [37] Krause, T., and Ulke, B. *Zahlentafeln für den Baubetrieb*. 9th ed., Springer Vieweg, Wiesbaden, 2016.

Sustainability in Construction Projects: Setting and measuring impacts

Ramprasad, Priyanka¹; Dave, Bhargav²; Ziliacus, Martin²; Patel, Viranj²

¹CEPT University, India

²Visilean, India

priyankabola@gmail.com, bhargav@visilean.com, martin@visilean.com, viranj.patel@visilean.com

Abstract –

The construction industry has proposed many frameworks to tackle its significant impact on sustainability. But there is a dearth of tools that help stakeholders quantify and understand the impact of their activities, particularly in the construction phase of a building. This study started with a literature review followed by interviews with field experts to find more about the problems in existing frameworks and the best way to bridge the gap between the concept of sustainability and the actual practice.

The outcome was a framework with quantifiable parameters that could help identify, track and measure sustainability targets incorporated in existing software. The Framework was used to create a tool that professionals in the field could easily use to assess the impact of the construction activities using dynamic inputs from the site. It helps the stakeholders comprehend the implications of variations in the construction processes and provides data to strategize and achieve their sustainability targets.

Keywords –

Dynamic, Sustainability impact assessment, Life cycle assessment framework, Construction phase

1 Introduction

Sustainability is broadly defined as the ability to meet our current needs without compromising the lack of future generations. Conventionally, sustainability is divided into three categories or pillars: environmental, social, and economic. The three pillars are interdependent, which means improvement of one can sometimes be at the cost of another. Recognizing this, United Nations, 2016, came up with 17 sustainable development goals, which act as a blueprint for all the nations to work on to achieve a more sustainable future.

1.1 Sustainable development goals and the construction industry

To tackle the growing environmental problems holistically, the United Nations developed sustainable

development goals (SDG) in 2015. After studying 60 recent publications on the role of the construction and real estate sectors in achieving sustainable development goals, it was concluded that 44% of agendas and ten critical goals under the 17 SDGs were dependent on construction activities, and ten critical goals were impacted by it. According to a report by the world economic forum, buildings consume 30% raw material and 12% potable water. It contributes to 25-40% of solid waste generation and about 20% of water effluents [14]. Because of this, the sector is increasingly being focused upon by governments, field experts, and practitioners, with the SDG providing them with a new way to approach the issues like waste generation and efficient resource usage [7].

As of 2021, the construction industry contributes nearly 5% of GDP in developed nations and up to 8% in developing countries. It accounts for about 39% of process-related emissions of carbon, making the field accountable for the future of sustainability. With an average global growth of 3.9 % per annum, its contribution will only increase.

1.2 Construction industry and sustainability

The existence of these issues in the construction industry is backed by studies that point toward high waste generation, inefficient usage of resources, and low productivity. Other typical problems include misuse of land, emissions of dust and gas, and pollution [12][13]. It also mentions that sustainable project management means the effective execution of a project to minimize the waste produced, which includes waste of materials and idle time. The entire life cycle of buildings needs to be considered to make the sector truly sustainable [12]. Thus, not only does sustainability help improve the working environment, but it also makes the process more efficient and beneficial for stakeholders.

Due to the adverse effects of its activity on the environment and the inherent benefits of inculcating sustainability in the process, the industry has tried to come up with various guidelines and frameworks for tracking it, with green building rating systems and Life cycle assessment (LCA) being the most notable ones.

While green building rating systems have been criticized for being qualitative, life cycle assessment has been recognized to be too complex for a regular stakeholder to understand.

1.3 Stakeholders and their role in sustainability

The use of stakeholders in the entire supply chain, from the vendors to the clients, architects, and contractors, can lead to the successful implementation of sustainability from the early stages of the design itself [11]. Definition of sustainability is not aligned among the project managers, making it difficult to aim for sustainability in buildings and assess it uniformly [13]. While PMBOK recognizes the inclusion of economic, social, and environmental factors as beneficial, it doesn't provide any guidelines to do so [13]. There is a need to create a verifiable quantitative framework that can be incorporated into the project management system that can be implemented on construction sites [3].

The study aims to identify and track the sustainable factors or indicators at the project and site level in the construction phase and develop a framework for the stakeholders. This can help them set sustainable goals and identify the impact of the decisions and processes on the goals by providing them with a tool to periodically track it and change the process or propose alternative if required.

2 Literature study

2.1.1 Existing Frameworks for assessing sustainability in construction projects

Different assessment systems of sustainability can be classified into the following, listing their drawbacks [4]:

1. **Performance-based design systems:** The emphasis is more on the outcomes of design, and the approach helps adopt any means to get that outcome. It helps accomplish the client's requirements and can be modified to be building-specific.

2. **Sustainable building rating and certification system:** The weightage for each of the common factors across all the sustainability evaluation tools might differ based on the local context. Having a universal weightage that can be adapted in all the countries and identifying the factors for each of the building typologies is a time-consuming process. Assessment of established green building rating systems like LEED and BREEAM stated that one of the problems with creating assessment methods is that there is no universally established objective assessment system of excellence in building sustainability performance 0.

3. **Life cycle assessment systems:** This process

requires a lot of background information on each of the building components involved. The data required for such an assessment is huge and might not always be available. The bigger the supply change, the more data-intensive it is.

There are more than 600 rating tools for the assessment of sustainability, with the number of indicators ranging from 6 to 70 [10][1]. Sustainability indicators Any of these approaches can be adapted, sometimes in conjunction with each other, and customized based on the requirement of the stakeholder to provide them with the best way to analyze the sustainability of the buildings.

2.1.2 Problems with Existing Frameworks for assessing sustainability in construction projects

Most of the sustainability evaluation tools used in construction projects are comprehensive though they do little to help practitioners apply them practically and strategize to improve sustainability at a project level. The drawbacks of most of the existing frameworks were the subjective nature of weights, the predominantly qualitative approach resulting in a subjective analysis of impact, and subjective methods of assigning weights0 [3]. Analysis of the existing sustainable review tools (SRT) by a study to identify drawbacks suggested that the comparability problems of the tools might be due to the different standards in different regions. Problems in using LCA as a basis of the Framework include problems with standardization leading to difficulty in comparison, as the building has a much longer life than general products. It also needs an extensive database, and the process needs expertise and time due to the complexity[2][6][9][11].

3 Methodology

In order to propose an effective system of sustainability tracking for stakeholders, the study started with a literature review to know the existing sustainability assessment frameworks in the field and the sustainability parameters or indicators that are used in frameworks. As seen in 2.1.2, Analysis was done to find out the gaps in the assessment system to derive the desirable characteristics or features for the proposed Framework to be effective. This was followed by an interview with field experts to better understand the desired characteristics of the new Framework and problems in the existing ones. Finally, an existing framework from 2.1.1 was identified as a reference framework from which a new one could be modelled based on identified desirable characteristics, keeping in mind the provisions of the existing software. The last stage is an application of the newly modelled Framework on a sample project to see if the outcomes accomplish the objective.

3.1 Semi-structured Interview

Further to the literature review, a semi-structured interview was conducted with three experts in the field to discuss the requirements that emerged from the literature study. The various tools available in the industry to measure sustainability were discussed, with emphasis on finding out if and how they were falling short of being the required tool for stakeholders to control and strategize sustainable processes. The current requirements of the stakeholders were identified. The First interviewee was an industry expert and environment technologist. Second, a LEED Fellow and Energy efficiency expert, and the third was an academician with expertise in Building Energy and Performance. The key takeaway points were that the current processes weren't dynamic enough to track and bring changes to processes on-site during the construction phase or to measure the impact of the many variations at the site. They also pointed out the lack of information on site and proposed a system that could help stakeholders control the amount of information to provide and a tool that could accommodate this feature and give the impact with available information. Essentially a tool that would have provision for different levels of detail.

3.2 Characteristics of Proposed LCA-based Framework

The frameworks' characteristics were proposed based on the literature study and outcomes of the semi-structured interviews with experts.

It was decided that the Framework should have universal parameters applicable to all projects across the globe and shouldn't be limited by geographical boundaries. The system should be quantifiable so that projects can be compared against each other with the least number of possible inputs. The proposed guideline should focus on the construction phase of the building due to the available support from existing software. Also, since very few frameworks address this phase in-depth in a dynamic way, this would be a point of focus and lead to proactive decisions rather than reactive ones. The level of detail needs to be introduced so that stakeholders can control the amount of information that is required to be put into the system and help them set sustainability targets as per their requirements. The Framework is being built for the stakeholders who need to understand the direct impact of their actions on sustainability. The proposed system should be user-friendly.

Having recognized the gaps in the existing frameworks, followed by the inputs from experts, Life Cycle Assessment (LCA) Framework was chosen as a basis for the new system as it addressed the desired characteristics.

3.3 Life cycle assessment and its applicability to the proposed Framework

Following the resolutions of the Kyoto Protocol, the construction industry introduced ways to include sustainability through tools such as building rating systems and, eventually, the concept of LCA in the construction industry around the 1980s [6]. The ISO International Organization for Standardization) created a guideline in 1997 to help people evaluate the buildings based on LCA and make them comparable. The ISO, along with EPD (Environmental product declaration), made it possible to standardize the parameters to assess the impact and quantify the same. LCA has four defined steps:

- Step 1: Goal and Scope
- Step 2: Life Cycle Inventory
- Step 3: Impact assessment
- Step 4: Interpretation

The features of LCA overcame the problems in existing frameworks identified through literature reviews and semi-structured interviews in the following ways:

1. **Sustainability and reduction in costs:** The use of LCA leads to a reduction in economic and environmental costs as it encourages the reduction use of energy-intensive resources, equipment, and processes[9].
2. **Universal Parameters:** The parameters to measure the impact of the construction industry are the same throughout the world. The impact factors are the same across all the typologies of buildings and geographies, providing a much more consistent basis for measuring compared to the other types of frameworks.
3. **Quantifiable:** The proposed Framework is based on the LCA or the life cycle assessment, which has several guidelines on the details of the procedure and has almost no qualitative factors. It is a science-based approach that is quantifiable.
4. **Use in the construction industry:** Though several tools exist to analyse the construction industry, though a few are modelled on LCA, none dynamically evaluate or emphasize the construction phase making it an area of interest.
5. **Level of details:** The various stages in LCA Framework help provide a basis for introducing the concept of different levels of detail, which was suggested by experts and was part of the desired characteristics. It will help stakeholders set the level of information they need to give, enabling control over the level of assessment of sustainability. It helps in effectively considering the alternative approaches to construction at multiple stages and setting targets as per the level of information that

can be provided.

3.4 Proposed Framework.

3.4.1 Modifications to the existing LCA framework

Step: 1 Goal and Scope

As per LCA, the following are the stages of the construction lifecycle:

- A1- Raw material extraction
- A2- Transport to the manufacturing site
- A3- Manufacturing
- A4- Transport to the construction site
- A5- Installation/ Assembly at the site.

Out of this, A1-A3 are the Product stage, and A4- A5 are the construction stage. Rest is B1- B7 – Use stage, C1- C4 end of life stage. The goal and scope stage is to decide what stages will be assessed for our/Users' Project. The experts recommended keeping the research limited to product and construction stage (A1-A5) so that it is more focused on actual execution.

Step: 2 Life Cycle Inventory

IMPACT CATEGORY	VALUES	DESCRIPTION
Global Warming Potential (GWP)	kg-CO ₂ eq	Global warming potential which results in climate change due to emissions
Acidification potential (AP)	kg-SO ₂ eq	Leads to lowering of Ph Value of water and soil, reducing the nutrients intake of plants .
Eutrophication Potential (EP)	kg-CFC ₂ eq	Emissions that increases nutrients leading to algae growth .
Ozone Depletion Potential (ODP)	kg-CFC ₂ eq	Indicates Damage caused to the ozone layer leading to increased UV radiation
Photochemical Ozone creation Potential	kg-C ₂ H ₄ eq	Emission which leads to creation of smog .
Abiotic Depletion Potential	kg	Indicates the reduction of non renewable raw materials .

Figure 1 Sustainability indicators and parameters

This stage is data collection, and the section explains the sources of information for each of our chosen stages. As per LCA, there are 6 parameters that are used to measure environmental impact, as shown in Figure 1. To reduce confusion, make it user friendly and understandable for layman, the suggestion of experts was considered, and the impact was mainly calculated and presented in terms of the GWP parameter or the carbon footprint since it is a well-known parameter.

The values of the six parameters are considered for the calculation of A1-A3 stages and are available on registered products EPD which are available both for free and at payable basis. These values from open-source database will be connected to the software for the backend emission calculation. The values for A4 and A5 will be calculated based on information provided in the software.

Step 3: Impact Assessment of the proposed Framework

Impact assessment is done using coefficients of emission for every parameter of material/ vehicle/ equipment, which is collected from EPDs along with the information provided by users from the site.

To calculate the impact of the process on the environment as per LCA, the steps followed are:

1. The quantity of material used in construction is multiplied by the emission factor of that material specification (extracted from EPD) to get the impact of the A1-A3 phase.
2. For A4 phase, the quantity of material being transported is multiplied by the coefficient of emission of transport being used (extracted from EPD), the number of vehicles, along with the transportation distance.
3. Finally, for A5 Phase, which uses on-site input for activity, is considered for the coefficient of emission. It is usually equipment. The coefficient of emission of that equipment (extracted from EPD) is then multiplied by the amount of time the equipment was used. The time depends on the quantity of the material.
4. The emissions so obtained in every phase of the activity are then added to get the final emission of the activity.

Accordingly, an example has been shown of the calculation of the impact of the construction of a 10 m³ slab in Table 1

Table 1 Impact calculation

Stage	Quantity	x	Coefficient of emission of material/ vehicle/ equipment (from EPD)	=	Total environmental impact of that phase
A1-A3 (Manufacturing)	(Manufacturing of M30 Concrete) 10 m ³	x	(Coefficient of emission of 1m ³ M30 concrete) 266.69 kgCO ₂ e/ m ³	=	2666.9 kgCO ₂ e
A4 (Transportation)	(Transportation of M30 Concrete for 11km) 10x 1.133-ton x 11km	x	(Coefficient of emission of 1m ³ M30 concrete in transit mixer) 0.13 kgCO ₂ e/ tonkm	=	16.2 kgCO ₂ e
A5 (Assembly/ Construction)	(Time taken for Pumping 10 m ³ of M30 Concrete @ 40 m ³ per hr) 0.25 h	x	(Coefficient of emission of diesel concrete pump) 16.28 kgCO ₂ e/h	=	4.07 kgCO ₂ e
Total emission from concreting of 10 m ³ of slab (From Phase A1-A5)				=	2687.17 kgCO ₂ e

Step 4: Interpretation of results

Interpretation of results comes in the end. This helps analyze the problematic areas of the construction activities and get insights as per the requirement of the user. An example of the result is shown in .

The interpretation of the results shown has been made in such a way that the user can identify the item they want to assess the sustainability of (activity, trade, element, location). They can set targets or phases to analyze (A1- A3, A4, A5) and calculate the impact using universal and quantifiable sustainable indicators (GWP, ADP, etc.) to eventually know the impact of variations in the process (change in material specification, change in

transportation distance, change in the transport vehicle, change in equipment used and change in the duration of work or quantity of material due to rework).

The aim was to provide an easily understandable quantifiable tool that can help the users know the impact and reduce the same. This tool has dynamic inputs provision in A1-A5 and based on the background of the user, the takeaway changes. A sample dashboard can be seen in Figure 2

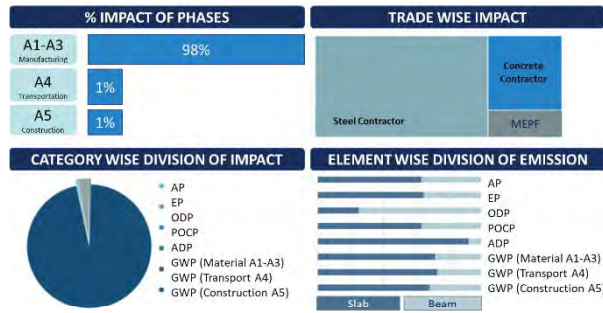


Figure 2 Interpretation of results

3.4.2 Information required in the proposed Framework

Parameter	BIM Model	Schedule	Dynamic Site inputs	Static Site inputs
Material				
Quantity of material				
Material specification				
Material Location				
Element and Location				
Mode of Transport				
Activity				
Duration of Activity				
Equipment				
Duration of equipment use				
Water				
Electricity				
Waste				

Figure 3 Inputs for the process

To enable dynamic tracking, Figure 3 shows the inputs required for the process, the sources of these inputs, and the exact parameters that need to be calculated from the site. The parameters required from the site are:

- A1-A3:** Material name, specification, and quantity
- A4:** Material quantity, the distance of transportation, mode of transport
- A5:** Equipment used, duration of use, water, electricity, and amount of waste collected

Information regarding water, hazardous, radioactive, and non-hazardous waste disposed off, which can be static inputs from site at frequent intervals from the project.

3.4.3 Difference between the existing LCA-based frameworks in the market and the proposed Framework

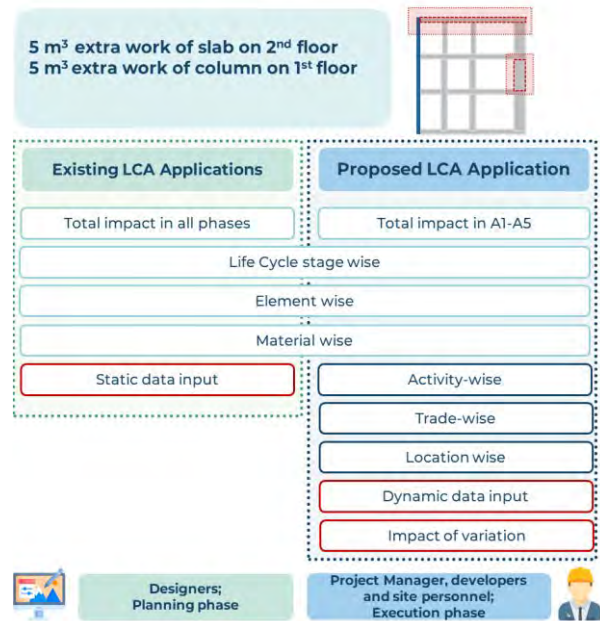


Figure 4 Difference between the results of existing LCA-based frameworks in the market and the proposed framework

If the example from Figure 4 is taken and there are changes in the highlighted elements in the form of 5 m³ of extra work on slab and column of different floors, the outputs in existing and proposed applications have been listed:

1. While the existing application shows the impact on all phases since it caters to the designers and planners, the proposed Framework gives importance to A1-A5 phases that are from the manufacturing of construction materials to the handover of the building/ This makes it easier to cater to the project managers and on-site personnel to help them make decisions at that stage.
2. The data input for existing LCA applications is static. They can either be done at the beginning or the end for them to be useful. The minute changes and impact of variations during construction activities will not be noticeable or highlighted. It also becomes tedious to collect and input the required data for the calculation. Lack of data input during construction activity makes it difficult for dynamic use and makes tracking variations or recording the advantage of using more sustainable alternatives virtually impossible. This will not be the case for the proposed Framework.

A problem user faces in existing applications is the difficulty in identifying the exact activity that affected the

expected impact and the root cause of problem. This is tackled in the proposed Framework by giving the impact results activity-wise, trade-wise, and location-wise. This can help the site personnel realize the root cause and exact impact of the variation in planned activities, making it easier for them to learn from their mistakes. This is not specific to the given example and is applicable in the case of finding the impact of any element and any kind of variance in the entire building and is scalable in nature as it is applicable to all kinds of buildings.

3.4.4 Flowchart of information for the proposed Framework

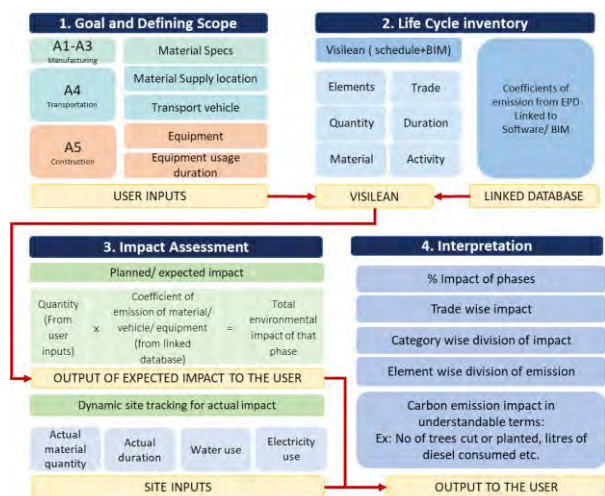


Figure 5 Flow of input

The flowchart in Figure 5 brings together the four steps of the LCA with the inputs and the outputs. Process flow can be explained as follows:

1. User input: The process starts with extra inputs from the user. This is where the level of detail or setting of sustainability targets can be selected depending on the amount of information user has. It helps stakeholders control the sustainability assessment. The information to be provided in various forms has been given in Figure 3.

2. Visilean: The input in the first step goes to Visilean, which already has a system of existing interlinked inputs from the user's schedule and BIM model. The user inputs will then be added as attributes to existing inputs like material/ duration. This step accomplishes part of the life cycle inventory (Step 1), where the information based on planned quantities is entered into the Framework.

3. Database: The emissions' information regarding given user inputs will be collected from the various EPD database that will be linked to the software will be linked to each activity.

4. Output of expected impact to the User: The information obtained in LCI from user inputs and emissions will be used to calculate the expected impact as per Table 1 to give the expected impact on

sustainability. Obtained depends on the level of the information fed by the user.

5. Site inputs: Dynamic site inputs as detailed out in Figure 3, help factor in the delays and rework. This is the key to realizing the dynamic part of the proposed sustainability assessment. The total electricity used, water used, and waste output, in the end, will finally give the total impact on the site of the construction activities listed in the schedule.

6. Output to the user: The final interpretation part of LCA can be accomplished by giving useful outputs regarding existing impacts and the impacts due to modification in a way that they can understand so that they can better control the impact and know the impact of inefficiencies in the processes dynamically, as shown in Figure 6



Figure 6 Carbon equivalents for better understanding of positive and negative impact on sustainability

3.4.5 Sample testing of the Framework

This proposed Framework has been tested by manually calculating the information extracted from a sample BIM model of a building and its schedule.

Scope: The activities considered were Concreting and steelwork of Slab, Beam, and columns of floor 7 of a sample residential project. The quantity and material specification can be extracted from the BIM model, the latter of which can also be taken as user input on software. The emission details and quantities from all the phases were brought together to calculate the expected impacts as explained in point 4 of 3.4.4

Changes in process were introduced to check if the Framework was successful in measuring the impact of variation. For this exercise, it was assumed that there was a rework of the slab, which increased the material quantity by five cum, and there was a reduction in the distance of steel transport by 5 km. Due to a change in the vendor. The factors that changed were:

1. The material quantity increased, due to which the impact in A1-A3 (manufacturing stage) and A5 (use of equipment duration in construction stage) increased as can be seen highlighted in red in Figure 7

2. Material transport distance was reduced due to which carbon impact was reduced in A4 (Transport stage) as can be seen highlighted in green in Figure 7

	A1-A3	A4	A5	A1-A5
Activity	GWP (Material)	GWP (Transport)	GWP (Construction)	GWP (Total)
Concreting of slab	290	0	1.19	291.5
Steelwork of Column	0	-13.87	0	-13.87
Steelwork of slab	181.5	-6.75	0	174.74
Steelwork of Beam	0	-7.78	0	-7.78
Grand total	471.5	-28.4	1.19	444.58
Increase in emission				
Decrease in emission				

Figure 7 Variation impact calculation and display

Only the carbon footprint has been calculated and presented in terms in which a layman can understand, as seen in Figure 6. The results show that while reducing transport distance (A4 phase) reduced expected impact (green), rework added to the impact (red) in both Manufacturing (A1-A3) and Construction phase (A5). It can also be seen that the most impact percentage is of manufacturing phase, which can be mitigated by stakeholder by opting for a material/ brand with lesser impact. The stakeholder also comprehends the impact of a minor rework, thus incentivizing the priority of quality, to help avoid it in future.

4 Integrating with existing software

The steps in the Framework were included at various points in the existing Visilean application. This has been explained in 3.4.4. and incorporated in the following ways:

a) Material specification: The material specification can be extracted from the BIM Model or from a list linked to EPD for the A1-A3 phase of the construction.

b) Location of the material: The material section will provide the list of materials being used. The material warehouse/ vendor location for the material chosen, with provision adding multiple pick up points, thus obtaining distance travelled till building. This is for the A4 phase of the construction.

c) Equipment used: The List of equipment to be used in construction activities with a large amount of power consumption or energy consumption can be listed. For example, a Crane for hoisting the rebars and a Concrete pump for concreting slabs can be listed. The type of fuel Ex: Diesel, based, Petrol based, or electricity-based, should be kept in mind and selected from options in linked EPD. This is important for the A5 phase of the construction.

After putting the information, the data can be linked to activities using the Gantt chart view or scheduler. The

emission for a particular activity will consider phases. Along with the total impact on all the elements calculated as described in Table 1. The impact can be seen in the following categories: Phase wise; Trade wise; Activity, wise and the same can be seen in sample dashboard of software in Figure 8. Carbon impact is used to measure and represent as in Figure 6 easier comprehension.

Furthermore, the user can track the impact of variation using a sustainability tracker, as seen in Figure 7. Here, the input can be taken for specific weeks with every activity having variation listed. The ones with positive changes will be highlighted in green along with the difference, and the activity with the negative changes will be highlighted in red.

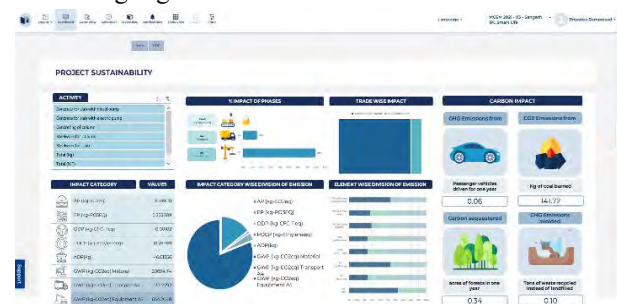


Figure 8 Screenshot of the sample dashboard of sustainability tracking in Visilean software

4.1.1 Data Enhancement for the proposed Framework

Despite reducing the amount of data required, the proposed system will still be a time-consuming process. To make it more efficient, growing technologies like Artificial Intelligence and Machine Learning can be leveraged to develop an engine that would facilitate the automatic linking of the plan and the BIM model in software to enable seamless data integration, making dynamic input of required sustainable parameters possible. The planned duration and quantities for scheduled activities can be directly extracted from the AI Linked BIM model, thus reducing the amount of user input required to just the actual duration and material variation during execution, thereby making dynamic monitoring and sustainability tracking much more efficient.

5 Conclusion

The research found that construction industry impacted about sustainability due to inefficiencies in the industry that resulted in increased material consumption and waste. There was a dearth of tools for field personnel that would help them easily understand the impact and come up with measures to reduce the same. Through a combination of literature reviews and interviews with

field experts, the Framework of the characteristics required was summarized. It was to be quantifiable and universal in nature; they had to include the construction phase, be user-friendly, and needed to provide the option to set the level of assessment based on the amount of accessible information. A dynamic system was also desirable for active tracking of the variations that might come up in the processes. LCA was chosen as the ideal Framework that includes all of these, but it came with its own set of challenges which include the complexity of the system and the data-intensive nature of the Framework, which made it difficult to comprehend the process and the impact.

The proposed Framework has overcome these by creating a system that involves using existing software which has the required data and by adding limited, easily accessible quantifiable user inputs to calculate LCA. In the dashboard, the impact is calculated according to the elements of a building, different phases, or across the materials used in a building. This information can be used by user to relook at the inefficient parts of process and replan, to make sure that sustainability is the aim at every phase regardless of its part in the life cycle, even during construction. In the future, the tool can be developed to cover the entire lifecycle for better assessment.

6 References

- [1] Berardi, U. (2012). Sustainability Assessment in the Construction Sector: Rating Systems and Rated Buildings. *Sustainable Development*, 20(6), 411–424. <https://doi.org/10.1002/sd.532>
- [2] Bilec, M. M., Ries, R. J., & Matthews, H. S. (2010). Lifecycle Assessment Modeling of Construction Processes for Buildings. *Journal of Infrastructure Systems*, 16(3), 199–205. [https://doi.org/10.1061/\(asce\)is.1943-555x.0000022](https://doi.org/10.1061/(asce)is.1943-555x.0000022)
- [3] Borja, L. C. A., César, S. F., Cunha, R. D. A., & Kiperstok, A. (2018). A quantitative method for prediction of environmental aspects in construction sites of residential buildings. *Sustainability (Switzerland)*, 10(6), 1–38. <https://doi.org/10.3390/su10061870>
- [4] Bragança, L., Mateus, R., & Koukkari, H. (2010). Building sustainability assessment. *Sustainability*, 2(7), 2010–2023. <https://doi.org/10.3390/su2072010>
- [5] BRE Global Limited. (2019). *CEEQUAL Version 6 Technical Manual*. 187. <https://www.ceequal.com/version-6/>
- [6] Buyle, M., Braet, J., & Audenaert, A. (2013). Life cycle assessment in the construction sector: A review. *Renewable and Sustainable Energy Reviews*, 26, 379–388. <https://doi.org/10.1016/j.rser.2013.05.001>
- [7] Fei, W., Opoku, A., Agyekum, K., Oppon, J. A., Ahmed, V., Chen, C., & Lok, K. L. (2021). The critical role of the construction industry in achieving the sustainable development goals (Sdgs): Delivering projects for the common good. *Sustainability (Switzerland)*, 13(16). <https://doi.org/10.3390/su13169112>
- [8] Hope, A., Ebbesen, J. B., & Hope, A. (2016). Re-imagining the Iron Triangle: Embedding Sustainability into Project Constraints . Re-imagining the Iron Triangle: Embedding Sustainability. *PM World Journal*, II(MARCH 2013), 1–13.
- [9] Joaquin Diaz, L. A. A. (2014). *Sustainable Construction Approach through Integration of LCA and BIM Tools*. 283–290.
- [10] Matar, M. M., Georgy, M. E., & Ibrahim, M. E. (2008). Sustainable construction management: Introduction of the operational context space (OCS). *Construction Management and Economics*, 26(3), 261–275. <https://doi.org/10.1080/01446190701842972>
- [11] Palumbo, E., Soust-Verdaguer, B., Llatas, C., & Traverso, M. (2020). How to obtain accurate environmental impacts at early design stages in BIM when using environmental product declaration. A method to support decision-making. *Sustainability (Switzerland)*, 12(17), 1–24. <https://doi.org/10.3390/SU12176927>
- [12] Shen, L. Y., Li Hao, J., Tam, V. W. Y., & Yao, H. (2007). A checklist for assessing sustainability performance of construction projects. *Journal of Civil Engineering and Management*, 13(4), 273–281. <https://doi.org/10.1080/13923730.2007.9636447>
- [13] Silvius, A. J. G., & Schipper, R. P. J. (2014). Sustainability in project management: A literature review and impact analysis. *Social Business*, 4(1), 63–96. <https://doi.org/10.1362/204440814x13948909253866>
- [14] World Economic Forum. (2016). Environmental Sustainability Principles for the Real Estate Industry. January, 1–23. <https://www.weforum.org/> Yu, W. Der, Cheng, S. T., Ho, W. C., & Chang, Y. H. (2018). Measuring the sustainability of construction projects throughout their lifecycle: A Taiwan Lesson. *Sustainability (Switzerland)*, 10(5). <https://doi.org/10.3390/su10051523>

State of the art Technologies that Facilitate Transition of Built Environment into Circular Economy

Aparna Harichandran¹, Søren Wandahl¹ and Lars Vabbersgaard Andersen¹

¹Department of Civil and Architectural Engineering, Aarhus University, Denmark

aparnaharichandran@cae.au.dk, swa@cae.au.dk, lva@cae.au.dk

Abstract –

The construction industry is highly energy intensive and causes significant environmental impacts and reduction in natural resources. A radical change in current practices is necessary for achieving a circular economy in the construction sector. Structural holes in the supply chain, coordination of diverse stakeholders, and resource management at the end of life of buildings are some of the key challenges for implementation. Technologies that spearhead the industry transition and their contributions to realizing a circular built environment are reviewed in this study.

Keywords –

Circular Economy; Construction Industry; Digitalization; Sustainability.

1 Introduction

Conventional construction practices in the linear manner that follow “take, make, use, dispose” result in a considerably high consumption of natural resources and greenhouse gas (GHG) emissions [1]. With the built environment currently responsible for about 35% of the global energy consumption and 38% of carbon dioxide-equivalent (CO₂e) emissions [2], decarbonizing the sector is one of the most cost-effective ways to mitigate the worst effects of climate breakdown [3]. If global warming has to be contained to less than 1.5° C increase by the year 2050, the built environment needs to reduce the CO₂e emission by around 60 Gt [4]. In this context, there is a compelling need to adopt a regenerative and sustainable business model for the construction industry.

Circular Economy (CE) emerged as one of the holistic solutions for addressing resource requirements, climate challenges and developing a sustainable built environment. CE is rooted in several sustainability concepts such as industrial ecology, cradle-to-cradle (C2C), regenerative design and the blue economy system as illustrated in Figure 1 [5]. Numerous definitions of CE by researchers and industrial experts over the period

often tend to create misunderstanding and lack of consensus. Therefore, Kirchherr et al. [6] analysed 114 definitions of CE for a comprehensive conceptualization. They have found that the definition by the Ellen MacArthur Foundation (EMF) is the most used among the 114 definitions. According to the EMF [7], CE is “an industrial system that is restorative or regenerative by intention and design. It replaces the ‘end-of-life’ concept with restoration, shifts towards the use of renewable energy, eliminates the use of toxic chemicals, which impair reuse, and aims for the elimination of waste through the superior design of materials, products, systems, and, within this, business models.” Introducing such a system in construction sector requires digitalization. This study presents the enabling technologies for CE in built environment. The role of each technology, their interdependencies and drawbacks are also evaluated.

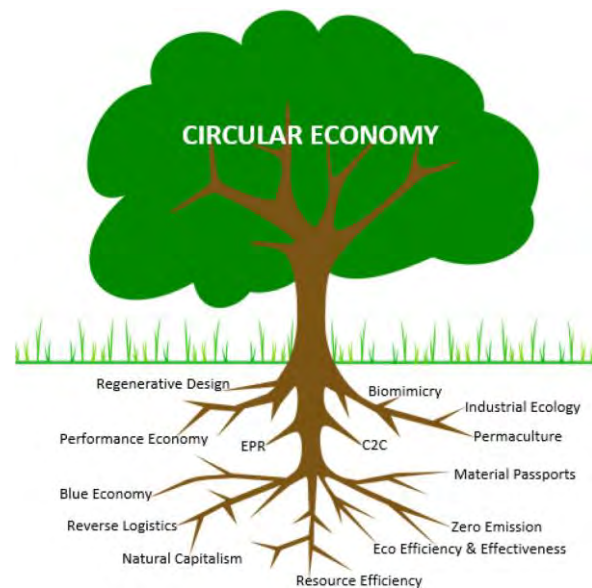


Figure 1 Sustainability concepts form the roots of circular economy [5]. (EPR: Extended Producer Responsibility, C2C: cradle-to-cradle)

The remaining parts of this paper are organised as follows. Section 2 describes a circular built environment framework. The methodology of this study is given in Section 3. The technologies that enable the transition of the built environment into a circular economy are provided in Section 4 and Section 5 concludes the paper.

2 A Circular Economy Framework for the Built Environment

Developing an integrated CE framework emphasising environmental sustainability is challenging due to the uniqueness of every construction project. A recent study proposed a comprehensive framework for implementing CE as illustrated in Figure 2 [8]. Building design aided by Building Information Modelling (BIM) enables accurate estimation of material quantities and the selection of sustainable alternatives of materials [9]. Sourcing materials from disassembled buildings and modularising and/or prefabricating new building components ensure material circularity [10]. Besides, the new design of building components should focus on deconstruction and disassembly at the end of life. The environmental impact caused by transporting raw building materials can be reduced by sustainable sourcing [11].

Firstly, material circularity can be incorporated during the service life of the building by using recycled materials from other cycles for refurbishing purposes [8]. Towards the end of the life of a building, the emphasis of CE shifts towards managing Construction and Demolition (C&D) waste. Developing an effective CE business model, controlling waste materials from the source, adopting strategic incentive plans and implementing technological innovations are some of the strategies for managing C&D waste [12]. Since the

concepts of deconstruction are already incorporated during design, the building components can be retrieved at the end of life of the building. These components can be adequately repaired or retrofitted before supplying back to the materials selection stage for the next cycle. The C&D waste materials other than building components, such as recycled aggregates, scrap steel and wood, must be handled separately. These materials are subject to onsite sorting and screening before being recycled or reused for producing appropriate secondary materials. In the end, these sustainably sourced materials are either directly utilized for the next cycle of building construction or to produce prefabricated elements. Therefore, industrial ecology concepts have a direct influence on material circularity for the CE.

The development of a new CE business model for the built environment requires combined efforts from various stakeholders such as governments, researchers, designers, manufacturers, construction companies, recyclers, and suppliers. Each of these stakeholders contributes to diverse aspects from policy formulation, product design, and technology development to sustainable sourcing and construction practices.

3 Methodology

This study applied a systematic literature review to identify the key technologies that enable a circular built environment. The Scopus database is selected for searching the relevant literature. The scope of this study is limited to literature that explicitly mentions the term ‘circular economy’ along with the keywords for each technology. For example, “circular economy” AND (building OR construction) AND “blockchain”. After the initial search, the relevant articles were identified and analysed to assess the role of technologies in developing

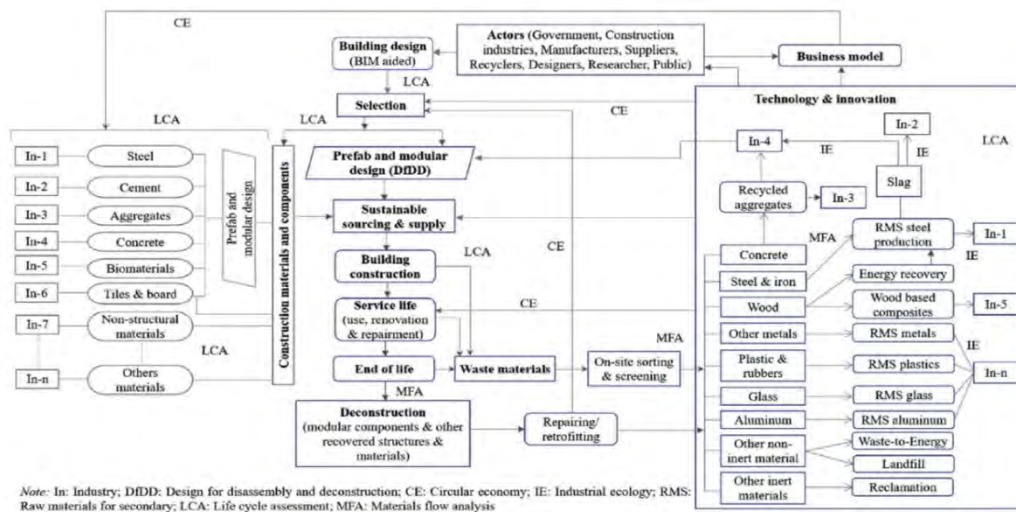


Figure 2 The framework for implementing CE in the built environment [8]

circular building strategies.

4 Enabling Technologies for Circular Economy in Built Environment

The conservative and fragmented nature of the construction industry is one of the significant barriers to CE. Several emerging technologies can accelerate the transformation of the industry [13]. Some of the most common and critical technologies identified from the literature are summarized in this section.

4.1 Artificial Intelligence

Due to the extensive applications in diverse fields of study, Artificial Intelligence (AI) has several definitions and understandings among scientific communities. In general, “AI leverages computers and machines to mimic the problem-solving and decision-making capabilities of the human mind” [14]. Several subdisciplines with diverse computing techniques constitute the continuously emerging discipline of AI. Machine Learning (ML) is a subfield of AI that trains algorithms to learn from data, while Deep Learning (DL) is a subfield of ML based on neural network algorithms [15]. Some of the existing and potential applications of AI in the construction industry include structural health monitoring, life cycle analysis, automated construction monitoring and material circularity [16], [17].

The EMF and Google identify that designing circular products, operating circular business models and optimizing infrastructure are the ways in which AI can assist in transforming to CE [18]. Çetin et al. [19] categorize the enabling functions of AI into three: 1) design optimization, 2) fault detection and requirement identification for buildings, and 3) applications to support end-of-life activities. Design optimization with ML can identify the best solution from numerous design alternatives based on desired performance criteria [20]. Besides, ML models can predict the carbon footprint of building designs at the early design stage [21]. Computer vision techniques are widely applied to identify faults in buildings through DL models [22]. Researchers have developed methods to identify the energy demands of buildings [23] and predict service life through ML models [24]. Categorizing demolition waste [25], estimating building component reusability [26], and detecting recycled aggregate composition [27] are some of the various ways AI supports end-of-life activities. The application of AI technologies for CE has several barriers such as the high cost of technology implementation, lack of technical expertise, need for large amounts of good quality data, and possibility of biases caused by training data.

4.2 Material Passports and Material Databanks

Comprehensive information on building resources at the end of life is unavailable. This lack of information is one of the greatest challenges for recycling and reusing construction materials [28]–[30]. According to some researchers, storing and maintaining the information of building components and materials in a digital environment from the early design stage to demolition is a solution [29], [31]. The concept of the Material Passport is formulated based on this idea. Material passports are digital datasets of objects that contain details such as properties, location, and ownership of the object. They are created and operated at various levels from city to building components in BIM or another digital platform. This concept is demonstrated by BAMB, an EU-funded project, by creating a platform with more than 300 material passports at three levels of detail [32]. Material passports were used to estimate environmental impacts of design alternatives [31], material quantities in a locality [33] or building circularity level [34]. Another concept introduced to address the lack of building resource information is material databank. The “material and component bank” proposed by Cai and Waldmann [30] is a BIM-based database run by an independent contractor. This database facilitates transferring demolition materials from one site to another for construction. Material passports and material databanks are new technology and have several challenges in adoption such as lack of standardisation, low adoption rate, need for data security and accurate information, and high implementation cost.

4.3 Building Information Modelling

BIM provides a comprehensive digital representation of products and processes related to built assets for facilitating interoperability during design, construction and management [35]. Engineers, architects, consultants, and other actors in the construction industry utilize BIM for numerous tasks such as quantity estimation, design alterations, planning and facility maintenance. Several contributions of BIM directly foster sustainable practices. One such example is enabling effective communication and information exchange between stakeholders to support alignment of project tasks and outcomes. Reducing the wastage of building resources through design optimization is another major contribution [36]. Sustainable design solutions can be generated with the help of existing commercial BIM software and their enhanced capabilities through plugins. Incorporation of Life Cycle Assessment (LCA) in the design phase [37] and performance optimization through analysis of the indoor environment are some of the significant contributions [38]. During the service life of a building,

BIM can be used for performance monitoring [39], managing and tracing resources [40], and asset maintenance [41]. In addition to that BIM acts as the source of information that enables material passports and databanks [19]. Implementing BIM requires high cost, time, and resources. Besides, the outcome of BIM is affected by the quality of data input.

4.4 Digital Twins

Digital Twins (DT) are the digital version of physical assets that can provide decision support and control feedback for monitoring and maintaining physical assets. According to Arup [42], “A digital twin is the combination of a computational model and a real-world system, designed to monitor, control and optimise its functionality. Through data and feedback, both simulated and real, a digital twin can develop capacities for autonomy and to learn from and reason about its environment.” This emerging technology has wide applications in various industries such as manufacturing, aerospace, consulting, and construction. However, the level of details, maturity and possible extent of control varies with the complexity of the physical systems. The DT can be developed for components, assets, processes, systems or networks of systems [42]. A construction process DT may differ from the DT for aircraft maintenance. The construction DT combines geometric information from BIM and data from sensor networks for data analysis and decision support with intelligent algorithms. The service life of buildings can be extended by predictive maintenance. Integrating material passports with DT enables predictive maintenance [43]. Besides, combining these technologies also helps in reusing material during deconstruction [19]. The DT also supports flexible space utilization in buildings. For example, the DT platform of the EDGE Olympic Office allows people to customize their working spaces [44]. Digital Twin technology is relatively new, and some drawbacks include the lack of standardisation, limited scalability in large projects, the complexity of DT models, and privacy concerns caused by cyber-attacks.

4.5 Big Data Analytics

Big Data Analytics (BDA) applies advanced analytic techniques on exceptionally large datasets that are diverse in composition, source, and structure to derive meaningful information for decision support. Big data refers to the datasets that cannot be processed or managed by conventional relational databases with low latency due to their size or type [45]. In addition to size, heterogeneity, authenticity, value, and speed of processing are some other distinguishing characteristics of big data [46]. Each stage of construction generates a large amount of data from various sources including BIM,

monitoring devices and sensors. Combining other technologies such as BIM, AI and the Internet of Things (IoT), BDA can offer several solutions for material wastage, resource constraints and energy expenditure [47]. Machine Learning algorithms improve their performance while trained with good-quality big data. These algorithms can be applied for creating low-carbon building designs [48] and for assisting tools for generative designs [47]. Besides, ML algorithms fuelled by big data provide decision support during the design [49] and operational phases of a building [50]. The decisions during the design phase may include selecting the right parameters, while for the operation phase they may direct towards improving the energy performance or extending the service life by predictive maintenance. Time-intensive analysis, limited availability of data, high cost of implementation, and low quality of construction data are some of the challenges for employing BDA.

4.6 Blockchain

Blockchain technology offers secure electronic transactions of tangible and intangible assets without intermediaries. Distributed ledgers that allow access to all participants, immutable records that cannot be altered, and smart contracts with stipulated conditions which automate business logic are the key characteristics of blockchain [51]. Transparent and secure transactions with the consensus of all the stakeholders through blockchain enable good business collaborations. The potential of blockchain technology has been extensively focused on developing cryptocurrencies in the earlier days. This technology can be explored for various applications in the construction industry such as tracking the revisions of BIM models, managing material passports, keeping ownership records of assets and automating stakeholder transactions [52]. The fragmented supply chain of the construction industry can be improved by transparent value transactions and efficient information management through blockchain technology [53], [54]. Coupled with the IoT, blockchain can deliver intelligent product services for prefabricated construction [55]. The most significant impact of blockchain is enabling material passports by transparent information flow across supply chain networks at various stages of the building lifecycle [56]. Trustful and collaborative trading networks can be created through this technology by offering secure transactions. One such example is a user-friendly community-based energy trading platform called Pando [57]. The adoption of blockchain requires significant computing power and money. Additionally, it may raise regulatory challenges including cyber security and legal liability.

4.7 The Internet of Things

The IoT refers to the technology that enables equipment connected with sensors or identifiers to communicate with the user or with other equipment through interoperable networks [58]. These networks of connected devices are created through various techniques including cloud computing and wireless sensor networks. Home automation with smart devices and security systems is one of the ubiquitous applications of the IoT. Tracing the building components throughout the building lifecycle is one of the biggest challenges to be addressed for material circularity. Researchers have identified the potential of IoT technology combined with Radio Frequency Identification System (RFID) for tracing the building components physically and digitally [55], [59]. The connected devices in the IoT network produce numerous data that can be utilized to generate meaningful information through BDA. Optimizing the energy performance of a building through IoT enabled lighting system is an example [60]. Assessing the conditions of a building through an embedded sensor system and predicting the maintenance requirements can prolong the service life of buildings [61]. Flexible use of building spaces through monitoring occupancy [62] and improving thermal comfort through controlling HVAC (Heating, Ventilation, and Air Conditioning) systems are other applications of IoT technology [63]. In addition to the high implementation cost and maintenance cost, IoT poses challenges such as the management of large quantities of data, environmental impacts due to high power consumption and discarding of IoT devices, and reliability issues caused by malfunctioning devices.

4.8 Extended Reality

Immersive technologies have grown beyond the realm of entertainment and reached to complex and innovative applications in other industries. According to Unity [64], Extended Reality (XR) refers to “technology-mediated experiences that combine virtual and real-world environments and realities” and stands as a generic terminology for Virtual Reality (VR), Augmented Reality (AR), and Mixed Reality (MR). Digital contents are overlaid in the real world to create AR. The users fully immerse in digitally created visuals that replace the real world to experience VR. The MR technology blends the real world and digital content to allow seamless interactions between these entities. The construction industry is yet to exploit the immense potential of XR for creating various sustainability solutions that involve visualisation and interaction. The XR technology aids immersive visualisation of the design alternatives and building models generated through BIM. This improves communication and consensus among stakeholders and allows correction in the early stages of design and avoids

reworks during construction [65]. The contractors, foremen, and workers can take scheduled virtual tours of the construction sites to reduce mistakes in the upcoming construction activities and associated wastages of materials. Construction safety training assisted by VR technology teaches the labours to navigate various construction accidents in a way that is not possible by conventional training methods [66], [67]. In addition to productivity improvement, loss of time and wastage due to construction accidents or injuries can be avoided by these advanced training techniques. The XR technology can also assist in various end-of-life activities such as planning deconstruction and material logistics between construction sites [68]. The demerits of XR technology include the need for specialised equipment and skillset, the high cost of implementation and maintenance, and sustainability concerns caused by the production and disposal of equipment.

5 Conclusions

Consumeristic and user-centric practices in the construction industry have resulted in significant environmental impacts and reduction in natural resources. A paradigm shift towards the circular economy is necessary for the built environment. Several studies propose theoretical frameworks for implementing circularity principles. Structural holes in the supply chain, coordination of diverse stakeholders, and management of resources at the end of life of buildings are some of the key challenges for implementation. Several independent studies were conducted to apply various technologies in the construction industry. However, only a few of the studies have focused on identifying the technologies and how they facilitate the transition of the built environment into a circular economy. Therefore, this study provides a review of the state of the art technologies and how they enable a circular built environment.

References

- [1] G. L. F. Benachio, M. do C. D. Freitas, and S. F. Tavares, “Circular economy in the construction industry: A systematic literature review,” *J. Clean. Prod.*, vol. 260, 2020.
- [2] United Nations Environment Programme, “2020 Global Status Report for Buildings and Construction: Towards a Zero-emissions, Efficient and Resilient Buildings and Construction Sector - Executive Summary,” 2020.
- [3] S. Wandahl, C. T. Pérez, S. Salling, H. H. Neve, J. Lerche, and S. Petersen, “The impact of construction labour productivity on the

- renovation wave,” *Construction Economics and Building*, vol. 21, no. 3. Australian Institute of Quantity Surveyors, pp. 11–32, 2021.
- [4] H. Wang, W. Chen, and J. Shi, “Low carbon transition of global building sector under 2- and 1.5-degree targets,” *Appl. Energy*, vol. 222, pp. 148–157, 2018.
- [5] O. E. Ogunmakinde, W. Sher, and T. Egbelakin, “Circular economy pillars: a semi-systematic review,” *Clean Technol. Environ. Policy*, vol. 23, no. 3, pp. 899–914, 2021.
- [6] J. Kirchherr, D. Reike, and M. Hekkert, “Conceptualizing the circular economy: An analysis of 114 definitions,” *Resour. Conserv. Recycl.*, vol. 127, pp. 221–232, 2017.
- [7] Ellen MacArthur Foundation (EMF), “Towards the circular economy Vol. 1: an economic and business rationale for an accelerated transition,” 2012.
- [8] M. U. Hossain, S. T. Ng, P. Antwi-Afari, and B. Amor, “Circular economy and the construction industry: Existing trends, challenges and prospective framework for sustainable construction,” *Renew. Sustain. Energy Rev.*, vol. 130, 2020.
- [9] L. A. Akanbi *et al.*, “Salvaging building materials in a circular economy: A BIM-based whole-life performance estimator,” *Resour. Conserv. Recycl.*, vol. 129, pp. 175–186, 2018.
- [10] H. Helander, A. Petit-Boix, S. Leipold, and S. Bringezu, “How to monitor environmental pressures of a circular economy: An assessment of indicators,” *J. Ind. Ecol.*, vol. 23, no. 5, pp. 1278–1291, 2019.
- [11] M. U. Hossain, A. Sohail, and S. T. Ng, “Developing a GHG-based methodological approach to support the sourcing of sustainable construction materials and products,” *Resour. Conserv. Recycl.*, vol. 145, pp. 160–169, 2019.
- [12] B. Huang, X. Wang, H. Kua, Y. Geng, R. Bleischwitz, and J. Ren, “Construction and demolition waste management in China through the 3R principle,” *Resour. Conserv. Recycl.*, vol. 129, pp. 36–44, 2018.
- [13] F. Elghaish, S. T. Matarneh, D. J. Edwards, F. Pour Rahimian, H. El-Gohary, and O. Ejohwomu, “Applications of Industry 4.0 digital technologies towards a construction circular economy: gap analysis and conceptual framework,” *Constr. Innov.*, vol. 22, no. 3, pp. 647–670, 2022.
- [14] IBM, “What is Artificial Intelligence (AI)?,” *IBM Cloud Education*, 2020. <https://www.ibm.com/cloud/learn/what-is-artificial-intelligence> (accessed Aug. 02, 2022).
- [15] IBM, “AI vs. Machine Learning vs. Deep Learning vs. Neural Networks: What’s the Difference?,” *IBM Cloud*, 2020. <https://www.ibm.com/cloud/blog/ai-vs-machine-learning-vs-deep-learning-vs-neural-networks> (accessed Aug. 04, 2022).
- [16] S. K. Baduge *et al.*, “Artificial intelligence and smart vision for building and construction 4.0: Machine and deep learning methods and applications,” *Autom. Constr.*, vol. 141, p. 104440, 2022.
- [17] A. Harichandran, B. Raphael, and A. Mukherjee, “Equipment activity recognition and early fault detection in automated construction through a hybrid machine learning framework,” *Comput. Civ. Infrastruct. Eng.*, vol. 38, no. 2, pp. 253–268, 2023.
- [18] Ellen MacArthur Foundation (EMF) and Google, “Artificial intelligence and the circular economy - AI as a tool to accelerate the transition,” 2019.
- [19] S. Çetin, C. De Wolf, and N. Bocken, “Circular digital built environment: An emerging framework,” *Sustain.*, vol. 13, no. 11, 2021.
- [20] V. J. L. Gan, I. M. C. Lo, J. Ma, K. T. Tse, J. C. P. Cheng, and C. M. Chan, “Simulation optimisation towards energy efficient green buildings: Current status and future trends,” *J. Clean. Prod.*, vol. 254, p. 120012, 2020.
- [21] M. Płoszaj-Mazurek, E. Ryńska, and M. Grochulska-Salak, “Methods to Optimize Carbon Footprint of Buildings in Regenerative Architectural Design with the Use of Machine Learning, Convolutional Neural Network, and Parametric Design,” *Energies 2020, Vol. 13, Page 5289*, vol. 13, no. 20, p. 5289, 2020.
- [22] Arcadis, “Artificial Intelligence in the AEC Industry – a Code of Practice.” <https://www.arcadis.com/en/knowledge-hub/blog/global/susanne-knorr/2020/the-future-of-architecture,-engineering,-and-construction-is-digital-and-intelligent> (accessed Aug. 29, 2022).
- [23] M. U. Mehmood, D. Chun, Zeeshan, H. Han, G. Jeon, and K. Chen, “A review of the applications of artificial intelligence and big data to buildings

- for energy-efficiency and a comfortable indoor living environment,” *Energy Build.*, vol. 202, p. 109383, 2019.
- [24] W. Z. Taffese and E. Sistonen, “Machine learning for durability and service-life assessment of reinforced concrete structures: Recent advances and future directions,” *Autom. Constr.*, vol. 77, pp. 1–14, 2017.
- [25] P. Davis, F. Aziz, M. T. Newaz, W. Sher, and L. Simon, “The classification of construction waste material using a deep convolutional neural network,” *Autom. Constr.*, vol. 122, p. 103481, 2021.
- [26] K. Rakhshan, J. C. Morel, and A. Daneshkhah, “A probabilistic predictive model for assessing the economic reusability of load-bearing building components: Developing a Circular Economy framework,” *Sustain. Prod. Consum.*, vol. 27, pp. 630–642, 2021.
- [27] J. D. Lau Hiu Hoong, J. Lux, P. Y. Mahieux, P. Turcry, and A. Aït-Mokhtar, “Determination of the composition of recycled aggregates using a deep learning-based image analysis,” *Autom. Constr.*, vol. 116, p. 103204, 2020.
- [28] M. Honic, I. Kovacic, G. Sibenik, and H. Rechberger, “Data- and stakeholder management framework for the implementation of BIM-based Material Passports,” *J. Build. Eng.*, vol. 23, pp. 341–350, 2019.
- [29] M. R. Munaro, A. C. Fischer, N. C. Azevedo, and S. F. Tavares, “Proposal of a building material passport and its application feasibility to the wood frame constructive system in Brazil,” in *IOP Conference Series: Earth and Environmental Science*, 2019, vol. 225, no. 1, p. 012018.
- [30] G. Cai and D. Waldmann, “A material and component bank to facilitate material recycling and component reuse for a sustainable construction: concept and preliminary study,” *Clean Technol. Environ. Policy*, vol. 21, no. 10, pp. 2015–2032, 2019.
- [31] M. Honic, I. Kovacic, and H. Rechberger, “Improving the recycling potential of buildings through Material Passports (MP): An Austrian case study,” *J. Clean. Prod.*, vol. 217, pp. 787–797, 2019.
- [32] L. Luscuere, R. Zanatta, and D. Mulhall, “Deliverable 7- Operational Materials Passports,” Brussels, Belgium, 2019.
- [33] O. Oezdemir, K. Krause, and A. Hafner, “Creating a Resource Cadaster—A Case Study of a District in the Rhine-Ruhr Metropolitan Area,” *Build. 2017, Vol. 7, Page 45*, vol. 7, no. 2, p. 45, 2017.
- [34] Madaster, “Madaster - The Materials Cadastre.” <https://madaster.com/> (accessed Aug. 30, 2022).
- [35] C. Eastman, P. Teicholz, R. Sacks, and K. Liston, *BIM Handbook: A Guide to Building Information Modeling for Owners, Managers, Architects, Engineers, Contractors, and Fabricators*, 3rd ed. Hoboken, NJ, USA: John Wiley and Sons, 2018.
- [36] K. din Wong and Q. Fan, “Building information modelling (BIM) for sustainable building design,” *Facilities*, vol. 31, no. 3, pp. 138–157, 2013.
- [37] K. Xue *et al.*, “Bim integrated lca for promoting circular economy towards sustainable construction: An analytical review,” *Sustain.*, vol. 13, no. 3, pp. 1–21, 2021.
- [38] S. Habibi, “The promise of BIM for improving building performance,” *Energy Build.*, vol. 153, pp. 525–548, 2017.
- [39] J. M. Davila Delgado and L. O. Oyedele, “BIM data model requirements for asset monitoring and the circular economy,” *J. Eng. Des. Technol.*, vol. 18, no. 5, pp. 1269–1285, 2020.
- [40] Y.-H. He *et al.*, “BIM and Circular Design,” *IOP Conf. Ser. Earth Environ. Sci.*, vol. 225, no. 1, p. 012068, 2019.
- [41] X. Gao and P. Pishdad-Bozorgi, “BIM-enabled facilities operation and maintenance: A review,” *Advanced Engineering Informatics*, vol. 39, pp. 227–247, 2019.
- [42] Arup, “Digital Twin towards a meaningful framework.” <https://www.arup.com/perspectives/publications/research/section/digital-twin-towards-a-meaningful-framework> (accessed Aug. 11, 2022).
- [43] F. Kedir, D. F. Bucher, and D. M. Hall, “A Proposed Material Passport Ontology to Enable Circularity for Industrialized Construction,” *Proc. 2021 Eur. Conf. Comput. Constr.*, vol. 2, pp. 91–98, 2021.
- [44] EDGE, “EDGE Olympic Amsterdam.” <https://edge.tech/developments/edge-olympic-amsterdam> (accessed Sep. 01, 2022).
- [45] IBM, “Big Data Analytics.” <https://www.ibm.com/analytics/big-data-analytics> (accessed Aug. 30, 2022).

- [46] S. Yin and O. Kaynak, "Big Data for Modern Industry: Challenges and Trends," *Proc. IEEE*, vol. 103, no. 2, pp. 143–146, 2015.
- [47] M. Bilal *et al.*, "Big Data in the construction industry: A review of present status, opportunities, and future trends," *Adv. Eng. Informatics*, vol. 30, no. 3, pp. 500–521, 2016.
- [48] M. Płoszaj-Mazurek, E. Ryńska, and M. Grochulska-Salak, "Methods to Optimize Carbon Footprint of Buildings in Regenerative Architectural Design with the Use of Machine Learning, Convolutional Neural Network, and Parametric Design," *Energies 2020, Vol. 13, Page 5289*, vol. 13, no. 20, p. 5289, 2020.
- [49] G. Bressanelli, F. Adrodegari, M. Perona, and N. Saccani, "Exploring How Usage-Focused Business Models Enable Circular Economy through Digital Technologies," *Sustain. 2018, Vol. 10, Page 639*, vol. 10, no. 3, p. 639, 2018.
- [50] C. Fan and F. Xiao, "Mining big building operational data for improving building energy efficiency: A case study," *J. Build. Serv. Eng. Res. Technol.*, vol. 39, no. 1, pp. 117–128, 2017.
- [51] IBM, "What is Blockchain Technology? - IBM Blockchain." <https://www.ibm.com/topics/what-is-blockchain> (accessed Aug. 30, 2022).
- [52] J. J. Hunhevicz and D. M. Hall, "Do you need a blockchain in construction? Use case categories and decision framework for DLT design options," *Adv. Eng. Informatics*, vol. 45, p. 101094, 2020.
- [53] A. Böckel, A. K. Nuzum, and I. Weissbrod, "Blockchain for the Circular Economy: Analysis of the Research-Practice Gap," *Sustain. Prod. Consum.*, vol. 25, pp. 525–539, 2021.
- [54] A. Shojaei, "Exploring applications of blockchain technology in the construction industry," *ISEC 2019 - 10th Int. Struct. Eng. Constr. Conf.*, 2019.
- [55] C. Z. Li *et al.*, "A blockchain- and IoT-based smart product-service system for the sustainability of prefabricated housing construction," *J. Clean. Prod.*, vol. 286, p. 125391, 2021.
- [56] Arup, "Blockchain and the built environment." <https://www.arup.com/perspectives/publications/research/section/blockchain-and-the-built-environment> (accessed Sep. 01, 2022).
- [57] Pando, "LO3 Energy." <https://lo3energy.com/> (accessed Sep. 01, 2022).
- [58] A. B. Lopes de Sousa Jabbour, C. J. C. Jabbour, M. Godinho Filho, and D. Roubaud, "Industry 4.0 and the circular economy: a proposed research agenda and original roadmap for sustainable operations," *Ann. Oper. Res.*, vol. 270, no. 1–2, pp. 273–286, 2018.
- [59] I. Bertin, R. Mesnil, J. M. Jaeger, A. Feraille, and R. Le Roy, "A BIM-Based Framework and Databank for Reusing Load-Bearing Structural Elements," *Sustain. 2020, Vol. 12, Page 3147*, vol. 12, no. 8, p. 3147, 2020.
- [60] Interact, "Interact IoT lighting." <https://www.interact-lighting.com/global> (accessed Sep. 02, 2022).
- [61] A. Katona and P. Panfilov, "Building Predictive Maintenance Framework for Smart Environment Application Systems," pp. 460–470.
- [62] Deloitte, "MAPIQ." <https://www.resources.mapiq.com/customer-story/deloitte> (accessed Sep. 02, 2022).
- [63] Deloitte, "GR15: The edge of tomorrow." <https://www2.deloitte.com/sk/en/pages/about-deloitte/articles/gx-the-edge-of-tomorrow.html> (accessed Sep. 02, 2022).
- [64] Unity, "Glossary of Terms & Acronyms for Immersive Technology." <https://unity.com/how-to/what-is-xr-glossary> (accessed Aug. 29, 2022).
- [65] E. Jamei, M. Mortimer, M. Seyedmahmoudian, B. Horan, and A. Stojcevski, "Investigating the Role of Virtual Reality in Planning for Sustainable Smart Cities," *Sustain. 2017, Vol. 9, Page 2006*, vol. 9, no. 11, p. 2006, 2017.
- [66] A. Harichandran and J. Teizer, "A Critical Review on Methods for the Assessment of Trainees' Performance in Virtual Reality-based Construction Safety Training," in *29th EG-ICE International Workshop on Intelligent Computing in Engineering*, 2022, pp. 439–448.
- [67] A. Harichandran and J. Teizer, "Automated Recognition of Hand Gestures for Crane Rigging using Data Gloves in Virtual Reality," in *39th International Symposium on Automation and Robotics in Construction (ISARC 2022)*, 2022, pp. 304–311.
- [68] T. M. O'grady, N. Brajkovich, R. Minunno, H. Y. Chong, and G. M. Morrison, "Circular Economy and Virtual Reality in Advanced BIM-Based Prefabricated Construction," *Energies 2021, Vol. 14, Page 4065*, vol. 14, no. 13, p. 4065, 2021.

A review on the Smartwatches as IoT Edge Devices: Assessing the end-users continuous usage intention using structural equation modelling

Udit Chawla¹, Hena Iqbal², Harsh Vikram Singh³, Varsha Mishra⁴, Sarabjot Singh⁵, Vishal Choudhary⁶.

¹University of Engineering and Management, Kolkata, India

²Ajman University, Ajman, UAE

³Techno India University, Kolkata, India

⁴Royal Holloway, University of London, London, United Kingdom

⁵Vellore Institute of Technology, Chennai, India

⁶The Heritage Academy, Kolkata, India

dr.uditchawla@gmail.com, dr.hena.iqbal@gmail.com, harsh16438@gmail.com, mishravarsha.vm@gmail.com, sarabjotsingh2624@gmail.com, chowdharyvishal0904@gmail.com

Abstract – The goal of this study is to identify people's intentions to use smartwatches and how their use of these devices is affected by the advantages and disadvantages of the IoT. For the research work, five cities were chosen, Delhi, Mumbai, Kolkata, and Chennai. These cities were chosen as a study focus primarily because these cities have seen the biggest increases in smartwatch usage in India. These cities have a significant contribution to the global smartwatch market. They provide a number of data points that are important for the research project, enabling it to provide satisfactory results. Structured questionnaires were used to collect data from the respondents. Convenience sampling method was used for the survey. The sample size for the data collection was 249, and it included men and women from a range of age groups, economic levels, and occupational backgrounds. From the findings, it has emerged that six factors influencing customer intention to use smartwatches are “Perceived usefulness”, “Perceived ease of use”, “Perceived connectivity”, “Continuous usage intention”, “Data risk”, and “Performance risk”. The technological characteristics of the Internet of Things, such as perceived connectivity, act as powerful stimulants for smartwatches, favorably affecting customers' perception and the behavioral effects of smartwatch use. The usefulness of smartwatches is unaffected by IoT concerns like data and performance, but the ease of use is negatively impacted by data risks. Furthermore, usefulness and ease of use have a positive influence on the intention to use.

Keywords – Internet of things (IoT); Smartwatch; Benefits; Risks

Introduction

Smartwatches are expanding into the area of the network edge, which will be important for future IoT systems [26]. The monitoring component of the IoT, including human activity, is best served by smartwatches. For example, the Apple Watch Series 8 has a number of built-in sensors, including an accelerometer, gyro, heart rate, barometer, always-on altimeter, compass, SpO2, VO2max, temperature (body), temperature sensing (0.01 accuracy), natural language commands, and dictation (talking mode). As being used for a variety of different purposes such as, tracking your fitness, managing your work, and booking appointments, smartwatches have become indispensable aspects of everyday life [27, 9, 10]. As a result, the development of smartwatches has sparked academic research on the variables affecting the use and acceptance of the device, with a focus on the function of the smartwatches' functional features [14, 18].

Today's modern smartwatch processors are very powerful and can easily execute deep-learning algorithms. For instance, using a special kind of machine called a Restricted Boltzmann Machine, researchers were able to show that it might be possible for someone to manually identify actions on a smartwatch [33]. Smartwatches have been growing in popularity lately, and they are often better than smartphones in terms of features and performance. For instance, action categorization was built and carried out on both smartphones and smartwatches systems by [12]. Their findings demonstrated that gesture action categorization on the smartwatch performed much better than on the smartphone, including an accurate gain of around twenty percent. This is primarily due to the fact that the inertial readings from smartwatches tend to be more precise compared to smartphones because the watch

is much more closely related to the wearer and is physically attached to the hand [30].

As inter-processor efficiency has increased, smartwatches are using wireless networks such as 4G/LTE, which can potentially sustain maximum connection speeds of Fifty Mbits/second. However, because of their short battery lives, smartwatches still have difficulty comprehending and sending information from their sensing devices [11]. For instance, some smartwatch models don't have sensors that can take pictures or videos because it's hard to get accurate information in difficult conditions and it takes a lot of time to do morphological operations for visual information [42]. As smartwatches integrate into the IoT and begin transmitting copious quantities of real-time or nearly real-time information, these problems will grow more severe [17]. To overcome this issue, edge analytics have been suggested. The fundamental concept is to lessen the quantity of sensory information provided in order to minimize energy usage and, as a result, increase battery capacity. To decrease the amount of information delivered, techniques including quantization, screening, and modification can be utilized [10].

In this study, the essential characteristics of visual attraction are benefits, risks, and connectivity. Previous studies separately examined every one of these factors that affect potential users' acceptance of technologies [5, 6, 43, 1]. This study, however, looks at the benefits, risks, and connectivity of smartwatches in order to determine how they are visually attractive and how that affects their use and acceptance. Additionally, it examines how wristwatch owners mediate the influence of visual attractiveness on purchasing behavior and usage behavior considering that different people have different views and attitudes about technology [41, 35, 13]. This research addresses two significant research questions.

RQ1. What variables are co-related with the intention of using a smartwatch?

RQ2. What relationship exists between customer use behavior and the intention to use?

Theoretical Background

2.1 Perceived usefulness

Perceived usefulness is a measure of how much an individual knows that using certain technological tools will improve their productivity [7]. It is based on an individual's external intentions and expectations from a psychological standpoint [19]. The concept has a favorable link with acceptance intent, especially in a range of job scenarios [24, 37]. It is necessary to re-describe perceived usefulness because the current research places a strong emphasis on the terminal viewpoint when it comes to technological usage [28, 20]. In accordance with this research, the more useful a

smartwatch is to its users, the more productive they will be [6]. Therefore, the more advantages customers receive, the happier they will be and the more likely it is that they will keep using smartwatches.

H1. Perceived usefulness is directly associated with the smartwatch continuous usage intention.

2.2 Perceived ease of use

The extent to which an individual experience that utilizing a certain technology might not require any effort is referred to as perceived ease of use [7]. In the moderate sector, the phrase "ease of use" may describe products whose self-service capabilities are widely used and whose simplicity of use by customers is seen as a key factor in their decision-making [29]. The acceptance of a new technology may be predicted using data on a person's perceived ease of use and their intended subsequent behavior. Technology is considered useful when it makes our lives easier. The idea of "ease of use" describes how easy technology is to use, without having to do any extra work [40]. Therefore, in the context of a smartwatch, perceived ease of use can be defined as the simplicity with which users pick up new interactive methods, such as natural language processing or gesture detection, and use them to interact with the device.

H2. Perceived ease of use is directly associated with the smartwatch continuous usage intention.

2.3 Perceived connectivity

A person's opinion of the effect of other people on their decision to accept new technologies is measured by societal influence, according to [41]. The Theory of Reasoned Action provides evidence of how people's opinion is influenced by arbitrary standards and sentiments. According to Rogers [31], the degree of acceptance and enthusiasm for new technologies is tied to their adoption rate. Perceived connectivity, which measures the number of individuals who use the same technologies, is a key factor that determines user acceptability, according to Luo, Gurung, and Shim [23]. The adoption of virtual technology is significantly influenced by perceived connectivity [36]. In fact, user acceptance of advanced technologies can be influenced by how widely it is used by others, particularly close family members or friends. According to Lu, Luo and Strong [22], a significant proportion of consumers are needed to develop potential relationships and recognition. Clearly, the perceived number of consumers, such as neighbors, relatives, or families, will influence how valuable a product is perceived to be in its use [37].

H3. Perceived connectivity is directly associated with the smartwatch continuous usage intention.

2.4 Performance risk

Performance risk entails the chance that goods will not function as planned. This significantly affects users' intentions to purchase specific items, such as smart wristbands. For instance, Hwang, Chung, and Sanders [16]

discovered that customers' perceptions of the performance risks associated with smart apparel had a negative impact on their attitudes about it and, as a result, decreased their desire to purchase the item. A further study found that respondents' increased perceptions of performance risk resulted in a poorer sense of the value of fitness-tracking wearables and this may discourage people from purchasing smartwatches [21]. Smartwatches can continually track a person's everyday behavior and actions, which is one of its main tasks. As a result, whether such a smartwatch can reliably identify and quantify the objective variables is a crucial efficiency problem [32, 34].

H4. Performance risk is directly associated with the smartwatch continuous usage intention.

2.5 Data risk

Privacy risks are especially acute when smartwatch functions monitor personal data, emotions, and extremely personal actions [3]. Whether the user is aware of it or not, the smartwatch can gather and send private pieces of information to third parties. The privacy issue around the gathering, publication, and utilization of information produced by an individual's private smartwatch during their everyday activities could be especially relevant, as the watch is personalized, common, and near to the body. Privacy concerns are raised when it comes to the potential invasion of privacy in virtual communities and social media platforms. These concerns can be humiliating, and they can be exacerbated by private information technology (IT) gadgets that capture extremely private details [4]. Smartwatch reputations may be compromised when people worry that their personal details can be disclosed to or utilized inappropriately by other entities [25]

H5. Data risk is directly associated with the smartwatch continuous usage intention.

2.6 Continuous usage intention

Behavioral intention is defined as a person's consciously stated goal to engage in a particular activity [2, 39]. According to Dehghani and Tumer [8], consumers can choose and consume goods and services through a decision-making process known as consumer intent. It is described as "a user's desire to continually use the immediate good or service being used" to use a common example [15]. The immersive responses of wearable technologies can be regulated, modified, or rapidly changed according to the user's behavioral goals. It could also be used to improve the user's communicative talents [38].

3 Findings & Analysis

Demographic survey-Gender: Female- 40.7% and Male- 59.3%. Age: 18-25- 7.4, 26-30- 34.6, 31-35- 28.9, 36-40- 22.6, >40- 6.5. Educational Qualification- ICSE/CBSE- 8.1, High School- 20, Graduation- 47, PG-

24.2, Others-0.7. Occupation: Service- 27, Business-22.9, Student-49.4, Others-0.7. Income- <25k- 1.7, 25k-50k- 38.2, 50k-75k- 30.5, 75k-1LAC- 18.2, >1LAC- 11.4.

EFA was performed for initial knowledge development of the construct.

CFA was also performed and we got the desired results.

From the Table 1 (Constructs with Variables), we can identify the variables of the respective Constructs. EFA is an Exploratory Factor Analysis and it's done to identify factors affecting Continuous Usage Intention. Confirmatory Factor Analysis (CFA) was performed after EFA.

Table 1 Constructs with Variables

Perceived usefulness
Perceived usefulness refers to how useful a person believes a technology or product to be.
Perceived usefulness can vary depending on the person's needs and preferences.
Perceived usefulness is a key factor that can influence a person's decision to adopt and continue using a smartwatch.
Perceived usefulness is important for the acceptance and continued use of technology.
Perceived usefulness is positively related to a consumer's intention to continue using a smartwatch.
If a consumer perceives a smartwatch as being helpful and useful, they are more likely to continue using it.
Smartwatches are becoming popular due to their many useful features like fitness tracking, etc.
A smartwatch can make your life easier by letting you stay connected without having to pull out your phone.
Perceived ease of use
Perceived ease of use refers to how easy or user-friendly a product is perceived to be by the users.
Smartwatches with well-perceived ease of use will be intuitive and simple for the user to operate.
User Interface (UI) design is important for making a user interface easy to use.
The physical design of the smartwatch affects the perceived ease of use.
Factors that can affect a user's perception of ease of use are the battery life, display size, features, and menu.
Consistent layout, readable text, and intuitive gesture commands can make a user interface more user-friendly.
Perceived connectivity
Smartwatches include additional sensors that can be used to track activity, detect falls, and measure altitude.
Smartwatches have various apps that can be downloaded and used to personalize and enhance the user's experience.
Smartwatches can be used as a tool for self-expression and personal style.
Smartwatches are a versatile technology that can do more than just receive notifications or track fitness.
Performance risks
The main performance risk associated with a smartwatch is its battery life.
The performance risk associated with smartwatches is the accuracy of their sensors and tracking features.
The performance risk of using a smartwatch is related to the cost of repairs or replacements.
The performance risk associated with smartwatches is related to the quality and reliability of the device.
Data risks
There is a risk that this personal data can be accessed or stolen by unauthorized parties.
Smartwatches often have GPS sensors, which can be used to track the wearer's location.
Many smartwatches include sensors that can track things like heart rate, sleep, and exercise.
Continuous usage intention
The important aspect for continuous usage is the compatibility and the ecosystem of the smartwatch.

Using structural equation modelling, the hypotheses H1, H2, H3, H4, and H5 are tested. As a result, a structural model using AMOS 22.0 was created (Figure 1), which shows the factors that affect the continuous usage intention of smartwatches.

According to the results, the model well fits the data (Chi-square value is 141.645, df = 54, p 0.001); CMIN/DF = 2.62; GFI = 0.94; AGFI = 0.92; NFI = 0.93; CFI = 0.97; and RMSEA = 0.045.

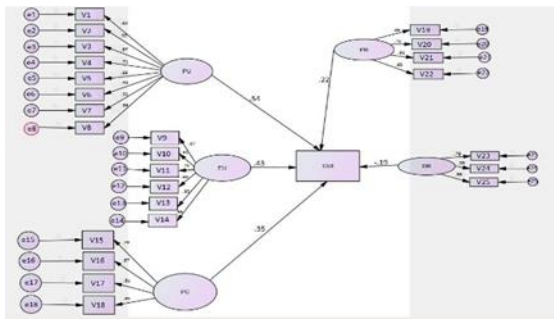


Figure 1. Structural Equation Modelling

The structural model suggests that Perceived usefulness (PU), Perceived ease of use (EU), Perceived connectivity (PC), and Performance risks (PR) have a positive influence on the Continuous Usage Intention of Smartwatches by Consumers. The construct Perceived usefulness (PU) is the most significant factor of Continuous Usage Intention as the regression weight is 0.54. The construct Perceived ease of use (EU) and Perceived connectivity (PC) are the second and third most significant factors of Continuous Usage Intention as their regression weights are 0.43 and 0.35. The construct Performance risks (PR) is the least significant factor of Continuous Usage Intention as its regression weight is 0.22. The Construct Data risk has a negative influence on Continuous Usage Intention as its regression weight is -0.19. Thus, it may be hypothesized that customers in general consider continuous usage intention with respect to the factors Perceived usefulness (PU), Perceived ease of use (EU), Perceived connectivity (PC), and Performance risks (PR). There is only a negative influence with the factor Data risks.

4 Managerial Implication and Conclusion

The phrase "perceived ease of use" relates to how someone feels about using a technical system. PEU has a favorable impact on people's attitudes toward adopting IoT. The more straightforward someone thinks using a smartwatch is, the more favorably that person will see the item and have an attitude toward using it. PEU hence has a favorable link with the continuous usage intention of smartwatches. The smartwatch is more beneficial to consumers as a result of their perception that it is simple to use. Thus, Perceived usefulness has a significant and positive relationship with smartwatch continuous usage intention. The perceived connectivity has a significant impact on how well-liked digital devices are. User acceptability may be influenced by how others, particularly close family or friends, utilize technology. The number of users—such as coworkers, friends, or family—will have an effect on how valuable technology

is thought to be. Using a smartwatch and PC regularly are positively related. However, if people perceive fitness-tracking wearables to have a higher risk of malfunctioning, they are less likely to value them and buy smartwatches. Therefore, performance risk is crucial when choosing a wristwatch. As a result, PR and continuous usage intention of a smartwatch are positively correlated. The term "data risk" describes a person's worries about a potential invasion of privacy. Such losses of personal data can be more unpleasant with IT gadgets that capture private information. Smartwatch identity may be weakened when people worry that their personal information could be disclosed to or used inappropriately by other parties. So, privacy issues will make it harder for someone to identify with their wristwatch. As a result, data risk has a detrimental effect on the continuous usage intention of smartwatches. The purpose of this study is to evaluate the impact of smartwatch technology on both planned and actual use. Unlike previous studies focusing on consumer preferences, this research examined risks and benefits of smartwatches.

References

- [1] Adapa, A., Nah, F. F. H., Hall, R. H., Siau, K., & Smith, S. N. "Factors influencing the adoption of smart wearable devices," *Int. J. Hum. Comput. Interact.*, vol. 34, no. 5, pp. 399–409, 2018.
- [2] Agudo-Peregrina, Á. F., Hernández-García, Á., & Pascual-Miguel, F. J. "Behavioral intention, use behavior and the acceptance of electronic learning systems: Differences between higher education and lifelong learning," *Comput. Human Behav.*, vol. 34, pp. 301–314, 2014.
- [3] Bellotti, V., & Sellen, A. "Design for privacy in ubiquitous computing environments," in *Proceedings of the Third European Conference on Computer-Supported Cooperative Work 13–17 September 1993, Milan, Italy ECSCW '93*, Dordrecht: Springer Netherlands, pp. 77–92, 1993.
- [4] Choi, B. C., Jiang, Z., Xiao, B., & Kim, S. S. "Embarrassing exposures in online social networks: An integrated perspective of privacy invasion and relationship bonding," *Inf. Syst. Res.*, vol. 26, no. 4, pp. 675–694, 2015.
- [5] Choi, J., & Kim, S. "Is the smartwatch an IT product or a fashion product? A study on factors affecting the intention to use smartwatches," *Comput. Human Behav.*, vol. 63, pp. 777–786, 2016.
- [6] Chuah, S. H. W., Rauschnabel, P. A., Krey, N., Nguyen, B., Ramayah, T., & Lade, S. "Wearable technologies: The role of usefulness and visibility in smartwatch adoption," *Comput. Human Behav.*, vol. 65, pp. 276–284, 2016.
- [7] Davis, F. D. "Perceived usefulness, perceived ease

- of use, and user acceptance of information technology,” *MIS Q*, vol. 13, no. 3, p. 319, 1989.
- [8] Dehghani, M., & Tumer, M. “A research on effectiveness of Facebook advertising on enhancing purchase intention of consumers,” *Comput. Human Behav.*, vol. 49, pp. 597–600, 2015.
- [9] Dehghani, M., & Dangelico, R. M. “Smart wearable technologies: state of the art and evolution over time through patent analysis and clustering,” *Int. J. Prod. Dev.*, vol. 22, no. 4, p. 293, 2018.
- [10] Gaura, E. I., Brusey, J., Allen, M., Wilkins, R., Goldsmith, D., & Rednic, R. “Edge mining the internet of things,” *IEEE Sens. J.*, vol. 13, no. 10, pp. 3816–3825, 2013.
- [11] Conti, F., Palossi, D., Andri, R., Magno, M., & Benini, L. “Accelerated visual context classification on a low-power smartwatch,” *IEEE Trans. Hum. Mach. Syst.*, vol. 47, no. 1, pp. 1–12, 2016.
- [12] Weiss, G. M., Timko, J. L., Gallagher, C. M., Yoneda, K., & Schreiber, A. J. “Smartwatch-based activity recognition: A machine learning approach,” in 2016 IEEE-EMBS International Conference on Biomedical and Health Informatics (BHI), pp. 426–429, 2016.
- [13] Ha, T., Beijnon, B., Kim, S., Lee, S., & Kim, J. H. “Examining user perceptions of smartwatch through dynamic topic modeling,” *Telemat. Inform.*, vol. 34, no. 7, pp. 1262–1273, 2017.
- [14] J.-Hong, J. C., Lin, P. H., & Hsieh, P. C. “The effect of consumer innovativeness on perceived value and continuance intention to use smartwatch,” *Comput. Human Behav.*, vol. 67, pp. 264–272, 2017.
- [15] Hong, J., Lee, O. K., & Suh, W. “A study of the continuous usage intention of social software in the context of instant messaging,” *Online Inf. Rev.*, vol. 37, no. 5, pp. 692–710, 2013.
- [16] Hwang, C., Chung, T. L., & Sanders, E. A. “Attitudes and purchase intentions for smart clothing: Examining U.S. consumers’ functional, expressive, and aesthetic needs for solar-powered clothing,” *Cloth. Text. Res. J.*, vol. 34, no. 3, pp. 207–222, 2016.
- [17] Kumar, K., Liu, J., Lu, Y. H., & Bhargava, B. “A survey of computation offloading for mobile systems,” *Mob. Netw. Appl.*, vol. 18, no. 1, pp. 129–140, 2013.
- [18] Kalantari, M., & Rauschnabel, P. “Exploring the early adopters of augmented reality smart glasses: The case of Microsoft HoloLens,” in *Augmented Reality and Virtual Reality*, Cham: Springer International Publishing, pp. 229–245, 2018.
- [19] Kim, H. W., Chan, H. C., & Gupta, S. “Value-based Adoption of Mobile Internet: An empirical investigation,” *Decis. Support Syst.*, vol. 43, no. 1, pp. 111–126, 2007.
- [20] Kulviwat, S., Bruner II, G. C., Kumar, A., Nasco, S. A., & Clark, T. “Toward a unified theory of consumer acceptance technology,” *Psychol. Mark.*, vol. 24, no. 12, pp. 1059–1084, 2007.
- [21] Li, J., Ma, Q., Chan, A. H., & Man, S. S. “Health monitoring through wearable technologies for older adults: Smart wearables acceptance model,” *Appl. Ergon.*, vol. 75, pp. 162–169, 2019.
- [22] Lou, H., Luo, W., & Strong, D. “Perceived critical mass effect on groupware acceptance,” *Eur. J. Inf. Syst.*, vol. 9, no. 2, pp. 91–103, 2000.
- [23] Luo, X., Gurung, A., & Shim, J. P. “Understanding the determinants of user acceptance of enterprise instant messaging: An empirical study,” *J. Organ. Comput.*, vol. 20, no. 2, pp. 155–181, 2010.
- [24] Marangunić, N., & Granić, A. “Technology acceptance model: a literature review from 1986 to 2013,” *Univers. Access Inf. Soc.*, vol. 14, no. 1, pp. 81–95, 2015.
- [25] Montgomery, K. C., Chester, J., & Kopp, K. *Health Wearable Devices in the Big Data Era: Ensuring Privacy, Security, and Consumer Protection*. Democraticmedia.org. [Online]. Available: <https://www.democraticmedia.org/CDD-Wearable-Devices-Big-Data-Report>. [Accessed: 26-Jun-2023].
- [26] P. Lamkin, “Smartwatch popularity booms with fitness trackers on the slide,” *Forbes*, 22-Feb-2018. [Online]. Available: <https://www.forbes.com/sites/paullamkin/2018/02/22/smartwatch-popularity-booms-with-fitness-trackers-on-the-slide/>. [Accessed: 26-Jun-2023].
- [27] Park, E., E. Park, K. J. Kim, K. J. Kim, S. J. Kwon, and S. J. Kwon. “Understanding the Emergence of Wearable Devices as Next-generation Tools for Health Communication.” *Information Technology & People* 29 (4): 717–732, 2016.
- [28] Park, Y., Chen, J.V.: Acceptance and adoption of the innovative use of smartphone. *Ind. Manag. Data Syst.* 107(9), 1349–1365 (2007)
- [29] Pavlou, P. A., and M. Fygenson. “Understanding and Predicting Electronic Commerce Adoption: An Extension of the Theory of Planned Behavior.” *MIS Quarterly* 30: 115–143, 2006.
- [30] R. Rawassizadeh, B. A. Price, and M. Petre, “Wearables: has the age of smartwatches finally arrived?,” *Communications of the ACM*, vol. 58, no. 1, pp. 45–47, Dec. 2014.
- [31] Rogers, E. M. *Diffusion of innovation* (5th ed.). New York: Free press, 2003.
- [32] Rupp, M. A., Michaelis, J. R., McConnell, D. S., & Smither, J. A. The role of individual differences on perceptions of wearable fitness device trust, usability, and motivational impact. *Applied Ergonomics*, 70, 77–87, (2018).
- [33] S. Bhattacharya and N. D. Lane, “From smart to

- deep: Robust activity recognition on smartwatches using deep learning,” in 2016 IEEE International Conference on Pervasive Computing and Communication Workshops (PerCom Workshops), pp. 1–6, 2016.
- [34] Shih, P. C., Han, K., Poole, E. S., Rosson, M. B., & Carroll, J. M. Use and adoption challenges of wearable activity trackers. Proceedings of the IConference 2015. Retrieved from <http://hdl.handle.net/2142/73649>, 2015.
- [35] Sohail, M. S., and I. M. Al-Jabri. “Attitudes Towards Mobile Banking: Are There any Differences between Users and Non-Users?” *Behaviour & Information Technology* 33 (4): 335–344, 2014
- [36] Strader, T. J., Ramaswami, S. N., & Houle, P. A. Perceived network externalities and communication technology acceptance. *European Journal of Information Systems*, 16(1), 54–65. doi:10.1057/palgrave.ejis.3000657, 2007.
- [37] Tarhini, A., Arachchilage, N.A.G., Masa’deh, R., Abbasi, M.S.: A critical review of theories and models of technology adoption and acceptance in information system research. *Int. J. Technol. Diffus.* 6(4), 1–20 (2015)
- [38] Turhan, G. “An Assessment Towards the Acceptance of Wearable Technology to Consumers in Turkey: The Application to Smart Bra and T-shirt Products.” *Journal of the Textile Institute* 104 (4): 375–395, 2013.
- [39] Venkatesh, V., J. Y. Thong, and X. Xu. “Consumer acceptance and use of information technology: Extending the unified theory of acceptance and use of technology,” *MIS Q*, vol. 36, no. 1, p. 157, 2012.
- [40] Venkatesh, V., Morris, M.G., Davis, G.B. and Davis, F.D. “User acceptance of information technology: toward a unified view”, *MIS Quarterly*, Vol. 27 No. 3, pp. 425-478, 2003.
- [41] Verkasalo, H., C. López-Nicolás, F. J. Molina-Castillo, and H. Bouwman. “Analysis of Users and Non-users of Smartphone Applications.” *Telematics and Informatics* 27 (3): 242–255, 2010.
- [42] Y. Ai, M. Peng, and K. Zhang, “Edge computing technologies for Internet of Things: a primer,” *Digital Communications and Networks*, vol. 4, no. 2, pp. 77–86, Apr. 2018.
- [43] Yang, H., J. Yu, H. Zo, and M. Choi. “User Acceptance of Wearable Devices: An Extended Perspective of Perceived Value.” *Telematics and Informatics* 33 (2): 256–269, 2016.